GEOMORPHOLOGICAL STUDY OF FLUVIAL FEATURES, FARAH VALLIS, MARS

Dissertation submitted to Christ College (Autonomous), Irinjalakuda, Kerala, University of Calicut in partial fulfillment of the degree of

Master of Science in Applied Geology

By,

AATHIRA P SANTHOSH

Reg. No: CCAVMAG001

2021-2023

DEPARTMENT OF GEOLOGY AND ENVIRONMENTAL SCIENCE CHRIST COLLEGE (AUTONOMOUS), IRINJALKUDA, KERALA, 680125

(Affiliated to University of Calicut and re-accredited with by NAAC with A++ grade)

SEPTEMBER 2023

DEPARTMENT OF GEOLOGY AND ENVIRONMENTAL SCIENCE

CHRIST COLLEGE (AUTONOMOUS) IRINJALAKUDA

CERTIFICATE

Certified that the dissertation work entitled "**GEOMORPHOLOGICAL STUDY OF FLUVIAL FEATURES, FARAH VALLIS, MARS**" is a bona fide record of work done by M.s AATHIRA P SANTHOSH of fourth semester M.Sc. Geology in this college during 2021-2023.

Dr. Anto Francis K

The Co-Ordinator

Dept. of Geology and Environmental science

Christ College (Autonomous) Irinjalakuda

Kerala- 680125

Place: Irinjalakuda

Date: ……

External Examiners;

1…….

2…….

CERTIFICATE

This is to certify that the dissertation entitled – **GEOMORPHOLOGICAL STUDY OF FLUVIAL FEATURES, FARAH VALLIS, MARS**, is a bona fide record of work done by Ms. Aathira P Santhosh (Reg. No. CCAVMAG001), MSc Applied Geology, Christ College (Autonomous) Irinjalakuda, under my guidance in partial fulfillment of requirements for the degree of Master of Science in Applied Geology during the year 2021-2023.

Mr. Gopakumar. P. G

Assistant Professor

Dept. of Geology and Environmental science

Christ College (Autonomous) Irinjalakuda

Kerala- 680125

Place: Irinjalakuda

Date: ……

DECLARATION

I hereby declare that this dissertation work – **"GEOMORPHOLOGICAL STUDY OF FLUVIAL FEATURES, FARAH VALLIS, MARS"** is a work done by me. No part of the report is reproduced from other resources. All information included from other sources has been duly acknowledged. I maintain that if any part of the report is found to be plagiarized, I shall take the full responsibility for it.

AATHIRA P SANTHOSH

CCAVMAG001

Place: Irinjalakuda

Date: ……

ACKNOWLEDGEMENT

I take this opportunity to thank everyone who made this a meaningful exercise. First and foremost, I would like to express my sincere gratitude to my guide **Mr. Asif Iqbal Kakkassery**, Assistant Professor Department of Geology, Government College Kasaragod, for his enthusiastic guidance, valuable suggestions, and inexhaustible encouragement which inspired me to complete this work.

I express my heartfelt gratitude to **Mr. Gopakumar. P.G**, Department of Geology and Environmental Science, Christ College (Autonomous), Irinjalakuda for his guidance, cooperation and valuable support throughout the course of work.

Dr. Linto Alappat, Dean of Reasearch and Development of TLC (Former Head, Department of Geology and Environmental Science, Christ College (Autonomous) Irinjalakuda), **Tharun. R,** Head, Department of Geology and Environmental Science, Christ College (Autonomous) Irinjalakuda, for rendering all the help and facilities available in the department.

I am deeply thankful to **Dr. Anto Francis K**, the Co-Ordinator of M.Sc. Applied Geology, and other faculty members of Department of Geology and Environmental Science, Christ College (Autonomous), Irinjalakuda, for their support, guidance.

I would like to extend my thanks to **Mr. Ayyappadas C.S**. for the continuous support provided for the completion of the dissertation.

I'd like to take this opportunity to thank all of my classmates and friends who supported me in completing this dissertation work, whether directly or indirectly. I am grateful to the entire Christ College family for their love, support, and guidance. I also express my gratitude to my parents and family members for their unwavering support and prayers throughout my life.

Above all, I express my gratitude to God, the Almighty, for his divine generosity and blessings showered upon me.

Aathira P Santhosh

ABSTRACT

Fluvial activities are dominant in the Martian surface which has extensively modified the planet from early times. Farah vallis is a small valley. Studies provide observations of the topography and geomorphology of this paleolake outflow valley and connected tributary valleys in order to determine when the Farah Vallis system was incised. It's critical to quantify the lake levels in Gale Crater in order to describe the hydrologic and climatic history of the sedimentary layers that Curiosity has discovered. We suggest that there were at least three significant lake stands in Gale, each of which lasted for more than a thousand years, and all of which appeared after Mount Sharp reached close to the topographic form it currently has. The highest lake level, which had a mean depth of 700 m, is defined by deltaic deposits off the southern rim of Gale, resulting from the incision of Farah Vallis, and comparable deposits off the southern flank of Mount Sharp. Near Gale, canyons with a shape resembling Farah Vallis enter craters and/or the crustal dichotomy from the south, indicating that the largest lake was fed by a massive flow system.

The main objective of the study is to identify geomorphological features of Farah Vallis by digitizing the features using ArcGIS 10.8. The MRO context camera (CTX) images of Farah Vallis were downloaded from The Geosciences Node of NASA's Planetary Data System (PDS) archives which distributes digital data related to the study of the surfaces and interiors of terrestrial planetary bodies.

From the geomorphological mapping of the Farah Vallis, the prominent geological features identified are main Vallis, Tributary Vallis, delta etc. The features are formed in the south west region of the Gale Crater. The various feature seen in the Farah Vallis tells us about the fluvial activity that is ongoing on its surface.

TABLE OF CONTENTS

List of Figures

CHAPTER 1

INTRODUCTION

1.1 MARS

Mars is one of the eight Planets of the solar system that appears to be red-orange in color due to the presence of iron oxide. The next planet after Earth is Mars, which is the fourth planet from the Sun. It is a terrestrial planet and is second smallest in the entire solar system. Mars has been observed, studies and recorded throughout the history using Earth-based and orbiting telescope. Even before the development of telescope astronomers have noted the movement of Mars across the sky. With the development of technologies over the last 40 years greater studies of Martian surface is possible today; the recent observation being the presence of water and its major role in the climatic conditions of Mars.

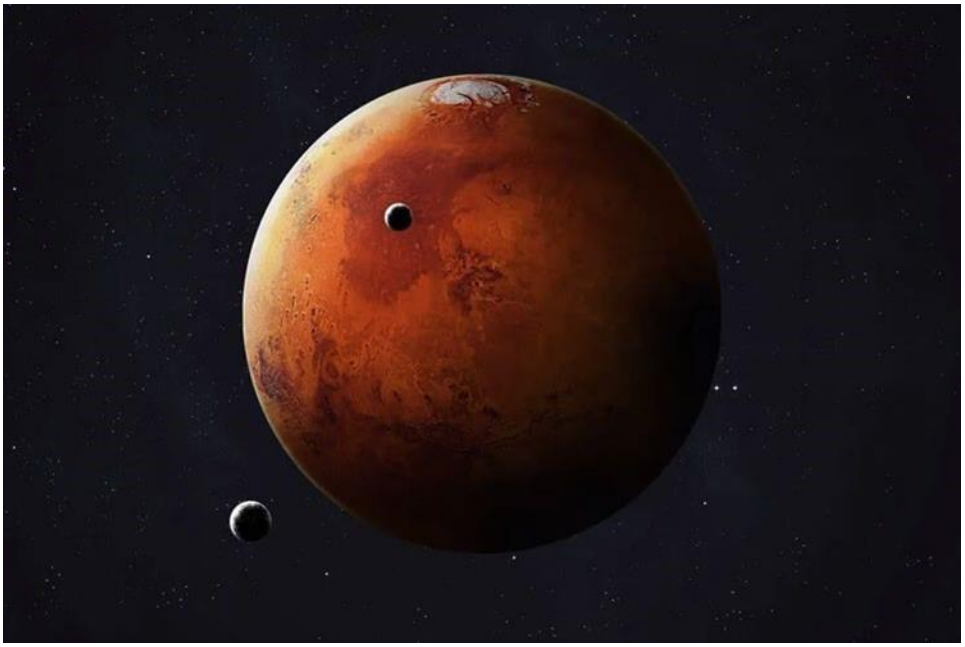

Figure 1.1: Shot of Mars taken from open space – (image www.telescopenights.com)

Today Mars has thin CO_2 atmosphere and is very cold and dry with respect to the Earth; nevertheless, it is likely that the planet may have experienced a warmer and wetter climate in the past. Due to the presence of a thicker atmosphere able to generate a greenhouse effect capable to stabilize liquid water on the Martian surface (Sagan et al., 1973; Pollack et al.,1987; Kargel, 2004; Car, 2006).

Mars is at an average distance of 2.279×10^{28} km (1.3237 astronomical unit) from the sun. Its orbit is inclined about 1.851 degree to the elliptical planet. Its orbit is more elliptical compared to others with an eccentricity of 0.0934. It is also called red planet due to the abundance of iron oxide in the surface of Mars. Mars has two small moons, outermost Phobos (FOE-bosh) and innermost Deimos (DEE-mosh).

Figure 1.2: Phobos, Mars' largest moon. (Image Credit: NASA)

Mars is formed along with the rest of solar system around 4.5×109 years (109 years=1Ga) ago from the protoplanetary nebula (cloud of gas and dust). Different elements condensing in

different locations due to variation of temperature pressure throughout the solar system. Iron oxides should be present in the solar nebula where Mars is formed. The materials that still remained after the planet formation contributed to heavy bombardment creating impact craters on the bodies of solid surfaces. In the inner solar system, Mercury, the Moon, and Mars all have heavily cratered surfaces.

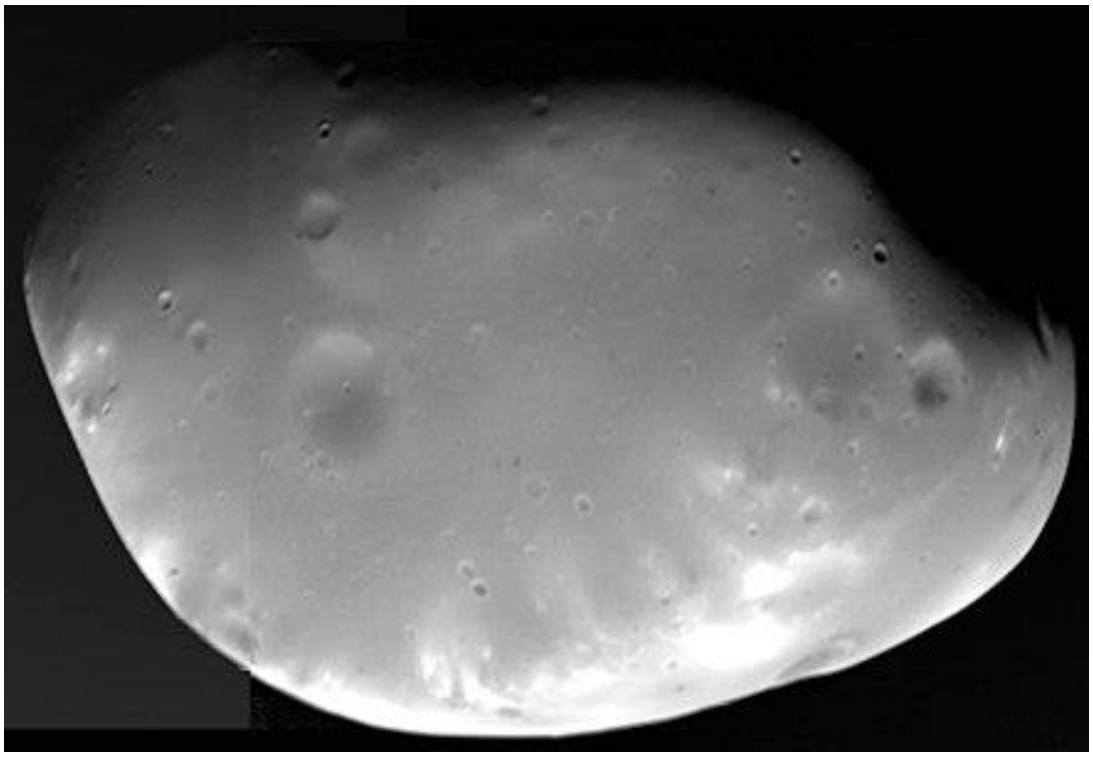

Figure 1.3: Mars' smaller moon, Deimos (Image credit: NASA)

The surface of Mars is rocky and covered in craters, canyons, volcanoes, and dried lake beds. Red dust covers most of its surface. And it has clouds and wind just like Earth. Mars' atmosphere is far thinner than Earth's. People would not be able to breath the air on Mars because it contains more the 95% carbon dioxide and much less than 1% oxygen. The surface erosion of Mars is extremely lower compared to the Earth, so very ancient to recent Martian landscapes are preserved and are available for observation. The angle of repose of Mars is about 33 degrees; the same as in the Earth. The planet's geological history is visible which makes the studies potential to provide deeper insights into early evolution of the planet. The lack of precipitation, vegetation & human influence have preserved the landforms on the Mars.

These findings, along with the assumption that almost all geological processes seen on Earth also occurred on Mars, make it a potent laboratory for comparing geomorphological processes.

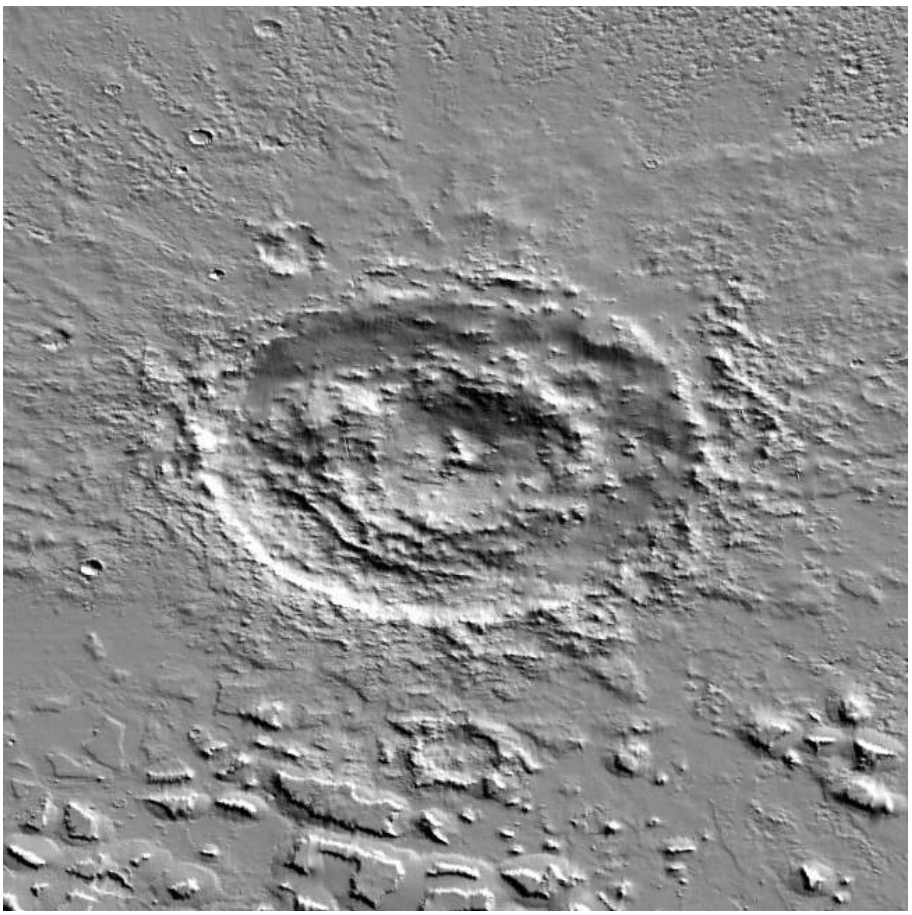

Figure 1.4: Loyt Crater, located at 50.38^N 29.33^E (Viking mosaic image, NASA/JPL).

1.2 AGES OF MARS

With no samples it is difficult to study about the history of the red planet. Scientist calculate the age of Mars by the presence of craters present on them; with larger number of impact craters indicate older terrain. But there is difficulty because of the extensive volcanism Mars suffered along with the erosion by glaciers, wind and running water and widespread deposition of sediments that buries the older craters.

On the basis of studies of largest impact craters and impact history of the solar system the southern highlands if Mars represent the oldest crust. They are believed to have formed prior

to 3.8 billion years ago. The northern plains that are less heavily cratered are newer because they contain fewer, smaller craters and developed after the end of the big bombardment.

The Martian geological history of has been divided in to three main periods each named after a region of Mars. An earlier, pre-Noachian, period has also identified, even though no physical evidence for its existence remains. As fresh information is discovered, the story's dates and specifics are continuously changed.

1.2.1 Pre-Noachian Epoch (4.5- 4.1 billion years ago)

Scientists believe that Mars experienced an extraordinarily high rate of impact during the planet's early history, which began 4.5 billion years ago with the development of its crust. During Pre-Noachian Era Martian surface has suffered extremely high impact formation of has an age about 4.13 billion years (or earlier). A cluster of very large low land making basin occurred during this time.

The earliest, extremely dense atmosphere of this time period. Which is formed due to the result of asteroid or comet impacts and outgassing of the planet’s mantle, started to cooldown. Then slowly the water vapor in the atmosphere would have condensed into vast ocean, perhaps even a global ocean, that existed at high temperature. This large body of water started to cool down, resulting in a first window for the possible emergence of life around 4.4 to 4.3 billion years ago.

The atmosphere which was formed after the solidification of an early Martian magma outgassed volatile could have been lost thermally during this era and Mars could have been wet and hot with surface CO2.

1.2.2 Noachian epoch (4.1- 3.7 billion years ago)

The Noachian Period is characterized by the oldest, densely cratered units in the highlands covering a time range of older than 3.97 Gyr ago (Tanaka et al., 1992; Hartmann and Neukum, 2001). During the early Noachian epoch, the well-preserved Hellas, Argyre & Isdis basin were formed after all the global magnetic field died. The Noachian Period is named after the ancient highland area known as Noachis Terra, which is situated in the southern hemisphere between

the massive Argyre and Hellas impact basins. These basins are the largest impact basin still visible on the planet.

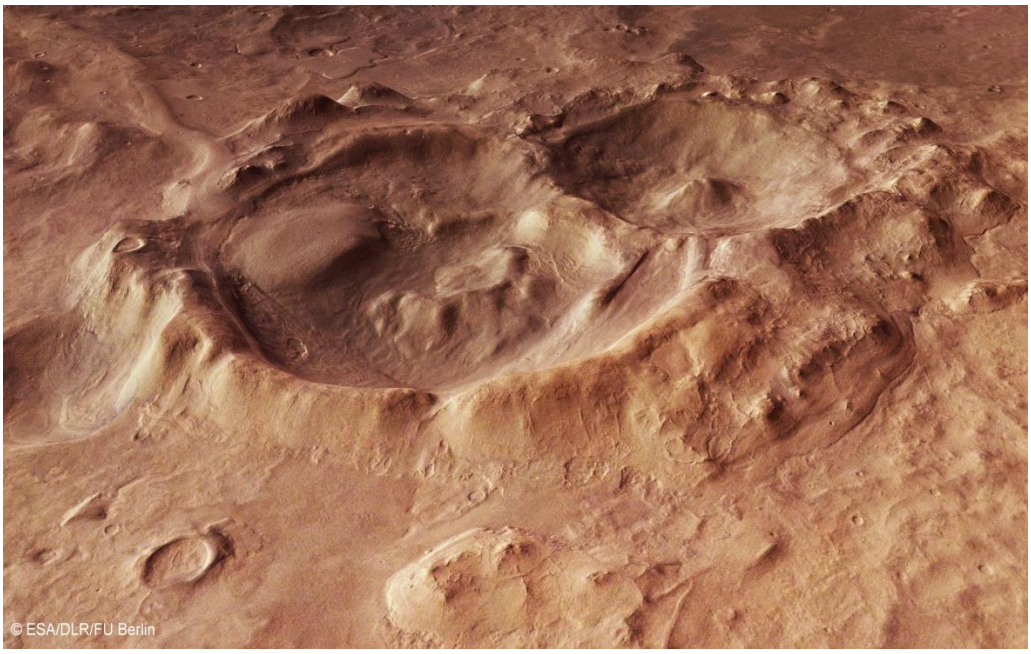

Figure 1.5: Craters within the Hellas Basin. Credit: ESA/DLR/FU

Noachian is still period of heavy bombardment and large-scale volcanic activity took place in the Tharsis region and parts of highlands. Tharis bulgre is home to Arsia Mons, Pavonis Mons and Ascraeus Mons; some of the largest volcanoes in the solar system. Growth of Tharis bulge coincides with widespread fracturing of the surface and the creation of the giant rift valley system known as Valles Marineris with the continuing volcanic eruption ash and gases accumulated into the atmosphere and the blanket of air got thicker trapping more solar heat which heated the planet. This further probably leads to clouds development and precipitation rained to the ground. Lakes seem to have formed in many basins and craters and many of the valley networks on Mars date from this period. There may even have been a shallow ocean converging at least part of the northern lowlands. Meanwhile, when the planet's interior cooled and its magnetic dynamo went down, Mars lost its global magnetic field. Habitable environments gradually became smaller and more localised, but Noachian surface conditions continued to be favourable for the emergence pf life.

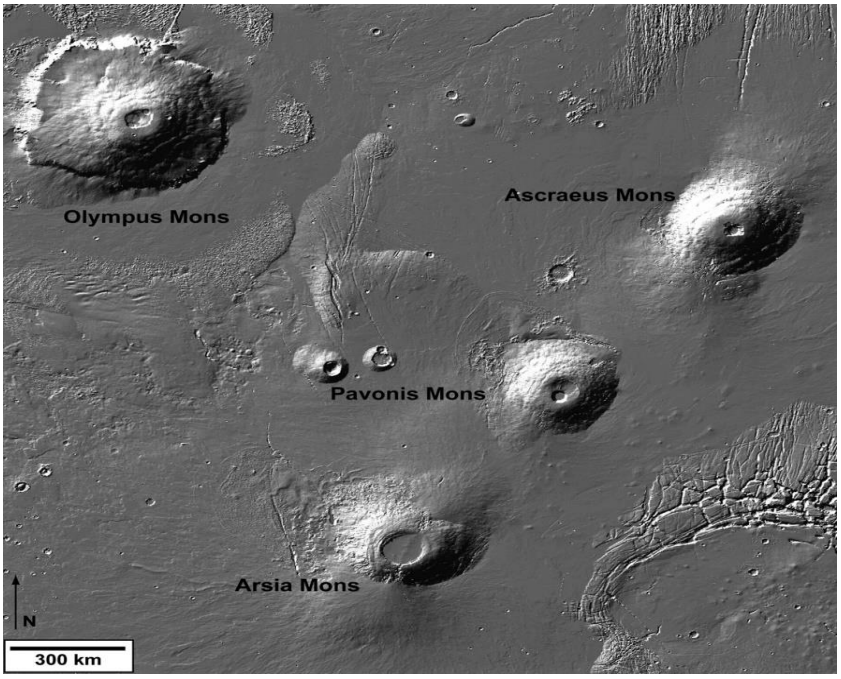

Figure 1.6: Shaded relief image of Tharis Montes and Olympus Mons derived from Mars Orbiter Altimeter data which flew on board NASA's Mars Global Surveyor.

1.2.3 Hesperian epoch (3.7- 2.9 billion years ago)

The era was named after the Hesperia planum a region of ridged plain located North- East of the Hellas Platina impact basin and last amount 800 million years.

During the era the impact cratering rates were significantly low compared to Noachian period. There were still considerable volcanism and the global geological activity was slowing down. According to studies, volcanic plains were common, especially in the northern lowlands, and at least 30% of Mars resurfaced during this time.

The Hesperian Period, which spans from 3.74 billion years ago to 2.9 billion years ago, is separated into the Early and Late Hesperian epochs and is distinguished by the Hesperia Planum ridged plains material northeast of the Hellas Planitia impact basin. The Early Hesperian period covers the age range of 3.74 to 3.65 Gyr ago (Hartmann and Neukum, 2001). The late Hesperian, which spanned 3.65 to 2.9 Gyr in the past, (Hartmann and Neukum, 2001).

Figure1.7: A large elliptical impact crater in the Hesperia Planum region of Mars. Image credit: ESA

1.2.4 Amazonian Epoch (2.9 billion years ago to present)

The most recent period of Martian history is named after the smooth plains of Amazonis Platina in the northern hemisphere. The Amazonian covers at least half of the planet's entire history, although the dating of the period is very uncertain: most estimates place its start date at about 2.9 billion years ago.

The Amazonian Period is commonly defined by processes related to extensive resurfacing of the northern lowlands. The Amazonian Period is characterised by absence of large-scale features such as climatic changes and geological changes, the planet’s surface has been dry and arid. The rocks have been altered slowly due to weathering, wetter conditions, short-lived etc.

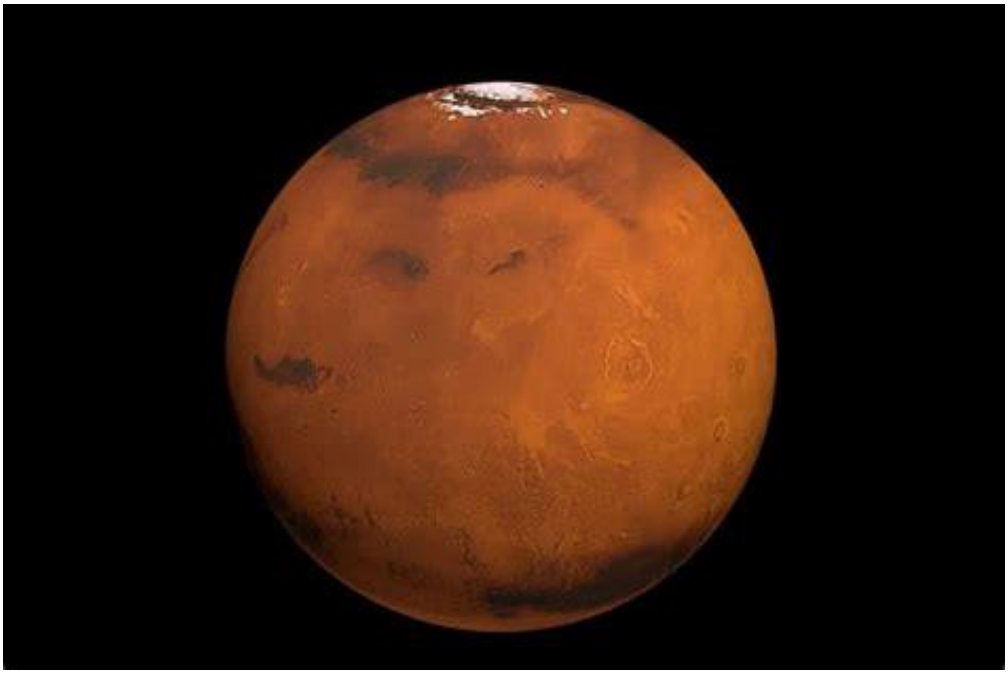

*Figure 1.8: Mars-with-white-polar-*cap *(image: www.telescopenights.com)*

1.3 History of Martian Exploration

Mars exploration, which is one of the closest planets to Earth that is also like it, is the second-hottest areas of deep space exploration after lunar exploration(Dengyun et al., 2016). As the neighbor of the Earth, the Mars evolution is of significant importance for understanding the history and future evolution of the Earth(Li et al., 2021) . Martian exploration has been ongoing for centuries, with the first records of the planet being made by the ancient Greeks. In modern times, exploration of Mars has been conducted by both human astronauts and robotic spacecraft. Robotic exploration of Mars began in 1960 with the launch of the Soviet Union's Sputnik 24 mission. Since then, numerous robotic spacecraft have been sent to explore Mars, including orbiters, rovers, and landers. These missions have provided us with a wealth of data about the planet's atmosphere, geology, potential for habitability, and climate etc.

The exploration of Mars began in the 16th century when astronomer Galileo Galilei first observed the planet through a telescope. In the 19th century, astronomers such as William Herschel and Giovanni Schiaparelli made detailed observations of the planet's surface features. This was followed by a series of increasingly sophisticated robotic spacecraft, including rovers, orbiters, and landers sent by NASA and other space agencies throughout the

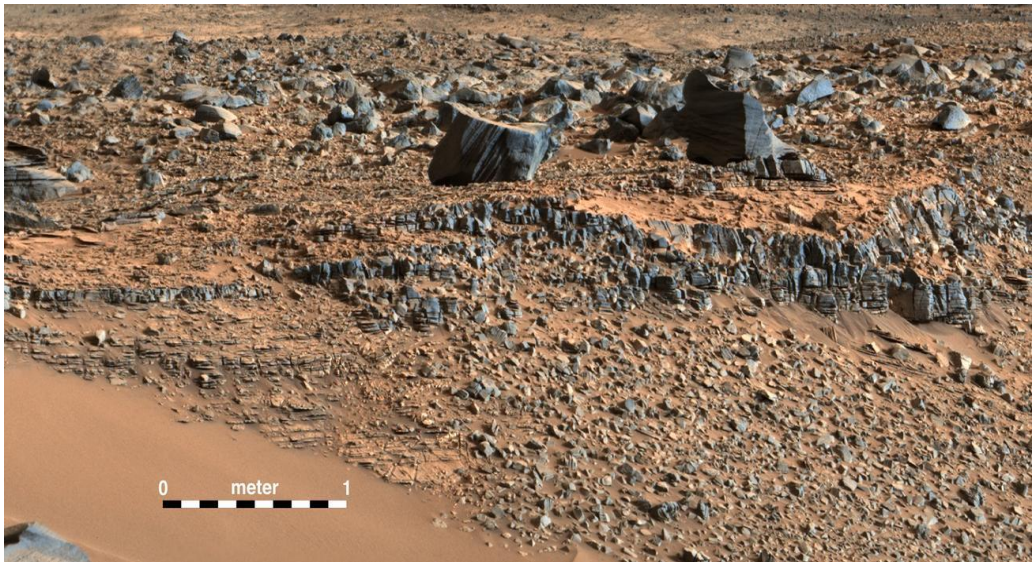

Figure 1. 9: Martian Layers, NASA Mars Exploration

1970s and 1980s. The NASA Mars Exploration Rover (MER) mission will land a pair of rovers on the surface of Mars in 2004(Maki et al., 2003).

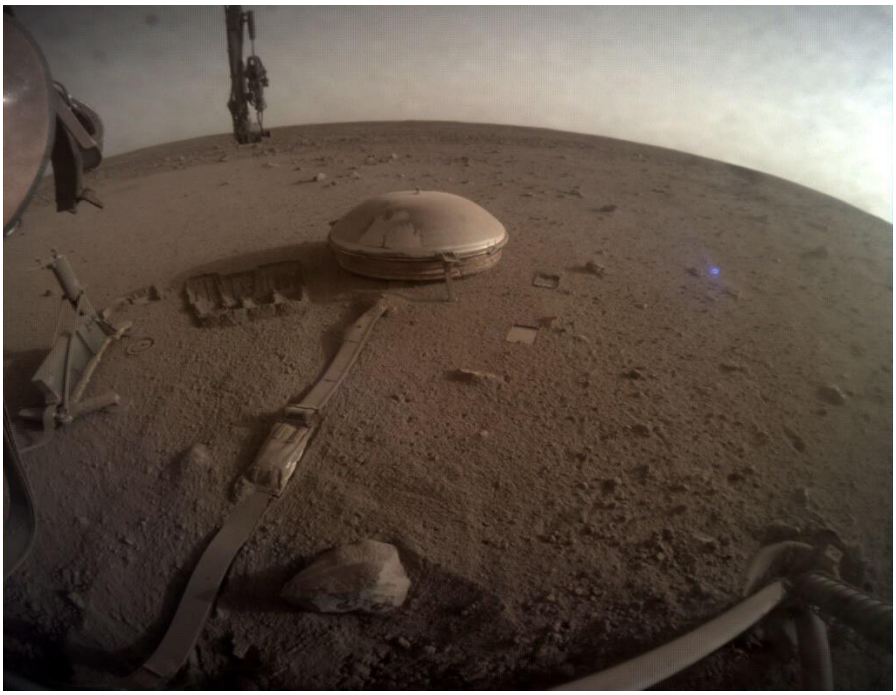

Figure 1.10: This is one of the last images ever taken by NASA's InSight Mars lander. Captured on Dec. 11, 2022, the 1,436th Martian day, or sol, of the mission, it shows InSight's seismometer on the Red Planet's surface. Image credits: NASA/JPL-Caltech.

Human exploration of Mars is still in its infancy. The first human exploration efforts, scientists are also studying Martian meteorites that have landed on Earth in order to gain insight into the planet's history and composition. By combining data from all these sources, scientists hope to gain a better understanding of our neighbouring planet and its potential for future exploration and habitation.

1.4 Fluvial history of Mars

The surface of Mars displays abundant evidence for fluvial activity (Pieri, 1980, Carr, 1987, Fassett and head, 2008b). Mars has >200 hydrologically open paleolake basins spread across the ancient southern highlands of the planet (Cabrol & Grin, 1999, 2001, 2010; Fassett & Head, 2008a; Goudge et al., 2016). The fluvial history of Mars is a fascinating topic that has been studied for many years. It is the study of the role of water on the planet Mars. It is believed that Mars once had a much wetter climate than it does today, and evidence of this can be seen in the many river valleys and other features on the planet's surface.

Impact crater-contained paleolakes on Mars have been recognized for several decades, including in many key contributions from studies of Viking data (Goudge et al., 2015).

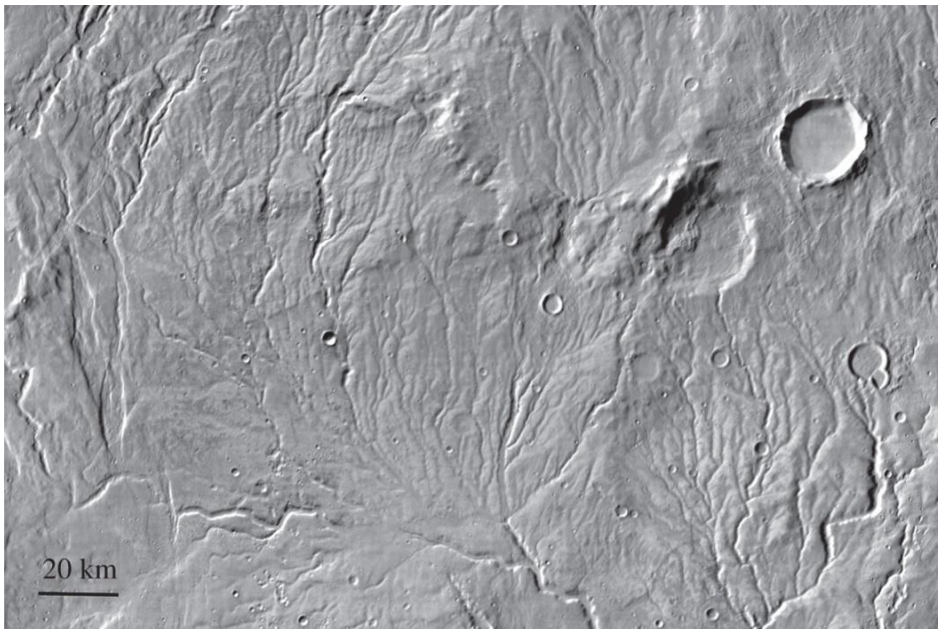

Figure 1.11: Fluvial History of Mars (https://doi.org/10.1098/rsta.2011.0500)

- Early Martian History: Around 4.6 billion years ago, Mars formed, and its early history included a period of heavy bombardment by asteroids and comets. During this time, the planet's surface was likely too hot to sustain liquid water.
- Ancient River Channels: Evidence suggests that Mars experienced significant fluvial activity during the Noachian period, roughly 4.1 to 3.7 billion years ago. This era saw the formation of large river channels and valley networks on the Martian surface. These ancient river channels, such as the Ares Vallis and Valles Marineris, indicate the presence of liquid water and a more substantial atmosphere than today.
- Climate Change: Over time, Mars underwent significant climate change, transitioning from a wetter and warmer environment to drier and colder one. It is hypothesized that is Mars lost its global magnetic field, the solar wind stripped away much of its atmosphere, resulting in a reduced greenhouse effect and the loss of liquid water.
- Outflow Channels: During the Hesperian period, approximately 3.7 to 3.0 billion years ago, Mars experienced massive flooding events that carved out extensive outflow channels. These channels, such as Kasei Valles and Ma'adim Vallis, indicate catastrophic releases of groundwater or sub-surfaces reservoirs, resulting in large-scale erosion.
- Polar Ice Caps: Mars has permanent polar ice caps composed mainly of water ice and some carbon dioxide ice. These ice caps experiences seasonal variations, with the ice melting and reforming in response to the planet's axial tilt. The melting of these ice caps could contribute to temporary liquid water flows, forming transient gullies and channels on the Martian surface.
- Recent Fluvial Activity: In recent times, Mars has shown some evidence of present-day fluvial activity.

Overall, the fluvial history of Mars reveals a complex interplay of geological processes and the role of water throughout the planet's history. Understanding these past fluvial systems helps scientists' piece together the puzzle of Mars' climate, geology, and the potential for habitable environments in its ancient past.

1.4.1 Various type of channels on Mars

There are several types of channels on Mars. The most common type is the outflow channel, which is created when water or ice flows from a source, such as a crater or lake, and cuts through the surface of the planet. Outflow channels can be hundreds of kms long and up to several hundred meters wide. Impact crater is another type of channel, which is created by asteroid or comet impacts on the surface of the Mars. These channels are usually much smaller than outflow channels and can be up to several hundred meters wide. The third type of channel is a meandering channel, which forms when water or ice slowly erodes away at the surface of Mars over time. These channels tend to be much wider than outflow channels and can span hundreds of kilo meters in length. Another type of channel is wind-eroded channels, that are formed due to wind erosion over time. These channels tend to be much narrower than other types of channels and can span up to several kilo meters in length.

The channels on Mars are divided into two main types, they are erosional and depositional. Erosional channels are those that have been carved out by the action of water, ice, or wind. Depositional channels are those that have been filled in with sediment or other material.

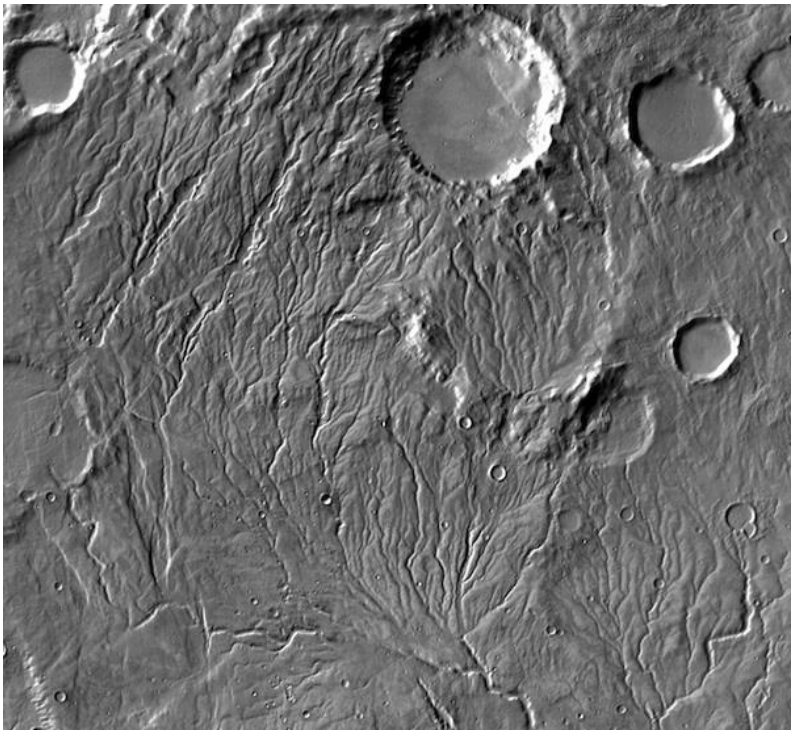

Figure 1.12: Dendritic channel pattern. Image credits: NASA/JPL-Caltech/Arizona State University

Different channels of various sorts have been seen and investigated on Mars. These channels offer insightful information on the planetary geological history and processes. Here are a few of the most common channel kinds on Mars.

1.4.1.1 Outflow channels on Mars

The Martian surface displays many landform assemblages associated with liquid flows. Martian outflow channels are one such feature (Gallagher & Bahia, 2021). They are very large, ancient riverbeds that were carved by water flowing across the surface of the planet. These channels are evidence of a warmer and wetter past on the surface. They are found in many regions of the planet. These large sinuous channels that were formed by catastrophic floods of liquid water. On Venus, there are also similar lengthy, sinuous wounds that were probably made by lava. And also, it resembles channels on Earth formed due to catastrophic glacial meltwater discharges (Gallagher & Bahia, 2021).

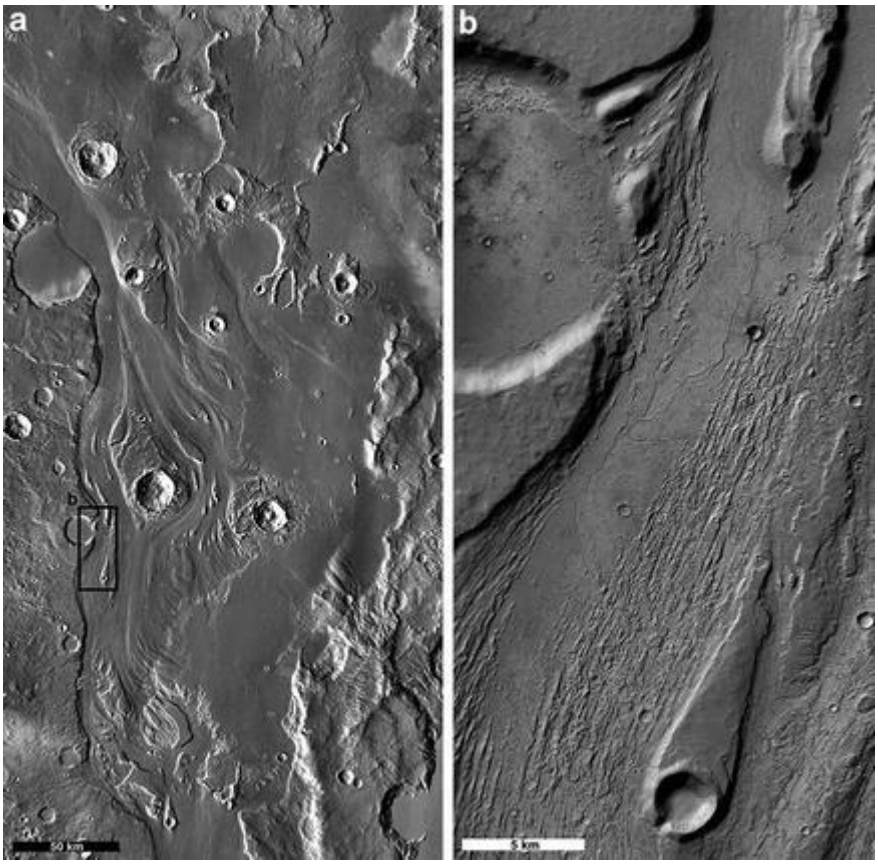

Figure 1.13: Outflow channel (Mars). Image credits: NASA/JPL/MSSS

The outflow channels on Mars were first discovered in the 1970s by the Viking spacecraft. Viking Orbiter and terrestrial satellite images were studied at similar resolution to compare features produced by the movement of ice on Earth many similarities were found, include the anastomoses, U-shaped cross profiles of valleys; hanging valleys, and grooves and ridges on valley floors (Baerbel K. Lucchitta, 1982). The channels are typically hundreds of kilo meters long and up to several kilo meters wide.

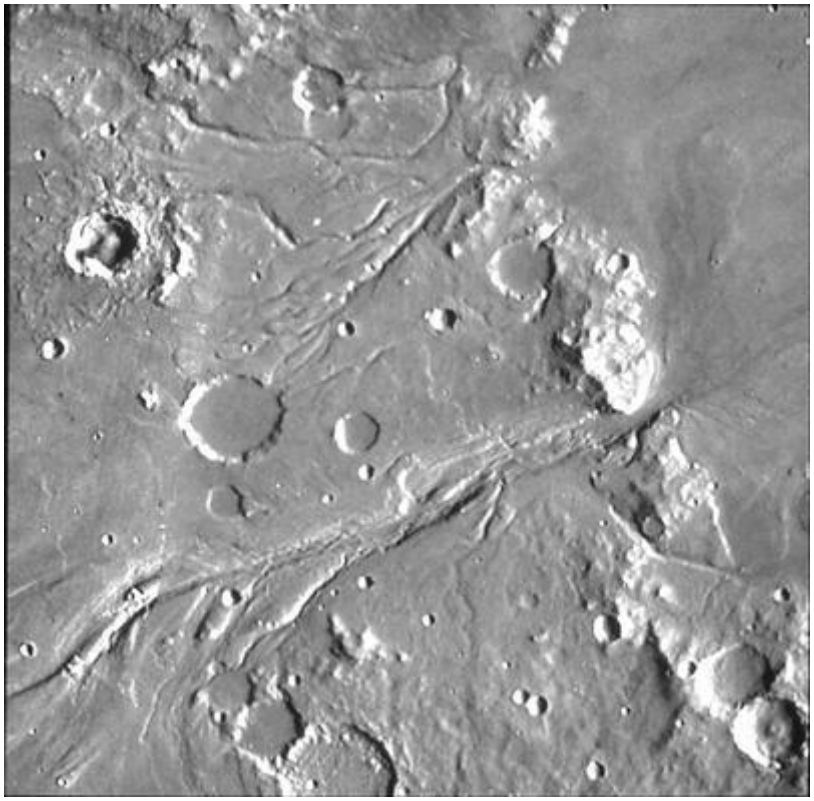

Figure 1.14: Outflow channels on Mars. Image credit: NASA/JPL-Caltech

1.4.1.2 Valley Networks

Valley networks, which mirror river valleys on Earth, are complex webs of interconnecting channels on Mars. These networks are widespread across the globe and have had a substantial impact on the geological history of Mars.

The appearance and morphology of the valley networks on Mars resemble the branching or dendritic patterns of Earth's river systems. They are made up of a main canal that is fed by

numerous smaller tributaries. The length of the Valley networks varies as well, ranging from a few kilometres to hundreds of kilometres. With widths often ranging from a few hundred metres to a few kilometres, they can be rather shallow and narrow. Additionally, the channels within valley networks frequently display features connected to fluvial erosion, such as steep cliffs, meandering patterns, and sediment deposits. These characteristics imply the historical presence of running water. On Mars, valley networks can be seen in a variety of landscapes, including the northern plains, the Tharsis volcanic region, and the southern highlands. This spread suggests that these networks were not localised and might have developed in a variety of environmental settings. There is ongoing discussion on the precise processes through which the valley networks on Mars formed. Some hypotheses contend that they were created by snowmelt or rainfall-related surface runoff, while others contend that groundwater seepage was responsible for their creation.

Example of Valley Networks: Ma’adim Vallis, The well-known Mars valley system known as Ma'adim Vallis is situated in the planet's southern highlands. It has both vast, flat-floored parts and narrower, sinuous waterways along its roughly 700-kilometre length.

Nirgal Vallis: Another well-known valley system is Nirgal Vallis, which is situated in Mars' southern hemisphere. It is 700 kilometres long and exhibits signs of several stages of channel creation, including erosion and deposition.

1.4.1.3 Gullies

Gullies on Mars are small, narrow channels that resemble the features of gullies found on Earth. They are primarily observed on the slopes of craters, cliffs, and other steep terrains. Gullies are intriguing geological formations on Mars, and their formation processes are still a subject of scientific investigation.

On Mars, gullies frequently have distinctive features, such as a narrow, trench-like appearance with steep sides. They frequently have a top alcove, a bottom channel, and a debris apron. The material that has eroded and gathered at the gully's bottom makes up the debris apron. On Mars, gullies have shown signs of very recent activity. Gully variations throughout time have been observed by orbiting satellites like NASA's Mars Reconnaissance Orbiter (MRO). During the warmer months, some gullies develop dark streaks that may indicate seasonal activity, maybe including the movement of a volatile fluid like water or carbon dioxide. The precise

mechanisms of gully development on Mars are currently being studied. There have been a number of explanations put forth, such as the sporadic flow of liquid water, dry mass movement (where loose material flows downslope without the presence of water), or other mechanisms involving the sublimation of volatile substances. It is significant to note that distinct gullies on Mars may have different precise mechanisms. Gullies have been spotted on Mars in a number of locations, including the poles, the mid-latitudes, and the southern highlands. They are frequently discovered on the slopes or walls of craters, where erosional forces caused by gravity and other environmental conditions may have played a role in their development. The formation processes of gullies on Mars, the

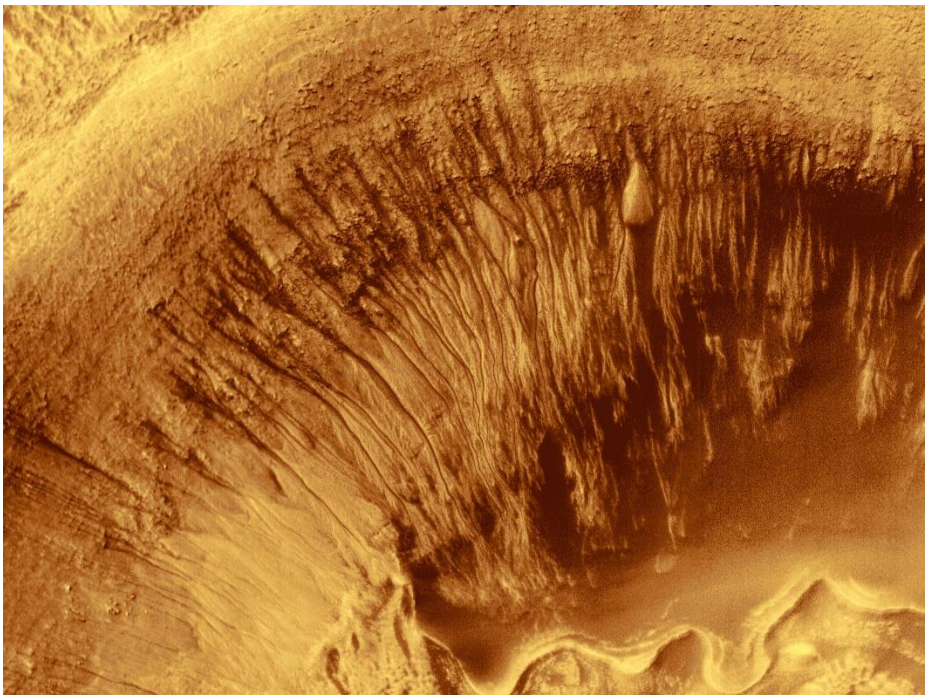

Figure 1.15: Gullies on Mars, Image credit: NASA Mars Exploration

probable involvement of volatiles like water, and the timescales of their activity are all still being studied by scientists. This study advances our knowledge of the planet's geological past, current dynamics, and potential for past or present habitability.

1.4.1.4 Polar Channels

On Mars, the term "polar channels" refers to structures that can be seen close to the planet's poles, generally in the shape of channels or grooves. These canals are frequently observed close to Mars' polar ice caps and are thought to be connected to seasonal ice melting and liquid water movement. The polar carbon dioxide ice (dry ice) and water ice can partially vaporise during Martian summers as temperatures rise, releasing gas. As a result of this process, pressure is created, which causes gas- and dust-filled jets or geysers to erupt. These eruptions may result in the underlying surface rupturing and ejecting material through channels or grooves. The channels seen on Mars can vary in size and shape, especially in the polar regions. Other channels may have meandering or branching patterns, while some are rather straight. From little channels to larger features that resemble gullies, the sizes might vary. These pathways indicate that liquid water may occasionally exist on Mars, although it is most likely briny or salty water given the extremely low temperatures and salts in the Martian soil. The channels offer insightful knowledge about the Martian water cycle's past and present activities as well as the planet's potential for habitability.

Even though it is well accepted that seasonal ice melting creates polar channels, the precise mechanisms and processes at play are still not entirely understood. The nature and genesis of these fascinating structures on Mars will continue to be better understood via further study and exploration, including missions like NASA's Mars Reconnaissance Orbiter and the future Mars Sample Return mission.

1.4.1.5 Reticulate Channels

Reticulate channels on Mars are a particular kind of surface geological feature. The term "reticulate" refers to these channels' branching pattern, which resembles a network or net-like structure. They were originally spotted in photographs obtained by NASA's Mariner spacecraft in the late 1960s and early 1970s, and then by later missions like Viking, Mars Global Surveyor, and Mars Reconnaissance Orbiter. It is thought that a variety of events, including water erosion and the collapse of subsurface holes, resulted in the formation of the reticulate channels on Mars. The thin atmosphere and low atmospheric pressure of the planet, which make the existence of massive, sustained bodies of water implausible, do limit the amount of liquid water that is now present on the Martian surface. Instead, it is believed that the channels were created

during sporadic times of elevated air pressure, which caused subsurface ice to melt more quickly and resulted in brief bouts of liquid water flow.

Scientists are fascinated by Mars' reticulate channels because they provide signs of the planet's past geological activity and hint at the possibility of water-related processes in its past. They act as a reminder of Mars' past potential for supporting liquid water on its surface and a more pleasant climate. We continue to learn more about the geological evolution of the planet and its potential for habitability as we continue to explore and analyse these channels and other Martian geological features.

1.4.1.6 Aim and objective

The main objective of the study is to identify geomorphological features of Farah Vallis by digitizing the features using ArcGIS 10.8.

To understand the fluvial features of the crater including various types of deltas, tributary vallis etc.

CHAPTER 2

2.1 STUDY AREA

Farah Vallis, a single, broad channel, cuts the southwest rim of the crater and connects the valley network system that surrounds Gale. Farah Vallis has a morphology consistent with other V-shaped Martian valley networks (Williams & Phillips, 2001) and is a few kilo meters wide and ~100 m deep. The upstream morphology of Farah vallis is partly buried by Gale ejecta, suggesting that the Gale impact disrupted it while it was active (Irwin et al., 2005).

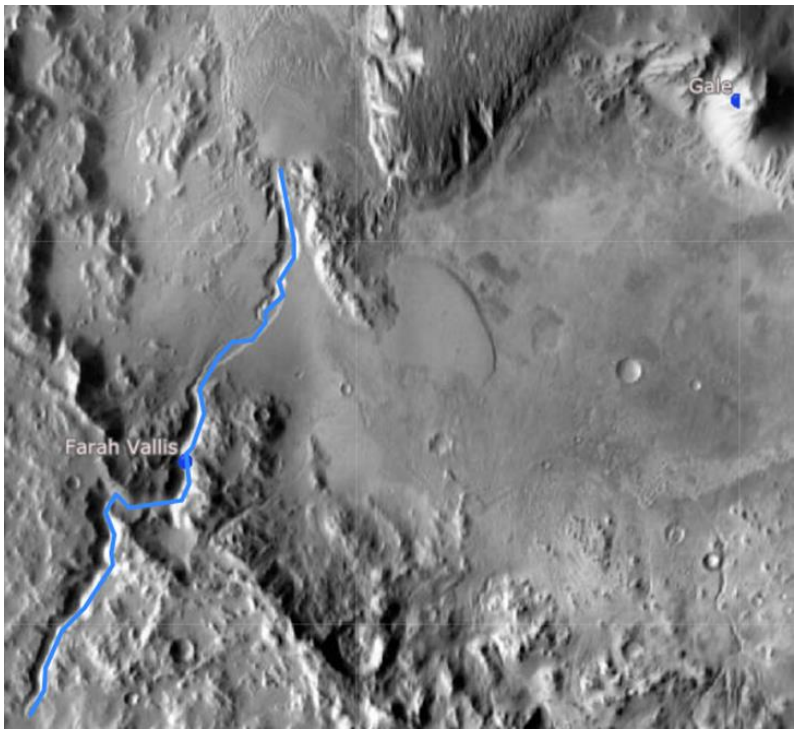

Figure 2.1: Study area: Geological Map of the Source Region of Farah vallis, Mars, several large fans (tan) and fan deltas (light blue), including a large delta feature in the southwestern corner of Gale [Irwin et al., 2005]

2.1.1 Geological history

On the planet Mars, Farah Vallis is a notable geological formation. It is a sizable valley situated in the Margaritifer Terra region of Mars' southern hemisphere. The valley was designated as a vallis, which is a term used to describe a valley-like structure on Mars, and was named after a town in Afghanistan. Farah Vallis' geological past can shed light on earlier processes that formed the Martian terrain. Scientists have conducted studies and produced judgements based on accessible data, including pictures and topographic measurements, even if our knowledge of exact features may be restricted.

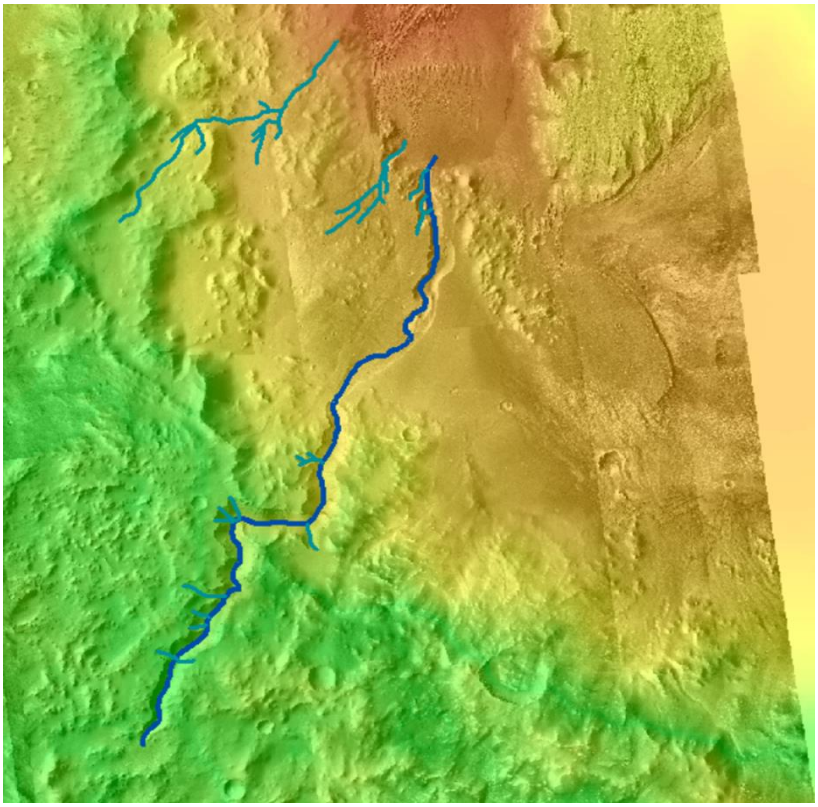

Figure 2.2: Image above shows the CTX image of the Farah Vallis and two Tributary Vallis (source ArcGIS 10.8)

Farah Vallis is thought to have created through a tectonic and erosional process combination. The stretching and faulting of the Martian crust is assumed to be the cause of the valley's formation. This tectonic activity led to the formation of a fracture system, which later served

as a pathway for water movement. Evidence points to a substantial role for water in the formation and structuring of Farah Vallis. The valley shows traits resembling those of old river routes on Mars. Landforms like point bars and oxbow lakes that are associated with meandering patterns show that water has been acting on the area for a long time.

Farah Vallis water supply may have come from subsurface glacier melting or groundwater discharge. It's possible that the water was spilled when tectonic or volcanic activity was at its peak. By eroding the surrounding land, this water flow gradually excavated and deepened the valley.

Erosion and modification: After Farah Vallis first formed, it was probably still being shaped by erosion processes like fluvial activity (connected to the passage of water). The valley may have seen periods of water flow over time, which would have carved out new channels, eroded the sides, and left silt in its wake.

Farah Vallis is only a small portion of the larger story of Mars' geological history, it is crucial to remember. Impact craters, volcanoes, and other valley networks, each with its unique history and creation processes, are some of the distinctive aspects of Martian geology. As new information is gathered by orbiters, rovers, and other missions exploring the surface of Mars, our understanding of the planet continues to advance. Studies that are currently being conducted and those that will be conducted in the future will help us understand Farah Vallis and the geological evolution of Mars better overall.

CHAPTER 3

REVIEW OF LITERATURE

3.1 Studies on Mars

Hartmann & Neukum, 2001 conducted a study on Mars to determine Cratering Chronology and the Evolution of Mars. The Noachian Period may only be considered to have begun before 3.5 Gyr due to the high crater concentrations of the Noachian. According to estimates, the Hesperian/Amazonian border occurred between 2.9 and 3.3 Gyr ago, while there is a smaller chance that it occurred between 2.0 and 3.4 Gyr. Because of the uncertainty surrounding the rate of Martian cratering, mid-age ages are less well-bound. Our dates and the data on resurfacing strongly suggest that the rates of volcanic, fluvial, and periglacial resurfacing were all significantly higher in the first third of Martian history. According to formal solutions, the Late Amazonian Epoch began between 300 and 600 Myr ago. Our work is compatible with meteorite evidence for Martian origins and Mariner 9-era speculations of extremely young lavas on Mars. Ages and resurfacing data can be compared to show that the rates of volcanic, fluvial, and periglacial resurfacing were all significantly higher in the first third of Martian history. According to formal solutions, the Late Amazonian Epoch began between 300 and 600 Myr ago. The crater retention ages of the youngest discovered Martian lava flows are on the order of 10 Myr or less. Also observe that several Martian meteorites show indications of river activity 700 Myr or more recent than the rocks themselves, which is confirmed by data on recent water seeps. The evidence of recent volcanic and aqueous activity, which comes from crater count data as well as meteorite data, places crucial restrictions on the geological evolution of Mars and points to a more active, complex Mars than some researchers have previously hypothesised.

According to the study of Dengyun et al., 2016 in Mars to determine the development process and prospects of Mars Exploration. This paper proposes possible research on Mars exploration that can be done and recommendations for China's Mars exploration missions based on a review of the history of Mars exploration, the exploration planning for the future, and the key technologies to face. In addition, the corresponding illumination and prospects are given.

Maki et al., 2003 conducted a study about Mars Exploration Rover Engineering Camers. According to this study, the scientific community will also be in need of the images captured by the engineering cameras for research on the morphology of rocks and soil. Each stereo pair of mast-mounted navigation cameras (Navcams, two per rover) has a 45° square field of vision (FOV) and an angular resolution of 0.82 milliradians per pixel (mrad/pixel). Four Hazard Avoidance Cameras (Hazcams, per rover) are positioned on the body, facing forward and backward, and each has a field of view (FOV) of 124° square with an angular resolution of 2.1 mrad/pixel. The lander-mounted Descent camera (one for each rover) has a 45° square field of view and will produce photos with a spatial resolution of about 4 m/pixel. The 1024 x 1024-pixel detectors and broadband visible filters are used by all engineering cameras.

Pieri, 1980 studied the Morphology, Distribution, Age, and Origin of Martian Valleys. According to this study there are no signs of rainfall-fed erosion creation in the valley networks on Mars' extensively cratered landscape. Instead, they advocate basal sapping for headward expansion. These valleys and the surrounding terrain's size-frequency patterns of impact craters indicate that valley creation has not taken place in billions of years.

Li et al., 2021 conducted on a study about China’s Mars exploration Mission and Science investigation. The scientific goals of previous and ongoing Mars exploration missions around the world are reviewed in this paper, along with the scientific goals, payloads, and initial scientific investigation plan of China's first Mars exploration mission. Expected scientific successes are also examined.

Fassett & Head, 2008 studied the distribution and implications for Noachian surface hydrology. According to this study there is evidence for a vertically integrated hydrological system, the absence of a global cryosphere, and direct interaction between the surface and subsurface hydrosphere of early Mars. Surface runoff and groundwater flow both seem to have been significant sources for lakes and lake chains.

Carr, 1980 discusses the geological features of Mars, focusing on the differences between the northern and southern hemispheres. The southern hemisphere is highly cratered and lofty, whereas the northern hemisphere is sparsely cratered and low. The Tharsis bulge is a wide uplift 8,000 kilometres across and 10 kilometres high at its peak. The southern hemisphere's terrain is made up of ancient crust with massive craters and younger intercrater plains. The northern hemisphere is covered with cratered plains, some of which are located around huge

volcanoes with volcanic flows, while others are located along lunar mare-like ridges. The inter-fingering structures on the boundary between the northern plains and the southern cratered terrain are intricate. In certain regions, there is mass wasting and a disordered landscape, implying catastrophic inundation. The Valles Marineris canyon system is formed by radial fractures from the Tharsis bulge that cut through much of the area. Mars' volcanoes are huge, resembling terrestrial shield volcanoes, especially in the Tharsis and Elysium regions. Ejecta strata surround impact craters, showing the presence of ground ice. Polar layered deposits are aeolian in origin, youthful, and volatile-rich. The north pole is surrounded by dunes, while aeolian modification elsewhere is modest despite global dust storms.

Carr, 2012 conducted on a study about Fluvial history of Mars. According to this study river channels and valleys on planets such as Venus, the Moon, Io, and Titan indicate historic or present liquid flows. Mars has a history of water-driven erosion and deposition, as evidenced by its wide branching valleys, deltas, and lake basins. Large outflow canals, most likely produced by water, can also be found. Some features have been impacted by glacial activity and volcanic events. Though the current Martian temperature is frigid, evidence suggests that water once flowed over its surface, dramatically changing the topography. The effect of flowing water on Mars' evolution is a critical subject of research.

3.2 Studies on Gale crater

Milliken et al., 2010 conducted a study about Gale Crater to determine the Paleoclimate of Mars as captured by the stratigraphic record in Gale Crater. According to the observed stratigraphic trends, the rocks of Gale Crater document a global transition from a climate that was conducive to the formation of clay minerals to one that was more conducive to the formation of sulphates and other salts**.**

Grant & Wilson, 2019 studied the evidence of late Alluvial activity in Gale Crater, Mars. The result obtained, Local alluvial deposits in Gale crater presumably predate more pervasive water-related deposits in Gale by less than 2 Ga. It's possible that the water connected to the younger alluvial deposits is a result of late-occurring diagenetic activity. When Aeolis Mons reached its current expression, alluvial deposits occurred, indicating late-occurring livable conditions within Gale.

Palucis et al., 2014 studied the origin and evolution of the Peace Vallis fan system that drains to the Curiosity landing area, gale Crater, Mars. And the result obtained, The Peace Vallis fan's distal end was close to the MSL landing, and the fan's form was compatible with fluvial processes. The fan sediment came from a valley incision into the colluvium.

Thomson et al., 2019 conducted a study about how much the sediment in Gale Crater's Central Mound was Fluvially transported. The result obtained, less than 20% of the volume of Aeolis Mons, the major mound in Gale crater, is due to fluvial processes. The vast bulk of the sediments that entered Gale crater were carried there by means other than flowing water. Aeolis Mons' sediments were presumably deposited mostly by aeolian airfall.

According to Palucis et al., 2016 study about Sequence and relative timing of large lakes in Gale crater (Mars) after the formation of Mount Sharp results incisional and depositional processes record a succession of lowering and then rising lake levels. Delta deposits inside Gale show a period of lake stands following the Mount Sharp formation. Lake water likely moved throughout time from a regional to a more local source.

CHAPTER 4

DATA & METHODOLOGY

4.1 DATA SET USED

The orbital data sets used for this study are the CTX images from MRO mission. Details of the instrument and mission are as follows.

4.1.1 Mars Reconnaissance Orbiter

Mars Reconnaissance Orbiter (MRO) is a spacecraft designed to search for the existence of water on Mars or to study geology and climate of Mars, serve as a scout for potential landing locations and transmit data from surface operations back to Earth. It was launched from Cape Canaveral on August 12, 2005, and reached Mars on March 10,2006. It is equipped with six scientific instruments, including a high-resolution camera, an imaging spectrometer, and a radar sounder. With the help of the MRO, the surface of Mars has been mapped in unprecedented detail, giving researchers important information about the geology and climate of the planet. The MRO has been used to look for signs of Mars' past or current life. Since its launch in 2006, the Mars Reconnaissance Orbiter, or MRO, has observed the atmosphere and geography of the Red Planet from space. It also acts as a vital data relay station for other Mars missions, such as the Mars Exploration Rover Opportunity.

The MRO is equipped with a suite of scientific instruments that enable it to gather data about Mars in high resolution and detail. Some of the important instruments are High-Resolution imaging science experiment (HiRISE), which can capture images of the Martian surface with unprecedented clarity, and the Compact Reconnaissance Imaging spectrometer for Mars (CRISM), which is used to analyse the composition of minerals on the planet.

The mission was the next phase in NASA's Mars Exploration Programme, and its main goals were to:

- Describe the climate on Mars at the moment and look at how it varies seasonally.
- Track the weather on Mars.

- Examine Mars' topography to find landforms that are related to water. Look for signs of hydrothermal activity and water.
- Look for water and ice beneath the earth.
- Examine potential landing and sampling locations. Transmit scientific data from Mars to Earth.

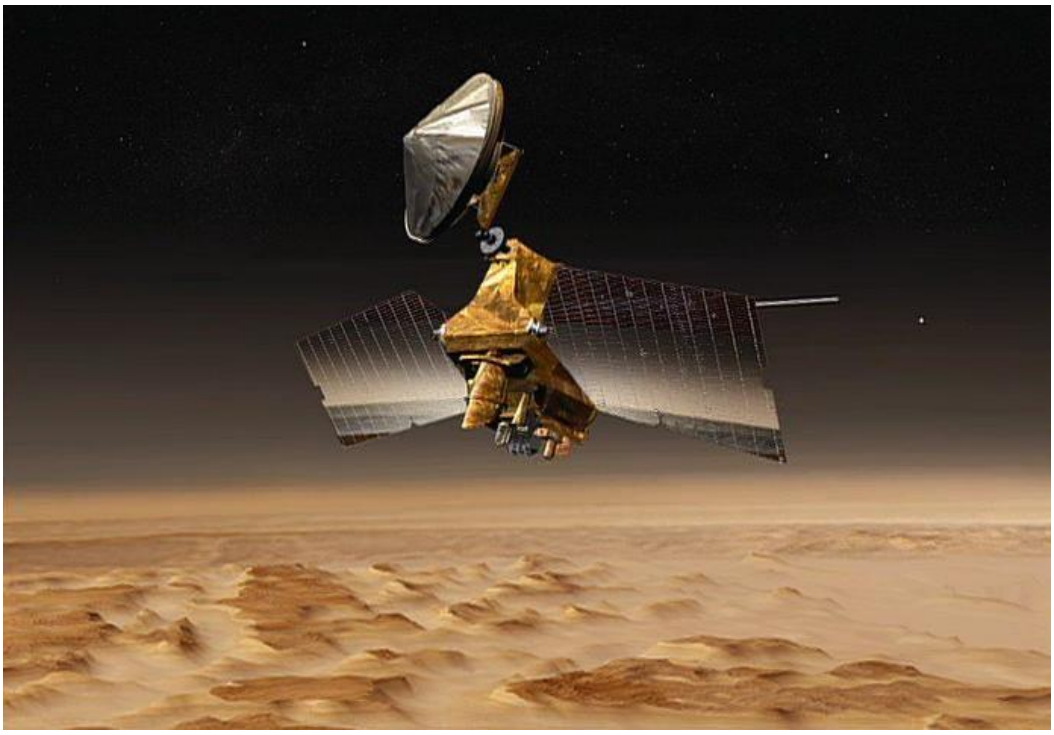

Figure 4.1: Mars reconnaissance Orbiter (MRO) image Credit: NASA

Science instruments

- High Resolution Imaging Science Experiment (HiRISE)
- Shallow Radar (SHARAD)
- Mars Climate Sounder (MCS)
- Compact Reconnaissance Imaging Spectrometer for Mars (CRISM)
- Mars Colour Image (MARCI)
- Accelerometer
- Context Imager (CTX)

New engineering payloads

- Ka-band Telecommunications Experiment
- Electra UHF communications and navigation package
- Optical Navigation Camera Experiment (ONC)

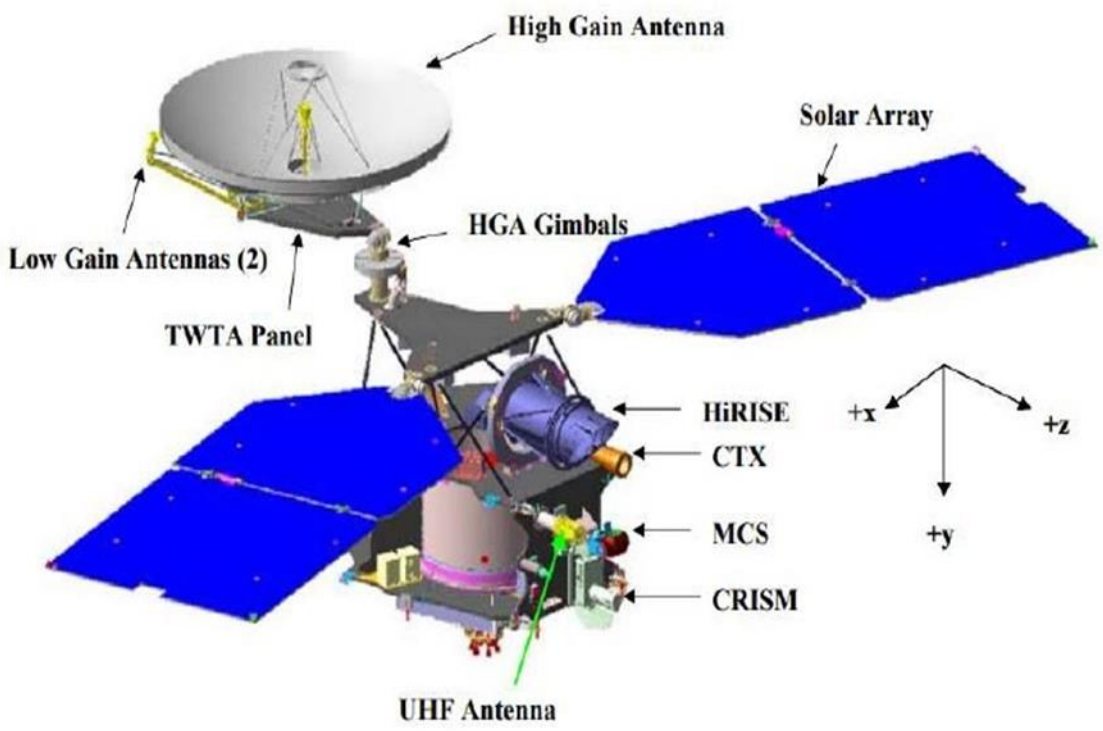

Figure 4.2: Sketch of the MRO spacecraft with various components and coordinate directions Image Credits: Mars Reconnaissance Orbiter. Deep Space Communications. (Taylor et al., 2016)

4.1.1.1 Context Camera (CTX)

The Mars Reconnaissance Orbiter's Context Camera, often known as CTX, offers a broad, backdrop image of the landscape around smaller rock and mineral targets. Its principal responsibility is to assist in setting the stage for high-resolution analysis. List significant Martian locations supplied by HiRSE and CRISM. It has a 6.6-pound weight and uses 5 Watts

while it is idle and 7 Watts when imaging. Black and White (grayscale) visible light with a wavelength range of 500 to 800 nano meters is used for the image's colour.

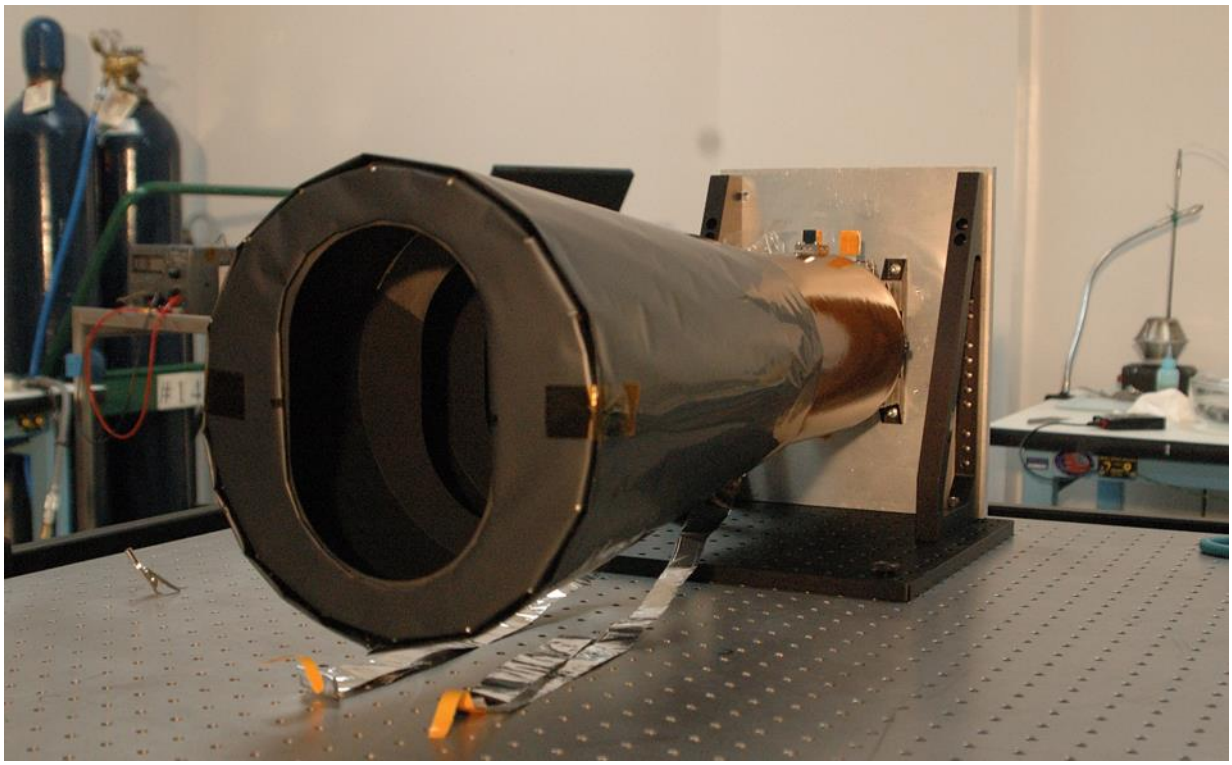

Figure 4.3: Image of the Context Camera payload seen here at the Malin Space Science System Laboratory before integration with the MRO spacecraft. Image Credits: NASA

In addition to the high-resolution photos taken by HiRISE and the data taken by the mineral-finding CRISM spectrometer, CTX (Context Camera) also conducts observations. As suggested by its name, CTX gives the information gathered by the other two instruments a wider perspective. With the other tools, scientists can investigate the specifics of the rocks and mineral fields, but CTX offers a more comprehensive perspective of the landscape. HiRISE, CRISM, and CTX are incredibly strong tools when used together. From 400 kilometres (250 miles) above Mars, CTX takes images spanning 30 kilometres (almost 19 miles) of terrain. The camera has a resolution of 6 meters per pixel

40 CTX images of Farah Vallis is used in the study are given below:

Sl.No	MRO-CTX (context) Image ID	Sl.No	MRO-CTX (context) Image ID
01	b02_010494_1737_xn_06s223w.tiff	21	g22_026779_1748_xn_05s223w.tiff
02	b10_013540_1747_xn_05s222w.tiff	22	g23_027201_1749_xn_05s223w.tiff
03	b21_017786_1746_xn_05s222w.tiff	23	g23_027280_1749_xn_05s222w.tiff
04	b21_017931_1746_xn_05s222w.tiff	24	j02_045504_1745_xn_05s223w.tiff
05	b22_018142_1743_xn_05s223w.tiff	25	j04_046348_1751_xn_04s223w.tiff
06	d05_029245_1757_xn_04s224w.tiff	26	j11_049130_1746_xn_05s222w.tiff
07	d09_030735_1746_xn_05s223w.tiff	27	j14_050119_1745_xn_05s223w.tiff
08	d10_031025_1752_xn_04s223w.tiff	28	j14_050330_1745_xn_05s223w.tiff
09	f06_038304_1753_xi_04s223w.tiff	29	j16_051108_1742_xn_05s223w.tiff
10	f09_039491_1746_xi_05s222w.tiff	30	j20_052598_1745_xn_05s222w.tiff
11	f21_043816_1748_xn_05s223w.tiff	31	k07_056198_1745_xn_05s223w.tiff
12	f23_044660_1746_xn_05s223w.tiff	32	k08_056475_1746_xn_05s223w.tiff
13	g04_019843_1746_xi_05s223w.tiff	33	n10_066471_1736_xn_06s223w.tiff
14	g04_019909_1746_xi_05s223w.tiff	34	n12_066880_1736_xn_06s223w.tiff
15	g05_020265_1746_xi_05s223w.tiff	35	p04_002530_1745_xi_05s223w.tiff
16	g12_022889_1746_xi_05s223w.tiff	36	p04_002675_1746_xi_05s222w.tiff
17	g12_022955_1746_xi_05s223w.tiff	37	p13_006143_1745_xn_05s223w.tiff
18	g14_023667_1741_xn_05s223w.tiff	38	t01_000881_1752_xi_04s223w.tiff
19	g18_025223_1739_xn_06s223w.tiff	39	u02_071642_1736_xn_06s223w.tiff
20	g21_026568_1751_xn_04s223w.tiff	40	u02_071787_1740_xn_06s223w.tiff

4.2 METHODOLOGY

The methodology adopted for the study initial identification and consequent feature mapping of the fluvial features.

Below is a flowchart that shows hoe the process was carried out.

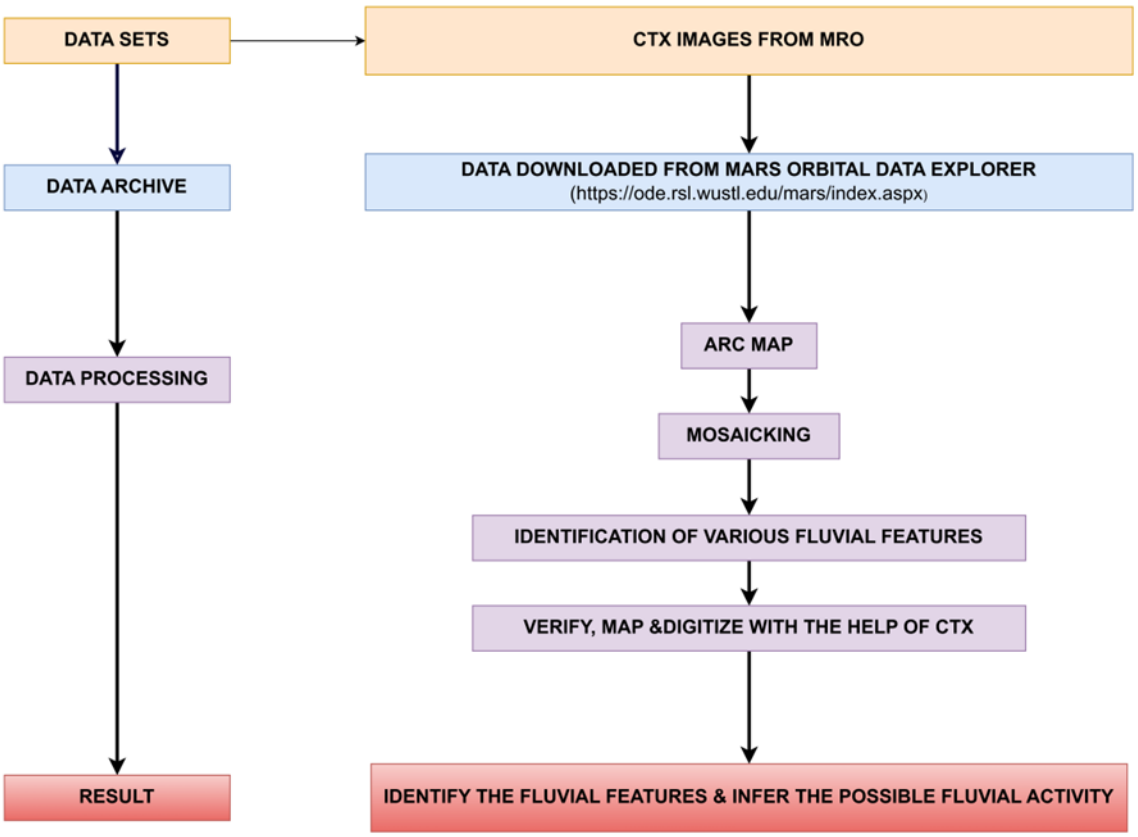

Figure 4.4: The methodological flowchart used in this study is shown in the figure up top.

4.2.1 Geological Map construction

The data were acquired from PDS Geosciences Node Mars Orbital Data Explorer (ODE) in order to create a geomorphological map of the study area. ArcMap 10.8 was utilised for additional morphological observations and building. The PDS Geosciences Node Mars Orbital Data Explorer (ODE) provides search, display, and download tools for the PDS science data

archives as well as for other data from the Viking Orbiter 1 and 2 as well as the Mars Express and ExoMars Trace Gas Orbiter missions of the European Space Agency.

Steps in mosaicking of the CTX image using ArcMap10.8

Each CTX image is inserted as a layer in ArcMap using the 'add data' function before mosaicking. And using the subsequent process, the area that had a null value was eliminated.

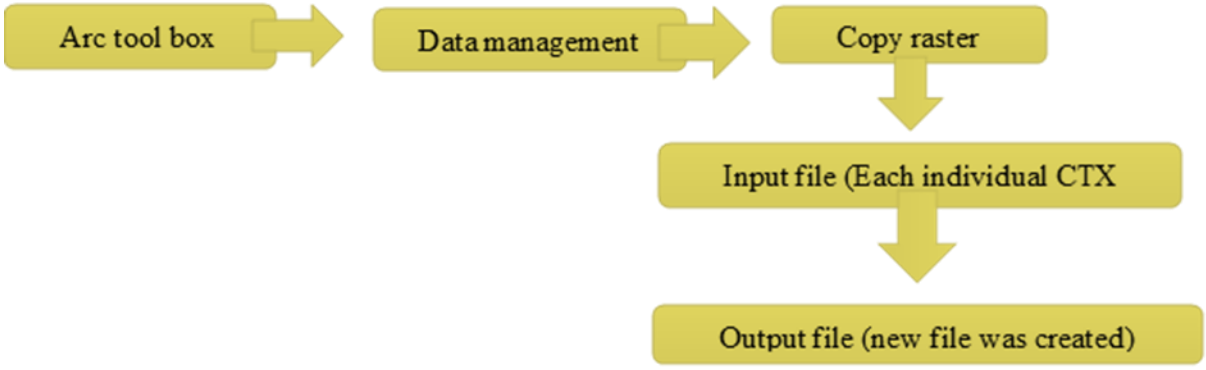

For each individual layer this step repeated. And after removing all null value mosaicking was done by following step;

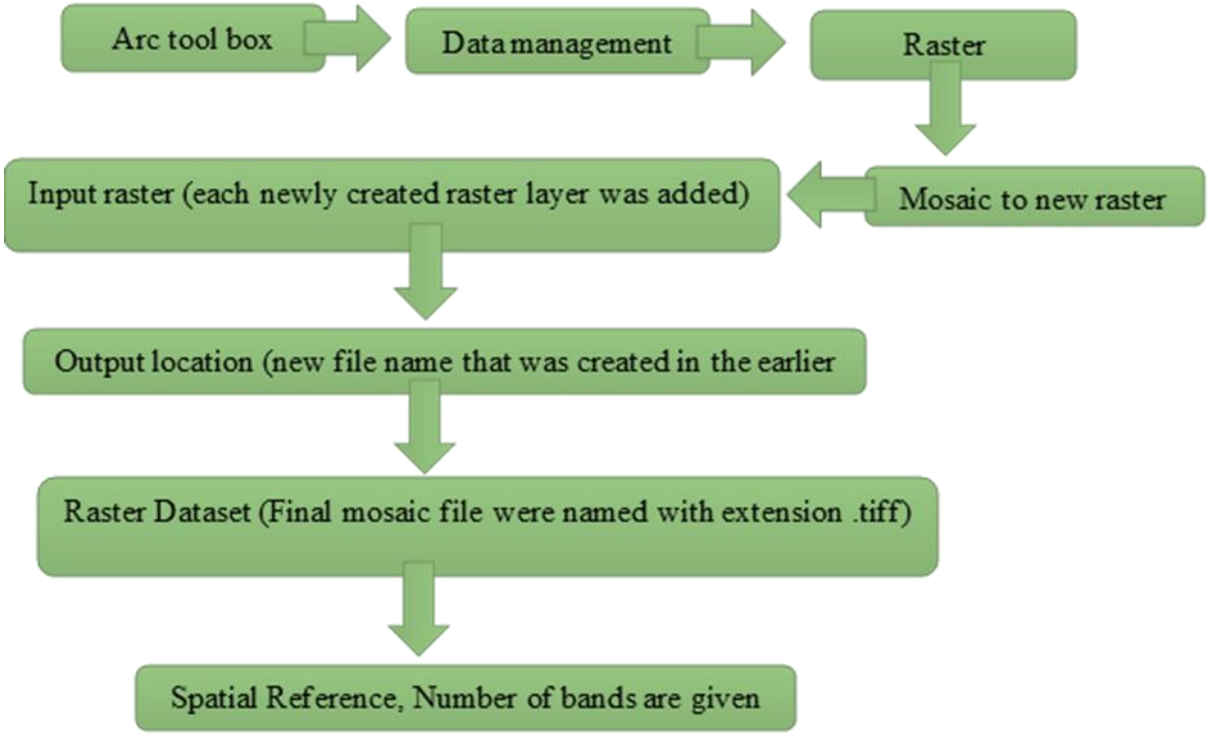

Creating Shape file

Shape file for each morphologic feature like fluvial features and crater boundary.

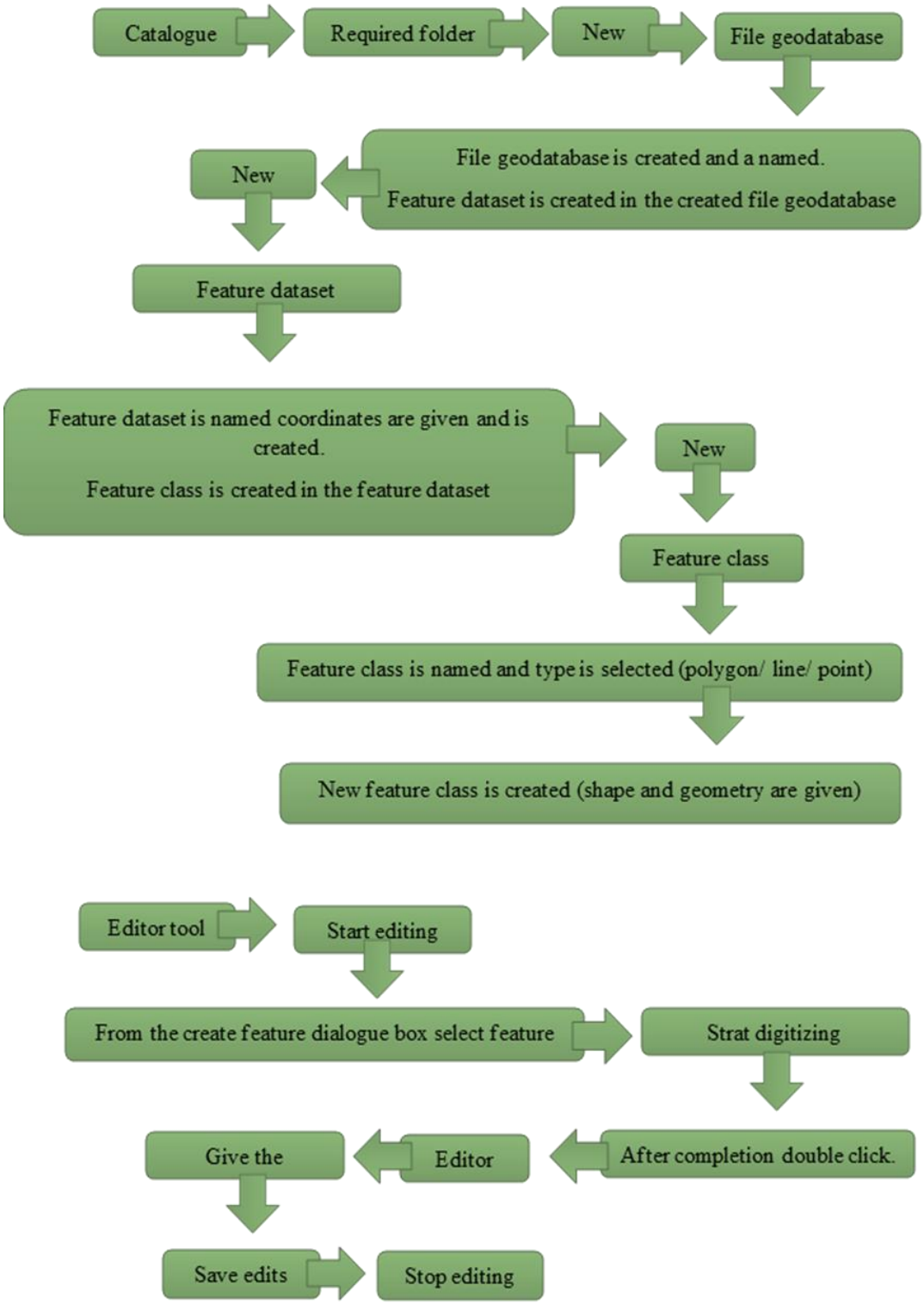

This step is repeated for each one**.**

Clipping map

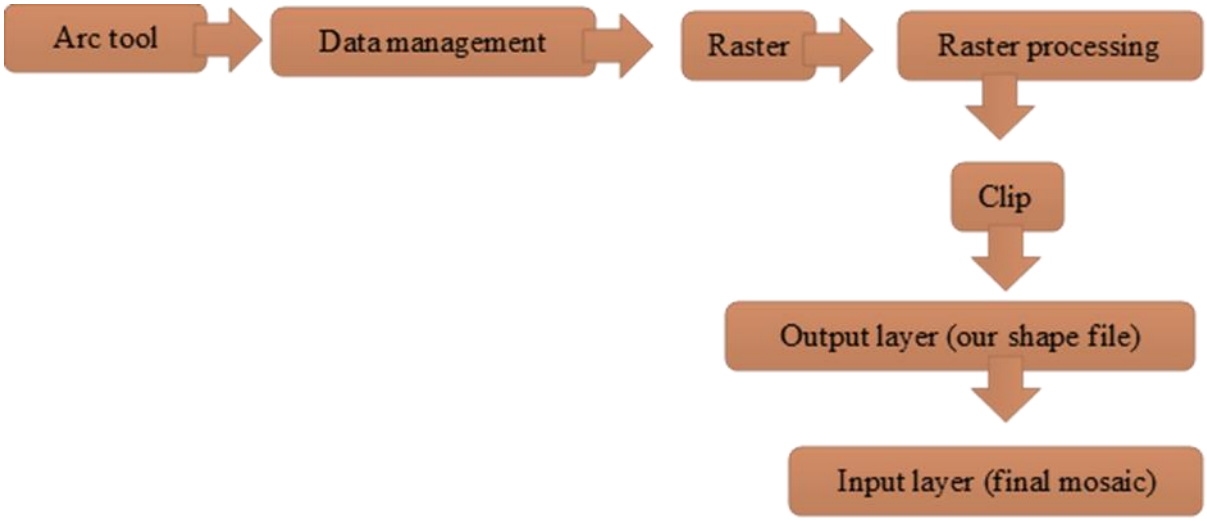

CHAPTER 5

OBSERVATIONS & DISCUSSIONS

5.1 IDENTIFICATION OF VARIOUS FLUVIAL GEOMORPHOLOGICAL FEATURES

The final findings and result of the study has been described in this chapter. For this study CTX Mosaic images and DEM are used. The work that had to be done is the identification of various geomorphological features from their physical appearance, surface texture terrain topography etc.

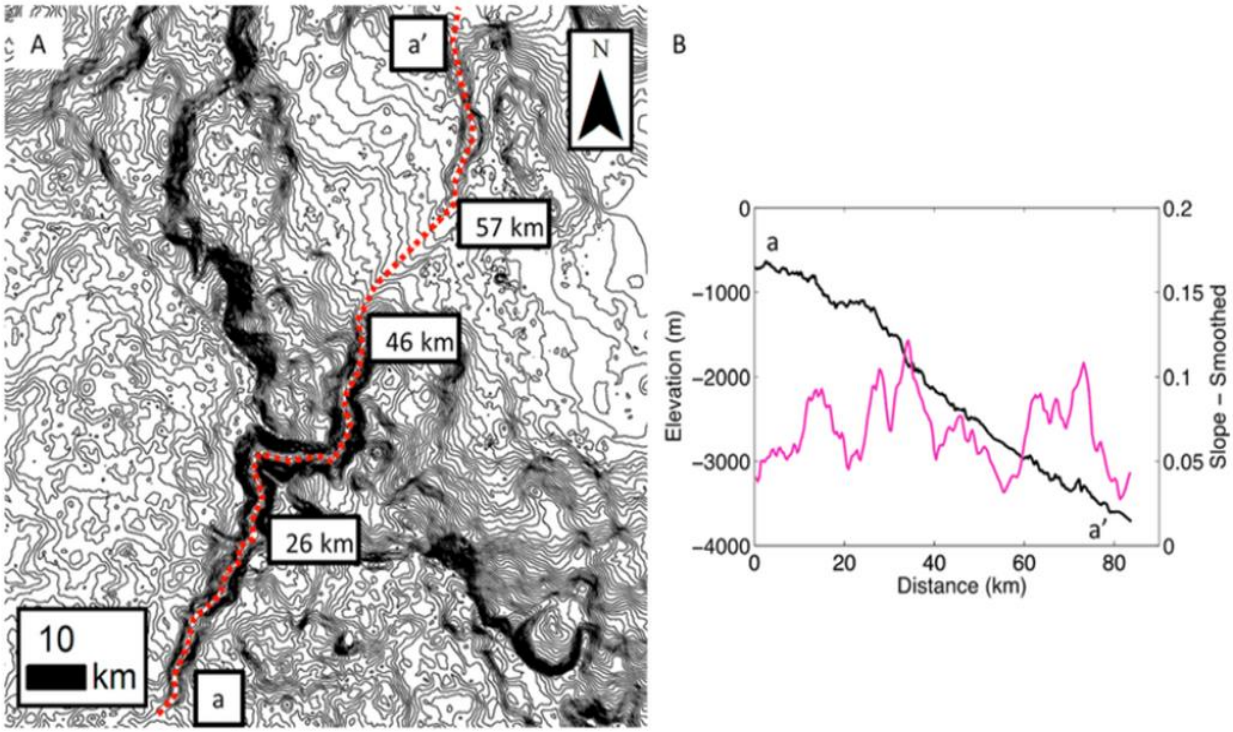

Figure 5.1: (a) 50m HRSE contours for the Farah Vallis region are shown, as is the location of the longitudinal profile. (b.) A longitudinal profile (black line) and slope profile (pink line) of Farah Vallis. (Palucis et al., 2016)

5.1.1 Farah Vallis

Farah Valley is a large canyon system on Mars that is located near the equator of the planet. It's over 4,000 kilo meters long and is thought to have been formed by water erosion billions of years ago. Water erosion, presumably from a massive river that ran through the area billions of years ago, is assumed to have built the canyon system. The valley is distinguished by sheer walls, terraces, and mesas, or flat-topped hills. The valley also has many big impact craters that are suspected to be the result of meteorite strikes.

The morphology of Farah Valley is trough. It is of fluvial origin and has a narrow dimension. where the geological unit of Farah Valley is known as the Middle Noachian highland unit. The primary characteristics of this unit are that it has an uneven to rolling topography, i.e., several high relief outcrops that extend hundreds to thousands of kilometres.

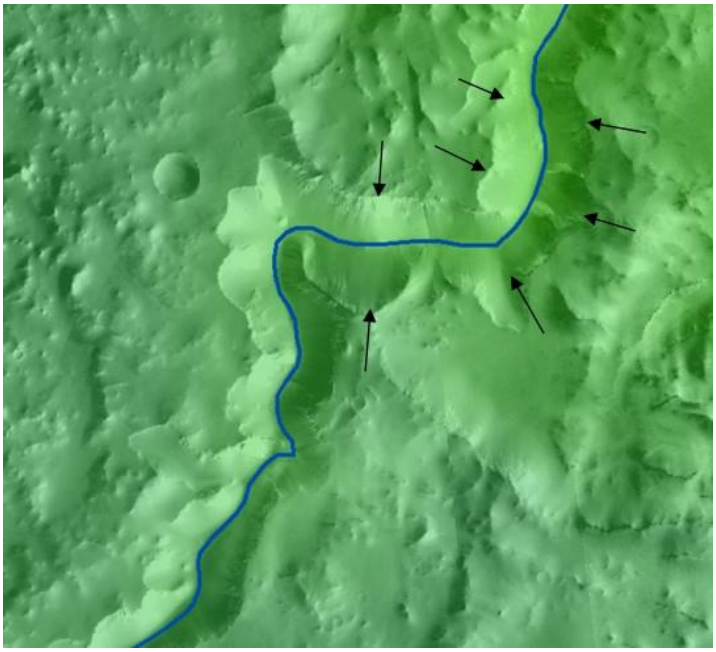

Figure 5.2: Examples of paired interior terraces (black arrows) within Farah Vallis. Main valley shown in blue. HRSE DEM mosaic overlain on CTX image.

These are commonly layered in the crater walls, and this layering may be more than hundreds of metres to more than a kilometre thick. Being extensive in the equatorial to southern highlands is an additional characteristic possessed by this unit. And it also consists of heavily cratered and marked by locally dense valleys, grabens, and wrinkle ridges. The Farah Vallis

terraces are paired, continuous for tens of kilo meters, and only outcrop at one level; i.e., there are not multiple flights of terraces (Figure 5.2).

5.1.2 The Farah Vallis-Pancake and Farah Vallis Delta-Fan Systems

On the SW wall of Gale, a number of deposits connected to Farah Vallis likewise seem to be quite young. Several well-preserved but abandoned channel segments that are shortened by more deeply incised portions define the upper surfaces. When headward incision eventually led to a single discharge channel that discharged water and sediment across an alluvial fan lower on the crater wall or floor, some of the abandoned segments may have terminated at locations of temporary stability during that time. It is challenging to trace the whole extent of the fan due to encroaching dunes from the north, although the fan otherwise embays other surfaces in the crater, such as the deposits in Peace Vallis and along the NW wall.

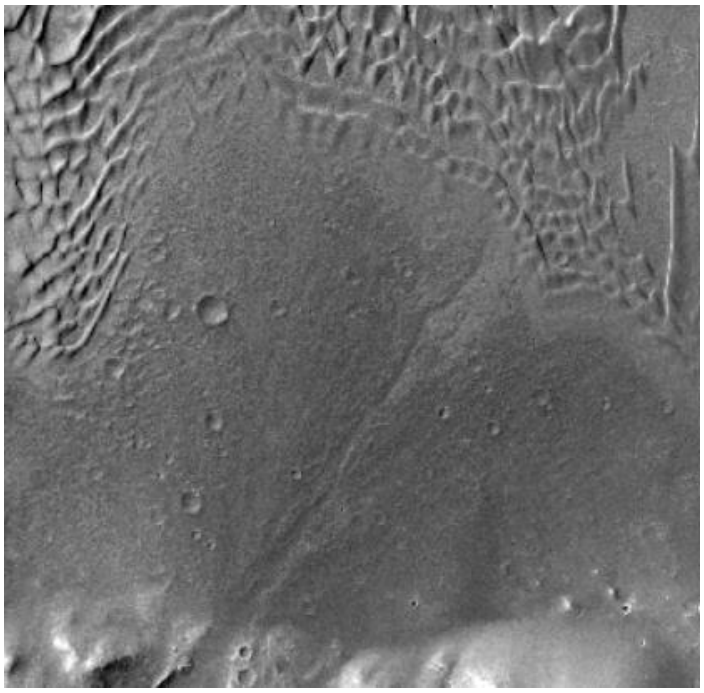

Figure 5.3: CTX image of the Farah Vallis Fan deposit, overlying the Farah Vallis delta deposit.

The Farah Vallis system is composed of a source canyon upstream, a fan, and then a delta deposit after more incision. A second, narrow, tiny fan was afterwards deposited on top of this delta deposit. Additionally, Farah Vallis sediment was moved east to the largest and maybe best-preserved delta seen in Gale.

Farah Vallis consists of 2 canyons; first canyon crosses the rim and cuts into ejecta and one that cuts in to deposits from the upslope canyon. There are two, short, stubby tributary valleys. And the relatively sharp-edged floor of Farah Vallis is covered with colluviam and dunes, also boulder-sized material found.

A minor delta-like feature emanating from a wide canyon on the south side of Mount Sharp is located to the east of the Farah Vallis delta-fan system. Milliken et al. [2014] discovered fan-like deposits radiating from canyons to the east of our delta-like structure, which are underlain by preserved bedforms comparable to those found beneath the Entrance Canyon deposits.

The overall eroded volume from Farah Vallis is 40.5 km^3, based on a combination of CTX and HRSC DEM data. The Pancake delta and its related deposits, which were later incised into, are 14 and 10 km^3 in size, respectively (5 km^3 was later eroded and deposited within the Farah Vallis delta). The Farah Vallis fan-delta deposit has a total volume of 23 km^3, with the fan being about 0.5 km^3. The Pancake delta, Farah Vallis fan-delta, and Wall fan coming from the upper half of Farah Vallis total 42 km^3 of material, which roughly corresponds to the 40 km^3 of material removed to form Farah Vallis.

5.1.3 Farah Vallis Lake Stand

The 3780 m HRSC contour defines the second highest lake level, which also corresponds to the upper Dulce delta (DD2) and the termination of about half of the gullies on the northern side of Gale crater. It is also close to the elevation at which the gully within the Entrance Canyon changes to a deposit. At this elevation, a lake would have had a surface area of 3617 km2 and a mean depth of 0.4 km. The lake's volume would have been 1583 km3(Palucis et al., 2016).

5.1.4 Tributary Valleys

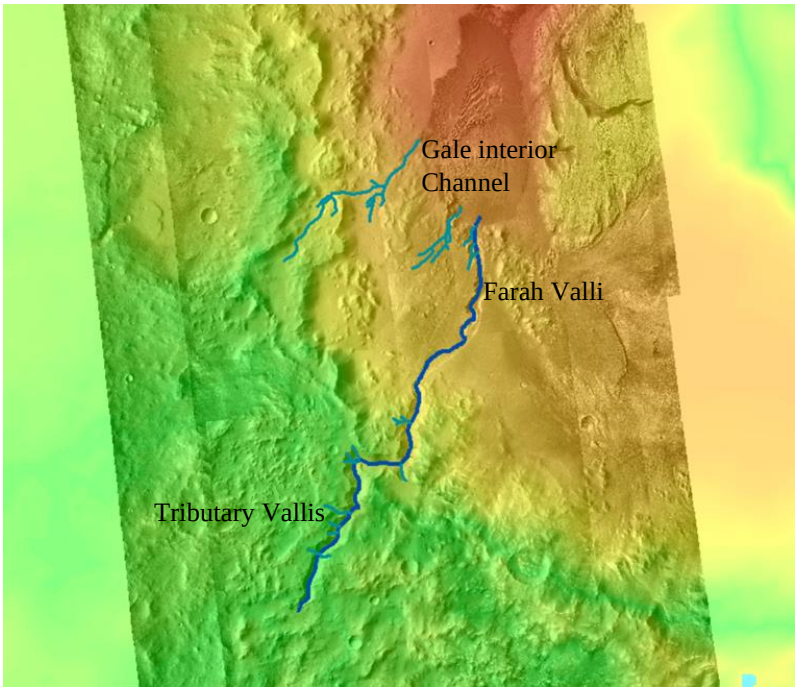

Figure 5.4: The image seen above shows the initial identification of various fluvial geomorphic features of Farah Vallis and interior channels on Mars.

From the study it is identified that Farah Vallis has 13 main tributary valleys, they flow towards Gale crater. Topographic profiles of the tributary valley show that the 10 most upstream tributaries have knickpoints along their length. The tributaries are flowing towards Gale crater and it shows dendritic pattern.

These tributaries must be divided into two groups: (1) those downstream of the likely overflow location of the first-generation, larger, intercrater paleolake basin, which have been influenced by two episodes of lake overflow flooding; and (2) those upstream of this point, which have only been influenced by the second-generation, smaller, intracrater paleolake basin's overflow flooding.

5.1.5 Gale interior channels

Based on the current topography, the total volume of material carried by flowing water into Gale is no more than 1.3 103 km3, which is 13% to 20% of the mound's current volume. The volume of the current mound clearly surpasses the volume of sediment mobilised by the contributory fluvial network and overland flow from Gale's catchment region by a factor of 5

or more. Other than river conveyance, other mechanisms are required to explain the remaining 80% to 87% of the mound's sedimentary budget. Fluvial, lacustrine, aeolian, and polar transit processes have previously been proposed.

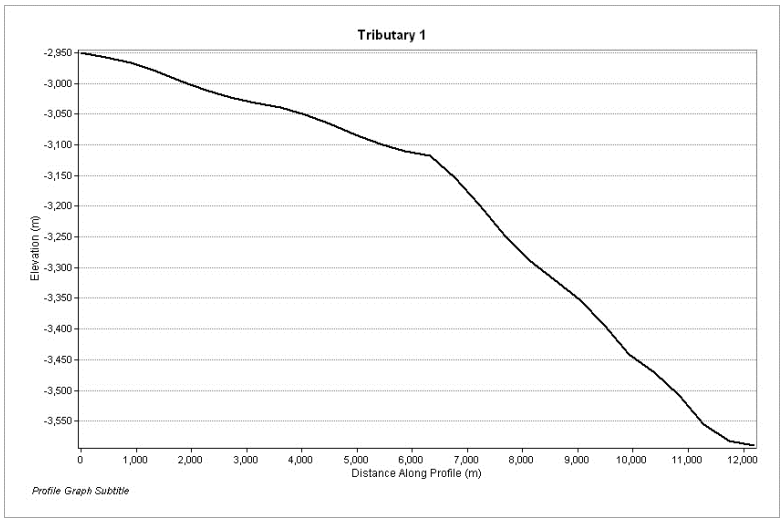

Figure 5.5: Elevation profile of Gale interior channel-1

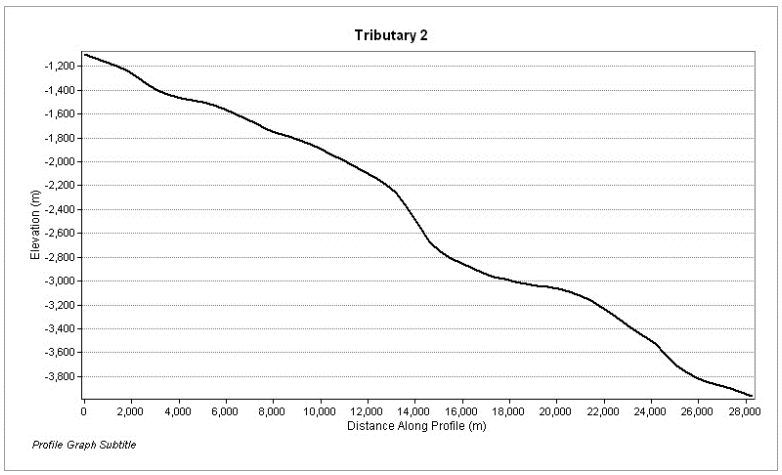

Figure 5.6: Elevation profile of Gale interior channel- 2

CHAPTER 6

CONCLUSION

From the geomorphological mapping of Farah Vallis the following conclusion can be arrived.

The observations and analysis revealed presence of fluvial landforms in the Farah Vallis and some part of Gale Crater that are distinct in terms of morphology, topography and scales of landforms. The southwest crater rim is pierced by the single, large channel known as Farah Vallis, which also links the valley network system that surrounds Gale. The morphology of Farah Vallis is similar to other networks of valleys on Mars that are V-shaped.

The surface of Mars displays abundant evidence for fluvial activity, it is believed that Mars once had a much wetter climate than it does today, the evidence of this can be seen in the many river valleys and other features on the Mar's surface. The fluvial features seen on the Farah Vallis include 13 Tributary Vallis, delta, and two other tributaries for another fluvial system. The Farah Vallis system is composed of a source canyon upstream, a fan, and then a delta deposit after more incision.

REFERENCE

- Carr, M. H. (1980). The morphology of the Martian surface. *Space Science Reviews*, *25*(3), 231–284. https://doi.org/10.1007/BF00221929
- Carr, M. H. (2012). The fluvial history of Mars. *Philosophical Transactions of the Royal Society A: Mathematical, Physical and Engineering Sciences*, *370*(1966), 2193–2215. https://doi.org/10.1098/rsta.2011.0500
- Dengyun Y. U., Zezhou S. U. N., Linzhi M., & Dong S. H. I. (2016). The Development Process and Prospects for Mars Exploration. 深空探测学报(中英文）, *3*(2), 108–113. https://doi.org/10.15982/j.issn.2095-7777.2016.02.002
- Fassett, C. I., & Head, J. W. (2008). Valley network-fed, open-basin lakes on Mars: Distribution and implications for Noachian surface and subsurface hydrology. *Icarus*, *198*(1), 37–56. https://doi.org/10.1016/j.icarus.2008.06.016
- Gallagher, C. J., & Bahia, R. (2021). Chapter 2—Outflow channels on Mars. In R. J. Soare, S. J. Conway, J.-P. Williams, & D. Z. Oehler (Eds.), *Mars Geological Enigmas* (pp. 13–40). Elsevier. https://doi.org/10.1016/B978-0-12-820245-6.00002-1
- Goudge, T. A., Aureli, K. L., Head, J. W., Fassett, C. I., & Mustard, J. F. (2015). Classification and analysis of candidate impact crater-hosted closed-basin lakes on Mars. *Icarus*, *260*, 346–367. https://doi.org/10.1016/j.icarus.2015.07.026
- Grant, J. A., & Wilson, S. A. (2019). Evidence for Late Alluvial Activity in Gale Crater, Mars. *Geophysical Research Letters*, *46*(13), 7287–7294. https://doi.org/10.1029/2019GL083444
- Hartmann, W. K., & Neukum, G. (2001). Cratering Chronology and the Evolution of Mars. *Space Science Reviews*, *96*(1), 165–194. https://doi.org/10.1023/A:1011945222010
- Li, C., Zhang, R., Yu, D., Dong, G., Liu, J., Geng, Y., Sun, Z., Yan, W., Ren, X., Su, Y., Zuo, W., Zhang, T., Cao, J., Fang, G., Yang, J., Shu, R., Lin, Y., Zou, Y., Liu, D., … Ouyang, Z. (2021). China's Mars Exploration Mission and Science Investigation. *Space Science Reviews*, *217*(4), 57. https://doi.org/10.1007/s11214-021-00832-9
- Maki, J. N., Bell III, J. F., Herkenhoff, K. E., Squyres, S. W., Kiely, A., Klimesh, M., Schwochert, M., Litwin, T., Willson, R., Johnson, A., Maimone, M., Baumgartner, E.,

Collins, A., Wadsworth, M., Elliot, S. T., Dingizian, A., Brown, D., Hagerott, E. C., Scherr, L., … Lorre, J. (2003). Mars Exploration Rover Engineering Cameras. *Journal of Geophysical Research: Planets*, *108*(E12). https://doi.org/10.1029/2003JE002077

- Milliken, R. E., Grotzinger, J. P., & Thomson, B. J. (2010). Paleoclimate of Mars as captured by the stratigraphic record in Gale Crater. *Geophysical Research Letters*, *37*(4). https://doi.org/10.1029/2009GL041870
- Palucis, M. C., Dietrich, W. E., Hayes, A. G., Williams, R. M. E., Gupta, S., Mangold, N., Newsom, H., Hardgrove, C., Calef III, F., & Sumner, D. Y. (2014). The origin and evolution of the Peace Vallis fan system that drains to the Curiosity landing area, Gale Crater, Mars. *Journal of Geophysical Research: Planets*, *119*(4), 705–728. https://doi.org/10.1002/2013JE004583
- Palucis, M. C., Dietrich, W. E., Williams, R. M. E., Hayes, A. G., Parker, T., Sumner, D. Y., Mangold, N., Lewis, K., & Newsom, H. (2016). Sequence and relative timing of large lakes in Gale crater (Mars) after the formation of Mount Sharp. *Journal of Geophysical Research: Planets*, *121*(3), 472–496. https://doi.org/10.1002/2015JE004905
- Pieri, D. C. (1980). Martian Valleys: Morphology, Distribution, Age, and Origin. *Science*, *210*(4472), 895–897. https://doi.org/10.1126/science.210.4472.895
- Thomson, B. J., Buczkowski, D. L., Crumpler, L. S., Seelos, K. D., & Fassett, C. I. (2019). How Much of the Sediment in Gale Crater's Central Mound Was Fluvially Transported? *Geophysical Research Letters*, *46*(10), 5092–5099. https://doi.org/10.1029/2018GL081727

QUALITATIVE ANALYSIS OF GROUNDWATER IN AND AROUND SOUTHERN CLAY MINES AT MANGALAPURAM, TRIVANDRUM DISTRICT

Dissertation submitted to Christ College (Autonomous), Irinjalakuda, Kerala, University of Calicut in partial fulfilment of the degree of

Master of Science in Applied Geology

By,

AKSHAYA PRAKASH

Reg. No: CCAVMAG002

2021-2023

DEPARTMENT OF GEOLOGY AND ENVIRONMENTAL SCIENCE

CHRIST COLLEGE (AUTONOMOUS), IRINJALAKUDA, KERALA, 680125

(Affiliated to University of Calicut and re-accredited by NAAC with A++ grade)

AUGUST 2023

QUALITATIVE ANALYSIS OF GROUNDWATER IN AND AROUND SOUTHERN CLAY MINES AT MANGALAPURAM, TRIVANDRUM DISTRICT

Dissertation submitted to Christ College (Autonomous), Irinjalakuda, Kerala,

University of Calicut in partial fulfilment of the degree of

Master of Science in Applied Geology

By,

AKSHAYA PRAKASH

Reg. No: CCAVMAG002

2021-2023

DEPARTMENT OF GEOLOGY AND ENVIRONMENTAL SCIENCE

EXAMINERS

1……

2……

Dr. ANTO FRANCIS. K

Co-ordinator

CERTIFICATE

This is to certify that the dissertation entitled - **QUALITATIVE ANALYSIS OF GROUNDWATER IN AND AROUND SOUTHERN CLAY MINES AT MANGALAPURAM, TRIVANDRUM DISTRICT**, is a bonafide record work done by Ms. Akshaya Prakash (CCAVMAG002), MSc Applied Geology, Christ College (Autonomous) Irinjalakuda, under my guidance in partial fulfilment of requirements for the degree of Master of Science in Applied Geology during the year 2021-2023

Dr. Vidhya.G.S

Junior Hydrogeologist

Ground Water Department

District office, Thiruvananthapuram

Place: Thiruvananthapuram

Date:

DECLARATION

I, AKSHAYA PRAKASH hereby declare that entitled **'QUALITATIVE ANALYSIS OF GROUNDWATER IN AND AROUND SOUTHERN CLAY MINES AT MANGALAPURAM, TRIVANDRUM DISTRICT'** submitted to Christ College (Autonomous), Irinjalakuda is an original research work done by me, and has not been submitted to any other university for the award of any degree, diploma, associateship and fellowship or any other similar title or recognition. It is a bonafide record carried out by me under the guidance of Dr.Vidhya.G.S, Junior Hydrogeologist, Thiruvananthapuram, Kerala, during April 2023 to August 2023.

Place : Thiruvananthapuram AKSHAYA PRAKASH

Date : Reg.No. CCAVMAG002

ACKNOWLEDGEMENT

First of all, I express my sincere gratitude and heartfelt thanks to the persons from whom I have received guidance, help, and encouragement in fulfilling the completion of this project work.

I would like to express my deep sense of gratitude to my guide **Dr.Vidhya.G.S**, **Junior Hydrogeologist, District office, Thiruvananthapuram**, for her guidance and whole support for completing the work. I am highly indebted to her for all valuable advices and guidance in all aspects of my dissertation work.

I also express my sincere gratitude for **Sudheer.A.S, District Officer**, **Thiruvananthapuram**, for his permission to carry out the project work in the department.

I also express my gratitude to the **National Hydrology Project Assistants, SGWB**, for helping me conduct field studies.

I would like to take this opportunity to express my deepest gratitude to **Dr.Anto Francis K, Co-ordinator**, Department of Geology and Environmental Science, Christ College (Autonomous), Irinjalakuda.

I record my deep sense of gratitude to **Gopakumar. P. G, Assistant Professor**, Department of Geology and Environmental Science, Christ College (Autonomous), Irinjalakuda, for all the help, suggestions and support throughout the course and dissertation. I also thank other faculty members of the for their continuous support and encouragement.

I am also thankful to **Ms. Rajalakshmi, Ms. Anju** and other staffs (technical and non-technical) of **National Centre for Earth Science Studies (Ministry of Earth Science, Government of India), Thiruvananthapuram, Kerala**, for helping me in the analysis of water samples.

Last but not the least, I express my sincere gratitude to my parents, friends and family for other support.

Above all, I want to thank the Almighty God for the blessings and generosity he's shown me.

AKSHAYA PRAKASH

ABSTRACT

This study aims to investigate the qualitative analysis of groundwater in and around clay mines in Mangalapuram. Groundwater is a vital resource for various purposes, and its contamination can pose significant risks to human health and the environment. The presence of clay mines in the vicinity raises concerns about potential groundwater pollution due to mining activities. The qualitative analysis will assess the physical and chemical, and parameters of the groundwater samples collected from different locations around the clay mines.

From the areas around the Mangalapuram clay mines, 17 open well samples were taken for the current investigation. The investigation focused on determining the concentration of anions, cations and trace metals. Additionally, the study will assess the impact of clay mining on groundwater quality by comparing the results with the existing water quality standards and guidelines. The study area shows abnormal pH values, which indicate a trend toward acidity. The water quality parameters such as pH, Total Dissolved Solids (TDS), Sodium (Na), Calcium (Ca), Iron (Fe) etc. were used for evaluating Water Quality Index. The Water Quality Index decline as a result of the impact of clay mining. The investigation indicate that the region is unsuitable for the production of drinking water.

The findings of this study are expected to provide valuable insights into the potential contamination of groundwater in and around clay mines. This information will be beneficial for mining industry to develop appropriate measures for protecting and managing groundwater resources effectively. Furthermore, the study will contribute to the existing knowledge in the field of environmental science and advance our understanding of the impact of clay mining on groundwater quality.

List of Tables
List of Figures

List of Photographs

LIST OF TABLES

LIST OF FIGURES

LIST OF PHOTOGRAPHS

CHAPTER 1

INTRODUCTION

1.1 INTRODUCTION

Water is a remarkable agent of change and transformation. Over millennia, it has sculpted the Earth's surface, shaping valleys, canyons, and coastlines through processes like erosion and weathering. Its incessant flow, whether as rivers or glaciers, carves through rocks, carrying away sediment and leaving behind breathtaking landscapes. Water's ability to dissolve minerals and carry them in solution further contributes to the formation of caverns and underground structures. Moreover, as water freezes and expands, it exerts immense pressure, cracking rocks and contributing to the disintegration of rock formations. Thus, water is an essential force in shaping the ever-evolving geology of our planet.

The Earth is unique in that as it is the only planet that has water in its three forms (solid, liquid and gas) and in sufficient quantity to maintain life on Earth. Oceans make up more than 70% of the surface of the earth. Total usable freshwater supply to ecosystem from river system, lakes, wetlands, soil moisture and groundwater is less than 1% of all freshwater and only 0.01% of all water on Earth. As per WHO estimates only 0.007% of all water on Earth is readily available for human usage. The water in rivers, lakes, marshes and oceans known as gravitational water, accounts for almost 97% of the total water reserves of the Earth. This indicates that freshwater on earth is finite and also unevenly distributed. The availability of freshwater results from the cycling of water (evaporation from ocean into atmosphere and precipitation from the atmosphere back to the land and oceans). The water falling over the land is stored as surface water and/or percolates down to fill underground reservoirs or aquifers. Human actions modify the hydrological cycle and can seriously pollute available water. Climate change also affects the hydrological cycle significantly thereby freshwater production and its distribution.

Water is elixir of life. Man needs water for all domestic needs like drinking, cooking, washing etc. Though Kerala state receives an average annual rainfall of 3100mm of rainwater annually, which is 2.8 times of the national average, the per capita availability of freshwater in the state is one of the lowest among the other states of India. To a certain extent, the peculiar nature of the topography of the state with deforestation and sand mining in rivers lead to an accelerated draining of water to the sea. This is evident from the fact that groundwater recharging has suffered and groundwater levels have steeply declined. The pollution levels in the water bodies and drinking water sources have gone up to an alarming rate. Factors like unscientific waste disposal, over usage of fertilizers and pesticides in agriculture, lack of alacrity to protect the rivers and other water bodies and unplanned construction of toilets in area of high density of population have led to a steady deterioration of water quality.

One of the nation's most valuable natural resources is groundwater, which is found in aquifers beneath the Earth's surface. This valuable resource is tapped by dug wells and

borewells drilled through hard rocks that only store or transmit water when weathered and/or fractured (Raju and Reddy, 1998). Since groundwater is typically heavily mineralized in its natural condition, it is generally less prone to contamination than surface water. The quality of groundwater is influenced by interactions between water and rock, in which geology and weathering can be significant factors as well as anthropogenic activities and climate. One of the most important elements influencing groundwater pollution is changes in land use.

The country has 18 percent of the world's population, but only 4 percent of its water resources, making it among the most water-stressed in the world. A large number of Indians face high to extreme water stress according to a recent report by the government's policy, the NITI Aayog. The National commission for integrated Water Resource Development Plan has estimated an overall water demand of 1180 billion cubic meters which was 710 in 2010. Aayog in their report has declared the current water scarcity as the worst water crisis in Indian history where about 60 crore people are facing high to extreme water stress. By 2030, the country's water demand is projected to be twice the available supply. This may have implications in terms of food security, farmer's livelihood and nation's economic development. Water scarcity already affects every continent. Around 1.2 billion people, or almost one-fifth of the world's population live in areas of physical scarcity and 500 million people are approaching this situation. Another 1.6 billion people, or almost one quarter of the world's population economic water shortage.

Keeping the quality of the world's groundwater is one of the biggest problems. The main reasons of drinking water scarcity in our nation are insufficient groundwater distribution and excessive groundwater extraction. Water-rock interactions, which can be significantly impacted by geology, weathering, anthropogenic activity, and climate, determine the quality of groundwater. Changes in land use are one of the most significant factors affecting groundwater pollution. (Benson et al.,2006). Nitrate is one of the key indicator of groundwater contamination. Groundwater deterioration caused by $NO3^-$ degrades the groundwater quality and impacts negatively on ecosystems. An increased nitrate ($NO3^-$) concentration in groundwater has been a rising issue on a global scale in recent years. Different consumption methods clearly demonstrate the harmful impact on human health in the various age categories children, males, and females. Nitrate contamination of ground water in various parts of the world has raised alarmingly. Nitrate levels have been increasing in drinking water supplies in most countries. Environmental Protection Agency (EPA) in 1990 indicated that 2,50,000 water supply sources had maximum contaminant levels (MCL) for nitrate.(Archna et al., n.d.)

There is an urgent need to generate greater social awareness about the right and responsibilities in the use of water and to put in place better management practices in the utilization of this valuable resource. Under these circumstances, we should be keener in doing research work in the allied field. More often than not, researchers focus their attention only on the quantity of water, but in the real state of affairs, the quality of water is as imperative as the quantity of water.

In India, people suffer from health disorders mainly from the occurrence of fluoride and arsenic in drinking water. Relatively, the health implications caused by F-contamination are far more widespread than those of arsenic contamination in the country (Subba Rao, 2011). Seventeen states in India have been identified as endemic for fluorosis (Mishra et al., 2006). Geochemically, fluorine is the most electronegative element and occurs primarily as a

negatively charged ion in water. A low amount of fluoride (0.3-1.0 mg/L) in drinking water helps in the prevention of dental caries and osteoporosis. However, a high intake of fluoride (>1.5 mg/L) in drinking water for a prolonged period can damage the teeth enamel and eventually lead to skeletal complications which ultimately can result in fluorosis (WHO 1984, ISI 1983). Thus, fluoride (F) concentration is an important aspect of hydrogeochemistry. Bureau of Indian Standards (BIS, 1991) has prescribed a limit between 1.0 and 1.5 mg/L of F- in drinking water. Potential sources of fluoride in groundwater include various minerals in rocks and soils, such as fluorite, apatite, amphiboles, and micas (Handa, 1975, Pickering 1985, Wenzel & Blum, 1992, Bardsen et al., 1996, Subba Rao & Devadas, 2003). High fluoride is reported from both phreatic and deeper aquifers in the eastern part of the Palghat district (Shaji et al., 2007), and sedimentary aquifers of Alleppey (Raj and Shaji, 2017). Concentration of fluoride in drinking water and its effects on human health is given in the table.

Fluoride mg/L	**Effects on human health**
Nil	Limited growth and fertility
<0.5	Dental Caries
0.5 – 1.5	Promotes dental health, prevents tooth decay
1.5 – 4.0	Dental Fluorosis (mottling & pitting of teeth)
4.0 – 10-.0	Dental and Skeletal Fluorosis
>10.0	Crippling Fluorosis

Fluoride in drinking water and its effects on human health

The environmental and socio-economic conditions of Kerala's midland and lowland regions have been impacted by the indiscriminate extraction of clay and sand-rich soil from paddy fields and other wetland systems for the production of bricks, tiles, and other clay products. Mining operations cause intolerable environmental damage unless they are adequately planned and managed. Rapid, unregulated, and occasionally biased mining activities lead to large-scale environmental damage through air, water, and noise pollution, soil degradation, health risks, the loss of agricultural land, well dryness, and rehabilitation issues. Finding a balance between mineral development on the one hand and environmental restoration on the other is crucial.

1.1.1 GLOBAL GROUNDWATER SCENARIO

The worldwide water withdrawal has increased seven times over the past century compared to a three-fold increase in human population. Due to rising population expansion and expanding economic development activities, freshwater removal from rivers, lakes, and groundwater aquifers has grown by 40% since 1940. As a result, the demand for freshwater resources has increased over the past several decades in many

parts of the world, and as a result, a number of regions have begun to experience issues with a lack of freshwater.

Several international initiatives have been made in recent years to address the issue of groundwater overexploitation, including the Transboundary Water Assessment Programme (TWAP), facilitated by the Global Environment Facility, and UNESCO's International Hydrological programme on International Shared Aquifer Resources Management. Both programmes concentrated on transboundary aquifers, or aquifers shared by two or more nations.

1.1.2 NATIONAL GROUNDWATER SCENARIO

The groundwater scenario in India is of particular concern due to its heavy reliance on groundwater for various sectors, including agriculture, industry, and domestic use. The Central Ground Water Board (CGWB) of India estimates that groundwater supplies provide around 40% of the nation's overall water needs. The groundwater scenario in India, however, faces a number of difficulties. In many areas of the nation, water levels are decreasing as a result of overuse of groundwater resources. Approximately 53% of the wells surveyed in India show a fall in groundwater levels, according to CGWB. About 90% of all groundwater withdrawals in India are used for agriculture, making it the largest consumer of groundwater. Groundwater reserves have been depleted as a result of excessive pumping for irrigation, which has decreased soil fertility and agricultural output. India's groundwater is also facing quality challenges, with the presence of contaminants like arsenic, fluoride, and nitrates in some regions. High levels of these contaminants pose significant health risks to people consuming such water. In coastal regions, overextraction of groundwater has led to the intrusion of saline water into freshwater aquifers. This has made the groundwater in these areas unfit for irrigation and drinking purposes, impacting agriculture and communities dependent on groundwater.

To address these challenges, several initiatives and policies have been implemented in India:

- **Jal Shakti Abhiyan**: Launched by the government of India, this campaign aims to promote water conservation and management, including groundwater, through various measures such as rainwater harvesting, watershed development, and efficient irrigation practices.

- **National Water Policy**: The National Water Policy of India emphasizes the need for sustainable groundwater management, encouraging the adoption of water-saving technologies, and regulating groundwater extraction through policies and legal frameworks.

- **Groundwater management**: The CGWB, along with state groundwater departments, monitors, assesses, and regulates groundwater resources. They undertake

measures such as mapping of aquifers, implementing groundwater recharge structures, and promoting water use regulations in critical areas.

- **Climate resilience**: Indian states are also focusing on climate resilience by promoting climate-smart agriculture, promoting drought-tolerant crops, and implementing strategies to reduce water demand and enhance water use efficiency.

- **Public awareness**: Various campaigns and educational programs are conducted to raise awareness among farmers and communities about sustainable groundwater practices, focusing on issues like rainwater harvesting, water conservation, and judicious water use.

1.1.3 KERALA GROUNDWATER SCENARIO

Kerala is known as "God's own country" because of its lush greenery, plenty of water resources, including forty-four rivers, a large number of lakes, and lagoons, as well as its regular rainfall. It is widely believed that the state has abundant water resources to meet all of its needs, although this is not currently the case. Despite having rainfall that is over 2.8 times more than the national average, the state, including Rajasthan, has one of the lowest per-person freshwater availability rates. Long-term groundwater levels in Kerala show a predominately rising trend throughout the pre-monsoon season. However, the Kerala Water Authority (KWA) reports that during the summer of 2003, 48% of the 45 million wells in the state dried up (Dr. Ajayakumar Varma, Groundwater Resource and Governance in Kerala Status, Issue and Prospects, 2017).

Groundwater availability varies significantly from location to location in Kerala depending on the local hydrogeological, geomorphological, and climatic circumstances. A hard crystalline rock that is completely devoid of primary porosity and has less ground water potential underlies about 88 percent of the land. The aquifer systems in alluvial deposits are numerous. Water quality may, on occasion, impose restrictions on the development of water resources. Over the past few decades, the state's utilisation of ground water resources has increased due to rising population and fast urbanisation. To preserve the long-term sustainability of Kerala's priceless natural resource, scientific management of ground water development and management has become essential. Recently, numerous blocks around the state have reported cases of groundwater contamination, groundwater overuse, and water table falls. According to the CGWB's report on groundwater management (2019), the state has two critical blocks and one overexploited block (the Chittoor block). In recent years, Kerala has seen a sharp rise in the number of problematic blocks.

1.2 OCCURRENCE OF GROUNDWATER

In hard rock terrain, comprising weathered crystallines and laterites, ground water occurs under phreatic conditions in the weathered residuum and the shallow fractures

hydraulically connected to it; below this semi-confined to confined conditions prevails in the deep fracture zones. In the alluvial terrain, ground water in the shallow systems is in phreatic condition. Granular zones in the Tertiary sedimentary formations at deeper levels and forms potential confined to semi-confined aquifers. (Dynamic Groundwater Resources of Kerala, March 2020). Fig.1 shows Principal Aquifers of Kerala.

1.2.1 CRYSTALLINE ROCK AQUIFER

The shallow aquifers of the crystalline rocks are made up of the highly decomposed weathered zone or partly weathered and fractured rocks. Thick weathered zone is seen along the midland area either beneath the laterites or exposed. In the hill ranges thin weathered zone is seen along topographic lows and area with lesser elevation and gentle slope. In areas along the hill ranges generally rock exposures are seen. The depth to water level in this aquifer varies from 2 to 16 mbgl and the yield of the well ranged between 2 to 10m^3 per day. Exploratory drilling carried out by Central Ground Water Board in the state in the crystalline formations has indicated that the fractures are encountered at depths ranging between 30 to 175mbgl with yield varying from less than 1 to as much as 35 litres per second (lps). In Charnockites, more than 40% of the wells have yielded more than 10lps or above indicating that in Kerala, Charnockite suite of rocks are better aquifers compared to Khondalite group. (Dynamic Groundwater Resources of Kerala, March 2020)

1.2.2 TERTIARY ROCK AQUIFERS

Groundwater occurs under phreatic condition in the shallow zone and under semi-confined to confined conditions in the deeper aquifers. The Tertiary formation of Kerala coast is divided into four distinct beds viz. Alleppey, Vaikom, Quilon and Warkali. These formations except the Alleppey beds seen as outcrops are lateritized wherever they are exposed. The maximum thickness of Tertiary sediments is found between Karunagapally and Kattoor and all the four beds are found in this area.

Groundwater is commonly developed through dug wells tapping the sandy zones at shallow depth in the Tertiary sediments. The depth to water level in this shallow zone ranges from 2.0 to 27mbgl and the yield of the wells range from 500 lps to 10 m3 per day.

The Vaikom and Warkali beds form the most potential aquifers in the Tertiary group. The Alleppey bed has been encountered at deeper levels in the bore holes drilled in the coastal tract of Alappuzha district and the formation water is found to be saline and hence, no tube well has been constructed tapping this formation.

In the Vaikom aquifers, the piezometric level is between 2 and 20 m above msl. The yield of the tube wells constructed in this formation ranges from 1 to 57 lps. This bed forms auto flow zones along the coast between Karunagapally in Kollam district and Nattika and Kaipamangalam in Thrissur district. The water is generally fresh south of Karuvatta in Alappuzha district. Also, exploration by CGWB proved that good quality groundwater pockets

are in existence in this formation in and around Cochin and NW of Kottayam around Kallara-Udayanapuram areas.

Warkali aquifers are the most developed aquifer system among the Tertiary group. The urban and rural water supply in the coastal area between Kollam and Alappuzha is mostly dependent on this. The piezometric head is about 3 m. above msl along the eastern part of the sedimentary basin whereas it is 10 m. below msl in and around Alappuzha. The yield of the wells tapping this formation ranges from 3 to 14 lps. The hydrogeological information on Quilon beds is very limited. The formation is a poor aquifer compared to Vaikom and Warkali beds. (Dynamic Groundwater Resources of Kerala, March 2020)

1.2.3 LATERITE AQUIFERS

Laterites are the most widely distributed lithological unit in the state and the thickness of this formation varies from a few meters to about 30 m. Laterite forms potential aquifers along topographic lows and valleys. The depth to water level in this formation ranges from 2 to 25 mbgl and the yield ranges from 0.5 to 30 m^3 per day. The occurrence and movement of groundwater in the laterites are mainly controlled by the topography. Laterite is a highly porous rock formation, which can form potential aquifers along topographic lows. However, due to the porosity, groundwater is drained from elevated places and slopes immediately after monsoon and hence water scarcity is experienced in the elevated places and hill slopes. (Dynamic Groundwater Resources of Kerala, March 2020)

1.2.4 ALLUVIAL AQUIFERS

The alluvial deposits form potential aquifer along the coastal plains and groundwater occurs under phreatic and semi-confined conditions in this aquifer. The thickness of this formation varies from few meters to above 100 m and the depth to water level ranges from less than a meter to 6 mbgl. Filter point wells are feasible wherever the saturated thickness exceeds 5m. This potential aquifer is extensively developed by dug wells and filter point wells throughout the state and the yield ranges from 5 to 35 m^3 per day. (Dynamic Groundwater Resources of Kerala, March 2020)

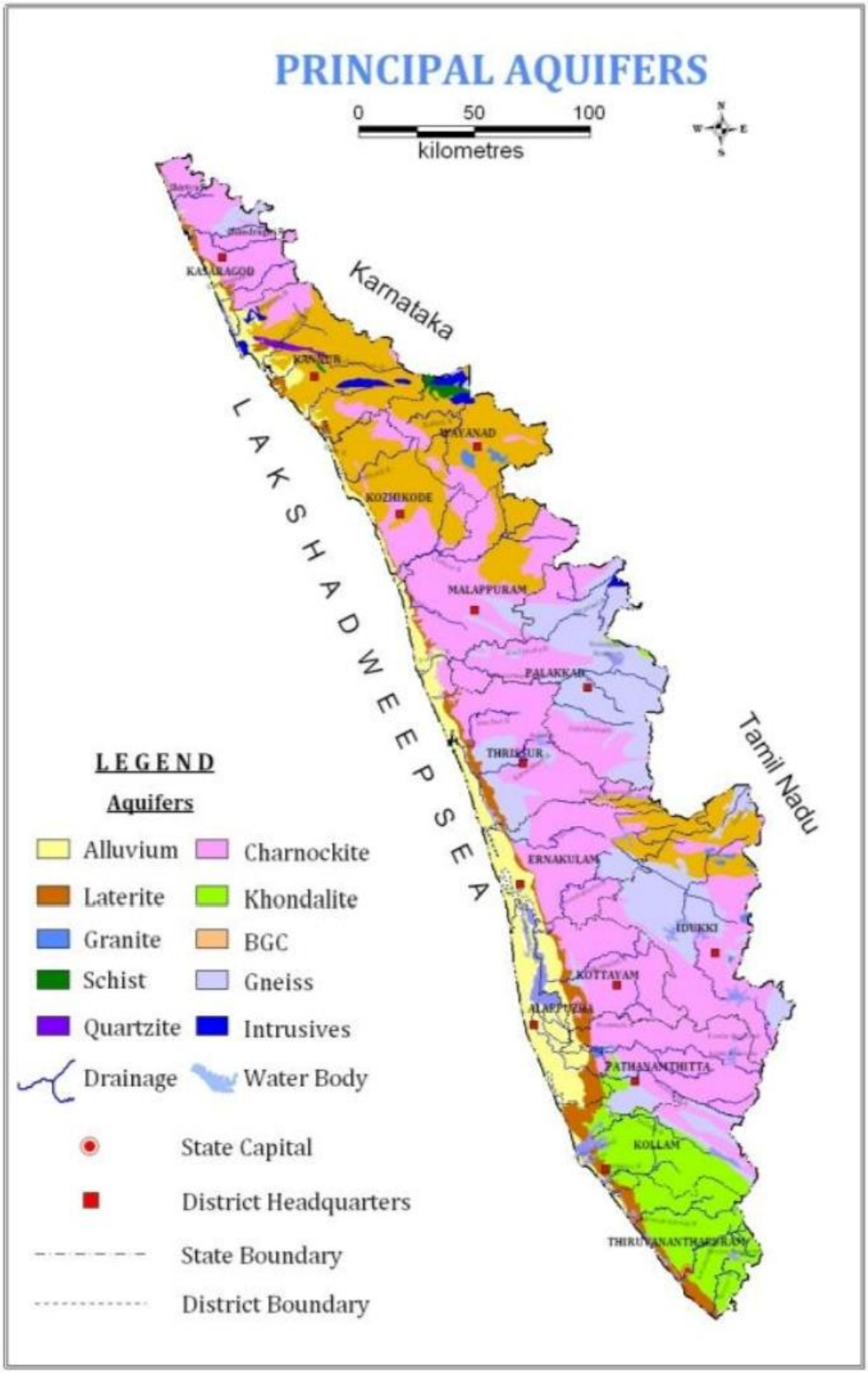

Fig.1 Principal Aquifers of Kerala

Source : Dynamic Groundwater Resources of Kerala, March 2020

1.3 GROUNDWATER RESOURCE ESTIMATION

The Ground Water Estimation Committee was constituted by both the Central Ground Water Board and the State Ground Water Department to facilitate realistic and coordinated estimation of groundwater resources. The groundwater resources of India were assessed as per the norms recommended by the above committee. Subsequently, with the objective of refining the assessment methodology, the "Groundwater Estimation Committee (GEC)" headed by the Chairman, Central Ground Water Board (CGWB), came into existence. Based on the information gathered during the studies carried out by CGWB, the committee formulated the detailed methodology for the estimation of groundwater resources in 1984 (GEC-84). The methodology was reviewed in 1997, and a modified methodology was formulated in 1997 (GEC-97) for the computation of groundwater resources. This GEC-1997 methodology was modified subsequently, and GEC-2015 norms were issued

In GEC-2015, the water level fluctuation method and the rainfall infiltration method were both advised for use in estimating ground water recharge. The concept of storage change as a result of variations in numerous input and output components serves as the foundation for the water level fluctuation method. The term "input" refers to subsurface inflow into the unit of assessment as well as recharge from rainfall and other sources. Groundwater extraction, evapotranspiration, base flow to streams, and subsurface discharge from the unit are all considered output. It is preferable to use basin/subbasin/watershed as the unit for groundwater evaluation since the inflow/outflow across these boundaries may be regarded as minor because data on subsurface inflow/outflow are not readily available. (Groundwater Resource Estimation Report, 2022)

The annual extractable groundwater recharge was determined in accordance with the standards outlined in the 2015 methodology by subtracting unaccounted losses and natural discharge during the non-monsoon season from the total annual recharge available. In Kerala, the annual extractable groundwater recharge is 5.19 billion cubic metres (BCM). Kerala's district-level availability ranges from 189.06 MCM in Idukki to 589.82 MCM in Palakkad.

In Kerala, groundwater extraction mostly serves domestic needs and irrigation. Various methods exist for calculating extraction for domestic use (GE_{DOM}), irrigation usage (GE_{IRR}), and industrial use (GE_{IND}). An estimated 1.55 BCM of groundwater is extracted for domestic usage. 1.17 BCM is thought to be the amount of groundwater extracted for irrigation usage. The estimated amount of groundwater extracted for irrigation is 0.01 BCM. The annual groundwater extraction for all uses in Kerala is in the order of 2.729 BCM, varying from 55.46 MCM in the Wayanad district to 339.35 MCM in the Palakkad area. (Groundwater Resource Estimation Report, 2022)

According to the criteria suggested in the GEC-2015 methodology, the assessment units have been classified as "over exploited," "critical," "semi-critical," and "safe" based on the stage of ground water extraction and the long-term decline of average ground water levels in the assessment unit's observation wells.

According to Ground Water Resource Estimation Report of 2020 and 2022, out of 152 assessed units, 3 blocks (Chittur and Malampuzha blocks of Palakkad district and Kasaragod block of Kasaragod district) have been classified as critical; 29 blocks are "semi-

critical," and 120 blocks are in the "safe" category. For the purpose of categorising the blocks, the Stage of Ground Water Extraction and the block-wise long-term (2008–2019) water level trends of the observation wells being monitored by the Central Ground Water Board and the State Ground Water Department for pre and post-monsoon were taken into account.

The classification of groundwater quality based on the level of groundwater extraction is given in the table.

Stage of Ground Water Extraction	Category
≤70%	Safe
>70% and ≤90%	Semi-critical
>90% and ≤100%	Critical
>100%	Over Exploited

According to GEC Report, there are 11 blocks in the Thiruvananthapuram district, of which 5 (Athiyannur, Chirayinkil, Nedumangad, Parasala and Pothencode) are semi-critical blocks and 6 are safe blocks. The study area is coming under the **semi-critical Pothencode block**. Percentage of Ground Water Extraction in Pothencode Block is **86.68.**

Thiruvananthapuram district's annual extractable ground water recharge is 272.86 MCM, while current gross ground water extraction is 172.08 MCM. Ground water extraction is at stage 63.06 %

Stage of groundwater development in Thiruvananthapuram District (CGWB)

Category	2022	2020	2017	2013
Safe	6	6	6	8
Semi-critical	5	5	5	3
Critical	0	0	0	0
Over Exploited	0	0	0	0

1.4 STUDY AREA

The study area is demarcated by 2 watersheds of Vamanapuram river basin having an aerial extension of 8.6 km.sq, where clay mining activities are predominant. The study primarily focused on Pothencode and Mangalapuram panchayats within the Pothencode block of Thiruvananthapuram district. The study area covers Thonnakal, Kalloor, Manjamala, Koithoorkonam, Kalluvetti and Mangalapuram. The area lies between 8°37'12.73" and 8°39'44.83" North Latitude and 76°56'24.89" and 76°52'59.13" East Longitude. The area falls in parts of Survey of India toposheet 58 D/14. The area occupies NW part of Thiruvananthapuram district of the state of Kerala. Thiruvananthapuram district is bordered by Arabian sea (Lakshadweep Sea) in the west, Kollam and Pathanamthitta districts in the north, Tirunelveli and Kanniyakumari districts in the east and south.

The clay mines operating in the study region are Thonnakal China Clay Mines and English Indian Clay Ltd (Photo no 3&8). The English Indian Clays Ltd. has been running a China clay mine near Thiruvananthapuram since 1966. The processing facility there produces several grades of refined Kaolin, Metakaolin, and Calcined Kaolin (Clays) for the paper, paint, rubber, plastic, fibreglass, cement, and ultra-marine industries. The facility has the largest capacity in South East Asia at 190,000 metric tonnes per year. (Joji. V.S, 2017). The study area is shown in Fig.2

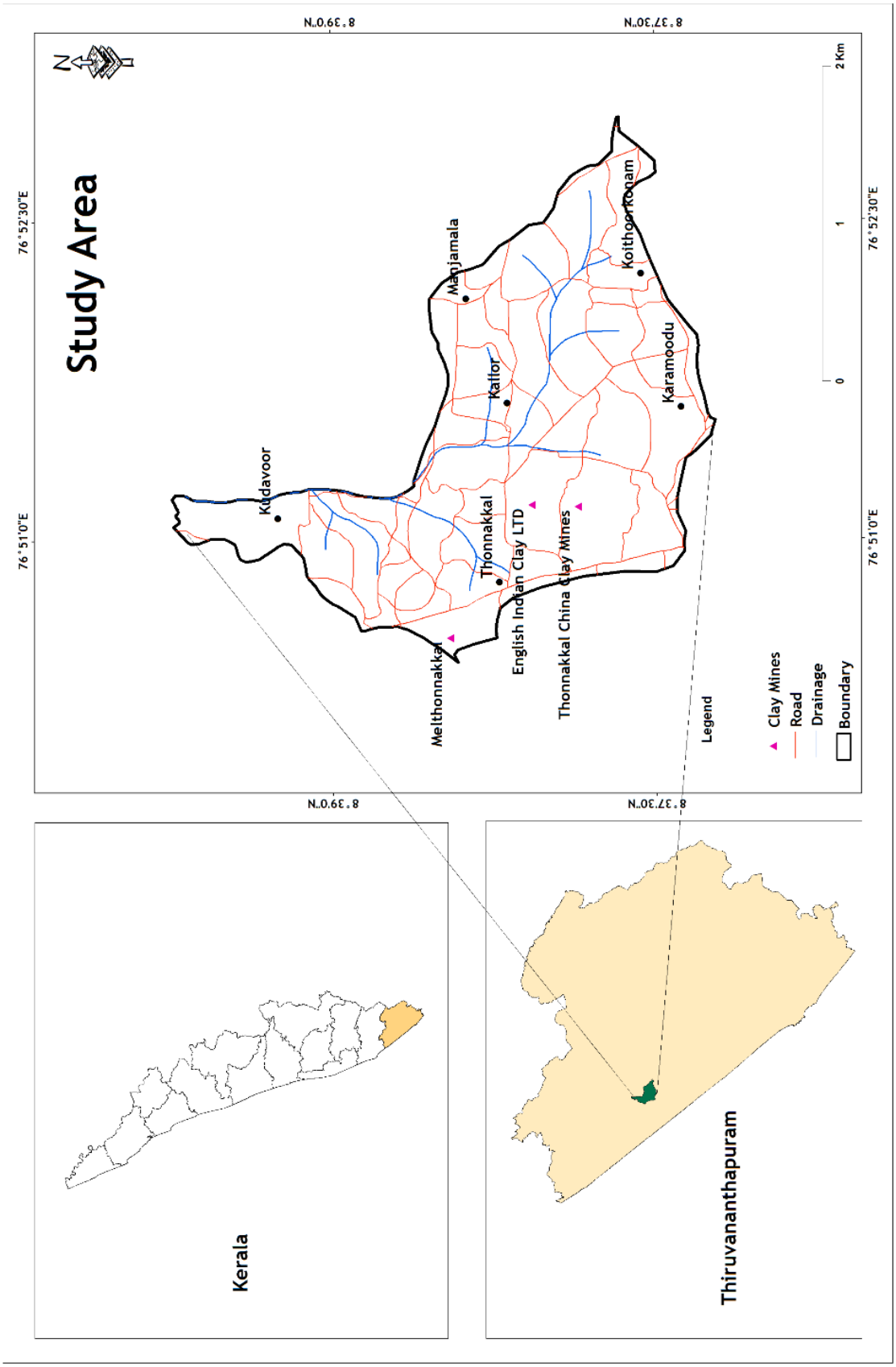

Fig.2 Location Map of the Study Area.

1.4.1 CLAY AND ITS MINING ACTIVITIES

Kerala is the third-largest producer of china clay in the nation, and the best paper coating type reserves are found in the villages of Mel Thonnakkal, Veiloor, Pallipuram, Andoorkonam, and Azhoor in the Thiruvananthapuram District. Around 3,97,188.565 tonnes of china clay were produced in this region in 2012–2013. China clay deposits of primary and secondary origin resulting from weathering of bed rocks, gneisses and sedimentary clays, are found mostly in two belts in Kerala: the northern belt in Kannur-Kasaragod districts and the southern band in Thirvananthapuram and Kollam districts (A.Prabhakumar et al., 2014).The clay resource of the Kerala is divided into three, namely

a) Residual or primary china clay
b) Sedimentary or secondary china clay and ball clay
c) Tile and brick clay

Tile and brick clay are often of Quaternary age, china clay is typically of Tertiary age. Siliceous and ferromagnesium mineral impurities are frequently found in the residual clays. On the other hand, organic matter is an impurity in the sedimentary clays of the ball clay type.

The clay minerals, which are made up of layers of crystalline aluminium silicates. Alkali feldspar-rich rocks like granite or gneiss undergo hydrothermal or residual weathering to produce primary kaolins, whereas sedimentary processes produce secondary kaolins. The results of the physical and chemical tests performed on clay samples show that the china clay is of a high grade and acceptable for use in the manufacturing of synthetic zeolites, paper coating materials, and pharmaceutical sectors. For the establishment of a sizable clay-based industrial unit, the reserve and quality of china clay are sufficient (A.Prabhakumar et al., 2014).

China clay in Kerala is confined to two southern districts (Thiruvananthapuram and Kollam) and two northern districts (Kasargod and Kannur) and hence in generally referred to as Southern Clay Belt (SCB) and Northern Clay Beit (NCB) respectively. While the SCB is rich in sedimentary china clay derived from khondalite rocks, the NCB is predominantly residual china clay, developed over charnockite basement. (Directorate of Mining and Geology, 2005). Presently, more than 30 large and small surface mines are operating in the district. China clay in Thiruvananthapuram and Kollam is generally referred to as Southern Clay Belt (SCB). It is rich in sedimentary china clay derived from khondalite rocks. The kaolinised gneisses at the base of the Tertiaries have given rise to good quality china clay at several places in the Thiruvananthapuram district.

The upper Tertiary sedimentary sequence in Trivandrum district, south Kerala belonging to the Warkalli beds of Mio-Pliocene age contains a column of kaolin clays over the current bedded variegated sandstones, grits, lignite beds etc (Foote 1883; Menon 1966). The kaolin clay beds attain a maximum thickness of about 4-5m at Thonnakkal in Trivandrum district and the adjoining areas and prove to be of refractory quality raw material (Soman 1984). In some of the clay mines at Thonnakkal, more than one bed of kaolin is observed, and the clay bed in most cases is covered by a laterite cover with a maximum thickness of up to 8-10m. Clay mines around Thonnakal is shown in Photo no.1

Photo no.1 Views of Clay mines around Thonnakal

The midland fringes of the study area along Mangalapuram have a comparatively greater thickness of this surface clay.

Aquifer Properties of Clay

Grain Porosity(mm)	Porosity (%)	Specific Yield	Permeability(cm/s)
< 0.002	33-60	2 to 5 %	10-9 to 10 - 6

These characteristics of the clay imply that it is a poor aquifer and, for the most part, an aquitard with very little potential for groundwater.(Mini Chandran et al., 2014.)

1.4.2 DEPTH TO WATER TABLE

The depth to the water table is the vertical distance between the ground surface and the water table. Regional variations in the depth of the water table are influenced by how much water seeps into the ground. The depth-to-water table map displays these variations for various

wells in a given area. The groundwater level varies from 0.7m to 23m with an average of 8.65m. The southern party of the study area has the greatest depth to the water table, which include the area of Thonnakal, Kalloor, Karamood. Greater depth of 23m is found in Karamood. Most of the northern and eastern parts of the study area, which include the regions of the Manjamala, Koithoorkonam and, Pattathil experience lowest depth. Spatial variation of depth to water table is shown in Fig.8

1.4.3 EFFECTS ON GROUNDWATER

The clay reserves at the Mangalapuram clay mines, which are well known, can significantly affect the water table, which include:

- **Depletion of groundwater**: Clay mines require continuous water pumping for various purposes, such as washing the clay and controlling dust. This extraction of water from the ground can lead to a significant drop in the water table over time, resulting in the depletion of groundwater resources.

- **Reduced availability of water sources**: The decline in the water table caused by clay mining can also affect nearby water bodies, such as ponds, lakes, and rivers. These surface water sources often rely on groundwater replenishment, so a drop in the water table may lead to a reduced amount of water flowing into these water bodies, impacting their availability for local communities and ecosystems.

- **Disruption of neighbouring wells**: The decline in the water table can impact the functioning of wells in surrounding areas. Shallow wells used for domestic purposes or agriculture may experience reduced water availability or even run dry as the groundwater levels drop. This can affect the livelihoods and daily lives of people depending on these wells for their water supply.

- **Increased vulnerability to drought**: Lowering of the water table due to clay mining can make the area more susceptible to drought conditions. During periods of low rainfall or prolonged dry spells, the already reduced groundwater levels may not be able to sustain the local population, agricultural activities, and other water-dependent industries.

- **Changes in hydrological processes**: Clay mining can alter the natural hydrological processes in the region. Excavation activities and the formation of large mining pits can disrupt the natural flow of water, leading to changes in drainage patterns and groundwater recharge dynamics. This can impact the overall water balance and hydrological cycle in the area.

- **Ecological impacts**: A decrease in the water table caused by clay mining can negatively affect local ecosystems. Wetlands, marshes, and other groundwater-

dependent habitats may suffer from reduced water availability, leading to diminished biodiversity and the loss of plant and animal species that rely on these habitats for survival.

When surface mines are excavated into aquifer materials, they simply remove a portion of the aquifer, which might be considered a loss of resource in and of itself. The depth of mining and aquifer characteristics have the greatest influence on the local groundwater regime while mining for clay. The clay mining area's effect zone is where the impact is primarily felt. In the long run, this will cause the hydraulic gradient to reverse, causing an increase in the flow of ground water from the aquifer into the mines, deepening water levels, drying up shallow wells, and decreasing the sustainability of ground water abstraction systems(Mini Chandran et al.,2014).

It is important for mining companies and relevant authorities to implement responsible mining practices, such as efficient water management, proper land reclamation, and groundwater monitoring, to minimize the adverse effects on the water table and the surrounding environment. Additionally, engaging in sustainable extraction practices and considering alternative materials can help reduce the dependency on clay mining and its associated impacts on water resources.

1.4.4 GEOLOGY

The study area predominantly characterised by sedimentary rocks with some intrusive and metamorphic rock. Major rocks are sandstone and clay with lignite intercalation which covers an area of 3.7km, Khondalite group of rocks which covers an area of 3.6km, and Laterite with an area of 1.34km. In crystalline terrain, the typical laterite profile is composed of lateritic soil at the top, soft laterite, lithomargic clay, and weathered crystalline rocks. The Tertiary-derived laterites are light, homogenous, soft, and they are found below the alluvium. In the khondalitic terrain, the laterite capping's thickness ranges from 15 to 20 metres. Warkali, Quilon, Vaikom, and Alappy beds are the four separate beds that make up Tertiary sedimentary formations (Mini Chandran et al.,2014) Regional geology of the study area in shown in the table.

Era	Age	Formation	Lithology
Quaternary	Recent	Alluvium	Sands and clay along the coast, flood plain deposits, river alluvium and valley fill deposits.
	Sub-recent	Laterites	Laterites and lateritic clays derived from Tertiary sediments and crystalline rocks.
Tertiary	Lower Miocene	Warkalli beds	Sandstone and clay with thin bands of lignite
…….unconformity……..			
-	Undated	Intrusive	Dolerite, gabbro, pegmatites and quartz veins
Precambrian	Archean	Migmatite Group	Granite gneisses, Charnockites, Biotite gneisses and Garnet Sillimanite gneiss, Graphite gneiss.

Regional settings of study area

1.4.5 ACCESSIBILITY

The study area is located along a national highway about 24 km north of Kerala's capital city, Thiruvananthapuram district. connected by a good road system. These roads lead to several destinations in the study areas. The National Highways (NH-47 and Bypass) are the primary thoroughfares that traverse the study area. National rail networks are in close proximity.

1.4.6 TOPOGRAPHY

The study area falls mainly in the midland and lowland areas of Thiruvananthapuram district of Kerala. The coastal plain forms a narrow strip of land in the western portion of the study area and the general width is less than half a kilometer. The coastal plain extends from Kadinamkulam in the South to Varkala in the North in Thiruvananthapuram district. The midland fringes along the lowlands are characterized by a synclinal basin with Cenozoic deposits. This occurs along Mangalapuram, Thonnakkal and Sasthavattom areas of Thiruvananthapuram district.

1.4.7 PHYSIOGRAPHY AND VEGETATION

The terrain is typically 40 metres above mean sea level. The landscape is made up of broading valleys and gently sloping hills. The stream that emerges from the region runs northwesterly and merges with the Sarkara river. The southern slopes of the area where the Kadinamkulam lake connects are drained by tiny streams. The three main crops are paddy, rubber, and coconut. Mangalapuram town is where most people live and conduct business. The

area's geomorphology shows a rolling landscape. The maximum elevation is 75 m and the minimum is 10 m above mean sea level. Small streams from the region enter the Mamam river in a north-easterly direction. Small streams join the Kadinamkulam kayal on the southern slope.

1.4.8 DRAINAGE

The Vamanapuram river and some of its tributaries serve as the study area's primary drainage system. Backwaters in the study locations include Kadinamkulam Kayal and Mungottu Kayal. The Chemunjimotta hills of Kerala's Western Ghats are the source of the Vamanapuram River. The river is also known by the name Attingal River. One of the principal rivers in Thiruvananthapuram District, the Vamanapurum flows roughly 80 km westward and has a drainage area of 687sq.km. These river's tributaries include the upper Chittur and Manjaprayar. Through the village of Attingal, the river meanders its way to the Achuthuthengu back waters. Spatial variation is drainage is shown in Fig. 10

1.4.9 CLIMATE

A tropical monsoon climate characterises the area, and the rainy season runs from May to November. Thiruvananthapuram, the closest meteorological station, records an average annual rainfall of 1838.7mm, of which 540mm (or 29.4%) and 864mm (or 47%) come from the NE monsoon, respectively. There is usually a dry season between the two monsoons, lasting from August to October. Even though it makes up just 29.4% of the total contribution, the NE is crucial for preserving the groundwater regime because any disturbance to this monsoon leads to drought conditions in the area. An early conclusion to the SW monsoon and a late start to the NE monsoon both contribute to near-drought conditions. During the SW monsoon phase, the temperature of Thiruvananthapuram ranges from 26° to 13°C; the mean air temperature is roughly 27.6°C. The district receives regular rainfall of 2001.6mm per year, or 1947mm on average.

1.4.10 LAND USE

The study area exhibits a mix of land use patterns, including residential, agricultural, commercial, and industrial areas. The various land use patterns in the study area are paddy fields, coconut groves, mixed crops, rubber plantations, arable fallow land, roads, ditches, canals, etc. Mixed crops are those that are planted in a field with other crops like coconut, gourd, banana, vegetables, and tubers. The primary crop is coconut because panchayat's geography is ideal for this type of agriculture. Mixed farming comes in second. In a single field, multiple crops such coconuts, gourds, bananas, vegetables, and fruit trees are grown in a practise known as mixed farming.Local farmers engage in traditional agricultural practises and may also adopt modern techniques to enhance productivity. The area has a growing commercial sector, with several local markets and shops. Its evolving urbanisation has resulted in the

growth of residential areas and commercial establishments, while agricultural activities and open spaces continue to shape its character.

The land that was mostly used for agricultural is being invaded by the clay mining industry, which is rife in the area. In these places, there have been observable changes in the land use pattern, including the cessation of paddy farming and modifications to the cropping pattern.(Mini Chandran et al.,2014.)

1.4.11 NATURE OF EXPOSURE

The clay mines are mostly exposed in the midland fringes along the lowlands and the prevalent tropical climate was conducive for their formation and deposition in a synclinal basin as evident from the exploration data of CGWB and Mining & Geology Department. The Promising Clay Deposits occur along this synclinal basin along Mangalapuram, Andoorkonam and Azhoor Panchayaths of Thiruvananthapuram district.

1.5 PREVIOUS STUDY

In the district, thorough hydrogeological investigations and exploration were conducted between 1983 and 1988 as part of the Central Ground Water Board's Coastal Kerala Groundwater Project, which received funding from SIDA. In the years 1997–1998 and 2004–2005, CGWB conducted a number of hydrogeological assessments and short-term Water Supply Investigations in the Thiruvananthapuram district. Periodically, the Mining & Geology Department conducted exploration to evaluate the potential of Clay Beds. In 1983, research was conducted on the clay and laterite profiles of South Kerala by the Centre for Earth Science Studies. Other studies include Impact of clay mining on the ground water regime in parts of Thiruvananthapuram district, Kerala by Mini Chandran et al; Characterization, Classification and Evaluation of Groundwater in are around the Open Cast Mining of Clay Deposits of Thonnakal, South India by Joji.V.S (2017) and Origin and depositional environment of the china clay deposits in South Kerala by K. Soman and Terry Machado(1986). Students of the Geology Department, University of Kerala have carried out many studies as part of the dissertation works in the area.

1.6 PRESENT WORK

The Groundwater Estimation Committee (GEC) was established by Government of India to assess and estimate the quantity and availability of groundwater resource potential in India. In the Thiruvananthapuram district, there are 11 blocks in total, five of which are considered semi-critical. According to the GEC 2022 report, the study area is located in the Pothencode block, a semi critical block.

The primary objective of present work is to document the hydrogeology of the area and to analyse the impact of clay mining in the groundwater regime of the area.

1.6.1 METHODOLOGY

The methodology of the study includes:

- Detailed hydrogeological survey to assess the quality of groundwater resources.
- Groundwater level monitoring.
- Groundwater sample collection from the phreatic zone (dug wells).
- Physical and chemical analysis of groundwater samples.

CHAPTER 2

GEOLOGY AND GEOMORPHOLOGY OF KERALA

2.1 INTRODUCTION

Kerala State lies as a narrow strip of land in the southwest of India, surrounded on the east by the Western Ghats and on the west by the Lakshadweep Sea. Mahe, a Pondicherry coastal outpost, is surrounded by Kerala, which shares borders with Karnataka and Tamilnadu in the southeast and southwest, respectively. The state is located between the North latitudes of 81730 and 12 47 40 and the East longitudes of 74 51 57 and 77 1310. The state comprises an area of 38864sq.km, with a maximum width of 120 km from east to west and a length of 75 km from north to south.

Even the earliest geology professionals were intrigued by Kerala's geology. After researching the quarries close to Angadipuram in the former Malabar, Buchanan coined the term "laterite" in 1800. In the nineteenth century, Bruce Foote (1883) and William King (1875, 1878, 1882) of the Geological Survey of India traversed the State and documented their findings on the geology and mineral resources. Previously thought to have formed during the Archean, the peninsular shield (South Indian Shield) is now viewed as a mosaic of different crustal blocks with diverse geologic and geochronologic characteristics that range in age from Archean to Proterozoic. However, the rocks from the craton and the nearby mobile belt dominate the geology of the South Indian shield. Kerala, forming a part of the South Indian granulite mobile belt mainly exposes charnockites and gneisses which occasionally contain included remnants of metamorphosed alder rocks, ancient supracrustals, especially towards the northern Kerala.

2.2 PHYSIOGRAPHY OF KERALA

Physiographically, Kerala can be divided into four large sections running longitudinally from East to West. (Fig.3). Those are the steep foothills of the Western Ghats range in elevation from 200 to 600 m, with the steeply rising Western Ghat hill ranges reaching heights of up to 2500 m. The low-lying coastal strip bordering the Lakshadweep Sea with its distinctive lagoons and estuaries and the midland defined by laterite cappings with an altitude ranging from 30 to 200m.

Kerala has a coastline that is around 580km long. Kerala features 27 estuaries and 7 lagoons in total, with the Vembanad lake being the largest at 205sq.km. There are 44 rivers in Kerala, 41 of which flow into the Arabian Sea. They originate in the Western Ghats and move westward to the Arabian Sea or the backwaters. The rivers are mostly perennial in nature and are mostly fed by the monsoon season. Rivers run turbulently during the monsoon season, and the largest rivers frequently rise 3 to 4 m over their danger level, producing widespread flooding in the midland and coastal communities. About 2,50,000 million cubic feet, or 5% of India's total water potential is lost through the run-off of the rivers of Kerala. Of the overall area, 35.955 sq. km are made up of hard rock crystalline, and the remaining area is made up of

soft sediments. Most of the sediments are found along the coast. The state is known to contain the minerals bauxite, clay, rare earth elements, glass sand, iron ore, limestone, gold, graphite, and chrysoberyl.

i. Mountains and Peaks

The majority of mountain range crests and the interstate border are formed by the peaks and mountains of the Western Ghats, which climb over 1800 metres. They are sparse in number and only cover 0.64 percent of the state's total land. (GSI, Kerala's Geology and Mineral Resources, 2014).

ii. The highlands (Western Ghats)

The Western Ghats, which are represented by the severely scarped hills and ridges, make up the highland. Precipitous hills, deep valleys, and gorges that are covered in dense forest make up the eastern boundary. The majority of rivers in the state have their beginnings in this area. The Palghat Gap, with a displacement of 50 km along the crest line, is the main rift in this area. The Western Ghats rise from very low elevations of just a few hundred metres up to around 2000 metres. The "Anamudi" mountain (2695m), located in the High Range of the Kottayam District, is the highest point in the West Ghats. Within this region are the Plateaus of Wayanad and Munnar. The highlands make up approximately 20.35% of the state's total area. It extends from the far north, running parallel to the shore, to Kozhikode's east.

iii. The midlands

The midland, which spans Central Kerala between the lowlands and the mountain slopes to the west of the mountains and foothill slopes, is made up of undulating hills and valleys. In the northern section of the State, the midland region is made up of plateaus scraped by laterite. Nearly 8.44% of the State's total area is made up by the midland. While the midlands make up the majority of Kannur District's eastern regions, their area decreases towards the west of the Wayanad plateau, along with steep slopes. Midland, in the Central Region, is a heavily farmed area where the hills are not very steep and the valleys are large.

iv. The Lowland

Beaches, sand dunes, ridges, riverine deposits, backwaters, and the Arabian Sea's coastline make up the Lowland or coastal region. The region is within the 10-300 m altitudinal range, with a maximum area of 54.17%. The main sources of income for the

local population in this region are fishing and coir. The narrow coastal plain's northern portion is more appropriately referred to as the Konkan Coast or simply Konkan, while the southern portion is known as Malabar or Malabar coast.

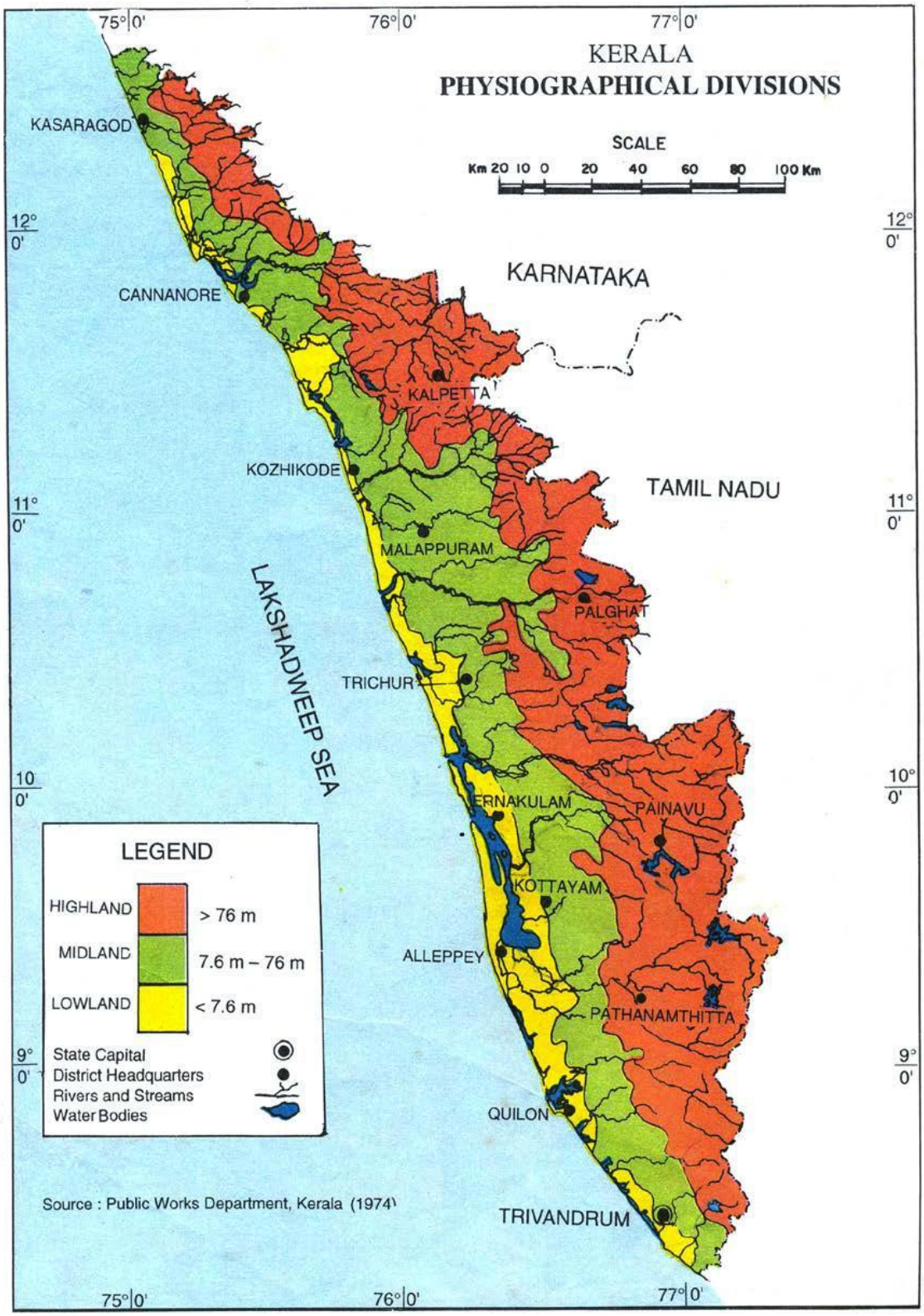

Fig :3 Physiographic divisions of Kerala

2.3 GEOLOGY OF KERALA

The Precambrian South Indian Granulite Terrain includes the state of Kerala as a significant component. Pre-Cambrian crystalline makes up the majority of the state's three primary geological units- Pre Cambrian crystalline, Quaternary deposits and Neogene sediments. High-grade crystalline rocks from the pre-Cambrian period make up the majority of Kerala state. A section of the Neogene sediment and pre-Cambrian crystalline sediment are lateralized at the top. The last geological formation, quaternary sediments is the least studied of the three, despite the fact that it contains valuable resources including heavy mineral placers, lime shell, building-grade sand, drinking water, etc. The primary components of the Archean continental crust preserved in Kerala state are Dharwarian equivalents.

Most of the state's exhumed continental crust designated the region that is best suited for research on granulite petrogenesis. Khondalite-Charnockite assemblages are a collection of migmatised metasedimentary and meta igneous rocks that are exposed in the southern section of the state, south of the Achankovil shear zone. The rocks are mostly charnockites, charnockitic gneisses, and a variety of other gneisses from north of the Achankovil shear zone up to the southern flank of the Palghat gap. Occasional assemblages of metasediments can be found in the Idukki-Munnar region, which represents the western continuation of the Madurai block in Tamil Nadu. Charnockitic patches and hornblende-biotite gneisses predominate in the southern portion of the Palghat Gap. Migmatitic gneisses (hornblende-biotite gneisses) and sporadic areas of amphibolites, calc-granalites, and granite are seen in the middle and northern portions of the Gap.

A metasedimentary succession of khondalites and calc-granulite with crystalline limestone bands makes up the northern flank of the Gap. The northernmost region of the state is made up of granulites, schists, and gneisses that have acid and alkaline plutons intruding upon them. Precambrian rocks make up the majority of the rocks in Kerala, particularly the granulites and related gneisses. These rocks are intruded by sparodic late precambrian early Paleozoic granites, together with related pegmatites and Meso-Cenozoic dykes. Only the Neogene period contains the onland sedimentary deposit. Only the Neogene period contains the onland sedimentary deposit. This shows that the geologic column of the area is far from complete, with only a little representation of rocks from the Paleozoic, Mesozoic, and early Cenozoic eras on the geologic time scale.

The lithology of Kerala can be divided into 3:

1. Precambrian
2. Tertiary
3. Quaternary

Geological map of Kerala is shown in figure 4.

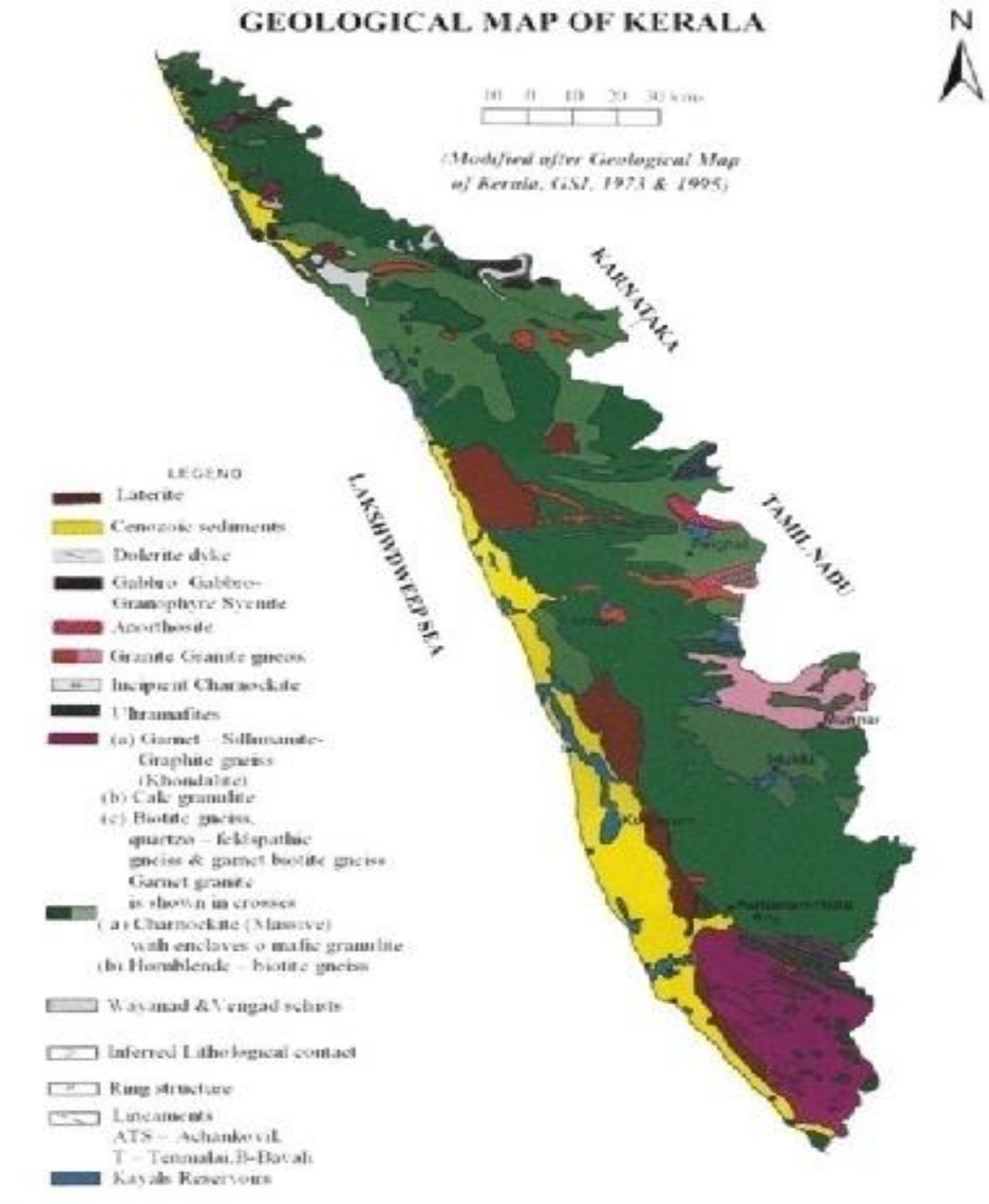

Fig 4: Geological map of Kerala

(Source : https://www.researchgate.net/figure/Geological-map-of-Kerala-After-GSI-1973-1995_fig19_295548580

2.3.1 PRECAMBRIAN ROCKS

Kerala, which encompasses the Western Ghats, the Midlands, and a portion of the coastal belt, is primarily made up of precambrian rocks. Some lengths expose Early Proterozoic rocks, mostly in Southern and Central Kerala. Small intrusive igneous masses of late Proterozoic rocks are visible in a number of locations (GS1,2014). The various rock types that make up Kerala's Precambrian crystalline rocks include ancient supracrustals, charnockite-gneiss associations, associations, khondalite, intrusive rocks, granitoids, and related rocks

2.3.1.1 ANCIENT SUPRA CRUSTALS

The Charnockites or Charnockitic gneisses, the oldest dated rock in Kerala, feature a number of enclaves of schistose rocks. These are the southward extensions of the schistose sequence in Karnataka, and they appear as linear en-echelon bands and enclaves extending from Sultan Bathery, close to the Karnataka border, through Manantoddy in the Wayanad plateau to Taliparambu and Payyannur, and to the eastern parts of Kasargod district. The schistose rock's lithology enables their identification with the Sargur complex of Karnataka, which is thought to be the region's oldest rock assemblage and is made up of a collection of sediments and related intrusives. These rocks can also be attributed as being the oldest rock assemblage in Kerala due to field relationships and age comparisons with the schists of Karnataka.

2.3.1.2 CHARNOCKITE-GNEISS ASSOCIATION

In Kerala, charnockites and related gneisses are the most common kinds of rocks. The Western Ghats and the state's midland regions, particularly in central and north Kerala, are largely made up of these pyroxene-bearing granulites and gneisses. In the Kerala Khondalite Belt, substantial bands of charnockites have also been noted. These are the oldest rocks that have been dated thus far in Kerala, according to the geochronologic information that is currently available on a charnockite (massive) sample from Nedumannur in southern Kerala. In several places, charnockites also contain enclaves of mafic granulites. The two most significant characteristics of charnockites are their granular texture and the constant inclusion of rhombic pyroxene in their constituents. The huge charnockites' ages range between 2155 and 2930 ± 50Ma, according to the available age information, indicating that they are older (Soman, 1997). The textural, mineralogical, and geochemical features of charnockites from diverse places vary.

2.3.1.3 KHONDALITE

Khondalite is a gneiss made up of garnet and sillimanite with various proportions of graphite, quartz, and orthoclase Its occurrences are widespread all over the state. The largest

patch, which is connected to garnet-biotite gneiss and garnetiferous quartzo-feldspathic gneiss, is found in South Kerala. Between charnockite massifs, this appears as a linear belt. Another linear belt is seen along the Palghat Gap's northern flank, where it is associated with calc-granulite and crystalline limestone. Essentially, this is a metasedimentary series from the amphibolite-granulite facies of higher metamorphism. Distinct depositional and provenance circumstances may be indicated by the sequence's lithological variation in different segments. The available data indicates that the rocks in this group range in age from 2830 to 2100 Ma, while Crawford claimed an older whole-rock Rb-Sr age of 3070 Ma (1969). The former also supports the field relation and shows that the Khondalite is younger in age (Soman 1997).

2.3.1.4 INTRUSIVE ROCKS

In the Kerala region, examples of the intrusive phase include a range of younger granites (late Precambrian to early Palaeozoic age) with associated pegmatites, later dolerite dykes, and Cretaceous Palaeocene Deccan Basalt Magmatism. These basic and ultrabasic masses and dykes originate from the Lower-Middle Proterozoic. The Pan-African tectono-magmatic event is when the majority of these intrusive rocks, which are younger granites and related pegmatites, were formed. These are the pink granite, syenite, and gabbro granophyre of the charnockite terrain, whereas the white garnet granites of the Khondalite terrain (as in South Kerala) predominate. The pegmatite phase, which is closely linked to the younger granite phase, is particularly apparent in the Khondalite terrain of South Kerala, where it includes gem-quality chrysoberyl mineralization.

Dolerite dykes, which may be found in both charnockites and gneisses and range in age from 141 to 61 Ma, make up the main phase. These dykes developed at the same time as the Deccan Basalt Magmatism. However, the largest dyke swarm in Kerala occurred over a 100 x 25 km area in the state's centre and was NW-SE directed. The west coast faulting is dated to the deployment of the dyke. The phase correlation of quartz veins in the Wayanad region is either syn-or post-pegmatite emplacement.

2.3.2 THE TERTIARIES

The Tertiary sedimentary strata of Kerala are located unconformably above the Precambrian crystallines in a north-south linear basin along the state's coastal regions. These sedimentary strata are exposed in the southern and northern parts of Kerala's coastal region.

Paulose and Narayanawamy (1968) identified two deposition basins in Kerala based on the distribution:

1) Between Trivandrum and Ponnani is the south and central Kerala with a maximum width of 16 km between Quilon and Kundara.
2) Between Cannanore and Kasargod in the north with a maximum width of 10km at Cheruvathoor.

In the coastal region of Kerala, King (1882) and Foote referred to the Tertiary sequence's marine carbonate and continental clastic facies as the Quilon and Warkalli Beds, respectively (1883). For further study, the Central Ground Water Board split the Upper Tertiary strata into three distinct formations. Underneath the youngest of these, the Warkalli Formation, with a thickness of around 80 m, is the limestone of the Quilon Formation, which has a maximum thickness of 70 m. The Vaikkom Formation, regarded as the oldest sedimentary formation, supports these (Raghava Rao, 1976). The Warkalli Formation extends in a short strip between the coastal and midland regions, from Thiruvananthapuram to Kasargod, with crystalline rock promontories in between. The main areas for the Quilon formation are the Kollam and Alappuzha districts in the state's southern region. The greatest inferred thickness of the Tertiary Sedimentary Sequence is 30 metres, which is greater than 600 metres (Bose and Kartha, 1977).

King (1882) separated the Tertiary rocks in the Quilon-Varkala area into beds made up of sandstone, clays, and lignite in the Warkalli beds and beds made up of limestone and calcareous clays in the Quilon beds. After examining the Karruchal laterite-capped sandstone, Foote (1883) concluded that it was comparable to King's proposed Warkalli layers. The sedimentary terrain was later the subject of studies by Jacob and Sastri (1952), Narayanan (1958), and Desikachar and Subramanyam (1959). A general stratigraphic sequence of these sedimentary strata has been proposed by Paulose and Narayanaswami (1968), as shown in the table. However, investigations into the lithology of these sediments by Central Ground Water Board staff members, backed by exploratory borehole data, show that the Upper Tertiary sediments in Kerala are made up of three separate formations. Rocks from the Quilon Formation, which have a maximum thickness of 70 m, lie beneath the Warkalli, which has a thickness of almost 80 m.

2.3.2.1 VAIKKOM FORMATION

Thin strata of lignite, together with very coarse to coarse gravel, grey clay, and carbonacious clay, are present in the Vaikkom formation. The lowest unit of the sequence is known as the Vaikkom formation because it may be seen in the laterite quarry nearby. they encircle the crystalline rocks that have worn, and they can be as thick as 100 metres.

2.3.2.2 QUILON FORMATION

The Quilon Formation is a marine sequence with interbedded continental elements. Its main component is calcareous facing material, which is composed primarily of an intermixture of fossiliferous limestone, fossiliferous marl, clay, and sand (Paulose and Nair, 1965). It is considered that Padappakara is the formation's type region. The full succession of the Quilon formation is exposed along a cliff section that borders the Astamudi estuary (Menon 1967). A thin bed of non-calcareous sandy clay lies directly beneath the limestone, and that clay itself immediately follow by a thin deposit of carbonaceous clay. This carbonaceous clay is flexible, vaguely laminated, worn and friable. it is also brownish. laminated shale rich in

carbonaceous material is found beneath the carbonaceous clay. (GSI, 2014, Geology and Mineral Resource).

Stratigraphy of Quilon Formation

Unit	Thickness (m)
Detrital Laterite	2.00
Laterite	11.00
Limestone	0.60
Sandy Clay I	0.15
Carbonaceous Clay	0.50
Carbonaceous Shale	0.50
Sandy Clay II	1.00

2.3.2.3 WARKALLI FORMATION

This is the youngest of the Tertiary Formations conformably overlying the Quilon Formation and it occurs as patches along the coast. This formation is exposed in the cliff section of Varkala, fringing the coast, extending from Edava in the north to Taingapatanam in the south (GSI, 2014). it attains a maximum exposed thickness of 60m along the sea cliff. other Warkalli formation exposures can be found in the southern regions Vettur, Kundara, Thamarakulam and Puliyur, as well as the northern regions of Cheruvathur, Pazhayangadi, Ramapuram, Nileswaram, Kanhangad. its arial extend is 200sq Km. unconsolidated sands of coloured clays, white clastic clays and carbanecous makeup the sedimentary deposits, which also contains lignite seems and lenses that are not permanent. these have marcasite nodules embedded in them.Despite the fact that there is no obvious unconformity between the Quilon formation and the surrounding Warkalli formation, it is very important since it separates the two.

Lithology	Thickness (m)
Laterite with sandstone masses, sand, and sandy clay	18
Lithomarge	23
Alum clay	14
Lignite bed	5

Stratigraphy of Warkalli formation

2.3.3 QUATERNARY FORMATIONS

The aerial distribution of quaternary sediments is around 3000 sq.km, with unconsolidated layers resting unconformably over the earlier rocks. Shell deposits, lagoonal clays, and sands. Unconformably above Neogene strata are Teri sands and other Quaternary deposits. The Thrissur and Alappuzha districts each have sedimentary strata that are 30 and 80 metres thick, respectively.

2.3.3.1 RECENT TO SUB RECENT SEDIMENTS

In the low-lying region between Quilon, Kayamkulam, Kottayam, Ernakulam, Ponnani, Cannore, and Nileswaram, sub-recent formation made up of thick layers of sand with shell pieces, sticky black clay, and peat beds can be found. The placer minerals are widely scattered in the coastal sands of southern Kerala, particularly in Chavara and nearby locations near Quilon. Garnet, illmenite, leucoxenite, rutile, monazite, and sillimanite are a few of the important minerals that can be found in them. Polymict pebbles, which are typical of Kerala, differentiate this deposit from Tertiary rocks. The term "Teri sands" refers to rising beaches along coastal sections that are composed of fine-grained, Aeolian-origin reddish sandy loam.

2.3.3.2 LATERITE

Kerala is a specific location where laterite is formed. About 60% of the state's surface is covered in laterite or items made from it. Laterite relics, particularly hard crusts, are found at higher altitudes and may be an indication that the landmass has been uplifted. It occurs as a sub aerial byproduct of chemical weathering on Precambrian crystalline and tertiary sediments all throughout Kerala. The word "laterite" was first used in 1807 by Francis Hamilton Buchanan. In the final step of land surface reduction, laterite typically forms and protects the former surface with a cap rock. Both detrital and residual forms of it can be discovered, and it has evolved on all different kinds of rocks, including more recent sediments. Along the edges of both lateritic and non-lateritic hillocks, detrital laterite is transported, deposited, and reconsolidated in river valleys. The appearance of detrital laterite as the cap of the lone hillocks is a sign of topographic inversion. In humid environments, laterites are produced by the gradual, continuous action of water and humic acids. They are identified by goethite, haematite, aluminium hydroxides, kaolinites, and quartz and typically contain REE and silica. But it differs from clays because it contains less silica than aluminium. They are excellent groundwater aquifers and quite permeable.

The laterite mineral is a significant economic mineral, according to recent studies. Recently, along with bauxite, iron, nickel, and other minerals, gold has been found nearby laterites. Potential gold ores have been found in the Nilambur laterites in north Kerala.

	Pebble bed	
Quaternary	Periyar Formation	Fluvial sand
	Viyyam Formation	Fluvio-marine sand
	Kadappuram Formation	Marine sand
	Guruvayoor Formation	Paleo-marine sand
Mio-Pliocene	Laterite	
	Warkalli Formation	Sandstone and clay with lignite intercalations
	Quilon Formation	Fossiliferous limestone and calcareous marl.
Mesozoic (61 – 144 Ma)	Mafic intrusives	Dolerite, gabbro
PROTEROZOIC	Felsic and alkaline Intrusive(550-90 Ma)	Quartz veins and pegmatite Alkali granite, granite, syenite plutons
	Charnockite (younger) (550 Ma)	Incipient charnockite, cordierite charnockite
	Basic and Ultrabasic Intrusives (700 – 600 Ma)	Gabbro, diorite and anorthosite
	Mafic dykes (2100 – 1600 Ma)	Dolerite
	Vengad Formation	Quartz-mica schist, conglomerate
	Migmatitic Complex (2500-2200 Ma)	Biotite gneiss, hornblende-biotite- gneiss, and associated migmatites.
NEO ARCHEAN	Khondalite Group	Garnet-biotite gneiss, garnet-biotite-sillimanite-cordierite gneiss, calc granulite, quartzite, leptynite
		Older quartz veins
	Charnockite(~2500 Ma)	Charnockite and banded charnockite
	Peninsular Gneissic Complex(≥2500 Ma)	Hornblende-biotite gneiss, granite gneiss
	Layered ultramafic-mafic rocks(2500Ma)	Anorthosite Peridotite, dunite, pyroxenite
ARCHEAN	Wayanad Supracrustal Complex (>2500 Ma)	Quartz-mica schist ± kyanite, kyanite/sillimanite schist, felsic volcanics, banded magnetite quartzite/magnetite quartzite, talc-tremolite schist,metapyroxenite, amphibolite, mafic granulite, pyroxene granulite

Stratigraphy of Kerala

Source: Geology and Mineral Resources of Kerala, GSI.2014

2.4 GEOMORPHOLOGY OF KERALA

Kerala is located between the western ghats to the east and the Arabian Sea to the west and covers 38,863 km2 (1.18 percent of India's landmass). Kerala's coastline is 580 km long and ranges in width from 35 to 120 km. Kerala is geographically divided into three main climate-wise regions. These include the western lowlands, the central midlands (rolling hills), and the eastern highlands (rough and cool mountainous terrain) (coastal plains). The majority of the state, with the exception of isolated places, is subject to relatively little seismic or volcanic activity because of its location in the very southernmost point of the Indian subcontinent and close to the centre of the Indian tectonic plate (the Indian Plate). The majority of Kerala's terrain is made up of Precambrian and Pleistocene foundations geologically. Kerala, a location in the tropical monsoon belt, has alternately dry and rainy climates; as a result, weathering and denudation dominate the geomorphic processes. Although Precambrian crystalline rocks make up the majority of the state.

2.5 BACKWATERS AND LAGOONS

The backwaters of Kerala are particularly well-known due to their unusual occurrence. A system of interconnected brackish canals, lakes, estuaries, and rivers meant for the coastal plains provides a reticulate drainage pattern. The shallow lagoons, colloquially referred to as "kayals", serve as water conduits for the discharges of modern rivers. They extend a considerable distance along the seashore. There are 34 kayals, the largest of which, Vembanad, spans more than 200 kilometres between Alappuzha and Kochi. Due to the fact that it is perpendicular to the coast and is another large lake, Ashtamudi is regarded as an estuary. Major freshwater lakes are Sasthamkotta Kayal and Vellayani Kayal (Thiruvananthapuram district). The prevalence of different sized and shaped coast parallel lagoons suggests various evolutionary processes during the Late Quaternary.

2.6 SOIL

In the Thiruvananthapuram district, red loams, coastal alluvium, riverine alluvium, laterite soil, brown hydromorphic soil, and forest loam are the main types of soil. The midland of the area is where lateritic soil, which is primarily reddish brown to yellow red in colour, is found. Brown hydromorphic soils, which include characteristics like a grey horizon, mottling streaks, hard organic matter deposition, iron and manganese concretions, etc., are primarily restricted to low-lying coastal strip areas and valley bottoms in the middle of the country. Red loamy soils, which are mostly found in the southern portion of the district, are very porous, friable, and poor in organic content. Alluvium, which ranges in texture from sandy loam to clayey loam, predominates throughout the lowland region. River alluvium is found primarily along the banks of rivers and their tributaries, whereas coastal alluvium is mostly found near the coastline. Fluvial loams, which are byproducts of the weathering of crystalline rocks, are what

give the district's eastern portion its distinctive look. These soils have a loam to silty loam texture and are dark reddish brown to black in colour. Ten different types of soil are found in the district, according to a recent ICAR survey. Despite the district housing the state capital, there has been very little industrial growth there. (GSI, 2016)

2.7 CLIMATE

Kerala, a tropical paradise in India, is located in the country's southwestmost point. The State enjoys a tropical climate all year. In April and May, it's hot and humid, while in December and January, it's cool. Kerala is known for its abundant rainfall. In the summer, the maximum temperature is 33°C, and in the monsoon, it is 18°C.

2.8 RAINFALL

Kerala experiences two monsoon seasons, the southwest season, which runs from June to September, and the northeast season, which runs from October to May. These are referred to in the local community as "Edavappathi" and "Thulavarsham," respectively. While the southwest monsoon is responsible for 85.3 percent of the annual total rainfall, the northeast monsoon only contributes 8.9 percent. Maximum rainfall in the Western Ghat areas of the Wayanad district is about 3588 mm. The State averages 360 cm of rainfall in its northernmost sections, and 180 cm in its southernmost regions (Soman, 1997). Kerala experiences annual rainfall ranging from 1250 to 5000 mm.

2.9 DRAINAGE

The Western Ghats are the source of 44 rivers that enter Kerala. All other rivers run west and empty into the Lakshadweep sea, with the exception of those that flow east: Kabani, Bhavani, and Pambar. The Kaveri river is formed when the east-flowing rivers of Tamil Nadu and Karnataka come together. Most rivers are small, fast flowing, with variable degrees of gradation, cascades, and waterfalls at the higher parts, maturing downhill. Drainage map of Kerala is shown in Figure.5

The five main rivers in the state drain almost 40% of the state's total land. Pamba, Chaliyar, Periyar, Bharathapuzha, and Chalakkudi Periyar is the longest river in Kerala, measuring 344 kilometres in length and draining 5395 square kilometres. The Bharathapuzha River is the second-longest river in Kerala, measuring 209 kilometres in length with a catchment area of over 4400 kilometres. Pamba, the third-longest river, is 176 km long and has a catchment area of 2235 sq km. The Chaliyar River is the fourth longest river in India, with a catchment area of 2923 square kilometres and a length of 169 metres. The 130-kilometer-long drainage area surrounding Chalakkudi is 1704 square kilometres in size. (Geology and Mineral Resources of Kerala)

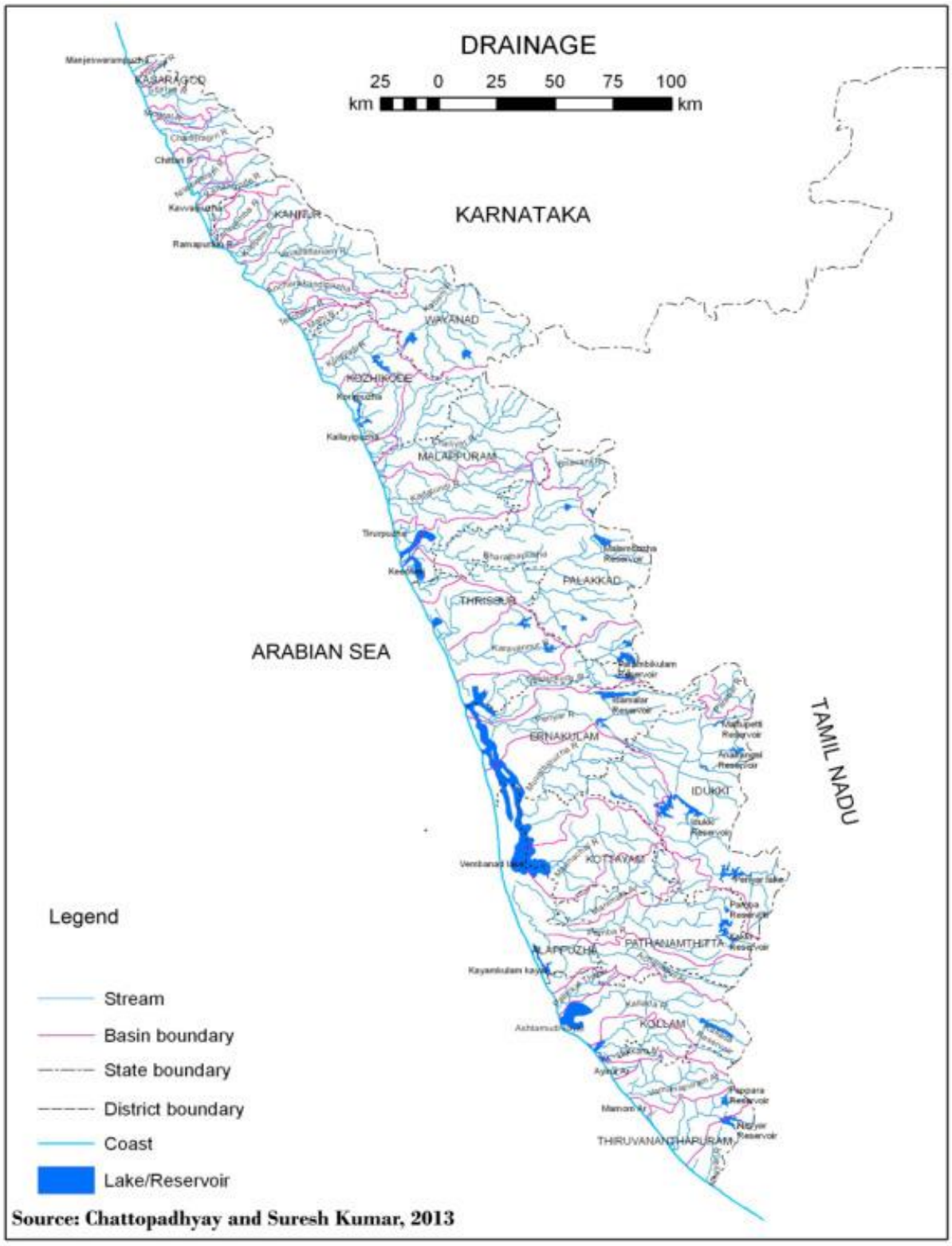

Fig.5: Drainage Map of Kerala

2.10 GEOLOGY AND GEOMORPHOLOGY OF POTHENCODE BLOCK

2.10.1 INTRODUCTION

Trivandrum, the southernmost district of Kerala State, is located between 8° 16' 59" and 8° 49' 59" in the north and 76° 28' 59" and 77° 16' 59" in the east. It has a geographic area of 2192 sq. km. and is included in Survey of India degree sheets 58 D and H. The district is 76 km long and borders the Lakshadweep Sea on its western shore, the Kollam District on its northern border, the Tamil Nadu districts of Tirunelveli and Kanyakumari on its eastern and southern borders, respectively. The Trivandrum district can be roughly divided into 4 taluks, or administrative divisions, which are Trivandrum, Neyyatinkara, Chirayinkil, and Nedumangad. Each taluka has 11 blocks, 84 panchayats, 4 municipalities, and 1 corporation.

Trivandrum taluk consist of 11 blocks, including Parassala, Permkadavila, Athiyannoor, Nemom, Pothencode, Vellanad, Nedumangad, Vamanapuram, Kilimanoor, Chirayinkeezhu and Varkala. The study area lies in **Pothencode block.**

2.10.2 GEOLOGY OF POTHENCODE BLOCK

Pothencode block has a total area of 133.38 sq.km. The main type of rock formation is Alluvium, which covers total geographical area of 74.15 sq.km.China clay is mostly present there. The china clay is associated with crystallines. The main deposit known is at Aakulam which is being mined by English India Clays Ltd. The china clay is white, soft and free from iron and titanium.

The Charnockite group of rocks, which occupy an area of 33.0 Ha and 31.09 Ha, are part of the Pothencode block's lithology. Andoorkonam (326.05 Ha), Azhoor (177.21 Ha), Mangalapuram (738.86 Ha), and Pothencode all contain the Khondalite group of rocks (1979.41 Ha). Laterite is mainly found at Pothencode(281.57Ha) and Mangalapuram (62.78Ha). There are only Migmatites in the Pothencode region (38.34Ha). Sandstone and clay with lignite intercalations are present in Andoorkonam, Azhoor, Kadinamkulam, Mangalapuram and Pothencode regions. (Natural Resources Data Bank, Thiruvananthapuram, 2013)

2.10.3 GEOMORPHOLOGY OF POTHENCODE BLOCK

The highlands, midlands, and lowlands are the three geographical divisions of the Thiruvananthapuram district. Lowland makes for 114 km^2 (5.22%) of the district's overall area. High land covers 574.3km^2 (26.27%) and the midland 1497.7km^2 (68.51%). Pothencode block lies in midland and lowland regions. The midland regions lying between the Western Ghats and

lowlands is made up of small and tiny hills and valleys. This is an area of intense agricultural activities. This region is rich such as paddy, tapioca, rubber, eucalyptus, spices and cashews.

The regions of Andoorkonam, Azhoor, Kadinamkulam, and Mangalapuram contain coastal plains. Lower Laterite Plateaus can be found in the following locations: Andoorkonam (10.62.06 Ha), Azhoor (797.92 Ha), Kadinamkulam (5.89 Ha), Mangalapuram (1792.09 Ha), and Pothencode (2263.04Ha). In Azhoor, Kadinamkulam, Mangalapuram, and Andoorkonam, mudflats can be found. In the Pothencode region, residual mount spans 65.82Ha. 256.72 Ha in Andoorkonam, 102.29 Ha in Azhoor, 1 Ha in Kadinamkulam, 195.94 Ha in Mangalapuram, and 151.27 Ha in Pothencode are covered by valley fills. (Natural Resources Data Bank, Thiruvananthapuram, 2013)

CHAPTER 3

HYDROGEOCHEMISTRY

3.1 INTRODUCTION

As crucial as groundwater quality is its quantity. The purest type of water is rainwater. Water is a great solvent, so as it flows over the surface or below the surface, both becomes contaminated with a variety of dissolved or suspended substances. It receives its annual replenishment from precipitation, unlike any other mineral resource. About 97.2 percent of the world's water supply is found in the oceans, and only 2.8 percent of it is accessible freshwater. 2.2 percent of the world's fresh water supply is available as surface water, and 0.6 percent is found underground. At the moment, groundwater resources provide almost a fifth of all water used. The presence of groundwater relies on the physiography, climate, and geological characteristics of a location.

Due to the demand from numerous industries, there is an intense strain on the groundwater resource, endangering its purity. Groundwater pollution has become a serious issue for society at large due to the significant regional variability of its properties and the strong anthropogenic influence it has in many parts of the world. Due to the demand from numerous industries, there is an intense strain on the groundwater resource, endangering its purity. Groundwater pollution has become a serious issue for society at large due to the significant regional variability of its properties and the strong anthropogenic influence it has in many parts of the world. (Bardossy, 2006)

For sustainable development and efficient management of groundwater resources in each particular terrain, it is crucial to understand the hydrogeochemistry of groundwater and water quality. Any aquifer's groundwater has a distinct chemistry that it acquired as a result of the system's replenishing meteoric water being chemically altered (Back, 1996; Drever, 1982). The cumulative effects of groundwater interaction with rocks, the dissolution of soluble mineral species, ion exchange reactions, and numerous anthropogenic activities are what primarily regulate the groundwater chemistry (Faure, 1998). Water is categorised as either hard or soft depending on the Mg and Ca content. In contrast to hand water, soft water readily forms a lather with soap. Anthropogenic and natural activities together determine the quality of the groundwater. Before using water for domestic, agricultural, or industrial purposes, it is crucial to take into account its chemistry. The minimum allowable quantity for a certain usage determines whether natural water is suitable for that use. Because of this, the quality criterion for drinking water, irrigation water, and industrial water differs. Cations, anions, pH, TDS, and EC are all determined as part of the quality examination of the water sample. Hydrochemical data of groundwater (Pre-monsoon) is shown in Table no.2.

3.2 FACTORS AFFECTING GROUNDWATER QUALITY

Ever since there have been living beings on the planet, water has been a necessity for survival. Understanding the variables that influence groundwater quality can aid in selecting the proper well depth and water quality for a given application. Groundwater quality is influenced by a number of variables, including depth below the surface, the permeability and chemical composition of the sediments through which groundwater passes, as well as climate changes.

- **Depth from the surface**: The best and most plentiful solvent in the planet is water. Most things it comes into contact with are attempted to disintegrate by it. As a result, groundwater becomes more mineralized as it moves through sediments over a longer period of time. As a result, shallow groundwater aquifers have lower total dissolved solids (TDS) levels than deeper aquifers do. Since deeper groundwater aquifers must travel farther to reach their destination, their water is frequently more mineralized. Although shallow wells have lower TDS levels than deeper wells, they do contain higher quantities of calcium, magnesium, and iron. The term "hard" refers to the water's high mineral content. Higher sodium and lower hardness levels in deeper wells result in "softer" water. The explanation for this is that deeper sediments and rock formations have higher sodium concentrations, and when water descends through the sediment and rock formation, an ion exchange process naturally takes place. In the sediment and rock formations, sodium is traded for calcium, magnesium, and iron in groundwater. The end result is groundwater that contains more sodium and has little to no hardness.

- **Permeability of sediments**: Groundwater moves somewhat slowly through materials like clay that have low permeability. This gives minerals more time to dissolve. Sand, on the other hand, and other sediments with high permeability enable groundwater to travel more quickly. Since minerals have less time to dissolve, groundwater often has lower concentrations of dissolved minerals. Dissolved solids differ between groundwater in recharge zones and water in outflow zones, as well. Upland areas known as recharge zones are where precipitation easily seeps into the ground through permeable, sandy sediments. Water in recharge zones often has little mineralization. Discharge zones are low places where groundwater eventually returns to (or is very close to) the ground surface. Mineral concentrations in the groundwater in certain regions, including sodium, sulphate, and chlorides, can be exceedingly high. Saline springs, sloughs, and lakes are a few examples.

- **Chemical composition of sediments**: The chemical composition of minerals is another element influencing groundwater quality. Some chemicals are more likely to dissolve in water because they are more soluble than other substances. For instance, groundwater will mineralize more quickly than it would if other chemicals were present when it comes into touch with sediments that contain high amounts of sodium, sulphate, and chloride.

- **Climatic variations**: Groundwater quality is also significantly influenced by climatic variance, such as yearly rainfall and evaporation rates. Discharging groundwater frequently evaporates when it nears the surface in semi-arid areas. A salt accumulation results from the minerals from the water being deposited in the soil. The salts could be redissolved by precipitation that seeps through the soil and return to the groundwater

- **Seawater Intrusion**: Sea water may transverse the flow toward the sea in coastal areas where the water table has dropped. Saltwater intrusion is the term for seawater migrating inland. Alternately, salt from mineral beds may naturally erode into the groundwater.

- **Groundwater Pollution**: Not all groundwater issues are brought on by excessive exploitation. contaminants that have been released into the earth seep into groundwater. The pollutant is dispersed across a larger region by the movement of water and dispersion inside the aquifer, where it can subsequently come into contact with groundwater wells or make its way back into the surface water, endangering the safety of the water supplies. The local stratigraphy is crucial to the movement of these contaminants in the area. For drinking water supply, agricultural irrigation, trash disposal, and other ecological challenges, water table conditions are crucial.

3.3 FIELD SAMPLING

The entire study area has undergone methodical field work for the collection of samples, for laboratory analysis, and to familiarise the study region with its surrounding environment. To assess the quality of the water for drinking and household use, samples of water were taken from 17 dug wells and three tube wells. Data on well inventories was gathered from 108 locations (Table no.1). Sections of the wells were observed and recorded. The observations included well's diameter, total depth and depth to water table level. Each well's water table depth was calculated using a measuring tape. To get the depth from ground level, the parapet height was subtracted. Random water samples are gathered for analysis. 20 water samples were taken from various sites within the study area.

A 1 L polythene container is used to collect samples for physical and chemical investigation. The can was properly labelled with the sampling number and locations. The bottles are then kept airtight. Each sample has named with numbers. The datasheet contained information about each location's sample number, name, latitude, longitude, elevation, total depth, and depth to the water table below the surface. Using a portable GPS, the geographic location of each well was identified.

3.4 EXPRESSION OF RESULTS

The milligram per litre (mg/l) is the standard unit of measurement for analytical results. Parts per million (ppm) refers to the weight-to-weight ratio. In the context of one litre of water weighing 1 kg, the word "mg/l" is equivalent to parts per million. The weight technique uses parts per million (ppm) to express the relative weights of the solute and the solution. The analytical findings are displayed in tables 1 and 2, and the mean range value of samples of open well water taken in accordance with BIS criteria is displayed in table.3.

3.5 METHODS OF STUDY

The main goal of laboratory water analysis is to produce precise data that reveals the physical and chemical properties of the water samples being examined. All programmes designed to guarantee the consistency of analytical data must include quality assurance. Water samples from Mangalapuram and the surrounding areas were taken in order to evaluate the quality of the groundwater. 20 samples in all have been taken from the study area throughout the months of April 2023.

3.6 GIS ANALYSIS

The field of geographic information systems (GIS), which is still relatively young, has the potential to greatly improve the analytical capabilities in the area of water resources. Unlike conventional mapping, geospatial mapping offers digital information that may be used to make a unique map that is personalised to our requirements. Data are gathered, examined, and presented in relation to a particular location using geographic information systems (GIS), a rapidly developing computer-based technology.

Arc GIS software is used to prepare the geospatial maps of water sample locations, depth to water table, pH, EC, TDS, cations, anions, geology and geomorphology of the study area.

3.7 ANALYTICAL TECHNIQUES USED

Microwave Plasma – Atomic Emission Spectroscopy (MP-AES4210) :

Na, K, Ca, Mg and Fe are major cations present in the surface water system. These cations are analysed by MICOWAVE PLASMA- ATOMIC EMISSION SPECTROSCOPY (MP-AES- 4210). MP-AES is an atomic emission technique. It uses the fact that once an atom of a specific element is excited, it emits light in a characteristic pattern of wavelengths-an emission spectrum, as it returns to the ground state. Source for atomic emission include the microwave plasma (MP) and the inductively coupled argon plasma (ICP) both of which are high temperature sources, and therefore excellent excitation sources for Atomic Emission

Spectroscopy. The nitrogen fuelled microwave plasma reaches temperatures nearing 5,000 K. At these temperatures, atomic emission is strong, producing excellent detection limits and linear dynamic range for most elements. Inside a MP-AES instrument, microwave energy form an industrial magnetron is used to form plasma form nitrogen that has been extracted from compressed air by Agilent's Nitrogen Generator. Effectively, the MP-AES runs on air. Using a magnetic field rather that an electronic one for excitation generates a very robust plasma-capable of handling a wide range of sample types. An optimized microwave waveguide creates concentrated electromagnetic fields at the torch. Then an axial magnetic field and a radial electrical field focus and contain the microwave to create plasma.

MP-AES 4210 Instrument

Continuous Flow Analysers (CFA):

Continuous flow analysers (CFAs) are automated instruments used to analyze chemical species in liquid samples. They operate based on flowing a sample and reagents through interconnected tubing and reactors, with analyte concentrations measured using a detector. CFAs offer several advantages over other analytical instruments, including high sample throughput, high precision and accuracy, continuous monitoring, automatic sample handling, minimal sample preparation, lower cost per sample, flexibility, ease of use, reduced waste generation, and improved safety. CFAs are widely used in various industries, including environmental, food and beverage, pharmaceutical, agricultural, chemical manufacturing, petrochemical, medical, and biotechnology.

Continuous Flow Analyser (CFA)

Eutech pH Tutor:

The pH meter is used to measure the hydrogen ion or the hydroxide ion concentration in water sample. It usually consists of a probe which is dipped inside the sample for obtaining the values. Probe consist of a thin glass bulb (Measuring electrode) and reference electrode both submerged in neutral KCl solution and having a silver alloy wire. The eutech pH tutor was used for determining the pH. values and specifications of the model is given below:

Model Name	:	Cyber Scan pH Tutor pH/°C
pH Range	:	0.00 to 14.00
pH Resolution	:	0.01
Temperature Default	:	25°C
pH Buffer Options	:	US Standard (pH 4.01, 7.00, 10.01)
pH accuracy	:	±0.01 pH
Display	:	Custom Dual line LCD

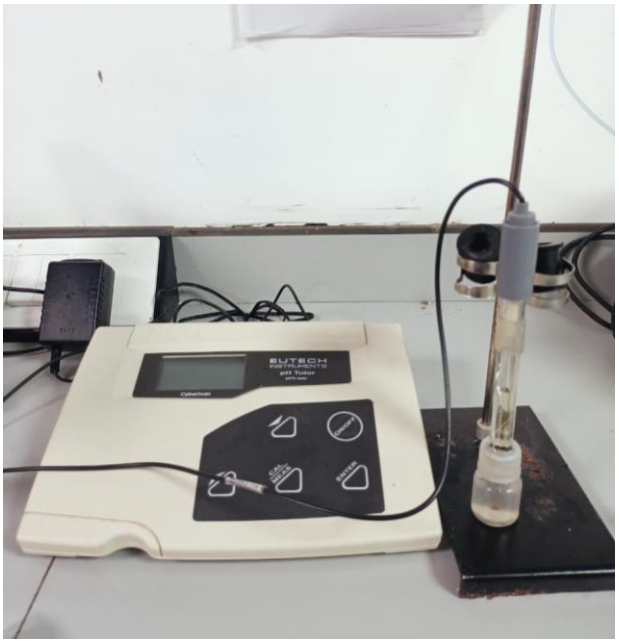

Eutech pH Tutor

Eutech PC 2700 :

This instrument was used for analysing EC and TDS.

Eutech PC 2700

3.8 ANALYSIS OF WATER

3.8.1 HYDROGEN ION CONCENTRATION (pH)

The pH is the hydrogen ion concentration, which expresses the scale of intensity of acidity or alkalinity of water. The pH value of natural water is a measure of its net alkalinity and acidity. The letter p indicates potential and the letter H represents hydrogen. Mathematically pH is the logarithm to the base 10 of the reciprocal of Hydrogen ion concentration. Thus, pH = -log10 H, where H the concentration of Hydrogen ion in moles per litre. The pH values range from 0 to 14. If the pH is below 7 (pH< 7) then the water is acidic and the pH is above 7 (pH>7) then the water is basic in nature.

Anomalous pH values were observed in the study area. The Variation is from a low pH value 3.6 to 6.99 with a mean of 6 indicating an acidic trend. It is prominent to note that the BIS limit is ranging from 6.5 to 8.5. Lowest pH value of 3.6 was obtained from Thonnakal and highest pH value of 6.9 from Vavaraambalam. The total pH variation in the study area is 6.1 from Koithoorkonam, 4.9 from Karamood, 4.3 from Pattathinkara, 6.3 from Manjamala, 5.6 from Kannakankulam, 6.4 from Edayavanam and 5.7 from Kudavoor. Measured pH values of open well water samples indicate that almost all the water samples in the study area lies within the permissible limits of BIS (6.5 to 8.5) and showing an acidic inclination. Strikingly low pH values obtained in the open well samples convey a message that this is not at all suitable for drinking purpose in the existing form. So, it needs some kind of water treatment mechanism to make the water suitable to drink. The spatial variation map of pH is shown in Fig.14.The spatial variation map of pH reveals that the southern region of the study area, which include areas of Karamood, Thonnakal, Pattathinkara and Kudavoor shows low acidic nature

3.8.2 ELECTRICAL CONDUCTIVITY (EC)

Electrical Conductivity of water is owing to the actuality that water is an electrolytic solution. EC is unswervingly proportional to the quantity of dissolved salts. Distilled water does not conduct electric current. The EC denotes the characteristic of a medium to the passage of electricity. In water quality determination, conductivity is defined as the conductance of a cube of one centimeter side of a substance expressed in mohs/cm now used as Siemens (S)/cm. When expressed in mohs/cm, the conductivity of most of the natural water is less than unity. Hence for convenience, the conductivity is expressed in micromobs/cm (µS/cm), which is equal to one million times the value given in mohs/cm. Electrical conductance of water is a function of temperature, type and concentration of various ions. The EC readings are usually adjusted to a temperature 25°C. So that variations in conductance is a function of concentration and type of dissolved constituents present. measured using calibrated (with 0.01m KCI solution) conductivity meter equipped with conductivity cell and resistance measuring device.

The electrical conductivity values of the samples vary from 67.13-755.7 with an average 261.28µS. The lowest value is obtained from Kannakankulam and the highest value of

EC is recorded from Thonnakal. The BIS value of EC 200 to 600 µS. One sample show EC value above the permissible limit with value of 755.7µS is obtained from the open well from Thonnakal. Most of the samples are within the permissible limit. The spatial variation map of the EC is given in Fig.15. The spatial variation map of the electrical conductivity shows that a high value is observed in the northern part of the study area and most of the EC values from the central part of the study area is within the permissible limit. Low EC values are randomly distributed with in the study area which includes area of Karamood, Kalloor, Kabarady Nagar and, Michabhoomi.

3.8.3 TOTAL DISSOLVED SOLIDS (TDS)

TDS refers to all solid materials present in solution either in ionized state or in non ionized state and exclude the suspended colloids or dissolved gases. Quality of drinking water will be affected by the presence of soluble salts. TDS indicate general nature of water quality or salinity. Therefore, the level of TDS is one of the characteristics which decide the quality of drinking water. When TDS in water is more than 500 ppm, deliciousness of water decreases and way cause gastro intestinal irritation (Park and Park, 1980). High TDS indicates that the water is highly mineralized and this water is not suitable either for drinking or for industrial purposes. The concentration of TDS above 2000 ppm produces laxative effects. Bulk of the total dissolved solids includes bicarbonates, sulphates and chloride of calcium, magnesium, sodium and silica. Potassium chloride and nitrate form a minor part of the dissolved solids in groundwater.

The total dissolved solids in the study area range between 44.38-504.8 ppm respectively with an average of 173.55 ppm. The desirable limit BIS value for TDS is 500ppm for drinking water and the maximum permissible limit is up to 2000ppm. The lowest value of TDS is 44.38 ppm, which is obtained from Kannakankulam and highest value of TDS 504.8 ppm was obtained from Thonnakal. Fig.16 shows spatial variation map of TDS. The map shows that the major portion of the study area is characterized by samples having medium TDS value. Highest TDS value is obtained from northern part of the study area.

3.8.4 DETERMINATION OF CATIONS

SODIUM, POTASSIUM, CALCIUM, MAGNESIUM, IRON

Na, K, Ca, Mg and Fe are major cations present in the surface water system. These cations are analysed by MICOWAVE PLASMA- ATOMIC EMISSION SPECTROSCOPY (MP-AES- 4210).

Principle

MP-AES is an atomic emission technique. It uses the fact that once an atom of a specific element is excited, it emits light in a characteristic pattern of wavelengths-an emission spectrum, as it returns to the ground state. Source for atomic emission include the microwave plasma (MP) and the inductively coupled argon plasma (ICP) both of which are high temperature sources, and therefore excellent excitation sources for Atomic Emission Spectroscopy. The nitrogen fuelled microwave plasma reaches temperatures nearing 5,000 K. At these temperatures, atomic emission is strong, producing excellent detection limits and linear dynamic range for most elements. Inside a MP-AES instrument, microwave energy form an industrial magnetron is used to form plasma form nitrogen that has been extracted from compressed air by Agilent's Nitrogen Generator. Effectively, the MP-AES runs on air. Using a magnetic field rather that an electronic one for excitation generates a very robust plasma-capable of handling a wide range of sample types. An optimized microwave waveguide creates concentrated electromagnetic fields at the torch. Then an axial magnetic field and a radial electrical field focus and contain the microwave to create plasma.

Procedure

- Sample Introduction

Just like a flame AA instrument, an aerosol is created from a liquid sample using a nebulizer and a spray chamber. The aerosol is then introduced into the centre of the hot plasma. The aerosol dries, decomposes and is then atomized. The atoms continue to be excited and emit light at wavelengths characteristic for each as they return to lower energy states.

- Optical system

Emission from the plasma is directed into a fast scanning monochromator. The selected wavelength range is imaged onto the high efficiency charged couple device (CCD) detector. This measures both spectra and background simultaneously for optimum precision

- Quantification

Just like flame AAS, MP-AES quantifies the concentration of an element in a sample by comparing its emission to that of known concentrations of the element, plotted on a calibration curve. The final result is the concentration of the element in the sample.

- **SODIUM**

In the study area, sodium concentration of water sample ranges from 17.67ppm to 158.2ppm with a mean of 58 ppm. According to BIS, the maximum permissible limit of sodium is 200ppm. All the samples from the study area are within the permissible limit. The highest value of Sodium is reported from Thonnakal and lowest value of sodium is obtained from Michabhoomi road. Spatial variation map of sodium is shown in Fig. 17

- **POTASSIUM**

The potassium concentration in water sample from the study area ranges from 1.15ppm to 87.62ppm with a mean of 15.04ppm. The maximum permissible limit of potassium in drinking water based on BIS is 40ppm All the samples from the the study area, except one, falls within the permissible limit. Spatial variation map of potassium is shown in Fig.18. The highest value of Potassium is reported from Thonnakal, which is outside the permissible limit and lowest value of sodium is obtained from Karamood.

- **CALCIUM**

In the study area, concentration of calcium in the water sample ranges from 0.88ppm to 18.8ppm with a mean value of 5.82ppm. The highest desirable limit of calcium based on BIS standards is 75ppm. All the samples from the study area are within the desirable limit. From the spatial variation map of calcium, the higher value for calcium fall in the central part of the study area which is Thonakkal. The lowest value is marked from north, south and eastern part of the study area which include places such as Karamood, Pattathinkara and Kabaradi Nagar. Spatial variation map of Calcium is shown in the Fig.19.

- **MAGNESIUM**

In the study area, the concentration of magnesium in the water sample ranges from 1.74ppm to 27.97ppm with a mean value of 7.59ppm. The desirable limit of magnesium in drinking water recommented by BIS is 30 ppm. From the data, all the samples in the study area falls within the highest desirable limit. The spatial variation map (Fig.20) of magnesium shows that the higher concentration of magnesium is seen in the south eastern part of the study area which is Koithoorkonam and lowest value is obtained from Pattathinkara, Kudavoor and Kabaradi Nagar.

- **IRON**

In the study area, the concentration of Iron in the water sample ranges 0.25ppm to 0.67ppm with a mean value of 0.305ppm. The desirable limit of Iron content in drinking water recommented by BIS is 0.3 ppm. From the data, concentration of iron in water sample from Thonnakal(1) and Kannankulam are higher than the desirable limit. The spatial variation map of Iron (Fig.21) is shows that highest concentration of Iron is seen in western part of the study area, which is Kannakankulam and lowest values falls in the majority of the study area in north, south and east directions including Koithoorkonam, Karamood, Koppam, Manjamala and Vavaraambalam.

3.8.5 DETERMINATION OF ANIONS

CHLORIDE(Cl^-)

It is estimated by Argentometric method. Cl_2 in aqueous solution is not stable and chlorine content of the sample decreases rapidly.

Procedure

25 ml of sample was taken in a clear conical flask. Add 3 drops of K_2CrO_4 as indicator and titrate against standard $AgNO_3$ end point is the disappearance of yellow colour to dirty orange colour. $AgNO_3$ is standardized with standard NaCl. Repeat the titration with distilled water as blank.

Calculation

$$\text{Amount of } Cl_2 \text{ as mg/L} = \frac{\text{N of AgNO3} \times (A-B) \times 35450}{\text{Volume of sample}}$$

Where , A = ml titration for sample

B = ml titration for blank

In the study area, Chloride concentration ranges from 1.52ppm to 167.12ppm with a mean value of 46.83ppm. According to BIS. the desirable limit of chloride in water is 250 ppm. It is clear that all the samples are within the highest desirable limit. The highest value of chloride is present in Thonnkal and lowest value at Kannakankulam.

SULPHATE (SO_4^{2-})

Principle

Sulphate ion is one of the major anions occurring in natural waters. Sulphate is precipitated with $BaCl_2$, so as to form Barium Sulphate crystals of uniform size.

$BaCl_{2(excess)} + SO_4^{2-} \rightarrow BaSO_4$

Light absorbance of $BaSO_4$, suspension is measured by spectrophotometer. The wavelength is at 420 nm.

Procedure

The $SO4^{2-}$ concentration is determined by comparison of reading with standard one. 0.02 N H_2SO_4 is taken as standard solution in which three standards are prepared with

corresponds to 1 ml=1 mg, 2 ml =2 mg, and 3 ml=3 mg, which is diluted to 25 ml distilled water in a graduated tube and add small amount of $BaCl_2$. A white precipitate is developed. The absorbance of std-1. std-2, and std-3 are measured. The same procedure is followed for sample and blank.

In the study area, the concentration of Sulphate value ranges from 0.01ppm to 118.07ppm with a mean of 16.98ppm. All the samples are under BIS highest desirable limit of sulphate (200ppm). Sulphate having highest value in the Pattathinkara and lowest value in Karamood.

PHOSPHATE (PO_4^{3-})

Weathering of rocks liberates phosphorous as soluble alkali phosphates and colloidal calcium phosphates are carried by many sources which reach the water. In addition to this, anthropogenic inputs of fertilizers (superphosphate) and detergents (alkyl phosphates) which increase amount of phosphorous in water.

Principle

The automated procedure for the determination of total UV digestible phosphate is based on the following reaction; the sample is mixed with a potassium peroxodisulfate. The organic phosphates are destructed by means of UV radiation. Sulphuric acid is added to the sample stream and the solution is heated to 110°C. Complex inorganic phosphates are digested to orthodox-phosphate. Sodium hydroxide is added to neutralize the solution. Hereafter the solution is dialysed against distilled water. Ammonium heptamolybdate catalysed by potassium antimony (III) oxide tartrate reacts in an acidic medium with diluted solutions of phosphate to form a phosphor-molybdic acid complex. This complex is reduced in an intensely blue coloured complex by L(+) ascorbic acid. This complex is measure at 880 nm. Reagents used are; potassium peroxodisulfate, sulphuric acid solution, sodium hydroxide solution, ascorbic acid solution, ammonium heptamolybdate.

In the study area, the concentration of phosphate content varies from -0.00047ppm to 0.0215ppm with a mean value 0.0038ppm. The maximum permissible limit of BIS for phosphate is 5ppm. It shows that all the samples are within the desirable limit.The highest value for phosphate is marked in Kaniyapurath Vila.

NITRATE

Nitrogen in the atmosphere converted to nitrate by lightning and is carried to the water by rain. and run off. In addition to this, anthropogenic inputs of nitrate as fertilizer which makes various forms of nitrogen in water. Nitrate is reduced to nitrite, and ammonia under anoxic condition.

Principle

The automated determination of Nitrite is based on the following reaction; the diazonium compounds formed by diazotizing of sulphanilamide by nitrite in water under acid conditions is coupled with N-(1-naphthyl) ethylene diamine dihydrochloride to produce a reddish-purple colour which is measured at 540 nm. Ammonia was determined by mixing the sample with alkaline solution. This solution is dialyzed through Teflon membrane. Hereafter the sample reacts with orthophtaldialdehyde (OPA) and Sulphate. This reaction produces an intense fluorescent product which is measured fluorometrically. The excitation wavelength is 370 mm and the emission wavelength is 452 nm.

In the study area, the concentration of nitrate ranges from 0.26ppm to 19.365ppm with a mean value 6.87ppm. The maximum permissible limit of BIS for nitrate is 6.87ppm. It shows that all the samples are within the desirable limit. The highest value for nitrate is marked from Koithoorkonam and lowest value is from Pattathinkara.

Graphical representation of anions is depicted below.

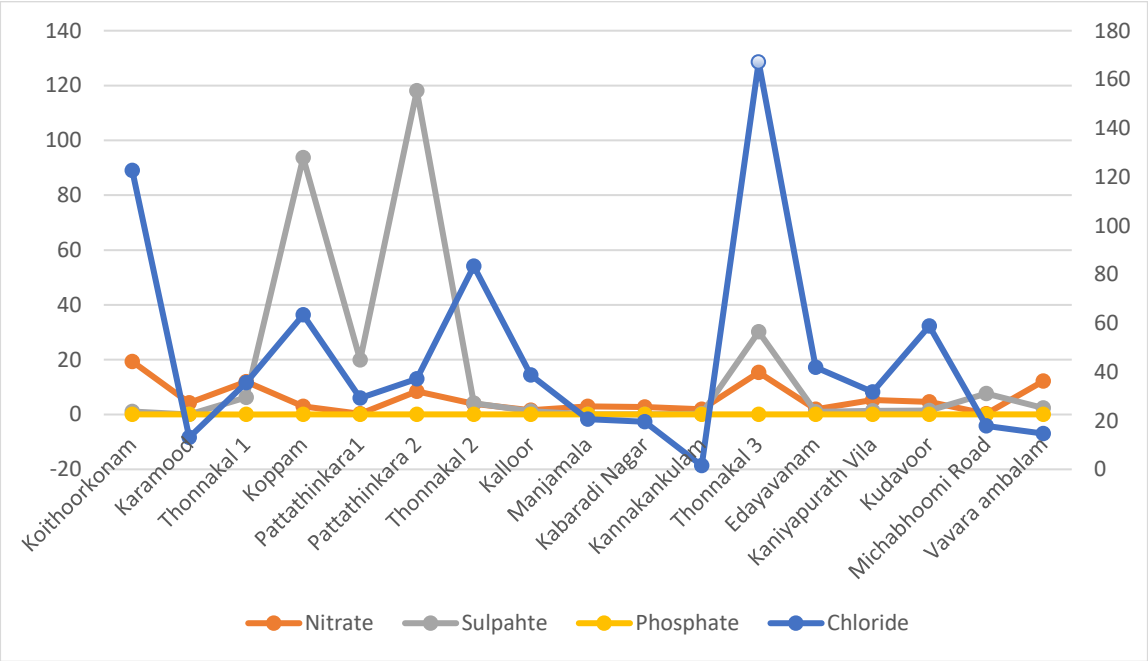

3.8.6 TRACE METALS

Analysis of trace metals such as Lead, Zinc, Cadmium and Chromium is done by MP-AES instrument by changing the standards. The blank used in the determination trace elements is 5% HNO_3.

Heavy metals are toxic to people even at low concentrations because they tend to bioaccumulate in the body, bind to cell membranes, and interfere with all biological processes. A great universal industrial solvent, water has a high dielectric constant, is polar, and is tiny.Water molecules' asymmetric nature allows them to both absorb and adsorb various substances from their surroundings. Water molecules are therefore not in their purest form in nature and are picking up impurities as a result of both natural and manmade activity (WHO 2007; Bhol and Pravindra 2017: Mendie 2005). The two main anthropogenic sources of heavy metals in ground water samples are weathering of rocks and industrial, agricultural, and fertiliser businesses. Heavy metals are frequently found in the earth's crust and can sometimes be dissolved naturally into groundwater.

In addition, landfill leachates, discharge from the steel, paper, and pulp industries, batteries, sewage from mine tailings, deep well disposal of liquid wastes, seepage from industrial waste lagoons, and industrial spills and breaches can all cause heavy metal contamination of groundwater (Evanko and Dzombak 1997). The carcinogenic and teratogenic effects that toxic heavy metals have on humans, animals, and plants make them dangerous environmental contaminants. Even at low concentrations, they are hazardous and have both phytotoxic and synergistic impacts on living things (Momodu and Anyakora 2010; Bhol and Pravindra 2017).

Trace elements present in water sample and the Mean and range values of Trace elements are shown in Table no 5 and 6.

- **LEAD**

In the study area, Lead concentration ranges from 0.02 ppm to 0.06 ppm with a mean value of 0.03 ppm. According to WHO, the desirable limit of lead in water is 0.1 ppm. It is clear that the samples are within the desirable limit. The highest value of Lead can be seen in Thonnakal and lowest value at Edayavanam and Koppam.

- **ZINC**

In the study area, Zinc concentration ranges from 0.01 ppm to 0.65 ppm with a mean value of 0.13 ppm. According to WHO, the highest desirable limit of zinc in water is 5 ppm. It is clear that the samples are within the desirable limit. The highest value of zinc can be seen in Thonnakal and lowest value at Vavaraambalam and Koithoorkonam.

- **CHROMIUM**

In the study area, concentration of chromium is below detection level.

- **CADMIUM**

In the study area, concentration of cadmium ranges from 0.54 ppm to 0.76 ppm with a mean value of 0.64 ppm. According to WHO, the highest desirable limit of cadmium in water is 0.01 ppm. It is clear that the samples are outside the desirable limit. The highest value of cadmium can be seen in Kalloor and lowest value at Thonnakal. Graphical representation of Trace metals is depicted below.

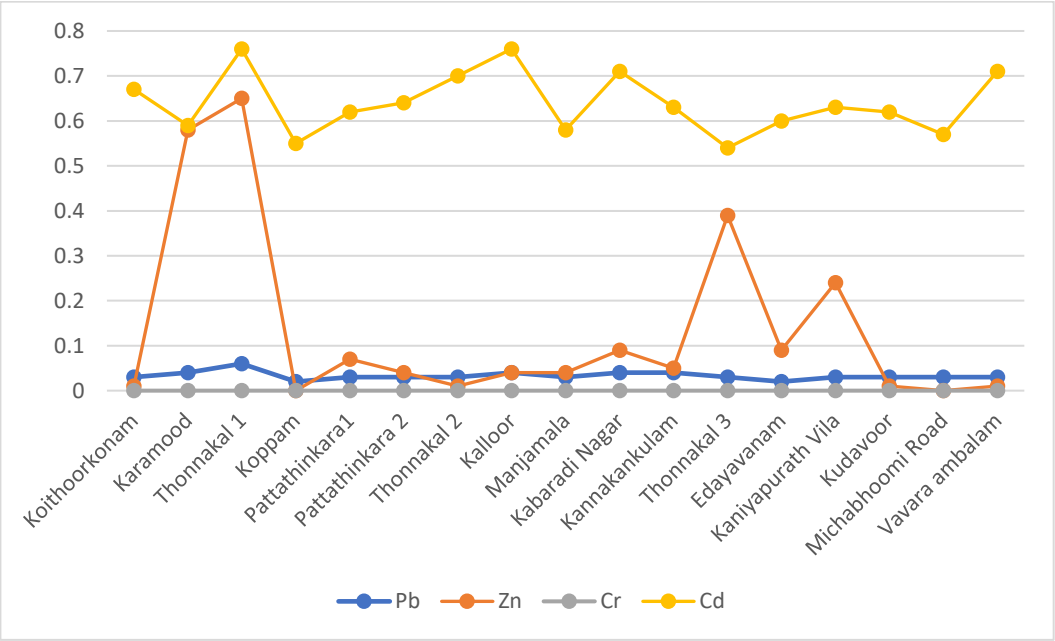

3.9 DOMESTIC AND DRINKING WATER QUALITY STANDARDS

Drinking water used in the home should be clear and devoid of colour, turbidity, odour, and germs. However, they do not fit into the category of chemical purity. Chemically, the water should ideally be soft, have a low concentration of dissolved solids, and be devoid of any toxic elements. The hydrochemical characteristics of groundwater in the research region are compared with the fundamental values advised by the Bureau of Indian Standards to determine if groundwater is suitable for drinking and public health purposes (BIS). The potential disturbance in relation to the water quality indicator is shown in Table 3.

DRINKING WATER QUALITY (As per BIS Standards)

Chemical Nature	Highest Desirable	Maximum Permissible
pH	6.5-8.5	No relaxation
TDS	500	2000
Total Hardness	300	600
Calcium (ppm)	75	200
Magnesium (ppm)	30	100
Chloride (ppm)	250	1000
Sodium (ppm)	-	200

3.10 WATER QUALITY INDEX (WQI)

Water quality index is an indicator and a single numerical expression, which reflects the composite influence of a number of water quality parameters, which are significant for a specific beneficial use. This management tool helps to asses for the overall water quality of. Series of mathematical equations mostly based on the mean methods like arithmetic, harmonic, logarithmic and mean multiplicative are widely adopted by various authors in developing water quality indices. In the present study the water quality parameters are studied from the point of view of suitability of ground water for human consumption. The permissible values of various pollutants for the drinking water recommended by World Health Organization (WHO).

WQI is calculated by using Arithmetic Mean Method (Brown et al., 1972)

The water quality index was prepared by using parameters such as pH, EC, TDS, sodium, calcium, iron, chloride, nitrate, and sulphate.

Step: 1

Calculate the unit weight (W) factors for each parameters by using the formula

$$Wn = K /(Sn)$$

where,

$$K = \frac{1}{\frac{1}{S_1}+\frac{1}{S_2}+ \ldots\ldots\ldots\ldots\ldots\ldots\ldots\ldots\ldots\ldots\ldots\ldots\ldots\ldots\ldots\ldots+1/S_n} = \frac{1}{\sum 1/S_n}$$

Sn = Standard desirable value of the n^{th} a parameters

On summation of all selected parameters unit weight factors, W_n=1(unity)

Step: 2

Calculate the Sub-Index (Q value by using the formula

$$Q\ n = [(Vn - Vo)] / [(Sn – Vo)] *100$$

Where,

V_n = concentration of the nth parameters

S_n = Standard desirable value of the n^{th} parameters

V_o = Actual values of the parameters in Pure water

(Generally V_o= 0 for most parameters except for pH and DO)

where pH=7and DO= 14

Step: 3

Combining Step 1 & Step 2, WQI is calculate as follows

Overall WQI = $\Sigma W_n Q_n$

WQI developed by Brown et al, (1972)

Water Quality Index Parameters

Water Quality Index	Water Quality Status
0-25	Excellent
26-50	Good
51-75	Poor
76-100	Very Poor
>100	Unfit for consumption

Water Quality Index of Ground Water

No.	Location	Water Quality Index	Water Quality Status
1	Koithoorkonam	72.89	Poor
2	Karamood	71.81	Poor
3	Thonnakal 1	80.61	Very Poor
4	Koppam	64.61	Poor
5	Pattathinkara1	76.81	Very Poor
6	Pattathinkara 2	75.64	Very Poor
7	Thonnakal 2	70.61	Poor
8	Kalloor	71.32	Poor
9	Manjamala	78.31	Very Poor
10	Kabaradi Nagar	80.36	Very Poor
11	Kannakankulam	145.72	Unfit
12	Thonnakal 3	69.72	Poor
13	Edayavanam	67.12	Poor
14	Kaniyapurath Vila	70.52	Poor
15	Kudavoor	112.98	Unfit
16	Michabhoomi Road	137.01	Unfit
17	Vavaraambalam	74.01	Poor

CHAPTER 4

CONCLUSION

A sizeable and frequently overwhelming percentage of the drinking water source is groundwater. In Kerala State, open-dug wells are the only source of drinking water, particularly in rural areas where surface water-based protected water delivery systems are lacking. This priceless resource's availability has recently decreased due to contamination from several sources as well as overexploitation.

Hydrological studies of the groundwater quality in and around clay mines of Mangalapuram, Thiruvananthapuram district was carried out. The area is located between 8^{o}37'12.73" and 8^{o}39'44.83" North Latitude and 76^{o}56'24.89" and 76^{o}52'59.13" East Longitude. The study area falls mainly in midland and lowland areas of Thiruvananthapuram district of Kerala. Clay mining activity is dominant in the study area. Approximately thirty clay mines are located within the area. English Indian clay Ltd is one of the big clay mining company and its mine is located at Thonnakal.

The major rock type of the study area are predominantly characterised by sedimentary rocks with some intrusive and metamorphic rocks. Major rocks are sandstone and clay with lignite intercalation, Khondalite group of rocks, and Laterite.

The present work was carried out with the objective to understand the impact and effects of clay mining in groundwater. The entire area was investigated to access the quality of water for drinking and household use. 17 water samples were collected from dug wells and 3 from tube wells. Well inventory data were collected from 108 locations, reveals that the water levels in the study area ranges from 0.7mbgl to 23mbgl. The deepest water level is reported from places near clay mines. The deepest water level is recorded at Karamood and Thonnakal regions. The depth of well ranges from 1.5 to 24.5m. Comparison of water chemistry with BIS standards are discussed in the third chapter reveals that groundwater at most of the places are unsafe for drinking. In the study area, lower pH values were observed from nine of the samples, in which the samples from Thonnakal and Pattathinkara has the lowest value 3.59 and 4.38 respectively. The low pH values are observed near the clay mines.

The presence of iron sulphide (pyrite), which is present in the deep clay horizon and becomes exposed during mining, is what causes the acidity. This oxidation results in the formation of sulphate and hydrogen ions. Low pH values are found in groundwater retrieved from deep wells. According to the chemical information, the pH of the groundwater gathered from Karamood and Thonnakal is low. It was noted that these wells were extremely deep. As a result, the distance from mine pits where deep water levels exist can be linked to low pH in groundwater. Low pH can cause gastrointestinal disorders like hyper acidity, ulcers, stomach pain, burning sensation etc in the users and also can trigger corrosion in pipes, thereby releasing toxic metals such as Zinc, Lead, Cadmium and Copper (Trivedy Goel, 1986).

Ironic chloride, an acidic and easily soluble chemical, is created when the iron in the laterite reacts with the chloride content of the groundwater that is flowing around it. The pH of the groundwater may become increasingly acidic if ferric chloride is present. Acidic groundwater is seen in connection with lateritic aquifers, which supports this observation.

The highest value of EC is observed from Thonnakal which is near the clay mines. The anomalous values are due to clay mining activities in the proximity. The highest Iron value was reported from from Kannakankulam (0.67ppm) which is exceeding the permissible limit indicating the contamination of groundwater by clay mining activites. The highest value of Potassium is reported from Thonnakal. The values of remaining cations and anions lies within the BIS limit. The concentration of trace metals such as Lead, Zinc, Chromium and Cadmium were also studies. Only values of Cadmium are outside the permissible limit. In and near the Mangalapuram clay mines, the groundwater has low pH and trace metal concentrations as a result of mining. It is evident that the research area's groundwater quality is rapidly declining.

WQI stands out as a very useful approach to the valuation and management of water quality. It also provides a profoundly thoughtful explanation of the water quality of the study area. Arithmetic Mean method used for the Water Quality Index shows more than 17% of water samples are unfit for consumption. The samples of contaminated water come from Manjamala, Thonnakal, and Kabaradi Nagar. 29% of the water quality index of samples belongs to very poor water quality status. The extremely poor-quality water will soon become unfit for consumption It suggests immediate need for appropriate water quality management strategy that tackles the issue.

The environmental issues associated with clay mining include reduction in agricultural production, loss of rich soil, and creation of fallow lands. They also involve water level decline and quality deterioration in wells seasonally near to mining sites, particularly during the summer. The regional hydrogeological conditions have been impacted by indiscriminate clay mining activities that lacked proper depth control. Due to changes in land use caused by mining, productive paddy fields that were once a dependable source for recharging the aquifer system have been converted to clay mines or other cropping patterns that are relatively less favourable to recharge.

Based on interactions with the public, it was determined that the majority of the dug wells in these locations dry up in the summer and lack water supply plans to meet the needs of the local population. People began to violently protest the clay mining businesses as a result of this. Due to clay mining activities, open wells are non-perennial in the study area and the groundwater is unfit for human consumption. To meet their demands, the majority of the people in the region relies on public water supply schemes. Additionally, clay mining companies provide appropriate arrangements for the supply of drinking water.

Clay formations are often not suited for artificial recharge, however sites where the aquifer is accessible at greater depths more than 20 m, can employ rainwater harvesting techniques. Depending on the amount of runoff available, a shallow shaft with dimensions of 2 to 5 m in diameter and 3 to 5 m in depth may be built.

LIST OF TABLES

Table.1

WELL INVENTORY DATA

Sl.No.	Well Type	Location	Latitude	Longitude	Well Diameter (m)	Height of parapett	Water Level	Total Depth
1	OW1	Vavaraambalam	8.62747	76.88133	1.7	0.853	9.266	12.583
2	OW2	Piriyattukonam	8.627333	76.88133	1.5	0.914	7.9861	10.058
3	OW3	Vavaraambalam	8.62747	76.88141	1.6	0.7619	18.1961	20.391
4	TW1	Elluvila	8.62725	76.87922	0	0	0	53.339
5	OW4	Vavara	8.629611	76.87933	1.8	0.67	12.177	13.868
6	OW5	Pothencode	8.63147	76.87847	1.9	0.761	10.547	12.801
7	OW6	Manjamala	8.631722	76.87719	1.1	0.761	2.119	3.931
8	OW7	Koithoorkonam	8.631417	76.87661	1.1	0.914	1.219	4.602
9	OW8	Anaikodu	8.631444	76.87464	1.2	0.701	2.834	4.511
10	OW9	Koithoorkonam	8.629611	76.87422	1.2	0.731	9.632	12.039
11	OW10	Koithoorkonam	8.628389	76.87367	1.6	0.792	8.648	11.216
12	OW11	Mannara	8.626444	76.87325	1.3	0.335	14.082	15.554
13	OW12	Koithoorkonam	8.626083	76.87081	1.5	0.822	10.793	12.313
14	OW13	Koithoorkonam	8.627333	76.86958	1.5	0.609	10.82	14.081
15	OW14	Naranathkonam	8.629139	76.87089	1.1	0.914	2.469	5.974
16	OW15	Kunnukad	8.629222	76.86864	1.1	0.64	14.539	17.983
17	OW16	Koithoorkonam	8.630139	76.86894	1.9	0.883	14.082	18.013
18	OW17	Kunnukal	8.632028	76.86961	1.6	0.761	3.018	8.077
19	OW18	Mohanapuram	8.624556	76.86458	1.2	0.701	16.245	20.452
20	OW19	Karamood	8.623028	76.86033	1.5	0.64	23.012	1.584
21	OW20	Thonnakal	8.626417	76.853	1.5	0.761	16.939	19.385
22	OW21	Mangalapuram	8.627806	76.85467	1	0.883	0.979	4.724
23	OW22	Thonnakal	8.628972	76.85447	1.1	0.609	1.158	7.619
24	OW23	Pattathinkara	8.632306	76.85522	1.5	1.066	4.725	6.37
25	OW24	Pattathinkara	8.63525	76.85383	1.2	0.807	9.281	13.228
26	OW25	Thonnakal	8.640694	76.85331	1	1.188	6.157	10.972
27	OW26	Kalloor	8.636444	76.86067	1	0.944	4.146	6.918
28	OW27	Manjamala	8.639583	76.86883	1.8	0.838	11.11	12.496
29	OW28	Kabaradi Nagar	8.632389	76.63239	1.5	0.761	10.55	12.923
30	OW29	Kannakankulam	8.637111	76.84664	1.5	0.792	3.813	8.107
31	OW30	Thonnakal	8.644889	76.84733	1.2	0.88	11.91	15.845
32	OW31	Edayavanam	8.649861	76.85122	1.5	0.731	8.229	11.277
33	OW32	Kudavoor	8.654167	76.85167	1.5	0.731	7.833	11.826
34	OW33	Kudavoor	8.659917	76.85069	1.6	0.822	11.65	14.72
35	OW34	Mangalapuram	8.640611	76.84392	1.2	0.36	2.71	6.64
36	TW2	Thonnakal	8.632389	76.84886	0	0	0	106.6
37	BW3	Thonnakal	8.626194	76.86061	0	0	0	91.44
38	OW35	Manjamala	8.628583	76.86406	1.5	0.762	9.90	11.88

39	OW36	Vavaraambalam	8.629278	76.87839	1.5	0.792	9.84	13.47
40	OW37	Koithoorkonam	8.626167	76.86794	1.7	0.60	11.06	12.22
41	OW38	Mohanapuram	8.622694	76.86486	1.8	0.822	12.89	16.45
42	OW39	Mohanapuram	8.623917	76.86331	1.5	0.762	18.53	23.46
43	OW40	Thonnakal	8.624167	76.861	1.5	1.005	18.53	22.34
44	TW4	Karamood	8.622694	76.85908	0	0	0	76.20
45	TW5	Mangalapuram	8.624194	76.8555	0	0	0	54.86
46	TW6	Mangalapuram	8.624889	76.8505	0	0	0	60.96
47	OW41	Mangalapuram	8.626111	76.85036	1.6	0.792	16.67	22.12
48	OW42	Thonnakal	8.627278	76.84972	1.5	0.829	10.33	13.62
49	OW43	Mangalapuram	8.629917	76.85114	1.6	0.822	13.41	16.06
50	OW44	Kunnuvila	8.628889	76.84981	1.4	0.731	11.49	17.06
51	OW45	Mohanapuram	8.626556	76.86333	1.5	1.005	10.63	15.30
52	OW46	Thonnakal	8.627083	76.86242	1.8	0.883	11.73	15.66
53	OW47	Koithoorkonam	8.629778	76.86311	1.5	0.701	10.30	13.41
54	OW48	Koithoorkonam	8.631111	76.86317	1.7	0.822	10.60	13.44
55	OW49	Melthonnakal	8.630611	76.86506	1.15	0.853	0.731	6.004
56	OW50	Koithoorkonam	8.630806	76.86725	1.5	0.731	9.05	12.67
57	TW7	Koithoorkonam	8.631389	76.87639	0	0	0	60.96
58	OW51	Kalloor	8.636417	76.86667	1.1	0.762	7.46	9.75
59	OW52	Manjamala	8.637583	76.86694	1.6	0.792	11.49	13.01
60	OW53	Kalloor	8.637417	76.86433	1.6	0.762	8.47	11.704
61	OW54	Manjamala	8.63725	76.86822	1.6	0.762	7.31	13.198
62	OW55	Manjamala	8.639389	76.86839	1.5	0.762	11.27	12.49
63	OW56	Kalloor	8.638139	76.859	2	0.701	7.49	16.49
64	OW57	Kalloor	8.640139	76.85867	1.3	0.792	4.02	6.18
65	OW58	Kalluvetti	8.642167	76.85942	1.6	0.643	13.46	14.93
66	OW59	Kalluvetti	8.640556	76.86139	1.5	0.792	10.08	14.53
67	OW60	Manjamala	8.63775	76.86953	1.5	0.701	8.71	13.106
68	OW61	Manjamala	8.636222	76.87267	1.5	0.883	9.81	12.52
69	OW62	Manjamala	8.634167	76.87167	1.5	0.701	9.38	12.55
70	OW63	Manjamala	8.635722	76.87117	1.2	0.670	5.91	9.41
71	OW64	Manjamala	8.639556	76.86669	1.2	0.670	7.10	10.09
72	OW65	Manjamala	8.642389	76.86806	1.8	0.731	5.7	12.61
73	OW66	Manjamala	8.64175	76.86589	1.3	0.701	7.95	9.44
74	OW67	Kalloor	8.640139	76.86283	1.5	0.792	8.59	10.24
75	OW68	Kalloor	8.639389	76.85714	1.2	0.914	1.58	5.608
76	OW69	Manjamala	8.642806	76.85661	1.1	0.9753	3.017	5.516
77	OW70	Thonnakal	8.637111	76.85719	1.4	0.914	3.16	8.199
78	OW71	Kabarady	8.634889	76.85806	1.6	0.822	10.02	11.003
79	OW72	Thonnakal	8.631306	76.85881	1.1	1.005	2.98	6.065
80	OW73	Mohanapuram	8.629528	76.86236	1.5	1.310	8.9	12.375
81	OW74	Thonnakal	8.638722	76.85331	1.6	0.67	7.86	14.874
82	OW75	Thonnakal	8.643667	76.85342	1.5	0.762	11.15	13.35
83	TW8	Mangalapuram	8.637972	76.85061	0	0	0	91.44
84	OW76	Pattathil	8.643028	76.84525	1.5	0.792	7.68	24.44
85	OW77	Thonnakal	8.648444	76.85033	1.5	0.792	3.931	8.382
86	OW78	Mangalapuram	8.651306	76.85175	1	0.731	0.82	5.21

87	OW79	Kudavoor	8.652556	76.85125	1.6	0.822	2.86	4.26
88	OW80	Kudavoor	8.655806	76.86111	1.6	0.643	11.03	14.11
89	OW81	Thonnakal	8.657139	77.05361	1.1	0.914	1.43	3.96
90	OW82	Chembakamangalam	8.649833	76.84803	1.8	0.822	8.93	15.02
91	OW83	Thonnakal	8.649806	76.84803	1.7	0.731	12.10	14.47
92	OW84	Poikayil	8.647889	76.84675	1.6	0.701	3.81	8.83
93	OW85	Kudavoor	8.647361	76.84928	1.5	0.670	4.96	6.736
94	OW86	Poikayil	8.648111	76.84581	1.2	1.097	3.23	8.016
95	OW87	Thonnakal	8.647833	76.84383	1.6	0.853	13.04	19.11
96	OW88	Poikayil	8.646639	76.84569	1.6	0.762	9.11	14.41
97	OW89	Thonnakal	8.647083	76.844	1.6	0.914	2.89	7.498
98	OW90	Poikayil	8.645361	76.84483	1.8	0.762	8.10	13.80
99	OW91	Kannankarakonam	8.642972	76.84889	1.5	0.792	10.85	14.44
100	OW92	Thonnakal	8.642861	76.84978	1.3	1.219	8.26	13.47
101	OW93	Kannankarakonam	8.640611	76.84783	1.2	0.914	4.87	8.29
102	OW94	Thonnakal	8.640306	76.84567	1.2	0.91	3.35	7.924
103	OW95	Thonnakal	8.638333	76.846	2.1	0.762	9.601	13.28
104	OW96	Thonnakal	8.636917	76.84875	1.5	0.82	12.009	15.84
105	OW97	Pattathinkara	8.6335	76.85589	1	0.914	1.67	6.43
106	OW98	Thonnakal	8.629861	76.85742	1.5	0.701	11.308	14.29
107	OW99	Karamood	8.626972	76.85906	1.3	0.792	16.33	21.21
108	OW100	Koithoorkonam	8.626056	76.86664	1.7	0.914	9.14	11.61

Table.2

HYDROCHEMICAL DATA OF GROUNDWATER (PRE-MONSOON)

No:	Location	pH	EC µS	TDS ppm	Na^{+} ppm	K^{+} ppm	Ca^{2+} ppm	Mg^{2+} ppm	Fe^{2+} ppm	Cl^{-} ppm	NO_3^{-} ppm	SO_4^{2-} ppm	PO_4^{3-} ppm
1	Koithoorkonam	6.13	512.8	338.9	122.5	22.29	3.84	27.97	0.27	122.66	19.3529	1.09	0.00121
2	Karamood	4.92	89.55	60.03	26.41	1.15	1.34	3.31	0.26	13.11	4.2148	0.01	0.00013
3	Thonnakal 1	3.59	278.8	187	33.74	13.9	5.74	9.3	0.32	35.52	11.942	6.22	-0.00079
4	Koppam	6.94	501.1	333.8	87.3	12.37	10.3	12.8	0.25	63.42	3.0186	93.71	0.00085
5	Pattathinkara1	6.94	180.3	119	43.4	2.98	1.95	1.74	0.29	29.21	0.26221	19.86	0.0359
6	Pattathinkara 2	4.38	440.9	290.9	142.1	5.14	6.86	8.42	0.28	37.13	8.414	118.07	0.00047
7	Thonnakal 2	6.86	386.2	256.7	94.7	11.88	18.8	8.94	0.25	83.39	3.869	4.15	0.00089
8	Kalloor	6.51	176.2	117.6	39.04	11.49	4.88	4	0.26	38.71	1.5159	1.19	-0.00052
9	Manjamala	6.38	119.4	79.19	34.57	4	3.52	4.41	0.28	20.62	2.9203	0.06	0.001
10	Kabaradi Nagar	6.57	109.3	72.36	23.26	15.19	1.66	2.93	0.29	19.57	2.7631	0.1	0.00159
11	Kannakankulam	5.64	67.13	44.38	17.96	4.58	0.88	2.03	0.67	1.52	1.953	0.23	0.00031
12	Thonnakal 3	6.3	755.7	504.8	158.2	87.62	11.6	13.29	0.27	167.12	15.2914	30.22	-0.00047
13	Edayavanam	6.46	180.2	119.9	30.42	15.28	7.86	5.33	0.25	41.81	1.9407	0.97	0.0011
14	Kaniyapurath Vila	6.65	188.5	123.9	33.66	10.48	6.74	5.09	0.25	31.76	5.30396	1.38	0.0215
15	Kudavoor	5.74	174.6	116.2	42.24	15.65	1.02	4.59	0.45	58.75	4.6537	1.47	0.00097
16	Michabhoomi Road	6.62	83.76	55.64	17.67	5.55	6.42	4.89	0.3	17.79	0.286	7.67	0.00033
17	Vavara ambalam	6.99	197.4	130.1	38.97	16.15	5.6	10.14	0.26	14.66	12.2334	2.39	0.00076

Table.5

TRACE ELEMENTS OF GROUNDWATER

No.	Location	Lead	Zinc	Chromium	Cadmium
1	Koithoorkonam	0.03	0.01	BDL	0.67
2	Karamood	0.04	0.58	BDL	0.59
3	Thonnakal 1	0.06	0.65	BDL	0.76
4	Koppam	0.02	BDL	BDL	0.55
5	Pattathinkara1	0.03	0.07	BDL	0.62
6	Pattathinkara 2	0.03	0.04	BDL	0.64
7	Thonnakal 2	0.03	0.01	BDL	0.7
8	Kalloor	0.04	0.04	BDL	0.76
9	Manjamala	0.03	0.04	BDL	0.58
10	Kabaradi Nagar	0.04	0.09	BDL	0.71
11	Kannakankulam	0.04	0.05	BDL	0.63
12	Thonnakal 3	0.03	0.39	BDL	0.54
13	Edayavanam	0.02	0.09	BDL	0.6
14	Kaniyapurath Vila	0.03	0.24	BDL	0.63
15	Kudavoor	0.03	0.01	BDL	0.62
16	Michabhoomi Road	0.03	BDL	BDL	0.57
17	Vavaraambalam	0.03	0.01	BDL	0.71

Table 6

MEAN AND RANGE VALUES OF TRACE ELEMENTS IN GROUND WATER

Parameters	Range	Mean	WHO	Highest desirable
Pb	0.02-0.06	0.03	0.1	0.1
Zn	0-0.65	0.13	-	5
Cr	-		0.05	0.05
Cd	0.54-0.76	0.64	0.01	0.01

Table.3

MEAN AND RANGE VALUES OF OPENWELL WATER SAMPLES

Parameter		Pre-monsoon	BIS standard	
			Highest Desirable	Maximum Permissible
Ph	Range	3.59-6.99	6.5 – 8.5	No relaxation
	Mean	6.095		
EC (µS)	Range	67.13-755.7		
	Mean	261.28		
TDS (ppm)	Range	44.38-504.8	500	2000
	Mean	173.55		
Ca^{2+}(ppm)	Range	0.88-18.8	75	200
	Mean	5.82		
Mg^{2+}(ppm)	Range	1.74-27.97	30	100
	Mean	7.59		
Na^{+}(ppm)	Range	17.67-158.2		200
	Mean	58.008		
K^{+}(ppm)	Range	1.15-87.62		40
	Mean	15.04		
Fe^{2+}(ppm)	Range	0.25-0.67	0.3	No relaxation
	Mean	0.305		
Cl^{-}(ppm)	Range	1.52-167.12	250	1000
	Mean	46.83		
SO_4^{2-}(ppm)	Range	0.01-118.07	200	400
	Mean	16.98		
PO_4^{3-} (ppm)	Range	-0.00047-0.0215		5
	Mean	0.0038		
NO_3^{-} (ppm)	Range	0.26-19.35	45	100
	Mean	6.87		

TABLE 4

DETAILS OF POSSIBLE DISORDERS

No	Chemical Nature	Highest Desirable	Maximum Permissible	Possible disorder if in higher amounts
1	pH	6.5	8.5	Taste difference and intestinal problems. Also cause rusting of pipes
2	Hardness (ppm)	300	600	Do not lather soap, diseases to kidney, thickening of blood vessels.
3	Total Dissolved Solids (ppm)	500	2000	Taste difference and Intestinal problems
4	Chloride (ppm)	250	1000	Affects taste and not good for those with heart and kidney disease
5	Calcium (ppm)	75	200	Kidney diseases.
6	Magnesium (ppm)	30	100	Diarrhea, increases with production of enzymes.
7	Sulphate (ppm)	200	400	Intestinal and stomach disorders
8	Sodium (ppm)	_	200	Affect heart, kidney, and blood circulation.
9	Potassium (ppm)	No guidelines		Diarrhea
10	Phosphate (ppm)	_	5	Vomiting and diarrhea. It affects thyroid glands and bones.

FIGURES

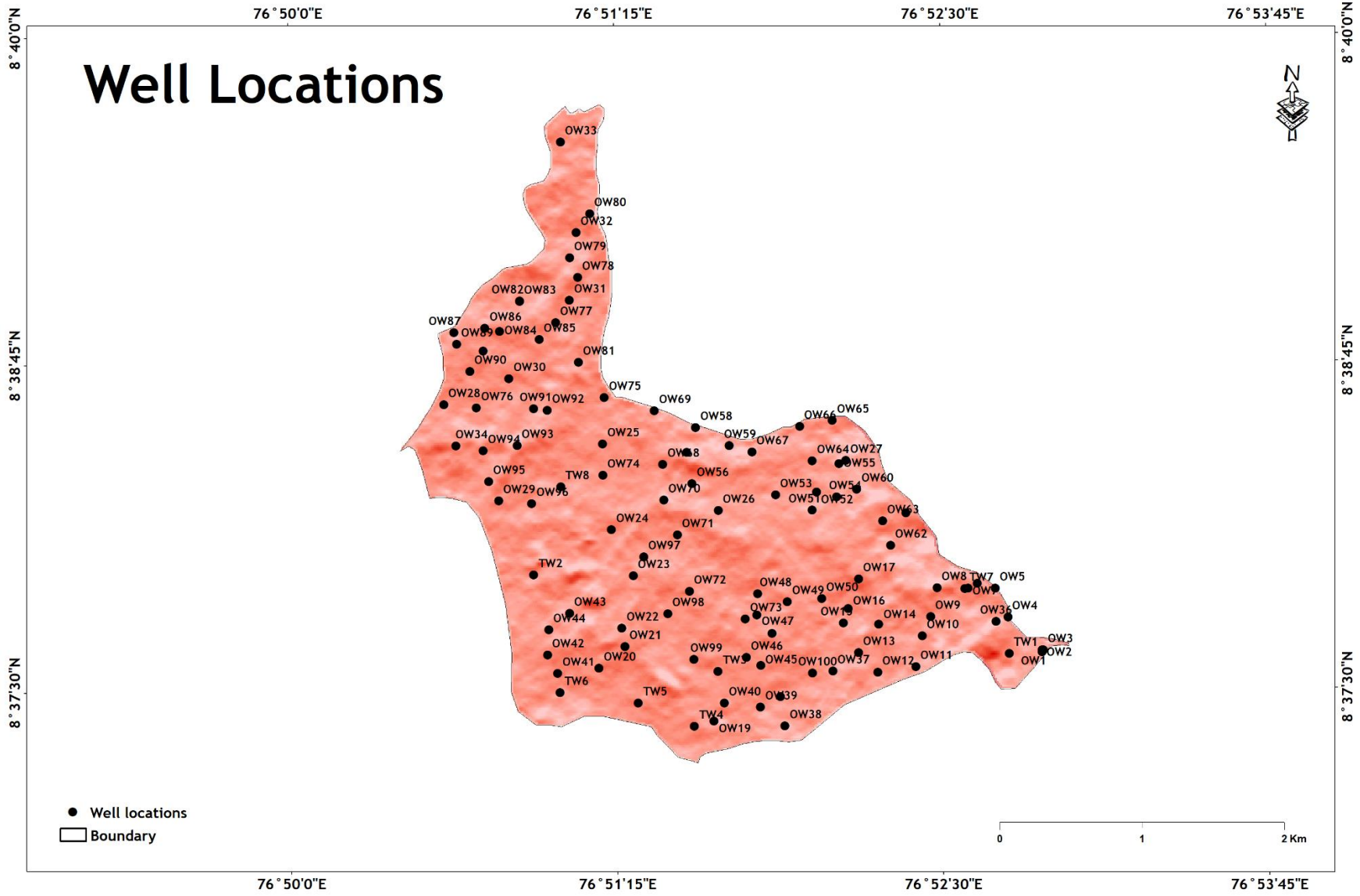

Fig 6. Spatial variation of well locations

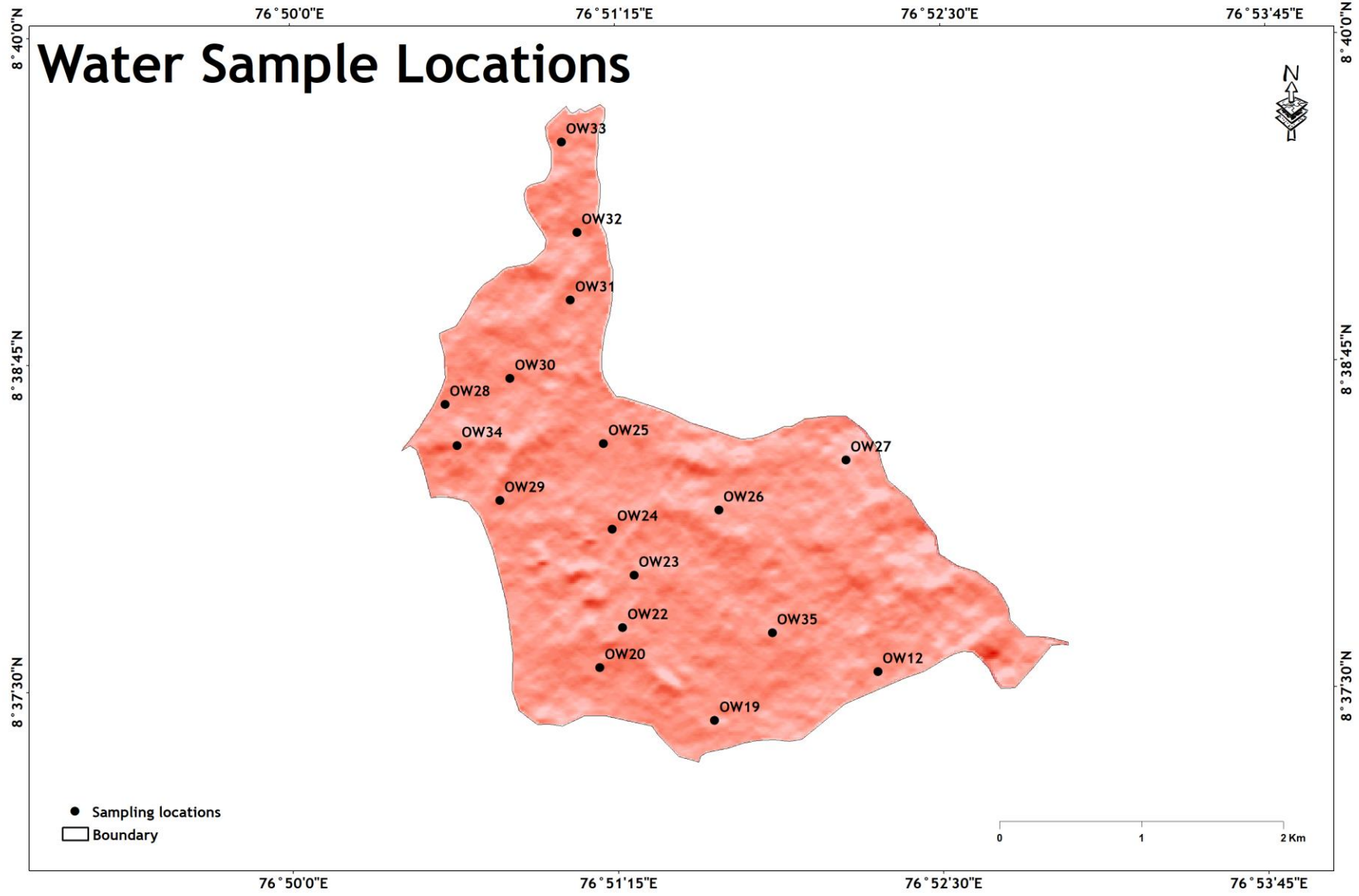

Fig. 7 Spatial variation of water sample locations

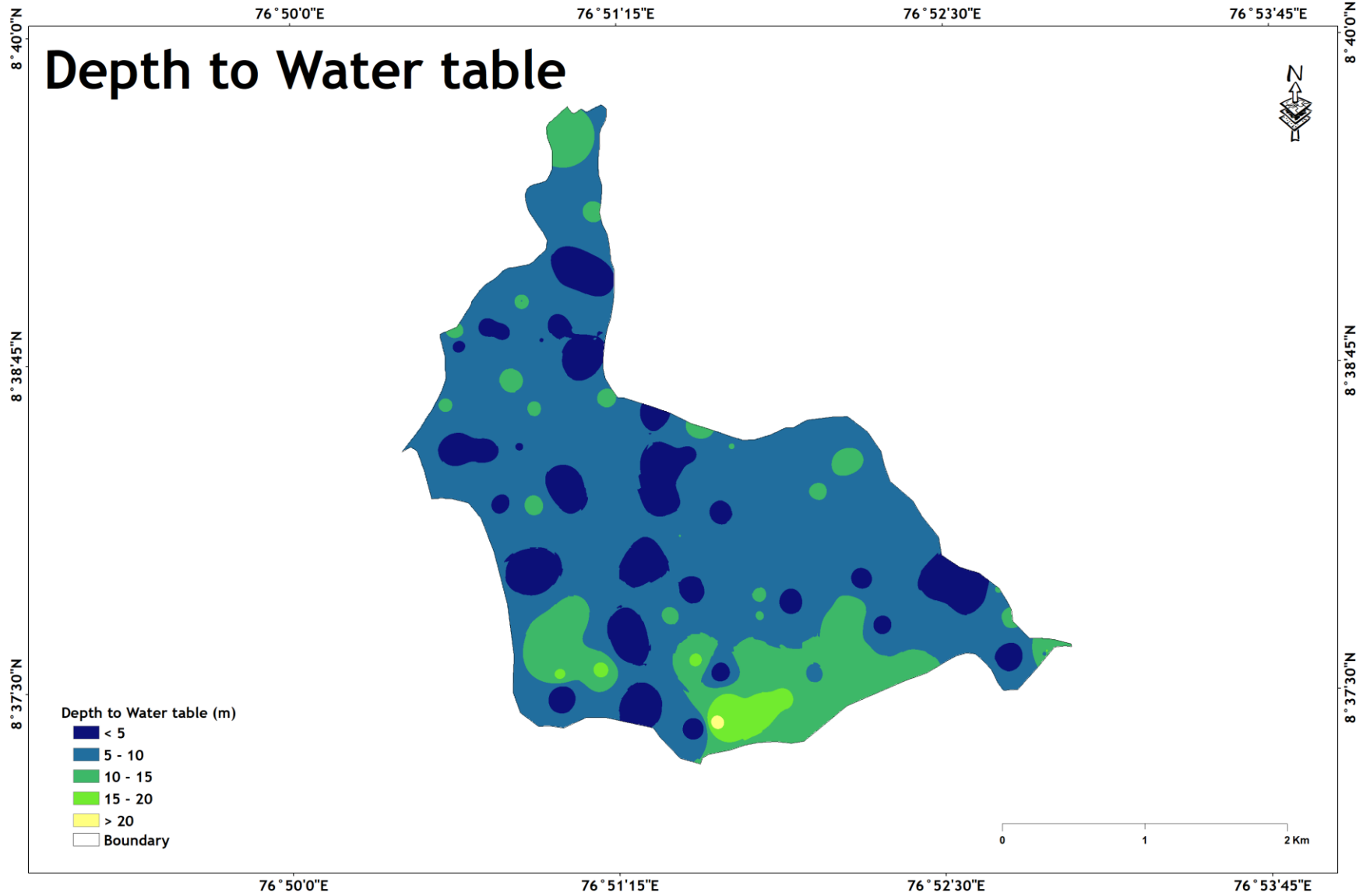

Fig.8 Spatial variation of Depth to water table

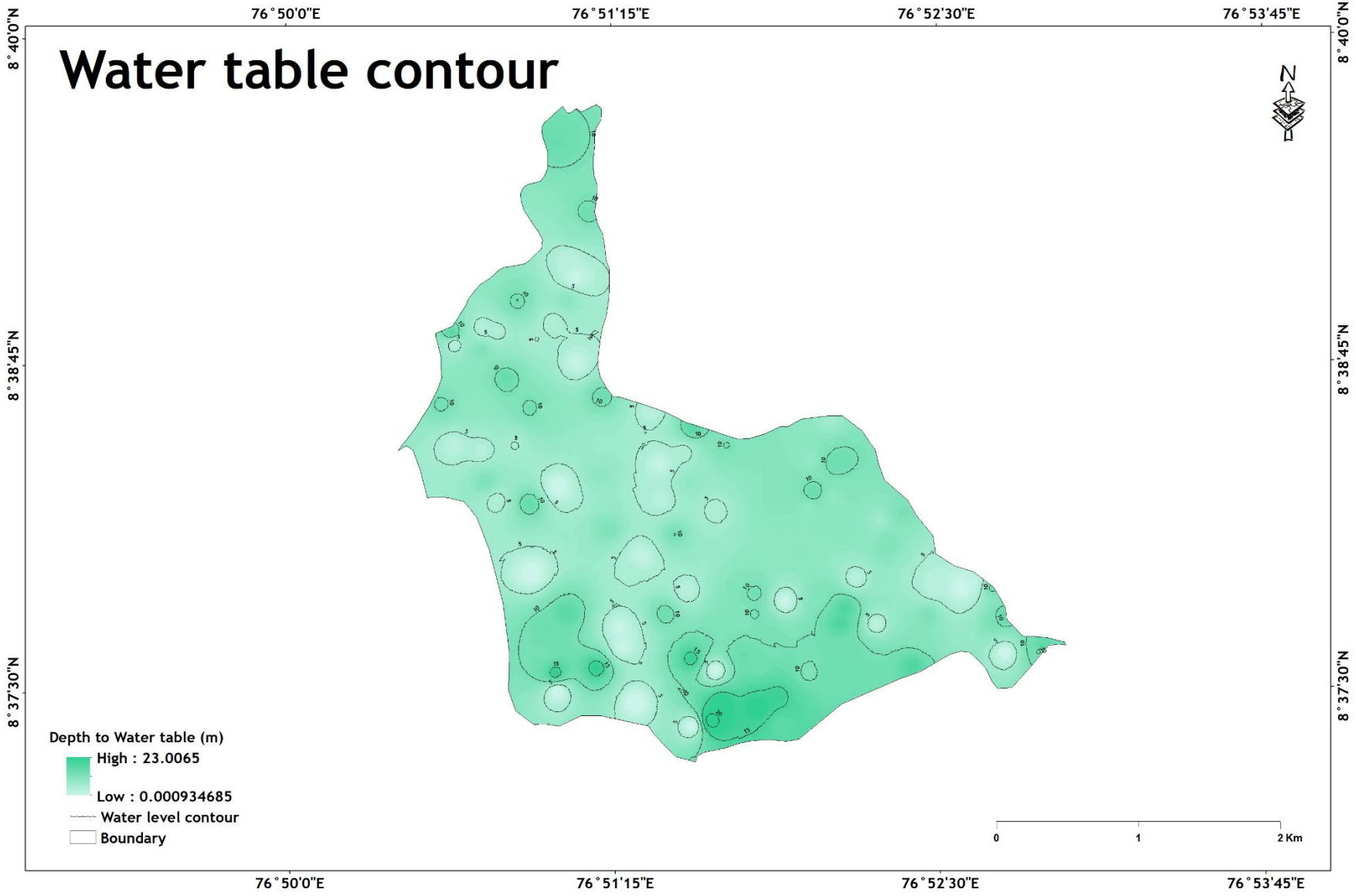

Fig.9 Spatial variation of Water table contour

Fig.10 Spatial variation of Drainage

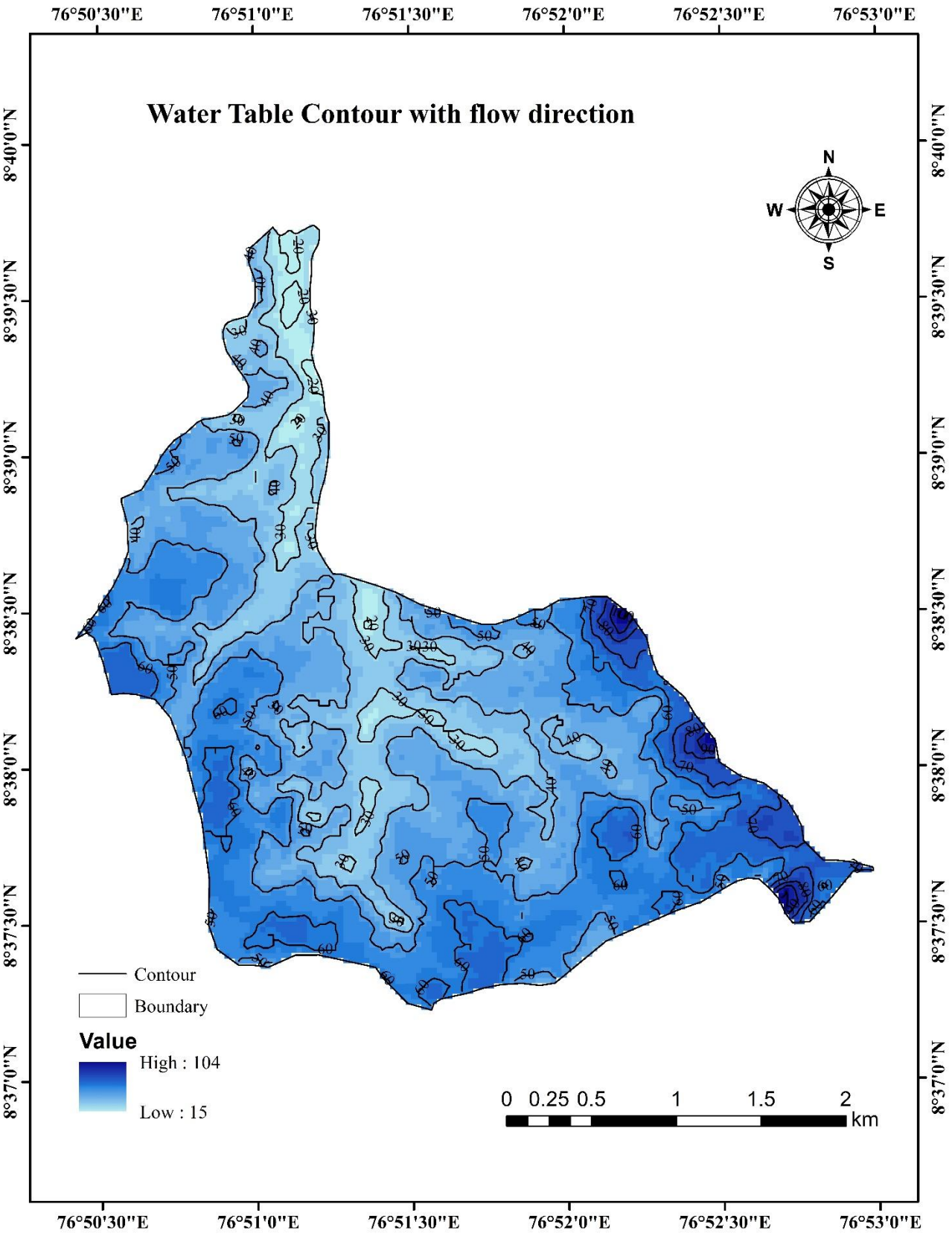

Fig.11 Spatial variation of water table contour with flow direction.

Fig.12 Geological map of the study area

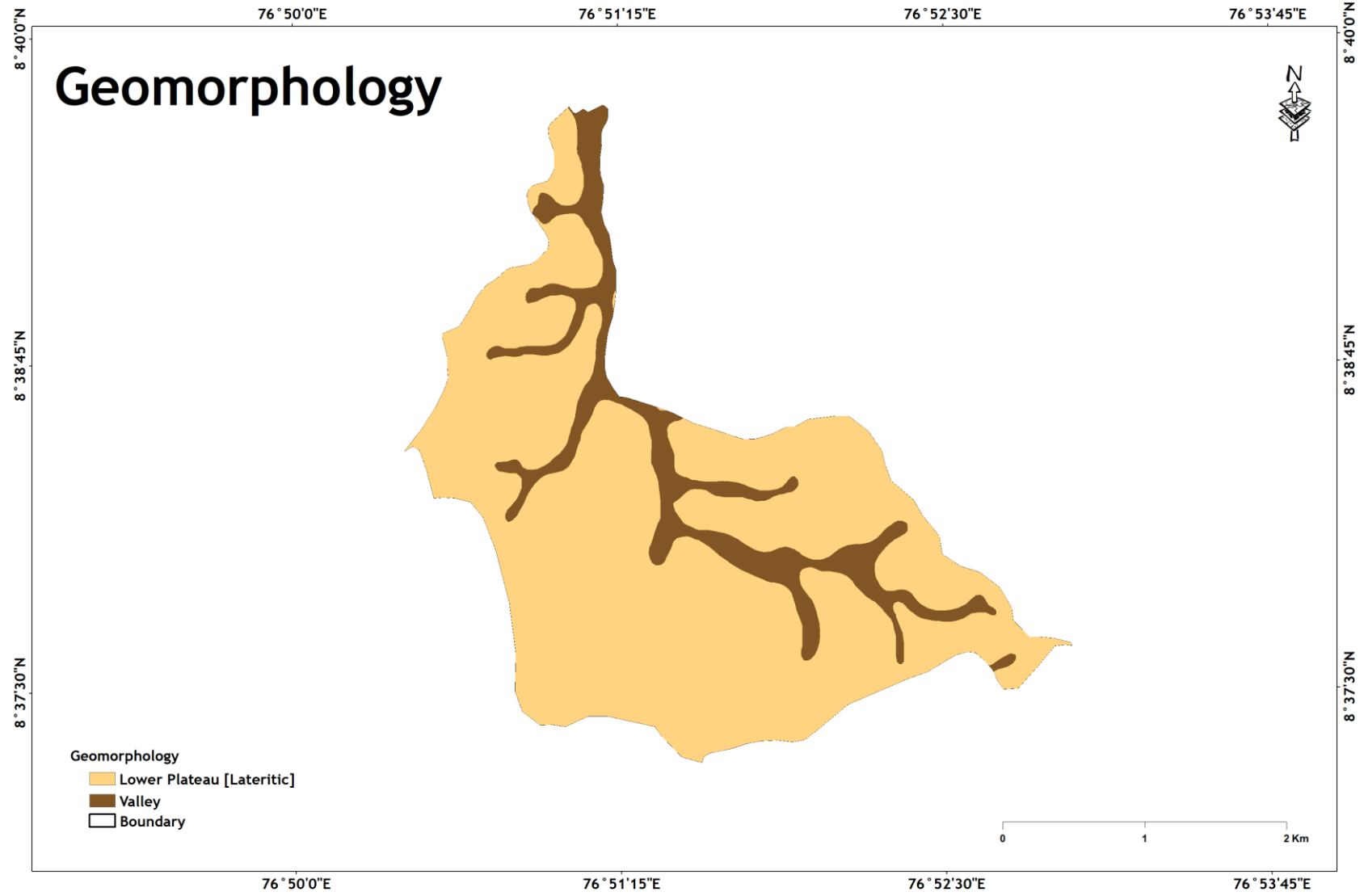

Fig.13 Geomorphology of the study area

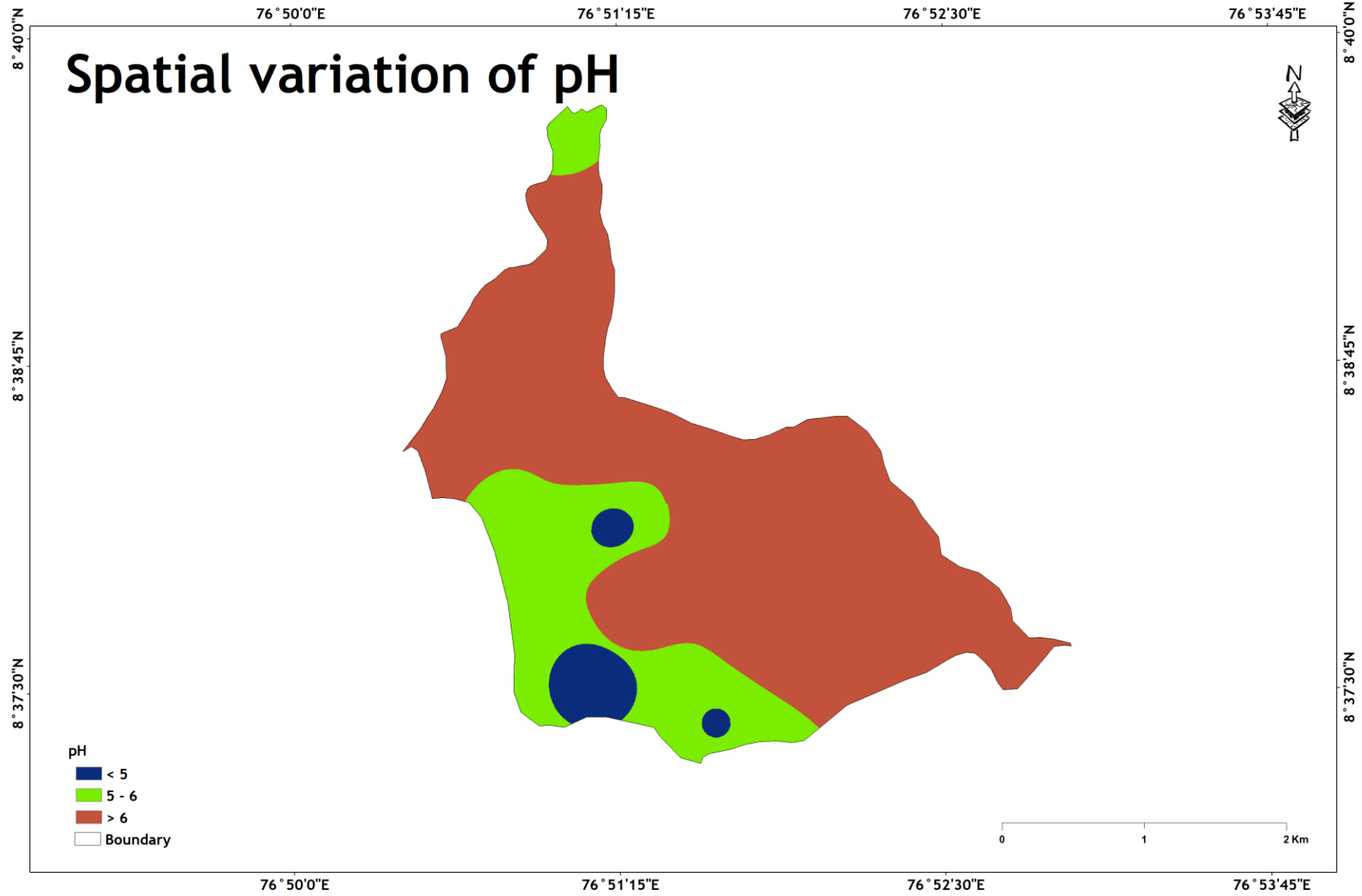

Fig.14 Spatial Variation of pH

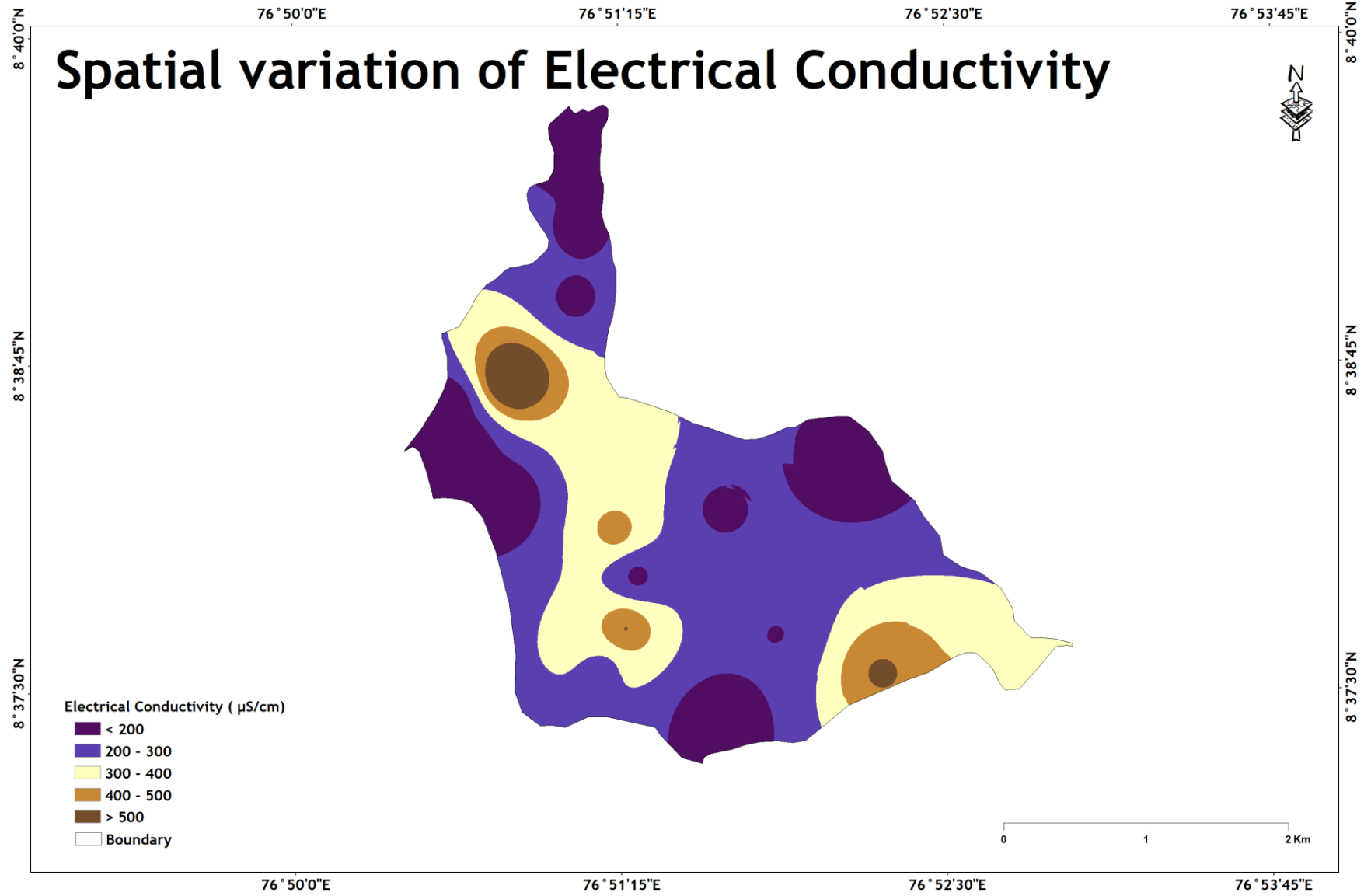

Fig.15 Spatial Variation of EC

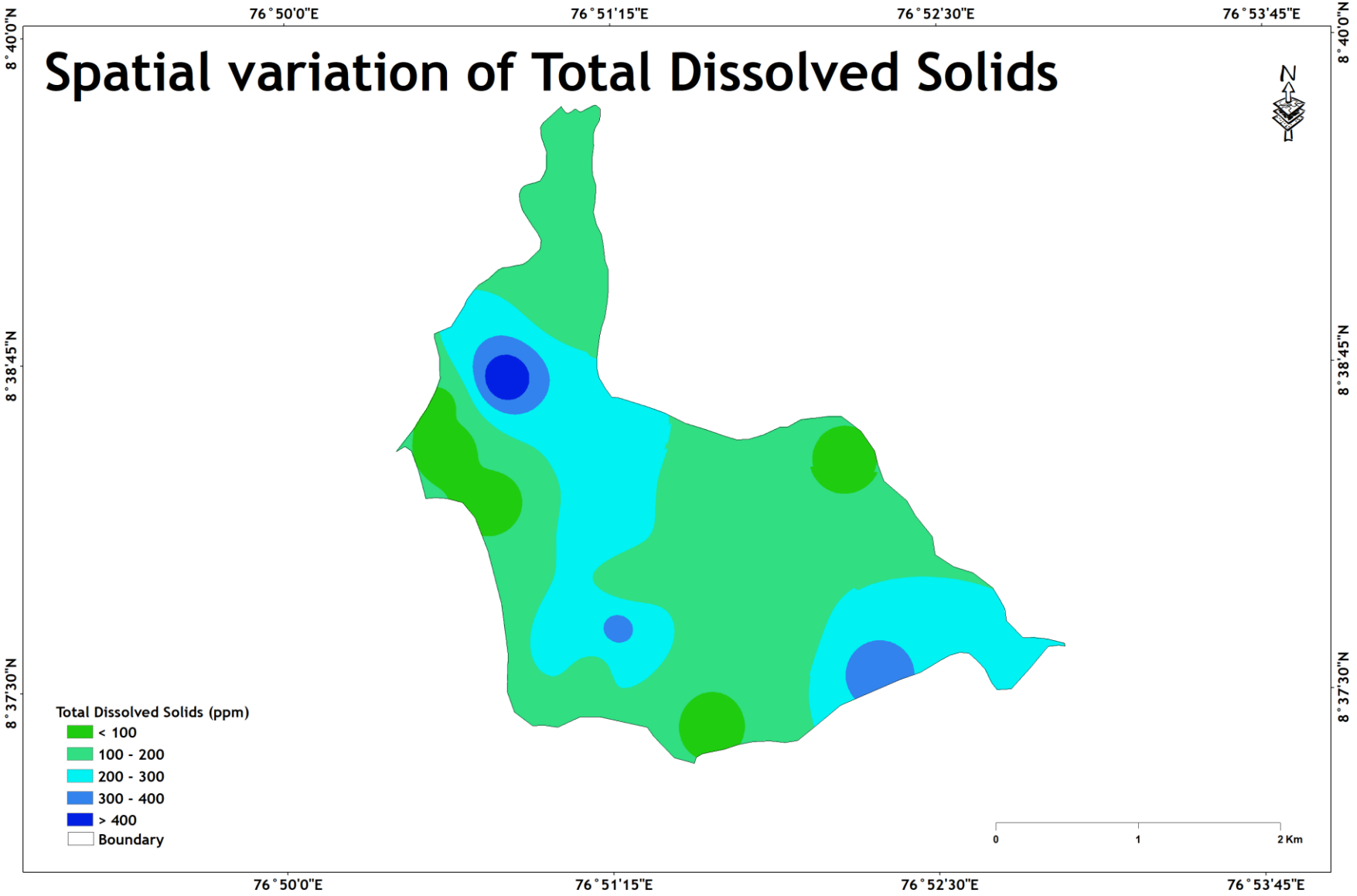

Fig. 16 Spatial variation of TDS

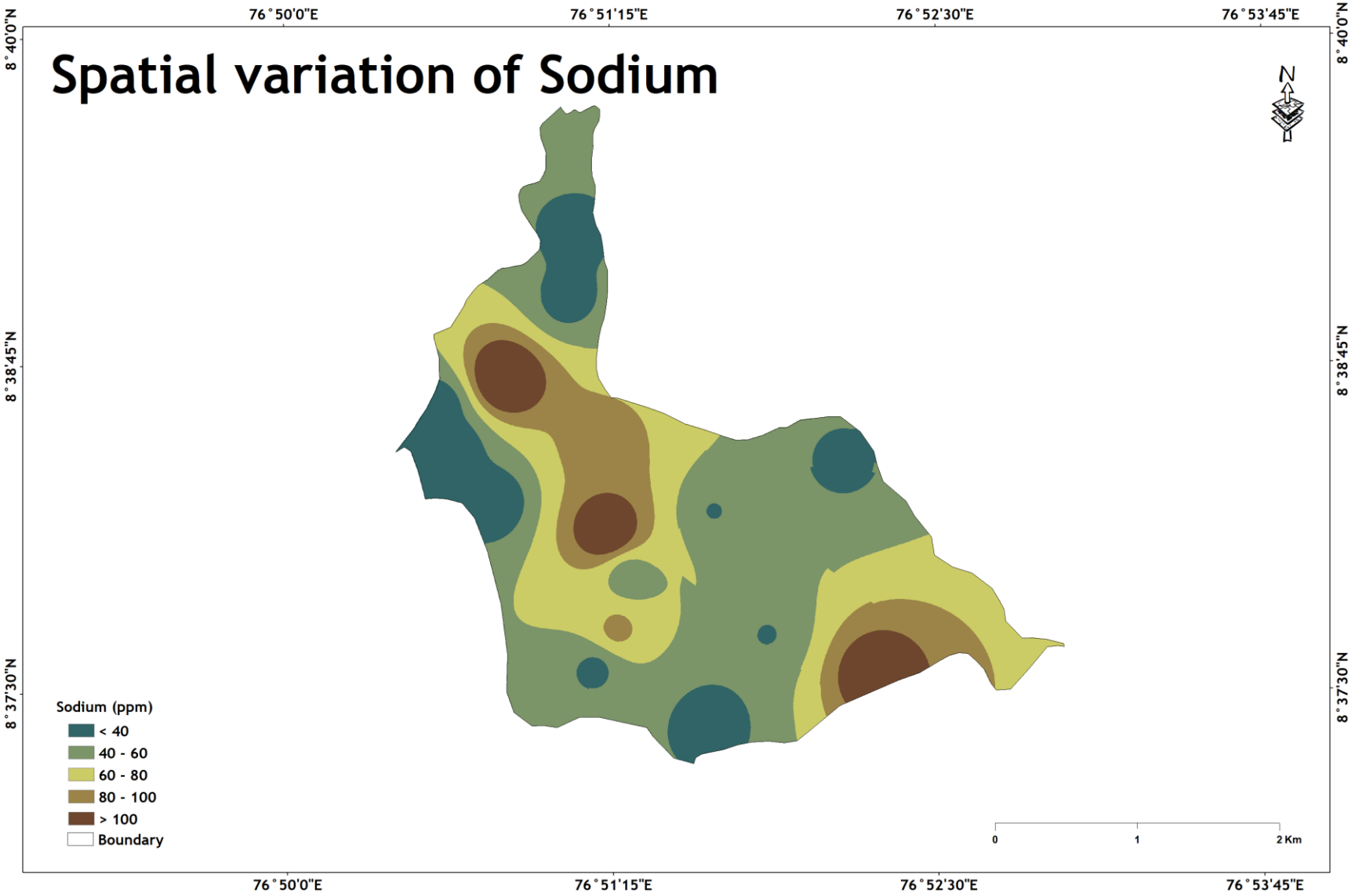

Fig.17 Spatial Variation of Sodium

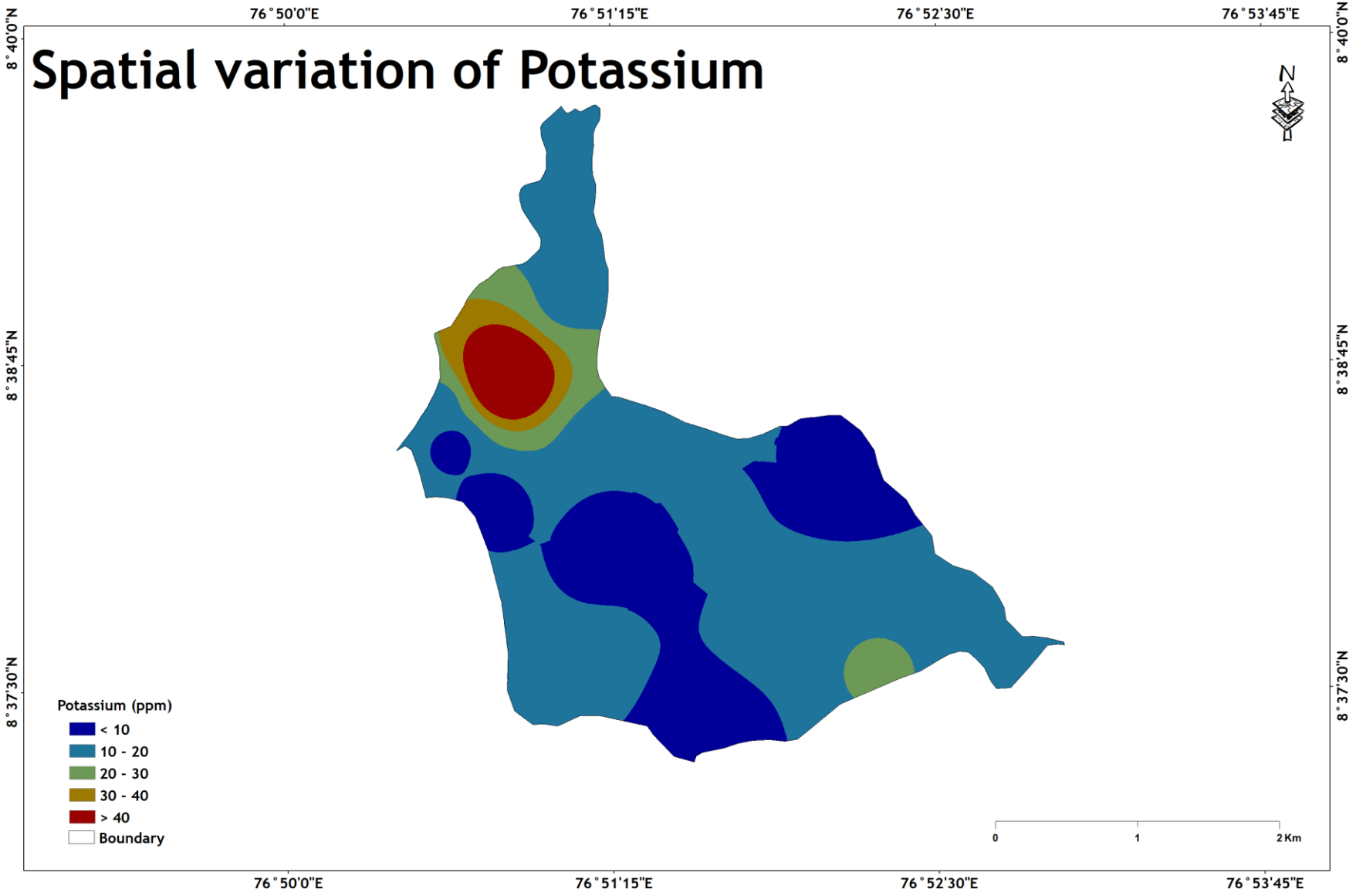

Fig .18 Spatial Variation of Potassium

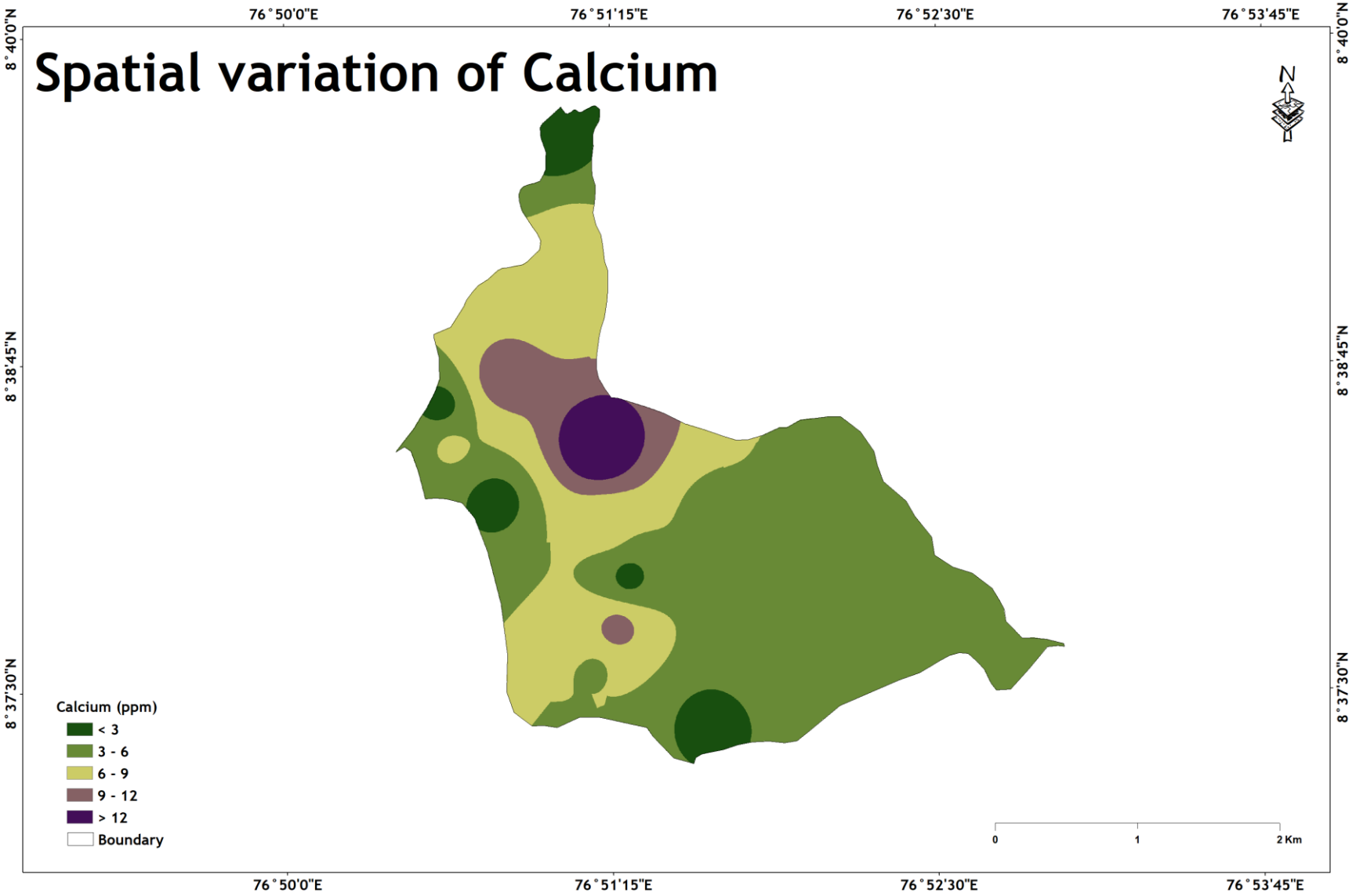

Fig.19 Spatial variation of Calcium

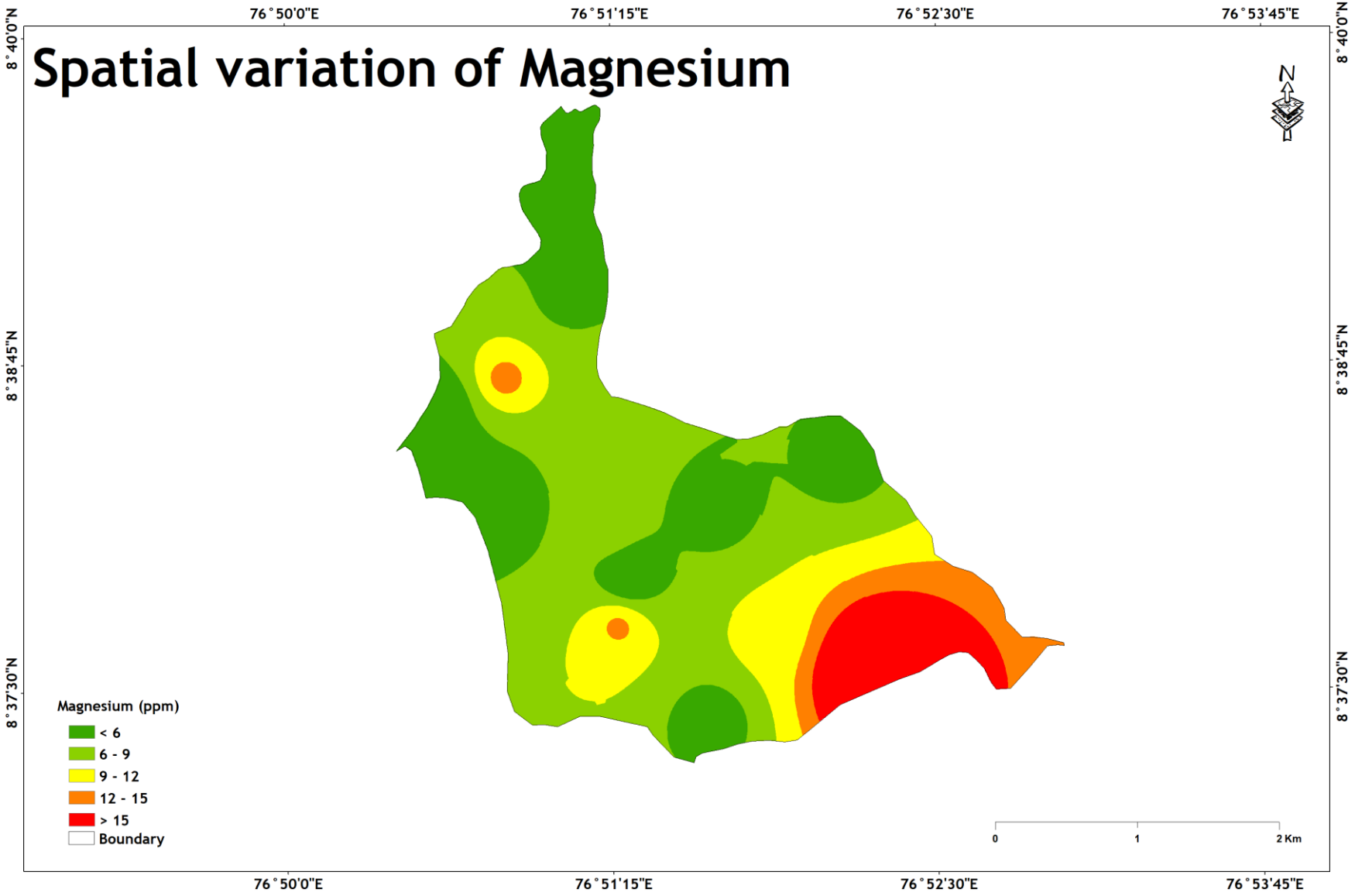

Fig.20 Spatial variation of Magnesium

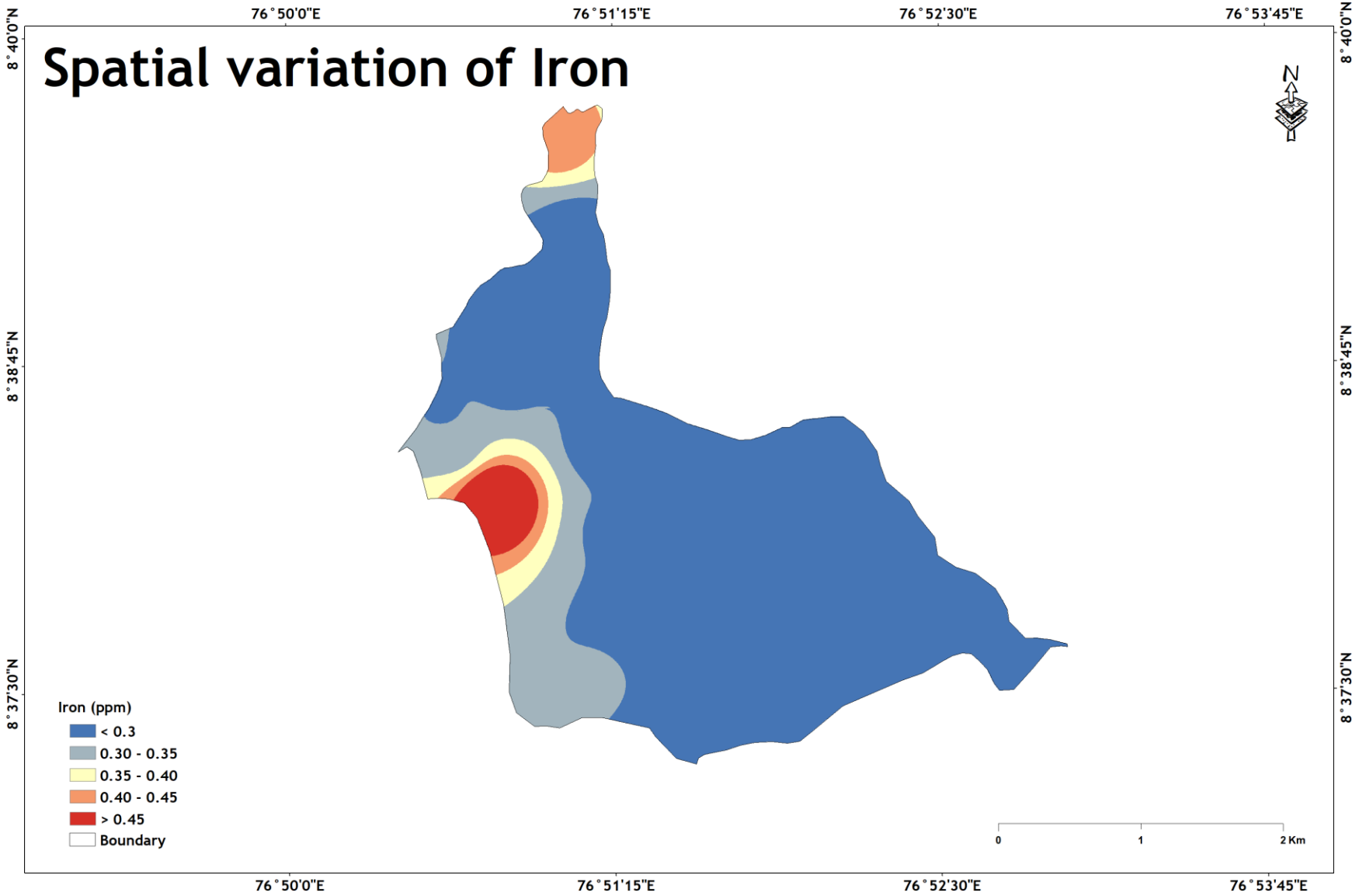

Fig.21 Spatial Variation of Iron

Fig 22. Spatial variation of Water Quality Index

PHOTOGRAPHS

Photo 2: Monitoring the water level

Photo 3: A working clay mine at Thonnakal

Photo 4: Dumping of clay waste at Thonnakal

Photo 5: Dried well at Thonnakal due to clay mining activities.

Photo 6: English Indian Clay Limited

Photo 7: Quality deterioration noted in Thonnakal

Photo 8: Thonnakal China clay mine

Photo 9: Abandoned well

Photo 10: Iron precipitation in marshy land

Photo 11: Reclimed paddy field

Photo 12 : Pool of groundwater in the clay mine

Photo 13 Analysis of water samples in NCESS

REFERENCE

A. Prabhakumar, & Sughada Pradeep. (2014). Exploration of china clay in and around Mangalapuram,Thiruvananthapuram district, Kerala.

Anju.P.S, & Jaya.D.S. (2022). Impacts of Clay Mining Activities on Aquatic Ecosystems; A Critical Overview. International Journal of Engineering and Advanced Technology, 128–134.

A.P.H.A. (1995) Standard methods for the examination of water and wastewater. (1995). American Public Health Association, Washington DC.

Archna, Surinder k, Sharma, & Ranbir Chander Sobti. (n.d.). Nitrate Removal from Ground Water : A Review. 9.

Bhola. RG, & Pravindra K. (2017). Environmental pollution monitoring modeling and control. Studium Press LLC USA.

BIS, (1991) Indian Standard specification for drinking water, Bureau of Indian Standards, New Delhi. (n.d.).

CGWB. (2013). Ground water resources and development potential of Trivandrum district, Kerala. 1–30.

Claudia Herbert, & Petra Doll. (2019). Global Assesment of Current and Future Groundwater stress with a Focus on transboundary Aquifers. Water Resources Research, 55(6).

David Keith Todd, & Larry W. Mays. (1980). Groundwater Hydrology. John Wiley & Sons.

District Survey Reports of Minor Elements. (2016).

Dr. K. Soman. (2016). Status Report on Ground Water Potential and Use in Trivandrum District with Special Emphasis on Trivandrum City.

Dynamic Ground Water Reaources of India. (2013).

Dynamic Ground Water Resource of Kerala. (2020).

Dynamic Groundwater Resources of India. (2017). Central Ground Water Board.

E.Shaji, Bindu, J.Viju, & D.S.Thambi. (2007). High fluoride in groundwater of Palghat District, Kerala. Current Science, 92.

E.Shaji, Gomez-Alday.J.J, Hussein.S, Deepu.T.R, & Anilkumar.Y. (2018). Salinization and Deterioration of Groundwater Quality by Nickel and Fluoride in Chittur Block, Kerala. Geological Society of India, 92, 337–345.

Gautam Mahajan. (n.d.). Evaluation and Development of Ground Water. Ashish Publishing House, 50–51.

Geology and Mineral Resource of Kerala, GSI. (2014).

Ground Water Information Booklet of Trivandrum District, Kerala State. (2013).

Ground Water Resources of Kerala. (2022).

Joji. V.S. (2017). Characterization, Classification and Evaluation of Groundwater in and around the Open Cast Mining of Clay Deposits of Thonnakal, South India .

K. Soman. (2002). Geology of Kerala. Geological Society of India, Banglore.

King.W. (1882). General Sketch of Geology of Travancore, Geological Survey of India. 15, Part 2.

K.K.Menon. (1967). Lithology and sequence of Quilon beds. Indian Academy of Sciences, 20–25.

K.Soman. (2002). Geology of Kerala, Geol.Soc.India, Banglore.

K.Soman. (2013). Geology of Kerala, Geological Society of India. 3.

K.Soman, & Terry Machado. (1986). Origin and depositional environment of the china clay deposits of South Kerala. Proc. Indian Acad. Sci, 95.

Mendie U. (2005). The Nature of Water. The theory and practice of clean water production for domestic and industrial use. Lacto-Medals Publishers, Lagos.

Mini Chandran, T.S. Anitha Shyam, P.Nandakumaran, & E.Shaji. (n.d.). Impact of clay mining on the groundwater regime in parts of Thiruvananthapuram district, Kerala.

Mohammad Salim Mohammad Tarawneh, M.R. Janardhana, & Mohamed Muzamil Ahmed. (2019). Hydrochemical Processes and groundwater quality ssessment in North eastern region of Jordan Valley, Jordan. HydroResearch, 2.

N. Subha Rao, Ch. Srihari, B. Deepthi Spandana, M. Sravanthi, T. Kamalesh, & V. Abraham Jayadeep. (2019). Comprehensive understanding of groundwater quality and hydrogeochemistry for the sustainable devopment of suburban areas of Visakhapatnam, Andhra Pradesh, India.

Natural Resources Data Bank, Thiruvananthapuram. (2013). Kerala State Land Use Board.

Report of the Ground Water Resource Estimation Committee (GEC). (2005).

Sonu Sasidharan, & D.S. Jaya. (2021). Metal Contamination of Groundwater Sources in the Environs of a Tropical Estuary in South India.

WHO (2011). Guidelines for drinkingwater quality. 4.

Zhengqiu Yang, Litang Hu, Haiyan Ma, & Wang Zhang. (2023). Hydrochemical Characteristics of Groundwater and their Significance in Arid Inland Hydrology.

SEDIMENT TEXTURE AND MICROFOSSIL ASSEMBLAGES OF THE SUBSURFACE SEDIMENTS OF CENTRAL KERALA: IMPLICATIONS OF HOLOCENE LAND-SEA INTERACTIONS

Dissertation submitted to Christ College (Autonomous), Irinjalakuda, Kerala, University of Calicut in partial fulfillment of the degree of

Master of Science in Applied Geology

By,

ANJANA AJITH

Reg. No: CCAVMAG003

2021-2023

DEPARTMENT OF GEOLOGY AND ENVIRONMENTAL SCIENCE

CHRIST COLLEGE (AUTONOMOUS), IRINJALAKUDA, KERALA,680125

(Affiliated to University of Calicut and re-accredited with by NAAC with A^{++} grade)

SEPTEMBER 2023

DEPARTMENT OF GEOLOGY AND ENVIRONMENTAL SCIENCE

CHRIST COLLEGE (AUTONOMOUS) IRINJALAKUDA

CERTIFICATE

Certified that the dissertation work entitled "**SEDIMENT TEXTURE AND MICROFOSSIL ASSEMBLAGES OF THE SUBSURFACE SEDIMENTS OF CENTRAL KERALA: IMPLICATIONS OF HOLOCENE LAND-SEA INTERACTIONS**" is a bonafide record of work done by Ms. Anjana Ajith (Reg. No. CCAVMAG003), MSc Applied Geology in the college during 2022-23.

Dr. Anto Francis K

Co-Ordinator (Geology Self-financing)

Christ Christ College (Autonomous) Irinjalakuda

Place: Irinjalakuda

Date:

External examiners

1.

2.

CERTIFICATE

This is to certify that the dissertation entitled – "**SEDIMENT TEXTURE AND MICROFOSSIL ASSEMBLAGES OF THE SUBSURFACE SEDIMENTS OF CENTRAL KERALA: IMPLICATIONS OF HOLOCENE LAND-SEA INTERACTIONS**", is a bonafide record of work done by Ms. Anjana Ajith (Reg. No. CCAVMAG003), MSc Applied Geology, Christ College (Autonomous) Irinjalakuda, under our guidance in partial fulfillment of requirements for the degree of Master of Science in Applied Geology during the year 2021-2023**.**

Dr. Linto Alappat
Dean of Research and Development of TLC,
Assistant Professor, Dept. of Geology and Environmental science
Christ College (Autonomous) Irinjalakuda,
Kerala - 680125

Place: Irinjalakuda

Date:

External examiners

1.

2.

DECLARATION

I thus certify that this dissertation – "**SEDIMENT TEXTURE AND MICROFOSSIL ASSEMBLAGES OF THE SUBSURFACE SEDIMENTS OF CENTRAL KERALA: IMPLICATIONS OF HOLOCENE LAND-SEA INTERACTIONS**"- is my own work. The report contains no quotations from external sources. All information derived from external sources has been properly credited. I maintain that if any element of the report is discovered to be plagiarised, I will accept full responsibility. Dr. Linto Alappat, Department of Geology and Environmental Science, Christ College (Autonomous), Irinjalakuda, Kerala, has provided necessary supervision for the completion of the work. I followed best practises and scientific study ethics. This work is presented to Christ College (Autonomous), Irinjalakuda, University of Calicut, Kerala, in partial satisfaction of the Master of Sciences in Applied Geology degree requirements.

Place: Irinjalakuda ANJANA AJITH

Date: Reg.NO: CCAVMAG003

ACKNOWLEDGEMENT

This report is official documentation of dissertation work carried out in the Vallarpadam Island, Kerala. It is a privilege for me to convey my gratitude and respect to those who guided and inspired the project's completion.

I would like to express my heartfelt thanks to my mentor, **Dr. Linto Alappat, Dean of Research and Development of TLC, Assistant Professor, Department of Geology and Environmental Science, Christ College (Autonomous) Irinjalakuda**, for including me, making timely comments, and guiding me through the completion of my research.

Tarun R, Head, Department of Geology and Environmental Science, Christ College (Autonomous) Irinjalakuda, for rendering all the help and facilities available in the department.

I would also like to thank **Dr. Sijin Kumar, Associate Professor, Central University of Kerala**, for allowing me to conduct this research at this institution and preparing thin section as well as identifying the microfossils.

I am grateful to **Dr. Anto Francis K**, **Co-Ordinator of the M.Sc. Applied Geology**, and the other faculty members of the Department of Geology and Environmental Science, Christ College (Autonomous), Irinjalakuda, for their encouragement, direction, and affection.

I'd like to express my gratitude to **Mrs. Shaima M.M** and **Mr. Ayyappadas C.S** for their continued support and assistance in completing the dissertation. I would like to take this opportunity to thank all of faculty, my classmates and friends who helped me finish this dissertation, either directly or indirectly. I am grateful to the entire Christ community. Thank you to my college family for their love, support, and advice. I would also like to thank my parents and family members for their everlasting support and prayers throughout my life.

Above all, I thank God, the Almighty, for his wonderful kindness and the benefits that have been bestowed upon me.

ANJANA AJITH

ABSTRACT

Vallarpadam Island is located in the Vembanad Lake of Ernamkulam District of Central Kerala. The area possess a unique opportunity to study the palaeogeography and land sea interactions due to its geographic location in the coastal plain. A 15m deep sediment core was raised using mechanically operated auger to sample the sub-surface sediments of the area. The core sediment from Vallarpadam Island was subjected to textural and micropaleontological analysis. Wet sieving is used for textural analysis. Paleontological analysis was carried out by making a fossil slide. These pieces of evidence revealed the Island's diverse depositional history, which included marine- marginal marine, intertidal, littoral, and supratidal environments.

Presence of the fossil foraminifera indicate that the depositional environment of the sediment occurs under marginal marine to marine condition due to marine transgression and regression during the Holocene. The majority of the fossil foraminifera discovered in the research area were benthic in nature; however, planktic forms were also discovered. Ammonia beccarii was the most frequent species found here. The presence of spores in a specific sequence suggests the presence of vegetation in the past.

Presence of peat layers, leaf impressions and fossil shells in the Holocene sediments indicating the geomorphic history of the region that was initiated by transgression which is followed by a regression. All of these indicating that the shoreline is initially migrated towards the east and was later towards the west at the stage of deposition

CONTENT

LIST OF TABLES

LIST OF FIGURES

LIST OF PHOTOGRAPHS

CHAPTER 1

INTRODUCTION

1.1. Quaternary Period

The Quaternary time period is the most recent geologic era in Earth's history, spanning from about 2.58 million years ago to the present day. It is part of the Phanerozoic Eon, which began around 541 million years ago and continues to the present. The period is divided into two epochs: the Pleistocene and the Holocene. The Northern Hemisphere glacial period began approximately 2.6 million years ago, and the Holocene is the most recent of the geochronological time periods that make up the quaternary period (Zalasiewicz et al., 2015).

The Quaternary period is more commonly known as the ‘Age of Man" or the ‘Great Ice Age’. The Pleistocene Epoch encompasses the time from about 2.58 million years ago to around 11,700 years ago, and was marked by more than 50 large-scale cycles of climatic oscillations, including the cold glacial interval and the warm interglacial period. The Holocene Epoch represents the period from 11,700 years ago to the present. Now the earth is experiencing the warm interglacial period after the civilization of humans. The shortest epoch in the history of the earth is commonly known as the Holocene.

The Quaternary period holds immense geological significance due to several key factors and events that have shaped the Earth's surface, climate, and ecosystems. It includes glacial and interglacial cycles, sea-level fluctuations, sedimentary records of landform evolution and environment, climate change, fossil records etc. These cycles are responsible for most of the global climatic changes, including the distribution of the flora, fauna, and human populations. It is, perhaps, the most important period of time because, despite its brevity relative to earlier periods, its materials cover much of the present landscape and provide soils and resources for agriculture and other human activities. As well as the subsequent evolution of hominids, it experienced the rise of Homo sapiens. It is, therefore, a time span on Earth that is both intrinsically and practically quite interesting and fascinating.

The quaternary period is characterized by number of glacial- interglacial cycles and associated landform modifications. The most recent glaciation, known as the Last Glacial Maximum, occurred approximately 26,500 to 19,000 years ago when ice sheets were at their peak extent. The Holocene Epoch marks a relatively stable and warm period. The advances and retreats of ice sheets during glacial and interglacial periods also led to significant sea-level fluctuations. As ice accumulated on land during glaciations, sea levels dropped, and when the ice melted during interglacial periods, sea levels rose. The changing sea levels influenced coastal environments and shaped sedimentary deposits found in coastal regions. The sedimentary records preserve valuable information about past climate, sea-level changes, and environmental conditions. Fossils found in Quaternary sediments provide essential information about the diversity and distribution of various species and provide insights in to the sedimentary environments in which they deposited.

Throughout the quaternary period, the earth experiences fluctuations in sea levels, changes in atmospheric composition, and shifts in global weather patterns. These climatic changes shaped the environment and influenced the evolution of species. As we know, the evolution of humans began prior to the quaternary period, but the species Homo sapiens evolved and thrived during this time. The first member of the Homo species evolved in Africa about 2 million years ago, which subsequently expanded and colonised every corner of the globe. With changes in their environment, these hominins changed their adaptation.

The Quaternary saw significant evolution of mammals. At this time, the majority of living species emerged, and many of them exhibit adaptations to the unusual Quaternary settings. The final stage includes the construction of lakes and offshore islands, as well as the continental steppe and tundra. Whereas some species have evolved flexible adaptations that enable them to occupy a variety of niches and deal with considerable environmental changes, others have evolved fixed adaptations to specific habitats. Pre-adaptation of mammal species to the longer-term cyclical changes of the Quaternary likely involved adaptation to short-term habitat change(Lister, 2004).

The geological processes and events of the Quaternary continue to have a profound impact on the modern environment and serve as crucial reference point for understanding Earth's history and predicting its future. Quaternary studies have attained great attention today because they not only reconstruct the history of the events but also analyse the work of present-day landscape formation and give an idea about future climatic changes. As a result, many scientists from

various disciplines, including geomorphologists, geologists, archaeologists, oceanographers, and climatologists, are now showing an interest in this field. Consequently, numerous institutions and organisations worldwide are currently conducting research on Quaternary geology, climatic changes, and sea-level alterations.

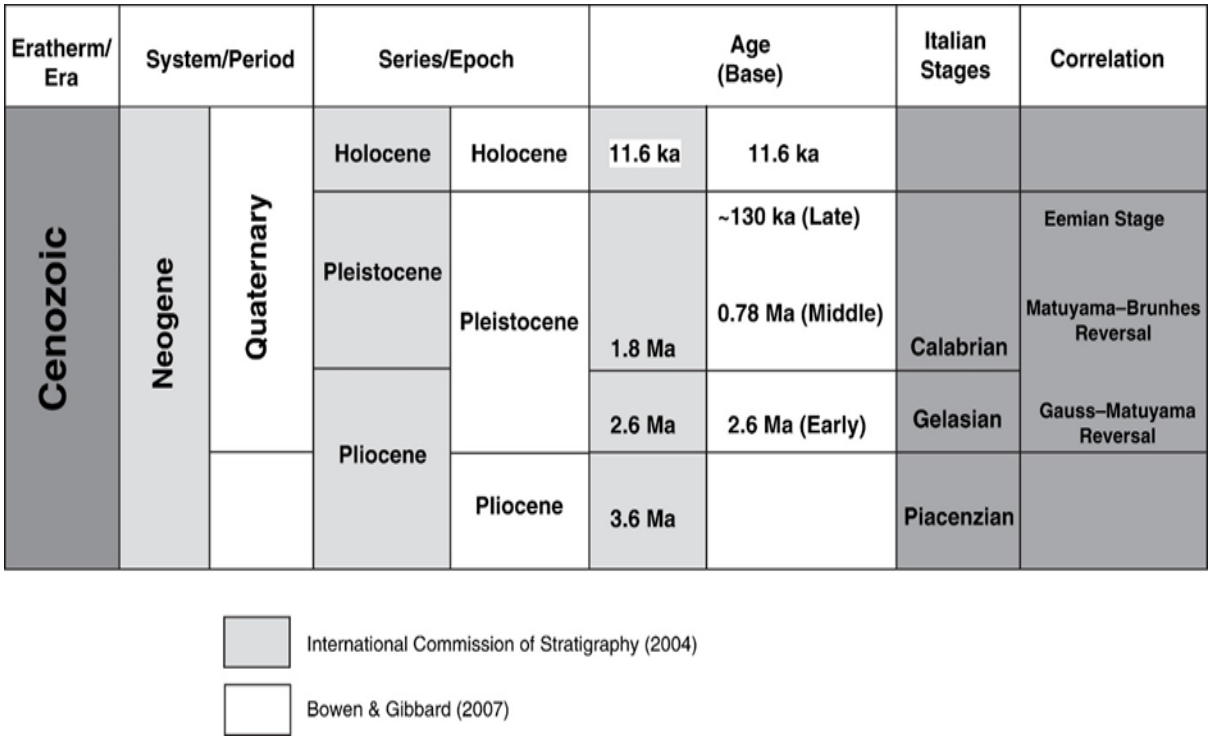

Figure 1. Quaternary period (Gradstein et al., 2004) and Bowen & Gibbard (2007).

1.1.1. Quaternary Sea Level Changes

The nature of the quaternary records varies with the environment of formation, which is widely marked between continental and marine environments. Interaction between Holocene climate and sea level changes has had notable effects on the geomorphic evolution of coastal environments. Throughout geologic time, sea levels have fluctuated, occasionally intruding or retreating across coastal plains (Lambeck & Chappell, 2001). The regions near the poles have experienced large changes in sea level, while those near the equator have experienced smaller oscillations.

The vertical movement of the land and change in ocean volume are the key factors that create changes in the relative positions of sea and land. Vertical movement of the land is caused by processes such as plate tectonics, volcanic activity, or isostatic adjustments due to the redistribution of mass on Earth's surface. Changes in ocean volume are mainly caused by the

melting or formation of ice sheets and glaciers as well as the pattern of precipitation and temperature. All of these actions were quite common in the quaternary period.

Earth's climate system changes due to both natural and anthropogenic processes. The statement "present is the key to the past" becomes more meaningful by studying and understanding the quaternary sediments. Geomorphic evolution in the coastal environment is a result of Holocene climate and sea level interactions. The early Holocene period saw the carving out of most of the coastal land due to transgressive sea and later land accretion by regression, and this geomorphic evolution had an impact on human history. Changes in sea level have influenced the evolution of coastal ecosystems such as lagoons, estuaries, and barriers, as well as the regulation of sedimentation rates in the coastal environment, over the Holocene.

Understanding the relationship between the surface deposit and deposits that date from one cycle of relative sea level fluctuations is made possible by the study of Quaternary deposits on the continental margins (Posamentier et al., 1988). Although modern processes have had an impact, late Pleistocene paleo topography appears to be a fundamental component in determining the areal distribution of Holocene deposits. The Holocene Sea level variations, the layout of the coastal land, and the sediment intake from the rivers are some of the additional significant elements that affect the Holocene sedimentation. In recent years, there has been a focus on tackling climate change associated with sea level oscillation, particularly in coastal lowlands and nearby areas in late quaternary deposits (Loveson et al., 2019).

1.1.2. Coastal Landforms

The coastal zones provide valuable and important ecosystem services and forms as a transitional space between terrestrial and marine environments (Crossland Christopher J. and Baird, 2005) 40% of world population live within 100 km of a coastal zone, and 60% of major cities are situated in coastal regions (Nicholls et al., 2007). Coastal depositional environments are the result of continental and marine processes. Interaction between waves, tides, and other oceanic and atmospheric processes are responsible for the formation of coastal landforms. In addition to natural processes, human activities have a significant impact on how the world's coastline is degrading (Stanchev et al., 2015). Some of the natural forces that cause change in the landscape include sea level rise, changes in the sediment rate, aeolian activity, incident wave energy, etc. (Psuty et al., 2018).

The transitional zone between oceans and continents where sediments are deposited is commonly termed the ocean margin," which extends from the coastal zone across the shelf and the continental slope to the continental rise. Intertidal zones are located along marine coastlines, which include both rocky shores and sandy beaches. Due to constant and drastic changes at this region causes emergence of the extreme ecosystem. Across the gradient of elevation within the intertidal zone, species have a tendency to develop their own communities, depending on the climate. The basal part of this zone consists of several plant species, usually benthic, to resist the wave energy. The portions that are submerged under the water are known as subtidal zones. Zones that are close to the ocean but above the peak of the tide so that salt water only enters during the greatest tides or storms are called supratidal zones. The bathymetry is shown in Fig. 2 below.

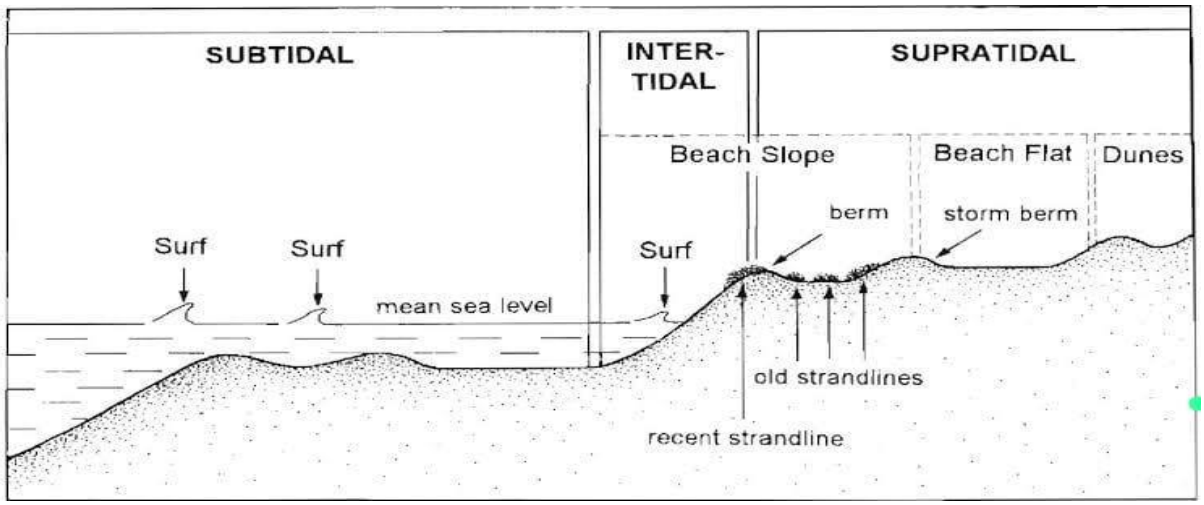

Figure 2. Coastal environment

There are two types of facies arrangements: those associated with transgressive depositional sequences and those related with regressive sequences. Transgressive sequences are associated with both prograde and stationary barrier types and are generated during the Postglacial Marine Transgression. In the Northern Hemisphere, the thickness of nearshore facies is frequently greater than corresponding units beneath barriers on lower energy beaches and for less steep inner shelf gradients. The interaction of numerous variables inside embayment's has resulted in the creation of several barrier types, including prograde, fixed, receding, and episodic dune, all of which share some sedimentary characteristics with similar kinds recognised elsewhere in the world (Thom, 1984).

Barrier islands are extremely dynamic coastal systems that are typical of these transitional habitats. They are impacted by variations in sea level and the buildup of transgression deposits as the shoreline moves inland. Late Quaternary clastic transgressive coasts often consist of typical barrier-lagoon systems that migrate landwards as the sea level rises, and these are representing coastline retreat; thus, they may occur with high frequency and amplitude due to glacio-eustacy.

Microfossils are abundant in coastal deposits, as their small size allows the collection of significant populations using core samples. The high preservation capability of coastal sediments allows for reconstructions that span thousands of years. Microfossils are particularly efficient as a proxy for marine inundation in coastal sequences because to their various ecological niches, which span the full environmental gradient given by the coastal zone, from marine to freshwater conditions. Diatoms and foraminifera are environmental indicators. Diatoms survive well in sedimentary records and in temperate to cold climates. Foraminifera exist freely on sediment (benthic forms), on rocks, shells, and corals (attached benthic forms), and within the water column (planktic forms) from brackish to marine habitats. Testate amoeba and salt-marsh foraminifera can be used to provide information on freshwater sources in the coastal zone. A predictable distribution of agglutinated assemblages restricted to vegetative marshes and calcareous assemblages dominantly found on mudflats and sandflats is a feature of benthic foraminifera in the intertidal zone (Pilarczyk et al., 2014).

1.1.3. Global Quaternary Scenario

With each pulse, glaciers from the poles advance and retreat, sculpting and reshaping the landscape, and with every glacial- interglacial cycle, the sea level drops and rises. Humans develop into their present forms, wander the planet, and have an impact on almost every aspect of the environment, including the temperature.

During Ice ages, large ice sheets covered many parts of the northern and southern hemispheres. The most recent periods of widespread glaciation occurred during the late Pleistocene epoch, which reached its peak during 18 ka ago. The advancing and retreating of the glaciers are responsible for sculpting and moulding the land. These dynamic movements have given rise to valuable geological features like U-shaped valleys, moraines, and fjords.

Study and comprehension of the interactions between ancient creatures and their surroundings are commonly termed "paleoecology," and when the studies occur 2.7 million years ago, they are subsequently known as "quaternary paleoecology. It will facilitate an understanding of how organisms evolve. Large animals like mammoths, mastodons, giant ground sloths, sabre-toothed cats, and short-faced bears were driven to extinction as a result of the land bridge's creation during the Pleistocene epoch. The other causes of these extinctions include rapid climatic changes and the evolution of humans (Wicander and Monroe et al., 2000). The interaction between the geosphere and biosphere has given rise to various sea level changes in the earth's history. A different stage of sea level change, including both transgression and regressive phases, was seen during the quaternary. Changes in global warming and other natural sources are the main factors.

The impact of individual volcanic eruptions on regional and global meteorological conditions was originally identified by Franklin (1789) and has since been thoroughly investigated by Lamb (1972). The higher-scale quaternary glacial changes could have been caused by volcanic activity. (Zielinski et al., 1996; McGuire et al., 1997).

Various types of quaternary deposits can be found all over the world. Some are listed below:

The Holocene evolution of coastal systems was caused by complex relationships and temporal shifts in the relative contributions of sea-level variations, climate change, and sedimentary processes. Despite continued, rather rapid sea-level rise, Wadi sediment intake, aided by a period of wetter climate in the early to mid-Holocene, drove the closure of coastal embayment's. This bay was the principal trading port for ancient Egyptians along the Red Sea coast. During the late Holocene, sea-level fall, driven by isostatic processes, dominated coastline progradation. These findings show how multiple global sea level, regional climate, and local bathymetry controls influenced the Red Sea's coastline evolution, and how these variables influenced the response of a complex civilization (Hein et al., 2011) .

Several parts of the Brazilian coast have relative sea-level curves marked. It shows that the central Brazilian coast had a submergence phase that lasted until 5600 Cal year BP, followed by a reduction in sea level. This decrease in sea level was not continuous, but was broken up by two high frequency oscillations (Martin et al., n.d.).

(Banerji et al., 2017), studied sediment cores raised from an active mudflat on Diu Island, off the coast of Southern Saurashtra in Gujarat, which indicated warm and humid conditions during the Holocene Climate Optimum between 4105 and 2640 Cal yr BP as a result of monsoon intensification, followed by arid conditions between 2640 and 1930 Cal yr BP Later, approximately 1930-355 cal yr BP, the region experienced a return to warm and humid conditions. The mudflat responded to global climate perturbations throughout the last 2000 years. Furthermore, cold and humid climatic conditions continued during the Little Ice Age, followed by the Modern Warming Period observed during the last 300 years.

1.1.4. Indian Quaternary Scenario

In India, where a wide range of archives across a large geographic area have a rich manifestation of the Quaternary period and contributed to shaping the development of various landscapes, The Himalaya, Ganga basin, Bay of Bengal, Thar desert, coastal, and marine records are major resources of the Quaternary deposits in India. The significant features of the Indian Quaternary are as follows:

Glaciation: Glaciers adapt to the climate system by shifting their mass balance and thus serve as a proxy for quantifying the changes on both a regional and global level (Yao et al., 2012). The Quaternary glaciation of India is well defined in the Himalayan region. The studies (Sati et al., 2014; Shukla et al., 2018) give an idea about the past climate of India and the extent of the glacial period in the past. Since successive glaciations have reshaped and altered the topography that was originally carved over 2.6 million years by hundreds of preceding glaciations, the majority of these preserved landscape signatures date to the late Quaternary epoch.

Landforms: Quaternary rocks give rise to various landscapes in India. Common formations during the quaternary period are the, alluvial plains, Brahmaputra River, Ganges, and Narmada graben. This terrain of today is the outcome of certain processes like weathering, erosion, and mass wasting. There are a few distinct occurrences of Quaternary deposits throughout the peninsular India, all along the western and eastern coasts. Thick deposits of Quaternary strata are found in the central part of India, primarily along the banks of the Narmada and Tapti River Valleys, in the Bengal Basin, and in areas of Rajasthan and Gujarat. The Deccan Plateau's flat-topped hills were generated by the uplift of fault-bounded blocks during the late Quaternary

epoch. The Quaternary formations in the Himalayas are the youngest portions of the Siwalik Group (A. B. Roy & Purohit, 2021).

Evolution of humans: About 73,000–55,000 years ago, the first humans appeared in India, which commonly migrated from Africa. The known species that evolved here were Homo erectus, including the acclaimed Java man and Pecking man, which were followed by Homo sapiens about 80,000–65,000 years later. Most of the traces of human evolution were found in South India (Jain & Anantharaman, 1996).

Paleoclimate and paleoenvironmental changes: Dynamic conditions in the environment leave geological signals in the sediment records that can be employed to interpret paleo-ecological and paleoenvironmental backgrounds (Meyers & Teranes, n.d.). Diatoms, foraminifers, speleothems, stalactites, stalagmites, phytoliths, and sediments have all been used in the reconstruction of paleo-monsoon records from the Late Quaternary to the Holocene in the Indian subcontinent (Agarwal et al., 2023; Carter, 2007; KEERTHINAIR et al., 2014; Kotlia et al., 2018).

The Quaternary period of India witnessed plenty of significant environmental changes along with the emergence of human civilization and with the extinction of large mammals (Jukar et al., 2021). Researchers are now more concerned about the earth's history and our current state of life on the planet as a result of numerous investigations conducted regarding the geological and paleontological evidence that took place in India throughout this time.

1.1.5. Kerala Quaternary Scenario

The formation of the Indian subcontinent as a separate landmass during this time, which started around 50 million years ago and was largely finished by the end of the Quaternary period, had a significant impact on the area's climate, terrain, and biodiversity. The Kerala coast has an assortment of peculiar geomorphic traits that originated from interaction between land and sea across the Late Quaternary. A transgression (8000-6000 Y.B.P) and regression (3000-5000 Y.B.P) event that triggered in an extensive peat and shell deposit across the Kerala's coast during the Holocene. These events resulted in the establishment of Kerala's backwater system.

Quaternary sediments of Kerala were well distributed in Quilon, Kottayam, Trichur, Alleppey, Ernakulam, Calicut, Cannanore, and Kasargod districts. A polymictic pebble bed, then separate these inland sediments from the tertiary sediments. During the quaternary period, the Kerala

coast noticed an array of major shifts, opening with a climate like that of a tropical rainforest but less hot and arid. The rainforest has been displaced by more open woodlands and grasslands as a result of an evolving climate that became dryer and cooler over time.

The Western Ghat had an enormous influence on the region's ecology and biodiversity due to their work as a barrier dividing Kerala from the drier regions to the east. The western ghats are thus a home to an abundance indigenous animal and plant species.

The origin of Homo sapiens was witnessed in the Indian subcontinent, with significant evidence also found in the southern part of India, especially those part of Kerala due to the vast forest and wetlands.

Kerala's Quaternary sediments include alluvium, beach sand deposits, lime shell deposits, red sands, peat beds, and calcareous clays with shells, all of which are underlain by laterite in the coastal area, indicating an unconformity with Mio-Pliocene sediments. These sediments are widely spread in low-lying areas (C. P. et al., 1989). During the Quaternary period, sea level and climatic variations had a significant impact on the geomorphic and sedimentation processes in coastal locations. During the Holocene, sea level variations influenced the evolution of coastal ecosystems such as estuaries/lagoons and barrier complexes, as well as controlling sedimentation in coastal areas. Although Pleistocene paleo-topography appears to be the most important element in regulating the areal distribution of Holocene deposits, current processes have also played a role. Other key elements that influence Holocene sedimentation include Holocene Sea level variations, coastal land layout, and river sediment intake(A. Narayana, Research, et al., n.d.).

During the late Quaternary period along the Kerala coast, SW India, recurring sea-level variations are represented in the construction of coastal landforms such as estuaries, lakes, lagoons, and barrier beaches. To reconstruct the late Quaternary environment, the sediment core from these landforms was examined for sediment lithofacies, geochemical parameters, and associated foraminiferal assemblages. The textural properties of this substance imply a swampy/marsh and shallow marine to lagoon environment. The late Pleistocene (40 Kyr's BP) sediment sequence is overlain by a layer of coarse sandy material. The sediment was deposited in a variety of energy regimes, ranging from violent to quiet. An abundance of Ammonia beccarii, A. tepida, E. discoidale, and N. scaphum in the sediments demonstrates their high tolerance and adaptation to changing environments. Sediment studies show a stronger monsoon in the early Holocene, resulting in high-water levels, higher river discharge, and bottom

scouring, whereas a weak monsoon and arid environment prevailed during the Last Glacial Maximum (Tiju et al., 2021).

Overall, Kerala's history as well as the history of the larger Indian subcontinent underwent substantial change and modification during the Quaternary period. The region's terrain and biodiversity were shaped by the geological, climatic, and ecological changes that took place throughout this time, setting the groundwork for Kerala's rich cultural and natural history that is still there today.

1.2. Foraminifera

Protozoans, commonly known as foraminifera, are monocellular protoplasmic cells with one or more nuclei. These unicellular organisms are available in sizes ranging from 0.01 cm to 8 cm. These microorganisms are found below the ocean at a depth of about 5–5000 m. Forams have existed since the Cambrian. Foraminifera is a Latin word that means hole bearers. D'Orbigny (1826) released the first comprehensive descriptions of planktic foraminifera. The Challenger voyage of 1872–1876 brought about advancements in foraminiferal investigations.

Foraminifera could be found in both planktonic and benthonic forms. Currently, there are about 40 different varieties of planktonic foraminifera in the ocean. Thus, 1% of the foraminifera species are still in existence. The remaining 99% are benthic foraminifera (Heinz et al., 2002). Planktonic forms mainly inhibit the open ocean and are rarely abundant in coastal waters, whereas benthonic foraminifera exist on substrates ranging from abyssal plains to high intertidal zones.

Planktonic foraminifera are often known to be planktonic forams and are primarily classified on the basis of the morphology and ultrastructure of the tests. Some of the early forms only have cells without tests. Foraminifers switched to a planktonic mode around 200 million years ago, during the Jurassic. There was a rapid growth of forams throughout the Cenozoic, especially during the Cretaceous; hence, they became ideal stratigraphic markers.

Benthic foraminifera and their ecology have gained great importance over the last 40–50 years (Murray, 2007).It is a group of meiofaunal organisms that are widely distributed in marine environments. Changes in temperature and salinity, which are the most striking properties of ocean water, cause the diversification of forams. While other notable changes in the forams are

caused by depletion in the amount of dissolved oxygen, this will help in the correlation of the modern environment with past oxygen-depleted habitats.

Foraminiferal test is mainly composed of calcareous, arenaceous, chitinous, siliceous, or gelatinous matter that is secreted by the animals or is formed by the process of agglutination of exotic particles like sand, coccolith, sponge spicules, etc. Among these, calcium carbonate ($CaCO_3$) is increasingly popular and preserved. Chitinous shells do not occur as fossils. Tests are usually made up of numerous cavities termed "chambers," and the first chamber of the foraminiferal tests is known as the proloculus.

Kingdom: Protista

Phylum: Protozoa

Superclass: Sarcodina

Class: Reticularia

Subclass: Rhizopoda

Order: Foraminiferida

shallow water Foraminifera are the most beneficial for sea-level examinations because their life range is more easily linked to sea level. Foraminifera may exist in the topmost intertidal zone. Another distinguishing advantage of using Foraminifera as sea-level indicators is that abundance is often high in salt marshes while species diversity is low. The agglutinated species found in the higher regions of salt marshes are also well preserved in fossil deposits. Foraminifera are less valuable in sediments from the lower intertidal zone. Calcareous species (e.g., Ammonia) are found here, and these are not well preserved in sediments due to dissolution, especially when the sediments are organic in nature and acidic conditions are present. The natural processes which generate intertidal zonation become less significant in deeper seas, thereby reducing Foraminifera's sea-level indicative value (Gehrels, 2013).

Foraminifera are abundant in the current oceans, and in water that extends from the continental shelf out to a depth of at least 2000 metres, their testing contributes to the formation of the dense globigerina slime that covers the ocean floor. Benthic foraminifera are commonly found in the sands of tropical beaches, and in shallow water, their abundance creates obstructive shoals. Benthic foraminifera balance planktic species in coastal locations, and their

assemblages are frequently depth dependent, with various species preferring different water depths. This is especially true in intertidal settings, where agglutinated foraminiferal assemblages' depth dependent has been applied to reconstruct relative sea-level change. Foraminifera are durable and can withstand transport and post-depositional activities, in addition to being numerous in tiny sample sizes and possessing species assemblages that can reflect sediment provenance and biological context (Hawkes, 2020).

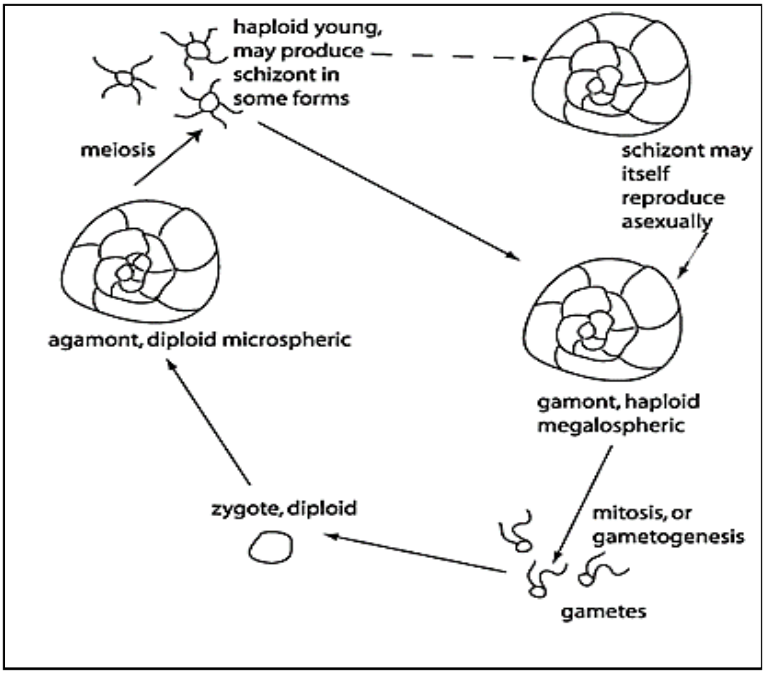

Figure 3. Life cycle of foraminifera (Redrawn from Goldstein et al., 1999)

1.2.1. Foraminifera as Paleoenvironmental Indicators

Due in part to recent studies on the dead and live assemblages in marine marginal settings, benthic foraminifera have long been known as valuable tools for reconstructing paleoenvironments (Murray, 2001). Foraminifera species diversity, abundance, and distribution can all reveal important details about previous environmental circumstances.

It's notable to note that despite the large number of long-term seasonal studies that have been conducted for populations of benthic foraminifera, practically all of them have only addressed changes in the live population. None have thoroughly addressed changes in the matching total assemblages (Tiju et al., 2021). According to Murray, only assemblages of extant benthic foraminifera can provide information on the paleoenvironment. Foraminifera can be employed in the following ways to reconstruct the paleoenvironment:

Paleoecology: Foraminifera species vary in their ecological preferences, which include things like water depth, temperature, salinity, and nutrient availability. Researchers can determine the palaeoecological conditions of the past by examining the foraminiferal assemblages preserved in sediment cores or fossil deposits. For instance, the presence of specific species may indicate a shallow- or deep-water environment, and variations in the species composition may signal changes in temperature or nutrient availability.

Paleoclimate: The climatic conditions of the past can be deduced from foraminifera. Some species are very sensitive to temperature changes, which makes them useful proxies for estimating historical sea surface temperatures. Analyses of the oxygen and carbon isotopic compositions of the foraminiferal samples can also reveal details on previous climate variables like ice volume, ocean circulation, and productivity.

Palaeoceanography: Oceanographic conditions from the past can be reconstructed using foraminifera. It is recognised that certain species live in particular oceanic areas, such as upwelling zones or places impacted by nutrient-rich currents. Scientists can retrace previous oceanic circulation patterns, upwelling events, and alterations in nutrient availability by examining the distribution patterns of foraminifera in sediment cores.

Sea level changes: Using foraminifera, you may retrace historical sea-level changes. The vertical distribution of some species within sediment cores can change over time, and these changes can reveal information about historical sea-level changes. Some species are indicative of particular water depths. Researchers can reconstruct relative sea-level fluctuations and deduce tectonic or eustatic processes by examining foraminiferal assemblages in conjunction with other sea-level indicators, such as microfossils and sediment types.

Environmental pollution: The past levels of pollution in marine habitats can be evaluated using foraminifera. Pollutants like organic pollutants or heavy metals can be especially harmful to some species. Researchers can retrace the history of pollution episodes and gauge how human activities have affected marine ecosystems by examining the presence or lack of organisms that are tolerant of pollution or have a typical morphology in foraminiferal assemblages.

Foraminifera are frequently used to define and connect particular geologic time periods because they are index fossils. An index fossil is a fossilised creature that serves as a marker for a specific geological era or time period. In general, index fossils are widely distributed

geographically, numerous in the rock record, and have a brief existence. They can be used to date and correlate sedimentary layers and rocks in various places. Some of the common species known to be index fossils are:

Globigerina bulloides: As an indicator fossil for the Pleistocene era, this species of foraminifera is frequently employed. Deep-sea cores and coastal regions are just two examples of the many places where it can be found in marine sediments (Shrivastava et al., 2016).

Globigerina falconensis: It is a planktonic foraminifera species in the genus Globigerina. The species are mainly found in marine sediments. Globigerina falconensis is remarkable for being used as a bio stratigraphic marker in geological research. Globigerina falconensis found in sediment cores or outcrops can help geologists determine the age and correlation of those deposits (Fabbrini et al., 2022).

Nummulites: The Eocene epoch's key index fossil is from the genus Nummulites. These massive, coin-shaped foraminifera were widely distributed around the world and can be discovered in a variety of sedimentary strata from that epoch (Monjezi & Saeedi Razavi, 2021).

Ammonia beccarii: The Holocene epoch, which corresponds to the current geological epoch, is often employed as an index fossil thanks to Ammonia beccarii. It is a foraminiferal species that is widely distributed and abundant in estuarine and marine habitats (Debenay et al., 1998a).

Globorotalia: Numerous species in the genus Globorotalia serve as indicator fossils for various geological eras. For the Pliocene epoch, Globorotalia menardii is utilised as an index fossil, whereas Globorotalia truncatulinoides is employed for the Pleistocene epoch (de Vargas et al., 2001).

Heterohelix globulosa: An essential indicator fossil for the Cretaceous era, it is frequently discovered in sediments from the ocean and is used to date biological strata (Abramovich et al., 1998) .

Nonion subturgidum: It is a foraminiferal species found in marine sediments that is benthic. It is a member of the Nonionidae family, which comprises a wide range of shell forms and ornamentation. These foraminifera are important in paleo-oceanography and paleoclimatology because they can be used as bioindicators to recreate historical environmental conditions (Debenay & Luan, 2006) .

Bolivina acerosa: Is a species that coming under genus Bolivina. Is a widespread group of benthic foraminifera found in marine settings all over the world. Foraminifera in the genus Bolivina typically have a coiled or planispiral shell, and the shape, decoration, and size of the shell vary depending on the species. These animals are key indicators in paleo-oceanography and paleoenvironmental studies because they play a vital role in marine ecosystems (Obiosio, 2013).

Among these, the most notable species is Globorotalia, which was abundant in marine environments. Depending on the locality and the geological era being investigated, different species may be used as index fossils.

Some of the most common foraminiferal species discovered on Kerala's southwest coast (Gandhi & K.Jisha, 2016; Radhakrishnan et al., 2016), includes:

Ammonia beccarii

Ammonia beccarri is a widely distributed species. It is most commonly seen in littoral and neritic environments. It is most common in marine environments with salinities greater than 33 ppm. The ammonia test is sparsely decorated, with no distinct beading, furrowing, or either spiral or umbilical sides. Ammonia beccarii, on the other hand, has prominent spiral side decoration and deeply etched sutures. Which can only be found in a marine environment. In the intertidal zone, one can find the alga Corallina officinalis. As a result, it is in phytal form. A closer examination reveals that it is found under moderate-to-strong energy conditions rather than very powerful energy. Free-living species are uncommon.

The tests are biconvex and trochospiral, with about 10 angular chambers on the umbilical side in the last whorl. Granules are formed in adults. Deeply carved sutures with noticeable thickening on the umbilical and spiral sides provide gaps between subsequent whorls and an open interlocular area. It lives in an epipelic or shallow endopelic habitat as well as an epiphytic habitat. Sediment containing this foram cannot be dated beyond a generic late Miocene-recent time frame. (Debenay et al., 1998b)

Bolivina sp.

The aperture of Bolivina sp. is narrow. Extend a test that may have been compacted. Chambers are broad and low, and they are biserially distributed throughout; the basal margin of the chambers has a retral process, or backward-directed chamber overlap. The shell is usually made

of calcium carbonate. The suture is perforated and radial. Extend the loop on the chamber face. They are benthic. Marine, freshwater, and terrestrial environments are all home to this species. In other words, these species are best observed in low-oxygen bottom water or pore water. Typically, the species are present form Holocene – Recent (Obiosio, 2013).

Nonion subturgidm

Nonion subturgidm is a common species found in the marine environment. The tests are bilaterally symmetrical, compressed, and last produced coils with 8 to 9 chambers. The length is rapidly rising. Round on the periphery. The sutures are gently recessed. The face of the aperture is substantially rounded. Secondary material is frequently used to fill the umbilical area.

Typically, they live in shallow-water environments, primarily on the shelf. They are benthic organisms. Presented throughout the Holocene epoch**.**

Nonion sp.

Nonion sp. is a common species found in the maritime environment. They had a planispirally coiled shape that was involute and finely perforated. It has a simple opening and is found at the base. The chambers range in shape from triangular to trapezoidal.

The age ranges from the Holocene to the Recent.

Globigerina bulloids

Globigerina bulloids has the following characteristics: Tests are free, varied in size, low to medium trochospiral, firmly lobulate, chambers are spherical to slightly oval and well separated, size increasing gradually, sutures deep, consistently and densely perforated calcareous wall, simple, circular-sectioned spines, umbilical aperture. It mainly occurs in subpolar regions, but it is also frequent in upwelling zones and boundary currents in low-latitude regions with strong surface production. It mainly happens in upwelling areas of cold subpolar water. The age ranges from Pliocene to the Recent (Shrivastava et al., 2016).

1.3. AIM AND OBJECTIVE

The main of the study is to analyse:

1. Microfossil assemblage and textural characteristics of shallow subsurface sediments of Vallarpadam to identify the paleoenvironmental changes in the area.
2. Identify the changes in Holocene Sea level changes using the microfossil assemblages in the sediment core.

CHAPTER 2

STUDY AREA

2.1 Location

The study area is located in the Ernakulam district of Kerala State in the Indian subcontinent. The district is divided into three physiographic zones: the coastal plains in the west, the midland region in the east, and the steep to very steep hills in the easternmost part.

The coastal plains, which have a maximum elevation of around 10 metres, are low-lying regions with backwaters, marshes, sand flats, alluvial plains, and the unusual beach-ridge swale complex. During monsoon, the area is vulnerable to floods. The geography of the midland region is rolling, with low hills and narrow valleys. The low hills are often covered in laterite caps or lateritic soils, while the valleys are relieved.

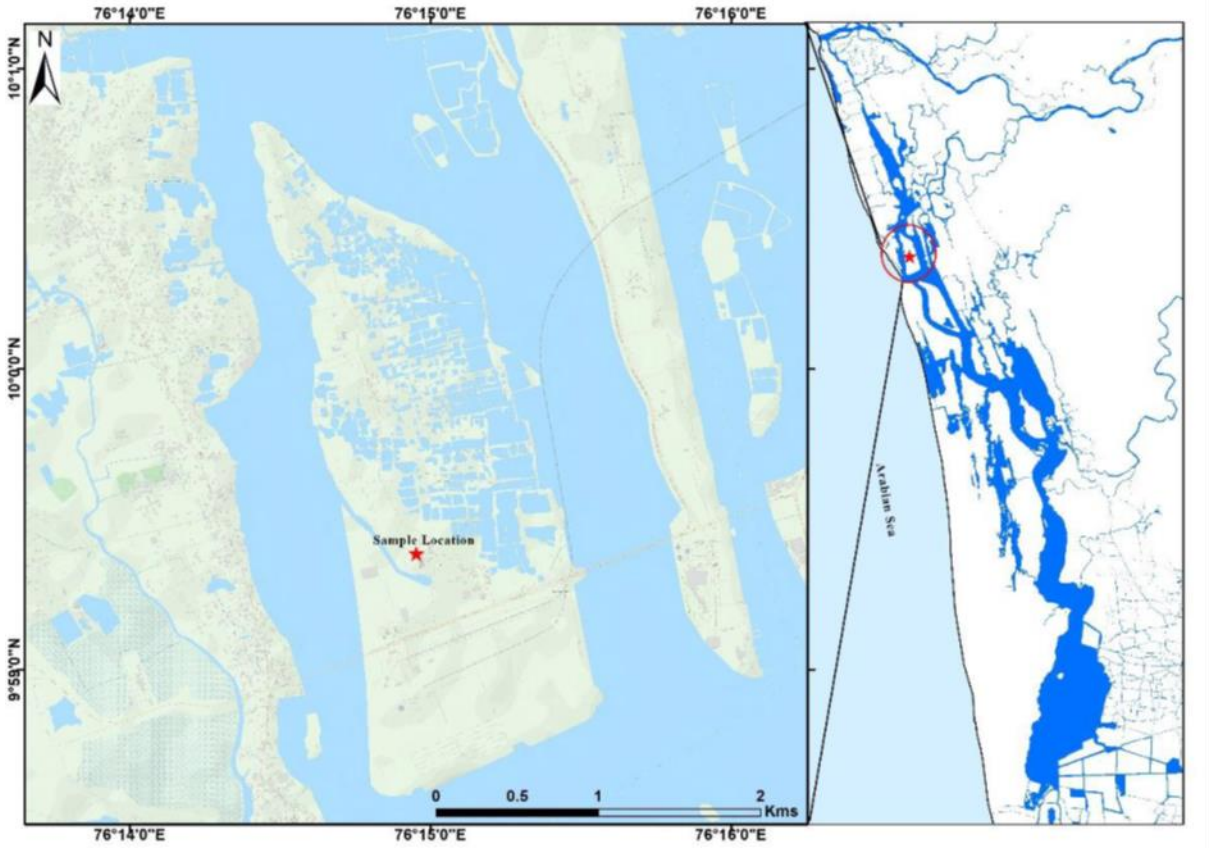

Fig 4. Study area map showing core location in the Vallarpadam Island

The area is having gentle to moderate slope from east to west. The district's easternmost region is made up of rough terrain with steeply sloping hills and tiny summits that make up the foothills of the Western Ghats. The elevation of the area is typically greater than 300 metres above mean sea level.

Our study is concentrated on the coastal plains of the western Ernakulam district, especially on Vallarpadam island (Lat: 9.989772, Long: 76.249231), one of the two islands around which the port of Kochi is situated. It is placed in the Vembanad Lake, sometimes referred locally as Kochi Lake. The area is having a population of over 10,000 .

2.2. Vallarpadam Island

The Vembanad lake has several islands, one of which is called Vallarpadam, which is connected via the Goshree bridges with the city of Ernakulam and Vypin Island. Paddy fields make up over 70% of the island, and traditional fishing techniques and rice farming are the main economic activities.

Vallarpadam Island is located in the coastal plains of the Ernakulam district and is covered in Quaternary sediments such as beach sand, paleo-beach ridge deposits (sand), flood plain deposits (sand, silt, clay), and tidal deposits (clay, mud), among others. With an average annual rainfall of 3000 mm, the area experiences a moist monsoonal climate. It is a low-lying area close to the mouth of the Cochin Estuary that is covered in wetlands and mangroves. Vallarpadam Island, which together with Mulavukad Island make up the Mulavukad Panchayat, has a significant impact on the development of Cochin and offers a vast road network for the movement of commodities.

Kerala experiences monsoon season twice a year. The main rainy season is the Southwest monsoon, which occurs from June to August and experiences an average of 2,923.7 mm of rain., and the Northeast monsoon, also known as the retreating monsoon, occurs between October and November and experience an average of 380 mm which creates a network of rivers and estuaries that come from the Western Ghats. From the highlands and midlands, these rivers transport sediment to the plains, where it is released into the Arabian Sea. The lagoon system and landforms of Kochi are directly shaped by the interaction between river discharge and tidal forces. These wetlands, which reveal the physiographic condition of Vallarpadam Island, are

the result of dry ground slowly seeping into the flood basins of canals, watercourses, and estuaries.

2.3. Vembanad Lake

On India's southwest coast, there is a vast estuarine system of backwaters, the greatest of which is the Vembanad Lagoon and is India's largest estuary system and famous for its uniqueness and diverse fisheries. In 1981, UNESCO declared it a Ramsar site near the Iranian city of Ramsar. In addition, the Indian Ministry of Environment and Forests classified it as an ecologically sensitive zone due to its ecological value and high biodiversity.

The Vembanad wetland system and the drainage basins that it is connected to are located in the humid tropical region between 09°00' and 10°40' N and 76°00' and 77°30' E. Generally, it stretched from Alleppy in the south to Munambam in the north for around 90 km in a NW-SE direction. The lake has a depth range of 49–54 m and a width range of 500 m–4 km (Narayana et al., 2002). The Vembanad Wetland has an area of 2033 km^2, whereas the complex's combined catchment area is 6126.5 km^2. The Vembanad lake's water surface area was measured in 1990 and was 213.3 km^2 (Alappat et al., 2021a).

Estuaries are the product of numerous transgressional and regressive processes that occurred during the Holocene (Black and Baba et al., 2001). Vembanad Lake has been severely altered by a variety of anthropogenic and natural factors (Balachandran et al., 2005; Laturaj et al., 2006). The large backwaters and low-lying wetlands that make up the Vembanad water basin in central Kerala are Kochi's most distinguishing physical features

The Vembanad Lake complies with the concept of an estuary provided by Pritchard in 1967 as a “bar-built estuary”. During the Holocene, an extended tract's subsidence created the Vembanad (Soman et al., 2002). It is the largest body of water in, which holds 30% of the state's surface water resources and drains 40% of its land area. The population within the region's borders is 1.6 million. The productivity of Vembanad Lake has been noted to be continuously strong all year (Murthy and Veerayya et al., 1972).

Vembanad estuaries acts as a best depositional centre for the quaternary deposit and surface sediments are made up of a combination of sand, silt, and clay. Peat deposits have been discovered at various depths between the sedimentary facies of sandy clay and clayey sand.

Desiccated clays found below peat deposits imply an arid climate existed before the humid climate of 40,000 years ago (A. Narayana, Priju, et al., n.d.). The region, which is composed primarily of charnockites, gneisses, hornblende-biotite schists, khondalites, and intrusive rocks. The lake is divided into three sections: the northern section is made up of silty and clayey sand; the centre region is made up of clayey and sandy silt; and the southern section is made up of silty and clayey sand (Priju et al., n.d.).

(Alappat et al., 2021)(Alappat et al., 2021b)(Alappat et al., 2021b)The lake is bordered by spits that act as barriers between it and the Arabian Sea. Both the Muvatupuzha River (121 km) and the Lagoon receive runoff from the Periyar River, which empties into both locations. The six rivers Meenachil (78 km), Manimala (90 km), Achankovil (128 km), and Pamba (176 km) empty into the southern lagoon and contain sediment without producing deltas.

The Periyar River travels through the districts of Idukki, Kottayam, and Ernakulam before joining Vembanad Lake. It is the largest river in Kerala and the second-longest river in South India. The Meenachil River, which is a tributary of the Pamba River, traverses the Kottayam and Alappuzha districts before merging with Vembanad Lake. The Pamba River, which is the third-longest river in the state of Kerala, traverses the districts of Pathanamthitta and Alappuzha before it empties into Vembanad Lake. The Manimala River, which serves as a tributary to the Pamba River, traverses the Kottayam and Pathanamthitta districts prior to its confluence with the Pamba River. Subsequently, the combined flow of both river discharges into Vembanad Lake. Prior to its confluence with the Pamba River, which subsequently drains into Vembanad Lake, the Achankovil River, a subordinate watercourse of the Pamba River, traverses the Pathanamthitta and Alappuzha districts. Prior to flowing into Vembanad Lake, the Muvattupuzha River traverses the districts of Ernakulam and Kottayam, both located in the central region of the Indian state of Kerala.

CHAPTER 3

REVIEW OF LITERATURE

3.1. Quaternary Sea Level Change

Benjamin et al., 2017, examines major evidence and discussions concerning relative sea-level variations in the Mediterranean Basin since the Last Interglacial (roughly the last 132,000 years) and their consequences for historical human populations. The study demonstrates a relationship between coastal geomorphology, human migration, and sea level variations; this will help to explain how the environment impacts human civilizations living in the coast. It analyses geological sea level indicators and explain how archaeological features are often used as proxies to figure out previous sea levels, including both slow variations and catastrophic occurrences.

De Deckker & Yokoyama, 2009, work on recalibration of the chronology by documenting the history of sea level changes as determined by microfossil studies. The study concluded that the shallow oceans encircling Northern Australia, far from ancient ice sheets and on a tectonically stable coast, are optimal for sea-level reconstructions because to the low hydro-isostatic effects. Ostracods and foraminifera are thoroughly examined to provide a complete account of the sea level transgression that occurred towards the end of the Last Glacial Maximum.

Colman & Mixon, 1988, examine how the Chesapeake Bay region has responded to significant quaternary sea level variations. The study reports details about maximum and minimum sea level stands as well as complete sedimentary records of three significant transgressions.

Zazo et al., 2013, describes the coastal geomorphic reactions to the numerous sea-level variations that occurred throughout Spain's Mediterranean and Atlantic coasts over the Quaternary period. A special focus is placed on the geomorphic and stratigraphic record of the changes in amplitude, duration, and frequency associated with both the rapid and abrupt Late Pleistocene and Holocene climate changes as well as the gradual climate changes seen in marine cores and ice oxygen-isotope records during the Early and Middle Pleistocene

Bulletin & 1961, n.d., shows the location of the sea level throughout the quaternary period. According to some data, the sea level was roughly 8 fathoms when the last glacial interstadial

occurred (30,000 years ago). Following that, the sea level may have fallen to 65 fathoms. Between 15,000 and 7,000 B.P. (before the present), there was a rapid rise in sea level and a warming of the climate. Unlike the 11,000 B.P. warming that has been claimed, this warming was spread out over a period of time with climatic and sea level oscillations.

Padmalal et al., 2014, studied the sedimentological, palynological, and stable isotopic (13C and 15N) evidence of paleoclimate and sea level records in the Holocene sedimentary archives of the coastal lowlands of the Periyar-Chalakudy river systems of Central Kerala. Palynological and non-pollen palynomorph research show that Holocene sedimentation occurred in the area under variable climatic conditions with significant variations in climate and sea level. There is additional evidence of human habitation, which was later buried by fluvio-marine sediments in the Late Holocene.

Roy et al., 1980, discloses the genesis of the Holocene depositional phases on Australia's southern coast. According to the study, it is a high-energy coast with embayment that have various degrees of infilling with 'fluvial' and 'marine' sediments. To account for their many stages of development, an evolutionary model is given, which shows that with extreme or extended wave erosion, barriers may be removed and estuarine deposits reworked to form mixed "fluvial" and "marine" sediments. When an estuary entirely fills and river sand is fed to the coast, similar polygenetic sediments are formed.

Rao et al., 2003, made a try to update the compilation of radiocarbon ages of relic deposits on India's western margin therefore summarises results on sea level variations in connection to glacio-eustatic sea level and the impact of sea level or environmental changes on sediment depositional environments throughout the late quaternary. From this study, it was understood that relic carbonate deposits are found in the form of dolomite crusts, aragonite sands (pelletal and oolitic), aragonite-cemented limestones, oyster shells, corals, encrusted coralline algae, and foraminiferal-dominated nodules that serve as sea level indicators along India's western margin. The age of these deposits was determined, and a depth vs. age graph was created. These graphs show that the early Holocene saw the elevation of the Gulf of Kachchh and the subsidence of the Carbonate Platform. The early Holocene monsoon season was indicated by ecological succession.

Narayana et al., 2006, analyses the evolution of coastal landforms throughout the central Kerala coast and their importance in the deposition of coastal clastic deposits. The study concludes

that numerous causes, such as fluvial, marine, tectonic, and climatic factors, have had an important influence on the evolution of landforms and sedimentary ecosystems along the central Kerala coast.

Dash et al., 2020, examines the correlation between the paleo-sea level variations and the paleo-fluvial morphological changes in the Mahanadi delta. The study illustrates the various stages of maritime transgression and regression based on several indicators. Over the course of the Holocene Transgression, the river mouth had shifted. Fluctuations in sea level throughout the late Quaternary affected the geomorphology of rivers. The majority of the river relocated from the coastline as the sea level rose.

Alappat et al., 2021, studied early Holocene transgression from the sediment deposits of Central Kerala and constrain its chronology using optically stimulated luminescence (OSL) as well as radiocarbon dating. The study shows an initial rise in sea level along the central Kerala coast, which drowned significant areas of today's inland regions, establishing estuaries, tidal channels, and embayment in the area.

Shaji et al., 2022, studied the climatic and marine disturbances around the Vembanad lagoon, Kerala, SW India. The study obtained a high sea level as well as a warm and rainy environment due to the Indian summer monsoon, which confirms the Holocene environment as optimal. The high sea level suggests that the core location was a southward extension of the Vembanad lagoon, which became part of the terrestrial system due to gradual sea regression during the mid-late Holocene period, followed by the deposition of alluvial sediments from the hinterland rivers.

Vishnu Mohan et al., 2017investigated the Holocene climate and sea level changes in response to the coastal sedimentary processes of India's southwestern coast, which is thought to be the gateway for the Asian Summer Monsoon (SW monsoon) to the Indian subcontinent. The study concluded that a significant rainfall event occurred in the early half of the Holocene, giving rise to the Bay Head Delta in the estuary's fluvial end. Palynological contents below the level show a facies transition as freshwater and terrestrial materials predominate over marine contents.

Rosentau et al., 2021, investigated available Holocene relative shore level database for the Baltic Sea basin and the Kattegat area. The study concluded that relative shore line data from

locations with negative tendencies, but projections for the mid-Holocene in the eastern Baltic clearly overestimate the relative shore line and fail to restore the mid-Holocene relative shore line high stand determined from proxy reconstructions.

Tiju et al., 2021, focuses on the lithological differences, foraminiferal assemblages, and geochemical relationship proxies of sediment cores from the coastal plain, estuary-lagoon, and offshore locations of Kerala in order to interpret marine transgression-regression episodes. that the evidences from sediments supported a stronger monsoon in the early Holocene, resulting in the invasion of high-water levels, increased flow discharge, and bottom scouring, although a moderate monsoon and arid climate prevailed during the Last Glacial Maximum (LGM).

3.2. Foraminifera as a proxy for sea-level changes

De Araújo & De Jesus Machado, 2008, evaluated the foraminiferal faunas and their relationships to sediment texture and composition in reef areas from the shore to the 30-m isobath between the cities of Corumbau and Nova Viçosa in the extreme south of the state of Bahia. The study found a link between foraminifera and grain size. Amphistegina lessonii and Peneroplis carinatus were frequent in sandy carbonate deposits, while Ammonia beccarii, Elphidium poeyanum, Pyrgo subsphaerica, Quinqueloculina disparilis curta, and Q. lamarckiana were plentiful in mixed sand and mud, whether carbonate or mixed carbonate and siliciclastic. The variation in the richness score among samples suggested microenvironmental zones that were unfavourable for some foraminiferal species. Local hydrodynamic circumstances occur in settings with more energy where finer sediments and many foraminiferal species have been eliminated.

Rossi & Horton, 2009, investigated the ability of a foraminifera-based transfer function to recreate the Holocene paleo-bathymetric history of the Po Delta area (northern Adriatic Sea). With sufficiently accurate reconstructions, the Northern Adriatic Transfer Function predicts a significant correlation between the observed and foraminifera-predicted water depths. The inner shelf deposits at the base of the marine succession have the deepest reconstructed water depths. According to the shallowing-upward, progradational trend, the uppermost layers are characterised by the shallowest paleowater depths. These findings imply that paleobathymetric reconstructions of subsurface deposits in contemporary deltaic systems can be aided by subtidal foraminifera-based transfer functions.

Horton et al., 2007, investigated the ability of subtidal foraminifera to reconstruct Holocene relative sea levels from Australia's central Great Barrier Reef shelf. There are two zones of subtidal foraminiferal assemblages. The distributions of subtidal foraminifera are related to water depth according to the zonations of the research regions and the relative abundances of individual species.

Massey et al., 2006, examined surface sediments from mudflats and salt marshes in the south Devonian estuaries of Erme and Salcombe-Kingsbridge to develop an intertidal foraminifera-based transfer function for retracing Holocene sea-level rise in southwest England, UK. The study's findings demonstrate that foraminiferal assemblages in estuaries show a distinctive and comparable vertical zonation. The evidences were used to calculate the height of Holocene sea-level index points from southwest England, as shown by foraminiferal assemblages from a Holocene core.

Horton et al., 2003, shows the total abundance of dead foraminifera from a 12-month examination of surface samples from Cowpen Marsh, but there are significant seasonal fluctuations in the relative abundance of agglutinated and calcareous species. The findings imply that accurate reconstructions of historical sea levels are feasible; however, their accuracy changes throughout the year. Because the foraminiferal assemblages are dominated by agglutinated and calcareous species, respectively, the highest precision is obtained using samples taken during the winter, and the poorest precision is obtained during the summer.

Nigam & Khare, 1999,investigated the biodiversity and composition of foraminifera. The study also focused on the local region's paleoclimatic changes. In the study, morpho-groups like angular-asymmetrical and rounded-symmetrical are quantified and distributed spatially. An inverse association between angular-asymmetrical morpho-groups and river discharge (low salinity water) is indicated by the distribution, which showed a lower abundance of angular-asymmetrical forms at the river mouth.

Nigam, 1986, studied aspects of forecasting net sediment transport as well as for designing and planning for offshore projects. Three main assemblages of Ammonia annectens, Ammonia papillosus-Asterorotalia dentata, and Ammobaculites persicus are identified by the study. The amount of organic matter in the sediments and fresh water flow influence these assemblages. The distribution of significant assemblages in living and dead experiments reveals a current and an east-southeast migration of sediment.

MANASA et al., 2016, analysed the proxy to reconstruct previous monsoon strength from the Arabian Sea using temporal variations in benthic foraminiferal morpho-groups. While calcareous benthic foraminiferal abundance rises away from the riverine influx zones, agglutinated foraminifera dominate shallow water, low salinity locations. Comparatively little impact on the distribution of fauna is exerted by food availability, as determined by the quantity of organic carbon in sediments, in the northwest Bay of Bengal. The study came to a conclusion that the distribution of benthic foraminiferal morpho-groups in the northwest Bay of Bengal is influenced by parameters related to freshwater influx, and that this can be utilised to reconstruct previous monsoon strength from the Bay of Bengal.

Maeda et al., 2022, studied the abundances and assemblages of the planktic foraminifers, and the factors controlling the assemblages and their potential as markers of climate and ocean activities in the sedimentary record. In general, the summer and winter monsoon seasons saw the highest fluxes of planktic foraminifer testing, while the inter monsoon seasons, particularly from March to May, saw the lowest fluxes. A rapid rise in Globigerina bulloides flux was associated with periods of increased primary production during monsoons, whereas nutrient shortage in the top ocean in spring resulted in subsurface small size plankton production and low planktic foraminifer test fluxes. Seasonal surface and subsurface primary production was primarily responsible for controlling the seasonality of foraminiferal assemblages and fluxes.

3.3. Vembanad lake sediments and palaeogeographical reconstructions

A. C. Narayana et al., 2021, attempted to figure out the magnetic characteristics' relationship to metal pollution from the Vembanad lagoon sediments. The investigation came to the conclusion that the upper layers of cores have a significant magnetic record.

Kunte et al., 2013, studied the offshore turbidity patterns, and quantitative estimation of suspended sediments in determining the size and direction of sediment flows. Analysing coastal drift indicators and shoreline alterations based on multitemporal satellite photos allowed researchers to better understand the littoral drift regime along India's northeastern coast. According to the study, sediment transport along the coast is bidirectional and dependent on the monsoon, as shown by the characteristics of coastal landforms and sedimentation processes. The remote sensing technology is used to comprehend the coastal morphometric changes, long-term sediment transport, coastline alterations, offshore turbidity distribution pattern, and the consequences for the transfer of sediment-associated contaminants.

Alappat et al., 2021 attempted to identify early Holocene transgression signs in the region and constrain its chronology using optically stimulated luminescence (OSL) and radiocarbon dating. The study found that the fluvial layers were made up of huge fossil tree trunks and clay and sand sequences rather than peat deposits. The peat unit was created between 8 and 7 ka BP, according to the radiocarbon dates of the peat itself and the OSL age of a sand layer beneath it. The peat unit's pollen examination shows that it was created by Rhizophoraceae mangrove plants, suggesting that the studied region was close to the shore. Wet climatic conditions in the area are shown by the predominance of wet evergreen forest species in the non-mangrove pollen of the peat. The presence of massive tree trunks buried in the fluvial succession and fossilised wood stumps indicates that the trees were submerged in water throughout the transportation of the flood or in situ in the growth position.

3.4. Textural Analysis of sediments

To assess the depositional conditions and paleoflood occurrences from the late Pleistocene epoch, a study comprising grain size analysis was conducted by Raja et al., 2018, from the Parsons valley lake deposit, Nilgiris, India**.** According to the study, changes in the grain size distribution are primarily caused by local climate factors.

In their study, Priju et al., n.d., described the textural features and Tanner's bivariate plots of grain size parameters to explain the depositional processes in a lagoonal system throughout the Late Holocene. The northern and southern portions of the lagoon noticed high energy conditions, particularly in regions near the river mouths. The energy regime in other areas of the lagoon is low to moderate. It is emphasised in the study that the bivariate plot is a very helpful tool for identifying open- and closed-basin conditions in coastal areas.

Basu, 1976, investigated the petrology of Holocene River sand generated from granitic plutons in the moist Appalachian Mountains and the dry Rocky Mountains of the United States to comprehend the impact of climate on these sands and also to identify their source. According to the study, the abundance of the four primary minerals that make up first cycle sand—quartz, feldspar, rock fragments, and accessory minerals—varies depending on the grainsize and is largely influenced by the climate.

CHAPTER 4

METHODOLOGY

4.1. Sampling Method

For a better understanding of the local topography, physiography, geomorphology, and other fundamental factors, a number of field reconnaissance studies were held in the region. The site near the northern tip of Vallarpadam Island (N 9.989772; E 76.249231) was then selected for the coring and sample collection. The samples were taken up to a depth of 15 metres from the surface. Core sampling was carried out, and subsurface samples were taken using a hand auger method and a commercially available augur drilling system every 20 cm interval up to a depth of 15 m. A total number of 132 samples were obtained. The samples were numbered as VLD-1, VLD-2, VLD-3, and so on up to VLD-132 from surface to the depths.

The augers are dug into the borehole, rotated into the soil until they are full, and then raised out and emptied. The samples were taken from each portion and placed in polythene sip-lock bags and named in the field. Each sample was first carefully examined, with the sediment texture and additional features visually identified and noted. Shells, wood fragments, leaf imprints, peat, and other organic remains were searched for in the sediment for additional study and identification. Certain stratigraphic levels were found to contain the noxious odour of sulphur.

Materials required:

1. Field note
2. Camera
3. Pocket lens
4. Measuring Tape
5. Zip lock covers

Photograph 1. Manual auguring for sample collection

4.2. Laboratory Method

4.2.1. Grain Size Analysis

Sediment is an organic material that develops naturally as a result of the weathering and erosion of rock and is carried to the site of deposition by water, wind, ice, or mass movement. Particle or grain size is a fundamental attribute or physical property of particulate samples or sediments and sedimentary rocks (Folk, 1980; Friedman and Sanders, 1978). A sediment's grain size can reveal properties including sorting, sphericity, angularity, and the texture of the surface.

Investigating a sediment reveals the origin of the rock's constituent particles as well as the processes of erosion and transport that enable the particles to migrate from their point of source to their sink. The size of particles is directly dependent on the type of environmental setting, transporting agent, length and time during transport, and depositional conditions, and hence it possesses significant utility as an environmental proxy (McManus, 1988; Stanley-Wood and Lines, 1992). A wide range of extrinsic factors operating at the local or regional level are related to grain size.

Basically, sediment may be broken down into three major categories: gravel, sand, and mud. On the basis of their mineralogical aspects, these are later split into silt and clay. The maximum grain diameter is used to quantify particles. Grade scale is the term for the geometric scale that is employed. The commonly used grade scale is Wentworth or Udden-Wentworth scale (Udden, 1914; Wentworth, 1922). That divides the grains size from boulders (> 200 mm) to clay (< 0.004 mm). The Krumbein scale (Krumbein and Sloss, 1963) is a modified version of the Udden-Wentworth scale that uses round values that can be easily calculated to avoid dealing with millimetre fractions.

4.2.1.1 Sieve analysis

The method that is commonly used to determine the grain size is sieve analysis. Separating the sample will be challenging if there is a larger concentration of sand than clay particles. In these situations, wet sieving is more frequently used than the dry sieving procedure. Washing the smaller particles through smaller sieves with a stream of water is the simplest technique to distinguish between clay and sand particles. The sample that is still in the sieve can be used to estimate the sand's weight. The pipette method is used to determine the remaining proportion of clay and silt. Stokes law is used to calculate the time and depth of pipetting based on the temperature of the suspension and the settling sizes. Stokes law involves a consideration of the physical forces that influence the behaviour of a particle in a fluid (Speed, 2022).

The purpose of this type of investigation is to (1) learn about environmental condition of deposition of sediments, (2) reconstruct previous sedimentary transport records, , sediment provenance, or (3) thoroughly investigate a catastrophic event (Lopez, 2017).

4.2.2. Pipette Method

Apparatus required

1. Weighing balance
2. 230 ASTM sieve
3. Cylindrical flask
4. Pipette
5. Beaker
6. Hot air oven

Procedure

The collected sample of 10 g was dried and taken for sieve analysis. This measured sample undergoes preliminary treatment. As stated by Ingram in 1970, it involves the removal of carbonates by HCl (10%) and the removal of organic materials by H_2O_2 (30%). For disintegration, each sample was dispersed overnight in a 0.025 N Sodium Hexametaphosphate solution. Approximately 5 g of the dried sample were then collected, placed on the 230 ASTM (opening = 0.063 mm) sieve mesh, and washed until clear water passed through it.

The material retained in the mesh is generally referred to as sand with a grain size greater than 1/16 mm. After drying, the weight of the sand is recorded. The pipette method is used to determine the weight of finer materials such as silt and clay. For this, the sieved suspension is collected in a 1 L graduated measuring jar. If the suspension collected in the jar after complete washing was less than 1 L, distilled water was added to obtain a 1 L sample. The suspension in the measuring jar was then vigorously agitated with a stirring mechanism in order to achieve uniform particle dispersion in the suspension exactly after 2 hours and 3 minutes of agitation. The solution was pipetted into a 50-ml beaker using a 20-ml pipette that was plunged into the solution to a depth of 10 cm. A hot air oven was used to dry the sample. Following complete drying, the residue will resemble the clay's weight. By comparing the weights of the sand and clay, one can determine how much silt is present in the sample.

Data is entered into an Excel spreadsheet in order to provide tabular results. The soil texture calculator programme is used to determine the sediment's texture at different depths. This

utility uses Microsoft Excel macros to compute and visualise different texture classes based on the percentages of sand, silt, and clay. contains the optional sand fractions utilised with sandy loam, loamy sand, and sand textures.

Photograph 2. Pipette Analysis

CALCULATIONS

$$\% \text{ Sand} = \frac{\text{Final weight of beaker} - \text{Initial weight of beaker}}{\text{Weight of sample}} \times 100$$

$$\% \text{ clay} = \frac{\text{Final weight of beaker} - \text{Initial weight of beaker}}{\text{Weight of sample}} \times 100$$

$$\% \text{ silt} = 100 - (\% \text{ Sand} + \% \text{ Clay})$$

4.2.3. Micropalaeontology Analysis

The foraminifera's exterior morphology is frequently well preserved, yet it is occasionally insufficient for identifying the specimen. Additionally, sectioning can be used to determine the

internal structure of some groupings of foraminifera. However, for a few reasons, it is not satisfactory (Dunbar and Hembest, 1942; Douglass, 1960,1965; Honjo, 1960; Hofker, 1965).

A slow-setting, glass-clear plastic can be used to embed a specimen accurately while also enabling the observation and photography of morphological structures during sectioning. The method has been effectively used with both fossil and recent foraminifera, and it is especially helpful for very small specimens (Zeidler, 1972).

a) Hot air oven

b) Weighing balance

c) Otto splitter

d) Binocular microscope

e) Chapman Side

Photograph 3. Images of instrument used for Micropalaeontology analysis

Apparatus required

1. Petri dish
2. Weighing balance
3. Hot air oven
4. 230 ASTM sieve
5. Otto splitter
6. Binocular microscope
7. Glass slide

Procedure

Washing: Using the cone and quarter method, 5 g of the original sample were taken. A clean, marked container is used to carefully put the sample inside. The container is then placed into an oven set to a normal drying temperature of 50 to 70 degrees Celsius. The sample should be dried until it is entirely desiccated. The dry sample is once more weighed before being soaked in the distilled water. The sample should continue to soak with periodic stirring until all of the components have separated. The sample can now be sieved.

Sieving: A set of sieves with the necessary mesh width is employed. Mesh sizes as common as 600, 150, 125, and 63 microns. Wet sieves are typically used in the case of foraminifera and have micron sizes of 125 and 63. The sample is put into the sieve and given a light water wash. Never use your finger to massage a sample in a sieve; instead, clean it with a stream of water. The sample is gently placed into the container after washing is complete. After that, the container was tagged, and it was dried in the oven over 50 deg C. The dried sample is then weighed, tagged, and placed in the little polythene vials. If the sample contains organic contaminants, it will be treated with H_2O_2 one more time before being washed and dried once more.

Picking: The dried sample is next placed in an Otto splitter, which splits it to make the selection process easier. The divided sample was then transferred onto the Chapman slide, a 24-chamber assembly slide, where foraminifera were subsequently picked out with a brush under a stereo zoom binocular microscope (NOVEX-Holland). The species are divided up into their own squares on the assemblage slide.

Identification and photography: After the foraminifera have been completely transferred, species identification is complete. In order to determine the abundance, the number of fossils is now counted. The identified sample is now mounted on the stereomicroscope stage (LEICA M2025C). The foraminifera photos were obtained with the Leica Application Suite X (LAS X) software.

Photograph 4. Performing micropalaeontology analysis of microfossils

CHAPTER 5

RESULT AND DISCUSSION

5.1. RESULTS

5.1.1. Sediment Texture Studies

5.1.1.1 Stratigraphic core logging

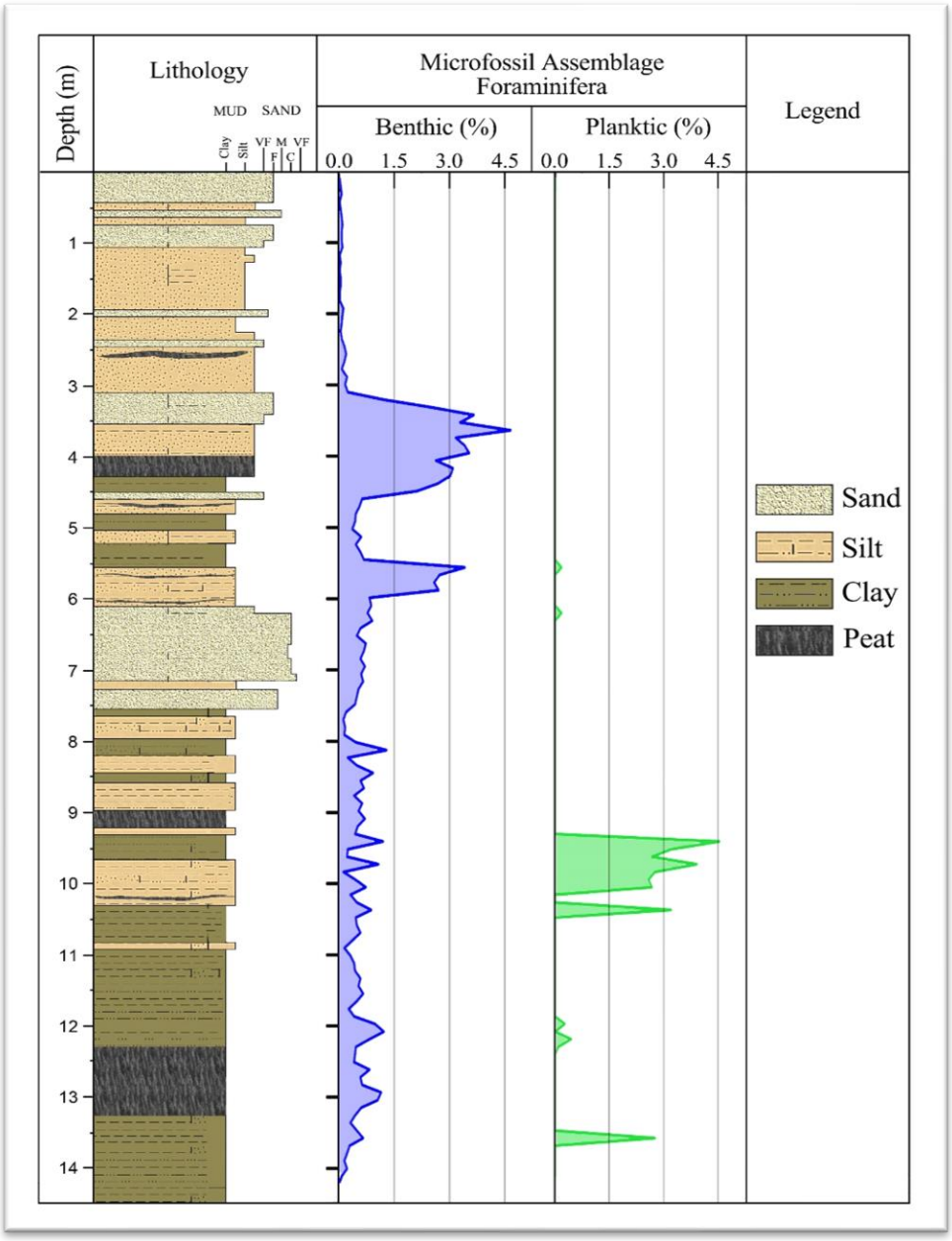

Figure 5 : Core log of Vallarpadam core 1

The core samples were logged in detail and core log was prepared. Samples were examined for texture, colour, the presence of shells, wood fragments, peat, leaf impressions, and organic content. The initial examination uses visual interpretation to determine the variation sediment deposits up to 15 m depth of the core.

The upper part is made up of fine sand that was deposited by the aeolian process and is distinguished by its uniform and well-sorted nature. The succession consists of medium-to-fine sand and silt with carbonised wood, tree twigs, and leaf impressions. The core also contains supra-tidal mixed siliciclastic deposits. Analysis revealed that the shell's preservation ranged from 74.8 cm to 14 m. Samples taken at depths of 3 to 4 m point to a marshy area that is intertidal to subtidal. This was followed by coarse sand in the sedimentary unit at a depth of ~5 metres with shell fragments . After this, there is an increase in peat content as well. The core section at a depth of 5–7 m reveals a thick sequence of silty clay with abundant shell and peat, which could be an intertidal deposit. Medium-to-fine sand with an abundance of shell pieces were found at depths of 7 to 8 m. The lower part of the core (8 to 15 m) is mostly clay and silt, with peat at depth intervals of 8.9 to 9.9 m and 11.6 to 12.8 m. A general increase in grain size was observed at a depth of 5 m and then starts to decrease at 7 m.

The subsurface sediments revealed the presence of several shell types, including Pirenella cingulata, Timoclea cohensis, Mereteix aurora, Dentalium, Tricula java, Dohax cuneatus, Pseudominalia biangulosa, and Sunetta sp.

5.1.1.2 Pipette Analysis

The table 1 below shows the data of pipette analysis. The results shows that the samples were mostly sand, sandy clay, silt, silty clay, and clay.

Sl NO.	VLD CORE 1					
	SAMPLE NO	DEPTH (cm)	WEIGHT PERCENTAGE (%)			TEXTURE
			SAND	SILT	CLAY	
1	VLD 1	10.69	81.36	6.64	12	Sandy Loam
2	VLD 2	21.38	77.94	13.06	9	Sandy Loam
3	VLD 3	32.07	80.36	5.64	14	Sandy Loam
4	VLD 4	42.76	79.44	14.56	6	Loamy Sand
5	VLD 5	53.45	53.04	16.96	30	Sandy Clay Loam
6	VLD 6	64.14	90.76	7.24	2	Sand
7	VLD 7	74.83	80.18	2.82	17	Sandy Loam
8	VLD 8	85.52	66.2	13.8	20	Sandy Clay Loam
9	VLD 9	96.21	77.3	19.7	3	Loamy Sand
10	VLD 10	106.9	67.06	5.94	27	Sandy Clay Loam
11	VLD 11	117.59	85.52	0.48	14	Loamy Sand
12	VLD 12	128.28	71.62	9.38	19	Sandy Loam
13	VLD 13	138.97	69.5	5.5	25	Sandy Clay Loam
14	VLD 14	149.66	63.2	9.8	27	Sandy Clay Loam
15	VLD 15	160.35	64.36	9.64	26	Sandy Clay Loam
16	VLD 16	171.04	66.35	13.65	20	Sandy Clay Loam
17	VLD 17	181.73	68.34	17.66	14	Sandy Loam
18	VLD 18	192.42	69.7	20.3	10	Sandy Loam
19	VLD 19	203.11	62.92	9.08	28	Sandy Clay Loam
20	VLD 20	213.8	69.78	20.22	10	Sandy Loam
21	VLD 21	224.49	70.94	13.06	16	Sandy Loam
22	VLD 22	235.18	67.44	1.56	31	Sandy Clay Loam
23	VLD 23	245.87	68.1	12.9	19	Sandy Loam
24	VLD 24	256.56	69.18	3.82	27	Sandy Clay Loam
25	VLD 25	267.25	70.44	4.56	25	Sandy Clay Loam
26	VLD 26	277.94	69.18	10.82	20	Sandy Clay Loam
27	VLD 27	288.63	71.74	4.26	24	Sandy Clay Loam
28	VLD 28	299.32	65.52	9.48	25	Sandy Clay Loam
29	VLD 29	310.01	69.56	16.44	14	Sandy Loam
30	VLD 30	320.7	63.1	5.9	31	Sandy Clay Loam
31	VLD 31	331.39	71.98	0.02	28	Sandy Clay Loam
32	VLD 32	342.08	73.66	7.34	19	Sandy Loam
33	VLD 33	352.77	67.24	0.76	32	Sandy Clay Loam
34	VLD 34	363.46	25.3	0.7	74	Clay
35	VLD 35	374.15	61.34	28.66	10	Sandy Loam
36	VLD 36	384.84	69.88	24.12	6	Sandy Loam
37	VLD 37	395.53	56.9	1.1	42	Sandy Clay
38	VLD 38	406.22	61.16	8.84	30	Sandy Clay Loam
39	VLD 39	416.91	64.04	1.96	34	Sandy Clay Loam
40	VLD 40	427.6	52.8	15.2	32	Sandy Clay Loam
41	VLD 41	438.29	14.3	13.7	72	Clay
42	VLD 42	448.98	22.42	16.58	61	Clay
43	VLD 43	459.67	15.02	75.98	9	Silt Loam
44	VLD 44	470.36	32.78	5.22	62	Clay
45	VLD 45	481.05	87.68	1.32	11	Loamy Sand
46	VLD 46	491.74	25.48	51.52	23	Silt Loam
47	VLD 47	502.43	18.6	19.4	62	Clay
48	VLD 48	513.12	51.64	23.36	25	Sandy Clay Loam
49	VLD 49	523.81	60.38	13.62	26	Sandy Clay Loam
50	VLD 50	534.5	31.94	11.06	57	Clay
51	VLD 51	545.19	34.78	22.22	43	Clay
52	VLD 52	555.88	26.86	2.14	71	Clay
53	VLD 53	566.57	53.8	39.2	7	Sandy Loam
54	VLD 54	577.26	8.74	14.26	77	Clay
55	VLD 55	587.95	65.12	14.88	20	Sandy Clay Loam
56	VLD 56	598.64	19.46	35.54	45	Clay
57	VLD 57	609.33	79.42	2.58	18	Sandy Loam
58	VLD 58	620.02	72.68	4.32	23	Sandy Clay Loam
59	VLD 59	630.71	79.6	7.4	13	Sandy Loam
60	VLD 60	641.4	63.02	33.98	3	Sandy Loam
61	VLD 61	652.09	24.58	3.42	72	Clay
62	VLD 62	662.78	77.58	11.42	11	Sandy Loam
63	VLD 63	673.47	91.64	1.36	7	Sand
64	VLD 64	684.16	61.3	3.7	35	Sandy Clay
65	VLD 65	694.85	68.72	19.28	12	Sandy Loam

66	VLD 66	705.54	68.48	20.52	11	Sandy Loam
67	VLD 67	716.23	69.06	8.94	22	Sandy Clay Loam
68	VLD 68	726.92	39.14	33.86	27	Clay Loam
69	VLD 69	737.61	72.62	15.38	12	Sandy Loam
70	VLD 70	748.3	66.3	29.7	4	Sandy Loam
71	VLD 71	758.99	6.24	23.76	70	Clay
72	VLD 72	769.68	0.46	69.54	30	Silt Clay Loam
73	VLD 73	780.37	36.6	43.4	20	Loam
74	VLD 74	791.06	6.24	9.76	84	Clay
75	VLD 75	801.75	24	66	10	Silt Loam
76	VLD 76	812.44	41.86	41.14	17	Loam
77	VLD 77	823.13	10.9	26.1	63	Clay
78	VLD 78	833.82	6.06	39.94	54	Clay
79	VLD 79	844.51	2.7	66.3	31	silty Clay Loam
80	VLD 80	855.2	2.44	19.56	78	Clay
81	VLD 81	865.89	6.6	38.4	55	Clay
82	VLD 82	876.58	22.9	76.1	1	Silt Loam
83	VLD 83	887.27	3.12	69.88	27	silty Clay Loam
84	VLD 84	897.96	5.62	65.38	29	silty Clay Loam
85	VLD 85	908.65	24.24	55.76	20	Silt Loam
86	VLD 86	919.34	3.38	85.62	11	Silt
87	VLD 87	930.03	1.8	55.2	43	Silty Clay
88	VLD 88	940.72	31.34	51.66	17	Silt Loam
89	VLD 89	951.41	11.1	44.9	44	Silty Clay
90	VLD 90	962.1	20.94	17.06	62	Clay
91	VLD 91	972.79	38.1	40.9	21	Loam
92	VLD 92	983.48	12.2	3.8	84	Clay
93	VLD 93	994.17	10.1	53.9	36	Silty Clay Loam
94	VLD 94	1004.86	27.74	42.26	30	Clay Loam
95	VLD 95	1015.55	1.42	24.58	74	clay
96	VLD 96	1026.24	0.18	37.82	62	clay
97	VLD 97	1036.93	21.2	13.8	65	clay
98	VLD 98	1047.62	1.66	28.34	70	clay
99	VLD 99	1058.31	0.92	17.08	82	clay
100	VLD 100	1069	16.88	41.12	42	Silty Clay
101	VLD 101	1079.69	3.26	18.74	78	Clay
102	VLD 102	1090.38	2.8	15.2	82	Clay
103	VLD 103	1101.07	6.56	50.44	43	Silty Clay
104	VLD 104	1111.76	5.52	13.48	81	Clay
105	VLD 105	1122.45	12.84	65.16	22	Silt Loam
106	VLD 106	1133.14	16.46	33.54	50	Clay
107	VLD 107	1143.83	2.44	7.56	90	Clay
108	VLD 108	1154.52	7.66	78.34	14	Silt Loam
109	VLD 109	1165.21	17.02	17.98	65	Clay
110	VLD 110	1175.9	2.74	2.26	95	Clay
111	VLD 111	1186.59	1.9	96.1	2	Silt
112	VLD 112	1197.28	10.16	18.84	71	Clay
113	VLD 113	1207.97	10.06	2.94	87	Clay
114	VLD 114	1218.66	6.94	23.06	70	Clay
115	VLD 115	1229.35	8.14	27.86	64	Clay
116	VLD 116	1240.04	22.32	0.68	77	Clay
117	VLD 117	1250.73	13.04	12.96	74	Clay
118	VLD 118	1261.42	35.92	7.08	57	Clay
119	VLD 119	1272.11	19.04	23.96	57	Clay
120	VLD 120	1282.8	4.3	30.7	65	Clay
121	VLD 121	1293.49	12.14	52.86	35	Silty Clay Loam
122	VLD 122	1304.18	3.28	7.72	89	Clay
123	VLD 123	1314.87	10.62	7.38	82	Clay
124	VLD 124	1325.56	19.8	20.2	60	Clay
125	VLD 125	1336.25	6.74	64.26	29	Silty Clay Loam
126	VLD 126	1346.94	6.92	82.08	11	Silt
127	VLD 127	1357.63	14.16	27.84	58	Clay
128	VLD 128	1368.32	8.12	72.88	19	Silt Loam
129	VLD 129	1379.01	13.68	73.32	13	Silt Loam
130	VLD 130	1389.7	10.24	15.76	74	Clay
131	VLD 131	1400.39	1.02	61.98	37	Silty Clay Loam
132	VLD 132	1411.08	5.78	37.22	57	Clay

Table 1. Data showing weight percentage of sand, silt, clay

5.1.2. Micropaleontology

5.1.2.1. Classification

Loeblich and Tappan, along with others, supplied the scientific world with the most thorough and authoritative compilation of taxonomic information on foraminifera in 1964, which became the foundation of the study. The study discovered that the majority of the samples contained 5 different species of foraminifera, including both benthic and planktonic foraminifera.

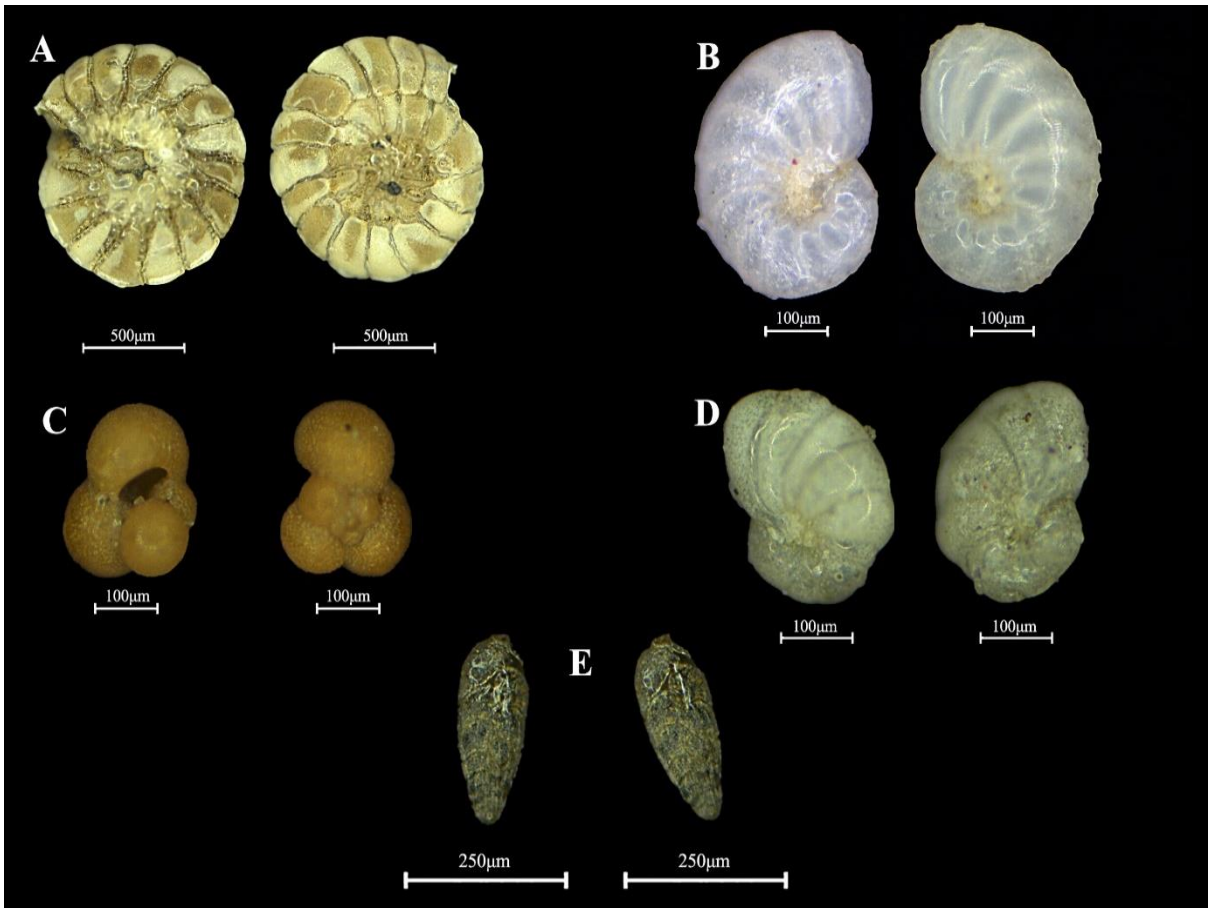

Figure 6: Different types of foraminifera found in the core sediments of Vallarpadam Island

List of species:

A. Ammonia beccarii
B. Nonion subturgidum

C. Globigerina bulloids
D. Nonion sp.
E. Bolivina sp.

The table 2 below displays the total abundance and population of the species identified in the research region. Analysing the table reveals that the current study area has 4436 fossils. It has 4105 and 331 benthic and planktic species, respectively. The abundance of the fossils varies according to depth. The first 3 metres consists of less than 10 fossils. The abundance rises between 3–4 m and 5.5–5.9 m. The greatest abundance of fossils in the whole core occurred at depth of around 3.6 m. The species density is modest at the range of 5.9–9.3 m and 10–12 m. An increase in the number of fossils increased at the depth of 9.4 m, whereas 13–14 m recorded fairly low abundance.

The whole analysis reveals a high abundance of benthic species, primarily Ammonia beccarii. The highest concentrations are reported at 3.6–4.4 m and 5.5–5.6 m. Globigerina bulloids, a planktic species, are abundant at 9.4–10.4 m. It is most abundant in upwelling zones and at low latitudes. A benthic species, known as Bolivina sp., which are typically found in low oxygen conditions, may be found at 13.5–13.6 m depth. That belongs to a deep ocean basin.

SL NO:-	SAMPLE NO	DEPTH	BENTHIC SPECIES				PLANKTIC SPECIES	ABUNDANCE
			Ammonia beccarii	Nonion sp.	Nonion subturgidum	Bolivina sp.	Globigerina bulloid	
1	VLD 1	10.69	1	0	0	0	0	1
2	VLD 2	21.38	2	0	0	0	0	2
3	VLD 3	32.07	3	0	0	0	0	3
4	VLD 4	42.76	1	0	0	0	0	1
5	VLD 5	53.45	2	0	0	0	0	2
6	VLD 6	64.14	3	0	0	0	0	3
7	VLD 7	74.83	4	0	0	0	0	4
8	VLD 8	85.52	3	0	0	0	0	3
9	VLD 9	96.21	3	0	0	0	0	3
10	VLD 10	106.9	4	0	0	0	0	4
11	VLD 11	117.59	1	0	0	0	0	1
12	VLD 12	128.28	2	0	0	0	0	2
13	VLD 13	138.97	1	0	0	0	0	1
14	VLD 14	149.66	2	0	0	0	0	2
15	VLD 15	160.35	2	0	0	0	0	2
16	VLD 16	171.04	1	0	0	0	0	1
17	VLD 17	181.73	1	0	0	0	0	1
18	VLD 18	192.42	5	0	0	0	0	5
19	VLD 19	203.11	4	0	0	0	0	4
20	VLD 20	213.8	3	0	0	0	0	3
21	VLD 21	224.49	2	0	0	0	0	2
22	VLD 22	235.18	3	0	0	0	0	3
23	VLD 23	245.87	6	0	0	0	0	6
24	VLD 24	256.56	8	0	0	0	0	8
25	VLD 25	267.25	6	0	0	0	0	6
26	VLD 26	277.94	3	0	0	0	0	3
27	VLD 27	288.63	9	0	0	0	0	9
28	VLD 28	299.32	3	4	0	0	0	7
29	VLD 29	310.01	7	3	0	0	0	10
30	VLD 30	320.7	46	4	0	0	0	50
31	VLD 31	331.39	92	10	0	0	0	102
32	VLD 32	342.08	130	11	9	0	0	150
33	VLD 33	352.77	90	33	12	0	0	135
34	VLD 34	363.46	180	9	2	0	0	191
35	VLD 35	374.15	100	26	4	0	0	130
36	VLD 36	384.84	125	15	0	0	0	140
37	VLD 37	395.53	141	3	1	0	0	145
38	VLD 38	406.22	99	6	3	0	0	108
39	VLD 39	416.91	125	2	0	0	0	127
40	VLD 40	427.6	117	5	2	0	0	124
41	VLD 41	438.29	86	15	9	0	0	110
42	VLD 42	448.98	66	18	3	0	0	87
43	VLD 43	459.67	19	4	3	0	0	26
44	VLD 44	470.36	15	6	2	0	0	23
45	VLD 45	481.05	8	6	5	0	0	19
46	VLD 46	491.74	17	1	0	0	0	18
47	VLD 47	502.43	5	9	1	0	0	15
48	VLD 48	513.12	16	5	4	0	0	25
49	VLD 49	523.81	19	0	0	0	0	19
50	VLD 50	534.5	22	2	0	0	0	24
51	VLD 51	545.19	20	4	4	0	0	28
52	VLD 52	555.88	122	10	8	0	2	142
53	VLD 53	566.57	102	9	1	0	0	112
54	VLD 54	577.26	95	5	6	0	0	106
55	VLD 55	587.95	97	11	3	0	0	111
56	VLD 56	598.64	30	3	1	0	0	34
57	VLD 57	609.33	33	2	1	0	0	36
58	VLD 58	620.02	29	3	0	0	2	34
59	VLD 59	630.71	37	0	0	0	0	37
60	VLD 60	641.4	23	1	0	0	0	24
61	VLD 61	652.09	20	0	0	0	0	20
62	VLD 62	662.78	25	4	1	0	0	30
63	VLD 63	673.47	26	1	1	0	0	28
64	VLD 64	684.16	22	0	2	0	0	24
65	VLD 65	694.85	18	6	5	0	0	29
66	VLD 66	705.54	20	3	2	0	0	25
67	VLD 67	716.23	19	8	0	0	0	27

68	VLD 68	726.92	12	8	2	0	0	22
69	VLD 69	737.61	20	0	0	0	0	20
70	VLD 70	748.3	16	0	2	0	0	18
71	VLD 71	758.99	8	0	0	0	0	8
72	VLD 72	769.68	5	0	0	0	0	5
73	VLD 73	780.37	6	1	0	0	0	7
74	VLD 74	791.06	6	0	0	0	0	6
75	VLD 75	801.75	17	1	1	0	0	19
76	VLD 76	812.44	15	38	0	0	0	53
77	VLD 77	823.13	10	0	0	0	0	10
78	VLD 78	833.82	18	1	1	0	0	20
79	VLD 79	844.51	30	0	8	0	0	38
80	VLD 80	855.2	21	2	1	0	0	24
81	VLD 81	865.89	25	2	1	0	0	28
82	VLD 82	876.58	5	12	0	0	0	17
83	VLD 83	887.27	17	5	4	0	0	26
84	VLD 84	897.96	22	0	0	0	0	22
85	VLD 85	908.65	20	0	9	0	0	29
86	VLD 86	919.34	20	1	0	0	0	21
87	VLD 87	930.03	15	3	0	0	0	18
88	VLD 88	940.72	44	3	2	0	51	100
89	VLD 89	951.41	9	1	0	0	36	46
90	VLD 90	962.1	8	1	0	0	30	39
91	VLD 91	972.79	40	4	0	0	44	88
92	VLD 92	983.48	5	0	0	0	31	36
93	VLD 93	994.17	14	3	1	0	29	47
94	VLD 94	1004.86	20	0	10	0	30	60
95	VLD 95	1015.55	11	1	1	0	0	13
96	VLD 96	1026.24	18	2	0	0	0	20
97	VLD 97	1036.93	28	0	8	0	36	72
98	VLD 98	1047.62	19	0	0	0	0	19
99	VLD 99	1058.31	17	3	0	0	0	20
100	VLD 100	1069	21	3	0	0	0	24
101	VLD 101	1079.69	15	0	0	0	0	15
102	VLD 102	1090.38	6	0	0	0	0	6
103	VLD 103	1101.07	4	9	0	0	0	13
104	VLD 104	1111.76	13	3	1	0	0	17
105	VLD 105	1122.45	17	1	0	0	0	18
106	VLD 106	1133.14	22	2	0	0	0	24
107	VLD 107	1143.83	21	0	1	0	0	22
108	VLD 108	1154.52	25	0	2	0	0	27
109	VLD 109	1165.21	18	2	0	0	0	20
110	VLD 110	1175.9	10	0	1	0	0	11
111	VLD 111	1186.59	12	5	0	0	0	17
112	VLD 112	1197.28	33	3	4	0	3	43
113	VLD 113	1207.97	36	9	5	0	0	50
114	VLD 114	1218.66	33	0	1	0	5	39
115	VLD 115	1229.35	7	5	7	0	1	20
116	VLD 116	1240.04	11	6	1	0	0	18
117	VLD 117	1250.73	15	1	1	0	0	17
118	VLD 118	1261.42	9	3	22	0	0	34
119	VLD 119	1272.11	20	2	2	0	0	24
120	VLD 120	1282.8	21	5	0	0	0	26
121	VLD 121	1293.49	8	5	34	0	0	47
122	VLD 122	1304.18	26	0	17	0	0	43
123	VLD 123	1314.87	13	0	12	0	0	25
124	VLD 124	1325.56	10	3	5	0	0	18
125	VLD 125	1336.25	8	5	0	0	0	13
126	VLD 126	1346.94	8	6	0	6	0	20
127	VLD 127	1357.63	8	1	10	8	31	58
128	VLD 128	1368.32	10	2	0	0	0	12
129	VLD 129	1379.01	9	0	0	0	0	9
130	VLD 130	1389.7	6	0	0	0	0	6
131	VLD 131	1400.39	8	1	0	0	0	9
132	VLD 132	1411.08	3	0	0	0	0	3
TOTAL			**4105**				**331**	**4436**

Table 2. Table showing abundance of foraminifera

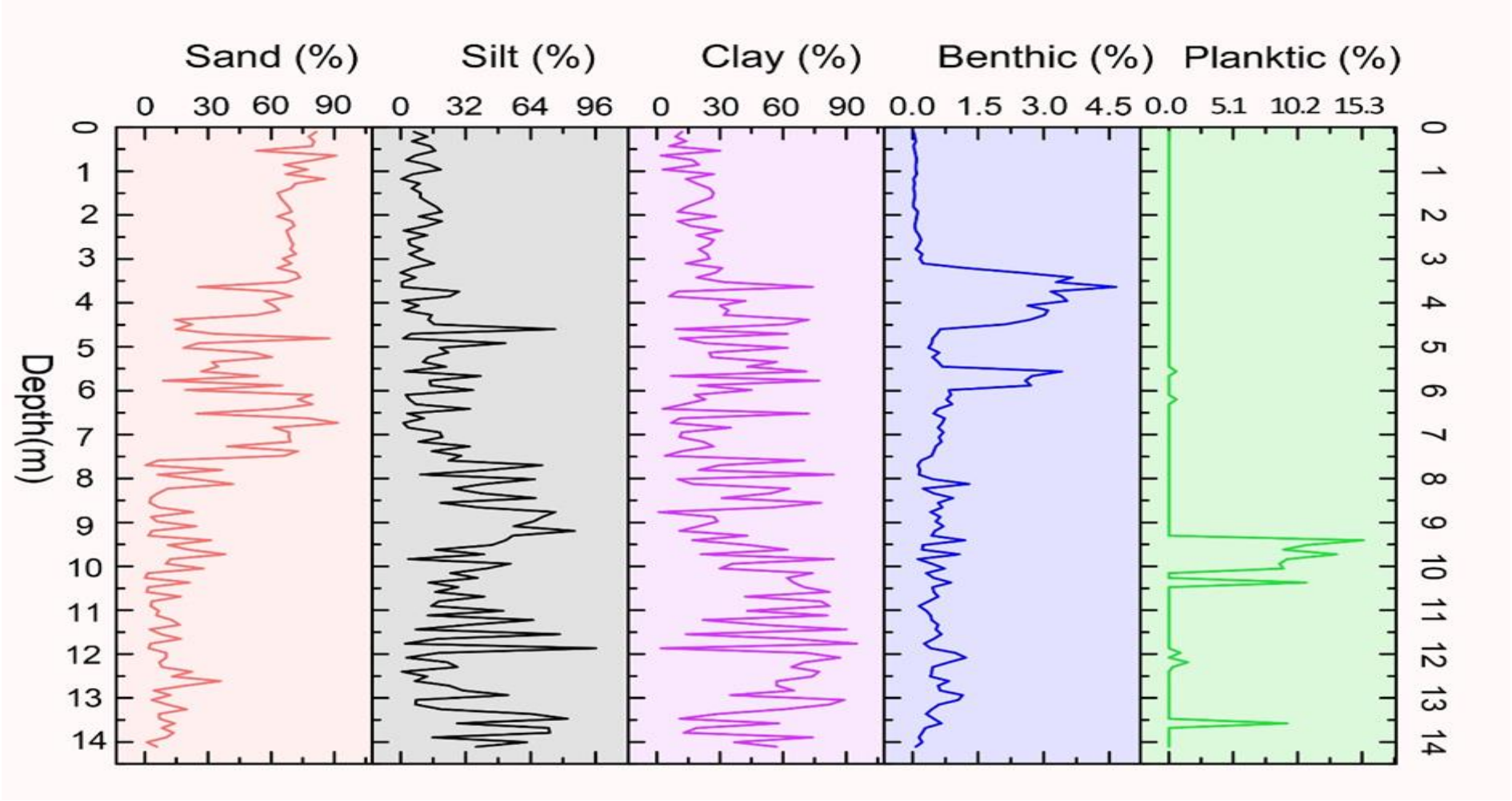

Figure 7. Graphical representation of texture and foraminiferal assemblages of VLD core 1

The figure 7 depicts a link between fossil assemblages and sediment, providing insight into coastal dynamics over the Holocene period. The graph demonstrates that the first three metres have a higher percentage of aeolian sand, indicating that they were generated in a highly weathered environment, which is also characterised by a smaller number of fossils and it contain 69% sand, 10% silt, and 20% clay. At 3 m, the abundance of benthic foraminifera named Ammonia beccarii increases. 5 to 6 m indicates a decrease in sand (33%), an increase in silt (17%), and a decrease in clay (52%). Below 8 m, the proportion of sand (11%) declines significantly as the amount of clay (50%) increases. The scarcity of fossils up to 13.5 m. At 13.5 m, there is a high abundance of planktic and benthic species, Bolivina sp. The lower section sediments has a lower number of forams with a high percentage of clay, but an abundance of marine mollusc shells and shell fragments indicate a marginal marine condition.

5.2. DISCUSSION

Aeolian sand from the topmost layer revealed that the uppermost region was deposited under backshore regime when the area was exposed to subaerial conditions The presence of leaf impressions at various depths in the core suggests that the area has a lot of organic materials and mangrove flora. Littoral sand is present at a depth of 6 m, which indicates a change in depositional conditions with a high-energy depositional environment. Peat is found in different layers and indicates an intertidal depositional environment, while shell fragments are abundant between 4 and 10 m and indicating a littoral depositional environment. Subsurface stratigraphy of the sediment core demonstrates that deposition in the area largely occurred through transgression in the lower part and regression in the top section. Thick sequence of silty clay with abundance of shells, peat and benthic foraminiferal species indicating a littoral to inter tidal deposit. Higher amount of clay and marine shells, implying a transgression of nature; also, marginal marine conditions prevailed in the area. Thus, we can deduce that there might be a transgression period after a phase of regression from coarsening of grains, shell fragments and increase in the peat content. Each strata's alteration in grain size and changes in the abundance of microfossil corresponds to a transgression period and a subsequent regression phase.

Textural studies reveal an increase in sand content in the upper part up to a depth of 4m with an average of 65-70% with low silt and clay content imply a higher energy environment of deposition. An increase in benthic foraminifera was also observed at depths of 3-4.5m and 6m depths. The sand content in the core at depths of 6-7m had shown a rapid change amounting up to 80%. Beyond 7m depth in the core, the sediments were largely composed of high

proportion of clay and silt. With minimal content of sand (<10%) implying a low energy depositional condition. The abundance of planktic species of foraminifera was observed at 10-11m interval and at 13.5m depth.

The microfossil assemblage of Vallarpadam core consists of both benthic species and planktic foraminifers, including Ammonia beccarii, Nonion sp., Nonion subturgidum, Bolivina sp. and Globigerina bulloid. It is observed that the abundance and distribution of microfossils are a function of substrate energy conditions and environmental variables. The presence of foraminifera of Nonion sp. are generally found associated with shallow inner shelf region in sandy sediments, whereas Ammonia beccarii in the middle shelf region with sandy to muddy substrate. The Bolivina sp. of foraminifera are found associated with the upper slope and within the muddy sand substrate with low dissolved oxygen in the bottom waters (Hari Krishnan and Senthil Nathan, 2023). The Nonion sp. found to show littoral characteristics and the depth of their occurrence and grain size characteristics gives evidences of littoral beach environment with high wave energy. Longshore transport by littoral drift and tidal current may mix the benthic foraminifera species of diverse shallow water affinity in an area (Hari Krishnan and Senthil Nathan, 2023). Similarly, Ammonia beccarii can be found associated with wide range of environments with varying salinity. Bolivina sp. is generally found confined to the oxygen deficient muddy environments and in the core, they are found at a depth of 13.4m associated with peat and clay substrate. The planktic foraminifera, Globigerina bulloid are thrived at 5-50m water depth where there is high productivity and food availability (Taylor et al., 2018).

The lack of fossils or their sparse distribution in the first 3 m indicates a sedimentary process that was unable to preserve the materials, which typically signifies erosion and could be a regressive phase. Changes in the environmental variables required to conserve fossils influenced the quantity of fossils and shell pieces. Spores found at a depth of 9.7 metres at VLD 91 point to the presence of a peat layer, which suggests that plants and greenery exist there.

Higher percentage of sand at a depth 3-4 m and the abundance of ammonia beccarii indicate littoral and neritic environment because this species is commonly found at this environment (Almogi-Labin et al., 1995). 4.5 m shows a decrease in fossil assemblages and could be due to a drop in sea level. At 9 m, planktic species increase, indicating a deep-water environment and this area is dominated by silty clay and the higher abundance of globigerina bulloids at this depth indicates upwelling zones (Shrivastava et al., 2016). Bolivina sp at bottom part are

indicating a deep ocean basin because the represents a low oxygen environment (Obiosio, 2013).

Previous work on sedimentological, palynological, and stable isotopic (13C and 15N) records in the Holocene sedimentary archives of the coastal lowlands of Central Kerala, (Padmalal et al., 2014),which is very close to the study area, gives an idea about the age, paleoclimate and sea level of the region. The organic-rich samples from the Varapuzha core at three levels, 3.5 m, 8.0 m, and 18.5 m, gave an age of 7550±70 years BP, 8340±120 years BP, and 10,110±80 years ago, respectively implying that the sediments were deposited throughout the Holocene. The transgression could have occurred between 8340±120 years BP ago. The comparison of the two cores Vallarpadam and Varapuzha reveals that the upper section is mostly sand dominated. According to the previous work, this sand is mainly derived from terrestrial input and extends to about 3 m. The presence of forams in the Varapuzha core indicates a marine affinity up to a depth of 3-5 m, also in the Vallarpadam core, the largest number of foram assemblages was observed between 3-5 m. Similarly, at a depth of 10 m in both cores, there is a high abundance of forams indicating the presence of marine sequence. Majority of the shells that have been identified from the core are found to be of marine origin and thus suggesting a marine to marginal marine depositional environment. Thus, it could be concluded that the sample that collected from the Vallarpadam core is deposited at Holocene period.

CHAPTER 6

CONCLUSIONS

The VLD sample is primarily used to study the land- sea interactions and paleoenvironmental conditions in Central Kerala. The sediment properties are identified through the textural analysis of the sample. Micropaleontological evidence provides information about the evolution of the area and its palaeo-geographic conditions. The following conclusions may be made from the present study:

1. The sediment in the core VLD at various depths suggests that the area was predominantly deposited in marine to marginal marine, intertidal, littoral, and supra-littoral conditions.
2. The visual interpretation of sediment, which includes sediment texture, leaf impression, peat, shells, and other materials, reflects the geomorphological changes in the study area, largely moderated by events of transgression followed by a regression.
3. The presence and abundance of microfossils of foraminifera in the subsurface sediments provides further evidences of sediment depositional settings, mainly marine to marginal marine environments. The greater number of these fossils, both benthic and planktic, indicates that the area was once submerged or experienced higher sea levels. Increases in planktic foraminifera, in particular, may indicate the expansion of the photic zone.
4. The lower abundance of these fossils at upper levels indicates a drop in sea level, which represents the regression phase.
5. The higher the ratio of marine fossils and clay, the more likely it is to have a maritime incursion phase which was later followed by a regression phase

Future Directions:

A detailed examination and systematic investigation of texture, carbon dating, palynological analysis, and other biological proxies would provide a better understanding of the region's evolutionary history. The fossil spores present in the subsurface sediments and characterization of peat units would shed light in to the palaeo-vegetation in the area. The detailed investigation of fossil shells and microfossils along with its dating would yield understanding on the land-sea interaction over time in the past.

REFERENCE

- Abramovich, S., Almogi-Labin, A., & Benjamini, C. (1998). Decline of the Maastrichtian pelagic ecosystem based on planktic foraminifera assemblage change: Implication for the terminal Cretaceous faunal crisis. *Geology*, *26*(1), 63–66. https://doi.org/10.1130/0091-7613(1998)026<0063:DOTMPE>2.3.CO;2
- Agarwal, S., Shukla, S. K., Srivastava, P., & Sundriyal, Y. (2023). Peat sequence diatoms from Kedarnath, Central Himalaya, used to reconstruct mid-late Holocene hydroclimatic conditions. *Palaeogeography, Palaeoclimatology, Palaeoecology*, *612*, 111381. https://doi.org/https://doi.org/10.1016/j.palaeo.2022.111381
- Alappat, L., Frechen, M., Tsukamoto, S., Anupama, K., Prasad, S., Gopakumar, P. G., & Kumar, S. S. (2021a). Evidences of early to mid-Holocene land–sea interactions and formation of Wetlands of Central Kerala in the south west coast of India. *Regional Studies in Marine Science*, *48*, 102009. https://doi.org/https://doi.org/10.1016/j.rsma.2021.102009
- Almogi-Labin, A., Siman-Tov, R., Rosenfeld, A., & Debard, E. (1995). Occurrence and distribution of the foraminifer Ammonia beccarii tepida (Cushman) in water bodies, recent and quaternary, of the Dead Sea rift, Israel. *Marine Micropaleontology*, *26*(1), 153–159. https://doi.org/https://doi.org/10.1016/0377-8398(95)00013-5
- Banerji, U. S., Bhushan, R., & Jull, A. J. T. (2017). Mid–late Holocene monsoonal records from the partially active mudflat of Diu Island, southern Saurashtra, Gujarat, western India. *Quaternary International*, *443*, 200–210. https://doi.org/https://doi.org/10.1016/j.quaint.2016.09.060
- Basu, A. (1976). Petrology of Holocene fluvial sand derived from plutonic source rocks; implications to paleoclimatic interpretation. *Journal of Sedimentary Research*, *46*(3), 694–709. https://doi.org/10.1306/212F7031-2B24-11D7-8648000102C1865D
- Benjamin, J., Rovere, A., Fontana, A., Furlani, S., Vacchi, M., Inglis, R. H., Galili, E., Antonioli, F., Sivan, D., Miko, S., Mourtzas, N., Felja, I., Meredith-Williams, M., Goodman-Tchernov, B., Kolaiti, E., Anzidei, M., & Gehrels, R. (2017). Late Quaternary sea-level changes and early human societies in the central and eastern Mediterranean Basin: An interdisciplinary review. *Quaternary International*, *449*, 29–57. https://doi.org/https://doi.org/10.1016/j.quaint.2017.06.025
- Bulletin, J. C.-G. S. of A., & 1961, undefined. (n.d.). Late Quaternary sea level: a discussion. *Pubs.Geoscienceworld.Org*. Retrieved June 21, 2023, from https://pubs.geoscienceworld.org/gsa/gsabulletin/article-abstract/72/11/1707/5278

- C. P., R., Rajagopalan, G., & Narayanaswamy. (1989). Quaternary geology of Kerala: evidence from radiocarbon dates. *Journal - Geological Society of India*, *33*, 218–222.
- Carter, J. A. (2007). PHYTOLITHS. In S. A. Elias (Ed.), *Encyclopedia of Quaternary Science* (pp. 2257–2265). Elsevier. https://doi.org/https://doi.org/10.1016/B0-44-452747-8/00212-X
- Colman, S. M., & Mixon, R. B. (1988). The record of major quaternary sea-level changes in a large coastal plain estuary, Chesapeake Bay, Eastern United States. *Palaeogeography, Palaeoclimatology, Palaeoecology*, *68*(2), 99–116. https://doi.org/https://doi.org/10.1016/0031-0182(88)90033-8
- Crossland Christopher J. and Baird, D. and D. J.-P. and L. H. and B. R. W. and D. W. C. and M. B. A. and S. S. V. and S. D. P. (2005). The Coastal Zone — a Domain of Global Interactions. In H. H. and L. H. J. and M. C. J. I. and L. T. M. D. A. Crossland Christopher J. and Kremer (Ed.), *Coastal Fluxes in the Anthropocene: The Land-Ocean Interactions in the Coastal Zone Project of the International Geosphere-Biosphere Programme* (pp. 1–37). Springer Berlin Heidelberg. https://doi.org/10.1007/3-540-27851-6_1
- Dash, C., Jaiswal, M. K., Pati, P., Patel, N. K., Singh, A. K., & Shah, R. A. (2020). Fluvial response to Late Quaternary sea level changes along the Mahanadi delta, east coast of India. *Quaternary International*, *553*, 60–72. https://doi.org/https://doi.org/10.1016/j.quaint.2020.07.033
- De Araújo, H. A. B., & De Jesus Machado, A. (2008). BENTHIC FORAMINIFERA ASSOCIATED WITH THE SOUTH BAHIA CORAL REEFS, BRAZIL. *Journal of Foraminiferal Research*, *38*(1), 23–38. https://doi.org/10.2113/gsjfr.38.1.23
- De Deckker, P., & Yokoyama, Y. (2009). Micropalaeontological evidence for Late Quaternary sea-level changes in Bonaparte Gulf, Australia. *Global and Planetary Change*, *66*(1), 85–92. https://doi.org/https://doi.org/10.1016/j.gloplacha.2008.03.012
- de Vargas, C., Renaud, S., Hilbrecht, H., & Pawlowski, J. (2001). Pleistocene adaptive radiation in Globorotalia truncatulinoides: genetic, morphologic, and environmental evidence. *Paleobiology*, *27*(1), 104–125. https://doi.org/DOI: 10.1666/0094-8373(2001)027<0104:PARIGT>2.0.CO;2
- Debenay, J.-P., Bénéteau, E., Zhang, J., Stouff, V., Geslin, E., Redois, F., & Fernandez-Gonzalez, M. (1998a). Ammonia beccarii and Ammonia tepida (Foraminifera): morphofunctional arguments for their distinction. *Marine Micropaleontology*, *34*(3), 235–244. https://doi.org/https://doi.org/10.1016/S0377-8398(98)00010-3
- Debenay, J.-P., & Luan, B. T. (2006). Foraminiferal assemblages and the confinement index as tools for assessment of saline intrusion and human impact in the Mekong Delta

and neighbouring areas (Vietnam). *Revue de Micropaléontologie*, *49*(2), 74–85. https://doi.org/https://doi.org/10.1016/j.revmic.2006.01.002

- Fabbrini, A., Greco, M., Ezard, T., Wade, B., & Kucera, M. (2022, August). *Unravelling the Globigerina falconensis plexus: a journey from the Miocene to the present*.
- Gandhi, M. S., & K.Jisha. (2016). Foraminiferal and Sediment geochemistry studies in and around Cochin backwaters, southwest coast of India. *Indian Journal of Geo-Marine Sciences*.
- Gehrels, W. R. (2013). SEA LEVEL STUDIES | Microfossil-Based Reconstructions of Holocene Relative Sea-Level Change. In S. A. Elias & C. J. Mock (Eds.), *Encyclopedia of Quaternary Science (Second Edition)* (Second Edition, pp. 419–428). Elsevier. https://doi.org/https://doi.org/10.1016/B978-0-444-53643-3.00137-0
- Hawkes, A. D. (2020). Chapter 12 - Foraminifera in tsunami deposits. In M. Engel, J. Pilarczyk, S. M. May, D. Brill, & E. Garrett (Eds.), *Geological Records of Tsunamis and Other Extreme Waves* (pp. 239–259). Elsevier. https://doi.org/https://doi.org/10.1016/B978-0-12-815686-5.00012-2
- Hein, C., FitzGerald, D., Milne, G., … K. B.-, & 2011, undefined. (2011). Evolution of a Pharaonic harbor on the Red Sea: Implications for coastal response to changes in sea level and climate. *Pubs.Geoscienceworld.OrgCJ Hein, DM FitzGerald, GA Milne, K Bard, R FattovichGeology, 2011•pubs.Geoscienceworld.Org*. https://doi.org/10.1130/G31928.1
- Heinz, P., Hemleben, C., & Kitazato, H. (2002). Time-response of cultured deep-sea benthic foraminifera to different algal diets. *Deep Sea Research Part I: Oceanographic Research Papers*, *49*(3), 517–537. https://doi.org/https://doi.org/10.1016/S0967-0637(01)00070-X
- Horton, B. P., Culver, S. J., Hardbattle, M. I. J., Larcombe, P., Milne, G. A., Morigi, C., Whittaker, J. E., & Woodroffe, S. A. (2007). RECONSTRUCTING HOLOCENE SEA-LEVEL CHANGE FOR THE CENTRAL GREAT BARRIER REEF (AUSTRALIA) USING SUBTIDAL FORAMINIFERA. *Journal of Foraminiferal Research*, *37*(4), 327–343. https://doi.org/10.2113/gsjfr.37.4.327
- Jain, P. C., & Anantharaman, M. S. (1996). *Palaeontology, Evolution and Animal Distribution*. Vishal Publications.
- Jukar, A. M., Lyons, S. K., Wagner, P. J., & Uhen, M. D. (2021). Late Quaternary extinctions in the Indian Subcontinent. *Palaeogeography, Palaeoclimatology, Palaeoecology*, *562*, 110137. https://doi.org/https://doi.org/10.1016/j.palaeo.2020.110137
- KEERTHINAIR, B., BABEESH, C., & HEMA, A. (2014). LATE QUATERNARY-HOLOCENE PALEOENVIRONMENTAL RECONSTRUCTION AND HYDRODYNAMICS BASED ON SOME LAKES AND MARINE. *Journal o f Geological Society o f Sri Lanka*, *16*, 159–170. http://viduketha.nsf.gov.lk:8585/slsijn/JGSSL-VOL-16-2014/JGSSL-VOL-16-2014-159.pdf

- Kotlia, B. S., Singh, A. K., Joshi, L. M., & Bisht, K. (2018). Precipitation variability over Northwest Himalaya from ~4.0 to 1.9 ka BP with likely impact on civilization in the foreland areas. *Journal of Asian Earth Sciences*, *162*, 148–159. https://doi.org/https://doi.org/10.1016/j.jseaes.2017.11.025
- Kunte, P. D., Alagarsamy, R., & Hursthouse, A. S. (2013). Sediment fluxes and the littoral drift along northeast Andhra Pradesh Coast, India: estimation by remote sensing. *Environmental Monitoring and Assessment*, *185*(6), 5177–5192. https://doi.org/10.1007/s10661-012-2934-0
- Lambeck, K., & Chappell, J. (2001). Sea Level Change Through the Last Glacial Cycle. *Science*, *292*(5517), 679–686. https://doi.org/10.1126/science.1059549
- Lister, A. (2004). Correction for Lister, The impact of Quaternary Ice Ages on mammalian evolution. *Philosophical Transactions of The Royal Society B: Biological Sciences*, *359*, 1953–1954. https://doi.org/10.1098/rstb.2004.2000
- Loveson, V. J., & Nigam, R. (2019). Reconstruction of Late Pleistocene and Holocene Sea Level Curve for the East Coast of India. *Journal of the Geological Society of India*, *93*(5), 507–514. https://doi.org/10.1007/s12594-019-1211-z
- Maeda, A., Kuroyanagi, A., Iguchi, A., Gaye, B., Rixen, T., Nishi, H., & Kawahata, H. (2022). Seasonal variation of fluxes of planktic foraminiferal tests collected by a time-series sediment trap in the central Bay of Bengal during three different years. *Deep Sea Research Part I: Oceanographic Research Papers*, *183*, 103718. https://doi.org/https://doi.org/10.1016/j.dsr.2022.103718
- MANASA, M., SARASWAT, R., & NIGAM, R. (2016). Assessing the suitability of benthic foraminiferal morpho-groups to reconstruct paleomonsoon from Bay of Bengal. *Journal of Earth System Science*, *125*(3), 571–584. https://doi.org/10.1007/s12040-016-0677-y
- Martin, L., Dominguez, J., Research, A. B.-J. of C., & 2003, undefined. (n.d.). Fluctuating Holocene sea levels in eastern and southeastern Brazil: evidence from multiple fossil and geometric indicators. *JSTORL Martin, JML Dominguez, ACSP BittencourtJournal of Coastal Research, 2003•JSTOR*. Retrieved August 31, 2023, from https://www.jstor.org/stable/4299151
- Massey, A. C., Gehrels, W. R., Charman, D. J., & White, S. V. (2006). AN INTERTIDAL FORAMINIFERA-BASED TRANSFER FUNCTION FOR RECONSTRUCTING HOLOCENE SEA-LEVEL CHANGE IN SOUTHWEST ENGLAND. *Journal of Foraminiferal Research*, *36*(3), 215–232. https://doi.org/10.2113/gsjfr.36.3.215
- Meyers, P. A., & Teranes, J. L. (n.d.). *9. SEDIMENT ORGANIC MATTER*.

- Monjezi, N., & Saeedi Razavi, B. (2021). Biostratigraphy of the Asmari Formation in Gachraran oilfield, Southwestern Iran. *Scientific Semiannual Journal Facies*, *13*(2), 239–251. https://doi.org/10.22067/sed.facies.2021.46954
- Murray, J. W. (2001). The niche of benthic foraminifera, critical thresholds and proxies. *Marine Micropaleontology*, *41*(1), 1–7. https://doi.org/https://doi.org/10.1016/S0377-8398(00)00057-8
- Murray, J. W. (2007). Biodiversity of living benthic foraminifera: How many species are there? *Marine Micropaleontology*, *64*(3), 163–176. https://doi.org/https://doi.org/10.1016/j.marmicro.2007.04.002
- Narayana, A. C., Ismaiel, M., & Priju, C. P. (2021). An environmental magnetic record of heavy metal pollution in Vembanad lagoon, southwest coast of India. *Marine Pollution Bulletin*, *167*, 112344. https://doi.org/https://doi.org/10.1016/j.marpolbul.2021.112344
- Narayana, A., Priju, C., Science, G. R.-C., & 2002, undefined. (n.d.). Late Quaternary peat deposits from Vembanad Lake (lagoon), Kerala, SW coast of India. *JSTOR*. Retrieved June 21, 2023, from https://www.jstor.org/stable/24106893
- Narayana, A., Research, C. P.-J. of C., & 2006, undefined. (n.d.). Evolution of coastal landforms and sedimentary environments of the late quaternary period along central Kerala, southwest coast of India. *JSTOR*. Retrieved June 21, 2023, from https://www.jstor.org/stable/25743091
- Nicholls, R. J., Wong, P. P., Burkett, V., Codignotto, J., & Hay, J. (2007). *Coastal systems and low-lying areas*. https://ro.uow.edu.au/scipapers/164/
- Nigam, R. (1986). Foraminiferal assemblages and their use as indicators of sediment movement : a study in the shelf region off Navapur, India. *Continental Shelf Research*, *5*(4), 421–430. https://doi.org/https://doi.org/10.1016/0278-4343(86)90069-5
- Nigam, R., & Khare, N. (1999). Spatial and temporal distribution of Foraminifera in sediments off the central west coast of India and use of their test morphologies for the reconstruction of paleomonsoonal precipitation. *Micropaleontology*, *45*(3), 285–303.
- Obiosio, E. (2013). Biostratigraphy and Paleoenvironment of Bolivina Fauna from the Niger Delta, Nigeria. *Earth Science Research*, *2*. https://doi.org/10.5539/esr.v2n2p80
- Padmalal, D., Kumaran, K. P. N., Limaye, R. B., Baburaj, B., Maya, K., & Vishnu Mohan, S. (2014). Effect of Holocene climate and sea level changes on landform evolution and human habitation: Central Kerala, India. *Quaternary International*, *325*, 162–178. https://doi.org/10.1016/J.QUAINT.2013.12.032
- Pilarczyk, J. E., Dura, T., Horton, B. P., Engelhart, S. E., Kemp, A. C., & Sawai, Y. (2014). Microfossils from coastal environments as indicators of paleo-earthquakes, tsunamis and

storms. *Palaeogeography, Palaeoclimatology, Palaeoecology*, *413*, 144–157. https://doi.org/https://doi.org/10.1016/j.palaeo.2014.06.033

- Priju, C., OF, A. N.-J.-G. S., & 2007, undefined. (n.d.). Particle size characterization and late Holocene depositional processes in Vembanad Lagoon, Kerala: inferences from suite statistics. *Researchgate.Net*. Retrieved June 29, 2023, from https://www.researchgate.net/profile/Priju-P/publication/287690867_Particle_size_characterization_and_Late_Holocene_depositional_processes_in_Vembanad_lagoon_Kerala_Inferences_from_suite_statistics/links/5851895208ae7d33e013bcc2/Particle-size-characterization-and-Late-Holocene-depositional-processes-in-Vembanad-lagoon-Kerala-Inferences-from-suite-statistics.pdf
- Psuty, N. P., Ames, K., Habeck, A., & Schmelz, W. (2018). Responding to coastal change: Creation of a regional approach to monitoring and management, northeastern region, U.S.A. *Ocean & Coastal Management*, *156*, 170–182. https://doi.org/10.1016/J.OCECOAMAN.2017.08.004
- Radhakrishnan, R., N.R, N., Menon, N., & Musaliyarakam, N. (2016, September). *REPORTS OF SOME RECENT BENTHIC FORAMINIFERA FROM THE INNER SHELF OF KERALA COAST*.
- Raja, P., Achyuthan, H., Geethanjali, K., Kumar, P., & Chopra, S. (2018). Late Pleistocene Paleoflood Deposits Identified by Grain Size Signatures, Parsons Valley Lake, Nilgiris, Tamil Nadu. *Journal of the Geological Society of India*, *91*(5), 547–553. https://doi.org/10.1007/s12594-018-0903-0
- Rao, V. P., Rajagopalan, G., Vora, K. H., & Almeida, F. (2003). Late Quaternary sea level and environmental changes from relic carbonate deposits of the western margin of India. *Journal of Earth System Science*, *112*(1), 1–25. https://doi.org/10.1007/BF02710040
- Rosentau, A., Klemann, V., Bennike, O., Steffen, H., Wehr, J., Latinović, M., Bagge, M., Ojala, A., Berglund, M., Becher, G. P., Schoning, K., Hansson, A., Nielsen, L., Clemmensen, L. B., Hede, M. U., Kroon, A., Pejrup, M., Sander, L., Stattegger, K., … Subetto, D. (2021). A Holocene relative sea-level database for the Baltic Sea. *Quaternary Science Reviews*, *266*, 107071. https://doi.org/https://doi.org/10.1016/j.quascirev.2021.107071
- Rossi, V., & Horton, B. P. (2009). THE APPLICATION OF A SUBTIDAL FORAMINIFERA-BASED TRANSFER FUNCTION TO RECONSTRUCT HOLOCENE PALEOBATHYMETRY OF THE PO DELTA, NORTHERN ADRIATIC SEA. *Journal of Foraminiferal Research*, *39*(3), 180–190. https://doi.org/10.2113/gsjfr.39.3.180
- Roy, A. B., & Purohit, R. (2021). Quaternary Changes in the Indian Subcontinent: Implications on Neotectonics. *International Journal of Advanced Research in Science, Communication and Technology (IJARSCT)*, *7*(2). https://doi.org/10.48175/568

- Roy, P. S., Thom, B. G., & Wright, L. D. (1980). Holocene sequences on an embayed high-energy coast: an evolutionary model. *Sedimentary Geology*, *26*(1), 1–19. https://doi.org/https://doi.org/10.1016/0037-0738(80)90003-2
- Sati, S. P., Ali, S. N., Rana, N., Bhattacharya, F., Bhushan, R., Shukla, A. D., Sundriyal, Y., & Juyal, N. (2014). Timing and extent of Holocene glaciations in the monsoon dominated Dunagiri valley (Bangni glacier), Central Himalaya, India. *Journal of Asian Earth Sciences*, *91*, 125–136. https://doi.org/https://doi.org/10.1016/j.jseaes.2014.05.008
- Shaji, J., Banerji, U. S., Maya, K., Joshi, K. B., Dabhi, A. J., Bharti, N., Bhushan, R., & Padmalal, D. (2022). Holocene monsoon and sea-level variability from coastal lowlands of Kerala, SW India. *Quaternary International*, *642*, 48–62. https://doi.org/https://doi.org/10.1016/j.quaint.2022.03.005
- Shrivastava, A., Singh, A., Sinha, D., Kaushik, T., Singh, V., & Mallick, K. (2016). Significance of Globigerina Bulloides D'orbigny: A Foraminiferal Proxy for Palaeomonsoon and Past Upwelling Records. *Journal of Climate Change*, *2*, 99–110. https://doi.org/10.3233/JCC-160021
- Shukla, T., Mehta, M., Jaiswal, M. K., Srivastava, P., Dobhal, D. P., Nainwal, H. C., & Singh, A. K. (2018). Late Quaternary glaciation history of monsoon-dominated Dingad basin, central Himalaya, India. *Quaternary Science Reviews*, *181*, 43–64. https://doi.org/https://doi.org/10.1016/j.quascirev.2017.11.032
- Speed, D. E. (2022). 11 - Environmental aspects of planarization processes. In S. Babu (Ed.), *Advances in Chemical Mechanical Planarization (CMP) (Second Edition)* (Second Edition, pp. 257–320). Woodhead Publishing. https://doi.org/https://doi.org/10.1016/B978-0-12-821791-7.00002-2
- Stanchev, H., Stancheva, M., & Young, R. (2015). Implications of population and tourism development growth for Bulgarian coastal zone. *Journal of Coastal Conservation*, *19*(1), 59–72. https://doi.org/10.1007/s11852-014-0360-x
- Thom, B. G. (1984). Transgressive and regressive stratigraphies of coastal sand barriers in southeast Australia. *Marine Geology*, *56*(1), 137–158. https://doi.org/https://doi.org/10.1016/0025-3227(84)90010-0
- Tiju, V. I., Prakash, T. N., Sheela Nair, L., Sreenivasulu, G., & Nagendra, R. (2021). Reconstruction of the paleoenvironment of the late Quaternary sediments of the Kerala coast, SW India. *Journal of Asian Earth Sciences*, *222*, 104952. https://doi.org/https://doi.org/10.1016/j.jseaes.2021.104952
- Vishnu Mohan, S., Limaye, R. B., Padmalal, D., Ahmad, S. M., & Kumaran, K. P. N. (2017). Holocene climatic vicissitudes and sea level changes in the south western coast of India:

Appraisal of stable isotopes and palynology. *Quaternary International*, *443*, 164–176. https://doi.org/https://doi.org/10.1016/j.quaint.2016.07.018

- Yao, T., Thompson, L., Yang, W., Yu, W., Gao, Y., Guo, X., Yang, X., Duan, K., Zhao, H., Xu, B., Pu, J., Lu, A., Xiang, Y., Kattel, D. B., & Joswiak, D. (2012). Different glacier status with atmospheric circulations in Tibetan Plateau and surroundings. *Nature Climate Change*, *2*(9), 663–667. https://doi.org/10.1038/nclimate1580
- Zalasiewicz, J., Waters, C. N., Williams, M., Barnosky, A. D., Cearreta, A., Crutzen, P., Ellis, E., Ellis, M. A., Fairchild, I. J., Grinevald, J., Haff, P. K., Hajdas, I., Leinfelder, R., McNeill, J., Odada, E. O., Poirier, C., Richter, D., Steffen, W., Summerhayes, C., … Oreskes, N. (2015). When did the Anthropocene begin? A mid-twentieth century boundary level is stratigraphically optimal. *Quaternary International*, *383*, 196–203. https://doi.org/https://doi.org/10.1016/j.quaint.2014.11.045
- Zazo, C., Goy, J. L., Dabrio, C. J., Lario, J., González-Delgado, J. A., Bardají, T., Hillaire-Marcel, C., Cabero, A., Ghaleb, B., Borja, F., Silva, P. G., Roquero, E., & Soler, V. (2013). Retracing the Quaternary history of sea-level changes in the Spanish Mediterranean–Atlantic coasts: Geomorphological and sedimentological approach. *Geomorphology*, *196*, 36–49. https://doi.org/https://doi.org/10.1016/j.geomorph.2012.10.020

DISTRIBUTION OF MICROPLASTICS FROM SURFACE SEDIMENTS IN BRAHMAPURAM AREA, ERNAKULAM DISTRICT

Dissertation submitted to Christ College (Autonomous), Irinjalakuda, Kerala, University of Calicut in partial fulfilment of the degree of

Master of Science in Applied Geology

By,

APARNA RAJAN

Reg. No: CCAVMAG004

2021-2023

DEPARTMENT OF GEOLOGY AND ENVIRONMENTAL SCIENCE

CHRIST COLLEGE (AUTONOMOUS), IRINJALAKUDA, KERALA,680125

(Affiliated to University of Calicut and re-accredited with by NAAC with A++ grade)

AUGUST 2023

CERTIFICATE

This is to certify that the dissertation entitled- **DISTRIBUTION OF MICROPLASTICS FROM SURFACE SEDIMENTS IN BRAHMAPURAM AREA, ERNAKULAM DISTRICT** is a bonafied record of work done by Ms. APARNA RAJAN (CCAVMAG004) M.Sc. Applied Geology, Christ College (Autonomous), Irinjalakuda under my guidance in partial fulfilment of requirements for the degree of Master of Science in Applied Geology during the academic year 2021-2023.

Ivine Joseph .
Internal Supervisor

Dr. Anto Francis K.
Coordinator Geology

Christ College (Autonomous), Irinjalakuda

Kerala - 680125

Place: …….

Date: ……..

External Examiners:

1……..

2……..

DECLARATION

I hereby **Aparna Rajan** declare that this dissertation work — **DISTRIBUTION OF MICROPLASTICS FROM SURFACE SEDIMENTS IN BRAHMAPURAM AREA, ERNAKULAM DISTRICT,** is a work done by me. No part of the report is reproduced from other resources. All information included from other sources has been duly acknowledged. I maintain that if any part of the report is found to be plagiarized, I shall take the full responsibility for it.

Place: Irinjalakuda APARNA RAJAN

Date: Reg. No. CCAVMAG004

ACKNOWLEDGEMENT

In the first place, I thank God Almighty greatly, by whose grace I'm able to complete this work.

I place my earnest thanks to **Ms. Ivine Joseph**, Assistant Professor, Department of Geology, Christ College (Autonomous), Irinjalakuda, who guided and encouraged me with her constant support, guidance and suggestions throughout the programme to make it a great success.

I would like to take this opportunity to express my deepest gratitude to**, Dr. Linto Alappat**, Dean of Research and Development of TLC (former HOD), Department of Geology, Christ College (Autonomous), Irinjalakuda. **Dr**. **Anto Francis K.** Co-ordinator (SF), Department of Geology, Christ College (Autonomous), Irinjalakuda and **Mr. Tharun R**. Head of Department of Geology and Environmental Science, Christ College (Autonomous), Irinjalakuda.

I express my sincere gratitude to **Ms. Roshini. P.P, Dr. Anso M.A, Mrs. Shaima M.M,** Assistant Professors, Department of Geology, Christ College (Autonomous), Irinjalakuda, who guided me internally for completion of my work. I also thank other faculty members of the department for their continuous support and encouragement.

I would like to acknowledge the Research Scholar, **Mr. Ayyappa Das C.S**, Department of Geology, Christ College (Autonomous), Irinjalakuda, for his advice and valuable guidance.

Last, but not the least, I would like to show my sincere gratitude to my parents for their sustained prayer, financial and moral support in the completion of my work.

I take this opportunity to thank my friends and classmates and all those who have directly and indirectly contributed their time, material and encouraged me during the course of my investigation.

APARNA RAJAN

CONTENTS

LIST OF FIGURES

LIST OF TABLES

ABSTRACT

The present study is a distribution pattern of microplastic, percentage of organic carbon and a textural characteristics of river bank sediments in Brahmapuram area, Ernakulam district. This is focused on the quantity of microplastic present in the soil, presence of organic carbon relation with microplastic, and the related textural classification. Sediments were collected from Brahmapuram waste plant and nearby areas. Brahmapuram has led to a concern about the contamination of waste. By using trilinear plot, percentage of the texture of sample were identified and classified into different types. Maximum organic matter and microplastic is identified in sample number 10. The study is an integrated approach showing the relationship between organic matter, microplastic, and soil texture.

CHAPTER 1

INTRODUCTION

1.1 GENERAL

The presence of microplastic, which was defined as small piece of plastic less than 5 mm in size. Aquatic environment has become global concern there days. The microplastic accumulate in basin sediments either directly by sinking through the water column or indirectly by current or sediment transport by water. Main source of microplastic in soil sludge and waste water irrigation. Microplastic can have ecological impact on soil biota and even threaten human health. Microplastic came from a variety of source including larger particles piece that have broken synthetic textiles are the single greatest contributors of microplastic.

One in aquatic environment microplastic might float in the water column or sink in to the bottom, depend up on the particle density. Microplastic could sink in bottom as result of biofouling which can increase its density [Biofouling – undesirable accumulation of microorganisms, plants, algae and animals are submerged structure]. Sediments have considered to be major sink of microplastic and accumulation in sediments can bring harm to marine and human life. The morphological characteristics of microplastic is shape, colour, and size. Microplastic were identified in all sediment. Microplastics can come in many different forms, such as bigger plastic pieces that have broken up, resin pellets used in the production of plastic, or microbeads, which are tiny, produced plastic beads used in cosmetic and health products. Microplastics and their impact on human health are still an early stage of research, thus little is known about them. The research on this subject is being spearheaded by the NOAA Marine Debris Programme. There are now standardised field techniques that are being tested for the collection of sediment, sand, and surface-water microplastic samples. The first step in understanding the ultimate distribution, effects, and fate of this debris is to compare the amount of microplastics discharged into the ecosystem on a worldwide scale using field and laboratory techniques. Microplastics are considered to be carbon and hydrogen atoms bound together in polymer chains and others are phthalates, polybrominated diphenyl ethers and Tetra bromo bisphenol A are present. These chemicals are lech out of the plastic and entering into the environment. Primary and secondary microplastics are the two types of microplastic. Primary

consist of microbeads found in personal care products, plastic pellets manufacturing of industries and plastic fibres used in synthetic textiles. Primary plastics are directly entered into sediments and secondary plastics are form from breakdown of larger particles. Microplastic are not in sediments but also in water, beer, and food products including sea food and table salt. To reduce the amount of microplastic in environment to use of microorganism capable of breaking down chemicals like polystyrene, polyester polyurethane and polyethylene. These microorganisms are applied in sewage waste water and other contaminated environment. Microplastics are typically linked to anthropogenic sources, although there is mounting proof that they can also appear naturally in sediments. There is less research on natural sources of microplastics in sediments than there is on anthropogenic sources. Natural processes like abrasion, erosion, and weathering can break down rocks and minerals, producing particles of various sizes. In environments with high-energy processes like rivers, glaciers, and wind, these natural micro-sized particles can be certain natural polymers like chitin, found in the exoskeletons of crustaceans and insects, can break down into small particles. While these particles are not plastics, they may resemble microplastics in terms of size and shape generated and transported into aquatic systems, eventually becoming part of sediment deposits. Volcanic eruptions can release ash and lava fragments that, upon cooling and solidifying, can be broken down into micro-sized particles. These volcanic particles can eventually be transported by water and deposited in sedimentary environments. Natural plant materials, such as leaves, stems, and wood, can degrade over time, producing small particles that might resemble microplastics. These particles can be carried by water and wind and eventually settle in sedimentary environments.

The traces of once living creatures and their carbon-containing metabolites are referred to as organic matter. Dead plants, animals, microbes, and other organic compounds including cellulose, lignin, and proteins are included in this category. Because it helps with nutrient cycling, soil structure, and general ecosystem health, organic matter is an essential part of soil, sediment, and aquatic ecosystems. Organic material can appear in sediment in a number of ways, including: detritus, peat, humus, microbial biomass. Organic material in sediment can have a number of significant effects, including:

1. Cycling of nutrients: Nitrogen and phosphorus, two vital nutrients, are found in organic matter. These nutrients are released into the water and sediment as it decomposes, fostering the development of plants and microbes.

2. Structure of Sediment: By holding particles together, organic materials can strengthen the structure of sediment and soil. This improves aeration and water retention, both of which are crucial for plant growth.
3. Carbon Sequestration: By storing carbon over long periods of time, organic matter that collects in sediment can aid with carbon sequestration, which helps to slow down the effects of climate change.
4. Support for Ecosystems: Organic material in sediment serves as a food supply for a variety of aquatic creatures, enhancing the biodiversity and efficiency of aquatic ecosystems.

Various kinds of organic matter accumulate under various conditions, therefore the presence and makeup of organic matter in sediment can reveal information about the evolution of an. In order to comprehend current ecological dynamics, influences of humans, and historical environmental changes, scientists frequently investigate organic sediments.

Organic matter in sediments is considered carbon and nutrients in the form of carbohydrate, protein, fat, and nucleic acid. In the sediments, the organic matter is formed from plant and animal detritus, bacteria or plankton were formed in situ, or derived from natural and anthropogenic source in catchments. The Total Organic carbon (TOC) is considered as organic matter in sediments. The amount of organic matter in sediments is the function of the sediments reaching the surface and different type of organic matter is degrade by microbial processes during burial. The organic matter in sediments indicate that organic life, based on geology, a fossil. Organic carbon is more important and abundant with the development and diversification of life. 0rganic matter in sediments is a source of recycled nutrients for water column productivity, food and energy and its nutritional balance. Organic decomposition is increases as nitrogen and phosphorous is also increase. Organic matter is accumulated mostly in fine grained sediments. Sediments absorb minerals and helps to preserve organic matter. Accumulation of organic matter is in the way of water which control the organic matter by the process of transport and deposition. In a variety of marine depositional situations, more than 90% of the total organic material cannot be physically separated from the mineral matrix.

Sediment develops when rocks, minerals, and organic compounds from the Earth's surface are eroded and weathered. These materials can be transported by wind or water as they are broken down into smaller particles. The sediment particles settle out of the fluid and assemble on the surface of the ground or in bodies of water when the carrying force decreases or

disappears. Sedimentary rocks can be created when the accumulated sediment layers are compressed and cemented together over extended periods of time. These rocks can offer crucial hints about historical environmental circumstances, such as details on the kinds of species that existed there, the climate at the time, and geological events that affected the terrain.

Textural classification of sediments will be providing valuable information of source of sediments. Most of the sediments are fairly sorted at the backshore and reasonably well sorted at the foreshore. The majority irinof the sediments along the shore are symmetrical and mesokurtic, indicating that the majority of the sediments are properly sorted. Textural classification is influenced by sedimentary process and also environmental factors. Majority of the land is covered by soil, loose substance.

Based on the dominant particles, soil can be divided into sand, clay, silt, peat, chalk and long type of soil. Sedimentation is carried out by water, winter, and other agencies. In river bank areas water is the major agency to carry sediments in different size, it is due the influence of flow rate of water. The flow rate is slow, more mud, silt, and sand are dumped in to the river or the vicinity. Water flow is influencing the range in size of particles from boulders to sand particles. sedimentation frequently occurs along waterfall bottoms, riverbank, and deltas. Came in variety of sizes. The smallest particle has the size less than 0.002 mm is clay. Silt size up to 0.002 to 0.05 mm and sand size is 0.05 to 2.0 mm.

1.2 AIM AND OBJECTIVES

Aim:

The aim of the study is to investigate the textural characteristics and microplastic abundance in the surface sediments near Bhramapuram landfill, Ernakulam

Objectives:

- To identify the source and path way of microplastic pollution and understand the extent of microplastic pollution in the ecosystem
- To correlate the influence of organic matter on microplastics.
- To analyse the textural characteristics of the surface sediments.

CHAPTER 2

REVIEW OF LITERATURE

Plastic is changed our way of life. It can be used at a wide range of temperature, has low thermal conductivity, a high strength to weight ratio. As a result, the global plastic production has grown exponentially over since its mass production started in the 1950s with 288 million tonnes produced worldwide in 2012 plastic are present in the environment in various size from metres to micrometeors. The smallest form of plastic is called MICROPLASTIC.

At present there is no universally accepted definition of size of microplastic. Firstly, described in 2004. The term microplastic was adopted to refer to microplastic debris in the 20 μm**.** Region definition fragments smaller than 5mm was made in 2009.microplastic is reported in the water. Column and marine sediments worldwide which the 1st reported in surface water already date back to early 1970s. Sediments are suggested to be a long-term sink for microplastic. Plastic with a density that exceeds that of sea water will sink and accumulate in the sediment, while low density particles tend to float on the sea surface or in the water column. The first report of microplastic associate with sediments date back to the late 1970s.This early observation comprised industrial resin pellets on beaches in New Zealand, Canada, Bermuda, and Spain.

To study microplastic pollution samples are often take from deep ocean sediments, coast and sea beds microplastic are swallowed by a wide range of biological species from single called to marine mammals. During the consumption of their waste. Several problems like distribution and decrease nutritional ability, reduce fertility and reproduction death have been occurred. Studies have also revealed that microplastic pollution is increasing in worldwide in river and lake. Microplastic are composed mainly of poly vinyl chloride, nylons and polythene terephthalate and those made of polythene, polypropylene and polystyrene which float on the surface of water. Microplastic studies are late focused on temporal and spatial variation understanding, biological effect and analytical method of microplastic in sediments, transportation, transformation and accumulation of microplastic is due to the anthropogenic input and environmental process. The biological effect of microplastic is based on the field

research and laboratory test. Density separation method for separation of microplastic in sediments is the most commonly used. Component identification is by optical analysis.

Microplastic pollution was investigated in sediments and surface water in West Dong ting lake and South Dongping lake for the first time. The abundance of microplastic ranged from 616.67 to 22167.67 items /m^3 and 716.67 to 2316.67 items /m^3 only the marine microplastic pollution have given more attention. Inland fresh water bodies are also face their problems. More than 95% of plastic waste remained into terrestrial environment. People keep variety of plastic items and dispose to soil or water bodies and they are gradually transported to fresh water systems.

China is the largest produce and consumer of plastic in the world. Dong ting lake is the second largest fresh water lake in China. Its average depth is 6.4 m and its volume is 1.67 billion $m^{3.}$ Lake is covering an area about 2625km^2 and is divided in to three parts due to the influence of lake reclamation and siltation. Dons ting lake is an important agricultural bare and tourist spot. More than 11 million permanent residents, accounting for 20% of population of human provenance.

In the maritime environment, microplastics are universal, and sediments are thought to be one of their main sinks. Worldwide findings regarding evidence of microplastics in marine sediments and the water column have been made (Claassens et al., 2011, Law et al., 2010, Moore et al., 2001, Thompson et al., 2004). The first records of plastic pellets on beaches were made in the early 1970s (Carpenter et al., 1972; Carpenter and Smith, 1972), but it was another five years (Gregory, 1977; Gregory, 1983; Shier, 1979); and another thirty years (Thompson et al., 2004) before the first reports of microplastics (1 mm) in sediments were made. As a result, since widespread manufacturing of plastic began in the 1950s, it has increased drastically, reaching 288 million tonnes in 2012 (Plastics Europe, 2013). Plastic has unchangeable social advantages, but there are also significant environmental problems to consider (Andrade and Neal, 2009). It has been projected those millions of tonnes of plastic garbage (4.8-12.7 million tonnes in 2010) wind up in the marine environment, even though some of the plastic debris is appropriately managed (via recycling or combustion) (Jam beck et al., 2015).

Claessence et. al in 2011 and Matsuguma et at. 2017 is conducted a comparison focusing on the spatial variation of microplastic in surface sediments. Limited number of studied about chronological changes that require core sediments and analysis of microplastic

in sediments in different horizons. In different geographic region have substantial increase in concentration of microplastic in sediments. Due the increase of microplastic in sediments ecological damage is also increase. Bour et. al in 2018, Li et al. in 2018 and Su et. al carried to evaluate the effect of microplastic on aquatic organism.

Microplastic is affect all environments, include river and recently number of microplastic studies in river has strongly increased. Still many questions are regarding the source, pathways, and the role of land use patterns. Depending on their size category, studies have shown that microplastics have a harmful influence on the environment and ecosystems. Plastics of any size and particles directly and indirectly release toxic chemicals in to the environment and affect the food chain. It strongly affects the pollution and quality of water and also affect the absorb and adsorb of organic pollutants in environment. Microplastics in the marine environment have received a lot of attention in the past, while aquatic ecosystems have received little. The results show that anthropogenic factors relate to the abundance of microplastics in rivers, and more abundances are frequently found in regions with high people densities and urban land cover. This problem was studied across the world, Europe, Asia, Australia, and North America.

The occurrence, distribution and impact of MPs had already been studied and detected in marine habitats from different part of the world. Sediment in Cox's Bazar in Bangladesh from sea salt, fish species, and presence of MPs was documented. Is focused on the hazards due to microplastic. Kuakata sea beach, also known as Shagor Kannya (Daughter of the Sea), is the second-largest sandy beach on Bangladesh's Bay of Bengal coastline. Around the peak vacations season (November-March), around 115,000 domestic and international visitors visit this beach (Rahman et al., 2015). However, coastal hotels, restaurants, and tourist activities generate a large number of plastic debris, which frequently ends up on the beach. The three major rivers in Bangladesh (the Padma, Meghna, and Jamuna) may be able to facilitate this migration, but currents may also carry MPs from other regions of the Bay of Bengal into the coastline and beaches. As a result, it is critical to understand the incidence of MPs as well as their possible implications on the environment and the health risks to humans and species. So far, no scientific study of MP contamination in Kolkata beach's coastal water and beach sediment has been completed. As a result, this study was the first step in determining the presence and spatial distribution of MPs particles in beach sands from Kolkata, Bangladesh. Furthermore, the ecological risk assessment of MPs, as well as the relationship between sand particle size and MPs distribution at Kolkata beach, were studied. Beach sediments of Kuakata

were primarily composed of very fine sands (39%) and mud (35%), followed by fine sand (24%), medium sand (1.5%), and coarse sand [0.5 (Figure 5)]. However, a positive correlation was found between the MPs abundance and the finer grain size distributions from each sampling point ($p = 0.055$; $r = 0.7$). McLachlan and Brown (2006) stated that beach sediments work as pollution traps that non-specifically adsorb particles carried by tides and currents. In this first experiment, we discovered a greater MPs incidence in finer sediment grain size, supporting the theory that finer sediments operate as MP pollution traps on beaches. Nonetheless, no link between MPs occurrence and finer sediment grain size has hitherto been reported on tidal beaches. The investigation PET, polyethylene (PE), and polypropylene (PP) were found in sediment samples from Kuakata, Bangladesh. PET was discovered to be the most abundant polymer type, accounting for 45.5% of the total samples identified using FTIR analysis, whereas PP was discovered to be the least abundant (18.2%). Figure 6 depicts the FTIR spectra of various polymers. Some identical peaks of those plastic polymers were not identified in the FTIR spectrum due to ageing, natural weathering, and degradation of MPs. Polymers are common in microplastic in the coastal ecosystem. The abundance and type of MPs suggest that they are obtained from terrestrial sources. PLI studies revealed that the Kuakata beach sediments were in category I of the pollution index, which means they were slightly polluted. This discovery can assist guide better management of local and regional plastic trash. More long-term and comprehensive research on the effects of MPs on marine life, habitats, and, eventually, human health is advised.

Plastic production has increased dramatically over the previous 70 years over the world, to the point where we may claim we live in a plastic world. It is very difficult to determine the content of plastic in the environment and human health associated with massive production of plastic and disposal of plastic. After the COVID pandemic the use of plastic items is chaos in the environment. 2021 De Sousa studied how single use plastic items like disposal can make variable problems in environment like mask. From this study, the disposal plastic led to the death of organisms like Magallanes penguin. Due to the incineration of infected plastic. Plastics are highly persistent in nature due to which their degradation occurs at a slower rate and their accumulation at a faster pace (Barnes et al. 2009). In the present scenario, worldwide prevalence of smaller fraction of plastics, i.e., microplastics (MPs) and nano plastics (NPs), is gaining significant attention of the researchers globally due to their serious environmental consequences. There is no doubt that MPs have been present in the environment for many years. They are found in aquatic systems, on the land surface, inside biological creatures,

human consumables, and even in the air. The plastics sector in India is rapidly expanding, with Western India being the greatest consumer (47%) with considerable consumption in the states of Gujarat, Maharashtra, Madhya Pradesh, Daman and Diu, Chhattisgarh, and Dadra and Nagar Haveli. Many scientists are investigating the prevalence of MPs in various components of the Indian environment as a result of the weathering and fragmentation of this plastic trash.

In 2011 study by Cole et al. that covers several facets of microplastics in the marine environment. Microplastics, which are microscopic plastic particles less than 5 millimetres in size, have grown to be a major problem because of their pervasiveness and potential negative effects on the environment. The study likely discussed how microplastics are defined and classified, along with their sources. Microplastics can originate from various sources, including the breakdown of larger plastic items, microbeads from personal care products, fibres from textiles, and industrial processes. The study may have explored how microplastics find their way into the marine environment. This can occur through direct littering, runoff from land, industrial discharge, and other pathways. Wind and water currents can also transport microplastics from one location to another. evaluated different methods used to detect and quantify microplastics in marine environments. These methods could include visual surveys, net trawling, sediment sampling, and spectroscopic techniques to identify and characterize microplastic particles. highlighted the potential negative impacts of microplastics on marine ecosystems. Microplastics can adsorb and concentrate harmful pollutants from the surrounding water, making them vectors for transporting these contaminants through the food chain. Marine organisms, including filter feeders and larger animals, may ingest microplastics, leading to potential health effects and bioaccumulation of plastics and associated toxins. The study's results indicate that microplastics are widespread and found in various marine environments, from coastal areas to open oceans. This ubiquity emphasizes the need to address microplastic pollution comprehensively. The study might have mentioned that the fate of microplastics in the marine environment, including their long-term behaviour and impact, was not well understood at the time. Additionally, the potential for microplastics to release toxic additives or adsorb harmful chemicals from the water could further exacerbate their environmental impact. findings likely suggest that microplastics can enter the marine food web. This occurs when marine organisms, from plankton to larger fish, consume microplastics either directly or indirectly. As these organisms are consumed by higher trophic levels, microplastics and associated contaminants can be biomagnified through the food chain, ultimately affecting humans who consume seafood. Overall, the study by Cole et al. sheds light on the complex

issue of microplastics in the marine environment, emphasizing the need for further research, better waste management practices, and policy interventions to mitigate their effects.

Study by Andrady from 2017, which focuses on the characteristics of microplastics and their ecological impact. The study by Andrady assesses the relevance of certain characteristics of plastics that make up microplastics to their potential role as pollutants with ecological impacts. These characteristics might include properties like size, shape, composition, and surface chemistry. Discusses the concept of fragmentation leading to the creation of secondary microplastics. This refers to the process by which larger plastic items break down into smaller microplastic particles over time due to environmental factors such as UV radiation, mechanical stress, and wave action. Found that certain characteristics of microplastics, such as average molecular weight, structural chemistry, and crystallinity, can influence their fate in the ocean. This means that these characteristics might affect how microplastics interact with the marine environment, including how they disperse, degrade, and potentially impact ecosystems Andrady mentions that the fragmentation of plastics can also occur in the natural environment, not just in controlled settings. This process can generate a significant number of smaller microplastic particles, often referred to as "daughter microplastics". study highlights the complexity of microplastic pollution and its potential ecological impact. The study emphasizes the importance of understanding the characteristics of microplastics and how they behave in the marine environment, particularly through processes like fragmentation and surface ablation. These insights contribute to our understanding of the various factors that play a role in the persistence and distribution of microplastics in oceans and ecosystem.

The study conducted by Sarkar et al. in 2020 aimed to investigate the presence and distribution of meso and microplastics in sediments in the lower stretch of the Ganga River. Sediment samples were collected from seven different locations along the river: Buxar, Patna, Bhagalpur, Nabadwip, Barrackpore, Godakhali, and Fraserganj. The analysis of the collected sediment samples revealed the presence of both meso and microplastics in all of the samples. Meso and microplastics are larger plastic fragments and smaller plastic particles, respectively. The study utilized Fourier-transform infrared spectroscopy (FTIR) to analyses the composition of microplastics in the sediment samples. The analysis determined that the major contributing plastic debris in the sediments was polyethylene terephthalate (PET), followed by polyethylene. The study light on the presence of plastic pollution in the sediments of the Ganga River's lower stretch. The fact that mesa and microplastics were found in all samples highlights the widespread contamination of these plastic particles in the environment. The identification

of the major plastic types, PET and polyethylene, provides insight into the types of plastics that are most prevalent in this specific area of the river. This study contributes to our understanding of the distribution and composition of plastic pollution in aquatic ecosystems and their potential environmental impacts.

Soil have organic matter, is a fraction of the soil that contain plant or animal tissue in various stages of break down. Organic matter is made up of different components. Plant residues and living microbial biomass, active soil organic matter and stable soil organic matter. The first two forms of organic matter contribute to soil fertility since their breakdown produces in Nitrogen and other plant nutrients are released. Phosphorus, potassium, and so forth. Organic matter is present more in surface than deeper in the soil. By this top soil is more productive than subsoil that become exposed by erosion or mechanical removal of soil layers. When the plants die or sheds leaves or branches, thus depositing residues on the surface, earthworms and insects help incorporate the residues on the surface deeper than into the soil. High concentration of organic matter in soil is remain with one feet of the surface. Soils with higher levels of fine silt and clay usually have high level of organic matter. 2% of the organic matter in sandy soil is good and difficult to reach. 2% of clay indicate depleted situation. Organic matter can come from various sources including, Plants and Animals: Leaves, stems, roots, shells, bones, and other organic materials from plants and animals that lived in or near the water body can contribute to the organic content of sediments microscopic algae and phytoplankton. This includes dead and decaying organic material, such as fallen leaves, twigs, and other debris. On contribute organic matter to sediment when they die and sink to the bottom of water bodies. Bacteria and other microorganisms play a role in breaking down organic matter, releasing various compounds and gases in the process. The accumulation of organic matter in sediments is influenced by factors such as water depth, sediment type, and local environmental conditions. Over time, layers of organic-rich sediments can become buried and compacted, eventually forming sedimentary rock layers like shale. Organic material in sediments performs a number of crucial tasks. Carbon, nitrogen, and phosphorus are among the nutrients found in organic matter that are cycled through ecosystems as they break down. These nutrients are crucial for the development of aquatic animals and plants. Microbes that participate in the breakdown of organic materials and their transformation into simpler chemicals can obtain energy from organic matter. Organic matter in sediments has the capacity to store carbon for a considerable amount of time, contributing to the carbon cycle and affecting the amounts of carbon dioxide

in the atmosphere. Organic matter can offer a variety of creatures habitats and shelter, resulting in a complex and varied ecosystem inside sediments.

While organic matter in sediments serves important ecological roles, there are also limitations and challenges associated with its presence. Some of these limitations, Organic material in sediments has the potential to release nutrients when it breaks down. The discharge of too many nutrients, especially nitrogen and phosphorus, can cause eutrophication, where too many nutrients encourage the growth of too many algae and aquatic plants, potentially compromising water quality and creating ecological imbalances. Anoxic Conditions: Microbial activity can cause sediment oxygen levels to drop when organic matter breaks down. Anoxic (low oxygen) conditions may result from this, resulting in "dead zones" where many aquatic creatures cannot survive. Habitat Alteration: Excessive organic matter buildup in sediments can change the habitat's physical characteristics, which in turn affects the variety and distribution of benthic (bottom-dwelling) creatures. Dense accumulations of organic-rich sediments have the potential to suffocate species and alter their environments. Organic materials may have an impact on the cohesiveness and stability of sediment. High quantities of organic matter may occasionally result in less stable sediment, which raises the possibility of erosion and sediment transport during water flow episodes. When disturbed or resuspended, organic matter can release carbon into the water column or atmosphere, despite the fact that it can trap carbon under specific circumstances (such as disturbance or dredging). This might affect the carbon cycle and increase carbon emissions. Microbial Activity: Microbial activity can cause the decomposition of organic waste to produce byproducts like sulphides, Transport of Contaminants: Heavy metals and persistent organic pollutants can both be transported by organic materials. The wider ecosystem may be impacted if these toxins are adsorbed onto organic matter particles and carried within sediments. which can poison aquatic creatures and have a detrimental effect on the quality of the water. High quantities of organic matter can make sediment remediation activities more difficult since they have an impact on how well sediment treatment techniques and technologies work. Paleoenvironmental Reconstructions: Using sediment cores for these reconstructions might be challenging when organic material is present. The original composition of the organic matter can vary due to decomposition and diagenesis (physical and chemical changes during burial), which has an impact on how we interpret previous environmental conditions. Oxygen is used up during the decomposition of organic materials, or the biological oxygen demand. Large levels of organic matter in sediments may increase biological oxygen demand, which may result in oxygen deprivation and adverse

effects on aquatic species. For the purpose of preserving healthy aquatic ecosystems, controlling water quality, and making educated decisions on environmental management and restoration initiatives, it is crucial to manage and comprehend the limitations of organic matter in sediments. For the purpose of preserving healthy aquatic ecosystems, controlling water quality, and making educated decisions on environmental management and restoration initiatives, it is crucial to manage and comprehend the limitations of organic matter in sediments.

The amount of organic matter in sediments tends to decline with time for a variety of reasons. Although organic matter is a crucial part of sediment ecosystems, both natural and human-made processes can cause it to degrade or disappear. Several factors contribute to the decline of organic matter in sediments Oxidation. Oxidation: Organic material can be broken down and released carbon dioxide and other byproducts when exposed to oxygen. This process can cause the loss of organic material from sediments and is more likely to occur in well-oxygenated situations. It's crucial to remember that, depending on the situation, the loss of organic matter in sediments can have both beneficial and negative effects. The availability of nutrients and habitats for benthic species may be impacted by lower organic matter concentration, which can also increase sediment stability and minimise eutrophication potential. Effective ecosystem management and conservation depend on balancing the natural dynamics of sediment ecosystems and comprehending the effects of changes in organic matter. Compression and Burial: Organic matter may get compressed over time as a result of sediment deposition, compaction, and burial. It is possible for pressure and temperature to increase as sediments are buried deeper below the Earth's crust, which could help organic materials transform into more stable forms like kerogen or fossil fuels Microorganisms are essential to the biodegradation process, which breaks down organic materials. In sediments, microbial and bacterial communities break down organic materials as they eat it for nutrients and energy. Microbial activity can cause organic materials to gradually deteriorate over time. Physical Disturbance: Physical disturbances such as erosion, dredging, and sediment resuspension can disrupt the accumulation of organic matter in sediments. These disturbances may cause sediment layers and the organic material contained within them to be removed or redistributed. Water Flow and Currents: In aquatic ecosystems, strong water flow, currents, and wave action can move organic matter away from places where silt deposits. Layers of silt that are rich in organic matter may be removed as a result. Bioturbation, or the mixing of sediments by organisms that dig underground, can introduce organic material to the sediment-water

interface. As a result, the organic material may be exposed to oxygen, hastening its decomposition. Land Use Modifications: Human activities including agriculture, urbanisation, and deforestation can worsen soil erosion and sediment runoff into bodies of water. This influx of silt may change sediment properties and diminish the number of organic materials. Climate Change: The preservation and decomposition of organic matter may be impacted by changes in temperature, precipitation patterns, and water quality brought on by climate changes. These changes may also have an impact on the rates of sedimentation and microbial activity. The availability of nutrients can alter microbial activity and the rate of breakdown. Increased nutrient levels can encourage microbial development and speed up the decomposition of organic waste. Natural Decomposition: Over time, organic matter in sediments will naturally disintegrate by physical, chemical, and biological processes, even in the absence of particular disturbance factors.

Numerous investigations have been made into the composition, origins, effects on ecosystem processes, and pollution caused by organic matter in sediments. Composition and Sources of Organic Matter: Studies identify the origins of organic matter in sediments, such as land plants, aquatic algae, and human contributions, using techniques including stable isotope analysis and molecular biomarkers. To comprehend the makeup of organic matter in sediments and its possible origins, researchers compare the ratios of various organic substances, such as lipids, carbohydrates, and protein. Decomposition and diagenesis: Studies concentrate on the diagenetic processes that follow the decomposition of organic matter in sediments and convert organic compounds into more stable forms throughout time. Researchers look at how microbial activity, environmental factors (such temperature and oxygen availability), and the decomposition of organic materials are related.

Textural classification of sediments refers to categorizing sediment particles based on their size and sorting characteristics. Sediments are naturally occurring particles that settle out of water or air, and they can range in size from clay particles (very small) to boulders (very large). The classification is an essential aspect of sedimentology, which is the study of sedimentary rocks and their formation. The Wentworth scale, which classifies sediments into various size categories, is the most often used classification system for sediment textures: Clay: Particles with a diameter of less than 0.002 mm. Silt: Particles with a diameter of between 0.002 and 0.0625mm. Sand: Substances with a diameter of 0.0625 to 2 mm. Fine, medium, and coarse sand are the further divisions made for sand. Granules: Particles with a diameter of 2 to 4 mm. Pebbles: Substances with a diameter of 4 to 64 mm. Cobbles: Substances with a diameter

of 64 to 256 mm. Boulders: Substances with a diameter more than 256 mm. The homogeneity of particle sizes within a sediment sample is referred to as sorting, and it is another method for classifying sediments: Clearly arranged: Particles in the sediments.

The well-known Wentworth scale, a system for categorising the size of clastic sediment particle sizes, was first established in Wentworth's paper titled "A Scale of Grade and Class Terms for Clastic Sediments," which was published in 1922. Clastic sediments are made up of bits of previously existent minerals and rocks that have been eroded and moved by different natural processes. Wentworth acknowledged the necessity for a uniform method of describing the size of sediment particles in geology in this study. According to their diameter, he established a logarithmic scale that divides sediment particles into discrete size classes. The scale includes very small particles like dirt and very large particles like stones. The size classes on the Wentworth scale are as follows, Clay: Particles with a diameter of less than 0.002 mm. Silt: Particles with a diameter of between 0.002- and 0.0625-mm. Sand: Substances with a diameter of 0.0625 to 2 mm. Fine, medium, and coarse sand are the further divisions made for sand. Granules: Particles with a diameter of 2 to 4 mm. Pebbles: Substances with a diameter of 4 to 64 mm. Cobbles: Substances with a diameter of 64 to 256 mm. Boulders: Substances with a diameter more than 256 mm. Regardless of their geographical location or topic of study, geologists were able to communicate about sediment sizes more effectively thanks to Wentworth's scale. The scale has since gained widespread use and serves as the foundation for

The 1980 publication of Mazzullo and Boothroyd's study, "The Effect of Sorting on Sediment Textural Analysis," was named. This work focuses on how particle sorting affects sediment texture analysis precision, especially with regard to grain size distribution. Sorting, which is the homogeneity of particle sizes within a sediment sample, can affect how sedimentary environments and processes are understood. Mazzullo and Boothroyd carried out laboratory tests in this work to investigate how changes in particle sorting affect the outcomes of sediment texture analysis. They employed a collection of natural sediment samples that had undergone varying degrees of sorting before being put through particle size analysis procedures. Understanding whether and how sorting influences the precision of grain size distribution measurements was the main objective. Revealed that grain size analysis results can be greatly influenced by the degree of particle sorting present in a sediment sample. Poorly sorted samples resulted in more variability in grain size distribution measures, whereas well-sorted samples tended to yield more precise and consistent results. There was a tendency to overstate the quantity of smaller particles in samples that weren't properly separated.

Sedimentologists could make assumptions about higher energy conditions than are actually present, which could lead to incorrect interpretations of sedimentary settings. The study emphasised the significance of taking sorting effects into account when evaluating depositional settings and sedimentary processes. The degree of sorting can reveal information about the energy levels during deposition, the modes of transit, and the origins of sedimentary deposits. The study emphasised the value of taking sorting effects into consideration when analysing sediment texture. For proper interpretation of sedimentary environments and processes as well as for drawing trustworthy geological and environmental conclusions based on sediment features, it is essential to understand how sorting affects grain size distribution data.

"Grad stat: A Grain Size Distribution and Statistics Package for the Analysis of Unconsolidated Sediments," a paper by Blott and Pye, was released in 2001. This paper introduces the "Grad stat" software programme, which was created to make it easier to analyse grain size distributions in unconsolidated sediments. Researchers can learn more about sedimentary processes and environmental circumstances using the software's tools for analysing and evaluating sediment texture data. Grad stat is a user-friendly software programme that the authors created to assist sedimentologists in analysing grain size distributions from sediment samples. The programme was designed to make it easier to compute numerous statistical characteristics and visualise the textures of silt. The grain size metrics that can be calculated using Grad stat include mean grain size, sorting indices, skewness, and kurtosis. These variables shed light on the asymmetry, dispersion, and central tendency of the grain size distribution. The programme has statistical analysis features such the ability to compute percentiles, cumulative frequency curves, and grain size distribution moments. Researchers can compare and quantitatively define sand samples using these technologies. Grad stat offers histograms, cumulative frequency curves, and probability plots as graphical representations of grain size distributions. Understanding the distribution of particle sizes inside a sediment sample is made easier with the use of these visualisations. The authors wanted to develop an approachable and user-friendly software programme that would enable sedimentologists with various degrees of technical expertise to undertake sediment texture analyses effectively. This study demonstrates the many uses of Grad stat, such as its usage in detecting sediment sources, characterising sedimentary ecosystems, and evaluating the effects of human activity on sediment compositions. The authors contributed to the availability of tools for sediment texture analysis by making Grad stat freely available to the scientific community. In their publication, Blott and Pye offer Grad stat as a useful tool for

sedimentologists and geologists who study sediment grain size distributions. Grad stat seeks to improve the precision and effectiveness of sediment texture analysis by offering a user-friendly interface and a variety of analytical tools. Enabling academics to learn more about sedimentary processes and environmental circumstances.

CHAPTER 3

STUDY AREA

1.1 TOPOGRAPHY

In the Indian city of Kochi, Kerala. There is an overflowing trash disposal site called Brahmaputra land fill. The cochin municipal corporation is the governing body and operator of the solid waste plant.110 arc footprint and is located at 9.992449 latitude and 76.365823 longitude. It has been 16 years since garbage dumping at the brahma Puram dump in Kochi. In 2007, 15 arc swamp was reclaimed and plant was built in that area. The plant was inaugurated in 2008 capacity is changed to 250 tonnes per day.

More than 60 tons of waste are generated in Kochi, and the brahma Puram solid waste plant., almost 100 tons of that waste are converted into organic manner. Apart from the Kochi Corporation, Kalamassery, Aluva, Angamali, Thrikkakara, Thripunithara, municipalities and the Cheranallur, Vadavukod puthankurish panchayats also dump their watse at the Brahmapuram waste plant.390 tonnes of waste is dumped. 64 percent of this is biodegradable and non-degradable are mixed.

Figure 1. Map of the area

1.2 GEOLOGY OF AREA

Brahmapuram landfill is waste dumping site is situated in Indian city of Kochi, Kerala. Owned and operator by Kochi Corporation. The location is a significant contributor to environmental pollutants, fire dangers, and problems with public health and safety. The city produces more than 600 tons of waste per day. 100 tons of its decomposed at Brahmapuram solid plant. The area is close to the backwaters and also include hydromorphic saline soils. Area is divided into three physiographic zones; the midland region in the east, the steep to extremely steep hills, and coastal plain in the west. The valleys are hill, while the hills are typically covered in laterite or lateritic soils. sleep is very gently to moderately from east to west. In valley bottom hydromorphic soil. The soil is filled with black nutrients and clay. Graphite and China clay are the minerals found in the area. The khondalite rock group is associated with presence pf graphite.

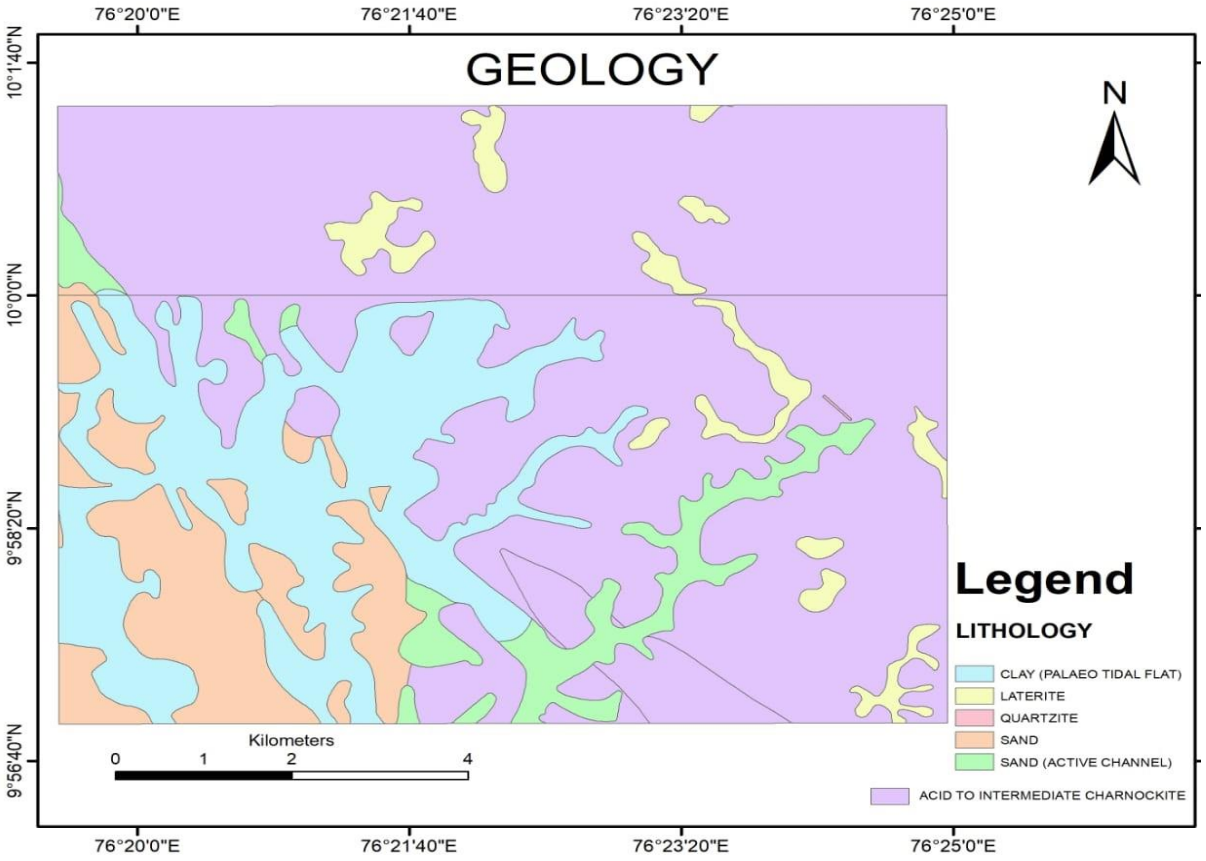

Figure 2. Geology of the area

3.3 GEOMORPHOLOGY OF THE AREA

The coastal status, backwaters, and the Eastern Ghats Mountain range all have an impact on Ernakulam's geomorphology. The Ernakulam district has the following significant geomorphological characteristics. The Ernakulam district has a sizable coastline that runs along the Arabian Sea. Sand beaches, tidal flats, and estuaries define the coast. Continuous processes that continuously shape the shoreline are coastal erosion and deposition. The district is well-known for its intricate network of backwaters and estuaries, which are created by the intricate interaction of freshwater rivers and tidal waters from the sea.

These backwaters have enriched the cultural and economic fabric of the area by acting as vital channels and providing a base for age-old pursuits like fishing and tourism. The Western Ghats Mountain range has an impact on the district's eastern portion. A notable geological formation, the Ghats are famous for their abundant biodiversity. The Western Ghats' hills and slopes have a role in the region's drainage patterns since rivers that originate here travel west to the Arabian Sea. The district is also home to a number of lakes and lagoons, including Vembanad Lake and the estuarine system of the Periyar River. These bodies of water are crucial for aquatic biodiversity, flood control, and water storage. Mudflats, sandbars, and marshes are common landforms in the deltaic regions at the mouths of rivers, such as the Periyar River. Due to tidal action and continual silt deposition, these places are dynamic and variable. The geomorphology of Ernakulam has been significantly impacted by urbanisation, infrastructure development, and population growth. Land reclamation, development, and land use changes have affected some of the natural landscapes in the district.

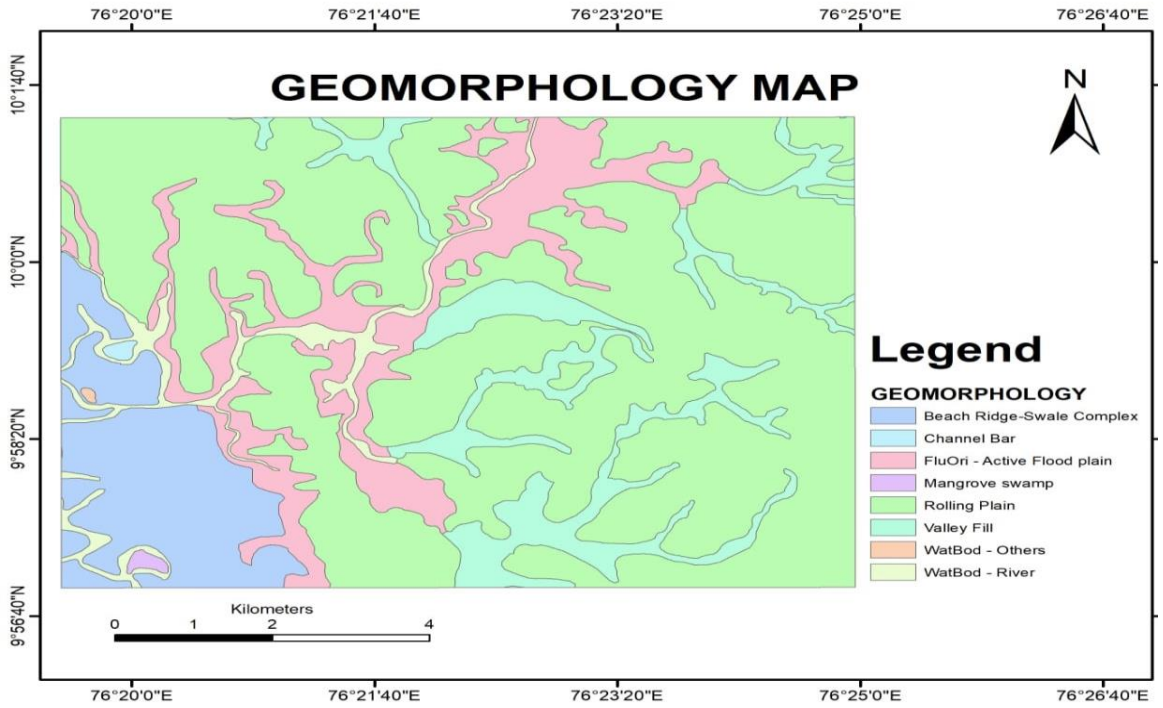

Figure 3. Geomorphology of the study area

CHAPTER 4

METHODOLOGY

4.1 GENERAL PROCEDURE

4.1.1 RIVER BANK SEDIMENT COLLECTION

The sample is collected through river bank and nearby areas of plant. Sample is collected with the scooper and Ziplock cover of 1 kg. Half kg sediments are collected from each location. About 25cm of the top soil is removed before collecting the actual sample. Sample 1-3 is collected from Brahmapuram waste plant,4 and 5 is collected from back side of the Rajagiri college of engineering.

Figure 4. Photograph showing sample collection

4.1.2 CONE AND QUADRANT METHOD

Well dried sediments are mixed well for even distribution of particles. Following the cone and quadrating method. 70gm of sample is taken in a butter paper and mixed together by

using long scale in homogenous manner. Then divided in to 4 portions, two of the opposite quadrants were removed continuing this until we get 10gm of sediments.

4.1.3 PHYSIOCHEMICAL PARAMETERS

The method is used for sediments analysis is wet sieving, using a 230 ASTM sieve mesh. For this analysis sediments where dried in the sunlight for 72 hours. Then sufficient amount of H_2O_2 added to a 200ml beaker to remove organic matter. Then it allows to settle down for overnight. Sodium hexa meta phosphate is added to the same on the next day to dissolve the particles foe 14 hour at 64ºC. This is then grounded in to fine grained powder with a glass rod. This powdered sediments in then used for further analysis.

The previously powdered sample weighed into 5gm then washed in the 230-ASTM sieve mesh (opening=0.063mm) made of phosphor-bronze wire mesh plate and the base plate until the water gets clear with sand, then sand is removed to a beaker and let it dry. Then rest of the clay and silt are made in a1000ml cylindrical flask till the mark and agitated well and stirring device in order to have uniform distribution of the particles throughout the standard flask. Allow to settle for 2 hours and 3 minutes. After the exact time 20ml pipet is used to pipette out the clay by dipping 10cm depth from the mark. It is transferred into a beaker and let it dry in the oven.

Figure 5. Pipette analysis

4.1.4 CALCULATION

The beaker along with sand and clay weight is measured for all eight samples and then weight of the beaker without sand and clay is also measured after cleaned and drying it. Then calculated the percentage of sand and clay.

Final weight of the beaker – initial weight of the beaker*100

Weight of the sample

% of silt = 100 - (% of sand + % of clay)

4.1.5 ANALYSIS OF ORGANIC CARBON METHOD

Procedure:

Take 0.5 gm of powdered sample is taken in a 500 ml of conical flask. Add 10 ml of potassium di chromate solution nicely into the flask. Then add 20ml of silver sulphate solution. Mix nicely and rotating the flask for 3 minutes. Wait for 30 minutes. And after 30 minutes add

200ml add distilled water. Add 10 ml of orthophosphoric acid solution. And add pinch of NaF (sodium fluoride). Add 0.5ml of Diphenylamine indicator solution. Titrate the solution with Ferrous Ammonium Sulphate solution. The colour change from BLACKISH BLUE TO PURE GREEN. RUN A BLANK. (Walkey-Black method (1947), adopted and modified from Jackson, 1958)

calculation:

% organic matter (readily oxidizable) = $10\ (1\text{-}T/S) \times F$

Where,

S - Standardization blank titration, ml of ferrous solution

T - Sample titration, ml of ferrous solution

F - Factor derived as follows:

$F = 1.0\ N \times 12/4000 \times 1.72 \times 100/\text{sample weight}$

(- 1.03 when sample weight is exactly 0.5 g)

where,

12/4000 - milli equivalent wt. carbon

1.72- Factor for organic matter from organic carbon.

Replicate analyses (10) of a sample with an average of 0.30% organic matter give a standard deviation of 0.03% (coefficient of variation of 9%).

Figure 6. Titration method for organic carbon analysis

4.1.5 ANALYSIS OF MICROPLASTIC

40 grams of sample is taken in a beaker and add 5.5 g/l sodium hexametaphosphate solution and soak the sample for 24 hours. Place the solution in a rotary shaker at 250 RPM for 60-90 minute. Sieve the sample using 0.3 mm and 5 mm sieves, separating them into different beakers.

Density separation:

Prepare a solution of 933.3 g of zinc chloride in 1 litter distilled water, allow to settle the solution overnight. Sieve half of the beaker content to extract the microplastics. sodium chloride or sodium bromide can also be used, but they are not effective for extracting high-density microplastic.

Removal of microplastic:

200 ml of hydrogen peroxide is added to the sample and produce effervescence. Stop the adding of hydrogen peroxide until effervescence stopes. Zinc chloride is added to the sample and allow to settle overnight. Collect the residue on filter paper (Whatman paper) and identifies the microplastic. Organic decomposition is increases as nitrogen and phosphorous is also increase. Organic matter is accumulated mostly in fine grained sediments. Sediments absorb minerals and helps to preserve organic matter. Accumulation of organic matter is in the way of water which control the organic matter by the process of transport and deposition.

Figure 7. Microscopic analysis

CHAPTER 5

RESULT AND DISSCUSSION

5.1 TEXTURAL ANALYSIS

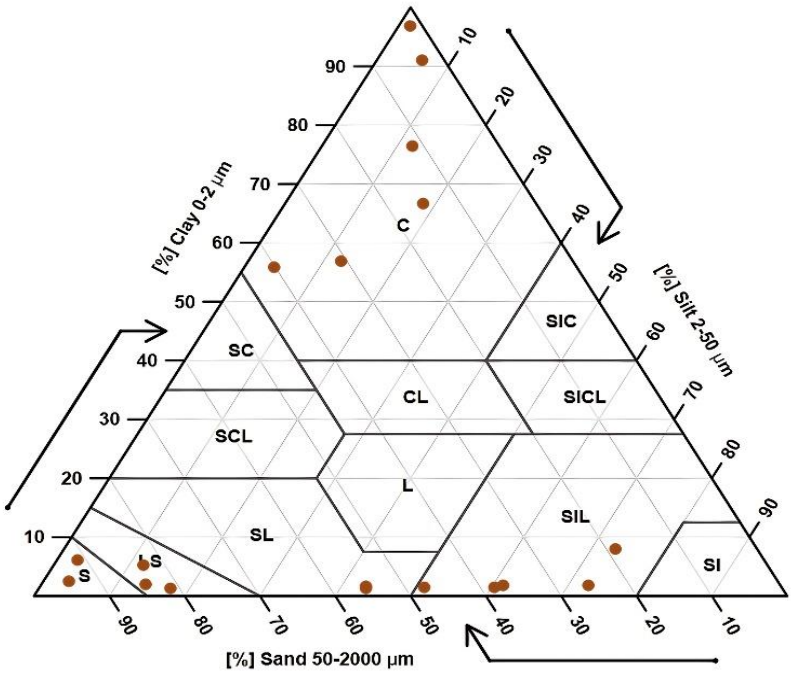

Figure 8. Trilinear plot, (after Trefethen,1950.)

SAMPLE NO	WEIGHT PERCENTAGE			TYPE OF TEXTURE	PLACES COLLECTED
	SAND	SILT	CLAY		
1	38.72	61	0.28	Silt loam	Brahmapuram plant
2	1.12	0.88	98	Clay	Brahmapuram plant
3	48.4	51.6	0.3	Silt loam	Brahmapuram plant
4	30.96	12.04	57	clay	Rajagiri college back side
5	2.6	5.4	92	clay	Rajagiri college back side
6	40.38	3.62	56	clay	Kakkanad boat jetty
7	11.4	11.6	77	clay	Chitrapuzha bridge
8	83.8	12	4.2	loamy sand	Chitrapuzha bridge
9	56.3	43.7	0.4	sandy loam	Chitrapuzha bridge
10	92.2	2.8	5	sandy	Chitrapuzha bridge
11	56.1	43.9	0.1	sandy loam	Chitrapuzha river side
12	65.8	3.4	1.4	sandy loam	Chitrapuzha river side
13	98.8	73.4	0.7	sand	Chitrapuzha river side
14	14.88	18.12	67	clay	Chitrapuzha river side
15	19.16	73.84	7	Silt loam	Chitrapuzha river side
16	38.1	61.9	0.7	Silt loam	Chitrapuzha river side

17	86	14	0.8	sand	Chitrapuzha river side
18	82.4	17.6	0.1	loamy sand	Chitrapuzha river side

Table 1. Table showing wet sieve data

5.2 ORGANIC MATTER IN SOIL

Analysing the following graph (Figure 8) it will give an idea about the variation in the organic carbon abundance,gives an idea about the percentage of the organic matter, which will help to determine the effects that caused by organic matter in the sediment.

It is noted that difference in the organic content of the sediments. Each peak shows the maximum and minimum number of organic matters in sediments. Location (1) Brahmapuram waste plant, location (8) under the Chitrapuzha bridge, location (10) near the Chitrapuzha bridge, and location (14) also 5meter away from the Chitrapuzha bridge are showing the maximum percentage of the organic matter in sediments. Location (4) and Location (5) Rajagiri college back side, Location (13) Chitrapuzha river side showing minimum percentage of organic matter. Sediment organic carbon content is important for many biological and environmental processes, example nutrient cycle, sediment structure and stability, contaminant sorption, microbial activity and diversity and aquatic habitat quality etc. Nutrient cycle: Microorganisms in sediments use organic carbon as a source of nutrients. The organic waste is broken down by bacteria and other decomposers, releasing nutrients like nitrogen and phosphorus. The development of aquatic plants and phytoplankton, which serve as the foundation of aquatic food webs, depends on these nutrients. Sediment structure and stability of Sediment can be increased by the ability of organic materials to bind sediment particles together.

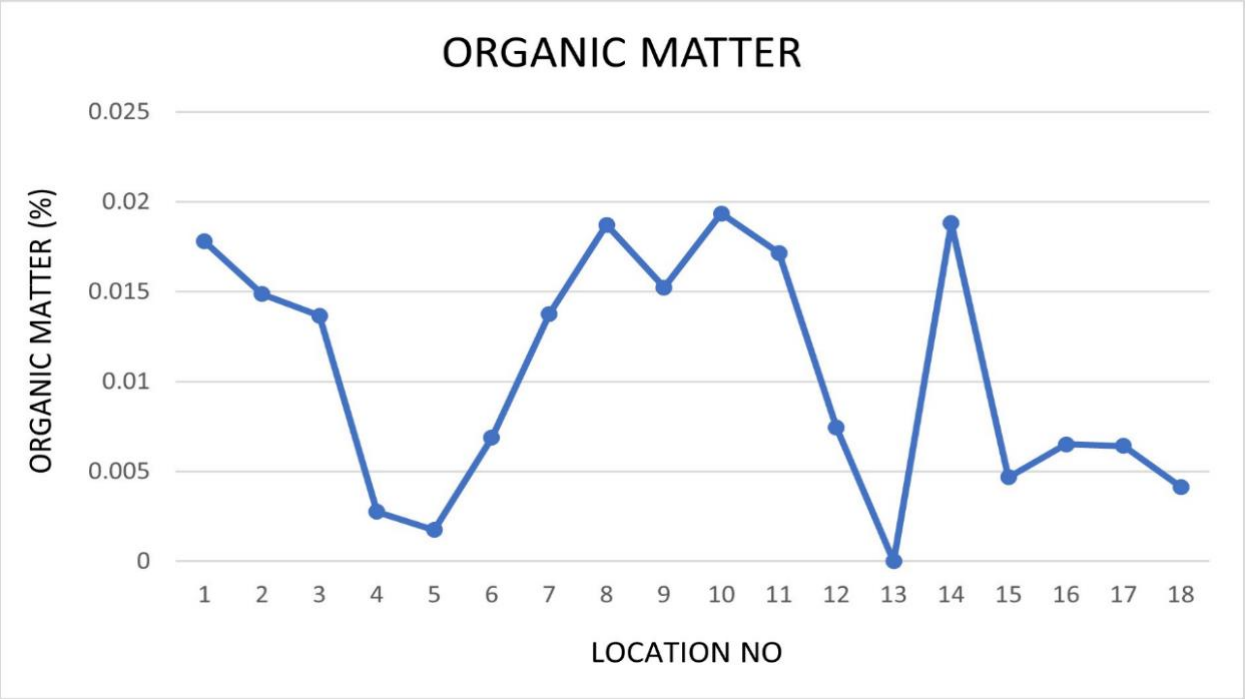

Figure 9. Graph showing abundance of organic matter

5.3 MICROPLASTIC ANALYSIS

This graph is showing the abundance of microplastic in sediments in different locations. Highest peak is location 10 and 11 is collected from nearby areas of chitrapuzha bridge and chitrapuzha river bank. Location 2,7, and 13 are minimum no of microplastic in plant, chithrapuzha bridge and chithrapuzha river side. Depending on variables including the kind and size of the microplastics, the properties of the sediment environment, and the species living there, the maximum amount of microplastics present in sediments can have a variety of consequences. Sediment contamination, change in sediment properties, reduced oxygen exchange, and spread of contaminants etc.

Sediment contamination: adsorbing contaminants and chemicals into sediment increases along with the amount of microplastics. The quality of the sediment may be impacted, and organisms that live there may be disturbed. Change in sediment properties: High microplastic concentrations can have an impact on the sediment's porosity, permeability, and water-holding capacity. This might have an impact on habitat accessibility, nitrogen cycling, and sediment stability. Reduced oxygen exchange: Microplastic buildup in sediments can obstruct oxygen exchange between the sediment and water column, possibly resulting in hypoxic conditions that are harmful to organisms that live in the sediment. Economic implications: Fisheries and other industries dependent on healthy sediment ecosystems could experience financial losses if the amount of microplastics in sediments rises to levels that have a negative impact on economically significant species. Spread of contaminants: Microplastics have the ability to disperse pollutants across wider areas by minimum number of microplastic in sediments is essential for maintaining the health of aquatic ecosystem and minimizing potential negative impact on organisms and the environment. Improving water treatment, proper waste management etc.

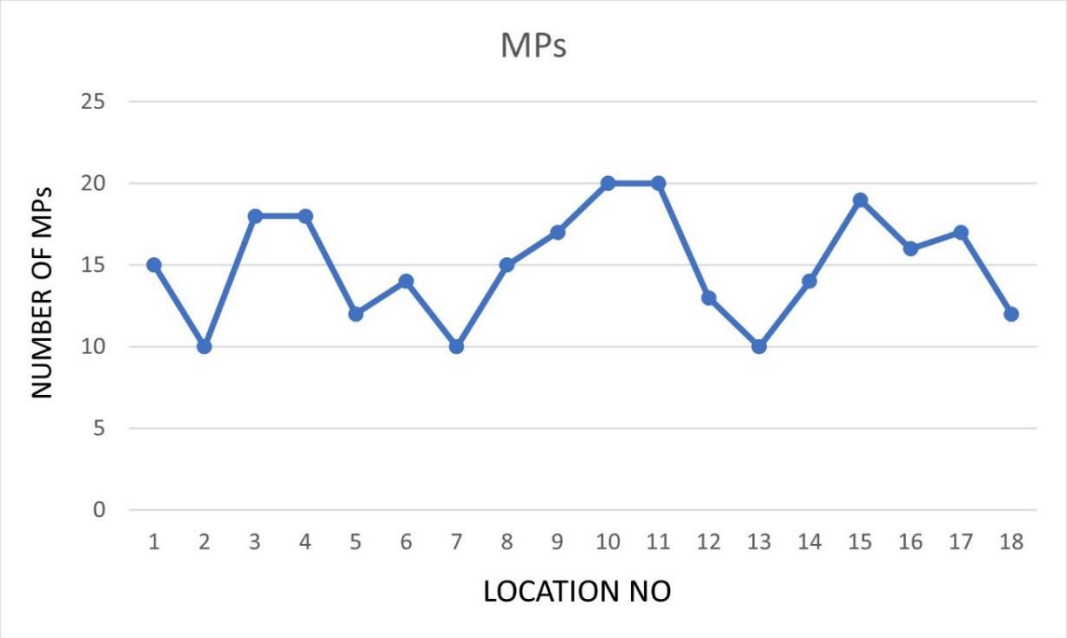

Figure 10. Graph showing the abundance of microplastic

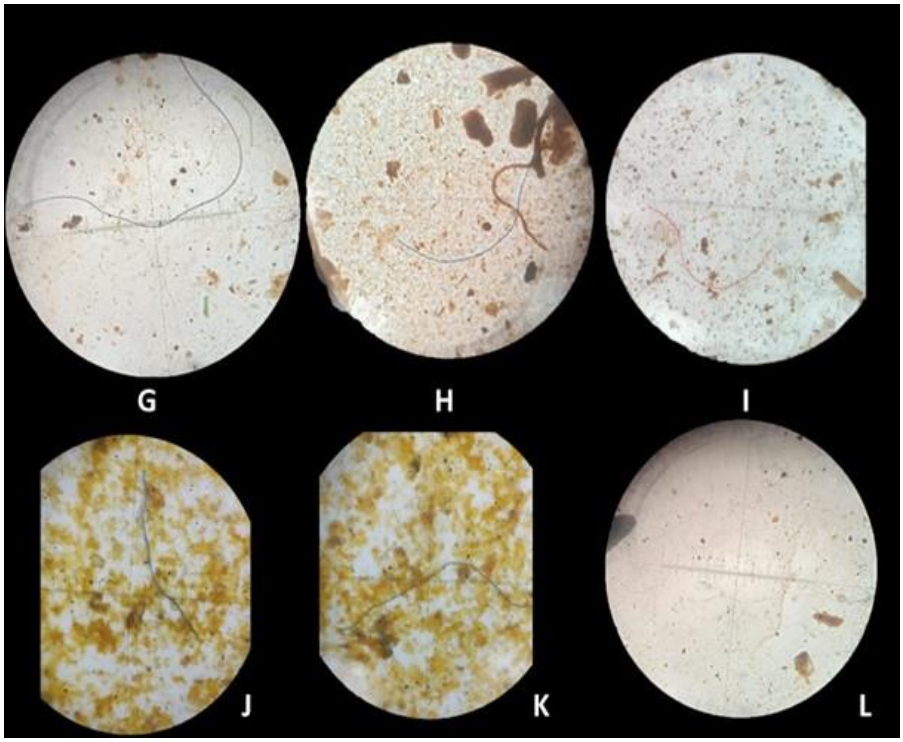

Fig 11. Microplastic in microscopic view

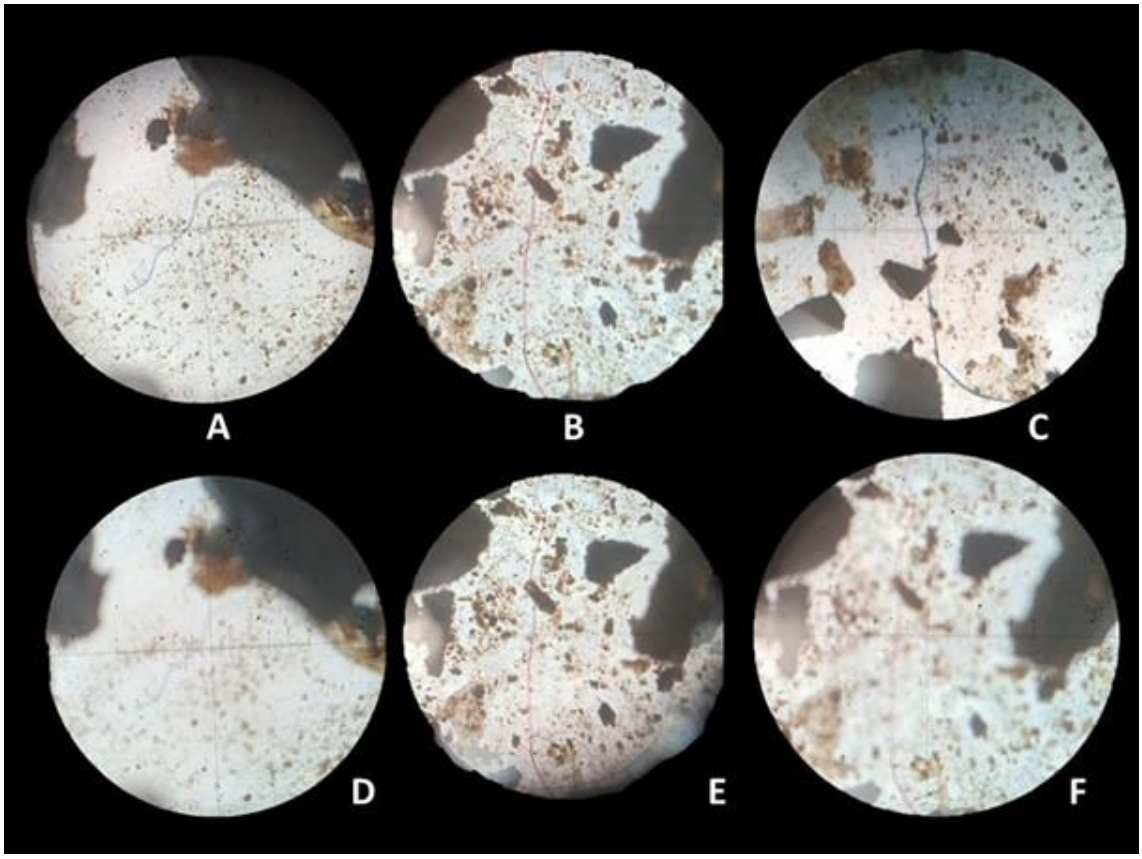

Fig 12. Microplastic in microscopic view

Sample no:	**Texture**	**No: of microplastics**	**Organic matter**
1	Silt loam	15	High
2	Clay	10	Medium
3	Silt loam	18	Medium
4	Clay	18	Low
5	Clay	12	Low
6	Clay	14	Medium
7	Clay	10	Medium
8	Loamy sand	15	High
9	Sandy loam	17	Medium
10	Sandy	20	High
11	Sandy loam	20	Medium
12	Sandy loam	13	Medium
13	Sand	10	Zero
14	Clay	14	High
15	Silt loam	19	Low
16	Silt loam	16	Medium
17	Sand	17	Medium

18	Loamy sand	12	Low

Table 2. Table of result

High amount of organic compound is in clay. Because the sand is more aerated thus organic matter will decompose easily in sand and clay contain more organic matter than sand. If the organic matter is high in soil, it will disintegrate microplastics and the content of microplastics will also increases. Sample 1-3 is collected from Brahmapuram waste plant and is highly contaminated. The samples 4-7 is clay, which is collected from Chitrapuzha river bank, here the organic matter is from low to medium range and its microplastic content is also less. The decrease in organic matter content is due to pollution in that area. The Sample 8-12 is sandy material here the organic matter is medium to high which is due to shifting of organic matter through erosion. Sample 13 is sand, here organic matter and microplastics are low, which shows the general trend. Sample 14 is clay, here the organic matter and microplastic content is high as in normal condition. Sample 15-18 is silt, here the organic matter and microplastic is medium to low, which also shows a general trend.

CHAPTER 6

CONCLUSION

The study indicates the distribution of microplastic from surface sediments. Microplastic and organic content revealed presence and contaminants in various soil texture. In majority of the sample the maximum and minimum loading for organic matter are respectively in clay and sand. From the sample number 5-12, it is visible from the study that the normal trend have been shifted due to the direct industrial input. From the surface sediments along with the nutrient supply the enhanced microplastic contamination can move on to the entire food chain level and this led to biomagnification and bioaccumulation. This study highlights the need for more education and preventative steps to reduce the release of microplastics into the environment. It also highlights the necessity for continued research to clarify the complex connections between microplastics and organic matter in distinct ecosystems.

REFERENCE

Ammendolia, J., Saturno, J., Brooks, A. L., Jacobs, S., & Jambeck, J. R. (2021). An emerging source of plastic pollution: environmental presence of plastic personal protective equipment (PPE) debris related to COVID-19 in a metropolitan city. Environmental Pollution, 269, 116160.

Ayyamperumal, R., Huang, X., Li, F., Chengjun, Z., Chellaiah, G., Gopalakrishnan, G., ... & Antony, J. K. (2022). Investigation of microplastic contamination in the sediments of Noyyal River-Southern India. Journal of Hazardous Materials Advances, 8, 100198.

Bayard, R., Kouyi, G. L., Gautier, M., Dumont, N., Lebouil, D., Moretti, P., & Larabi, C. (2021). Micro-particules organiques synthétiques: sources, transfert, quantification et impacts des micro-et nano-plastiques au sein des hydrosystèmes urbains-Etat de l'art des connaissances scientifiques (Doctoral dissertation, Agence de l'Eau Rhône Méditerranée Corse).

Bharath, K. M., Muthulakshmi, A. L., & Usha, N. (2022). Microplastic contamination around the landfills: Distribution, Characterization and Threats-A Review. Current Opinion in Environmental Science & Health, 100422.

Cordova, M. R., Ulumuddin, Y. I., Purbonegoro, T., & Shiomoto, A. (2021). Characterization of microplastics in mangrove sediment of Muara Angke Wildlife Reserve, Indonesia. Marine Pollution Bulletin, 163, 112012.

De Sá, L. C., Oliveira, M., Ribeiro, F., Rocha, T. L., & Futter, M. N. (2018). Studies of the effects of microplastics on aquatic organisms: what do we know and where should we focus our efforts in the future?. Science of the total environment, 645, 1029-1039.

Geyer, R., Jambeck, J. R., & Law, K. L. (2017). Production, use, and fate of all plastics ever made. Science advances, 3(7), e1700782.

Horton, A. A., & Dixon, S. J. (2018). Microplastics: An introduction to environmental transport processes. Wiley Interdisciplinary Reviews: Water, 5(2), e1268.

Hossain, M. B., Banik, P., Nur, A. A. U., & Rahman, T. (2021). Abundance and characteristics of microplastics in sediments from the world's longest natural beach, Cox's Bazar, Bangladesh. Marine pollution bulletin, 163, 111956.

Jambeck, J. R., Geyer, R., Wilcox, C., Siegler, T. R., Perryman, M., Andrady, A., ... & Law, K. L. (2015). Plastic waste inputs from land into the ocean. Science, 347(6223), 768-771.

Jambeck, J., Hardesty, B. D., Brooks, A. L., Friend, T., Teleki, K., Fabres, J., ... & Wilcox, C. (2018). Challenges and emerging solutions to the land-based plastic waste issue in Africa. Marine Policy, 96, 256-263.

Law, K. L., Starr, N., Siegler, T. R., Jambeck, J. R., Mallos, N. J., & Leonard, G. H. (2020). The United States' contribution of plastic waste to land and ocean. Science advances, 6(44), eabd0288.

Mu, J., Qu, L., Jin, F., Zhang, S., Fang, C., Ma, X., ... & Wang, J. (2019). Abundance and distribution of microplastics in the surface sediments from the northern Bering and Chukchi Seas. Environmental Pollution, 245, 122-130.

Vaid, M., Mehra, K., & Gupta, A. (2021). Microplastics as contaminants in Indian environment: a review. Environmental Science and PollutJi, X., Ma, Y., Zeng, G., Xu, X., Mei, K., Wang, Z., ... & Shang, X. (2021). Transport and fate of microplastics from riverine sediment dredge piles: implications for disposal. Journal of hazardous materials, 404, 124132.ion Research, 1-28.

Van Cauwenberghe, L., Devriese, L., Galgani, F., Robbens, J., & Janssen, C. R. (2015). Microplastics in sediments: a review of techniques, occurrence and effects. Marine environmental research, 111, 5-17.biological effects, and analytic methods. Quaternary International, 519, 274-281.

Wang, Y., Zou, X., Peng, C., Qiao, S., Wang, T., Yu, W., ... & Kornkanitnan, N. (2020). Occurrence and distribution of microplastics in surface sediments from the Gulf of Thailand. Marine Pollution Bulletin, 152, 110916.

Yao, P., Zhou, B., Lu, Y., Yin, Y., Zong, Y., Chen, M. T., & O'Donnell, Z. (2019). A review of microplastics in sediments: Spatial and temporal occurrences,

Yao, P., Zhou, B., Lu, Y., Yin, Y., Zong, Y., Chen, M. T., & O'Donnell, Z. (2019). A review of microplastics in sediments: Spatial and temporal occurrences, biological effects, and analytic methods. Quaternary International, 519, 274-281.

Zhang, D., Liu, X., Huang, W., Li, J., Wang, C., Zhang, D., & Zhang, C. (2020). Microplastic pollution in deep-sea sediments and organisms of the Western Pacific Ocean. Environmental Pollution, 259, 113948.

HYDROCHEMICAL AND TRACE METAL ANALYSIS IN MINOR WATERSHED OF MAMAM RIVER BASIN- UPPER REACHES OF KADINAMKULAM LAKE, KERALA

Dissertation submitted to Christ College (Autonomous), Irinjalakuda, Kerala,

University of Calicut in partial fulfilment of the degree of

Master of Science in Applied Geology

By,

APARNA.G

Reg. No: CCAVMAG005

2021-2023

DEPARTMENT OF GEOLOGY AND ENVIRONMENTAL SCIENCE

CHRIST COLLEGE (AUTONOMOUS), IRINJALAKUDA, KERALA, 680125

(Affiliated to University of Calicut and re-accredited by NAAC with A++ grade)

AUGUST 2023

HYDROCHEMICAL AND TRACE METAL ANALYSIS IN MINOR WATERSHED OF MAMAM RIVER BASIN- UPPER REACHES OF KADINAMKULAM LAKE, KERALA

Dissertation submitted to Christ College (Autonomous), Irinjalakuda, Kerala,

University of Calicut in partial fulfilment of the degree of

Master of Science in Applied Geology

By,

APARNA.G

Reg. No: CCAVMAG005

2021-2023

DEPARTMENT OF GEOLOGY AND ENVIRONMENTAL SCIENCE

EXAMINERS

Dr. ANTO FRANCIS. K

Co-ordinator

1……

2……

CERTIFICATE

This is to certify that the dissertation entitled - **HYDROCHEMICAL AND TRACE METAL ANALYSIS IN MINOR WATERSHED OF MAMAM RIVER BASIN- UPPER REACHES OF KADINAMKULAM LAKE, KERALA**, is a bonafide record work done by Ms. Aparna.G (CCAVMAG005), MSc Applied Geology, Christ College (Autonomous) Irinjalakuda, under my guidance in partial fulfilment of requirements for the degree of Master of Science in Applied Geology during the year 2021-2023

Dr. Vidhya.G.S

Junior Hydrogeologist

Ground Water Department

District office, Thiruvananthapuram

Place: Thiruvananthapuram

Date:

DECLARATION

I, Aparna.G hereby declare that entitled **'HYDROCHEMICAL AND TRACE METAL ANALYSIS IN MINOR WATERSHED OF MAMAM RIVER BASIN- UPPER REACHES OF KADINAMKULAM LAKE, KERALA'** submitted to Christ College (Autonomous), Irinjalakuda is an original research work done by me, and has not been submitted to any other university for the award of any degree, diploma, associateship and fellowship or any other similar title or recognition. It is a bonafide record carried out by me under the guidance of Dr.Vidhya.G.S, Junior Hydrogeologist, Thiruvananthapuram, Kerala, during April 2023 to August 2023.

Place : Thiruvananthapuram APARNA. G

Date : Reg.No. CCAVMAG005

ACKNOWLEDGEMENT

While bringing this project to its final form, I came across a number of people whose contributions in various ways helped my field of research and they deserve special thanks. It is a pleasure to convey my gratitude to all of them.

For the successful completion of this project work, I would like to extend my thanks and cordial sense of gratitude to **Mr. John Samuel IAS, Director, State Ground Water Department** for giving permission to do the project work under State Ground Water Department. I extend my gratitude to **Mr. Sudheer AS, District Officer, Trivandrum** for giving an opportunity to do my project work under District office and for the suggestion, support given from an early stage of this project work.

I record my deep sense of gratitude and indebtedness to my guide **Dr. Vidya GS, Junior Hydrogeologist, State Ground Water Department,** for developing the project's framework and providing regular support and supervision throughout the duration of the project. I am deeply thankful to **Dr. D Bindu, Rtd Superintendent Hydrogeologist (NHP) and Nodal Officer** for the valuable support.

I also express my sincere thanks to **Ms. Anju, Ms. Rajalekshmi** and other technical and Non-technical staff of **National Centre for Earth Science Studies (Ministry of Earth Science, Government of India), Thiruvananthapuram, Kerala**, for helping the hydrochemical analysis of water samples.

I would like to take this opportunity to express my deepest gratitude to **Dr. Anto Francis K, Co-ordinator**, **Department of Geology and Environmental Science, Christ College (Autonomous), Irinjalakuda**.

I extend my gratitude to **Dr. Linto Alappat, Assistant Professor, Department of Geology and Environmental Science, Christ College (Autonomous), Irinjalakuda** for his sincere support.

I am deeply thankful to **Mr. Sibin Sebastian, Assistant Professor, Department of Geology and Environmental Science, Christ College (Autonomous), Irinjalakuda,** for all the help, support throughout the work. I also thank other faculty members of Department of Geology.

Last but not the least, I express my sincere gratitude to my family and friends for their support.

Above all, I want to thank the Almighty God for his divine blessings showed upon me.

APARNA.G

ABSTRACT

Study on hydrochemical and trace metal analysis of groundwater provide very useful information about its quality for domestic and irrigational purposes. Water quality is defined as the characteristic of water that influences its suitability for specific use. Most important parameters for the quality analysis of groundwater are its physical and chemical parameters such as pH, EC, TDS , Cations and Anions. Trace metal analysis is also important because the contamination of groundwater is one of the critical environmental problems, among which trace metal contamination of groundwater cause significant pollution. In the present study 19 open well samples were collected from minor watershed of Mamam river basin and upper reaches of Kadinamkulam Lake. Physical, chemical and trace element analysis was carried out at NCESS, Thiruvananthapuram.

The study showed that the area is not suitable for drinking water purpose. Anomalous pH values were observed in the study area which shows an acidic trend. The interaction of Fe in laterite with Cl producing ferric chloride which is acidic, use of fertilizers for paddy and rubber , the presence of clay mine and concrete industry may be a reason for this. The iron content is higher in the areas near Kadinamkulam lake which may be due to the leaching of effluents from the retting of coconut husk or may due to the leaching of sewage from the houses. Cadmium and zinc are above highest desirable limit which makes the water toxic. This may be due to the industrial and domestic waste water entering in to the waterbody. Source of these trace metals are due to the anthropogenic activities. The sandy aquifer enhances the interaction between groundwater and surface water resources. The suitability of irrigation was studied by Wilcox and USSL diagram which shows that most of the areas are suitable for irrigation.

CONTENTS

LIST OF TABLES

LIST OF FIGURES

LIST OF PHOTOGRAPHS

CHAPTER 1

INTRODUCTION

1.1 INTRODUCTION

"Water is life". It is how water has been characterized in the European Union (EU) Water Policy document. Such characterization is apt, as life on Earth had its origin in water, and life is not possible without water. The world's water resources are locked in the hydrological cycle, whereby evaporation of ocean water becomes entrained into the atmosphere. Precipitation provides water to the lakes, streams and wetlands. Ultimately, all these continental waters flow back to the ocean and become recycled again. Ocean with 97.2% of all water dominate the hydrosphere. There is less than 1% of water that is possibly available to mankind for its various uses (Soman ,2016) Riverine sources are a meager part of the above. Because of the limited nature of freshwater availability and the increasing demand for various purposes, besides resource depletion due to pollution, water resource estimation had become a major concern of Governments in the developed countries for national planning. Surface water evaluation is relatively easy, whereas ground water recharge estimation requires application of multiple techniques to increase reliability of recharge estimate (Scanlon et al., 2002). Global warming and climate change have all the ingredients to add to the woes of recharge estimation that can offset the water resource projections, affecting life and economy of nations. Today ground water is the source of about one third of global water withdrawals and provides drinking water for a large portion of global population (Kundrewicz and Doll, 2009). Further, ground water resources are continuously recharged under favorable geo-climatic conditions, and are considered safe storage for use in difficult times (Soman, 2016)

Groundwater is the most abundant source of freshwater on earth, accounting for approximately 97% of non-frozen fresh water. Groundwater sustains ecosystems, maintains base flow of rivers and stabilizes land in areas with easily compressed soils. The natural storage of groundwater

buffers the impacts resulting from long-term and short-term climatic variations (Varma, 2017). Approximately 50% of the world's population drinks groundwater every day, especially the rural populations who are located away from water supply infrastructure. Further, groundwater contributes to over 40% of the world's production of irrigated crops, irrigating nearly 100 million hectares of arable land. Overall, the economic benefits of abstracting groundwater exceed those of surface water per unit volume. This is because of local availability of the resource, reliability during droughts, and the fact that groundwater generally requires little treatment (IGRAC, 2014). The role of groundwater is very significant for achieving universal access to drinking water, sanitation and hygiene as highlighted in the Sustainable Development Goals to be achieved by the year 2030 (Resolution adopted by the General Assembly, United Nations, September 25, 2015).

From a physical perspective, groundwater is different from surface water for two main reasons (Custodio, 2000). First, it is typified by a large storage volume per unit of inflow (as compared with low ratios of storage to flow as in surface water). This makes groundwater's availability less sensitive to annual and interannual rainfall fluctuations than surface water. The often-vast spatial extents of aquifers also make its distribution highly ubiquitous, underlying most of the earth's surface rather than confined to narrow channels or lakes as is surface water. Second, groundwater typically moves much more slowly than surface water often at rates measured in meters per year or decade rather than per second. Groundwater's physical properties contribute to its special function in human systems (Giordano,2009). Aquifer recharging by filtration through the soil tends to remove and block impurities and creates a source for high-quality drinking water for domestic use. For both domestic and agricultural uses, aquifers serve a natural storage function, providing a substitute for surface reservoirs and a source of supply in the dry season when surface supplies or rainfall are insufficient (Morris et al., 2000). Groundwater tables are falling at phenomenal rates, often more than one meter per year, in many parts of the world. Formerly perennial rivers and streams whose base flow was supplied by groundwater are becoming seasonal or disappearing altogether. Wetlands are drying up. Salt water is intruding inland in many coastal areas, and land is subsiding under cities. Pollution is increasingly threatening those supplies that are available (Llamas, 1975) (Kayj,2007). Studies show that no water body is free from pollution (Ahluwalia , Sunitha2009) . Any changes in the water body, it may be physical, chemical or biological properties that hurts living things, is termed as water

pollution (WHO 1997). Among the common pollutants that degrade water quality, industrial effluents play a leading role. The chemical composition of groundwater is controlled by several factors that include the composition of precipitation, anthropogenic activities, geological structure and mineralogy of the watersheds, aquifers, and geological processes within the aquifer (Ander L et al 2005).

1.2 GLOBAL SCENARIO

Throughout the world, regions that have sustainable groundwater balance are shrinking by the day. Three problems dominate groundwater use: depletion due to overdraft; waterlogging and salinization due mostly to inadequate drainage and insufficient conjunctive use; and pollution due to agricultural, industrial and other human activities. In regions of the world, especially with high population density, dynamic tube-well-irrigated agriculture and insufficient surface water, many consequences of groundwater overdevelopment are becoming increasingly evident. The most common symptom is secular decline in water tables (Shah T et al., 2000). Unplanned groundwater exploitation can wreak havoc on fragile ecologies such as wetlands. A good example of how groundwater overexploitation can ruin ecologies is offered by the Azraq Oasis in the heart of the Jordanian Badia. The Azraq, a Ramsar wetland of over 7,500 hectares, has provided a natural habitat for numerous, unique, indigenous, aquatic and terrestrial species; and the oasis was acclaimed internationally as a major station for migratory birds until it dried up completely as a result of groundwater overexploitation upstream through mechanical pumps for irrigation and for feeding the city of Aman (Fariz et al., 1996). Groundwater is also emerging as a critical issue for cities and towns around the world. At the heart of the urban groundwater problem is population density; cities just do not have a large enough recharge area to support the needs of their inhabitants on a sustainable basis(www.facingthefuture.org).

1.3 NATIONAL SCENARIO

Groundwater is a common-pool resource used by millions of farmers across the country. Hence, this resource is managed both by the government and private entities. The nature and relative ease and convenience of decentralized access to groundwater make it the backbone of India's

agriculture and drinking water security. It remains the only drinking water source for most of India's rural households. With an estimated 30 million groundwater structures, India is fast hurtling towards a serious crisis of groundwater overuse and quality deterioration (Varma, 2017). The report of the Expert Group on Groundwater Management and Ownership of the Planning Commission (2007) states, that in 2004, 28% of India's blocks were showing alarmingly high levels of groundwater use. A study under the GRACE satellite mission (NASA) and hydrological models indicated that the northern India region and surroundings lost groundwater at a rate of 54±9 km3/year between April 2002 and June 2008 (Tiwari, Wahr & Swenson, 2009). This amounts to a decline in the water table to the tune of 0.33 metres per annum and is also said to be equivalent to the contribution from the melting of Alaskan glaciers to the rise in the sea level. This is probably the largest rate of groundwater loss in any region of a comparable area on earth and is attributed to excessive extraction. In addition to depletion, many parts of India report severe water quality problems (Varma et al., 2017).

If current trends continue, 60% of all the groundwater aquifers of India will be in critical condition by 2032 (World Bank, 2012). India is the largest user of groundwater in the world as it uses an estimated 230 km3 per year that works out to be over a quarter of globaltotal. Groundwater is an annually replenishable resource, but its availability is non-uniform in space and time (Varma et al., 2017).

1.4 KERALA SCENARIO

Kerala is a tiny strip of land located at the south-western tip of India between North latitudes 8°18′ and 12°48′ and East longitudes 740°52′ and 77° 22′, occupying only 1.2% of India's land area. Geographically, it can be described as an elongated strip of land cushioned between the Western Ghats in the east and the sandy shores of the Arabian Sea in the west. Its land area is 38,863 km2 with a length of 560 km and width ranging between 11 km and 124 km (Varma et al.,2017). Though Kerala forms only 1.2% of the total area of India (3,287,263 km2), 3% of the country's population inhabits the state. As per the 2011 Census, about 62% of the population of Kerala depends on groundwater for the purpose of drinking alone. The latest estimate (2008-09) of the Groundwater Resource Potential of Kerala by the Groundwater Evaluation Committee (2012) indicates that the total available resource is 6029 Mm3 and the average level of development is 47% annually. The level of development is highest in Kasaragod district (71%)

and lowest in Wayanad district (17%). The long-term groundwater levels during the pre-monsoon period show a predominantly rising trend in Kerala. However, the Kerala Water Authority (KWA) reported that during the year 2003, 48% of the total 45 lakh wells in the state dried up during the summer. The hydrological importance of river systems, wetlands, ponds, tanks, irrigation canals, etc. in sustaining the groundwater system is either not understood or not taken seriously at the grassroots level, and therefore the environmental abuse of these systems is on the rise. The thick and highly porous and permeable sand bed in rivers is now more or less removed, because of which the riverbed storage of water for the lean season is almost lost. As a result, the perennial flow in rivers is on the decline and the groundwater levels even in wells on the riverbanks are lowering dangerously (Varma et al.,2017). Various studies by the Centre for Water Resources Development and Management (CWRDM), Kozhikode also highlight that 90% of the open wells in Kerala are subjected to bacteriological contamination. The studies also confirm localised issues with respect to excessive iron and fluoride and low pH (Harikumar, 2016).Different groundwater problems, including declining groundwater groundwater table, contamination of groundwater, seawater intrusion, etc., have been reported across the state over last few years (Goldin, 2016).As per the recent reports of CGWB there are one over exploited block (Chittoor) and two critical blocks (Malampuzha and Kasargod) in the state. They also discovered 30 semicritical blocks in kerala. These reports mark the changing scenario of groundwater in kerala.

1.5 THE OBJECTIVE OF THE STUDY

The objective of the present study is to carry out a physical and chemical quality analysis of groundwater in the watershed coming under Mamam River which includes two panchayat Azhoor and Mangalapuram. Most of the people in the study area depend on open well for their daily needs because it is a sedimentary terrain where open well tapping is from laterite aquifer. Data charts were prepared and compared with the BIS and WHO specifications to evaluate the quality status of water resource used for drinking and irrigational purposes.

1.6 STUDY AREA

The study area falls between the coordinates (8°38’36.78’’-8°35’46.24’’N and 76°47’50.51’’-76°50’58.80’’E) of India toposheet 58D/14. The nearest railway station Murukumpuzha and

Perunkuzhi. The total study area is about 13.12 km² .Azhoor Gramapanchayat is about 25Kms from the Trivandrum city which include 18 wards. Azhoor(8.648 N°76.8277E°)is a coastal village in Thiruvananthapuram district in the state of kerala,India. It is one of the "A" grade panchayath in Thiruvananthapuram. This gramapanchayath falls under the 'Coastal Sandy Zone' as the centers are classified into 13 agro-climatic zones of kerala on the basis of average above sea level,rainfall, and topography. The Azhoor Gramapanchayat is situated in the coastal tract of Kadinamkulam Lake, one of the major retting zones in the coastal belt of kerala(Sasidharan et al., 2020). The Kadinamkulam estuary is a temporary estuary lying in the southern part of Kerala, South India (Lat 8° 35′–8°40′N; Long 76°44′–76°51′E) is the largest of its kind in Thiruvananthapuram district connected with the Anchuthengu Kayal in the north and the Veli Kayal in the south. This temporary estuary has no direct connection with the Arabian Sea, but seasonally it becomes connected through the opening of the sand bar at Perumathura. Kadinamkulam lake is the major coir- retting area in South Kerala (Sasidharan et al.,2021). Mangalapuram Gramapanchayat is a land lying about 24kms north of Thiruvananthapuram including 20 wards. The land is blessed with fertile soil as it is a land that collects rainwater,there is not a single piece of land in this village that is not suitable for agricultural purpose. Mangalapuram Panchayat can be divided into two parts according to its topography. The hilly region in the east and the coastal region in the west. Both these lands were suitable for agriculture till ancient times. Coconut cultivation is abundant in the coastal wards of Murukumpuzha, Kozhimada, Mullashery, Mundaikkal, Edavilakam and Veilur in the panchayat. The study area is shown in the figure below.

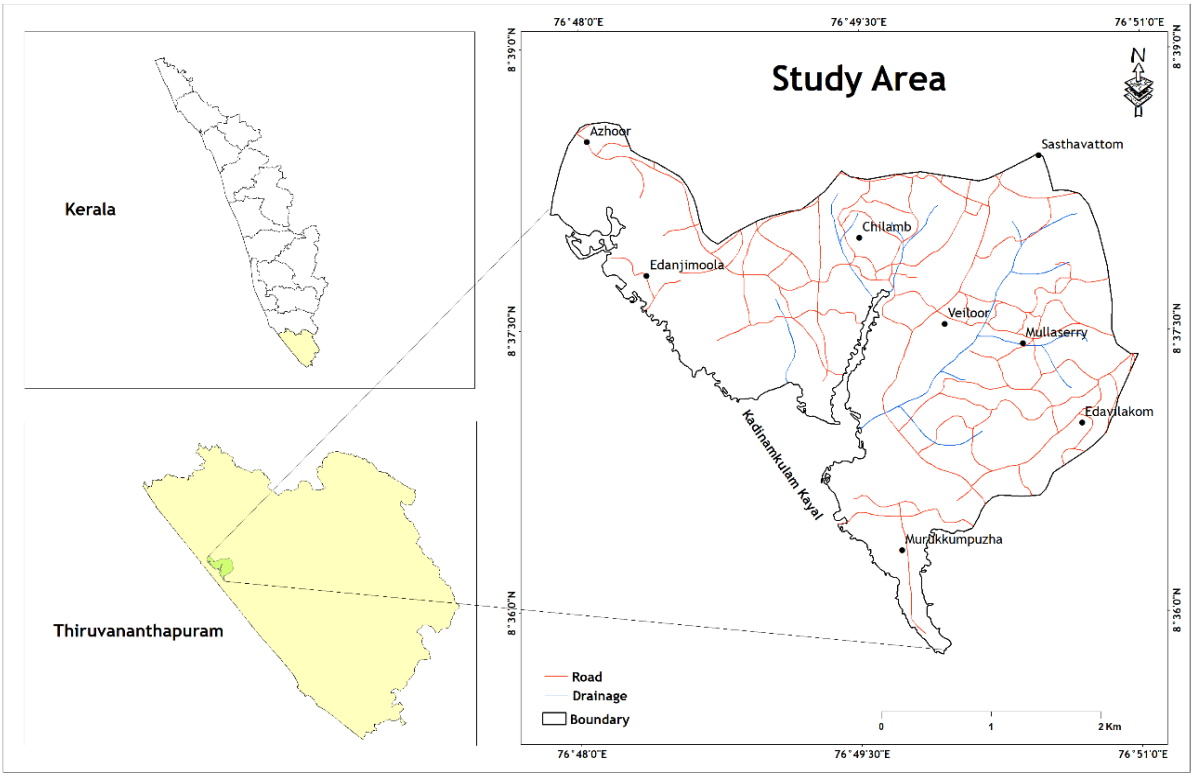

Fig 1- Map of the study area

1.6.1 GEOLOGY

The area has a basement of Precambrian crystalline rocks (Khondalite group) overlain unconformably by a thick sequence of the Warkalli Formation of Miocene age followed by laterites and alluvium. The sedimentary formation consists of sandstone and clay with lignite intercalation and sand and silt on old coastal plains. The basement rock is garnetiferous - quartzo feldspathic gneiss (Leptynite) partially kaolinised forming residual clayzone underlying the sedimentary rocks. The top portions of the sedimentary sequence are lateritised and form a blanket (Mini Chandran et al). The china clay found in Thonakkal,Mangalapuram ,shasthavattom, the midland fringes of the study area, are of sedimentary origin and is developed over the Archean gneissic rocks in the midland fringes of the study area. Laterites of Sub Recent age occur as residual deposits, developed due to weathering of the crystallines and sedimentary

rocks. The typical laterite profile seen in crystalline terrain consists of lateritic soil at the top followed by soft laterite, lithomargic clay and weathered crystalline rocks. The laterites derived from the Tertiary formations are light, homogeneous, soft, and occur below the alluvium. The thickness of laterite capping varies from 15 to 20 m in the khondalitic terrain. The Warkalai formation is only encountered in the study area as Tertiary. The alluvial formations are represented by back water and lagoonal deposits (Mini Chandran et al.,2014). Map of the geology of study area is given in **Figure- 2**

1.6.2 GEOMORPHOLOGY

Physiographically the study area falls mainly in the lowland of Trivandrum which consisting of lower plateau, old coastal plain, Valley, Kayals/estuaries and old mud flats. In the study area lower plateau(laterite) occupies an area of 6.81 km², old coastal plain 5.01 km², valley 1.15 km², kayals/estuaries 0.1 km² and old mud flats 0.05 km². Map of Geomorphology is given in the **Figure- 3**

1.6.3 DRAINAGE

The main drainages in the study area are the Vamanapuram River and its tributaries. There are small streams originating from the area flows north-easterly and join the Mamam river. On the southern slope small streams join the Kadinamkulam kayal. The Drainage Map is given in the **Figure- 4**

1.6.4 CLIMATE

Climate specifies the average weather condition of a particular area for a time period. The study area experiences a tropical humid climate. The two major monsoon seasons are the south-west monsoon (June-August) and the south-west monsoon (September-November). The total annual average rainfall of the district is about 1500 mm per annum (KSLUB 2013). The study area has a mean temperature of 22°C to 35°C. The terrain experiences a dry climate from the end of February to the beginning of June.

1.6.5 LAND USE PATTERN

The study area mainly consists of cultivation such as coconut, paddy, vegetables and fruits, black pepper, cashew etc. Mangalapuram is purely an agricultural village. Coconut is the main crop in Mangalapuram Gram Panchayat, 6,5806 square kilometers (30,381) percent) of the land area is cultivated. This is also the main crop in the watersheds of Paatathinkara and Veiloor Ela. The main reason for this is that the topography of the panchayat is very suitable for this agriculture. Second is mixed farming. Mixed farming is the cultivation of different crops such as coconut, gourd, banana, vegetables and fruit trees together in the same field. This is 26.499 percent of the panchayat's land area (5.7397 sq km). Rubber is cultivated as a sole crop in an area of 3.8522 sq km. Also, bananas (0.1703 square km), tubers (0.0599 square km), cowpea (0.0200 square km), black pepper (0.0279 square km), mixed trees (0.1523 square km), vegetables and cashew are cultivated.0.3773 sq km area of the Panchayat is under paddy cultivation. The main cultivation of Azhoor panchayat is paddy, at present the production of paddy is 10 hector which is less than past. Saltwater intrusion to the paddy fields is a main reason for the decrease in paddy cultivation. According to the topography of Azhoor Gramapanchayat, there is more hand farming than paddy cultivation, and projects to protect and promote paddy cultivation are being given importance. Other crops include cassava, banana, sorghum, cashew, ginger, coconut, banana, palm and organic vegetables.

1.6.6 ACCESSIBILITY

This area is served by a good network of road and rail connections. The area is highly accessible from NH 47 and is connected by motorable roads branching from Mangalapuram to Azhoor. The nearest railway stations are Murukkumpuzha and Perunkuzhi. Thiruvananthapuram International Airport is the nearest Airport.

1.6.7 PREVIOUS STUDY

A study conducted by Sonu Sasidharan and D S Jaya (2020) on Metal contamination of groundwater sources in the residential areas in the surroundings of kadinamkulam estuary shows that 16.66% of groundwater sources in Azhoor and 21.73% in Kadinamkulam gramapanchayaths

are in the low category and the remaining wells are classifed in the high and medium category. The correlation analysis revealed that the sources of metals in groundwater in the study area are the leachates from the Kadinamkulam estuary, agricultural activities and solid wastes dumped in the nearby residential area.They also conducted a study on Quality Assessment of Groundwater in vicinity of Coir Retting areas of Kadinamkulam estuary(2020). Study shows that recorded values for colour,PH,Phosphate,Calcium,Magnesium and Hydrogen Sulfide were above permissible limits of drinking water during monsoon season , this may be due to leaching of effluents from the coir retting activity in kadinamkulam estuary and due to the disposal of solid waste. A study of Characterization, classification and Evaluation of Groundwater in and around the opencast mining of clay deposits of Thonnakkal was done by Joji VS (2017).The impact studied include changes happened to the qualitative and quantitative aspects related to the ground water. It is found that changes occurred in depth to the water level (decline of water level), lowering pH of ground water in the area, high sulfate, and trace metals in the ground water.

CHAPTER-2

GEOLOGICAL AND PHYSICAL SETTINGS OF KERALA

2.1 INTRODUCTION

Kerala is a tiny strip of land located at the south-western tip of India between North latitudes 8°18′ and 12°48′ East longitudes 74°52′ and 77° 22′, occupying only 1.2% of India's land area. Geographically, it can be described as an elongated strip of land cushioned between the Western Ghats in the east and the sandy shores of the Arabian Sea in the west. Its land area is 38,863 km2 with a length of 560 km and width ranging between 11 km and 124 km. Though Kerala forms only 1.2% of the total area of India (3,287,263 km2), 3% of the country's population inhabits the state. The state is subdivided into 14 districts, 21 revenue divisions, 75 taluks and 1635 revenue villages for administrate convenience and into 152 blocks, 6 city corporations, municipalities and 941 grama panchayats for decentralised governance (Varma et al., 2017).

2.2 PHYSIOGRAPHY OF KERALA

Physiographically the state can be divided into four domains from east to west, viz., the Western Ghats, the foothills, the midland and the coastal low land.

Western Ghats - The hill ranges of the Western Ghats rise to an altitude of over 2500m above the MSL and the crest of the ranges marks the inter-state boundary in most of the places. A breach in the continuity of the ranges marks the Palghat Gap with a sinistral shift of 50 km between the shifted crests. The Wynad plateau and the Munnar (10°57'00": 77°31'00") upland fall within this zone.

Foothills - The foothills of the Western Ghats comprise the rocky area from 200 to 600m.above MSL. It is a transitional zone between the high-ranges and midland.

Midland region - This forms an area of gently undulating topography with hillocks and mounds. Laterite capping is commonly noticeable on the top of these hillocks. The low flat-topped hillocks forming the laterite plateau range in altitude from 30-200m and are observed between coastal low-land and the foothills.

Coastal low – Coastal low-land is identified with alluvial plains, sandy stretches, abraded platforms, beach ridges, raised beaches, lagoons and estuaries. The low- land and the plains are generally less than 10m above MSL.

Rivers - Kerala is drained by 44 rivers, many of which orginate from the Western Ghats. Except Kabini, Bhavani and Pambar which are east- flowing, the rest of rivers are west- flowing and join the Arabian Sea. A few of them drain into the backwaters. Most important rivers (with their length in km in paranthesis) of the state, are Chandragiri (105). Valapatnam (110), Achankovil (120) Kallada (121), Muvattupuzha (121), Chalakudy (130), Kadalundi (130), Chaliyar (169), Pampa (176),Bharathapuzha (209) and Periyar (244).

The backwaters form an especially attractive and economically valuable feature of Kerala. They include lakes and ocean inlets which stretch water into the Vembanad Lake, some 200 sq.km. in area, which opens out into the Arabian Sea at Cochin Port. The Periyar, Pamba Manimala, Achenkovil, Meenachil, and Movattupuzha rivers drain into this lake. The other important lakes are AnjuThengu,Edava, Nadayaram Paravoor, Ashtamudi (Quilon), Kayamkulam, Kodungallor, (Cranganore) and Cheruva. The deltas of the rivers interlink the backwaters and provide excellent water transportation in the lowlands of Kerala. A navigable canal, 367 Km long, stretches from Thiruvananthapuram, the capital of Kerala, to Tirur in the far north.

2.3 CLIMATE

Kerala, which lies in the tropic region, is mostly subject to the type of humid tropical wet climate experienced by most of Earth's rainforests. Meanwhile, its extreme eastern fringes experience a drier tropical wet and dry climate. Kerala receives an average annual rainfall of 3107 mm – some 7,030 crores of water. This compares to the all-India average is 1,197 mm. Parts of Kerala's lowlands may average only 1250 mm annually while the cool mountainous eastern highlands of Idukki district comprising Kerala's wettest region – receive in excess of 5,000 mm of orographic

precipitation (4,200 crore of which are available for human use) annually. Kerala's rains are mostly the result of seasonal monsoons. As a result, Kerala averages some 120–140 rainy days per year. In summer, most of Kerala is prone to gale-force winds, storms urge, and torrential downpours accompanying dangerous cyclones coming in off the Indian Ocean. Kerala's average maximum daily temperature is around 37 °C; the minimum is 19.8 °C (IJCRT, Anaida Ann Jacob 2021).

2.4 RAINFALL

Kerala receives normal annual rainfall of 3060 mm, received mainly during the Southwest Monsoon period, extending from May to September, followed by the Northeast Monsoon in the months of November and December. The period between May and October accounts for about 87 percent of the annual rainfall. This period has been considered as monsoon season for computation of monsoon rainfall recharge. The amount of rainfall received shows a gradual decrease from North to South(Dynamic Ground Water Resource of Kerala, 2014).

2.5 GEOLOGY OF KERALA (Geological Survey of India,T.N Rajan et al 2005)

Of the total area 35,955 sq km is constituted by hard crystalline rock and the rest by soft sediments. The crystalline comprise charnockite, gneiss, granite, Meta sediments, gabbro and dolerite to mention the major ones. The sedimentary occur mostly in the coastal areas. Mineral deposits of clay, bauxite, rare earth sands, glass sands, iron ore, limestone, gold, graphite, chrysoberyl, etc are known to occur in the state.

The geology of Kerala kindled the interest of even the earliest workers in the field. Buchanan in 1800 coined the term laterite after a study quarry near Angadipuram in east Malabar. General Cullen between 1840-60 discovered graphite occurrence in Travancore and was earliest to study the sedimentary formation around Kollam. In the later part of the 19th century, Bruce Foote (1883) and William King (1875, 1878, 1882) of the Geological Survey of India (GSI) took traverses across the state and recorded their findings on geology and mineral resources. In 1907

a Geology department was formed in Travancore for systematic survey of minerals. Chacko (1922) and Masilamani (1914) made significant contributions to the geology of Kerala.

Geology of the South Indian field is dominated by the rocks belonging to the craton and the surrounding mobile belt. The remaining parts of metamorphosed older rocks of ancient supracrustal especially are present towards Northern Kerala. The major rock of Kerala region can be divided into three, based on the age of the formation- They are.

- The Archeans
- The Warkalli bed of Tertiary age

The recent deposits, these have North South alignment Geologically, Kerala is occupied by Precambrian crystalline, acid to ultrabasic intrusions of Archean to Proterozoic age, Tertiary (Mio-Pliocene) sedimentary rocks and Quaternary sediments of fluvial and marine origin. Both the crystalline and the Tertiary sediments have extensively undergone lateritization.

Geology of kerala is shown in the figure below:

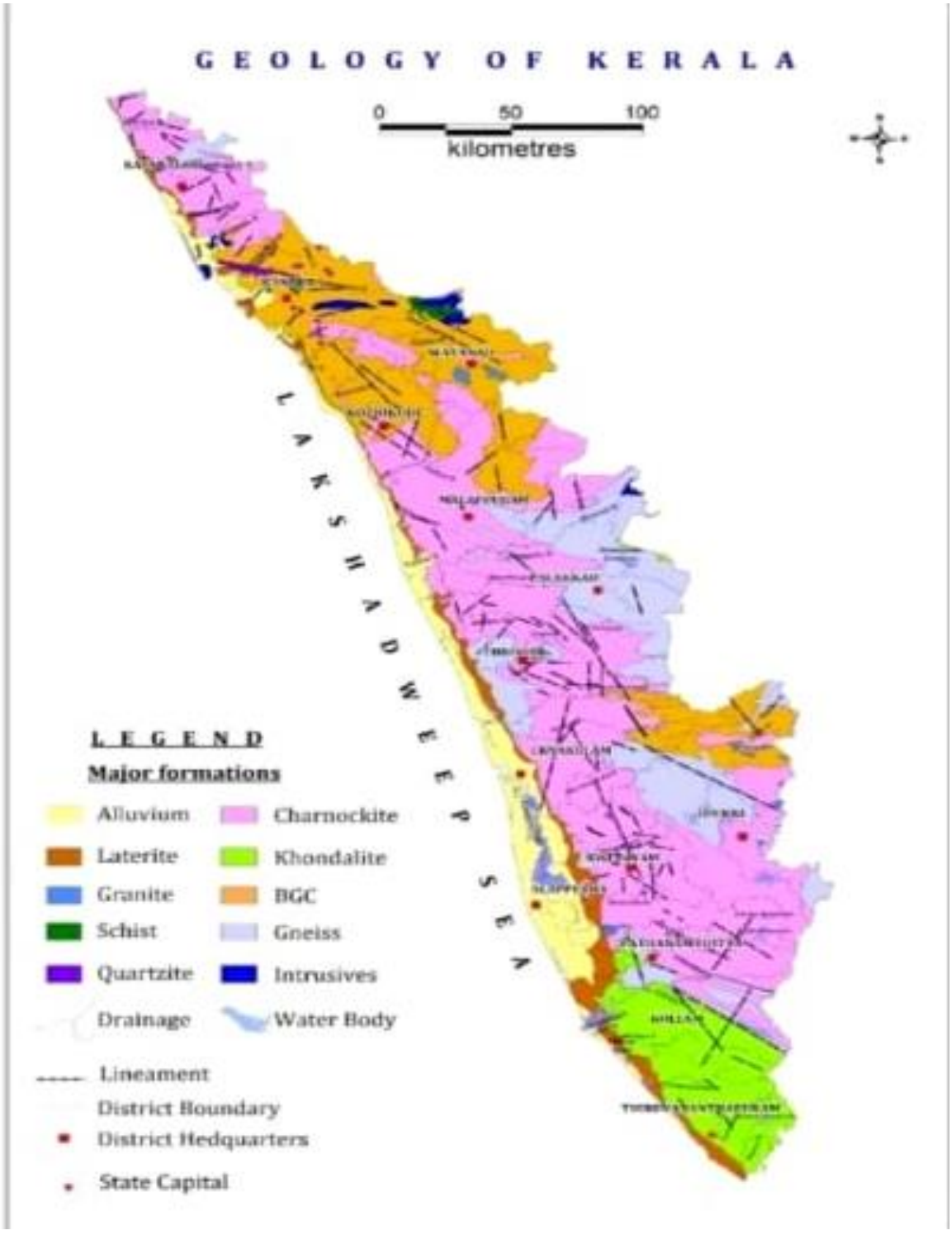

GEOLOGICAL SUCCESSION OF KERALA

Based on the detailed studies by GSI during the last three decades, the following stratigraphic sequence has been suggested.

CENOZOIC	Quarternary	Recent Holocene	Pebble bed Kadappuram Formation Periyar Formation Guruvayur Formation Viyyam Formation
	Tertiary	Neogene	Laterite Warkalli Formation Quilon Formation
	Mesozoic		Gabbro/Dolerite Dyke
PROTEROZOIC	Younger granites Charnockite Ultrabasic/Basic Basic Intrusive Migmatite/Gneiss Granitoid		Alkaline granites, granophyres, and other acid intrusive Massive charnockite Incipient charnockite Charnockite Perinthitta-Anothosite, Kartikulam gabbro, Adakkathodu gabbro, Bengur Diorite Agali-Anakatti dyke Garnet-Biotite-Gneiss with associated magma Quatzo-Feldspathic Gneiss, Hornblende Gneiss, Hornblende Biotite Gneiss, Quartz Mica Gneiss
ARCHEAN	Vengad Group Charnockite Khondalite group Peninsular gnessic complex Layered ultrabasic –basic complex Wayanad schist complex		Quartz mica schist and quartzite, conglomerate Mafic granulites, pyroxene granulites, banded magnetite, quartzite and gneissic charnockite Quartzite, mafic granulite, calc-granulite, garnet biotite-sillimanite, corderite gneiss, garnet biotite gneiss, leptynite, foliated garnet, hornblende gneiss, pink garnet, biotit gneiss Peridotite, dunite, pyroxenite, anorthosite Talc-Tremolite schist, fuschite quartzite, amphibolites calc-granulites, quartz, sericite, schist Kyanite, quartzite, kyanite-mica schist

2.5.1 THE ARCHEANS

Rocks of Archean Era encompass a wide spectrum of lithological assemblages ranglng from Khondalite, Charnockite gneiss and meta-sedimentary rocks occupying the Western Ghats including the foothill region. The khondalite and charnockite group are correlated with Eastern Ghats supergroup based on the overall similarity in lithology and geochronology.

2.5.1.1 Wayanad Supracrustal

The high grade sedimentary and ultramafic rocks occurring in the Wyanad district comes under the Sargur schist complex of the Karnataka. The schistose rocks are characterized by intense deformation, medium to high grade metamorphism, migmatisation and lack of sedimentary structures. The schist complex consists of meta-ultramafic, schist, meta gabbro, meta pyroxenite, serpentine, talc tremolite rock and amphibolite.

2.5.1.2 Layered ultrabasic complex

Remains of layered basic — ultra basic complex are reported from Attapadi area. The ultramafic are represented by meta-pyroxinites, meta-dolerite, peridotites with chromite and meta gabbro- The anorthosites of Attapadi are only a few meters thick.

2.5.1.3 Peninsular Gneissic complex

The rocks of PGC are exposed in the northern parts of Kerala adjoining Karnataka. These consist of heterogenous mixture of granitoid materials. The equivalent rocks of PGC in kerala include hornblend - biotite gneiss (sheared), biotite hornblend gneiss, foliated granite and pink granite gneiss.

2.5.1.4 Khondalite Group

The khondalite group of rocks includes calc-granulites, quartizites and para-gneisses of peletic parentage. Para-gneisses are well developed in the southern part of this state, particular in the Trivandrum and Kollam districts. Calc- granulite and quartzite occurs as bands within the paragneisses- Granetiferous- biotite- sillimanite gneiss is well developed in the southern part of the state- It occurs with the close association with the migmatitic gneisses, charnockite gneisses.

Calc-granulite occurs as linear bands mainly in the eastern part of Kollam and Thiruvananthapuram District, northeast and east of Munnar in Idukki district and in parts of Palakkad District. The rock is generally medium to coarse-grained, inequigranular and granoblastic in texture. It consists of diopside and plagioclase. Minerals like wollastonite, scapolite, calcite, garnet, spinel, sphene, quartz and apatite are also present in different proportions.

Quartzite occurs as linear bands amidst the khondalitic gneiss, charnockite and migmatitic gneisses. These hands are exposed between Pathanamthitta (9°15'45":76°47'00"), Muvattupuzha (9°59'00": 76°35'00") in Ernakulam District. The rock is coarse-grained and generally white in color with a brownish coating on the weathered surface. It consists of granular quartz with subordinate feldspar, garnet and iron oxide.

Garnetiferous biotite-sillimanite gneiss is well-developed in the southern part of the state. It occurs in close association with the migmatitic gneisses, charnockite and charnockite gneisses, mostly as weathered outcrops. Sillimanite rich bands occur alternating with gamet - rich portions or with quartzo-feldspathic layers and iron oxides are the common accessory minerals.

2.5.1.5 Charnockite Group

Charnockite Group shows great diversity in lithology comprising pyroxene granulite, hornblende pyroxenite, magnetite quartzite, charnockite and hypersthene- diopside gneiss and cordierite gneiss. Chanockite and chanockitic gneiss have preponderance over all other crystalline rocks covering 40-50% of the total area of the State. The charnockites are well-exposed in the central and northern parts of Kerala including the high hills of the Western Ghats. Charnockite has lesser predominance in Thiruvananthapuram and Kollam districts. In Attappady, the Bhavani Shear Zone is limited by the charnockite massif of the Nilgiri plateau on the north. Though the interrelationship of the Charnockite and the Khondalite is not clear, in many places there are intercalations rather than interlayering of one with the other. In Palakkad District, the Khondalite Group of rocks structurally overlie the charnockite. The occurrence of pyroxene granulite as fine and linear bodies within the charnockite of Tirur, suggests that chanockite is a product of migmatisation of pyroxene granulite (Vidyadharan and Sukumaran, 1978). Charnockite and

charnockitic gneiss consist of quartz, feldspar and biotite. Garnet-bearing variants are also observed. The basic charnockite is more granulitic and contains clino- and ortho- pyroxenes. feldspar, biotite and gamet whereas the acid variety (alaskite/ enderbite) is greenish black, coarse-grained, massive to poorly foliated rock consisting of quartz, feldspar and pyroxenes, Basic charnockite has low- potash feldspar and more clinopyroxene. This is devoid of garnet and graphite, hut shows a little amount of biotite (Chacko, 1922). Due to the polygenetic nature of the rock, geochemical and mineralogical variations do exist between charnockites reported from Kerala. The available age data indicate that the massive charnockites are older and their ages range between 2155 and 2930 +50 Ma (Soman ,1997).

2.5.1.6 Vengad Group

A succession of schistose rocks in parts of Tellichery Taluk in Kannur district is described as vengad group of rocks(Nair,1976). The vengad group of rocks comprises of basal Conglomerate, quartzite and quartz mica schist. The conglomerate shows graded bedding and quartzite shows current bedding.

2.5.2 THE PROTEROZOIC

2.5.2.1 Young Granite

The granite and its variant occur around Chengannur in Alappuzha and Pattanamthitta districts, Munnar in Idukki district, Peralimala in Kannur district and Kalpatta and Ambalavayal in Wayanad district- Many of the granites occur as later emplacements along crustal fractures and faults- The Achenkovil —Tamraparni tectonic zone, the Attapadi shear zone, Bhavani shear zone and Moyar shear zone are all marked by granitic emplacements.

2.5.2.2 Charnockite (younger)

The area of south of Palakkad exposes charnockite over large areas -The charnockites are represented by acid microperthic charnockite and intermediate gneissic charnockite occurring association with granetiferous biotite gneiss and khondalite- It is medium to coarse grained and shows xenoblastic texture. It is composed of quartz, feldspar, pyroxene, garnet with accessories like biotite, zircon, apatite and monazite.

2.5.2.3 Basic Intrusive

Basic dyke emplacement within the Archean crystalline rocks of Kerala is spread throughout the entire length and breadth of the State- Of these dolerite dykes occurring north of Palakkad gap had given Proterozoic age.

2.5.3 TERTIARY SEDIMENTS

It is interesting that Paleozoic and Mesozoic have not been represented so far from Kerala.The Cenozoic rock represented by the tertiary succession from the coastal sedimentaries Of Kerala. Several geologists from abroad as well as from India have worked on the stratigraphy of Tertiaries of Kerala. W King in 1882 and Bruce foot in 1883 were the pioneers of the study Of Kerala geology.

2.5.3.1 Vaikom Formation

This formation consists of gravel to very coarse sand with greyish clay, carbonaceous clay and with seams of lignite. The lower limit of the sequence is exposed in the laterite quarries at Vaikom.

2.5.3.2 Quilon Formation

The Quilon formation consists of fossiliferous limestone, sand and clay. The type of area of the formation at Padappakara is about 20 km east of Quilon (Kollam city). Padappakara is near Kundra. The type of area of the Quilon formation is exposed in a cliff section fringing the Ashtamudi Lake. Lignite fragments are also sometimes seen in limestone. The Quilon limestone contains numerous fossils of foraminifera, corals, echinoids and molluscs. The Lower Miocene

age for lower stratigraphic horizons and the Upper Miocene age for the topmost beds of the Quilon Formation indicate the lower and upper age limits of these marine sediments. The predominance of black clays, sandstone, bluish grey brackish water shell limestone and nodular limestone clearly indicate deposition in a lagoonal condition.

2.5.3.3 Warkalli Formation

The Warkalli formation occurs along the coastal belt of kerala.It conformably overlies the Quilon formation.The type area is exposed at papanasham beach.Warkalli is generally taken as a type area.It is considered to be shallow water shoreline littoral deposits.

2.5.3.4 Laterite

Kerala is the home of the laterite as it was first named by the Dutch traveller, Buchanan 1807. Laterite is widespread in its distribution in the midland region of Malappuram, Kannur and Kasaragod districts where it forms well-defined mesas. The Archaean crystalline rocks and the Tertiary sedimentary rocks are extensively lateritised. The laterite has wide areal distribution in the State and occurs at all levels upto 2000 m, height though mostly restricted to an altitude of 50-150 m above MSL. in the coastal and midland regions. A few bauxitic patches also occur within the laterites. The thickness of laterite cappings varies from a few metres to 50 metre at places. At Chovvara (8°21′30: 77°01'30") in Thiruvananthapuram District,Chattannur (8°50'30": 76°4630") and Kundara (8°5700": 76°40′30") in Kollam District, a zone of about 2 m thick bauxite is recognised at the contact between the crystallines and the overlying sedimentary rocks. The overlying sedimentary column is also blanketed by laterite of varying thickness. The bauxite at the base of the sedimentaries indicates an earlier pre-Warkalli spell of lateratisation. Further, the erosional features on the top part of the bauxite horizon corroborates the antiquity of the earlier spell of lateritisation (Mallikarjuna and Kapali, 1980).

Generally, the laterite after the crystalline rocks is compact and the top crust moderately indurated. The dark brown crust passes downward to pink and buff coloured soft laterite. Quartz veins, joints and fractures can be traced from the top to the bottom of the laterite profile.

2.5.4 QUATERNARY SEDIMENTS

Recent to sub-recent sediments of costal sands, sticky black clay with carbonized wood, silty alluvium and lagoonal deposits are observed mostly in the low-lying areas from Kollam to Ponnani and between Kannur and Nileswaram. Alluvium is observed along the major river valley At places along coastal tracts, there are raised sandy beaches composed of fine grained reddish sandy loam known as 'teri" sands. Palaeo-beach ridges alternate with marshy lagoonal clay in the coastal area.

The sandy stretches are widest between Alappuzha (9°30': 76°20') and Kottayam (9°35': 76°31'), upto 25 km inland from the shoreline. The Quatemaries of the coastal plain have been classified into (i) the Guruvayur Formation representing the earlier strandline deposits with an elevation of 5-10 m; (ii)the Viyyam Formation of tidal plain deposits; (iii) Periyar Formation being mainly of fluvial deposits and (iv) the Kadappuram Formation representing the beach deposits (Krishnan Nair, 1989).

2.6 GEOMORPHOLOGY

Relief distribution in Kerala is asymmetric. As much as 62% of the total geographical area is below 100 m (Chattopadhyay and Mahamaya, 1995). The coastal plain is wide in the central part, especially around Vembanad Lake where it coincides with a sedimentary basin, and tapers both towards north and south. From the coastal plain, elevation increases in a stepped manner, justifying the nomenclature of 'Ghats'. The average rise of land is 27 m for every kilometre from the coastline towards east and the relief amplitude increases with the rise in altitude. Seventy per cent of landmass in Kerala fall in the slope category of >15% (Chattopadhyay and Mahamaya, 1995). The crest line of the Western Ghats reaches the maximum altitude of 2695 m at Anamudi, which is the highest point in south India. The monolithic Western Ghats is broken by the 30 km

wide Palghat Gap at the altitudinal level of 100 to 200 m. This Gap connects Kerala plains with the Tamil Nadu plains, and has pronounced influence on the climate, culture and economy of the State. The Western Ghats and the Eastern Ghats merge at the Nilgiri Hills in Tamil Nadu, an extension of which is the Kunda Hill ranges in Kerala. About 23% of the land lying above 600 m altitude is the source area for all the rivers in the State and is the primary source zone for sediment and water. The abrupt rise of the Western Ghats from 100 m upward with precipitous slope is a characteristic feature of Kerala's topography that controls hydrology, climate, land use, infrastructural development and settlement distribution(Chattopadhyay,S. 2017).

2.7 SOIL AND VEGETATION

The topo-lithosequence of Kerala along with variation in rainfall, temperature and alternate wet and dry conditions particularly from the western coast to high ranges in the east and swift flowing rivers lead to the development of different types of natural vegetation and soil. The soils of Kerala can be broadly grouped into coastal alluvium, mixed alluvium, acid saline, kari, laterite, red, hill, black cotton and forest soils. Coastal alluvium soils are of marine origin and are identified along the coastal plains and narrow strips, coconut is the major crop in the area. Cashew and other fruit trees are also grown. Mixed alluvium are developed from fluvial sediments of marine, lacustrine and riverine sediments or its combination. Paddy, other annuals and seasonal crops like banana, tapioca and vegetables are grown here(Department of soil survey and soil conservation). Acid saline soils are present throughout the coastal area in patches with very little extent. Major area of this soil is identified in the coastal tract of Ernakulam, Thrissur and Kannur districts. Paddy is the only crop that can be cultivated. Laterite and laterite soil are the weathering products of rock in which several course of weathering and mineral transformations take place. It is mainly cultivated with coconut, arecanut, banana, tapioca, vegetables, yams, pepper, pineapple, fruit trees etc. Blackcotton soil are identified in alluvial plains, terraces and undulating plains of chittur, Palakkad. A variety of crops such as coconut, sugarcane, cotton, chilly, vegetables are grown here. Red soils are found mostly on the southern part of Thiruvananthapuram and in pockets in catenary sequence along the foot slopes of laterite hills and mounds. A variety of crops such as coconut, arecanut, banana, yams, pineapple, vegetables, fruit trees etc., can be grown under proper management. The hill soil mostly occurs

above an elevation of 80m MSL. Crops such as banana, pepper, pineapple, vegetables can be grown in foot slopes. Forest soil soils are developed from crystalline rocks of archaean age under forest cover.Forest trees, shrubs and grasses are grown here(Department of soil survey and soil conservation).

2.8 OCCURRENCE OF GROUNDWATER IN KERALA

In hard rock terrain, comprising weathered crystalline and laterites, ground water occurs under phreatic conditions in the weathered residuum and the shallow fractures hydraulically connected to it, whereas it is under semi-confined to confined conditions in the deep fracture zones. In the alluvial terrain, ground water in the shallow systems is in phreatic condition. Granular zones in the Tertiary sedimentary formations at deeper levels form potential confined to semiconfined aquifers (Ground water resources of kerala 2017).

Crystalline Rock Aquifers- The shallow aquifers of the crystalline rocks are made up of the highly decomposed weathered zone or partly weathered and fractured rocks. Thick weathered zone is seen along the midland area either beneath the laterites or exposed. In the hill ranges thin weathered zone is seen along topographic lows and area with lesser elevation and gentle slope. In areas along the hill ranges generally rock exposures are seen. The depth to water level in this aquifer varies from 2 to 16 mbgl and the yield of the well ranged between 2 to 10 m3 per day.

Tertiary Rock Aquifers- Groundwater occurs under phreatic conditions in the shallow zone and under semi-confined to confined conditions in the deeper aquifers. The Tertiary formation of the Kerala coast is divided into four distinct beds viz. Alleppey, Vaikom, Quilon and Warkali. These formations except the Alleppey beds are outcrops and they are lateritized wherever they are exposed. The maximum thickness of Tertiary sediments is found between Karunagapally and Kattoor and all the four beds are found in this area. Groundwater is commonly developed through dug wells tapping the sandy zones at shallow depth in the Tertiary sediments. The depth to water level in this shallow zone ranges from 2.0 to 27 m.bgl and the yield of the well's ranges from 500 lpd to 10 m3 per day. The Vaikom and Warkali beds form the most potential aquifers in the Tertiary group. The Alleppey bed has been encountered at deeper levels in the bore holes drilled

in the coastal tract of Alappuzha district and the formation water is found to be saline and hence, no tube well has been constructed tapping this formation. Warkali aquifers are the most developed aquifer system among the Tertiary group. The hydrogeological information on Quilon beds is very limited. The formation is considered to be a poor aquifer compared to Vaikom and Warkali beds.

Laterite Aquifers- Laterites are the most widely distributed lithological unit in the State and the thickness of this formation varies from a few meters to about 30 m. Laterite forms potential aquifers along topographic lows and valleys. The depth to water level in this formation ranges from 2 to 25mbgl and the yield ranges from 0.5 to 30 m3 per day. The occurrence and movement of groundwater in the laterites are mainly controlled by the topography. Laterite is a highly porous rock formation, which can form potential aquifers along topographic lows. However, due to the porosity, groundwater is drained from elevated places and slopes at shortest duration after monsoon and hence water scarcity is experienced in the elevated places and slopes.

Alluvial Aquifers- The alluvial deposits form potential aquifer along the coastal plains and groundwater occurs under phreatic and semi-confined conditions in this aquifer. The thickness of this formation varies from few meters to above 100 m and the depth to water level ranges from less than a meter to 6 mbgl. Filter point wells are feasible wherever the saturated thickness exceeds 5m. This potential aquifer is extensively developed by dug wells and filter point wells throughout the State and the yield ranges from 5 to 35 m3 per day (Ground water resources of kerala, 2017).

2.9 SOURCE OF GROUNDWATER

HYDROLOGICAL CYCLE

The hydrological cycle denotes the circulation of water from the oceans to the atmosphere, the atmosphere to the lithosphere, and lithosphere to the oceans through complex and interdependent processes including precipitation, runoff, groundwater flow, evaporation,transpiration,etc. The part of the precipitation reaching the ground may be absorbed, evaporated, transpired by plants,

or may flow over ground. The water absorbed in the ground infiltrates downward through interstices to reach the saturated groundwater medium. It completes the hydrological cycle by emergence as springs or by subsurface flow into streams and oceans. The region of Kerala flanked by the Western Ghats and Lakshadweep has a characteristic hydrological cycle dominated by high monsoonal rainfall(Varma, 2017).

Kerala received the highest Annual Average Rainfall (AAR) of 3070 mm among the 35 agro-climatic zones of India based on rainfall data for the last 100 years. There are about 120–140 rainy days, having about 1–2 hours of rainfall on an average. On an average, Kerala receives about 70% of the AAR during the southwest monsoon (SWM) (June to September), 16% during the northeast monsoon (NEM) (October to December), 1% during the winter (January – February), and 13% during summer months (March to May). Almost 50% of the SWM rainfall occurs during 30–40 hours with an intensity of 50–60 mm per hour. The rainfall intensity recorded at Thiruvananthapuram, Kochi and Munnar during the SWM period is 46–144 mm/hr; 97–223 mm/hr and 44–133mm/hr, respectively (Sasikumar, Sampath, Vinayak & Harikumar,2007). Whereas southern Kerala receives almost comparable rainfall during both the monsoons, northern Kerala is devoid of significant rainfall after the SWM. Therefore, northern Kerala experiences water shortage long before the summer sets in.

CHAPTER 3

HYDROCHEMISTRY

3.1 INTRODUCTION

Groundwater contains a wide variety of dissolved inorganic constituents as a result of chemical interactions with geological materials and to lesser extent contributions from the atmosphere. The study of hydrochemistry is of prime importance in deciding about the quality of groundwater supply. Hydrochemistry helps to evaluate hydrogeochemical processes responsible for temporal and spatial changes in the chemistry of groundwater. Groundwater chemistry is affected by many factors such as movement through the rocks, recycling by irrigation practices, natural or artificial recharge and discharge. As water flows, it assumes a diagnostic chemical composition as a result of interaction with lithological and stratigraphical frameworks. Hydrochemical results provide a basis for the characterization of groundwater within each hydrogeological unit. From this information, it is possible to draw inferences concerning the processes that may occur within the aquifers, the effect of groundwater abstraction on the aquifer, host rock, and the suitability of ground waters for use (Shunmugam, 2022). This chapter includes all the methodologies or procedures which are followed for the hydrochemical analysis of groundwater. It includes the procedures done before and after the fieldwork and collection of data. The methodology adopted for the present study is a quality-based analysis. The parameters are measured by volumetric analysis and certain equipments.

3.2 GENERAL BACKGROUND

The study area falls between the coordinates (8°38’36.78’’-8°35’46.24’’N and 76°47’50.51’’-76°50’58.80’’E) of India toposheet 58D/14. In the present study, a total of 20 groundwater samples were collected from 20 location situated in different parts of the study area. Physical and chemical analysis were carried out in the chemical lab of National Centre for Earth Science Studies Thiruvananthapuram.

3.3 METHODOLOGY

3.3.1 Depth to Water Table Analysis (April-May 2023)

For the analysis of water level trend in the study area 105 observation wells has been examined by dividing the study area with an interval of ½ km distance. Data regarding water level, dimensions of well, and the address of the owners were noted according to the well inventory procedure. Depth to water table map and water table contour map were prepared using Arc Gis. Well inventory data is given in the **Table- 1** , the map of well location is shown in the **Figure- 5** and Water table contour map is shown in **Figure- 6**

3.3.2 Sample Collection

To determine the water quality 19 open well samples were collected from the study area during April-May 2023. Water samples were collected in new polyethylene bottles. Before sampling , these bottles were cleaned with pure water and also rinsed with the groundwater sample to be taken. The collected samples were properly labelled with sample location, location number, date and time. Each samples location was also marked in location grid map to prepare sample location map.The coordinates were marked using GPS Essentials.. Samples were transported to the laboratory for further analysis. The map of sample location is given in the **Figure – 7**

3.3.3 Laboratory Work

After sampling the samples were analysed in the laboratory to find out the physical and chemical parameters present in them. There are various methods and instruments used for analysing different parameters.

3.4 PHYSICAL PARAMETERS OF WATER

3.4.1 HYDROGEN ION CONCENTRATION(pH)

pH is the hydrogen ion concentration in water. The ph value indicates acidity or alkalinity of a given solution.

Instrument used- The ph meter is used to measure the hydrogen ion or the hydroxide ion concentration in water sample. it usually consists of a probe which is dipped inside the sample for obtaining the values Probe consist of a thin glass bulb (Measuring electrode) and reference electrode both submerged in neutral KCI solution and having a silver alloy wire. The eutech pH in a tutor was used for determining the pH values and the model name of the instrument is Cyber Scan pH Tutor pH/°C with pH range 0.00 to 14.00. It is having a pH resolution of 0.01 with temperature 25°C. pH buffer options US Standard (pH 4.01, 7.00,10.01), Accuracy ±0.01 pH,Display of Custom Dual Line LCD.

pH Meter

3.4.2 ELECTRICAL CONDUCTIVITY

The conductivity of water comes from ionisable of the dissolved salts and inorganic compounds in it. It was measured in the unit of µS $cm^{-}1$. EC and TDS is determined using the same equipment by changing the electrode. The equipment is EUTECH PC 2700.

3.4.3 TOTAL DISSOLVED SOLIDS (TDS)

TDS refers to all solid materials present in solution either in ionized State or in non-ionized state and exclude the suspended colloids or dissolved gases. Quality of drinking water will be affected by the presence of soluble salts. TDS indicate general nature of water quality or salinity. Therefore the level of TDS is one of the characteristics which decide the quality of drinking water. When the TDS in water is more than 500 ppm, deliciousness of water decreases and may cause gastrointestinal irritation (Park and Park, 1980). High TDS indicates that the water is highly mineralized and this water is not suitable either for drinking or for industrial purposes. The concentration of TDS above 2000 ppm produces laxative effects. The bulk of the total dissolved solids include bicarbonates, sulphates and chloride of calcium, magnesium, sodium and silica. Potassium chloride and nitrate form a minor part of the dissolved solids in groundwater.

EUTECH PC 2700

3.5 CHEMICAL PARAMETERS OF WATER

3.5.1 MAJOR CATION ANALYSIS

Na, K. Ca, Mg and Fe are major cations present in the surface water system, These cations are analysed by MICOWAVE PLASMA- ATOMIC EMISSION SPECTROSCOPY (MP-AES)

Principle

MP-AES is an atomic emission technique, It uses the fact that once an atom of a specifie element is excited, it emits light in a characteristic pattern of wavelengths-an emission spectrum, as it returns to the ground state. Sources for atomic emission include the microwave plasma (MP) and the inductively coupled argon plasma (ICP) both of which are high temperature sources, and therefore excellent excitation sources for Atomic Emission Spectroscopy. The nitrogen fuelled microwave plasma reaches temperatures nearing 5,000 K. At these temperatures, atomic emission is strong, producing excellent detection limits and linear dynamie range for most elements. Inside a MP-AES instrument., microwave energy form an industrial magnetron is used to form plasma form nitrogen that has been extracted from compressed air by Agilent's Nitrogen Generator. Effectively, the MP-AES runs on air. Using a magnetie field rather that an electronic one for excitation generates a very robust plasma-capable of handling a wide range of sample types, An optimized microwave waveguide ereates concentrated electromagnetic fields at the torch. Then an axial magnetie field and a radial electrical field focus and contain the microwave energy to create plasma.

Procedure

Sample Introduction-

Just like a flame AA instrument, an aerosol is created from a liquid sample using a nebulizer and a spray chamber. The aerosol is then introduced into the centre of the hot plasma. The aerosol dries, decomposes and is then atomized. The atoms continue to be excited and emit light at wavelengths characteristic for each element as they return to lower energy states.

Optical system-

Emission from the plasma is directed into a fast scanning monochromator. The selected wavelength range is imaged onto the high efficiency charged couple device (CCD) detector. This measures both spectra and background simultaneously for optimum precision.

Quantification-

Just like flame AAS, MP-AES quantifies the concentration of an element in a sample by comparing its emission to that of known concentrations of the element, plotted on a calibration curve. The final result is the concentration of the element in in the sample.

3.5.2 MAJOR ANION ANALYSIS

3.5.2.1 Chloride

The chloride content in rainwater is usually less than 10 ppm. The chloride content of rainwater may be high in coastal areas this can be attributed to the high chloride content of ocean water to the order of about 13,000 ppm. Cl is a natural substance present in potable water and usually occurs in sewage as metallic acid. Its concentration in fresh water is quite low and generally less than that of sulphate and bicarbonates. General source of chloride is animal organic matter, sewage from drainage and refuse. Chloride cannot be removed biologically in treatment of water, as it is highly soluble with cations and does not sediment and precipitate. The important mineralogical sources of chloride are sodalite, apatite, micas and hornblende. Chloride in water is a stronger oxidizing agent than oxygen and Cl with oxygen slowly decomposes water. High concentrations may be injurious to people suffering from disease of heart or kidney (Khurshid et al, 1998). High concentration of Cl can also corrode concrete by extracting calcium in the form of calcides. As per BIS (1991) the highest desirable value is 250 ppm and maximum permissible limit for chloride in drinking water is 1000 ppm. However, concentration above 100 ppm itself can cause physiological damage. Chloride is determined volumetrically by titration against standard AgNO3 solution in the presence of potassium chromate as indicator.

Method: Argentometric titration

Reagents:

1) Potassium Chromate Indicator: Dissolve 50 g K_2CrO4 in distilled water. Add AgNO3 till definite red precipitate is formed. Allow to stand for 12 hrs. Filter and dilute to 1000 ml.
2) Silver nitrate 0.014 N: Dissolve 2.395g silver nitrate and dilute to 1000 ml.
3) Standardize against sodium chloride, 0.014 N

Procedure

Take 20 ml of sample in a conical flask and add 2 ml of K_2Cr_2O4 solution and then titrate it against 0.05 N AgNO3 until a persisted red tinge appears.

Calculation

4) (ml x N) of AgNO3 x 1000 x 35.5 Ml of sample
5) Chloride, mg/l

3.5.2.2 SULPHATE ($SO4^2$)

The sulphate content of atmospheric precipitation is only about 2 ppm. Sulphur is not a major constituent of most of the rocks; however sulphate is abundant in most groundwater. This happens through oxidation, reduction, precipitation, solution and concentration processes as water traverses through rocks. Natural water contains higher levels of sulphate contributed from the weathering of rocks. In addition to this, domestic sewage and industrial effluents also add sulphate to aquatic ecosystem and hence high level of sulphate is an indicator of organic pollution. Fragrant condition is easily created when water is over loaded with organic wastes to the point that oxygen is removed and the SO4 formed. The sources of sulphate are sulphur minerals, sulphide of heavy metals which are of common occurrence in the igneous and metamorphic rocks and gypsum and anhydrite found in some sedimentary rocks. Also the oxidation and hydrolysis of pyrite produce sulphuric acid and soluble sulphate. Apart from these natural sources, sulphates can be introduced through the application of sulphatic soil conditioners. Climate has an important bearing on the accumulation of sulphate in the soil and groundwater. In humid regions the sulphate may be removed with the runoff, whereas in arid and semi-arid regions the sulphates may accumulate in the surface and in groundwater due to low precipitation and inadequate drainage. At concentration around 1000 ppm, it is laxative and

cathartic (U.S.E.P.A, 1971). Sulphate with sodium interferes with the normal functioning of the intestine. Sulphate is determined by using Perkin Elmer Lambda 25 UV-Visible Spectrophotometer. Sulphate ion is precipitated in the form of barium sulphate by adding barium chloride in hydrochloric acid medium. The concentration of sulphate can be determined from the absorbance of light by barium sulphate and then comparing it with a standard curve. Reagents used are NaCl, HCl, ethyl or isopropyl alcohol, glycerol, Barium chloride crystals, Na2SO4 and H_2SO4 to 100ml with distilled water.

Reagents used

1) Conditioning reagent - Mix 75 g of NaCl, 30 ml concentrated HC1, 100 ml 95% ethyl or isopropyl alcohol in 300 ml distilled water. Add 50 ml glycerol to this solution and mix thoroughly.

2) Barium chloride crystals.

Procedure

1) Take 100 ml of water in a conical flask and add 5 ml of conditioning reagent.

2) Stir the sample on a magnetic stirrer and during stirring; add a spoonful of $BaCl_2$ crystals. Stir for only 1 minute after addition $BaCl_2$ crystals.

3) Take the reading on a spectrophotometer at 420 nm exactly after 4 minutes. Find out the concentration of sulphate from the standard curve.

4) Prepare standard graph by diluting appropriate volumes of sulphate working solutions from 0 ppm to 25 ppm in the intervals of 5 ppm.

3.5.3 ANALYSIS OF TRACE ELEMENTS

Heavy metal is harmful to humans even at low concentraation due its trend to accumulate in the human body leading to bioaccumulation and bind to the cell membrane and distrupt all biological activities. Weathering of rocks and anthropogenic activities such as industrial, agricultural and fertilizer industries are the major sources of heavy metals in grounduwater samples.

Analysis of trace metals such as Zn, Cd, Ni, As, Cu, Co, Pb, Th, Mn, Al can be analysed by MP-AES instrument by changing the standards. The blank used in the determination of trace elements

is 5% HNO. The result and the desirable limits of trace elements under the specification of BIS and WHO drinking standards are given in the **Tables - 6**

3.6 DOMESTIC AND DRINKING WATER QUALITY STANDARDS

Water using in home for drinking purpose should be free from colour,odour,microorganisms and other harmful contents. However, they do not fall in the realm of chemical quality. Chemically, the water should preferably soft,low in dissolved solids and free from poisonous constituents.To assess the suitability of groundwater for drinking and public health purposes, the hydrochemical parameters of groundwater of the study area are compared with the guideline value recommended by Bureau of Indian Standards

DRINKING WATER QUALITY (AS PER BIS STANDARDS)

Chemical Nature	Highest Desirable	Maximum Permissible
Ph	6.5 – 8.5	No relaxation
TDS (ppm)	500	2000
Calcium (ppm)	75	200
Magnesium (ppm)	30	100
Chloride (ppm)	250	1000
Sulphate (ppm)	200	400
Nitrate (ppm)	45	100
Sodium (ppm)	-	200
Phosphate(ppm)	-	5

3.7 IRRIGATIONAL WATER QUALITY STANDARDS

3.7.1 SODIUM ADSORPTION RATIO (SAR)

Sodium concentration in groundwater is important since increase of sodium concentration in waters effect deterioration of the soil properties reducing permeability. Sodium adsorbed on the clay surface as substitute for calcium and magnesium may damage the soil structure making it compact and impervious. The processes leading to the cation exchange reactions in soil may be studied from sodium adsorption ratio (SAR) is expressed as

$$\mathrm{SAR} = \frac{Na^{+}}{\sqrt{\frac{1}{2}(Ca^{2+} + Mg^{2+})}}$$

Where, the concentrations are expressed in equivalents per million (epm). Classification of water with reference to SAR (Herman Bouwer,1978) is presented in the table

SAR	QUALITY
0-6	No problem
6-9	Increasing problem
>9	Severe problem

3.7.2 INTEGRATED EFFECTS OF EC AND SAR

US Salinity Laboratory Diagram based on SAR v/s specific conductance values, the two significant parameters of sodium and salinity hazards indicate usability for agricultural purposes. Twenty categories are demarcated in the diagram in terms salinity hazards and also in terms of sodium hazards, these are given below

SALINITY HAZARD

Conductivity Classification			Sodium Classification		
C1	Low salinity water	Good	S1	Low sodium water	Good
C2	Moderate salinity water	Good for soils of medium permeability for most plants.	S2	Medium sodium water	Good for coarse grained permeable soils.Unsatisfactory for highly clayey soils with low leaching.
C3	Medium to high salinity water	Satisfactory for plants having moderate salt tolerance, on soils of moderate permeability with leaching.	S3	High sodium water	Suitable only with good drainage, high leaching and organic matter addition. Some chemical additives in water may help if epm is low.
C4	High salinity water	Satisfactory for salt tolerant crops on soils of good permeability with special leaching.	S4	Very high sodium water	Unsatisfactory
C5	Excessive salinity water	Not fit for irrigation.	S5		

3.7.3 PERCENT SODIUM

In all natural waters percent sodium content is a parameter to assess it suitability for agricultural purposes (Wilcox, 1948). Sodium combining carbonate can lead to the formation of alkaline soils, while sodium combining with chloride form saline soils. Both these soils do not help growth of plants. A maximum of 60% sodium in groundwater is allowed for agricultural purposes (Ramakrishna, 1998)

Sodium ions have a tendency to be adsorbed on soil colloids. As the proportion of sodium to other cations in irrigation waters increases, sodium replaces the soil calcium and magnesium. This action, called Base Exchange, alkalises the soil, due to which granular and permeable soil are converted into sticky clays of low permeability which dry up into hard lumps and are difficult to plough. An excess of calcium and magnesium ions over sodium in irrigation waters inhibits Base Exchange so that the soil does not loose its permeability. Hence various ratios of sodium to calcium, magnesium have been used to depict the suitability of water for irrigation. Wilcox (1948) defined a sodium percentage in terms of epm of the common cations;

$$SSP = \frac{(Na + K) \times 100}{Ca + Mg + Na + K}$$

Where all ionic constituent are expressed in epm. Wilcox (1955) classified irrigation water into different categories based on the percent sodium.

Na%	**Quality**
0 - 20	Excellent
20 – 40	Good
40 – 60	Permissible
60 – 80	Doubtful
>80	Unsuitable

The chemical quality water samples were studied from percent sodium vs Specific conductance on the Wilcox diagram.

3.8 GIS Analysis

The thematic maps prepared are the spatial variation maps of PH,EC,TDS,Cations and Anions.

CHAPTER 4
RESULTS AND DISCUSSION

4.1 SUITABILITY OF DRINKING WATER

Hydro chemical data of groundwater is given in **Table- 2** and water chemistry in comparison with the drinking water standards are given in **Table-3**

4.1.1 pH

In the present study the pH value ranges from 3.73-7.36 with a mean value of 5.99. It is found that pH of most of the openwells are much lower than the highest desirable limit of pH recommended by BIS. It is found that water in the study area is more acidic in nature. Out of 19 samples 11 samples have more acidic trend which is not suitable for drinking.The low pH value can cause gastro intestinal disorders like hyperacidity, ulcers, stomach pain and burning sensation on users and also cause corrosion in pipes that will release toxic metals such as zinc, lead, cadmium etc. From the spatial variation map prepared in Arc GIS it shows that more acidic values for pH are seen in the Northeastern and southern part of the study area including places like Mullassery, Thonakkal, Chilambil and Murukumpuzha. The spatial variation map of Ph is given in the **Figure- 8**

4.1.2 ELECTRICAL CONDUCTIVITY (EC)

In the present study EC values range from 55.2-350.3 µs/cm with a mean of 201.54 µs/cm. The spatial variation map of Electrical Conductivity shows that the higher EC value is seen in the Southern, Southeastern, Northwestern and central parts of the study area which include places like Perunkuzhi, Edavilakam, Murukumpuzha and Thalamuk. EC is the lowest in the chilamb region on the northern part. More conductivity means there are a greater number of ions present and this will affect the purity of water. Spatial variation map of EC is given in the **Figure- 9**

4.1.3 Total Dissolved Solids(TDS)

In the study area TDS of open well varies from 36.72-231.3 ppm with a mean value of 125.26 ppm. The lowest value of TDS is 36.72 ppm which is obtained from chilambil((ow21) and

highest value 231.3 from Edavilakam(ow1). All the open well samples collected from the study falls under the highest desirable limit (500ppm) as per the specification of BIS. The spatial variation map of total dissolved solids shows that the higher TDS values are seen in the South south eastern, East south eastern,North western and central part of the study area like Perunkuzhi,Thonakkal, Edavilakam and Murukumpuzha. The spatial variation map of TDS is given in the **Figure- 10**

4.1.4 CHLORIDE

In the present study, Chloride concentration ranges from 9.83-95.26 ppm with a mean value of 37.47 ppm. According to BIS, the desirable limit of chloride in water is 250 ppm. It is clear that all the samples are within the highest desirable limit. The highest value of chloride can be seen in the southeastern part of the study area which is Edavilakam (ow1) and lowest value at the northern part chilambil (ow21).

4.1.5 SULPHATE

Sulphate value ranges from 0.08-68.93ppm with a mean of 11.94ppm. All the samples are under BIS highest desirable limit of sulphate (200ppm). Sulphate is having highest value in the southern part of the study area which is Thalamuk(ow8) and lowest value in the chilambil (ow21) area which is in the north.

4.1.6 SODIUM

In the present study the sodium concentration of water sample ranges from 13.56-106.1ppm with a mean of 35.81ppm. According to BIS,the maximum permissible limit of sodium is 200 ppm and the samples are within the limits. The highest value of sodium is reported from Edavilakam (ow 1) and lowest at chilambil(ow21). From the spatial variation map the highest concentration of iron can be detected in the southeast region which is Edavilakam and lowest concentration at north northwest and south south-southwest direction including Chilambil and Murukumpuzha. The spatial variation map of sodium is shown in the **Figure-11**

4.1.7 CALCIUM

In the present study, the calcium concentration on the water sample ranges from 0.59-19.7 ppm with a mean value of 5.37 ppm. The lower value 0.59ppm was obtained from Mullassery (ow17)

and highest value 19.7 from Thalamuk (ow8) . The highest desirable limit of calcium based on BIS standards is 75ppm and all the samples are within the desirable limit. From the spatial variation map of calcium, the higher value for calcium falls in the southern and northeastern part of the study area which is Thonakkal (ow24) and Thalamuk (ow8). The lowest limit is marked on the northwestern and continuous trend from the central part to east and west directions and the places are Mullassery, Thonakkal, Chilambil, Kannankarakonam, Shasthavattom, Perunkuzhi and Thannerkonam. The spatial variation map of calcium is shown in the **Figure-12.**

4.1.8 MAGNESIUM

In the present study the magnesium concentration in the water sample ranges from 3.5-14.69ppm with a mean value of 8.21ppm where highest value 14.69ppm is obtained from Perunkuzhi (ow30) and lowest value 3.5ppm from Murukumpuzha (ow10). The desirable limit of magnesium contentin drinking water recommented by BIS is 30 ppm. From the data all the samples in the study area fall within the highest desirable limit. The spatial variation map of magnesium shows that the higher concentration of magnesium is seen in the north western part of the study area which is perunkuzhi and lowest value fall from the central part and continuous trend to northwest and at northeast,south western part including areas such as Mullassery, Chilambil, Thonakkal, Edavilakam and Murukumpuzha. The spatial variation map of magnesium is shown in the **Figure-13.**

4.1.9 POTASSIUM

The potassium concentration in water sample from the study area ranges from 0.96-22.56ppm with a mean of 5.81ppm. The highest value 22.56ppm was obtained from Murukumpuzha (ow5) and lowest value 0.96ppm from Chilambil (ow20). The maximum permissible limit of potassium in drinking water based on BIS is 40ppm and all the values in the study area fall within the permissible limit. From the spatial variation map the highest values of potassium is marked on south eastern part of the study area which is Murukumpuzha(ow5) and lowest values are marked in the map with a continuous trend of potassium from central to east and western direction,at the wast north western part and south south western part which including places such as Mullassery, Chilambil, Kannankarakonam, Thonakkal, Perunkuzhi, Edanjimoola,Thannerkon, Edavilakam and Murukumpuzha. The spatial variation map of potassium is shown in the **Figure-14.**

4.1.10 IRON

In the present study the Iron concentration in the water sample ranges from 0.25-0.47ppm with a mean value of 0.28 ppm.The desirable limit of Iron content in drinking water recommented by BIS is 0.3 ppm. From the data OW 17, OW21, OW22 and OW5 in the study area falls higher than desirable limit. Beyond the highest desirable limit taste/appearance are affected and has adverse effects on domestic uses and water structures and promotes iron bacteria.The spatial variation map of iron shows that the higher concentration of iron is seen in the north north eastern part of the study area which is kannankarakonam and lowest value falls in the majority region of the study area in east,west,north and south directions including places like veiloor, Thonakkal, Chilambil, Knnankarakonam, Perunkuzhi, Edanjimoola, Thannerkonam, Edavilakam, Thalamuk, Murukumpuzha . The spatial variation map of Iron is shown in the **Figure-15**

Details of possible disorders due to the higher concentration of physical and chemical constituents are shown in the **Table - 4**

4.1.11 TRACE METALS

Trace metal data of the analysis of groundwater samples are given in the **Table- 5** and its range values with desirable limits are shown in **Table- 6**

4.1.11.1 ZINC

In the present study the zinc concentration in the water sample ranges from 0-0.81ppm where the highest value 0.81ppm is reported from Thonakkal (ow 24). The highest desirable limit of zinc based on BIS standard is 5ppm and all the samples are within the limit.

4.1.11.2 CADMIUM

In the present study the range of cadmium concentration is 0.51 – 0.7ppm. The highest desirable limit of cadmium concentration on the specification of BIS and WHO standard is 0.003ppm. All the samples are above the highest desirable limit, the highest value 0.7 ppm was obtained from Perunkuzhi (ow31) and lowest value 0.51 from Chilamb (ow20). Beyond this limit the water becomes toxic. Cadmium is a non-essential element in the human body, and this can severely affect kidney, a small concentration of cadmium can adversely cause changes in arteries and

cadmium reacts with enzymes and other biological compounds, cause a painful disease called Itai-itai (Mohan et al. 1998; WHO 2011).

4.1.11.3 LEAD

The lead concentration ranges from 0.02-0.04ppm. The highest desirable limit of lead concentration on the specification of BIS and WHO drinking water standard is 0.01ppm. All the water samples in the study area are above the highest desirable limit, the highest value 0.04 ppm is obtained from Mullassery (ow17), Chilamb (ow21), Kannankarakonam (ow 04), Perunkuzhi (ow25,26,29), Edanjimoola (ow27), Edavilakam (ow1) and the lowest value 0.02 is obtained from Murukumpuzha (ow10). Beyond the highest desirable limit, the water became toxic and has many health issues. It will adversely affect the kidney and can interfere with the production of red blood cells that carry oxygen to parts of the body.

4.1.11.4 NICKEL

The concentration of Nickel in the study area ranges from 0-0.02ppm where the highest value is obtained from Thonakkal (ow24). The highest desirable limit of nickel in drinking water under BIS standard is 0.02 and under WHO health-based guideline value is 0.07. The sample is at the highest desirable limit. Except ow24 all other open well is not having the presence of nickel.

4.2 SUITABILITY OF IRRIGATIONAL WATER OF THE STUDY AREA

Irrigational water quality standards (epm) are shown in the **Table-7.**

4.2.1 SODIUM ADSORPTION RATIO

Based on classification of water with reference to SAR (Herman Bouger,1978) out of 19 samples 18 samples are in no problem category and only one sample which is from Edavilakam (ow1) has been recognized with Increasing problem. It is shown in the table below

SAR Values	Quality	Number of samples
0-6	No problem	18
6-9	Increasing problem	1
>9	Severe problem	No sample

4.2.2 INTEGRATED EFFECT OF EC AND SAR

The calculated SAR values and analytical EC values are plotted in USSL Diagram (Fig 17) and the results are presented in the table below with respect to suitablilty of groundwater for irrigation purposes.

Quality	Number of samples
C1S1 Low salinity-Low sodium	13
C2S1 Moderate salinity and Low sodium	6

Out of 19 samples 13 samples belong to (C1S1) region which indicates low salinity hazard and low sodium hazard. 6 samples fall in (C2S1) that is the region of moderate salinity hazard and low sodium hazard.

4.2.3 PERCENTAGE SODIUM

Based on the Wilcox (1955) classification based on percent sodium the samples were classified and the results inferred from the classification is given below

Quality	Number of samples
Permissible	10
Doubtful	8
Unsuitable	1

Out of 19 samples 10 samples belong to permissible limit where they are suitable for agriculture and 8 samples belong to Doubtful category and one sample which is in Edavilakam (ow1) is unsuitable for irrigation purpose.

4.2.4 INTEGRATED EFFECT OF EC AND PERCENT SODIUM

The chemical quality of water samples were studied from percent sodium v/s specific conductance on the Wilcox diagram (Fig 18). The results inferred from the diagram are summarized in the table below.

Quality	Number of samples
Excellent to Good	18
Permissible to Doubtful	1

Out of 19 samples 18 samples belong to excellent to good category which conclude that most of the water in the area under study is suitable for agricultural purposes. The sample collected from Edavilakam (ow1) is found to be permissible to doubtful, which is found to be unsuitable for agricultural purposes.

4.3 Depth to Water Table Analysis (April-May 2023)

From depth to water table analysis the actual water level in the study area ranges from 0.3048 m bgl – 37.3989 m bgl with a mean of 10.329 m bgl . The study area contains both shallow and deep depth open wells. From the spatial variation map of depth to water table the highest water table depth can be seen in northwest, southeast and northeast portions and lower water tables on the old coastal stretches. Water table having high depths are seen in Edavilakam, Nellimood, Mullassery and veiloor, these areas are mosly having clay. Depth to water table map is shown in the **Figure- 16**

CHAPTER 5
SUMMARY AND CONCLUSION

Water is one of the essential factors to support all forms of plant and animal life (WHO 2011), and it is obtained from two sources such as surface water (lakes, rivers, streams) and groundwater (borewells, Tubewells, dug wells) (McMurry and Fay 2004; Mendie 2005). Previous studies (Aminiyan and Hosseinifard 2015; Huggenberger et al. 2013) show that groundwater sources are the primary sources for fresh drinking water in rural and urban areas. The availability of an adequate supply of freshwater is very important for a sustainable development in any region.

Any changes in the water body it may be physical, chemical, or biological properties that hurts living things is termed as water pollution (Ahluwalia and Sunitha 2009). The chemical composition of groundwater is controlled by many factors that include the composition of precipitation, anthropogenic activities, geologic structure and mineralogy of the watersheds, aquifers and geological processes within the aquifer (Ander L, Francesschi M and Pouchan p, Atteia o 2005). The contamination of groundwater is one of the critical environmental problems, among which heavy metal contamination of groundwater causes significant pollution (Marcovecchio et al.2007; Mamodu and Anyakora 2010).

The present work was carried out with an objective to analyse, understand and to assess the quality of groundwater resources for domestic and irrigation purposes in and around Mamam watershed area, Trivandrum district. A major part of the study area was close to Kadinamkulam kayal. The study started with geological field work in and around the watershed which includes Azhoor and Mangalapuram Gramapanchayat. The main geology of the area is identified as sedimentary including sandstone, sand, silt and clay with lignite. Water samples collected from the study area were analyzed systematically to determine various parameters such as pH , EC, TDS, major anions, cations and Trace metals. Anomalous pH values were observed in the study area which shows an acidic trend. The interaction of the laterite aquifer with the circulating groundwater may be the reason for the low pH value. The Fe in the laterite react with the Cl content of the circulating groundwater and produce compound called Ferric chloride which is acidic. Also, use of fertilizers for cultivation can be a cause for low pH, the two panchayat has

major cultivation of rice and rubber. For rubber, fertilizers are introduced by constructing pits in the ground and this can infiltrate it into the groundwater during monsoon. The presence of clay mine and concrete industry in Thonakkal and Shasthavattom can also give more acidic character to water. The acidity is due to the presence of Iron sulphide (pyrite) present in the deep clay horizon which gets exposed during mining, resulting in its oxidation, the end products being sulphate and hydrogen ions. Most parts of the study area have a low pH value which is not suitable for drinking water purposes. While in the study area near to estuary there is a decline in acidic trend due to the interaction with kadinamkulam lake.

Measured EC, TDS of openwells falls within the BIS limits. Analytical report of openwell water samples shows that except iron all other samples are within the highest desirable limit. The iron content is higher on the areas near to Kadinamkulam estuary, the retting of coconut husk has resulted in the formation of more contaminants in the water, the residential time of calcium and magnesium is higher in the estuary so there is a high contamination of iron in open wells. The colour change of water near estuary was due to the presence of organic matter associated with the presence of iron either as natural or as corrosion products. Another reason for the iron contamination may be due to the leaching of sewage from the house in the vicinity of Kadinamkulam estuary. Consumption of high concentration of iron in drinking water may lead to a liver disease called haermosiderosis(Rajgopal 1984).

Trace metal analysis of the study area revealed that Cadmium and Zinc are above the highest desirable limit of BIS and WHO standards of drinking water. Leena (2006) conducted a study on trace metals in the Kadinamkulam estuary and reported that the heavy metal accumulation in Kadinamkulam estuary comes from agricultural, industrial, and domestic wastewater entering this water body. The main sources of cadmium contamination in groundwater sources are plastic batteries, fertilizers, and industries. Cadmium even at low concentration adversely causes changes in arteries of the human kidney. Zinc contaminations are due to the mining activity, waste dump and wastewater release. The metal contamination in groundwater samples in the study area implied that source of these metals is due to anthropogenic activities such as wastewater from the Kadinamkulam estuary and leaching of solid waste from the residential area. The sandy aquifers in Gramapanchayath may cause the mobility of heavy metals to the

groundwater sources in the study area. The study conducted by Kumar et al.,2012 states that the sandy aquifer enhances the interaction between the groundwater source and surface water.

The suitability of water for agricultural purposes was studied by USSL and Wilcox diagram. With respect to percentage sodium factor all the samples except one lies within excellent to good, indicating suitability for agricultural purposes. Based on SAR value all the samples except one are having good quality.

The present study is a preliminary assessment of water quality in the study area. Lower pH, high Fe content and presence of Zinc and Cadmium contamination is a very serious issue. The presence of trace metals make the drinking water toxic; the low pH enhances the corrosion in pipes thereby releasing toxic metals. Mass awareness programme should organize at panchayat level to conserve the precious natural resource. The groundwater development in the study area is found to be more. The water level in the area is showing a falling trend especially in all seasons which is from public responses. Hence large-scale future groundwater development is restricted in the area. More stress should be given to watershed management. A community survey has to be conducted to find the health condition of people in highly contaminated areas. The study strongly recommends that groundwater quality monitoring shall be conducted in Azhoor and Mangalapuram Gramapanchayath in every six months and proper acid neutralizing mechanisms needs to be adopted to overcome the situation thereby ensuring safe supply of drinking water to the people.

REFERENCES

- Ahluwalia VK, Sunitha M. In: Environmental science, Ane Books Pvt. Ltd., New Delhi. 2009;351
- Anaida Ann Jacob (2021).An analysis of the Impact of climate change on Kerala's agriculture with special reference to Palakkad District, Vol. 9
- Ander L, Franceschi M, Pouchan P, Atteia O. Using geochemical data and modeling to enhance the understanding of ground water flow in regional deep aquifer, Aquitain Basin, south west of France. Journal of Hydrology. 2005;305: 40-62
- Ander L, Franceschi M, Pouchan P, Atteia O. Using geochemical data and modeling to enhance the understanding of ground water flow in regional deep aquifer, Aquitain Basin, south west of France. Journal of Hydrology. 2005;305: 40-62
- BIS (2012). Indian Standard: Drinking Water-Specification. Second Revision. Bureau of Indian Standards (BIS), New Delhi. 18p
- Bruce foote,R., 1883 .A note on the geology of south Travancore., Rec. GSI, v. XVI,Pt.1, pp. 20-35.
- Buchanan, H.F., 1807 . A journey from Madras through the countries of Mysore,Canara and Malabar.(London, 1807-3 Vols.) v. 2, pp. 436-437.
- Chacko, I.C 1922 . A sketch of the geology of Travancore., Rec. of Dept. of Geology, Travancore State, v. 1.
- Chandran, M., Shyam, T.A., Nandakumaran, P. and Shaji, E., 2014. Impact of clay mining on the ground water regime in parts of Thiruvananthapuram district, Kerala. MINERAL RESOURCES OF KERALA, p.126.
- Chattopadhyay S and Chatopadhyay M. (1995). Terrain analysis of Kerala- Concept, method and application. State Committee on Science, Technology and Environment, Government of Kerala, 79p.
- Chattopadhyay, S. 2017. Geomorphological Field Guide Book on Laterites and Backwaters of Kerala (Edited by Amal Kar). Indian Institute of Geomorphologists, Allahabad.

- Custodio E. 2000. The complex concept of groundwater over-exploitation. In Papeles Proyecto Aguas Subterr´aneas, A1:1–45. Santander, Spain: Fund. Marcelino Botin.
- CWRDM (1995). Water atlas of Kerala. Centre for Water Resources Development and Management (CWRDM), Kozhikhode. 82p.
- CWRDM (1998). Water Scenario of Kerala. In E.J. James (Ed.), Water related environmental problems of Kerala.Compendium on Water Resources Development and Management State Committee on Science, Technology and Environment, Kerala, 101pp
- Department of soil survey and soil conservation,Types of soils in kerala
- Environmental science, Ane Books Pvt. Ltd., New Delhi. 2009;351.3. WHO, Water Pollution Control - A Guide to the Use of Water Quality Management principles. Great Britain: WHO/UNEP; 1997
- Fariz G, Hatough-Bouran A. 1996. Jordan. In Water and Population Dynamics: Case Studies and Policy Implications, ed. A de Sherbnin, V Domka, pp. 105–35. Washington, DC: Am. Assoc. Agric. Sci
- GEC (2012). Dynamic Groundwater Resources of Kerala (2008-09). Report by Groundwater Estimation Committee (GEC), Kerala. Central Ground Water Board, Thiruvananthapuram. 269p
- GEC (2014). Dynamic Groundwater Resources of Kerala . Report by Groundwater Estimation Committee (GEC), Kerala. Central Ground Water Board, Thiruvananthapuram.
- Giordano, M., 2009. Global groundwater? Issues and solutions. Annual review of Environment and Resources, 34, pp.153-178.
- Guidelines for drinking-water quality: fourth edition incorporating the first addendum. Geneva: World Health Organization; 2017. Licence: CC BY-NC-SA 3.0 IGO
- Harikumar, P.S. (2016). Water quality management of Kerala- Issues, challenges and solutions. Report by Working Group on Environment, Kerala State Planning Board. p. 9.
- Hartmann, A., Weiler, M., Wagener, T., Lange, J., Kralik, M., Humer, F., Mizyed, N., Rimmer, A., Barberá, J.A., Andreo, B. and Butscher, C., 2013. Process-based karst modelling to relate hydrodynamic and hydrochemical characteristics to system properties. Hydrology and earth system sciences, 17(8), pp.3305-3321.

- Hosseinifard, S.J. and Mirzaei Aminiyan, M., 2015. Hydrochemical characterization of groundwater quality for drinking and agricultural purposes: a case study in Rafsanjan plain, Iran. Water Quality, Exposure and Health, 7, pp.531-544.
- IGRAC (2014). Groundwater in the sustainable development goals: Including groundwater in the draft goals. Position paper-Ten years of assessing the World's Groundwater (2003-13), International Groundwater Resources Assessment Centre (IGRAC), 7p
- Indian Standard drinking water — specification (second revision),2012 bureau of indian standards manak bhavan, 9 bahadur shah zafar marg new delhi 110002.
- King, W., 1875. Preliminary note of the gold fields of southwest Wynad, Madras Presidency, Rec. GSI., v. 8, Pt. 2, pp. 29-45.
- King, W., 1878. Note on the progress of the gold investigation in Wynad, Nilgiri district, Madras Presidency, Rec. GSI, v. 11, pp. 235-246.
- King, W., 1882 . General sketch of the Geology of Travancore State, Rec. GSI v. 15, Pt. 2, pp. 87-93.
- King, W., 1882. The Warkalli beds and reported associated deposits at Quilon in Travancore. Rec. GSI. V. 15, Pt. 2, pp. 93-102.
- Krishnan Nair, K., 1989. Quaternary geology and geomorphology in parts of Alleppey, Kottayam and Pathanmthitta districts, Kerala; Rec.Geol.Surv.India. v. 122, pt.5, pp-191-193.
- Kumar PJS, Delson PD, Babu PT.Appraisal of heavy metals in groundwater in Chennai City using a HPI model. Bull Environ Contam Toxicol. 2012;89:793–798
- Leena Grace, B., 2006. Trace metal concentration in the sediments of KadinankulamEstuary-south west coast of India. Poll, Res, 25(3), pp.613-616.
- Llamas MR. 1975. Non-economic motivations in ground water use: hydroschizophrenia. Ground Water 13:296–300.
- Mallikarjuna, C and Kapali, P.,1980. Studies on stratigraphy and regional assessment of clay potential of the Tertiary sediments in Trivandrum district
- Marcovecchio, J.E., Botté, S.E. and Freije, R.H., 2007. Heavy metals, major metals, trace elements. Handb Water Anal, 2, pp.275-311.
- Masillamani, E., 1914. Geology of Travancore State : Annual report of the State Geologist, Travancore State for 1913-1914., 36 p.

- McKay J. 2007. Groundwater as the Cinderella of water laws, policies and institutions in Australia. See Ref. 141, pp. 321–27
- McMurry J, Fay RC (2004) Hydrogen, oxygen and water. In: Hamann KP (ed) McMurry fay chemistry, 4th edn. Pearson Education, New Jersey, pp 575–599
- Momodu, M.A. and Anyakora, C.A., 2010. Heavy metal contamination of ground water: The Surulere case study. Res J Environ Earth Sci, 2(1), pp.39-43.
- Morris BL, Lawrence ARL, Chilton PJC, Adams B, Calow RC, Liknck BA. 2003. Groundwater and its susceptibility to degradation: a global assessment of the problem and options for management.Early Warn. Assess. Rep. Ser. RS. 03–3. UN Environ. Program., Nairobi, Kenya
- Nair, M.M.,1976. Conglomerate horizons in the precambrians of Tellicherry area and its significance. In Geology and Geomorphology of Kerala., Miscellaneous publication No.5.
- Planning Commission (2007). Groundwater management and ownership. Report of the Expert Group, Planning Commission, Government of India, 70p
- Rajan,N., Anilkumar,PS., 2005. Geology and mineral resources of the state of India Geological Survey Of India miscellaneous publication no. 30 part ix – kerala.
- Rajgopal (1984) Groundwater quality assessment for public policy in India. 1st Annual report. Department of Geography, IOWA University,
- Sasidharan, S. and Jaya, D.S., 2020. Quality Assessment of Groundwater in the Vicinity of Coir Retting Areas of Kadinamkulam Estuary, South India. Current Journal of Applied Science and Technology, 39(21), pp.118-128.
- Sasidharan, S. and Jaya, D.S., 2021. Metal contamination of groundwater sources in the environs of a tropical estuary in South India. Bulletin of Environmental Contamination and Toxicology, 106, pp.342-348.
- Sasikumar, V., Sampath, S., Vinayak, P.V.S.S.K. and Harikumar, R. (2007). Rainfall intensity characteristics at coastal and high altitude stations in Kerala. Journal of Earth System Science, Vol. 116 (5), pp. 451-463.
- Shah T, Molden D, Sakthivadivel R, Seckler D. 2000. The Global Groundwater Situation: Overview of Opportunities and Challenges. Colombo, Sri Lanka: Int. Water Manag. Inst.

- Shunmugam, K., 2022. Hydrogeochemistry and ionic ratios for identification of salinity sources in parts of Coromandel Coast of Pondicherry, South India. In Groundwater Contamination in Coastal Aquifers (pp. 245-260). Elsevier.
- Soman, K. (1997). Geology of Kerala. Geological Society of India, Bangalore, 280p
- Tiwari, V.M., Wahr, J. and Swenson, S. (2009). Dwindling groundwater resources in northern India from satellite gravity observations. Geophysical Research Letters, Vol. 36, L18401 (1-5).
- Todd K. Groundwater hydrology. John Wiley & Sons, New York, Chichester;1980.
- Vidyadharan K.T and Sukumaran, P.V., 1978. Geological mapping and mineral resources of parts of South Wynad and calicut distt.,Ernad taluk, malappuram distt. Unpub. GSI report
- WHO (2011). Guidelines for drinkingwater quality, Fourth Edn, ISBN 9789241548154.
- World Bank (2012). India Groundwater: A valuable but diminishing resource.

IDENTIFICATION AND CHARACTERIZATION OF MICROPLASTICS IN THE SEDIMENTS IN THE BHARATHAPUZHA RIVER FROM ITS SOURCE TO SINK

Dissertation submitted to Christ College (Autonomous), Irinjalakuda, Kerala,

University of Calicut in partial fulfillment of the degree of

Master of Science in Applied Geology

By,

ARJUN PRADEEP M

Reg. No: CCAVMAG006

2021-2023

DEPARTMENT OF GEOLOGY AND ENVIRONMENTAL SCIENCE

CHRIST COLLEGE (AUTONOMOUS), IRINJALAKUDA, KERALA, 680125

(Affiliated to University of Calicut and re-accredited with by NAAC with A++ grade)

SEPTEMBER 2023

DEPARTMENT OF GEOLOGY AND ENVIRONMENTAL SCIENCE

CHRIST COLLEGE (AUTONOMOUS) IRINJALAKUDA

CERTIFICATE

Certified that the dissertation work entitled "IDENTIFICATION AND CHARACTERIZATION OF MICROPLASTICS IN THE SEDIMENTS IN THE BHARATHAPUZHA RIVER FROM ITS SOURCE TO SINK" is a bonafide record of work done by Mr. ARJUN PRADEEP M of fourth semester M.Sc. Applied Geology in this college during 2022-23.

Dr. Anto Francis K

Co-Ordinator (Geology Self-financing)

Christ College (Autonomous) Irinjalakuda

Place: Irinjalakuda

Date: ……

External Examiners;

1…….

2…….

CERTIFICATE

This is to certify that the dissertation entitled – **IDENTIFICATION AND CHARACTERIZATION OF MICROPLASTICS IN THE SEDIMENTS IN THE BHARATHAPUZHA RIVER FROM ITS SOURCE TO SINK**, is a Bonafide record of work done by Mr. Arjun Pradeep M (Reg. No. CCAVMAG006), MSc Applied Geology, Christ College (Autonomous) Irinjalakuda, under our guidance in partial fulfillment of requirements for the degree of Master of Science in Applied Geology during the year 2021-2023.

Dr. V. Neetha

Assistant Professor

Department of Zoology

Sacred Heart College Thrissur

Kerala 680307

Dr. Linto Alappat

Dean of Research and Development of TLC

Department of Geology and Env. science

Christ College (Autonomous) Irinjalakuda

Kerala- 680125

DECLARATION

I hereby declare that this dissertation work – **IDENTIFICATION OF CHARACTERIZATION OF MICROPLASTICS IN THE SEDIMENTS IN THE BHARATHAPUZHA RIVER FROM ITS SOURCE TO SINK** is a work done by me. No part of the report is reproduced from other resources. All information included from other sources has been duly acknowledged. I maintain that if any part of the report is found to be plagiarized, I shall take the full responsibility for it.

Place: Irinjalakuda ARJUN PRADEEP M

Date: Reg.NO.CCAVMAG006

ACKNOWLEDGEMENT

This report is an official documentation of dissertation work carried out in Bharathapuzha River basin, Kerala. This report would not have been possible without guidance, encouragement and support of many well-wishers and my colleagues who helped me in many ways.

Firstly, I record my deep sense of gratitude and indebtedness to my guide **Dr. Linto Alappat, Dean of Research and Development of TLC (former HOD), Christ College (Autonomous) Irinjalakuda**, for developing the project's framework and providing regular support and supervision throughout the duration of the course of the study.

Next, I would like to thank **Tharun R, Head, Department of Geology and Environmental science, Christ College (Autonomous) Irinjalakuda**, for providing all the facilities and help available from the department.

I would like to express my gratitude to **Dr. V. Neetha, Assistant Professor, Department of Zoology, Sacred Heart College, Chalakudy,** for the guidance and supervision in the completion of the dissertation.

Next, I would like to thank **Dr. Sijinkumar and Dr. Sandeep. K, Assistant Professors at Central university of Kerala**, for giving me permission to carry out my work in this institution.

I am deeply thankful to **Dr. Anto Francis.K, the Co-ordinator of M.Sc. Applied Geology**, and other faculty members of Department of Geology and Environmental Science, Christ College (Autonomous), Irinjalakuda, for their support, guidance and love.

I would like to extend my thanks to Mr. **Ayyappadas C.S.** for the continuous support provided for the completion of the dissertation. Also, I'd like to take this opportunity to thank all of my classmates and friends who supported me in completing this dissertation work, whether directly or indirectly. I am grateful to the entire Christ College family for their love, support, and guidance. I also express my gratitude to my parents and family members for their unwavering support and prayers throughout my life. Above all, I express my gratitude to God, the Almighty, for his divine generosity and blessings showered upon me.

ARJUN PRADEEP M

ABSTRACT

This investigation mainly focused on the identification and quantification of microplastics in the surface sediments of Bharathapuzha river, Kerala. Various chemical procedures were done in the methodology of the work. Microplastics were detected in all the samples taken from the study area from the source to the sink of the river. The abundance of microplastics was increasing and decreasing from the sink and it was not in a definite order. The maximum number of microplastics was obtained from sample BP S13 and BP S22, which were taken from Ottappalam and Ponnani beach respectively and the least amount of microplastics was from the sample BP S1 and BP S2, which where taken from the source of the river. Microscopic examination showed that a type of microplastic called fibres was found in abundance in total microplastic count obtained. The black coloured microplastics was the abundant coloured microplastics. The increase in the percentage of coloured microplastics in the river increases the probability of damage to the aquatic life. Microplastics can cause serious effect to aquatic organism when they ingest it. The abundance of microplastics in the study area point towards different sources of contaminations like anthropogenic activities like fishing and waste disposal, and due to the hydrogeomorphology of the river like sediment type, flow velocity and discharge of the river.

CONTENT

LIST OF TABLES

LIST OF FIGURES

CHAPTER 1

INTRODUCTION

1.1 Microplastics

Microplastics (MPs) are small sized plastic particles which are formed due to commercial product development and due to the breaking down of bigger plastic materials. MPs are generally of the size less than 5mm (0.2 inch). They are present in a variety of products, from cosmetics to synthetic clothing to plastic bags and bottles. Many of these products readily enter the environment along with waste water. The proportion of species able to consume MPs rises as their quantity increases and as fragment size decreases (Hale et al., 2020).

Microplastics are seen in almost every place including oceans, river, land, and also in plants and animals. In oceans, microplastics mainly come from marine plastic litter break down, run-off from plumbing, leakage from production facilities and other sources. The amount of microplastics in some oceanic compartments is predicted to double by 2030 (Hale, et al., 2020). On land, microplastics come from inappropriate plastic disposal in soil, waste materials from industries etc. These microplastics mixed in soil and ocean will be ingested along with food by living organisms and as a result, they enter into their bodies. Due to their abundance and persistent nature, microplastics pose serious hazards to terrestrial ecosystems. Microplastics unavoidably come into contact with higher plants, an essential component of the terrestrial ecosystem. They are absorbed by plants from the soil along with water and nutrients (Li et al., 2022).

1.1.1 Impacts of MPs

MPs can cause toxic effects in the living organisms like reduced food intake, suffocation, behavioral changes and genetic alteration. It enters an organism’s body, not only through the food chain but also by inhalation from air, consumption of water, and also absorbed through skin. Microplastics also have the ability to concentrate and adsorb harmful substances from the environment. These substances may include endocrine disruptors, heavy metals, and persistent organic pollutants (POPs). These hazardous compounds may migrate into marine species' tissues along with the ingested MPs, thereby impairing their physiological and reproductive functions. On the seafloor, microplastics can accumulate and change the structure and content

of marine environments. They can suffocate benthic organisms, impede sedimentary processes, and alter the marine life's access to food and shelter. MPs can also harbor dangerous diseases and bacteria, posing new dangers to the ecosystem.

Microplastics consist of carbon and hydrogen atoms bound together in polymer chains. Other chemicals, such as phthalates, polybrominated diphenyl ethers (PBDEs), and tetrabromobisphenol A (TBBPA), are typically also present in microplastics. Many of these chemical additives leach out of the plastics after entering the environment. Despite having a wide range of chemical components, polymers including polyethylene (PE), polypropylene (PP), and polyethylene terephthalate (PET) make up the majority of microplastics. While PP is utilized in food containers and textiles, PE is present in products like shopping bags and packaging materials. PET is frequently used in polyester fabrics and drink bottles. Ethylene for PE, propylene for PP, and terephthalate and ethylene glycol for PET, are repeating units of specific monomers. These monomers are combined and arranged in a certain way to give microplastics their distinct characteristics, which also contribute to their persistence and possible environmental effects. Common polymer types include lightweight polymers and those produced in large amounts, such as polyethylene, polypropylene, and polystyrene (Shim et al., 2018).

1.1.2 Sources of MPs

There are different sources from which microplastics are formed. Some of the sources are:

- Fragmentation of larger plastic items: mechanical forces like wave action can cause large plastic goods like bottles, bags, and packaging materials to break down. This fragmentation process results in the production of MPs.
- Microbeads: Tiny plastic particles known as microbeads are used in body washes, toothpaste, and other personal care and cosmetic products. These microbeads can reach water bodies after passing through wastewater treatment facilities and are frequently made to wash down the sink.
- Shedding of Synthetic Fibers: When synthetic textiles, such as polyester, nylon, and acrylic, are washed, microfibers fall off. As they travel via wastewater systems, these microfibers may eventually end up in rivers, lakes, and oceans.
- Road dust and tire wear: Friction between a vehicle's tires and the road surface causes its wear over time. Microplastic particles are created by wear and tear and either become airborne or are washed into bodies of water by rain.

- Industrial Processes: A number of industrial procedures, including the production, processing, and recycling of plastic, have the potential to release microplastics into the environment. For instance, plastic pellets that are used as raw materials to make plastic products may become lost during handling or shipping and wind up in bodies of water.
- Agricultural Practices: Using plastic mulch films for farming or applying fertilizers based on plastic might cause microplastics to be released into the soil and water systems.
- Paints & Coatings: When paints, coatings, and other surface treatments with plastic components degrade, tiny plastic particles may be produced and released into the environment.
- Atmospheric deposition: MPs can also travel through the air and end up as atmospheric deposition, which can occur in both terrestrial and aquatic ecosystems. They may come from a number of places, such as airborne plastic waste, urban runoff, and atmospheric fallout of microplastics from industrial pollutants.

1.1.3 Types of MPs

MPs are mainly classified into two types. Primary microplastics and secondary microplastics. Primary microplastics are tiny particles designed for commercial use, such as cosmetics, as well as microfibers shed from clothing and other textiles, such as fishing nets. Nurdles, which are little pellets of plastic resin, are another source of primary microplastics. These pellets are used as the building blocks for making plastic, and they may end up in water bodies as a result of unintentional spills during transit, poor production site handling, or insufficient waste management systems. Primary microplastics enter the environment directly through any of various channels, for example, product use (e.g., personal care products being washed into wastewater systems from households), unintentional loss from spills during manufacturing or transport, or abrasion during washing (e.g., laundering of clothing made with synthetic textiles).

Secondary MPs are particles that result from the breakdown of larger plastic items. Sources of secondary MPs include water and soda bottles, fishing nets, plastic bags, microwave containers, teabags and tire wear. This breakdown is caused by exposure to environmental factors, which typically happens when larger plastics undergo weathering, through exposure to wave action, wind abrasion, and ultraviolet radiation from sunlight. Due to weathering, wind erosion and the movement of soil and sediment, plastic debris that has been dumped on land

may also deteriorate and fragment. These processes reduce plastic materials into secondary MPs and other smaller particles, which can then be carried to water bodies by the wind, runoff, or other causes. Secondary microplastics can also be produced during plastic recycling procedures including shredding and grinding. When plastic garbage is mechanically broken down for recycling, these microplastics may be discharged.

Methods to reduce MPs include regulations, better waste management, and responsible plastic usage to lower the amount of microplastics released into the environment and address their origins. As a part of this venture, microbeads in personal care products must be banned, precautions must be taken to prevent plastic pellet spills during handling and transportation, sustainable alternatives to single-use plastics must be promoted, recycling systems must be improved to prevent plastic contamination, and public awareness of the dangers of microplastics and the value of proper waste disposal must be raised. By putting these preventive measures in place, we can lessen the amount of microplastics produced and released into the environment, safeguarding ecosystems and lowering the dangers they bring to animals and public health. Implementing strategies to reduce plastic waste, improve recycling practices, raise awareness, and develop innovative technologies are crucial steps toward mitigating the impacts of secondary microplastics and promoting a more sustainable future.

1.2 Aim and objective

The main aim of the study is to determine the presence, amount and forms of microplastics in the source to sink of the Bharathapuzha river basin.

The following objectives were to be completed during this study. They are:

- To determine the presence of microplastics in the source to sink in Bharathapuzha river basin.
- To identify the most polluted area in the Bharathapuzha river basin.
- To determine the different forms of microplastics like fibers, fragments etc. in the river basin.

CHAPTER 2

STUDY AREA

2.1 Location

There are 41 west flowing rivers in Kerala and Bharathapuzha is one of them. Bharathapuzha is also called as Nila. It is the second longest river present in Kerala after Periyar. It has a length of 209 km (Soman, 2002). It lies between North Latitudes of 10°30' to 11°00' and east longitude of 76°00' to 77°30'. This river covers an area of 6186 km² and two thirds of its basin lies in state Kerala and the remaining lies in Tamil Nadu. The river rises in the Anamalai hills in Western Ghats at an altitude of 1100m above the mean sea level. Bharathapuzha flows through Malappuram, Thrissur and Palakkad districts of Kerala and through Coimbatore district of Tamil Nadu, before entering into the Arabian sea. The four major tributaries present are Kalpathypuzha, Gayathripuzha, Thoothapuzha, and Chitturpuzha.

There are 13 reservoirs along the course of the river and out of it, the largest one is the Malampuzha dam. Some of the other dam includes Walayar, Pothundi, Meenkara, Chulliyad etc. Water from all these reservoirs are mainly used for irrigational purposes.

Bharathapuzha river main stream is a seventh order stream and basin consist of four sub-basins (Nikhil Raj and Azeez, 2012). The river has a dendritic pattern which indicates homogenous and horizontal underlying strata. During the monsoons, the river will be fully filled and will be navigable for long lengths, but in hot and dry climatic conditions, the river bed will be nearly dry (Soman, 2002). The river consists of well devoloped fluvial terrace and floodplain of recent origin and major rock types in the area include charnockite, gneiss and schists of Archean age and also include Tertiary formation, sub-recent laterites and recent alluvium.

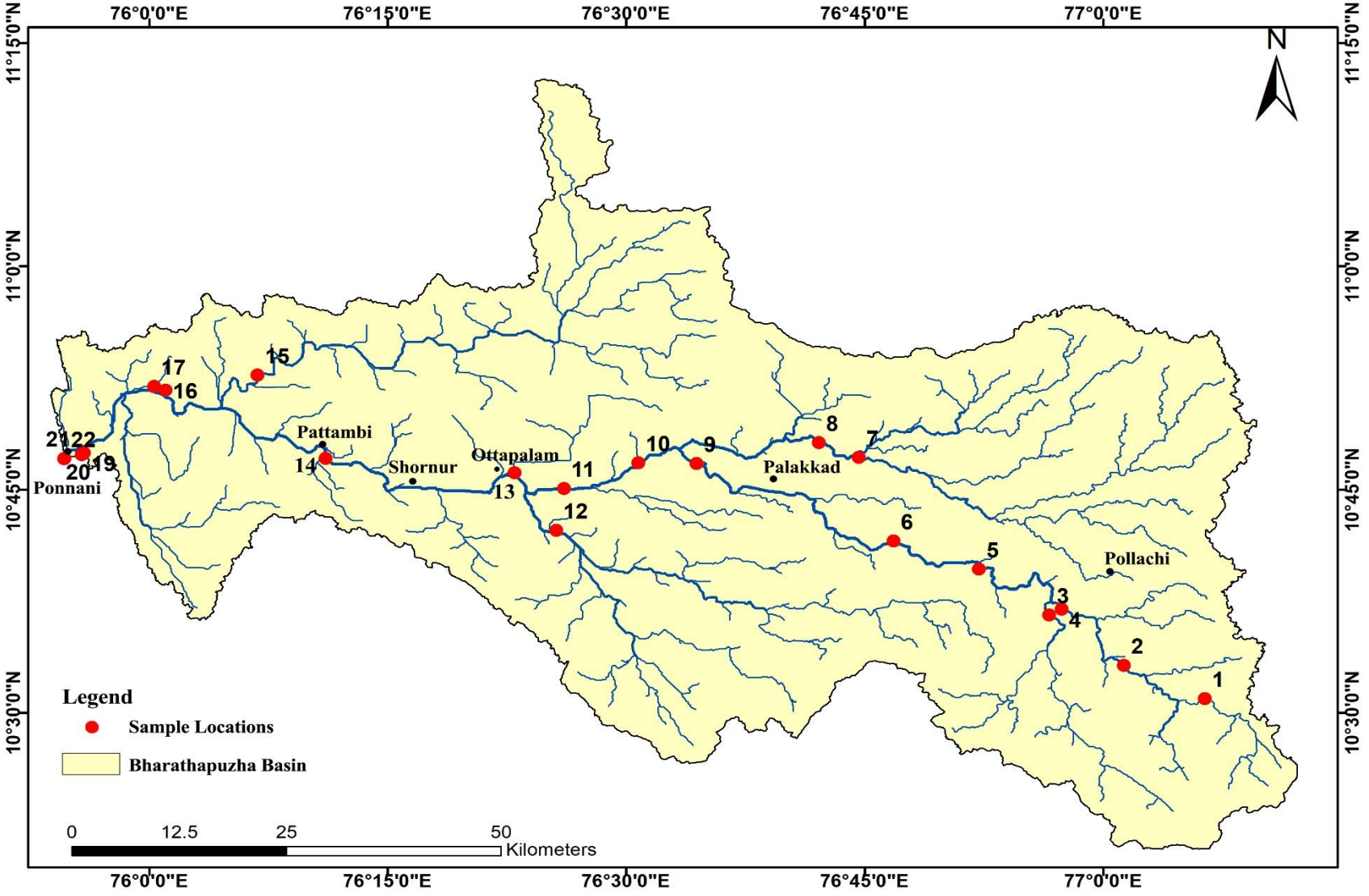

Fig 1. Map showing the locations of samples taken from the Bharathapuzha river basin.

2.2 Climate

The study area experiences tropical climate and faces two types of seasons per year; a wet season ranging from June to February and a hot season ranging from March to May. Rainfall in this area is mainly from Northwest and Southwest monsoons. Out of these, the major contribution of rainfall is from Southwest monsoon and it begins in the first week of June.

The temperature rises in the months of February and reaches a maximum during the month of March and April. From March onwards, relative humidity rises to reach a maximum of 92% in July, whereas least relative humidity has been recorded in the month of January. The minimum monthly temperature in the Bharathapuzha river basin is recorded as an increase of 0.012°Cper year from 1901 to 2013 (George, 2020). The wind direction in Bharathapuzha is westwards and maximum speed of wind is normally associated with the monsoons (Das, 1986).

The Bharathapuzha basin experiences a non-uniform climate across its whole area. This is due to the presence of Palghat Gap. Palghat Gap is a low mountain pass in the Western Ghats between Coimbatore in Tamil Nadu and Palakkad in Kerala. It has an average elevation of 140m. The pass is located between the Nilgiri Hills to the north and Anaimalai Hills to the south. Due to this gap, the basin's upstream region experiences a semi-arid climate while the downstream region experiences intense rainfall (Reddy et al., 2021).

2.3 Physiography

The primary physiographic divisions of Kerala are well represented in Bharathapuzha basin, that is, the coastal plains (0-10m), lowlands (10-20m), midlands (300-600m), and the highlands (600-1800m). The Bharathapuzha river basin is bordered on the north by the Western Ghats and in the south by Anamalai hill ranges (Brijesh, 2006).

2.4 Geology of the area

The Bharathapuzha basin is a part of Pre-Cambrian shield of Indian peninsula. It is underlain dominantly by Archean crystalline rocks of granulite and amphibolite facies. Younger formation consists of laterite and alluvium. The region is characterized by diverse geological formations. This area is composed of several types of rocks, including ancient Pre-Cambrian rocks, such as gneisses, schists and granites. These rocks are estimated to be around 2500

million years old and form the foundation of the basin. Rocks like charnockite, pyroxene granulites and migmatites are found in the major parts of the basin. Some part of the basin consists of quartzo-feldspathic gneiss, biotite-hornblende gneiss, pink granite and quartz syenite. The river itself has eroded through these ancient rocks, creating a variety of landforms within the basin. The upper reaches of the Bharathapuzha Basin are marked by steep valleys and gorges as the river descends from the mountainous terrain of the Western Ghats. As it progresses towards the lower reaches, the river meanders through broader valleys, forming floodplains and deltas.

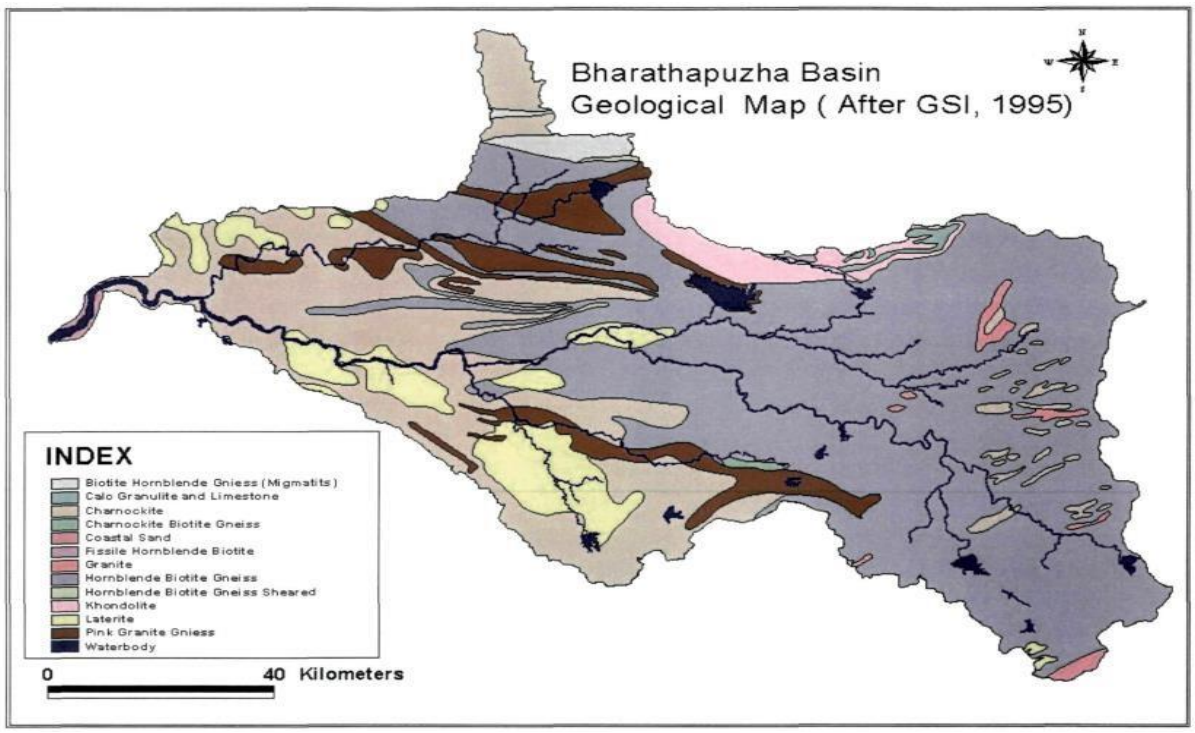

Fig 2. Geological map of Bharathapuzha river basin after Brijesh, 2006.

The west region of the basin and also the Palghat Gap is covered by hornblende-biotite gneiss. Acidic rock intrusions like norite, granulite pyroxene and basic rocks like gabbro, dolerite etc. are found in many places. The western part of Ottapalam is mainly composed of laterite. In Walayar, crystalline limestones are found as thin patches. These rocks had been affected with differential weathering and has developed a grooved appearance along the foliations. Also, thick alluvial soil cover is developed in areas like Kuttipuram, Thiruvegapuram etc.

A three-fold division of Bharathapuzha basin has been proposed by Rao and Sreenivasan (1980) They are:

i. The area south of Palghat gap dominated by charnockite and granite gneisses.
ii. The area north of Palghat gap with khondalite suite of rocks.
iii. The Palghat gap underlain mainly by hornblende-biotite gneiss.

The geology of the Bharathapuzha Basin has a direct impact on the region's hydrology, soil composition, and vegetation patterns. The river carries significant amounts of sediment, including sand, silt, and clay, which contribute to the fertile soils in the basin. The basin supports a variety of ecosystems, including forests, wetlands, and agricultural lands, which are highly dependent on the river and its geological features. The basin is also influenced by the coastal plains of Kerala. The river eventually meets the Arabian Sea, and the coastal areas are characterized by estuaries, backwaters, and tidal zones. These coastal regions are rich in sediment deposition and play a significant role in the overall geomorphology of the basin.

2.4.1 Desamangalam fault

At the Desamangalam quarry, a fault zone has been located (Rajendran, C. P., Rajendran, K., 1996). It is discovered that the course of this fracture zone corresponds to the isoseismic elongation of the earthquake in 1994. It is a fault zone with three parallel fractures that is 5.5–6 metres broad. Fracture F1 does not exhibit much displacement despite passing through a region with a high concentration of biotite. According to Rao et al. (2002), the fracture F2 exhibits a slip plane with audible signs of movement. The grooves and striations of the slip plane's long axis show an oblique reverse sensation of movement.

Crushed rocks and voids are also present along the contact surface, some of which include secondary minerals. A 6 cm thick gouge zone has also formed at the fault contact. This zone contains two sets of striations that stand for oblique and perfect reverse movement, respectively. The F3 fracture parallels the F2 fracture and occurs at a higher level. The striations seen within this fracture indicate a northward oblique reversal movement (Rao et al., 2002).

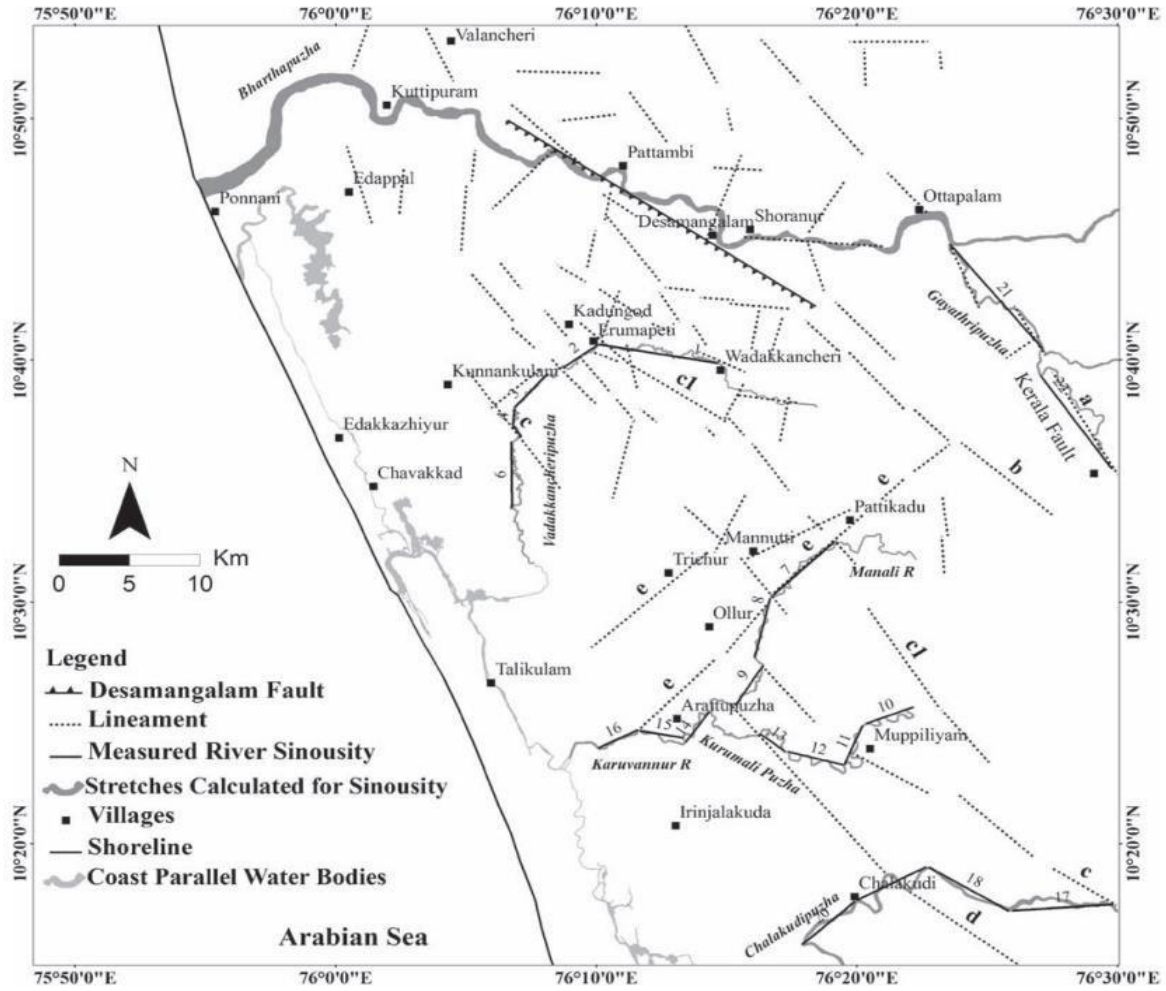

Fig 3. Map representing Desamangalam fault (Singh et al., 2016)

2.4.2 Idamalayar lineament

It is a NW-SE lineament located in the eastern part of Bharathapuzha river. It influences the Bharathapuzha river course at Ottapalam and it follows the river Gayathripuzha (Singh, et al., 2016). Dolerite dykes are observed in southeast Wadakkancherry along this lineament which is dated as 76 Ma (Subramaniam, 1976). It suggests that this lineament may be associated with the initial stages of Deccan volcanism.

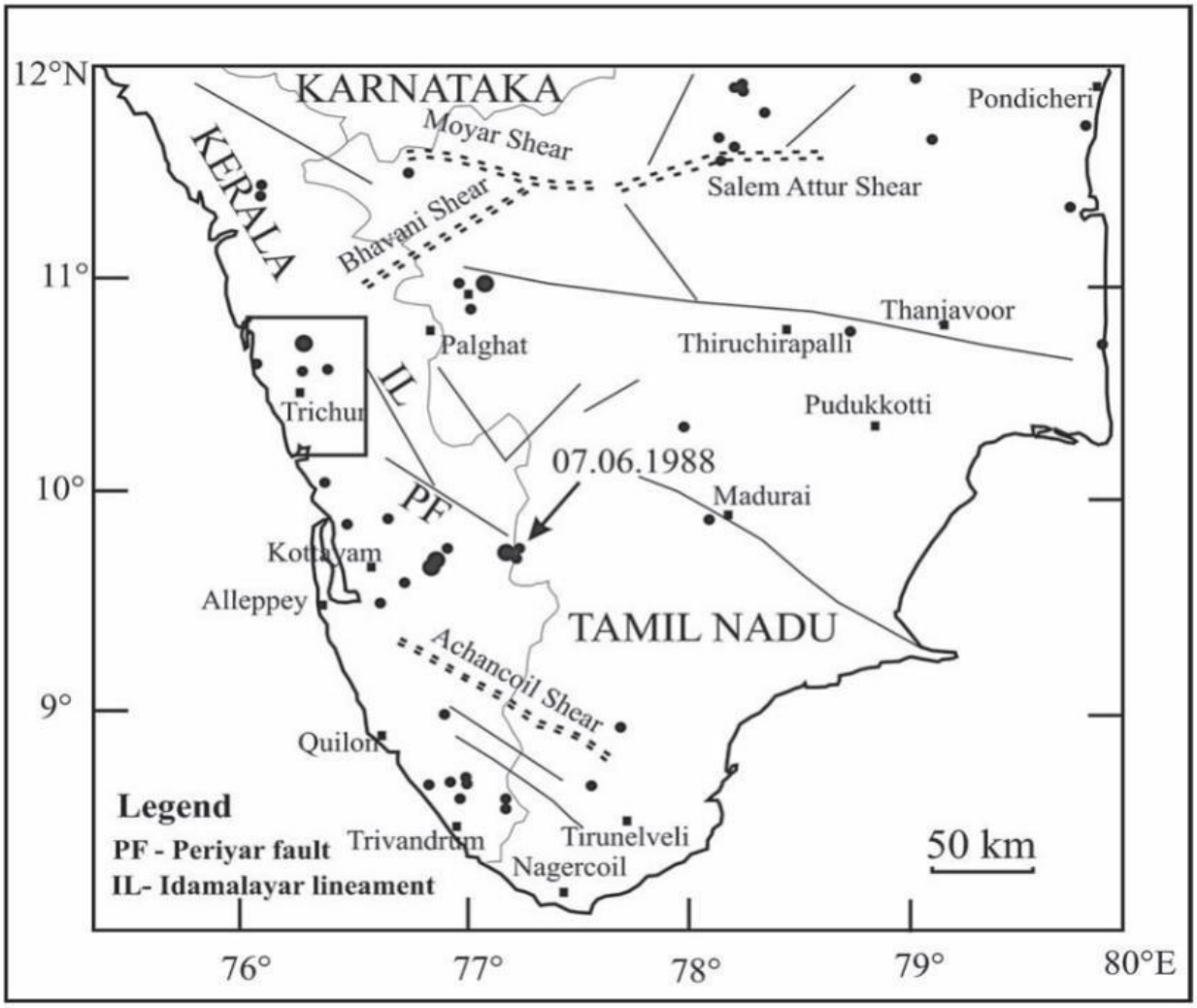

Fig 4. Map representing Idamalayar lineament (Singh et al., 2016)

CHAPTER 3

REVIEW OF LITERATURE

This chapter describes review of previous literatures about microplastics and their implications. Various studies of Bharathapuzha river basin as well as literatures about textural characteristics of sediments are also discussed in this chapter.

3.1 Studies on analysis of Microplastics

Khaleel et al., 2022, focused on the occurrence and distribution of MPs present in the beach sediments of St. Mary's Island, a geological heritage site located in the south-eastern part of the Arabian sea. It was found that microplastic densities were determined for each of the eight sites surveyed along SMI.

Following the 2018 floods, Nikhil et al., 2023 conducted research on the spatial and temporal distribution of microplastics along Kerala's nearshore surface waters. Results indicated a seven-fold increase in its mean concentration post deluge and average abundance was highest during pre-monsoon. They also show high ecological risks due to the presence of PVC and PU. Surface morphology of microplastics indicates severe weathering.

Cole et al., 2011, discussed about the nomenclature and source of Microplastics, route by which microplastics enter the marine environment, evaluated the method by which microplastic are detected in the marine environment and also about the environmental impacts by microplastics. He concluded that MPs are ubiquitous within the marine environment. It can adsorb waterborne contaminants or leach toxic additives. His study revealed that MPs can enter the food web.

In a study by Andrady, 2017 on the relevance of selected characteristics of plastics that composes the microplastics, their role as a pollutant with potentially serious ecological impact was assessed. Fragmentation leading to secondary MPs was also discussed underlining the likelihood of a surface ablation mechanism that can lead to preferential formation of smaller sized microplastics. From this study, it is found that average molecular weight, structural chemistry and crystallinity can influence the fate of MPs in the ocean. He further mentioned that, fragmentation of the plastics in the field can also occur via surface ablation generating large number of daughter MPs.

In a study by Podbielska & Szpyrka, 2023, the effects and impacts of MPs and co-existing pollutants on algal population were observed. It showed that plastic of a smaller size and with a positive surface charge have a higher toxic effect on algae. MP's toxicity to algae strongly depends on their concentration and becomes more severe as its level increases. Effect of pollutant MP complexes are more often found to be antagonistic than synergetic, in consequence of toxic substance adsorption on the MPs surface and their lower bioavailability to algae. Also, longer exposure of algae to the MPs lead to their adaptation and resistance.

Devi et al., 2020, studied about the ingestion of microplastics by the alien fish, Pirapitinga that escaped Vembanad Lake, the largest brackish water lake in the southwest coast of India, from the aquaculture system during the 2018 flooding. 123 fishes were analyzed and microplastics were separated from the gut of 32 of these fishes. The attained microplastics include fibers, foam and fragments. The presence of MPs in the gut content of alien fish could reflect the increase in microplastic pollution in the estuaries and backwaters along the southwest coast of India.

Boots et al., 2019, in their study of the effect of different types of microplastics on plant growth. Conventional high-density polyethylene (HDPE) and microplastic clothing fibers were added to soil containing the endogenic rosy-tipped earthworm and planted with perennial ryegrass to assess the biophysical soil response in a mesocosm experiment. The result was, when exposed to fibers or microplastics, fewer seeds germinated. There was also a reduction in shoot height. The biomass of rosy-tipped earthworm exposed to HDPE was significantly reduced compared to controlled samples. Also, there was a decrease in soil ph. Also, the soil stability was potentially altered. This study provided evidence that microplastic like HDPE and PLA can affect the development of perennial ryegrass, health of rosy-tipped earthworm and also impacts on soil ecosystem functioning.

Dowarah & Devipriya, 2019, in their research work, they studied about the microplastic prevalence in the beaches of Puducherry and also its correlation with fishing and tourism was also included. They monitored about 6 beaches of Puducherry coast was the presence of MPs. They reported 13 polymers (PP, LDPE, HDPE, PS, PVC etc.) and two polymer dyes were identified with Raman spectroscopy and also, a strict correlation was found between fishing activity and microplastic abundance.

A study by Gopinath et al., 2020, was the first to analyze the microplastic contamination in red hill lake, Chennai. Of the 32-sediment sample and 6 water samples collected the most abundant

microplastics are fibers, fragments, pellets and films. The common types of microplastics were found to be high-density polyethylene, low-density polyethylene, polypropylene, and polystyrene.

Veerasingam et al., 2016, studied about the source, distribution and age of microplastic pellets in sediments along Chennai coast before and after Chennai floods which were characterized using a stereoscopic microscope and FTIR spectroscopy methods. The result obtained was that white coloured PP and PE (Polyethylene and Polypropylene) were dominant in all sampling locations. Also, three-fold increase in amount of microplastic was noted after the Chennai floods. The microplastic pellets found in Chennai coasts was found to be land as well as ocean based.

S. K. & Varghese, 2020, analysed the microplastic pollution in Nattika beach, Kerala and also devised an environmental forensic investigation strategy for identifying the pathways and sources of microplastics. The microplastics collected from the location was subjected to analysis in FTIR and SEM for characterisation. The result of the forensic investigation indicated that the pollutants were from the nearby area. Fibrous microplastics, found from this location was sourced from fishing nets, which was used for fishing in nearby shore area.

Maneesh Kumar et al., 2023 quantified the MPs in the surface waters of Chalakudy river. The results showed the presence of MPs in the river water. Maximum amount was found in site near Chalakudy temple and the least was found in site near Muthakkunnam bridge. MP of size less than 20 nanometre and an abundance of coloured plastics were also found in their study area which caused damage to aquatic life. Also, the Raman spectrum analysis conducted in the samples showed the abundance of low-density Polyethylene as the dominant plastic present here.

Sundar et al., 2021 conducted a study on the abundance of microplastic in the southernmost coast of India, Kanyakumari. Sediments were collected from harbours, residential beaches, tourist beaches and also from undisturbed coastal areas. Dry sediments were evaluated and microplastic presence was identified in eight different stations. Also, all of the found MPs were secondary microplastics and most of them were transparent. It was concluded that the tourist beaches had the greatest number of MPs followed by harbours and the least amount was found in the undisturbed beaches. From these results it was understood that this microplastic presence is due to anthropogenic activities.

Patel et al., 2020 studied about the microplastic presence and abundance in Sabarmati river in Gujarat, India. In this study, the samples were collected from four different locations through the stretch of Sabarmati river. Gravimetric analysis and SEM analysis was done to identify the presence of MPs as well as for studying the morphology of different MPs. From the study, it was observed that the abundance of MPs was increasing from upstream to downstream of Ahmedabad city.

Sarkar et al., 2020, sediments at the lower stretch of river Ganga was studied for finding the distribution of meso and microplastics. Sediments was collected from seven different locations, Buxar, Patna, Bhagalpur, Nabadwip, Barrackpore, Godakhali and Fraserganj. Analysis found that all of the collected samples contained meso as well as microplastics. Analysis of the mesoplastics with FTIR revealed polyethylene terephthalate as the major contributing plastic debris in the sediments followed by polyethylene.

Cox et al., 2019, assessed the amount of microplastic particles in frequently consumed foods in relation to their recommended daily intake, with an emphasis on the American diet. It was also investigated whether microplastics might be inhaled and how the source of drinking water would influence their ingestion. Over 3600 processed samples totalling 402 data points from 26 investigations were used in our study. From their study, they calculated the yearly microplastic consumption ranges from 39000 to 52000 particles depending on age and sex, accounting for roughly 15% of the caloric intake of Americans. When inhalation is considered, these estimates rise to 74000 and 121000 respectively. Additionally, it was understood that compared to people who only drink tap water, people who consume the recommended amount of water from bottled sources may be swallowing an additional 90,000 microplastics annually.

Van Cauwenberghe et al., 2015 focused on the study about microplastics in sediments. The main studies conducted were, about the effectiveness of current microplastic extraction methods, the prevalence and geographic distribution of microplastics in sediments, and a thorough evaluation of the potential negative impacts of this form of pollution on marine animals. From this study, he concluded that there is a definite need for standardised procedures, unified reporting units, and more accurate effect assessments based on this study and suggest future research needs.

3.2 **Literature on Bharathapuzha river basin**

Magesh et al., 2013, carried out a morphometric analysis of Bharathapuzha river basin using geoprocessing techniques in GIS. According to Strahler's technique of categorization, the extracted drainage network was categorised, and the results show that the terrain has a dendritic to sub-dendritic pattern.

John & C. P., 2008, studied about the geomorphic indicators of neo tectonism in the Bharathapuzha basin. From their study, it was identified that a regional seismic structure was present in the vicinity of Palghat gap. This is identified as an active fault trending in WNW-ESE direction which is capable of producing moderate seismic events.

Nikhil Raj & Azeez, 2012, using GIS and remote sensing tools, performed a morphometric analysis of Bharathapuzha basin to study about the morphometric characteristics of the basin and its sub basin. From their study, it was identified that Bharathapuzha river was a seventh order stream with 4 basins and also is of dendritic drainage pattern.

Rajendran et al., 1996 conducted a geochemical study in lower Bharathapuzha sediments and also analysed the heavy mineral presence in it. Heavy metal distribution was also examined and the order of abundance was Fe>Mn>Ni>Cr>Zn>Pb>Cu>Cd. Bulk samples show the lowest content. For Ni and Pb, the difference in metal abundance between HM and mud fraction is merely minor. In HM, Cd, Cu and Zn content are very low whereas Cr, Mn and Fe are enriched. Cu, Zn, Cr, and Mn EF (Enrichment Factor) values are close to crustal abundance, although Cd and, to a lesser extent, Pb show relatively high values that may be attributable to anthropogenic contributions.

Anirudhan, 1989 focused on the study about the sediments of Bharathapuzha. The texture and grain shape of the sediments was also analysed. The result has attained using the scheme of McLaren and Bowles (1985). The result of analysis of textural parameters revealed the existence of Case B trend in the direction of transport for mainstream (Bharathapuzha) and two high gradient tributaries viz., Gayathripuzha and Thuthapuzha. Further, Fourier amplitude spectra estimated from digitized data of grain boundaries of the sand grade sediment from selected samples and the Waddell's sphericity and roundness indices demonstrate that influx of sediment from tributaries does not alter the size or shape distribution trends of the mainstream sands to any extent.

Anirudhan et al., 1994 defined the climate, physiography and geologic setting of the Bharathapuzha river basin. Also, Biju Kumar et al 2006, studied about the faunal species in the river basin. And in 201, he also presented a comprehensive account of diversity, distribution, and threats for the fishes of the Bharathapuzha river.

CHAPTER 4

METHODOLOGY

In this chapter, we discuss about the methods by which the samples were collected as well as the different laboratory works and procedures done for analysing the grain size of sediments from Bharathapuzha, Kerala. The different laboratory works like determination of moisture content of sediments, sieve analysis, chemical treatment of the sample for removing organic component as well as for separating microplastics are also well defined in detail.

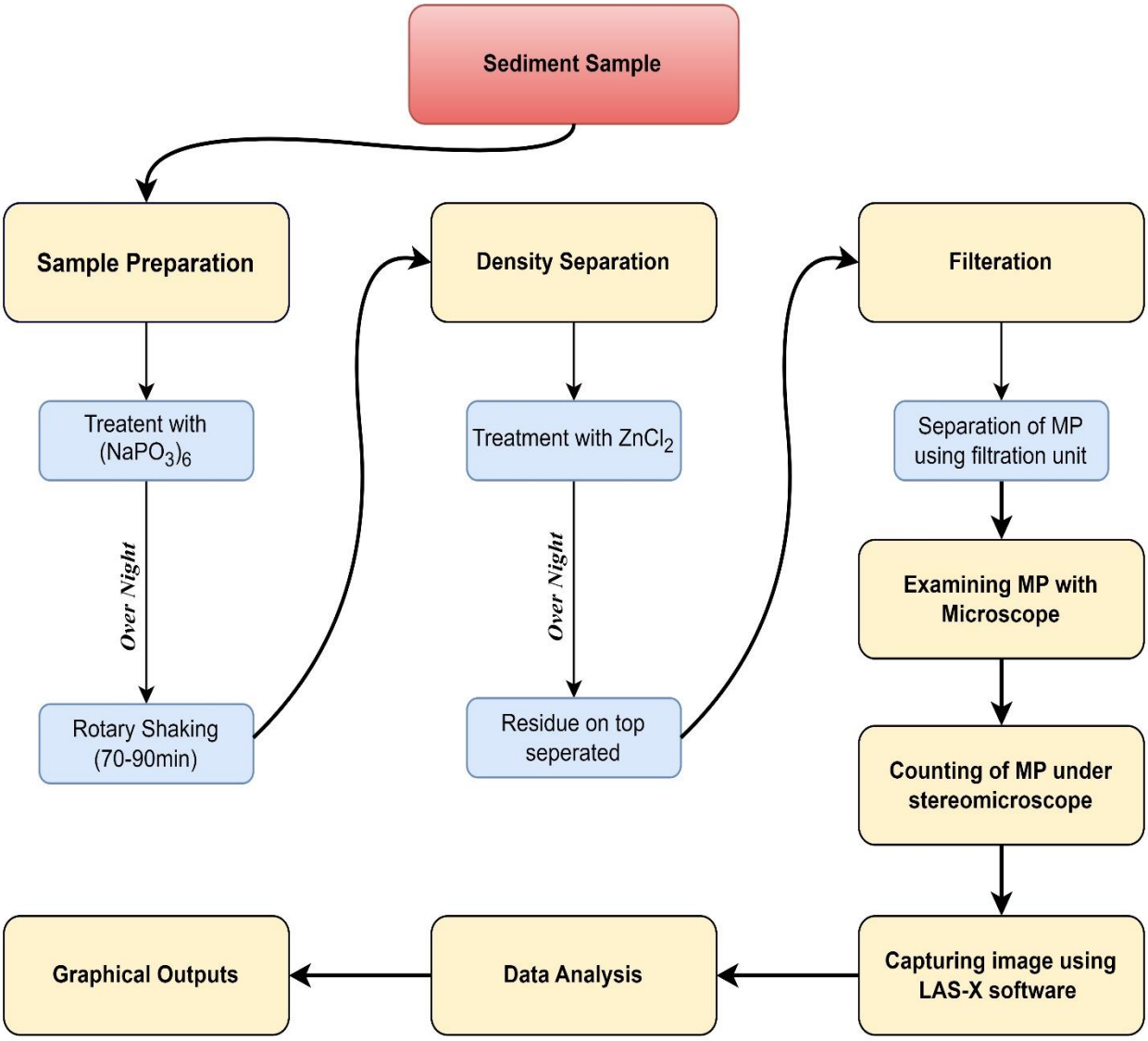

Fig 5. Flowchart showing the methodology of separation and characterization of Microplastics.

4.1 Sampling Method

The study was done with sediment samples which have been already collected from the Bharathapuzha river. A total number of 22 samples were collected across the river starting from the origin of the River along the entire stretch of the river till it joined the Arabian Sea, i.e from the source to the sink of the Bharathapuzha River. All the samples collected for this study are surface samples. Samples were also collected from the mouth of the tributaries of the river before they join the mainstream and also from mainstream after convergence. All the 22 samples were labelled individually as BP S1, BP S2, BP S3 and up to BP S22, BP S1 being the first sample collected from the origin of the river and BP S22 being the last sample collected from the mouth of the river.

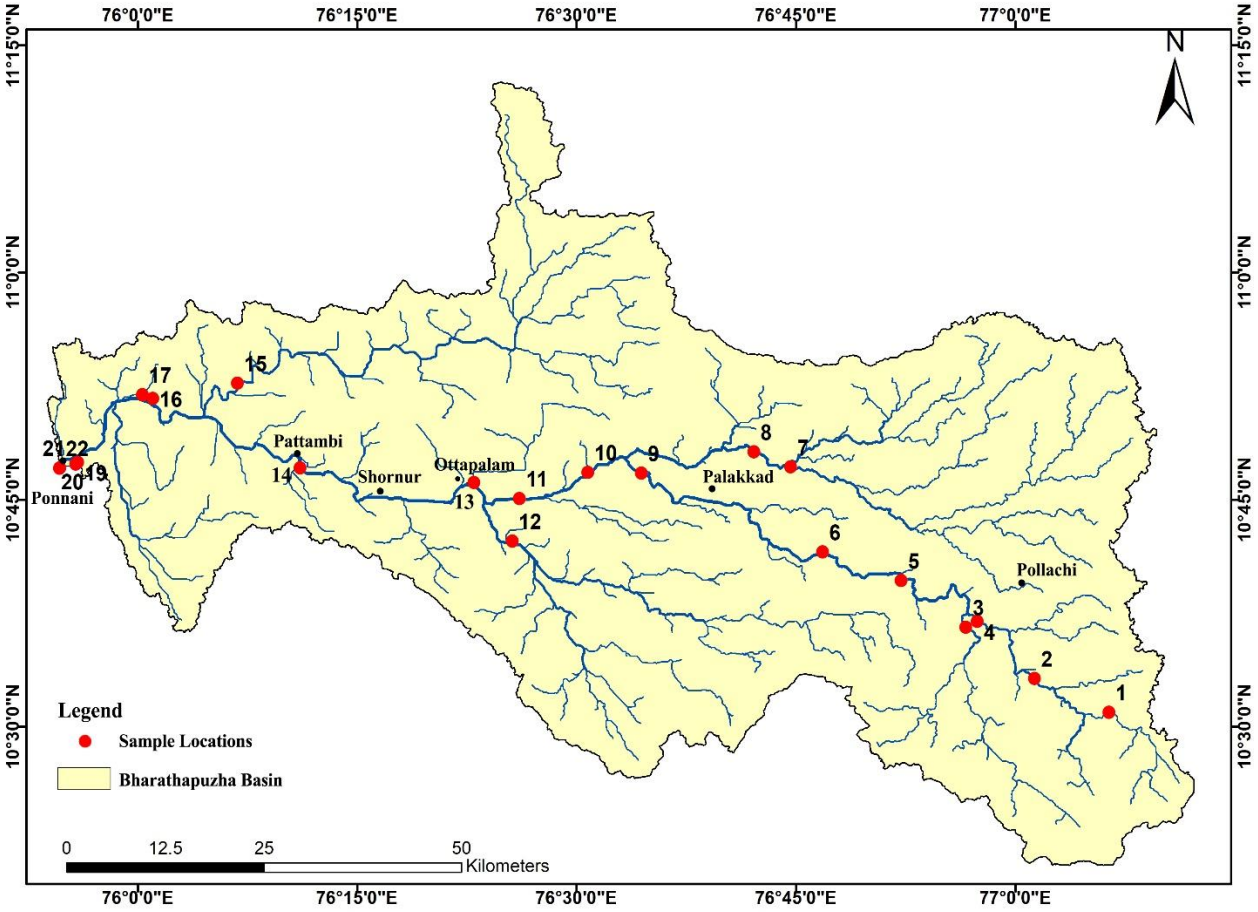

Fig 6. Map showing the locations of sample collection

SAMPLE NUMBER	LOCATION
BP S1	**TIRUPPUR** (10°30'56.08"N, 77°62'4.3"E)
BP S2	**THORAYUR** (10°33'10.6"N, 77°11'9.2"E)
BP S3	**UPPAARU RIVER(TBT)** (10°36'33.3"N, 76°56'37.8"E)
BP S4	**SINGANALLUR** (10°36'57.8"N, 76°57'24.12"E)
BP S5	**MOOLATHARA** (10°39'37.09"N, 76°52'12.33"E)
BP S6	**PERUMATTY** (10°41'32.08"N, 76°46'49.26"E)
BP S7	**KORAYAR RIVER(TBT)** (10°47'9.25"N, 76°44'38.77"E)
BP S8	**KALPATHY RIVER(TBT)** (10°488.63N, 76°42'7.87"E)
BP S9	**PARALI** (10°46'45.21"N, 76°34'25.71"E)
BP S10	**KALIKAVU** (10°46'47.64"N, 76°30'46.91"E)
BP S11	**PAMPADY** (10°45'3.5"N, 76°26'5.9"E)
BP S12	**GAYATHRI RIVER(TBT) (**10°42'15.5"N, 76°25'36.3")
BP S13	**OTTAPPALAM** (10°46'7.62"N, 76°22'58.76"E)
BP S14	**CHERUKKAD** (10°47'4.9"N, 76°11'6.5"E)
BP S15	**KUNTHI RIVER(TBT)** (10°52'40.79"N, 76°6'48.71"E)
BP S16	**KUTTIPPURAM** (10°51'40.14"N, 76°1'2.34"E)
BP S17	**RANGATHUR** (10°51'55.9" N, 76°0'18.6"E)
BP S19	**KEEZHILLAM** (10°47'28.6"N, 75°55'54"E)
BP S20	**KEEZHILLAM** (10°47'20.83"N, 75°55'45.92"E)
BP S21	**PONNANI BEACH** (10°47'4.90"N, 75°54'40.40"E)
BP S22	**PONNANI BEACH** (10°47'3.89"N, 75°54'38.55"E)

Table 1. table showing locations from where samples were taken.

*****TBT- Tributary

4.2 Laboratory method

4.2.1 Sediment sample analysis

Almost 400g of samples were collected from each of the 22 locations at the Bharathapuzha river basin. Out of the samples, 100g of samples of each location were separated from it. The samples were then dried using hot air oven for removing the excess moisture content present in it. Then, subsamples of 40g each were taken using a weighing machine, and put into conical flasks for further analysis conical flasks which are numbered similar to the sample number.

4.2.1.1 Sample preparation

Sodium hexametaphosphate solution is needed for this process. 1 litre of distilled water is taken into a beaker and 5.5g of sodium hexametaphosphate is added to it and stirred well to completely dissolve it. This solution is then poured in all the 22 samples which were placed in the conical flask until all the solution are soaked well in sodium hexametaphosphate solution. The solution is then kept to aside without any disturbance for 24 hours. This ensures that the samples are completely soaked in the solution.

After 24 hours, the conical flask containing the sample solution was placed into a rotary shaker for shaking the solution to ensure through mixing of the sample with the sodium hexametaphosphate. The speed of the shaker was kept at 250 RPM and the timer of the rotary shaker was kept at a range of 70-90 minutes. The samples were removed from the shaker after 90 minutes.

4.2.1.2 Density separation

Zinc chloride solution is needed for the separation of microplastics by density separation. 1 litre of distilled water was taken in a beaker and then, 933.3g of solid zinc chloride was added to it. The mixture is then stirred for 5-10 minutes using a long glass rod until all the solid zinc chloride completely dissolves in it. The reaction being exothermic releases a lot of heat which makes the solution very hot due to the chemical reactions occurring in it. The solution is therefore kept aside for almost 5-10 minutes to cool down the solution.

The 22 samples are then collected into 22 cylindrical flasks of 100ml quantity and zinc chloride solution is poured into it in such a way that the samples are completely covered by the solution. This mixture is then kept to rest overnight. The heavy materials in the solution sink and light

materials like microplastics and other substances float above the solution. Then, the supernatant is separated from the sample and transferred to another beaker. This solution is poured one by one into a filtration unit containing a 47 mm filter paper. A new filter paper is used for every sample. The light residues in the supernatant which were present on the top of the solution are trapped on the filter paper. These filter papers with the trapped residues are then used for further analyses.

4.2.2 Microscopical examination

For detailed microscopic examination, the samples were mounted on the stage of a stereomicroscope (LEICA M2025C). This microscope has a camera, which is connected to an external computer for viewing and capturing images of various microscopic objects seen through the microscope. The filter paper containing residues of each respective sample was mounted on the stage of the microscope and observed. The images of different types of microplastics were captured with the help of a software called as Leica Application Suite X (LAS X).

Using the images captured from the microscope, the quantity of microplastics in each sample was counted. The various coloured microplastics were identified and counted and sorted according to their colour. The different forms of microplastics which include fibres, fragments, filament etc. were present and identified in most of the samples and the presence and number were noted and counted. The data was entered in an excel sheet with the total count of microplastics, the count of different coloured microplastics and different forms of MPs. The data set is represented graphically.

CHAPTER 5

RESULTS AND DISCUSSION

In this chapter, the final findings and results of the present work has been described. 22 samples were collected from the Bharathapuzha river basin, starting from the source to the sink of the river. These samples were named as BP S1, BP S2, BP S3…etc. These samples were chemically treated, the MPs collected on filter papers were then observed through a microscope. Various types of MPs of different colours and types were observed and these were counted and data set prepared.

5.1 RESULTS

5.1.1 Microplastics Analysis

As the first step, the total amount of microplastics present in each sample were counted and noted. The presence of microplastics was observed in all the samples, with some samples having greater number and variety of MPs. Also, different coloured microplastics which include black, blue, red, pink etc coloured microplastics were observed. All these were counted, sorted and noted down separately. Similarly, different forms of microplastics like fibres, fragments, filaments were seen in some of the samples. This was closely observed and the photographs were captured. The count was also calculated and noted down based on their different forms. These data were entered in an excel sheet from which graphical and diagrammatical representations were plotted showing the form, colour and total abundance of the MPs in the sediment samples collected.

MICROPLASTICS IN BHARATHAPUZHA RIVER SEDIMENTS							
LOCATION NO.	**COLOURS OF MPs**						**TOTAL NO OF MPs**
	BLACK	BLUE	RED	PINK	GREEN	VIOLET	
BP S1	6	1	2	0	0	1	10
BP S2	4	2	1	0	2	0	9
BP S3	14	9	5	5	0	2	35
BP S4	6	1	0	4	0	3	14
BP S5	4	2	1	2	0	1	10
BP S6	53	10	2	0	2	28	95
BP S7	6	6	3	0	0	0	15
BP S8	10	0	3	0	1	1	15
BP S9	22	3	0	0	0	5	30
BP S10	10	12	5	3	3	5	38
BP S11	9	4	3	5	2	1	24
BP S12	44	11	6	12	14	8	95
BP S13	84	43	12	27	17	7	190
BP S14	56	7	12	2	12	1	90
BP S15	8	5	3	0	1	0	17
BP S16	16	20	5	2	2	0	45
BP S17	5	10	4	0	0	1	20
BP S18	51	4	11	0	17	1	84
BP S19	78	1	5	0	4	6	94
BP S20	24	2	3	0	1	1	31
BP S21	33	3	6	0	4	1	47
BP S22	68	36	17	0	19	3	143
TOTAL	611	192	109	62	101	76	1151

Table 2. showing the number of MPs observed based on colour

	TYPES OF MICROPLASTICS				
LOCATION NO	POTENTIAL FIBRES	UNCERTAIN FIBRES	LINES	FRAGMENTS	TOTAL
BP S1	5	1	4	0	10
BP S2	4	2	3	0	9
BP S3	13	7	15	0	35
BP S4	6	6	2	0	14
BP S5	4	4	1	1	10
BP S6	35	25	10	25	95
BP S7	6	4	4	1	15
BP S8	7	4	2	2	15
BP S9	12	8	5	5	30
BP S10	14	13	5	6	38
BP S11	13	7	2	2	24
BP S12	40	32	2	21	95
BP S13	62	59	5	64	190
BP S14	38	21	0	31	90
BP S15	9	3	1	4	17
BP S16	18	12	0	15	45
BP S17	11	2	1	6	20
BP S18	37	21	1	25	84
BP S19	28	6	3	57	94
BP S20	14	6	0	11	31
BP S21	27	8	0	12	47
BP S22	62	33	3	45	143

Table 3. Table showing the number of microplastics based on shape in sediment samples collected along the Bharathapuzha river basin

From the 22 samples collected from the Bharathapuzha river, it was found that all the 22 samples showed the presence of MPs and almost all of the samples had variations in colours and types of MPs. BP S1 was the sample collected from the source of the river, only 10 MPs were found in this sample which was dominated by potential fibres and lines. Whereas, BP S2 recorded the least number of MPs in the whole 22 samples, only 9 MPs dominated by potential fibres and lines was found from this sample. In BP S3, a peak in the number of MPs occurred, recording 35 pieces of MPs and lines were found more in this sample followed by potential fibre. 14 MPs were present in BP S4 having more potential and uncertain fibres. In BP S5, the number of uncertain and potential fibres was higher, with a total of 10 MPs. In BP S6, an increase in number of MPs was observed, having 95 MPs and this was dominated by potential fibres and fragments. BP S7 and BP S8 contained 15 MPs each and both samples were dominated by potential fibres. In BP S9 was observed a total of 30 MPs in which potential fibre was more and also, lines and fragments were also seen in this sample, but were less in number. BP S10 recorded 38 MPs having both potential and uncertain MPs more in number. In BP S11 also, potential fibre is the dominant one and the total MP count is recorded at 24. In BP S12, total of 95 MPs were found and this constituted potential and uncertain fibres and also the fragments, whereas, lines were very less in number. BP S13 was the sample which recorded the greatest number of MPs among all the samples. This sample recorded 190 pieces of MPs and the dominant type in this sample is fragments, followed by potential and uncertain MPs, but still, lines are very less in number in this sample. BP S14 showed 90 MPs having more fibres and fragments. A large decline in number of MPs occurred in BP S15, showing only 17 MPs, having more potential fibres in it. BP S16 had 45 MPs and most in number were fibres and fragments. A total of 20 MPs were found in BP S17 and high in number were potential fibres. In BP S18, an increase in number of MPs occurred having a total of 84 MPs and this sample is dominated by potential fibres and fragments. The sample, BP S19 consisted a total of 94 MPs and fragments are the dominated type in this sample. In BP S20, a total of 31 MPs were seen, having potential fibres and fragments more in number. 47 MPs were contained in the sample BP S21, and the most seen type were potential fibres. The final sample BP S22, which was collected from the mouth of the Bharathapuzha river, consisted the second the greatest number of MPs in all the locations. This sample recorded 143 MPs and most dominant type of MP in this sample also is potential fibres, followed by fragments.

From the obtained data, it can be understood that all of the total 22 samples showed the presence of MPs in various forms and colours and the total count of microplastics obtained from all the samples was 1151. Out of all the samples, it was seen that the sample BP S13, which was taken from Ottapalam town area, has the greatest number of microplastics, that is 190 and it has been followed by the sample BP S22, which is the last sample taken from the sink of the river, having 143 number of microplastics. This sample was taken from Ponnani beach area. Lesser number of microplastics were seen in the samples which were taken from the origin of the river basin, that is, in BP S1 and BP S2 having the total count of microplastics as 10 and 9 respectively. BP S1 was taken from the origin point of the river in Tamil Nadu and BP S2 was taken from an area near Thorayur Bridge in Tamil Nadu.

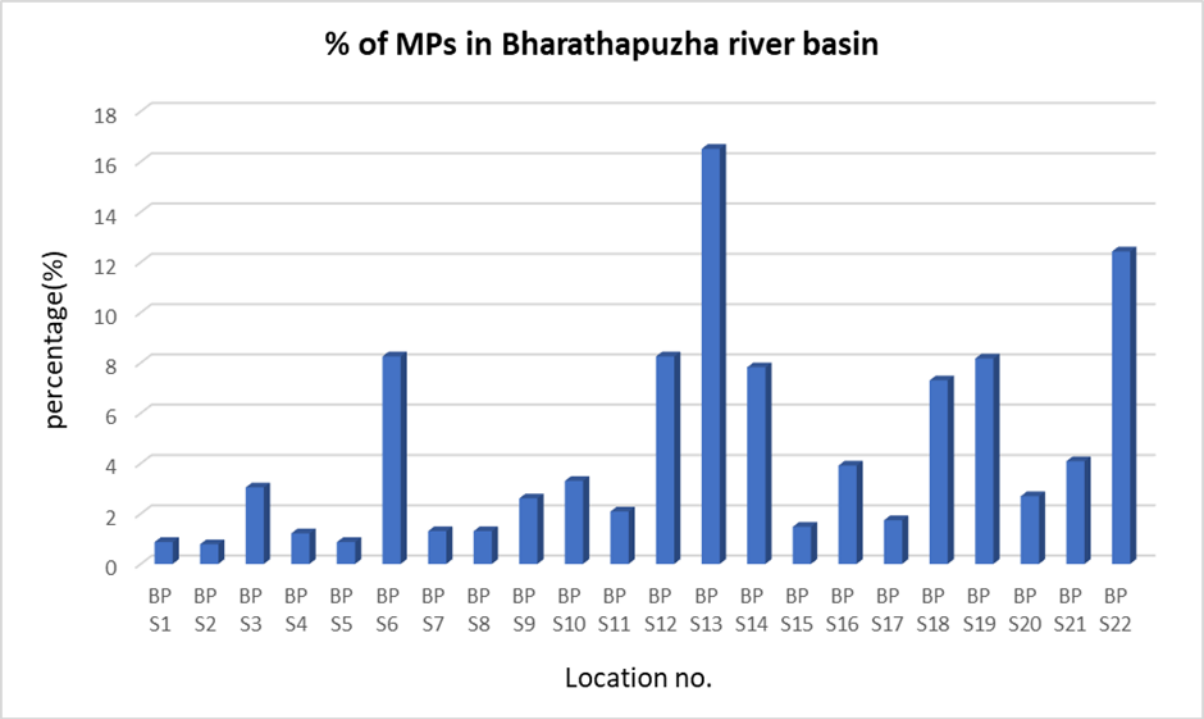

Fig 7. graph showing % of MPs in locations of Bharathapuzha river basin

From these observations it can be seen that there is a great variation in the amount of microplastics in the different samples. The amount of microplastics in the samples do not show a specific pattern of increase or decrease, but shows an irregular increase and decrease in the amount of microplastics in each location. There is no gradual increase or decrease either, for example the sample having most amount of microplastics is BP S13, and BP S14 which is the next location has lower number of MPs. This clearly indicates that it is the anthropogenic activities in certain areas of the river basin that causes the increase in the number microplastics

observed. Such activities include dumping of plastic wastes into the river, MPs from fishing harbours, from plastic covers and bottle wastes etc. Since Ottapalam is a township, there is a higher chance of MPs entering the region due to such anthropogenic activities. This can be clearly seen in the results which shows high number of MPs in the sample BP S13 which was taken from Ottapalam area.

The percentages of microplastics found in the respective tributaries of Bharathapuzha river basin is shown below. Out of the total samples, 5 samples are taken from tributary rivers. They are BP S3, BP S7, BP S8, BP S12 and BP S15. Out of this, the greatest number of MPs was found in the sample BP S12, which recorded a number of 95 MPs and followed by the sample BP S14 consisting of 90 MPs. All the other tributary samples comparatively recorded lesser number of MPs.

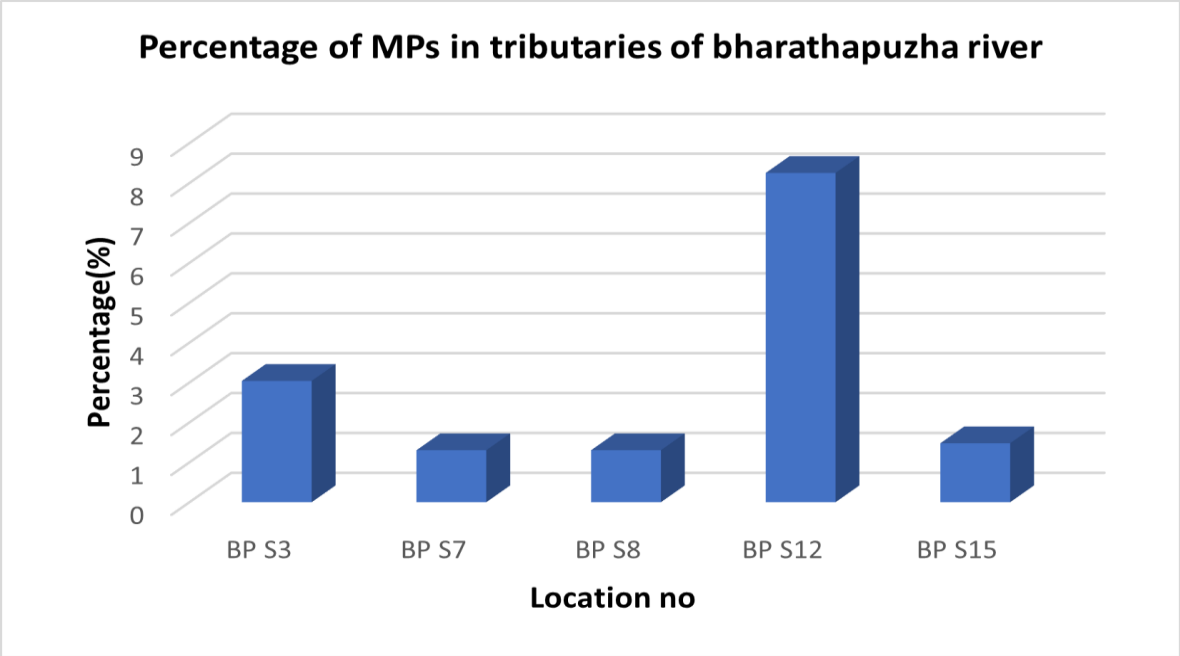

Fig 8. Graph showing % of MPs in tributaries of Bharathapuzha river

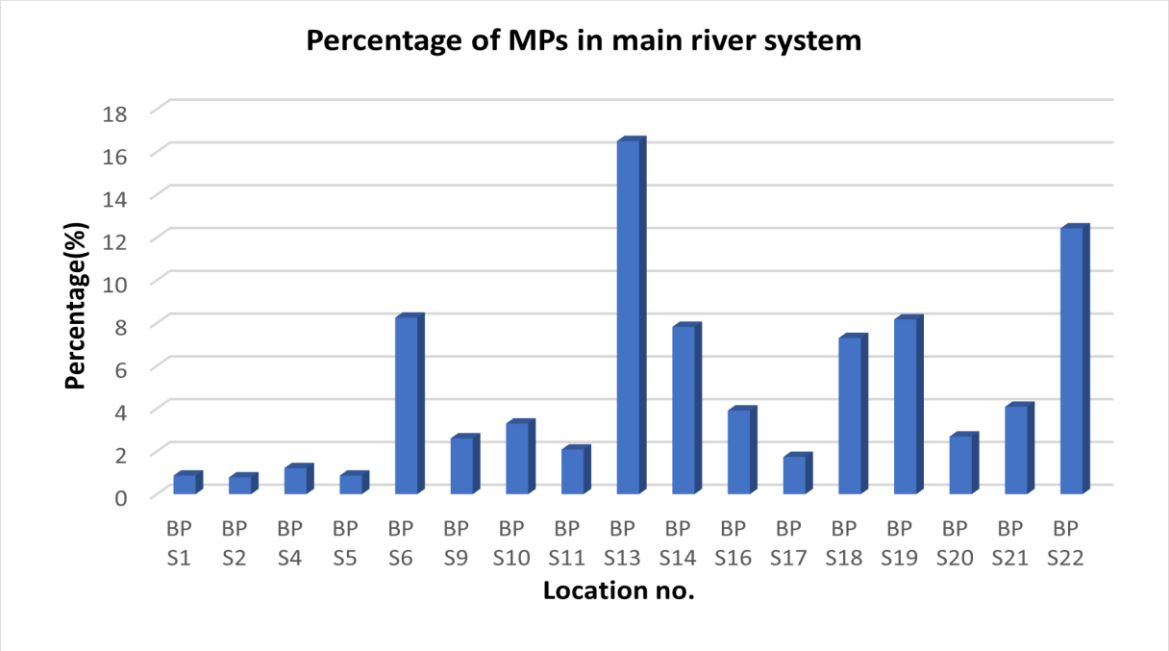

Fig 9. graph showing % of MPs in main river system of Bharathapuzha river basin

5.2 Discussion

All of the total 22 samples showed the presence of MPs. It is shown that all the samples shown only 4 forms of MPs. They are potential fibres, uncertain fibres, fragments and lines. These are found in the river mainly due to anthropogenic activities like fishing and waste discharge and also due to the hydrogeomorphology of the river which include sediment type, flow velocity, discharge of the river etc (Tjaša Matjašič, 2023). The fibres obtained from the sample may be discharged from fishing nets and lines during fishing and also secondary microplastics which were formed from the plastic wastes disposed by humans into the river. The sample BP S1 and BP S2, which contained lesser number of MPs in all the samples was taken from the origin of the river and that area wasn't highly populated and the anthropogenic activities were very very low. Maximum MPs were collected from S13 (Ottapalam town area) indicating that the MPs in this region may be related to the population density. Similar results were reported by Kunz et al 2023, in which they showed that there is a strong positive correlation between abundance of MPs and population density and land use patterns. Thus, it concludes the effect of anthropogenic activity in the increase of MPs at that location. Another crucial aspect of MPs is their colour because marine species have been observed to consume MPs that resemble their food in terms of colouring. [Ory et al 2017, Marti et al 2020].

Microplastics come in a variety of colours [Rochman et al 2019] which are chemicals that were added to the plastics during their manufacture. According to earlier research, the two single colours that are most frequently observed in environmental MPs are transparent (clear) and blue [Maynard et al 2021, Minor et al 2020]. Black and blue particles also prevailed in this analysis (Table 2). The increase in the amount of coloured microplastics shows a high probability of decrease in aquatic life (Maneesh Kumar, 2023). Because smaller MPs can be eaten by both terrestrial and aquatic animals, particle size plays a significant role in the assessment of MP hazards to biota [Cole et al 2014, Sheng et al 2021]. Also tiny particles are of concern since they can absorb a range of pollutants due to their relatively high surface-to-volume ratio [Tourinho et al 2019]. For further study it is therefore essential to determine the size of MPs and their composition as well.

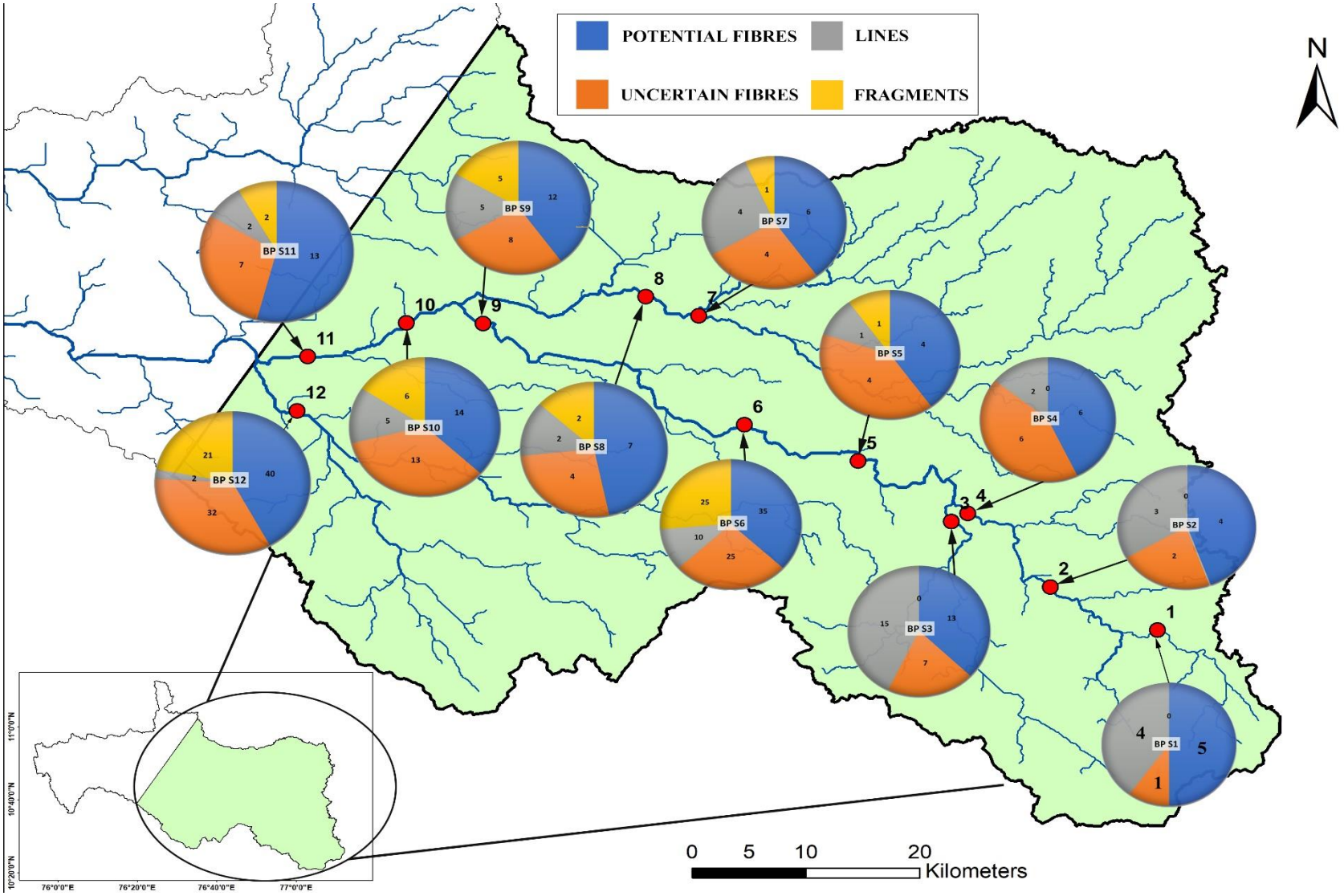

Fig 10. Spatial map showing pie chart of forms of MPs in Bharathapuzha river(upstream)

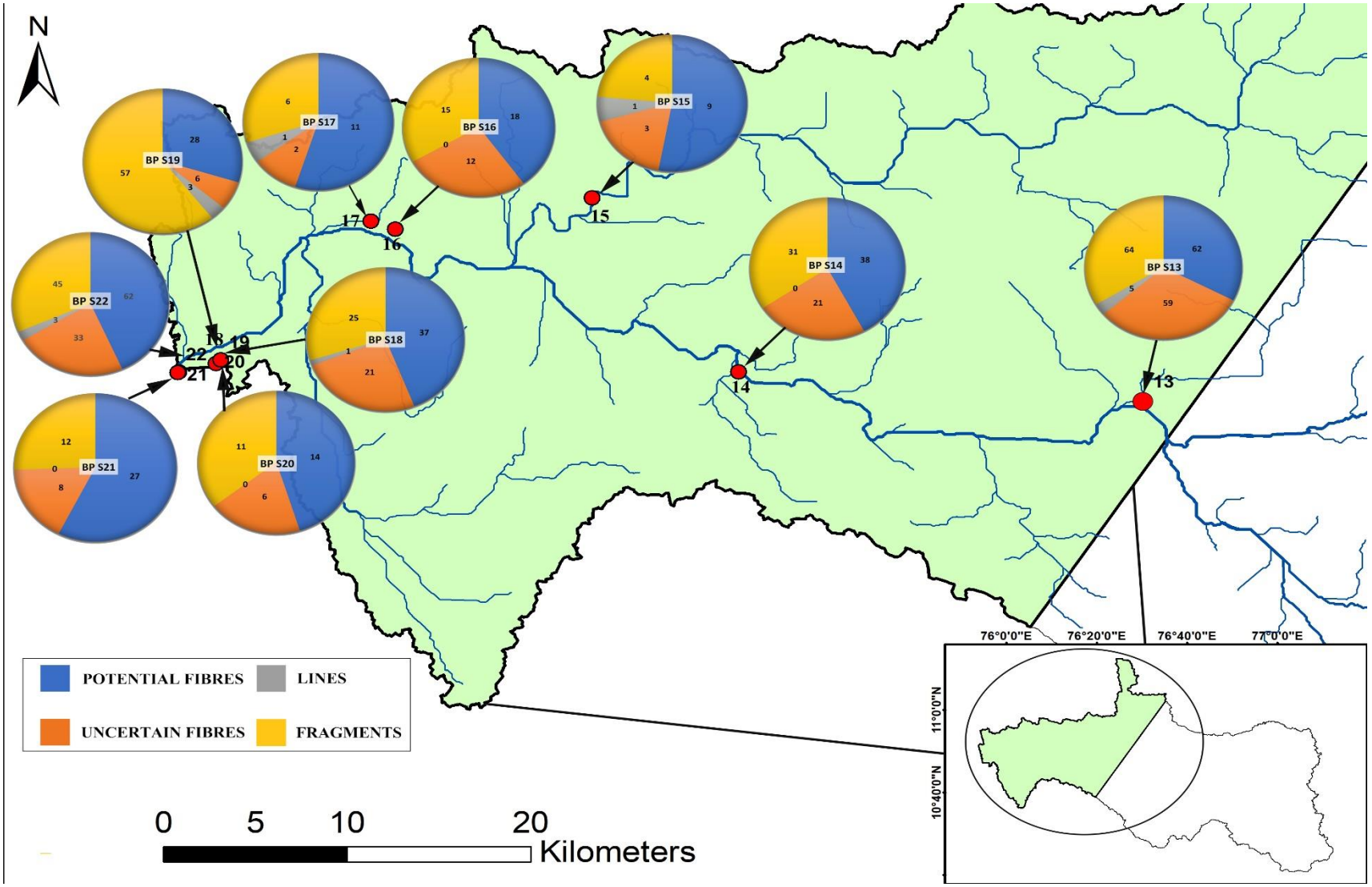

Fig 11. Spatial map showing pie chart of forms of MPs in Bharathapuzha river(downstream)

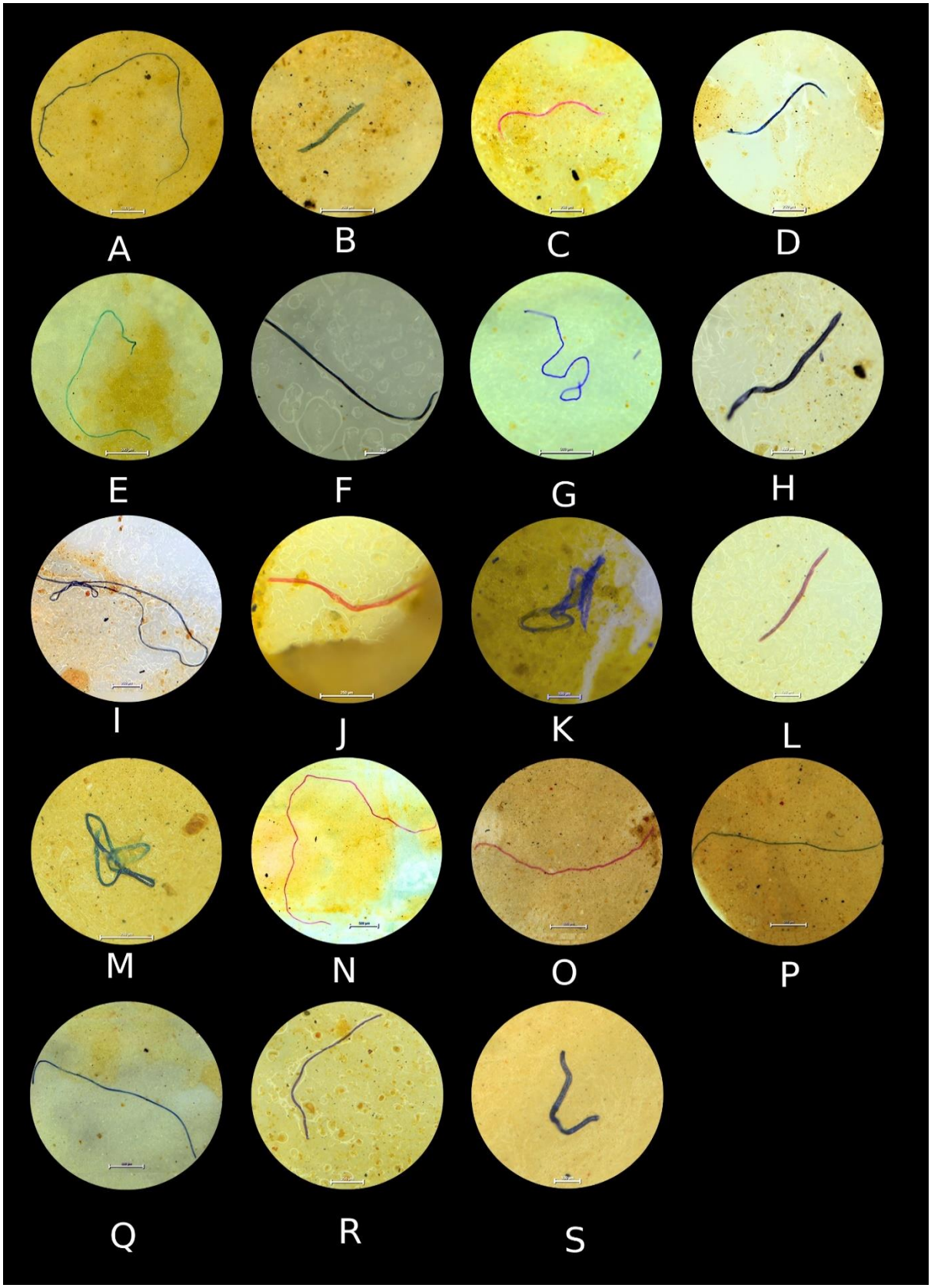

Fig 12. Photoplate showing different type of MPs in Bharathapuzha river. A, B- BP S2; C, D- BP S4; E, F- BP S3; G, H, I- BP S10; J, K, L- BP S13; M, N, O- BP S19; P- BP S20; Q, R- BP S21; S- BP S22.

CONCLUSION

The present study was carried out for investigating the presence and amount of microplastics in the sediments from the Bharathapuzha river and also to determine the different forms and colour variants of the microplastics present in the source to sink region of Bharathapuzha river basin. For that, a total of 22 samples were collected from different part of the river basin starting from the beginning to the end of the river basin.

From the study, it is concluded that the presence of MPs is seen in every sample collected from the Bharathapuzha river basin. This shows the contamination rate of the river basin.

Different types of MPs were identified throughout the study which includes: potential fibres, fragments, uncertain fibres and lines. This points towards the different sources of pollution which may include wastes from fishing hubs like fishing nets, fishing lines etc and wastes from townships and also from other anthropogenic activities.

The greatest number of MPs were shown in the sample BP S13, which was taken from Ottapalam town area, Palakkad. Hence, we can conclude that Ottapalam is the most polluted location in the study area. The second most polluted area is Ponnani beach area, from which the sample BP S22 was collected. This sample showed the second the greatest number of MPs. The least number of MPs was seen in the sample BP S2, which was taken from an area near Thorayur bridge in Tamil Nadu and the next lesser number of MPs was seen in the sample BP S1, taken from the origin of the river in Tamil Nadu. This point towards the fact that these are the least polluted areas in the Bharathapuzha river.

Regulations, trash management, and ethical plastic use can reduce microplastics and address their causes. Microbeads in personal care products must be banned, plastic pellet spills must be prevented during handling and transportation, sustainable alternatives to single-use plastics must be promoted, recycling systems must be improved to prevent plastic contamination, and public awareness of microplastic dangers and proper waste disposal must be raised. These preventive approaches can reduce microplastic production and discharge, protecting ecosystems and reducing animal and public health risks. Reduce plastic waste, increase recycling, raise awareness, and create innovative technology to mitigate secondary microplastics and promote a sustainable future.

REFERENCE

- Andrady, A. L. (2017). The plastic in microplastics: A review. *Marine Pollution Bulletin*, *119*(1), 12–22. https://doi.org/10.1016/j.marpolbul.2017.01.082
- Anirudhan, S. (1989). *Textural and mineralogical variations of sediments of Bharathapuzha river system*.
- Anirudhan, S., Thiuvikramji, K. P., & Chacko, P. T. R. (1994). Roles of Relief and Climate on Composition of Detrital Sediments of Bharathapuzha Basin, Kerala. *Geological Society of India*, *43*(4), Article 4.
- Boots, B., Russell, C. W., & Green, D. S. (2019). Effects of Microplastics in Soil Ecosystems: Above and Below Ground. *Environmental Science & Technology*, *53*(19), 11496–11506. https://doi.org/10.1021/acs.est.9b03304
- Cole, M., Lindeque, P., Halsband, C., & Galloway, T. S. (2011). Microplastics as contaminants in the marine environment: A review. *Marine Pollution Bulletin*, *62*(12), 2588–2597. https://doi.org/10.1016/j.marpolbul.2011.09.025
- Cox, K. D., Covernton, G. A., Davies, H. L., Dower, J. F., Juanes, F., & Dudas, S. E. (2019). Human Consumption of Microplastics. *Environmental Science & Technology*, *53*(12), 7068–7074. https://doi.org/10.1021/acs.est.9b01517
- Devi, S. S., Sreedevi, A. V., & Kumar, A. B. (2020). First report of microplastic ingestion by the alien fish Pirapitinga (Piaractus brachypomus) in the Ramsar site Vembanad Lake, south India. *Marine Pollution Bulletin*, *160*, 111637. https://doi.org/10.1016/j.marpolbul.2020.111637
- Dowarah, K., & Devipriya, S. P. (2019). Microplastic prevalence in the beaches of Puducherry, India and its correlation with fishing and tourism/recreational activities. *Marine Pollution Bulletin*, *148*, 123–133. https://doi.org/10.1016/j.marpolbul.2019.07.066
- Gopinath, K., Seshachalam, S., Neelavannan, K., Anburaj, V., Rachel, M., Ravi, S., Achyuthan, H., K R, M., Kannaiyan, N., & Srinivasalu, S. (2020). *Quantification of microplastic in Red Hills Lake of Chennai city, Tamil Nadu, India*.
- Jacob, K., & Narayanaswamy, S. (1954). The structural and drainage patterns of the Western Ghats in the vicinity of the Palghat Gap. *Proc. Nat. Inst. Sci. Ind*, *20*(1), 104–118.

- John, B., & C. P., R. (2008). Geomorphic indicators of neotectonism from the Precambrian terrain of Peninsular India: A study from the Bharathapuzha Basin, Kerala. *Journal of the Geological Society of India*, *71*, 827–840.
- Khaleel, R., Valsan, G., Rangel-Buitrago, N., & Warrier, A. (2022). Hidden problems in geological heritage sites: The microplastic issue on Saint Mary's Island, India, Southeast Arabian Sea. *Marine Pollution Bulletin*, *182*, 114043. https://doi.org/10.1016/j.marpolbul.2022.114043
- Li, J., Yu, S., Yu, Y., & Xu, M. (2022). Effects of Microplastics on Higher Plants: A Review. *Bulletin of Environmental Contamination and Toxicology*, *109*(2), 241–265. https://doi.org/10.1007/s00128-022-03566-8
- Magesh, N. S., Jitheshlal, K. V., Chandrasekar, N., & Jini, K. V. (2013). Geographical information system-based morphometric analysis of Bharathapuzha river basin, Kerala, India. *Applied Water Science*, *3*(2), 467–477. https://doi.org/10.1007/s13201-013-0095-0
- Maneesh Kumar, S. K., Kartha, A. R., Rajathy, S., Ratheesh Kumar, C. S., Chandini, P. K., Vidya, P. V., Madhuraj, P. K., Sajith, K. S., & Anamika, S. (2023). Characterization of suspended microplastics in surface waters of Chalakudy River, Kerala, India. *Chemistry and Ecology*, *39*(3), 268–287. https://doi.org/10.1080/02757540.2023.2178648
- Nikhil Raj, P., & Azeez, P. A. (2012). Morphometric Analysis of a Tropical Medium River System: A Case from Bharathapuzha River Southern India. *Open Journal of Modern Hydrology*, *2*, 91–98. https://doi.org/10.4236/ojmh.2012.24011
- Nikhil, V. G., Ranjeet, K., & Varghese, G. K. (2023). Spatio-temporal evaluation and risk assessment of microplastics in nearshore surface waters post-2018 Kerala deluge along the southwest coast of India. *Marine Pollution Bulletin*, *192*, 115058. https://doi.org/10.1016/j.marpolbul.2023.115058
- Patel, A., Bhagat, C., Taki, K., & Kumar, M. (2020). *Microplastic Vulnerability in the Sediments of the Sabarmati River of India* (pp. 127–138). https://doi.org/10.1007/978-981-15-4668-6_7
- Podbielska, M., & Szpyrka, E. (2023). Microplastics – An emerging contaminants for algae. Critical review and perspectives. *Science of The Total Environment*, *885*, 163842. https://doi.org/10.1016/j.scitotenv.2023.163842

- Rajendran, S., Karthikeyan, P., & Seralathan, P. (1996). Heavy mineral and geochemical studies of Lower Bharathapuzha sediments, Kerala. *Geological Society of India*, *48*(3), 319–324.
- S. K., A., & Varghese, G. K. (2020). Environmental forensic analysis of the microplastic pollution at "Nattika" Beach, Kerala Coast, India. *Environmental Forensics*, *21*(1), 21–36. https://doi.org/10.1080/15275922.2019.1693442
- Sarkar, D. J., Sarkar, S., Manna, R., Samanta, S., & Das, B. (2020). Microplastics pollution: An emerging threat to freshwater aquatic ecosystem of India. *Journal of the Inland Fisheries Society of India*, *52*, 05–15. https://doi.org/10.47780/jifsi.52.1.2020.106513
- Shim, W. J., Hong, S. H., & Eo, S. (2018). Chapter 1—Marine Microplastics: Abundance, Distribution, and Composition. In E. Y. Zeng (Ed.), *Microplastic Contamination in Aquatic Environments* (pp. 1–26). Elsevier. https://doi.org/10.1016/B978-0-12-813747-5.00001-1
- Subramanian, K., & Muraleedharan, M. (1985). Origin of the Palghat Gap in South India-a synthesis. *Geological Society of India*, *26*(1), 28–37.
- Sundar, S., CHOKKALINGAM, L., Roy, P. D., & Usha, T. (2021). Estimation of microplastics in sediments at the southernmost coast of India (Kanyakumari). *Environmental Science and Pollution Research*, *28*. https://doi.org/10.1007/s11356-020-10333-x
- Van Cauwenberghe, L., Devriese, L., Galgani, F., Robbens, J., & Janssen, C. R. (2015). Microplastics in sediments: A review of techniques, occurrence and effects. *Marine Environmental Research*, *111*, 5–17. https://doi.org/10.1016/j.marenvres.2015.06.007
- Veerasingam, S., Mugilarasan, M., Venkatachalapathy, R., & Vethamony, P. (2016). Influence of 2015 flood on the distribution and occurrence of microplastic pellets along the Chennai coast, India. *Marine Pollution Bulletin*, *109*(1), 196–204. https://doi.org/10.1016/j.marpolbul.2016.05.082
- Matjašič, T., Mori, N., Hostnik, I., Bajt, O., & Viršek, M. K. (2023). Microplastic pollution in small rivers along rural–urban gradients: variations across catchments and between water column and sediments. Science of The Total Environment, 858, 160043.
- Cole, M., Webb, H., Lindeque, P. K., Fileman, E. S., Halsband, C., & Galloway, T. S. (2014). Isolation of microplastics in biota-rich seawater samples and marine organisms. Scientific reports, 4(1), 4528.

- Sheng, Y., Liu, Y., Wang, K., Cizdziel, J. V., Wu, Y., & Zhou, Y. (2021). Ecotoxicological effects of micronized car tire wear particles and their heavy metals on the earthworm (Eisenia fetida) in soil. Science of The Total Environment, 793, 148613.
- Maynard, I. F. N., Bortoluzzi, P. C., Nascimento, L. M., Madi, R. R., Cavalcanti, E. B., Lima, Á. S., ... & Marques, M. N. (2021). Analysis of the occurrence of microplastics in beach sand on the Brazilian coast. Science of The Total Environment, 771, 144777.
- Minor, E. C., Lin, R., Burrows, A., Cooney, E. M., Grosshuesch, S., & Lafrancois, B. (2020). An analysis of microlitter and microplastics from Lake Superior beach sand and surface-water. Science of The Total Environment, 744, 140824.
- Ory, N. C., Sobral, P., Ferreira, J. L., & Thiel, M. (2017). Amberstripe scad Decapterus muroadsi (Carangidae) fish ingest blue microplastics resembling their copepod prey along the coast of Rapa Nui (Easter Island) in the South Pacific subtropical gyre. Science of the Total Environment, 586, 430-437.
- Martí, E., Martin, C., Galli, M., Echevarría, F., Duarte, C. M., & Cózar, A. (2020). The colors of the ocean plastics. Environmental Science & Technology, 54(11), 6594-6601.
- Rochman, C. M., Brookson, C., Bikker, J., Djuric, N., Earn, A., Bucci, K., ... & Hung, C. (2019). Rethinking microplastics as a diverse contaminant suite. Environmental toxicology and chemistry, 38(4), 703-711.
- Tourinho, P. S., Kočí, V., Loureiro, S., & van Gestel, C. A. (2019). Partitioning of chemical contaminants to microplastics: Sorption mechanisms, environmental distribution and effects on toxicity and bioaccumulation. Environmental Pollution, 252, 1246-1256.

REGIONAL STUDY OF MICROPLASTICS IN SURFACE WATER OF BRAHMAPURAM AREA, ERNAKULAM DISTRICT

Dissertation submitted to Christ College (Autonomous), Irinjalakuda, Kerala,
Under University of Calicut in partial fulfilment of the degree of

MASTER OF SCIENCE IN APPLIED GEOLOGY

By,

CHANDINI S

REG NO: CCAVMAG007

2021-2023

DEPARTMENT OF GEOLOGY AND ENVIRONMENTAL SCIENCE

CHRISTCOLLEGE (AUTONOMOUS), IRINJALAKUDA, KERALA,680125

(Affiliated to university of Calicut and re-accredited by NAAC with A^{++} grade)

CERTIFICATE

This is to certify that the dissertation entitled- '**Regional study of microplastics in surface water of Brahmapuram area, Ernakulam district**' is a bonafide record of work done by**. Ms. Chandini S** (Reg. No. CCAVMAG007), M.Sc. Applied Geology, (Christ College (Autonomous), Irinjalakuda) under the guidance of **Mrs. Roshini P.P**, Assistant professor, (Dept. of Geology and Environmental Science, Christ College (Autonomous) Irinjalakuda) in partial fulfilment of requirements for the degree of Master of Science in Applied Geology during the academic year 2021-2023.

Project in charge

Mrs. ROSHINI P.P

Assistant professor

Dept. of Geology and Environmental Science

Christ College (Autonomous),Irinjalakuda

Dr. Anto Francis K.

Co-ordinator (Geology Self-financing)

Christ College (Autonomous),Irinjalakuda

Place: ……

Date: ……

External Examiners;

1. ……

2. ……

DECLARATION

I **CHANDINI S**, hereby declare that the work incorporated in this dissertation report entitled '**Regional study of microplastics in surface water of Brahmapuram area, Ernakulam district**' has been composed solely by me and that it has not been submitted, in whole or in part, in any previous application for a degree. Except where stated by reference, the work presented here is entirely my own. It was carried out under the guidance and supervision of **Mrs. Roshini P.P,** Assistant Professor, Dept. of Geology and Environmental Science, Christ college (Autonomous) Irinjalakuda, Kerala. I have followed best practice and ethics of scientific study. This work is submitted to Christ College (Autonomous), Irinjalakuda, Kerala in partial fulfilment for the award of degree of Master of Sciences in Applied Geology.

Place: CHANDINI S

Date: Reg No: CCAVMAG007

ACKNOWLEDGEMENT

This work would not have been possible without guidance, encouragement and support of other people. I would like to extend my sincere gratitude to all those who helped me in this project. First and foremost, I thank my project guide **Mrs. Roshini P.P**. (Assistant professor, Dept. of Geology and Environmental Science, Christ College (Autonomous) Irinjalakuda for designing framework of the project, support and supervision throughout the work. I am deeply grateful to **Dr. Linto Alappat**(Deen of Research and Development of TLC and former HoD), **Mr. Tharun R** (Head of the Department), and **Dr. Anto Francis K** (Co-ordinator, Geology Self-financing) of Department of Geology and Environmental Science for their constant motivation throughout the course and in giving guidance in all possible ways to carry out the analysis.

I would like to extend my gratitude to **Dr. Anso M. A**, and **Ms. Ivine Joseph** (Assistant Professors, Dept. Of Geology and Environmental Science) for their constant guidance and support throughout the work and all other faculty members of Dept. of Geology and Environmental Science, Christ College, for their guidance during the academics. I would like to thank **Mr. Ayyappadas C S** (Research Fellow Christ (College Autonomous) Irinjalakuda) who gave technical support for my project and Christ college family for their support, guidance and love.

I also acknowledge with reverence, my warm regards towards my parents and my family members for their moral support and guidance. Last but not the least I extend my thanks to all of my friends who directly or indirectly helped me to complete this dissertation report.

Above all I would like to express my gratitude to God almighty for showering His blessings on me to complete my project in efficient manner.

ABSTRACT

Since surface water is easily accessible than ground water, it is relied on for many human uses. Brahmapuram is one of the prominent industrial areas in Ernakulam district, so assessment of surface water quality and microplastic contamination is of high demand.17 samples were collected as part of this investigation. Analysis of physico-chemical parameters of samples was carried out. In case of most parameters sample 2 recorded lowest value and samples 15, 16 &17 show highest values. Samples were analyzed using filtration unit for the determination of microplastics. This research provides the first step in understanding microplastic contamination in the river and its proximity to the water cycle.

CONTENTS

LIST OF TABLES

LIST OF FIGURES

CHAPTER 1
INTRODUCTION

1.1 SURFACE WATER

Water is an essential substance; all life on earth depends on water. It is odorless and colorless liquid. Water covers about 71% of earth's surface. Surface water accounts only 1.2% of freshwater available on the earth and 69% of that surface water is trapped in permafrost and ground ice. Water has many unique properties. Hydrosphere is considered to be an important agent of geologic change. Two major components of hydrosphere are surface water and ground water. The movement of water between land, atmosphere and oceans through different processes like precipitation, evaporation, runoff and condensation is known as water cycle on Earth. This cycle maintains water accessibility for a variety of anthropogenic and natural activities. Water is an important factor for human survival, and it has been used for different purposes, including agriculture, drinking, energy production and industry. Surface water is a vital element of water cycle. It is necessary for maintaining a variety of ecosystem.

Surface water acts as a source of shelter and nutrition for numerous animals and plants. The changes in availability of surface water and its quality can have major impacts on the environmental health. Surface water is also used as fresh water, for household purposes, for cooking. Surface water is highly important because of it's social, ecological, economic, environmental and cultural significance.

1.2 SURFACE WATER CONTAMINATION

The analysis of surface water pollution has concentrated primarily on lakes and streams. Freshwater is effortlessly contaminated. As soon as contaminated to the extend, freshwater can be considered polluted. Freshwater quality is hard and costly to restore. Surface water pollution is described as the toxicity of hazardous pollutants and compounds in streams, ponds, rivers, lakes and other surface water bodies. These pollutants or compounds can arise from different sources including urban runoff, agricultural activities, improper waste disposal, industries etc. It comprises of domestic waste water. Surface water contamination can trigger harmful effects on human health and aquatic ecosystems. Pollution of surface water can cause threats to human

health when contaminated water is consumed for drinking, other activities like swimming. It can also result in waterborne diseases such as gastrointestinal illness. In addition to this it can also cause respiratory infections, skin infection etc. As this contaminated water contains toxic chemicals it can cause neurological disorders, cancer and other health problems. Surface water which is contaminated can reduce agricultural productivity and soil quality, can also damage crops. It can also destroy fish and other aquatic life, which declines fish population.

The physical and chemical features of surface water are what describes its suitability for various sources. Quality of surface water may be induced by human activities as well as natural activities which bring pollutants into water bodies. In order to protect human health, surface water quality monitoring and management are necessary. The occurrence of various chemicals regulates the surface water quality. The physical features such as dissolved oxygen, temperature and turbidity also influence quality of surface water.

1.3 MICROPLASTICS IN SURFACE WATER

Microplastic (MP) is a prevalent pollutant seen in biota, sediment and water all over the world. Though, the research regarding the extent to which mankind are exposed to this pollutant is very feeble. Recently researches have suggested the fact MP are found in surface water, ground water, bottled water, tap water etc. Microplastics are described as tiny plastic fragments of size less than 5 millimeters long which is harmful to our entire mankind. There are 2 kinds of microplastics; primary and secondary. Primary microplastics are defined as small particles induced for commercial purpose, which includes microfibers that shed from clothes and other textiles, like nets used for fishing. Whereas secondary microplastics are particles that form from the breaking of large plastics items, like water bottles. This breakdown is mainly due to exposure of those plastics to environmental factors, such as ocean waves, sun’s radiation etc.

According to the shape, there are different types of microplastics. This includes, fibers, fragments, films etc. There are potential MP like fibers, it can be blue, black, pink colored. Uncertain MP like fibers which is colorless. Potential MP like fragments and films are another type of microplastics. Polymer type in microplastics is determined by Fourier Transform Infrared

Spectrometer (FT-IR). Using FT-IR polymer types are identified as polyethylene, polypropylene, polyethylene terephthalate, ethylene vinyl acetate copolymer etc.

Microplastics have been determined in aquatic organisms from whales to plankton, in drinking water and seafood etc. All traces of microplastics cannot be eradicated by standard water treatment amenities. Areas with high population density has highest microplastic pollution. Microplastics being hazardous pollutant is a serious threat to both aquatic ecosystem and human health. So, regarding this issue appropriate measures has to take for proper waste management and its disposal.

1.4 AIM AND OBJECTIVE OF THE STUDY

The study aims to determine spatial distribution of physico- chemical parameters and microplastic abundance in surface water near Brahmapuram area, Ernakulam district. The objectives of the study include: -

- To determine the physico-chemical characteristics and spatial variation of surface water.
- To study the distribution of microplastics in surface water.

1.5 NEED FOR THE STUDY

A massive fire accident has happened on March 2at Brahmapuram solid waste management plant, Kakkanad, Kochi. Due to this incident, there is higher chance of water quality contamination at the same time Kadambrayar river is also affected. On this perspective, quality of surface water study over Kadambrayar river is highly appreciable. People over there uses this water for their daily needs, agricultural purposes and even for drinking too. After contamination of waste and plastics in water occurred by fire accident, the people over there have been suffering from suffocation from chock and drinking water quality. Hence the people and aquatic ecosystem has been adversely affected. The number of fish and other aquatic life has been greatly reduced. Locals in the area are reporting several troubles including dry cough, breathing difficulties, and irritation and dryness in the eyes.

CHAPTER 2

LITERATURE REVIEW

Imogen E Napper et al.,2021 this study mainly concentrated on the abundance and characters of microplastics in surface water transboundary Ganges River. About 140 microplastics were identified, out of this pre-monsoon samples possess higher concentration (71.6%) than post-monsoon. So, this study firstly helps in knowing the contamination of microplastics in the Ganges and its addition to the microplastic oceanic load. Most of the identified microplastics are fibers (91 %) and the rest of them were fragments (9%).

Mei Han et al., 2020 this research is focused on the distribution of microplastics of yellow river's surface water. Composition of microplastics were investigated in this work, identified as polyethylene, polypropylene and polystyrene. About 93.12 percentage microplastics in surface water were fibers. Concentration of microplastics in surface water is reduced linearly with distance from the estuary of Yellow River. The work highlights that in Yellow River microplastic fibers less than 200 micrometers were dominant.

Mingxiao Di, Jun Wang et al., 2018 in this research microplastic pollution in surface water of largest reservoir in China were studied. They discovered fibers were the most dominant microplastics. Microplastic concentrations are affected by residential and sewage treatments.

S K Maneesh Kumar et al., 2022 the study focused on suspended microplastics characterization in surface water of Chalakudy River, Kerala. This study area is abundant with microplastics of size less than 20 micrometer. The chance of damage of aquatic life is indicated by the microplastic pollution in surface water.

Ajith Nithin et al., 2022 this work emphasis on the seasonal microplastic distribution in the surface water and sediments of the Vellar estuary, Parangipettai, southeast coast of India. In this study area fiber, film, pellet, fragment, and glitter were discovered. Microplastics of ten colors were found, among them black was more abundant. From surface water 4 polymers were obtained, among them LDPE was most abundant. So, this study reveals the fact vellar estuary is contaminated with microplastics.

R janakiram et al., 2023 the study is carried out in surface water of north Indian ocean to identify the seasonal distribution of microplastics. For the first time microplastic seasonal distribution is done in open sea. Surface water samples are collected from the Arabian sea and Bay of Bengal. The dominant polymers were polyethylene and polypropylene. In 2018-2019 seven expeditions were done in pre-monsoon, monsoon and in post monsoon. About 86 percentage fibers were obtained from the samples. Of all particles colored particles account for 67 percentage. Movement of microplastics are affected by the hydrodynamic conditions.

Wenfang wang et al., 2018 this work is concentrated on the distribution of microplastics in surface water of Hong Lake and Dongting lake, China. The study investigated properties and occurrence of microplastics present in surface waters of two dominant lakes in the middle reaches of the Yangtze River. Fibers were the most dominant kind of microplastics. Especially in China the world's leading producer of plastics has no enough knowledge regarding the presence of microplastics in freshwater ecosystem. The reason for the presence of microplastics in both lakes is due to fishery activity. The samples consist of microplastics with particles less than 2 mm were dominant. Majority of the particles is being occupied by the colored items. Particles sized less than 330 micrometer consists of greater than 20 percentage of total microplastics that has been taken from the 2 lakes. The major components of identified microplastics are polypropylene and polyethylene.

S. Haddout et al., 2021 microplastics are important pollutant which affects the environmental and human health. This research highlights the distribution of surface water and sediment microplastics present in the Atlantic Coast and Sebou Estuary, Morocco. The quantification, occurrence, and characteristics were identified. The identified microplastics are separated into fragments, films, fibers and granules. Most of the discovered microplastics size range from 0.1 to 0.5 mm, followed by 0.5 to 1 mm. Most of the identified microplastics in sediments and surface waters were fragments. The Sebou Estuary is being a hotspot on the Atlantic Coast which has been suggested by the results for the size, color and type of the identified microplastics.

Bingxu Nan et al., 2020 this includes distribution and discovery of microplastics in surface water and Paratya australiensis Australian freshwater shrimp in Victoria, Australia. Microplastics were found in surface waters of all sites. The most common type of microplastics found were fibers. Blue fibers were dominant in both surface water and shrimp samples. In water samples polymers

were the dominant plastic types where as in shrimp samples it is found to be rayon kind of plastic. When comparing with water samples, shrimp samples contain wide variety of plastic types.

Firdha Cahya Alam et al., 2019 focused on the occurrence of microplastics in surface water and sediment river along industrial area and slum of Ciwalengke River, Majalaya district, Indonesia. This work is concentrated in slum area which gains importance recently. Both surface water and sediment samples from lake were collected from 10 locations and grouped into 6 segments location on the basis of different land use on the river bank. Using binocular microscope microplastic particles were identified and classified by size and shape. The dominant kind of microplastic type identified were fibers. The reason for the abundance of fibers were derived from the fabric washing process and direct clothing of residents in the river in the textile industries. The microplastic particles were gone through Raman spectroscopy test and showed the type of microplastic were polyester and nylon.

Daofen Huang et al., 2021 the occurrence of microplastics in West River downstream, in the south of China were investigated. Freshwater is the potential source and transport routes for plastic matter to the oceans. The characteristics and distribution of microplastics in the downstream area of West River were investigated. Both surface water and sediments dominated with fibers of less than 0.5 mm. Using Fourier transform infrared spectrometer the identified polymer types of microplastics were polyethylene, polyethylene terephthalate, polypropylene, and polyvinyl chloride. So, the distribution of microplastics can be corelated with different use of land. The highest abundance of microplastics were found in public or commercial or recreational areas than residential, natural, and industrial areas. Their result shows the occurrence of high dominance of microplastics in river is due to the impact of human activities. The presence of microplastics in water samples were less than that of sediments.

Pathompong Vibhatabandhu et al., 2022 assessed the impact of seasonal changes on the distribution of microplastics in the surface water of Inner Gulf of Thailand. About 100-1000L of surface water samples were collected from 70 to 74 sites in Inner Gulf of Thailand. The samples were collected during both wet and dry seasons in order to know the relation between environmental variables and spatiotemporal dispersal of microplastics. The presence of microplastics in dry season was less than that of the dry season. The dominance of microplastics

in river estuaries and seasonal current circulations were revealed by spatial distribution. The microplastics identified primarily consist of polymers such as polypropylene and polyethylene. The chemical structure of discovered microplastics include new functional groups such as hydroxyl, carbonyl, vinyl groups. River is the important factor in the movement of microplastics to the coastal sea which is confirmed by the quantity of freshwater runoff and the negative link with salinity.

Cris Gel Loui A. Arcadio et al.,2023 investigated the presence of microplastics in surface water of Laguna de Bay. This is the first documented evidence on largest lake in the Philippines. On the surface water of lake 10 sampling stations were sampled using plankton net. Fourier-transform infrared spectroscopy used for analyzing and extracting the samples. From 10 sites about 100 microplastics were obtained with mean density 14.29 items/meter cube. Fibers were the dominant kind of microplastics. Among them blue colored microplastics predominated the water samples. About 11 types of polymers were identified in microplastics such as ethylene vinyl acetate copolymer, polyethylene terephthalate and polypropylene, which all together account for about 65 percentage of total microplastics in the areas. The result revealed the fact that there is high density of microplastics in areas having high population density. So, it is necessary to take proper measures regarding plastic waste management and to protect ecosystem of lake.

Gaoliang Wang et al., 2020 this work investigated surface water of Manas River Basin, China. The occurrence and characteristics of microplastic pollution were studied in this river. Microplastics being important type of pollutant seen in various environmental conditions and their effect on aquatic life are great concern on society. Still the investigation of microplastic pollution characteristics is rare in inland rivers in China. Most of the samples were rich in fibrous microplastics. Their size ranged between 0.1- and 1.0-mm. Black and white colored fibers were mostly found. In addition to this flaky type of microplastics were also detected. Polyethylene, polyethylene terephthalate is dominant kind of polymers seen in microplastics which is identified using infrared spectral analysis.

Faika Tasnim Ayshi at el., 2008 water bodies selected in and around Dhaka city were studied by characterization and qualification of microplastic distribution. From Dhanmondi and Ramna Lakes, hatirjheel, Turag and Buriganga rivers samples were collected during both winter and

summer season for the quantification of microplastics. In both summer and winter season the amount of microplastics in 2 peripheral rivers -Turag and Buriganga is comparatively higher than that of inland waterbodies – Dhanmondi Lake and Ramna Lake. From morphological analysis the identified microplastics were found to be irregular and rough in nature which indicate they are introduced into waterbodies a long time ago. Whereas some microplastics have large size and irregular/sharp edges particularly in Buriganga River and Dhanmondi River suggest that they have been added to respective water bodies recently. This investigation provides knowledge regarding the microplastic pollution in various water bodies of Dhaka city during two different seasons.

Huan Jing Ke Xue at el., 2020 Haizhou Bay, Lianyungang is the study area investigated for distribution and characteristics of microplastics in surface area and sediments. Recently microplastics is a new marine pollutant and which gained research importance nowadays. The microplastic distribution in Haizhou Bay of Jiangsu area was studied by both quantitative and qualitative methods. The size of the microplastics in both sediments and surface water ranged as 0.04-14.74 mm and 0.08-13.48 mm, respectively. 60 percentage of microplastics found in surface water and sediments has a size less than 2.00 mm. About 92 percentage of microplastics detected in Bay were fibrous shaped. The dominant colors were black and blue, accounting for 70 percentage. The materials were PET and man-made fibers which accounts for about 79.4 percentage. From the composition of microplastics and analysis of morphological characteristics they concluded the result that microplastics in Haizhou Bay come from coastal land sources and mariculture.

Joana Correia Prata at el., 2019 detection and sampling methods of microplastics in water and sediment were studied in this work. Samples of water can be collected by methods such as Neuston and Manta nets, plankton net, sieving, pumps. Whereas sediment can be collected by methods such as beach sediment collection, Seabed collection with the help of grab sampler, box corer, gravity core. Identification can be improved by removal of organic matter through digestion. Cross contamination should be reduced to get accurate results.

A.M.A.I.K. Athapaththu at el., 2020 investigated both microplastics and macroplastics in surface water of southern coastal belt of Sri Lanka. Distribution and characterization are done by FTIR. The accumulated plastics in coastal waters that have been selected were filaments. The rate of

plastic contamination mainly depends up on environmental factors and anthropogenic activities. Blue- colored microplastics were dominant in this coastal line. This kind of approach facilitate the need for programs that deal with regular plastic debris management.

Lishan Zhang at el., 2020 Qin River is the area of investigation studied for distribution of microplastics in surface water and sediments. From 12 sampling sites surface water and sediment samples were collected along the urban section of Qin River, China. Using Teflon pump system and plankton nets with different pore size water samples were collected. Polyethylene and polypropylene were the dominant kind of polymers present in microplastics. The reason behind accumulation of microplastics were identified as factors such as aquaculture activities, population density, and industrial structure. The study concluded that waste water treatment plants will effectively reduce the microplastic contamination in urban sewage.

Yutaka Kameda at el., 2021 worldwide attention has been gained regarding environmental behaviors of microplastics. This study assessed the source and polymer specific size distribution of fine microplastics in surface water in an urban river. They found about 18 polymer types of microplastics. Two primary sources of microplastics were identified by cluster analysis which include non-point sources and residential waste water at the headwater site. Microplastic's median particle size has been increased in urban areas at the downstream site and were larger than those in the influent and effluent. So, these results shows that the release of larger microplastics are from non-point sources in urban areas.

M.N. Uddin at el., 2014 this work focused on the assessment of river water quality parameters. Jamuna River is the study area. Water quality of a river has great importance because that water has been used for various purposes such as irrigation, drinking, and for other domestic purposes. Jamuna River is one of the most prominent rivers in Bangladesh. In plastic containers of 2 liters were used for the water sample collection. Samples were collected from 5 different locations during wet and dry season. Physical and chemical parameters were detected which include PH, TDS, COD, BOD, EC, temperature, Nitrate, Chlorides, Calcium, Sulphates, Ammonia. So, respective mean value of each parameter in both seasons was compared with the standards that has been set by the EQS guideline and the guideline of Department of Environment of Bangladesh.

A.K.M.L. Rahman at el., 2012 the author studied the water quality parameters in Turag River with seasonal variations. The aim of this work was to assess the extent of pollution in Turag River by detecting various physcio-chemical parameters. From the following locations Tongi Railway Bridge, Ashulia and Bishwa Ijtema field during wet and dry seasons water samples were collected 6 times per year. The measured physico-chemical parameters exceeded the permissible limit of the drinking water. The range of concentration of heavy metals and arsenic in ppb were as follows: cadmium (Cd)(0.043 to 2), lead (Pb)(2.29-18.62), zinc (Zn)(0.04-0.4), arsenic (As)(1.15 to 4.8). The detected PH range from 6.6 to 7.98 and EC from 160 to 1107 µs/cm. The recorded biological oxygen demand (BOD) ranges from 10 to 180 mg/L whereas chemical oxygen demand (COD) ranged from 21 to 220 mg/L. Because of increased values of parameters PH, BOD, COD, and free Carbon dioxide water from these places are not suitable for human intake without proper treatment.

A.K. Verma at el., 2012 this study demonstrated the prediction of water quality from simple field parameters. Water quality parameters like PH, temperature, total dissolved solids(TDS), dissolved oxygen(DO), total suspended solids(TSS), grease and oil, etc., are computed from the field like parameters like chemical oxygen demand(COD) and biological oxygen demand(BOD) are inferred through laboratory tests. Here, an attempt has been made to compute COD and BOD from simple field parameters such as TSS, PH, DO, etc., by means of Artificial Neural Network (ANN) method.

Mohammed AA Flora at el., 2016 studied the biological and physico-chemical properties of water from Meghna River, Bangladesh. Meghna is one of the most importantrivers in Bangladesh where it endures multi-species commercial fishery. Recently the study was done to asses biological and physico-chemical parameters of Meghna river's water in 3 spots.19 physico-chemical parameters were studied. This includes water temperature, water color, transparency, water depth, air temperature, total dissolved solids, free carbon dioxide, PH, NH3, odor of water, bottom type, biological oxygen demand, chemical oxygen demand, total hardness, total alkalinity, plankton community of zooplankton and phytoplankton were studied. From Bhairab region highest transparency were recorded. In Meghna ghat area free carbon dioxide found maximum of about 3.7 mg/L. Highest dissolved oxygen was found in Chandpur of about 3.7

mg/L. From results obtained they concluded water quality of Meghna River are safe for aquatic life.

Khurshid at el., 1998 waste disposal effect on water quality in parts of Cochin, Kerala. The increasing amount of chemicals in water bodies and other rivers, causing from increased discharge of municipal waste water and industrial effluents, has become main problem in affecting water quality. In their present study an approach has been made to assess the water pollution caused by prevailing industries in parts of Cochin. From Eloor to Cochin systematic study of the chemical nature of surface water bodies has been made with a view to evaluate the range of pollution of various trace elements. Around Eloor industrial belt the concentration of trace elements is higher than that of Vembanad lake.

Jai M Paul at el., 2018 this study is based on water quality index, a Water Quality Index(WQI) gives a single value on the basis of variety of water quality criteria that denotes overall quality at a certain time and location. The aim of WQIis to convert complex quality data into information that the general public can understand and use. In order to detect the WQI, 12 physico-chemical parameters have been used which includes, PH, Total Alkalinity, Electric Conductivity, Total Hardness, Sulphate, Chloride, Nitrate, Calcium, Magnesium, Fluoride, Turbidity and Dissolved Oxygen.

Singh et al., 2019 this study focused the distribution and the sources of heavy metals in the surface water of Ganga River in India. Water samples were collected from different locations along the river and examined them for heavy metal content. The author concluded the primary origin of heavy metal content in the river were mainly due to municipal wastewater and industrial discharges. This work also focuses the adverse effects of heavy metal pollution on human health and aquatic life.

Opuene et al., 2020 Niger Delta Region of Nigeria is the stud area, assessed for surface water quality which is highly impacted by gas and oil exploration activities. From different locations water samples were collected and detected high levels of pollutants such as heavy metals, total dissolved solids, hydrocarbons. From detailed study on this area author concluded that water quality in the region was severely damaged, causing serious threat to aquatic life and human health.

Kaur et al., 2019 this research paper demonstrated surface water pollution and its effects on human health. Here the author gives an outline of surface water pollution and its adverse impact on aquatic life and mankind. Study mainly discusses about the various pollutants that can contaminate surface water including heavy metals, pathogens, pesticides, and pharmaceuticals. The paper also deals with adverse health effects that has been faced by humans due to exposure to polluted water which include, cancer, neurological disorders and gastrointestinal illness etc.

Revathy Das et al., 2021 with special reference to drinking water potential water quality assessment has been done in 3 tropical freshwater lakes of Kerala, SW India. To assess the water quality of lakes for drinking purposes physico-chemical parameters and bacteriological examination were evaluated in surface waters of Vellayani,Pookot, and Sasthamkotta lakes. For this purpose, 20 samples from these three lakes were collected along S-N-W transects that cover the whole area. According to WQI most of the samples in 3 lakes on the basis of observed chemical constituents were dropping under good category but the real problem lies in the bacteriological contamination. There was huge count of coliforms in these 3 lakes, which should be zero for drinking water. So, the enhanced microbial population in all 3 lakes denote the unhealthy activities taking place near lake catchments. The author concluded that necessary steps have to be taken to develop the water quality of freshwater resources.

CHAPTER 3

STUDY AREA

3.1 INTRODUCTION

Major waste dump lawn in Kochi, Kerala is Brahmapuram landfill. Brahmapuram solid waste plant is managed and owned by Kochi Corporation. This waste plant is being foremost contributor to fire dangers, environmental pollution and problems affecting public safety and health. The solid waste of Kochi city has been received and transported through Brahmapuram plant. Firstly, waste is separated into different categories at the plant which includes plastics, organic waste, glass, metals etc. In a combusting unit this organic waste has been collected and processed into high quality compost that can be used as fertilizer for plants. Each day excess of 600 tons of waste has been delivered by Kochi city and almost 100 tons of waste has been decayed at this plant into natural manure. At last, the solid waste management service built in 2018 became a landfill. A major fire accident happened at Brahmapuram waste plant on March 2nd, 2023. Due to this many areas of the city were engulfed by toxic gas filled smoke for several days.

3.2 KADAMBRAYAR RIVER

The chief river flowing through the study area is Kadambrayar river and samples were collected from the same. This river begins from hill named Arakkappady. After passing through panchayats of Kizhakkambalam, Thrikkakara, Edathala, Kunnathunad the river joins Chitrapuzha. Kadambrayar river has a total length of 27 km and has catchment area of 115 km approximately. Natural canals like Vanachira thodu, Palakuzhythodu, Kunnipadam, Chandakkadavu thodu, Mundampalam, Valiya thodu, Pazhangattu chal, Paapparakkadavu thodu etc are some of the tributaries of the river.

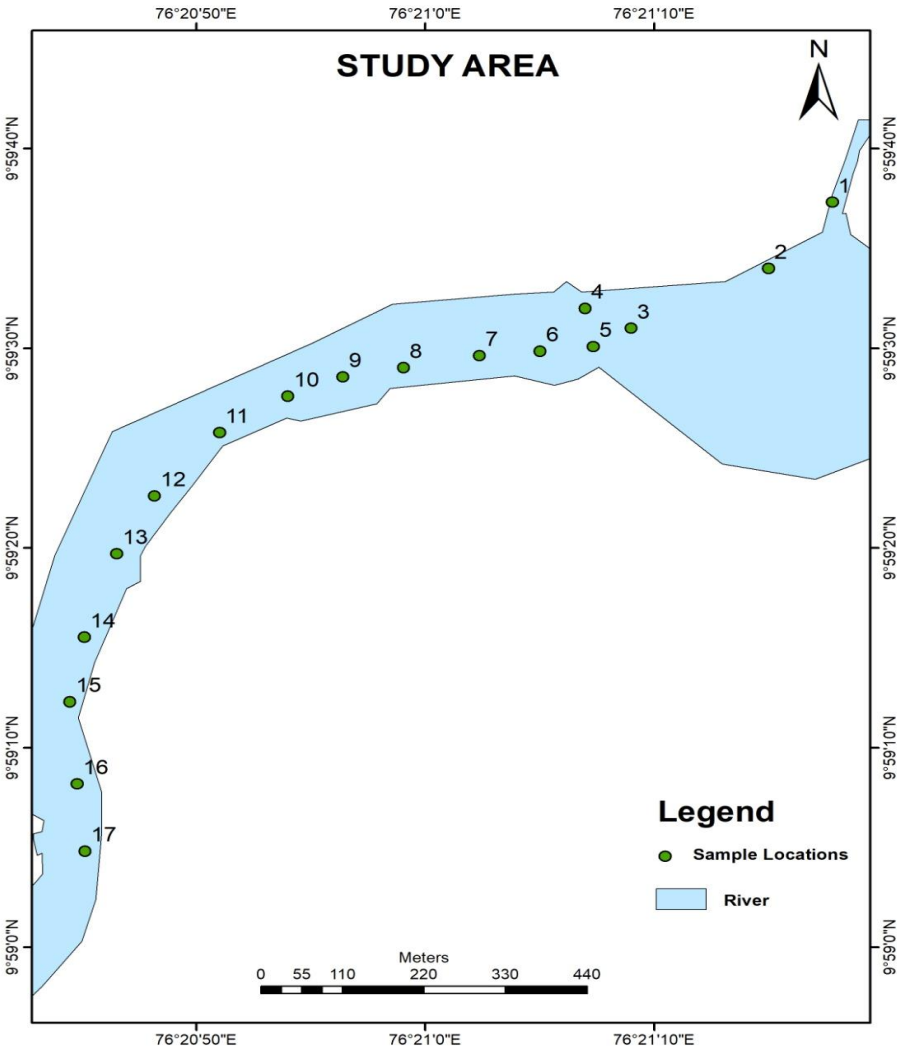

Figure 1: Study area map

3.3 GEOLOGY OF AREA

Kakkanad is a region in Kochi city of Ernakulam district which is located in south India. It is characterized by complex geological history as it is situated in the western ghats. The basement rock is identified as charnockite. This region is formed through various geomorphological and

geological processes. This region comprises of different types of rocks. The sedimentary rocks observed in this region includes laterite, shale, sandstone, clay etc. These rocks have been formed during Cretaceous and Tertiary Period.

3.4 GEOMORPHOLOGY

The district can be broken down into 3 physiographic zones: (i) the coastal plains in the west, (ii) the midland region in the east, and (iii) the steep to very steep hills in the easternmost part. With a maximum elevation of about ten meters towards the ocean, the coastal plain is a low-lying region. The eastern region, which is made up of sandy flats, marshy areas, backwaters, and alluvial plains that are subject to flooding during the monsoon season. The midland region has topography of narrow valleys and low hills. The valleys are alleviated and hills are covered with laterite or lateritic soil. The region has very gentle to moderate slope from east to west. Rugged terrain with small summits and steeply sloping slopes can be found in the easternmost region. Actually, it creates the Western Ghats' foothills. This terrain is typically elevated by more than 300 meters above mean sea level.

3.5 AGRICULTURE

Ernakulam is one of the most important agricultural centers in Kerala due to several factors such as favorable climate, fertile soil, and large number of water resources. Ernakulam district is the state’s largest producer of coconuts. The major crop grown in the area is coconut which approximately account for 39% of Kerala’s total production. Hybrid variety of coconut that is produced in the district is used for both commercial and domestic purposes. The district’s eastern portion is home to the most of rubber plantations due to soil conditions and favorable climate for rubber cultivation. Another important crop observed is rubber plantation which approximately accounts for 7% of state’s total rubber production.

3.6 CLIMATE

District usually experiences tropical monsoon weather. Climate over here is categorized as dry climate and tropical wet which is also known as tropical monsoon climate. Duration of monsoon is calculated from June to September during which the city obtains a lot of rain. During this time

the city encounters an average rainfall of 3000 millimeters. The fundamental wellspring of precipitation in Ernakulam is the southwest rainstorm. District also experiences relatively cool and dry winter from December to February, which is good time to visit due to the temperature which usually ranges from 22 °C to32° C. In Ernakulam mid-year season lasts from Spring to May. During this period temperature can shoot up to 35°C. In common, the district has humid and warm climate all year long, with lot of rain during monsoon season and comparatively cold and dry weather in winter.

3.7 INDUSTRIES

Major industries over the study area includes Philips Carbon, Nitta Gelatin India Ltd, Cochin Kadaalas, KINFRA, Wonderla, Infopark Phase-1, Phase-2, Hindustan Organics Chemicals Limited (HOCL), Fertilizers and Chemicals Travancore (FACT), Kochi Refinery Limited (KRL), Smartcity, and the Cochin Special Economic Zone (CSEZ). The effluents and contaminants have smelling salts, calcium sulphate, phosphate, nitrate, ammonium sulphate and other anthropogenic effluents and weighty metals effluents from these modern units alongside rural find their path into nearby stream at last into Cochin backwaters have a great threat to the surface water quality of the study area. Due to this polluted water locals over there complained that this polluted water kills aquatic life like fish and damages agricultural crops etc. At the same time this polluted water also affects the food chain. Each day about 33,600-meter cube of pollutant is dumped into the Kadambrayar river. This study assists us with investigating the effects of modern effluents and its effect on the surface water quality of the study area.

3.8 DRAINAGE

Vembanad Lake, Kerala's largest lake, forms the south-western border of the Ernakulam district. The districts of Alappuzha and Kottayam also border the lake, in addition to Ernakulam. The lake opens to the sea in Cochin and is separated from the Lakshadweep Sea by a small barrier island. and further north at Munambam. At the southern end of the lake, where it empties into the Sea, is where Kochi (Cochin), the port. The region between Kochi Azhi and Munambam Azhi is referred to as Varapuzha. The lake is connected to neighboring coastal lakes to the north and south via canals. Kochi kayal refers to the area of the Vembanad Lake that is on and near the Kochi mainland.The lake is home to numerous islands, including those in the Ernakulum area,

such as Vypin, Mulavukad, Vallarpadam, and Willingdon Island. The Vembanad-Kol wetland system, of which the lake is a component, has a length of little over 96.5 kilometers and stretches from Alappuzha in the south to Azheekkode in the north, making it by far India's longest lake. Ten rivers feed the lake, including the Achenkovil, Manimala, Meenachil, Muvattupuzha, Pamba, and Periyar, the six largest rivers in central Kerala. The lake drains 15,770 km2 in total, which is 40% of Kerala's total land area. With an annual surface runoff of 21,900 mm, it contributes over 30% of the state's total surface water resources.

3.9 HYDROGEOLOGY

In worn and broken crystalline rocks, laterites, and unconsolidated coastal sediments, groundwater usually forms under phreatic conditions. It takes place in the deeply seated fractured aquifer of the crystalline rocks and Tertiary sediments under semi-confined to confined conditions. The weathered zone in the lower crystallines serves as an effective groundwater storage area. The aquifer can be divided into hard rock aquifers and sedimentary aquifers depending on how it formed.

Hard crystalline formation-While it occurs under semi-restricted to confined conditions in the deep-seated fractures of the crystalline formation, groundwater occurs under phreatic conditions in the shallow weathered parts. Primary porosity is generally absent in hard rock formations. The water is kept in the secondary pores that weathering caused to form in cracks, fissures, joints, etc. The degree of the fractures' connectivity regulates how much groundwater moves.

Sedimentary formations- The Warkali and Vaikom beds are among the prospective aquifers that can occur at deep inside the sedimentary formations, which are restricted to the coastal belt.

CHAPTER 4

METHODOLOGY

4.1 GENERAL PROCEDURE

Near Brahmapuram in Kochi, Kerala, samples of surface water were taken at 17 different locations. Without adding any preservative, the samples were collected in the 1000 ml polythene bottles. To prevent contamination, the bottles were rinsed with the water that was collected directly. The physical and chemical properties of these surface water sample bottles were measured in the lab.

Table1: Details of sampling locations

Sample No	Latitude	Longitude	Location Name
1	N9°59'37.31"	E76°21'17.78"	Rajagiri valley, Chittethukara (side of rajagiri college of engineering)
2	N 9°59'34"	E 76°21'15"	Rajagiri valley, Chittethukara (opposite side of rajagiri college of engineering)
3	N 9°59'31"	E 76°21'09"	kakkanad ferry terminal
4	N 9°59'32"	E 76°21'07"	seaport airport road (near Chithrapuzha bridge,Chittethukara, Kakkanad.)
5	N 9°59'27"	E 76°21'07"	below Chithrapuzha bridge Ernakulam (1)
6	N 9°59'29"	E 76°21'07"	below Chithrapuzha bridge Ernakulam (2)
7	N 9°59'28"	E 76°21'07"	below Chithrapuzha bridge Ernakulam (3)
8	N 9°59'28"	E 76°21'00"	below Chithrapuzha bridge Ernakulam (4)
9	N 9°59'23"	E 76°20'23"	Riverside, Chitrapuzha river
10	N 9°59'21"	E 76°20'48"	Chungath Road, Kochi (1)
11	N 9°59'19"	E 76°20'47"	Chungath Road, Kochi (2)
12	N 9°59'19"	E 76°20'54"	Chungath Road, kochi (3) (opposite of astro-7

			football)
13	N 9°59'12"	E 76°20'44"	Serene cottage Road, Kakkanad
14	N 9°59'09"	E 76°20'45"	Serene cottage Road, kakkanad (50 m away from previous location)
15	N 9°59'07"	E 76°20'45"	North, Irubanam, Thripunithara
16	N 9°59'04"	E 76°20'47"	Chithrapuzha river, kochi
17	N 9°59'25"	E 76°20'50"	River side ,50 m away from previous location Chithrapuzha river, kochi

The Multiparameter (Eutech instrument) was used to test the physical characteristics of the water samples, including pH value, Electrical Conductivity [EC], and Total Dissolved Solids [TDS]. The accurate value is displayed on the digital screen of the Eutech meter.

4.2 PHYSICAL PARAMETERS

4.2.1 pH CALIBRATION

1. Turn on the Eutech meter and confirm that the pH mode is selected. If not, press the MODE key until the pH mode appears.

2. After rinsing, put the electrode in the 4.0 Buffer solution. The calibration status will be visible on the main screen.

3. The adjusted buffer value (dark) will be displayed on the meter after the electrode is steady. For reading, the value stays constant.

4. After rinsing the electrode, put the second buffer—which has a pH value of 7—into the system. Then, wait for a steady pH measurement.

5. Repeat these steps using a buffer with a value of 10.

6. As a result, the calibration of a Eutech meter is carried out using water that has a pH value of 4, 7, and 10 (acidic, neutral, and basic, respectively). The instrument is now prepared to measure pH.

4.2.2 pH MEASUREMENT

Procedure:

1. A beaker is thoroughly cleaned with distilled water before a sample that needs to be measured is added.

2. Use the distilled water to rinse the waterproof electronic.

3. Pour the sample beaker's contents into the waterproof electronic.
Make sure the tip is not in contact with the beaker's bottom.

4. Measure the pH level of the sample by pressing the F3 button.

5. When the pH value appears on the screen and is stable, note the value.

6. Continue in this manner until you get the pH values for all of the samples.

4.2.3 ELECTRICAL CONDUCTIVITY(EC)

Procedure:

1. A beaker is thoroughly cleaned with distilled water before being filled with a water sample that needs to be measured.

2. Use the distilled water to rinse the electrode.

3. Insert the electrode into the beaker containing the sample of surface water.

4. To test the conductivity of the sample that was obtained, press the F3 button to switch the meter's mode to conductivity.

5. Note the value for steady conductivity.

6. Keep doing this until you get the remaining samples' electrical conductivity.

4.2.4 TOTAL DISSOLVED SOLIDS(TDS)

Procedure:

1. A beaker is thoroughly cleaned with distilled water before being filled with a water sample that needs to be measured.

2. Use the distilled water to clean the electrode.

3. Dip this electrode into the beaker containing the sample for testing.

4. To switch the meter's mode to TDS (Total Dissolved Solids), use the F3 button.

5. Measure the Total Dissolved Solids.

6. Note the constant TDS value.

7. Keep going through this process until you have the total dissolved solids value for all of the samples.

4.3 CHEMICAL PARAMETERS

To evaluate chemical parameters such as alkalinity (the presence of carbonate and bicarbonate), total hardness (the concentration of calcium ions and magnesium ions), and the chloride content in the samples, multiple chemical analyses were performed on them. By applying titrimetric chemical analysis, they were identified.

4.3.1 ALKALINITY TEST

To determine the presence of carbonate and bicarbonate

Procedure:

1. Dilute 2.8 ml of$H_2SO_4$by mixing it with 1000 ml of purified water. Burette is filled with this H_2SO^4 solution.

2. Pour distilled water into the beaker and wash it before adding 50 ml of the sample solution.

3. Refill the conical flask with the sample solution after cleaning it with distilled water.

4. Add two drops of phenolphthalein to the sample solution in the conical flask. The pink color of the solution indicates the presence of CO_2; otherwise, CO_2 is absent (i.e., carbonate is not present).

5. Add three drops of methyl orange into the same sample solution.

6. Titrate the sample solution against H_2SO_4 solution which is filled in the burette till the straw yellow color changes to pale pink color.

7. Note down the burette readings.

8. Repeat the same procedure with the remaining samples.

4.3.2 TOTAL HARDNESS

Total hardness is a measurement of a water's capacity to precipitate insoluble calcium, magnesium, and other hard metals. In reality, it assesses water quality rather than pollution levels.

4.3.3 TOTAL Ca and Mg CONTENT

Procedure:

1. Fill the burette with EDTA (ethylenediaminetetraethanoic acid) solution.

2. Take 50ml of sample in a clean conical flask and add 1ml of ammonium buffer

solution and shake well.

3. Add 2 drops of EBT indicator (Erichrome Black-T) in the sample.

4. Titrate the sample solution against EDTA till the wine-red changes to steel blue.

5. Record the burette values.

6. Repeat this process with the remaining samples.

4.3.4 CALCIUM CONTENT

Procedure:

1. Make 1N sodium hydroxide and fill it in the burette (40g of NaOH pellets were

make up by adding 1000ml of distilled water).

2. Take 50ml of sample solution in a clean conical flask and add 20-40mg of

murexide indicator.

3. Titrate the sample solution against NaOH till the reddish-purple changes to

blue-purple color.

4. Note down the burette values.

5. Repeat this process with the remaining samples.

4.3.5 CHLORIDE DETERMINATION

Procedure:

1. The silver nitrate ($AgNO_3$) solution is added to the burette.

2. Take 50ml of sample solution in a clean conical flask and add 1ml of potassium chromate indicator.

3. Titrate the sample against burette having the silver nitrate solution. The end point is yellow to red.

4. Record the burette values.

5. Repeat this procedure with the remaining samples.

4.3.6 POTASSIUM DETERMINATION

Using flame photometer method determination of potassium was done.

Procedure:

1. Dissolve 1.9070 g of KCl in one litre of dissolved water to make 1000 ppm KCl standard solution.
2. 10 ml of standard solution is pipetted out to 100 ml volumetric flask and make up to 100 ml with distilled water to make 100 ppm standard solution.
3. Pipette 10 and 5 ml from 100 ppm solution to 100 ml volumetric flask and make up to 100 ml of flask with distilled water to make 10 and 5 ppm standard solution.

4. Set low concentration method in flame photometer.
5. 10 and 5 ppm standard solutions are used to calibrate flame photometer.
6. For every 10 samples calibration process should be done.
7. Note the reading of potassium present in the sample.

4.3.7 SODIUM DETERMINATION

Using flame photometer method determination of sodium was done.

Procedure:

1. Dissolve 2.5416 g of NaCl in one litre of distilled water to make 1000 ppm NaCl standard solution.
2. Pipette 4, 6, 8 and 10 ml from 1000 ppm standard solution to 100 ml volumetric flask and fill rest with distilled water to make 40, 60, 80, and 100 ppm standard solution.
3. Set high concentration method in flame photometer.
4. 40, 60, 80, and 100 ppm standard solutions are used to calibrate the flame photometer.
5. For every 10 samples calibration process should be done.
6. Note the reading of sodium present in the sample.

4.3.8 SULPHATE DETERMINATION

Using turbidimeter sulphate determination was done.

Procedure;

1. Take 50 ml of sample in cuvette after rinsing it with distilled water.
2. Add 10 ml of sulphate buffer and a pinch of barium chloride to it and shake well.
3. Cuvette is placed in turbidimeter.
4. Record the readings of the turbidimeter.
5. Repeat the procedure for remaining samples.

4.4 DETERMINATION OF MICROPLASTIC DISTRIBUTION IN SURFACE WATER

Procedure:

1. Filtration apparatus is rinsed with distilled water. After placing filter paper in filter holder 1000 ml of sample is added to the funnel which is attached to the filter holder then to a 1000 ml conical flask which is secured with a clamp. Filter paper used for this has 47 mm diameter and pore size of about 0.45 micrometer.
2. Using a tube filter holder is connected to a vaccum-pressure motor pump.
3. Once the sample is added switch on the motor and the filtration unit starts working.
4. After completion of filtration the filter paper is taken from the apparatus.
5. Filter paper is viewed under microscope for microplastic distribution.
6. Repeat the procedure with the remaining samples.

Figure 2: Field and lab photos

CHAPTER 5

RESULT AND DISCUSSION

5.1 Quality parameters

According to different sources quality parameters can vary. Parameters are mainly divided into two physical and chemical parameters. EC, TDS, Ph are the physical parameters and chemical parameters include magnesium, sodium, potassium, calcium, chloride, bicarbonate, sulphate, total hardness.

Table2: Min-Avg-Max values of physico-chemical parameters

Parameters	Maximum	Minimum	Average
pH	6.38	5.92	6.14
EC (μS/cm)	294.5	101.5	175.47
TDS (mg/l)	1473	507.5	877.51
HCO_3(mg/l)	1.2	0.2	0.7
Cl(mg/l)	40	12.1	22.9
SO_4(mg/l)	35.1	4.4	16.12
Na(mg/l)	228.33	102.91	159.57
Mg(mg/l)	26.16	10.08	17.04
Ca(mg/l)	144	28	83.29
K(mg/l)	18.66	7.40	11.70
Total hardness	467.2949	146.0166	278.15

5.1.1 pH

One of the most important and often utilized water chemistry investigations is pH measuring. The strength of a solution's acidic or basic character at a specific temperature is indicated by pH or hydrogen ion activity. The pH idea was first proposed by the Danish biochemist Soren Peter Lauritz Sorensen in 1909. The equation can be given as: -

$$pH = -\log[H^+]$$

The physical parameter of pH is crucial for analyzing the acid-base stability of water. Alkaline concentration rises as pH values rise, while acid concentration falls as pH values fall. It also measures the alkaline and acidic conditions of water. All aquatic life has a range of pH tolerances, and changes in pH can have an impact on some substances' solubility and toxicity. The pH of surface water can vary depending on a number of factors, such as location, day of the week, season, and human activity.

In the current review pH value ranges from 5.92 to 6.38. The acceptable limit of pH is 6.5-8.5 (as per IS: 2296).and all samples have pH below the permissible limit. So, all samples are considered as acidic according to pH scale.

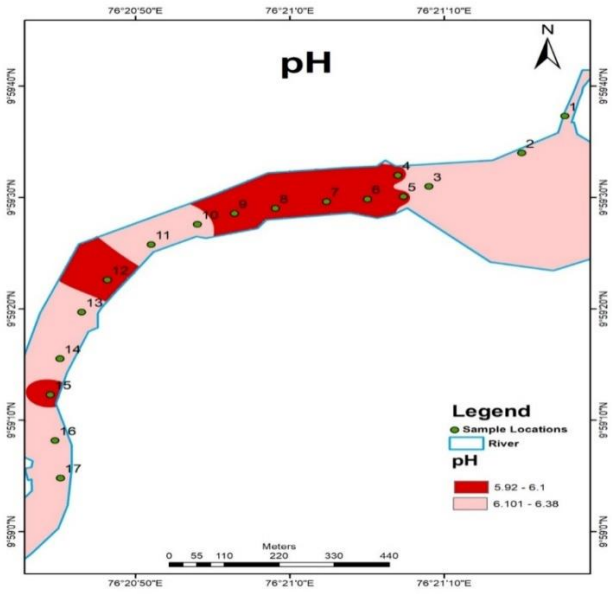

Figure 3: Spatial distribution of pH

In this investigation red color shows the sample with very-low pH and pink color shows the samples with low pH.

In the year 2016 and 2017, the average pH value of Kadambrayar river at Brahmapuram area was 6.65 and 6.35 respectively (ACTION PLAN FOR RIVER KADAMBRAYAR – KERALA (OA No.673/2018). The average value of the current study is 6.14, which shows that the pH loadings are tend to become more acidic over the years. It may be due to the influence of industrial inputs and the less alkaline nature of the study area. The lower pH in the surface water will eventually influence the unconfined aquifers by infiltration. Thus, the periodic change in pH must be monitored otherwise, the quality shift in surface water will ultimately deteriorate the quality of groundwater as well.

5.1.2 ELECTRICAL CONDUCTIVITY (EC)

The ability of a substance to conduct electricity through itself is measured by the dissolved material's Electrical Conductivity (EC), which is found in an aqueous solution. Seimens per unit area are the units used to measure EC. SI units for "siemens per meter" The nature and quantity of ionic species present affect the movement of ions in solutions, which controls a solution's capacity to conduct an electrical current. A solution's conductivity and the quantity of current it can carry are inversely related to its resistance. In addition, the temperature of the solution and the quantity, mobility, valence, and type of ions present all play a role. The concentration of TDS in a sample is inversely related to its specific conductance. The type of ions present, their relative quantities, the water's ionic strength, dissolved carbon dioxide, turbidity, and temperature all have an impact on how conductivity is measured.

Pure water has a relatively limited electrical conductivity. River water conducts electricity because ionic species are present. As the ion concentration rises, the sample's conductance rises as well. Rivers receive ions from a variety of sources, which are reflected in the different conductance levels they have, including industrial effluents, municipal trash, mining operations, farm runoffs, and other sources.

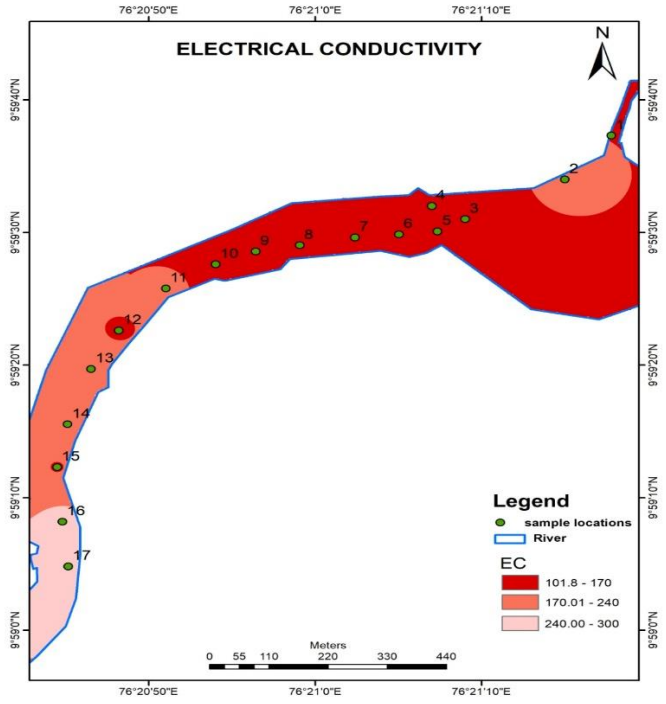

Figure 4: Spatial distribution of electrical conductivity

Pink color indicates samples with highest electrical conductivity. Red color represents the samples with low EC when compared with other samples. EC increases with increase in ion concentration so sample 16 marks the highest EC 294.5 (µS/cm) due to high concentration of different ions. Sample 4 recorded the lowest electrical conductivity 101.5(µS/cm) is due to low concentration of ions compared to all other samples.

5.1.3 TOTAL DISSOLVED SOLIDS (TDS)

The amount of organic and inorganic substances dissolved in water is measured using a TDS. High TDS levels can cause a water sample to taste or smell unpleasant and can also indicate the presence of heavy metal contaminants. Inorganic and some organic minerals, as well as various salts, such as potassium, calcium, sodium, bicarbonates, chlorides, magnesium, sulfates, and others, can be dissolved by water. Natural sources, sewage, animal waste, urban runoff, industrial wastewater, and chemicals employed in the water treatment process are all sources of

TDS in surface water. These minerals give water an unpleasant flavor and color. This crucial method is employed to ensure the safe use of water. The presence of any of the aforementioned minerals in significant concentrations in water shows that it is highly mineralized.

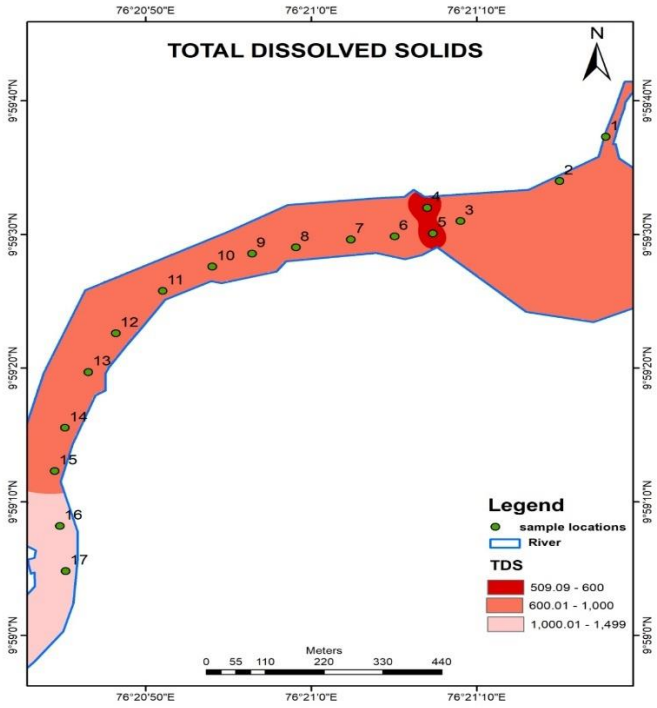

Figure 5: Spatial distribution of total dissolved solids

In this investigation, TDS of all samples are within the limits. Pink color in map represents samples with highest TDS whereas dark red color shows the samples with low TDS. Light red indicates samples with TDS intermediate between the other ones. Sample 16 has highest TDS 1473 mg/l is due to increased number of dissolved solids in water it can be organic, inorganic matter, various salts and industrial wastewater etc. Also sample 16 has recorded highest amount of sodium, potassium, calcium. Sample 4 has lowest TDS 507.5 mg/l is due to reduced number of dissolved solids in water. Dissolved solids can produce hard water soaps and detergents do not produce as much lather in hard water than soft water.

5.2 CHEMICAL PARAMETERS

5.2.1 CHLORIDE

All kinds of water contain the inorganic anion chloride (Cl^-), which is one of the anions. The saltiness of the water depends on the amount of chloride present in it. A water sample with 250 mg Cl^-/L might leave behind a distinctly bitter flavor if the cation is sodium.

All bodies of water contain chloride, but concentrations are normally modest. In most surface waters, chloride concentrations are safer than sulphate or bicarbonate values.

Anomalies include waterways that accumulate high-chloride groundwater, radioactive wastewater, or are impacted by ocean tides.

One of the main ions in surface water is chloride. The presence of chloride ions in water is caused by the strong ion mobility and high solubility of the chloride salt. As the mineral content rises, the chloride content typically follows. Chloride in surface water can come from a variety of places, including the weathering and leaching of sedimentary rocks and soils, seawater infiltration, the discharge of household and commercial waste, municipal effluents, irrigation drainage, the dissolution of salt deposits, etc. The chemical makeup of the water determines how salty chloride ions taste. Chloride is typically a conservative characteristic and can be used as a measure of pollution coming from primary sources like industrial and municipal outputs in natural freshwater.

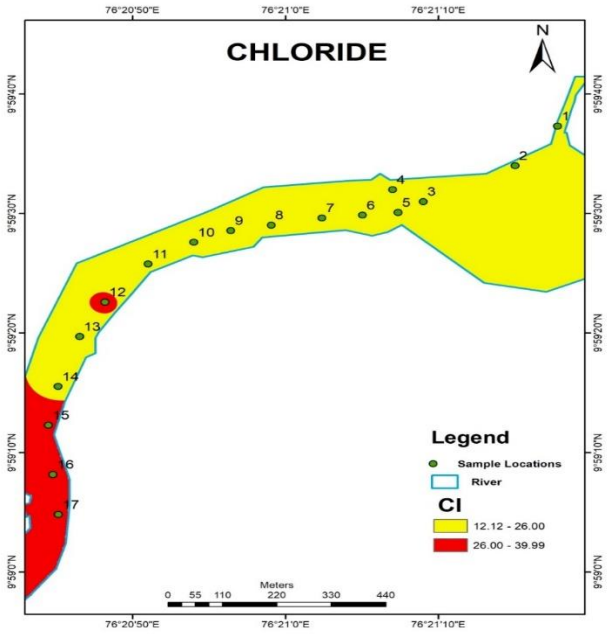

Figure 6: Spatial distribution of chloride

Sample 16 has highest chloride value about 40 mg/l and sample 4 recorded lowest chloride value12.1 mg/l. red color represents samples with highest chloride values compared to other samples. Yellow color indicates samples with low chloride values. Sample 16 shows high chloride value may be due to anthropogenic activities such as industrial effluents, animal feeds, irrigation drainage, use of inorganic fertilizers etc.

5.2.2 CALCIUM

Ca is thought to be abundant in the earth's crust at 4.9 percent, in soils at 0.07 to 1.7 percent, in lakes at about 15 mg/L, and in groundwater at 1 to 500 mg/L.

A key component in many geochemical processes is calcium. Streams flowing over dolomite, limestone, gypsum, and other calcium-containing rocks and minerals are a natural source of calcium. Surface water has large amounts of calcium and magnesium, which can also be found as bicarbonate, chloride, and sulfate. In freshwater, calcium is the cation that is most frequently observed. Calcium can be easily dissolved from rocks or leached from soil.

In the treatment of wastewater and drinking water, lime (Cao), hydrated lime ($Ca(OH)_2$), and limestone ($CaCO_3$) are frequently used to raise pH levels and precipitate metal pollutants. Pharmaceuticals, lights, lime, deicing salts, colorants, fertilizers, insecticides, and plasters all require calcium compounds. pH and dissolved CO_2 control the solubility of calcium carbonate.

Calcium is an essential component of both plants and animals' diets and is found in bones, shells, and plant tissues. Marine creatures are less exposed to some metals in water when calcium is present. Numerous studies demonstrate that water hardness protects against cardiovascular disease.

One possible negative effect of consumption of elevated calcium concentrations for prolonged periods of time may be an increased chance of kidney stones. Very low levels of calcium can raise the damaging effects of sodium in water irrigation by raising the SAR (Sodium Adsorption Ratio).

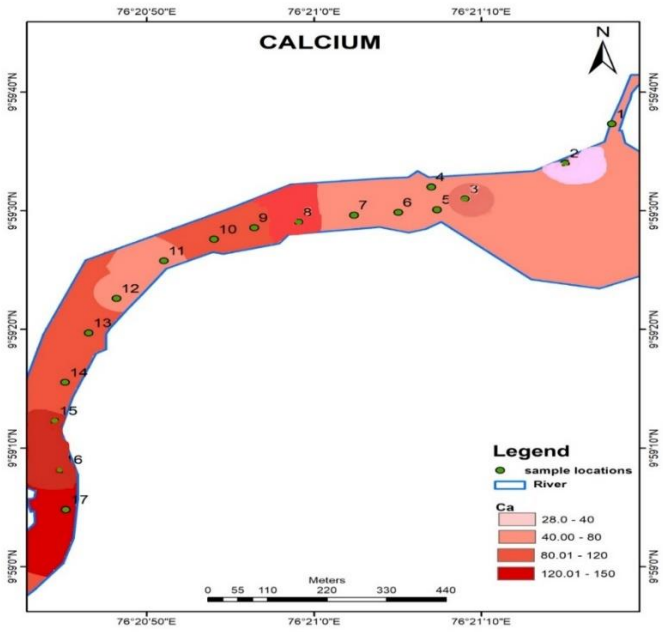

Figure 7: Spatial distribution of calcium

From spatial map given below it is understood sample 3 has lowest calcium value 28 mg/l and samples 16,17 has highest about 144 mg/l. Anthropogenic activity and due to waste from Brahmapuram plant may cause these changes in rivers. The increase in calcium value in these samples may be due to the gradual weathering of their watersheds and the leaching of calcium from soils and rocks by river and runoff. As calcium increases in surface water also increases the hardness of the water. Light pink in the map shows the samples with lowest Ca value and dark red represents samples with highest value.

5.2.3 MAGNESIUM

The average amount of magnesium in the earth's crust is 2.1%; in soil, it ranges from 0.03 to 0.84%; in lakes, it is 4 mg/L; and in earth waters, it is 0.5 mg/L.

Magnesium is utilized in the textile, tanning, and paper industries. Molds, castings, extrusions, luggage, and sheets and sheets of rolling and plating, mechanical handling, small tools, household goods all frequently use lightweight magnesium alloys. Magnesium carbonates, chloride, hydroxides, oxides, and sulphates are used in the production of metal magnesium, refractories, fertilizers, ceramics, weaponry, and pharmaceutical items. Magnesium is a naturally occurring element that can be found in the earth's crust.

Natural water rarely possesses conditions that are favorable for rapid dolomite aggregation, and equilibrium associations of magnesium carbonate are more challenging than those of calcium. When boiled, magnesium salts break down, creating scale in boilers and greatly increasing the hardness of the water.

Magnesium has emerged as a crucial mineral for both plants and animals due to its role in the development of bones and cells. The substance is found in bone (700–1800 mg/kg), sea algae (6300–21000 mg/kg), marine fish (1250 mg/kg), mammalian (900 mg/kg), and tissue containing calcareous diet (750–5600 mg/kg). One of the main soft tissue cations is magnesium. Red blood cells and chlorophyll are crucial components. Magnesium is frequently beneficial in water; however, some magnesium salts can be dangerous when ingested or inhaled.

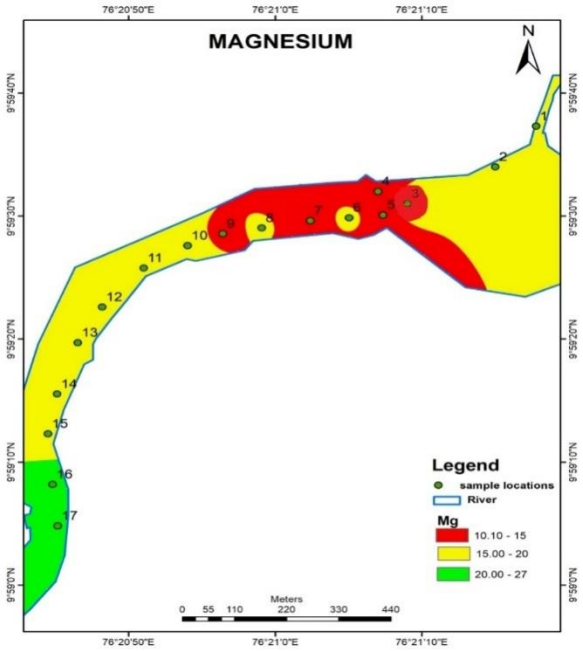

Figure 8: Spatial distribution of magnesium

In this investigation red color represents the samples with lowest magnesium values that have been recorded. Green color indicates the samples with highest magnesium values compared to other samples. Yellow represents the intermediate samples. Sample 3 and sample 16 recorded lowest 10.08 mg/l and highest magnesium 26.16 mg/l values respectively.

5.2.4 BICARBONATE

The main source of subsurface water is bicarbonate. The alkalinity of water is a measure of its ability to neutralize. Depending on the presence of dissolved CO_2 and carbonic acid, the carbonate minerals present along the path will be dissolved during infiltration of rainwater and irrigation water. During the recharge process, HCO_3 and Ca will be released into the groundwater. Another polyatomic ion is bicarbonate (HCO_3), although it has a 1-negative charge. It has one hydrogen atom, one carbon atom, and three oxygen atoms. When carbon dioxide dissolves in water and interacts with a base, like sodium hydroxide, bicarbonate is created. It is frequently present in natural waterways and contributes significantly to the water's ability to act as a buffer, keeping pH levels within a certain range. Water can contain carbonate

and bicarbonate, both of which can change the chemical composition of the liquid. For instance, bicarbonate can make water more alkaline and therefore more resistant to pH shifts.

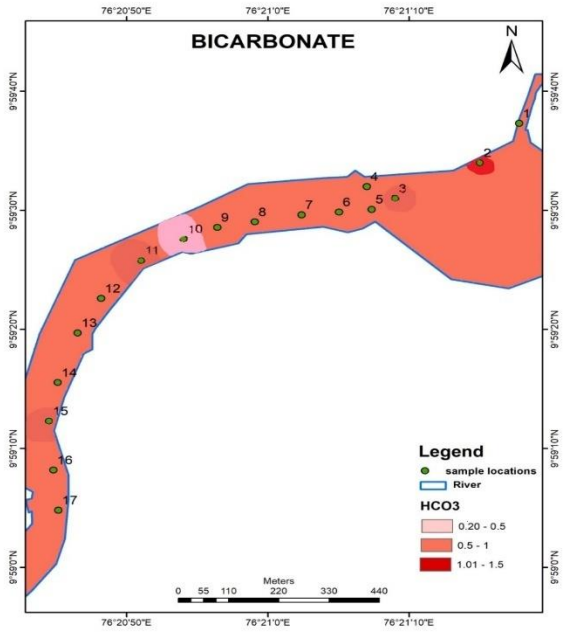

Figure 9: Spatial distribution of bicarbonate

From spatial distribution map of bicarbonate, it is understood that sample 2 recorded highest value 1.2 mg/l and sample 10 has lowest value of about 0.2 mg/l. The reason for this could be excessive waste from Bhramapuram plant and industrial effluents. Anthropogenic activities are another fact which affect these values.

5.2.5 TOTAL HARDNESS

The ability of water to precipitate insoluble calcium and magnesium as well as heavy metal salts of higher fatty acids from soap solution is known as hardness. Water hardness is a measure of water quality rather than pollution. Calcium and magnesium, together with bicarbonate, carbonate chloride, and sulfate, are the primary cations responsible for hardness. In regions with heavy topsoil and limestone formations, hard waters first appear. High hardness levels have physio-chemical implications. Water with a high hardness content deposits scale in boilers, utensils, and water supply pipes, and excessive soap use is followed by scum formation.

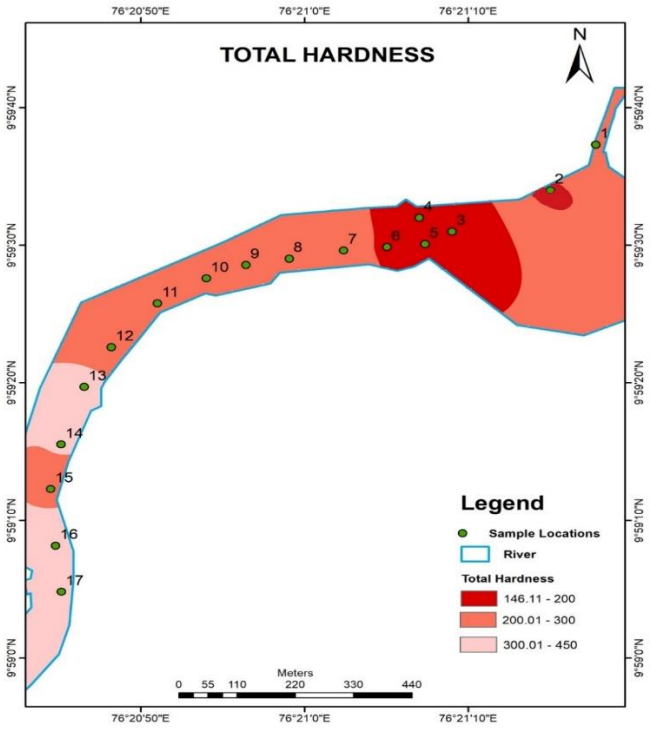

Figure 10: Spatial distribution of total hardness

From spatial distribution map of total hardness shows that pink color indicates samples with high total hardness values whereas red color shows samples with low values. Light red represents samples with intermediate values. Sample 2 and sample 16 has lowest 146.01 mg/l and highest 467.29 mg/l values respectively. The variation in total hardness is mainly dependent upon the calcium and magnesium values. Sample 2 has lowest calcium and magnesium values compared to other samples due to this it has recorded lowest total hardness, vice versa in case of sample 16. Total hardness of river may be affected by the activities of humans and due to several nearby industries.

5.2.6 SODIUM

Sodium is one of the cations that can be found naturally. Na is thought to be abundant on the earth's surface at a rate of 2.5%, in soils at a rate of 0.02 to 0.62 percent, in lakes at a rate of 6.3 mg/L, and in groundwater at a rate of 5 mg/L. In salt deposits and silicates, sodium can be employed. Aqueous is strongly miscible with sodium salts and is softened by them. In terms of

quantity, sodium is found in the sixth place among the components in most natural water. Sodium ions enter water through the weathering of rocks. Domestic sewage is a significant source of sodium in river water.

Water that contains salt has a sour flavor, causes foaming, and corrodes metals. Higher sodium levels are bad for plants, people with kidney and heart problems, and even animals. The sodium-to-total-cation ratio plays a significant role in both productivity and land physiology. Permeability of the soil might be harmed by a high sodium ratio. Since it closes the soil's pores and makes it resistant to water circulation, water with a high salt level is bad for the environment. If there is a significant concentration of it, it will have an impact on those who have heart issues. The high sodium content of the water has an impact on the soil's physical condition. It is advised to use a controlling density of 2 to 3 mg/L in feed streams for high-pressure boilers.

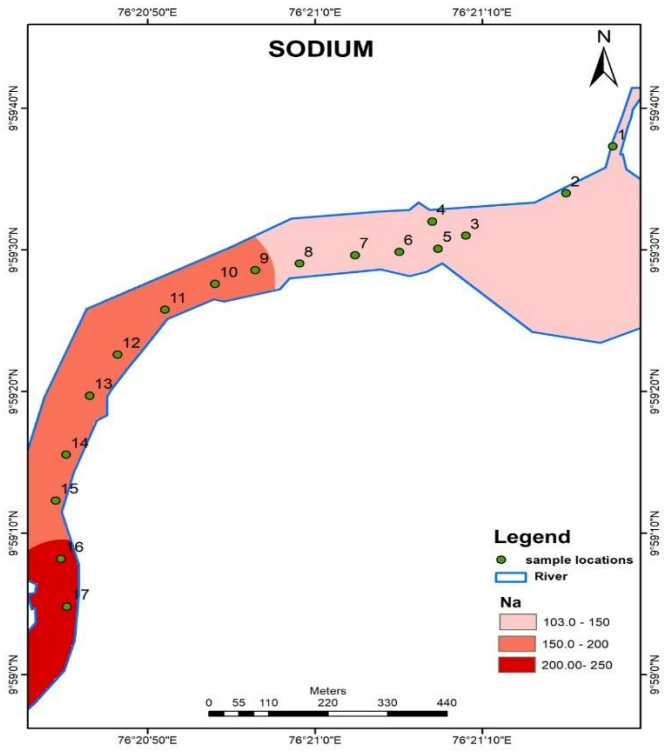

Figure 11: Spatial distribution of sodium

In this investigation of sodium samples marked pink shows values with low sodium values and dark red represents highest sodium values. Light red indicates intermediate values. Sample 4 and sample 16 recorded lowest 102.91 mg/l and highest 228.33 mg/l sodium values respectively. Sample 15 and 16 recorded highest values may be due to industrial impacts on the river and anthropogenic activities. As towards southern part of study area concentration of dissolved sodium and chloride ion increases that can replace other nutrients in the soil. Plants absorb chloride and sodium instead of potassium and phosphorus, leading deficiencies.

5.2.7 POTASSIUM

The abundance of potassium ranges from 0.1 to 2.6 percent in soils, 2.3 mg/L in lakes, and 0.5 to 10 mg/L in ground waters, with an average abundance of 1.84 percent in the earth's crust. In terms of super fluidity, potassium is the eighth most fluid element in most natural water.

Natural water contains potassium because of the weathering of rocks. It is a K_2O type and is present in flash. Feldspars are an example of an alumina-silicate mineral that contains potassium. In comparison to sodium, calcium, and magnesium concentrations, potassium concentrations in marine environments are often substantially lower. The amounts of sodium and potassium are only equal in water with little mineral content. The chemistry of potassium is somewhat similar to that of sodium, and it mostly remains in solution without precipitating. Potassium ions, which are incorporated into a variety of clay-mineral formations, are absorbed by plants. Two things contribute to the lack of potassium ions in water: the vulnerability of potassium minerals to weathering and the fixation of potassium ions in clay minerals.

Containers, fertilizers, baking powder, soft beverages, bombs, pigments, and other goods all include potassium compounds that eventually wind up in rivers. Being a crucial component of nutrients, potassium must be present in natural water. It is a significant nutrient for both plants and people.

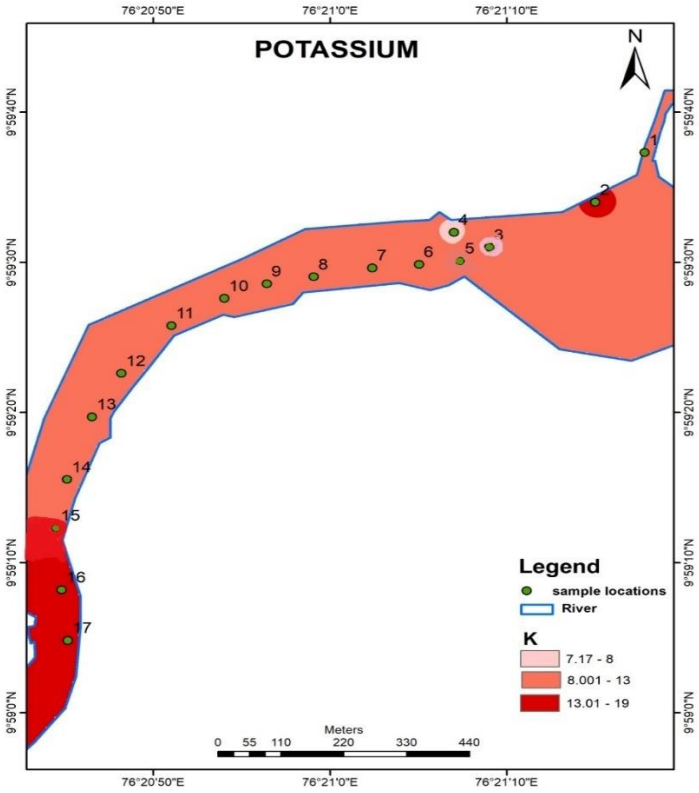

Figure 12: Spatial distribution of potassium

In this investigation pink color in spatial distribution map given below indicates the samples with low potassium value whereas dark red shows the samples with highest potassium values compared with other all samples. Light red indicates the intermediate values. Sample 4 recorded lowest value of 7.40 mg/l. Sample 16 has recorded the highest value 18.66 mg/l, is due to excessive waste dumped by near factories and because of anthropogenic activity.

5.2.8 SULPHATE

Sulfur can exist in a variety of oxidation states, ranging from $S2^-$ to $S6^-$, and the redox characteristics of aqueous environments have a significant impact on how it behaves chemically. In its most intensely oxidized state, the sulfur ion's effective radius forms a stable four-coordinate structure with oxygen. Iron is abundant and extensively distributed, and iron sulphones have a considerable impact on the geochemistry of sulfur. The output of growing plants and animals depends on the element.

Sulfur is oxidized when sulfide minerals weather in the presence of aerated water, producing sulfate ions that dissolve in the water. Hydrogen ions are created in significant quantities during this oxidation process. Many sedimentary rocks contain pyrite crystals, which add ferrous iron and sulphate to the ground water.

The oxidation of metal sulphates released from numerous factories may be to blame for the river's high sulfate level. The lead, barium, and strontium sulphates are the outliers since they are insoluble in water.

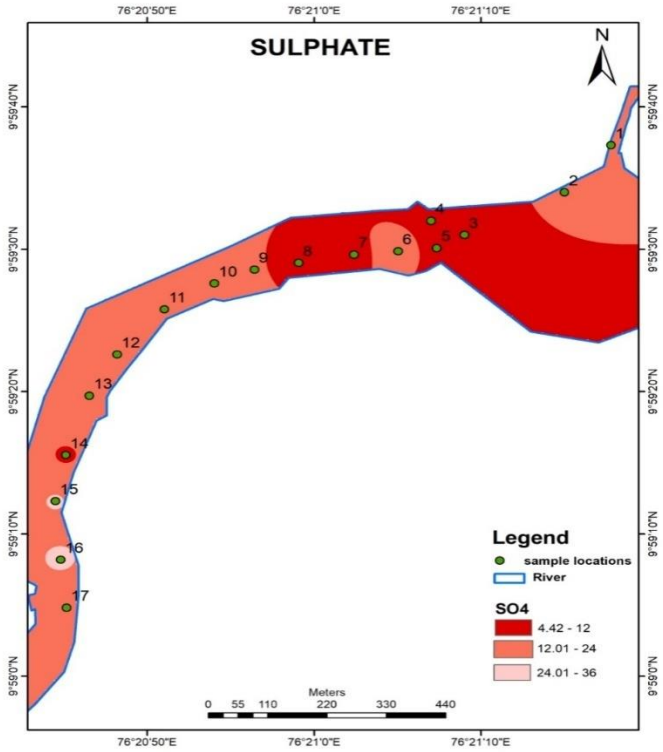

Figure 13: Spatial distribution of sulphate

Pink color shows the samples with high sulphate values compared to other samples. Red color indicates samples with low sulphate values. Light red represents intermediate values. Sample 2 recorded 4.4 mg/l being lowest recorded value. Sample 17 recorded highest sulphate value 35.1 mg/l due to industrial effluents that reaches the river. In other viewpoint sulphate values can be varied by anthropogenic activities. Industries near river has great impact on sulphate values.

5.3 IRRIGATION WATER CRITERIA (USSL DIAGRAM)

Irrigation water criteria mainly depends on the type of plants, soil, climate and amount of the irrigation water used. The salinity hazard can be estimated by measuring the electrical conductivity. Besides potential chargers from high salinity range and boron sodium hazard may exist. The two prone effects of sodium hazards are hardening of the soil and reduction of soil permeability. Both effects are caused by the replacement can be estimated by the sodium adsorption ratio (SAR) which is represented by the formula:

$$SAR = \frac{Na +}{\sqrt{\frac{Ca2+ + Mg2+}{2}}}$$

where the amounts of sodium, calcium, and magnesium are represented in milliequivalents/litters of representative ions. SAR values are widely used for the irrigation water classification as recommended by U.S Salinity Lab (USSL). This diagram enables the quality rating of irrigation water.

Table3: SAR values

ID	EC (µS/cm)	Na (meq/l)	Ca (meq/l)	Mg (meq/l)	SAR
1	188.9	6.35	4.2	1.49	3.764719209
2	166.8	5.93	1.4	1.51	4.916128167
3	105.8	4.5	2.8	0.82	3.344823658
4	101.5	4.47	2.2	0.88	3.602028649
5	158.1	5.77	2.6	1.33	4.116181684
6	122.2	4.88	3.6	0.98	3.22479477
7	157.2	5.77	3.4	1.25	3.784115072
8	149.6	6.95	4.6	1.16	4.095326774
9	167.7	7.4	4.6	1.39	4.275956775
10	174.3	7.62	3.8	1.47	4.69423321
11	167.8	7.38	3.8	1.45	4.555034891
12	194.4	8.08	4.8	1.61	4.51333265
13	189.5	7.9	4.6	1.41	4.557270982
14	168.6	7.3	4	1.33	4.47171641
15	252.4	9.03	6	1.88	4.549248278
16	294.5	9.92	7.2	2.14	4.590428549
17	223.7	8.55	7.2	1.55	4.087681844

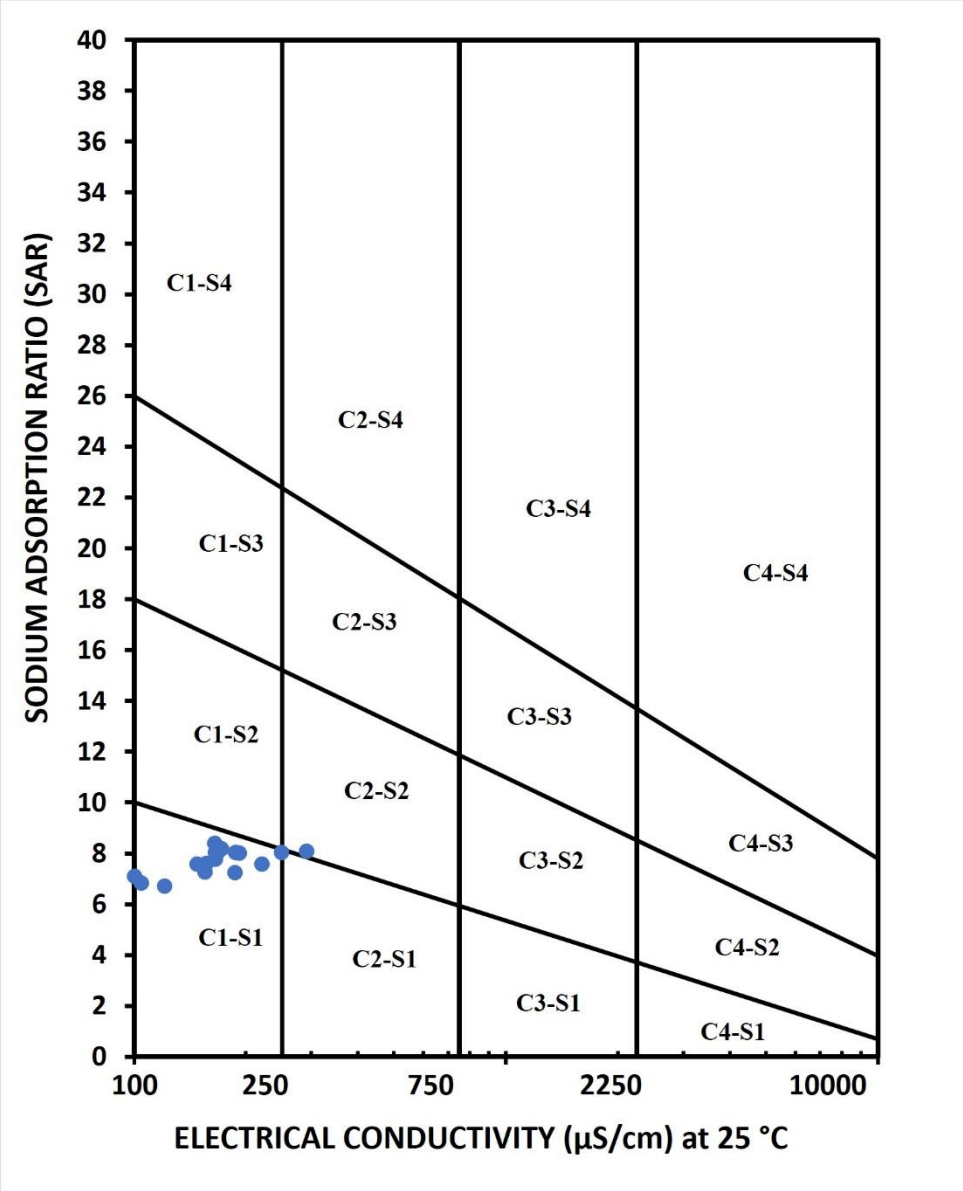

Figure 14: USSL DIAGRAM

Table 4: Explanations of USSL diagram

Explanations	
Based on Sodium Adsorption Ratio (SAR) and Electrical Conductivity (EC) (µs/cm) The irrigation water quality is classified as follows:	
EC (µs/cm)	C1 stands for Low Salinity Hazard
	C2 stands for Medium Salinity Hazard
	C3 stands for High Salinity Hazard
	C4 stands for Very High Salinity Hazard
SAR	S1 stands for Low Sodium (alkali) Hazard
	S2 stands for Medium Sodium (alkali) Hazard
	S3 stands for High Sodium (alkali) Hazard
	S4 stands for Very High Sodium (alkali) Hazard

Class	Explanation
C1-S1	Very good quality
C2-S1	Good quality
C3-S1	Medium quality
C4-S1	Bad quality
C1-S2	Good quality
C2-S2	Good quality
C3-S2	Bad quality
C4-S2	Bad quality
C1-S3	Medium quality
C2-S3	Medium quality
C3-S3	Very bad quality
C4-S3	Very bad quality
C1-S4	Bad quality
C2-S4	Bad quality
C3-S4	Very bad quality
C4-S4	Very bad quality

According to USSL diagram most of the samples falls on the C1-S1 class which indicates the water is very good quality for irrigation except sample 15 and 16. Sample 15 and 16 falls on the

C2-S1 class indicates the water is good quality for the purpose of irrigation. Overall water over there can be used for irrigation purposes.

5.4 HILL -PIPER'S TRILINEAR DIAGRAM

The classification for cation and anion facies, in terms of major ion percentages and water types, is according to the domain in which they occur on the diagram segments (Back, 1966). To define composition class, Back and Hanshaw (1965) suggested subdivisions of the tri-linear Diagram

Hill Piper's Trilinear diagram has two lower triangular fields and a central diamond shaped field. Cations expressed as a single dot in uniquely related to the total ion concentration. Similarities and differences among water sample can be inferred from triangular diagram. Water of same qualities will tend to plot together as a group.

Distinct water quality can be quickly distinguished by their plotting in certain areas of the diamond shaped field. The field is drained into 9 such areas: -

Table 5: Subdivision of diamond of Piper diagram

Subdivision of the diamond	Characteristics of the corresponding subdivisions of diamond shaped field
1	Alkaline earth (Ca + Mg) exceeds alkalis (Na + K)
2	Alkalis exceed alkaline earths
3	Weak acids (CO_3+HCO_3) exceed strong acids (SO_4+Cl)
4	Strong acids exceed weak acids
5	Magnesium bicarbonate type
6	Calcium- chloride type
7	Sodium-chloride type
8	Sodium-bicarbonate type
9	Mixed type (no cation-anion exceed 50%)

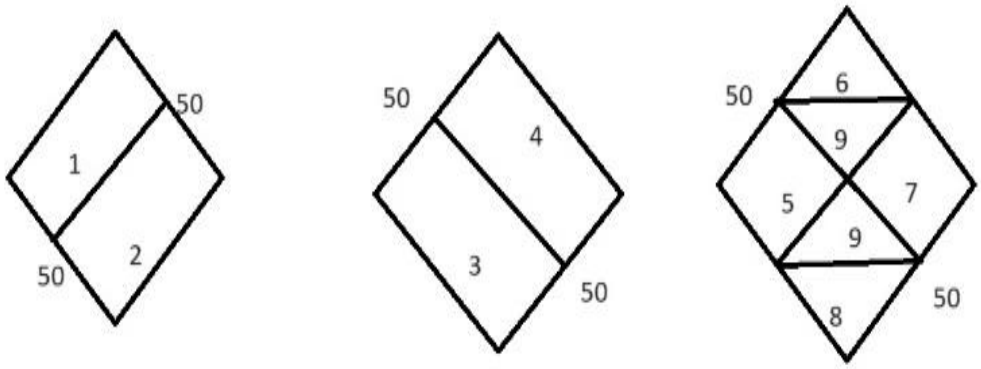

Figure 15: Subdivision of diamond of Piper diagram

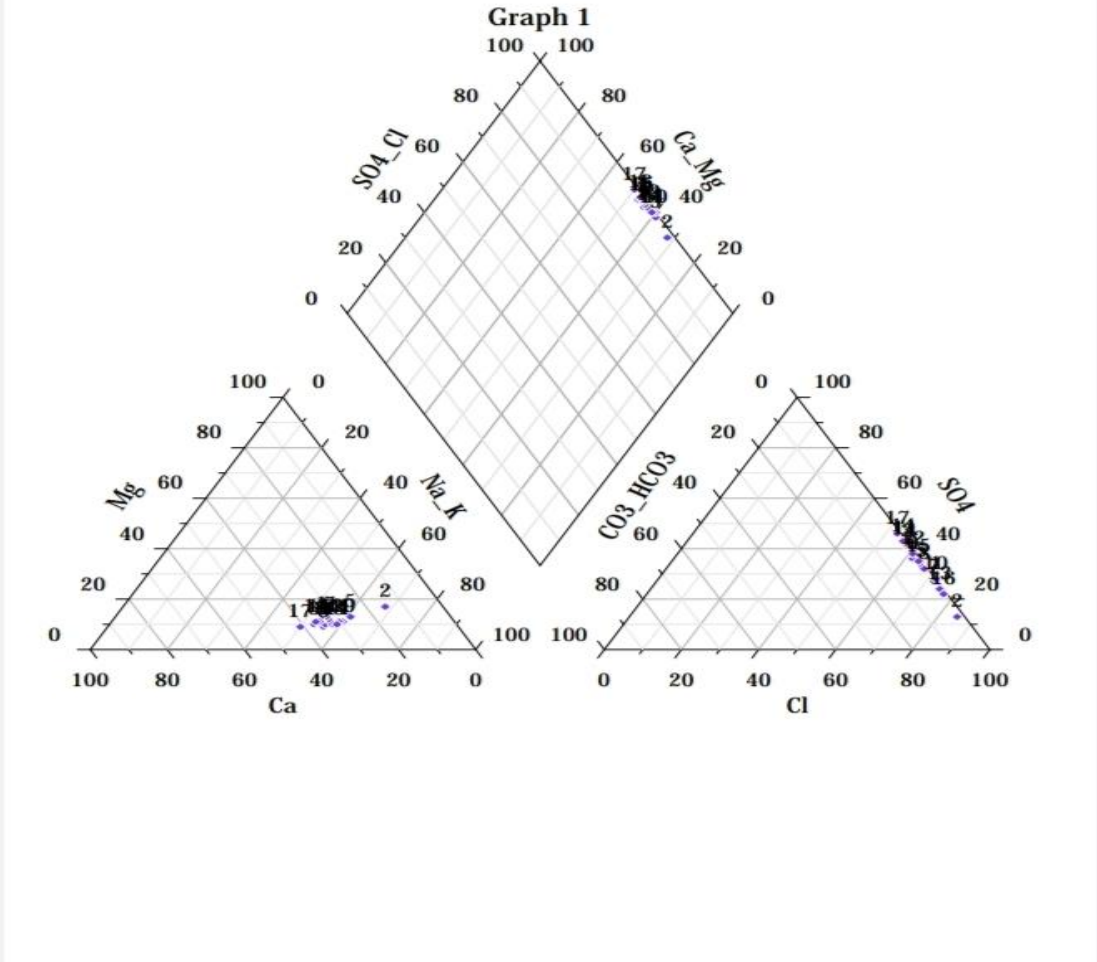

Figure 16: Hill Piper's Trilinear Diagram

According to hill piper's trilinear diagram the water samples fall on the 7th area which indicates it is of sodium chloride type water. From this diagram it is also inferred that alkalis exceeds alkaline earths and also strong acids exceeds weak acids.

5.5 ANALYSIS OF MICROPLASTICS

The total amount of microplastics was initially measured, and visual evidence was recorded. All of the samples included microplastics. Microplastics were seen in a range of hues, including black, blue, green, pink, and purple. The samples showed a high fiber content. Additionally, each of these artifacts was carefully catalogued and categorized in accordance with their colour. The colour of the microplastics served as the basis for the study, and an Excel spreadsheet was used to generate a graphical representation of the microplastics present in surface water samples.

SAMPLE NO	FIBER					FILAMENT	
	black	blue	pink	green	purple		Total
1	6	0	3	5	0	0	14
2	6	1	1	0	0	0	8
3	7	0	0	1	1	0	9
4	3	0	0	0	0	0	3
5	1	0	1	1	0	0	3
6	5	2	2	0	3	0	12
7	2	0	1	0	0	0	3
8	7	1	2	2	0	0	12
9	5	2	6	0	0	0	13
10	5	1	4	0	0	0	10
11	6	0	5	1	0	2	14
12	4	0	2	0	0	0	6
13	5	0	1	0	0	0	6
14	2	1	0	0	1	0	4
15	9	0	0	0	1	0	10
16	3	2	1	0	1	0	7
17	4	0	1	0	0	2	7
TOTAL	80	10	30	10	7	4	141

Table6: Table showing colours and count of Microplastics

Based on their colour, all of the water samples' fibers were categorized, measured, and identified. No additional information was provided on the fibers' precise makeup. Over 141 microplastics were collected overall during the treatment. With 80 occurrences, the colour black displayed the highest degree of dominance. After that, there were 10 occurrences of blue, 30 occurrences of pink, 10 occurrences of green, and only 7 occurrences of purple. The most microplastics are

present in sample number 11 and 14, total 14 particles. The least amount of microplasticsis found in Sample 4,5,7, total 3 particles.

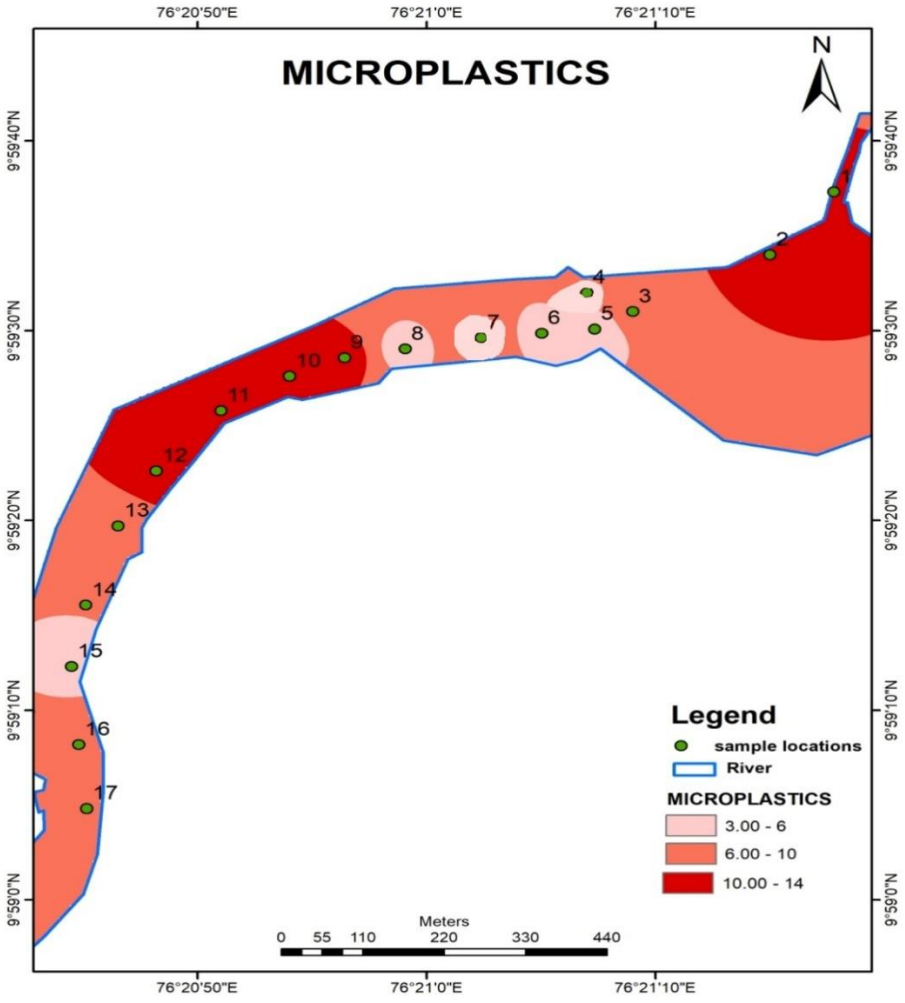

Figure 17: Spatial distribution of microplastics

From spatial map of microplastics it is understood that dark red represents the samples with highest number of microplastics and pink shows samples with microplastics ranging 3 to 6. Light red shows intermediate values. Sample 1 and 11 has highest number of microplastics about 14 items per litre. Excessive waste from Brahmapuram power has great influence over this

distribution of microplastics. Anthropogenic activities also have significant role in addition of microplastics over the river.

Microplastics found in surface water is a serious threat to aquatic life and causing reduction in their population. At the same time people will suffer from microplastic contamination as fishes are part of food chain. Gradually, it causes the destruction of entire ecosystem.

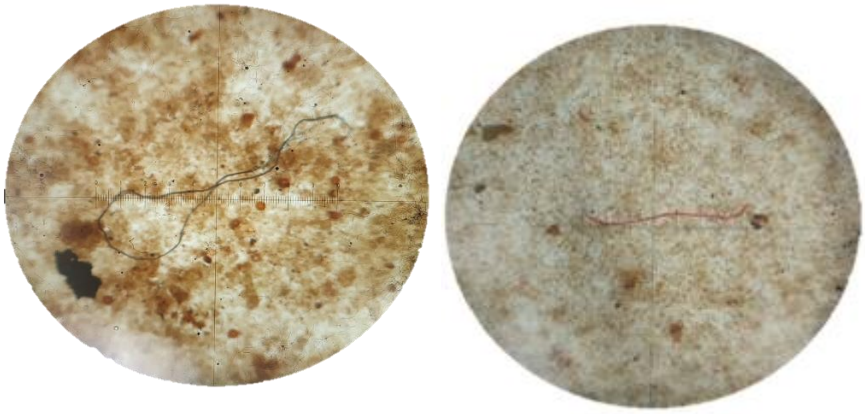

Figure 18: Photos of microplastics

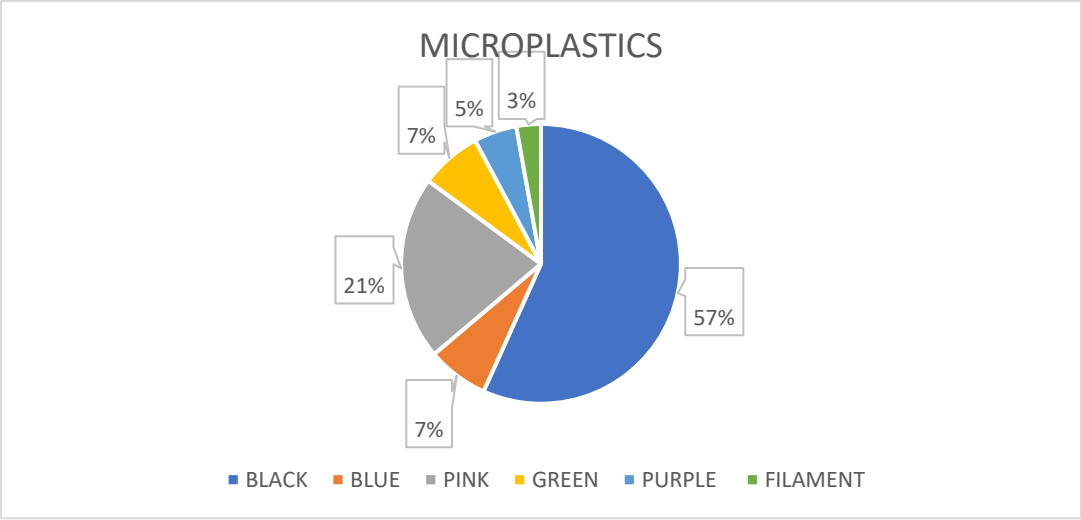

Figure 19: Pie chart representing distribution of microplastics

Following blue at 7%, pink at 21%, green at 7%, purple at 5% and filament at 3 %, it can be deduced from the analysis of the data gathered from the primary survey that black microplastic accounts for 57% of the total. The gathered sample's colour differences are caused by the microplastic's varied chemical composition. The average number of microplastic particles per litre in our samples is between 6 and 8.

Numerous health issues, including respiratory issues brought on by inhalation, gastrointestinal issues brought on by ingesting, changes in endocrine function, inflammatory and immunological reactions, an increased risk of cancer, and potential organ damage have all been linked to microplastic

CHAPTER -6

CONCLUSION

The study aims to determine spatial distribution of physico-chemical parameters and microplastic abundance in surface water near Brahmapuram area, Ernakulam district. Geology of the area mainly constitutes laterite, clay, charnockite basement. In the year 2016 and 2017, the average pH value of Kadambrayar river at Brahmapuram area was 6.65 and 6.35 respectively. The average value of the current study is 6.14, which shows that the pH loadings are tend to become more acidic over the years. It may be due to the influence of industrial inputs and the less alkaline nature of the study area. The lower pH in the surface water will eventually influence the unconfined aquifers by infiltration. Thus, the periodic change in pH must be monitored otherwise, the quality shift in surface water will ultimately deteriorate the quality of groundwater as well. Acidic nature of river results in bioaccumulation and biomagnification. Towards south of the study area concentration of ions increases due to industrial impact that can be observed in samples 15, 16 and 17 and may be continued in the course of river. In such case it can result in acidification of ocean. According to USSL diagram, the water samples fall over C1-S1 (88%) and C2-S2 (12%) class of very good and good quality water for irrigation respectively. As per water irrigation criteria water over the study area can be used for irrigation purposes. All samples recorded high sodium and chloride values. As a result in Piper plot samples fall under sodium chloride type area and also strong acids exceeds weak acides. It also indicates alkalis exceeds alkaline earths.

Industrial inputs have significant role in the abundance of microplastics in surface water. Samples recorded an average of 8 microplastics per litre.During monsoon period, the discharge from the landfill and sites through the surface water increase the chances of microplastic contamination and it eventually infiltrate into the groundwater system. Thus it accounts for bioaccumulation and biomagnification. Proper disposal of waste and plastics are necessary for the protection of rivers and enitre ecosystem.If everyone takes an active role, recycling and reusing plastic products will be very effective.We must develop and implement strategies that will prevent the export of microplastics from cities and the environment, safeguard water resources from pollution, repair damaged aquatic ecosystems. If not, it causes serious threat to surface water and declines the quality of groundwater as well.

REFERENCES

- Alam, F. C., Sembiring, E., Muntalif, B. S., & Suendo, V. (2019). Microplastic distribution in surface water and sediment river around slum and industrial area (case study: Ciwalengke River, Majalaya district, Indonesia). *Chemosphere*, *224*, 637-645.
- Arcadio, C. G. L. A., Navarro, C. K. P., Similatan, K. M., Inocente, S. A. T., Ancla, S. M. B., Banda, M. H. T., ... & Bacosa, H. P. (2023). Microplastics in surface water of Laguna de Bay: First documented evidence on the largest lake in the Philippines. *Environmental Science and Pollution Research*, *30*(11), 29824-29833.
- Athapaththu, A. M. A. I. K., Thushari, G. G. N., Dias, P. C. B., Abeygunawardena, A. P., Egodauyana, K. P. U. T., Liyanage, N. P. P., ... & Senevirathna, J. D. M. (2020). Plastics in surface water of southern coastal belt of Sri Lanka (Northern Indian Ocean): Distribution and characterization by FTIR. *Marine Pollution Bulletin*, *161*, 111750.
- Das, R., Krishnakumar, A., Kumar, M. R., & Thulseedharan, D. (2021). Water quality assessment of three tropical freshwater lakes of Kerala, SW India, with special reference to drinking water potential. *Environmental Nanotechnology, Monitoring & Management*, *16*, 100588.
- Di, M., & Wang, J. (2018). Microplastics in surface waters and sediments of the Three Gorges Reservoir, China. *Science of the Total Environment*, *616*, 1620-1627.
- Flura, M. A., Akhery, N., Mohosena, B. T., & Masud, H. K. (2016). Physico-chemical and biological properties of water from the river Meghna, Bangladesh. *International Journal of Fisheries and Aquatic Studies*, *4*(2), 161-165.
- Haddout, S., Gimiliani, G. T., Priya, K. L., Hoguane, A. M., Casila, J. C. C., & Ljubenkov, I. (2022). Microplastics in surface waters and sediments in the sebou estuary and Atlantic Coast, Morocco. *Analytical Letters*, *55*(2), 256-268.
- Han, M., Niu, X., Tang, M., Zhang, B. T., Wang, G., Yue, W., ... & Zhu, J. (2020). Distribution of microplastics in surface water of the lower Yellow River near estuary. *Science of the total environment*, *707*, 135601.
- Huang, D., Li, X., Ouyang, Z., Zhao, X., Wu, R., Zhang, C., ... & Guo, X. (2021). The occurrence and abundance of microplastics in surface water and sediment of the West River downstream, in the south of China. *Science of the total environment*, *756*, 143857.

- Janakiram, R., Keerthivasan, R., Janani, R., Ramasundaram, S., Martin, M. V., Venkatesan, R., ... & Sudhakar, T. (2023). Seasonal distribution of microplastics in surface waters of the Northern Indian Ocean. *Marine Pollution Bulletin*, *190*, 114838.
- K., Vidya, P. V., ... & Anamika, S. (2023). Characterization of suspended microplastics in surface waters of Chalakudy River, Kerala, India. *Chemistry and Ecology*, *39*(3), 268-287.
- Kameda, Y., Yamada, N., & Fujita, E. (2021). Source-and polymer-specific size distributions of fine microplastics in surface water in an urban river. *Environmental Pollution*, *284*, 117516.
- Khurshid, S., Basheer, A., & Zaheeruddin, S. M. (1998). Effect of waste disposal on water quality in parts of Cochin, Kerala. *Indian Journal of Environmental Health*, *40*(1), 45-50.
- Li, Z., Gao, C. M., Yang, J. L., Wu, L. Z., Zhang, S., Liu, Y. H., & Jin, D. D. (2020). Distribution characteristics of microplastics in surface water and sediments of Haizhou Bay, Lianyungang. *Huan Jing ke Xue= Huanjing Kexue*, *41*(7), 3212-3221.
- Maneesh Kumar, S. K., Kartha, A. R., Rajathy, S., Ratheesh Kumar, C. S., Chandini, P.
- Nan, B., Su, L., Kellar, C., Craig, N. J., Keough, M. J., & Pettigrove, V. (2020). Identification of microplastics in surface water and Australian freshwater shrimp Paratya australiensis in Victoria, Australia. *Environmental Pollution*, *259*, 113865
- Napper, I. E., Baroth, A., Barrett, A. C., Bhola, S., Chowdhury, G. W., Davies, B. F., ... & Koldewey, H. (2021). The abundance and characteristics of microplastics in surface water in the transboundary Ganges River. *Environmental Pollution*, *274*, 116348.
- Nithin, A., Sundaramanickam, A., & Sathish, M. (2022). Seasonal distribution of microplastics in the surface water and sediments of the Vellar estuary, Parangipettai, southeast coast of India. *Marine Pollution Bulletin*, *174*, 113248
- Pathompong, V., & Sarawut, S. (2022). Abundance and Characteristics of Microplastics Contaminating the Surface Water of the Inner Gulf of Thailand. *Water, Air and Soil Pollution*, *233*(2).
- Rahman, A. K. M. L., Islam, M., Hossain, M. Z., & Ahsan, M. A. (2012). Study of the seasonal variations in Turag River water quality parameters. *African Journal of pure and applied Chemistry*, *6*(10), 144-148.

- Shadia, N., Sharmin, S., Ayshi, F. T., & Ali, M. A. (2020). Occurrence and quantification of microplastics in the selected waterbodies of Dhaka city. In *5th International Conference on Civil Engineering for Sustainable Development (ICCED), Bangladesh. Khulna*.
- Verma, A. K., & Saksena, D. N. (2010). Assessment of water quality and pollution status of Kalpi (Morar) River, Gwalior, Madhya Pradesh: with special reference to conservation and management plan. *Asian J. Exp. Biol. Sci*, *1*(2), 419-429.
- Wang, G., Lu, J., Tong, Y., Liu, Z., Zhou, H., & Xiayihazi, N. (2020). Occurrence and pollution characteristics of microplastics in surface water of the Manas River Basin, China. *Science of The Total Environment*, *710*, 136099.
- Wang, W., Yuan, W., Chen, Y., & Wang, J. (2018). Microplastics in surface waters of dongting lake and hong lake, China. *Science of the Total Environment*, *633*, 539-545.
- Zhang, L., Liu, J., Xie, Y., Zhong, S., Yang, B., Lu, D., & Zhong, Q. (2020). Distribution of microplastics in surface water and sediments of Qin River in Beibu Gulf, China. *Science of the Total Environment*, *708*, 135176.

QUALITATIVE ANALYSIS OF GROUNDWATER ON WATERSHED OF KARAMANA RIVER BASIN: A CASE STUDY IN AND AROUND VILAPILSALA SOLID WASTE TREATMENT PLANT, KERALA

Dissertation submitted to Christ College (Autonomous), Irinjalakuda, Kerala, University of Calicut in Partial fulfillment of the degree of

Master of Science in Applied Geology

By,

GREESHMA GANESH

Reg. No: CCAVMAG008

2021-2023

DEPARTMENT OF GEOLOGY AND ENVIRONMENTAL SCIENCE

CHRIST COLLEGE (AUTONOMOUS), IRINJALAKUDA, KERALA, 680125

(Affiliated to University of Calicut and re-accredited with by NAAC with 'A++')

AUGUST 2023

QUALITATIVE ANALYSIS OF GROUNDWATER ON WATERSHED OF KARAMANA RIVER BASIN: A CASE STUDY IN AND AROUND VILAPPILSALA SOLID WASTE TREATMENT PLANT, KERALA

Dissertation submitted to Christ College (Autonomous), Irinjalakuda, Kerala,

University of Calicut in Partial fulfillment of the degree of

Master of Science in Applied Geology

By,

GREESHMA GANESH

Reg. No: CCAVMAG008

2021-2023

DEPARTMENT OF GEOLOGY AND ENVIRONMENTAL SCIENCE

CHRIST COLLEGE (AUTONOMOUS), IRINJALAKUDA, KERALA, 680125

(Affiliated to University of Calicut and re-accredited with by NAAC with 'A++')

AUGUST 2023

EXAMINERS **Dr. Anto Francis K**

1…… **Co - ordinator**

2……....

ACKNOWLEDGEMENT

This report is an official documentation of dissertation work carried out in and around Vilapilsala solid waste treatment plant, Kerala. This report would not have been possible without guidance, encouragement and support of many well-wishers and my colleagues who helped me in many ways.

Firstly, I record my deep sense of gratitude and indebtedness to my guide **Dr. Vidhya G.S, Junior Hydrogeologist, District office of Ground Water Department, Thiruvananthapuram**, for developing the project's framework and providing regular support and supervision throughout the duration of the course of study.

I extend my gratitude to **Sudheer A.S,** District officer of Ground Water Department, Thiruvananthapuram, for granting me permission to conduct my dissertation work in the department.

I thank National Hydrology Project Assistance , SGWB, for their support in the field studies and sampling.

I am deeply thankful to **Dr. Anto Francis K,** Co-ordinator, Department of Geology and Environmental Science, Christ College (Autonomous), Irinjalakuda, for the support and guidance.

I would like to extend my thanks to **Ms. Roshini P.P.**, for the continuous support and guidance.

I extend my sincere gratitude to **Ms. Rajalakshmi and Ms. Anju**, **National Centre for Earth Science Studies (NCESS), Thiruvananthapuram,** for helping me in my analysis of water samples.

I'd like to take this opportunity to thank all of my classmates and friends, who supported me in completing this dissertation work, whether directly or indirectly. I am grateful to the entire Christ College family for their love , support, and guidance. I also express my gratitude to my parents and family members for their support and prayers throughout my life.

Above all, I express my gratitude to God, the Almighty, for his divine generosity and blessings showered upon me.

GREESHMA GANESH

ABSTRACT

This study seeks to explore and analyze the qualitative characteristics of groundwater, especially around the Vilapilsala solid waste treatment plant. The plant has been shut down since past 11 years. Vilapilsala is a densely populated area where groundwater is a crucial source of drinking water for the local community. The aim of this study is to assess the quality of the groundwater in this region and identify any potential risks or contaminants that may affect its suitability for consumption or other uses.

The research will employ a qualitative research design, including both primary and secondary data sources. Primary data will be collected through the sampling and analysis of groundwater samples, 18 open wells and 2 bore wells were taken from different locations within Vilapilsala for this investigation. The samples will be analyzed for various physicochemical properties such as pH, electrical conductivity, total dissolved solids and levels of specific ions. This analysis will provide insights into the overall quality and suitability of the groundwater for various purposes.

Secondary data sources will include official reports, previous research studies, and historical data on water quality in the region. These sources will provide valuable context and allow for comparisons to be made over time.

The findings of this study will help in understanding the current state of groundwater quality in Vilapilsala and the potential risks associated with its use. The study will also identify any potential sources of contamination and recommend measures to address these issues. The results will be beneficial to local authorities, water management agencies, and the community in implementing appropriate measures to protect and preserve the groundwater resources in this region.

CONTENTS

LIST OF TABLES

LIST OF FIGURES

LIST OF PHOTOGRAPHS

CHAPTER I

INTRODUCTION

Water is an essential and finite resource that sustains all life on Earth. While over 70% of the planet is covered with water, only a tiny percentage is suitable for human consumption. Groundwater, which accounts for about 30% of the world's freshwater, plays a crucial role in meeting the needs of billions of people worldwide. Water is vital for various purposes, including domestic use, agriculture, industry, energy production, and maintaining the environment. Groundwater, which is water stored beneath the Earth's surface, serves as the primary source of drinking water for almost half of the global population. It also supplies water for irrigating crops, particularly in regions where surface water is scarce. Furthermore, groundwater supports the ecological balance of ecosystems, ensuring the preservation of biodiversity and natural habitats.

Water and groundwater face numerous challenges that put them at risk of depletion and contamination. Overexploitation due to an increasing population and excessive consumption patterns has strained water resources. Substantial groundwater pumping, especially in areas like California's Central Valley, has caused aquifers to become depleted faster than they can be naturally replenished.

Industrial activities and improper waste management contribute to water pollution. Chemicals, heavy metals, and agricultural runoff contaminate water bodies, making them unsafe for human consumption and damaging ecosystems. Moreover, climate change exacerbates these issues by altering precipitation patterns, reducing snowpack's, and intensifying droughts, affecting water availability around the world.

Efficient water management is crucial to ensure the long-term sustainability of water and groundwater resources. Measures must be taken at individual,

community, and governmental levels to preserve and protect these invaluable resources.

Conservation practices, such as water-efficient technologies, rainwater harvesting, and improved irrigation methods, can significantly reduce water consumption. Encouraging behavioral changes like shorter showers and fixing leaky faucets can also make a collective difference.

Regulating and managing groundwater extraction is essential to maintain the equilibrium between recharge and withdrawal rates. Implementing groundwater monitoring systems and establishing limits on withdrawal rates can prevent overexploitation and the depletion of aquifers.

Addressing water pollution demands stricter regulations on industrial discharges, improving wastewater treatment plants, and implementing sustainable agricultural practices to minimize chemical use and runoff. Public awareness campaigns and education are crucial to promoting responsible waste disposal and water pollution prevention.

Investing in climate change adaptation strategies is also essential. These can include expanding water storage infrastructure, adopting innovative water-saving technologies, and implementing drought-resistant agriculture practices.

Water and groundwater are finite resources that are fundamental to sustainable development and the well-being of all living beings. The protection and preservation of these resources require a coordinated effort from individuals, communities, industries, and governments. By implementing conservation practices, regulating groundwater extraction, addressing pollution, and mitigating the impacts of climate change, we can ensure the availability of water and groundwater for future generations.

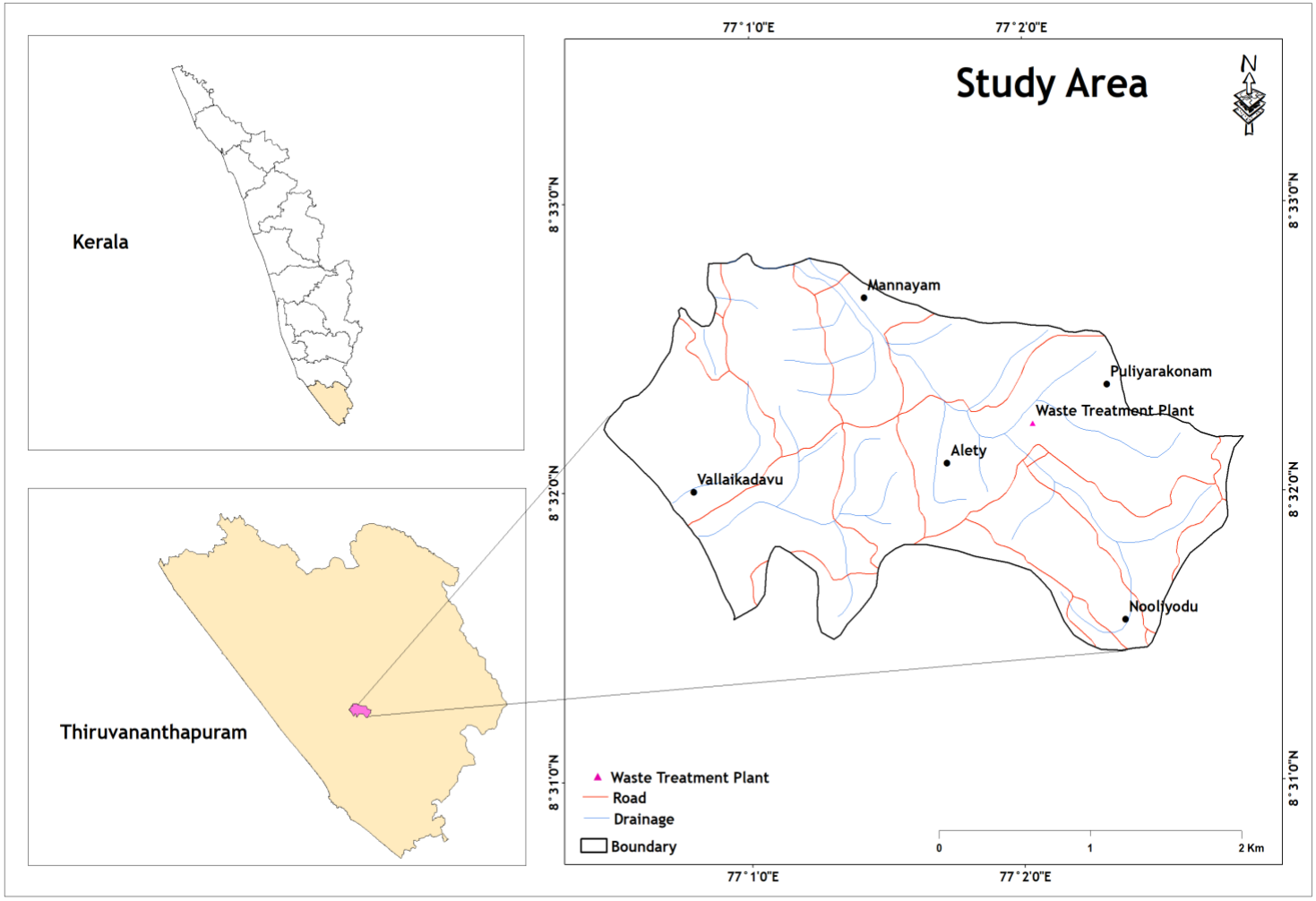
Kerala
Thiruvananthapuram
Study Area
N
77°1'0"E
77°2'0"E
8°33'0"N
8°32'0"N
8°31'0"N
Mannayam
Puliyarakonam
Waste Treatment Plant
Alety
Vallaikadavu
Nooliyodu
Waste Treatment Plant
Road
Drainage
Boundary
0
1
2 Km

1.1 LOCATION

The area investigated is located in and around Vilapilsala in Vellanad block, which is in the eastern part of the Thiruvananthapuram district. It lies between parallels of the North latitude 8° 31′ 26.59″ - 8° 32′ 49.64″ and East longitude 77° 0′ 27.72″- 77° 2′ 48.68″ in the Survey of India topo-sheet number 58H/2 in 1: 50,000 scale. The area selected for study falls in two small watershed having an area of 6.41 km² which comes under the Karamana River Basin. The major locations of the study area include Chowalloor, Nooliyode, Puliyarakonam, Aletty and Mayiladi.(**Fig: 1**)

1.2 ACCESSIBILITY

Accessibility to Vilapilsala is primarily through road transport. It is about 14 km from Thiruvananthapuram towards eastern direction. The nearest major highway is the NH-66. Most of the roads are metalled and in some locations un-metalled roads are also present.

1.3 TOPOGRAPHY

Vilappilsala is situated in a hilly region with lush green surroundings. The area is part of the Western Ghats, a mountain range known for its biodiversity. The terrain is undulating and consists of small hills and valleys. Vilappilsala is known for its calm and serene atmosphere due to its location away from the hustle and bustle of the city. The surrounding areas are predominantly rural with agricultural fields and coconut groves. The region also has several freshwater streams and rivers, which add to its natural beauty.

1.4 DRAINAGE

The drainage of Vilapilsala is primarily characterized by the Karamana River and the tributary of Parvathy Puthanar River.

The Karamana River, also known as the Paradise River, flows through Vilapilsala and is one of the major rivers in Trivandrum district. It originates from the Chemunchi hills and passes through various regions before merging with the Arabian Sea.

The Parvathy Puthanar flowing through the study area. It originates from the Western Ghats and flows through Vilapilsala, eventually joining the Arabian Sea.

Apart from these rivers, Vilapilsala also has several smaller tributaries and streams that further contribute to its drainage system. These water bodies, along with the natural topography of the area, determine the overall drainage patterns and water flow in Vilapilsala, shown in the (**fig: 6)**

1.5 CLIMATE AND RAINFALL

The climate is characterized by high temperatures, heavy rainfall, and high humidity throughout the year.

The average annual rainfall of the district is 2197 mm. It is significant that the area gets benefits of both monsoon-southwest monsoon and northeast monsoon. Trivandrum is the first city along the path of southwest monsoon and gets its showers by end of May/beginning of June. The district also gets rain from receding northeast monsoon which hits the district by October. The southwest monsoon contributes more than the northeast monsoon to the total rainfall in the district. The dry season sets by December in the district. December, January and February are the coldest months while March, April and May are hottest. The normal rainfall of the district is 2001.6 mm. (CGWB Booklet of Trivandrum 2013).

Overall, Vilapilsala has a warm and humid climate with heavy rainfall. The monsoon season brings abundant precipitation, while the winter season offers more moderate temperatures and lower humidity levels.

1.6 VEGETATION

The vegetation found in this area primarily includes tropical trees and shrubs. Some of the commonly found tree species in the region are coconut palm, mango trees, jackfruit trees, and teak wood. Besides these, other vegetation includes small herbs, shrubs, and grasslands. The region also has a few patches of forest areas that form a part of the Western Ghats.

1.7 SOIL

The study area is enriched with lateritic soil, especially in the hilly regions of Vilappilsala. Laterite soil is a type of reddish-brown soil that is formed by the tropical weathering of rocks, and it is rich in iron and aluminum oxide.

The soil in Vilappilsala is suitable for a variety of crops including coconuts, paddy, rubber, bananas, and cashew nuts. With proper management and fertilization, farmers can grow a diverse range of crops and sustain a livelihood.

1.8 LAND USE PATTERN

Vilapilsala is a small village located in the Thiruvananthapuram district of Kerala. The land use in Vilapilsala primarily consists of agriculture and residential areas. Agriculture is one of the main sources of livelihood for the residents of Vilapilsala. The village is known for its paddy fields, where farmers cultivate rice crops. Other crops grown in the area include coconut, banana, vegetables, and spices. The fertile soil and favorable climate of the region make it suitable for agriculture. Apart from agriculture, there are also residential areas in Vilapilsala. The village has a mix of traditional homes and modern housing complexes. Many residents are engaged in various professions outside of agriculture, such as government service, small businesses, and the service sector.

Additionally, there are a few small-scale industries and businesses in Vilapilsala, mainly catering to the local population's needs. These include grocery stores, small shops, and locally-run businesses.

In past years, Vilapilsala has faced issues related to the management of treatment solid waste collected and dumped in the plant. The village was home to a major garbage treatment plant that was operational for several decades. However, due to concerns raised by the local residents regarding health and environmental hazards, the plant was shut down in 2012. This has led to ongoing discussions and efforts to find suitable alternatives for waste management in the area.

Overall, Vilapilsala is characterized by its agricultural activities, residential areas, and a few small-scale industries. The village's economy relies heavily on agriculture, and efforts are being made to address the waste management challenges faced by the community.

1.9 PREVIOUS WORK

The terrain was first mapped in the 1840.s by General Cullen, one of the earliest observers of Travancore (Varaden and Murthy, 1975). Geological Survey of India had conducted exploration for graphite during the period 1959-1962 and later in 1965 near Vellanad (Radhika et al., 1995). Later, organizations like CESS, Kerala State Dept. of Mining and Geology and KMEDP (with UN assistance) have studied the area (Muraleedharan, 1989) Students of the University of Kerala have mapped the present area during 1978, 1992 and 1999 Panicker (2001) and Shyam (2001) had reported anomalous variations in the chemistry of the surface water and groundwater of the Karamana river basin. The other groundwater issue in Trivandrum district is the pollution due to waste disposal particularly around Vilapilsala where the waste disposal factory resides. The E.Coli content is very high in this area whereas the other constituents are within the desirable limit. Other important issue is the water marketing mainly seen during summer months due to

heavy withdrawal resulting in decline of water table(CGWB Booklet of Trivandrum district, 2013). The groundwater in Vilapilsala is primarily used for drinking, irrigation, and domestic purposes. However, due to various anthropogenic activities, groundwater quality has been deteriorating over the years.

1.10 PRESENT WORK

The present work is motivated by the recognition of the importance of water quality for ensuring the health of a population and irrigation purpose. The study of water quality involves a description of the occurrence of different constituents in various water sources and the relation of these constituents to water use. An attempt has been made here to assess the quality of groundwater, especially around the Vilappilsala solid waste treatment plant. The plant has been working since 2000. The Government of Kerala as a part of its effort to effectively dispose the waste generated in the Trivandrum urban area had, through the Corporation of Trivandrum, arranged to set up a solid waste treatment plant at Vilappilsala. This plant was set up by M/s Poab Green of the Excel group of companies with an aim of converting the solid waste of Trivandrum city into bio- manure (Shyam, 2001). The plant used to treat the municipal solid waste collected from the city and convert it into bio manure and by-products. A large amount of waste was also generated in the process. Apart from this, the liquid effluent from the treatment plant has been found to be let off into a small stream (nullah) draining into the Karamana River, which in turn is the source of drinking water of the Trivandrum city. The plant has been shut down since February 2012 following opposition to its operation from the local population, who are agitated over the alleged pollution of water bodies by the leachate from the Poabs Solid Waste Management Plant. The area lies in and around the downstream part of an abandoned Solid waste treatment plant situated NE direction of the study area which is situated in Thiruvananthapuram district. The study area includes two watersheds of Karamana River Basin, which covers major parts of Vilapilsala and around the Solid waste treatment plant. The plant has been

shut down since past 11 years following the opposition to its operation from the local population. The plant used to treat the municipal solid waste collected from the city and convert it into bio manure and by-products. The condition of Meenampally thodu, a tributary of Karamana River were badly affected by this Solid waste treatment plant. At that time the groundwater from nearby areas including Mayiladi, Chowalloor and Puliyarakonam were became not suitable for drinking and irrigation purposes.

An attempt is carried out to embark the hydrogochemistry in and around the Solid Waste Treatment Plant. Quality criteria for groundwater use for domestic and drinking water quality as well as appropriateness for irrigational purposes were also studied. To assess the suitability of groundwater for drinking and other domestic purposes, the hydro-chemical parameters of groundwater of the study area were compared with the guideline values recommended by Bureau of Indian Standards (BIS).

CHAPTER II

GEOLOGY AND GEOMORHOLOGY

2.1 GEOLOGY OF KERALA

The state of Kerala is made up of a narrow strip of land of about 38863k m² area; extending between North latitudes 8°17′ 30" and 12° 27′ 40″ and between east longitude 74° 5' 57″and 77° 24′ 47″ . The shape of Kerala resembles a scalene triangle with its base on the long coast (560 km) and its apex on the Western Ghats. Mountains and peaks above 1800 m within the Western Ghats constitute only 0.64% of the total area of the state width of the state ranges from a minimum of 11km to a maximum of over line 124 km. The Arabian Sea on the west and the NNW-SSE trending Western Ghats in the East constitute the natural boundaries of Kerala. The state forms a part of the South Indian Granulite Terrain of geological significance.

The Kerala coast strips are marked by estuaries, barriers beaches and lagoons. The midlands are made up of laterite capped isolated mounds and hillocks of crystalline rocks like chanockites, khondalites, and gneiss. The high lands are characterised by mountains and the Western Ghats rise to more than 1500 m above mean sea level. Lowland or the coastal area is made up of beaches, sand dunes, ridges, riverine deposits, backwaters and coastline of the Arabian Sea. Numerous flood plains, alluvial terraces and valley fills are part of the lowland.

2.2 PHYSIOGRAPHY OF KERALA

The state can be sub-divided into three major units based on their Physiographic characteristics viz. the coastal plains/Lowlands, the midlands and the hill ranges/Highlands. The coastal plains have an elevation of less than 7.6m above mean sea level (a.m.s.l). The elevation of the midland region ranges from 7.6 to 76 m amsl and that of the hill ranges is more than 76 m above mean sea level. Along

the hill ranges two distinct plateau regions are seen, the important being the Wayanad plateau, covering major part of Wayanad district, with elevations above 700 m.amsl and the Munnar plateau, located along the northern part of Idukki district with a general elevation of about 1000 m.amsl are the prominent plateaus in the hilly region of the state.

Highlands: Highlands occupies 20.35% of the area of the state and forms an imperative physiographic province. From the extreme north, the ranges run parallel to the coast as far as Vavalmalai to the east of Kozhikode. The undulating western fringe of the highlands and the lateritised rocky spines projecting westward form the midland region. It covers nearly 8.44% of the total area of the state.

Midlands: The undulating western fringe of the highlands and the lateritised rocky spurs projecting westward and parts of the crustal breaks (passes) form the midland region. It covers nearly 8.44% of the total area of the state. While the midlands constitute most of the eastern parts of Kannur district, their area shrinks towards the west of Wayanad plateau where they occupy a narrow strip, coinciding with the steep slopes. From the west of Nelliampathi plateau to the north of the Cardamom hills, the elongated spurs separated by extensive ravines are seen to merge with the relatively gentler slopes of the lowlands.

Lowlands: The area falling under the altitudinal range of 10 - 300 m, and consisting of dissected peneplains constitute the lowlands. The altitudinal range is quite asymmetric with the maximum area of 54.17% falling within this unit. Numerous flood plains, alluvial terraces, valley fills, colluvium and sedimentary formations are part of the lowlands. In the northern and southernmost parts of the state, this unit merges with the coastal plains with the discernible steeper slopes than in the rest of the state. In the areas around Poovar-Vizhinjam stretch, Kadakkavur -Varkala stretch, north of Vadakara, Bekal - Kasaragod stretch, etc, this unit adjoin the sea without the intervening coastal plain. The vast low-lying area fringing the coast, is

not only important physiographic unit of the state, but also important in terms of economic activity and demographic distribution. It constitutes 16.40% of the area of the state. In central Kerala, most of the area shows elevations of 4 to 6 m above mean sea level, where as it is 4 to 10 m in north and south Kerala, except the coastal cliffs, promontories and sloping platforms. Beach dunes, ancient beach ridges, barrier flats, coastal alluvial plains, flood plains, river terraces, marshes and lagoons constitute this unit. It has maximum width in the Alleppey and Aluva – Kaladi.

2.3 GEOLOGY OF KERALA

Geologically Kerala forms the southwestern fringe of the south Indian peninsular shield. It consists of two major terrains

1. The cratonic part lying north of Palghat-Cauvery shear zone and 2. The mobile belt the Pandyan mobile helt formed of gneiss, charnockite and khondalite.

The southern part of the state, south of Achankovil shear zone, exposes an assemblage of migmatised meta-sedimentary and meta-igneous rocks (Khondalite-Charnockite assemblages). Granulites, schists and gneiss intruded by acid and alkaline plutons constitute the northernmost part of the state. A number of radiometric age determinations of rocks from the Kerala region have helped in classifying the rocks into broad age groups. The oldest rocks, so far dated in Kerala, are the charnockite (massive) which yielded U - Pb Zircon age of 2930±50 ma. Charnockite and associated gneisses occupy most part of the western and the midland regions of the state. The largest patch of khondalite group of rocks is noticed south of Achankovil shear in South Kerala.

The rock type falling within Kerala can be classified into four major age groups as belonging to Archean, Proterozoic, Cretaceous and Cenozoic.

1. High grade Archeansupracrustal sedimentary rocks of Tertiary and Quaternary age

2. Laterites capping the crystallines

3. The sedimentary rocks

4. Recent to sub-recent sediments forming the low lying areas and river valleys.

Geological map of Kerala (Figure : 2)

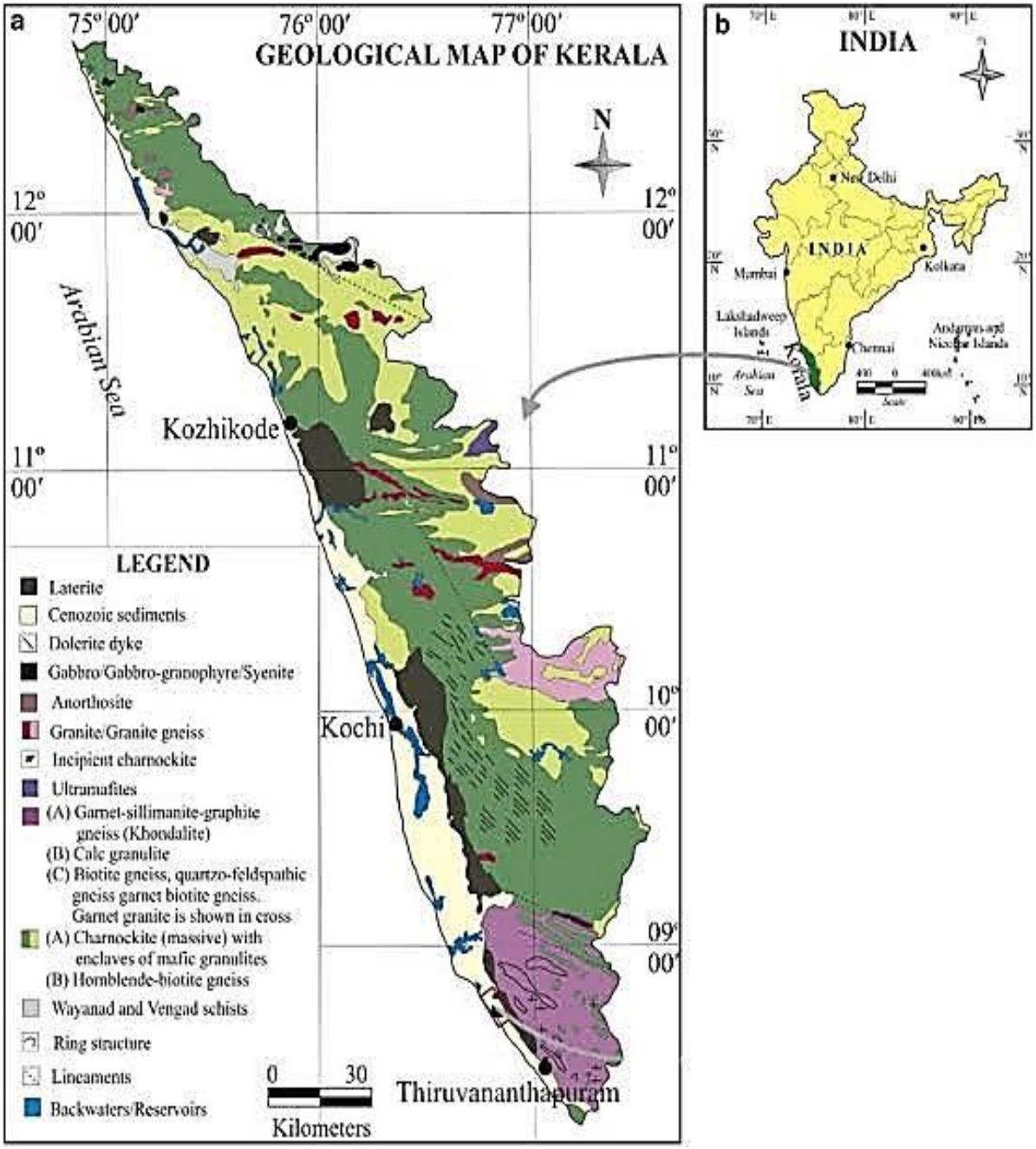

2.3.1 High-grade Archean supracrustals

A narrow arcuate lenticular band of supracrustals occurs in the northern part of Kerala. This formation has all the characteristics of an Archeanpolymetamorphic and poly. deformed terrain consisting of alternate bands of metasediments, granulite and gneisses. The rocks can be divided in to i) a shelf facies sedimentary group characterised by quartzite-carbonate pelitic association. ii) mafic-ultramafic group comprising amphibolite and ultramafites iii) migmatitic banded hornblende biotite gneiss in which the supracrustal rocks occur as enclaves and narrow belts. The mineral assemblages reflect a varying lower amphibolite facies in the west to upper amphibolite facies and at places granulite facies metamorphism to the east.

The charnockite – gneiss association

Major rock formation, outcropping within the Kerala region belongs to the charnockite and chanockite gneisses and younger incipient charnockite in various parts of the state. Most parts of Western Ghats especially the mountain peaks and the midland regions of the states are composed of charnockite and charnockite gneisses. Large bands of chamockite are also observed within the Kerala Khondalite Belt. In the Periyar valley region, in Idukki and Kottayam districts, pyroxenite and alaskite constitute the charnockite group (Nair and Selvan, 1976)

Khondalite group

The Khondalite group of rocks includes garnet sillimanite gneiss, graphite gneiss, calc granulite and quartzite. They are encountered at south of Achankovil shear in the southern part of the State. Major parts of Trivandrum and Quilon districts are underlain by rocks of Khondalite Group. Khondalite Group of rocks which represent the sedimentary sequences metamorphosed to granulite grade are exposed mainly in south Kerala tectonic block. South Kerala khondalites are intensely migmatised, while migmatisation is less observed in the Palghat Gap area, P-T conditions of

formation of the rocks also differ, with estimated higher values recorded for the northern occurrences. Garnet sillimanite gneiss containing varying amounts of graphite is designated as khondalite.

Intrusive rocks

Intrusive phase within the Kerala region includes sporadic occurrence of basic and ultra-basic bodies and dykes belonging to lower middle Proterozoic age, pegmatite of middle Proterozoic age, a host of younger granites with associated pegmatite, and later dolerite dykes contemporaneous with Cretaceous Palaeocene Deccan basalt magmatism of these younger granites and associated pegmatites constitute the bulk of intrusive rocks. Within the khondalite terrain these are white coloured garnet granites while within the charnockite domain, pink granite, syenite and gabbro-granophyre predominate**.**

Offshore sediments

The western, Atlantic-type, passive continental margin along the Kerala coast has a 50 km wide continental shelf, hosting the Kerala-Laccadive basin. The near-shore shelf part contains a clastic sequence of marine shale and sand with a very few limestone interbeds and Cretaceous-Palaeocene sediments. The major basin in the offshore contains sediments of over 4000 m thickness of late Cretaceous to Quaternary age and contains limestone, sandstone and a pile of volcanic.

2.3.2 TERTIARY SEDIMENTS

The tertiary sedimentary formations of Kerala basin unconformably overlie the Precambrian. The name Kerala basin denotes the southern most part of a great sedimentary province spread over a major part of the western continental margin of the Peninsula. Occurrence of marine and non-marine rocks in the land part of it was known since King (1882) and Foote (1883) who reported these rocks. Exposures are

seen mostly in the southern and northern parts of coastal Kerala and contain essentially Neogene and Quaternary sediments.

Based on the distribution of the Tertiary formations, Paulose and Narayanaswami (1968) recognized two major basins of deposition: (i) between Thiruvananthapuram and Ponnani in the south and central Kerala with a maximum width of 16 km between Quilon and Kundara, and (ii) between Cannanore and Kasargod in north Kerala with a maximum width of 10 km at Cheruvattur**.**

VAIKKOM FORMATION

The Vaikkom Formation consists of gravel, coarse to very coarse sand with grayish clay and carbonaceous clay, with them seems of light. The lowest unit of this sequence is exposed in the laterite quarries at Vaikkom and hence they are called the Vaikkom Formation. They attain a thickness of 200 m and overlie the weathered crystalline rocks.

QUILON FORMATION

The Quilon Formation, consisting of fossiliferous limestone, sand and clays, were originally believed to be of very limited extent, confined to the type locality at Padappakara, 11 km northeast of Kollam. Subsequently fossiliferous limestone has been reported from several other places in the south, especially at Nedungolam, Edava, Pozhikkara, Varkala and Kidangayara. Quilon limestone beds contain abundant Orbiculina malabaricus and other fossils amongst which are corals, lamellibranchs and gastropods. The limestones are also exposed in a cliff section near the coast in the vicity of Kollam the age of the Quilon Formation is Hurdigalian The strata above these are of Mi Plocene Later investigations have brought out similar occurrence at vares localities like Chathannur Nedumpolam and Edava

WARKALLI FORMATION

The Quilon Formation is conformably overlain by rocks of the Warkalli formation which occurs as patches all along the coast. The type section is located at Varkala, edging the sea shore, 22 km south of Quilon, where it attains a thickness of 60 m and has the following succession.

Sequence of Warkalli Formation at Varkala (after King, 1882)

UNIT	THICKNESS (in meters)
Laterite with sandstone masses	18.00
Sand and sandy clays	23.00
Alum clays	14.00
Lignite bed	5.00

The Warkalli Formation is nearly horizontal and has been traced almost in the entire coastal stretch from near Cape Comorin in the south to Kottayam and Ernakulam in the north bordering the backwater tract on the east, but obscured beneath the recent deposits of sand and silt and has an aerial extent of over 2000 sq. km. This formation occurs at Chilakkoor, Vettur, Kundara, Thamarakulam and Puliyur in the south and in the cliffs of Cheruvathur and china clay quarries at Palayangadi, Ramapuram, Nileshwaram and Kalanad in Kannoor districts and is lateritized down to a depth of 10-13m and in places where sandstones directly over the gneisses this is kaolinized down to a depth of 10m.

The carbonaceous lay and hinge no often impremated with arc and nodiles of manavite These are present kindly towards the base of the accession Plant focols are also reported in many places The Warkalli Group consists of (1) the Mayanad formation, made up of coarse-grained sandstone with intercalations of clay and

lignite with occasional lenses of limestone; (2) fossiliferous limestones, calcareous clays.

2.3.3 QUATERNARY FORMATIONS

The Quaternary formation include sandbars, marshy lagoonal clays, shell deposits, Teri sands and peat beds of both marine and fluvial environment which unconformably overlie the Neogene sediments. These are found in large areas in between Chavara and Cochin. Teris that are raised sand beaches, with fine-grained reddish sandy loam also can be included in this formation. The teri sands overlie both sedimentary and crystalline rocks. Mud flats include "Kari" and "Punja" lands in central Kerala and Kole lands in parts of Thrissur district. Shell deposits occur in Vembanad and Ashtamudi lakes, and also on land at Payyanur.

RECENT ALLUVIUM

The Recent Formations in Kerala include fringes of parallel sand bars and sandy flats alternating with marshy lagoonal clays and beach sand deposits. The different recent deposits include: i) Alluvium and ii) Teri sand (Red Loam).

Mud Banks

Records of existence of mud banks along Kerala coast are available from the year 1668 onwards. Patches of calm turbid water with high load of suspended sediments, appearing close to the shore along the Kerala coast during the southwest monsoon season are known as mud banks (Soman, 1997). The mud of the mud banks is probably derived from lagoonal basins, as the clays from Kuttanad and Vembanad estuary closely correspond to the clays from the mud banks area excepting for oil contents and shells of organisms. Mud banks have been reported from many places along the Kerala coast from Kannur to Quilon. The aerial extent and suspended sediment concentration gradually decrease in the non-monsoonal period. Further,

waxing and waning of mud bank peripheries during monsoon have been noticed as local meteorological conditions vary.

Laterite Formation

Laterite is a tropical weathering product of rocks, enriched in oxides of iron and aluminum. Francis Hamilton Buchanan is the person who reported laterite first from Angadipuram during his traverse to Malabar. In Latin laterite means 'brick stone' and is locally known as 'Ishtikakallu or Vettukallu'. Laterites of the state can be classified into two groups. Laterite originated from crystalline formation is primary laterite. Laterite originated from sedimentary formation is secondary laterite. All along the midlands and parts of the upland areas the crystalline rocks are laterised on the top to form in situ primary laterite. The secondary laterite is formed due to laterisation of Tertiary sediments due to its exposure in the atmosphere and the transportation of lateritic material and is known as 'detrital laterite'. At places the laterites are absent completely, may be due to the erosion after laterisation. The laterite derived from the sediments can be identified from those derived from crystallines by the presence of relict structures of parent rocks. Laterites consist mainly of the minerals kaolinite, goethite, hematite and gibbsite, of which the iron oxides goethite and hematite cause the red-brown colour of laterites. Many laterites contain quartz as relatively stable relict mineral from the parent rock. In Kerala, laterite of more than one generation is present and is confined to elevation of 600 m and below, over Precambrian and Tertiary sediments. While discussing on the laterite distribution in Kerala, it occurs almost everywhere in the midlands and low lands and can be broadly classified as primary or residual and secondary or detrital. Primary laterite is the product of insitu weathering.

Geological Succession of Kerala

PERIOD	AGE	FORMATION	LITHOLOGY
Quaternary	**Recent**	Alluvium	Sand, clay, riverine alluvium etc. and flood plain deposits of Kuttanad area
	Sub-recent	Laterite	Derived from crystalline and sedimentary rocks
Unconformity			
Tertiary	**Upper Miocene**	Warkalli	Sand stone, clays with lignite seams
	Miocene	Quilon	Limestone, marl and clay
	Oligocene to Eocene	Vaikom	Sandstone with pebbles and gravel beds, clay and lignite
	Eocene	Alleppey	Carbonaceous clay and fine sand
	Undated	Intrusives	Dolerite, Gabbro, Granites, Quartzo-feldspathic Veins
Unconformity			
Archean		Wayanad group	Granitic gneiss and schists
		Charnockites	Charnockites and associated rocks
		Khondalites	Khondalites suite of rocks and its associates

2.4 GEOLOGY AND GEOMORPHOLOGY OF THE STUDY AREA

The study area Vilappilsala belong to the Vellanad block, which is a region located in the Thiruvananthapuram district of Kerala. It is primarily characterized by its diverse geology and unique geomorphology.

Geology

The Vellanadu block is situated in the Southern Granulite Terrane, which is a part of the Indian Shield. The region is primarily composed of khondalite group of rocks

and migmatites, which are formed due to the process of intense metamorphism and partial melting of pre-existing rocks. Charnockites are also found in this region, which are coarse-grained rocks formed at higher temperatures, often associated with regional metamorphism. These rocks are predominantly composed of orthopyroxene, quartz, and feldspar minerals. In addition to khondaite, migmatites and charnockites, there is occurrences of graphic. Vellanadu is a main centre of gem bearing pegmatites. The study area, Vilapilsala located in Thiruvananthapuram district of Kerala. The geology of Vilapilsala is characterized by a variety of rock formations. The region predominantly consists of Khondalite group of rocks which is present around 5.88 km^2 and Charnockite group of rocks, it covers only 0.53 km^2 of the study area, shown in the (**fig:4**).

Geomorphology

The geomorphology of the Vellanad block is influenced by various processes such as weathering, erosion, and tectonic activities. The region exhibits several landforms, including hills, valleys, and plateaus.

The Vellanad block is mainly having Lower Plateau, which is Lateritic and Denudational structural hills. Residual mounts are distributed along this block.

The Vellanad block is also known for its valleys and plains formed by the erosion of rocks over time. Several rivers and their tributaries, such as the Karamana River and the Killiyar River, flow through these valleys, shaping the landscape further. These rivers have played a crucial role in the formation of fertile alluvial plains in the region.

The prominent geomorphic feature of Vilappilsala is the presence of hills and valleys. The village is nestled amidst the Western Ghats, a mountain range that stretches along the western coast of India. The area is characterized by undulating terrain with numerous small hills, which provide scenic beauty and shelter diverse flora and fauna.

Geomorphology of the study area characterized by its lateritic lower plateau (5.29 km^2), valley(1.05 km^2) and river channel (0.07 km^2). The region also contains several rivers and streams that add to its geomorphological significance. The unique geology and geomorphology of Vilappilsala have significant implications for the environment and local communities. The diverse rock formations contribute to the soil fertility, which supports agricultural activities in the region. The hills and valleys act as catchment areas for rainwater, crucial for sustaining groundwater availability and the local water supply.Shown in the (**fig: 5**)

Overall, the geology of the Vellanad block in Thiruvananthapuram is characterized by its khondalite, migmatites, charnockite and gneisses. The unique combination of these rocks contributes to the diverse geomorphology of the region, which includes hills, valleys, and plains shaped by various geological processes.

CHAPTER III

HYDROGEOCHEMISTRY

3.1 Introduction

Water is a fundamental resource for life. Ground water has become an increasingly important natural resource catering to the fresh water requirements of various sectors in India. Sustainable development and efficient management of this scarce resource has become a challenge. Groundwater has steadily emerged as the backbone of India's agriculture and drinking water security. Contribution of ground water is nearly 62% in irrigation, 85% in rural water supply and 50% in urban water supply. Ground water is an annually replenishable resource but its availability is non-uniform in space and time. Ground water available in the zone of water level fluctuation is replenished annually with rainfall being the dominant contributor. Hence, the sustainable utilization of groundwater resources demands a realistic quantitative assessment of ground water availability in this zone based on reasonably valid scientific principles. National Water Policy, 2012 has laid emphasis on periodic assessment of ground water resources on scientific basis. The trends in water availability due to various factors including climate change must also be assessed and accounted for during water resources planning. To meet the increasing demands of water, it advocates direct use of rainfall, desalination and avoidance of inadvertent evapotranspiration for augmenting utilizable water resources. The National Water Policy 2012 also states that safe water for drinking and sanitation should be considered as pre-emptive needs followed by high priority allocation for other domestic needs (including needs of animals), achieving food security, supporting sustenance agriculture and minimum eco-system needs. Available water, after meeting the above needs should be allocated in a manner to promote its conservation and efficient use.

Groundwater is the water that is stored beneath the Earth's surface in pores and crevices within rocks and soil. It forms through a process called infiltration, which occurs when precipitation, such as rainfall or snowmelt, soaks into the ground. As the water infiltrates, it fills up the spaces between soil particles, fractures in rocks, and porous layers known as aquifers.

The formation of groundwater starts with the water cycle. When rain falls on the Earth's surface, some of it evaporates back into the atmosphere, some is taken up by plants, and the remaining water either runs off into rivers and lakes or infiltrates into the ground. The rate at which water infiltrates depends on various factors, including the type of soil or rock, its saturation level, and the presence of impermeable layers.

Once the water infiltrates, it begins to percolate further down into the ground, driven by gravity. As it continues to flow through the soil and rocks, it undergoes processes of filtration and purification. The soil and rocks act as natural filters, removing impurities and contaminants from the water, making it cleaner and suitable for drinking.

The water continues its downward journey until it reaches an impermeable layer, such as a layer of clay or solid rock, which prevents it from moving further underground. At this point, the water accumulates, forming an aquifer – a saturated layer of rock or sediment that can store and transmit water.

The depth at which groundwater is found varies depending on the geographical location and the characteristics of the underground formations. Shallow groundwater is often found closer to the surface, while deep groundwater can be found hundreds of meters below the ground.

Groundwater is a vital resource for human consumption, agriculture, and industrial use. It is also crucial for sustaining ecosystems, as it supports streams, lakes, and wetlands, and provides a source of water for vegetation.

3.2 GROUNDWATER CONDITIONS IN KERALA

In hard rock terrain, comprising weathered crystal lines and laterites, ground water occurs under phreatic conditions in the weathered residuum and the shallow fractures hydraulically connected to it, whereas it is under semi-confined to confined conditions in the deep fracture zones. In the alluvial terrain, ground water in the shallow systems is in phreatic condition. Granular zones in the Tertiary sedimentary formations at deeper levels form potential confined to semi confined aquifers.

Crystalline Rock Aquifers

The shallow aquifers of the crystalline rocks are made up of the highly decomposed weathered zone or partly weathered and fractured rocks. Thick weathered zone is seen along the midland area either beneath the laterites or exposed. In the hill ranges thin weathered zone is seen along topographic lows and area with lesser elevation and gentle slope. In areas along the hill ranges generally rock exposures are seen. The depth to water level in this aquifer varies from 2 to 16 m.bgl and the yield of the well ranged between 2 to 10 m3 per day.

Exploratory drilling carried out by Central Ground Water Board in the State in the crystalline formations has indicated that the potential fractures are encountered at depths ranging between 30 to 175 m.bgl with yield varying from less than 1 to as much as 35 litres per second (lps). In Charnockites, more than 40% of the wells have yielded more than 10 lps or above indicating that in Kerala, Charnockite suite of rocks are better aquifers compared to Khondalite group. Tertiary Rock Aquifers

Groundwater occurs under phreatic condition in the shallow zone and under semi-confined to confined conditions in the deeper aquifers. The Tertiary formation of Kerala coast is divided into four distinct beds viz. Alleppey, Vaikom, Quilon and

Warkali. These formations except the Alleppey beds are outcrops and they are lateritized wherever they are exposed. The maximum thickness of Tertiary sediments is found between Karunagapally and Kattoor and all the four beds are found in this area.

Groundwater is commonly developed through dug wells tapping the sandy zones at shallow depth in the Tertiary sediments. The depth to water level in this shallow zone ranges from 2.0 to 27 m.bgl and the yield of the wells range from 500 lpd to 10 m3 per day.

The Vaikom and Warkali beds form the most potential aquifers in the Tertiary group. The Alleppey bed has been encountered at deeper levels in the bore holes drilled in the coastal tract of Alappuzha district and the formation water is found to be saline and hence, no tube well has been constructed tapping this formation.

In the Vaikom aquifers, the piezometric level is between 2 and 20 m above msl. The yield of the tube wells constructed in this formation ranges from 1 to 57 lps. This bed forms auto flow zones along the coast between Karunagapally in Kollam district and Nattika and Kaipamangalam in Thrissur district. The water is generally fresh south of Karuvatta in Alappuzha district. Recent exploration by CGWB proved that good quality groundwater pockets are in existence in this formation in and around Cochin.

Warkali aquifers are the most developed aquifer system among the Tertiary group. The urban and rural water supply in the coastal area between Kollam and Alappuzha is mostly dependent on this. The piezometric head is about 3 m. above msl along the eastern part of the sedimentary basin whereas it is 10 m. below msl in and around Alappuzha. The yield of the wells tapping this formation ranges from 3 to 14 lps.

The hydrogeological information on Quilon beds is very limited. The formation is considered to be a poor aquifer compared to Vaikom and Warkali beds.

Laterite Aquifers

Laterites are the most widely distributed lithological unit in the State and the thickness of this formation varies from a few meters to about 30 m. Laterite forms potential aquifers along to pographic lows and valleys. The depth to water level in this formation ranges from 2 to 25 mbgl and the yield ranges from 0.5 to 30 m3 per day. The occurrence and movement of groundwater in the laterites are mainly controlled by the topography. Laterite is a highly porous rock formation, which can form potential aquifers along topographic lows. However, due to the porosity, groundwater is drained from elevated places and slopes at shortest duration after monsoon and hence water scarcity is experienced in the elevated places and slopes.

Alluvial Aquifers

The alluvial deposits form potential aquifer along the coastal plains and groundwater occurs under phreatic and semi-confined conditions in this aquifer. The thickness of this formation varies from few meters to above 100 m and the depth to water level ranges from less than a meter to 6 mbgl. Filter point wells are feasible wherever the saturated thickness exceeds 5m. This potential aquifer is extensively developed by dug wells and filter point wells throughout the State and the yield ranges from 5 to 35 m3 per day.

Principal Aquifers of Kerala (Figure 3)

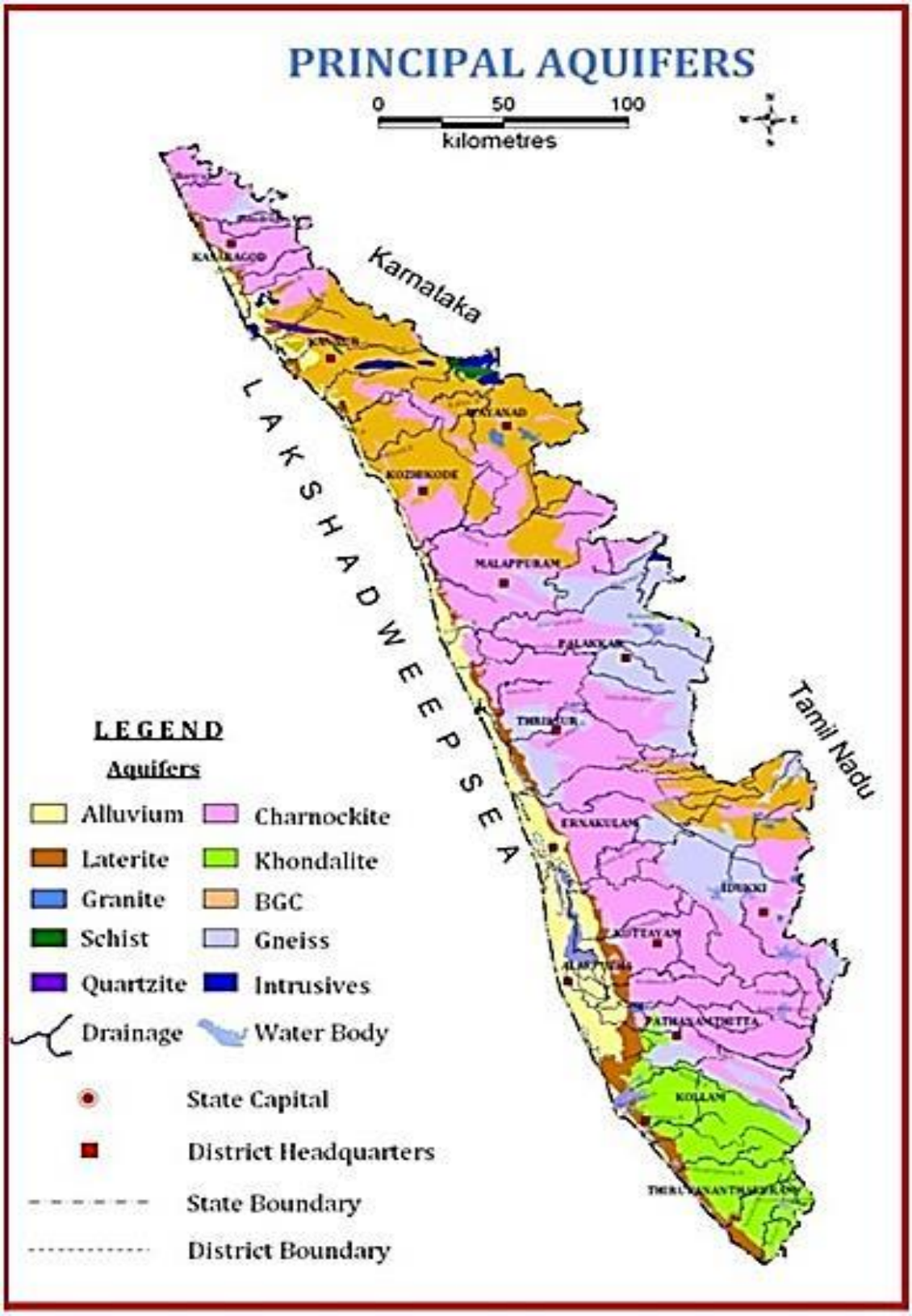

3.3 GROUNDWATER RECHARGE IN KERALA

Recharge of groundwater takes place soon on the onset of the monsoon which starts by the end of May or early June. The process prolong till the end of October. Although hallowed with profuse precipitation, because of the trait topography with steep slopes and wide network of rivers a major portion of water reaches the sea as surface run off within a few hours of precipitation, leaving inadequate time for infiltration. In consequence the aquifers fall short to get recharged to meet up the requirement during summer.

3.4 CHEMICAL UNIQUENESS OF WATER

Bearing in mind the veracity that groundwater occurs in harmony with geological materials containing soluble minerals, elevated concentration of dissolved salts are by and large is expected in groundwater relative to surface water. The type and concentration of salts depend on the geological environment, the source and movement of water. The natural chemical quality of groundwater is generally good, but elevated concentrations of a number of constituents can cause problems for water use. Chemical composition of minerals, through which infiltration takes place, plays a significant role in determining the quality of groundwater. Some chemicals are more soluble than others, making them more likely to become dissolved in water. Taking in to account of groundwater in contact with elements like sodium, sulphate and chloride will become mineralized at a faster rate than if other chemicals were present.

3.5 WATER QUALITY PARAMTERS

The important factors that affect the quality of water are climate variation, depth of water from surface, hydrologic parameters and chemical makeup of sediments through which the water moves. Water being an excellent solvent, it is imperative to be acquainted with the geochemistry of the dissolved solid constituents.

Groundwater quality is the sum of natural and anthropogenic influence. Multi-purpose monitoring may be directed towards a whole range of groundwater quality issues and embrace many variables. Other categories of monitoring may contemplate on a single quality issue such as agricultural pesticide, an industrial spill or saline intrusion.

3.6 FACTORS AFFECTING GROUNDWATER QUALITY

An understanding of the factors that affect groundwater quality can help us to make decisions on well depth and appropriate water quality for a particular application. There are several factors that affect groundwater quality which are depth from surface, permeability and chemical makeup of the sediments through which groundwater moves and also climatic variations.

Depth from surface: Water is the world's supreme and most abundant solvent. It endeavors to dissolve everything it comes in contact with. As a result, the longer groundwater takes to move through the sediments, the more mineralized it becomes. Thus, shallow groundwater aquifers have a lower level of mineralization, or total dissolved solids (TDS), than deeper aquifers. Water from deeper groundwater aquifers typically has a much longer trip to its target and thus it is usually more mineralized. While shallow wells have lower levels of TDS, they do have higher levels of calcium, magnesium and iron than deeper wells. High levels of these minerals make the water "hard." Deeper wells have higher levels of sodium and lower levels of hardness, making the water "soft." The reason is that deeper sediments and rock formations contain higher levels of sodium and as water moves downward through the sediment and rock formation. a natural ion exchange process occurs. Calcium, magnesium and iron in the groundwater are exchanged for sodium in the sediment and rock formations. The result is groundwater with higher levels of sodium and little or no hardness is produced.

Permeability of sediments: Movement of groundwater is relatively very slow through sediments with low permeability, such as clay. This allows more time for minerals to dissolve. In contrast, sediments with high permeability, such as sand, allow groundwater to move more quickly. There is less time for minerals to dissolve and thus the groundwater usually contains lower levels of dissolved minerals. There is also a difference in dissolved solids between groundwater in recharge zones and water in discharge zones. Recharge zones are uplands areas where precipitation readily enters the ground through permeable, sandy sediments. Generally, water in recharge zones has a low level of mineralization. Discharge areas are low areas where groundwater flow eventually makes its way back to (or near) the ground surface. Groundwater found in such areas can be extremely high in minerals such as sodium, sulphates and chlorides. Examples are saline seeps, sloughs and lakes.

Chemical makeup of sediments: Another factor affecting groundwater quality is the chemical makeup of minerals. Some chemicals are more soluble than others, making them more likely to become dissolved in the water. For example, groundwater in contact with sediments containing large concentrations of sodium, sulphate and chloride will become mineralized at a faster rate than if other chemicals were present.

Climatic variations: Climatic variations such as annual rainfall and evaporation rates also play an important role in groundwater quality. In semi-arid regions, discharging groundwater often evaporates as it approaches the surface. The minerals from the water are deposited in the soil, creating a salt buildup. Precipitation infiltrating through the soil can re-dissolve the salts, carrying them back into the groundwater.

Seawater intrusion: In coastal areas, lowered water table may induce sea water to reverse the flow toward the sea. Sen water moving inland is called saltwater

intrusion. Alternatively, salt from mineral beds may leach into the groundwater of its own accord.

Groundwater pollution: Not all groundwater problems are caused by over-extraction. Pollutants released to the ground can work their way down into groundwater. Movement of water and dispersion within the aquifer spreads the pollutant over a wider area, which can then intersect with groundwater wells or find their way back into surface water, making the water supplies unsafe. The stratigraphy of the area plays an important role in the transport of these pollutants. Water table conditions are of great importance for drinking water supplies, agricultural irrigation, waste disposal and other ecological issues.

3.7 UNAVOIDABILITY TO ANALYSE WATER

To examine the suitability of water for industrial and agricultural needs and also to make a decision the most effective treatment technique for different types of appraisal (physical, chemical, biological and microbiological) of water are necessary. Analysis becomes further significant because to determine whether any pollution has occurred in the water course and to trace the origin and degree of pollution and also to suggest a likely remedy. Other momentous factors endorse us to do analysis of water include to measure the effect of pumping, particularly when the wells are constructed near sea or an estuary where the tidal influence is possible. To find out whether infection of microbial organisms has occurred and to recommend defensive measures and effectual distinction procedures. In addition to the above mentioned reasons, water may perhaps also contain minerals, silicate and metals such as iron, manganese and small amount of phosphates. These all makes astuteness for the necessity of analyzing water.

3.8 FIELD SAMPLING

Careful collection of water samples from the field is very important to get reliable results of water chemistry. Hence the samples collected should be very carefully handled and it should not deteriorate or get contaminated during the transport to the laboratory. Adequate volume of samples is to be collected for the analysis of all required parameters. Selection of sampling point is of primary importance because representative samples need to be collected to ensure accuracy. In sampling ground. water or surface water for chemical analysis polythene bottles of 1-2 litre in volume are generally satisfactory. After rinsing the bottles with the water to be sampled, the sample is collected and securely sealed. The water should be stored in a cool place and transferred promptly to a laboratory for analysis.

Water samples were collected from open wells to analysis and assess the quality of the ground water. After the collection of water the samples, they were numbered and labelled. The location, measuring point static water level, total depth, diameter, geology etc. were noted. GPS reading is also recorded for the correct location in the map. The water samples were collected mainly from two watersheds covering the Vilappilsala area.

Water quality analysis involves the measurement and assessment of various physical and chemical parameters to determine the quality and suitability of water for a specific purpose. In order to analyze the quality of groundwater, water samples were collected from in and around Vilapilsala. A total of 20 groundwater samples (18 dug wells and 2 bore wells) have been collected from the study area during the pre-monsoon (April 2023).

Samples were analysed in the Chemical lab of NCESS (National Centre for Earth Science Studies) in Akkulam, Thiruvananthapuram. The collected water samples were subjected for to analyse the various parameters such as pH, EC, TDS and all

the major ions were analysed. Routine titremetric method and MP-AES were used for the analysis.

3.9 DEPTH TO WATERLEVEL

The depth to water level refers to the distance from the ground surface to the level of groundwater. It is an important parameter used to assess the accessibility and availability of groundwater resources. Monitoring the depth to water level helps determine the overall health of an aquifer system and provides useful information for various applications such as water resource management, hydrological studies, and environmental monitoring.

The depth to water level can vary spatially and temporally based on factors such as precipitation, evaporation, surface water dynamics, and local geology. It is typically measured using monitoring wells or piezometers, which are instruments specifically designed for groundwater level monitoring.

Several studies have been conducted on the depth to water level in different regions globally. These studies help in understanding the dynamics of groundwater systems and their response to various hydrological conditions. They also provide insights into the effects of climate change, land use changes, and groundwater pumping on groundwater levels.

Detailed well inventory was carried out dividing the study area into half kilometer square grid about 20 samples were collected and parameters such as height of parapet, water level, total depth and well diameter were noted (Table: 5).

In the study area, the open wells water level shows maximum of 13.25 m is obtained from Nedumpara and minimum water level of 0.61 m is obtained from Vilapil. The depth to water table map is shown in (**fig: 18**)

3.10 ANALATICAL TECHNIQUES USED

MP-AES

The water quality analyzer instrument MP-AES (Microwave Plasma-Atomic Emission Spectrometer) is a modern analytical instrument used for the analysis of water samples. It is a variation of the traditional Atomic Emission Spectrometry technique and offers several advantages such as enhanced sensitivity, lower detection limits, and reduced sample preparation requirements.

The procedure for using an MP-AES instrument for water quality analysis typically involves the following steps:

1. Sample preparation: Collect water samples from the desired location and ensure they are properly preserved and stored according to the required guidelines. Depending on the specific analytes of interest, water samples may need to be filtered or undergo pre-concentration steps.

2. Calibration: Prepare a series of calibration standards by diluting stock solutions of known concentration for each analyte. These standards cover the range of expected concentrations in the samples. The number of standards and their concentrations depend on the specific requirements and analytes being targeted.

3. Instrument setup: Ensure that the MP-AES instrument is properly calibrated and set up according to the manufacturer's instructions. This includes checking the plasma gas flow, auxiliary gas flow, and optimizing the instrument's operating parameters such as RF power, nebulizer gas flow, and torch position.

4. Sample analysis: Introduce the water samples into the MP-AES instrument using an appropriate sample introduction technique such as direct injection, flow injection analysis, or digestion. The instrument uses a high-frequency microwave-induced plasma to atomize and excite the elements in the sample.

5. Data acquisition and analysis: The MP-AES instrument detects and measures the emission wavelengths characteristic of various elements present in the sample. The instrument's software acquires and processes the emission spectra generated, and peak heights or areas are measured and correlated with the concentrations of the elements in the sample using the calibration curve.

6. Quality control: Implement quality control measures such as duplicate analysis, blank analysis, and analysis of external standards periodically throughout the analysis to ensure the accuracy and reliability of the results.

3.11 ANALYSIS OF WATER

HYDROGEN ION CONCENTRATION (PH)

pH value is a measure of the acidity or alkalinity of a solution. It is a scale ranging from 0 to 14, where a value of 7 is considered neutral, values below 7 are acidic, and values above 7 are alkaline.

The pH value of water is important for water quality as it can affect the chemical reactions and biological processes that occur in water. It can also impact the solubility and availability of certain nutrients and minerals in water. In drinking water, a pH range of 6.5 to 8.5 is typically considered suitable for human consumption. Water with a pH level that is too low or too high may have a negative impact on taste, health, and the effectiveness of disinfectants.

In the present study the pH value ranges from **4.76** to **7.45** with a mean of **6.1** indicating an acidic trend. The BIS standard for pH is ranges from 6.5 to 8.5. Lowest pH value of 4.76 was obtained from Puliyarakonam and highest pH value of 7.45 from Nooliyode, which lies NW and SE direction of the study area. The spatial variation map is shown in the (**fig :7**)

Instrument used: The ph. meter is used to measure the hydrogen ion or the hydroxide ion concentration in water sample. It usually consists of a probe which is

dipped inside the sample for obtaining the values Probe consist of a thin glass bulb (Measuring electrode) and reference electrode both submerged in neutral KCl solution and having a silver alloy wire. The eutech pH tutor was used for determining the pH. values and specifications of the model is given in (photo: 1)

Photo : 1 pH meter

ELECTRICAL CONDUCTIVITY (EC)

The electrical conductivity of water refers to its ability to conduct an electric current. Pure water is a poor conductor of electricity because it contains very few ions or charged particles that can carry the current. However, when certain substances are dissolved in water, such as salts or acids, they break up into ions and increase the water's conductivity. The conductivity of water is typically measured in units of siemens per meter (S/m) or microsiemens per centimeter (µS/cm). The conductivity of pure water at room temperature is very low, typically around 5.5 µS/cm. However, it can vary depending on factors such as temperature, pressure, and the presence of dissolved substances. Water with a higher concentration of dissolved substances will have a higher conductivity because there are more ions

available to carry the current. For example, seawater has a much higher conductivity than freshwater due to its higher concentration of dissolved salts. The EC readings are usually adjusted to a temperature 25°C. So that variations in conductance is a function of concentration and type of dissolved constituents present. A sudden increase in conductivity indicates addition of some pollutants to it (Trivedy and Goel, 1986). Systronics Water Analyser 371 was used for the determination of EC. The method is, conductivity of water sample is measured using calibrated (with 0.01 M KCl Solution) Conductivity meter equipped with Conductivity cell and resistance measuring device.

Electrical conductivity values of open well samples show slight variations in the study area. i.e. from 64.88 µS/cm at Puliyarakonam to 623.4 µS/cm at Nooliyode, with a mean value 214.36 µS/cm. The spatial variation map is shown in the (**fig:8**)

TOTAL DISSOLVED SOLIDS (TDS)

Total dissolved solids (TDS) in water refer to the total concentration of inorganic and organic substances that are dissolved in water. These substances can come from various sources, such as minerals, salts, metals, organic matter, and even human activities like agriculture and industrial processes.

TDS is usually reported in parts per million (ppm) or milligrams per liter (mg/L) and can have an impact on the taste, color, and quality of water. It is an important parameter to consider in determining the suitability of water for various purposes like drinking, irrigation, or industrial use.

Therefore the level of TDS is one of the characteristics which decide the quality of drinking water. When the TDS in water is more than 500 ppm, palatability of water decreases and may cause gastro-intestinal irritation (Park and Park, 1980). High TDS indicates that the water is highly mineralized and this water is not suitable either for drinking or for industrial purposes. The concentration of TDS above 2000 ppm produces laxative effects. The bulk of the total dissolved solids include

bicarbonates, sulphates and chloride of calcium, magnesium, sodium and silica. Potassium chloride and nitrate form a minor part of the dissolved solids in groundwater.

In the study area TDS of open well varies from 43.13 – 412.1 ppm with a mean value of 131.24 ppm. The lowest value of TDS is 43.13 ppm is obtained from Puliyarakonam and highest value of TDS 412.1 ppm was obtained from Nooliyode, which lies NE and SE direction of the study area. All the open well samples collected from the study fall inside the highest desirable limit (500 ppm) as per specification of BIS. The spatial variation map is shown in the (**fig:9**)

3.12 DETERMINATION OF ANIONS

CHLORIDE (Cl^-)

Chloride is a common anion found in water, often originating from natural sources or as a result of various human activities. It is an essential electrolyte for the human body to maintain fluid balance and to support proper nerve and muscle function. The concentration of chloride ions in water can vary depending on factors such as geological formations, industrial discharges, and agricultural practices. High levels of chloride in water can be detrimental as it can affect the taste and smell of water, corrode metal pipes and equipment, and impact the environment. To measure the chloride content in water, various analytical techniques are employed, including ion-selective electrodes, titration methods, and spectroscopic analysis. These methods enable precise detection and quantification of chloride ions in water samples. Water treatment processes, such as desalination and reverse osmosis, can effectively reduce chloride concentrations in brackish or saline water sources, making them suitable for drinking or industrial use. Chloride in water is a stronger oxidizing agent than oxygen and Cl with oxygen slowly decompose water. High concentrations may be injurious to people suffering from disease of heart or kidney (Khurshid et al, 1998). High concentration of C1 can also corrode concrete by

extracting calcium in the form of calcides. As per BIS (1991) the highest desirable value is 250 ppm and maximum permissible limit for chloride in drinking water is 1000 ppm. However concentration above 100 ppm itself can cause physiological damage.

In the present study chloride ion concentration ranges from 4.69 ppm to 98.19 ppm with a mean value of 37.10 ppm in the case of open well water samples. Lower chloride value 4.69 ppm is obtained from Velaikadavu and higher value 98.19 ppm is obtained from Nooliyode, which lies SW and SE direction of the study area. All the values fall within the BIS limit (250-1000).

SULPHATE (SO_4^{2-})

The sulphate content of atmospheric precipitation is only about 2 ppm. Sulphur is not a major constituent of most of the rocks; however sulphate is abundant in most groundwater. This happens through oxidation, reduction, precipitation, solution and concentration processes as water traverses through rocks. Natural water contains higher levels of sulphate contributed from the weathering of rocks. In addition to this, domestic sewage and industrial effluents also add sulphate to aquatic ecosystem and hence high level of sulphate is an indicator of organic pollution. Fragnant condition is easily created when water is over loaded with organic wastes to the point that oxygen is removed and the SO_4 formed.

The sources of sulphate are sulphur minerals, sulphide of heavy metals which are of common occurrence in the igneous and metamorphic rocks and gypsum and anhydrite found in some sedimentary rocks. Also the oxidation and hydrolysis of pyrite produce sulphuric acid and soluble sulphate. Climate has an important bearing on the accumulation of sulphate in the soil and groundwater. In humid regions the sulphate may be removed with the runoff, whereas in arid and semi-arid regions the sulphates may accumulate in the surface and in groundwater due to low precipitation and inadequate drainage. At concentration around 1000 ppm, it is

laxative and cathartic (U.S.E.P.A, 1971). Sulphate with sodium interferes with the normal functioning of the intestine.

In this study the amount of sulphate varies from -0.22 ppm to 19.97 ppm with a mean value of 3.45 ppm. The BIS standard value of sulphate for highest desirable limit is 200 ppm and the maximum permissible limit is 400 ppm. In the study area, no open well samples exceed the highest desirable limit.

PHOSPHATE (PO_4^{3-})

Phosphate is determined by means of Perkin Elmer Lambda 25 UV-Visible Spectrophotometer. For this, phosphate in water is allowed to react with ammonium molybdenite in acid medium, form a phosphomolybdenite complex which is reduced by ascorbic acid in presence of antimony ions (to accelerate the reaction) to form a blue colored complex containing 1:1 atomic ratio of phosphorous to antimony. The absorption of the complex is measured at 880 nm. In order to avoid the interference of silicate in the reaction pH is usually kept low.

In the study area phosphate content varies from -0.0005 to 0.0278 ppm with an average value of 0.0023 ppm.

NITRATE (NO_3^-)

Nitrogen is a very minor constituent of rocks, but is a major constituent of the atmosphere. The greatest contribution of nitrate to groundwater is from decaying organic matter and sewage wastes and nitrogen fertilizers. As such high concentrations of nitrate are found only in specific areas. Groundwater when not polluted, contain less than 5 ppm of nitrates, but polluted water may contains up to 100 ppm.

In the present study nitrate concentration of water samples varies from 0.018 ppm to 12.15 ppm with a mean value of 4.09 ppm. All the values fall within the BIS limit for drinking water quality which is 45 ppm (highest desirable) and 100 ppm

(maximum permissible). Hence with respect to nitrate level all water samples are safe for domestic purpose.

3.13 DETERMINATION OF CATIONS

CALCIUM (Ca^{2+})

Calcium is a common mineral found in groundwater and plays a crucial role in the overall mineral composition of water. It is one of the primary ions that contribute to water hardness. Calcium ions are present in the form of calcium carbonate (CaCO3) or calcium bicarbonate (Ca(HCO3)2) in natural water sources.

Calcium is a major constituent of most igneous, metamorphic and sedimentary rocks. Principal source of calcium in groundwater are some members of the silicate mineral group such as plagioclase, pyroxene, and amphibole. Sandstone, shale and other deposits usually contains calcium carbonate as the cementing material. Calcium is also present in the form of adsorbed ions on negatively charged minerals surfaces in soil and rock.

Calcium concentration of open well water samples in the study area varies from 0.1 ppm to 10.15 ppm with a mean value of 3.66 ppm. The highest value is obtained from Velaykadavu and lowest value is obtained from Nooliyode. The BIS standard of Calcium for drinking water quality is 75 ppm (highest desirable) and 200 ppm (maximum permissible). All the samples fall within the highest desirable limits. Hence all the samples are suitable for drinking purpose with respect to this parameter. The spatial variation map is shown in (**fig:10**)

MAGNESIUM (Mg^{2+})

Magnesium is another common mineral found in groundwater and is an essential element for both humans and plants. It is often present in water in the form of magnesium bicarbonate (Mg(HCO3)2) or as a divalent cation (Mg2+). The

concentration of magnesium in groundwater depends on various factors such as geology, pH levels, and the solubility of magnesium-containing minerals. Foremost mineral bearing magnesium are olivine, augite, biotite, hornblende, serpentine and talc. Even though in igneous and metamorphic rocks magnesium occurs in the form of insoluble silicates, weathering breaks them down into more soluble carbonates, clay minerals and silica. Hence the magnesium content in groundwater achieves abundant range.

Analytical report indicates that the magnesium concentration of the open well water in the study area ranges between 1.98 to 27.76 ppm with a mean value of 8.33 ppm. Higher value of magnesium of 27.76 ppm is obtained from Ootukuzhy and lower value from Padavancode. The BIS standard for drinking water quality is 30 ppm (highest desirable) and 100 ppm (Maximum permissible). All open well water samples are well within the highest desirable limits. The spatial variation map is shown in (**fig:11**)

SODIUM (Na^+)

Momentous magnitude of sodium is found in natural water. Virtually all sodium salts are highly soluble in water and once leached from rocks and soil they hang around in solution. Foremost source of Na^+ in groundwater is plagioclase feldspars, feldspathoids and clay minerals. Sodium has a propensity to get absorbed on the clay particles but may efficiently be exchanged by Ca^{2+} and Mg^{2+}.

In the present study measurements indicate that the sodium concentration varies from 15.1 ppm to 86.9 ppm with mean value of 35.95 ppm in the case of open well water samples. The lower value 15.1 ppm was obtained from Chowalloor and higher value 86.9 ppm was obtained from Aletty. As per the BIS limits the maximum permissible limit is 200 ppm and if we discuss on this basis all the samples are within the limits. The spatial variation map is shown in the (**fig:12**)

POTASSIUM (K^+)

The frequent source of potassium is the silicate minerals orthoclase, microcline, nepheline, leucite and biotite in igneous and metamorphic rocks. Though potassium is nearly as copious as sodium in igneous and metamorphic rocks, its concentration in groundwater is one-tenth to even one-hundredth that of sodium. Resistance of potassium minerals to decomposition and fixation of potassium in clay minerals are the reasons for the slighter amount of potassium.

The results obtained shows Potassium concentration varies from 2.47 to 43.93 ppm with a mean value 14.12 ppm. Higher value 43.93 ppm was obtained from Nooliyode. According to Karanth (1987), the concentration of potassium varies from 1 ppm or 10 ppm in potable water. Here the values of Potassium are considerably within limit. The spatial variation map is shown in the (**fig:13**)

3.14 QUALITY CRITERIA FOR GROUNDWATER USE

Nearly every groundwater is free from suspended impurities and pollutants and is of steady temperature; and hence it is considered superior to surface water. Unless the water supply points are located close to saline zones, the chemical quality of groundwater remains virtually steady. To establish the suitability of groundwater of any area for drinking, domestic and irrigation uses, it is very much essential to classify groundwater depending upon their hydrochemical properties.

3.15 DOMESTIC AND DRINKING QUALITY STANDARDS

Domestic water quality standards typically include parameters such as pH levels, turbidity, odor, color, and microbial contamination. These standards govern the quality of water used for various household purposes such as bathing, cleaning, and irrigation. The guidelines aim to protect public health and prevent the transmission of waterborne diseases.

Drinking water quality standards, on the other hand, focus specifically on the safety and potability of water that is consumed by humans. These standards specify the acceptable levels of various substances and contaminants in drinking water to ensure it does not pose any health risks when ingested.

To assess the appropriateness of groundwater for drinking and public health purposes, the hydrochemical parameters of groundwater of the study area are compared with the principle values recommended by Bureau of Indian Standards (BIS).

DRINKING WATER QUALITY (As per BIS standards)

Chemical Nature	**Highest Desirable**	**Maximum Permissible**
pH	6.5 – 8.5	No relaxation
TDS	500	2000
Calcium (ppm)	75	200
Magnesium (ppm)	30	100
Chloride (ppm)	250	1000
Sodium (ppm)	-	200

3.16 IRRIGATIONAL WATER QUALITY STANDARDS

Several chemical constituents affect the suitability of water for irrigation. That includes the total concentration of soluble salts, relative proportion of sodium to calcium and magnesium, concentration of boron and the relative percentage of bicarbonate to calcium and magnesium. The quality of irrigation water is judged by studying the respective graphic representations, which is functional for display purposes and for emphasizing similarities and differences. The dominant ions such as calcium, magnesium, sodium, potassium, carbonate, bicarbonate, sulphate and chloride in a water sample can be represented in several ways. For this purpose the

equivalents per million (epm) values are most commonly utilized. A variety of graphic techniques have been developed for showing the major chemical constituents. The values are shown in table 4.

3.17 SODIUM ABSORPTION RATIO

Sodium concentration in groundwater is important because increase in sodium concentration in water upshot deterioration of soil properties there by reducing permeability. Sodium adsorbed on the clay surface as substitute for calcium and magnesium may smash up the soil structure making it compact and impervious. The processes leading to the cation exchange reactions in soil may also be studied from sodium adsorption ratio (SAR) is expressed as

$$\text{SAR} = \frac{Na^{+}}{\sqrt{\frac{Ca^{2+}+Mg^{2+}}{2}}}$$

Where, the concentrations are expressed in equivalents per million (epm)

Classification of water with reference to SAR (Herman Bouwer, 1978) is presented in the table.

SAR Values	Quality	Number of samples
0-6	No problem	20 samples
6-9	Increasing problem	No samples
>9	Severe problem	No sample

3.18 INTEGRATED EFFECT OF EC AND SAR

US Salinity Laboratory (USSL) Diagram based on SAR v/s specific conductance values, the two significant parameters of sodium and salinity hazards indicate

usability for agricultural purposes. Assorted categories are demarcated in the diagram in provison of salinity hazards and also in terms of sodium hazards, these are listed below:-

Conductivity Classification

C_1 Low salinity water ─ Good

C_2 Moderate salinity water ─ Good for soils of medium permeability for most Plants.

C_3 Medium to high salinity water ─ Satisfactory for plants having moderate salt tolerance, on soils of moderate permeability with leaching.

C_4 High salinity water ─ Satisfactory for salt tolerant crops on soils of good Permeability with special leaching.

C_5 Excessive salinity water ─ not fit for irrigation.

Sodium Classification

S_1 Low sodium water ─ Good

S_2 Medium sodium water ─ Good for coarse grained permeable soils. Unsatisfactory for highly clayey soils with low leaching.

S_3 High sodium water ─ Suitable only with good drainage, high leaching and organic matter addition. Some chemical additives in water may help if epm is low.

S_4 Very high sodium water ─ Unsatisfactory.

The calculated SAR values and the analytical EC values are plotted on USSL Diagram (**fig: 19**) and the results are presented in the table below with respect to suitability of groundwater for irrigation purposes.

Quality	Number of samples
C_1S_1 Low salinity – Low sodium	14
C_2S_1 Moderate salinity – Low Sodium	6

3.19 PERCENT SODIUM

Sodium combining carbonate can lead to the formation of alkaline soils, while sodium combining with chloride form saline soils. Both these solids do not help growth of plants. In all natural waters percentage of sodium content is a parameter to assess it suitability for agricultural purposes (Wilcox, 1955). A maximum of 60% sodium in groundwater is allowed for agricultural purposes (Ramakrishna, 1998)

Sodium ions have a tendency to be adsorbed on soil colloids. As the proportion of sodium to other cations in irrigation waters increases, sodium replaces the soil calcium and magnesium. This action, called Base Exchange, alkalizes the soil, due to which granular and permeable soil are converted into sticky clays of low permeability which dry up into hard lumps and are difficult to plough. An excess of calcium and magnesium ions over sodium in irrigation waters inhibits Base Exchange so that the soil does not lose its permeability. Hence various ratios of sodium to calcium + magnesium have been used to depict the suitability of water for irrigation. Wilcox (1955) defined a sodium percentage in terms of epm of the common cations;

$$\% \text{ Na} = \frac{(Na+K)100}{Ca+Mg+Na+K}$$

Where all ionic constituents are expressed in epm.

Wilcox (1955) classified irrigation water into different categories based on the percent sodium. The chemical quality water samlples were studied from percent sodium v/s specific conductance on the Wilcox diagram (**Fig: 20**). The results inferred from the diagram are summarized in the chart given below.

Quality	**Number of samples**
Excellent to good	20 samples
Permissible to doubtful	Nil
Doubtful to unsuitable	Nil
Unsuitable	Nil

All the 20 samples belong to excellent to good category which conclude that most of the water in the area under study is suitable for agricultural purpose.

CHAPTER IV

SUMMARY AND CONCLUSION

The present study focuses on the groundwater resources around the Poabs Solid Waste Treatment plant at Vilappilsala, within the watershed of Karaman River Basin. Geomorphologically, the area has undulating topography and is well-drained by streams. Geologic mapping has revealed that the country rock is khondalite group of rocks. Small patches of charnockite are also found associated with this rock. The area is underlain by high-grade metamorphic rocks belonging to the Kerala Khondalite Belt.

Qualitative analysis in and around Vilapilsala, the area is coming under two small watersheds of Karamana River Basin. To check for the suitability of the groundwater in the area for domestic and agricultural utilities and also to decide the most effective treatment methods, physicochemical analysis of the water was undertaken. Inorder to assess the suitability of drinking and agricultural purposes qualitative analysis were carried out by collecting groundwater samples from the downstreams of Solid Waste Treatment Plant using MP-AES instrument and titrimetric method. The physical parameters analysed include pH, EC and TDS. The chemical parameters include major anions (Cl, SO, PO_4, NO_3) and cations (Ca^{2+}, Mg^{2+}, Na^{+}, K^{+}).

A total of 20 water samples were collected. Eighteen of the samples were dugwell samples and two borewell water samples. The BIS range of pH for drinking water ranges from 6.5 to 8.5. The analysis shows that 11 out of 20 groundwater samples have pH < 6.5. Anomalous pH values were observed in the open well water in numerous parts of the study area which indicates an acidic trend. Rubber plantation is the major vegetation grown in several parts, especially where the low pH values were obtained. Large scale application of fertilizers may be the cause for this. For rubber, fertilizers are introduced by constructing pits in the ground and during the movement of water through the pits, it will get flooded with water and will perform like an infiltration pit, recharging groundwater stock in the area. During the movement downward, the collected water in pits, will dissolve fertilizer and take away it in to the aquifer. This is the major reason for the anomalous pH values

obtained in the area. Apart from that for the pre-treatment of rubber, acid is also used, the excess acid will get spread in the soil around and subsequently get mixed with water and reach the groundwater reserve of the area. The interaction of the lateritic aquifer with the circulating groundwater may be the reason for the lower pH values. The ferrous chloride present in the laterite may be converted into ferric chloride due to the interaction with ground water. This ferric chloride can give an acidic nature to the ground water. Low pH is corrosive to metallic pipes and fixtures and this could lead to release of metal ions into the drinking water. Addition of neutralizing agents can bring the pH values within the BIS limits. The analysis also reveals that all other parameters of both ground water falls within permissible limit of BIS. So on a broad canvas the water resources in the study area are safe for drinking purpose except for the low pH in 11 ground water samples. Also there is no marked increase or decrease in pH in the groundwater in the vicinity of the waste treatment plant. Irrigational water quality indices like sodium adsorption ratio and percent sodium for the sampled waters indicate that they are suitable for irrigation purposes. Plots in the Wilcox diagram too reveal that the water in the study area can be used for irrigational purposes.

The previous studies in the area a decade back by Shyam (2001) and Panicker (2001) had found that the water samples from around the waste treatment plant at Vilapilshala contain high concentration of all physical and chemical parameters during the period the plant was in operation. But the present study does not show any anomalous departure of the parameters from the standards. This may be because of the closure of the plant and subsequent cessation of leachate contamination. Nevertheless the spatial variation maps still point to a relatively higher concentration of ions (but which are within BIS standards) from two watersheds covering Vilappilshala area. The remnants of pollutants might still be lingering in the waters, but slowly nature is nurturing the aquifer back to health and to its original condition, without any human interventions.

REFERENCES

- A.P.H.A. (1995) Standard methods of analysis of water and waste water, American Public Health Association, U. S. A, 14^{th} edition, Washington, D.C.
- BIS (1991) Indian Standard specification for drinking water, Bureau of Indian Standards, New Delhi.
- CGWB, Groundwater Information Booklet Of Trivandrum District (2013), Kerala Pp.15.
- Dynamic Groundwater Resources of Kerala, March 2020, GWD & CGWB.
- Foote, R.B. (1883) On the geology of South Travancore. Rec. Geol. Surv. India, V.16, pp.20-35
- Karanth, K.R. (1987) Ground Water assessment, Development and Management, Tata McGraw-Hill publishing company Ltd, New Delhi, 720p.
- Kerala Floods Worsen Plight of Vilappilsala Village, The New Indian Express, August 14, 2018.
- Kerala Land Use Board: Natural Resources Data Bank , Thiruvananthauram (2013).pp; 41
- King, W . (1882) General sketch of the geology of Travencore State, Rec. Geol. Surv. India, V. 15, part 2, pp. 93-102
- Menon, K. K. (1967) The lithology and sequence of Quilon beds. Proc. Indian Acad. Sci. V. 65, No 1, pp.20-25
- Muraleedharan.M.P (1989); Report on large scale mapping in parts of Thiruvananthapuram district for deciphering the controls for graphite mineralization in Southern Kerala. GSI unpublished report.pp.13.
- Nair and Selvan (1976); Stratigraphic analysis of Kerala Basin. Proc.Sym.on Geology and Geomorphology of Kerala. Geological Survey of India.
- Narayanaswami. S. (1968): The Tertiaries of Kerala coast.Mem. Geol. Soc. India, No.2, pp. 300-308
- Panicker. A.V. (2001); Geo Environmental impact of Solid waste Treatment Plant at Vilapilsala, Thiruvananthapuram District, Kerala.
- Park, J.E. and Park.K. (1980) Text book of preventive and social medicine, Bharadidas Bhanet, Jobalpur.

- Probe into Industries at Vilappilsala, The Hindu, January 7, 2020
- Radhika U.P, Santhosh. M and Wada (1995); Graphite occurrences in Southern Kerala; characteristics and gneiss. Jour. Geol.Soc. India. Vol.45.No.6, pp. 653-666
- Ramakrishna, (1998): Groundwater- Handbook, India, 556pp.
- Ravindra Kumar, G.R., Rajendran, C.P and Prakash. T.N (1990); Charnockite-Khondalite belt and Tertiary-Quarternary Sequences of Southern Kerala. Geological Society of India, Bangalore.
- S. Khurshid *et al*., Indian J. Environ , Health, 40(1): 45 (1998).
- Shyam A., (2001) Micro level pollution study in and around Vilappilsala waste disposal plant site, Vilappilsala GramaPanchayath, Thiruvananthapuram District. Project submitted to CGWB Thiruvananthapuram.pp. 10
- Soman, K. (2002) Geology of Kerala, Geol. Soc. India, Bangalore.
- Todd. D.K (1980); Groundwater Hydrology, John wiley and sons, Singapore, 535p.
- Trivedy, R.K. and Geol, P.K. (1986) Chemical and Biological Methods for water pollution studies, Environmental Publications, Karad, 248P.
- U.S. Salinity Laboratory Staff (1954): Diagnosis and Improvement of Saline and Alkali Soils. – Handbook 60. U.S. Department of Agriculture, Washington, D.C.
- USEPA, (1971) Water quality criteria, EPA, R, 3/73-033, Washington D.C.
- Varadan and Murthy Y.G.K (1975); Utilisation prospect of Graphite ores in Kerala. Mineral resources of Kerala and their utilization. Proc.of the Symosium held under the auspices of the Geoscience and Technology association of Kerala. Pp.115-118.
- Wilcox, L. V. (1955) Classification and use of irrigation water, U.S.Dept. of agriculture, pp.969.

TABLES

TABLE 1: HYDROCHEMICAL DATA OF WATER SAMPLES

Sample No	Location	pH	EC µS/cm	TDS (ppm)	Ca^{2+} (ppm)	Mg^{2+} (ppm)	Na^{+} (ppm)	K^{+} (ppm)	Cl^{-} (ppm)	SO_4^{2-} (ppm)	PO_4^{3-} (ppm)	NO_3^{-} (ppm)
OW1	Nooliyode	6.34	481.9	120.4	5.89	10.47	36.79	12.76	39.88	4.07	0.00133	2.13816
OW4	Vilapil	5.32	93	61.84	2.25	3.1	26.12	5.86	19.41	0.42	0.00793	2.82727
OW8	Ootukuzhy	6.57	372.5	247.8	3.35	27.76	41.99	32.59	62.17	19.97	0.00046	1.82794
OW17	Nooliyode	5.97	85.88	56.84	1.32	3.59	24.1	5.67	19.63	0.87	0.00073	1.4513
OW18	Nooliyode	7.3	623.4	412.1	9.4	14.52	39	43.93	98.19	1.83	0.00062	7.00885
OW19	Mayiladi	5.75	320	211.9	5.41	13.6	83.5	17.76	82.41	0.56	0.00096	12.15903
OW20	Puliyarakonam	5.76	64.88	43.13	1.97	5.25	16.73	4.28	9.73	0.46	0.00005	2.46592
OW22	Aletty	5.06	304	202.9	3.09	9.86	86.9	12.74	80.89	2.01	-0.00055	8.51974
OW23	Chowalloor	7.36	68.53	45.38	0.64	6.11	15.1	8.88	19.58	-0.22	-0.00002	1.52968
OW24	Puliyarakonam	4.76	167.1	110.5	0.56	8.66	35.01	17.95	26.09	2.43	0.0004	4.57071
OW25	Velaykadavu	7.1	163.6	109.3	10.15	12.53	27.63	8.66	4.69	12.02	0.0278	3.97893
OW26	Plavaramoola	6.66	137.1	91.33	2.47	8.55	29.08	13.45	8.43	1.42	-0.00017	4.15146
OW27	Thanimoodu	5.99	100.1	66.41	2.07	4.28	28.06	4.97	22	0.64	0.00051	0.01824
OW28	Mannayam	5.93	169.1	112.4	3.46	9.95	40.03	9.6	37.84	1.87	0.00092	4.23845
OW29	Puliyarakonam	6.78	172.9	115.2	6.94	5.33	35.51	2.47	24.86	1.39	0.00089	1.6435
OW30	Vanchiyoorkonam	5.73	172.6	115.2	0.45	2.37	32.72	40.07	37.76	12.35	0.0004	1.59036
OW31	Aletty	5.79	100.3	66.45	3.78	2.11	26.53	8.49	8.52	0.05	0.00004	3.35555
OW32	Padavancode	5.79	261.7	173.3	2.71	1.98	22.4	4.04	65.74	0.07	-0.00033	10.25465
BW1	Thozhuvara	6.72	122.5	81.2	6.12	6.73	26.45	7.04	4.33	0.68	0.00006	2.50212
BW2	Nooliyode	7.45	160	106.3	0.1	6.07	35.66	2.41	7.18	4.3	0.01318	2.83348

TABLE 2:

MEAN AND RANGE VALUES OF WELL WATER SAMPLES

Parameter		Values	BIS Standards	
			Highest Desirable	Maximum Permissible
pH	Range	7.45-4.76	**6.5-8.5**	**No relaxation**
	Mean	6.2		
EC (µs/cm)	Range	64.88-623.4	-	-
	Mean	207.05		
TDS (ppm)	Range	43.13-412.1	500	2000
	Mean	131.24		
Ca^{2+}	Range	0.1-10.15	75	200
	Mean	3.66		
Mg^{2+}	Range	1.98-27.76	30	100
	Mean	8.33		
Na^{+}	Range	15.1-86.9	-	200
	Mean	35.95		
K^{+}	Range	2.47-43.93	-	-
	Mean	14.12		
Cl^{-}	Range	4.69-98.19	250	1000
	Mean	37.10		
Fe	Range	0.37-0.25	0.3	No relaxation
	Mean	0.27		

TABLE 3: AGRICULTURAL UTILITY OF GROUNDWATER

Sl No	Sample no	Latitude	Longitude	Location	SAR	% Na
1	OW1	8.528111	77.03872	Nooliyode	2.977666	76.93346
2	OW4	8.527972	77.04172	Vilapil	3.749256	87.50355
3	OW8	8.536694	77.04256	Ootukuzhy	2.33484	68.48826
4	OW17	8.531028	77.03036	Nooliyode	3.488367	86.85426
5	OW18	8.539694	77.02869	Nooliyode	2.630432	77.22135
6	OW19	8.538917	77.02475	Mayiladi	6.163838	85.47436
7	OW20	8.536056	77.02403	Puliyarakonam	1.998744	75.9488
8	OW22	8.530111	77.02358	Aletty	7.694166	89.48027
9	OW23	8.540583	77.03656	Chowalloor	1.796592	76.78077
10	OW24	8.539361	77.01875	Puliyarakonam	3.539546	84.26083
11	OW25	8.534556	77.01506	Velaykadavu	1.938595	64.93264
12	OW26	8.531694	77.01478	Plavaramoola	2.782402	79.56041
13	OW27	8.540944	77.01578	Thanimoodu	3.617233	85.54566
14	OW28	8.545	77.02025	Mannayam	3.497724	80.034
15	OW29	8.540806	77.02356	Puliyarakonam	3.48706	80.38133
16	OW30	8.535083	77.02719	Vanchiyoorkonam	6.10433	95.7478
17	OW31	8.529639	77.02067	Aletty	3.834827	88.33241
18	OW32	8.531111	77.04072	Padavancode	3.568942	87.84872
19	BW1	8.535611	77.03592	Thozhuvara	2.482574	75.59578
20	BW2	8.526028	77.03669	Nooliyode	4.389909	86.5933

TABLE 4: DETAILS OF POSSIBLE DISORDERS

No.	Chemical Nature	Highest Desirable	Maximum Permissible	Possible disorders if in higher amounts
1	pH	6.5	8.5	Taste difference and intestinal problems. Also cause rusting of pipes.
2	Hardness (ppm)	300	600	Do not lather soap, diseases to kidney, thickening of blood vessels
3	Total Dissolved Solids(ppm)	500	2000	Taste difference and intestinal problems
4	Chloride (ppm)	250	1000	Affects taste and not good for those with heart and kidney disease
5	Calcium (ppm)	75	200	Kidney diseases
6	Magnesium (ppm)	30	100	Diarrhea, increases the production of enzymes
7	Sulphate (ppm)	200	400	Intestinal and stomach disorders
8	Nitrate (ppm)	45	100	Blue baby syndrome and stomach cancer.
9	Sodium (ppm)	-	200	Affect heart, kidney, and blood circulation
10	Potassium (ppm)	No Guidelines		Diarrhea
11	Phosphate (ppm)	-	5	Vomiting and diarrhea. It affects thyroid glands and bones.

TABLE 5: WELL INVENTARY DATA

SL. NO	Well No.	Location	Latitude	Longitude	Height of parapet	Water Level	Total Depth	Well Diameter (m)
1	OW1	Nooliyode	8.528111	77.03872	0.792	3.825	6.59	1.09
2	OW2	Chowalloor	8.529861	77.03839	0.579	5.943	7.55	1.34
3	OW3	Chowalloor	8.532833	77.03572	0.838	5.257	8.74	1.21
4	OW4	Vilapil	8.527972	77.04172	0.609	6.949	8.96	1.49
5	OW5	Kadavancode	8.530528	77.04286	0.64	6.09	7.1	1.37
6	OW6	Ootukuzhy	8.532972	77.04375	0.853	6.004	7.31	1.24
7	OW7	Vilapil	8.534472	77.04475	0.762	2.788	4.32	1.25
8	OW8	Ootukuzhy	8.536694	77.04256	0.609	0.609	2.49	0.91
9	OW9	Ootukuzhy	8.534472	77.0455	0.64	9.326	11	1.52
10	OW10	Nedumpara	8.536167	77.04503	0.609	13.258	15.48	1.7
11	OW11	Ootukuzhy	8.536056	77.04411	0.853	6.339	8.56	1.09
12	OW12	Padavankode	8.536472	77.04261	1.463	8.778	13.71	1.82
13	OW13	Edamala	8.533972	77.04114	3.931	1.283	7.77	0.33
14	OW14	Edamala	8.533639	77.03861	0.822	1.188	2.95	0.88
15	BW1	Thozhuvara	8.535611	77.03592	0	0	79.24	0
16	OW15	Chowalloor	8.536889	77.04964	0.883	1.996	5.6	0.64
17	OW16	Chowalloor	8.534861	77.03436	0.335	3.535	5.71	1.43
18	BW2	Nooliyode	8.526028	77.03669	0	0	91.44	0
19	OW17	Nooliyode	8.531028	77.03036	0.822	6.903	8.19	1.43
20	OW18	Nooliyode	8.539694	77.02869	0.731	3.794	6.09	0.96
21	OW19	Mayiladi	8.538917	77.02475	0.762	8.93	11.44	0.94
22	OW20	Puliyarakonam	8.536056	77.02403	0.64	8.138	10.21	1.67
23	OW21	Nagakode	8.534528	77.01958	0.792	13.076	16.03	0.88
24	OW22	Aletty	8.530111	77.02358	0.762	9.296	13.28	1.21
25	OW23	Chowalloor	8.540583	77.03656	0.914	11.704	15.91	1.52
26	OW24	Puliyarakonam	8.539361	77.01875	0.731	9.083	12.98	1.37
27	OW25	Velaykadavu	8.534556	77.01506	0.67	10.881	13.77	1.52
28	OW26	Plavaramoola	8.531694	77.01478	0.701	3.566	5.519	1.31
29	OW27	Thanimoodu	8.540944	77.01578	0.731	6.797	9.448	1.21
30	OW28	Mannayam	8.545	77.02025	0.822	6.157	9.54	1.52
31	OW29	Puliyarakonam	8.540806	77.02356	0.548	3.048	5.85	1
32	OW30	Vanchiyoorkonam	8.535083	77.02719	0.64	3.84	6.06	1.28
33	OW31	Aletty	8.529639	77.02067	0.64	10.366	15.48	1.64

34	OW32	Padavancode	8.531111	77.04072	0.64	6.98	2.499	0.91
35	OW33	Aletty	8.531	77.01636	0.822	9.022	11.82	0.97
36	OW34	Velaykadavu	8.533361	77.01283	0.762	6.675	8.44	1.15
37	OW35	Pulimoodu	8.537111	77.01547	0.701	4.818	8.71	1.76
38	OW36	Thittayathvila	8.536	77.01169	0.64	10.058	13.13	0.82
39	OW37	Aletty	8.532278	77.02042	0.853	1.95	5.608	0.97
40	OW38	Kunjukonam	8.533778	77.01731	0.731	2.255	5.516	0.85
41	OW39	Parambmukku	8.535417	77.01839	0.792	3.383	6.919	1.49
42	OW40	Puliyarakonam	8.53925	77.02103	0.579	3.383	6.919	0.85
43	OW41	Velaykadavu	8.5335	77.02072	0.67	8.077	11.734	1.4
44	OW42	Chirakakonam	8.534611	77.01739	0.701	5.791	9.418	1.24
45	OW43	Chirakakonam	8.545139	77.01819	0.762	11.369	13.563	1.46
46	OW44	Nelivila	8.546056	77.01578	0.64	2.895	4.907	0.64
47	OW45	Kappivila	8.545583	77.01436	0.792	10.119	12.192	1
48	OW46	Kappivila	8.543028	77.01442	0.792	3.535	8.168	3.65
49	OW47	Mayilamoodu	8.541278	77.01356	0.975	11.826	13.106	1.7
50	OW48	Puliyarakonam	8.539056	77.01672	0.335	7.193	8.686	0.91
51	OW49	Puliyarakonam	8.538444	77.02294	0.701	6.309	9.357	1.52
52	OW50	Mayiladi	8.541194	77.02475	0.335	8.321	9.784	1.67
53	OW51	Mayiladi	8.542444	77.02422	0.64	8.625	10.85	1.52
54	OW52	Thottumukku	8.5445	77.02397	0.883	7.071	10.759	1.52
55	OW53	Mayiladi	8.545861	77.02194	0.762	2.042	3.96	0.88
56	OW54	Mayiladi	8.540667	77.02642	0.762	6.035	8.991	0.94
57	BW3	Chekalakonam	8.542583	77.02628	0	60.96	60.96	0
58	OW55	Kavinpuram	8.533722	77.02581	0.822	9.967	12.1616	1.21
59	OW56	Kavinpuram	8.534167	77.02286	0.64	8.382	12.984	0.7
60	OW57	Puliyarakonam	8.537139	77.02175	0.579	3.721	5.9741	1.58
61	OW58	Kavinpuram	8.5325	77.02603	0.365	8.93	11.948	1
62	OW59	Kavinpuram	8.531639	77.02486	0.338	13.28	15.788	1.67
63	OW60	Kalluparamb	8.527	77.02342	0.883	2.346	7.2848	0.88
64	OW61	Aletty	8.527778	77.02206	0.822	1.615	4.4196	1.21
65	OW62	Puliyarakonam	8.532	77.02322	0.731	8.961	12.557	1.21
66	OW63	Nooliyode	8.527083	77.03922	0.822	3.566	5.882	1
67	OW64	Chowalloor	8.526556	77.04072	0.822	2.987	8.016	1.15
68	OW65	Korakottukonam	8.531222	77.01775	0.853	5.425	7.95	1.37

FIGURES

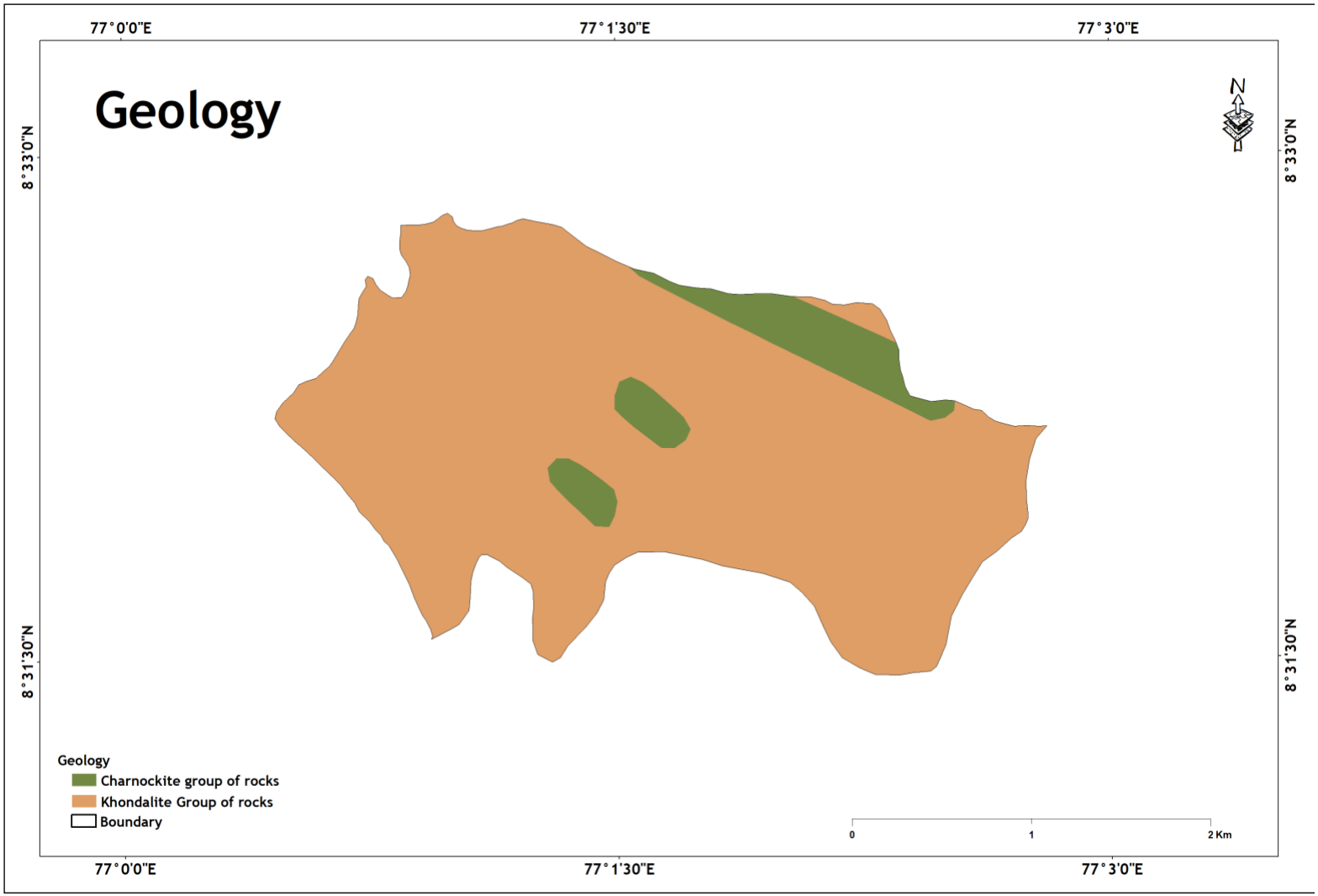

Fig 4 : GEOLOGICAL MAP

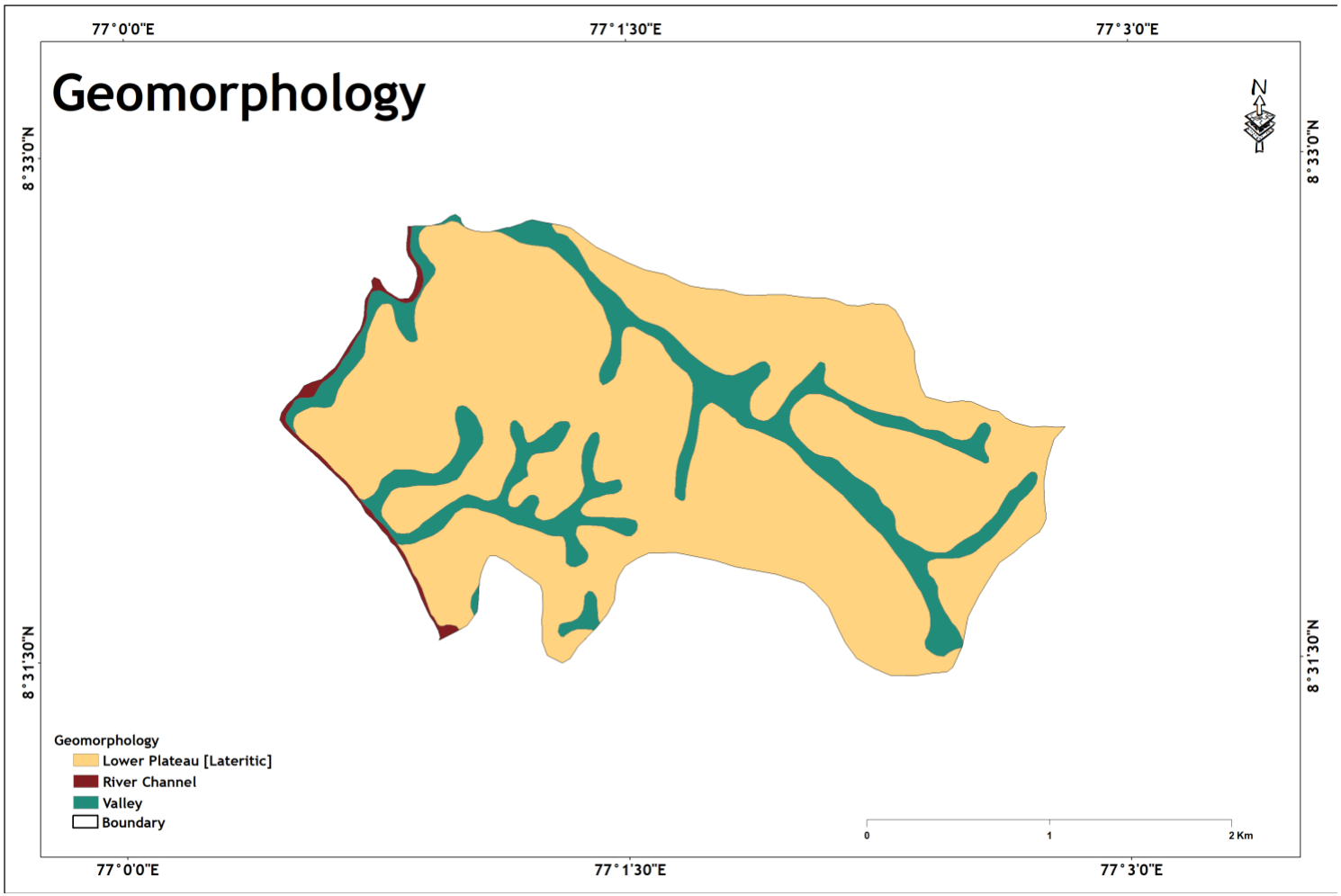

Fig 5 : GEOMORPHOLOGICAL MAP

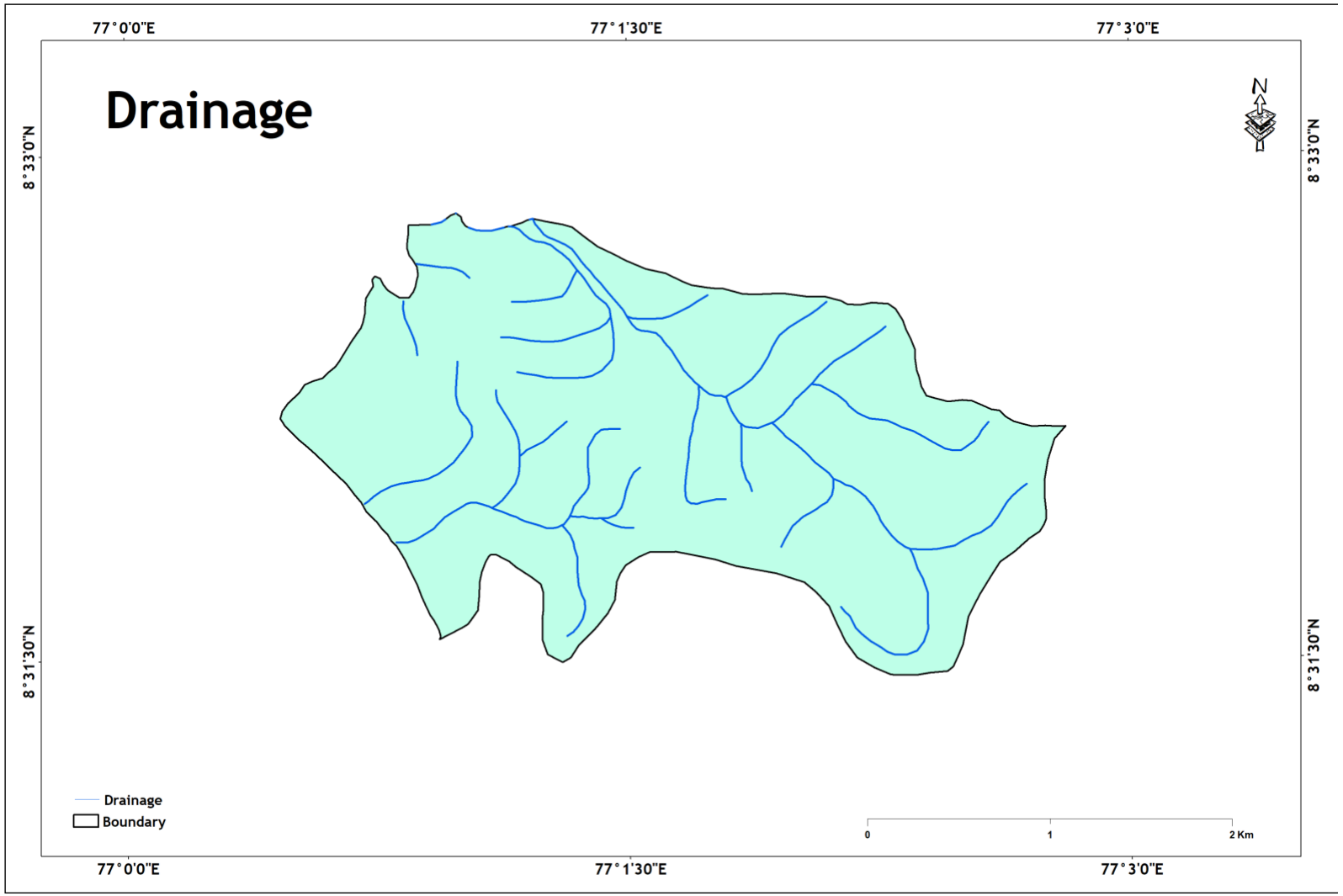

Fig 6 : DRAINAGE

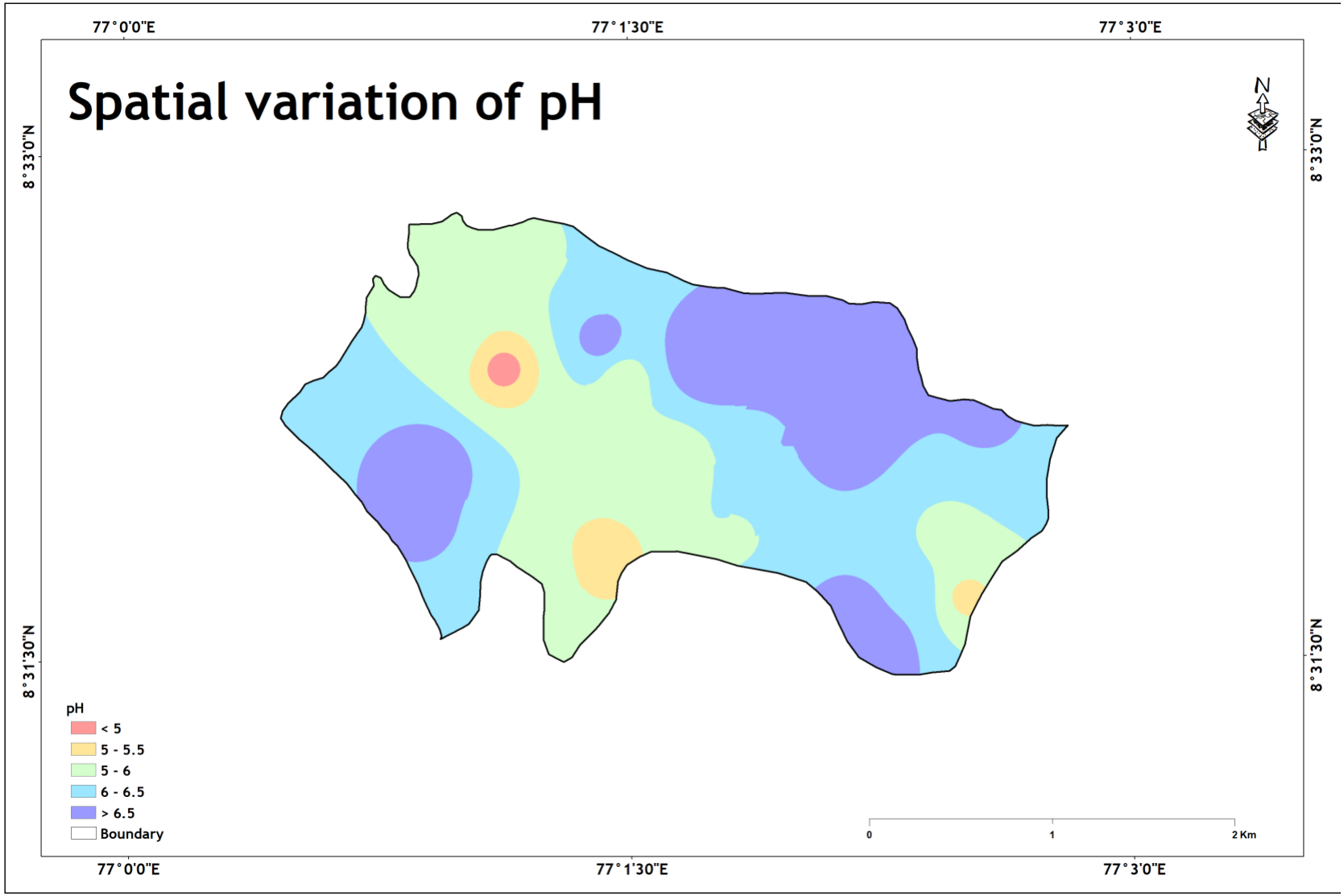

Fig 7 : SPATIAL VARIATION OF GROUND WATER pH

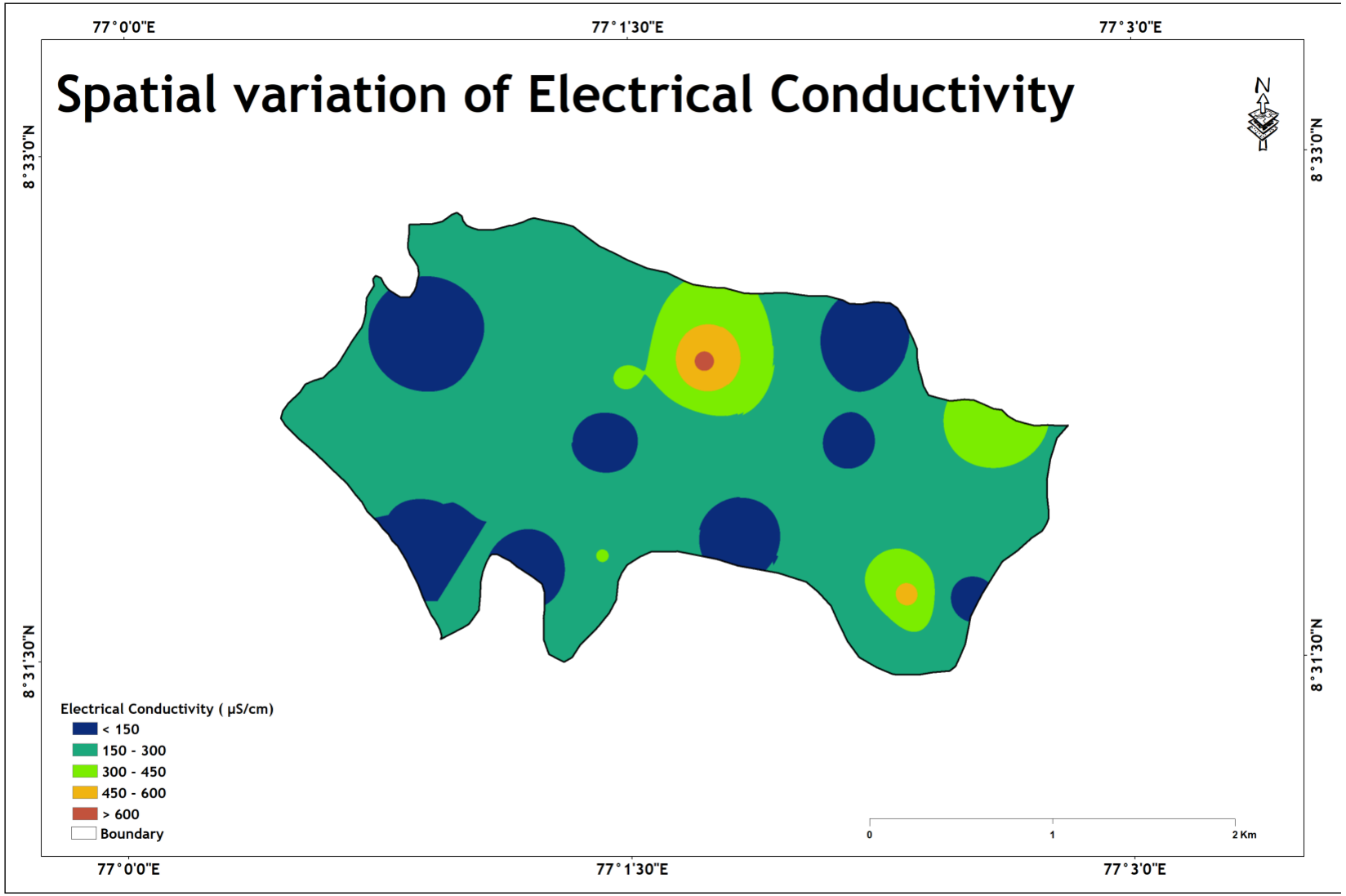

Fig 8 : SPATIAL VARIATION OF GROUNDWATER EC

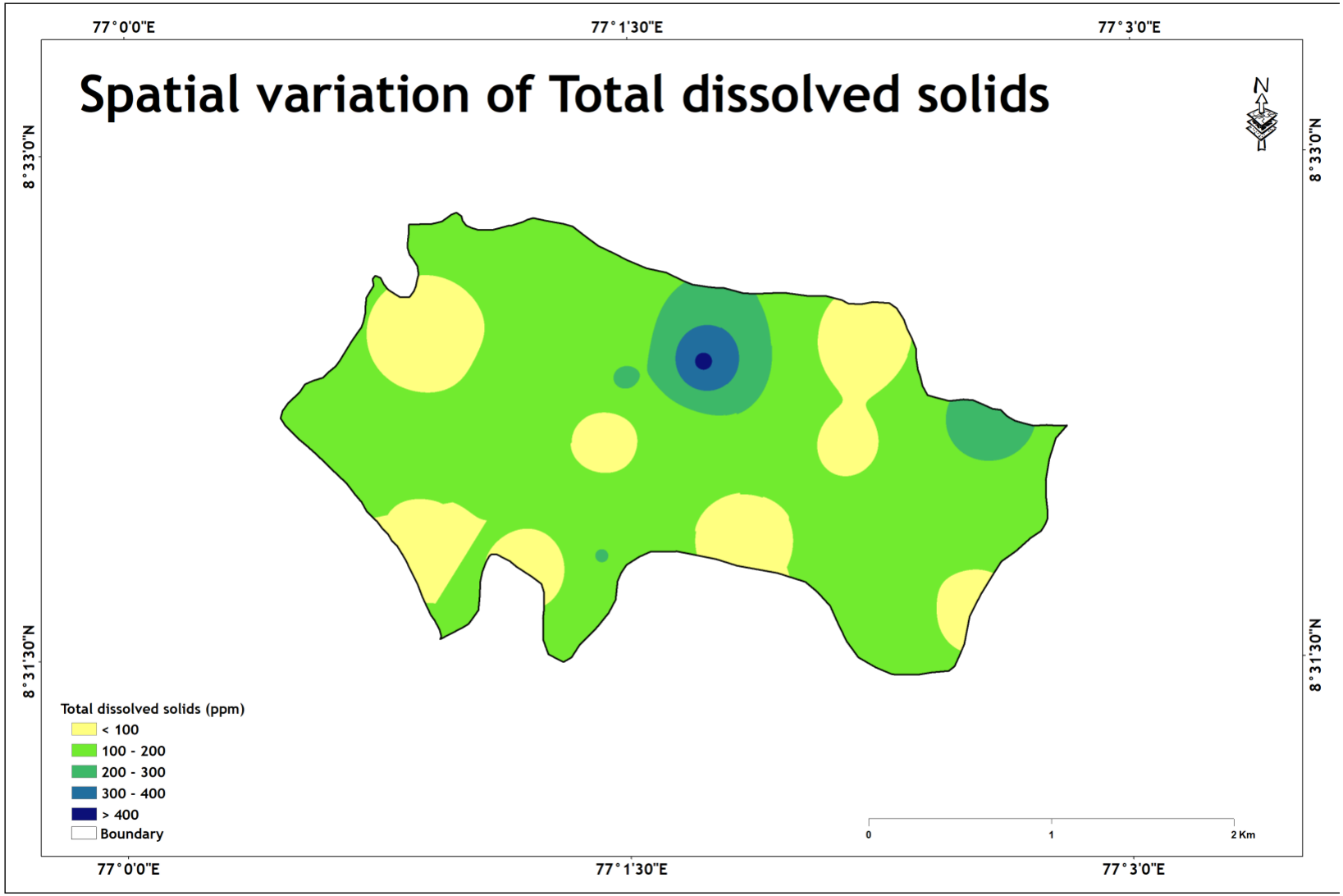

Fig 9 : SPATIAL VARIATION MAP OF GROUNDWATER TOTAL DISSOLVED SOIDS (ppm)

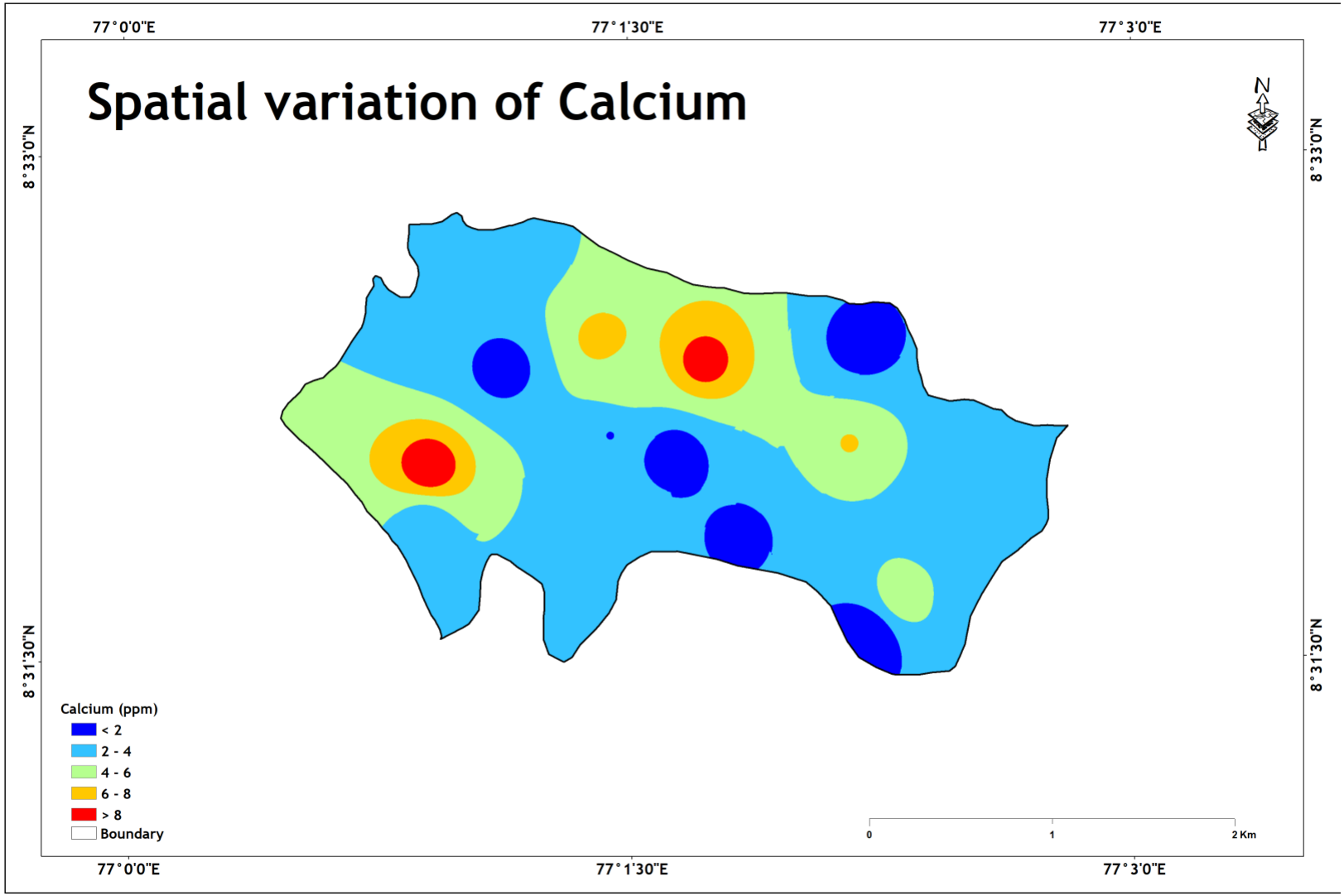

Fig 10 : SPATIAL VARIATION MAP OF CALCIUM (ppm)

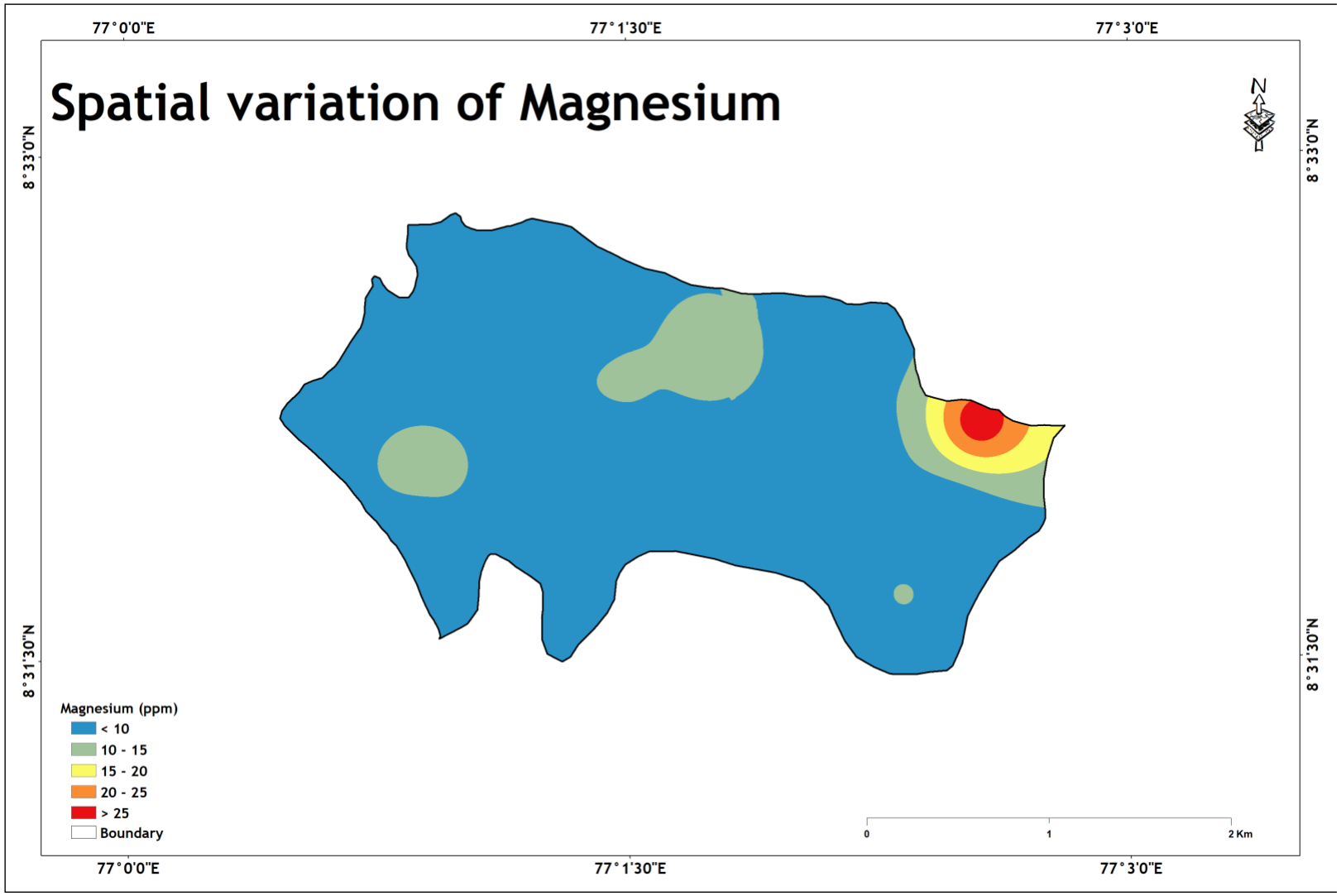

Fig 11 : SPATIAL VARIATION MAP OF MAGNESIUM (ppm)

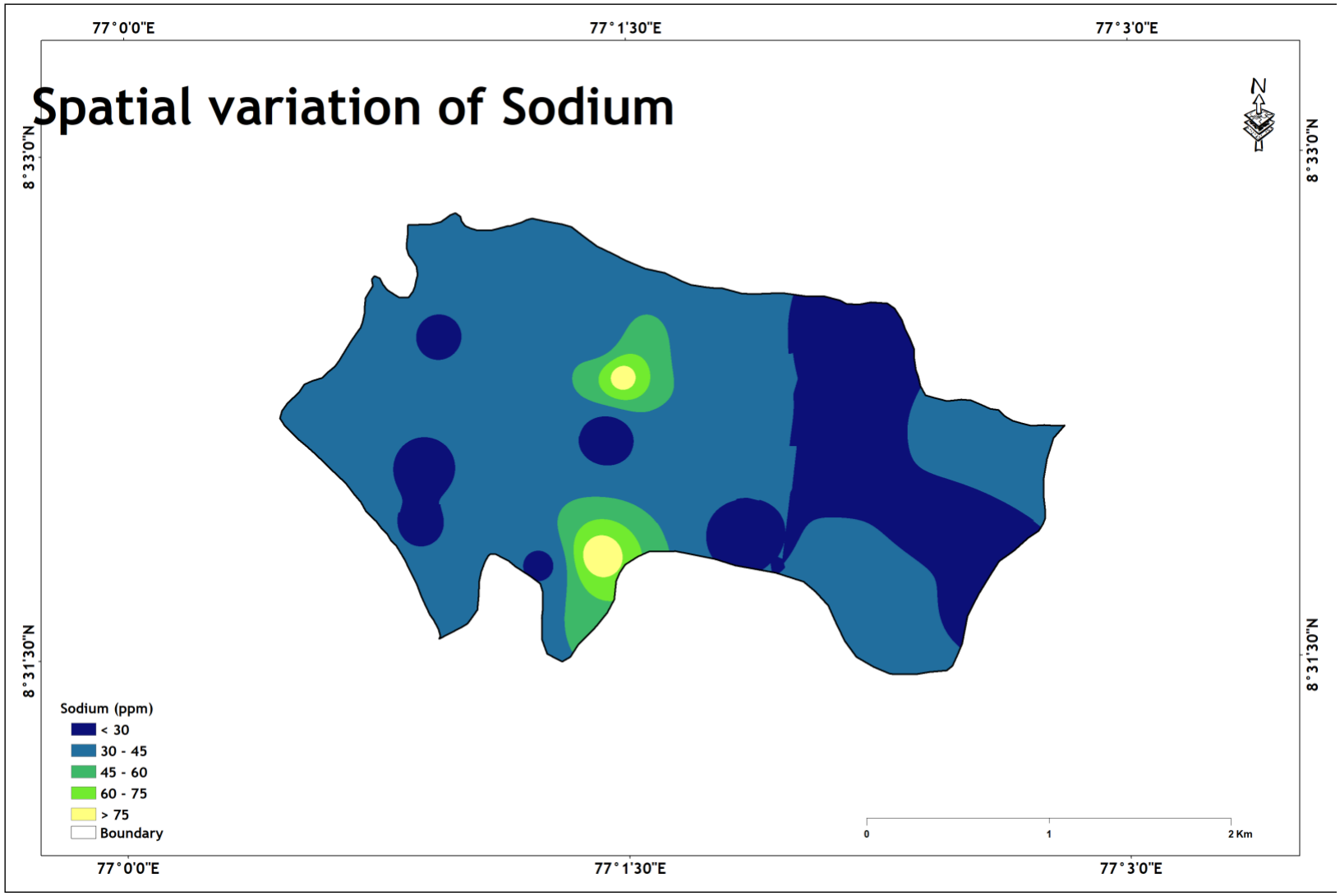

Fig 12 : SPATIAL VARIATION MAP OF SODIUM (ppm)

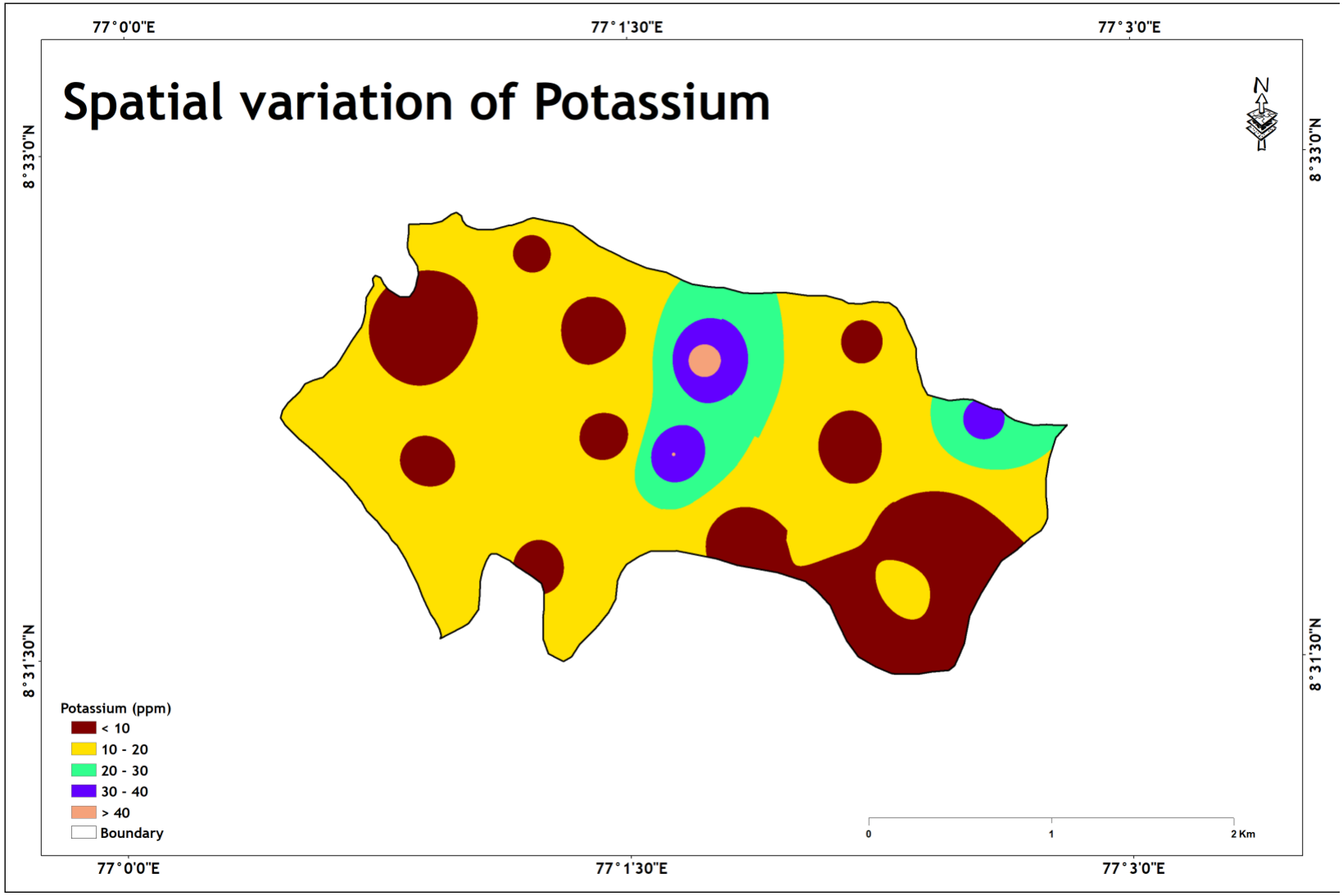

Fig 13 : SPATIAL VARIATION MAP OF POTASSIUM (ppm)

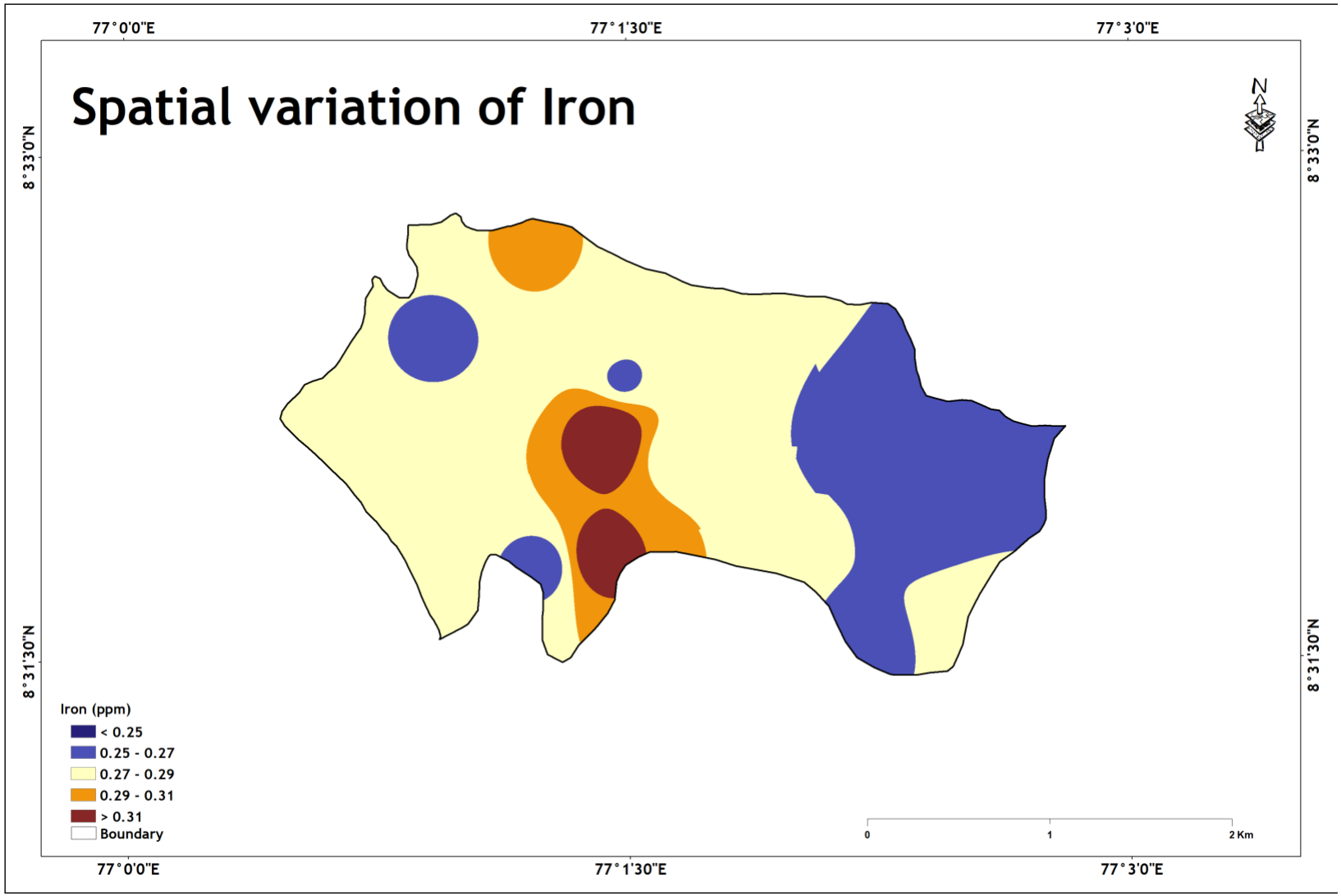

Fig 14 : SPATIAL VARIATION MA OF IRON (ppm)

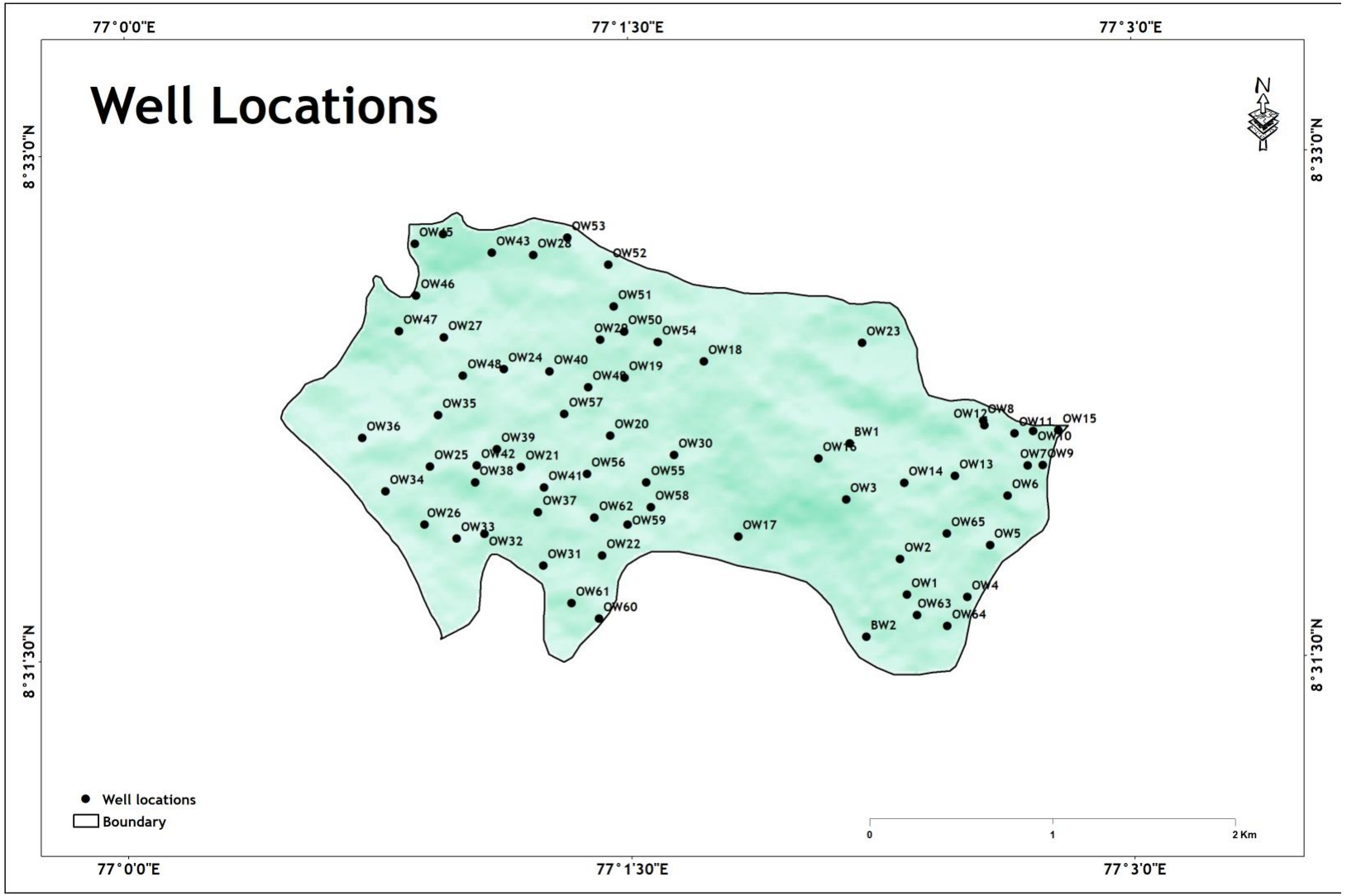

Fig 15 : WELL LOCATIONS OF

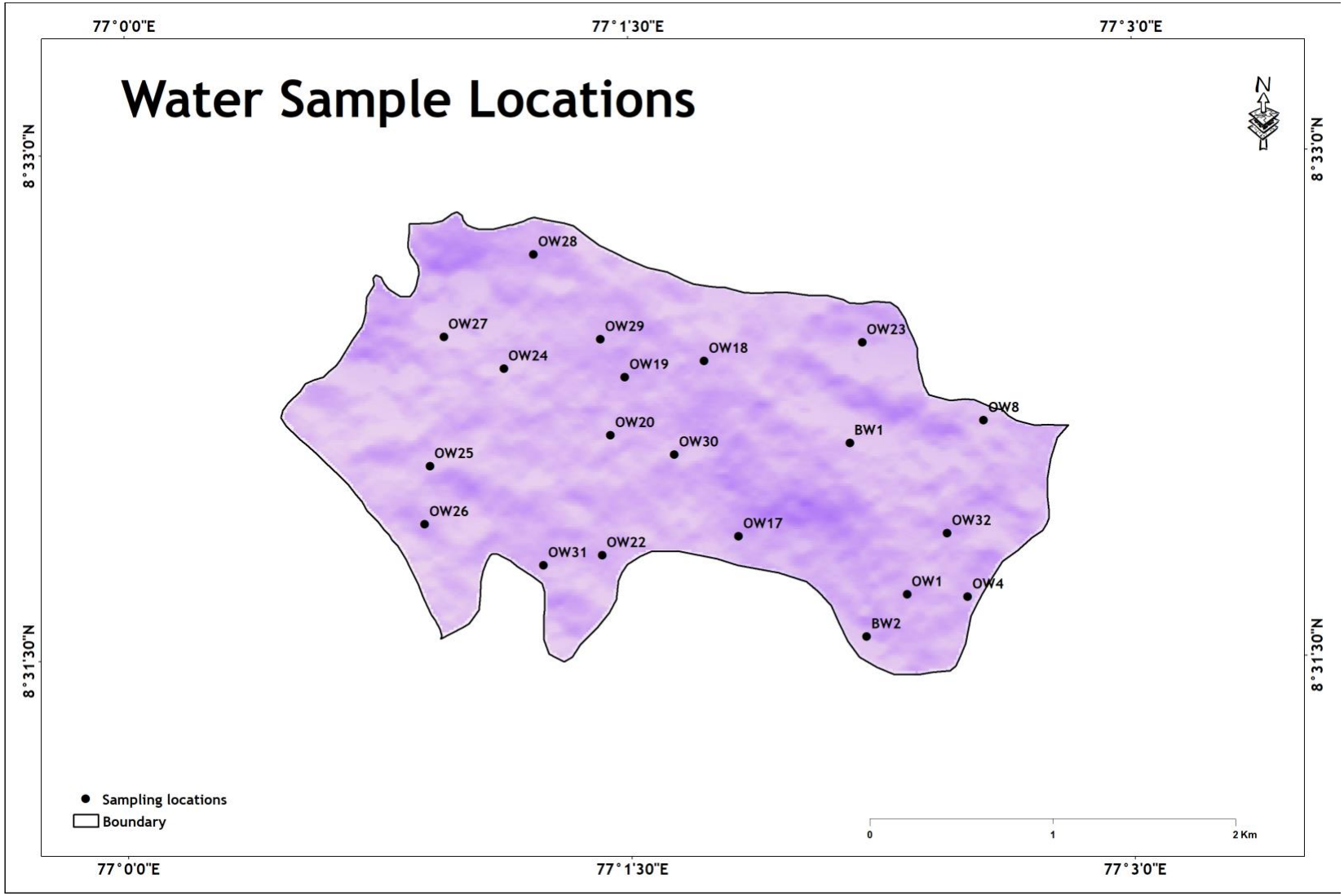

Fig 16 : WATER SAMPLE LOCATIONS

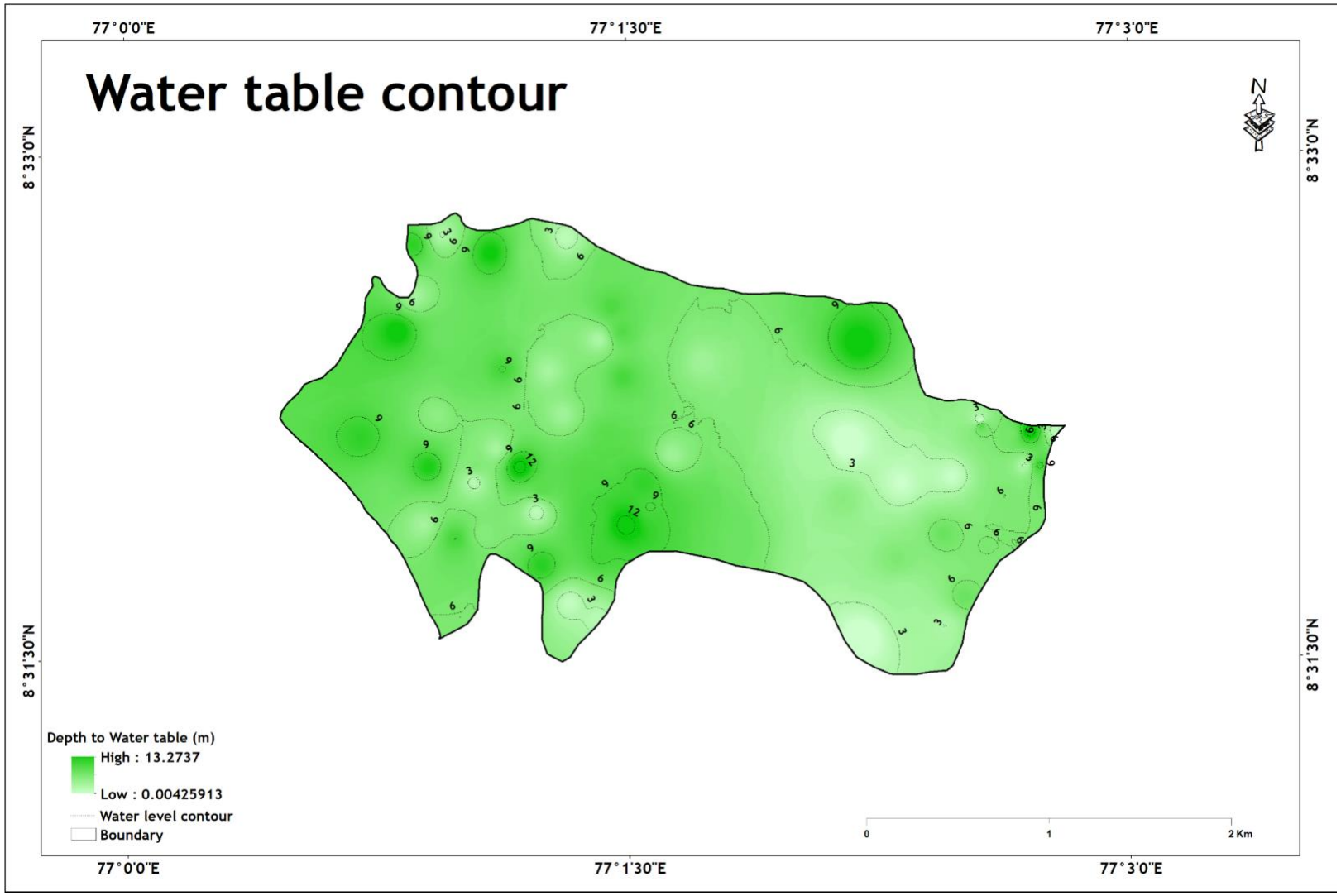

Fig 17 : WATER TABLE CONTOUR MAP

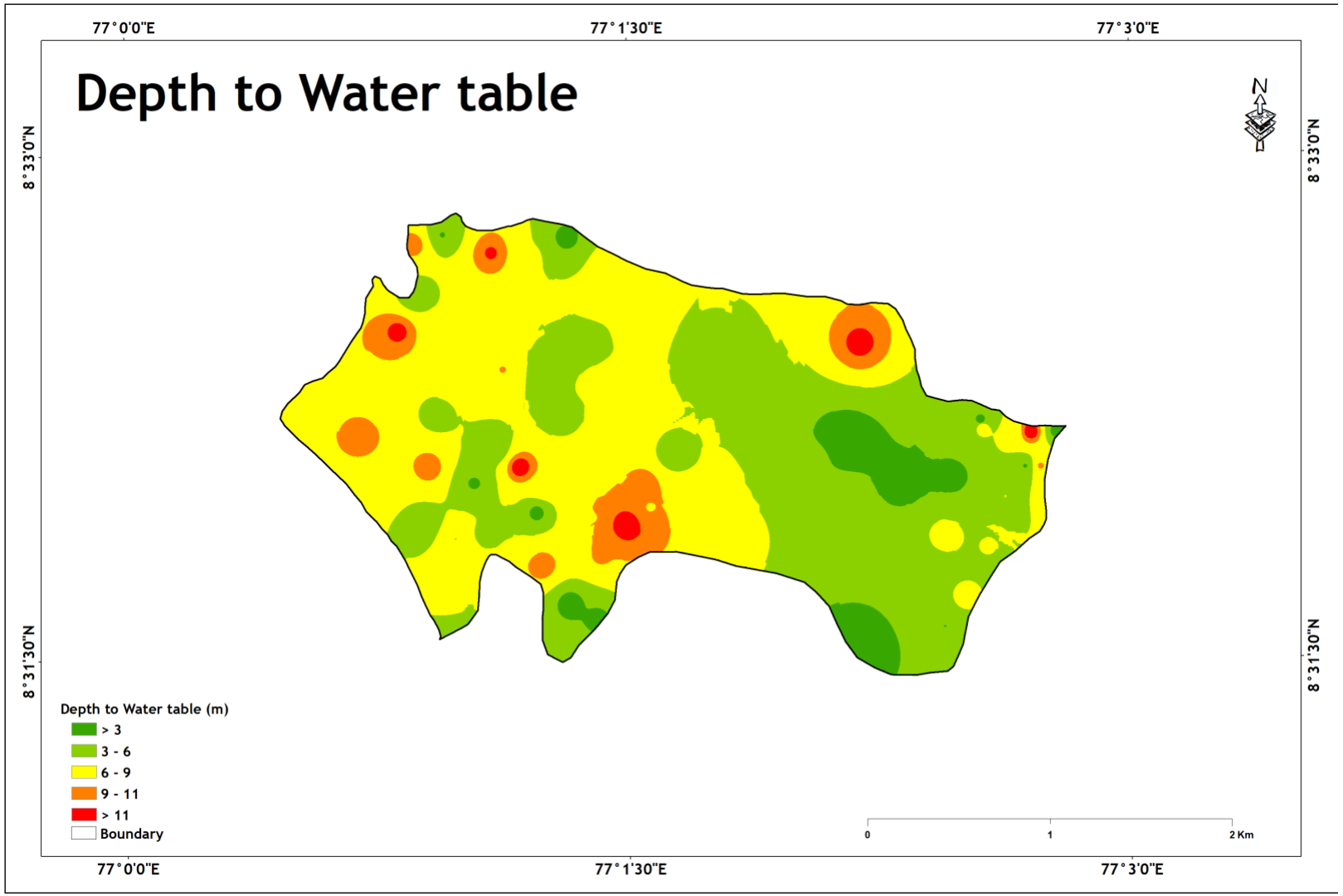

Fig 18 : DEPTH TO WATER TABLE

US Salinity Diagram

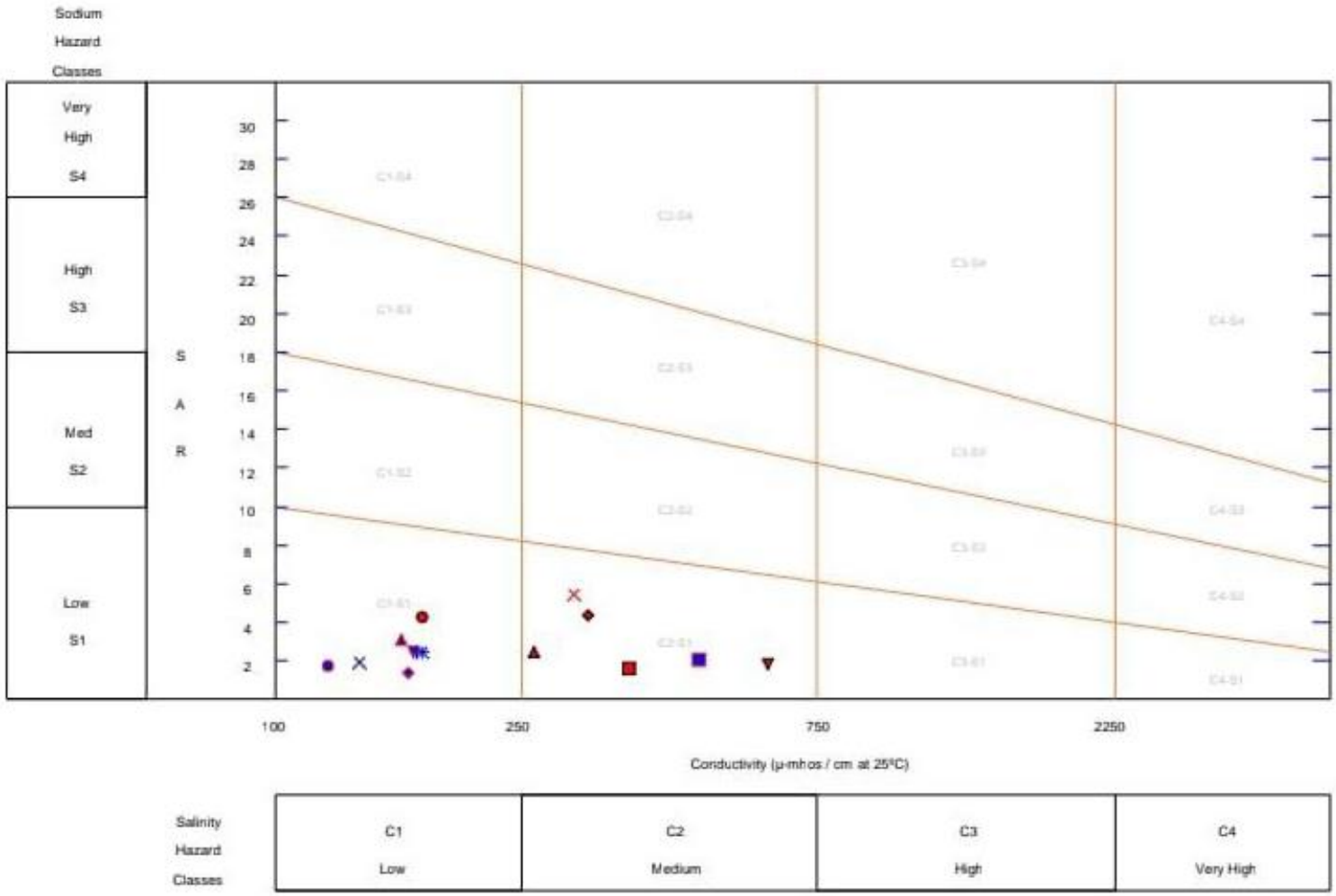

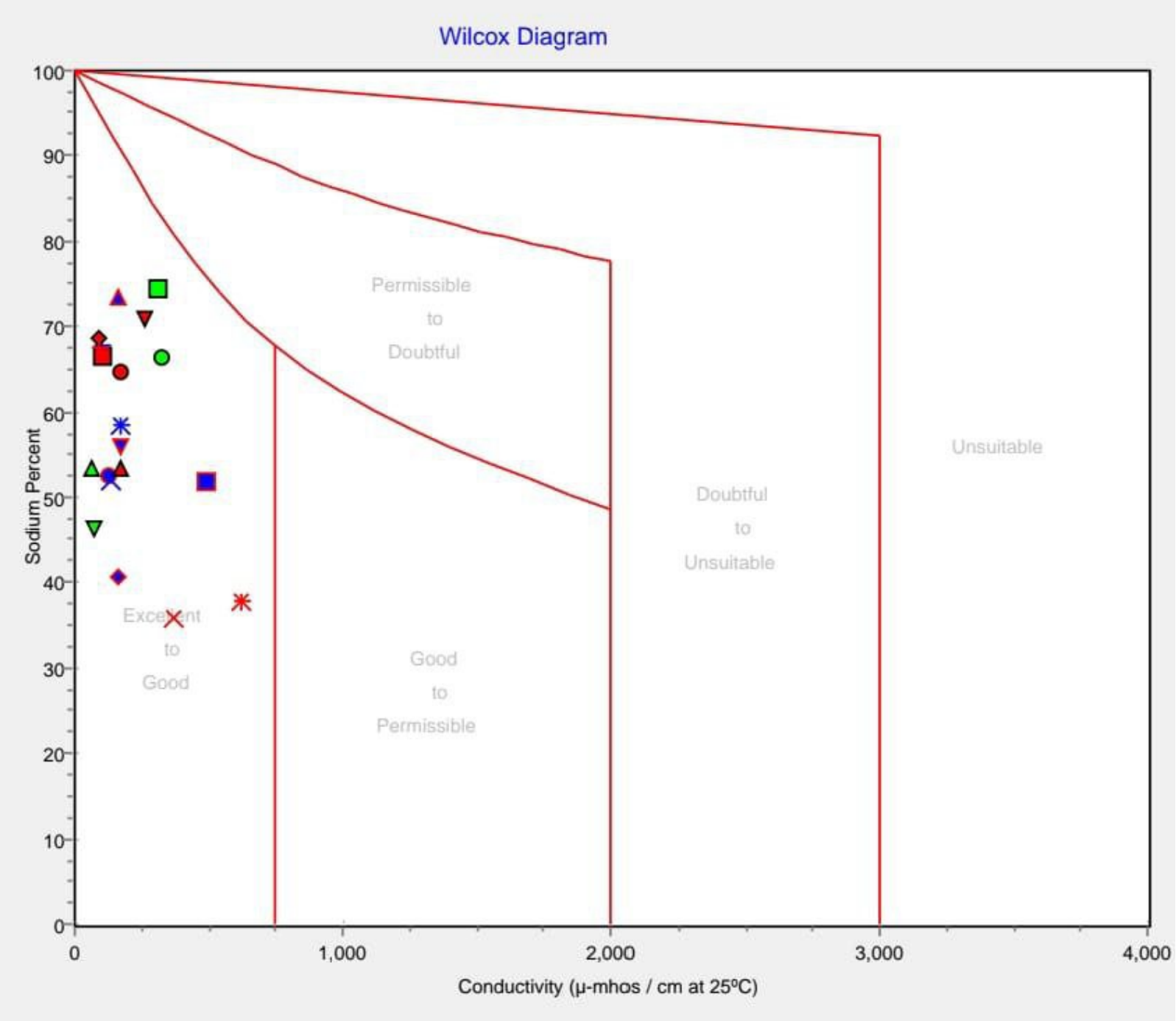
Wilcox Diagram
Sodium Percent
Conductivity (µ-mhos / cm at 25ºC)
100
90
80
70
60
50
40
30
20
10
0
0
1,000
2,000
3,000
4,000
Permissible
to
Doubtful
Unsuitable
Doubtful
to
Unsuitable
Excellent
to
Good
Good
to
Permissible

DISTRIBUTION OF OSTRACODA IN THE VANCHIPURA BEACH: IMPLICATION ON RATE OF SEDIMENTATION

Dissertation submitted to Christ College (Autonomous), Irinjalakuda, Kerala,

University of Calicut in partial fulfilment of the degree of

Master of Science in Applied Geology

By,

INDUSREE B RAJ

Reg. No: CCAVMAG009

2021-2023

DEPARTMENT OF GEOLOGY AND ENVIRONMENTAL SCIENCE

CHRIST COLLEGE (AUTONOMOUS), IRINJALAKUDA, KERALA, 680125

(Affiliated to University of Calicut and re-accredited by NAAC with A++ grade)

SEPTEMBER 2023

DISTRIBUTION OF OSTRACODA IN THE VANCHIPURA BEACH: IMPLICATION ON RATE OF SEDIMENTATION

Dissertation submitted to Christ College (Autonomous), Irinjalakuda, Kerala,

University of Calicut in partial fulfilment of the degree of

Master of Science in Applied Geology

By,

INDUSREE B RAJ

Reg. No: CCAVMAG009

2021-2023

DEPARTMENT OF GEOLOGY AND ENVIRONMENTAL SCIENCE

EXAMINERS **Dr. ANTO FRANCIS. K**

Co-ordinator

1……

2……

CERTIFICATE

This is to certify that the dissertation entitled- 'Distribution of Ostracoda in Vanchipura Beach: Implication on rate of sedimentation' is a bonafied record of work done by Ms. Indusree B Raj (Reg.No. CCAVMAG009), M.Sc. Applied Geology, Christ College (Autonomous), Irinjalakuda under my guidance in partial fulfilment of requirements for the degree of Master of Science in Applied Geology during the academic year 2021-2023.

Dr. Sunitha D
Internal Supervisor

Dr. Anto Francis. K
Co-ordinator

DECLARATION

I, Indusree B Raj, declare that the work included in my dissertation report named "DISTRIBUTION OF OSTRACODA IN THE VANCHIPURA BEACH: IMPLICATION ON RATE OF SEDIMENTATION" was composed entirely by me and that it has not previously been presented, in whole or in part, in any previous application for a degree. Except where otherwise noted, the work presented here is entirely my own. This work is presented to Christ College (Autonomous), Irinjalakuda, Kerala, in a partial fulfilment of the Master of Science in Applied Geology degree requirements.

ACKNOWLEDGEMENT

First, I want to express my gratitude to God Almighty, by whose mercy I am able to do this work. I wish to express my heartfelt gratitude and heartfelt thanks to, Dr.Linto Alappat, Dean of Research and Development of TLC (former HOD) Department of Geology and Environmental Science, Christ College(Autonomous) Irinjalakuda, Dr. Anto Francis. K, Co- Ordinator, Department of Geology and Environmental science, Christ College (Autonomous) Irinjalakuda,and Mr. Tharun R. Head of Department of Geology and Environmental Science, Christ College (Autonomous) Irinjalakuda, for developing the project's framework and providing regular support and supervision throughout the duration of the course study. A successful and ultimate conclusion of this project necessitated a great deal of advice and assistance, and I consider myself very grateful to have received this during all stages of my project work. Whatever I've accomplished is entirely due to such guidance and assistance, for which I am grateful. I would like to thank my project guide, Dr Sunitha, D (Assistant Professor, Department of Geology & Environmental Science) Christ College (Autonomous) Irinjalakuda, for creating the project guidelines and providing support and supervision throughout the project. I would prefer to take this opportunity to thank all of my classmates and friends who helped me finish my dissertation, whether directly or indirectly. I'm also thankful to the entire ChristCollege family for their love and support. I also express my gratitude to my parents and family members for their unwavering support and prayers throughout my life.

Indusree B Raj

ABSTRACT

In order to study the distribution of Ostracoda, the calcareous microfauna, occurring in the Vanchipura Beach samples, a total of 25 surface samples and one core sample were collected. Distribution pattern of individual taxon was examined and their sediment relationship was determined for ecologic/environmental interpretation. Sand-silt clay ratio estimation was carried out using the procedure of Krumbein and Pettijohn (1938). Estimation of CaCO3 was made by adopting the procedure proposed by Piper (1947) has been incorporated in this dissertation. Previous research work on Ostracoda has been reviewed and included in the separate chapter.

The main aim of the present study is to find the abundance and distribution of Ostracoda in Vanchipura Beach region. Individual taxon, distribution trends were studied, and their sediment relationships have been identified for ecologic/environmental assessmen and to discuss on carapace and open valve ratio, to know the rate of sedimentation. 4 Osracoda species were identified from the surface samples and 6 Osracoda species were identified from the core sample. The species belonging to Loxoconcha gruendeli and Xestoleberis antillea were abundant in the surface samples. The species belonging to Hemicytheridea paiki is comparatively less in number in the surface samples. On the other hand, in the core sample. Hemicytheridea paiki and Xestoleberis antillea found dominant, Ambocythere sp and Loxoconcha gruendeli found rare. The species were observed in shallow water condition.

Sedimentological characteristics were discussed by analysing the sand silt clay and the calcium carbonate percentage and the carapace and open valve ratio have also studied.

CHAPTER I

INTRODUCTION

1.1 GENERAL INTRODUCTION

Microfossils, which can be anywhere between one centimeter and one micron in size, are the subject of the relatively recent area of micropaleontology. A tiny sample of sedimentary rock or silt can yield hundreds of well-preserved specimens due to their small size, making them a useful tool for researching ecosystems and environmental changes. Foraminifera,Ostracoda, Nanoplankton, dinoflagellates, acritarchs, diatoms, and radiolarians are only a few of the different kinds of microfossils that are frequently utilized in biostratigraphic correlation, paleoenvironmental reconstruction, and paleoceanography. Micropaleontology has significantly advanced in the areas of taxonomy, biostratigraphy, and paleoecology during the course of the past century, attributed in large part to the petroleum industry's use of the field for subsurface correlation of geologic layers.

The 1970s saw a shift in emphasis towards the interpretation of deep-sea core sequences, which improved our understanding of the geologic time scale and elevated paleoceanography to the forefront of modern science. More recently, radioactive isotope ratios in microfossils have been found to vary through space and time, revealing changes in plate tectonics and paleoclimatology as well as other physical, chemical, and biological components of the global ecosystem

Microfossils are helpful for studying ecology and evolution in addition to these new fields, as well as for environmental monitoring of aquatic ecosystems that are impacted by urban and industrial pollutants. Using micropaleontology in forensic investigations is prevalent.

1.2. INTRODUCTION TO OSTRACODA

Organisms that offer a proxy record of changes are especially important in light of the growing focus on environmental and climatic change in the scientific literature. It is widely used as a palaeoenvironmental, palaeoclimatic, and biostratigraphic indicator because one group of tiny

crustaceans, the ostracods, has a good fossil record and is one of the few that can be equally (palaeo)environmentally informative in both the marine and non-marine realms. Ostracod applications span a variety of fields, including evolutionary biology, zoology, molecular biology, (palaeo-)ecology, (palaeo-)limnology, and (palaeo-)oceanography, in addition to geological and palaeontological ones, such as basin analysis. Palaeoclimatic applications of ostracods frequently combine and integrate several of these fields.

Only estimations of the overall number of species in the ostracoda have been reported; the richness of this group has not yet been thoroughly characterized. Although this includes subspecies and synonymies, more than 65,000 living and fossil ostracod taxa at or below the species level have been reported based on the database compilations of Kempf 1996 and Kempf 1997 (Ikeya et al., 2005). Only half of the 20,000 living species that are thought to exist have been formally described, with the bulk coming from marine and transitional waters; 2000 fictitious species are known from non-marine environments (Martens et al., 2008).

The longest fossil record of any arthropod, dating from the Ordovician to the present, belongs to the ostracods and spans roughly 450 million years (Ma). A Silurian planktonic ostracod represents the earliest known instance of a male metazoan (Siveter et al., 2003), and a non-marine family with a lengthy history of obligate parthenogenesis (probably more than 200 Ma) is exceptional as a "ancient asexual" lineage with a rich fossil record (Martens 1998, Martens et al., 2003, Martens 2008).

Ostracods were first mentioned between 1000 and 1150 A.D. by the Mogollon people of New Mexico, who depicted certain specimens (perhaps Chlamydotheca or Megalocypris) on some Pueblo pottery (Neale, 1988). The first ostracod was described by Linné in 1746, and Baker illustrated one in 1753, likely depicting a Cypris (Oertli, 1982). However, O.F. Müller made the most significant contribution to early ostracod studies by proposing the first linnean taxonomic assignment of an ostracod (Müller, 1776, in: Oertli 1982, Neale 1988; both are also useful for historical references).

The French scientist Pierre André Latreille gave the name of the Class Ostracoda; he first used the spelling "Ostracoda" in 1802 and then modified it to "Ostracoda" in 1806 (Oertli, 1982). Early descriptive studies were published in the nineteenth century, such as those by Baird (1850), and a higher taxonomy of the major groups was established by Sars (1866). These were followed by the first comprehensive investigation of British Pleistocene ostracods (Brady et al., 1874), as

well as classic monographic treatments of living ostracods collected during oceanic cruises as well as in coastal and inland waters (e.g., Brady 1868, Brady 1880, Brady and Norman 1889, Brady and Norman 1896, Müller 1894).

Important publications on ostracod taxonomy (Sars, 1923–1928), ecology (Elofson, 1941), and functional morphology (Skogsberg 1920, Cannon 1925, Cannon 1933) were published in the first half of the 20th century. The development of radiometric dating and the advancement of geochemical microanalyses later in the 20th century provided some of the foundation for the collaborative advancement of Recent and Quaternary ostracod studies. Recent assemblages can be thought of as "modern analogues" of fossil assemblages discovered in sediment core samples where the palaeoenvironmental signals may be interpreted in terms of climatic changes (Delorme and Zoltai 1984, Penney 1987, examples in De Deckker et al., 1988). This is possible because the autecology of many living species has been described in relation to key environmental parameters (e.g., McKenzie and Jones, 1993).

Ostracodologists, or specialists in ostracod research, have been particularly busy lately. The ostracodologists' periodical, CYPRIS, reported on roughly 150 prominent scholars between 2008 and 2009 (Brouwers and Frenzel, 2009). Significant contributions to ostracod research are compiled in the Proceedings of the 16th International Symposia on Ostracoda (ISO1, Naples, 1963 to ISO16, Brasilia, 2009), as well as in the 7th European Ostracodologists' Meetings (EOM1, Frankfurt, 1989 to EOM7, Graz, 2011). These publications, in addition to numerous publications in well-known international scientific journals.

Ostracods live in almost every known aquatic ecosystem, from the ocean's depths to transient inland waterways and even semiterrestrial habitats like leaf-littered soils. With the exception of the planktonic niche in brackish and non-marine waters, their ecological flexibility, which is based on tolerance of environmental limits and adaptability to varied feeding and reproduction types, allows them to fill the majority of ecological aquatic niches.

The calcitic carapace of the ostracod, which has two valves and encloses the soft body, shields the creature from potential threats in the aquatic environment in which it lives and also traps the geochemical and isotopic signal of the water during the time of biomineral precipitation. Ostracods are thought to have the most extensive palaeontological record of any arthropod, with a fossil record dating back at least 450 Ma due to the great possibility for this carapace to be retained in sediments.

1.2.1.APPLICATION

In a geological context, applications of ostracods include relative dating and correlation (biostratigraphy) as well as palaeoenvironmental and palaeoclimatic uses. With the exception of their use in Purbeck–Wealden (latest Jurassic to Early Cretaceous) stratigraphy where ostracod zonation is widely utilised (Horne, 1995), the value of the ostracods as biostratigraphical markers (biozones) is often regarded as less than that of planktonic foraminifers and nannoplankton (in marine settings)

1.3 SEDIMENMT ANALYSIS

Understanding the content, origin, and history of sediments requires the use of sediment analysis. Silt analysis, which focuses on the size distribution and properties of silt particles in a sediment sample, is a crucial component of sediment analysis. Typically described as particles with a diameter between 2 and 63 microns, silt particles are intermediate in size between sand and clay. Silt particles can reveal vital details about the ways that sediment is transported, where it comes from, and where it is deposited.

Techniques for sediment sieving, settling, and microscopy are frequently used in silt analysis. The silt fraction of sediment samples is first separated out using a sieve, and it is then given time to settle in water. The size and shape parameters of the settled silt particles are next determined by microscopical examination. Additional analytical methods, such as X-ray diffraction (XRD) to determine the mineralogical composition and scanning electron microscopy (SEM) to look at the shape and microstructure of silt particles, may be employed in addition to silt analysis. Sedimentology relies heavily on silt analysis, which is also helpful for deciphering the geological past of sedimentary environments.

Carbonate is a common mineral composition found in soils, sediments, and rocks, and it can be generated in both marine and terrestrial environments. As the largest inorganic carbon reservoir on Earth's surface, carbonate minerals in the ocean are primarily responsible for shallow carbonate platform sediments and deep ocean biogenic calcareous deposits. Numerous environmental and climatic variables, including temperature, pH, precipitation, biological productivity, microbial community, and hydrological circumstances, can have an impact on the types, concentrations, elements, and isotopic compositions of carbonate in sediments and

sedimentary rocks. Paleoceanography hence frequently uses proxies for sediments or sedimentary rocks that are connected to carbonate

1.4. OBJECTIVES

- **a.** To identify and illustrate calcareous microfauna such as Ostracoda, occuring in the VanchipuraBeach samples, using standard micropalaeontological techniques
- **b.** To determine the sedimentological parameters such as sand, silt and clay and calcium carbonate of the sediments collected from the beach samples in Vanchipuraand to correlate with distribution of Ostracodapopulation
- **c.** To discuss on carapace and open valve ratio, to know the rate of sedimentation.

CHAPTER II

REVIEW OF LITERATURE

2.1 STUDY OF OSTRACODS IN AND AROUND THE WORLD

There are several kinds of studies done on ostracoda, the studies are done by using several methods. The studies of the Use of Ostracods in Palaeoenvironmental Studies, or What can you do with an Ostracod Shell done by (Ian Boomer,David J. Horne andIanJ.Slipper)2017.Ostracods have emerged as reliable markers of ecosystem health, biodiversity, and environmental change in recent decades. Their utility extends to almost every aquatic and semi-aquatic habitat, from the deep ocean to high mountain springs, with applications ranging across the earth sciences (from modern pollution studies to sea-level change, basin evolution, plate tectonics, palaeoceanography) and related disciplines such as archaeology, ecology, and genetics. Their time span has now been determined to be the last 500 million years of Earth's history.The study of fossil ostracod assemblages follows traditional palaeontological lines of inquiry, such as taphonomy, morphometries, and diversity, but there are a number of ostracod-specific methodological approaches that make them potentially one of the most versatile organisms in the fossil record. Ostracods have been used to recreate historical habitats on a variety of temporal and geographical dimensions, from global geological-scale occurrences in the deep sea to smaller-scale studies of lakes and their archives of local environmental change over recent decades.Much information may be gathered from ostracod assemblages, but it is recent breakthroughs in the chemical and physical examination of single shells or carapaces that have pushed the value of these creatures to the forefront. This research examines the possible palaeoenvironmental information gained from an ostracod assemblage, a single species, or a single shell. The primary uses of ostracods for marine and non-marine habitats are discussed. Finally, the ostracods' function in reconstructing the Aral Sea's recent past is discussed.

Oxygen and carbon isotopes in current freshwater ostracod valves: determining essential offsets and autecological effects relevant to palaeoclimate investigations (Ulrich von Grafenstein a, Helmut Erlernkeuser b, Peter Trimborn)1999.The isotopic composition of modern benthic ostracod and mollusc carbonate, the oxygen isotope composition of lake water (18OW),

the carbon isotope composition of dissolved inorganic carbon (13CDIC), and water temperatures were all measured over a year in two lakes (Ammersee and Starnberger See, both in southern Germany). The goal was to see if the valves were constructed in isotopic equilibrium and how seasonal water temperatures were recorded in the shells. We observe regular deviations between the 18O of valve carbonate and the 18O anticipated for isotopic equilibrium calcite. Offsets are greater than +2 for many Candona species, +1.5 for Cytherissalacustris, and less than 0.8 for Limnocythereinopinata and Darwinulastevensoni.They appear to be temperature independent and consistent for all instars of a species. When the offsets are removed, the mean water temperatures of the calcification period are easily reflected in the valve-18O. The 13C of valve carbonate is mostly influenced by the 13C of dissolved carbonate in ambient lake water, although it appears to be influenced by micro-habitat effects and important offsets. The research gives information on the seasonality of valve creation, which might lead to the determination of temporal and geographical water temperature gradients from particular 18O recordings.

The chemistry of ostracod shells as an indicator for paleoenvironmental change(Nicole Börner a, Bart De Baere b, Qichao Yang c, Klaus Peter Jochum c, Peter Frenzel d, Meinrat O. Andreae)2013 Over the last several decades, the use of ostracod shell chemistry as a paleoenvironmental tool has risen. Most research have focused on Mg and Sr in ostracod shells as temperature and salinity proxies, and the use of a diverse range of trace elements as future paleoenvironmental indicators for lacustrine systems has yet to be explored. Trace metals, such as Cd, Ba, and Zn as paleonutrient indicators, or Mn, Fe, and U as redox and oxygenation indicators, have only been employed in a few exploratory investigations in paleolimnological studies.Foraminifera and corals are the most commonly utilised fossils in paleoceanography to recreate historical climatic conditions. Proxies for variations in sea surface temperatures, such as 18O, Mg/Ca, and Sr/Ca, are well-established. Furthermore, a large number of novel proxies, such as radiogenic isotopes and redox sensitive trace elements, have lately been produced. Ostracod shell chemistry is commonly utilised in paleolimnology to determine paleohydrological changes. Temperature and salinity changes in lake environments are frequently reconstructed using oxygen isotopes, as well as Mg/Ca and Sr/Ca ratios, but depending on the hydrological and geological settings of the lake system, local calibrations are required to determine which proxy is best suited to reflect which processes.New proxies must be tested using unique approaches that have lately become available. When compared to traditional ostracod shell chemistry

instruments, technologies such as Laser Ablation ICP-MS and NanoSIMS allow for single shell analysis and give high-resolution data. The paleolimnological potential of ostracods has not yet been thoroughly explored, but it may be developed by learning from paleoceanographic investigations.

Ostracod genomics (Ostracoda, Crustacea): Opportunities and Challenges(Isa Schön a b, Koen Martens a c)2016. Ostracods are excellent models for evolutionary studies. Classical genetic approaches were largely employed for phylogenetic investigations on Ostracoda, and they were hampered by a scarcity of adequate markers. Genomic technologies, despite their enormous promise, have seldom been used to this group of crustaceans. We present pertinent examples of genomic investigations on other organisms in order to suggest future directions for genomic ostracod research. At the same time, we propose answers to possible difficulties in ostracods that genomic approaches may offer.

Ostracods from ancient lakes, both modern and fossil (J. A. Holmes and A. R. Chivas)2002.Ancientlake systems have very rich records of ecological and environmental change from the past. Ostracods have long been connected with ancient lakes, owing to the fact that they are widespread in such environments, commonly fill specialised ecological niches, and can be researched relatively simply. Furthermore, because of their exceptional preservation capability, they usually have a lengthy fossil record, giving a simple approach of analysing temporal changes in the lake system. We use a combination of biological and geological criteria to classify ancient lakes and then review some of the evolutionary and palaeoclimatic issues that can be addressed with respect to ancient lake ostracod faunas through a series of case studies using both extant and fossil examples.We also highlight some of the present gaps in the field and ask for greater coordinated study, not just from a taxonomic and ecological aspect, but also in providing rigorous chronological control for fossil sequences. The possibility of combining present and fossil faunal data with new genetic analysis tools will keep ostracod studies at the forefront of palaeoclimatic and evolutionary study in ancient lake habitats.

Ostracod Taxa as Quaternary PalaeoclimateIndicators(Alan R. Lord, Ian Boomer, Elisabeth Brouwers, John E. Whittaker)2012.We discuss the use of ostracods for palaeoclimatic reconstruction at various taxonomic levels. Ostracods can give palaeoenvironmental information in a variety of ways. Their mineral shells' chemical and isotopic composition, as well as the

comparatively tiny organic component trapped within the carbonate lattice, may provide direct quantitative evidence of circumstances in their native environment. Morphological observations and comprehensive morphometric records of valve size, shape, and outline within a species might offer minor hints about environmental changes across habitats or stratigraphic intervals.Uniformitarian techniques may be used to classify species, genera, and suprageneric classifications, but with decreasing precision and growing uncertainty in palaeoenvironmental relevance (1) as the taxonomic unit increases and (2) as the material becomes older geologically. The standard practise of integrating individual species' habitat and environmental preferences to infer palaeoclimatic conditions is as applicable now as it was in the nineteenth century.

The use of ostracods from brackish and marginal marine environments as bioindicators of current and Quaternary environmental change (Peter Frenzel, Ian Boomer)2005.Ostracoda (microscopic aquatic Crustacea) from brackish waters have a significant potential for ecological monitoring and palaeoenvironmental studies in extremely changeable situations. This has been demonstrated in several papers over the last few decades, but their potential has yet to be completely realised or harnessed. The composition of ostracod assemblages, species distributions, eco-phenotypic variability, and analysis of stable isotopes and trace elements in ostracod shells provide valuable information on current and past water salinity, temperature and chemistry, hydrodynamic conditions, substrate characteristics, climate, sea level variations, oxygen and nutrient availability. This article gives an overview of the use of ostracods from brackish waters for Quaternary palaeoenvironmental reconstruction and environmental research in modern contexts.

The use of Ostracoda in sea-levelresearch (DavidN. Penny 1987).Ostracoda are likely stronger predictors of former sea level than previously thought. This is due to the presence of extremely distinct low diversity, high productivity faunas in the higher reaches of the estuary environment. Furthermore, there is a significant amount of understanding about their environment. The faunas found in different estuary facies are described in detail, as well as how death assemblages may be separated from life assemblages. In some NW European microtidal locations, sea level can be calculated with an accuracy of 50 cm to 100 cm, but further study on macrotidal shores is needed to see if they can be used to pinpoint sea level here. Examples of where Ostracoda have been useful in sea-level research include North Denmark and The Netherlands.

Distribution of Ostracoda in marine and marginal marine habitats off Tamil Nadu and adjoining areas, southern east coast of India and Andaman Islands: Environmental implications..Ostracods may live in practically every aquatic habitat, from deep seas to brackish water lagoons, estuaries, and even freshwater streams, lakes, and so on. Water temperature, salinity, and substrate are the primary determinants of ostracod population and dispersion in estuarine habitats and continental shelf zones. The distribution and ecology of marine ostracoda are discussed in this paper in relation to environmental parameters such as temperature, salinity, dissolved oxygen in bottom waters, organic matter, and CaCO3, as well as the sand-silt-clay ratio of sediments from the inner shelf sediment region off Karikkattukuppam (near Chennai), Rameswaram, Tuticorn, and Andaman Islands.Similarly, research on brackish water ostracods from the Adyar estuary, the Pitchavaram mangroves, and the Tamiraparani estuary have been reported. Work on ostracoda statistical factors such as carapace/valve ratio, ornamentation, and grain size to estimate the ecology of the research area from the Indian region is also presented.

Distribution of ostracode assemblages along the nearshore and offshore areas of Malabar coast, Kerala (west coast of India)(Gopalakrishnan K., Shabi. B, Bilwa L. Mahesh) In 76 sediment samples collected from 28 nearshore and 48 offshore sites off the Malabar Coast of Kerala, 61 ostracode species have been discovered. The ostracode assemblages of the nearshore sediments were analysed using a Q mode clustering method, and the results show that the entire nearshore assemblage can be divided into two clusters: Cluster I, which includes the blocks Kumbla (A1), Hosdurg (B1), and Mattul (D1), and Cluster II, which includes the blocks Payyannur (C1), Cannanore (E1), and Telicherry (F1). The variations in the depositional environment are presumably to blame for this grouping. Due to the mixing of freshwater from the surrounding land masses, the effect of the estuary environment is predominate in cluster I. The locations this cluster covers have a number of backwaters. The whole offshore off the Malabar coast may be analysed using cluster analysis of offshore assemblages, according toKumbla (A2) and Bekal (B2) blocks make up cluster I, whereas Neeleswaram (C2), Payyannur (D2), and Payangoti (E2) blocks make up cluster II. The fossil molluscan assemblages imply and further show the existence of shallow water ostracode species in cluster I that existed on nearshore sand and silty sand substrate under the impact of subtropical water currents. According to Q-mode cluster analysis and specifics on physical and biological characteristics, salinity, organic matter, and substrate all have a significant impact on the ostracode's distribution, variety, and abundance. As

a result, Kerala's Malabar coast is largely categorised as belonging to the maritime ecosystem/environment category.

2.3 SEDIMENT CHARACTERESTICS

Sediment accumulation in a coastal environment, an estuary or a shelf environment is mainly dependent on the type and rate of input and distribution of sediment types. Grain size parameters have been used commonly to characterize the sediments in the shelf environment (Nittrouer et al., 1983); moreover, the bottom topography of any modern environment is affected by the distribution and transport processes of the sediments present in the area (Swift, 1970; McCave, 1972). According to Koldijk (1968), analyses of textural parameters are indicators of the environmental condition as they environmental sensitive. Due to rapid industrial development, the estuaries and the inner shelf sediments receive a wide range of contaminants which are ultimately concentrated and deposited on and sink the estuary or inner shelf floor.

According to Loring and Rantala (1992), trace metalconcentrations usually increase with decreasing grain size of sediments, and to ascertain the paleoclimatic conditions and depositional environments, it is essential to study the distribution of grain size parameters in any area. Hence, grain size parameters expand importance with reference to geochemical studies.

Hashimi and Nair (1981) described the textural parameters in the sedimentsoff Mangalore and off Goa (MohanaRao et al. 1990) of the western continental shelf and Sreenivasa Rao et al., (1990) reported the occurrences of coarse sand deposits in the deeper parts of the inner shelf off Gopalpur, Visakhapatnam and Nizampatnam on the east coast of India and attributed their formation to a Holocene stagnation of the sea level at that depth. Likewise, Purnachander Reddy and DurgaPrasada Rao (1992)reported mid-Holocene strand line deposit from the inner shelf sediments off Cochin, where a linear belt of sandy sediments in the outer parts is encountered withmoderately sorted sands. Distributions of clay minerals in the shelf sediments of the northwestern part of Bay of Bengal were studied in detail by number of workers(Ramamurthy and Shrivastava1979, PurnachandraRao et al., 1998). According to Venkatesh Prabhu et al. (1997), the study of texturalcharacteristics from the sediments off Honnavar, southwest coast of India, revealed that the sediments are generally clayey in nature and poorly sorted. Recently,

depositional environments of beach and beach ridges of 158 km long coastal strip, extending from north of Pondicherry to Ennore, Tamil Nadu, southeast coast of India, have been classified based on grain size parameters by Mohan and Rajamanickam (1998). Selvaraj (1999), in his study on the shelf sediments off Kalpakkam coast, has revealed the presence of a pale beach at 50 m depth, where a linear stretch of sand deposit was encountered. Carbonate is often an important component of marine sediments and has been found to be an important indicator of provenance and dispersal of terrigenous material in the Gulf of St.Lawrence (Loring and Nota, 1973). In the present study, calcium carbonate was determined by the author using rapid titration method (Piper, 1947). The carbonate determined by this method includes other carbonates such as magnesium, which is negligible, and hence for all practical purposes the total carbonate is referred to as calcium carbonate in the present investigation.

2.4 CALICUM CARBONATE

Carbonate has been discovered to be a key indicator of the provenance and dispersion of terrigenous material in the Gulf of St. Lawrence (Loring and Nota, 1973). Carbonate is frequently a significant component of marine sediments. The author of the study used the quick titration method to ascertain the calcium carbonate concentration (Piper, 1947). The total carbonate is referred to as calcium carbonate in the current inquiry since the carbonate identified by this method contains additional carbonates, such as magnesium, which is negligible.

CHAPTER III

METHODOLOGY

3.1 METHODOLOGY

3.1.1. FIELD WORK

In order to study the various aspects of Ostracoda distribution,a field work has been carried out along the Vanchipura Beach ,Kerala .A total of 19 surface samples and 1 core sediment samples were collected by our team .The detail morphological ,microstructural characters criticallly studied using stereo- binocular microscope . Distribution pattern of individual taxon was examined and their sediment relationship was determined for ecologic interpretation.Sand-silt – clay ratio estimation was carried out using the procedure of Krumbein and Pettijohn(1938). The taxonomy and systematic study were dealt using ostracod treatises by Moore and Pitrat (Eds) (1961), Van Morkhoven (1963), Hartmann and Puri (1974) and other recent literature.

3.1. LABORATARY ANALYSIS

3.1 CORE SAMPLE

Core sample was collected and kept in a zip lock cover, each sample weighing 50 g.There were 25 core samples in total when the core was divided in 3 cm length.

Fig no.3.1 Showing the core sample taken from Vanchipura Beach

A) MICROPALEONTOLOGY

Washing: To make deflocculating easier, a small fraction (100g) of each sample was carefully transferred to a beaker and immersed in distilled water overnight. Each deflocculated sample was gently sprayed with distilled water to remove the fine mud (silt + clay) particles and prevent shell breaking before being rinsed through an ASTM 230 (63-m opening) screen. The components that had been caught on the sieve were carefully transferred to a watch glass and dried in an oven at 45°C for an entire night. Foraminifera separation: The dried samples were placed in little polythene vials, labeled, and then separated. After homogenizing the sample with cone and quartering, a representative fraction was taken and weighed. The known weight of the sample(10g) was spread on a picking tray and was scan under a stereo zoom binocular microscope (NOVEX-Holland), and foraminifers were hand-picked using a soft-bristled moist brush (preferably a 0.00 brush). Minimum of 100 specimens were picked from all the samples and mounted on a 24 punch micro-paleontological slide.

B) DETERMINATION OF SAND-SILT-CLAY RATIO

Offshore shallow water sediments are commonly composite types consisting ofparticles of size range from sand to claywith their different combinations. In general, however, particle size tends to decrease with increase in depth.

PROCEDURE

Each bottom sediment sample is completely dried in a hot air oven to eliminate the moisture content. A suitable quantity (weight determined) of each sample is then treated with 0.025N sodium hexametaphosphate (Calgon) solution in order to facilitate deflocculation. The sample thus disaggregated is washed through a 230 ASTM sieve (mesh opening = 0.063 mm) until clear water passes through, taking care that the washings do not exceed 1000 ml. The portion of the sample retained on the sieve is dried and weighed for obtaining the weight of the sand fraction. The fine fraction (silt and clay) in the washings is analysed by the pipette method in accordance with the procedure adopted by Krumbein and Pettijohn (1938, pp.166- 168). The suspension passing through the sieve is collected in a 1 litre graduated measuring cylinder. If, after complete washing, the suspension is less than 1000 ml, the already prepared sodium hexametaphosphate solution is added to make it up to 1000 ml. The suspension in the measuring cylinder is agitated

well using a stirrer in order to have uniform distribution of the particles in suspension. As soon as the agitation is stopped, the time is noted, and exactly after 2 hours and 3 minutes, a 20 ml pipette is slowly inserted up to a depth of 10 cm in the solution and the sample withdrawn with uniform suction to avoid any turbulence. The sample pipetted out is transferred to a preweighed 50 ml beaker and dried in an oven taking care to prevent boiling and splashing. After complete drying, the weight of the residue is determined from which the weight of the clay fraction is calculated. The weight of the silt fraction is determined by subtracting the combined weight of the sand and clay fractions from the known sample weight. The individual weights of the sand, silt and clay fractions are converted into weight percentages and plotted on a trilinear diagram. Trefethen's (1950) textural nomenclature has been used to describe the sediments in the present study.

Fig no.3.2. Showing the sand silt clay analysis

C) DETERMINATION OF CALCIUM CARBONATE

Carbonate is often an important component of marine sediments and has been found to be an important indicator of provenance and dispersal of terrigenous material in the Gulf of St.Lawrence (Loring and Nota, 1973). In the present study, calcium carbonate was determined by the author using rapid titration method (Piper, 1947). The carbonatedetermined by this method includes other carbonates such as magnesium, which is negligible, and hence for all practical purposes the total carbonate is referred to as calcium carbonate inthe present investigation.

PROCEDURE

The procedure for determining the calcium carbonate content in sediments is as follows: 5.0 g of soil is weighed and transferred to a tall 150 ml beaker. Then 100 ml of 1N hydrochloric acid is added to it making use of a pipette with an enlarged jet. The beaker is covered with a watch glass and stirred vigorously several times for a period of one hour. After allowing the mixture to settle, 20 ml of supernatant liquid is pipette out and transferred to a small Erlenmeyer flask. To it are added 6-8 drops of bromothymal blue indicator and titrated with N sodium hydroxide. With some samples, the colour of the indicator may fade as the end point – blue colour – is approached. In such cases, more indicator is added and the titration completed. A blank titration is carried out to obtain the titrevalue of hydrochloric acid. The percentage of calcium carbonate is known by the equation: Percentage of calcium carbonate = (Blank titration - actual titration) x 5

3.2. GEOLOGY OF STUDY AREA

Vanchipura Beach is located in the southwestern part of India, in the state of Kerala. The geological history of the area dates back to the Pre-Cambrian era, which spanned from about 4.6 billion years ago to about 542 million years ago.The rocks at Vanchipura Beach are mainly composed of granitic gneiss, which is a type of metamorphic rock formed from the transformation of pre-existing igneous or sedimentary rocks under high pressure and temperature conditions. The granitic gneiss at Vanchipura Beach is believed to have formed about 2.5 billion

years ago during the Archean period.The rocks at Vanchipura Beach have been subject to various geological processes such as weathering, erosion, and sedimentation over millions of years, which have contributed to the unique rock formations seen today. The rocks have been shaped by the action of the waves and the weather, resulting in the formation of interesting features such as caves, arches, and pillars.The reddish-brown color of the rockatVanchipura Beach is due to the presence of iron oxide minerals such as hematite and magnetite. These minerals have formed as a result of the weathering and alteration of the original rock.

Fig no.3.3. Showing images taken from the study area

LOCATION	LATITUDE	LONGITUDE
VANCHIPURA BEACH	N10.3351	E76.1146
M1	N 10 .3360	E76.1143
M2	N10.3369	E76.114
M3	N10.3377	E76.1137
M4	N10.3386	E76.1134
M5	N10.3395	E76.3411
M6	N10.3411	E76.1124
M7	N10.3419	E76.1121
M8	N10.3428	E76.1118
M9	N10.3436	E76.1115
M10	N10.3435	E76.1112
M11	N10.3445	E76.1109
M12	N10.3453.	E76.1105
M13	N10.3462	E76.1102
M14	N10.3470	E76.1103
M15	N10.3476	E76.1101
M16	N10.3488	E76.1094
M17	N10.3496	E76.1091
M18	N10.3522	E76.1082
M19	N10.3531	E76.1078

Table no.3.1 Showing the latitude and longitude of the study area

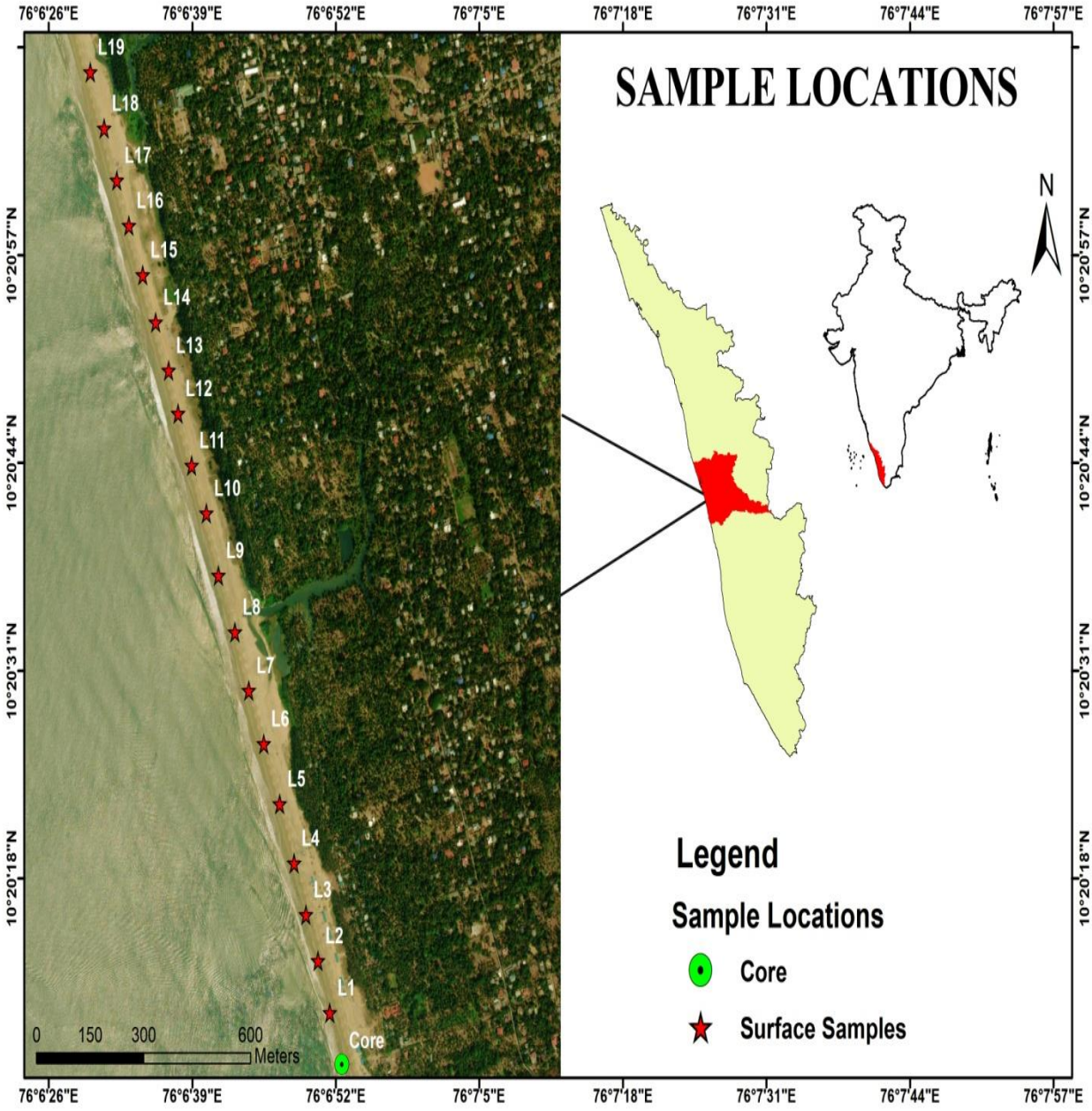

Fig no. 3.4 Showing the study area of Vanchipura Beach

CHAPTER IV

RESULT AND DISCUSSION

4.1. SYSTEMATIC PALEONTOLOGY

CLASSIFICATION

The widely utilized classification proposed by Alexander Liebau (2005) has been followed in the present study. In the following pages, 10 Ostracodal species belonging to 10 genera has been illustrated.

CHECK LIST OF OSTRACODA SPECIES

1. *Bairdoppilata alcyonicol*
2. *Cytherella vermilionensis*
3. *Hemicytheridea paiki*
4. *Xestoleberis antillea*
5. *Loxoconcha gruendeli*
6. *Ambocythere sp*
7. *Cytherella vermilionensis*
8. *Hemicytheridea paiki*
9. *Xestoleberis antillea*
10. *Loxoconcha gruendeli*

4.2.TOTAL POPULATION OF OSTRACODA IN SURFACE SAMPLES

In order to study the distribution of Ostracoda 19 surface samples and 1 core sample are collected from the Vanchipura Beach, Kerala. The population of Ostracoda in all the surface samples ranges from 8 to 14 and a total of 39 specimens per 100 g of wet sediment respectively.Out of the 19 surface sediment samples, sample locations 1,5,7 and 8 containing maximum Ostracoda and sample locations 2, 3 and 4 containing minimum Ostracoda populations.In that,ten different specimen sidentified from all samples.The population of core sample ranges from7 to 11 and a total of 120 specimens per 100 g of wet sediment respectively Out of the 25 surface sediment samples, sample locations 5,15 and18 containing maximum Ostracoda and sample locations 3,7, 14 and 16 containing minimum Ostracoda populations. The total population of surface samples in each samples shown in Table no 4.1 and Table no.4.2.

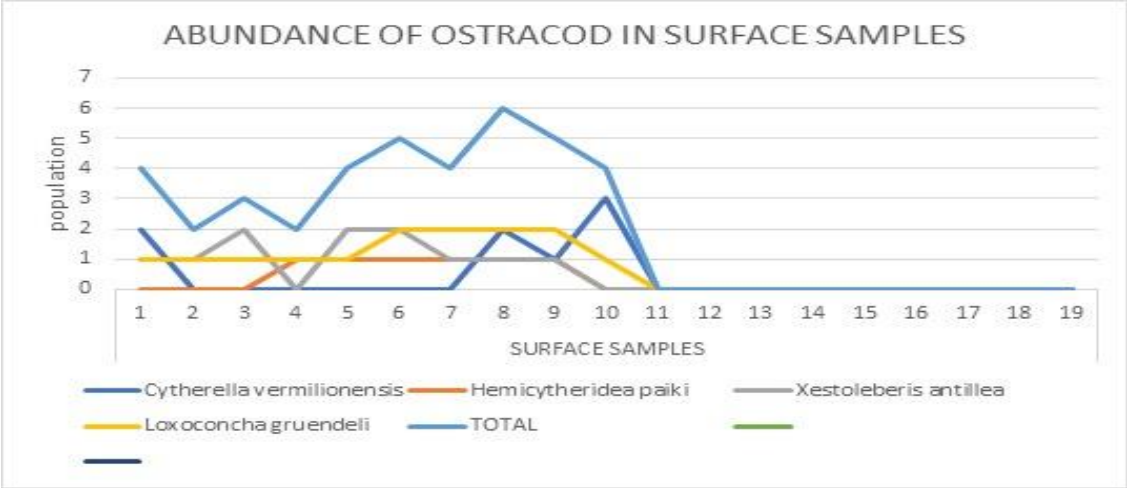

Fig 4.1.The total distribution of Ostracoda in surface samples.

	SAMPLE LOCATION																									
SPECIES	1	2	3	4	5	6	7	8	9	10	11	12	13	14	15	16	17	18	19	20	21	22	23	24	25	TOTAL
Bairdoppilata alcyonicol	3	2	2	0	1	1	2	0	0	0	2	1	2	1	2	1	1	2	0	2	0	1	1	1	0	28
Cytherella vermilionensis	3	1	2	0	3	1	1	0	0	0	1	1	1	0	2	0	1	2	0	1	0	1	1	2	2	26
Hemicytheridea paiki	1	1	0	0	2	1	1	0	0	0	2	1	1	0	2	0	1	2	0	1	0	1	1	1	2	21
Xestoleberis antillea	2	1	0	0	1	1	0	0	0	0	2	2	1	0	1	0	1	1	1	1	0	1	1	1	1	19
Loxoconcha gruendeli	1	0	0	0	1	1	0	0	0	0	1	1	1	0	1	1	1	1	1	0	0	0	0	1	1	13
Ambocythere sp	1	0	0	0	1	2	0	0	0	0	0	0	1	0	1	1	1	1	1	1	0	0	0	1	1	13
TOTAL	**11**	**5**	**4**	**0**	**9**	**7**	**4**	**0**	**0**	**0**	**8**	**6**	**7**	**1**	**9**	**3**	**6**	**9**	**3**	**6**	**0**	**4**	**4**	**7**	**7**	120

Table 4.1. The total distribution of Ostrcoda in core samples

	SAMPLE LOCATION																			
SPECIES	1	2	3	4	5	6	7	8	9	10	11	12	13	14	15	16	17	18	19	TOTAL
Cytherella vermilionensis	2	0	0	0	0	0	0	2	1	3	0	0	0	0	0	0	0	0	0	8
Hemicytheridea paiki	0	0	0	1	1	1	1	1	1	0	0	0	0	0	0	0	0	0	0	6
Xestoleberis antillea	1	1	2	0	2	2	1	1	1	0	0	0	0	0	0	0	0	0	0	11
Loxoconcha gruendeli	1	1	1	1	1	2	2	2	2	1	0	0	0	0	0	0	0	0	0	14
TOTAL	4	2	3	2	4	5	4	6	5	4	0	0	0	0	0	0	0	0	0	39

Table 4.2. Total Distribution in Ostracoda in surface samples.

SAMPLE NUMBER	CARAPACE	OPEN VALVE	TOTAL
1	2	2	4
2	0	2	2
3	2	1	3
4	1	1	2
5	3	1	4
6	4	1	5
7	3	1	4
8	3	3	6
9	3	2	5
10	3	1	4
11	0	0	0
12	0	0	0
13	0	0	0
14	0	0	0
15	0	0	0
16	0	0	0
17	0	0	0
18	0	0	0
19	0	0	0
TOTAL	24	15	39

Table no . Total Carapace distribution in Ostracoda.

SAMPLE NUMBER	CARAPACE	OPEN VALVE	TOTAL
1	5	6	11
2	3	2	5
3	2	2	4
4	0	0	0
5	5	4	9
6	5	2	7
7	2	2	4
8	0	0	0
9	0	0	0
10	0	0	0
11	5	3	8
12	4	2	6
13	3	4	7
14	0	1	1
15	7	2	9
16	1	2	3
17	3	3	6
18	4	5	9
19	2	1	3
20	4	2	6
21	0	0	0
22	2	2	4
23	1	3	4
24	3	4	7
25	5	2	7
TOTAL	66	54	120

In surface samples the the total number of Carapace present is 24 and the maximum abunda nce is in sample number 6 and the minimum abundance is in sample number 11 to 19. In core samples the the total number of open valves present is 15 and the maximum abundance is in sample number 8 and the minimum 11 to 19 abundance is in sample number 11 to 19.

In study area, carapace-open valve ratio is high, the sedimentation is rapid, which minimizes the disarticulation of carapaces into separate valves. In an environment where deposition of the sediment is low, the carapaces are likely to open up by bacterial action. But, in an environment where deposition is very rapid, the carapaces will sink into the soft bottom and will be quickly covered by sediments

4.3. SEDIMENT CHARACTERS

Ostracods are a diverse microfossil group that exist in non marine , marginal marine and marine environments and produce calcite valves that are easily fossilized .They are frequently transported , deposited and preserved in coastal overwash deposits.

4.3.1. CALCIUM CARBONATE

Shells and shattered shell pieces of animals, molluscs, as well as the dilution of biogenic calcite by detrital material in the sediments, are the main sources of carbonate in the research area's sediments. In their investigation of the sediments of the Mahe estuary on the West Coast of India, Sebastian et al. (1990) reported comparable findings. The combination of sand particles with CaCO3 suggests that shell fragments are the main contributor to the sand component. In the Gulf of Mannar, off Tuticorin, Hussain et al. (1997) found that a rise in CaCO3 favors maximum population size.

According to the current study, the calcium carbonate content of the core sample sediments of Vanchipura Beach ranges from 0.5% to 4%.The lowest value was recorded in station nos.11,12and 14 the highest values are recorded in station nos 1 and 19. The calcium carbonate content of the surface sample sediments of Vanchipura Beach ranges from 0.5% to 5.5%.The lowest value was recorded in station nos.9,21and 22 the highest values are recorded in station nos 1 and 3.

In the present Study, it has been found that the calcium carbonate in the sediments of Vanchipura Beach ranges from 0.5% to 4 % in core samples and 0.5% to 5.5%in surface samples. (Tableno.4.2.).The determined values are plotted in Fig.. The lowest value was recorded in station nos. 11, 12 and 14 the highest values are recorded in station nos. 1 nd 19 in core samples and the lowest value was recorded in station nos. 9, 21 and 22the highest values are recorded in station nos. 1 nd 3 in surface samples. It is understood that the calcium carbonate content in this area is one of the important parameters, which governs the population of Ostracoda, especially its spatial distribution. Here, the calcium carbonate content is found to be generally propotional to the population size.

SAMPLE NUMBER	Caco3 %
CORE SAMPLES	
VCB C2(1)	4%
VCB C2(2)	2.5%
VCB C2(3)	2%

VCB C2(4)	1.5%
VCB C2(5)	1.5%
VCB C2(6)	2%
VCB C2(7)	1.5%
VCB C2(8)	2%
VCB C2(9)	1%
VCB C2(10)	2.5%
VCB C2(11)	0.5%
VCB C2(12)	0.5%
VCB C2(14)	0.5%
VCB C2(15)	1.5%
VCB C2(16)	1%
VCB C2(17)	1%
VCB C2(18)	1%
VCB C2(19)	4%
MAXIMUM %	4%
MINIMUM %	0.5%
SURFACE SAMPLES	
VCB M1	5%
VCB M2	2.5%
VCB M3	5.5%
VCB M4	2.5%
VCB M5	4%
VCB M6	4.5%
VCB M7	3.5%
VCB M8	3.5%

VCB M9	1%
VCB M10	2%
VCB M11	2.5%
VCB M12	2%
VCB M13	1.2%
VCB M14	2%
VCB M15	1.5%
VCB M16	1.5%
VCB M17	1.5%
VCB M18	2.5%
VCB M19	3%
VCB M20	1.5%
VCB M21	1%
VCB M22	0.5%
VCB M23	3%
VCB M24	3.5%
VCB M25	2%
MAXIMUM%	5.5%
MINIMUM %	0.5%

Table no4.4.2. Showing calcium carbonate percentage

4.3.2 SAND-SILT-CLAY ANALYSIS

In the Vanchipura Beach samples, the sand-silt-clay ratio is carried out sand with a range of 31.52 % to 52.03%, silt with a range of47.9225% to 47.9225% to88.57% and clay with a range of 0.01% to0.0975%

respectively in core samples (Table.4.3). The sand-silt-clay ratio is carried out sand with a range of 46.33% to88.57% of silt with a range of 11.425 % to53.5725 % and clay with a range of 0% to0.0675% respectively in surface.samples. The trilinear diagram of sand-silt-clay ratio of surface samples is shown in Fig.4.2. In these areas the sediment type is observed as silty-sandy substrate only. From the above observations, it may be inferred that the most favourable sediment type for the population abundance is silty- sand.

SAMPLE NO	SAND PERCENTAGE	CLAY PERCENTAGE	SILT PERCENTAGE
CORE SAMPLE			
VCB C2(1)	46.63 %	0.13%	53.24%
VCB C2(2)	46.63 %	0.0075%	53.3925%
VCB C2(3)	31.52 %	0.0675%	68.4125%
VCB C2(12)	41.59%	0.345%	58.065%
VCB C2(13)	36.24%	0.0625%	63.6975%
VCBC2 (14)	52.03%	0.0475%	47.9225%
VCB C2 (23)	35.49%	0.01%	64.5%
VCB C2(24)	41.35%	0.13%	58.52%
VCB C2 (25)	41.16%	0.14%	58.7%
MAXIMUM%	52.03%	0.0675%	68.4125%
MINIMUM %	31.52 %	0.01%	47.9225%
SURFACE SAMPLES			
VCB M1	46.33%	0.0975%	53.5725%
VCB M2	78.97%	0.0075%	21.0225%
VCB M3	77.32%	0.0225%	22.6575%
VCB M12	69.4%	0.005%	30.595%
VCB M13	75.23%	0%	24.77%
VCB M14	63.94%	0.005%	36.055%
VCB M17	88.57%	0.005%	11.425%
VCBM18	74.74%	0.0075%	25.2525%
VCB M19	76.87%	0.005%	23.125%

MAXIMUM %	88.57%	0.0975%	53.5725%
MINIMUM %	46.33%	0%	11.425%

Table 4.3. Showing sediment charecterstics of Vanchipura Beach in core and surface samples.

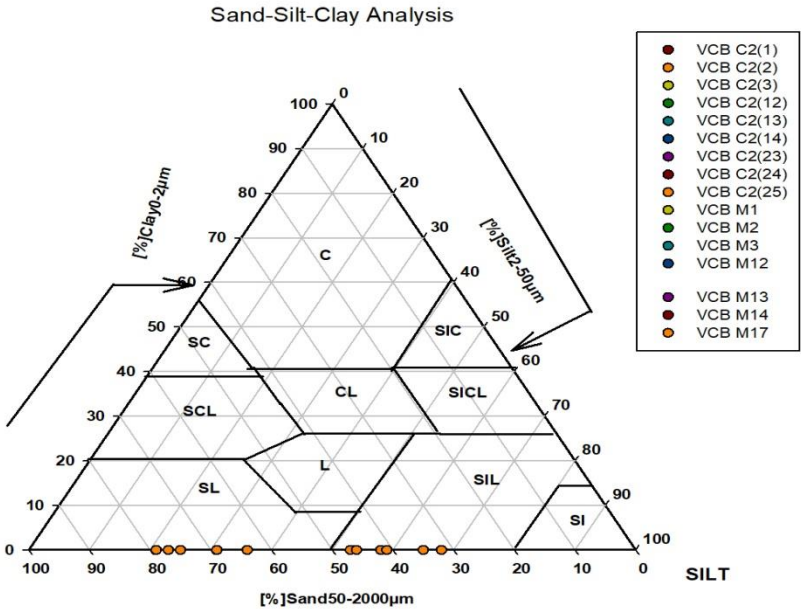

Fig 4. 2. Trilinear plots of sand-silt-clay percenentage.

CHAPTER V

SUMMARY AND CONCLUSION

The taxonomy and systematic study were dealt using ostracod treatises by Moore and Pitrat (Eds) (1961), Van Morkhoven (1963), Hartmann and Puri (1974) and other recent literature. Most ostracods are benthic, swimming, crawling or burrowing at sediment – water interface in muds or silts with abundant organic material. They are very useful for environmental reconstructions and, at some levels in the stratigraphic record, have been used for correlation.It is understood that the calcium carbonate content in this area is one of the important parameters, which governs the population of Ostracoda, especially its spatial distribution. Here, the calcium carbonate content is generally found to be directly proportional to the population size.From the distribution of the calcareous micofauna in the beach sediments, it may be inferred that the most favourable sediment type for the population abundance is sand.In the present work, the ratio between the carapaces and open valves has been taken into consideration for determining the rate of sedimentation in the study area.The distribution of carapaces and open valves reveals that the carapaces are outnumbered than the open valves. From the above observations, it may be concluded that moderately rapid rate of sedimentation prevails in the VanchipuraBeach.

REFERENCE

Benson, R. H., Chapman, R. E., & Deck, L. T. (1985). Evidence from the Ostracoda of major events in the South Atlantic and world-wide over the past 80 million years. *South Atlantic Paleoceanography*, *325*, 333.

Bate, R. H. (1977). Jurassic ostracoda of the Atlantic Basin. In *Developments in Palaeontology and Stratigraphy* (Vol. 6, pp. 231-244). Elsevier.

Neale, J. W. (1988). Ostracoda—A historical perspective. In *Developments in Palaeontology and Stratigraphy* (Vol. 11, pp. 3-15). Elsevier.

Maddocks, R. F. (1979). Two new examples of symbiosis or parasitism in cypridacean Ostracoda. *Crustaceana*, 1-12.

Zhao, Q., & Wang, P. (1988). Distribution of modern Ostracoda in the shelf seas off China. In *Developments in Palaeontology and Stratigraphy* (Vol. 11, pp. 805-821). Elsevier.

Neale, J. W. (1984). The freshwater ostracoda. In *Ecology and Biogeography in Sri Lanka* (pp. 171-194). Dordrecht: Springer Netherlands.

Maddocks, R. F. (1979). Two new examples of symbiosis or parasitism in cypridacean Ostracoda. *Crustaceana*, 1-12.

Hartmann, G. (1988). Distribution and dispersal of littoral Pacific island Ostracoda. In *Developments in Palaeontology and Stratigraphy* (Vol. 11, pp. 787-795). Elsevier.

Hartmann, G., & Hartmann-Schröuder, G. (1988). Deep-sea Ostracoda, taxonomy, distribution and morphology. In *Developments in Palaeontology and Stratigraphy* (Vol. 11, pp. 699-707). Elsevier.

Boomer, I., Horne, D. J., & Slipper, I. J. (2003). The use of ostracods in palaeoenvironmental studies, or what can you do with an ostracod shell?. *The Paleontological Society Papers*, *9*, 153-180.

Von Grafenstein, U., Erlernkeuser, H., & Trimborn, P. (1999). Oxygen and carbon isotopes in modern fresh-water ostracod valves: assessing vital offsets and autecological effects of interest for palaeoclimate studies. *Palaeogeography, Palaeoclimatology, Palaeoecology*, *148*(1-3), 133-152.

Börner, N., De Baere, B., Yang, Q., Jochum, K. P., Frenzel, P., Andreae, M. O., & Schwalb, A. (2013). Ostracod shell chemistry as proxy for paleoenvironmental change. *Quaternary International*, *313*, 17-37.

Schön, I., & Martens, K. (2016). Ostracod (Ostracoda, Crustacea) genomics—promises and challenges. *Marine genomics*, *29*, 19-25.

Frogley, M. R., Griffiths, H. I., & Martens, K. (2002). Modern and fossil ostracods from ancient lakes. *Washington DC American Geophysical Union Geophysical Monograph Series*, *131*, 167-184.

Lord, A. R., Boomer, I., Brouwers, E., & Whittaker, J. E. (2012). Ostracod taxa as palaeoclimate indicators in the quaternary. In *Developments in quaternary sciences* (Vol. 17, pp. 37-45). Elsevier.

Frenzel, P., & Boomer, I. (2005). The use of ostracods from marginal marine, brackish waters as bioindicators of modern and Quaternary environmental change. *Palaeogeography, Palaeoclimatology, Palaeoecology*, *225*(1-4), 68-92.

Penney, D. N. (1987). Application of Ostracoda to sea-level studies. *Boreas*, *16*(3), 237-247.

Gopalakrishnan K., Shabi. B, Bilwa L. Mahesh, et al. Distribution of ostracode assemblages along

the nearshore and offshore areas of Malabar coast, Kerala (west coast of India), Indian Journal

of Marine Sciences, 37(3) (2008).

SPATIAL DISTRIBUTION OF MICROPLASTIC CONCENTRATION IN AND AROUND BRAHMAPURAM LANDFILL SITE AND ITS POTENTIAL RISK ON GROUNDWATER

Dissertation submitted to Christ College (Autonomous), Irinjalakuda, Kerala, University of Calicut in partial fulfillment of the degree of

Master of Science in Applied Geology

By,

J KRISHNANUNNI

Reg Number: CCAVMAG010

2021-2023

DEPARTMENT OF GEOLOGY AND ENVIRONMENTAL SCIENCE

CHRIST COLLEGE (AUTONOMOUS), IRINJALAKUDA, KERALA,680125

(Affiliated to University of Calicut and re-accredited by NAAC with A++ grade)

SEPTEMBER 2023

CERTIFICATE

This is to certify that the dissertation entitled – **SPATIAL DISTRIBUTION OF MICROPLASTIC CONCENTRATION IN AND AROUND BRAHMAPURAM LANDFILL SITE AND ITS POTENTIAL RISK ON GROUNDWATER**, is a bonafide record of work done by Mr. J Krishnanunni (Reg. No. CCAVMAG010), MSc Applied Geology, Christ College (Autonomous) Irinjalakuda, under my guidance in partial fulfilment of requirements for the degree of Master of Science in Applied Geology during the year 2021-2023.

Project Guide

Dr. Anto Francis K
Co-ordinator (Geology Self-financing)
Dept. of Geology and Environmental science
Christ College (Autonomous) Irinjalakuda
Kerala- 680125

Dr. Anso M A
Assistant Professor
Dept. of Geology and Environmental science
Christ College (Autonomous) Irinjalakuda
Kerala- 680125

Place: Irinjalakuda

Date: ……

External Examiners;

1…….

2…….

DECLARATION

I hereby declare that this dissertation work – **SPATIAL DISTRIBUTION OF MICROPLASTIC CONCENTRATION IN AND AROUND BRAHMAPURAM LANDFILL SITE AND ITS POTENTIAL RISK ON GROUNDWATER** is a work done by me. No part of the report is reproduced from other resources. All information included from other sources has been duly acknowledged. I maintain that if any part of the report is found to be plagiarized, I shall take the full responsibility for it.

Place: Irinjalakuda

Date:

J KRISHNANUNNI

Reg.No. CCAVMAG010

ACKNOWLEDGEMENT

This report is an official documentation of dissertation work carried out in Ambalamukal Industrial Area, Kerala. This report would not have been possible without guidance, encouragement and support of many well-wishers and my colleagues who helped me in many ways.

I would like to express my sincere gratitude and appreciation to **Dr. Anso M A**, Assistant Professor in the Department of Geology and Environmental Science at Christ College (Autonomous) Irinjalakuda. He played a pivotal role in shaping the framework of this thesis and provided unwavering support and guidance throughout the entire duration of the study.

Dr. Linto Alappat, Dean of Research and Development of TLC (Former Head, Department of Geology and Environmental Science, Christ College (Autonomous) Irinjalakuda), **Mr Tharun R**, Head of the Department of Geology and Environmental Science, Christ College (Autonomous) Irinjalakuda, for rendering all the help and facilities available in the department.

I express my utmost gratitude to **Mr. Ayyappadas C.S**, a Research Scholar at Christ College (Autonomous) Irinjalakuda, for his invaluable assistance in the technical aspects of my study and his unwavering support during the completion of my dissertation.

I am grateful to **Dr. Anto Francis K**, Coordinator (Geology Self-financing), and the other faculty members of the Department of Geology and Environmental Science, Christ College (Autonomous), Irinjalakuda, for their encouragement, direction, and affection.

I'd like to take this opportunity to thank all of my teachers, classmates and friends who supported me in completing this dissertation work, whether directly or indirectly.

I am grateful to the entire Christ College family for their love, support, and guidance. I also express my gratitude to my parents and my sister for their unwavering support and prayers throughout my life. Above all, I express my gratitude to God, the Almighty, for His divine generosity and blessings showered upon me.

J KRISHNANUNNI

ABSTRACT

Although plastic is already a vital part of modern life and plays a significant role in human activity, it poses a serious threat to freshwater ecosystems. The aim of this study is to analyse the quality of ground water and to find the presence of microplastics in Ambalamugal area of Eranakulam District. Ambalamugal is one of the largest industrial areas in Eranakulam District. Total of 40 samples were taken before South West monsoon. The microplastic contamination in the groundwater samples ranged from 1 to 23 microplastics/L and included coloured microplastic particles in shades of white, black, green, pink, purple and blue. The quantification of the Physical parameters such as pH, electrical conductivity (EC) and total dissolved solids (TDS) also accounts for the severe ecological impacts over this area. Among the forty samples analysed, it was found that eight samples from the region exhibited pH levels within the allowed limit. Additionally, twelve samples met the acceptable standard for electrical conductivity (EC), while thirty-eight samples adhered to the allowable total dissolved solids (TDS) limit as specified by the Bureau of Indian Standards (BIS). All collected groundwater samples contained microplastics of various colours and morphologies, predominantly fibres. Among the 261 microplastics identified, black-coloured particles were most prevalent, with sizes ranging from 2 to 401 micrometres. The average microplastic concentration was 6 to 7 particles per litre, peaking at the Brahmapuram waste plant and decreasing with distance from this reference point. The investigation reveals that the water within the study region does not meet the permitted threshold, as evidenced by the presence of microplastics in the samples. This finding suggests that the water is unsuitable for consumption as drinking water.

CONTENTS

List of Figures

List of Tables

CHAPTER 1

INTRODUCTION

1.1 Groundwater

Groundwater refers to the water that is found beneath the Earth's surface in the spaces and crevices of rocks and soil. It is one of the Earth's most important natural resources and plays a crucial role in the planet's water cycle.

When it rains or when the snow melts, some of the water seeps into the ground and descends because of gravity. These areas are filled by the water, which also fills rock cracks and porous rock strata called aquifers. Groundwater is stored and moved through aquifers, which are subsurface reservoirs. Different subsurface depths contain groundwater. The water table is the highest level, where water has soaked the soil and rocks. Rainfall, geology, and human activity are a few examples of the variables that might affect the depth of the water table.

For a variety of uses, including drinking water, irrigation for agriculture, and industrial activities, groundwater is a crucial source of freshwater (Konikow and Kendy, 2005). It is frequently reached by drilling wells into aquifers, which enable the water to be pumped to the surface. Wells can be deep, drawing from deeper groundwater sources, or shallow, reaching the upper section of the aquifer. It is significant to remember that human activities like inappropriate waste disposal, industrial spills, or agricultural runoff can contaminate groundwater. Human health and ecosystems are at risk from contaminated groundwater (Redwan et al., 2020; Li et al., 2021). To preserve the sustainability and accessibility of groundwater resources for future generations, careful management and conservation are therefore crucial.

1.2 Significance of Groundwater Study

The rapid and mostly uncontrolled spread of groundwater exploitation provided tremendous social and economic benefits, but it has also recently encountered considerable issues. Current abstraction rates are not physically viable in certain cases over the long term, and there has been variable degrees of aquifer deterioration, environmental effect, or both in many others (Morris et al., 2003).

The study of groundwater holds significant importance for various reasons such as studies on groundwater offer vital data for managing water resources effectively (Kumar et al., 2005). Planning and making wise choices concerning the sustainable use of groundwater are made easier when one is aware of the quantity, quality, and availability of the resource. For many communities around the world, groundwater is a crucial supply of drinking water. The results of groundwater investigations are used to locate well-suited drilling sites, determine if groundwater is fit for human consumption, and, if necessary, put in place the necessary water treatment procedures. Studies of groundwater help to reduce risks associated with water, such as floods and droughts. To forecast and control the effects of extreme weather events, it is necessary to comprehend how groundwater systems behave, including aquifer features and recharge rates.

Groundwater is one of the major resources for agriculture, and irrigation using groundwater is extremely important. The availability and sustainability of water supplies for agriculture can be ascertained by studying groundwater. It helps determine how much groundwater crops need, how well to irrigate, and how to avoid over- or under-using groundwater, which can cause land subsidence and other negative effects.

1.3 Groundwater Contamination

The toxins that could be present in groundwater are virtually endless. The sources and causes of groundwater pollution are inextricably linked to human water use. The range of human activities affecting the hydrologic cycle results in a complex and interconnected series of changes to natural water quality.

The following are the primary sources and causes of groundwater pollution: municipal, industrial, agricultural, and miscellaneous (Li et al., 2021). The majority of pollution is caused by rubbish disposal on or into the ground. Waste can be disposed of in percolation ponds, on the ground surface, seepage pits or trenches, dry streambeds, landfills, disposal wells, and injection wells.

Contaminated groundwater used for drinking or irrigation can cause gastrointestinal diseases, reproductive problems, and long-term exposure to certain chemicals may potentially raise the risk of cancer (Rao et al., 2020). Pollution can have a significant influence on aquatic ecosystems that rely on groundwater. Toxins in the water can kill aquatic life as well as altering the entire ecosystem. The remediation of polluted groundwater can be expensive. Furthermore,

enterprises and livelihoods that rely on clean groundwater may suffer financial losses or suffer legal liabilities as a result of contamination.

1.4 Microplastics

Microplastics are barely visible plastic particles with a size of less than 5 millimetres (Moore, 2008). Microplastics can be classified into two type and they are primary microplastics and secondary microplastics (Chia et al., 2021).

The primary microplastics refer to intentionally manufactured plastic particles that are designed for everyday use. Primary microplastics encompass several types of particles, such as microbeads used in personal care products, pellets utilised in plastic production, and microfibers originating from synthetic textiles. Secondary microplastics are generated as a result of the degradation of larger plastic items by physical, chemical, or biological weathering mechanisms. Over a period of time, larger plastic waste items, such as bottles, bags, and packaging materials, have the potential to undergo disintegration, resulting in the formation of minuscule particles known as microplastics.

Microplastics can be absorbed directly or indirectly through the food chain by marine creatures such as fish, shellfish, and plankton. Ingestion of this substance can result in bodily injury, decreased feeding effectiveness, internal injuries, and even death. Microplastics can also build up in soil, impacting soil quality and perhaps entering the food chain via plants and soil-dwelling creatures.

1.5 Microplastics in Groundwater

Groundwater, an essential potable water resource for numerous communities, is susceptible to the infiltration of microplastics via diverse routes (Li et al., 2021). These particles have the potential to infiltrate groundwater through several mechanisms, including surface runoff and infiltration, wastewater discharge, agricultural practises, and the breakdown of plastic debris. Microplastics have the potential to endure in groundwater for prolonged durations as a result of the sluggish flow of groundwater and the scarcity of natural processes for their elimination.

The investigation into the potential ramifications of microplastics in groundwater is ongoing, although it elicits apprehension regarding the quality of water and the well-being of ecosystems (Kumar et al., 2021). The ingestion of microplastics by aquatic species inhabiting groundwater systems has the potential to introduce these particles into the food chain, so affecting both wildlife and human populations that depend on groundwater supplies for their drinking water.

In order to provide a thorough analysis of this matter, additional research is required to measure the magnitude of microplastic pollution in groundwater, ascertain the origins and mechanisms of its transportation, and evaluate the possible hazards it poses to both human health and the environment. The implementation of more effective waste management strategies, advancements in wastewater treatment methodologies, and more public knowledge regarding the issue of plastic pollution have the potential to mitigate the occurrence of microplastics in groundwater.

The widespread distribution of microplastics in groundwater is an increasing concern, despite the fact that study on this topic is still restricted in comparison to other environmental compartments such as oceans and surface waters. Microplastics can enter groundwater from a variety of source such as microplastic-contaminated surface water bodies may penetrate through the soil and reach groundwater (Padervand et al., 2020).

1.6 Health problems due to Microplastics

There exists a prevailing concern over the potential respiratory implications associated with the inhalation of microplastics, which may encompass the development of airway inflammation and irritation (Chia et al., 2021). Concerns have been raised over the potential accumulation of ingested microplastics within the gastrointestinal tract, which may give rise to inflammatory responses, disturbances in gut flora, and various digestive complications (Fackelmann and Sommer, 2019). Certain microplastics possess additives or chemicals that have the ability to interfere with the endocrine system, responsible for regulating hormonal activity within the human body. The potential consequences encompass a variety of health concerns associated with disruptions in hormonal equilibrium. The presence of microplastics has the potential to elicit inflammatory reactions within the human body, as the immune system endeavours to mount a response against these exogenous particles (Wright and Kelly, 2017). There exists a correlation between chronic inflammation and a multitude of health issues. Several studies have indicated that specific categories of microplastics may possess the ability to harbour carcinogenic compounds with hazardous properties (Saeed et al., 2023; Sun et al., 2021). Freshwater species can be predated by organisms at higher trophic levels; as a result, microplastics can transfer up the food chain (Wong et al., 2020). The possible long-term damage caused by the accumulation of microplastics in specific organs is a matter of concern. As an illustration, the build-up of microplastics in the liver or kidneys may impede their optimal

functionality. Microplastics also interact with toxic chemicals such as iron (Fe), manganese (Mn), aluminium (Al), lead (Pb), copper (Cu), silver (Ag), zinc (Zn), as well as hydrophobic organic contaminants (HOCs), also known as persistent organic pollutants (POPs) such as polyaromatic hydrocarbons (PAH), organochlorine pesticides (OCP) and polychlorinated biphenyls (PCB) can create adverse consequences to environment (Verla et al., 2019).

1.7 *Sources of Microplastics*

Microplastics are derived from several sources and can be introduced into the environment through deliberate or unintentional mechanisms.

Microbeads refer to diminutive plastic spheres employed in personal care commodities such as exfoliating scrubs, shower gels, and toothpaste. These items are specifically engineered to enhance tactile sensation, nevertheless they possess the propensity to be effortlessly flushed down drainage systems, so exacerbating the issue of water contamination. Microplastics are utilised in various industrial processes as abrasives, specifically in the production of cleaning agents, air blasting, and sanding applications. The following are the key sources of microplastics.

Over time, plastic objects of larger size, such as bottles, bags, and containers, undergo fragmentation into tiny particles as a result of exposure to environmental variables, including UV radiation and mechanical forces. Earthworms have the ability to enhance the rates of biodegradation of biodegradable polymers by establishing habitats that are favourable for the development of microorganisms. This phenomenon has the potential to facilitate the deterioration of plastics, as it amplifies the susceptibility of microplastic particles to a wide range of micro-organisms (Khaldoon et al.,2022). The operation of vehicles on roadways results in the generation of friction between the tyres and the pavement, which subsequently leads to the emission of tyre wear particles that contain microplastics. The particles are transported into water bodies by rainwater. Synthetic textiles such as polyester, nylon, and acrylic exhibit the phenomenon of shedding minuscule fibres after both laundering and regular usage. The microfibers are discharged into wastewater and have the potential to infiltrate rivers and seas. The introduction of plastic debris into marine and freshwater ecosystems can result in the fragmentation of these materials into microplastics, a process facilitated by many environmental conditions such as wave action and solar radiation. Plastic resin pellets, commonly employed as primary constituents in plastic manufacturing, has the potential to inadvertently disperse into aquatic environments as a result of transportation or handling

mishaps, hence augmenting the prevalence of microplastic contamination. The following are the primary contributors to the presence of secondary microplastics.

1.8 Aim and Objectives

The aim of this study is to analyse the quality of ground water and to quantify microplastic contamination in and around Brahmapuram landfill, Ambalamugal area of Ernakulam District.

- To determine the physical properties of groundwater.
- To determine the presence of microplastics in around Brahmapuram landfill, Ambalamukal industrial area.
- To emphasis on the health hazard due to groundwater contamination.

CHAPTER 2

REVIEW OF LITERATURE

Selvam et al. (2021) examined the potential hazards associated with microplastics and their role in facilitating the transport of heavy metals in both groundwater and surface water within the coastal regions of south India. The primary sources of heavy metal contamination are the disposal of solid waste, discharge of industrial waste, and municipal trash. This study investigates the presence and characteristics of microplastics (namely, those measuring 5 mm) in both groundwater and surface waters within the Punnakayal estuary, located in a heavily developed part of Tamil Nadu state in southern India. The size of microplastics in surface water was found to be larger compared to microplastics in groundwater. Polyamide, polyester, polypropylene, polyethylene, polyvinyl chloride, and cellulose were the polymers that were extensively utilised, albeit with varying capacities for heavy metal adsorption. Based on the aforementioned investigations, the findings indicate that microplastics serve as a prominent medium for the transportation of heavy metals within aquatic ecosystems.

Srihari S. et al., 2022 studied the characterisation, quantification, and spatial distribution of microplastics in surface water, groundwater, and coastal sediments throughout South India's highly populated Chennai coast. Microplastics contaminated groundwater samples as well, with a total of 315 particles in 25 samples obtained from various locations (an average of 13 particles/L). According to the FTIR data, the most common types of Microplastics were nylon, polyvinylchloride, and polyethylene terephthalate. The spatial variation map showed that a high concentration of Microplastics was observed on tourist beaches. Remediation technologies are highly effective in eliminating and preventing MP pollution in our environment.

Manikanda Bharath K et al., 2021 assessed the microplastic abundance, characteristics such as composite, size, colour, shape, and surface morphology, detection methods of plastic particles, and potential risk factors from the absorption of microplastic in groundwater. The microplastics found in groundwater samples in the South Indian municipal solid waste dump site of Perungudi and Kodungaiyur are identified, described, and quantified in the current study. The LB-340 Zoom Stereo Microscope with LED Illumination and ATR-FTIR equipped with SEM and an EDX analyser were used to classify microplastic particle. The groundwater samples

were found contaminated with microplastic particles in the range of 2–80 items/L with coloured particles: white, black, green, red, blue, and yellow. The polymer type was found to be nylon, pellets, foam, fragments, fibres, PVC, and polythene. Surface runoff, effluent, open dumping, and open burning are the major sources of microplastics entering groundwater at landfill sites. A significant risk factor for human health is particle size.

Hongyu Mu et al., 2022 investigated the occurrence of microplastics in groundwater sampled from five sites in the Jiaodong Peninsula, China. Laser direct infrared spectroscopy was used to determine the number, kind, and size of Microplastics in groundwater samples. All groundwater samples were found to contain polyethylene terephthalate and polyurethane in significant amounts. More than 90% of the Microplastics discovered in four sampling sites were found to be smaller than 100 m in size, which was probably due to their migration paths through surface water runoff and infiltration into groundwater environments.

Le Xuan Thanh Thao et al., 2022 study aims to preliminarily investigate the occurrence of microplastics in groundwater of five wells at a distance of 100–1000 m from the Khanh Son landfill site in Da Nang City, Viet Nam. The microplastic concentration and polymer composition in groundwater samples were identified by FTIR spectra using the Nicolet iN10 MX Infrared Imaging Microscope. The results showed that groundwater samples were found to have microplastic concentrations ranging from 2 to 21 particles/L. With the help of fibres and fragments, the two shapes of microplastics were established. Microplastics were discovered with diverse polymers, with polyethylene terephthalate (PET) being the most common polymer observed in groundwater.

Bin Wu et al., 2022 investigated occurrence and distributions of microplastics were investigated in shallow groundwater from an important water source district in Tianjin city of northern China. This study comprehensively characterised the abundance, physical form, chemical composition, and potential linkages of microplastics with human activities. A total of seven types of microplastics were determined with polyethylene, polyethylene terephthalate, and polystyrene as the main types. Polypropylene found substantial positive associations with polystyrene, indicating that they may have comparable sources. The determined Microplastics in groundwater were higher in locations with a high population density and high population activity, demonstrating a substantial link between human activity and microplastics.

Gokul Valsan et.al., 2023 assessed the prevalence of microplastics in pore water, groundwater, and sea water from four southwest Indian locales. Polymers such as polyester, low-density

polyethylene, and polystyrene were discovered using Fourier transformed infrared spectroscopy. Fishing, tourism, and coastal dwellers are all potential sources of microplastic. The risk assessment scores determined from microplastics show that ecosystems are in grave danger. Fibres were the most common type of microplastics discovered.

Mansi Vaid et al., 2021 studied by evaluating accessible scientific research, this review article attempts to convey current understanding of microplastic contamination in India's aquatic systems, terrestrial systems, atmosphere, and human consumables. This study is an attempt to discover information gaps and gaps in microplastic pollution in various compartments of the Indian ecosystem. The toxicity of these microplastics has not been widely studied, and the current condition of microplastic prevalence in Indian food and beverage items is unclear. The study also focuses on identifying gaps in current knowledge and highlighting potential research directions.

K. Amrutha et al. 2020 studied the source-to-sink characterisation of microplastics (5mm - 0.3mm) in a tropical Indian river, the Netravathi, which flows into the Arabian Sea. He presents a careful investigation of water, sediment, and soil samples gathered from the river catchment in this paper. The main categories collected from the catchment include fibres, films, and pieces. The microplastics found in the samples were largely transparent and white in colour, owing to the decomposition of plastic carry bags, packing materials, and fishing lines. The most abundant polymers in the samples are polyethylene and polyethylene terephthalate and minor amount of PVC were also present. According to the study, the Netravathi River is contaminated with microplastics from its source to its mouth. However, the spatial distribution and abundance of microplastic particles show the influence of population distribution, land use, and good waste management practises in some locations.

Ashwini S. K et al., 2019 measured microplastic pollution on Kerala's Nattika coast and developed an environmental forensic investigation approach for identifying microplastic pathways and sources. The microplastics were analysed using FTIR and SEM. The research revealed that the majority of the microplastics detected (90%) were secondary microplastics. Polyethylene was discovered to be a common type of microplastic in Nattika, and the polyethylene fibres found on the beach could nearly totally be traced back to their source. And the fibres were discovered were used for net mending yard and the boat pulling ropes. The research revealed that the beach is polluted, but there are no standards for comparison to represent the severity of the problem.

Dennis Brennecke et al., 2016 investigated under experimental manipulation, the adsorption of two heavy metals, copper (Cu) and zinc (Zn), leached from an antifouling paint to virgin polystyrene (PS) beads and old polyvinyl chloride (PVC) fragments in saltwater. The antifouling paint released heavy metals into the water, and both microplastic varieties absorbed the two heavy metals. As a result, they have discovered a strong connection between these forms of microplastics and heavy metals, which could have consequences for marine life and the environment. These findings significantly confirm recent discoveries that plastics might serve as vectors for heavy metal ions in the marine environment. And from these findings emphasise the necessity of monitoring marine litter and heavy metals, particularly those linked with antifouling coatings, in the context of the Marine Strategy Framework Directive (MSFD). As a result of this mechanism, microplastics become vectors of increased contamination, posing a significant concern to marine species as possible sources of heavy metals.

Lisbeth Van Cauwenberghe et al., 2015 studied over 100 articles from the last 50 years are reviewed with the following goals in mind such as to evaluate current microplastic extraction techniques, to discuss the occurrence and global distribution of microplastics in sediments, and to make a comprehensive assessment of the potential adverse effects of this type of pollution on marine organisms. While most extraction procedures are based on the same idea, namely density separation, there are numerous variants on this principle. Some are more efficient than others at extracting different types of microplastics but this comes at a cost in some cases. In general, sampling procedures will differ depending on the research subject being addressed. However, by describing the whole set of sampling details disparities between sampling methodologies can be avoided, and inter-study comparability can be facilitated. As a result, the suggested harmonisation will aid future, uniform microplastic abundance evaluations, as well as scientifically grounded regional comparison and time trend assessments.

Barbara E. Oßmann et.al 2018 investigated microparticle pollution was evaluated in mineral water samples. Microplastics were found in varying levels in water from all bottle types. Mineral water from reusable bottles (both PET and glass) contained more microplastics than water from single-use PET bottles. The main polymer in water from PET bottles was PET, indicating contamination from the bottle material. Various polymer forms, such as PE or a styrene-butadiene-copolymer, were discovered in water from glass bottles. Contamination sources include the bottle cap, washing machinery, and other processes in the filling process. Microplastic levels were higher in water from regularly reused PET bottles than in water from newer PET bottles. This could have been produced by the ageing of the bottle material. A few

particles of an antioxidant ingredient were also discovered in reusable PET bottles. These could be leached out of the bottle's substance.

Kakani Katija et al., 2017 studied Bathochordaeus stygius, a gigantic larvacean, was used in in situ feeding experiments of microplastic particles. We show that giant larvaceans can filter a variety of microplastic particles from the water column, swallow, and subsequently package microplastics into their faecal pellets by conducting in situ feeding trials with remotely operated vehicles. Microplastics can also easily attach to their houses, which have been found to sink swiftly to the seafloor and supply carbon pulses to benthic ecosystems. As a result of the quick sinking of faecal pellets and discarded dwellings, giant larvaceans can contribute to the vertical flux of microplastics.

Valentina Iannilli et al., 2019 investigated Gammarus setosus from the Svalbard Archipelago is the first to have consumed microplastics in its natural environment. Nile Red staining and Micro FT-IR spectroscopy were used to identify the plastic particles. If microplastic particles are available in the environment, the animal investigated ingests them, most likely mistaking them for food. The microplastic particles consumed may be available for ingestion by predators that consume this Arctic amphipod, thereby affecting the food web. The majority of the larger shards we've discovered are red coloured and appear to be flaking paint fragments from ships or naval equipment. Polyarylamide, a thermoplastic polymer used in mechanical components, electrical connectors, and fishing gear manufacturing, was detected among the fragments analysed alongside poly-methyl-acrylamide. Nylon was also found among the fragments, with likely sources being lost fishing gear such as fishing rope and nets.

Defri Yona et al., 2019 examine the amount of microplastics in the Java Sea's eastern water. The research locations are widely recognised for their high population density and industrial activity, both of which can contribute to plastic pollution. Microplastics were collected from surface sediments at five separate locations reflecting various local activities such as a fish landing place, a mangrove forest, an abandoned prawn pond, a river mouth, and the open sea. Plastic pieces were determined to be the most common kind of microplastic, followed by fibres and films. The mangrove area had the largest concentration of microplastics, which were mostly shards and fibres. Films were detected in the greatest number in the fish landing area, but their abundance was substantially reduced when compared to the other types of microplastics. Domestic garbage and fishing activities were the primary sources of microplastics in the research locations. The findings of this study demonstrated that

microplastic contamination is a severe problem that requires attention not just from the government but also from the general public. Waste management for plastics is required.

Sarah Reed et al., 2018 studied microplastic particle concentrations in soil samples collected at 20 locations up to 7 kilometres from Rothera Research Station. From the study found microplastic pollution in near-shore marine sediments collected near the research area. Microplastic concentrations were highest in silt collected near the station's sewage treatment plant outfall. The amounts were comparable to those found in shallow and deep-sea marine sediments outside of Antarctica. The identified microplastics have properties comparable to those usually created by laundry.

Anthony L. Andrady et al., 2011 studies the mechanics of creation and potential effects of microplastics in the ocean environment. Plastics degrade on beaches due to weathering, resulting in surface embrittlement and microcracking, which produce microparticles that are pushed into water by wind or wave action. Microplastics, unlike inorganic fines found in seawater, concentrate persistent organic pollutants by partitioning. Under maritime exposure circumstances, micro- and nano plastics are stubborn materials. While they make up a relatively minor proportion of the micro- and nano particulates in marine water, the demonstrated ability of plastics to absorb and concentrate POPs is a major worry.

Jamila Patterson et al., 2020 focuses on the presence and properties of microplastics, as well as the spatial distribution and pollution status of heavy metals in the water and sediments of coral reef ecosystems linked with the Tuticorin and Vembar groups of islands in the Gulf of Mannar, southeast India. MP concentrations are greater in water and sediment samples from the Tuticorin islands than in the Vembar islands. Certain metals associated with Microplastics appear to have higher levels than the surrounding sediments. This demonstrates the potential for Microplastics to act as heavy metal vectors and transport them over large distances. They may also leak harmful substances back into the environment as conditions change and drive desorption processes, or if they come into contact with other media for which they have a higher affinity. This implies that Microplastics could be a significant source, transport mechanism, and exposure route for this class of environmental contaminants.

S. Sruthy et al., 2017 studied microplastics in the sediments of Vembanad Lake, an Indian Ramsar site. Micro Raman spectroscopy was used to identify the polymer components of Microplastics. The current study indicates the presence of microplastic particles in the sediments of India's Vembanad Lake and estuary. The shape of the Microplastics found in this

study implies that they are the result of fragmentation of bigger plastic debris, indicating that their ultimate cause is the usage and disposal of plastics. Controlling Microplastics/plastics at the source is thus an option that should be seriously considered, because once Microplastics are released into the environment, there is little that can be done to limit their dispersion and impacts.

V. Anu Pavithran et al., 2021 attempts to categorise and quantify microplastics from selected parts of Kerala's northern coast, located on India's southwest coast. Deeply pigmented threads predominated in this investigation. Micro-Raman Spectroscopy was used to examine the chemical composition of the microplastic particle. Polypropylene was the dominant particle among the polymer and presence of Polyethylene-co-vinyl acetate, polyamide, polybutadiene and polyethylene were present. The presence of these particles in coastal seawaters causes major harm since these places include a diverse fauna that plays an important role in the food web. The existence of these polymers demonstrates poor waste management practises as well as a lack of proper recycling and management of abandoned plastic products. Because all of the small polymer particles discovered in this study are major components of packaging materials, fishing nets, and floats, it is obvious that the degraded secondary microplastic particles in coastal saltwater are the result of anthropogenic activity in these coastal locations.

Davis Ephsy et al., 2023 studying the geographical and seasonal dispersion of microplastics in Kumaraswamy Lake Coimbatore, Tamil Nadu. Samples were collected from the inlet, centre, and outlet during several seasons, including summer, pre-monsoon, monsoon, and post-monsoon. All sampling points contained microplastics made of linear low-density polyethylene, high-density polyethylene, and polypropylene. The water samples contained fibre, thin fragments, and film morphologies of microplastics, in which majority of which were black, pink, blue, white, translucent, and yellow in colour. Seasonally, the monsoon season had the highest microplastic concentration, followed by the pre-monsoon and post-monsoon seasons, while the summer season had the lowest. These findings highlight how the spatial and seasonal distribution of microplastics can have a negative impact on the fauna and flora that reside in lake ecosystems.

Kalpana Gopinath et al., 2020 investigate the distribution and source of microplastic contamination in Red Hills Lake, one of the freshwater systems supplying water to Chennai's northwestern suburbs. The most prevalent types of microplastics discovered in sediments and water include fibres, pieces, films, and pellets. FTIR analysis revealed that the most frequent

forms of microplastic were high-density polyethylene, low-density polyethylene, polypropylene, and polystyrene in both sediments and water samples. From their studies the microplastics revealed that several metals such as Al, Fe, Mg, Ca, Na, Si, Ti, K, Cl are present on the surface of the microplastics and might be absorbed by the microplastics. The current treatment plant does not prioritise the removal of microplastics from water; Chennai residents use the water directly or after boiling it, which does not remove the microplastics but increases the toxicity because heating releases metals into the water.

Isabella Gambino et al., 2022 studied the presence of microplastics in tap and bottled water was discovered in the studies examined, raising concerns for public health due to the potential toxicity associated with their polymeric nature, additives, and other substances or microorganisms adsorbed on their surface. The concentration of microplastics increased with particle size and was higher in bottled water than in tap water. Reusable PET and glass bottles had more microplastic contamination than other bottled water packaging. The lower microplastic abundance in tap water compared to natural sources suggests that microplastics are removed at a high rate in drinking water treatment plants.

D. Supriya Varshini et al., 2021 to investigate the prevalence and features of microplastics in the surface water of Puducherry, Tamil Nadu's largest lake and an important wetland, Ousudu Lake. All of the samples contained a high concentration of microfibers of various colours such as black, blue, pink, purple, translucent, and straw yellow were seen. The spatial distribution implies that microplastics predominate in the lake's centre and diminish in the banks. Raman spectroscopy verified polyethylene as the major plastic type, implying possible sources from bigger plastic debris.

Velusamy Selva Ganapathy et al., 2021 investigate to find out the distribution of microplastics in surface sediments and water from Chennai's Cooum River, Tamil Nadu. From the analysis 68% of the microplastics in water samples were coloured, while 32% were colourless. Fibres were the most common in overall distribution in Water, accounting for 87% of the total, followed by beads and fragments. Domestic garbage dumping near the river's banks, as well as the discharge of untreated waste water from industries, have a significant impact on the spread of microplastics in the Cooum River.

K. Radhakrishnan et al., 2021 the purpose of this study is to develop the characterization and distribution of microplastic in the estuarine surface sediments of the Kayamkulam estuary on India's southwest coast. To detect the separated polymer compositions, the Bruker Fourier-

transform infrared spectroscopy (FTIR) method was linked with Attenuated Total Reflectance (ATR) diamond crystal attachment. In the entire distribution, the fibre form of the microplastic was prominent in the sediments, followed by film and then fragment. Among the other polymer types studied, polyester, polypropylene, and polyethylene, polyester had the highest prevalence. The distribution of microplastics was mostly influenced by estuary flooding water and the test site's distance from the open sea.

Maimoona Raza et al., 2022 according to this review paper, they analysed the sources of microplastic are diverse and vast, and their occurrence, movement, fate, and health concerns in the environment are influenced by their physicochemical properties and natural causes. The marine environment is the primary focus of the limited research studies on microplastic pollution, and there is a need to bridge the data gap about microplastics in terrestrial soil and freshwater settings. Microplastics have been found in terrestrial soil and freshwaters in the form of pieces, fibres, and film forms, according to the literature. Previous research has reported on the relative abundances of PE and PP polymers. More research on the distribution, shape, and polymers of microplastics is required to better understand their health impacts.

Woody J. Drummond et al., 2022 examined the amount of microplastics in freshwater streams in Adelaide, Australia, to estimate their outflow into the Gulf of St Vincent. The most abundant microplastic type in all samples was fibres, which accounted for a quarter of all microplastics found. Beads, films, and foams each contributed substantially less to the microplastics discovered in the samples, with fragments being the second most frequent form. Translucent, blue, and black were the most prevalent colours. Other colours such as white, green, yellow, red, pink, purple, and brown were also present, but each represented a lower percentage of all microplastic colours discovered. The study found that freshwater streams in this area contribute to the transmission of microplastics into the marine environment, and it could serve as a foundation for future plastic waste management policies and initiatives in the area.

Austin Scircle et al., 2019 investigated to detect and quantify, microplastic by using fluorescence microscopy by staining them with nile red dye. Although a few fibres were found, the majority of the particles were categorised as fragments and beads. The mechanical operation of opening a bottle cap is thought to introduce microplastic fragments, while fibres may indicate sample contamination. Microplastics were detectable and counted in all samples, with mean counts ranging from 7 to 28 per litre. This was an exercise introduces students to microplastic pollution and to motivates and engages them to chemical research field.

CHAPTER 3

STUDY AREA

3.1 Introduction

The Brahmapuram landfill serves as a significant waste disposal location in the Ambalamugal area. Ambalamugal is a town in Kerala's Ernakulam district. It is located on the banks of the Periyar River, about 10 kilometres southeast of Kochi. Ambalamugal is well-known for its industrial presence, with several significant enterprises and factories located there. Ambalamugal's industrial presence has benefited the local economy and created job possibilities in the area. However, it is important to note that industrial operations might have an impact on the environment. Efforts are undertaken to control and manage industrial operations in order to reduce any potential negative environmental and public health repercussions. The Ministry of Environment and Forests designated Ambalamugal as a critically polluted area in 2010, putting a halt to further project approvals.

The Hindustan Organic Chemicals Ltd. (HOCL), a public sector firm under the Ministry of Chemicals and Fertilisers, Government of India, is one of the important establishments in Ambalamugal. HOCL manufactures a diverse range of pesticides, insecticides, and agricultural chemicals. The company has a manufacturing operation in Ambalamugal that serves India's agriculture sector. In addition to HIL, Ambalamugal is home to the Kerala Minerals and Metals Limited (KMML), another significant industrial organisation. KMML is a government-owned corporation that manufactures minerals and metals such as ilmenite, rutile, zircon, and synthetic rutile for use in paint, welding electrodes, and ceramics.

Figure 1: Study Area

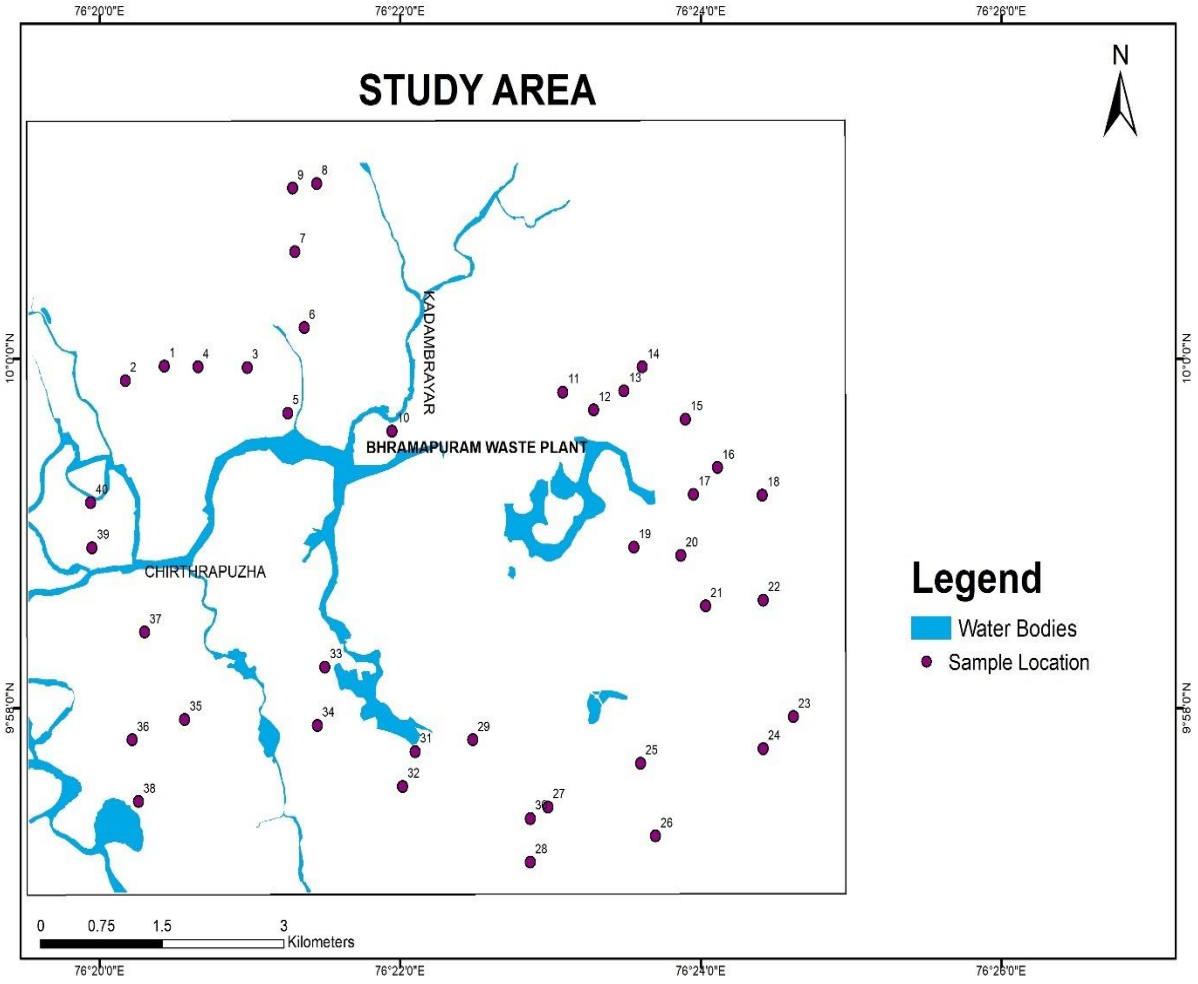

Source: Made by the author using ArcGIS

3.1.2. Kadambrayar River

The river Kadambrayar flows from a hill near Arakkappady in Perumbavoor Taluk's Vengola Panchayat. Near Ambalamugal, the river joins Chithrapuzha after passing through the panchayats of Edathala, Kizhakkambalam, Kunnathunad, and Thrikkakara. The river's catchment area is thought to be 115 km2, and its overall length is 27 km. For industrial zones including Kerala Industrial Infrastructure Development Corporation (KINFRA), Info Park Phase -1, Phase -2, Smart city, and Cochin Special Economic Zone (CSEZ), as well as for businesses like Nitta Gelatin India Ltd, Philips Carbon, Wonderla, and Cochin Kadaalas, among others, Kadambrayar serves as the supply of water.

3.1.3 Chitrapuzha River

On the southern coast, near the Amabalamugal town of Kochi, the Chitrapuzha River, one of the tributaries of the Periyar River, runs. At Thevara Ferry, Chithrapuzha flows south and joins Vembanad Lake. A range of effluents from the fertiliser, refinery, and other businesses are discharged into the river. Other significant industries in the Ambalamugal Kochi area are Kochi Refinery Limited (KRL) and Hindustan Organics Chemicals Limited (HOCL), in addition to Fertilisers and Chemicals Travancore (FACT).

3.1.4 Brahmapuram

Brahmapuram is situated in the northeastern region of Kochi, a prominent seaport city in the state of Kerala. The location of the area is within the Ernakulam district, adjacent to the banks of the Periyar River. The Brahmapuram Waste Management Plant stands out as a noteworthy characteristic of Brahmapuram. The aforementioned facility is under the management of the Kochi Municipal Corporation and functions as a vital hub for garbage management and disposal in the urban area of Kochi, as well as its neighbouring regions. The Brahmapuram Waste Management Plant encompasses a waste-to-energy facility that utilises contemporary technologies to transform solid garbage into a viable energy source and approximately 100 metric tonnes of plastic waste are deposited daily into the Brahmapuram Waste Management Plant. The facility produces electrical energy through the process of waste combustion, so making a significant contribution to fulfilling the energy requirements of the local area.

3.1.5 Geology of the Area

Ambalamugal's geology in Kerala, is distinguished by a mixture of sedimentary and igneous rocks that are influenced by the area's geological history. Sedimentary rocks predominate in the area surrounding Ambalamugal. Sandstone, shale, and limestone make up the majority of the sedimentary rocks in this region. Alluvial sediments have been deposited around Ambalamugal as a result of the Periyar River's presence. Alluvium such as sand, silt, clay, and gravel are present in the area. Alluvial deposits are frequently fertile and highly productive for farming. Some places near Ambalamugal also include laterite, a type of soil and rock created by severe weathering in tropical conditions. Igneous intrusions are found in a few locations in the Ambalamugal region. There could be granite and gneiss among the local igneous rocks.

Figure 2: Geological map of the area

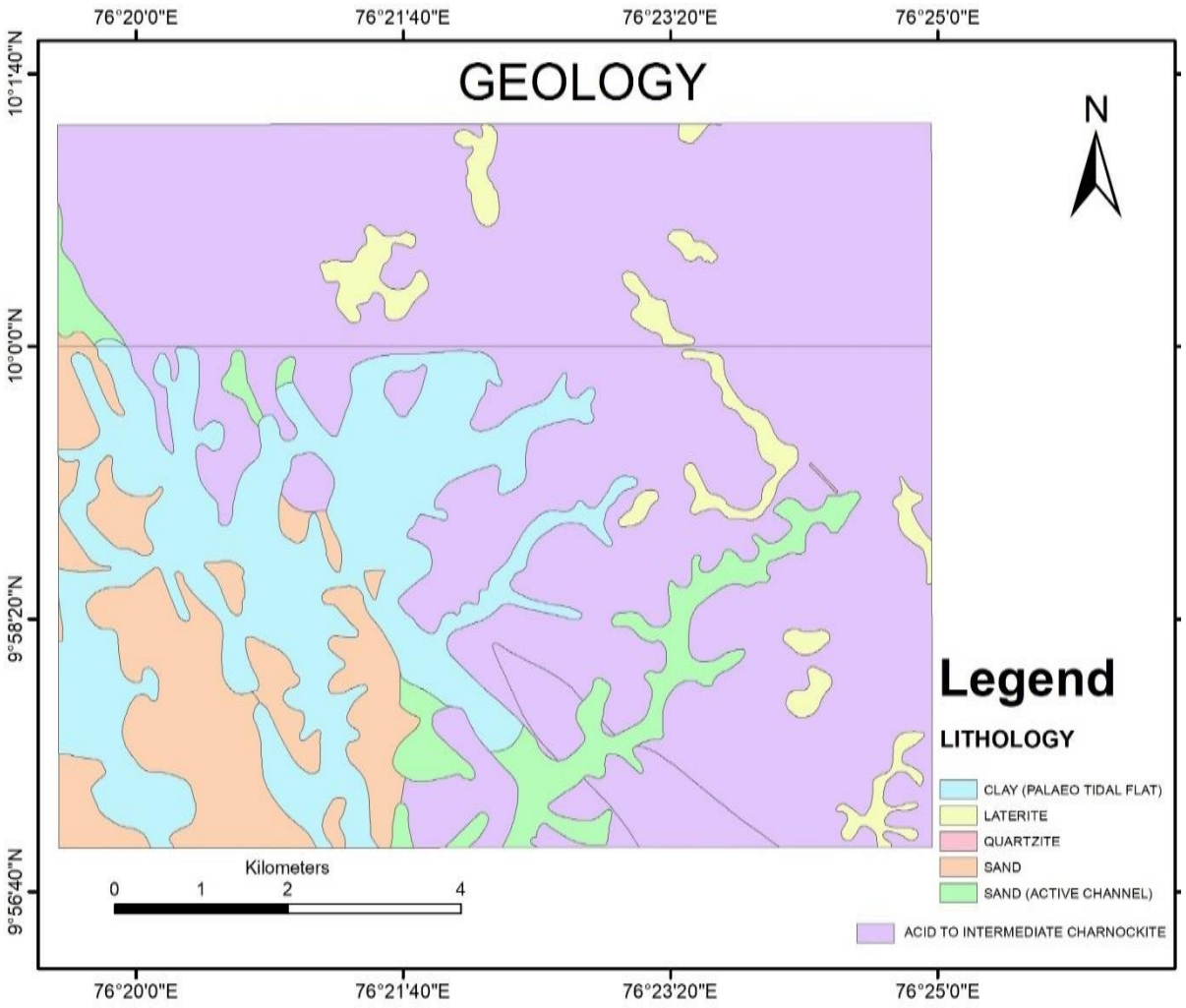

Source: Made by the author using ArcGIS

3.1.6 Climate

Ambalamugal, which is in the Indian state of Kerala, has a tropical monsoon climate. Ambalamugal's weather can be characterised as humid and warm throughout the year, with heavy rains during the monsoon season. Ambalamugal experiences a substantial quantity of rainfall from June to September, which is the monsoon season. The region receives a lot of rain thanks to the southwest monsoon, which moves in from the Arabian Sea. From October to November, Ambalamugal enjoys a post-monsoon period that is marked by sporadic downpours and gradually lessening rainfall. Ambalamugal experiences a moderate and pleasant winter that lasts from December to February. Ambalamugal experiences warm temperatures all year long. The typical annual temperature is between 25 and 35 degrees Celsius. The survey is carried out

during the pre-monsoon period, while there is a possibility of variations in the physical-parameters of groundwater during the post-monsoon period.

3.1.7 Geomorphology of the Area

Considering the geographical location of Ambalamugal inside the Ernakulam district, characterised by its proximity to the shore, it is plausible to anticipate the presence of several geomorphic attributes that are impacted by its coastal environment. However, it may be inferred that Ambalamugal, being situated further inland in comparison to the coastal regions of Ernakulam, is less likely to exhibit a prominent presence of coastal landforms in its geomorphology. Alternatively, it could encompass characteristics associated with elevated landforms, depressions, and watercourses.

Ambalamugal is situated in a region characterised by elevated landforms, such as hills or plateaus, which have been created by various geological processes, including erosion, weathering, and tectonic activity. The observed landforms might serve as indicators of the geological history of the area. Ambalamugal is characterised by the presence of rivers and associated geomorphological features such as river valleys, floodplains, and river terraces. The landscape may have been gradually altered by the rivers through the processes of erosion and silt deposition. Considering the status of Ambalamugal as an industrialised urban centre, it is plausible that human activities such as mining, construction, and industrial operations may have exerted an influence on the geomorphological characteristics of the surrounding area. These actions may have caused some degree of modification to the natural landscape.

Figure 3: Geomorphological map of the area

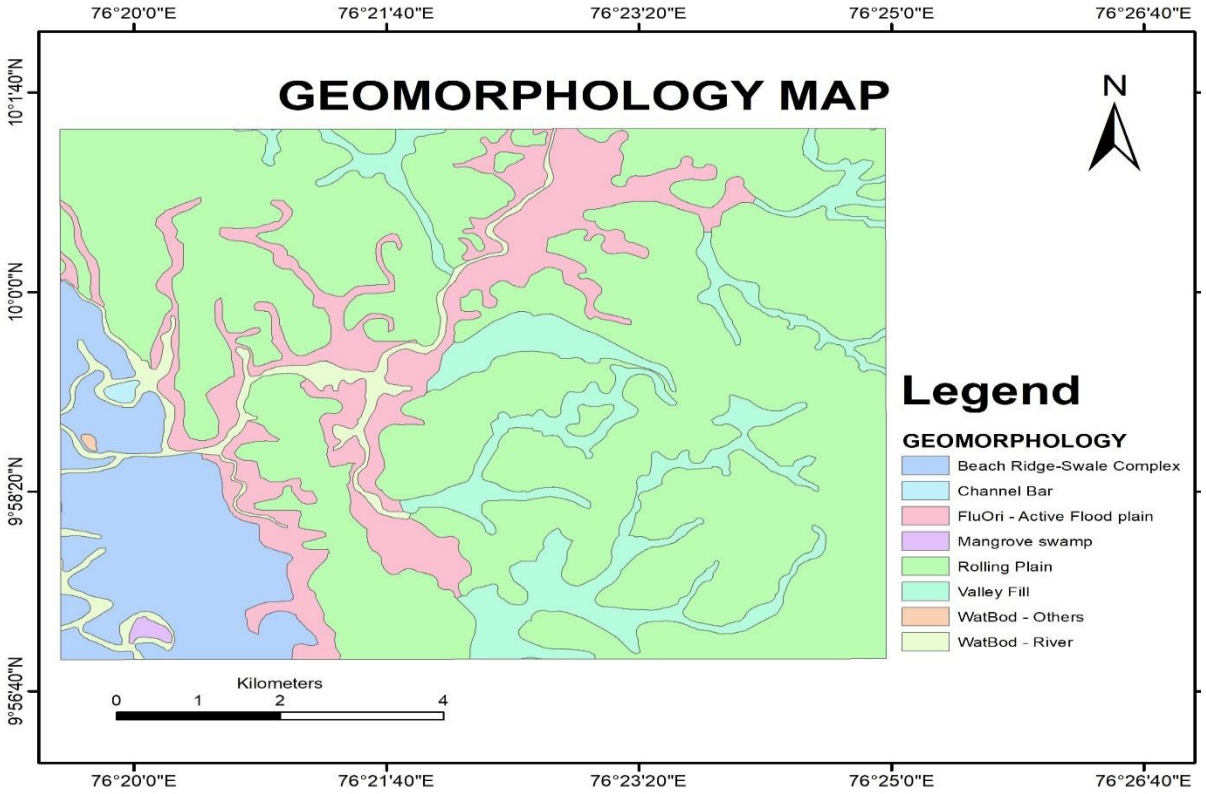

Source: Made by the author using ArcGIS

3.1.8 Industries

The main industries in the region are encompassed by Kerala Industrial Infrastructure Development Corporation (KINFRA), Info Park Phases 1 and 2, Smart City, and Cochin Special Economic Zone (CSEZ), as well as by companies like Nitta Gelatin India Ltd, Philips Carbon, Wonderla, and Cochin Kadaalas. Without any sort of treatment, Market's sewage is dumped into rivers. The water quality has declined as a result of some establishments dumping untreated or partially treated sewage into the drain that flows into the river. The Fertilisers and Chemicals Travancore Limited (FACT), Hindustan Organic Chemicals Ltd., and Kochi Refinery all discharge treated wastewater into this river. We can see domestic effluent outlets. Due to oxygen depletion and an increase in Biochemical Oxygen Demand (BOD), the Kadambrayar River's state is currently getting worse. On the bank of the confluence of the Kadambrayar and Chithrapuzha rivers in Brahmapuram is Kochi Corporation's Municipal Solid Waste (MSW) Plant.

CHAPTER 4

METHODOLOGY

4.1 Sample Collection

In the pre-monsoon month of April 2023, forty groundwater samples were taken prior to the south west monsoon from dug wells spaced one kilometre apart in various parts of the *Brahmapuram landfill, Ambalamugal, Ernakulam district.* Groundwater samples were collected according to American Public Health Association (APHA),2012, in which the pre-washed half litre polyethylene bottles were used for collecting the groundwater samples and pre-washed one litre polyethylene bottles were used for the collection of microplastics.

4.2 pH

Materials needed:

- pH Meter
- pH buffer solutions (pH 4.01 and pH 7.00)
- Distilled or deionized water
- Container for calibration (usually a small beaker or glass)

Procedure:

- Rinse the pH meter electrode with distilled or deionized water.
- Immerse the pH meter electrode into the pH 4.01 buffer solution.
- Wait for the pH reading to stabilize. This should take about 30 seconds.
- Adjust the pH meter reading to 4.01 using the adjustment knob or button on the meter.
- Rinse the pH meter electrode with distilled or deionized water again.
- Immerse the pH meter electrode into the pH 7.00 buffer solution.
- Wait for the pH reading to stabilize.

  Adjust the pH meter reading to 7.00 using the adjustment knob or button on the meter. Rinse the pH meter electrode with distilled or deionized water one more time immerse the PH meter and taken a measurement.

Potential Hydrogen, usually referred to as pH, is a metric for determining how acidic or alkaline a solution is. It shows how many hydrogen ions (H+) are present in the solution. The pH scale has a range of 0 to 14, with 7 being thought of as neutral. Acidity is indicated by a pH level

below 7, whereas alkalinity or basicity is indicated by a pH level above 7. The presence of dissolved minerals, the surrounding environment, and the geological makeup can all affect the pH of groundwater. In general, groundwater has a pH between 6 and 8, which is regarded as neutral and lies between the ranges of acidic and alkaline. The procedure follows the standard water quality procedures of APHA (2012).

4.3 Electrical Conductivity (EC)

Materials needed:

- Conductivity meter
- Conductivity standard solution (of known conductivity)
- Distilled or deionized water
- Container for testing (usually a small beaker or glass)

Procedure:

- Rinse the conductivity meter electrode with distilled or deionized water.
- Immerse the conductivity meter electrode into the conductivity standard solution of known conductivity.
- Wait for the conductivity reading to stabilize.
- Adjust the conductivity meter reading to match the known conductivity of the standard solution, using the adjustment knob or button on the meter.
- Rinse the conductivity meter electrode with distilled or deionized water again.
- Immerse the conductivity meter electrode into the sample water to be tested, wait for the conductivity metre reading to stabilize and record the conductivity reading.

Because it has a very low ion concentration, pure water in its purest form is a poor conductor of electricity. However, water easily dissolves a wide range of chemicals, including gases and minerals, which can increase its conductivity. Standard units for measuring electrical conductivity in water are Siemens per metre (S/m) or micro siemens per centimetre (S/cm). It is affected by a number of variables, including as temperature, the presence of dissolved compounds (such as salts, acids, and bases), and their concentration. The procedure follows the standard water quality procedures of APHA (2012).

4.4 Total Dissolved Solids (TDS)

Materials needed:

- TDS meter
- TDS standard solution (of known TDS)
- Distilled or deionized water
- Container for testing (usually a small beaker or glass)

Procedure:

- Rinse the TDS meter electrode with distilled or deionized water.
- Immerse the TDS meter electrode into the TDS standard solution of known TDS.
- Wait for the TDS reading to stabilize. This should take about 30 seconds.
- Adjust the TDS meter reading to match the known TDS of the standard solution, using the adjustment knob or button on the meter.
- Rinse the TDS meter electrode with distilled or deionized water again. Immerse the TDS meter electrode with again, immerse the TDS meter electrode into the sample water to stabilized.
- The drinking be tested.
- Record the TDS reading.

The combined concentration of all inorganic and organic elements dissolved in water is referred to as total dissolved solids (TDS). It serves as a gauge for how much solid matter is dissolved in water, including metals, salts, minerals, and other substances. TDS is commonly measured in parts per million (ppm) or milligrams per litre (mg/L). TDS can contain a variety of components, including organic debris, calcium, magnesium, sodium, potassium, bicarbonates, chlorides, sulphates, and other dissolved ions. The procedure follows the standard water quality procedures of APHA (2012).

Figure 4: Sample Collection from the study area

4.5 Microplastics

Materials Needed:

- Filter Unit
- vacuum pump
- Distilled or Deionised water
- one litre groundwater sample
- filter membrane(47mm)

Procedure:

- Wash the filter unit using distilled water, and fix the filter unit carefully
- Take one filter membrane or glass membrane(47mm) placed in the middle of the
- filter unit.
- Connect the vacuum pump (used for filtration make faster)
- pour one litre groundwater sample to it
- Started the filtration by switch on the vacuum pump.
- After finishing the filtration process, remove the filter membrane from the filter unit.
- Observe the filter membrane through stereoscopic microscope.
- Microplastics were present in the filter membrane, count the microplastics through the microscope and transfer the microplastics to the container.

Figure 5: Analysing physical properties of groundwater and detection of microplastics

CHAPTER 5

RESULT AND DISCUSSION

This chapter provides a description of the analysis of the data, the obtained results, and the subsequent discussion. A total of 40 samples were collected from several dug wells in and around Brahmapuram landfill and the vicinity of the Ambalamukal industrial area. The samples are subjected to filtration and microscopic observation, enabling differentiation based on their respective colours.

5.1 Result

5.1.1 Analysis of Groundwater

The collection of groundwater samples was initiated using pre-washed half-litre polyethylene bottles, followed by subsequent analysis performed within a controlled laboratory environment. The physical parameters, namely pH, TDS, and EC, have been assessed inside laboratory settings, and the resulting measurements have been when compared with the permissible thresholds provided by the Bureau of Indian Standards (BIS).

Table 1. Drinking Water Quality Standards (BIS 2012) And Estimated Values of Physical Parameters

Parameters	Indian standards (BIS 2012)	Maximum	Minimum	Average
pH	6.5-8.5	7.43	4.29	5.6
EC (μS/cm)	1500	1943	30.17	254.43
TDS (ppm)	500-2000	972.6	15.4	127.37

5.1.1.1 Hydrogen Ion Concentration (pH)

The pH scale is utilised to quantify the acidity or alkalinity of water. The numerical scale spans from 0 to 14, with the midpoint of 7 representing a state of neutrality. Acidity is indicated by pH values below 7, while pH values above 7 indicate alkalinity. The pH scale is a quantitative measure of the concentration of hydrogen ions (H+) and hydroxide ions (OH-) in an aqueous solution. Acidic water is characterised by a higher concentration of free hydrogen ions, while basic water is characterised by a higher concentration of free hydroxyl ions. The pH of water can be influenced by several chemical constituents, therefore rendering it a significant parameter for monitoring chemical alterations in water.

The solubility and biological availability of chemical elements, such as nutrients (phosphorus, nitrogen, and carbon) and heavy metals (lead, copper, cadmium, etc.), in water are influenced by its pH. Elevated pH levels result in a bitter flavour, the accumulation of deposits on water pipes and appliances, and a reduction in the efficacy of chlorine disinfection, necessitating the use of additional chlorine to compensate for the high pH. Water with a low pH level has the potential to induce corrosion or dissolution of metals and various other compounds.

Figure 6: Map representing spatial distribution of pH

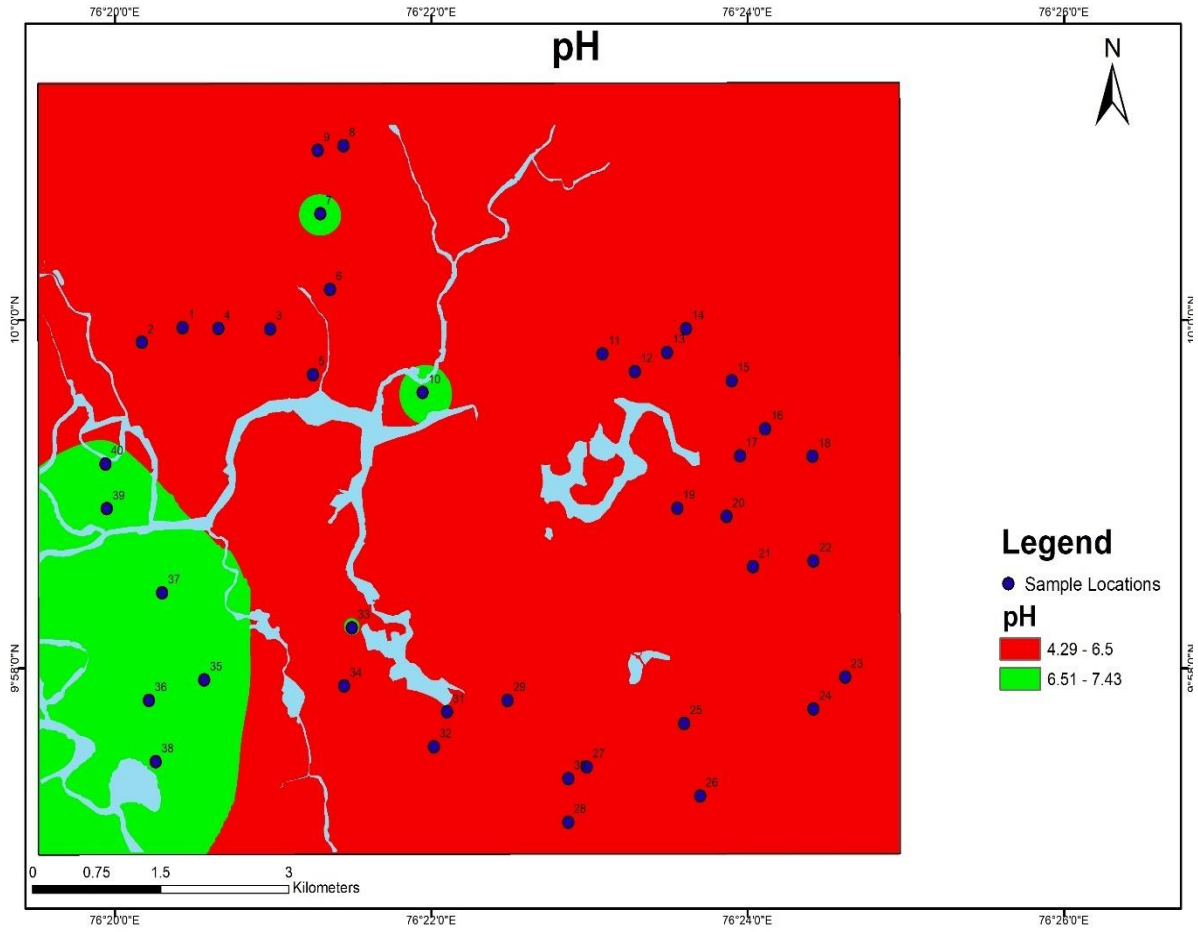

Source: Made by the author using ArcGIS

The present evaluation of the 40 samples indicates a pH range of 4.29 to 7.43, with an average pH value of 5.61. According to the standards set by the Bureau of Indian Standards (BIS) for drinking water, the acceptable pH range is between 6.5 and 8.5. Among the forty samples analysed, eight were found to meet the safety standards for drinking water, while the remaining thirty-two were determined to possess acidic properties. Based on the pH distribution map, it can be inferred that the southwestern region of the map exhibits favourable conditions for drinking water, whilst the majority of the remaining area demonstrates an acidic nature. The

presence of a low pH level has been associated with the development of various ailments, including dental complications, gastrointestinal disorders, skin irritation, and heavy metal toxicity. The green region represented on the map signifies the area inside the region that adheres to the allowed limit of water as defined by the Bureau of Indian Standards (BIS). The acidic character seen in the research area may be attributed to the presence of iron in laterites, orthopyroxene and feldspar in Charnockite, as well as the inadequate total alkalinity in the groundwater.

5.1.1.2 Electrical conductivity (EC)

The electrical conductivity is used to quantify the capacity of water to conduct the flow of an electrical current. The magnitude of the electrical current conducted in water is directly proportional to the quantity of dissolved charged substances. The movement of water is facilitated by the presence of electric charge, which imparts the necessary energy. Consequently, the motion of freely moving ions contributes to an increase in electrical conductivity (EC). The electrical conductivity of a solution is influenced by several factors, including the quantity, mobility, valence, and composition of ions, as well as the temperature of the solution. There exists a positive correlation between the specific conductance of a given sample and the concentration of total dissolved solids (TDS) within said sample. The World Health Organisation recommends that the EC value should not exceed 400 µS/cm and the BIS permissible limit is 1500 πS/cm.

The values of EC in this study ranged from 30.17 to 1943 µS/cm, with an average of 254.4338 µS/cm. The green area on the map indicates that the region falls within the permissible limit set by the Bureau of Indian Standards (BIS), while the white area represents regions that are below the BIS permissible limit. The brown-coloured region indicates that the levels significantly beyond the allowable limit established by the Bureau of Indian Standards (BIS). The observed groundwater quality limit in the study area has a similar pattern to that of surface water flows, specifically in relation to the Kadambrayar River and Chitrapuzha River. This suggests that the river has a significant impact on the electrical conductivity (EC) levels in the study area. The limited solubility of specific major ions in groundwater, such as calcium (Ca2+), sulphate (SO_4^{2-}), magnesium (Mg2+), strontium (Sr2+), and barium (Ba2+), depends upon the energy change, $\Delta E_{dissolve}$, that occurs when the ionic solid goes into solution as hydrated ions and the effect of the hydrated ions on the arrangement of the surrounding water molecules (Dill,2007).

Figure 7: Map representing spatial distribution of EC

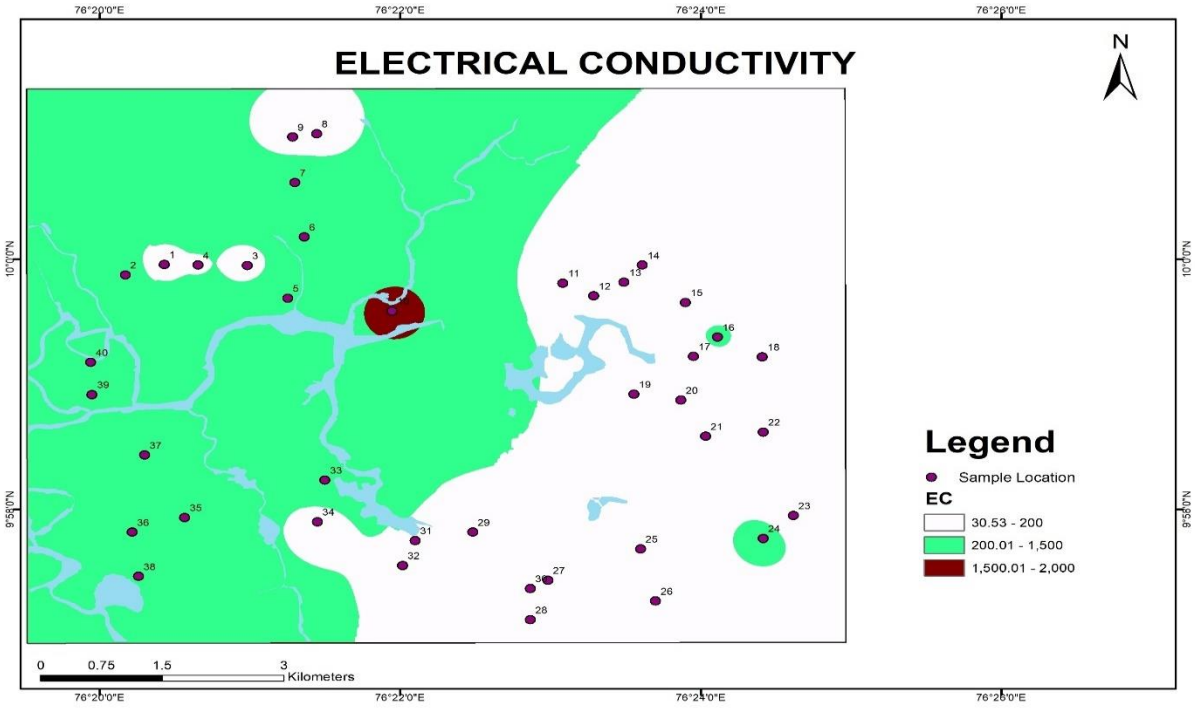

Source: Made by the author using ArcGIS

5.1.1.3 Total Dissolved Solids (TDS)

Figure 8: Map representing spatial distribution of TDS

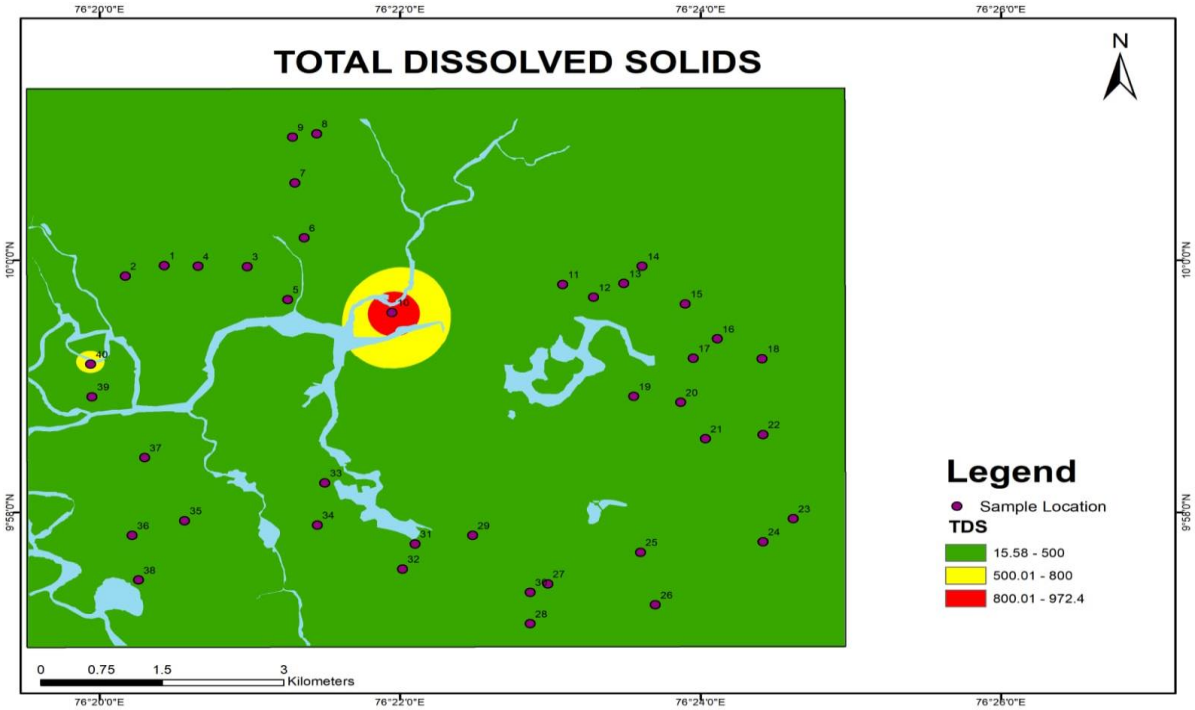

Source: Made by the author using ArcGIS

The term "Total Dissolved Solids (TDS)" refers to the overall level of dissolved compounds found in drinking water. TDS consist of inorganic salts along with a minor proportion of organic substances. Inorganic salts consist of cations with positive charges, including calcium, magnesium, potassium, and sodium, as well as anions with negative charges, such as carbonates, nitrates, bicarbonates, chlorides, and sulphates. The measurement of TDS pertains to the quantification of the concentration of dissolved substances in water. The high TDS value of the water indicates that it is highly mineralized.

The current assessment of the sample reveals that the TDS exhibit a range of values spanning from 972.6 to 15.4, with an average TDS concentration of 127.3718. In the examined sample, 38 specimens were determined to be drinkable, whereas 2 specimens were found to be unsuitable for consumption. The presence of a low TDS concentration in the research area suggests the potential occurrence of mineral deficiencies The presence of a low TDS concentration has been observed to contribute to the occurrence of corrosion problems, hence potentially posing health hazards. Figure 8 illustrates that the green region is deemed suitable for drinking purposes, as the water contained inside it falls under the allowed limit of Total Dissolved Solids. The region depicted in yellow and red signifies elevated total dissolved solids levels, rendering the water unsuitable for consumption. The observed groundwater quality limit in the study area has a similar pattern to that of surface water flows, specifically in relation to the Kadambrayar River and Chitrapuzha River. This suggests that the presence of these rivers has an impact on the TDS levels in the study area. The fact that the Brahmapuram Waste Facility exhibits the highest value (972.6 ppm) within the region is not due to geogenic activities but rather suggests a deficiency in waste management practices. As the distance from the sewage plant increases, there is a progressive decrease in TDS.

5.1.2 Microplastics Analysis

Initially, the aggregate quantity of microplastics was quantified and visual documentation was captured. Microplastics were observed in all of the samples. The different morphology and various coloured microplastics were present in the study area. Various colours of microplastics includes, black, blue, green, pink, and purple. The samples exhibited a prevalence of fibres. Furthermore, these items were meticulously recorded and categorised according to their respective hues. An Excel spreadsheet was utilised to provide a graphical representation of the microplastics contained in groundwater samples, with the colour of the microplastics serving as the basis for the analysis.

Table 2. Table showing colours and count of Microplastics

Sample No.	**Fiber**					**Total**
	Black	Pink	Green	Blue	Purple	
1	4	2	0	2	0	8
2	5	1	0	1	0	7
3	5	1	0	0	0	6
4	5	5	2	5	0	17
5	1	0	0	2	2	5
6	2	2	0	1	0	5
7	4	0	1	2	0	7
8	2	1	0	0	0	3
9	3	0	0	7	0	10
10	10	5	0	8	0	23
11	3	2	0	2	0	7
12	2	2	1	2	0	7
13	2	1	3	1	0	7
14	1	4	1	4	0	10
15	1	2	0	1	0	4
16	2	0	0	1	0	3
17	4	2	1	1	0	8
18	6	2	0	0	0	8
19	2	0	0	2	0	4
20	3	1	0	1	0	5
21	5	0	0	0	0	5
22	4	1	1	0	0	6
23	4	1	1	1	0	7
24	3	1	1	0	0	5
25	2	2	0	0	0	4
26	5	0	2	3	0	10
27	2	1	0	2	0	5
28	5	1	0	0	0	6
29	2	1	0	1	0	4
30	3	0	0	1	0	4
31	0	1	0	2	0	3
32	3	1	0	0	0	4
33	4	2	0	2	0	8
34	1	0	0	5	0	6
35	1	5	2	0	0	8
36	1	1	0	0	0	2
37	1	0	0	0	0	1
38	2	2	1	4	0	9
39	1	1	0	1	0	3
40	3	1	1	2	0	7
Total	119	55	18	67	2	261

Source: Based on Primary Survey conducted

The fibres in all water samples were classified based on their colour, quantified, and identified. A sum of 261 microplastics was acquired during the process of the procedure. The colour black exhibited the highest level of dominance, with a total of 119 occurrences. This was followed by blue, which had 67 occurrences, pink with 55 occurrences, green with 18 occurrences, and purple with only 2 occurrences. Sample number 10 has the largest concentration of microplastics, totalling 23 particles. Sample 37 has the lowest quantity of microplastics, totalling 1.

Figure 9: Spatial distribution of Microplastics

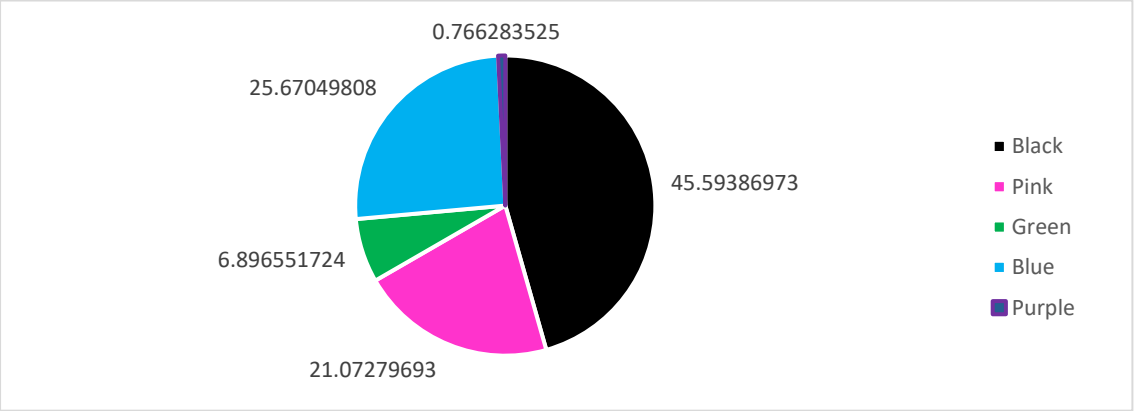

Source: Based on primary survey

Based on the analysis of the data collected from the primary survey, it can be inferred that the proportion of black microplastic constitutes 45.59% of the total, followed by blue at 25.67%, pink at 21.07 %, green at 6.89%, and finally purple at 0.76%. This colour variations in the collected sample are due to various composition of the microplastics. The microplastic length approximatly varies from 2 micrometre 401 micrometres. The average concentration of microplastics in our samples is approximately 6 to 7 particles per litre. Microplastics have been associated with several health concerns, such as respiratory troubles resulting from inhalation, gastrointestinal problems caused by ingestion, alteration of endocrine function, inflammatory and immunological responses, increased risk of cancer, and potential organ damage.

Figure 10: Microscopic Analysis of Microplastics

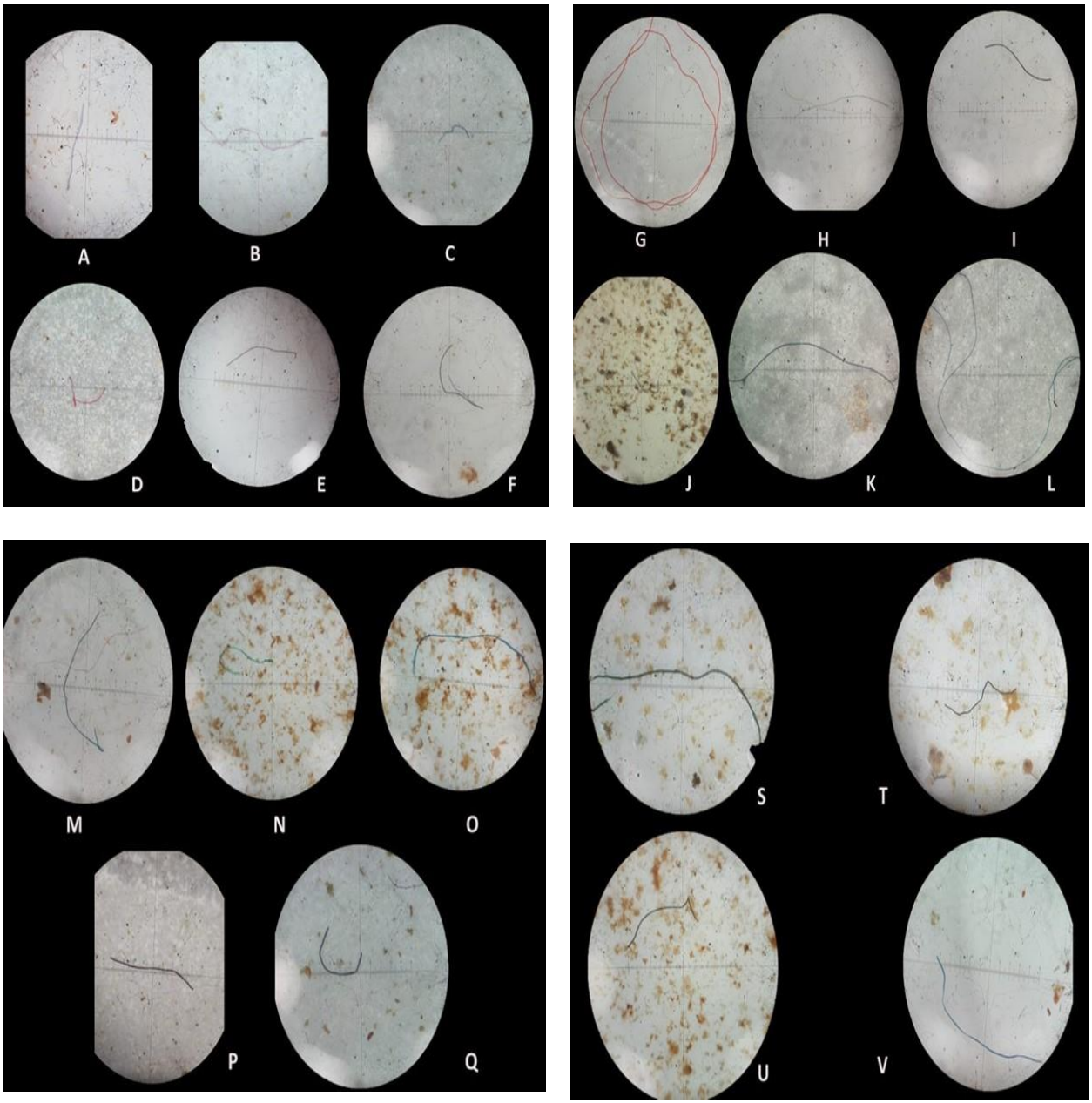

The above images illustrates the microscopic analysis of microplastic present in the groundwater samples collected during the primary survey.

Figure 11: Map representing abundance of microplastics

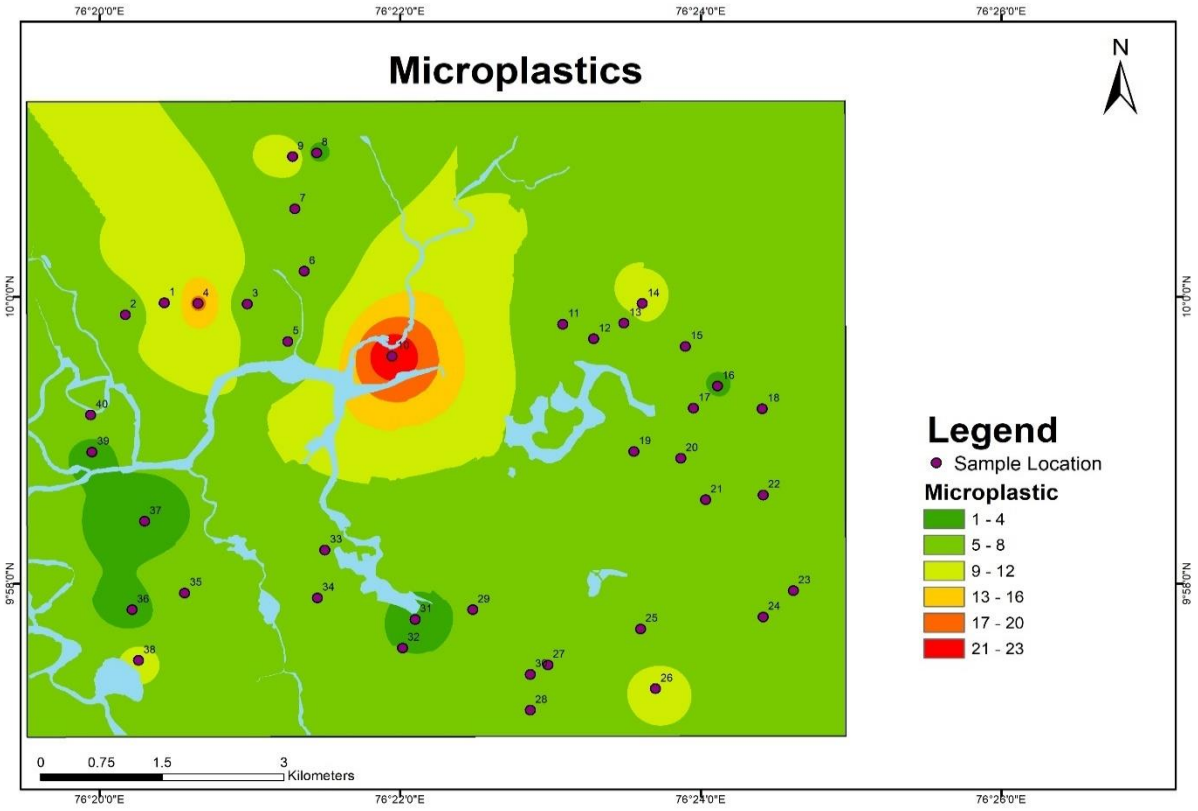

Source: Made by the author using ArcGIS

Through a comprehensive examination of the map, valuable insights can be gleaned regarding the spatial dispersion of microplastics within the designated research region. The abundance of microplastics can be ranked in decreasing order as follows: red exhibits the highest abundance, followed by orange, yellow, pale green, green, and dark green is the least abundant. Sample number 10 exhibits the highest concentration of microplastics, with the abundance reducing as the distance from the reference point (Brahmapuram) increases. The dissemination of microplastics in a given region is facilitated by the presence of rivers and groundwater. Based on the identification of Sample 10 as the Brahmapuram waste factory, it can be inferred that this particular facility serves as a significant contributor to the presence of microplastics. As we farther ourselves from the waste management facility, the level of abundance decreased.

The lithology of the study also plays a major role in the spread of microplastics. The spread from the landfill is progressing towards Northern and Eastern part compared to South-West,which accounts for the influence of clay in the South-Western part of the study area. Since clays are non-permeable layers have the least chance for the further progress of microplastics contamination. The predominant hue seen within the surveyed region is green, which serves as

an indicator of the existence of microplastic particles ranging from 5 to 8. The investigation was carried out during the pre-monsoon period, during monsoonal season the potential for contamination can observed to escalate as a result of flooding in the landfill area. Consequently, this process leads to the infiltration of microplastics into groundwater, resulting in the phenomena of bioaccumulation and biomagnification. Microplastics can infiltrate groundwater through various pathways, including surface runoff, infiltration, wastewater discharge, agricultural practises, and inadequate waste management at waste treatment facilities

CHAPTER 6

CONCLUSION

Groundwater has a crucial role in supporting several sectors such as potable water supply, agricultural practises, industrial operations, and ecological systems. Freshwater is a vital resource that offers a dependable supply of water, sustains ecosystems, and plays a crucial role in meeting our daily requirements. Consequently, it is considered a significant resource for both sustenance and economic development. The presence of microplastics in water, characterised by minuscule plastic particles with a size of less than 5 millimetres, has significant and wide-ranging implications for the ecosystem. The accumulation of these substances in aquatic ecosystems poses a hazard to marine life, as they are consumed by species and disturb the natural balance of food chains. Moreover, the escalating apprehension regarding the possible transmission of microplastics across the food chain to human beings has prompted inquiries regarding their influence on human health.

In this context, the primary objective of this study is to assess the groundwater quality and determine the occurrence of microplastics in the Brahmapuram landfill, Ambalamugal region of Ernakulam District. Ambalamukal is well recognised as one of the most prominent industrial regions in the state of Kerala. A total of forty samples were collected in the vicinity. The geological composition of the region mostly consists of laterites, clay, and charnockite as basement. The acidic character seen in the research area may be attributed to the presence of iron in laterites, orthopyroxene and feldspar in Charnockite, as well as the inadequate total alkalinity in the groundwater. Through the process of comparison, it becomes evident that there exists a direct relationship between EC and TDS. When compared to other areas within the Ambalamugal region, Brahmapuram, where the sole solid waste management plant is situated, stands out with the highest Total Dissolved Solids (TDS) value, suggesting that the area's elevated TDS levels are primarily attributable to inadequate waste management practises rather than natural factors. Therefore, the EC is also found to be increased in the Brahmapuram region. TDS is lowest in the eastern region of the study area. The observed groundwater quality limit in the study area has a similar pattern to that of surface water flows, specifically in relation to the Kadambrayar River and Chitrapuzha River. This suggests that the presence of these rivers has an impact on the TDS levels in the study area. The investigation reveals that the water

inside the study region does not meet complies to the permissible level, suggesting that it is unsuitable for consumption as drinking water.

All of the samples included microplastics. The research region contained microplastics of varied morphologies and colours. Microplastics come in a variety of colours, including black, blue, green, pink, and purple. Fibres dominated the samples. During the procedure, a total of 261 microplastics were collected. The colour black showed the most dominance. The length of microplastic varies between 2 and 401 micrometres. In our samples, the average concentration of microplastics is 6 to 7 particles per litre. Sample number 10 exhibits the highest concentration of microplastics, with the abundance reducing as the distance from the reference point (Brahmapuram) increases. The dissemination of microplastics in the given region is facilitated by the geology of the study area, rivers and groundwater. Based on the identification of Sample 10 as the Brahmapuram waste plant, it can be inferred that this particular facility serves as a significant contributor to the presence of microplastics. As we farther ourselves from the waste management facility, the level of abundance decreased. While the samples have been shown to contain microplastics, the amount of risk associated with their presence is out of scope of the present study. The investigation was carried out during the pre-monsoon period, during monsoon season the potential for contamination can observed to escalate as a result of flooding in the landfill area. Consequently, this process leads to the infiltration of microplastics into groundwater, resulting in the phenomena of bioaccumulation and biomagnification. Therefore, it enhances the odds of contamination during the post-monsoon season. This opens possibilities for further research in this area.

6.1 Recommendations

The mitigation of microplastic pollution necessitates the implementation of a comprehensive approach encompassing preventative and remedial strategies across several tiers, namely the individual, community, industrial, and governmental levels. The following are several remedial measures that can aid in the mitigation of microplastic pollution. In order to minimise the release of plastic materials into the natural environment, it is imperative to implement initiatives aimed at enhancing waste management infrastructure, improving recycling processes, and optimising disposal techniques. There is also a need to enhance the existing wastewater treatment infrastructure to more effectively catch and eliminate microplastics from effluent prior to its discharge into aquatic environments and also to institute policies aimed at mitigating littering and promoting conscientious waste management practises. It is also

important to promote the adoption of manufacturing practises within industries that prioritise the production with minimum plastic content that aim to minimise the release of microplastics. There is an essential requirement to advance the development of plastics that exhibit enhanced resistance to UV damage. These materials have the potential to be utilised in scenarios where conventional polymers are susceptible to degradation. One potential strategy for mitigating the degradation of microplastics caused by UV radiation involves implementing measures to prevent the exposure of microplastics to such radiation. It is recommended to allocate resources towards the advancement of research and development efforts aimed at the creation of novel materials that exhibit reduced susceptibility to degradation into microplastics. Developing landfill designs that effectively reduce oxygen availability inside the waste heap in order to decelerate microbial deterioration and decomposition. To mitigate environmental exposure and minimise the potential interaction between microorganisms, earthworms, and microplastics, it is crucial to employ efficient landfill cover and cap systems. These systems are designed to effectively contain garbage and prevent its dispersion into the surrounding environment. By implementing such measures, the risk of microplastics coming into contact with microorganisms and earthworms can be significantly reduced.

It is vital to facilitate community-led initiatives aimed at conducting environmental clean-up operations in coastal regions, riverbanks, and other ecologically significant locations, with the primary objective of eliminating pre-existing plastic debris. This proactive approach serves to impede the subsequent disintegration of such garbage into microplastics, thereby averting future ecological deterioration. In order to mitigate the issue of microplastic pollution caused by abandoned fishing gear, it is crucial to establish and enforce preventive measures. These measures should aim to avoid the loss and abandonment of fishing nets and lines in oceanic environments. To enhance comprehension of the dispersion, origins, and consequences of microplastics, it is imperative to engage in ongoing surveillance of their concentrations throughout various ecosystems. Utilise empirical scientific knowledge to effectively guide and shape policy-making processes. It is recommended to allocate resources towards the advancement of technological solutions aimed at the mitigation of microplastic pollution in aquatic environments. These solutions encompass the implementation of floating barriers and filtration systems to effectively capture and remove microplastics from water bodies.

REFERENCE

- Amrutha, K., & Warrier, A. K. (2020). The first report on the source-to-sink characterization of microplastic pollution from a riverine environment in tropical India. *Science of the Total Environment*, 739, 140377.
- Andrady, A. L. (2011). Microplastics in the marine environment. *Marine pollution bulletin*, 62(8), 1596-1605.
- Brennecke, D., Duarte, B., Paiva, F., Caçador, I., & Canning-Clode, J. (2016). Microplastics as vector for heavy metal contamination from the marine environment. *Estuarine, Coastal and Shelf Science*, 178, 189-195.
- Chia, R. W., Lee, J. Y., Kim, H., & Jang, J. (2021). Microplastic pollution in soil and groundwater: a review. *Environmental Chemistry Letters*, 19(6), 4211-4224.
- Drummond, W. J., Gascooke, J. R., Jones, R., Tuuri, E., & Leterme, S. C. Microplastics in Urban Freshwater Streams in Adelaide, Australia: A Source of Plastic Pollution in the Gulf St Vincent. Australia: A Source of Plastic Pollution in the Gulf St Vincent.
- Ephsy, D., & Raja, S. (2023). Characterization of microplastics and its Pollution load index in freshwater Kumaraswamy Lake of Coimbatore, India. https://doi.org/10.21203/rs.3.rs-2610640/v1
- Fackelmann, G., & Sommer, S. (2019). Microplastics and the gut microbiome: how chronically exposed species may suffer from gut dysbiosis. *Marine Pollution Bulletin*, 143, 193-203.
- Gambino, I., Bagordo, F., Grassi, T., Panico, A., & De Donno, A. (2022). Occurrence of microplastics in tap and bottled water: Current Knowledge. *International journal of environmental research and public health*, 19(9), 5283.
- Ganapathy, V. S., Radhakrishnan, K., & Prakasheswar, P. (2021). A Baseline Study On The Occurrence And Distribution of Microplastics In The Highly Polluted Metropolitan River Cooum, Chennai, India. https://dx.doi.org/10.2139/ssrn.4113873
- Gopinath, K., Seshachalam, S., Neelavannan, K., Anburaj, V., Rachel, M., Ravi, S., ... & Achyuthan, H. (2020). Quantification of microplastic in red hills lake of Chennai city, Tamil Nadu, India. *Environmental science and pollution research*, 27, 33297-33306.
- Iannilli, V., Pasquali, V., Setini, A., & Corami, F. (2019). First evidence of microplastics ingestion in benthic amphipods from Svalbard. *Environmental research*, 179, 108811.
- Katija, K., Choy, C. A., Sherlock, R. E., Sherman, A. D., & Robison, B. H. (2017). From the surface to the seafloor: How giant larvaceans transport microplastics into the deep sea. *Science advances*, 3(8), e1700715.
- Khaldoon, S., Lalung, J., Maheer, U., Kamaruddin, M. A., Yhaya, M. F., Alsolami, E. S., ... & Rafatullah, M. (2022). A review on the role of earthworms in plastics degradation: Issues and challenges. *Polymers*, 14(21), 4770.
- Konikow, L. F., & Kendy, E. (2005). Groundwater depletion: A global problem. *Hydrogeology Journal*, *13*, 317-320.
- Kumar, R., Sharma, P., Manna, C., & Jain, M. (2021). Abundance, interaction, ingestion, ecological concerns, and mitigation policies of microplastic pollution in riverine ecosystem: A review. *Science of The Total Environment*, *782*, 146695.

- Kumar, R., Singh, R. D., & Sharma, K. D. (2005). Water resources of India. *Current science*, 89(5), 794-811.
- Li, H., Lu, X., Wang, S., Zheng, B., & Xu, Y. (2021). Vertical migration of microplastics along soil profile under different crop root systems. *Environmental Pollution*, *278*, 116833.
- Li, P., Karunanidhi, D., Subramani, T., & Srinivasamoorthy, K. (2021). Sources and consequences of groundwater contamination. *Archives of environmental contamination and toxicology*, *80*, 1-10.
- Manh, D. T., Tuan, P. M., Thom, D. T., & Van Manh, D. (2022). Microplastics occurrence in groundwater of Da Nang City, Viet Nam. *Vietnam Journal of Science and Technology*, 60(5B), 39-49.
- Moore, C. J. (2008). Synthetic polymers in the marine environment: a rapidly increasing, long-term threat. *Environmental research*, 108(2), 131-139.
- Morris, B. L., Lawrence, A. R., Chilton, P. J. C., Adams, B., Calow, R. C., & Klinck, B. A. (2003). Groundwater and its susceptibility to degradation: a global assessment of the problem and options for management. *United Nations Environment Programme. http://www.unep.org/dewa/Portals/67/pdf/Groundwater_INC_cover.pdf*
- Mu, H., Wang, Y., Zhang, H., Guo, F., Li, A., Zhang, S., ... & Liu, T. (2022). High abundance of microplastics in groundwater in Jiaodong Peninsula, China. *Science of the Total Environment*, 839, 156318.
- Natesan, U., Vaikunth, R., Kumar, P., Ruthra, R., & Srinivasalu, S. (2021). Spatial distribution of microplastic concentration around landfill sites and its potential risk on groundwater. *Chemosphere*, 277, 130263.
- Oßmann, B. E., Sarau, G., Holtmannspötter, H., Pischetsrieder, M., Christiansen, S. H., & Dicke, W. (2018). Small-sized microplastics and pigmented particles in bottled mineral water. *Water research*, 141, 307-316.
- Othman, A. R., Hasan, H. A., Muhamad, M. H., Ismail, N. I., & Abdullah, S. R. S. (2021). Microbial degradation of microplastics by enzymatic processes: a review. *Environmental Chemistry Letters*, *19*, 3057-3073.
- Padervand, M., Lichtfouse, E., Robert, D., & Wang, C. (2020). Removal of microplastics from the environment. A review. *Environmental Chemistry Letters*, *18*, 807-828.
- Patterson, J., Jeyasanta, K. I., Sathish, N., Edward, J. P., & Booth, A. M. (2020). Microplastic and heavy metal distributions in an Indian coral reef ecosystem. *Science of the Total Environment*, 744, 140706.
- Pavithran, V. A. (2021). Study on microplastic pollution in the coastal seawaters of selected regions along the northern coast of Kerala, southwest coast of India. *Journal of Sea Research*, 173, 102060.
- Radhakrishnan, K., Sivapriya, V., Rajkumar, A., Akramkhan, N., Prakasheswar, P., Krishnakumar, S., & Hussain, S. M. (2021). Characterization and distribution of microplastics in estuarine surface sediments, Kayamkulam estuary, southwest coast of India. *Marine Pollution Bulletin*, 168, 112389.
- Raza, M., Lee, J. Y., & Cha, J. (2022). Microplastics in soil and freshwater: Understanding sources, distribution, potential impacts, and regulations for management. *Science Progress*, 105(3), 00368504221126676.
- Redwan, M., Moneim, A. A. A., Mohammed, N. E., & Masoud, A. M. (2020). Sources and health risk assessments of nitrate in groundwater, West of Tahta area, Sohag, Egypt. *Episodes Journal of International Geoscience*, *43*(2), 751-760.

- Reed, S., Clark, M., Thompson, R., & Hughes, K. A. (2018). Microplastics in marine sediments near Rothera research station, Antarctica. *Marine pollution bulletin*, 133, 460-463.
- Saeed, M. S., Fahd, F., Khan, F., Chen, B., & Sadiq, R. (2023). Human health risk model for microplastic exposure in the Arctic region. Science of The Total Environment, 895, 165150.
- Scircle, A., & Cizdziel, J. V. (2019). Detecting and quantifying microplastics in bottled water using fluorescence microscopy: A new experiment for instrumental analysis and environmental chemistry courses. *Journal of Chemical Education*, 97(1), 234-238.
- Selvam, S., Jesuraja, K., Venkatramanan, S., Roy, P. D., & Kumari, V. J. (2021). Hazardous microplastic characteristics and its role as a vector of heavy metal in groundwater and surface water of coastal south India. *Journal of Hazardous Materials*, *402*, 123786.
- SK, A., & Varghese, G. K. (2020). Environmental forensic analysis of the microplastic pollution at "Nattika" Beach, Kerala Coast, India. *Environmental forensics*, 21(1), 21-36.
- Srihari, S., Subramani, T., Prapanchan, V. N., & Li, P. (2022). Human health risk perspective study on characterization, quantification and spatial distribution of microplastics in surface water, groundwater and coastal sediments of thickly populated Chennai coast of South India. *Human and Ecological Risk Assessment*, 29, 1-12.
- Sruthy, S., & Ramasamy, E. V. (2017). Microplastic pollution in Vembanad Lake, Kerala, India: the first report of microplastics in lake and estuarine sediments in India. *Environmental pollution*, 222, 315-322.
- Subba Rao, N., Ravindra, B., & Wu, J. (2020). Geochemical and health risk evaluation of fluoride rich groundwater in Sattenapalle Region, Guntur district, Andhra Pradesh, India. Human and ecological risk assessment: An international journal, 26(9), 2316-2348.
- Sun, K., Song, Y., He, F., Jing, M., Tang, J., & Liu, R. (2021). A review of human and animals exposure to polycyclic aromatic hydrocarbons: Health risk and adverse effects, photo-induced toxicity and regulating effect of microplastics. *Science of The Total Environment*, *773*, 145403.
- Vaid, M., Mehra, K., & Gupta, A. (2021). Microplastics as contaminants in Indian environment: a review. *Environmental Science and Pollution Research*, 28, 68025–68052.
- Valsan, G., Warrier, A. K., Amrutha, K., Anusree, S., & Rangel-Buitrago, N. Microplastics in Subterranean Estuaries: The Karnataka Coast, Southwest India, as a Case Study. Southwest India, as a Case Study. https://dx.doi.org/10.2139/ssrn.4332426
- Van Cauwenberghe, L., Devriese, L., Galgani, F., Robbens, J., & Janssen, C. R. (2015). Microplastics in sediments: a review of techniques, occurrence and effects. *Marine environmental research*, 111, 5-17.
- Varshini, D. S., Ramesh, K., & Srinivasamoorthy, K. (2021). A Preliminary Study on Microplastic Occurrences in Surface Waters of Ousudu Lake, Pondicherry, India. *International Journal of Civil, Environmental and Agricultural Engineering*, 3, 35-48.
- Verla, A. W., Enyoh, C. E., Verla, E. N., & Nwarnorh, K. O. (2019). Microplastic–toxic chemical interaction: a review study on quantified levels, mechanism and implication. *SN Applied Sciences*, 1(11), 1-30.
- Wong, J. K. H., Lee, K. K., Tang, K. H. D., & Yap, P. S. (2020). Microplastics in the freshwater and terrestrial environments: Prevalence, fates, impacts and sustainable solutions. *Science of the total environment*, 719, 137512.

- Wright, S. L., & Kelly, F. J. (2017). Plastic and human health: a micro issue?. *Environmental science & technology*, 51(12), 6634-6647.
- Wu, B., Li, L. W., Zu, Y. X., Nan, J., Chen, X. Q., Sun, K., & Li, Z. L. (2022). Microplastics contamination in groundwater of a drinking-water source area, northern China. *Environmental Research*, 214, 114048.
- Yona, D., Sari, S. H. J., Iranawati, F., Bachri, S., & Ayuningtyas, W. C. (2019). Microplastics in the surface sediments from the eastern waters of Java Sea, Indonesia. *National Library of Medicine*, F1000Research, 8.

DATING PRE-AND POST-OCEAN DISAPPEARANCE EVENTS ON MARS USING CRATERSTAT

A dissertation submitted in partial fulfilment for the award of Degree of

MASTER OF SCIENCE

In

APPLIED GEOLOGY

By

KARTHIKA J.H.

(Register. No. CCAVMAG011)

Pursued in

Under the guidance of

Dr. SAJIN KUMAR K.S.

Assistant Professor, Department of Geology

University of Kerala, Karyavattom, Thiruvananthapuram

To

DEPARTMENT OF GEOLOGY AND ENVIRONMENTAL SCIENCE

CHRIST COLLEGE (AUTONOUMOUS), IRINJALAKUDA, KERALA

(Affiliated to Calicut University and re-accredited by NAAC with A++ grade) 2021-2023

CERTIFICATE

This is to certify that the dissertation entitled- **'Dating Pre-and Post Ocean disappearance events on Mars using Craterstat'** is a bonafied record of work done by Ms. Karthika J.H. (Reg.No. CCAVMAG011), M.Sc. Applied Geology, Christ College (Autonomous), Irinjalakuda under my guidance in partial fulfilment of requirements for the degree of Master of Science in Applied Geology during the academic year 2021-2023.

Ivine Joseph
Internal Supervisor

Dr. Anto Francis K.
Coordinator Geology (S)
Christ College (Autonomous), Irinjalakuda
Kerala - 680125

Place: …….

Date: ……..

External Examiners:

1……..

2……..

DECLARATION

I, Karthika J.H., hereby declare that the dissertation entitled "**Dating Pre-and-Post Ocean Disappearance Events on Mars using Craterstat"** is an authentic record of study and research work carried out by me, under the supervision and guidance of Dr. Sajin Kumar K.S., Assistant Professor, Department of Geology, University of Kerala, Thiruvananthapuram, in partial fulfilment of requirement for the award of the degree of Master of Science (M.Sc.) in Applied Geology of Calicut University, and that no part of this project work has been presented earlier for any degree or diploma in this or any other universities.

KARTHIKA J.H.

Reg. No: CCAVMAG011

ACKNOWLEDGEMENT

In the first place, I thank God Almighty greatly, by whose grace I'm able to complete this work.

I place my earnest thanks to **Dr. Sajin Kumar K.S, Assistant Professor**, **Department of Geology, University of Kerala, Trivandrum**, who guided and encouraged me with his constant support, guidance and suggestions throughout the programme to make it a great success.

I have the honour to extend my deep sense of gratitude to **Dr. E. Shaji, Associate Professor and Head, Department of Geology**, **University of Kerala**, for allowing me to do my dissertation work in this esteemed institute.

I would like to take this opportunity to express my deepest gratitude to, **Dr.Linto Alappat**, Dean of Research and Development of TLC (former HOD) Department of Geology and Environmental Science, Christ College(Autonomous) Irinjalakuda, **Dr. Anto Francis. K**, **Co-Ordinator**, Department of Geology and Environmental science, Christ College (Autonomous) Irinjalakuda,and **Mr. Tharun R.** Head of Department of Geology and Environmental Science, Christ College (Autonomous).

I express my sincere gratitude to **Ms. Ivine Joseph, Assistant Professor**, Dept. of Geology, Christ College (Autonomous), Irinjalakuda, who guided me internally for completion of my work. I also thank other faculty members of the department for their continuous support and encouragement.

I would like to acknowledge the Research Scholars, **Ms. Sadeeda Marjan.T, Ms. Devika Padmakumar and Mr. Rajaneesh. A**, Department of Geology, University of Kerala, for their advice and valuable guidance.

Last, but not the least, I would like to show my sincere gratitude to my parents for their sustained prayer, financial and moral support in the completion of my work.

I take this opportunity to thank my friends and classmates and all those who have directly and indirectly contributed their time, material and encouraged me during the course of my investigation.

KARTHIKA. J.H.

CONTENTS **Page no:**

LIST OF ABBREVATIONS

LHB	Late Heavy Bombardment
VBF	Vastitas Borealis Formation
CRISM	Compact Reconnaissance Imaging Spectrometer for Mars
CSV	Comma Separated Values
DIAM	Digital Imaging Adoption Model
JMARS	Java Mission-planning and Analysis for Remote Sensing
GIS	Geographical Information System
GEL	Global Equivalent Level
SFD	Size Frequency Distribution
Ga	Giga annum
yr.	year
km	kilometre

LIST OF FIGURES

ABSTRACT

The geologic history of the northern lowlands of Mars has been strongly debated, specifically, the Martian Ocean. Several hypotheses on the occurrence of ocean had been delineated by researchers, yet not with full clarity. In this work, we deal with the pre- and post-events of Martian Ocean and its disappearance from the northern lowland, mainly through dating denuded and fresh impact craters using Craterstat software. The geologic history of planetary surface can qualitatively and quantitatively be defined by crater counting method, that describes absolute ages and relative ages. We consider fresh craters of different diameter from the planitias of northern lowlands. Here, a comparison between two events had done to understand the time of existed ocean and its vaporisation. Formation of volcanic features, lava plains and resurfacing factors made considerable changes in production function in the Craterstat. This comparison will help to perceive the geologic history of the Martian Ocean. Studies suggest that the formation of ocean took place in the Hesperian period. Our studies on the ages of the northern Planitia implies also concur to the formation age of ocean in the Hesperian period and its vaporisation during the end of Hesperian. But if any Amazonis Ocean existed, then the crater counting on this surface will give more precise age of ocean evaporation, as few resurfacing occurred on this Planitia.

CHAPTER I

1. INTRODUCTION

Mars is the fourth planet from the Sun – a dusty, cold desert with a very thin atmosphere. It is considered as the second smallest planet in the Solar System having a mean radius of 3,389.5 km and gravity about 3.72 m/s^2. Mars had formed 4.5 billion years ago. The planet is seen in red colour due to the presence of finely grained iron (III) oxide, were it is also called as 'Red Planet'. Mars is a dynamic planet having different seasons, polar ice caps, canyons, extinct volcanoes and evidences suggesting that this planet was very much active during the past. Everything in the planet had changed over time, while looking at its history we can interpret its evolution in various region – surface, ocean, rivers, valleys and several others. The planet faced many impact phenomena and resurfacing events in its geological time period. Mars is found highly differential in its hemispheres – southern part is seen as heavily cratered while northern land is noticed as very smooth and gentle. All these factors make Mars a mysterious planet.

1.1 FORMATION OF MARS

It is believed that the formation of the Mars took place 4.5 billion years ago where gravity pulled the churning dust and hot gases which eventually condensed to form the fourth planet of our planetary system. Like Earth, Mars is composed of an outer crust, a silicate mantle and an inner liquid core (Carr and Head III (2010).

The geologic timescale of Mars includes following periods:

- Pre-Noachian Period: Formed about 4.5 Ga. Characterised by large impact basin - Hellas basin, dichotomy formation and expected to have magnetic field. But most of the evidence was erased by high impacts and erosion.
- Noachian Period: Formation of oldest enduring surface of Mars, 4.1 to 3.7 Ga. It is marked by large impact craters and accumulation of Tharsis – a volcanic upland. Named after Noachis Terra.

- ❖ Hesperian Period: formed between 3.7 to 3 Ga, marked by extensive lava plains and enhanced Tharsis growth. Named after Hesperian Planum.
- ❖ Amazonian Period: 3 Ga to present, identified by only few crater impacts. Named after Amazonis Planitia.

1.2 SURFACE OF MARS

Mars is a terrestrial planet. The character of the Martian terrain has been well established from spacecraft photography and altimetry. As it contains two hemispheres – northern and southern hemisphere. The northern hemisphere is appeared to be smoother and flatter than the southern hemisphere. Martian dichotomy is the most conspicuous feature of Mars, which is a sharp contrast between the northern and the southern hemisphere and was thought to be formed by the Late Heavy Bombardment (LHB). The northern hemisphere is flattened by lava flows whereas southern hemisphere is specified by cratered highlands.

Result from the Mars Exploration Rover and from the spectrometers on orbiting spacecraft show that the ancient highlands are compositionally distinct from the younger plains. The rocks on the plains are mostly typical basalts with only thin alteration rinds high in sulphur, chlorine and other volatile elements. The plains consist mostly of primary, unaltered basaltic minerals such as olivine and pyroxene. In contrast, alteration minerals such as clays are common throughout the ancient cratered terrain. The results indicate that surface conditions changed dramatically around 3.7 billion years ago.

Fluvial activity initiated at the end of Noachian period, most of the ancient cratered terrains were dissected by dry valleys and formed slow erosion by running water. These valleys ended up in northern plains and showed the presence of layered deposit of lakes, deltas and several other fluvial features. These valleys further eroded to form outflow channels, which is believed to be ended up as ocean in the northern lowlands. Valles Marineris, formed by faulting followed by erosion, is the Grand Canyon of Mars, which is the largest canyon on the solar system. Most of the fluvial channels terminate at Chrysae Planitia, a smooth circular plain in the northern equatorial region of Mars. The canyons of Valles Marineris culminate to the west of the Tharsis rise, where the largest volcano of the solar system, Olympus Mons, is found.

1.3 ATMOSPHERE AND CLIMATE

Earlier, the climate of Mars had warm surface conditions and a dense atmosphere with high carbon dioxide content and water, with secondary greenhouse gases. Now the condition is reversed, the atmosphere become less dense mainly due to high impact rates and volcanic eruptions. The climate of Mars is similar to earth due to similar tilt of two planets' rotational axes. Length of the season is twice that of the earth as it is greater distance from the Sun (Lewis, S. et al. 1999). The climate gradually changed to cold and dry conditions, when the planet began to lose its atmosphere. Due to lack of magnetosphere, there had a direct influence of solar wind which affected the Martian atmosphere. Mars contain 96% of CO_2, 1.93% of Ar along with the traces of oxygen and water. The temperature ranges from -110ºC to 35ºC. The Martian atmosphere is quite dusty and had a pink hue due to iron (III) oxide particles suspended on it (Zurek R. et al. 1992).

1.4 STUDY AREA

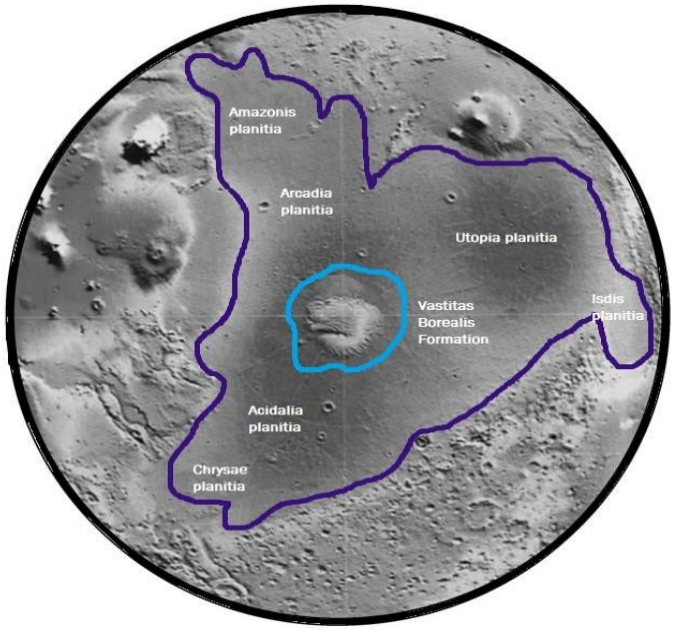

Figure:1, Northern hemisphere of Mars, showing different planitias of Martian Ocean, is taken as the study area for dating pre-and post-ocean disappearance events.

The area under investigation is the northern lowland, were Martian Ocean existed (Fig:1). There were several hypotheses regarding the origin of the northern ocean. For the purpose of

measuring the crater size-frequency distribution, we chose typical type regions giving special focus on different planitias on the northern plains. They include – Chrysae Planitia, Arcadia Planitia, Acidalia Planitia, Utopia Planitia, Isdis Planitia, Vastitas Borealis Formation and Amazonis Planitia. Studies imply that these planitias were formed during different geologic events. Surface morphologies and their evolutionary history of these regions can affect the crater size frequency distribution. Different regions of this planitias are densely cratered while other regions are sparsely cratered. Selecting the craters with specified morphologic characters can give accurate ages of the northern ocean. The age obtained from the crater count can be used to compare the time of ocean occurrence and their vanishing period.

1.5 OCEAN HISTORY OF MARS

Primarily, the Martian timescale can be divided into three periods – Noachian, Hesperian and Amazonian on the basis of crater impacts. The base of the Noachian period is marked by pre-Noachian basement, formed about 4.5 Ga when the planet differentiated into crust, mantle and core. Probably global dichotomy formed earlier. Only Hellas basin can be noticed from this period whereas other evidences were wiped out due to heavy impacts and high erosion. Studies suggest that earlier Mars had a magnetosphere that got abated due to meteorite bang on the Martian surface and the large impact basins that formed would have had devastating environmental effects.

The Noachian period (4.1 – 3.8 Ga) initiated with high cratering, valley formation, erosion and accumulation of most of Tharsis (Ivano 2001). Crater density ranged about >100 km in diameter. Ejecta from the crater influenced the hydrothermal activity around the impact sites. Noachian crater (500 – 1000 km in diameter) formed ejecta of 300 m which depends on the impact of the crater (Storm et al. 1992 and Segura et al. 2002). Formation of Tharsis also affected the Martian lithosphere. Noachian volcanism also enhanced the formation of the Utopia Planitia, which is the largest recognised impact basin in the Solar system. On comparing the Noachian craters with Hesperian craters, it is found that the Noachian craters are deformed by high and active sedimentation rate, having eroded rims and partially filled interiors. Valley networks were formed, groundwater sapping was common, craters were filled with water and the evaporation indicated the presence of Cl deposits (Carr, 01 June 2001). Open basin lakes were found in the Argyre basin; flood was rare. Presence of surface runoff patterns and open

basin lakes indicate episodic precipitation and warm surface conditions. Noachian is evident for the warm periods indicating there may had an ocean, which is controversial. If such ocean existed, then its evidence may be erased by erosion and burial (Craddock and Howard, 2002). So, if Noachian period had water, then it contained a warm and dry condition. Geomorphic evidence of lakes and rivers, groundwater movement and Cl rich deposits in lows indicate warm condition. Crater impact and volcanism enhanced precipitation i.e., large impact would heats up the Martian surface. At the end of the Noachian, climate changed, formed thick cryosphere and is uncertain (Carr, 2006).

Hesperian Period (3.7 – 3Ga) is characterised by low rate of valley formation and erosion, formation of extensive lava plains by volcanism, canyons, outflow channels which eventually terminate to sea or lakes (Carr, 01 June 2001) . Volcanism is evident mainly in the form of ridged plains and was widespread in Hesperian and resulted in resurfacing 30% of the planet (Kreslavsky and Pratt, 2002). Outflow channels were not formed by immediate precipitation but by the rapid release of large volume of stored water (Tanaka et al. 2005) and these water sources may be trapped below the cryosphere. Flood can be developed when the confined aquifer under the great pressure below the cryosphere burst out. Presence of dykes, melting or cracking of cryosphere can supply water i.e., large groundwater eruption is rare in Noachian due to absence of thick cryosphere. This groundwater eruption changed the surface condition and lead to the growth of thick cryosphere at the end of Noachian, thus valley formation declined. At the end of the Hesperian, water depleted below the cryosphere. Hesperian period is marked by the formation of Valles Marineris (Sharp, 1973) that caused flood and temporary presence of large bodies of water in northern plains. Increased atmospheric concentration of volcanically degassed SO_2 and H_2S account for the presence of liquid water in Noachian – Hesperian. Later, SO_2 was rapidly removed and changed the atmospheric condition and temperature dropped and formed the cryosphere. The fate of water is uncertain, but much of it has been transported to polar cold traps (Head and Pratt, 2001).

Amazonian period (3 Ga to present) constitutes very few impact craters, volcanism and tectonism. Erosion continued from Hesperian but in a low rate. Action of wind and ice was more evident. Volcanism formed numerous primary volcanic structures (Wilson et al. 2001). Ice is being observed above 60ºlatitude. Ice deposits were left in the low areas after large Hesperian floods. Crater count indicate that ice has been occurring at least for several 100 million years. As this ice could have been deposited at early Hesperian, as a consequence of

large floods or surface condition at the end of Noachian. Outflow channels ended at the end of Hesperian, only few valleys and channels were found. Gullies were present, those are formed by the temporary melting of mid latitude snow or ice (Malin and Edgett, 2001). Determining the age of gullies is difficult due to their smaller area. From the recent studies it is noted that aeolin processes and dust activities were dominant in the Martian surface. Mars' molten core began to cool down, due to high action of solar wind, it began to lose its water and atmosphere, eventually the remaining water condensed to form ice. In time, Mars become cold and dead planet (Carr and Head III, 2010).

Today, the state of the planet is solid, rocky and hyperarid. It has got a thin layer of active atmosphere, but the surface of the Mars' is not active, as the volcanoes are almost dead. Over the years, there were many spacecraft missions accomplished by scientist since 1970s. NASA has sent five robotic vehicles, called rovers to Red Planet – Sojourner, Spirit, Opportunity, Curiosity and Perseverance. The main objective is to study the surface of Mars, ancient habitability and potential for life. These researches are conducted to get a fix on the ancient and the latest activity undertaking the whole planet. A hypothetical procedure has been introduced 'Terraforming of Mars' which has a goal on transforming the planet from hostile environment to tellurian sphere to sustain the lifeforms.

1.6 NORTHERN LOWLANDS OF MARS

The northern lowlands, also called northern plains, is a smoother plain and younger in age (Parker and Bills, 2021), and holds geologic history of Mars and is separated from the southern highlands by a crustal dichotomy. It has an elevation of 5 km lower than the southern cratered highlands and have a thin crust of 30-40 km, whereas highlands have 60-70 km thickness. It preserves long-term geologic record of Mars – heavily cratered Noachian basement, Hesperian flow channels and Amazonian surface. It is believed that the effects of Late Heavy Bombardment resurfaced the northern plain of the planet, which occurred between 4.1 to 3.8 billion years ago. The stratigraphy of northern lowland is dominated by : Noachian-aged remnants, old degraded crater rims, a collection of domes interpreted to be old degraded Noachian crust, the Hesperian-aged Vastitas Borealis Formation, an unusual unit interpreted to be degraded lava flows and sediments, Hesperian-aged outflow channel deposits at the margins of the lowlands in Chryse Planitia, various local Amazonian-aged plains units, Elysium channel

and flow deposits, the north polar cap, consisting of Late Amazonian ice and layered terrain deposits, and Amazonian-aged circumpolar mantling material (Alberto.G.Fairen & James M Dohm, April 2004).

The northern lowland has fewer craters when compared with the southern highlands. The number of craters in the lowlands indicates, most of the surface is Upper Hesperian or younger in age. Presence of low hills in the plains represents the remnants of large craters that were formed during the Noachian age. Subdued craters were common, these depressions overlie the ancient craters, where it is covered by the northern plain deposits. Low regions of the northern lowlands were compared with Earth's abyssal plain, as they are flat and smooth in nature. The flattest region on the plain is the Amazonis Planitia, containing young lava flows and volcanic deposits. The lowlands are highly textured in nature as they show – pitted cones, polygonal cracks (James.C.Pechmann, May 1980), wrinkle ridges, thumbprint terrains, curvilinear ridges and degraded impact craters. Formation of these features indicates the floors of northern plain were once tectonically active site. Wrinkle ridges are mainly formed by tectonic activity, were the lava cools and solidify to shape the ridges. Thumbprint terrain of the northern plains of Mars may be caused by differential solution of large carbonate deposits occupying low-lying areas. Polygonal fractures result due to desiccation and compaction of sediments deposited in water bodies that formed at the end of channels (Fig:2). Igneous and mud volcanism process triggered the formation of pitted cones in the northern region of Mars. Curvilinear ridges can be formed by the action of fluvial and volcanic processes (Smith et al. 1998). By analysing these facets, we can say that, northern lowlands of Mars were highly active during the past (Parker and Bills, 2021).

a) 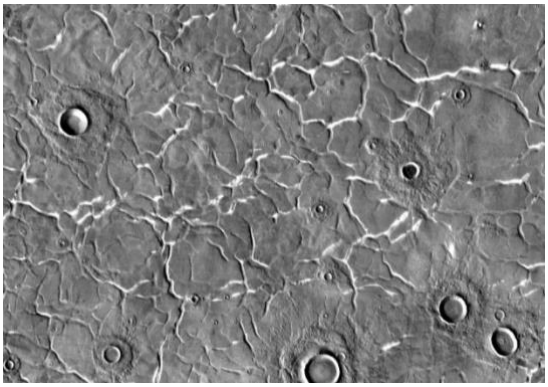 b) 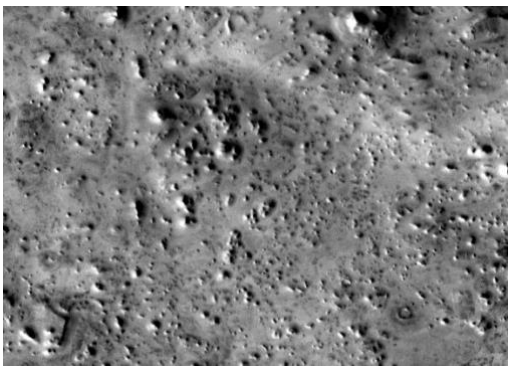

c) 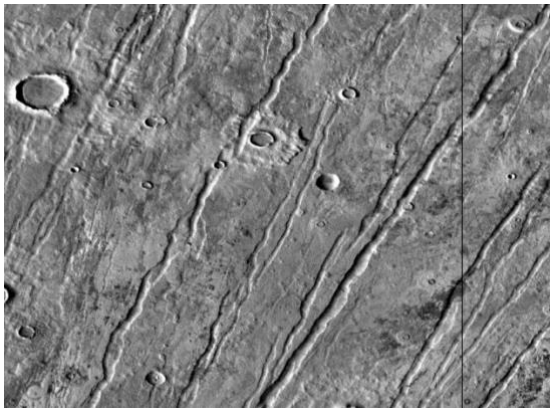 d) 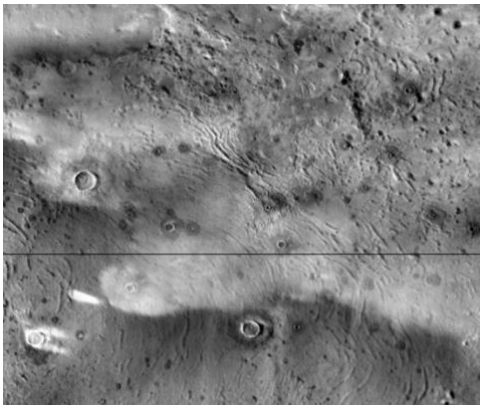

Figure:2, The figure representing different surface features on the Martian lowland. a) polygonal terrain, b) knob structure, c) ridges, d) thumbprint terrain

To understand more details about the northern plains, CRISM images associated with impact craters are surveyed. Impact craters can excavate subsurface materials and expose them within the crater central peak or ring structure, crater walls, ejecta blanket, and on the crater floor, making it possible for us to access the subsurface stratigraphy to varying degrees using orbital data. Craters of different sizes may expose distinctive mineralogy in the ejecta and reveal the depths of subsurface units by physical constraints on the maximum excavation depth (Nadine G. Barlow, 2010). Central peaks of large complex craters sometimes expose the deepest stratigraphy brought to the surface by the impact. Inverted flaps exposed on the crater walls access the shallow subsurface. Thus, the geologic context of hydrated mineral detections must be examined to understand their origins. Through analyses of the origins of detected minerals in craters and their association with impact crater size and morphology, it will be able to construct the basic stratigraphy, constrain scenarios for lowland-wide evolution, discover region-specific geology that was previously unknown, and unravel the buried record of geologic and aqueous activity within the northern lowlands of Mars.

It is known that the northern plains are relatively smooth and flat. Many outflow channels from the highlands terminate at the lowlands, indicating that this region once hold an open body lake or ocean. Outflow channel activity was peak during Hesperian age, along with the formation of Valles Marineris, which created intense flood. All these channels, valleys, deltas, lakebeds ended up in the vast northern plain. Gullies and slope lineage along with cliffs and crater walls suggest that the flowing water shaped the surface of Mars. So, we can say that this plain had an ocean during the past. There are also some heavy craters – Pohl and Lomonosov, that created

mega tsunami and Martian flood about 3.4 billion years ago. Thus, Hesperian period was highly active during the geologic history of Mars and had a warm condition. But where does all this water went?

1.7 WATER ON MARS

Today there is no large standing body of water existing on the planet and is found as ice at the poles. Earlier 1/3rd of the planet was covered with ocean (Robert et al. 2000). Development of water on Mars can be associated with atmosphere. Pre-Noachian (4.5 to 4.1 Ga) contained a dense atmosphere which was reduced to 60% by meteoritic impact. In the Noachian age, a secondary atmosphere, was formed by the outgassing of the Tharsis volcanoes that significantly formed the H_2O, CO_2 and SO_2. This period was warmer in nature and leads to precipitation and valley formation. The end of this period coincides with the termination of the internal magnetic field and a spike in meteoritic bombardment. The cessation of the internal magnetic field and subsequent weakening of any local magnetic field allowed unimpeded atmospheric stripping by the solar wind. Along with the solar wind, crater impacts also affected the atmosphere. From Hesperian to Amazonian (3.7 Ga to present) was marked by the sporadic outgassing events that leads to warm and wetter periods, also followed by interglacial periods. During Amazonian, the atmosphere becomes dry and arid, forming ice at the polar regions of the planet. When the planet undergoes episodic warming, these ice melts and carve the valley networks located at the lower elevation. This warming occurs by volcanism, impacts or CH_4 burst. It should be noted that all episodic events do not generate water on Mars (MaCauley et al. 1972, Milton 1973). The current environment at the Martian surface is dry, probably presenting an insuperable obstacle for living organism. Mars lack thick atmosphere, ozone layer and magnetic field, allowing the solar and cosmic radiation to strike the surface, which are the prime limiting factor on the survival on life on Mars (Baker et. al, 2001).

1.8 MARTIAN OCEAN

According to the Mars Ocean theory, an ocean of liquid water covered over a third of Mars' surface early in the planet's geologic history. The northern hemisphere basin Vastitas Borealis, which is located 4-5 km below the mean planetary elevation, would have been filled with this ancient ocean, between 4.1 and 3.8 billion years ago. Geographical characteristics that

resemble ancient shorelines and the chemical composition of the Martian soil and environment provide evidence for the existence of this ocean. To maintain liquid water at the surface, early Mars would have needed a denser atmosphere and a warmer temperature (Maria.T.Zuber, 28 March 2018).

Pictures taken by Mariner 9 in 1969 showed outflow canals that may transport water into the northern lowlands. These lowlands, known as Vastitas Borealis, appeared to have developed beneath an ocean because they were flat and smooth. Additionally, it was discovered that the channels' age and Vastitas Borealis' age were comparable. It was therefore reasonable to suppose that massive outflow channels provided the water needed to create an ocean that covered one third of the planet.

The Vastitas Borealis Formation material appears to be covering the northern lowlands, where the ocean formerly lay. Since many of these craters appeared to be covered by some form of deposit on the ocean floor, they were sometimes referred to as ‘stealth’ craters. This deposit could be made up of elements that have been eroded from the outflow channels. The Vastitas Borealis Formation's volume and the amount of eroded material from the channels are practically identical, providing evidence for this link. Additionally, more water was needed than would be in a Martian Ocean for the development of Mars' valley networks, outflow channels, and delta deposits. This suggests that there was enough water present to support an ocean. A group of scientists set out in 2009 to determine the precise number of stream channels that existed on Mars. They created a computer programme to look at topographical information. The programme searched for U-shaped structures since water-carved channels would often have that shape. They discovered several other channels, and in some locations the density of the valleys was comparable to that of the Earth. The planet's high channel density makes rain possible. It’s possible that a sizable ocean was required to produce enough moisture for rain. The distribution of several waterways throughout the planet might be attributed to a northern ocean. For instance, valleys tend to get shallower in the south, maybe as a result of their distance from the ocean. Also, it appears that valleys have a southern limit beyond which less water from a northern ocean may be transported.

1.8.1 Size of the Ocean

The extent of an ancient ocean on Mars has been estimated differently by several experts. The ocean volume is comparable to the amount of water required to carve many canals on Mars, therefore many of these estimations are acceptable in this regard. All of the water in the ocean might therefore be contained in the planet. Regarding the size of the ocean, there is disagreement. Two distinct shorelines were first suggested – Arabia and Deuteronilus shoreline (Citron, Hemingway and Manga, 2018). The size of the ocean can be determined by the shoreline extension. Arabia contact is found to be older than Deuteronilus, also the areas of Arabia shoreline had deformed by Tharsis growth and other geological events. Deuteronilus contact is found more prominent in the Chrysae region. Since there are much less height fluctuations along the beach, the shoreline of the smaller ocean seems more believable. The ocean's volume was formerly estimated to be 19,000,000 km^3 (1.9 X 107). This amount of water would cover the whole planet in 130 metres. The highest estimate for the size of the ocean is 23,000,000 km^3 (2.3 X 107) or 156 metres GEL.

1.8.2 Source of water

Today Mars is extremely arid and chilly. Many people think that there was once more carbon dioxide in the atmosphere, which would have made it much thicker and led to global warming. But long-term climate change models suggest that Mars may have always been a frigid, dry place. The fact that the sun wasn't much intense is a significant factor. Perhaps it was seldom above the freezing on average. If so, several channels on Mars may have created during much localised, brief events, such as impacts or volcanic activity. Today, we mostly accept the theories put forward in a lengthy study by Clifford (2001), who suggested that the planet was encircled by a thick layer of ice known as a cryosphere. It is anticipated that there are hundreds of metres of GEL in this frozen cryosphere. Water in the Mars froze to the base of this ice sheet as the planet cooled, forming an aquifer under intense pressure. Then, presumably as a result of an asteroid impact breaking the cryosphere, the water in the aquifer was abruptly released. Great outflow canals were formed by enormous, catastrophic floods that emerged from chaotic areas and brought water to a northern ocean.

1.8.3 Fate of water

The water would first freeze. The ice would have eventually sublimated—that is, converted into a gas—into the thin, chilly atmosphere of Mars. The vaporised water would have moved to the poles, where it would have melted the ice caps' bases and frozen into the cryosphere. The

ice, however, may have persisted for a very long period if dust had covered it. The ice caps, also known as the stratified polar deposits, are the source of the most water at this time. They barely account for 25 m of GEL, according to scientists. 17–22 m of GEL are the most recent estimations. It could, however, be smaller given that radar measurements from orbit have determined that the northern cap has just 821,000 km^3, or less than 6 m GEL (Carr, 2003).

1.8.4 Water lost to space

Recent advances in our understanding of the Martian atmosphere are very important in helping us to understand where the water went. In essence, several processes caused the majority of the atmosphere and water to be lost into space. The ratio of molecular hydrogen to deuterium measured in the upper atmosphere of Mars in 2001 revealed a rich water supply on primaeval Mars that has since been destroyed. A hefty, uncommon isotope of hydrogen is deuterium. Being heavier, it tends to remain for a longer period of time. A 2015 study on water and deuterium led to the conclusion that Mars had lost the same amount of water similar to the quantity of the Arctic Ocean. This finding was made by comparing the water-to-deuterium ratio in the current Martian atmosphere to the ratio observed on Earth and obtained from telescopic observations. Deuterium is eight times more concentrated in the polar regions of Mars, according to telescopic measurements made from the Earth, indicating that Mars formerly had far more water. Additionally, dust storms enhance water loss. The Mars Reconnaissance Orbiter analysis of dust storms suggests that dust storms may have contributed 10% of the water loss from Mars. Water vapour is carried to extremely high altitudes by dust storms, where it can be dissociated by UV radiation from the Sun, by the process called photodissociation. The hydrogen in the water molecule then travels to the universe (Jakosky et al. 2018).

1.9 EVIDENCE OF MARTIAN OCEAN

Scientists was suspected for decades that ancient Mars was much warmer, wetter environment, but estimates of how much water Mars has lost over its four and half billion-year history vary widely. Researchers have made the best estimate to date by measuring the atmospheric ratio of normal to heavy water molecules near the Martian polar caps. The new measurements suggest that the 20% of the Martian surface was once covered by water. Over time, 90% of this ocean was lost to space, with the remainder locked up today in Mars' north and south polar caps. There were three stages in emplacement of a large body of water:

- **A warm convecting stage** – It is the heat transfer. Convective system will maintain warm surface condition and causing an ocean. It depends on the depth of the ocean and temperature. In the case of shallow ocean i.e., 100 m depth the convecting stage lasts only few years.

- **Freezing stage** – When convection stops, ice cover form and heat loss from the surface is reduced. For instance, 1 km deep lake takes 10^5 years to freeze which depends on ice albedo and wind speed. Sediment deposition will take place within the 1st stage by convection and gets deposited on the floor.

- **Sublimating stage** – Here the ice deposit sublimates and get covered with the aeolian deposits. Clear polar ice will sublimate at 0.8 mm/yr. For strong winds, it sublimates at 0.5 mm/yr. Ice buried under rock or soil will be stable as temperature never gets above freezing point. If ice is clean it would sublimate in a few 100 – 1000 yrs. (even if it is 1 km thick), or the ice is covered with debris about 10cm, then it will remain for the lifetime of the planet.

Scientists have hypothesized that the northern lowlands of Mars are a dried-up ocean bottom. Since the majority of Mars' northern hemisphere is flat and lower in height than its southern hemisphere, it resembles Earth's Ocean basins in appearance. The shore of the imaginary ocean would have been the boundary between the lowlands and the highlands. By looking at sediment accumulation, the direction of erosion and other stratigraphic evidence, researchers were able to determine that the ridges were likely eroded river deltas, or the remains of an ancient Martian shoreline. The fact that sediments from another basin flow in, fill this one slowly over time, and liquid water collects there provides very strong evidence that this one was once an ocean of liquid water. In addition, this offers quite strong proof of a warm and rainy phase in Mars' past. If conditions on Mars were as they are now, the gradual, steady filling of this northern basin would not have been possible. It implies that the atmosphere was considerably thicker, trapping heat from the sun to maintain a temperature at which liquid water could exist.

1.10 Objective of the work

- The aim of the project is to find the age of Martian Ocean by using Craterstat.
- The intention of the work is to derive the time when ocean existed on the Martian surface and the evaporation of water from the northern surface.
- Comparison between the ages of the prevailed ocean and the timeline of ocean disappearance which were done by crater counting and then representing them in Craterstat software.

CHAPTER II

LITERATURE REVIEW

2.1 Introduction

Large quantities of water must have previously filled the northern plains during the Late Hesperian era if the vast outflow canals were eroded by widespread floods. According to Clifford and Parker (2001), the size of bodies of water in the northern lowlands can reach 3 x 108 km^3. The objective is to evaluate the observational support for post-Noachian waters in Mars' northern plains in the light of new information from the Mars Global Surveyor nominal mission. We concentrate on the post-Noachian era due to the potential link between the emergence of any seas and that of the major outflow channels, the majority of which are Hesperian in age (Kreslavsky and Head, 2002).

2.2 MARTIAN LOWLANDS

The northern lowlands of Mars make up about one-third of the planet's surface and are the centre of a larger drainage basin that has made up roughly two-thirds of the surface for most of the planet's history (Smith et al., 1998; Zuber et al., 1998). The northern lowlands may have held a sizable body of water at one point in the planet's history (Parker et al., 1989, 1993; Baker et al., 1991).

According to Scott and Tanaka 1986 (Tanaka and Scott, 1987; Greeley and Guest, 1987), the exposed surface units of the northern lowlands are dominated by Noachian-aged remnants, including a small unit divided by channels in Acidalia Planitia, old degraded crater rims, a group of domes thought to be old degraded Noachian crust, the Hesperian-aged Vastitas Borealis Formation, the north polar cap, which is made up of Late Amazonian ice and layered terrain deposits, the Hesperian-aged outflow channel deposits at the margins of the lowlands in Chryse Planitia, the various local Amazonian-aged plains units, the Elysium channel and flow deposits, the Amazonian-aged circumpolar mantling material, and so forth (Tanaka, Hare, Wenker and Skinner, 2003).

2.3 EVOLUTION OF MARTIAN HYDROSPHERE

We examine the consequences for the evolution of the Martian hydrosphere of the hydraulic and thermal conditions that gave birth to the high source regions of the Late Hesperian outflow channels. If the outflow channel floods came from a sub-permafrost aquifer, it is likely that up to one third of the planet's surface was covered in frozen water and ice during the first billion years of its history. The majority of this water would have been present as an ice-covered ocean on the northern plains after the emergence of the global dichotomy. The following climatic and geothermal history of the globe was a natural result of the ongoing crustal absorption of this early surface pool of water. The progressive cold-trapping of H_2O into the expanding cryosphere is expected to have significantly reduced the initial groundwater inventory in response to the long-term decline in planetary heat flow; this development may well account for the apparent decline in outflow channel activity seen during the Amazonian. Although the research is purely theoretical, the results are strikingly congruent with the geomorphic and topography evidence that Mars originally had a primordial ocean and that a sizable remnant of that body now exists as vast ice deposits in the northern plains (Clifford and Parker, 2010).

2.4 OCEAN ON MARS

By Parker et al. (1989, 1993) hypothesized that seas were formerly existent on the northern plains was developed in some depth. They observed several characteristics on the plains and surrounding them are believed to be remnants of previous shorelines. These included massifs with stepped slopes, cliffs and onlap relations in the fretted terrain, plains with muted parallel ridges or thumbprint textures, terraces on fretted valley walls, backflow evidence in the lower reaches of some outflow channels, and abrupt termination of outflow channels as they debouch onto the plains. With the use of these observations, scientists located two abrupt contacts that they inferred to be shorelines. An inner contact 2 lay almost entirely within the plains, while an outside contact 1 roughly aligned with the plains-upland boundary. Similar criteria they interpreted the discontinuous shorelines in terms of many small bodies of water rather than a single big ocean in the northern plains. Later, Parker and colleagues discovered a number of new shorelines, both inside and outside the previous contact 1 (Parker, 1998; Parker et al. 2001; Grant and Parker, 2001).

In order to explain unusual landform assemblages, such as potential glacial characteristics of the Amazonian era in the southern hemisphere (Kargel and Storm 1992) and Hesperian and

Amazonian age valley networks (Gulick and Baker, 1989, 1990), Baker et al. (1991) accepted the ocean theory. They proposed that Mars' climatic conditions have mostly remained the same since the end of the Noachian, but that these protracted cold periods have occasionally been broken by fleeting warm episodes. Massive floods that created transient oceans and released copious amounts of water and carbon dioxide into the atmosphere were the root cause of the warm episodes, which altered the climate on a worldwide scale. After the ocean-forming processes, they hypothesised, the carbon dioxide was removed from the atmosphere, the water seeped into the porous subsurface, and the planet returned to its previous frozen state (Zuber, 2018).

After considering the hydraulic and thermal circumstances that gave rise to the high source areas of the Late Hesperian outflow channels, Clifford and Parker (2001) utilised their findings to examine the implications for the makeup and development of Mars' hydrosphere. Clifford and Parker (2001) came to the conclusion that early Mars history must have been characterised by at least one third of the surface being covered by standing bodies of water and ice, most specifically, an ice-covered ocean in the northern lowlands, and that the outflow channel sources emerged from groundwater sources beneath a cryosphere.

2.5 FATE OF THE HESPERIAN OCEAN

Floodwaters often flowed into the northern basin during the mid- to late Hesperian under climatic circumstances similar to todays (Tuber and Forget, 2019). We suppose that each flood formed an ice layer that stayed in place until the following flood in a geologically little amount of time. Over time, successive ice layers began to fill up the basin. After the basin was filled, the ice slowly sublimated into the atmosphere, where it was lost to space or accumulated in a variety of cold traps close to the surface, such the polar layered deposits. Due to the thick cryosphere and low heat flow values, very little water was lost from the surface to the global groundwater system. Since the mid-Hesperian, around 5m of water had been outgassed to the surface (Carr, 2003).

CHAPTER III

METHODOLOGY

The main aim of this project is to derive the surface age of Martian Ocean and its vaporising events using Craterstat. Primarily, the work started with collecting information from previous journals. A good understanding from these papers provides a better way to acknowledge the subject and give details about Martian surface and the past geological events. Researchers had expounded their perceptions and abstractions on different aspects about Martian Ocean.

We had already discussed about the Mars and its surface. The northern hemisphere is a lowland and studies say that was once covered with an ocean. A global dichotomy is the boundary that divides both the hemisphere, where northern lowlands are seem to be flat and smooth. Later, due to change in atmospheric condition and crater events, the water in the northern plain began to vaporize. There are many controversies on this topic like how Mars had lost its atmosphere? Where does all this water went? What is the cause of ocean vaporisation? Some researches figured out that this event caused due to impact craters, which lead to sporadic glacial and interglacial period that occurred during Hesperian age, highly marked with flooding, tsunami and also formation of shorelines. All this evidence suggests, Mars was covered with a Hesperian Ocean. Absence of magnetosphere and presence of thin atmosphere also caused imbalances on Mars, high concentration of CO_2, effects of solar wind and dust devils weakened the planet apparently. Scientist signifies furtherly, only few percentages of water had lost to atmosphere, while major concentration of water is said to have accumulated at the polar regions. Studies show that water was lost by sputtering, photolysis and recombinant dissociation processes from the veneer of the Mars. It is evident that Mars had warm and wet period, where water existed as well.

3.1 CRATERS ON MARS: FORMATION AND DETERMINING THE SURFACE AGE

There are currently no samples from known sites on Mars, planetary scientists must make an educated guess as to how ancient the surface is by counting the number of visible craters: larger

number and high density of craters implies an older terrain. Mars' considerable volcanism, erosion by glaciers, wind, and flowing water as well as the broad deposition of sediments that buried earlier craters (Fig. 3) poses challenges. The surface of Mars is marked by numerous impact craters some of which are among the largest on the solar system. These craters provide valuable information about the planet's geological history including the processes that have shaped its surface and the age of various features.

Impact craters on Mars are created when a meteoroid or asteroid collides with the planet's surface. The impact causes a powerful explosion that excavates material from the surface leaving a circular depression or crater behind. The size and shape of the crater depend on several factors including the size and speed of the impacting object and the composition of the surface material. Larger fast-moving objects will create immense and more complex craters, while softer materials will create shallower craters than harder materials. Determining the age of Martian surface feature can be a complex process. One of the most common methods used by scientists is to estimate the density of impact craters in a particular area. The more craters there are the older will be the surface. By counting the number of craters per unit area and comparing it to the number of craters on the other surfaces with known ages, scientist can estimate the age.

However, this method can be complicated by a number of factors, for instance, the density of impact craters can vary depending on the location on the planet. Areas with thicker atmosphere or more geological processes such as volcanic activity may have fewer craters than areas with thinner atmosphere and less geological activity. Additionally, erosion and other processes can obscure or erase craters over time making it more difficult to determine their age. Another method used to determine the age of Martian surface feature is through the study of planet's geology by examining the layers of rock and sediment in a particular place. Scientists can gain insights into the history of geological processes in that region. In conclusion, the study of impact craters on Mars provides valuable information into the planet's history and processes that have shaped its surface overtime. By examining the size, shape and density of craters as well as the planet's geology, scientists can determine the age of the Martian surface features and gain better understanding of the planets' past and potential for future exploration and habitation.

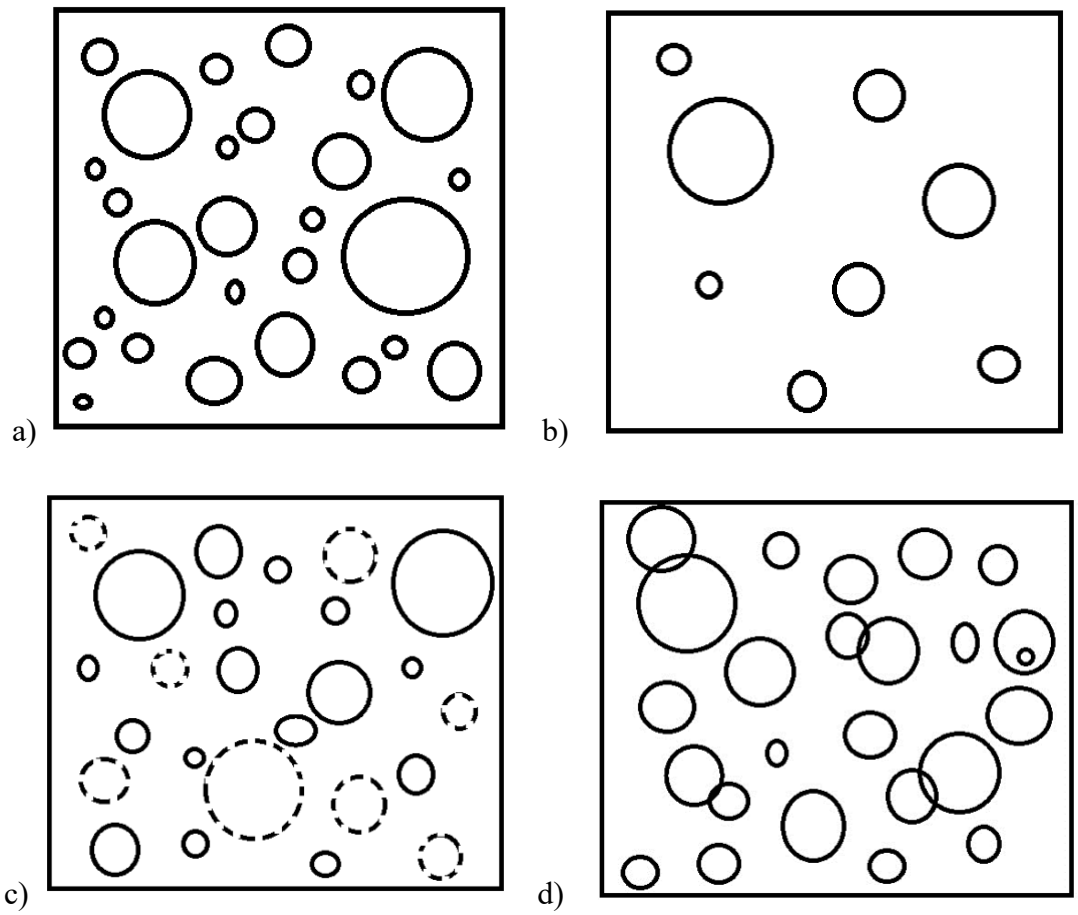

Figure:3, Schematic representation a) Cratered surface, b) surface affected by erosion, c) same surafce with continued cratering, d) here, older and younger crater is difficult to distinguish due to continous cratering.

Now, the Red Planet is cold and arid with huge dust storms and totally seen as a barren land. Probing on Mars is still augmenting. Determining the age of Mars is a crucial phase. Earlier, the age was derived by counting the number of craters present on the surface, manually, which was quiet challenging. Then researchers had developed crater counting techniques to acquire the surface age. Here, in this project, crater counting is done by using a software application called JMARS (Java Mission Planning and Analysis for Remote Sensing).

3.2 CRATER CHRONOLOGY

The term ‘impact’ refers to a basic geologic event, and the resulting imprints, known as impact craters, are typical geological structures that may be seen on the surfaces of many different planetary objects and are present throughout the solar system. Knowing the origin of the impactors since the formation of our solar system is crucial for employing impact crater density as a chronologic tool. Our solar system's primary impact cratering phase may have been

influenced by the LHB catastrophe. Following that, the flux of impactors for the terrestrial planets has remained essentially steady, with most of them coming from the asteroidal belt. As a result, there are essentially two populations of impactors: those who visited during the LHB and those who came subsequently. The Law of Order of Superposition is used to determine the relative ages of planetary surfaces that are in contact with one another, with the older surfaces having a higher crater density than the younger surfaces (Barlow, 1988).

The crater chronology technique for an area is executed in the following sequence:

1. **Determination of Crater size frequency distribution**: The size frequency distribution (SFD) of craters provides a quantitative measurement of the number of craters per unit area as a function of crater size. The size of individual craters and the frequency with which they are distributed throughout a surface are the two main variables that control the density of craters on a given surface.

2. **Fitting Production function**: The number of craters of a certain size relative to the number of craters of any other size is described by different production functions devised by Neukum and Hartmann (2001). For the total number of craters with diameters greater than a certain diameter, Neukum devised a polynomial fit.

3. **Estimating the age from the Chronology function**: After plotting the production function with respect to the diameter of the craters, the production function for 1km diameter crater is derived from the SFD plot and that value is calculated to derive the surface age (Srivastava and Indhu Varthrajan, 2013).

3.3 CRATER COUNTING

Ages are key piece of knowledge in geology and planetary science, which unravels the history of a planetary body. Crater counting is a technique for determining the age of a planet's surface based on the suppositions that impact craters are absent from freshly formed planetary surface and that they collect through time at a predictable pace. Therefore, calculating the number of craters of different sizes in a certain region enables one to determine how long they have collected and, as a result, how long ago the surface originated (Benedix. et al, 2020). The existence of separate craters is necessary for the crater counting approach. The primary impact point on a planet's surface is represented by independent craters, whereas the secondary impact point is represented by secondary craters (Russell and Daubar, 2014) (Fig:4).

3.4 SELECTION OF CRATERS

It is necessary to understand the type of crater to be selected, while determining the surface age. Different craters exhibit different properties as they show age of specific period and the time of geological activity. Therefore, crater selection is a crucial stage and plays an important role in determining the age of the Martian surface. We already discussed that the surface of Mars may contain craters of impact as well as volcanic origin. During crater counting, it should be noted that only impact craters are taken for counting process, whereas volcanic craters and craters formed by other geological activities should be avoided. During a crater impact, primary craters are chosen, that form from high-velocity impacts whose foundational shock waves must exceed the speed of sound in the target material, whereas, secondary craters impact at low velocity. These secondary craters are seen as clusters or chain surrounding the primary crater. While crater counting, secondary craters should be avoided, as they are considered as contaminants, which will affect the surface age of the Mars.

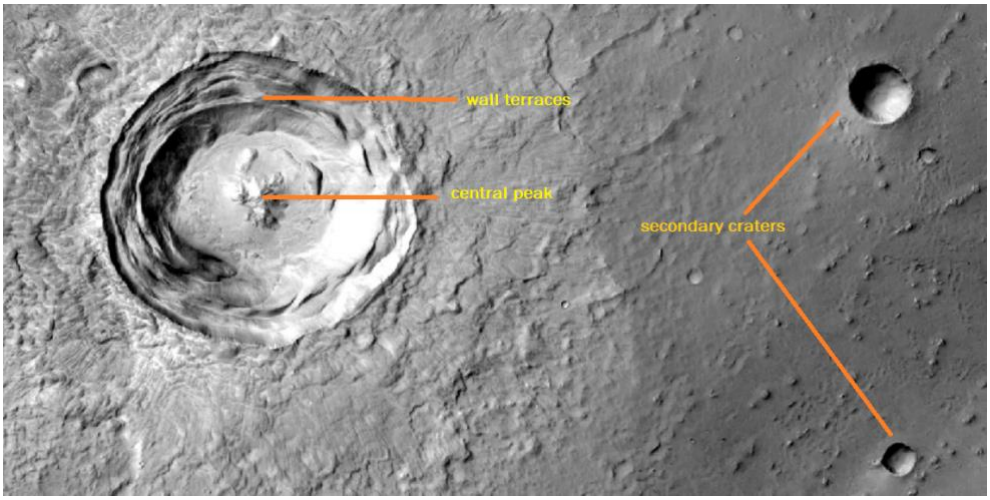

Figure:4 Martian surface showing primary and secondary craters, were crater with larger diameter, along with wall terraces and central pits is assumed to be primary crater, whereas the craters found scattered around the primary ones are secondary craters.

3.4.1 Factors affecting crater size frequency distribution

- **Magmatic flooding**: Lava flows can completely obliterate tiny craters, partially bury craters of intermediate sizes, and have minimal impact on the larger craters after eruption. Therefore, a count of the larger craters in a region provides information about the age of the older basement rocks, and a count of the smaller craters provides information about the age of exposure of the current surface.

- **Ejecta Blanketing**: When a new crater is created on the surface of a planet, it ejects material radially outward and away from the crater, creating a massive ejecta blanket that relies on the impactor's velocity as well as the parameters of the target.
  Depending on how far from the original crater they are, these ejecta particles can cover their surroundings in a thick layer up to hundreds of metres high. As a result, they could cover previously produced craters and exhibit abnormal SFD behaviour.

- **Secondary Cratering**: Formed as a result of primary craters by heavy impacts. They can be identified by their shape, shallow in nature, form in clusters and chain, usually flatter than the primary craters. During crater counting, secondary craters should be avoided.

- **Superposition, abrasion and infilling**: Superposition occurs when a new crater overlies the previous crater, thus destroying the details of the previous crater. Abrasion deals with eroding or surface events, as age of crater is directly proportional to abrasion. Infilling is caused by the ejecta of the new craters into the older ones.

- **Mass wasting**: This can affect the density of the crater in an area.

- **Volcanic craters**: Having irregular shape, broken rims and subdued appearance should be avoided while crater counting (Srivastava and Indhu Varthrajan, 2013).

Crater morphology is another important aspect while selecting a crater. The surface of Mars contains different varieties of craters ranging in different size and density. Choosing appropriate crater for counting is a quest. Selection of unfitting crater can affect the surface age. It is obligatory to find for the fresh craters while counting.

To find the recent craters we have to understand the morphological features of the fresh craters (Fig. 5). Those craters will be formed after the most of the intense erosion and do not had undergone any resurfacing phase. A fresh crater contain bowl shaped with sharp, raised rims, usually lacking flat floors. This morphology remains approximately 5 to 10 km in diameter. Deviation from this diameter (10 – 15 km) may shows craters with wall terraces, central peaks and flat floors will be prominent. If diameter ranges from 10 – 40 km, then well-developed terraces become more prominent and flat floors grow in proportion to the rim.

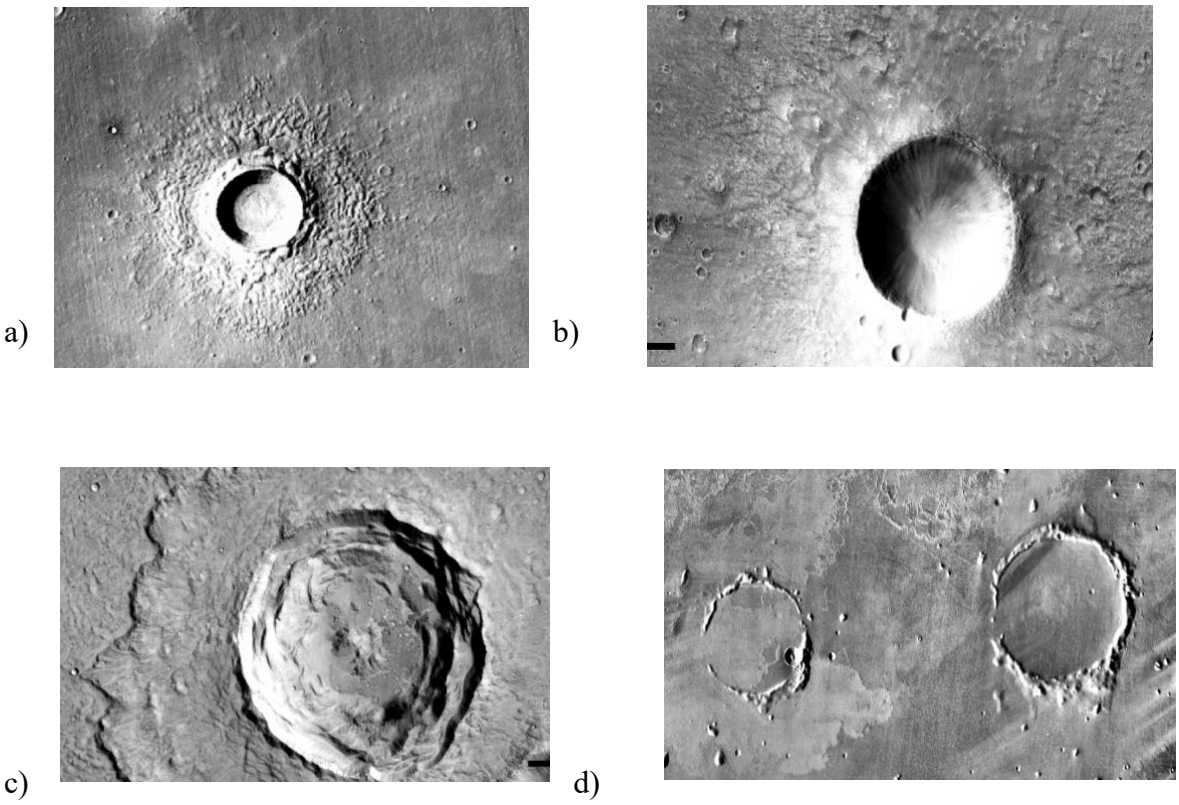

Figure:5 Different types of craters found on northern plains. a) and b) Representing crater with fresh ejecta and raised rims, c) Crater with developed wall terraces and central pits, d) highly eroded crater.

We know that the northern lowlands of Mars contain a smaller number of craters when compared to the southern highlands. It is also evident that these lowlands contain lava flows and have volcanic and tectonic features. Counting craters on these areas will give only age of that particular feature, so while crater counting, we have to avoid such areas that will alter the surface age.

After selecting suitable crater, by using JMARS, we have to mark the diameter of various craters. Crater with perfect and raised rims with good ejecta blankets are preferred. Different craters of different size and shape can be seen. In this work we divide the Martian Ocean into various Planitias based on their size (km). These planitias cover the northern lowlands, where each of them had formed at distinct time period, experiencing different type of crater impacts and resurfacing events.

3.5 PLANITIAS OF NORTHERN LOWLAND

The northern hemisphere of Mars comprises widespread basins, which are formed by crater impacts, outflow channel activities and so on. They are – Utopia Planitia, Chrysae Planitia, Isdis Planitia, Arcadia Planitia, Acidalia Planitia, Amazonis Planitia and Vastitas Borealis Formantion (VBF), the largest lowland in Mars. Crater counting on these region helps to determine surface ages by analysing the number of fresh carters. Geologic history (Noachian to Amazonian) of Mars reveals that the planet had undergone different events, which reshaped the planet.

Utopia Planitia covers an area of 3600 km and is one of the largest impact basins. Utopia Planitia, Acidalia Planitia and Arcadia Planitia line almost in the same latitude and these three stretches to VBF, encircling the pole area. Chrysae Planitia, Isdis Planitia and Amazonis Planitia were found close to the global dichotomy.

Firstly, we separate the planitias, by using ‘Custom Shape Layer’ in JMARS and divide the them into polygons, based on the area they covered.

3.6 CRATER COUNTING WITH JMARS TOOL

JMARS is a GIS application that makes it easy to access and work with planetary datasets from various NASA missions (Fig. 6). Originally developed for Mars, JMARS now supports work on data from many different solar system bodies, including Earth, Moon, and other planets. As a GIS application JMARS allows us to display one or more layers of spatially – organised data and use various tools to make measurements and do other analyses of the data. Here, we will

be focussing on crater counting using JMARS, i.e., to count the number of craters of various sizes in order to determine age of Martian Ocean.

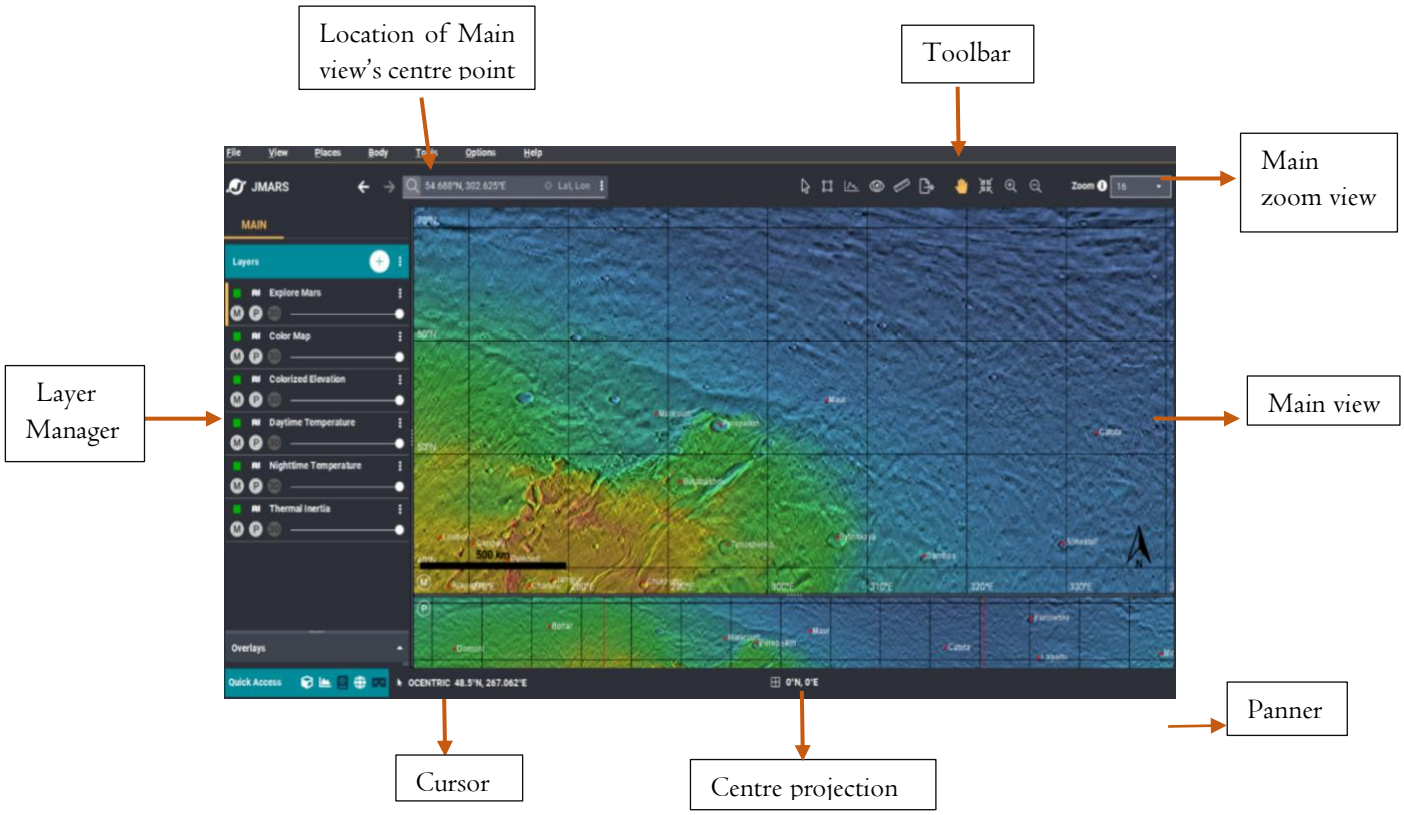

Figure.6 showing the basics of JMARS software

Steps included in working of JMARS:

- Open JMARS and select the area to be analysed
- Add Crater Counting Layer to the JMARS session
- Adjust crater tool settings to mark different size categories of craters
- Mark all the craters that needed to be analysed
- To calculate area of view, measure the width and height using a ruler tool
- Export the crater data as CSV file and image of marked up view
- Then export the data as DIAM file, to function in Craterstat

Our aim is to derive the age of Martian Ocean and its vaporising event. Here, we divided the northern lowlands into planitias. We already discussed about different basins on the northern hemisphere. Next we divide them into separate areas (Fig. 7), for that choose “Custom Shape Layer” → “Toolbar” → “ Draw Shape” → “Polygon”. This enables us to select a desired area.

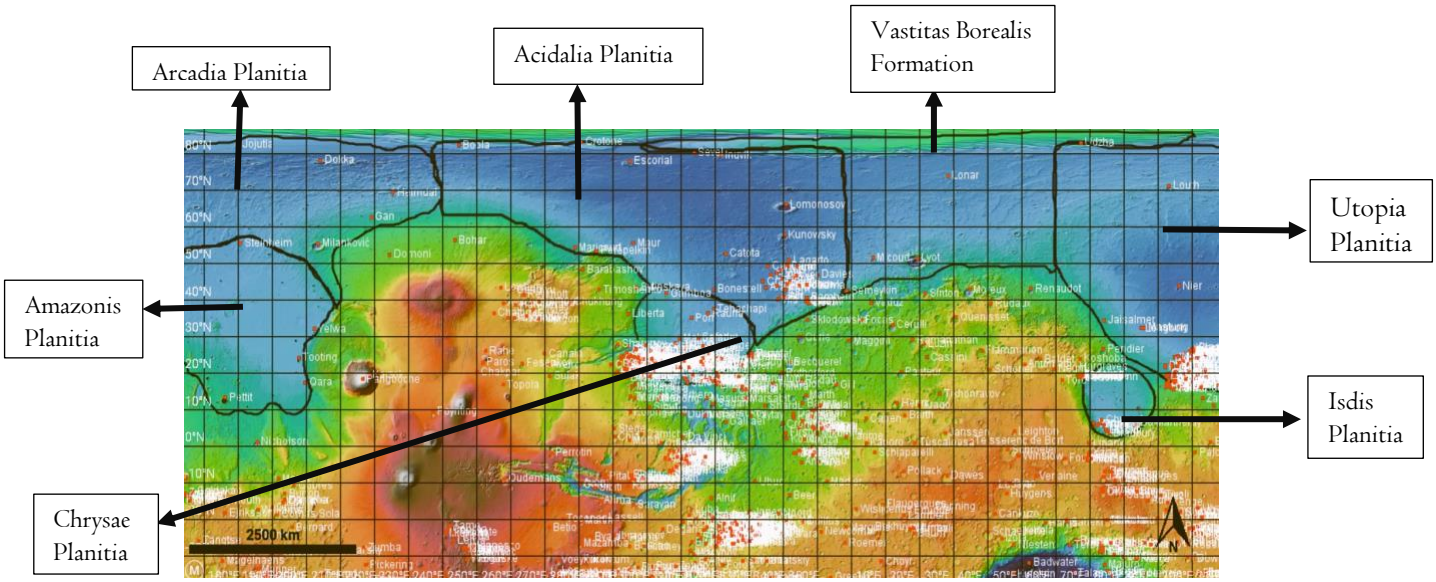

Figure.7 JMARS representing different planitias of northern part of Mars

After dividing the Planitias into polygons, crater counting can be started. For that we have to select “Crater Counting” → “ Open Docked” → “Crater Tool” (Fig. 8). Here, we can select the suitable crater of different diameter by adjusting the size of crater using crater tool. We already mentioned the conditions while selecting a crater.

a)

b)

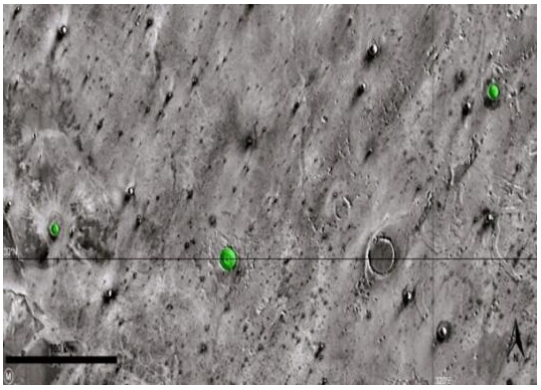

Figure.8, Crater counting on JMARS a) representation of crater count settings b) selected craters are marked in green colour.

Planitias will show different crater properties based on the impact. On moving towards higher latitude, craters can be seen as 'expanded craters', as they are ice covered and have subdued and broken rims. Therefore, such type of craters should be avoided. Following the crater counting, we have to export the crater data as CSV file (simple comma-separated text files or csv files are frequently exported from spreadsheet programmes like Microsoft Excel. It may represent point data as well as a countless number of extra information fields). Next step is exporting DIAM file directly to Craterstat.

The acquired data from JMARS now have to be imported to Craterstat, which is a modified programme for calculating surface ages and visualizing crater counts. The programme creates isochron fits to both cumulative and differential data and presents isochrons in cumulative, differential, R-plot and Hartmann representation.

There are several steps involved in Craterstat (Fig. 9):

- Step [1]: Firstly, browse the crater data which is stored as DIAM files
- Step [2]: Change the planetary body to Mars
- Step [3]: Select ''cumulative'' function
- Step [4]: Change the ''crater count'' to ''cumulative fit'', which shows the production curve
- Step [5]: Set the diameter range for the craters

- Step [6]: Enable all the selected function (shown below) to display age
- Step [7]: Duplicate the data to represent ages of different craters
- Step [8]: Enable isochron, to display ages in giga annum
- Step [9]: Export the obtained Craterstat data as “Image”

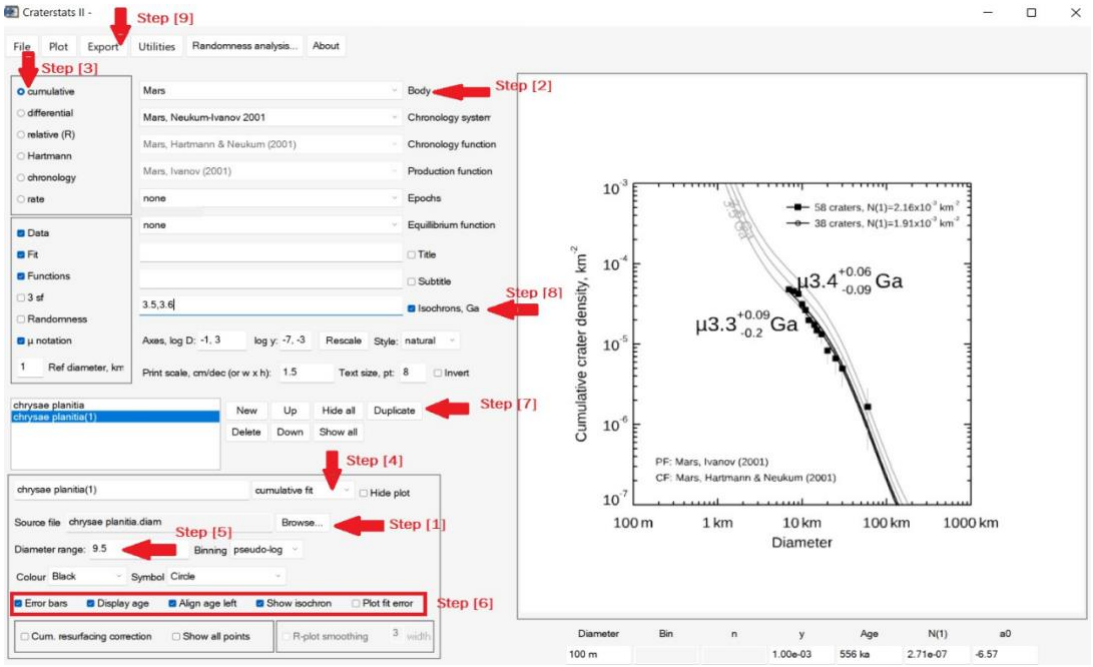

Figure. 9, figure showing the functioning of Craterstat and the representation of age of a particular surface

CHAPTER IV

RESULT AND DISCUSSION

Determining a surface's geologic history most efficiently relies on not just geologic mapping, which delineates materials by surface and natural breaks in the rock sequence, but also crater counting, which gives a quantitative tool for establishing relative ages and modelling absolute ages (Clifford and Parker, 2001).

The work had been done by dividing the northern lowlands into different zones, focusing the planitias of varying size. The existence of water and its vaporisation from these different lowland areas depict distinct ages. We want to plot past geological ages of ocean, that existed once, and the time when the ocean vanished, in the Craterstat.

4.1 CRATER COUNTING ON NORTHERN PLANITIAS

4.1.1 Pre– Events

Craters are not uniformly distributed over the Martian surface. Noachian period holds most of the large craters. Formation of valleys, active channels created large water bodies in the Early Hesperian. Crater counting on the Hesperian surface could tell the time of existence of ocean on lowlands. But many geological activities resurfaced the Hesperian surface and accumulated only small craters. In order to determine the pre-events of ocean disappearance, we have to consider fresh craters (diameter >5 km), with good ejects and raised rims (NB: eroded craters and modified craters should be avoided).

Chrysae region (30º West longitude) is a topographic depression of 1500 km in diameter and is an area of prominent outflow channels, so the chances of forming an open body lake or an ocean is high in this zone (M.R.Salvatore & P.R.Christensen, 2014). Crater counting can be used to describe the timing of evolution in this area. Absolute ages and crater size frequency distribution statistics measured on Chrysae Planitia shows water existed in this region about 3.4 Ga. Past geological age of Chrysae region is 3.4 Ga, representing Hesperian period, which depicts most of the bulk materials from Maja Valles, Kasei Valles, Valles Marineris got

deposited on the lowland of Chrysae basin. Therefore, crater size frequency distribution in this region shows an older age (Fig. 10).

Acidalia Planitia situated at 49.8ºN, 339.3ºE, is lying in same latitude as Utopia Planitia. It covers an area of 3400 km and has numerous mud volcanoes and flow channels, mostly from the Chrysae region. Acidalia region holds the traces and remnants of an ancient ocean that covers a part of northern lowlands. Dating craters from this region suggests that the zone comprises an age of 3.5 Ga to 3.7 Ga. This variation can be due to change in morphologic characteristics.

Isdis Planitia is an impact basin and is 1200 km in size, situated at 12ºN 87ºE towards the highlands. This large basin was formed during Noachian period. Lava flows were dominant in this basin, therefore chance of modification of this Planitia is very high. Crater counts on the Isdis floor provide an age of 3.1 Ga, but the actual age of basin is 3.96 Ga (Werner, 2008). The age from the crater count can implies the presence of ocean and the water present on this basin reveal ages ranging from 3.1 to 2.8 Ga, where 2.8 Ga represent the latest pre-event activity that resurfaced the basin.

Utopia Planitia is the largest impact basin in the northern plains, which covers an area of 3600 km and is centered at 47ºN 118ºE. Crater variation in Utopia region is quiet puzzling. In this area craters of different sizes are present. Rampart craters, having fluidized ejecta blanket, indicate the presence of volatiles like water ice or subsurface water (Carr.et al., 1977). Variety of craters with different shapes were analysed, these variations were correlated with giant polygons (Pechmann, 1980) and other surface structures, which denote a resurfacing event (McGill, 1986). The obtained age of Utopia Planitia range between 3.5 Ga to 3.7 Ga, this variation appears due to the presence of craters with different diameters.

Arcadia Planitia, having a smooth terrain and young lava flows, is situated 47.2ºN 184.3ºE. The southern region of this Planitia contains almost old craters, when compared to the northern parts. Crater ages in this Planitia are 3.6 to 3.4 Ga, which indicate the presence of Hesperian Ocean.

Amazonis Planitia is the flattest region in the northern lowland, which is recently formed, lying at 26ºN 163ºW and have an area of 2800 km. Crater events were very less and most of the craters are young in age. This region represents the youngest of the Martian stratigraphic periods. Crater ages of Amazonis Planitia ranges about 1.2 Ga, the mere existence of ocean and the remained water had transformed into ice caps.

Vastitas Borealis Formation, largest lowland in the northern hemisphere, found at 87º 44´N, 32º32´E, almost towards the pole area. It represents one of the final stages of water related sedimentary activity. Chrysae region was episodically active during Martian history (Tanaka, 1989). The active outflow channel deposits of Chrysae region have fine grained sediments, which are found in VBF, so there should be a source capable of transporting these materials from Chrysae to VBF. By extrapolating the observation, we could say that a huge water body or ocean might be the carrier of the particles. Crater count on the VBF shows almost similar age with Chrysae Planitia, range between 3.5 and 3.7 Ga, so we can say that both these basins coexisted at Hesperian age.

a)

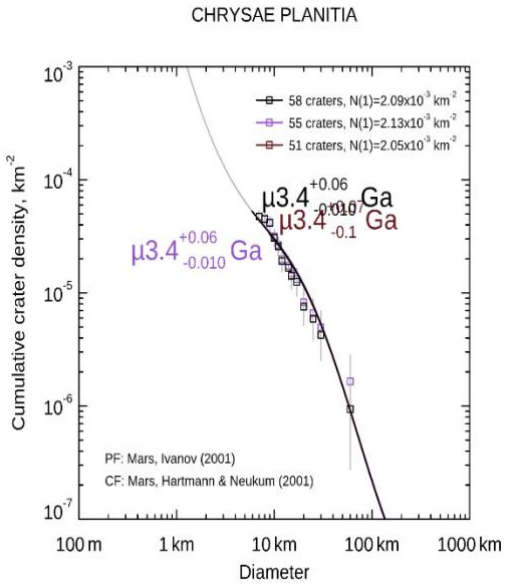

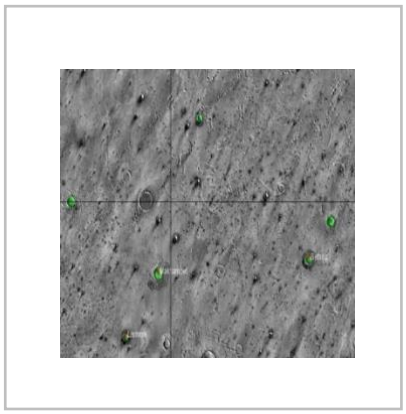

b)

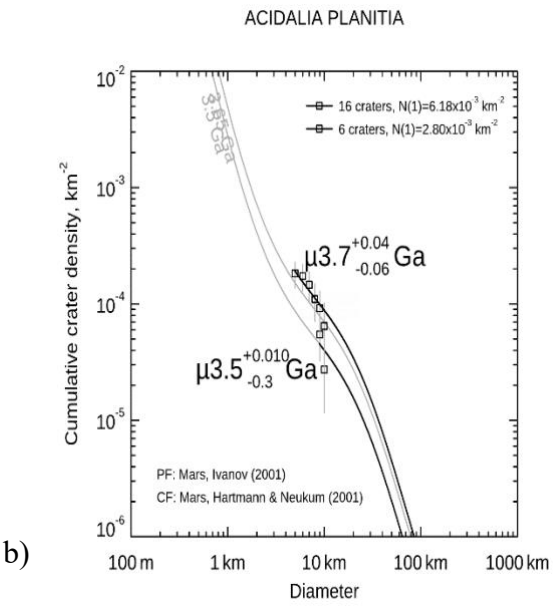

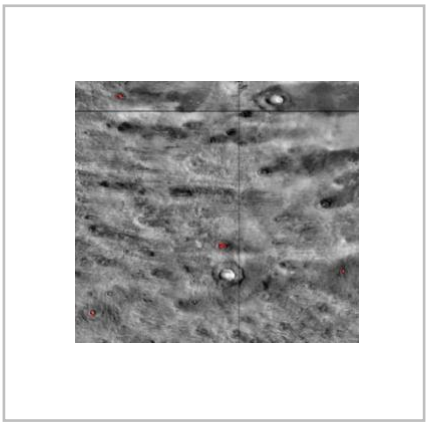

c)

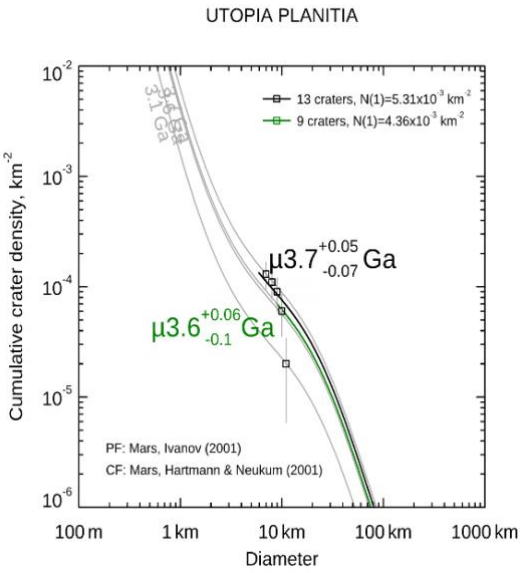
UTOPIA PLANITIA
13 craters, N(1)=5.31x10^-3 km^-2
9 craters, N(1)=4.36x10^-3 km^-2
μ3.7 +0.05 -0.07 Ga
μ3.6 +0.06 -0.1 Ga
PF: Mars, Ivanov (2001)
CF: Mars, Hartmann & Neukum (2001)
Cumulative crater density, km^-2
Diameter
100 m
1 km
10 km
100 km
1000 km

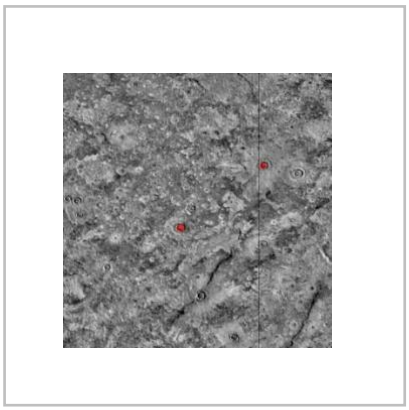

d)

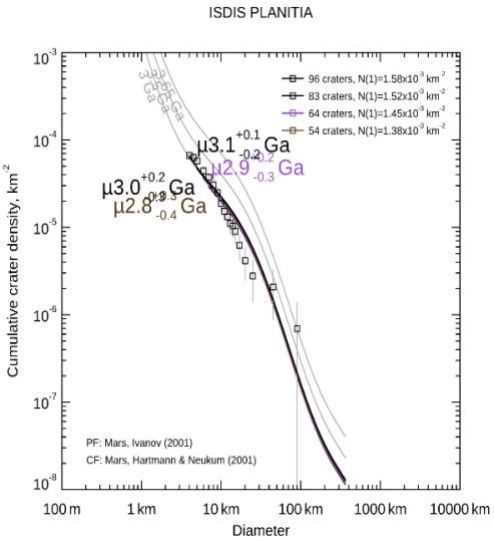
ISDIS PLANITIA
96 craters, N(1)=1.58x10^-3 km^-2
83 craters, N(1)=1.52x10^-3 km^-2
64 craters, N(1)=1.45x10^-3 km^-2
54 craters, N(1)=1.38x10^-3 km^-2
μ3.1 +0.1 -0.2 Ga
μ2.9 -0.3 Ga
μ3.0 +0.2 -0.3 Ga
μ2.8 -0.4 Ga
PF: Mars, Ivanov (2001)
CF: Mars, Hartmann & Neukum (2001)
Cumulative crater density, km^-2
Diameter
100 m
1 km
10 km
100 km
1000 km
10000 km

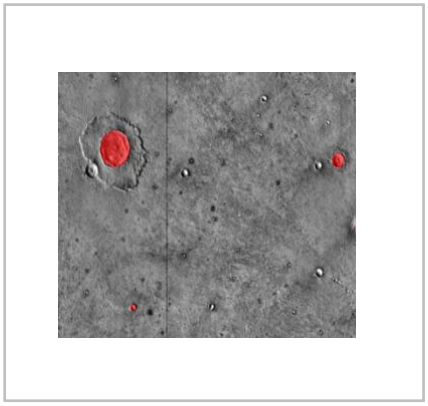

e)

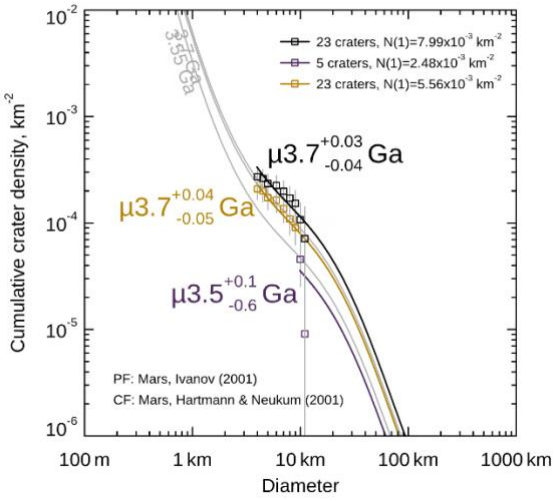
VASTITAS BOREALIS FORMATION
23 craters, N(1)=7.99x10^-3 km^-2
5 craters, N(1)=2.48x10^-3 km^-2
23 craters, N(1)=5.56x10^-3 km^-2
μ3.7 +0.03 -0.04 Ga
μ3.7 +0.04 -0.05 Ga
μ3.5 +0.1 -0.6 Ga
PF: Mars, Ivanov (2001)
CF: Mars, Hartmann & Neukum (2001)
Cumulative crater density, km^-2
Diameter
100 m
1 km
10 km
100 km
1000 km

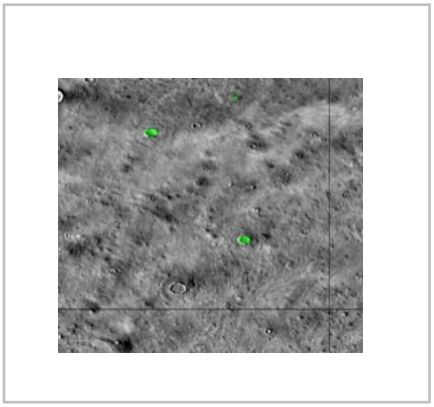

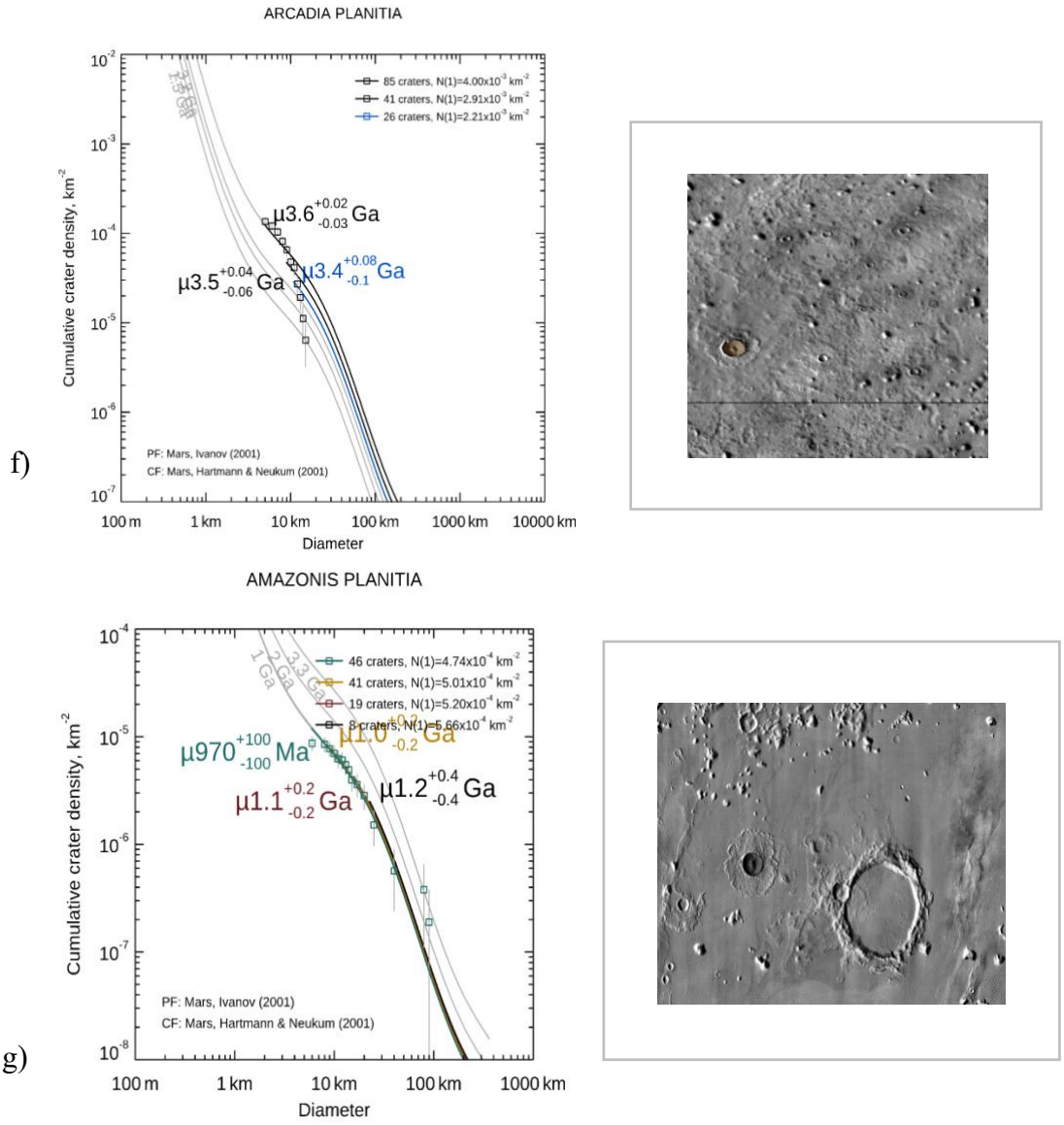

Figure. 10 Crater size frequency distribution of each Planitia, represented in the Craterstat, exhibiting pre-events of the Martian Ocean a) Chrysae Planitias' age delinated in Craterstat along with marked crater counts on the surface of Chrysae region in JMARS. Similarly, b) Acidalia Planitia, c) Utopia Planitia, d) Isdis Planitia, e) Vastitas Borealis Formation, f) Arcadia Planitia, g) Amazonis Planitia.

4.1.2 Post-Events

It deals with the disappearance of Martian Ocean. We are detecting the time of ocean evaporation through Craterstat. In order to find this vaporising event, we count craters that are extremely fresh. To determine the age of post-events, we have to check for craters, having diameter less than 5 km, which imparts fresh ejecta, raised rims, where central peaks and wall

terraces will be absent. By analysing the fresh craters, we can figure out the recent age of Martian northern lowland surface and the time ocean vanished.

To find the post-events, the same procedure of pre-events was performed. It encompasses considering the seven basins of the northern lowland and counting the number of fresh craters, which were later displayed it in the Craterstat (Fig. 11).

The obtained age from each Planitia depicts the time of ocean vaporisation in million years. Surface of every Planitia is found to be highly resurfaced due to the activity of lava plains and the presence of bulk materials, enhanced the vanishing of northern ocean at Chrysae region. Craters of smaller diameter reveal the latest age of each planitia. Presence of polygonal fractures in the Utopia Planitia and Acidalia Planitia indicate desiccation, which is the process of removal of moisture. By detecting this feature, we could say that there might existed a paleo-ocean that completely vapourised. Likewise, the age determined from each Planitia indicate the disappearance of Martian Ocean. Amazonis Planitia, the smoothest and flattest of all, reveals the recent age of vaporizing event, as it is affected with less crater activity and resurfacing processes. The similar morphologies of Utopia and Acidalia Planitia suggest a large basin fill that have occupied the northern lowlands for at least brief periods of geologic time. Also, the presence of unaltered mafic minerals in the shallow subsurface indicates the rapid evaporation of northern ocean, before the alteration could occur.

a)

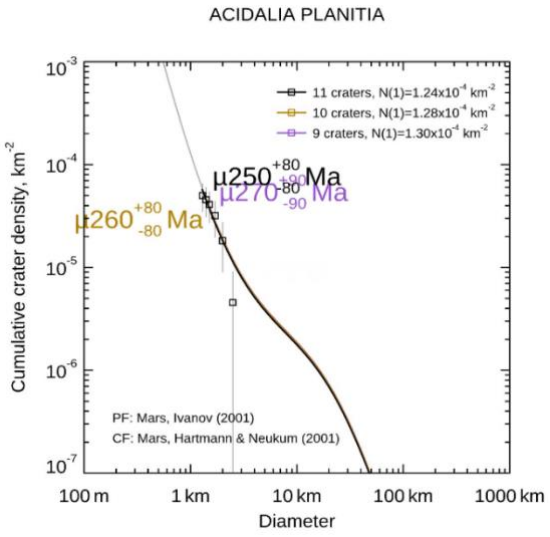

b)

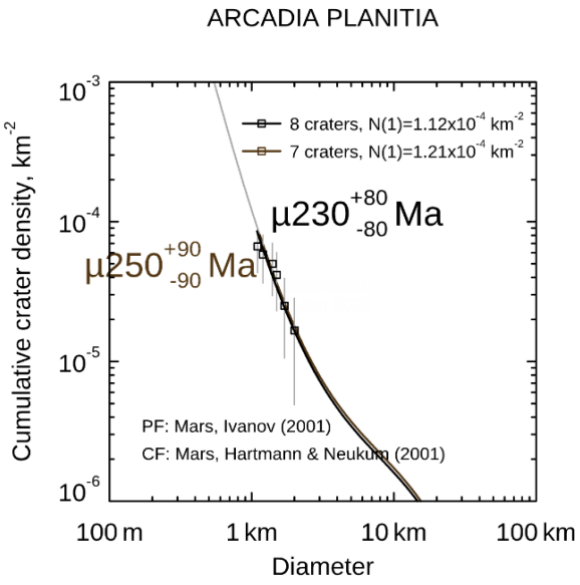
ARCADIA PLANITIA
Cumulative crater density, km-2
8 craters, N(1)=1.12x10-4 km-2
7 craters, N(1)=1.21x10-4 km-2
μ230+80-80 Ma
μ250+90-90 Ma
PF: Mars, Ivanov (2001)
CF: Mars, Hartmann & Neukum (2001)
100 m
1 km
10 km
100 km
Diameter

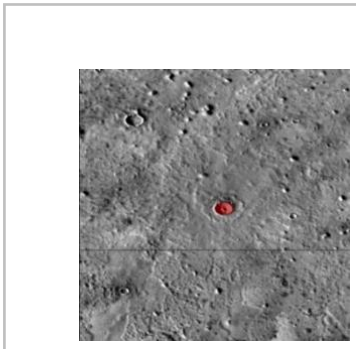

c)

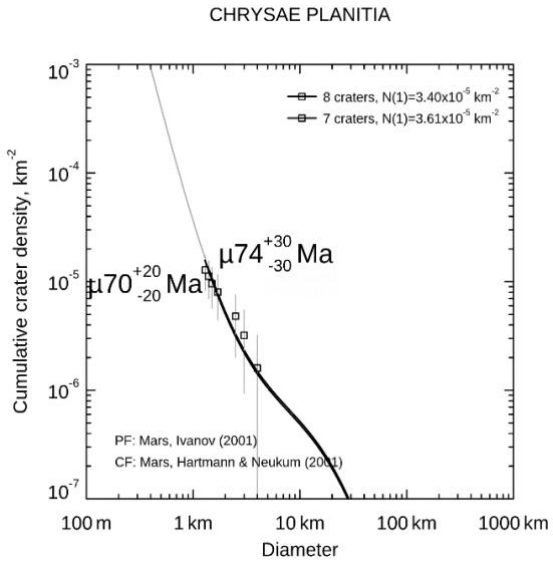
CHRYSAE PLANITIA
Cumulative crater density, km-2
8 craters, N(1)=3.40x10-5 km-2
7 craters, N(1)=3.61x10-5 km-2
μ74+30-30 Ma
μ70+20-20 Ma
PF: Mars, Ivanov (2001)
CF: Mars, Hartmann & Neukum (2001)
100 m
1 km
10 km
100 km
1000 km
Diameter

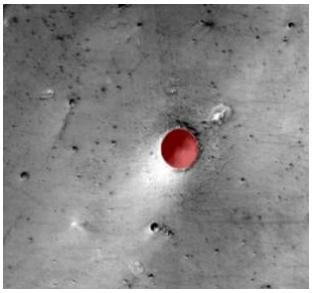

d)

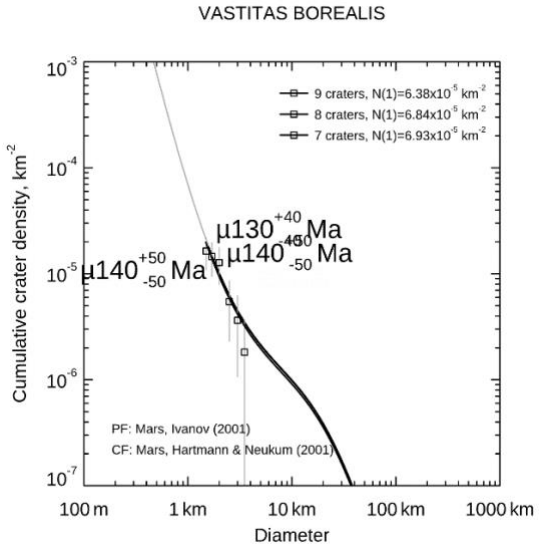
VASTITAS BOREALIS
Cumulative crater density, km-2
9 craters, N(1)=6.38x10-5 km-2
8 craters, N(1)=6.84x10-5 km-2
7 craters, N(1)=6.93x10-5 km-2
μ130+40-40 Ma
μ140+50-50 Ma
μ140+50-50 Ma
PF: Mars, Ivanov (2001)
CF: Mars, Hartmann & Neukum (2001)
100 m
1 km
10 km
100 km
1000 km
Diameter

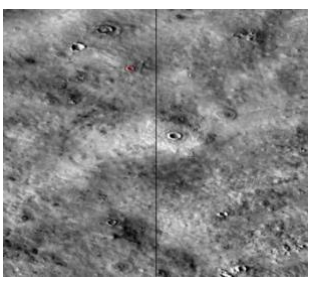

e)

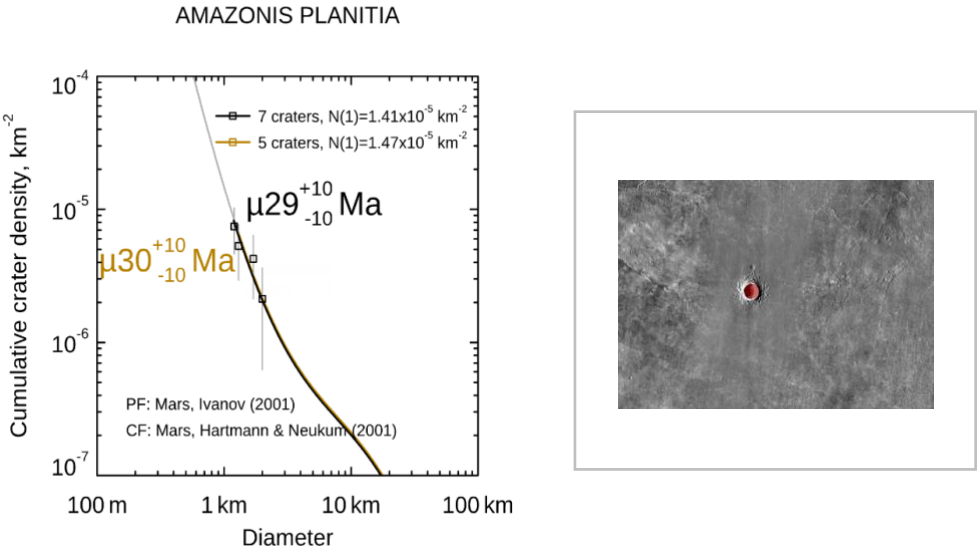
AMAZONIS PLANITIA
7 craters, N(1)=1.41x10-5 km-2
5 craters, N(1)=1.47x10-5 km-2
μ29+10-10 Ma
μ30+10-10 Ma
PF: Mars, Ivanov (2001)
CF: Mars, Hartmann & Neukum (2001)
Cumulative crater density, km-2
Diameter
100 m
1 km
10 km
100 km

f)

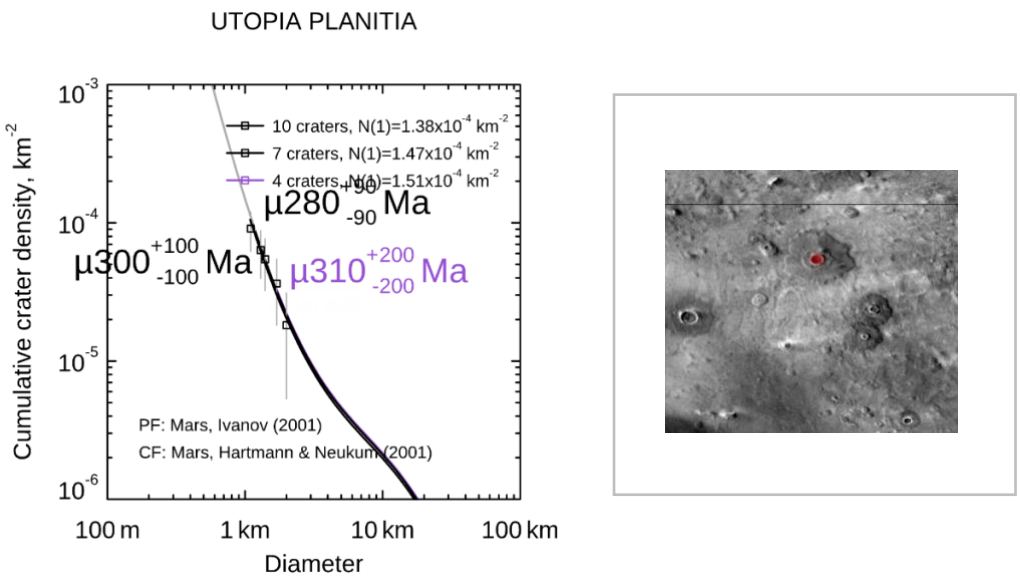
UTOPIA PLANITIA
10 craters, N(1)=1.38x10-4 km-2
7 craters, N(1)=1.47x10-4 km-2
4 craters, N(1)=1.51x10-4 km-2
μ280+90-90 Ma
μ300+100-100 Ma
μ310+200-200 Ma
PF: Mars, Ivanov (2001)
CF: Mars, Hartmann & Neukum (2001)
Cumulative crater density, km-2
Diameter
100 m
1 km
10 km
100 km

g)

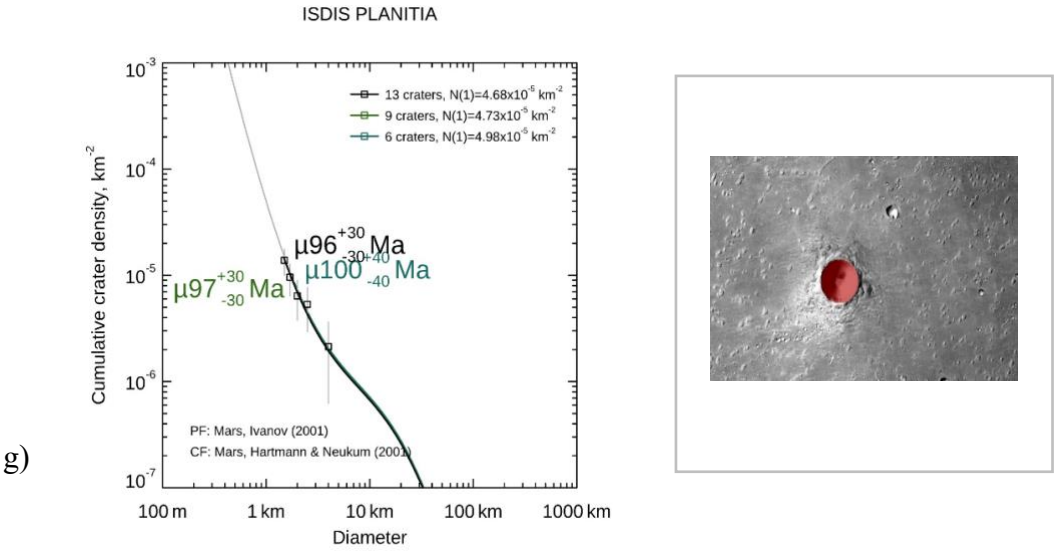
ISDIS PLANITIA
13 craters, N(1)=4.68x10-6 km-2
9 craters, N(1)=4.73x10-5 km-2
6 craters, N(1)=4.98x10-5 km-2
μ96+30-30 Ma
μ100+40-40 Ma
μ97+30-30 Ma
PF: Mars, Ivanov (2001)
CF: Mars, Hartmann & Neukum (2001)
Cumulative crater density, km-2
Diameter
100 m
1 km
10 km
100 km
1000 km

Figure. 11 Representation of post events in the Martian lowlands. Each planitias of northern lowland are represented in the Craterstat, indicating the time of ocean disappearance. a) Acidalia Planitia, b) Arcadia Planitia, c) Chrysae Planitia, d) Vastitas Borealis Formation, e) Amazonis Planitia, f) Utopia Planitia, g) Isdis Planitia

4.2 WHAT HAPPENED TO THE NORTHERN OCEAN?

Significant volume of liquid water was required to generate the observed geologic units, regardless of the timing, episodicity or duration of ocean activity. The water from the northern plain can be eliminated by several factors – shallow infiltration and storage as lenses of ice, deep subsurface infiltration, evaporation or sublimation and eventual loss to space by dissociation and atmospheric escape.

The current Martian atmospheric pressure and temperature can evaporate or freeze a large body of standing water. Also, water from the subsurface could easily be freeze before it evaporates. The fate of water is dependent upon the climatic conditions, where the water might be permanently lock in cryosphere or left and lost to spaces.

4.3 DISCUSSION AND IMPLICATIONS

Our approach focuses on the Martian Ocean and its evolution. The formation of this primordial ocean was an unavoidable result of Mars' huge water inventory and the hydraulic and thermal conditions assumed to have occurred during the first billion years of its history. The freezing solid and subsequent assimilation of the resulting frozen ocean, a rise in the global groundwater table, and the catastrophic breakout of groundwater and reflooding of the northern lowlands during the Hesperian would be natural consequences of the evolution of the post-Noachian climate and heat flow. The details would depend on the unique climatic circumstances existing in the Late Noachian, but the evolution of this hypothetical northern lowlands' ocean following its freezing would follow the same patterns and timelines as those stated for the Hesperian. The frozen Noachian-aged Ocean deposits that are now thought to be buried beneath the Upper Hesperian Vastitas Borealis Formation and the Lower Hesperian ridged plains may yet be preserved.

From the obtained result we could confirm that an ocean existed in the northern lowlands during the Hesperian age. This ocean had gone through various phases – formation of outflow channels, warm ocean phase, freezing of ocean, later constituting a frozen ocean, sublimation and loss to space. Formation of extensive craters in the northern lowland were generally >5 km, were ended about 3.4 to 3.7 Ga, can be assumed as the time of occurrence of Martian Ocean. A progressive change in the northern plain occurred in 3.1 to 2.8 Ga can be considered as younger units. This implies a gradual water retreat or other resurfacing processes. Craters present on the Amazonis Planitia can be compared with the other Planitia, as this region denotes the youngest surface where no resurfacing occurred. So, the disappearance of Martian Ocean can be more precisely associated with Amazonis Planitia. Presence of polygonal fracture in Utopia and Acidalia Planitia are consistent with the existence of a postulated water or ocean in the northern lowlands. These dates are compatible with the latest time period projected for any form of Martian Ocean to exist.

CHAPTER V

CONCLUSION

Summarizing the results from our investigation, we conclude that the northern hemisphere of Mars, which was reshaped after the LHB had an ancient ocean. The Noachian climate enhanced the hydrologic cycle, which eventually formed a Hesperian Ocean. The age of ocean is constrained to be mid–Hesperian i.e., 3.5 Ga, where huge outflow activity and large body of standing water existed. Towards the end of Hesperian, the water from the plains evaporated. This activity of ocean is determined by crater counts that describes the age of Martian Ocean to be about 3.6 to 3.1 Ga, whereas vaporisation of ocean took place at the end of the Hesperian period. The latest crater counts on the planitias can be considered as the recent activity occurred on the northern plains. This crater counts implies the latter processes that happened on the surface of Mars. The age obtained from the fresh crater count of each Planitia indicate fewer resurfacing activities, specifically Amazonis Planitia, where its latest age obtained is 30 Ma. Presence of polygonal terrain in Utopia and Acidalia Planitia shows an evidence of ocean vaporisation. So, we can round off that the derived ages from different planitias on the northern lowland implies prevailed ocean that existed can typically be about 3.2 Ga and the timeline of disappearance of ocean can standardly concluded around 160 Ma.

VI. References

1. Alberto.G.Fairen, & James M Dohm. (April 2004). Age and origin of the lowlands of Mars. *Icarus*, pages277-284.

2. Baker, V. R. (12 July 2001). *Water and the martian landscape.* Nature volume 412, pages228–236 (2001).

3. Carr, M. H. (01 June 2001). Martian oceans, valleys and climate. *Oxford Academic*, Astronomy & Geophysics, Volume 41, Issue 3, June 2000, Pages 320–326.

4. E.Arvidson, R. (July 1974). Morphologic classification of Martian craters and some implications. *Icarus*, 264-271.

5. G.K.Benedix, A. Lagain, K.Chai, S.Meka, S. Anderson, C.Norman, . . . M.C.Towner. (20 February 2020). Deriving Surface Ages on Mars Using Automated Crater Counting. *Earth and Space Science*.

6. H.Rickmann, M.I.Blecka, J.Gurgurewicz, U.G.Jorgensen, E.Slaby, S.Szutowicz, & N.Zalewska. (February 2019). Water in the history of Mars: An assessment. *Planetary Science and Space*, 70-89.

7. III, J., Mikhail.A.Kreslavsky, & Stephen Pratt. (29 January 2002). Northern lowlands of Mars: Evidence for widespread volcanic flooding and tectonic deformation in the Hesperian Period. *Journal Of Geophysical Research*.

8. Ingrid.J.Daubar, C.Atwoodstone, S.Byrne, A.S.McEwen, & P.S.Russell. (10 November 2014). The morphology of small fresh craters on Mars and the Moon. *JGR Planets*.

9. James.C.Pechmann. (May 1980). The origin of polygonal troughs on the Northern Plains of Mars. *Icarus*, 185-210.

10. K.L.Tanaka, J.A.Skinner Jr, T.M.Hare, T.Joyal, & A.Wenker. (30 April 2003). Resurfacing history of the northern plains of Mars based on geologic mapping of Mars Global Surveyor data. *Journal of Geophysical Research*.

11. M.R.Salvatore, & P.R.Christensen. (16 October 2014). On the origin of the Vastitas Borealis Formation in Chryse and Acidalia Planitiae, Mars. *JGR Planets*, 2437-2456.

12. Maria.T.Zuber. (28 March 2018). Oceans on Mars formed early. *nature*.

13. Michael Manga, Douglas.J.Hemingway, & Robert I.Citron. (19 March 2018). Timing of oceans on Mars from shoreline deformation. *nature 555*, 643-646.

14. Michel.H.Carr, & James .W.Head III. (June 2010). Geologic history of Mars. *Earth and Planetary Science Letters*, 185-203.

15. Michel.H.Carr, J. W. (20 May 2003). Oceans on Mars: An assessment of the observational evidence and possible fate. *Journal of Geophysical Reaserch Planet.*

16. Mikhail.A.Ivanov, H.Hiesinger, G.Erkeling, & D.Reiss. (15 January 2014). Mud volcanism and morphology of impact craters in Utopia Planitia on Mars: Evidence for the ancient ocean. *Icarus*, 121-140.

17. Mikhail.A.Kreslavsky, & James.W.Head. (07 December 2002). Fate of outflow channel effluents in the northern lowlands of Mars: The Vastitas Borealis Formation as a sublimation residue from frozen ponded bodies of water. *Journal of Geophysical Research*, 4-1-4-25.

18. Nadine.G.Barlow. (01 May 2010). What we know about Mars from its impact craters. *GSA Bulletin*.

19. Parker, T. J., & Bruce.G.Bills. (28 May 2021). Chapter 3 - Mars northern plains ocean. *Mars Geological Enigmas*, 41-59.

20. Parker, T., Donn.S.Gorsline, R. Stephen Saunders, David.C.Pieri, & Dale.M.Schneeberger. (25 June 1993). Coastal geomorphology of the Martian northern plains. *Journal of Geophysical Research*, Pages 11061-11078.

21. S.M, C., & T.J., P. (December 2001). *The Evolution of the Martian Hydrosphere.* American Geophysical Union, Fall Meeting 2001, abstract id.P12E-04.

22. Stephen.M.Clifford, & Timothy.J.Parker. (November 2001). *The Evolution of the Martian Hydrosphere: Implications for the Fate of a Primordial Ocean and the Current State of the Northern Plains.* Science Direct.

23. Turber, M., & F.Forget. (05 April 2019). *The paradoxes of the Late Hesperian Mars ocean.* Scientific Reports 9, Article number: 5717 (2019) .

24. Nadine.G.Barlow. (August 1988). Crater size-frequency distributions and a revised Martian relative chronology. *Icarus*, 285-305.

25. Srivastava, N., & Indhu Varthrajan. (January 2013). Crater Chronology: A tool for planetray surface dating. *Planex*.

PETROGRAPHY AND FLUID INCLUSION STUDIES IN METAPELITES OF COORG AND MERCARA, SOUTHERN GRANULITE TERRAIN, SOUTHERN INDIA

Project report submitted to the Christ College (Autonomous), Irinjalakuda, affiliated to University of Calicut, in partial fulfilment of the degree of

Master of Science in Applied Geology

Submitted By

Rahul Raj R

Reg. No. CCAVMAG012

2021-2023

Under the Supervision of,

Dr Amaldev .T

Assistant Professor

Department of Marine Geology and Geophysics

Cochin University of Science and Technology

Kochi-16, Kerala

DEPARTMENT OF GEOLOGY AND ENVIRONMENTAL SCIENCE

CHRIST COLLEGE (AUTONOMOUS), IRINJALAKUDA, KERALA, 680125

(Affiliated to University of Calicut and re-accredited with by NAAC with A++)

AUGUST 2023

DECLARATION

I, Rahul Raj R., student of MSc. Applied Geology, Department of Geology and Environmental science, Christ College (Autonomous) Irinjalakuda, Kerala, have completed my dissertation work entitled "Petrography and Fluid Inclusion Studies in Metapelites of Coorg and Mercara, Southern Granulite Terrain, Southern India". This work is solely based on the research work carried out by me from 9th May 2023 to August 10th, 2023, under the guidance of Dr. Amaldev T., Assistant Professor, Department of Marine Geology and Geophysics, Cochin University of Science and Technology, Lakeside Campus, Kochi-16. No part of the report is reproduced from other resources. All information included from other sources has been duly acknowledged. I maintain that if any part of the report is found to be plagiarized, I shall take full responsibility for it.

Place: Irinjalakuda — Rahul Raj R

Date: — Reg. No. CCAVMAG012

CERTIFICATE

This is to certify that the thesis entitled ***"Petrography and Fluid Inclusion Studies in Metapelites of Coorg and Mercara, Southern Granulite Terrain, Southern India"*** *was the work done by Mr. Rahul Raj R (Reg No. CCAVMAG012), MSc. Applied Geology, Department of Geology and Environmental science, Christ college (Autonomous) Irinjalakuda during the period 9th May 2023 to August 10th, 2023, at School of Marine Science, Cochin University of Science and Technology, Kochi-16, Kerala. The work was carried under my supervision in partial fulfillment of requirement for the award of degree of Master of Science in Applied Geology during the academic year 2021-2023 of Christ college (Autonomous) Irinjalakuda, Kerala.*

Dr Resmy K J

Internal Supervisor

Dr Anto Francis K

Co-ordinator

Department of Geology and

Environmental Science

Christ College (Autonomous) Irinjalakuda

Kerala-680125

Place : …….

Date : ……..

External Examination

1. ……

2. ……

ACKNOWLEDGEMENT

I am grateful to my supervisor Dr. Amaldev T, Assistant Professor, Department of Marine Geology and Geophysics, Cochin University of Science and Technology, Kochi-16, for the guidance, constant encouragement and for providing invaluable time, data and facilities that enable me to successfully complete my project.

I convey my sincere sense of gratitude to the Head, Department of Marine Geology and Geophysics, Cochin University of Science and Technology, Kochi-16, for providing necessary facilities required for the research work. I express my sincere gratitude to Dr. Resmy K.J Assistant professor Christ College (Autonomous) Irinjalakuda, Kerala, for her guidance and support. I express my heartfelt gratitude to Dr. Linto Alappat, Head of the Department, Department of Geology and Environmental science, Christ College (Autonomous) Irinjalakuda, for his guidance and valuable support throughout the work.

My heartfelt thanks to Mr. Rajkumar P.B, Research scholar, Department of Marine Geology and Geophysics, School of Marine Science, CUSAT, Kochi-16 for his technical help and necessary supports throughout my work. I would like to thank all the staff members of CUSAT for their support during the project. My sincere gratitude to all my teachers and staff members of the Department of Geology and Environmental science, Christ College (Autonomous) Irinjalakuda for their encouragement and help throughout the course of work.

I acknowledge my sincere gratitude to DST-SERB, Govt of India for financially supporting the work through the Scientific Social Responsibility Scheme of the funded project (File No.EEQ/2021/000992) "High-pressure granulites in the Archean crustal blocks of Southern Granulite Terrain, southern India" implementing in the Department of Marine Geology and Geophysics, Cochin University of Science and Technology.

Last but not the least, I would like to thank my family and friends for supporting me and for being by side in all ups and downs. I ascribe millions of gratitude to the Almighty for the abundant blessing poured upon me.

TABLE OF CONTENTS

LIST OF FIGURES

LIST OF TABLE

ABSTRACT

The Southern granulite terrain (SGT) is a classical granulite terrain in the world for the deep crustal studies and Archean tectonics. SGT is separated from Dharwar craton by Fermor line also known as orthopyroxene isograde, the transition of Amphibolite facies to granulite facies metamorphism from north to south. The Southern granulite terrain is categorized into several tectonic blocks, when moving from north to south, these blocks are named as follows: Coorg Block, Nilgiri Block, Salem Block, Madras Block, Madurai Block, Trivandrum Block (referred to as the Kerala Khondalite belt), and Nagercoil Block. These blocks are dissected by various major Proterozoic shear/suture zones, including the Mercara suture zone (MSZ), Moyar-Bhavani shear zone (MBSZ), Salem-Attur shear zone, Palghat-Cauvery suture zone (PCSZ), and Achankovil suture zone (ACSZ) and different minor shear zones. Apart from this the Coorg block of southern granulite terrain is one of the oldest blocks, which is renowned for its Mesoarchean magmatic rocks and is considered the oldest crustal block in the SGT. Studies reviled as Coorg block is an exotic microcontinent which is sandwiched between western Dharwar craton in the north and Neo-Archean-Proterozoic crustal blocks in the south.

The present study relies on field investigation, petrography and fluid inclusion analyses of rock samples of metapelites collected from different localities in and around Coorg block and Mercara shear zone. Field investigation and petrographic studies provides critical information's to the metamorphic processes subsequent to various tectonic activities emplaced in the region. Microthermometric studies reveals the presence of pseudosecondary type inclusions which is identified as CO_2 type fluid, indirectly indicating the dry nature and peak granulite metamorphism occur along the Coorg and Mercara.

CHAPTER 1

INTRODUCTION

1.1 GENERAL INTRODUCTION

Gondwana is also known as 'Gondwanaland' was a super continent which was formed during the breaking apart of earlier super continent Rodina. Gondwanaland which consists the landmasses that make up the present-day continents of South America, Africa, Antarctica, Australia, and the Indian subcontinent. These landmasses were once connected as part of Gondwana but later drifted apart due to the tectonic movement. Indian subcontinent covers approximately 5,000,000 sq.km. The geological history of Indian subcontinent is incredibly diverse and spans over billions of years, resulting in a wide variety of landforms, mineral resources, and geological hazards. Landforms includes Himalayan-mountain system, northern plains, peninsular plateau, Indian deserts and coastal region. Apart from this Indian subcontinent which comprises major craton blocks such as Aravalli, Bundelkhand, Singhbhum, Bastar, Eastern Dharwar and Western Dharwar cratons. Cratons are the oldest and tectonically most stable part of the continental crust which is large and relatively flat landforms which consists thick layers of Precambrian rocks. Cratons were intruded by various age granitoids, mafic dykes and ultramafic bodies.

Apart from these cratons there is a high-grade metamorphic terrain below the Dharwar cratons which is called the Southern Granulite terrain (SGT) in the bottom of the peninsular India. The southern granulite terrain is separated from Dharwar craton by Fermor line which is also called orthopyroxene isograd. Here we can see the transition of Amphibolite facies to granulite facies metamorphism across the Fermor line from north to south. In early time it is believed that SGT is a part of Dharwar cratons, but the petrographic and geochemical study of recent decades shows the lithological variation and change in the metamorphic grade of rock form Dharwar to Southern granulites. In Dharwar, two distinct facies of metamorphism are observed: Greenschist and Amphibolite facies. However, below the Fermor line, the metamorphic grade in the SGT increases significantly, reaching the Granulite facies. This indicates that the metamorphic rocks in the Southern Granulite Terrain were formed under high-grade pressure and temperature conditions. Underplated mafic magmas are the heat source of many high grade metamorphic terrane (Bohlen and Mezger, 1989). The Southern granulite terrain is categorized into several tectonic blocks, when moving from north to south, these blocks are named as follows: Coorg Block, Nilgiri Block, Salem Block, Madras Block, Madurai Block, Trivandrum Block

(referred to as the Kerala Khondalite belt), and Nagercoil Block. These blocks are dissected by various major Proterozoic shear/suture zones, including the Mercara shear zone (MSZ), Moyar-Bhavani shear zone (MBSZ), Salem-Attur shear zone, Palghat-Cauvery suture zone (PCSZ), and Achankovil suture zone (ACSZ) and different minor shear zones.

Petrology involves studying the petrography and petrogenesis of different rocks formed under varying conditions. Metamorphic petrology, a branch of petrology, focuses on the comprehensive examination of mineralogical and textural alterations in precursor rocks. Metamorphism is predominantly regional and typically occurs in the deeper segments of orogenic belts. The grade of metamorphic rocks varies depending on how much of temperature and pressure they experience. In Eskola's classification the granulite facies rocks are formed under high pressure and high temperature metamorphism. The granulite mobile belts are distinguished by a wide range of rock types, including charnockite, layered mafic complexes, and quartzo-feldspathic gneisses, among others. These terrains comprise diverse suites of both mafic and felsic rocks. Studies of those metamorphic terrains are usually concentrated in four general areas such as (i)Thermometry and Barometry (ii) The nature and composition of fluids (iii) Geochemical and Geochronological studies (iv) Tectonic modeling based on the field relationship-petrography-mineral reaction textures- pressure temperature- dating data.

Fluid inclusion studies are a crucial aspect of geology and mineralogy that focus on investigating the tiny pockets of fluid trapped within minerals, known as fluid inclusions. These inclusions can contain various substances, such as water, hydrocarbons, or gases, and provide valuable information about the geological processes that occurred during the formation and evolution of rocks and minerals. Depending on the timing of the formation of inclusion in the crystals they are classified as primary, secondary and pseudo-secondary. The inclusions occur as isolated, clustered and trail bounds. It decode the temperature, pressure, salinity, density, depth of trapping, composition and evolution of fluids that were present in Earth's crust throughout geological history. The information obtained from fluid inclusion studies is essential for understanding geological processes such as ore formation, metamorphism, and the evolution of hydrothermal systems. Additionally, these studies play a crucial role in mineral exploration and resource assessment, as they can provide insights into the geological history and potential mineral deposits in a given

area. Geologists and mineralogists considered as valuable tool for to unlock the secrets of Earth's history and better understand the processes that shaped our planet over millions of years.

The current study focuses on the Coorg block, one of the oldest blocks within the Southern Granulite Terrain (SGT). This block is renowned for its Mesoarchean magmatic rocks and is considered the oldest crustal block in the SGT. Unlike the surrounding blocks, the Coorg block lacks the later Neoarchean tectono-thermal imprints (Santosh et al., 2015). Previous research has suggested that the Coorg block is a higher-grade Southern extension of the Western Dharwar craton and Biligiri Rangan hills. Granulite facies rocks dominate the Coorg block, forming massive areas of significant extent (Asha Manjari and Malur, 1997). While the Dharwar Craton and many crustal blocks in the Southern Granulite Terrain have been extensively studied in recent years, there is very limited information available about the Coorg block and the nearby shear zones, especially in the area of fluid inclusion. Identification of entrapped fluids during the formation of high pressure granulite or the post deformation process using fluid inclusion studies is a tool to extract more information about Coorg block and framing the tectonic history.

1.2 SOUTH INDIAN GEOLOGY

Southern India has a complex geological history, which has fascinating geological features developed by various tectonic and orogenic activates over millions of years. The southern region of peninsular India is primarily composed of the Dharwar craton and Southern granulite terrains. Geologists worldwide have a significant interest in the Archean cratons and Archean crustal blocks within this area. Their primary focus is to investigate the correlation between crust-mantle interactions and the evolution of ancient continental crust.

1.2.1 Dharwar Craton

Cratons are stable portions of the Earth's crust which remains relatively stable and unchanged for long periods of time. Dharwar craton is one of the oldest cratons in the earth which is mainly dominated by TTG's (Tonalite-Trondhjemite-Granodiorite) and various rock types including younger granites and granitic gneisses. Basement of Dharwar cratons is of Tonalite-Trondhjemite-Granodiorite (TTG) groups of rock, which is the oldest

group of rocks in India about 4.1 billion years old rocks. Dharwar craton is one of the important Precambrian greenstone-granite terrain (Swaminath et al., 1976) among the cratonic blocks of peninsular Indian shield.

The Dharwar craton is divided into two tectonic blocks, Western Dharwar craton and Eastern Dharwar craton. These two cratons are separated by Chitradurga shear zone and Closepet granite. The Dharwar craton is bounded on the north by Proterozoic sedimentary rock and Deccan traps and towards east it is bounded by Eastern Ghat mobile belts and west it is Arabian Sea, south is of Southern Granulite Terrain. The division of the eastern and western Dharwar cratons are based on the abundance of Archean Greenstones, as well as the age of surrounding basements and also the degree of regional metamorphism.

The Archean Tonalitic-Trondhjemitic-Granodioritic Gneisses are found throughout the Western Dharwar craton. It is bounded on the east by Eastern Dharwar craton and to the west by Arabian Sea, the northern boundary is buried under the younger sediments and Cretaceous Deccan trap and south by Southern granulite terrain. The Western Dharwar shows an increase in regional metamorphic grade from greenschist to amphibolite in the north and granulite facies in the south. Generally shows intermediate pressure (kyanite-sillimanite type) metamorphism. Mostly comprise of ultramafic to mafic volcanic rock. Western Dharwar craton is occupied by vast area of peninsular gneiss. The western crustal block is collectively called Peninsular gneiss, these gneissic complexes were interlayered and then overlayed with volcano-sedimentary greenstone sequences and contain patches of stratiform Gabbro-Anorthosite complexes (Swami Nath et al., 1976). According to earlier studies two generations of greenstone volcanism and plutonism have happened in the Western Dharwar craton.

The Eastern Dharwar Craton is bounded to the north by the Deccan Traps and the Bastar Craton, to the east by the Cuddapah basin and Eastern Ghats Mobile Belt, and to the south by the Southern Granulite Terrain (Balakrishnan et al., 1987) and west by Western Dharwar. Based on the lithology and ages of rock units Eastern and Western Dharwar are separated. The craton is composed of the Dharwar Batholith (dominantly granitic), greenstone belts, intrusive volcanics, and middle Proterozoic to more recent sedimentary basins. Eastern Dharwar is relatively younger than the Western Dharwar craton and the metamorphic grade generally increases from west to east. This increase in metamorphic

grade from west to east is a result of the tectonic history of the region. Different geological processes, including regional metamorphism, have affected the rocks over time, leading to the observed variation in metamorphic grades across the Dharwar craton.

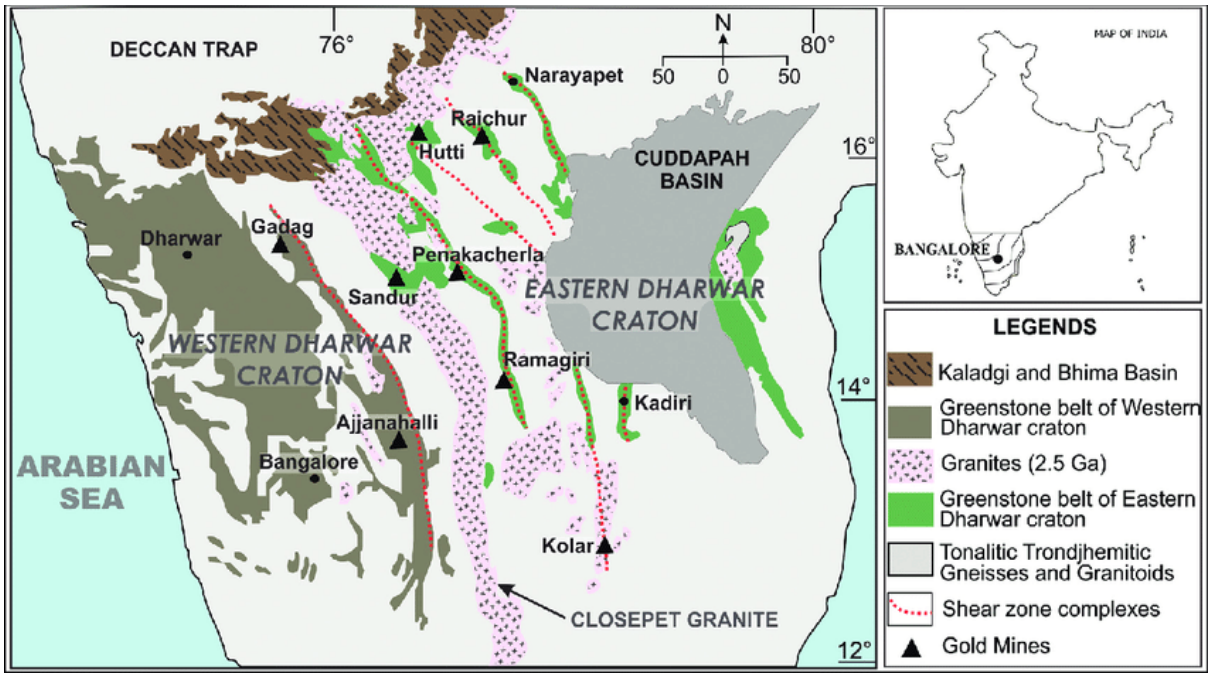

Figure 1 | Regional geology and tectonic framework of Dharwar craton (Manikyamba et al., 2004).

1.2.2 Southern Granulite Terrain

The Southern Granulite Terrane is the wedge shaped southern termination of Peninsular India, is a mosaic of several crustal blocks (Santosh. 2019), which is characterized by a unique assemblage of rocks known as granulite's, which are high-grade metamorphic rocks formed under high temperature and high pressure conditions and is one of the few terrains in the world that has preserved Archean and Proterozoic crust with extensive high grade granulite facies rock. The SGT is adjacent to the Dharwar cratons in the northern region. As one moves from north to south in this geological region, the metamorphic grade progressively intensifies, transitioning from Amphibolite to granulite facies. This transformation is demarcated by the Fermor line, also known as the ortho pyroxene (OPX) isograd, serving as a significant boundary that indicates the shift in metamorphic grade within the area. Also this is the largest exposed Precambrian deep continental crust consisting of multiply deformed Archean and Neoproterozoic high grade metamorphic rock.

Petrographically Southern Granulite Terrain is characterized by granulite facies rocks such as Charnockite, Khondalite, Mafic granulites, Meta gabbro, Meta pyroxenite, Metapelites and various types of Gneisses and Migmatites. These rocks are characterized by their medium to coarse-grained texture, displaying bands or foliated patterns. They predominantly consist of major minerals like quartz, feldspar, kyanite, sillimanite and mafic minerals such as amphibole and pyroxenes.

The formation of the Southern Granulite Terrain is associated with the collision and amalgamation of various crustal blocks during the Mesoarchean-NeoProterozoic-Cambrain periods. Generally Southern granulite terrain is divided into series of tectonic blocks with distinct protolith origins and tectono-thermal histories. From north to south they are Coorg Block, Nilgiri block, Salem Block (Sometimes called northern granulite terrain), Madras Block, Madurai Block, Trivandrum Block (also known as Kerala Khondalite belt) and Nagercoil Block. These terrains are dissected by Proterozoic shear/suture zones such as Mercara shear zone (MSZ), Moyar-Bhavani shear zone (MBSZ), Salem-Attur shear zone Palghat-Cauvery suture zone (PCSZ) and Achankovil suture zone (ACSZ). The terrain blocks are separated on the basis of age, rock type and major shear/suture zones. From north to south of SGT, the age of rocks decreases from Paleoarchean to Neoproterozoic. Above Palghat-Cauvery suture zone, age of the rocks are mostly of Archean when compared to south Madurai block. Charnockite is the dominant rock type in most of the crustal blocks of the SGT.

COORG BLOCK

From the recent studies, Coorg block is an exotic microcontinent which is sandwiched between Western Dharwar craton in the north and Neo-Archean – Proterozoic crustal blocks in the south. Form the detailed studies this block is bounded on the north by Mercara suture and south by western extension of Moyar suture zone. Coorg block is the oldest crustal block in SGT which mainly consists of Mesoarchean magmatic rocks includes Charnockites, gneisses, mafic granulites and TTG's (Tonalite-Trondhjemite-Granodiorite). High pressure-Ultra high temperature metapelitic and mafic rocks are also present in Coorg block and adjoining suture zones. The oldest charnockites in the SGT is from Coorg block and it dominantly composed of hypersthene, biotite, K-feldspar, plagioclase, ilmenite and minor garnets. Previous studies considered the Coorg block is higher

grade Southern extension of the Western Dharwar craton and Biligiri Rangan hills. However Santosh et al, 2015 reported Coorg block is an exotic crustal entity might be fragment of any microcontinent and interestingly the Coorg block lacking later Neoarchean tectonothermal imprints common in the surrounding blocks of SGT.

NILGIRI BLOCK

The Nilgiri Block is considered as a deep crustal exposure (~35 km), thrusted over the Dharwar Craton between 2700 to 2500Ma ago **(**Janardhan et al., 1994; Raith et. al., 1999; Samuel et al., 2014). This triangular block composed of medium to coarse grained late Archean charnockites, kyanite gneiss, quartzite and gabbroic to anorthositic pyroxinites, (Raith et al., 1999). The southern part of the block is mainly consist of charnockites. An abundance of mafic granulites/metagabbros, pyroxene granulites, amphibolites and pyroxenites towards the northern portion of the block is well established (Raith et al., 1999; Samuel et. al., 2014). A geochemical and isotope study by Samuel et al. (2014) confirms that Neoarchean arc magmatism led to the formation of massif charnockites and mafic-ultramafic rocks in this terrane. All the rocks are associated with Archean magmatic suites. Nilgiri block is bounded on the north and south by Moyar- Bhavani shear zone and is wedged between the segments of the Palghat-Cauvery shear zone.

SALEM BLOCK

The Salem block, also known as the Northern block, is located at the southern edge of the Dharwar craton. It is bounded by the Fermor line to the north and the Palghat Cauvery shear zone to the south. Within the Salem block, we can find various types of rocks, such as Charnockites, mafic granulites, granite gneisses, and migmatites. It is probable that these northern granulites are the metamorphosed equivalent of the Dharwar craton as the boundary between the two is progressive with no distinct lithological or tectonic contact (Fermor, 1936; Janardhan et al., 1982: Mojzsis et al., 2003: Hansen and Harlov, 2007).

MADRAS BLOCK

The Madras Block is located above the eastern margin of the Palghat-Cauvery suture zone. It is predominantly composed of charnockites and gneisses. The block is inter-

sected by the eastern extension of the Salem-Attur shear zone. The geological features in the area include broad doming, complex folding, and significant variations in hinge lines. These geological phenomena are a result of Neoproterozoic-Ordovician suturing along the Palghat Cauvery, extending beyond the Madras (Chetty and Rao, 2006). Retrograde amphibolite facies rocks appear at the boundaries of the shear zone (Santosh et al., 2002).

MADURAI BLOCK

Madurai block is the largest block of Southern granulite terrain bounded on the north by Palghat Cauvery suture zone and south by Achankovil shear zone. From west to east age of Madurai block decreases from Neoarchean to Paleoproterozoic. Karur-Kambam- Painavu–Trichur (KKPT) is a Neoproterozoic shear zone passing through the northern region Madurai block, which act as a boundary between Neoarchean and Paleo-proterozoic rocks of Madurai block. Charnockite massifs are present widely on the west-ern region of Madurai block, the presence of sapphirine- spinel – quartz which represent ultrahigh temperature and metamorphism on these bodies. The eastern region of Madurai block consists of gneiss and its related Meta sedimentary rocks. Southern parts of Madurai block present Mesoproterozoic to Neoproterozoic rock assemblages. Charnockite present in the block is mainly coarse to medium grained (Santosh et al., 2009), along with it char-nockites, granites and migmatite gneisses are also concentrated. The Madurai granulite block can be lithologically divided into a western region and an eastern region; Madurai block in Kerala (MBK) and Madurai block in Tamil Nadu (MBTN) (Cenki and Kriegsman, 2005). Based on recent studies Madurai block is amalgamated on the south of Salem block during late Neo Proterozoic – Cambrian time, along with Palghat-Cauvery suture zone (PCSZ) which is consider as the final amalgamation of the Gondwana supercontinent (Santosh et al., 2009, Collins et al., 2014, Li et al., 2016).

TRIVANDRUM BLOCK

Trivandrum block is at the southern end of SGT, which is separated from Madurai block by Achankovil shear zone. Trivandrum block is also known as Kerala Khondalite Belt (KKB), because of the presence of garnet-cordierite-sillimanite gneisses (Khondalites), which shows Ultra High Temperature (UHT) condition. They are granulite facies metapelites. Also this tectonic block is dominated by metasedimentary rocks consists the

presence of garnet-orthopyroxene granulites, garnet biotite gneisses, calc silicates etc. Protoliths of metasedimentary gneisses of Trivandrum block is aged between Neoarchean to Paleoproterozoic. The southern boundary of the Trivandrum Block is defined by the Nagercoil charnockite massif at the southern tip of the Indian Peninsula.

NAGERCOIL BLOCK

The Nagercoil block which is at the southern tip of Indian subcontinent. Dominated by Charnockite massifs, metapelites and felsic gneisses. Age spectra of zircons and monazites from the charnockites are similar to those from metasedimentary gneisses of the Trivandrum block (Santhosh et al., 2006c). Recent studies by Rajesh et al., (2011) the origin of charnockite is from granitic pluton that were the result of high temperature melting of hydrous basalt in a subduction setting. Only few studies are carried out to constrain the condition of metamorphism in the Nagarcoil block but they are assumed to be similar to those experiences by the adjoining Block (Santhosh et al., 2003a, 2006c).

Major Suture/Shear Zones in SGT

Mercara Suture Zone

Mercara shear zone is sandwiched between the Western Dharwar craton and the Coorg block in the Southern granulite terrain. It extending from western coast of south India and converging with Moyar suture zone (Amaldev et al., 2016). From the recent studies the extension of Mercara suture zone is about 100 km and width of 20-30km. Charnockites, gneisses, TTG (tonalite- trondhjemite-granodiorite), mafic granulites, kyanite-sillimanite bearing metapelites, metagabbro are the major rock types. Mercara suture zone act as a dividing boundary between Dharwar craton and Southern granulite terrain.

Moyar Bhavani Shear Zone

The Moyar shear zone (MSZ) is WNW-ESE trending shear zone having a length of 150km. It is bounded on the north by Coorg block and south by Nilgiri block. The Bhavani shear zone (BSZ) is NE-SW trending shear zone marking the southern boundary of Nilgiri block. Both Moyar and Bhavani shear zones merge at the Bhavanisagar, just below the Salem block. BSZ is also characterized by a zone of intense mylonitic fabrics, in turn overprinted by late brittle to brittle ductile structures with sheared gneisses of steeply dipping

with sparse sub-vertical stretching lineation's (Ghosh et al., 2004). The presence of Mylonitic gneiss and granitoids that shows the Neoproterozoic tectonothermal imprint on these shear zones.

Palghat Cauvery Suture Zone (PCSZ)

It is a suture zone that extent about 400 km in E-W trend on southern part of peninsular India. It having a maximum width of 10 km, which act as a suture between Madurai block and northern block. In other words it act as a boundary between Archean granulites rocks on the north and Neoproterozoic rocks on the south. PCSZ is consider as the major terrane boundary in the last stage of Gondwana amalgamation. This shear zone has been correlated with the Bongolava-Ranotsara shear zone (de Wit et al., 1998: Clark et al., 2019), the Madagascar axial high grade zone (Windley et al., 1994). Dominant rock types occurred along the suture zone includes, charnockites, migmatitic gneisses, metapelite, mafic granulites and minor occurrences of ultramafic and mafic rocks especially eclogites and gabbros. The rocks of PCSZ have been the subject of recent studies proposing that they experienced high pressure (> 15kbar) eclogite-facies metamorphism prior to UHT conditions during a single metamorphic cycle (Shimpo et al., 2006; Tsunogae and Santosh, 2006; Sato et al., 2009). Sapphirine plus quartz assemblages have been reported from the PCSZ that are the one of the more indicative assemblage of UHT metamorphism (Kelsey, 2008).

Achankovil Shear Zone

Achankovil shear zone is bounded between Madurai block in the north and Trivandrum block in the south. This shear zone having a trend of NW-SE having 120 km length and 50 km wide. Major lithology of Achankovil shear zone includes garnet-sillimanite- graphite bearing metapelites which is known as Khondalites, highly migmatized garnet-biotite gneisses, pyroxene granulites, calc – silicates rocks. This shear zone is considered by Naganjaneyulu and Santosh (2010) to be a continuation of the Bongolava – Ranotsara shear zone in Madagascar.

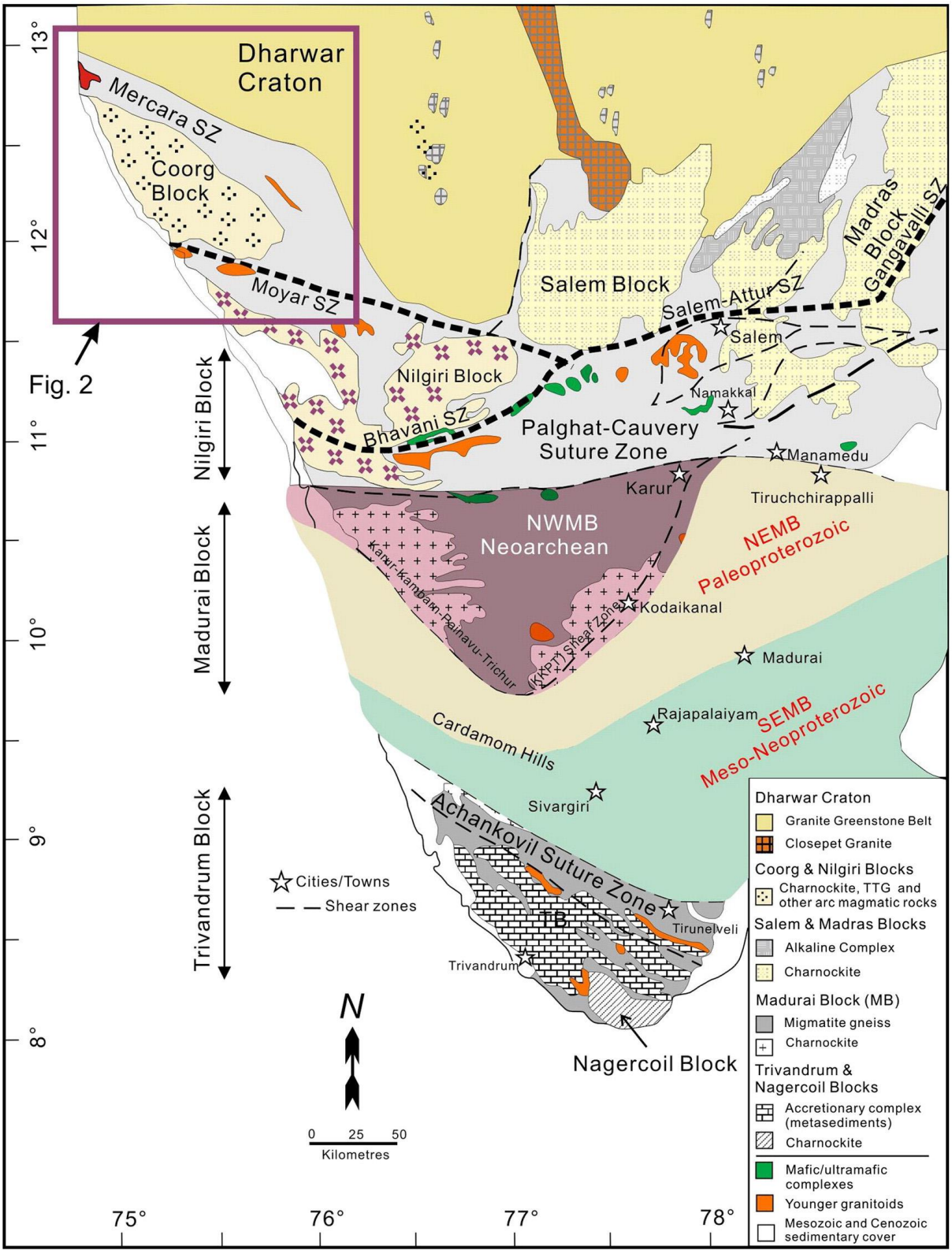

Figure 2| Generalized geological and tectonic framework of Southern India (after Collins et al., 2014; Santosh et al., 2015).

1.3 OBJECTIVES OF THE STUDY

The focus of current research is to extract petrological and fluid inclusion data from metapelites located in the Coorg block and Mercara suture zone, Southern Granulite Terrain, South India. This study comprises several objectives. Firstly, it search to gain an understanding of the lithological assemblage and petrographic characteristics of the Coorg block and Mercara, employing detailed geological mapping and systematic sample collection methods. Secondly, a detailed petrographic investigation will be conducted to analyse mineral phases and textural features, accompanied by the subsequent nomenclature of different rock samples through thin section analysis under a petrological microscope.

Furthermore, the research aims to identify entrapped fluids that occurred during the formation of high-pressure granulite or as part of the post-deformation process through fluid inclusion studies. Lastly, the study will involve the evaluation of the chemical and physical properties of fluid inclusions, this will include identification of nature, type and density of fluid by applying heating and homogenization techniques using a fluid inclusion stage. Overall this research provide valuable insights into the petrology and fluid dynamics of the Coorg block and Mercara shear zone, shedding light on their geological history and evolution.

1.4 Previous Studies

The Precambrian terrain of South India, often referred to as the Peninsular Shield, represents a geological treasure trove of diverse crustal blocks, each with a tectonic history spanning from the Archean to the Proterozoic era. These shields are demarcated by a series of significant shear and suture zones, further highlighting the complexity and evolution of the region's geological framework. On the south of Archean TTG-granite-greenstone provinces of the Dharwar craton, intensely metamorphosed granulite facies series of discrete crustal block are exposed, generally termed as Southern Granulite Terrain (SGT) which including Coorg, Nilgiri, Salem and Madras blocks, defined by the Fermor line (Drury et al., 1984). Coorg block in the southern granulite terrain is separated from the western Dharwar craton by Mercara suture zone and it is bounded south by WNW-ESE trending Moyar shear zone (MSZ) (Chetty et al., 2012). This block is the oldest

crustal block of SGT and also believed as the deepest exhumed crust on Indian peninsular (Raith et al., 1999). The Southern granulite terrain extended over 2×10^5 km^2 area, covering entirely the states of Tamil Nadu and Kerala and a small portion of Southern part of Karnataka. Crustal blocks of SGT separated by shear zones (Beckinsale et al., 1980; Drury et al., 1984). A number of prominent ductile shear zones and suture zones dissect the SGT. Shear zones having regional extension ranges from microscopic scale to few hundred kilometres. Those shear zones are important structural discontinuity surface in the earth crust and are highly deformed compared to surroundings. The remnants of subduction zones are the suture zones and those terrains are joined together are interpreted as the fragments of paleo continents and tectonic plates. Granulite rocks are well exposed throughout the SGT; except the linear stretches along the coasts where they are overlain by Mesozoic and Tertiary sedimentary formations. SGT comprises juxtaposed crustal blocks, which are fragmented and dismembered (Chetty et al., 2006). Palghat – Cauvery shear zones separates Southern granulite terrane from Northern granulite terrane. Nilgiri block in the northern region of SGT is a triangular shaped crustal province consisting mostly garnetiferous biotite gneiss, enderbitic granulites. It is sandwiched between Moyar shear in the north and Bhavani shear zone in the south. Samuel et al. 2014, defined that the Nilgiri block has been evolved through Neoarchean arc magmatism in a convergent margin. It is believed to be the deeply exhumed crust on the Indian peninsula after Coorg. The Madras block north of the Moyar–Bhavani shear zone, which evolved throughout the Precambrian Period mainly consists of high-grade metamorphic rocks (Poornachandra et al., 2006). Broad doming, complex folding, and extreme hinge line variation caused by Neoproterozoic-Ordovician suturing along the Palghat Cauvery extending beyond the Madras block (Chetty and Rao, 2006).The Madurai block is the largest crustal block in southern India, occurs immediately south of Palghat-Cauvery shear zone (PCSZ) and extends to the Achankovil within Madurai Granulite Block (Ghosh et al., 1998, 2008). Achankovil shear zone separates Madurai block from the Trivandrum block. Trivandrum block is subdivided into three tectonic units; The Kerala Khondalite belt (KKB), The Nagercoil unit and the Achankovil metasediments. Nagercoil block is on the southern tip of Indian peninsula as well as southern margin of Trivandrum block.

Within the Southern granulite terrain, a majority of the crustal blocks are characterized by a considerable presence of diverse and abundant fluid inclusions. According to

Roedder et al., 1984, fluid inclusions can be categorized into primary and secondary inclusions. Inclusions trapped during or along the growth of the mineral is termed as primary or pseudosecondary inclusions. They are commonly distributed along crystal-growth surfaces and are found as scattered or isolated inclusions in the sections. Secondary inclusions are those that formed after the complete crystallization of a mineral. Fluid inclusions often provide a wealth of information on the genetic and evolutionary history of the mineral assemblages in a rock or ore formation. Trapped fluids within the mineral provide one of the potential tools to detect the nature and activity of fluids. These microgeochemical systems offer important clues on the composition and density of the fluids, pressure-temperature conditions of equilibration of mineral assemblages, and exhumation history of rocks (Santosh et al., 2003). C–O–H-bearing fluids play a crucial role in the lower crustal and crust-mantle interaction processes (Satish Kumar, 2005; Santosh and Omori, 2008a; Santosh and Omori, 2008b; Santosh et al., 2009a; Tsunogae et al., 2008).

A Late Archean (2.4–2.7 Ga) garnet granulite from the southern margin of the south Indian craton preserves fluid inclusions with the highest density CO_2 yet reported from lower crustal rocks. The rock comprises garnet, clinopyroxene (salite), plagioclase, amphibole (pargasite), orthopyroxene (hypersthene), biotite, scapolite, and quartz with accessory K-feldspar, ilmenite, apatite (Santosh and Tsunogae, 2003).The dominant category in all these minerals are composed of monophase carbonic inclusions with melting temperatures close to −56.6°C, indicating a CO_2-rich composition for the fluid (Santosh M., 2003). Most of the crustal blocks of Southern granulite terrain is comprises of CO_2 rich fluid inclusions and along with that minor proportion of H_20 is also present. Locally CH_4 and N_2 occur as trace components. On the charnockite rocks of Maduri and other crustal blocks of SGT, grains of garnet and quartz contain high density carbonic fluids. Fluid inclusions in quartz from the charnockites show distinct distribution patterns consistent with three generations of inclusions. The early monophase type records entrapment of high-density CO_2-rich fluid (0.95–1.0 g cm^{-3}), a subsequent monophase type with lower-density CO_2-rich fluid (0.65–0.75 g cm^{-3}) coexists with CO_2, H_2O inclusions having an average degree of filling of 0.2 (H_2O = 20%; CO_2 = 80%), Late aqueous biphase inclusions show coexistence with a second category of CO_2, H_2O inclusions showing a degree of filling of 0.6 (H_2O = 60%; CO_2 = 40%) (Santosh et al., 1986). Characterization and quantification of fluid inclusions in graphite bearing charnockites from the south-western part of the Madurai Granulite Block

in southern India reveals a probable relation with the formation and break down of graphite during the high-grade metamorphism (Baiju et al., 2009).The southern Indian granulite terrain has been a key area in understanding the nature and role of fluids in deep crustal processes in the past three decades (e.g., Newton et al., 1980, Santosh et al., 1991, Satish-Kumar, 2005, Santosh and Omori, 2008a, Santosh and Omori, 2008b, Clark et al., 2009). The role of CO_2-rich fluids in granulite formation process was initially hypothesized in this region. In the Madurai Granulite Block (MGB), which is a prominent tectonic block of the central region of the Southern Granulite Terrain where the role of CO_2-rich fluids in charnockitization process was proposed by many early workers derived support from the common occurrence of high-density CO_2 inclusions in various minerals (e.g., Santosh, 1986a, Santosh, 1998, Srikantappa et al., 1992, Mohan et al., 1996, Santosh and Tsunogae, 2003, Sukumaran et al., 2005).

The majority of micro thermometry studies have primarily concentrated on the Madurai block, specifically in the quest for high-density CO2-rich fluids. However, other blocks within the SGT (Southern Granulite Terrain) region have not received as much attention in terms of inclusion research. Notably, Srikantappa and Hensen (1991) reported the presence of CO_2-rich fluid inclusions in the Coorg granulites. Nevertheless, comprehensive investigations have been lacking in the Coorg block, which represents a crucial missing link in understanding the pressure-temperature conditions under which mineral assemblages reached equilibrium and the subsequent exhumation history of the rocks. By expanding research efforts to include the Coorg block, a more comprehensive understanding of these aspects can be achieved.

CHAPTER 2

STUDY AREA

2.1 THE COORG BLOCK

Coorg block lies between 11.919862 N to 12.7546368 N latitude and 74.820486710 E to 75.83082211 E longitude. This exotic microcontinent which is sandwiched between Western Dharwar craton in the north and Neo-Archean-Proterozoic crustal blocks in the south. Two major shear zones entirely covers the Coorg block (i) Mercara shear zone in the WNW (ii) Moyar shear zone in the ESE trending. Coorg block is the oldest crustal block of SGT and also believed the deepest exhumed crust on Indian peninsular (Raith., et. Al, 1999), which mainly consists of Mesoarchean magmatic rocks includes Charnockites, Mafic granulites and TTG's (Tonalite-Trondhjemite-Granodiorite). The dominant rock type found in the Coorg block is granulite facies, forming massive areas over a large extent (Asha Manjari and Malur, 1997). High pressure-Ultra high temperature Meta pelitic and Meta mafic rocks are also present in Coorg block. The rocks were metamorphosed under granulite facies at P-T conditions of 760 - 800 °C and 7.1-8.4 Kilobars. Grade of metamorphism increases from amphibolite facies to granulite facies from Dharwar to Coorg block. The oldest charnockites in the SGT is from Coorg block it dominantly composed of ortho pyroxene, clino pyroxene, biotite, K-feldspar, plagioclase, ilmenite and minor garnets. Coorg block is separated from Dharwar cratons by Mercara suture zone in the north and bounded on the south by Moyar shear zone and Nilgiri block. The Geophysical prospecting along Mercara suture zones suggested that the extension of suture is upto Mohorovicic discontinuity (Moho). In earlier research, it was suggested that the Coorg block represents a higher-grade extension of the Western Dharwar craton and Biligiri Rangan hills towards the south. Interestingly, the Coorg block is considered exotic because it lacks the later Neoarchean tectonothermal imprints commonly observed in the surrounding blocks (Santosh et al., 2015). This peculiarity adds to the intrigue and geological significance of the Coorg block, making it an essential area of study to understand the complex geological history of the region. The high-grade massifs of Coorg block preserve imprints of tectonic and metamorphic activity from Mesoarchean to Neoproterozoic-Cambrian (Santosh et al., 2003 , 2009; Plavsa et al., 2012 ; Endo et al., 2012 ; Collins et al., 2014 ; Praveen, 2013 ; Samuel et al., 2014 ; Shaji et al., 2014 ; Kroner et al., 2015 ; Santosh et al., 2015 ; Santosh, 2020 ; Yu et al., 2020).

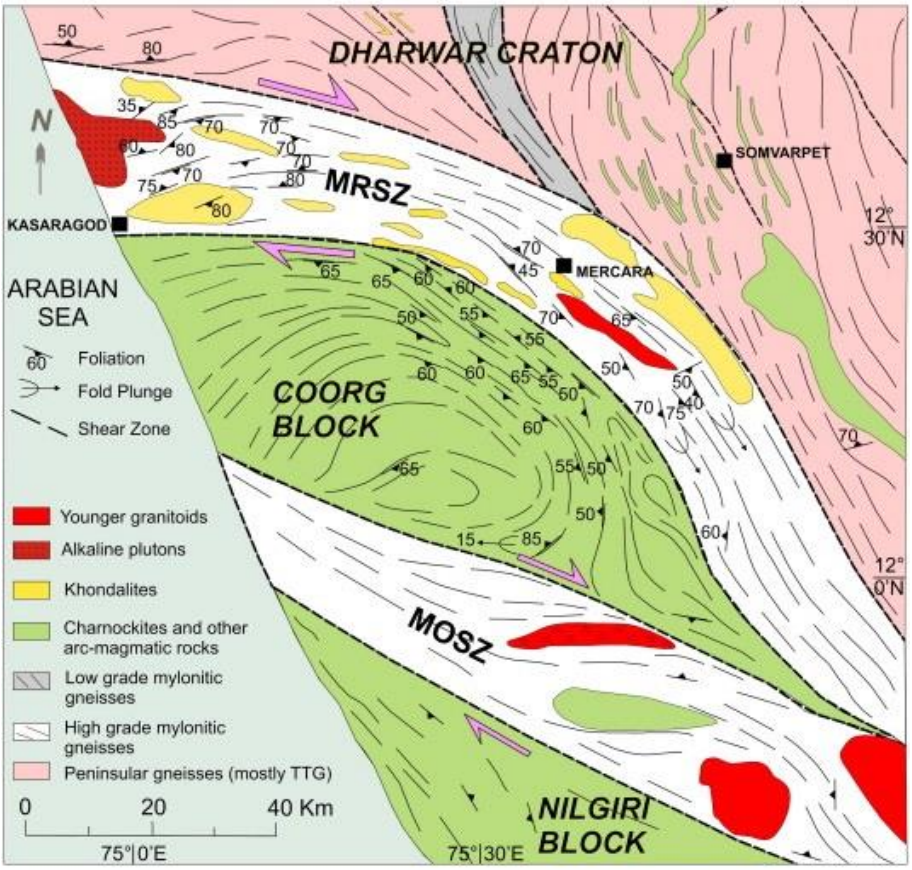

Figure 3| The Coorg block and the adjoining suture zones (Santosh et al., 2015)

Detailed field investigations and systematic sampling is conducted in and around Coorg and Mercara. List of samples collected from the study area is given in the Table 1

Table 1 | Location, rock type and minerology of samples selected for present study

Sl No:	Sample Name	Sample Location	Rock Type	Mineral assemblage
1	SPL-A1	N12° 20′ 26.4″ E75° 49′ 8.4″	Metapelite	Grt Qtz Pl Kfs Bt
2	SPL-A2	N12° 20′ 26.4″ E75° 49′ 8.4″	Granulite	Ky Grt Qtz Pl Kfs Bt

CHAPTER 3

METHODOLOGY

3.1 METHODOLOGY

Different materials and methods used in sample preparation for petrography and fluid inclusion studies. Detailed overview of instruments and working of those instruments and their analytical methods to obtain various geological data are explaining here.

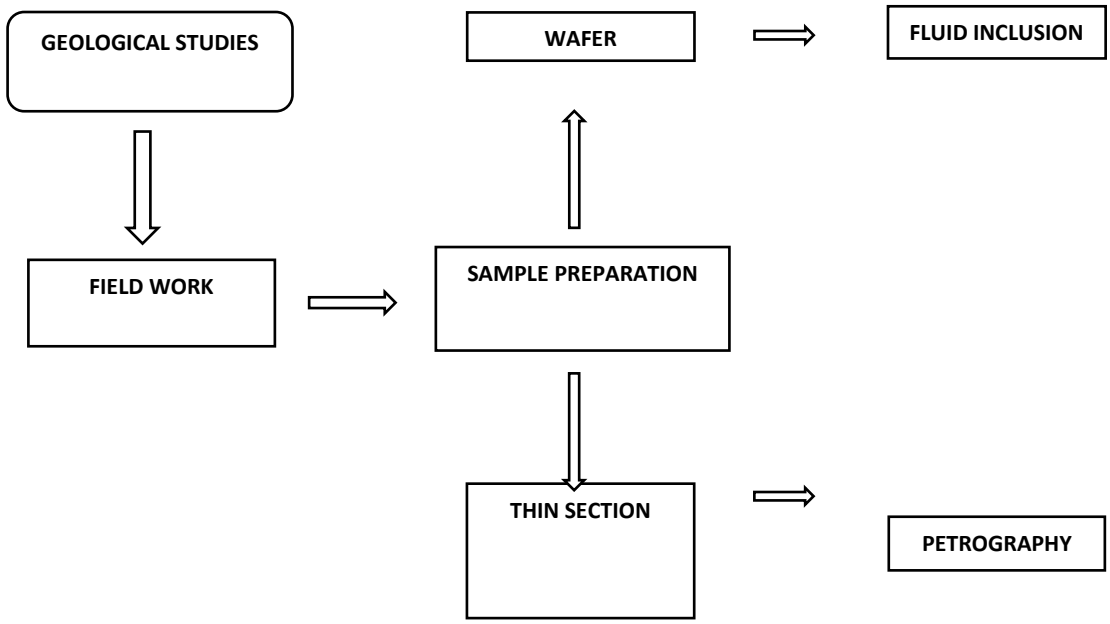

Figure 4| Flow chat display the different methodology used in the studies.

3.2 FIELD WORK

A detailed literature study was conducted before the field work. Collected all the previous and available reports from the study area. Through which a comprehensive knowledge was gained about the 'Coorg block 'and 'Mercara Suture zone' which is the study area. Knowledge about the major lithology and structural features are gained from the existing publications and geological maps. During the fieldwork, a series of activities were undertaken. These included megascopic identification of rock samples, detailed mapping of the structural features, and systematic collection of samples.

Throughout the fieldwork geological maps (Figure: 5a) and GPS (global positioning system) (Figure: 5b) are used to trace the location of lithological features. Rock samples are collected from the field by measuring latitude and longitude. Those coordinates are then plotted on the geological map to get the exact location of specific sample. Brunton compass (Figure: 5c) and clinometer (Figure: 5d) were used for measuring the strike and dip of the formations. Rock samples are collected by using Estwing geological hammers (Figure:5e) and chisel. Hand lens (Figure:5f) are used for the close observation of mineral grains present in the rocks during sampling. This equipment is also used as scale for taking field photographs. For taking field photographs digital cameras are used

Figure 5| Showing tools used for geological field investigation (a) Geological map (b) GPS (c) Brunton compass (d) Clino meter (e) Geological hammers (f) Hand lens

3.3 PETROGRAPHIC STUDIES

Petrographic studies are carried out by the analysis of rock sample under a microscope. These studies help to determine the minerals texture, structure and composition of rock samples, providing valuable information about their geological history and formation process of rocks. The initial step in petrographic studies involves the preparation of thin sections.

3.3.1 PREPERATION OF THIN SECTION

After collecting rock samples from the study area, they are sent to the petrological laboratory at the Department of Marine Geology and Geophysics, Cochin University of Science and Technology (CUSAT), Kochi. In this laboratory, thin section preparation takes place, allowing for a detailed study of the optical properties of minerals under a microscope. The rock slice which is attaching on the thin sections slide should have a thickness of 0.03 mm and the dimension of thin section slide is of 26 mm X 46 mm. Steps for the preparation of thin section are given below.

In the process of preparing rock samples collected from the field for further analysis, the first step involves dealing with their larger and heavier size. To fit these samples into the sample holder of the Primary Cutter or Hi-Tech Diamond 6-inch Trim saw (figure 6a), they need to be broken into smaller, more manageable sections. This can be achieved using either a geological hammer, which breaks the larger rock blocks into smaller pieces, or by manually pushing the entire rock block into the diamond blade of the Primary Cutter for cutting into smaller rectangular or cubical blocks. Once these smaller blocks are obtained, they can be comfortably placed in the sample holder of the Primary Cutter. This cutter is designed to cut and trim rocks, minerals, and other hard materials into thin sections or smaller pieces, which are then suitable for further analysis and petrographic studies. The cutting blade having an RPM of 3,450. While cutting the rock sample water is exerts on the diamond blade to reduce the friction. Once it is suitable for placing into the sample holder we proceed to cut into small rectangular or cubical block. The next step involves polishing the face of the rock sample to be mounted on the glass slide. This is achieved by using silicon carbide powder with different grit sizes, including 80, 120, 200, 400, 600, 800, and 1200. The polishing process is carried out using a glass plate. This ensures that the rock sample's surface becomes smooth and suitable for mounting on the glass slide (figure 6b).

Different epoxies like Canada balsam and araldite gum (figure 6c) are used to mount the polished face of rock sample on the glass slide. Ideal refractive index of epoxy is 1.54. While using Canada balsam we need to heat the glass slide and polished rock sample in a 'hot plate oven' at 140 to 150 Degree Celsius. At this temperature, Canada balsam began to melt and then we need to paste it on the entire glass slide. After a few seconds fix the polished face of rock sample on the glass slide containing epoxy, then allow time to stick the rock sample on the glass slide. In the case of araldite there is no need for heating the epoxy. Places one or two drop of araldite on the glass slide and fix the polished face of rock sample carefully and squeezed to avoid air bubble. Then allow time to stick the rock sample on the glass slide (hardly 10 minutes)

Then precision cutter or secondary cutter (figure 6d) (Buehler's Thin sectioning system) is used for further cutting and grinding process to get desired thickness. This precision cutter comes with a diamond cutting blade and a diamond grinding cup, for cutting and grinding of the thin section. There are two precision micrometers are there for adjust the distance of thinning for both cutting blade and grinding cup. Prepared glass slide is placed on the vacuum chuck and water is applied there as lubricant. Then the arm of the vacuum chuck is introduced first into the cutting blade to reduce the thickness and after that the arm of vacuum chuck introduce to the grinding cup to slice the thickness of rock section approximately to 0.03mm. After that the glass slide is taken from the vacuum chuck by releasing pressure. Next step after grinding is the polishing of thin section with silicon carbide powder with mesh size 1200 microns and observe the sample under petrological microscope. The interference color scheme of quartz grain in the sample has been used as a gauge to assess the correct thickness of sample which is prepared. Finally diamond polishing was done with diamond paste for the final touch (figure 6e). After getting the sample ready, we examine it with a special microscope for rocks. We use a LEICA DM750P microscope that's in our petrology lab. This helps us figure out what minerals are in the collected rocks.

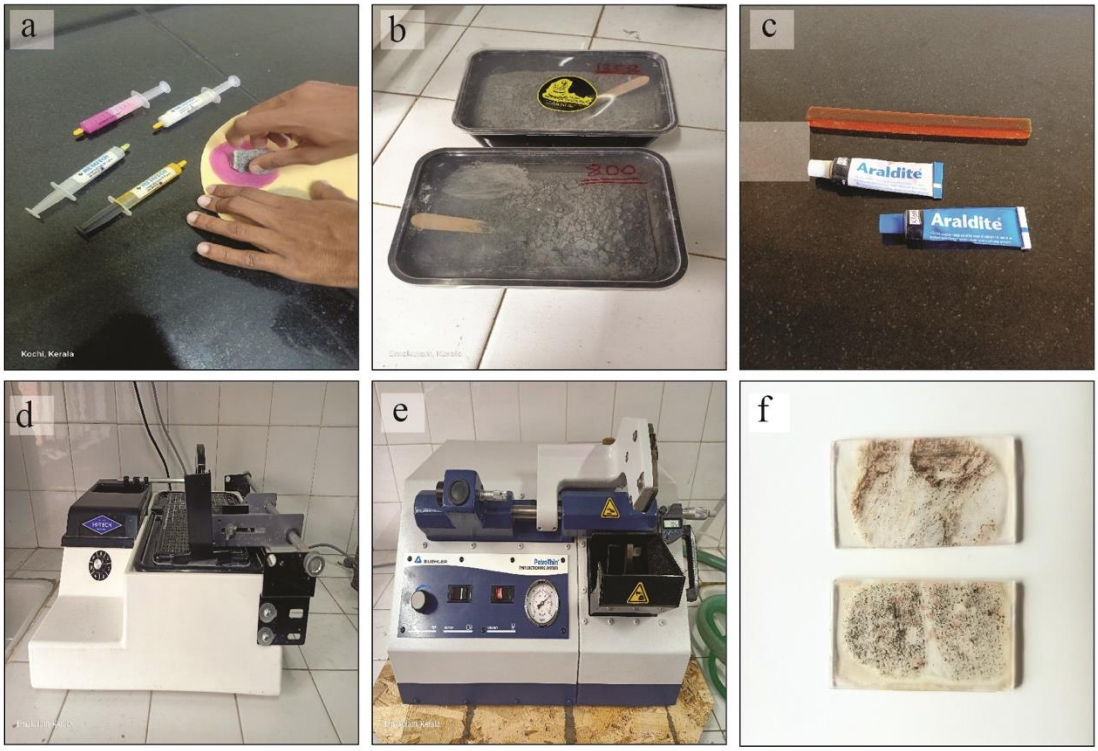

Figure 6 | Tools used for preparation of petrographic thin section (a) Diamond past. (b) Silicon carbide powder (c) Epoxy's (d) Primary Cutter (e) Precession cutter (f) Thin section slide

3.4 FLUID INCLUSION STUDIES

Fluid inclusion studies are the study of microscopic fluids which are trapped in the mineral grains during the formation of rocks. Those fluid inclusion occur in very small volume. Using micro thermometry, detailed fluid inclusion petrographic studies can take place. It provides information about the temperature, pressure, salinity, density and depth of entrapment of fluids. Thereby it provides direct evidence of condition of minerals and rocks are formed. Depending on the timing of the formation, fluid inclusion is classified into primary, secondary and pseudo secondary. Those inclusion occur as isolated, clustered and trail bounds based on their origin.

H.C. Sorby (1858) coined the term "Fluid Inclusion" for deciphering the temperature of past geological events. Inclusions, which are trapped at the time of growth of host mineral termed primary. The primary inclusions may represent samples of original fluids and re-

veal important information regarding the conditions of ore transportation and deposition. (Roedder., 1980). However, secondary inclusions do not reliably give information on the nature of ore forming fluids or conditions. But, they may provide some clues into post-depositional conditions. The secondary fluids formed as a trail after crystal growth usually along healed cracks and micro facture and forms pseudo secondary when the healed cracks terminate as the grain boundaries. The inclusions can be monophase (single phase of liquid/gas) or biphase (mixture of more than one phase). The composition of these fluids can be H_2O, CO_2, CH_4, N_2, Na, Cl, K and so on. The typical host minerals in which the fluid inclusions are observed include sphalerite, cassiterite, quartz, calcite, dolomite, fluorite, garnet, biotite and barite. Fluid inclusions in quartz and garnet exhibits forms of groups or isolated clusters, and are classified as groups of synchronous inclusions (GSI) following the scheme proposed by Touret (2001). Most of them are concentrated either towards the centre of the mineral grains or in other domains that are away from fractures or cracks therefore these inclusions are considered to be primary monophase inclusions and denoted as **type – I** inclusion. Some of the groups of monophase inclusions occur along trails that pinch out within individual grains. These groups of inclusions are considered to be **type-II** pseudo secondary inclusions. This type-II inclusions also formed along microcracks that develop during the partial growth of the crystal and form arrays/trails that pinch out with grains. Secondary inclusions are those that formed after the crystallisation of a mineral, thus if the mineral is fractured in the presence of a fluid subsequent to its growth, the fluid enters the fracture and rehealing of the fracture would result in inclusions aligned along linear arrays that cut across crystal, these groups of inclusions are generally occur as monophasic inclusion and are considered to be **type – III** inclusions. Fluid inclusion studies play a significant role in different aspects of geology and resource exploration. They are extensively utilized in economic geology to gain insights into the genesis of ore deposits, including valuable metals and minerals. Additionally, these studies are essential for understanding the intricate workings of hydrothermal systems, shedding light on the conditions responsible for the formation of geothermal fluids, hot springs, and hydrothermal veins. In the petroleum industry, fluid inclusion studies are instrumental in deciphering the historical evolution and migration of hydrocarbons. Moreover, by analysing ancient fluid inclusions preserved in minerals and rocks, scientists can

reconstruct the environmental conditions and tectonic processes that shaped the Earth's geological past.

In the study of fluid inclusions, doubly polished wafers of representative samples are commonly used for analysis. Rocks can contain a vast number of fluid inclusions per cubic centimeter, making it crucial to intelligently select specific fluid inclusions for detailed examination. Even within the same type of rock (lithology), fluid inclusions may exhibit significant variations (as noted by Van den Kerkhof et al. in 1994**)**. Therefore, a careful fluid inclusion petrographic study is conducted to identify the phases, size, and shape of the fluid inclusions. The intelligent selection of fluid inclusions for detailed analysis helps to ensure that the most informative and representative samples are studied, contributing to more accurate interpretations and conclusions in fluid inclusion studies.

3.4.1 METHODS OF FLUID INCLUSION STUDIES

First step for the fluid inclusion study is the detailed petrographic studies to understand the mineral assemblage, because in some mineral like garnet, quartz, feldspar, sillimanite, kyanite, omphacite, zircon and diamond the presence of fluid inclusion is reported. Late generation of fluids within the host rock may be altered in their composition and density due to deformation and they became inaccurate for study, Diamond (1990). A single rock sample contains numerous fluid inclusions within a cubic centimeter. Those fluid inclusion shows considerable variation even with in the same lithology. Therefore, detailed observation is needed before selection of sample for fluid inclusion analysis.

Ordinary petrological microscopes are used for the fluid inclusion petrographic analysis along with purposefully designed fluid inclusion stage for heating and cooling of the sample (figure 7a). Then wafers (doubly polished loose plate) (figure 7b) are prepared for the detailed studies under the micro thermometry. Wafers are much thicker than the ordinary thin section made for petrographic studies. The ideal thickness of wafers is between 90 and 120 nano meters. Fluid inclusion study under the micro thermometry, is done by heating and cooling of the stage. The device is capable to increase and decrease temperature between -200 degree Celsius and +1500 degree Celsius approximately. Cooling is mostly done with liquid nitrogen and heating is done by any light source. Stage of micro thermometer is placed on a microscope so that change in the phase and temperature

at which these changes are take place can be observed. Like the minerals, fluid inclusions do not tell us about one particular episode of rock forming processes (Van den Kerkhof and Hein, 2001), but generally about different stages of its evolution (Roedder, 1984). Apart from micro thermometric studies, Raman spectroscopy is also used for the fluid inclusion studies. Which provide direct result of the composition of fluids which are entrapped the crystals (Quantitative approach)

3.4.2 MICROTHERMOMETRY

Micro thermometric experiments were conducted on fluid inclusion wafers in the Department of Marine Geology and Geophysics at Cochin University of Science and Technology (CUSAT), Kochi. These experiments were performed using a Linkam stage, which was attached to a petrological microscope. The Linkam stage allows precise temperature control during the experiments, enabling the observation and measurement of fluid inclusion behaviour under different temperature conditions.

To calibrate the micro thermometric setup, three specific temperature points were used:

1. The triple point of H_2O at 0°C, which is the temperature and pressure where solid ice, liquid water, and water vapor coexist in equilibrium.

2. The triple point of CO_2 at -56.6 °C, which is the temperature and pressure where solid CO_2 (dry ice), liquid CO_2, and CO_2 vapor coexist in equilibrium.

3. The critical point of pure H_2O at 374.1 °C and a density of 0.317 g/cc. At this point, the distinction between liquid and vapor phases disappears, and water exists as a supercritical fluid.

During the heating and cooling experiments, we measured the melting temperature (*Tm*) and homogenization temperature (*Th*) of two-phase (gas-vapor) fluid inclusions. The melting temperature is the temperature at which the solid phase of the fluid inclusion changes into a liquid phase, while the homogenization temperature is the temperature at which the two phases of the fluid inclusion (gas and vapor) merge into a single phase (liquid or vapor).

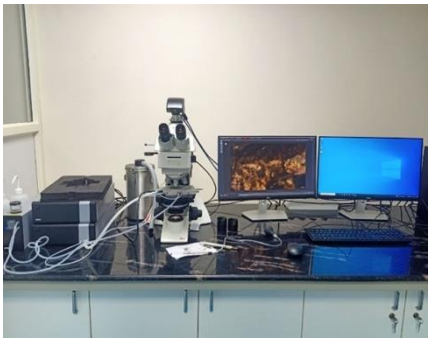

(a)

(b)

Figure 7| Methods for fluid inclusion studies (a) Fluid inclusion stage with petrographic microscope (b) Doubly polished wafer.

CHAPTER 4

RESULT AND DISUSSION

4.1 PETROGRAPHIC AND FIELD FEATURES OF STUDY AREA

Petrography involves the study of rocks and their mineralogical and textural properties under a petrographic microscope. The word "petrography" is derived from two Greek words: "petros" which means rock and "graphien" which means to describe or write. Petrography plays a crucial role in understanding the origin, composition, and geological history of rocks. By examine the thin sections of rocks, which are slices of rock samples that are so thin that they are transparent when viewed under a polarizing microscope. These thin sections allows to study the mineralogical composition, texture, fabric of rocks at a microscopic scale, its formation conditions and its geological history. Optical properties of the minerals are viewed under a polarized light microscope. Each mineral has its own behaviour towards plane polarized light and crossed polarizers, which help us to the identification of the particular mineral. Texture of the rocks are the arrangement and size of mineral grains, as well as any visible structures or features within the rock. Different textures provide information about the rock's formation processes, such as cooling rates, pressure, and deformation history. Petrography plays a crucial role in categorizing rocks into different groups according to their mineral composition, texture, and how they were formed. The main rock categories encompass igneous, sedimentary, and metamorphic rocks. To conduct in-depth petrographic analyses, thorough field investigations of the study area are indispensable.

The Coorg block is primarily distinguished by its dominance of Mesoarchean Magmatic rocks, notably Charnockites and TTG's (Tonalite-Trondhjemite-Granodiorite). Additionally, there is a dispersion of various mafic and ultramafic formations along its strike direction. Furthermore, the region contains high-pressure to ultra-high-temperature metamorphic pelitic and mafic rocks. The prevailing metamorphic conditions in the Coorg block are predominantly granulite facies, evident from the prevalence of anhydrous minerals. A brief account of representative samples selected from the different domains of Coorg block and Mercara is given below.

4.1.1 MEGASCOPIC ANALYSIS

SPL-A1 (Metapelite)

The specimen exhibits a massive and holocrystalline structure, displaying a mesocratic colour index. Its texture is phaneritic, and the grain size ranges from medium to coarse. The prominent minerals within are Garnet, Quartz, and Biotite. Garnet grains stand out due to their larger size and distinctive cherry-red colour. Quartz is recognizable by its white colour, glassy lustre, and conchoidal fracture pattern. Biotite is discernible through its deep brown colour, vitreous to pearly lustre, and platy habit in Basel section. Notably, the specimen features bands of a few millimetre's thickness that traverse its composition.

SPL-A2 (Garnet Kyanite Granulite)

The specimen is massive and holocrystalline, displaying a mesocratic colour index. Its texture is phaneritic, with a coarse grain size. Prominent minerals include Garnet, Kyanite, Quartz, and Biotite. Kyanite and garnet grains are notably larger in size. Garnet is recognizable by its cherry-red appearance, distinctive fracture, and lack of cleavage. Kyanite's bladed habit and bluish-green colour make it easily identifiable. Quartz is characterized by its vitreous lustre, absence of cleavage, and conchoidal fracture pattern. Biotite stands out due to its dark brown colour, platy cleavage, and vitreous to pearly lustre.

(a) (b)

Figure 8 | Megascopic images of collected samples (a) SPL-A1 (b) SPL-A2.

4.1.2 MICROSCOPIC ANALYSIS

Samples collected from the Coorg and Mercara vicinity are transformed into petrographic thin sections within the petrology laboratory at the Department of Marine Geology and Geophysics, Cochin University of Science and Technology, Kochi. The comprehensive petrographic portrayal of rocks within the study region is provided below:

SPL-A1 (Metapelite)

Quartz - Under plain polarised light (PPL) it is colourless with low relief and no cleavage. Under cross polarized light (XPL) it displays low interference colour, colour changed from grey to yellow and exhibit wavy extinction.

Garnet - Under plain polarised light (PPL) it shows light pink to light red colour, absence of cleavage with high relief, multi number of fractures are visible. Under cross polarized light (XPL) it is dark because of its isotropic in nature.

Biotite - Biotite exhibits moderate relief and a pale to deep greenish brown or brown colour with moderate to strong pleochroism with pale yellow to dark brown. Biotite has a high birefringence which can be partially masked by its deep intrinsic colour. Under cross-polarized light, biotite exhibits extinction approximately parallel to cleavage lines.

Pyroxene - Under plain polarised light (PPL) it is distinguished by two directional cleavage at approximately 87° to 90° and pale green to pink colour pleochroism with moderate relief. Under cross polarized light (XPL) it shows parallel extinction at 90°and strong interference colour.

Plagioclase -Plagioclase is identified with its colourless nature, low relief, medium to coarse grained and good cleavage under plain polarised light (PPL) along with polysynthetic twinning in XPL.

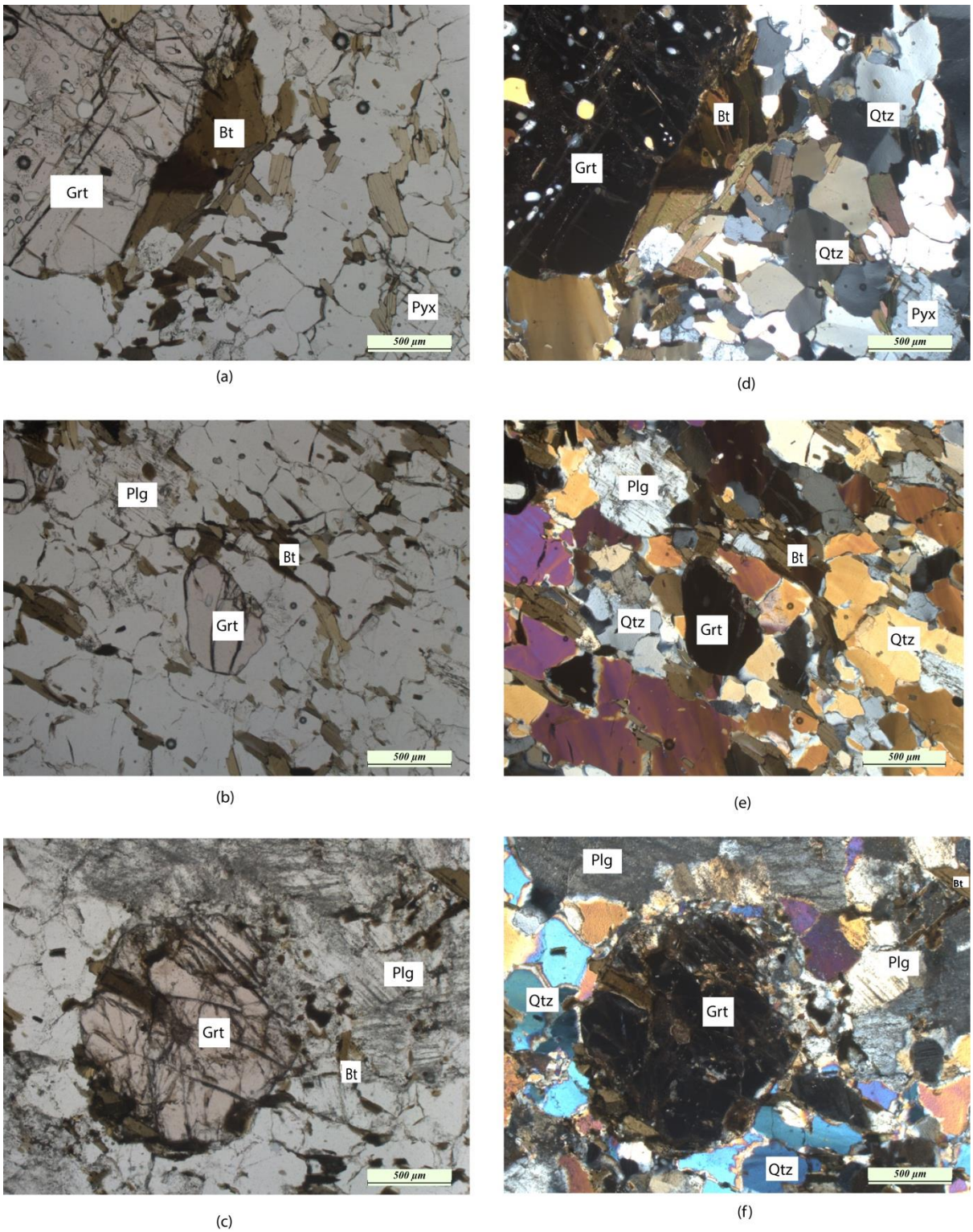

Figure 9| Photomicrographs of samples discussed in this study. (a), (b), (c), (d) are Garnet+ Biotite+ Pyroxene+ Quartz + Plagioclase assemblage in SPL-A1 (Metapelites) under plane and cross polarized light.

SPL-A2 (Garnet Kyanite bearing metapelites)

Quartz

Under plain polarised light (PPL) it is colourless with low relief and no cleavage. Under cross polarized light (XPL) it displays low interference colour, colour changed from grey to yellow and exhibit wavy extinction.

Garnet

Under plain polarised light (PPL) it shows light pink to cherry red colour with sets of fractures, shows high relief and absence of cleavage. Under cross polarized light (XPL) it is dark because of its isotropic in nature.

Biotite

Under plain polarised light (PPL) it is identified by brownish in colour, pleochroic with dark brown to pale yellow colour, and shows one set of perfect cleavage. Moderate relief usually seen lath like in cross section. Under cross polarized light (XPL) it shows parallel extinction.

Kyanite

Under plain polarised light (PPL) identified by its bluish colour and bladed habit, shows one set of perfect cleavage. In cross polarizer kyanite has bright interference colour.

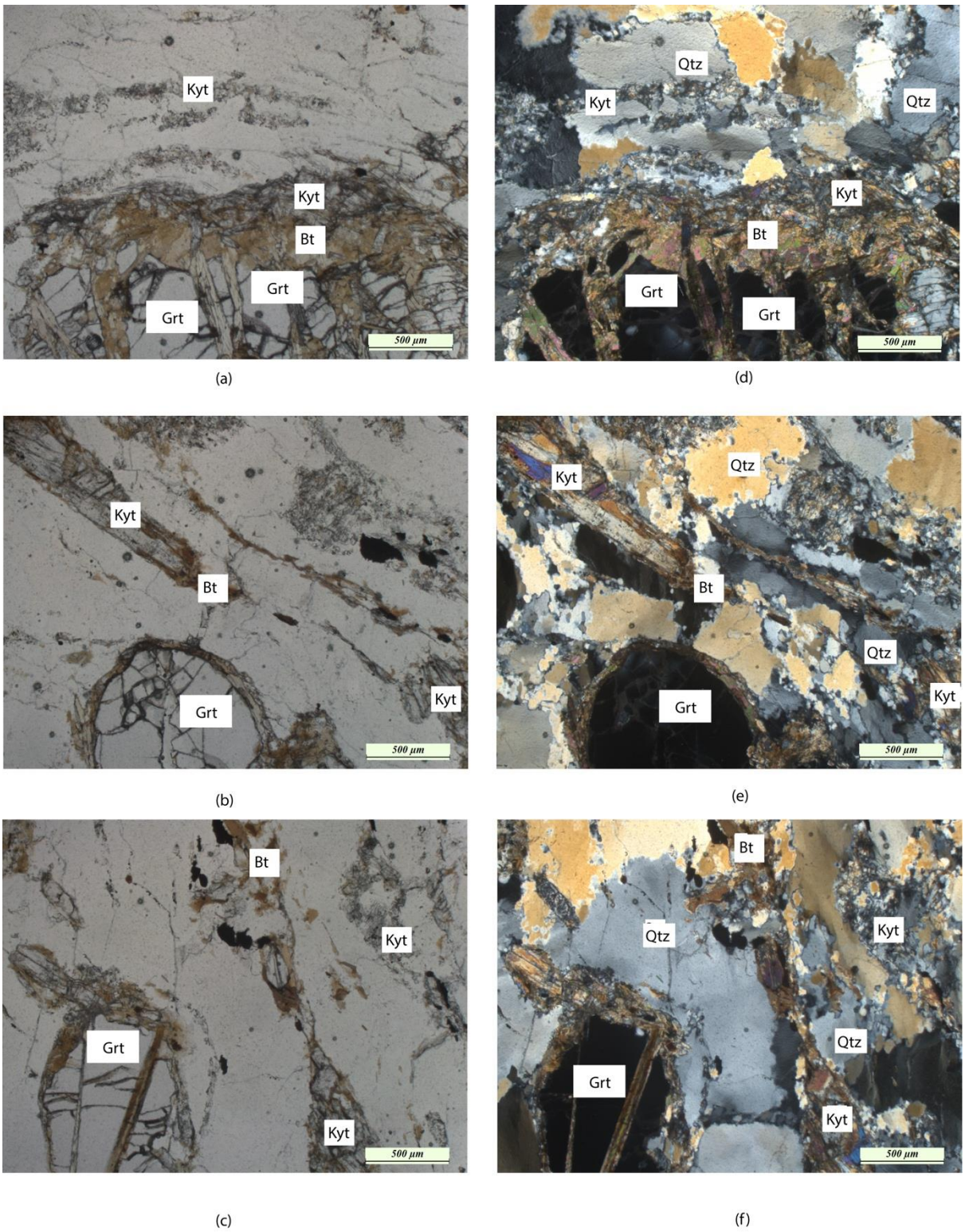

Figure 10| Photomicrographs of samples discussed in this study. (a), (b), (c), (d) are Garnet+ Biotite+ Quartz+ Kyanite assemblage in SPL-A2 (Garnet kyanite bearing metapellites) under plane and cross polarized light.

4.2 FLUID INCLUSION ANALYSIS

Fluid inclusions are present mostly in the quartz mineral grain. Those inclusion provide information about the Pressure - Temperature condition of rocks at various depth, especially from the lower to upper crustal level. Quartz is the only leucocratic mineral that participate in the prograde and retrograde mineral reactions during a regional metamorphism also considering its lack of alternation fluids are preserved in it. Trapped records of fluids in metamorphic rocks will give reliable information for the grade of metamorphism in which the rocks have undergone. Hence fluid inclusion data form high grade metamorphic rocks can be exclusively derived from quartz grains (Srikantappa et al., 2008). Fluid identification in a series of minerals allows a more precise estimation of the P-T evolution of the rocks as the different host minerals show different capabilities for preserving fluid inclusion (Horlov et al., 2012). This approach of petrographic study is carried out mainly for the identification of phases, size, shape, and degree of fill in order to classify the fluid inclusions by following the techniques outlined by Roedder (1984), Shepherd et al., (1985), Van den Kerkhof and Hein (2001), Kerkhof (2001), and Touret (2001). Fluid inclusions were observed in different minerals in all of the examined samples, although their size, relative abundance, and distribution patterns vary among the various rocks.

Microthermometric experiments were performed with a Linkam Heating/Freezing system, which was attached to a petrological microscope (Leica microscope with fluid inclusion stage) in the Department of Marine Geology and Geophysics at Cochin University of Science and Technology (CUSAT), Kochi. The calibrations was undertaken and in the heating/cooling experiments, the melting temperature (*Tm*) and homogenization temperature (*Th*) of two phases (gas-vapour) inclusions were measured. Heating rate of the sample were 1° C/min for *Tm* and 5 ° C/min for *Th.* Fluid densities and isochores were calculated using AQSO, BULK and ISOC programs, available in the package FLUIDS (Bakker, 2003). For this purpose, the equations of state of Thiéry et al. (1994a) and Duan et al. (1992) for CO_2 ±CH_4 system and those of Archer (1992) and Zhang and Frantz (1987) for H_2O – NaCl system were used. Garnet Kyanite metapelites (SPL -A2) and Metapelite (SPL -A1) collected from Siddapura and adjacent regions in Coorg block were selected for detailed fluid inclusion studies. Fluid characteristics of those litho unit are described below.

4.2.1 METAPELITE (SPL-A1)

Fluid inclusions are rare in the garnet-bearing metapelite from Siddapura, Mercara. However, some pseudosecondary trail-bound inclusions were detected in both garnet and quartz grains. These inclusions were observed to consist of biphase substances, but they were remarkably small, measuring less than 1 μm in size. Though microthermometric experiment was conducted on this trail bound inclusions, phase transitions are not identified due to the very small size of inclusions.

4.2.2 GARNET KYANITE METAPELITE (SPL-A2)

Fluid inclusions were not abundant in the Garnet kyanite metapelites. Only some pseudo secondary trails bound inclusions are identified in quartz grains. This consists of biphase inclusion. Apart from this, few inclusions are visible under microscope at higher magnification but majority of them are smaller than 1μm in size and unable to identify phase transition. Through micro thermometric experiment was conducted on this trail bound inclusion, phase transitions are observed only in one inclusion. Primary and secondary inclusions are absent in the grains of the sample due to its pelitic in nature.

Pseudosecondary trail bound inclusions can be seen in Quartz grain and are present in the form of isolated curved trail bound inclusion. But the trails are too small and the inclusion in trails have a size of about 5 to10 μm (Fig.11). The size of Pseudosecondary inclusion becomes smaller to larger from moving one end to another of the trails usually from left to right. Brownian movement is absent at room temperature. Inclusion has a square shaped outer phase and round inner phase.

Experiment was carried out on large biphase inclusions (Fig.12). The biphase inclusion was initially cooled to -195°C and the inclusion froze into a single phase. Then the sample was slowly heated. The first melting temperature is noted at -55 .8 °C with a peak range lies between -55.8 °C and -55.4 °C, which is close to the triple point of pure CO2 (-56.6°C) (Table 4.1). The homogenisation temperature of pseudosecondary fluid inclusion in Quartz is reached at around 31.0 °C. The composition of fluid, and the temperature and phase of homogenization allows a precise estimation of the density of the fluid. The result summarized in Table 4.1 which corresponds to 0.773445 g/cc. The density of carbonic fluid inclusion can be translated into CO2 isochore in *P-T* space (Fig 13).

Table 2| Microthermometric results of fluid inclusion in Garnet Kyanite metapelites.

Mineral	Type of Inclusion	Phase	Size and Shape of Inclusion	First melting Temperature (T_m)	Homogenization Temperature (T_h)	Density (g/cc)	Remark
Quartz	Pseudo secondary	Biphase	5-15 μm Round inner phase Square shaped outer phase	-55 .8 °C	31.0 °C.	0.773445	Presence of trapped CO2

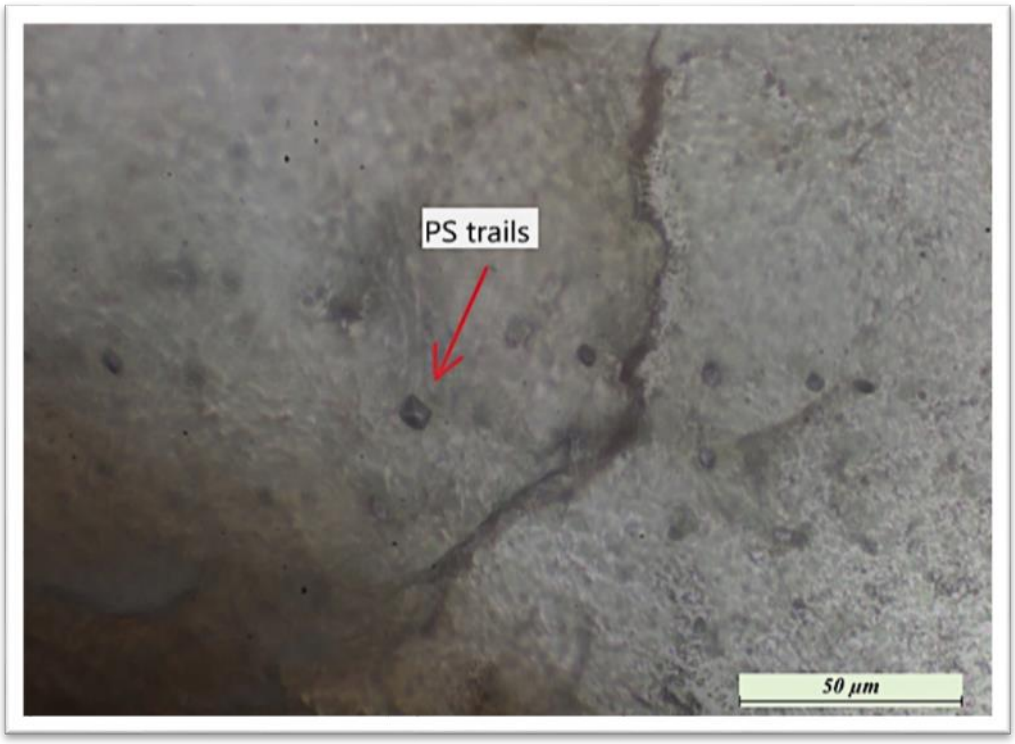

Figure 11 | Pseudosecondary (PS) trails in quartz (50x)

Figure 12 | Pseudosecondary (PS) trails in quartz (20x)

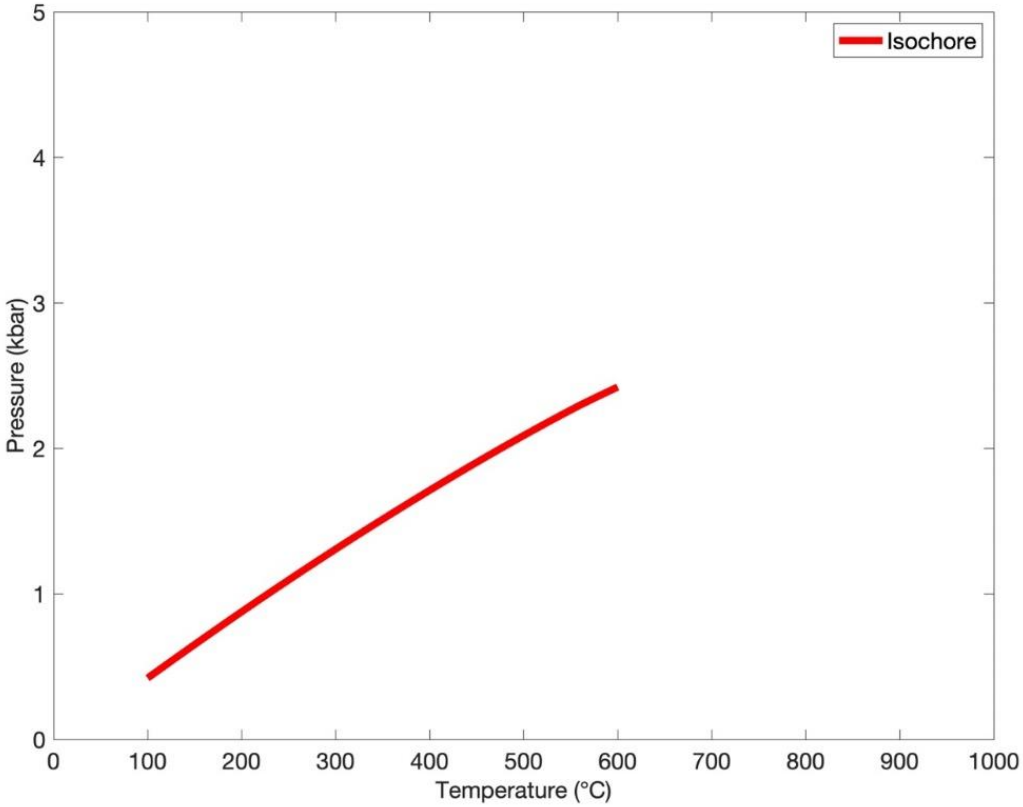

Figure 13| Isochore of CO2 inclusion in Garnet Kyanite metapelite

CHAPTER 5

CONCLUSION

5.1 CONCLUSION

The present study focus on understanding of petrological and fluid inclusion data from metapelites located in the Coorg block and Mercara suture zone, Southern granulite terrain, South India. Field investigation was conducted and major lithounits identified are high pressure to ultra-high temperature pelitic and mafic rocks. The prevailing metamorphic conditions in the Coorg block are predominantly granulite facies, evident from the prevalence of anhydrous minerals. Metapelites from Siddapura (SPL-A1) appear mesocratic and have a medium to coarse texture. However, they show gneissic foliation in which bands are few millimetre thick clearly indicate intensive shearing .On the other hand, Garnet Kyanite-bearing granulite (SPL-A2) from the same Siddapura location looks different. It has a similar coarse texture but contains larger kyanite and garnet crystals compared to SPL-A1. Unlike SPL-A1, this rock doesn't have any gneissic bands but quartz veins are visible. Petrographic study from microscopic analysis of both samples revels the presence of both felsic and mafic minerals such as quartz, plagioclase, biotite, garnet and pyroxene. In addition to this SPL-A2 have additional kyanite mineral and presence of porphyroblastic garnet in both sample. The mineral assemblages point to a high-pressure, medium-temperature setting, and the presence of biotite suggests a retrogressive phase. Fluid inclusion studies conducted in both samples. Inclusions are rare in garnet-bearing metapelite (SPL-A1). Both primary and secondary inclusions are totally absent in the doubly polished wafers studied, however, some pseudosecondary trail-bound inclusions were detected in both garnet and quartz grains but they were remarkably small, measuring less than 1 μm in size. In contrast, pseudo secondary trails bound inclusions are identified in quartz grains from Garnet Kyanite-bearing granulite (SPL-A2). This consists of biphase inclusion. Apart from this, few inclusions are visible under microscope at higher magnification but majority of them are smaller than 1μm in size and unable to identify phase transition. By conducting microthermometric experiments on pseudo secondary trails bound inclusions, phase transitions are observed in SPL- A2. The composition of the fluid was identified as CO2 based on the observed melting temperature (*Tm*) and homogenization temperature (*Th*). Fluid present in sample has indicate moderate density of 0.773445 g/cc, which shows that fluid in the rock trapped almost the peak metamorphic condition.

Also Fluid inclusion study shows that both the SPL-A1 (Metapelites) and SPL-A2 (Garnet Kyanite-bearing granulite) are devoid of primary and secondary inclusions. This would indicate the dry nature of rock at the peak metamorphism and its pelitic origin.

5.2 FUTURE WORK

The present study is a preliminary investigation on the fluids phases' present and petrographic investigation in and around Coorg and Mercara suture zone. Future works include detailed fluid inclusion study on more samples particularly their density, estimating pressure temperature conditions of entrapment and evaluation of the isotopic composition of the inclusion to ascertain their source characteristics. Also Laser Raman spectroscopy was employed to determine the precise composition of fluids. This technique accurately identifies the composition of the trapped fluid within the inclusion and provides molar ratios of gas phases present in each fluid inclusion. A detailed field sampling, petrographic studies together with major and trace element geochemistry and isotopic studies are necessary for a better understanding of the evolution of Coorg and Mercara suture zone.

REFERENCES

Amaldev, T., Santosh, M., Tang, L., Baiju, K. R., Tsunogae, T., & Satyanarayanan, M. (2016). Mesoarchean convergent margin processes and crustal evolution: Petrologic, geochemical and zircon U–Pb and Lu–Hf data from the Mercara Suture Zone, southern India. Gondwana Research, 37, 182-204.

Baiju, K. R., Nambiar, C. G., Jadhav, G. N., Kagi, H., & Satish-Kumar, M. (2009). Low-density CO2-rich fluid inclusions from charnockites of southwestern Madurai Granulite Block, southern India; implications on graphite mineralization. Journal of Asian Earth Sciences, 36(4-5), 332-340.

Balakrishnan, S., & Rajamani, V. (1987). Geochemistry and petrogenesis of granitoids around the Kolar Schist Belt, south India: constraints for the evolution of the crust in the Kolar area. The Journal of Geology, 95(2), 219-240.

Beckinsale, R. D., Reeves-Smith, G., Gale, N. H., Holt, R. W., & Thompson, B. (1982). Rb-Sr and Pb-Pb whole rock isochron ages and REE data for Archaean gneisses and granites, Karnataka State, South India. INDO-US Workship on Precambrian of South India, 35-36.

Bohlen, S. R. (1987). Pressure-temperature-time paths and a tectonic model for the evolution of granulites. The Journal of Geology, 95(5), 617-632.

Bohlen, S. R., & Mezger, K. (1989). Origin of granulite terranes and the formation of the lowermost continental crust. Science, 244(4902), 326-329.

Cenki, B., & Kriegsman, L. M. (2005). Tectonics of the Neoproterozoic southern granulite terrain, South India. Precambrian Research, 138(1-2), 37-56.

Chetty, T. R. K., & Rao, Y. B. (2006). The Cauvery shear zone, Southern Granulite Terrain, India: a crustal-scale flower structure. Gondwana Research, 10(1-2), 77-85.

Chetty, T. R. K., & Rao, Y. B. (2006). The Cauvery shear zone, Southern Granulite Terrain, India: a crustal-scale flower structure. Gondwana Research, 10(1-2), 77-85. V

Chetty, T. R. K., & Santosh, M. (2013). Proterozoic orogens in southern Peninsular India: contiguities and complexities. Journal of Asian Earth Sciences, 78, 39-53.

Chetty, T. R. K., Mohanty, D. P., & Yellappa, T. (2012). Mapping of shear zones in the Western Ghats, Southwestern part of Dharwar Craton. Journal of the Geological Society of India, 79, 151-154.

Collins, A. S., Clark, C., & Plavsa, D. (2014). Peninsular India in Gondwana: The tectonothermal evolution of the Southern Granulite Terrain and its Gondwanan counterparts. Gondwana Research, 25(1), 190-203.

Collins, A. S., Clark, C., & Plavsa, D. (2014). Peninsular India in Gondwana: The tectonothermal evolution of the Southern Granulite Terrain and its Gondwanan counterparts. Gondwana Research, 25(1), 190-203.

Collins, A. S., Clark, C., & Plavsa, D. (2014). Peninsular India in Gondwana: the tectonothermal evolution of the Southern Granulite Terrain and its Gondwanan counterparts. Gondwana Research, 25(1), 190-203.

de Wit, M. J., Bowring, S. A., Ashwal, L. D., Randrianasolo, L. G., Morel, V. P., & Rambeloson, R. A. (2001). Age and tectonic evolution of Neoproterozoic ductile shear zones in southwestern Madagascar, with implications for Gondwana studies. Tectonics, 20(1), 1-45.

Diamond, L. W. (1990). Fluid inclusion evidence for PVTX evolution of hydrothermal solutions in late-Alpine gold-quartz veins at Brusson, Val d'Ayas, Northwest Italian Alps. American Journal of Science, 290(8), 912-958.

Drury, S. A., Harris, N. B. W., Holt, R. W., Reeves-Smith, G. J., & Wightman, R. T. (1984). Precambrian tectonics and crustal evolution in South India. The Journal of Geology, 92(1), 3-20.

Endo, S., Wallis, S. R., Tsuboi, M., Torres De León, R., & Solari, L. A. (2012). Metamorphic evolution of lawsonite eclogites from the southern Motagua fault zone, Guatemala: insights from phase equilibria and Raman spectroscopy. Journal of Metamorphic Geology, 30(2), 143-164.

Ghosh, J. G., de Wit, M. J., & Zartman, R. E. (2004). Age and tectonic evolution of Neoproterozoic ductile shear zones in the Southern Granulite Terrain of India, with implications for Gondwana studies. Tectonics, 23(3).

Hansen, E. C., & Harlov, D. E. (2007). Whole-rock, phosphate, and silicate compositional trends across an amphibolite-to granulite-facies transition, Tamil Nadu, India. Journal of Petrology, 48(9), 1641-1680.

Janardhan, A. S., Jayananda, M., & Shankara, M. A. (1994). Formation and tectonic evolution of granulites from the Biligiri Rangan and Niligiri hills, S. India: Geochemical and isotopic constraints. Geological Society of India, 44(1), 27-40.

Janardhan, A. S., Newton, R. C., & Hansen, E. C. (1982). The transformation of amphibolite facies gneiss to charnockite in southern Karnataka and northern Tamil Nadu, India. Contributions to Mineralogy and Petrology, 79, 130-149.

Kelsey, D. E. (2008). On ultrahigh-temperature crustal metamorphism. Gondwana Research, 13(1), 1-29.

Kröner, A., Santosh, M., Hegner, E., Shaji, E., Geng, H., Wong, J., & Nanda-Kumar, V. (2015). Paleoproterozoic ancestry of Pan-African high-grade granitoids in south-

ernmost India: Implications for Gondwana reconstructions. Gondwana Research, 27(1), 1-37.

Manikyamba, C., Kerrich, R., Naqvi, S. M., & Mohan, M. R. (2004). Geochemical systematics of tholeiitic basalts from the 2.7 Ga Ramagiri-Hungund composite greenstone belt, Dharwar craton. *Precambrian Research*, *134*(1-2), 21-39.

Manjari, A. (1997). Petrogenesis of gneiss to granulite transition: evidence from the Coorg granulite complex, southern India. Geology in South Asia-II, 41.

Manjari, A. (1997). Petrogenesis of gneiss to granulite transition: evidence from the Coorg granulite complex, southern India. Geology in South Asia-II, 41.

Mezger, K., Hanson, G. N., & Bohlen, S. R. (1989). High-precision U-Pb ages of metamorphic rutile: application to the cooling history of high-grade terranes. Earth and Planetary Science Letters, 96(1-2), 106-118.

Mohan, A., Prakash, D., & Sachan, H. K. (1996). Fluid inclusions in charnockites from Kodaikanal massif (South India): PT record and implications for crustal uplift history. Mineralogy and Petrology, 57(3), 167-184. Sukumaran, S., Kumar, G. R., & Srikantappa, C. (2005). Charnockite forming metamorphism in Palghat, southern India: a fluid inclusion study of gneiss, charnockite, charno-enderbite and pegmatite. JOURNAL-GEOLOGICAL SOCIETY OF INDIA, 66(6), 679.d.

Mojzsis, S. J., Devaraju, T. C., & Newton, R. C. (2003). Ion microprobe U-Pb age determinations on zircon from the late Archean granulite facies transition zone of southern India. The Journal of Geology, 111(4), 407-425.

Newton, R. C., Smith, J. V., & Windley, B. F. (1980). Carbonic metamorphism, granulites and crustal growth. Nature, 288(5786), 45-50.

Pattrick, R. A. D. (1986). TJ Shepherd, AH Rankin and DHM Alderton A Practical Guide to Fluid Inclusion Studies. Glasgow and London (Blackie), 1985. xi+ 239 pp. Price£ 26. Mineralogical Magazine, 50(356), 352-353.

Plavsa, D., Collins, A. S., Foden, J. F., Kropinski, L., Santosh, M., Chetty, T. R. K., & Clark, C. (2012). Delineating crustal domains in Peninsular India: age and chemistry of orthopyroxene-bearing felsic gneisses in the Madurai Block. Precambrian Research, 198, 77-93.

Raith, M. M., Srikantappa, C., Buhl, D., & Koehler, H. (1999). The Nilgiri enderbites, South India: nature and age constraints on protolith formation, high-grade metamorphism and cooling history. Precambrian Research, 98(1-2), 129-150.

Raith, M. M., Srikantappa, C., Buhl, D., & Koehler, H. (1999). The Nilgiri enderbites, South India: nature and age constraints on protolith formation, high-grade metamorphism and cooling history. Precambrian Research, 98(1-2), 129-150.

Raith, M. M., Srikantappa, C., Buhl, D., & Koehler, H. (1999). The Nilgiri enderbites, South India: nature and age constraints on protolith formation, high-grade metamorphism and cooling history. Precambrian Research, 98(1-2), 129-150.

Raith, M. M., Srikantappa, C., Buhl, D., & Koehler, H. (1999). The Nilgiri enderbites, South India: nature and age constraints on protolith formation, high-grade metamorphism and cooling history. Precambrian Research, 98(1-2), 129-150.

Rao, G. P., & Rao, J. M. (2006). A palaeomagnetic study of charnockites from Madras block, southern granulite terrain, India. Gondwana Research, 10(1-2), 57-65.

Roedder, E. (1984). Volume 12: fluid inclusions. Reviews in mineralogy, 12, 644.

Roedder, E., & Bodnar, R. J. (1980). Geologic pressure determinations from fluid inclusion studies. Annual review of earth and planetary sciences, 8(1), 263-301.

Sain, K., Rajesh, V., Satyavani, N., Subbarao, K. V., & Subrahmanyam, C. (2011). Gas-hydrate stability thickness map along the Indian continental margin. Marine and Petroleum Geology, 28(10), 1779-1786.

Samuel, V. O., Santosh, M., Liu, S., Wang, W., & Sajeev, K. (2014). Neoarchean continental growth through arc magmatism in the Nilgiri Block, southern India. Precambrian Research, 245, 146-173.

Santosh, M. (1986). Carbonic metamorphism of charnockites in the southwestern Indian Shield: a fluid inclusion study. Lithos, 19(1), 1-10.

Santosh, M. (2020). The southern granulite terrane: a synopsis. Episodes Journal of International Geoscience, 43(1), 109-123.

Santosh, M., & Tsunogae, T. (2003). Extremely high density pure CO2 fluid inclusions in a garnet granulite from southern India. The Journal of geology, 111(1), 1-16.

Santosh, M., & Tsunogae, T. (2003). Extremely high density pure CO2 fluid inclusions in a garnet granulite from southern India. The Journal of geology, 111(1), 1-16.

Santosh, M., Maruyama, S., & Omori, S. (2009). A fluid factory in solid Earth. Lithosphere, 1(1), 29-33.

Santosh, M., Maruyama, S., & Omori, S. (2009). A fluid factory in solid Earth. Lithosphere, 1(1), 29-33.

Santosh, M., Maruyama, S., & Sato, K. (2009). Anatomy of a Cambrian suture in Gondwana: Pacific-type orogeny in southern India? Gondwana research, 16(2), 321-341.

Santosh, M., Yang, Q. Y., Shaji, E., Tsunogae, T., Mohan, M. R., & Satyanarayanan, M. (2015). An exotic Mesoarchean microcontinent: the Coorg block, southern India. Gondwana Research, 27(1), 165-195.

Santosh, M., Yang, Q. Y., Shaji, E., Tsunogae, T., Mohan, M. R., Satyanarayanan, M. 2015. An exotic Mesoarchean microcontinent: the Coorg Block, southern India. Gondwana Research, 27(1), 165-195.

Santosh, M., Yang, Q. Y., Shaji, E., Tsunogae, T., Mohan, M. R., & Satyanarayanan, M. (2015). An exotic Mesoarchean microcontinent: the Coorg block, southern India. Gondwana Research, 27(1), 165-195.

Santosh, M., Yokoyama, K., Biju-Sekhar, S., & Rogers, J. J. W. (2003). Multiple tectonothermal events in the granulite blocks of southern India revealed from EPMA dating: implications on the history of supercontinents. Gondwana Research, 6(1), 29-63.

Santosh, M., Yokoyama, K., Biju-Sekhar, S., & Rogers, J. J. W. (2003). Multiple tectonothermal events in the granulite blocks of southern India revealed from EPMA dating: implications on the history of supercontinents. Gondwana Research, 6(1), 29-63

Satish-Kumar, M. (2005). Graphite-bearing CO2-fluid inclusions in granulites: Insights on graphite precipitation and carbon isotope evolution. Geochimica et Cosmochimica Acta, 69(15), 3841-3856.

Shaji, E., Santosh, M., He, X. F., Fan, H. R., Dev, S. D., Yang, K. F., & Pradeepkumar, A. P. (2014). Convergent margin processes during Archean–Proterozoic transition in southern India: Geochemistry and zircon U–Pb geochronology of gold-bearing amphibolites, associated metagabbros, and TTG gneisses from Nilambur. Precambrian Research, 250, 68-96.

Shimpo, M., Tsunogae, T., & Santosh, M. (2006). First report of garnet–corundum rocks from southern India: implications for prograde high-pressure (eclogite-facies?) metamorphism. Earth and Planetary Science Letters, 242(1-2), 111-129

Sorby, H. C. (1858). On some peculiarities in the microscopical structure of crystals, applicable to the determination of the aqueous or igneous origin of minerals and rocks. Quarterly Journal of the Geological Society, 14(1-2), 242-242.

Srikantappa, C., & Malathi, M. N. (2008). Solid inclusions of magmatic halite and CO2^ H2O inclusions in the Closepet Granite from Ramnagaram, Dharwar Craton, India. Indian Mineralogist, 42, 84-89.

Srikantappa, C., Raith, M., & Touret, J. L. R. (1992). Synmetamorphic high-density carbonic fluids in the lower crust: evidence from the Nilgiri granulites, southern India. Journal of Petrology, 33(4), 733-760.

Srikantappa, C., Raith, M., & Touret, J. L. R. (1992). Synmetamorphic high-density carbonic fluids in the lower crust: evidence from the Nilgiri granulites, southern India. Journal of Petrology, 33(4), 733-760.

SWAMI, N., Ramakrishnan, M., & MN, V. (1976). Dharwar stratigraphic model and Karnataka craton evolution.

Thiéry, R., Van Den Kerkhof, A. M., & Dubessy, J. (1994). vX properties of CH4-CO2 and CO2-N2 fluid inclusions: modelling for T< 31 C and P< 400 bars. European Journal of Mineralogy, 6(6), 753-771.

Touret, J. L. R. (2001). Fluids in metamorphic rocks. Lithos, 55(1-4), 1-25.

Tsunogae, T., & Santosh, M. (2006). Spinel–sapphirine–quartz bearing composite inclusion within garnet from an ultrahigh-temperature pelitic granulite: implications for metamorphic history and P–T path. Lithos, 92(3-4), 524-536.

Tsunogae, T., Santosh, M., & Dubessy, J. (2008). Fluid characteristics of high-to ultrahigh-temperature metamorphism in southern India: a quantitative Raman spectroscopic study. Precambrian Research, 162(1-2), 198-211.

Van den Kerkhof, A. M., & Hein, U. F. (2001). Fluid inclusion petrography. Lithos, 55(1-4), 27-47.

Windley, B. F., Razafiniparany, A., Razakamanana, T., & Ackermand, D. (1994). Tectonic framework of the Precambrian of Madagascar and its Gondwana connections: a review and reappraisal. Geologische Rundschau, 83, 642-659.

GEOCHEMICAL ASSESSMENT OF GROUNDWATER QUALITY IN AND AROUND OF BHRAMAPURAM WASTE PROCESSING PLANT ERNAMKULAM DISTRICT, KERALA

Dissertation submitted to Christ College (Autonomous), Irinjalakuda, Kerala, University of Calicut in partial fulfillment of the degree of

Master of Science in Applied Geology

By,

SREELAKSHMI N S

Reg. No: CCAVMAG013

2021-2023

DEPARTMENT OF GEOLOGY AND ENVIRONMENTAL SCIENCE CHRIST COLLEGE (AUTONOMOUS), IRINJALKUDA, KERALA, 680125

(Affiliated to University of Calicut and re-accredited with by NAAC with A++ grade)

SEPTEMBER 2023

CERTIFICATE

This is to certify that the dissertation entitled – **GEOCHEMICAL ASSESSMENT OF GROUNDWATER QUALITY IN AND AROUND OF BHRAMAPURAM WASTE PROCESSING PLANT ERNAMKULAM DISTRICT, KERALA**, is a bonafide record of work done by Ms. Sreelakshmi N S (Reg. No. CCAVMAG013), MSc Applied Geology, Christ College (Autonomous) Irinjalakuda, under my guidance in partial fulfilment of requirements for the degree of Master of Science in Applied Geology during the year 2021- 2023.

Project Guide

Dr. Anto Francis K
Co-ordinator (Geology Self-financing)
Dept. of Geology and Env. science
Christ College (Autonomous) Irinjalakuda
Kerala- 680125

Dr. Anso M A
Assistant Professor
Dept. of Geology and Env. science
Christ College (Autonomous) Irinjalakuda
Kerala- 680125

Place: Irinjalakuda
Date: ……

External Examiners;

1……

2……

DECLARATION

I hereby declare that this dissertation work – **GEOCHEMICAL ASSESSMENT OF GROUNDWATER QUALITY IN AND AROUND OF BHRAMAPURAM WASTE PROCESSING PLANT ERNAMKULAM DISTRICT, KERALA**, is a work done by me. No part of the report is reproduced from other resources. All information included from other sources has been duly acknowledged. I maintain that if any part of the report is found to be plagiarized, I shall take the full responsibility for it.

Place: Irinjalakuda SREELAKSHMI N S

Date: ……. Reg. No. CCAVMAG013

ACKNOWLEDGEMENT

This report is an official documentation of dissertation work carried out in Ambalamukal Industrial Area, Kerala. This report would not have been possible without guidance, encouragement and support of many well-wishers and my colleagues who helped me in many ways.

I would like to express my sincere gratitude and appreciation to **Dr. Anso M A**, Assistant Professor in the Department of Geology and Environmental Science at Christ College (Autonomous) Irinjalakuda. He played a pivotal role in shaping the framework of this thesis and provided unwavering support and guidance throughout the entire duration of the study.

Dr. Linto Alappat, Dean of Research and Development of TLC (Former Head, Department of Geology and Environmental Science, Christ College (Autonomous) Irinjalakuda), Mr **Tharun R**, Head of the Department of Geology and Environmental Science, Christ College (Autonomous) Irinjalakuda, for rendering all the help and facilities available in the department. I express my utmost gratitude to **Mr. Ayyappadas C.S**, a Research Scholar at Christ College (Autonomous) Irinjalakuda, for his invaluable assistance in the technical aspects of my study and his unwavering support during the completion of my dissertation.

I am grateful to **Dr. Anto Francis K**, Coordinator (Geology Self-financing), and the other faculty members of the Department of Geology and Environmental Science, Christ College (Autonomous), Irinjalakuda, for their encouragement, direction, and affection.

I'd like to take this opportunity to thank all of my teachers, classmates and friends who supported me in completing this dissertation work, whether directly or indirectly.

I am grateful to the entire Christ College family for their love, support, and guidance. I also express my gratitude to my parents and my sister for their unwavering support and prayers throughout my life. Above all, I express my gratitude to God, the Almighty, for His divine generosity and blessings showered upon me.

SREELAKSHMI N S

ABSTRACT

Water is an essential element for the life of all living beings. Water has special qualities that make it an important part of the Earth's biosphere. As a result, determining water quality is critical to understanding the ecosystem's equilibrium status. In this regard, the current investigation was carried out in and around the Brahmapuram waste processing plant in Ernakulam to assess the quality of the groundwater. The landfills, pollutions from nearby industries, unattended environmental issues may have detiorated the quality of groundwater around Brahmapuram. Laterites, sandstone, shale, and clay dominate the lithology of the Brahmapuram area, with charnokite as the basement rock. The aim of the study is to quantify the physcio-chemical parameters of the study area and thereby to check the groundwater quality in around Bhramapuram area. Forty water samples were collected for observations. The groundwater in the study area is mostly acidic in nature. According to the EC spatial distribution map, the eastern section of the research area has the lowest EC and TDS values. The surface water influence from Kadambrayar river is evident in the groundwater quality of the area. The content of bicarbonate, sodium values range from 2.4–64.66 mg/l and 115.73 to 2.06 mg/l respectively. The correlation table shows that alkalinity has a positive correlation with pH. The low concentration of calcium and magnesium accounts for the least total hardness in the study area. The Piper diagram, Wilcox diagram, Gibbs plot, correlation analysis and factor analysis details chemometrics of the current study which in-turn help to understand hydrogeochemical setting in and around the Brahmapuram waste processing plant.

TABLE OF CONTENTS

LIST OF FIGURES

LIST OF TABLES

CHAPTER 1

INTRODUCTION

1.1 Groundwater

Groundwater is our most valuable natural resource. It provides around one-third of the water used in municipal water systems across the country, as well as nearly 90% of the drinking water used in rural towns that prefer not to use local water departments. The primary source of groundwater is precipitation. Rainfall penetrates the soil zone beneath the ground's surface. When the soil zone becomes saturated, water percolates downward. In a saturation zone, all of the interstices fill with water. There is also an aeration zone, in which air and water alternately fill the interstices (C R Fitts 2002). Rain, snow, sleet, or hail that falls to the ground can continue its journey in one of three ways: it can settle on a body of water and travel with the stream; it can run off the land and into a body of water or storm drain; or it can soak into the ground. Water seeps into the ground downhill through the spaces between soil particles due to gravity until it reaches a soil depth where the pore spaces are already saturated or filled with water(P L Younger 2009). When water enters the saturated zone, it becomes a component of groundwater. The top of this saturated zone is the water table. When there is a body of water nearby, the water table is frequently near the surface. Precipitation that falls on the ground's surface has a number of consequences. As it moves through the land, some of the water drains into streams, lakes, or the ocean. Water seeps into the earth from the surface soil if it is permeable, a process called infiltration. Water that enters the soil is attracted to soil particles and may be absorbed into the developing plant roots. Once the water has been consumed by the plant, it is released into the atmosphere as a vapor. Excess soil moisture is drawn downward by gravity. The depth at which soil or rock pores get saturated with water might vary depending on the area. The permeability of the soil or rock in the saturated zone determines the rate at which groundwater flows. A saturated zone formed of a less permeable material, such as clay, causes water to move more slowly. Groundwater can travel at speeds ranging from several feet per day to one foot every century. If permafrost or another barrier prevents groundwater from blooming, the water may find alternative methods to get around it. Aquifers are the underground structures that hold groundwater (S Mandel 2012). An aquifer is a geological structure, or a portion of one, that is constructed of permeable material and has the ability to store or produce vast volumes of water. Aquifers can be composed of a range of materials, such as loose sands and gravels, permeable sedimentary rocks such as sandstones or limestones,

broken volcanic and crystalline rocks, and so on. Rain and snowfall, as well as water that seeps through the bottoms of some lakes and rivers, naturally replenish groundwater. Groundwater can be recharged when water distribution systems break and crops are watered with more water than necessary. There are methods for controlling aquifer recharge and increasing groundwater infiltration.

1.2 Significance of groundwater

1.Groundwater is an important source of drinking water for millions of people worldwide. Many communities rely on groundwater wells as their primary source of safe drinking water, particularly in rural areas.

2.Agricultural Irrigation. Groundwater is vital in agriculture because it provides a continuous and steady source of water for irrigation. It helps crop development during dry periods and in places with limited surface water supplies.

3.Industrial and Commercial uses : Groundwater is used in a variety of industrial and commercial processes, including manufacturing, cooling, and cleaning. Groundwater is widely used in industries that require large amounts of water, such as power generation and food processing.

4.Ecosystem Support. Groundwater sustains wetlands, springs, streams, and rivers during periods of low precipitation or drought. These environments are crucial for biodiversity, wildlife habitat, and maintaining ecological equilibrium.

5.Groundwater recharge. Groundwater serves as a natural storage reservoir that replenishes over time through methods such as rainwater penetration. It helps to maintain river baseflow and contributes to overall water availability.

6.Drought Resilience: Groundwater can be used as a buffer during times of drought when surface water supplies become scarce or unreliable. Groundwater access can assist communities and agriculture during times of water constraint.

7.Geothermal energy : In areas with abundant geothermal resources, groundwater can be a source of geothermal energy, providing direct heat or power generation.

8.Contaminant Filtration: Water naturally filters through soil and rock strata, which can help eliminate or reduce some contaminants. Groundwater can act as a natural filter in some instances, improving water quality.

9.Research and Exploration: Groundwater systems provide vital insights into hydrogeology, geology, and the flow of subterranean fluids. A groundwater study can help us better understand Earth's processes and history.

10.Sustainability and management : Groundwater resource management is crucial to guaranteeing their long-term viability. Sustainable groundwater management solutions aid in reducing overexploitation and aquifer depletion.

11Emergency water Supply. When surface water supplies are disrupted due to natural catastrophes or pollution issues, groundwater wells can provide a reliable source of emergency water supply.

12.Climate Resilience: Groundwater can help mitigate the consequences of climate change by acting as a buffer against shifting precipitation patterns and supporting ecosystems during dry spells.

13.Recreation and Aesthetics:. Groundwater-fed springs, lakes, and streams are frequently used for leisure purposes such as swimming, fishing, and animal viewing. These natural traits also contribute to the psychological appeal of landscapes.

14.Given their importance, sustainable management and ethical use of groundwater resources are important to maintaining their availability for future generations as well as the health of ecosystems and civilizations that rely on them.

1.3 Potential Source of groundwater contamination

Storage tank : They could be above or below ground and could hold liquids such as chemicals, oil, petrol, or another kind. with 10 million storage tanks are thought to be buried in the United States; with time, these tanks may corrode, crack, and leak. Serious contamination may result if the toxins escape and enter the groundwater.

Septic system: Systems for disposing of wastewater on-site that are utilised by residences, workplaces, or other structures that are not connected to a municipal sewage system. Human waste is slowly and safely drained away underground by septic systems. Inadequate septic

systems can leach germs, viruses, household chemicals, and other toxins into the groundwater, posing major health risks.

Uncontrolled Hazardous Waste: Over 20,000 abandoned and unregulated hazardous waste sites are thought to exist in the United States as of right now, and the number continues to rise. If there are barrels or other containers lying around that are filled with hazardous materials, hazardous waste sites can cause groundwater pollution. These toxins have the potential to eventually seep into the groundwater if there is a leak.

Landfills: Our waste is transported to landfills where it is buried. To keep toxins from contaminating the water, landfills are intended to have a barrier at the bottom. However, if there isn't one or it is broken, toxins from the trash, such as paint and household cleansers, might seep into the groundwater.

Chemicals and Road salt: Another potential source of groundwater contamination is the extensive use of chemicals and deicing agents. Chemicals include items used in homes and businesses as well as items used on lawns and farm fields to kill weeds, insects, and fertilise plants. These substances may leak into the ground during rainstorms and finally reach the water. In the winter, road salts are used to melt ice on the roadways to prevent cars from swerving. The salt is washed off the roadways and finally finds its way into the water as the ice melts.

Atmospheric Contaminants: As a component of the hydrologic cycle, groundwater is susceptible to contamination from other sections of the cycle, such as the atmosphere or bodies of surface water.

1.4 AIM AND OBJECTIVES

The aim of this study is to analyse the quality of ground water in and around of Brahmapuram landfill area of Ernakulam District.

1 To study the spatial variation of physicochemical properties of groundwater.

2. To identify the suitability of groundwater for irrigation purposes.

3. To delineate the natural processes from the chemometrics.

CHAPTER 2

REVIEW OF LITERATURE

M.Ackah et.al., 2011 In the Ga East Municipality (Ghana), a large farming community, the acceptability of groundwater quality for drinking and agricultural purposes was evaluated. To evaluate the quality of the groundwater in 16 wells in the Teiman-Oyarifa community, various water quality metrics were established. Standard physicochemical analysis techniques were used. Water samples from boreholes, hand-dug wells, and pipes were gathered throughout the area and examined. Results showed the temperature range of 19.5o C-26.7o C, pH range of 4-7.4, conductivity range of 214-2830 µS/cm, total dissolved solids, 110-1384 mg/L, bicarbonate,8.53-287.7mg/L, chloride, 28.41-813.8 mg/L, Flouride, below detection limit -0.4667mg/L, Nitrate 1.9-4625 mg/L, sulphate, 16.35-149.88mg/L. The results of an investigation employing atomic absorption spectroscopy revealed that the metal concentrations of Fe, Mn, and Ca were respectively 0.212–3.396 mg/L, 0.01-0.1 mg/L, and 0.39–9.97 mg/L. The primary cations and anions' relative ionic dominances were Na+>K+>Mg+>Ca+ and Cl->HCO3->SO42->NO3-, in that order. The majority of the samples examined fell under the drinking water guidelines established by both national and international authorities. The majority of the groundwater samples fit into the US Salinity Laboratory's C2-S1 (medium salinity-low SAR) classification.

C Sarala,P Ravi babu 2012Except in a few rare instances where total hardness and fluoride concentrations are high, the analysis shows that the concentration of key constituents is often well within the acceptable limits of IS (10500-1994).It has been determined from the examination that the groundwater is contaminated over the whole research region. Due to this, during the monsoon season, rainwater drains into the solid waste, polluting the land leachate that already exists in the nearby areas and in the low lying places. Surface and groundwater use for drinking, industry, and agriculture has multiplied over the past few years, but as a result, it has been found that the water is polluted and has an adverse impact on the environment, livestock, soil nutrients, and biomass in some areas.Consequently, a study on the quality of the available groundwater has been conducted.

Venkateswara Rao et.al 2011 Water samples from various places were collected to study the physicochemical parameters of groundwater and municipal water in Vijayawada Rural and Town. During April and May of 2010, groundwater samples were collected for the study. The

findings were compared to WHO and ISI 10500-91 criteria. A total of 15 parameters were examined. At a few test sites, including Akunuru, Auto Nagar, and Vijayawada, it was discovered that the subterranean water was contaminated. The sampling locations Patamata Lanka and Madduru revealed physicochemical values within the water quality criteria, indicating that the water quality is good and fit for drinking.

P.Hemant et.al 2012 During a two-year period, water samples from ponds and reservoirs were tested for 15 physicochemical parameters, including water temperature, color, conductivity, turbidity, total solids, total dissolved solids, pH, alkalinity, and chlorides. During different seasons, total hardness, dissolved oxygen, biological oxygen demand, chemical oxygen demand, iron, and fluoride levels were measured. Ground water testing showed deviations, indicating ground water pollution. The water collected in Patamata Lanka and Madduru was proven to be safe to drink.

P.C Mane et.al 2017 Water-borne infections cause high rates of mortality and morbidity in India. As a result, the quality of drinking water must be examined on a frequent basis. The current study examines selected nutrients and metals in Manikdoh dam water during the 2016 pre-monsoon season. Calcium, phosphate, sulphate, nitrate, iron, manganese, selenium, zinc, chromium, and nickel were the parameters studied. When compared to the allowed limits for drinking water established by the Indian Standards (IS), the results show a considerable rise in some nutrients and metal levels. Calcium, phosphate, sulphate, iron, manganese, selenium, and nickel levels are significantly higher than the recommended levels.

Devendra Dohare et.al (2014) The quality of groundwater was assessed in various Indore City wards. The current study aims to calculate the water quality index (WQI) for groundwater in Indore City and its surrounding industrial region. Groundwater samples from all of the wards' designated stations were collected for physiochemical study. The following 27 parameters have been evaluated for calculating current water quality status by statistical evaluation and the water quality index Viz. pH, color, and total dissolved solids are all important factors to consider. calcium, chromium, zinc, manganese, nickel, total alkalinity, total hardness.The water quality assessment that the parameter slightly more in wet season compare to dry season.

Fikret Ustaoglu et al, 2021 The current study aims to offer a detailed picture of the river's water quality situation and pollution sources. Standard methodologies were used to examine some physicochemical characteristics of the river's surface water throughout time. Major elements

and heavy metal concentrations (Na, Mg, K, Ca, Al, Cr, Fe, Co, Mn, Ni, Zn, Cd, Cu, Pb, and As) were measured in water samples. The relationships between physicochemical data were examined using multivariate statistical analysis (MSA) methodologies. $Ca^{2+} > Mg^{2+} > Na^{+} > K^{+} > NH_4^{+}$ (32.66, 26.82, 13.29, 6.45, 0.305; mg/L), and anions: $SO_4^{2-} > NO_3^{-} > F^{-} > NO_2^{-}$ (7.88, 3.988, 1.01, 0.0316; mg/L).

Gagan Matta et al, 2015 Maximum turbidity, total solids, free CO_2, total hardness, pH, nitrate, nitrite, biochemical oxygen demand, chemical oxygen demand, and phosphate were measured during the investigation, while minimum velocity, transparency, and dissolved oxygen were measured at site 2 in comparison to site 1. When the mean values of these parameters were compared to WHO and ISI criteria, significant differences (p 0.05) in the mean values of turbidity, total solids, pH, dissolved oxygen, free CO_2, and total hardness with sampling locations were discovered.The result of their study to indicated that physiochemical parameters from Ganga canal system were within or comparitably with the ISL and WHO permissible limit of drinking water.So by the final conclusion says that it is suitable for domestic purposes.

R Ullah et al,2009 The purpose of this study was to evaluate the quality of groundwater in relation to heavy metal pollution and its impact on human health. The groundwater quality of Sialkot, a Pakistani industrial city, was assessed using water samples obtained from 25 different locations during October and November 2005. Twenty-two physiochemical parameters including pH, Electric Conductivity (EC), Total Dissolved Solids (TDS), Salinity, Temperature, Turbidity, Sulfate (SO_4) Chloride (Cl), Total Hardness, Iodide, Fluoride, Ferric (Fe^{+3}), Nitrate (NO_3), Manganese (Mn), Total Chlorine, Alkalinity, Zinc (Zn), Lead (Pb), Iron (Fe), Copper (Cu), Nickel (Ni) and Chromium (Cr) were recorded. The findings were compared to World Health Organization (WHO) and Pakistan Standard Quality Control Authority (PSQCA) groundwater quality standards. The results revealed that the groundwater in the research area is not of excellent quality since it is highly turbid (57% of total sites) and contains high levels of Zn, Fe, and Pb that exceed WHO and PSQCA allowed limits. Geographic Information System (GIS) was used to create spatial distribution maps of water quality metrics.

K.A. Yusuf et al., 2007, the water demands of Lagos are satisfied by the utilisation of both surface and groundwater resources. The city in question, situated in the southwestern region of Nigeria, is characterised by its industrial nature and high population density. However, it faces challenges related to resource constraints and issues pertaining to migration. Nevertheless, a significant portion of the population is dependent on well water as their primary supply of

drinking water. Consequently, a study was undertaken to investigate the inorganic composition of water extracted from wells that access shallow aquifers inside the urban area. The findings of this study indicate that a portion of the groundwater examined surpasses the drinking water quality standards set by the World Health Organisation. Regardless of the origin of the pollution, the study observed that 50% of the samples exceeded the limit for total dissolved solids, 27.8% exceeded the limit for conductivity, 38.9% exceeded the limit for lead, 44.4% exceeded the limit for pH, and 11.1% exceeded the limits for sodium and calcium.

Krishna Kumar et.al., 2009 investigation into the quality of the groundwater in the Manimuktha river basin in Tamilnadu and Kerala was carried out. There were a total of twenty-six bore well samples that were examined for geochemical variation and water quality. using the utilisation of a Piper trilinear diagram. It was determined that there are four primary hydrochemical facies, and they are Ca–HCO3, Na–Cl, Mixed Ca–Na–HCO3, and mixed Ca–Mg–Cl. The results of the geochemical analysis, when compared with the drinking water standards established by the Environmental Protection Agency of the United States, the World Health Organisation, and the Indian Standard Institution, indicate that all groundwater samples, with the exception of a few, are suitable for use as irrigation water and as drinking water.

Salihou Djari et al., 2018, assessed results of the groundwater quality study in the Tillabery Region are worrying because high levels of nitrites, nitrates, electrical conductivity, carbonate hardness, sodium concentration, dissolved iron, and total manganese can be bad for human health. When used for long periods of time, these factors can lead to the spread of diseases and illnesses. The groundwater quality study shows that 7 parameters, including nitrites, nitrates, electrical conductivity, carbonate hardness, sodium concentration, dissolved iron, and total manganese, do not meet the World Health Organization's standards for drinking water quality. The study shows that 10 of the 38 samples are in the "Good water quality" class, which means the water is safe to drink, and 16 samples are in the "Medium high water quality" class, which means the water is good enough to drink with little or no treatment. But 10 samples are in the "Medium low water quality" class, which means that the water needs a lot of work to meet the rules for drinking water.

E. Barth-Naftilana et al., 2018, looked into how shale gas development (SGD) might affect the quality of groundwater in the Marcellus Shale. The researchers put in eight multilevel tracking wells in bedrock aquifers of a 25-km2 area that was going to be used for SGD. Each month for two years, they took samples from 24 separate points in these wells. Before, during, and after

seven shale gas wells were drilled, hydraulically fractured, and put into production, groundwater levels were also measured.Also, salinity went up at the same time as [CH4], which rules out pollution by gas phase migration of escaping methane from gas wells with weak structures. These observations show that SGD was probably not the source of the methane in the valley wells, and that the concentration and composition of naturally occurring methane in valley settings, where regional flow systems interact with local flow systems, is more variable in time and space than was thought before.

Qiwen Xia et al., 2022 studied looked at how the re-use of water affects the chemistry of groundwater in the Jian and Chaobai Rivers in Beijing over time. The results showed that long-term infiltration of reclaimed water led to a significant increase in Na+, Cl–, and K+ and a drop in Ca2+, Mg2+, and HCO3- concentrations in the groundwater. The hydrochemical changes in Jian River and Chaobai River were very different. Jian River's groundwater changed to be more like recovered water, while Chaobai River's groundwater went in a different direction. The changes in hydrochemical evolution were thought to be caused by sediment thickness and geochemical processes like mixing and sulphate reduction. The study also shows the possible risks of using recycled water to restore river ecosystems, as well as the need for proper monitoring and control practises.

Tamás Mester et al., 2020 assesses with the help of three water quality measures, the study looked at how the quality of groundwater changed before and after a sewerage network was built. Before the sewerage network was built, the groundwater was heavily polluted. According to Brown's index, 90% of wells were either polluted or heavily polluted, 70% according to the contamination index Cd by Rapant, and 80% according to the Canadian Council of Ministers of the Environment Water Quality Index. But after the sewage network was built, there were big changes in the water quality. The number of wells that were very polluted went down, and the number of wells that were "good" or "acceptable" went up.

Peiyue Li et al., 2017, the goal of the study was to figure out what the hydrochemical properties of groundwater were in a grassy plain in northwest China that was next to a paper wastewater irrigation zone. Samples were taken from 14 groundwater monitoring wells at three different times of the year, and statistical analysis and Chadha diagrams were used to describe the water's chemical properties. Most of the groundwater samples had a hydrochemical facies called SO4 Cl- Na. Some of the samples also had HCO3- Ca- Mg, HCO3- Na, and Cl, SO4-, Ca-, Mg hydrochemical facies. The study found that the major ions and toxins in the groundwater are

controlled by many things, such as hydrogeological conditions, rock weathering, interactions between water and rock, and human activities. Since pH, TDS, and TH readings went down during the monsoon season, it was seen that the water quality got a little better.

Subba Rao et al., 2018, the study involved the analysis of groundwater samples obtained from thirty different locations within the Prakasam district of Andhra Pradesh, India. These samples were examined for a range of chemical parameters, including pH, electrical conductivity (EC), total dissolved solids (TDS), calcium (Ca2+), magnesium (Mg2+), sodium (Na+), potassium (K+), bicarbonate (HCO−3), chloride (Cl-), sulphate (SO2−4), nitrate (NO−3), and fluoride (F−). The alkaline nature of the groundwater is seen, and it is primarily characterised by the presence of Na+–HCO−3 and Na+–Cl− facies. The chemical composition of groundwater is primarily influenced by the process of rock weathering, and it is further altered by human activities.

Milad H. Z. Masoud et al., 2018 aimed to assess the influence of flash flood recharge on the quality of groundwater and its appropriateness for various purposes within the Wadi Baysh Basin located in Western Saudi Arabia. The examination of groundwater samples obtained prior to and subsequent to a sudden and intense flood occurrence revealed a notable reduction in total dissolved solids (TDS), magnesium (Mg), sodium (Na), chloride (Cl), nitrate (NO3), and electrical conductivity (EC) following the event. The research conducted revealed that the introduction of surface water through flash flood recharge exerted a noteworthy impact on the chemical composition of groundwater. The predominant water types observed were a combination of calcium-magnesium-chloride, sodium chloride, and calcium-chloride. The predominant categorizations of the water samples were C3S1, C4S2, and C3S2, indicating their appropriateness for the purpose of irrigating crops that are tolerant to saline conditions. The research findings indicate that the implementation of check dams in arid valleys has the potential to enhance the quality of groundwater in the region.

Yongjun Jiang et al,2008 The impact of land-use change on groundwater quality in the Xiaotjiang watershed, China, was studied from 1982 to 2004. Groundwater samples were obtained from 30 monitoring stations throughout the watershed and were typical of the numerous changes identified using remote sensing and geographic information systems. According to the findings, 610 km2 (60% of the total watershed area) experienced land-use change over the study period. The conversion of 135 km2 of wooded land to cultivated land and 211 km2 of unused land to cultivated land were the most significant developments. The

main damage was attributed to diffuse contamination from fertilizers applied to newly farmed land and from construction development. Overall, the pH of groundwater increased

. K .Saravanakumar and R Ranjith Kumar 2011 Water pollution affects all land surfaces, including Ambattur. Because all metabolic and physiological activities and life processes of aquatic species are often influenced by polluted waste, it is critical to research the physico-chemical features of water.The result of the water investigation ,water of their study area highly contaminated with Total Dissolved Solids,Higher TDS loses.The potability and decrease the solubility of oxygen in water.water of the study area affected the hard and contaminated.Because of this,the population of the Ambattur area are prove by the immediate health problems such as stomach disease ,gastric troubles.

K.A. Yusuf et al., 2007, the water demands of Lagos are satisfied by the utilisation of both surface and groundwater resources. The city in question, situated in the southwestern region of Nigeria, is characterised by its industrial nature and high population density. However, it faces challenges related to resource constraints and issues pertaining to migration. Nevertheless, a significant portion of the population is dependent on well water as their primary supply of drinking water. Consequently, a study was undertaken to investigate the inorganic composition of water extracted from wells that access shallow aquifers inside the urban area. The findings of this study indicate that a portion of the groundwater examined surpasses the drinking water quality standards set by the World Health Organisation. Regardless of the origin of the pollution, the study observed that 50% of the samples exceeded the limit for total dissolved solids, 27.8% exceeded the limit for conductivity, 38.9% exceeded the limit for lead, 44.4% exceeded the limit for pH, and 11.1% exceeded the limits for sodium and calcium.

Krishna Kumar et.al., 2009 investigation into the quality of the groundwater in the Manimuktha river basin in Tamilnadu and Kerala was carried out. There were a total of twenty-six bore well samples that were examined for geochemical variation and water quality. using the utilisation of a Piper trilinear diagram. It was determined that there are four primary hydrochemical facies, and they are Ca–HCO3, Na–Cl, Mixed Ca–Na–HCO3, and mixed Ca–Mg–Cl. The results of the geochemical analysis, when compared with the drinking water standards established by the Environmental Protection Agency of the United States, the World Health Organisation, and the Indian Standard Institution, indicate that all groundwater samples, with the exception of a few, are suitable for use as irrigation water and as drinking water.

Salihou Djari et al., 2018, assessed results of the groundwater quality study in the Tillabery Region are worrying because high levels of nitrites, nitrates, electrical conductivity, carbonate hardness, sodium concentration, dissolved iron, and total manganese can be bad for human health. When used for long periods of time, these factors can lead to the spread of diseases and illnesses. The groundwater quality study shows that 7 parameters, including nitrites, nitrates, electrical conductivity, carbonate hardness, sodium concentration, dissolved iron, and total manganese, do not meet the World Health Organization's standards for drinking water quality. The study shows that 10 of the 38 samples are in the "Good water quality" class, which means the water is safe to drink, and 16 samples are in the "Medium high water quality" class, which means the water is good enough to drink with little or no treatment. But 10 samples are in the "Medium low water quality" class, which means that the water needs a lot of work to meet the rules for drinking water.

E. Barth-Naftilana et al., 2018, looked into how shale gas development (SGD) might affect the quality of groundwater in the Marcellus Shale. The researchers put in eight multilevel tracking wells in bedrock aquifers of a 25-km2 area that was going to be used for SGD. Each month for two years, they took samples from 24 separate points in these wells. Before, during, and after seven shale gas wells were drilled, hydraulically fractured, and put into production, groundwater levels were also measured.Also, salinity went up at the same time as [CH4], which rules out pollution by gas phase migration of escaping methane from gas wells with weak structures. These observations show that SGD was probably not the source of the methane in the valley wells, and that the concentration and composition of naturally occurring methane in valley settings, where regional flow systems interact with local flow systems, is more variable in time and space than was thought before.

Qiwen Xia et al., 2022 studied looked at how the re-use of water affects the chemistry of groundwater in the Jian and Chaobai Rivers in Beijing over time. The results showed that long-term infiltration of reclaimed water led to a significant increase in Na+, Cl–, and K+ and a drop in Ca2+, Mg2+, and HCO3- concentrations in the groundwater. The hydrochemical changes in Jian River and Chaobai River were very different. Jian River's groundwater changed to be more like recovered water, while Chaobai River's groundwater went in a different direction. The changes in hydrochemical evolution were thought to be caused by sediment thickness and geochemical processes like mixing and sulphate reduction. The study also shows the possible risks of using recycled water to restore river ecosystems, as well as the need for proper monitoring and control practises.

Tamás Mester et al., 2020 assesses with the help of three water quality measures, the study looked at how the quality of groundwater changed before and after a sewerage network was built. Before the sewerage network was built, the groundwater was heavily polluted. According to Brown's index, 90% of wells were either polluted or heavily polluted, 70% according to the contamination index Cd by Rapant, and 80% according to the Canadian Council of Ministers of the Environment Water Quality Index. But after the sewage network was built, there were big changes in the water quality. The number of wells that were very polluted went down, and the number of wells that were "good" or "acceptable" went up.

Peiyue Li et al., 2017, the goal of the study was to figure out what the hydrochemical properties of groundwater were in a grassy plain in northwest China that was next to a paper wastewater irrigation zone. Samples were taken from 14 groundwater monitoring wells at three different times of the year, and statistical analysis and Chadha diagrams were used to describe the water's chemical properties. Most of the groundwater samples had a hydrochemical facies called SO4 Cl- Na. Some of the samples also had HCO3- Ca- Mg, HCO3- Na, and Cl, SO4-, Ca-, Mg hydrochemical facies. The study found that the major ions and toxins in the groundwater are controlled by many things, such as hydrogeological conditions, rock weathering, interactions between water and rock, and human activities. Since pH, TDS, and TH readings went down during the monsoon season, it was seen that the water quality got a little better.

Subba Rao et al., 2018, the study involved the analysis of groundwater samples obtained from thirty different locations within the Prakasam district of Andhra Pradesh, India. These samples were examined for a range of chemical parameters, including pH, electrical conductivity (EC), total dissolved solids (TDS), calcium (Ca^{2+}), magnesium (Mg^{2+}), sodium (Na^{+}), potassium (K^{+}), bicarbonate (HCO^{-}_{3}), chloride (Cl^{-}), sulphate (SO^{2-}_{4}), nitrate (NO^{-}_{3}), and fluoride (F^{-}). The alkaline nature of the groundwater is seen, and it is primarily characterised by the presence of Na^{+}–HCO^{-}_{3} and Na^{+}–Cl^{-} facies. The chemical composition of groundwater is primarily influenced by the process of rock weathering, and it is further altered by human activities.

Milad H. Z. Masoud et al., 2018 aimed to assess the influence of flash flood recharge on the quality of groundwater and its appropriateness for various purposes within the Wadi Baysh Basin located in Western Saudi Arabia. The examination of groundwater samples obtained prior to and subsequent to a sudden and intense flood occurrence revealed a notable reduction in total dissolved solids (TDS), magnesium (Mg), sodium (Na), chloride (Cl), nitrate (NO3),

and electrical conductivity (EC) following the event. The research conducted revealed that the introduction of surface water through flash flood recharge exerted a noteworthy impact on the chemical composition of groundwater. The predominant water types observed were a combination of calcium-magnesium-chloride, sodium chloride, and calcium-chloride. The predominant categorizations of the water samples were C3S1, C4S2, and C3S2, indicating their appropriateness for the purpose of irrigating crops that are tolerant to saline conditions. The research findings indicate that the implementation of check dams in arid valleys has the potential to enhance the quality of groundwater in the region.

Guanxing Huang et al.,2022, the primary objective of this study is to examine the alterations observed in groundwater with high iron content within the Pearl River Delta (PRD) region during the last twelve-year period. The Pearl River Delta (PRD) region exhibits a prevalence of marine sediments and a historical distribution of iron-rich groundwater. Nevertheless, there has been a notable decline in the presence of groundwater with high iron content in recent times. In the years 2006 and 2018, a series of groundwater samples were obtained and subjected to analysis. The findings of this investigation revealed a decline in the proportion of groundwater with high iron content, specifically from 19.3% in 2006 to 1.3% in 2018. In 2006, there was a higher occurrence of groundwater with elevated iron content in coastal-alluvial aquifers compared to other aquifers. In 2006, the existence of iron-rich groundwater in the Pearl River Delta (PRD) was primarily attributed to two significant anthropogenic factors: the penetration of industrial wastes and the irrigation with surface water containing high levels of iron.

Visant Madhav Wagh et al.,(2019) Hydrochemical characterization using the Durov plot, Chaddha diagram, Gibbs plot, and different scatter plots was used to determine how weathering, rock influence, precipitation and evaporation, reaction types, and so on influenced the region's groundwater composition. The chemistry of groundwater has mostly worsened as a result of agricultural and anthropogenic activities. The WQI spatial variation map shows that groundwater quality is primarily influenced in the research area's south and in a few places in the north.

Arjun peethambaran ,Anso M A et al., 2021 Chemometric analysis such as correlation matrix and factor analysis were used in the study, and the chemistry of groundwater was determined using Gibbs diagrams, Piper diagrams, and box and whisker diagrams. The findings indicate that the groundwater in the studied area is neutral to mildly alkaline in nature. According to the

Box whisker diagram, the order of abundance for cations is Ca2+> Na+ > Mg2+ and for anion is Cl- >HCO3 - > So4 2- for both seasons. The Gibbs diagram demonstrates that rock-water interaction is the dominant characteristic affecting the chemistry of groundwater during both seasons. The geogenic process is the key factor affecting the chemistry of groundwater during pre- and postmonsoons, based on factor analysis and correlation matrix.

Andres Marandi 2018 Many groundwater ion concentrations can be explained in great part by mixing and water-rock interactions. The network of flow channels, as well as the time each path spends in contact with various minerals and mixing with older waters at depth, govern key processes that create groundwater salinity. As a result, only ratios of Na/(Na + Ca) (or Cl/(Cl + HCO3)) are expressed on the Gibbs Diagram.

S Krishnakumar et al., 2017 The piper diagram shows that the bulk of the samples fall into the Ca-Mg-Cl, Na-Cl, and Ca-Cl fields and that the water quality in the research area is mostly regulated by anthropogenic activities, dissolution processes, and ion exchange processes. The LSI calculation findings show that the bulk of the samples are slightly corrosive with scale formation. Except for less than 5% of the samples, the irrigation water quality metrics revealed that the bulk of the water samples are appropriate for irrigation. The trace element concentration reveals that the slightly increasing trends of Fe and Mn in a few samples are most likely due to chemical weathering dissolution and the ferromagnetism process. The statistical results explain the ion association, which is dominated by anthropogenic activities such as weathering.

D Sujatha et al., 2003 The area has a semi-arid environment and is made up of igneous granites and pegmatites from the Archaean period. Forty-five representative groundwater samples were obtained from bore wells to study the water chemistry of several ions, including Ca+2, Mg+2, Na+, K+, CO3, HCO3, SO4, NO3, Cl, and F. The quantities of these ions were found to be over the allowable limits for drinking and irrigation. The contamination in terms of NO3, Cl, and F is mostly due to the intensive use of fertilizers and the large-scale discharge of municipal waste into the area's open drainage system.

Herman Bouwer 1987 Most state or federal guidelines address solely public health concerns, prescribing the treatment techniques or quality specifications that effluent must achieve before it may be utilized to irrigate a specific crop. However, crop and soil agronomic aspects must also be considered. Bacteria, viruses, and other pathogens; total salt content and sodium

adsorption ratio of water (soil and crop effects); nitrogen; phosphorus; chloride and chlorine; bicarbonate; heavy metals, boron, and other trace elements; pH; and synthetic organics (including pesticides) are all quality parameters to consider.

K Mathew (1982) Nitrogen removal was thoroughly investigated because it is a prominent pollutant in secondary sewage effluent, and soil adsorption is a crucial prerequisite for its removal. In order to simulate the total process and optimize nitrogen removal, a mathematical model based on the mechanisms contributing to nitrogen removal was constructed. For management purposes, a simplified but realistic model was developed.

Babu P Mynar 2017 Their study based on the Kotaih 1994 paper based, Water is a significant natural resource that is required for human health, socioeconomic development, and ecosystem function. Water's chemical constituents exist as dissociated particles, or ions. The chemistry of groundwater in terms of key elements and chemically linked properties has been determined in the current area of study. Calcium (Ca+2), sodium (Na+), potassium (K+), chloride (Cl), sulfate (So42), and nitrate (No3) are the primary cations. Total Dissolved Solids (TDS) and Total Hardness (TH) were also determined to have chemically linked characteristics. The integrated overlay technique aided in the preparation of the spatial distribution of groundwater quality for drinking purposes. In the research region, there are both potable and non-potable water sources.

CHAPTER 3

STUDY AREA

3.1 Introduction

Brahmapuram an Indian city of Kochi district is a significant contributor to the environmental pollutantsand the related health problems in Ernakulam District.More than 600 tons of waste are generated daily in Kochi, and at the Brahmapuram Solid Waste Plant, almost 100 tons of that waste are converted to organic manure.The facility, initially opened in 2008 to manage solid waste, eventually became a landfill. The landfill is expected to have 5.5 lakh tonnes of garbage distributed across 110 acres as of March 2023. The Brahmapuram waste factory experienced a large fire on March 2, 2023, which for several days covered various areas of the city in smoke and hazardous gas.

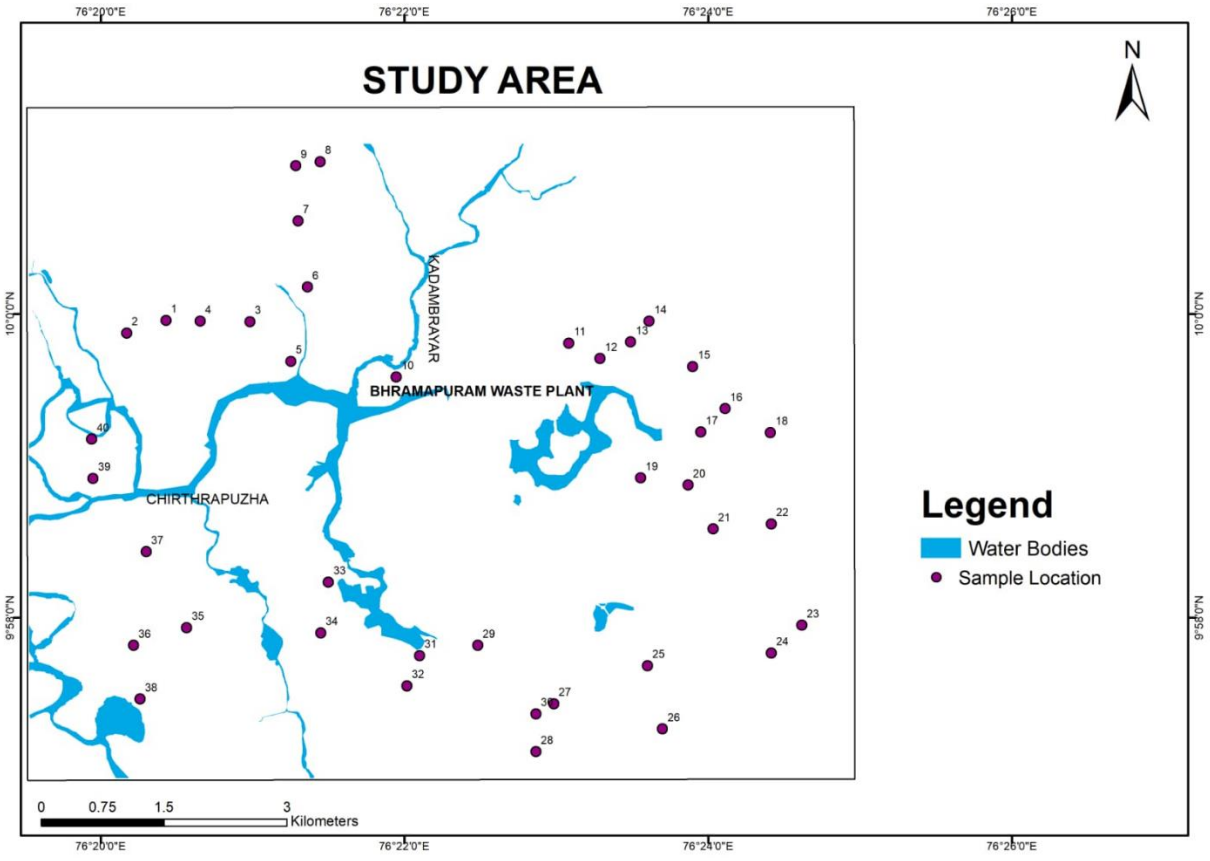

Figure 1: study area map

3.1.1 Drainage

Near Bhuthathankettudam, the river's major tributaries Cheruthoni and Idamalayar join it as it follows a nearly straight line course roughly in a northwestern direction. The Marthandavarma and Mangalapuzha branches of the river split off farther downriver at Aluva. The Marthandavarma branch flows south through the Udhyogamandal region and meets the Cochin backwater system (part of Vembanad Lake) at Varapuzha. The Mangalapuzha branch connects the Chalakkudy river and empties into the Lakshadweep sea at Munambam. The Periyar is a perennial river that provides drinking water to a number of significant communities.

At the southern end of the lake, where it empties into the Sea, is where Kochi (Cochin), the port. Varapuzha is the term used to describe the section from Kochi Azhito Munambam Azhi. The lake has canals connecting it to neighbouring coastal lakes to the north and south. Kochi kayal refers to the region of Vembanad Lake that is situated inside and around the Kochi mainland. Numerous islands can be found in the lake, including those in the Ernakulum district include Willingdon Island, Vypin, Mulavukad, and Vallarpadam. The lake, which is just over 96.5 km in length and is a component of the Vembanad-Kol wetland system that stretches from Alappuzha in the south to Azheekkode in the north, is by far the longest lake in India. Ten rivers feed the lake, including the Achenkovil, Manimala, Meenachil, Muvattupuzha, Pamba, and Periyar, the six largest rivers in central Kerala. The lake drains 15,770 km2 in total, which is 40% of Kerala's total land area. With an annual surface runoff of 21,900 mm, it contributes over 30% of the state's total surface water resources.

3.1.2 Kadamprayar River

The kadambrayar river, which originates from the hill at Arakkappady, is the main river that flows through the research area. After going through the panchayats of Edathala, Kizhakkambalam, Kunnathunad, and Thrikkakara, the river merges with Chithrapuzha close to Ambalamugal. The river has a total length of 27 kilometres and an estimated catchment area of 115 km. Natural canals like Palakuzhythodu, Chandakkadavu thodu, Valiya thodu, Paapparakkadavu thodu, Vanachira thodu, Mundampalam, Pazhangattu chal, Kunnippadam, and others are tributaries to the river. For industrial zones like KINFRA, Infopark Phase -1, Phase -2, Smartcity Cochin Special Economic Zone(CSEZ), and for businesses like Nitta Gelatin India Ltd, Philips Carbon, Wonderla, Cochin Kadaalas, etc., Kadambrayar serves as the supply of water.

3.1.3 Land Use

The district is divided into three parts based on the type of land used: arable, forest land, and waste land. A significant portion of the district is made up of agricultural land, both irrigated and unirrigated. The majority of the world's forests are in the east, where cashew and rubber plantations have been established in some locations. The midland region contains a great deal of hard laterite waste land that is unfit for farming. Lateritic soil covers the majority of the area. Alluvial soil is found along the coast, whereas forest loam soil is found in the east. The district's entire area is made up of roughly 83% cultivable land, 10% forest cover, including reserve forests and plantations, 5.3% water bodies, and nearly 2% built-up area.

In the district, irrigation is used to irrigate 26,825 hectares of land (net area). The Periyar Valley irrigation project, which uses the tail race water from Sengulam for its barrage at Bootathankettu, the Panniyur and Pallivasal hydroelectric projects, and the Chalakudy diversion project are the sources for canal irrigation in the district.Paddy, coconut, rubber, banana, and arecanut are the main crops irrigated in the district. More than one season is used to grow paddy. Coconut, paddy, banana, and rubber are the other main crops grown in the area. Additionally grown in the area are vegetables, oil seeds, areca nuts, and spices.

3.1.4 Rainfall and Climate

The Ernakulam district experiences a humid monsoon climate. The southwest monsoon season is followed by the northeast monsoon, which brings considerable rain to the district. The amount of rainfall is significantly less in the other months. The hottest months are March, April, and May. The coldest months are December through February.
Based on statistics from 1901 to 1999, the district experiences 3359.2 mm of rainfall annually. There are many locations throughout the district where the annual rainfall varies from 3233 to 3456 mm. The district's western region experiences less rainfall, which steadily increases towards the east. The eastern region's Neriamangalam area experiences the most rainfall, with an average annual rainfall of 5883 mm. While Kochi, which lies in the west, gets about 3233 mm of rain per year.

3.1.5 Geology

Geologically, the region is divided into two separate lithounits. Hard rocks from the Precambrian period make up the eastern portion, while soft rocks, or unconsolidated coastal alluvium, fill the western coastal tract.Precambrian rock collections called charnockite and

migmatite make up the majority of the area. Pyroxene granulite, magnetite quartzite, and charnockite make up the charnockite group. The extremely common mineral charnockite is granulitic, coarse-grained, and black in colour. Linear bands of magnetite quartzite and pyroxene granulite are found. The earliest rocks in the area are calc-gneiss and quartzite from the Khondalite group, which are visible as linear lensoidal masses inside the charnockites. The biotite gneiss and quartzofeldspathic gneiss of the migmatite group are found close to the charnockite that is prominent in the District Survey Report, Ernakulam District, Kerala State 9. Both acidic (syenite) and basic intrusive (gabbro and dolerite) have been seen intrusive into these earlier rocks. Warkalli beds, which are made up of pebble beds, grit, friable sandstone, and variegated clay, are found in patchy outcrops in the western region near Edappalli and Kalamasseri. Intense lateritization, which is limited to the midland region, affects both the Warkalli beds and the basement rocks. Quaternary sediments such as beach sand, palaeobeach ridge deposits (sand), flood plain deposits (sand, silt, clay), and tidal deposits (clay, mud) cover the coastal tract (Govt of kerala,District survey report of minor minerals ,Ernakulam district)..

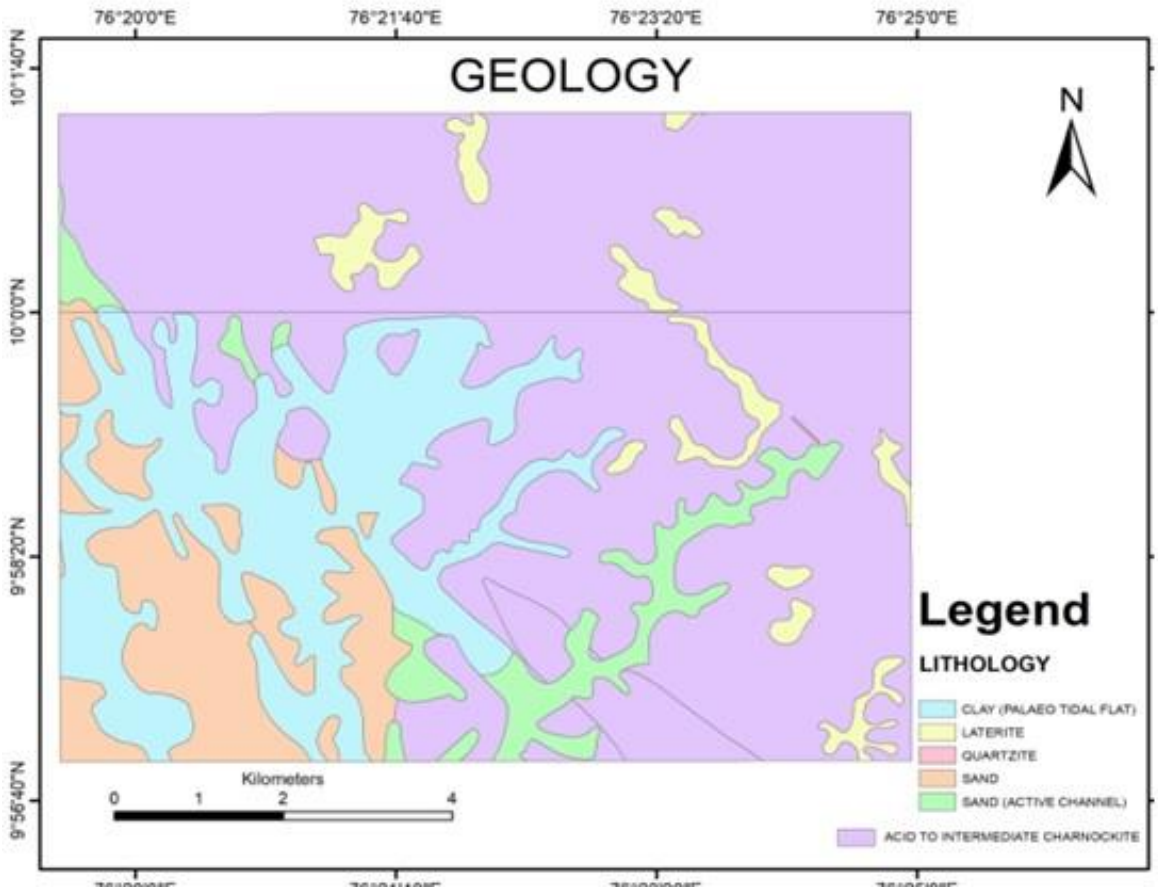

Figure 2: Geology map of the study area

3.1.6 Geomorphology

The district can be broken down into three physiographic zones: (i) the coastal plains in the west, (ii) the midland region in the east, and (iii) the steep to very steep hills in the easternmost part. The coastal plain is a low-lying region with a maximum elevation of around 10 metres towards the eastern side. It is made up of backwater bodies, marshy lands, sandy flats, and alluvial plains, all of which are susceptible to flooding during the monsoon season. The terrain of the midland region is rolling, with low hills and small valleys. The valleys are lessened, and the hills are typically covered in laterite or lateritic soils. From east to west, the area slopes very gently to moderately. Rugged terrain with small summits and steeply sloping slopes can be found in the easternmost area. In actuality, it creates the Western Ghats' foothills. This terrain is typically elevated by more than 300 metres above mean sea level. (Govt of kerala,District survey report of minor minerals,Ernakulam district).In the fig(3) gives that the most of the landforms are rolling plain. And the trend to the river area having the fluon active flood plains .As by the presence of channels which created channel bars over there.

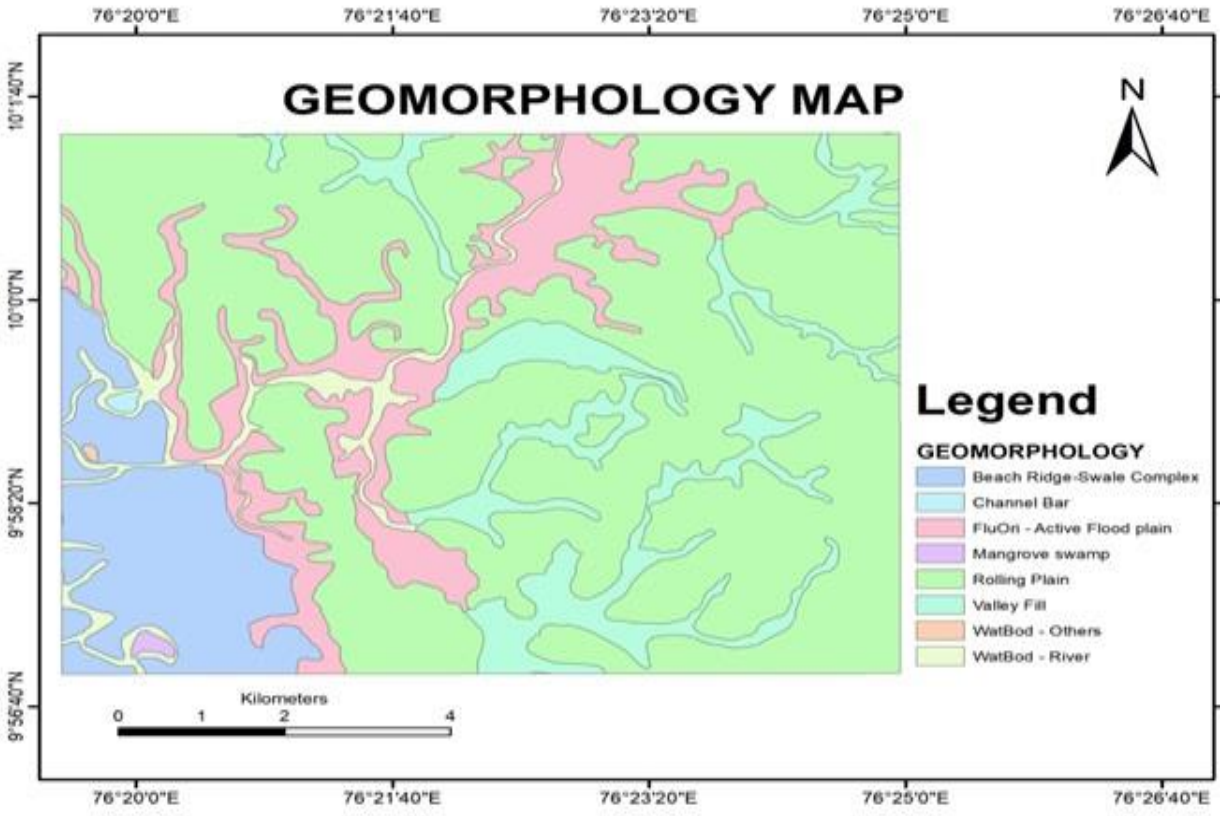

Figure 3: Geomorphology map of the study area

3.1.7 Industries

The major industries in the study area include Hindustan Organic Chemicals Limited (HOCL), Kochi Refinery Limited (KRL), Wonderla, Cochin Kadaalas, KINFRA, Infopark Phases 1-2, Smartcity, Fertilisers And Chemicals Travancore (FACT), and Cochin Special Economic Zone (CSEZ). Smelling salts, ammonium sulphate, phosphate, calcium sulphate, nitrate, and heavy metals are present in the pollutants and effluents. The groundwater quality of the research area is seriously threatened by the effluents from these contemporary units, together with rural and other anthropogenic effluents that eventually find their way into Cochin backwaters.The people have long complained about the filthy waters, claiming that it harms agricultural crops and kills fish. Each day, approximately 33,600 m3 of wastewater are discharged into the Kadambrayar River. This research helps us assess the impact of contemporary effluents on the study area's groundwater quality.

3.1.8 Hydrogeology

The majority of the time, laterites, utilised and cracked crystalline rocks, and unconsolidated coastal sediments are where groundwater typically occurs under phreatic conditions. It happens in crystalline rocks and Tertiary sediments in a deep, fractured aquifer under semi-confined to restricted circumstances. Groundwater can be effectively stored in the weathered zone in the crystalline rocks below. The aquifer can be divided into sedimentary and hard rock aquifers depending on how it formed.

3.1.9 Hard Crystalline Formation

Deep-seated fractures of the crystalline formation are where groundwater occurs under semi-restricted to confined conditions as opposed to shallow weathered parts where it occurs under phreatic conditions.In general, there is no fundamental porosity in hard rock formations. Water is kept in reserve in secondary pores that weathering-related cracks, fissures, joints, etc. have created. The degree to which the fractures are connected determines how groundwater moves. The depth of dug out wells in the shallow phreatic zone ranges from 3.4 to 14.8 mbgl. The wells' depths from the water's surface range from 1.82 to 12.05 mbgl

CHAPTER 4

METHODOLOGY

4.1 FIELD WORK

With an interval of one Kilometer fourty groundwater samples were collected to evaluate groundwater chemistry of the study area..samples were collected from dug wells from different location of the Brahmapuram area, Ernamkulam district prior to south west monsoon, 2023.Groundwater sample were collected according to APHA,2012 in which the pre washed one litre polyethylene bottle were used for collecting the groundwater sample.

Table 1: Field details

Sample no	latitude	longitude	Location name	Depth(m)	Type of well
1	9.999268	76.34051	Thukiyur	9	Dugwell
2	9.997872	76.3362	Palachuvadu(Vyasa Vidalaya)	3	Dugwell
3	9.999137	76.34972	Chittethukara	8	Dugwell
4	9.99919	76.34426	Thuthiyoor	5.5	Dugwell
5	9.99478	76.35447	Chittethukara	5	Dugwell
6	10.00287	76.356	Nilampathinjamugal	4.5	Dugwell
7	9.996741	76.38474	Parakkamugal	8	Dugwell
8	10.01659	76.35747	Kuzhikkatumoola	11	Dugwell
9	10.00694	76.36051	Parakkamugal	11.5	Dugwell
10	9.993056	76.36578	Bhramapuram Plant	12	Dugwell
11	9.996768	76.38472	Govt.JBS Bhramapuram schol	8	Dugwell
12	9.995087	76.38813	Vennithadam	9	Dugwell

13	9.999151	76.39353	Padathikkara	9.5	Dugwell
14	9.999077	76.40431	Pothanaparamb	7	Dugwell
15	9.989585	76.40186	Vellapara	11.5	Dugwell
16	9.989585	76.40186	Karimughal	11.75	Dugwell
17	9.98702	76.3992	Karimugal	3.5	Dugwell
18	9.98696	76.40685	Peechingachira	4.5	Dugwell
19	9.981986	76.3926	Ambalamedu	6	Dugwell
20	9.981211	76.3978	Vellor	1	Dugwell
21	9.976389	76.40056	Puttumanoor	2.7	Dugwell
22	9.976944	76.40694	Puttumanoor	5	Dugwell
23	9.965833	76.41028	Puthancruze	10	Dugwell
24	9.962778	76.410694	Varikoli	2.7	Dugwell
25	9.961389	76039333	Mattakuzhi	24.5	Dugwell
26	9.954444	76.395	Mattakuzhi	6	Dugwell
27	9.957222	76.38306	Kakkad	5.7	Dugwell
28	9.951944	76.38111	Mannala Kakkad	11	Dugwell
29	9.963611	76.37472	Adookara Chullichira	1.8	Dugwell
30	9.956111	76.38111	Chirapuzha	1.5	Dugwell
31	9.9625	76.36833	Irumpanam	4	Dugwell
32	9.959167	76.36694	Chithrapuzha	5	Dugwell
33	9.970556	76.35833	Irumpanam	9	Dugwell
34	9.965	76.3575	Irumpanam	7	Dugwell
35	9.96556	76.34278	Eroor	1	Dugwell

36	9.963611	76.33694	Aranjal road	1.2	Dugwell
37	9.973889	76.33833	Eroor	1.3	Dugwell
38	9.956667	76.33694	Kappattkavu	.5	Dugwell
39	9.981944	76.3325	Eroor	1.1	Dugwell
40	9.986667	76.3325	Aranjal Road	1	Dugwell

4.2 pH

Materials Needed

- PH meter
- PH buffer solution (PH 4.01 ans PH 7.00)
- Distlled or deionized water
- Container for calibration (beaker or glass)

procedure

- Rinse the Ph meter electrode with distilled water
- immerse the PH meter electrode into thepH4.01 buffer solution
- Wait for the ph reading to stabilize.This should take aout 30 seconds
- Adjust the Phmeter reading to 4.01 using the adjustment knob or button on the meter.
- Rinse the PH meter with distilled water
- immerse the ph meter electrode into the Ph 7.00 buffer solution
- Wait for the ph reading to stabilize

4.3 Electrical conductivity (EC)

Materials needed

- Conductivity meter
- Conductivity standard solution (of known conductivity)
- Distilled or deionized water
- Container for testing (usually a small beaker or glass)

Procedure:

- Rinse the conductivity meter electrode with distilled or deionized water.
- Immerse the conductivity meter electrode into the conductivity standard solution of known conductivity.
- Wait for the conductivity reading to stabilize.
- Adjust the conductivity meter reading to match the known conductivity of the standard solution, using the adjustment knob or button on the meter.
- Rinse the conductivity meter electrode with distilled or deionized water again.
- Immerse the conductivity meter electrode into the sample water to be tested.wait for the conductivity metre reading to stabilize and record the conductivity reading

4.4 Total dissolved solids (TDS)

Materials needed:

- TDS meter
- TDS standard solution (of known TDS)
- Distilled or deionized water
- Container for testing (usually a small beaker or glass)

Procedure

- Use distilled or deionized water to rinse the electrode on the TDS meter.
- Immerse the TDS meter electrode into the TDS standard solution of known TDS.
- Wait for the TDS reading to stabilize. This should take about 30 seconds.
- Adjust the TDS meter reading to match the known TDS of the standard solution, using the adjustment knob or button on the meter.
- Rinse the TDS meter electrode with distilled or deionized water again. Immerse the TDS meter electrode with again, immerse the TDS meter electrode into the sample water to stabilized. The drinking be tested. Record the TDS reading.

4.5 Calcium

Materials needed

- Calcium indicator solution (such as Eriochrome Black T)
- EDTA titrant solution (of known concentration)
- Buffer solution (such as ammonium chloride/ammonia buffer)
- Distilled or deionized water
- Erlenmeyer flask
- Burette
- Pipette

Procedure

- Prepare the calcium indicator solution by dissolving the indicator in distilled or deionized water, according to the manufacturer's instructions.
- Prepare the EDTA titrant solution by dissolving a known amount of EDTA in distilled or deionized water.
- Prepare the buffer solution by dissolving ammonium chloride and ammonia in distilled or deionized water, according to the manufacturer's instructions.
- Collect a sample of the water to be tested in an Erlenmeyer flask.
- Add a few drops of the calcium indicator solution to the flask and mix well.
- Add a few millilitres of the buffer solution to the flask and mix well.
- Titrate the solution with the EDTA titrant solution until the color of the solution changes from pink to blue. This indicates that all the calcium ions have reacted with the EDTA.
- Record the volume of EDTA titrant solution used for titration.

9.1 ml of 0.002 M EDTA = 0.0004 of Ca. A ml of 0.02 M EDTA = (0.0004xA) gm of Ca

10.Ca (Mg/l) =(0.0004x A ml × 10 ^6)/20

4.6 Magnesium

Material Needed

- Magnesium indicator solution (such as Eriochrome Black T)
- EDTA titrant solution (of known concentration)
- Buffer solution (such as ammonium chloride/ammonia buffer)
- Distilled or deionized water
- Erlenmeyer flask
- Burette
- Pipette

Procedure

- Prepare the magnesium indicator solution by dissolving the indicator in distilled or deionized water, according to the manufacturer's instructions.
- Prepare the EDTA titrant solution by dissolving a known amount of EDTA in distilled or deionized water.
- Prepare the buffer solution by dissolving ammonium chloride and ammonia in distilled or deionized water, according to the manufacturer's instructions.
- Collect a sample of the water to be tested in an Erlenmeyer flask.
- Add a few drops of the magnesium indicator solution to the flask and mix well.
- Add a few millilitres of the buffer solution to the flask and mix well.
- Titrate the solution with the EDTA titrant solution until the colour of the solution changes from wine red to blue. This indicates that all the magnesium ions have reacted with the EDTA.
- Record the volume of EDTA titrant solution used for titration.
- 1 ml of 0.02 M EDTA = 0.00024 of mg
- B-A ml of 0.02 M EDTA = 0.00024×(B-A)
- Mg (mg/L)= (0.00024-B-A × 10 ^6)/20

4.7 Carbonate and Bicarbonate

Materials Needed

- Phenolphthalein indicator solution
- Sulfuric acid solution (of known concentration)
- Sodium hydroxide solution (of known concentration)
- Distilled or deionized water
- Erlenmeyer flask
- Burette
- Pipette

Procedure

- Collect a sample of the water to be tested in an Erlenmeyer flask.
- Add a few drops of phenolphthalein indicator solution to the flask and mix well.
- Titrate the solution with sulfuric acid solution until the colour of the solution changes from pink to colourless. This indicates that all the bicarbonate and carbonate ions have reacted with the acid.
- Record the volume of sulfuric acid solution used for titration.
- Add a few drops of sodium hydroxide solution to the flask and mix well.
- Titrate the solution with sodium hydroxide solution until the colour of the solution changes from colourless to pink. This indicates that all the excess acid has been neutralized by the sodium hydroxide.
- Record the volume of sodium hydroxide solution used for titration.
- Calculate the carbonate and bicarbonate concentration in the water using the formula.
- .(Titration value * 0.02N * 1000/)50

4.8 Chloride

Materials needed

- Silver nitrate solution
- Potassium chromate
- Water sample

- .Burette
- Conical flask

Procedure

- The silver nitrate solution is added to the burette.
- Take 50ml 0f sample solution in a clean conical flask and add 1ml of potassium chromate indicator
- Titrate the sample against burette having the silver nitrate solution.The end point is yellow to red.
- Record the burette values.
- Repeat this procedure with the remaining samples.

4.9 Sulphate

Materials Needed

- Sulphate buffer solution
- Barium Chloride
- Water sample

Procedure

- Take 50ml of water sample solution in a beaker
- Add 10ml of sulphate buffer solution and pinch of barium chloride
- Mix it very well and transfer it into a bottle
- Measure the sulphate by using turbidimeter, transfer the bottle placed in the instrument and read the value. Repeat the process for other samples.

4.10 FLAME PHOTOMETRY

. The principle of flame photometer is based on the measurement of the emitted light intensity when a metal is introduced into the flame. The wavelength of the colour gives information about the element and the colour of the flame gives information about the amount of the element present in the sample.Flame photometry is one of the branches of atomic absorption spectroscopy.it is also known as flame emission spectroscopy. Currently, it has become a necessary tool in the field of analytical chemistry .Flame photometer can be used to determine

the concentration of certain metal ions like sodium, potassium, lithium, calcium and cesium etc. In flame photometer spectra the metal ions are used in the form of atoms.

4.10.1 Sodium and Potassium

Material Needed

- Flame photometer
- compressor
- LPG(gas connection)
- Distilled water
- groundwater sample
- standard solution
- small water containers
- 1000ml volumetric flask
- 100 ml standrad flask(4)
- weighing machine
- sodium chloride

procedure

- Firstly for making standard solution of sodium ,For making 1000ppm ;dissolve 2.5416 g NaCl and 1.907 g of KCl in one litre distilled water in a volumetric flasks.
- Pipette out 1ml,4ml,6ml and 8ml from 1000ppm sodium chloride solution and potassium chloride solution.
- Makeup into 100ml in standard flask upto the level by distilled water
- Now the 4 standards 10ppm,20ppm,60ppm and 8 ppm were ready for testing
- Started the new calibration by adding 10,20,30 and 80 ppm to the flame test
- The value were saved in the machine ;after all that the groundwater sample get placed for the flame test,after the aspiration over.
- Aspirating blank value ;using distilled water placed in a beaker in front of the machine,The nobe were put into the beaker filled with distilled water.
- After that the ground water sample ready for the flame test
- After 10 samples,calibrating the standards of 10ppm,20ppm,40ppm and 80 ppm is necesssary for the flame test.40 sample reading take place,always care about the flame,flame colour,and cone shape of the flame.

- Note the value get on the screen of the sample,note it and then turn to the blank value of distilled water

4.11 SPSS SOFTWARE

SPSS (Statistical Package for Social Sciences) is data analysis, manipulation, and visualization software. The software includes an easy-to-use interface that enables researchers to do a variety of statistical analyses, such as descriptive statistics, correlation analysis, regression analysis, and factor analysis. In this study, a correlation matrix was created using SPSS software, which aided in the interpretation of groundwater quality data.

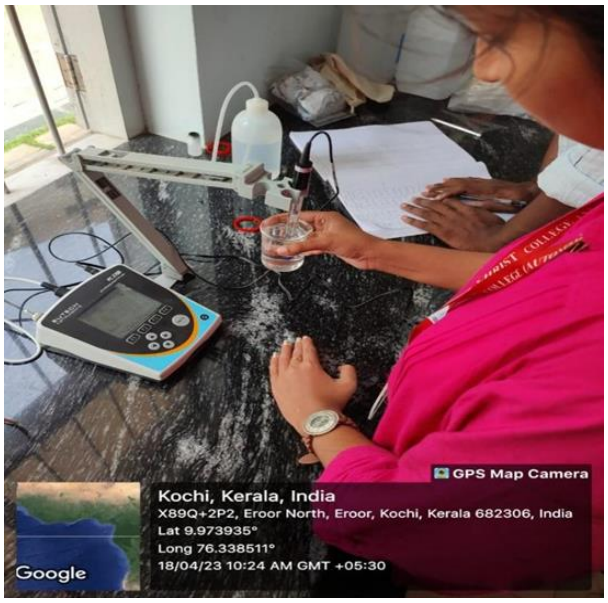

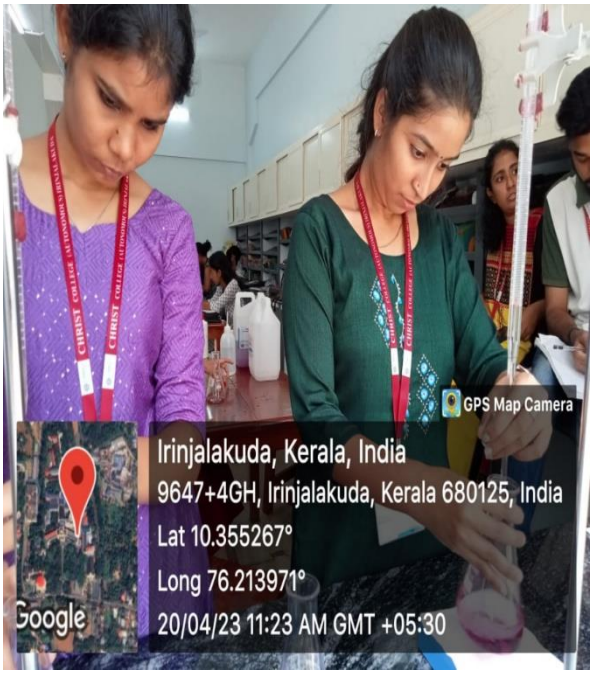

CHAPTER 5

RESULT AND DISCUSSION

5.1 Physico – chemical parameters

Water analysis was carried out for 40 samples collected during the month of April (2023) from the study area, are very essential to know the water qualities for drinking purpose. The parameters are differentiated as physical and chemical parameters. The physico parameters include pH, EC, TDS chemical parameters include ,sodium,potassium, calcium, magnesium, total hardness, chloride, sulphate, bicarbonate.The BIS and WHO standard values for several physicochemical characteristics in drinking water are presented.

Table 2: BIS values and minimum, maximum and average value of the study area

PARAMETER	**INDIAN STANDARD (BIS 2012)**	**MAXIMUM**	**MINIMUM**	**AVERAGE**
pH	6.5-8.5	7.43	4.29	5.621
EC (micro S)	1500	1943	30.17	254.43375
TDS(ppm)	500-2000	972.6	15.4	127.37175
Total Hardness(ppm)	200-600	203.7	3.97	35.847284
Ca(ppm)	75-200	79.6	0.4	10.115
Mg(ppm)	50-150	15.3	0.48	2.3805
Na(ppm)	200	115.73	2.06	18.7385
K(ppm)	-	44.09	0.72	4.577
HCO3(ppm)	200-600	64.66	2.4	11.285
SO4(ppm)	200-400	30.3	0.3	6.4
Cl(ppm)	200-600	312	0	38.15

5.2 pH

The pH scale determines how acidic or basic water is. The range is 0 to 14, with 7 representing neutrality. Acidity is indicated by pH values below 7, whereas baseness is shown by pH values above 7. In reality, pH is a measurement of the proportion of free hydrogen and hydroxyl ions in water. While water with more free hydroxyl ions is basic, water with more free hydrogen ions is acidic. Since chemicals in the water can change pH, pH is a crucial sign that the chemical composition of the water is changing. "Logarithmic units" are used to report pH. Each number corresponds to a 10-fold difference in the water's acidity or basicity. Ten times more acidic is water with a pH of five than is water with a pH of six.

The use of water might suffer from pH levels that are both excessively high and low. When pH is high, it impairs chlorine's ability to disinfect, which results in the need for more chlorine. High pH also causes a bitter taste deposits to build up in water pipes and on water-using appliances, and these effects all lead to the need for more chlorine. Metals and other things will dissolve or corrode in low-pH water. The majority of human interventions, agricultural drainages, and home waste water runoff are the causes of pH increases(Jain,1987). The pH of groundwater systems is impacted by changes in photosynthetic activity, the discharge of untreated wastewater, agricultural practices, and human activity (Kotaih, 1994).The groundwater ph value was significantly increased,as were the concentration of NH_4^+,SO_4^{2-},NO_3^-,NO_2^-,and Cl^- groundwater were the concentration of ca2+ and Hco3- declined(Yomgjun Jiang 2008).

In the present investigation, pH values varied from a minimum of 4.29, to a maximum of 7.43 with a mean value of 5.63. While 32 samples are acidic, only eight samples fall into the "safe" group. The groundwater's acidity is brought on by a least presence of alkalinity in the study area.The alkalinity in turn works as buffer solution to the system.If the buffer capacity is reduced with least alkalinity content are more probable for pH change.Thus it may catalyses the pH condition of the study area as acidic in nature. According to the Department of Water in Western Australia (2009), low pH in aquifers causes a host of ailments, including dental problems, gastrointestinal disorders, skin irritation, and heavy metal toxicity. The several areas of the study area, along with the reduced alkalinity the higher level of dissolved iron due to the influence of laterites also accounts for the acidic nature. From the spatial map, southwest samples are safer compared to rest of the samples.

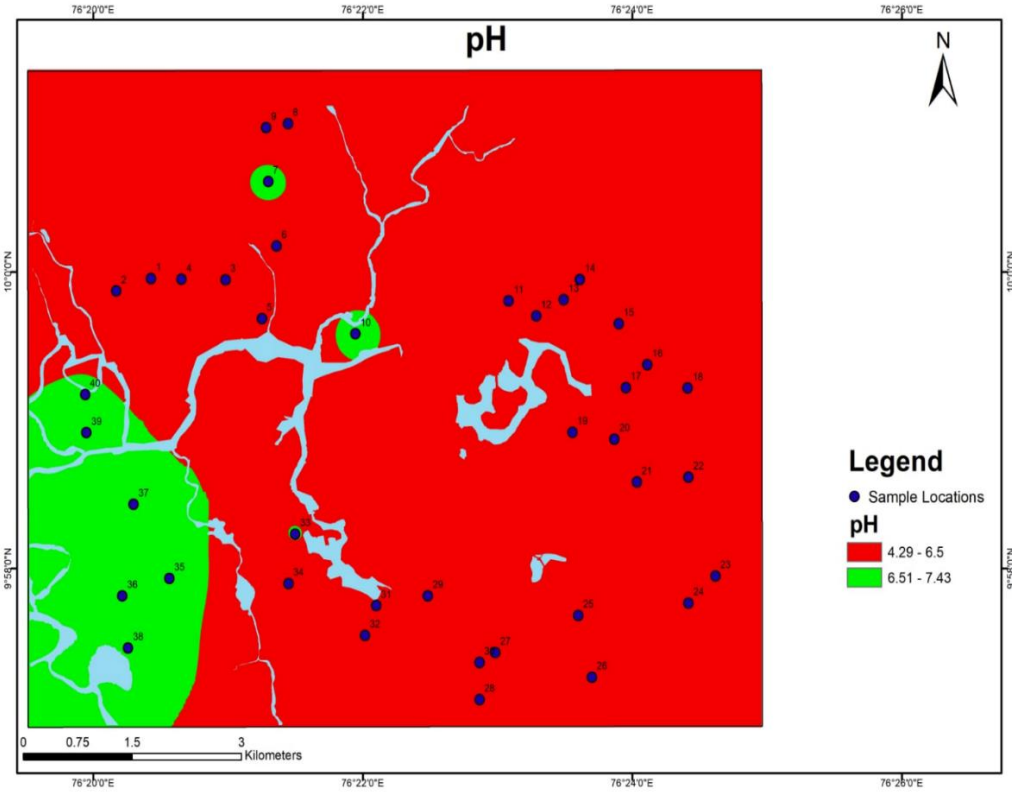

Figure 4: spatial map of pH

5.3 Total Dissolved Solids [TDS]

Water can dissolve a wide variety of inorganic and some organic minerals or salts, including potassium, calcium, sodium, bicarbonates, chlorides, and others. These minerals make water taste foul and seem cloudy. This is one of the most important criteria for water use. The water's high TDS measurement suggests that it is heavily mineralized. The recommended limit for TDS in drinking water is 1000 mg/l, with a preferred level of 500 mg/l. TDS convergence was seen in the scope between 114.7 and 121.2 mg/l in the current review. The mean total dissolved solids concentration at Wondo Genet campus was 118.19 mg/l, which is within WHO limits. TDS is directly related to EC since conductivity increases with the amount of soil dissolved.

In the studied region, the lowest concentration is 15.4 mg/l, the maximum is 972.6 mg/l, and the average concentration is 144.83 mg/l. 38 samples in the supplied sample fall within the allowed limit of 2000 mg/l. The decomposition of mineral-rich soil particles supports an increase in the TDS level in groundwater under slightly alkaline circumstances. (Rambabu et al., 1986; Shankar and Muttu Krishnan, 1994). As far as possible, establish that this water may be deficient in needed minerals in the water. There is a relationship between electrical

conductivity and total solids in water; the more the salts breakdown in the water, the higher the electrical conductivity.

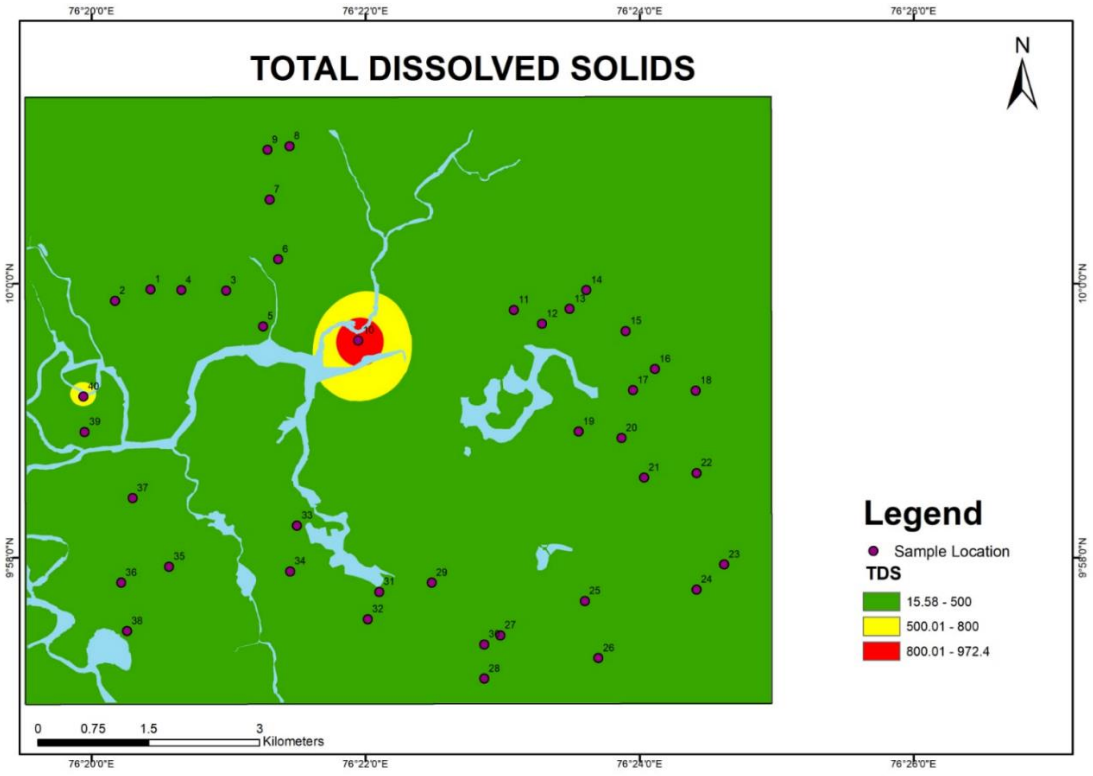

Figure 5: Spatial map of TDS

The fig (5) shows that the TDS distribution of groundwater in the Bhramapuram area.The area in which green marked as shown that the region within the BIS permissible limit. The permitted limit of groundwater quality in the study area follows the same trend as surface water flows, with the Kadambrayar River indicating a river effect over TDS in the study area. The increased loadings of TDS are associated with near surface water regions.The red areas exhibit highest TDS loadings, suggesting that the TDS of water in these regions is within the permissible limit in most places and is highest in the region where the Brahmapuram Waste facility is located. TDS levels fall away from the waste treatment plant. Even though the complete terrain is of low TDS, the TDS loadings at Brahmapuram suggests the influence of landfills in the groundwater quality. The lower loadings in TDS may probable for mineral deficency in the study area.

5.4 Electrical Conductivity [EC]

When evaluating the qualities and features of groundwater, electrical conductivity (EC) is a crucial measure to consider. It evaluates a solution's capacity to conduct an electrical current, in this case, groundwater. The quantity of dissolved ions, such as minerals and salts, that are present in the water has a major impact on the EC of groundwater.The electrical conductivity value is an index that represents the overall concentration of soluble salt in water (Purandara et al., 2003).

In this investigation, the EC values ranged from 30.17 to 1943 MicroS/cm, with an average of 289.29 MicroS/cm. The BIS acceptable limit is 1500 MicroS/cm, and one sample surpasses it. Ten of the samples are safe to use, while the remaining 29 exceed the limit. The bulk of inorganic salts, such as potassium nitrate, sodium chloride, and potassium sulfate, may leads for increasing groundwater EC values. The fig(6) shows the EC distribution of water in the Bhramapuram area.The area marked in green shows the region that has water with least EC. In most of the river associated regions have higher EC compared to other regions, shows the influence of surface water in the study area as well.

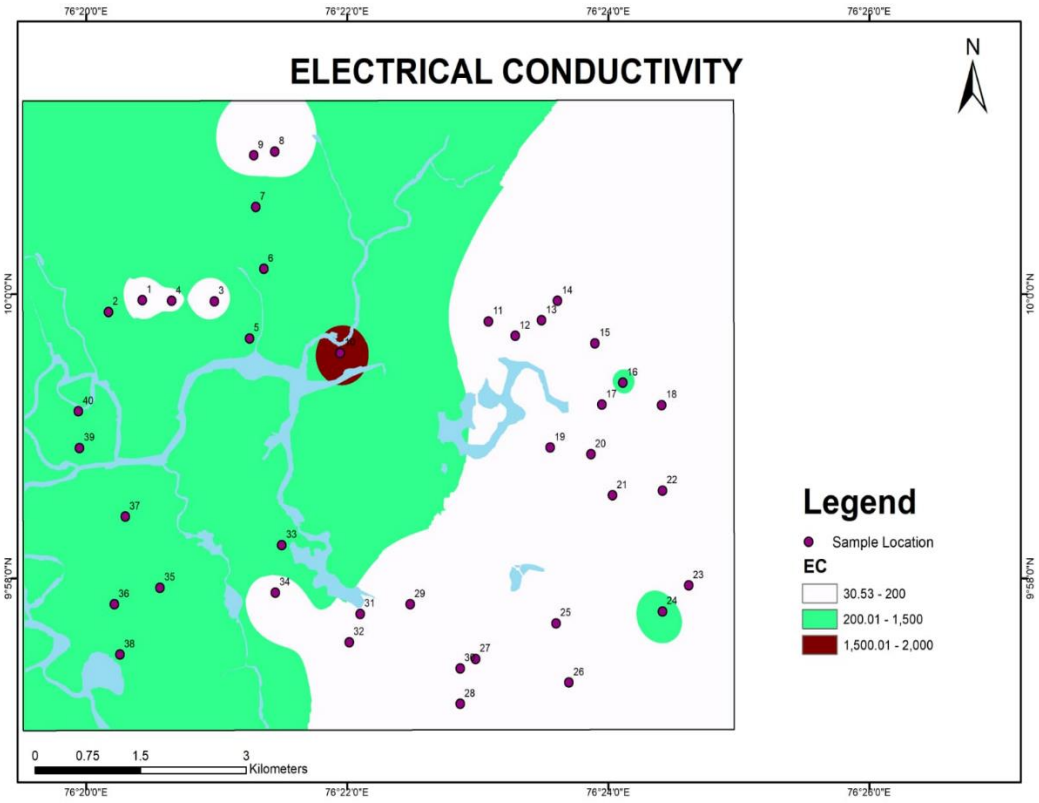

Figure 6: shows that the spatial map of EC

5.5 CHEMICAL PARAMETERS

5.5.1 Chloride

One of the principal ions found in groundwater is chloride. Chloride can be formed naturally through processes such as the weathering of rocks and minerals, as well as by agricultural and industrial methods. The concentration of chloride in groundwater varies according to location and underlying geology. Higher concentrations of chloride can have negative effects on the environment, human health, aquatic life, and so on. Chloride is a significant anion present in natural sources and waste water. As the mineral content increases, so does the chloride content.

In the current investigation, chloride levels ranged from 4 mg/l to 312 mg/l, with an average of 43.76 mg/l. Two samples in the study region exceed the acceptable level, whereas all other samples are within the permissible range.

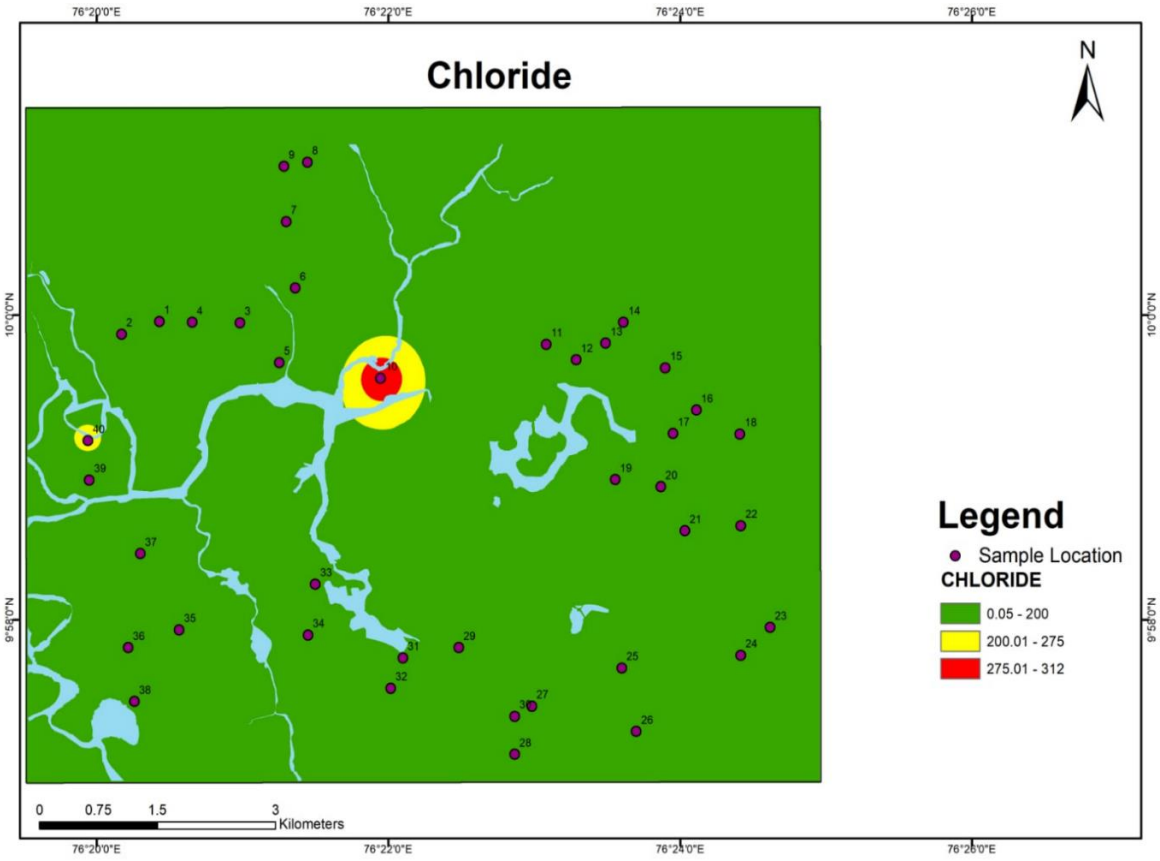

Figure 7: spatial map of Chloride

The given figure (7) shows that the chloride distribution of water in the Brahmapuaram region. The green area denotes the location with water within the BIS-allowed limit. In the

study area, most of the loadings are below desirable limit are due to the limited chlorination process as well as the unfavourable leaching condition of chloride ion into the aquifer system. The highest concentration of chloride is present at Brahmapuram Waste Plant with an loading of 312ppm. By examining the overall trend of the landscape, the greater the chloride concentration shows more pollution in the studied area. The high chloride content may cause gastrointestinal troubles, respiratory problems, skin and eye irritation, increased cancer risk, and other concerns.And the reduced content of Chloride in the groundwater may leads to lung diseases, Heart failure, metabolic alkalosis.

5.6 Bicarbonate

Bicarbonate (HCO_3) is similarly a polyatomic ion; however, it has a negative charge of 1. It has one carbon atom, three oxygen atoms, and one hydrogen atom. When carbon dioxide dissolves in water and interacts with a base, such as sodium hydroxide, bicarbonate is generated. It is often present in natural waterways and contributes significantly to water's buffering capacity, which aids in maintaining pH levels within a specified range. Water can contain both carbonate and bicarbonate, which can impact its chemical properties. The addition of bicarbonate, for example, can raise the alkalinity of water, making it more resistant to pH shifts. Carbonate, on the other hand, can react with specific molecules and ions in water to generate precipitates that can cause scaling and other problems.

As a result, it is critical to monitor the levels of carbonate and bicarbonate in water to ensure that it is safe and adequate for its intended usage. pH is defined as the concentration of acid protons [H+] in solution. The alkalinity of a solution is defined as its capacity to neutralize acids. Because alkalinity is responsible for keeping the pH of the water in check, it should be kept above a specified level. Alkalinity is made up of ions that incorporate acid protons into their molecules; therefore, they do not contribute to reducing the pH value of water, keeping it within the prescribed range.

In the current investigation, bicarbonate concentrations ranged from 4 mg/l to 312 mg/l, with an average value of 43.76 mg/l. The bicarbonate concentration of 39 samples in the research region falls within the minimum permissible range of 200–600 mg/l (BIS 2012), with only one sample, L10, above the acceptable threshold. Since alkalinity is the buffer for pH then, if the alkalinity of the water falls below a certain threshold, the pH of the study area may be affected,

and with a minor external input may change the pH in large scale. And thus may leads to corrosive to metals, may catalyses the dissolving nature etc

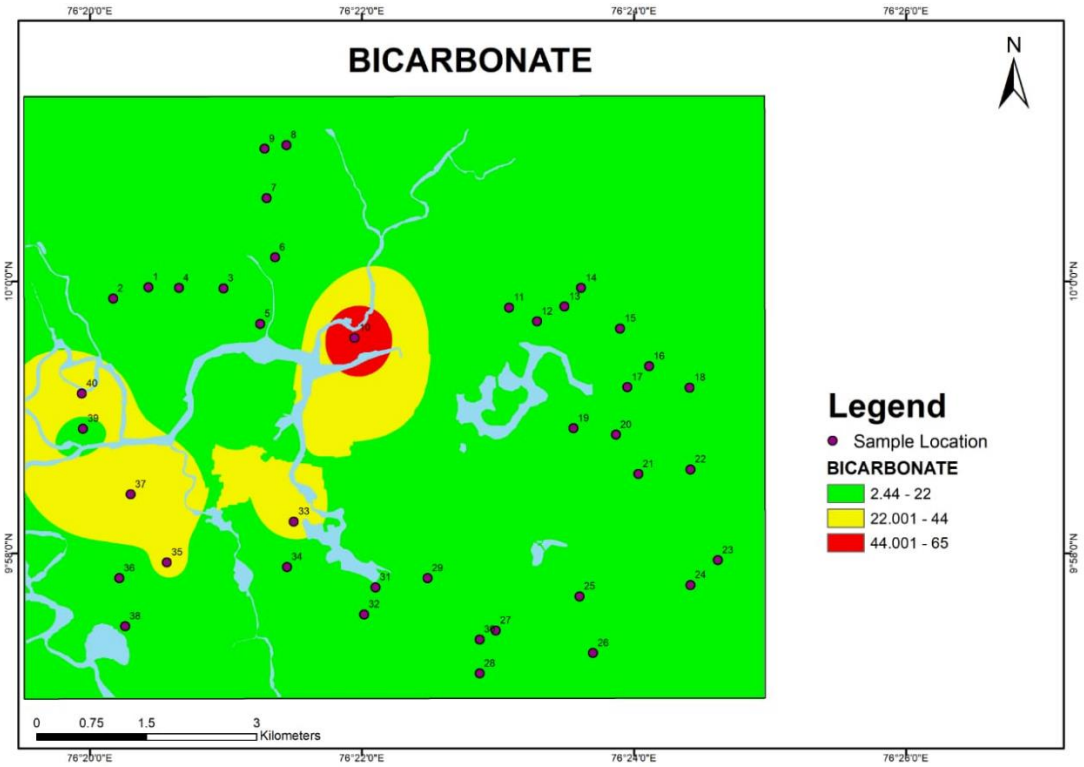

Figure 8: Spatial map of bicarbonate

5.7 Calcium

The main source of calcium is rock containing carbonates, such as limestones and dolomites, which are found in groundwater dissolved in carbonic acid. Calcium in groundwater will be caused by the chemical breakdown of feldspar and calcic-plagioclase feldspar. Calcium ion concentrations are in the range of 100–300 mg/liter; however, larger amounts are acceptable to consumers due to related anion. Hardness levels greater than 500 mg/liter are considered unsatisfactory. Groundwater is classified into four categories based on its calcium content. Very high (>180mg/litre), high(120mg/litre), medium(60mg/litre-119mg/litre) and low (<60mg/litre).

Calcium readings in the current investigation ranged from 0.4 mg/l to 79.6 mg/l, with an average value of 43.761 mg/l (Fig.). Except for sample no. 10, all of the remaining 39 samples are outside of the desirable-permissible level. The figure depicts the calcium distribution in the Brahmapuaram area. The zone highlighted in green contains water within the BIS's allowed

limit. Calcium loadings are are lowest in the eastern part of the study area. The lack of calcium-dominant country rock in the studied area is the primary cause of the low calcium concentration.

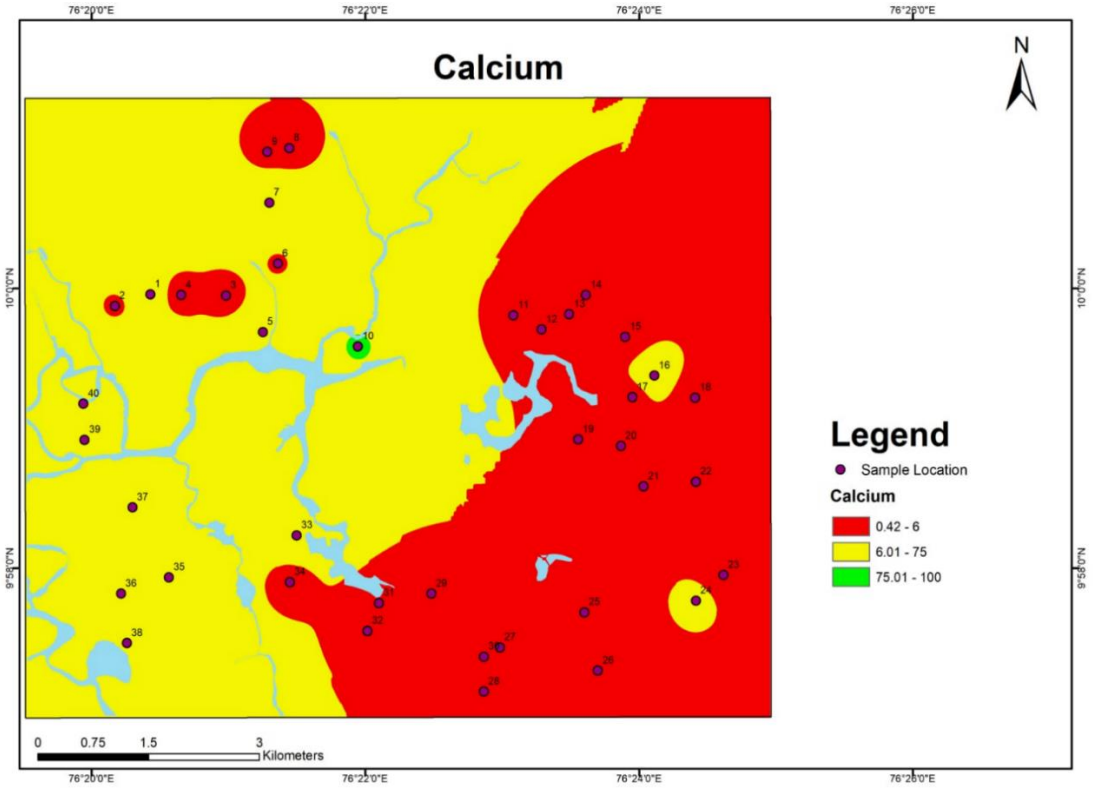

Figure 9: spatial map of calcium

5.8 Magnesium

Magnesium is a common mineral found in groundwater. It dissolves in groundwater as it percolates through rock formations. The presence of magnesium will have both beneficial and negative consequences. Magnesium-rich water can help supplement the body's magnesium levels. A high magnesium level in groundwater can cause hard water. Hard water is caused by dissolved minerals such as magnesium and calcium. On the other side, a high quantity of magnesium in drinking water might make it bitter. WHO recommends a magnesium level of 10–30 mg/L in drinking water. However, the level of magnesium in groundwater might vary based on local geological conditions and other factors. Few of the data points we collected are below the WHO-recommended range, which has good consequences such as reduced hardness, increased corrosion, negative effects on plant development, and potential health concerns. Magnesium concentrations in groundwater are mostly caused by the leaching of magnesium-

bearing minerals such as dolomite and magnesite, as well as other mafic and ultramafic rocks found in charnokite such as pyroxenite, peridotite, dunite, anorthosite, and hypersthene. Magnesium is also a critical macronutrient for humans. It aids in the treatment of acute illnesses such as insomnia.

The magnesium content in the current investigation ranged from 0.24 mg/l to 20.4 mg/l, with an average value of 2.88 mg/l, and none of the samples had magnesium concentrations within the allowable limits. All 40 samples are below the lower limit of the permitted magnesium limit, resulting in a magnesium deficit in the study region due to a lack of magnesium-bearing country rock in the study area. As a result, drinking of low-magnesium water on a regular basis .may result in hypertension, diabetes, coronary osteoporosis, and heart disease.

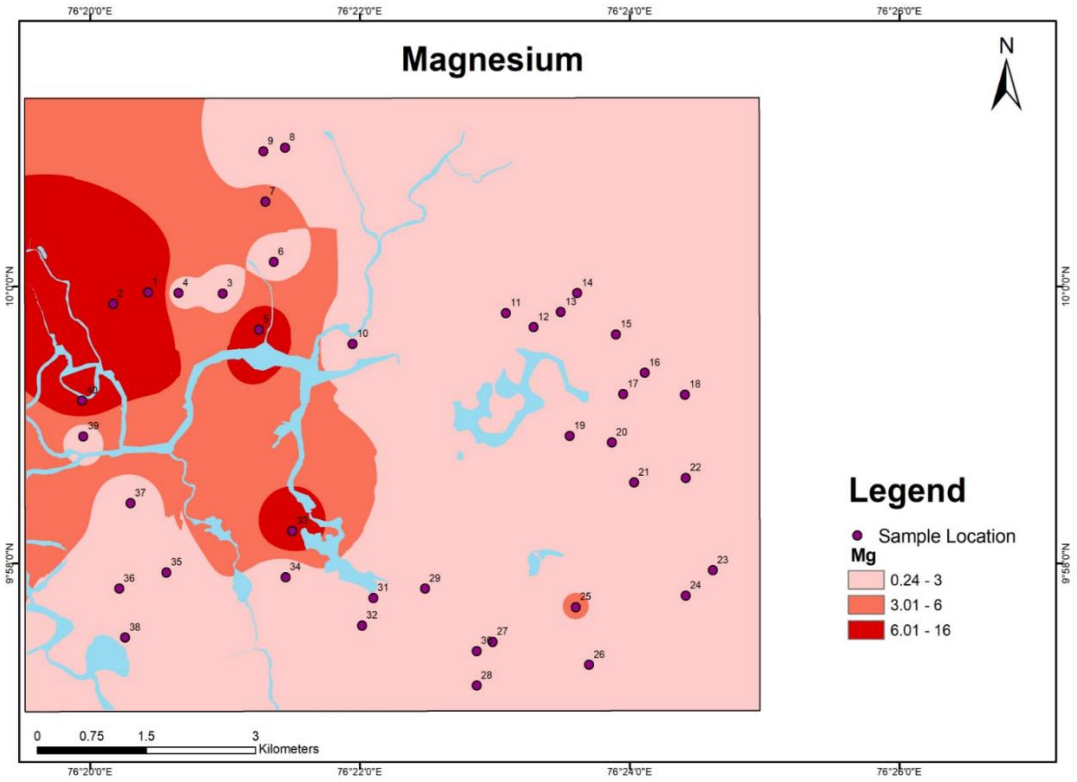

Figure 10: spatial map of magnesium

5.9 Total Hardness

The total hardness of water is defined as the concentration of dissolved calcium and magnesium ions in groundwater. Because they can impair the efficiency of soaps and detergents and generate scale deposits in pipes and appliances, these ions are often referred to as "hardness ions." The total hardness of groundwater is often measured in milligrams per liter (mg/L).

There are several methods for measuring overall hardness, but one of the most common is to use a titration method to determine how much calcium and magnesium are present in the water. Water hardness, for example, can make it less pleasant to drink and increase the expense of treating it for industrial activities. However, moderate degrees of hardness might be beneficial for agriculture since calcium and magnesium particles can provide essential supplements to establish development. The total hardness of groundwater can have important implications for its use in many applications, such as drinking water, modern cycles, and agriculture. Water hardness, for example, can make it less pleasant to drink and increase the expense of treating it for industrial activities. However, moderate degrees of hardness might be beneficial for agriculture since calcium and magnesium particles can provide essential supplements to establish development.

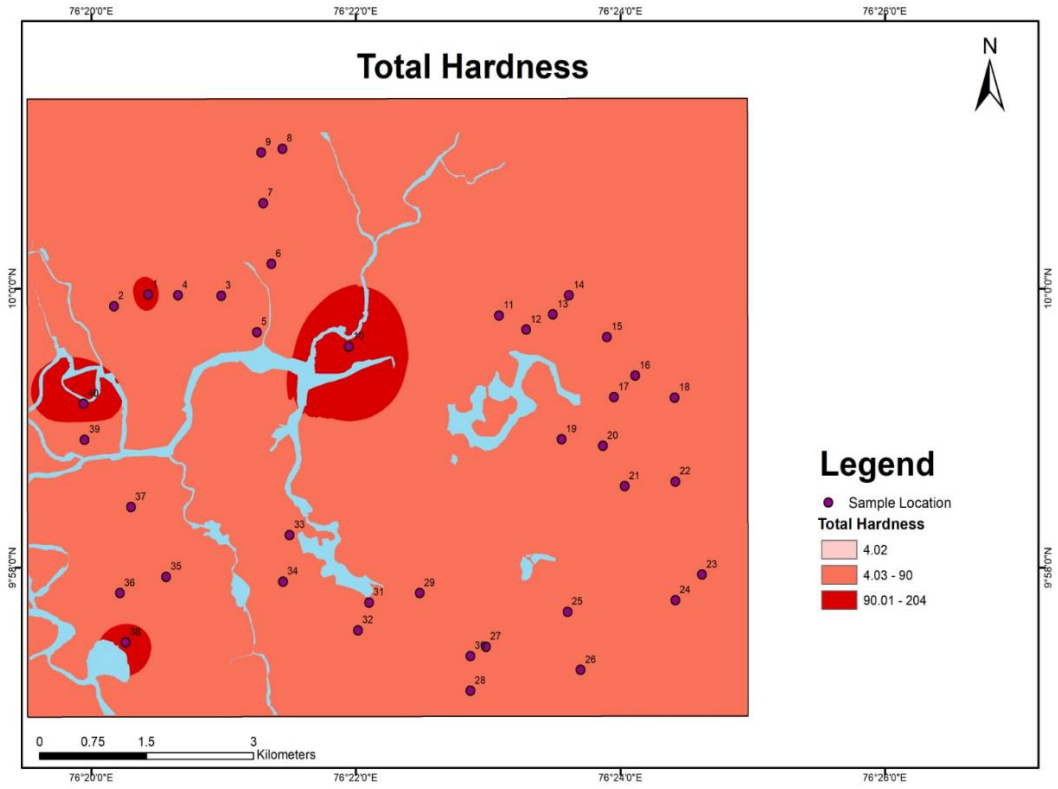

Figure 11: spatial map of Total Hardness

The figure 11, shows that the Total Hardness distribution in the study area.The area marked in red having comparatively higher total hardness. The Total Hardness value have a positive correlation for Ca and Mg values accounts for the influence of Mg and Ca in TH. The Bhramapuram plant have comparatively higher concentration than the rest of the sample area.

5.10 Sulphate

Sulphate is typically found in modest concentrations due to the slower decomposition of organic substances in weathered soil/water (Miller, 1979; Craig and Anderson, 1979; Sing et al., 1994). The majority of them are produced by the oxidation of sulphide ores, gypsum, and anhydrite. Sulphate concentrations in groundwater are often low in hard rock locations due to the amounts of sulphate obtaining minerals (Hem, 1985).

Sulphate is a significant anion found in natural waters. It may enter natural waters as a result of the weathering of sulphate-bearing sediments. It can be leached from sedimentary rocks, notably sulphate deposits like gypsum. Effluent from some industries, such as pulp and paper, may also be a major source of sulphate in receiving streams. Agricultural runoff, irrigation drainage, the breakdown of organic molecules in soil, leachable sulphates from fertilizers, and other human impacts are the primary drivers of high sulphate concentrations in fresh waters (Miller, 1979; Alexander, 1961).

Airborne industrial pollutants comprising sulphur oxides, which are transformed to sulphuric acid during precipitation, are another substantial source of sulphate in water systems. Sulphate can also be formed through bacterial or oxidizing action, such as the oxidation of organo-sulphur compounds. Sulphates are easily soluble in water because they are frequently associated to alkali and alkaline earth metals. Sulphate is critical in public water sources due to its cathartic impact on people when present in high concentrations. In the absence of dissolved oxygen and nitrates, sulphates serve as a source of oxygen for anaerobic bacteria's metabolic oxidations. Under anaerobic conditions, sulphate ions are converted to sulphide ions, which then create hydrogen sulphide in equilibrium with hydrogen ions. As a result, the amount of sulphate in water is an important consideration in evaluating the extent of difficulties that can develop from hydrogen sulphide reduction.

In the fig 12, shows that the sulphate content in groundwater from the area of Bhramapuram location with an average of 6.4ppm (min and max values are 0.3 and 30.3ppm). All among the samples are below the desirable limit and may leads to the chances of increased risk of autism. Among the 40 samples, the landfill site possess higher loadings. Lack of Sulphate rich country rock and the unsuitable meteorological-dissolving conditions may supress the concentration of sulphate in the groundwater

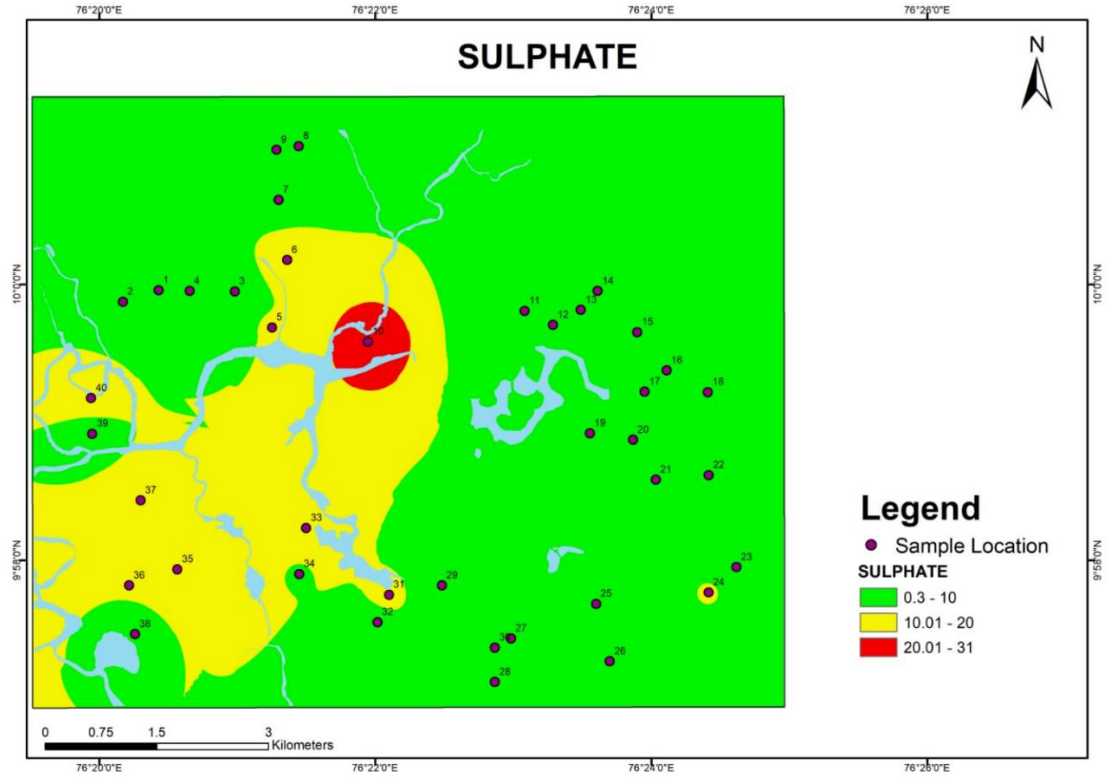

Figure 12: spatial map of sulphate

5.11 Sodium

Sodium is a frequent element found in nature, and it can be found as a dissolved ion in groundwater. The presence of sodium in groundwater can result from a variety of origins and consequences, including natural processes and human activities.

In the groundwater of the research area, sodium ions are the dominating cation after calcium. Sodium in groundwater is derived from both natural and manmade sources. Because of the disintegration of many rocks that create minerals, sodium is released into groundwater. The permitted limit for salt in drinking water is 200 mg/L (BIS, 2012). In natural waterways, sodium is present in variable levels and is the most frequent cation. Almost all sodium compounds are water soluble and tend to stay in aqueous solution. Water in contact with igneous rocks dissolves sodium from its natural source; other likely natural sources include clay minerals, feldspars, and minerals such as halite. Sodium enters natural streams via industrial and municipal waste discharges, as well as non-point sources such as agricultural runoff and cattle.

Excess sodium in drinking water would ordinarily have an adverse effect on water palatability, and water with up to 1000 mg/L may be physiologically tolerated. Excess salt in groundwater is detrimental to people who have heart, kidney, or circulation disorders. In human pathophysiology, the sodium total cation ratio (%Na) is significant (Prakash, Venkatesh Raju, and Somashekar, 2008). When evaluating water for agricultural use, the sodium-to-total-cation ratio is critical. High sodium concentrations may have a negative impact on soil structure and permeability, resulting in alkaline soils.

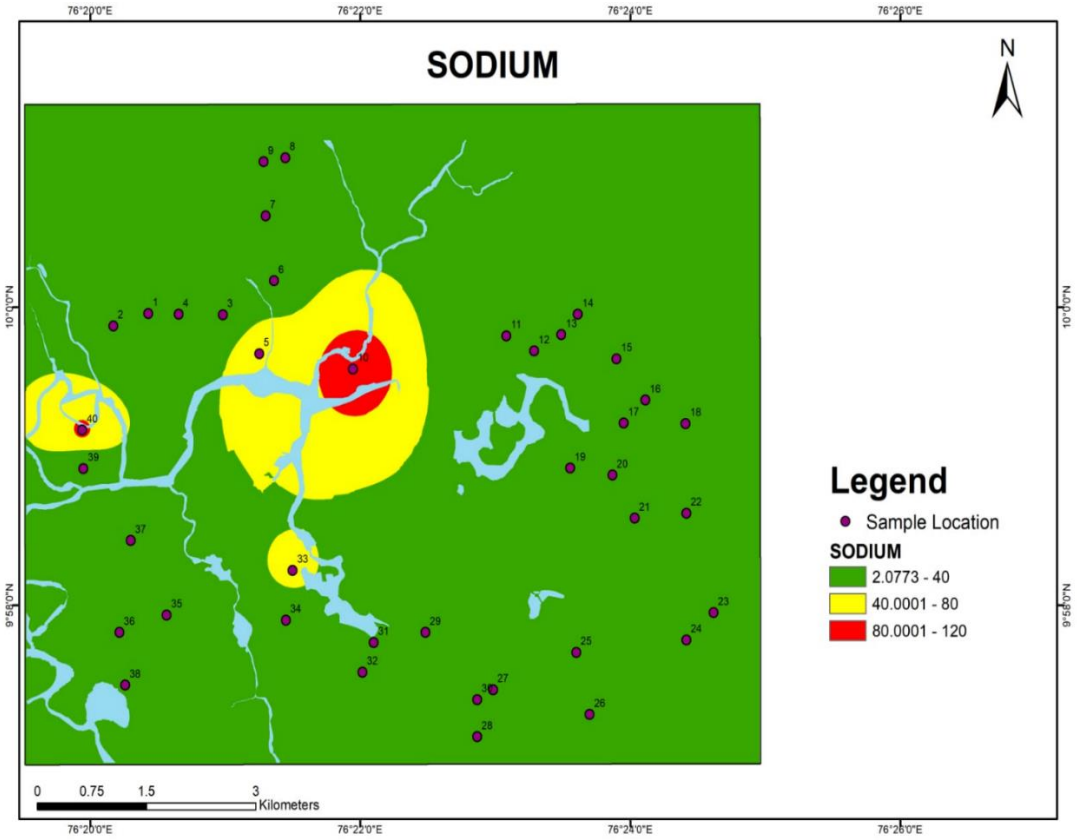

Figure 13: spatial map of sodium

In the fig 13 shows that the sodium concentration in Bhramapuram location. The sodium values range between 115.73 to 2.06 mg/l shows all samples are below the permissible limit.The comparative higher loadings of Na is at Bhramapuram land fill site.

5.12 Potassium

Potassium concentrations in groundwater are often low due to its limited mobility (Herman bouwer, 1987). It could be released as a result of the weathering of mica and orthoclase. feldspar Weathering releases K+ ions, which are normally used up in the production of

secondary minerals (Mathews, 1982). Feldspar, mica, and clay all contain significant levels of potassium. Contact with potassium-rich soils, industrial discharges, and agricultural runoff are all potential sources of potassium in ground water. Because of its low mobility, potassium concentrations in groundwater are frequently low (Herman bouwer, 1987). It could be released as a result of mica and orthoclase weathering. feldspar Weathering causes the release of K+ ions, which are generally consumed in the formation of secondary minerals (Mathews, 1982). Potassium is found in substantial amounts in feldspar, mica, and clay. Potassium in ground water can be found from contact with potassium-rich soils, industrial discharges, and agricultural runoff.

The figure shows the spatial distribution of potassium and all the samples are below the permissible limit.The sample number 10 act as hotspot for the spread of potassium. The least concentration emphasis the less dissolving nature of Potassium in groundwater.

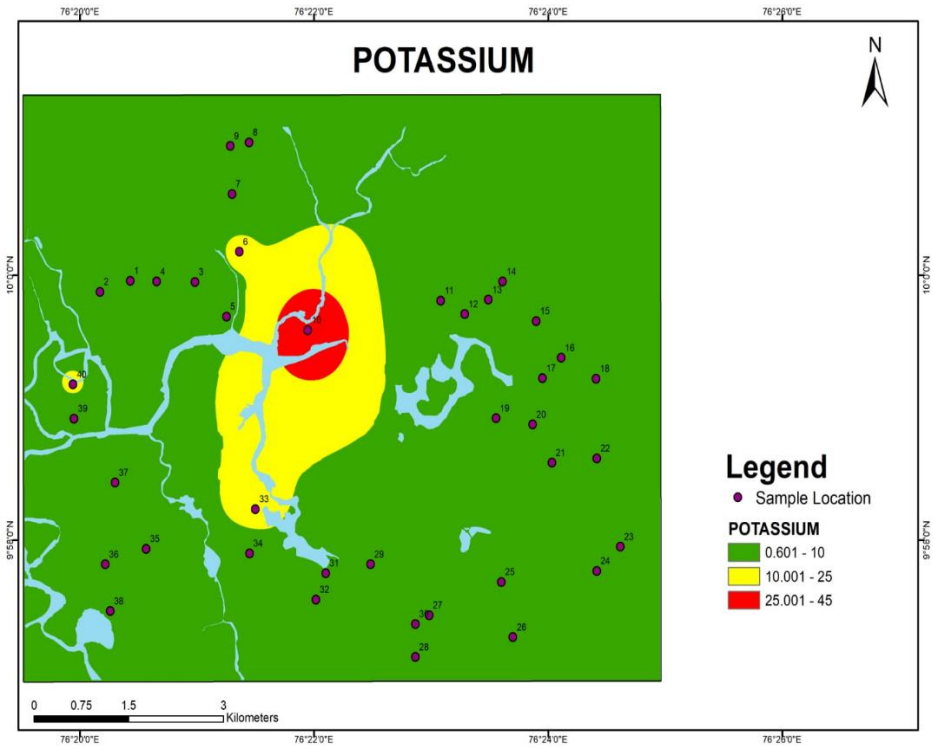

Figure 14: spatial map of potassium

CHAPTER 6

GROUNDWATER CLASSIFICATION

6.1 HYDROLOGICAL FACIES

The concentrations of key ionic constituents in groundwater samples were plotted in the Piper trilinear diagram (Piper, 1953) to determine the water type. In terms of major ion percentages and water types, cation and anion facies are classified according to the domain in which they occur on the diagram segments (Back, 1966). Back and Hanshaw (1965) proposed tri-linear diagram subdivisions to define composition classes. The cation and anion fields are merged to represent a single point in a diamond-shaped field, from which inference is derived using the hydro-geochemical facies concept.

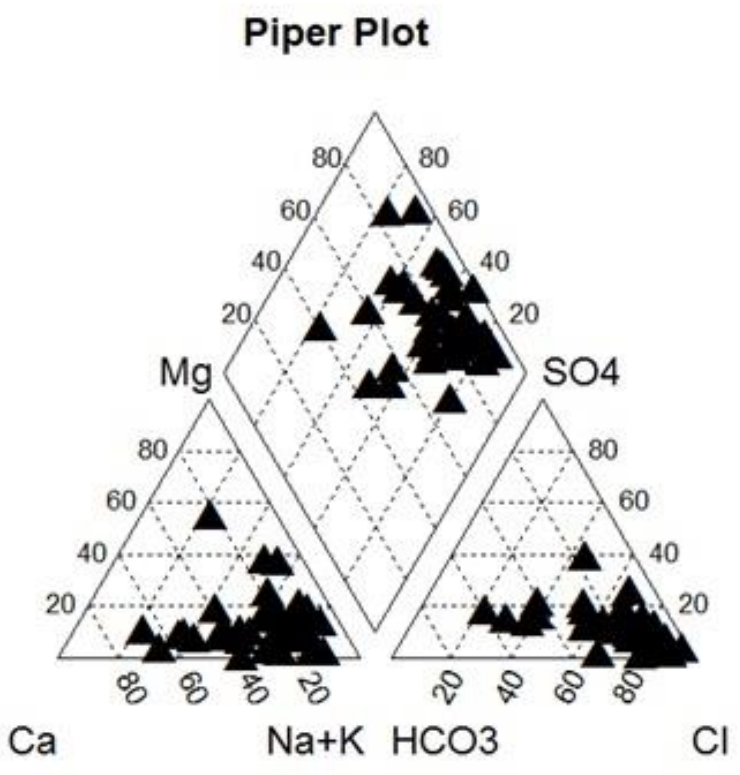

Figure 15: piper trilinear plot

Table 3: Characterization of groundwater for Piper tri-linear diagram

Subdivision of the diamond	Characteristisc of corresponding subdivision of diamond shaped fields	Percentage of sample in this category
1(5+6+9)	Alkaline earth(Ca+Mg)Exceed alkalies(Na+K)	30
2(8+9+7)	Alkalies exceeds alkaline earths	87.5
3(5+9+8)	Weal acids(C03+HC03)exceed Strong acids (S04+Cl)	25
4(6+9+7)	Strong acids exceed Weak acids	92.5
5	Magnesium bicarbonate type	7.5
6	Calcium chloride type	5
7	Sodium chloride type	67.5
8	Sodium bicarbonate type	0
9	Mixed type	20

Alkaline earth (Ca+Mg) Exceed alkalies (Na+K) to 30% and Weak acids (CO3+HCO3) exceed Strong acids (SO4+Cl) to 25%. Akalies exceeds alkaline earth is 87.5%.Second dominant type is Strong acids exceed weak acid of 92.5%. Alkalies exceeds alkaline earths . Magnesium bicarbonate,sodium chloride ,calcium chloride as30%,7.5%,67.5%,5% . Mixed type of having 20%. Thus piper diagram shows on the dominance of alkalies(Na+K) and Strong acids (S04+Cl) in the study area.

6.2 GIBBS DIAGRAM

The chemical connection of groundwater depending on aquifer lithology has been researched since Gibbs (1970). Viswanathaiah et al. (1978) interpreted the rock-water interaction in Karnataka groundwater chemistry. Rengarajan and Balasubramanian (1990), Sathyamoorthy (1991), Edwin Moses (1994), and Sreedevi (2004) have also applied this method to diverse places for the evolution of groundwater in various parts of India. The Gibbs diagram distinguishes three types of fields: precipitation, evaporation, and rock-water contact.

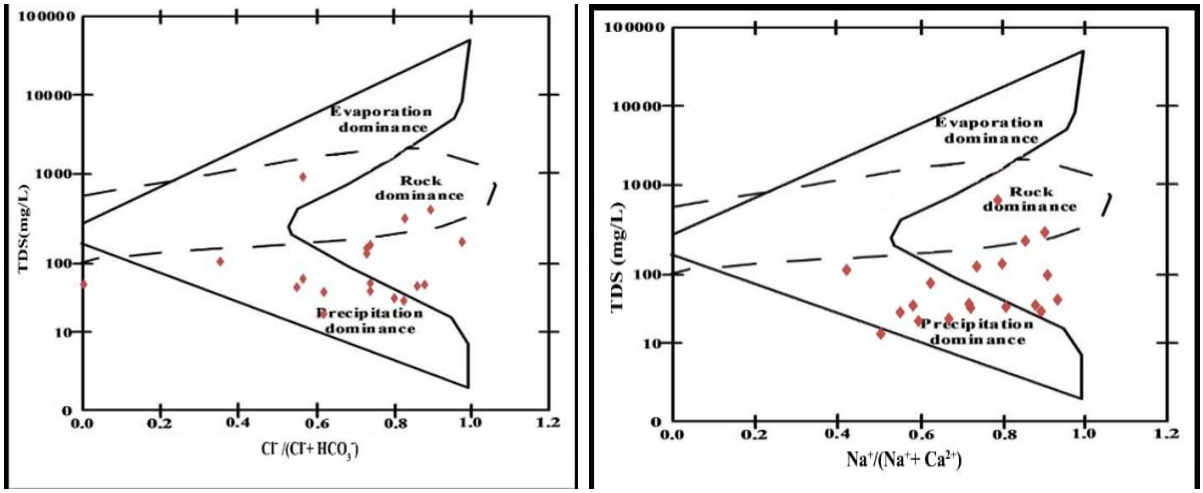

Figure 16: Gibbs diagram

Gibb's plots for groundwater quality data in the study area are presented in the fig(6.2).The Gibb's diagram shows that most of sample is in precipitation dominance,Because most of the sample falls in bottom of the gibbs diagram,which means the TDS value is less and the Na/Na+Ca and Cl/Cl+HCO3 are higher in amount. The groundwater chemistry of the study area is mainly influenced by precipitation, and rock water interaction respectively.Since the quality is depended to precipitation, the monsoonal effect has considerable impact on the quality of the study area. The precipitation effect also accounts for the least TDS in the study area.(Andres Maranadi 2018).

6.3 WILCOX DIAGRAM

The Wilcox diagram (1955) categorizes water samples based on their appropriateness for irrigation based on the sodium level. The sodium concentration is significant in classifying irrigation water because sodium reacts with soil, reducing its permeability. Alkali soils are formed when sodium is joined with carbonate as the main anion, while saline soils are formed when sodium is combined with chloride or sulphates as the predominant anion. A maximum of 60% Na in groundwater is permitted for agricultural use (Ramakrishna, 1998). Sodium% is the ratio of sodium total cations, which includes sodium, potassium, calcium, and magnesium. All concentration data is given in parts per million. Electrical conductance is displayed in eqm as abscissa and % sodium as ordinance in the Wilcox diagram and is separated into zones to indicate good and bad waters based on the standards established. Groundwater is graded as

excellent to good, good to permissible, permissible to doubtful, doubtful to unsuitable, and unsuitable in the diagram. The graphic depicts the sodium versus electrical conductivity values for all seasons.

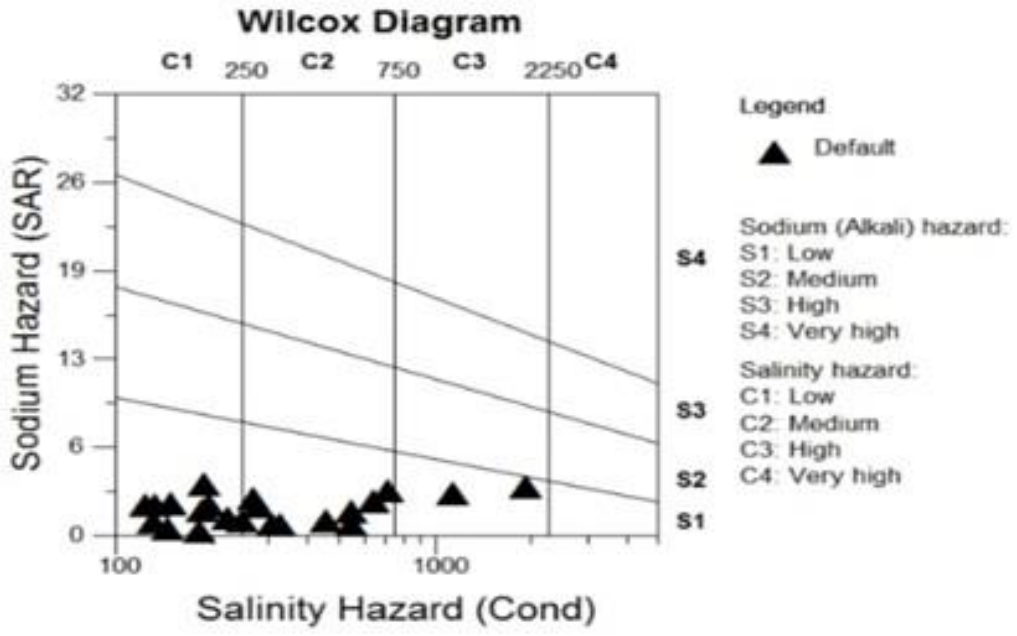

Figure 17: wilcox diagram

The groundwater samples are plotted in the Wilcox diagram fig(17).Among the samples most of the groundwater are fall in C1-S1 and C2-S1 which having 95%of the sample are Very Good and Good in their sodium content of the permissible limit.And 2 of the sample sample no10 and 40 which are lie in C3-S1 were are medium in purpose ,salinity content is very high compare to other samples.The increased concentration of salinity in location 10 and 40 needs immediate treatment and the rest of the samples are suitable for irrigation purpose.

6.4 BOX WHISKER PLOT

Box and whisker plots, often known as box plots, are an excellent graphic for displaying the distribution of data points across a specified metric. These graphs show ranges within variables that have been measured. Outliers, the median, the mode, and where the majority of the data points fall within the "box" are all included. These graphics are useful for comparing the distributions of numerous variables.John Wilder Tukey created the first box and whisker

graphs. In 1970, he developed the formula as part of his arsenal for exploratory data analysis as an American mathematician.

Box and whisker plots show the distribution of your data, as well as outliers and the median. The box within the chart shows where roughly half of the data points fall. It provides a five-point summary of a data set. The maximum is the mark with the highest value. It will almost certainly fall far outside the box. The minimum is the mark with the lowest value. It is very likely that it will fall outside the box on the opposite side of the maximum. The lower quartile, higher quartile, and median are all contained within the box. The median is the value that separates the upper and lower halves of a data sample, population, or probability distribution.

Box Whisker diagram mainly used to indicate the dominances of major ions in groundwater sample. The diagram includes a box that represents the 25th and 75th percentiles' upper and lower quartile values. The median is shown by the middle line, while the maximum and minimum values are shown by the vertical line (Machiwala and Jhab, 2015).Box and Whisker diagram(Fig 18) shows that the dominance of the major cations in groundwater in order of $Na^{2+}>Ca^{2+}>Mg^{2+}$ and for the anion is $Cl^{-}>HCO3^{-}>S04^{2-}$

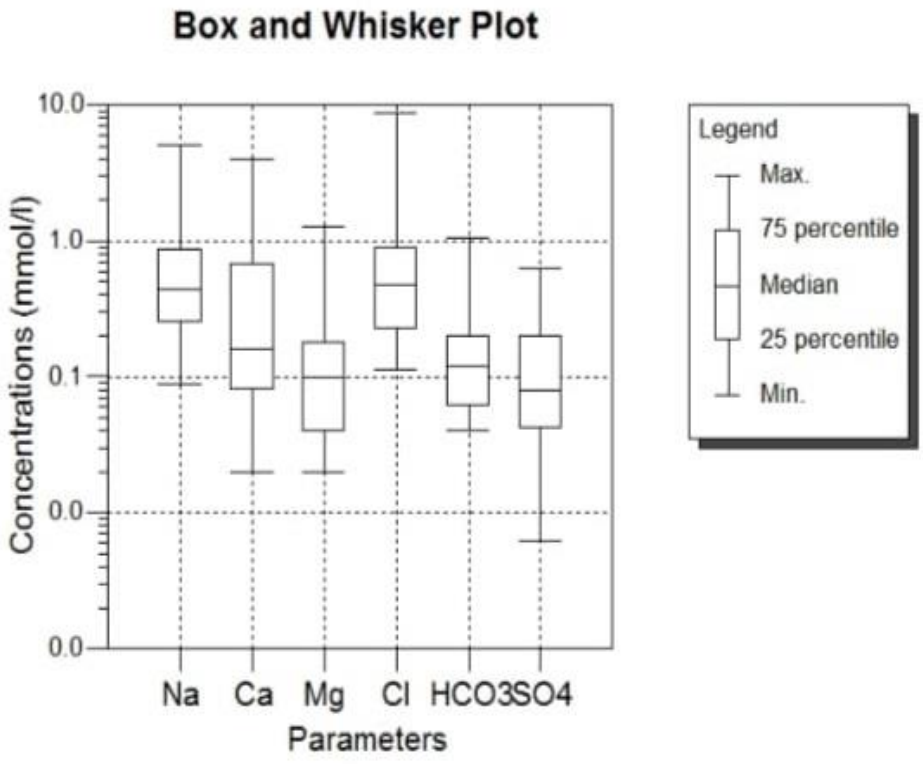

Figure 18: Box Whisker diagram

6.5 CORRELATION TABLE

Correlation matrix will help to identify the relationship between the series of water analyzed results or constituents.

Table 4: correlation table

Correlation Matrix												
		pH	EC	TDS	Total Hardness	Ca	Mg	Na	K	HCO3	SO4	Cl
Correlation	pH	1.000										
	EC	.449	1.000									
	TDS	.449	**1.000**	1.000								
	Total Hardness	.489	**.899**	**.899**	1.000							
	Ca	**.623**	**.946**	**.946**	**.926**	1.000						
	Mg	-.055	.315	.315	**.575**	.236	1.000					
	Na	.280	**.960**	**.960**	**.822**	**.827**	.401	1.000				
	K	.332	**.904**	**.905**	**.753**	**.816**	.192	**.863**	1.000			
	HCO3	**.601**	**.829**	**.829**	**.765**	**.833**	.190	**.736**	**.774**	1.000		
	SO4	.469	**.813**	**.813**	**.754**	**.769**	.312	**.777**	**.801**	**.803**	1.000	
	Cl	.297	**.960**	**.959**	**.838**	**.854**	.373	**.973**	**.836**	**.710**	**.716**	1.000

In the current study, pH is positively connected with HCO_3 and Ca but negatively correlated with Mg. EC is positively correlated with HCO_3, Cl, Ca, and TH and has a correlation value of one with TDS, indicating that the value of EC is directly proportional to the value of TDS because as the amount of solids dissolved in a particular quantity of liquid increases, so does the ability to conduct electricity because free ions are available for the movement of charge and conduct electricity. Most factors, including HCO3, Cl, Ca, and TH, are positively associated with TDS. HCO3 has a positive relationship with pH, EC, TDS, Cl, Ca, and TH. pH and HCO3 have a significant relationship with alkanity because it regulates the amount of H+ ions in a solution, which affects the pH value. Cl has a positive relationship with EC, TDS, HCO_3, Ca, and TH. Ca has a positive relationship with pH, EC, TDS, HCO3, Cl, and TH. Mg has a small positive correlation with all components and a negative correlation with only pH.. EC,TDS, HCO_3, Cl, Ca,Mg are all positively associated with TH. Ca and Mg

are clearly positively associated with TH since the sum of Ca and Mg equals total hardness.Except for Mg,most of the parameters shows high positive correlation among the parameters shows the least dominance of rock-water interaction,if the rock water interaction is dominant there we can see only selective correlation of parameters.Thus it also accounts for the influence of precipitation in the study area.

6.6 ROTATED COMPONENT MATRIX

A rotated component matrix, also known as a "rotated factor pattern" or "rotated factor loading matrix," is a notion used in factor analysis, a multivariate statistical method. Factor analysis is used to identify underlying latent variables that explain correlation patterns in observed data. The goal of factor analysis is to identify a smaller number of latent factors that may explain variation and covariance in a broader set of observed variables. The associations between these latent components and the observable variables are depicted in the factor loading matrix. The initial factor loading matrix, on the other hand, may not have a clear or interpretable structure.

Table 5: Rotated Component Matrix

Rotated Component Matrix[a]

	Component		
	1	2	3
pH	.183	**.958**	-.049
EC	**.936**	.289	.176
TDS	**.936**	.289	.175
Total Hardness	**.731**	.412	.496
Ca	**.809**	.512	.145
Mg	.173	-.044	**.978**
Na	**.943**	.093	.245
K	**.929**	.172	.015
HCO3	**.723**	**.552**	.071
SO4	**.750**	.394	.187
Cl	**.932**	.107	.231
Total	6.710	2.029	1.441
% of Variance	61.005	18.445	13.096
Cumulative %	61.005	79.450	92.546

In the factor 1 having the percentage of variance is 61.005% with high positive loading of Na(.943),EC(.936),TDS(.936),Cl(.932) and K(.929).TDS ,EC and the majority of the significant ions shows the geogenic influence in the study area (Tay etal.,2017). Factor 2 shows that the percentage of variance is 18.445% where pH (0.958), Ca^{2+} (.512),HCO_3(.552),The factor shows the importance in the shift of pH and are mainly due to the effects from bicarbonate and calcium content in the study area. Factor 3 shows 13.09% of percentage of variance were having highest loading on Magnesium and Total hardness and it itself is claimed that the hardness in this study area is depended mainly to Magnesium. Factor analysis concludes that the major factor influence to the groundwater quality is of geogenic origin especially due to the effects from precipitation.

CHAPTER 7

CONCLUSION

Ground water samples were analysed in the month of April 2023.The samples are collected in and around the location of Bhramapuram plant. The current study is being conducted to assess and monitor the geographical variation in groundwater quality over Brahmapuram in the Ernakulam district of Kerala, India. The geology of the area is dominated by laterites, clay, and Charnokite basement. The permitted groundwater quality limit in the research area follows the same pattern as the surface water flows. The acidic nature of the study area is exacerbated by the presence of iron in laterites and a lack of total alkalinity in the groundwater. The Comparative higher loadings of TDS are at Bhramapuram land fill site. The Gibbs diagram shows that the major influence is of precipitation thus accounts for the minimum TDS in the study area. Minimum calcium and magnesium levels indicate a lack of calcium- and magnesium-bearing country rock in the research area. In most of the samples, the physico-chemical parameters are below the desirable limit may results in mineral deficiency in the study area. The Gibbs diagram, correlation matrix and factor analysis accounts for the interionic relations responsible from geogenic processes as precipitation. The least concentration of potassium emphasis the less dissolving nature of Potassium.The wilocx diagram and sodium loadings shows that sample no 10 and 40 has higher loadings and it cannot be used for irrigation purposes.

The Box and Whisker diagram shows that the dominance of the major cations in groundwater in order of Na^{2+}>Ca^{2+}>Mg^{2+} and for the anion is Cl^{-}>$HCO3^{-}$>$S04^{2-}$.Gibbs diagram shows that groundwater chemistry of the study area is mainly influenced by precipitation and rock water interaction respectively. Correlation Matrix for TDS and EC shows high positive correlation towards the all major cations and anions. Ca and Mg are having positive correlation with Total Hardness and pH and total alkalinity shows appositive correlation about 0.61. In the Factor analysis marks the dominance of geogenic influence in the study area.

From the chemometrics and the spatial distribution, most of the physcio-chemical parameters are below the permissible limit and the higher loadings are at the Bhramapuram landfill area.Since the terrain is mostly of low tds and the higher loadings at landill site

attributes the anthropogenic or landfill influence.The comparative higher loadings of TDS except eastern side shows the influence of rivers in the study area.Thus, the influence of monsoon is critical for the Bhramapuram area, and it is substantiated with results from the precipitation effect from Gibbs diagram and river effect form tds spatial map and also the higher spread chances from the landfill sites during monsoon.

According to the current study, temporal monitoring of groundwater quality in and around the Brahmapuram Waste Processing Plant is critical, and this can be accomplished by checking the quality of water on a regular basis, recharging the wells, and closely monitoring the leaching of waste from the waste plant into the aquifer system.

REFERENCE

- Ackah, M., Agyemang, O., Anim, A. K., Osei, J., Bentil, N. O., Kpattah, L., ... & Hanson, J. E. K. (2011). Assessment of groundwater quality for drinking and irrigation: the case study of Teiman-Oyarifa Community, Ga East Municipality, Ghana. *Proceedings of the International Academy of Ecology and Environmental Sciences*, *1*(3-4), 186.
- Ahmed, M. J., Ahsan, A., Haque, M. R., Siraj, S., Bhuiyan, M. H. R., Bhattacharjee, S. C., & Islam, S. (2010). Physicochemical assessment of surface and groundwater quality of the greater Chittagong region of Bangladesh. *Pakistan Journal of Analytical & Environmental Chemistry*, *11*(2), 11.
- Amaliya, N. K., & Kumer, S. K. (2013). Evaluation of surface water quality of Kanyakumari district through water quality index assessment. *International Journal of Plant, Animal and Environmental Sciences*, *4*(1), 73-77.
- Babu, P. M., Sankar, G. J., Sreenivasulu, V., & Harikrishna, K. (2014). Hydrochemical Analysis and Evaluation of Groundwater Quality in Part of Krishna District, Andhra Pradesh-Using Remotesensing and GIS Techniques. *International Journal of Engineering Research*, *3*(8), 476-481.
- Bouwer, H., & Idelovitch, E. (1987). Quality requirements for irrigation with sewage water. *Journal of irrigation and drainage engineering*, *113*(4), 516-535.
- Babiker, I. S., Mohamed, M. A., & Hiyama, T. (2007). Assessing groundwater quality using GIS. *Water Resources Management*, *21*, 699-715.
- Balan, I., Shivakumar, M., & Kumar, P. M. (2012). An assessment of groundwater quality using water quality index in Chennai, Tamil Nadu, India. *Chronicles of young scientists*, *3*(2), 146-146.
- Dohare, D., Deshpande, S., & Kotiya, A. (2014). Analysis of ground water quality parameters: a Review. *Research Journal of Engineering Sciences ISSN*, *2278*, 9472.
- Hemant, P., Deepak, P., & Limaye, S. N. (2012). Studies on the physico-chemical status of two water bodies at Sagar city under anthropogenic influences. Advances in Applied Science Research, 3(1), 31-44.
- Huang, G., Sun, J., Zhang, Y., Chen, Z., & Liu, F. (2013). Impact of anthropogenic and natural processes on the evolution of groundwater chemistry in a rapidly urbanized coastal area, South China. *Science of the Total Environment*, *463*, 209-221.

- Jiang, Y., Zhang, C., Yuan, D., Zhang, G., & He, R. (2008). Impact of land use change on groundwater quality in a typical karst watershed of southwest China: a case study of the Xiaojiang watershed, Yunnan Province. *Hydrogeology Journal*, *16*(4), 727-735.
- Krishna Kumar, S., Hari Babu, S., Eswar Rao, P., Selvakumar, S., Thivya, C., Muralidharan, S., & Jeyabal, G. (2017). Evaluation of water quality and hydrogeochemistry of surface and groundwater, Tiruvallur District, Tamil Nadu, India. *Applied Water Science*, *7*, 2533-2544.
- Magesh, N. S., Krishnakumar, S., Chandrasekar, N., & Soundranayagam, J. P. (2013). Groundwater quality assessment using WQI and GIS techniques, Dindigul district, Tamil Nadu, India. *Arabian Journal of Geosciences*, *6*, 4179-4189.
- Mane, P. C., Kadam, D. D., Chaudhari, R. D., Pokale, S. S., Gawari, N. P., & Meher, S. (2017). EVALUATION OF SOME WATER QUALITY PARAMETERS WITH SPECIAL REFERENCE TO HEALTH–A CASE STUDY OF MANIKDOH DAM, JUNNAR, MAHARASHTRA.
- Matta, G., Srivastava, S., Pandey, R. R., & Saini, K. K. (2017). Assessment of physicochemical characteristics of Ganga Canal water quality in Uttarakhand. *Environment, development and sustainability*, *19*, 419-431.
- Mathew, K., Newman, P. W. G., & Ho, G. E. (1982). Groundwater recharge with secondary sewage effluent.
- Marandi, A., & Shand, P. (2018). Groundwater chemistry and the Gibbs Diagram. *Applied Geochemistry*, *97*, 209-212.
- Mester, T., Balla, D., & Szabó, G. (2020). Assessment of groundwater quality changes in the rural environment of the Hungarian great plain based on selected water quality indicators. Water, Air, & Soil Pollution, 231, 123
- Mohebbi, M. R., Saeedi, R., Montazeri, A., Vaghefi, K. A., Labbafi, S., Oktaie, S., ... & Mohagheghian, A. (2013). Assessment of water quality in groundwater resources of Iran using a modified drinking water quality index (DWQI). *Ecological indicators*, *30*, 28-34.
- Masoud, M. H., Basahi, J. M., & Rajmohan, N. (2018). Impact of flash flood recharge on groundwater quality and its suitability in the Wadi Baysh Basin, Western Saudi Arabia: an integrated approach. Environmental Earth Sciences, 77, 1-19.

- \Peethambaran, A., Anso, M. A., Salumol, T. S., Krishnamurthy, R. R., & Mahapatra, S. R. (2022). Classification and evaluation of groundwater in cheyyar watershed, Thiruvannamalai district, Tamil Nadu. *Materials Today: Proceedings*, *68*, 669-678.
- Premlata, V. (2009). Multivariant analysis of drinking water quality parameters of lake Pichhola in Udaipur, India. In *Biological Forum* (Vol. 1, No. 2, pp. 86-91). Satya Prakashan.
- Rao, B. V. (2011). Physicochemical analysis of selected ground water samples of Vijayawada rural and urban in Krishna district, Andhra Pradesh, India. *International journal of environmental sciences*, *2*(2), 710-714.
- Salihou Djari, M. M., Stoleriu, C. C., Saley, M. B., Mihu-Pintilie, A., & Romanescu, G. (2018). Groundwater quality analysis in warm semi-arid climate of Sahel countries: Tillabéri region, Niger. Carpathian J Earth Environ Sci, 13(1), 277-290.
- Sarala, C., & Ravi Babu, P. (2012). Assessment of groundwater quality parameters in and around Jawaharnagar, Hyderabad. *International journal of scientific and research publications*, *2*(10), 1-6.
- Saravanakumar, K., & Kumar, R. R. (2011). Analysis of water quality parameters of groundwater near Ambattur industrial area, Tamil Nadu, India. *Indian Journal of Science and Technology*, *4*(5), 660-662.
- Saravanakumar, K., & Kumar, R. R. (2011). Analysis of water quality parameters of groundwater near Ambattur industrial area, Tamil Nadu, India. *Indian Journal of Science and Technology*, *4*(5), 660-662.
- Sujatha, D., & Reddy, B. R. (2003). Quality characterization of groundwater in the south-eastern part of the Ranga Reddy district, Andhra Pradesh, India. *Environmental Geology*, *44*, 579-586.
- Sharma, M. K., & Kumar, M. (2020). Sulphate contamination in groundwater and its remediation: an overview. *Environmental monitoring and assessment*, *192*, 1-10.
- Subba Rao, N. (2018). Groundwater quality from a part of Prakasam district, Andhra Pradesh, India. Applied water science, 8, 1-18
- Wilkin, R. T., & DiGiulio, D. C. (2010). Geochemical impacts to groundwater from geologic carbon sequestration: controls on pH and inorganic carbon concentrations from reaction path and kinetic modeling. *Environmental Science & Technology*, *44*(12), 4821-4827.

- Tutmez, B., Hatipoglu, Z., & Kaymak, U. (2006). Modelling electrical conductivity of groundwater using an adaptive neuro-fuzzy inference system. *Computers & geosciences*, *32*(4), 421-433.
- Tiwari, A. K., & Singh, A. K. (2014). Hydrogeochemical investigation and groundwater quality assessment of Pratapgarh district, Uttar Pradesh. J Geol Soc India, 83(3), 329- 343.
- Xia, Q., He, J., Li, B., He, B., Huang, J., Guo, M., & Luo, D. (2022). Hydrochemical evolution characteristics and genesis of groundwater under long-term infiltration (2007—2018) of reclaimed water in Chaobai River, Beijing. Water Research, 226, 119222
- Ullah, R., Malik, R. N., & Qadir, A. (2009). Assessment of groundwater contamination in an industrial city, Sialkot, Pakistan. *African Journal of Environmental Science and Technology*, *3*(12).
- Ustaoğlu, F., Taş, B., Tepe, Y., & Topaldemir, H. (2021). Comprehensive assessment of water quality and associated health risk by using physicochemical quality indices and multivariate analysis in Terme River, Turkey. *Environmental science and pollution research*, *28*(44), 62736-62754.
- Wagh, V. M., Mukate, S. V., Panaskar, D. B., Muley, A. A., & Sahu, U. L. (2019). Study of groundwater hydrochemistry and drinking suitability through Water Quality Index (WQI) modelling in Kadava river basin, India. *SN Applied Sciences*, *1*, 1-16.
- Yusuf, K. A. (2007). Evaluation of groundwater quality characteristics in LagosCity. Journal of Applied Sciences, 7(13), 1780

DISTRIBUTION OF FORAMINIFERA IN THE VANCHIPURA BEACH: IMPLICATION ON PALEOENVIRONMENT

Dissertation submitted to Christ College (Autonomous), Irinjalakuda, Kerala, University of Calicut in partial fulfilment of the degree of

Master of Science in Applied Geology

By,

SUKRUTHA ANTONY

Reg. No: CCAVMAG014

2021-2023

DEPARTMENT OF GEOLOGY AND ENVIRONMENTAL SCIENCE

CHRIST COLLEGE (AUTONOMOUS), IRINJALAKUDA, KERALA, 680125

(Affiliated to University of Calicut and re-accredited by NAAC with A++ grade)

AUGUST 2023

DISTRIBUTION OF FORAMINIFERA IN THE VANCHIPURA BEACH: IMPLICATION ON PALEOENVIRONMENT

Dissertation submitted to Christ College (Autonomous), Irinjalakuda, Kerala,

University of Calicut in partial fulfilment of the degree of

Master of Science in Applied Geology

By,

SUKRUTHA ANTONY

Reg. No: CCAVMAG014

2021-2023

DEPARTMENT OF GEOLOGY AND ENVIRONMENTAL SCIENCE

EXAMINERS

Dr. ANTO FRANCIS. K

Co-Ordinator

1……

2……

CERTIFICATE

This is to certify that the dissertation entitled- '**Distribution of Foraminifera in Vanchipura Beach: Implication Of Paleoenvironment'** is a bonafied record of work done by Ms. Sukrutha Antony (Reg.No. CCAVMAG014), M.Sc. Applied Geology, Christ College (Autonomous), Irinjalakuda under my guidance in partial fulfilment of requirements for the degree of Master of Science in Applied Geology during the academic year 2021-2023.

Dr. Sunitha D
Internal Supervisor

Dr. Anto Francis K.
Coordinator Geology (S)
Christ College (Autonomous), Irinjalakuda
Kerala – 680125

DECLARATION

I, **Sukrutha Antony**, declare that the work included in my dissertation report named **"DISTRIBUTION OF FORAMINIFERA IN THE VANCHIPURA BEACH: IMPLICATION ON PALEO ENVIRONMENT"** was composed entirely by me and that it has not previously been presented, in whole or in part, in any previous application for a degree. Except where otherwise noted, the work presented here is entirely my own. This work is presented to Christ College (Autonomous), Irinjalakuda, Kerala, in a partial fulfilment of the Master of Science in Applied Geology degree requirements.

SUKRUTHA ANTONY

Reg. No. CCAVMAG014

ACKNOWLEDGEMENT

First and foremost, I want to express my gratitude to God Almighty, by whose mercy I am able to do this work. I wish to express my heartfelt gratitude and heartfelt thanks to, **Dr.Linto Alappat**, Dean of Research and Development of TLC (former HOD) Department of Geology and Environmental Science, Christ College(Autonomous) Irinjalakuda, **Dr. Anto Francis. K**, **Co- Ordinator**, Department of Geology and Environmental science, Christ College (Autonomous) Irinjalakuda,and **Mr. Tharun R.** Head of Department of Geology and Environmental Science, Christ College (Autonomous) Irinjalakuda, for developing the project's framework and providing regular support and supervision throughout the duration of the course study. A successful and ultimate conclusion of this project necessitated a great deal of advice and assistance, and I consider myself very grateful to have received this during all stages of my project work. Whatever I've accomplished is entirely due to such guidance and assistance, for which I am grateful. I would like to thank my project guide, **Dr Sunitha, D (Assistant Professor,** Department of Geology & Environmental Science) Christ College (Autonomous) Irinjalakuda, for creating the project guidelines and providing support and supervision throughout the project.

I also thank other faculty members for their support and encouragement. I would like to extend my thanks to **Mr. Ayyappadas C.S** and **Mrs. Shaima M.M** for the continuous support provided for the completion of the dissertation.

I would prefer to take this opportunity to thank all of my classmates and friends who helped me finish my dissertation, whether directly or indirectly. I'm also thankful to the entire Christ College family for their love and support.

I also express my gratitude to my parents and family members for their unwavering support and prayers throughout my life.

Sukrutha Antony

CONTENTS

LIST OF FIGURES

LIST OF TABLES

ABSTRACT

In order to study the distribution of foraminifera, the calcareous microfauna, occurring in the Vanchipura Beach samples, a total of 19 surface samples and one core sample were collected. The taxonomy and systematic study were deal using ostracod treatises proposed by Loeblich and Tappan, 1988 and other recent literature. Distribution pattern of individual taxon was examined and their sediment relationship was determined for ecologic/environmental interpretation. Sand-silt clay ratio estimation was carried out using the procedure of Krumbein and Pettijohn (1938). Estimation of $CaCO_3$ was made by adopting the procedure proposed by Piper (1947) has been incorporated in this dissertation. Previous research work on foraminifera has been reviewed and included in the separate chapter.

The main aim of the present study is to find the abundance and distribution of foraminifera in Vanchipura Beach region. Individual taxon, distribution trends were studied, and their sediment relationships have been identified for ecologic/environmental assessment. A total of 7 foraminiferal species were identified from the surface samples and 15 foraminiferal species were identified from the core sample. The species belonging to *Ammonia beccarii* and *Elphidium advenum* were abundant in the surface samples. The species belonging to *Elphidium norvangi* is comparatively less in number in the surface samples. On the other hand, in the core sample *Ammonia beccarii* and *Elphidium advenum* found dominant, *Sorites orbiculus* and *Trochammina mactescens* found rare. The species were observed in shallow water condition. Sedimentological characteristics were discussed by analysing the sand silt clay and the calcium carbonate percentage.

CHAPTER 1

INTRODUCTION

1.1 GENERAL INTRODUCTION

Micropalaeontology is a relatively recent subject that studies about microfossils, the morphology, the classification and environment. Microfossils are fossils that are less than 1 millimetre in size. Some remains of ancient life-forms are preserved as fossils in various sediments and provide information on the changing abundance and variety of species, but also on the environmental during past eras. The study of microfossil is mainly done by using a microscope. Micropaleontology, in general, involves successive sizes of microscopic fossils down to animals which need to be enlarged many times or more for seeing. The study of ultrasmall fossils is possibly the most rapidly growing branch of modern palaeontology, and it is reliant on modern laboratory gear such as electron microscopes. Today, micropalaeontologists started tackling current environmental and climate change challenges with microorganisms, whose fossilised remains used to be the primary focus of their research. It is composed of an extensive variety of fossils of organisms that are generally minute in size, which include Foraminifera, Ostracoda, Diatoms, and Radiolaria. The microfossil group consist of various types of skeletons that may be single celled aquatic organisms, which include (Foraminifera, Radiolaria, Diatoms, Calcareous fossils).

The practical significance of microfossils in several aspects of historical geology is enhanced by their small size, abundant occurrence, and wide geographic distribution in sediments of all ages and in most oceanic settings. Factors responsible for the entire preservation of the foraminiferal population include test composition and physico-chemical factors (rate of sedimentation, water depth, seawater upwelling, pore-water oxygen, and so on) at the foraminiferal occurrence site. The petroleum industry predominantly exploited micropaleontology for subsurface correlation of geologic layers, resulting in substantial advances in the discipline's taxonomic, biostratigraphic, and paleoecologic aspects.

Foraminifers are unicellular organisms, mostly they are found in marine environment. It can be either benthic or planktonic in origin. The unicellular protists have hard calcium

carbonate cover ie, test. The shell can be milky white, glassy, grey. Tests are also called allogromiids that's been made by tectin, which is soft and flexible organic matter. There are various types tests (simple, spiral, complex). Forams are mainly, effect to various physical and chemical changes that are been occurred in the surroundings, thus they can say that it is very useful for the paleoclimate study. The minor and major variation in the environment can be analysed by the morphological changes in the fossils. The main importance of the foraminifera is the use of fossil tests in biostratigraphy, paleoenvironment studies, isotope geochemistry. Foraminifers are abundant in seafloor sediments and can provide information on the presence and types of toxins in marine environments, so they're helpful for ecological and paleoecological applications as well as pollution studies. Almost 40 species are planktonic, that are floating in the water. And the others are living in the sand, mud, rocks and plants at the base of the ocean.

1.2 APPLICATION

Beyond enhancing our understanding of the diversity of life, the study of fossil foraminifera has various benefits. Biostratigraphy, paleoecology, paleobiogeography, and oil prospecting all benefit from fossil foraminifera.

1.2.1 BIOSTRATIGRAPHY

Foraminifera shows the relative ages of marine rocks. There are many reasons why fossil foraminifera are particularly useful for establishing the ages of marine rock layers. They have existed since the Cambrian period, nearly 500 million years ago. As they exhibit relatively constant evolutionary progress, various species can be found at different times. Forams are many and extensive occurring in all aquatic settings. Finally, even from deep oil wells they are little and easy to gather.

1.2.2 PALEOECOLOGY AND PALEO CLIMATE

Forams provide evidence of the past environment, that is due to different species of forams are found at various environment. Paleontologists uses the fossils to determine the past environment. Foraminifera are being used to map previous tropic distributions, determine ancient shorelines, and measure variations in global ocean temperature over the ice ages. If a fossil foraminifera sample contains a large number of extant species, the current distribution of those species can be used to estimate the environment at that site when the fossils were alive.

1.2.3 OIL EXPLORATION

The forams can be used to find petroleum, Certain species are geologically short-lived, whereas others are found only in particular locations. As a result, a palaeontologist can study the specimens in a small rock sample, such as those obtained during oil well drilling, and establish the geologic age and surroundings in which the rock developed. As a result, the oil industry has been a significant employment of palaeontologists who specialise in these minute fossils since the 1920s. Foraminifera stratigraphic control is so accurate that these fossils are employed to direct sideways drilling inside an oil-bearing horizon to boost well production.

1.3 OBJECTIVE

- To identify and illustrate calcareous microfauna such as foraminifera, occurring in the Vanchipura Beach samples, using standard micropalaeontological techniques.
- To determine the sedimentological parameters such as sand, silt and clay and calcium carbonate of the sediments collected from the beach samples in Vanchipura and to correlate with distribution of foraminifera population.
- To discuss on paleoenvironment of the Vanchipura Beach.

CHAPTER 2

REVIEW OF LITERATURE

2.1 STUDY OF FORAMINIFERA IN AN AROUND THE WORLD

There are several studies done on foraminifera by using various methods, the studies are been conducted in an around the world. The study of effective salinity variation on benthic foraminiferal species done by laboratory method done in Goa (Rajiv Nigam, Rajeev Saraswat, and Sujata R. Kurtarkar, 2006) In coastal areas, mixing of fresh water changes the features of marine water, affecting both living and dead foraminiferal species (Murray, 1991; Nigam et al. 1992, Nigam and Khare, 1994, 1999; Murray and Alve, 1999). Among the various changes brought about by the influx of fresh water, the most noticeable is a change in salinity (Liu et al. 2001). Thus, by studying a foraminiferal assemblage and its down core fluctuation, one might determine salinity variations in the past. This data can be used to infer the climatic changes that occurred in that region. However, knowledge of the precise response of the species or assemblage of species that will be used to infer before salinity fluctuations is required for such studies. The reaction of *Pararotalia nipponica* (Asano) to varied salinities and its salinity tolerance limitations were studied in a culture experiment. The specimen is kept in 33‰ saline water to achieve the growth. The field collection and laboratory analysis is been done. Within 25 days, specimens stored at 10‰ and 15‰ salinity began to become opaque and their tests dissolved. To determine the highest salinity tolerance limit, the salinity was gradually increased to 100 in the culture dishes containing specimens in 40 saline-water, and it was discovered that P. *nipponica* specimens were alive even at 100‰ salinity. It is established that lower salinities are substantially more harmful to foraminiferal tests than higher salinities. The salinity response of benthic foraminifera is being utilised for environmental evaluation, hence the results are notable.

Thejasino Suokhrie, R. Saraswat and Rajiv Nigam 2017 studied about the variability in the Indian monsoon during the last 2000 years as determined from benthic foraminifera. The effect of the surrounding environment on living benthic foraminifera was investigated from the shelf and slope of the central-western Bay of Bengal to assess the applicability of temporal changes in benthic foraminiferal morpho-groups to reconstruct past monsoon changes. An amount of 46 surface sediment samples and a gravity core were taken from the western Bay of Bengal. The sediments consist of 35 multi core top and 11 spade core top, the sample depth is about 27 m to 2494 m.

The result, organic carbon is limited in the inner shelf zone and rises as one approaches the slope. A high amount of organic carbon is observed in the northern region of Godavari River. And another type of organic carbon variation can be seen in the slope region of Krishna and Pennar River. The parameters influencing the relative abundance of angular asymmetrical and rounded symmetrical benthic foraminiferal morpho-groups in the central western Bay of Bengal have been investigated. The regional variation in relative abundance of benthic foraminiferal morpho-groups is influenced by riverine intake and concurrent alterations.

I. Mendes, Rajiv Nigam 2004 examined and studied about the Factors affecting recent distribution of benthic foraminifera on the Guadiana shelf (Southwestern Iberia). The studies mainly provided with the analysis of 24 sediment surface samples obtained at sea depths ranging from 9 to 103 m on the continental shelf off Guadiana River resulted in the identification of 270 species. The geographical distribution of assemblages is directly related to the sedimentary environments and bathymetry of the seafloor. The outflow of the Guadiana Estuary and local hydrodynamic factors greatly affect the number of benthic foraminiferal tests and the distribution of various nearshore species within the two shallowest assemblages. Deeper water assemblages, on the other hand, were found to be more connected with low tidal energy, low oxygen conditions associated with fine-grained sediments, and cold-water filaments associated with seasonal upwelling.

Frans J. Jorissen, 1987 the main aim of the study was to examine about the distribution of benthic foraminifera in the Adriatic Sea. The sediments were collected from bottom its about 287 grab samples. Based on a Q-mode principal components analysis, four major biofacial units have been identified; these are all distinguished by the frequency of one or more of the eight clusters of benthic foraminiferal taxa identified by an R-mode cluster analysis. The distribution pattern of benthic foraminifera in the Adriatic Sea differs significantly from that of many other marine basins in that it is strongly influenced by large amounts of nutrients from river runoff as well as a large variation in the nature of the substratum, resulting in extreme environmental and faunal differences over short distances.

Cluver and Buzas, 1981, Murray, 2006 each conducted substantial research on the distribution of foraminifera in the Gulf of Mexico. Much of the distributional and biodiversity study in the Gulf is based on two seminal papers (Gibson and Buzas, 1973; Poag, 1981). Phleger (1951) released his classic article on foraminiferal distribution based on 550 bottom samples from 12 traverses in the northwestern Gulf of Mexico. Parker (1954) published her

famous study on foraminiferal distribution in the northeastern Gulf of Mexico, based on 201 samples from 11 traverses. The data in the articles are easily comparable because Parker, one of the most distinguished foraminiferal taxonomists of the previous century, was the primary taxonomist on both studies. The northwestern study is divided into two parts: Phleger (1951), which focuses on ecology and distribution, and Phleger and Parker (1951), which focuses on taxonomy. Culver and Buzas (1981) provide a distribution of all species encountered in the Gulf of Mexico up to 1980.

Rajiv Nigam, 2005 done studies about the Addressing environment issues through Foraminifera case studies from the Arabian Sea. It was done almost about the few year's microfossils especially foraminifers, and it can be the main source to express the environmental issues. The major changes in the forams are due to the environmental conditions that have led to various development of techniques to understand the past sea level fluctuation. and other specific characters. Foraminifers have found application in marine pollution and archaeological investigations, in addition to being one of the most widely utilised indicators for paleoclimate fluctuations. There is a need and inclination for future development of foraminiferal helpful in environmental impact assessment. To maintain these procedures up to date with changing modern trends, traditional hard part investigations of foraminifera must be supplemented by a comprehensive foraminiferal - culture approach based on a molecular biological approach.

MG Anantha Padmanabha Shetty, Rajiv Nigam, 1982 Foraminiferal assemblages in sediments and their connection to organic carbon have been examined in a number of west coast near shore locations, including the Gulf of Kutch, the Bombay-Daman sector, the Vegurla-Dabhol sector, cola Bay, and Karwar. The study was conducted on the magnitude of relationship, correlation coefficients between organic carbon and by matter foraminiferal species were computed using TDC-316 computer. Gulf of Kutch lithology and organic carbon level - The Gulf of Kutch is a shallow region with a limited marine environment. Five samples from 14-42m depth are from the outside part of the Gulf, while ten samples from 14-39m depth are from the interior region, where there is only a thin veneer of sediments. The terrain at the mouth of the Gulf consists mainly of silty clay to clayey silt with some sand and includes diatoms (dead) miliolid and agglutinated foraminifera, ostracods, bivalves, and a high degree of carbonaceous (organic) debris. The inner Gulf is made up of very fine-grained greenish grey clayey silt to silty sand. It contains 0.46% organic carbon and contains young Foraminifera, bivalves, and gastropods.

Baggy (1905) described an assemblage of California foraminifera in a mudstone sample retrieved from the Miocene Monterey formation, many of them are borrowed from the European literature, as Cornteld (1920) first noted. Baggy assumed Chapman's assemblage was from the same geological unit based on its foraminiferal taxa. In 1925, Joseph A.Cushmun (1881 - 1949) named three new Siphogenerina species based on samples obtained for the Marland oil firm by Willian D. Kleinpell (1898 - 1959) from Highland School District to the south. Cushman (1926) added that he also possessed some of Branner's grave's creek material, which seemed to demonstrate that Bagg's three species were synonymous. Finger et al. (1990) recorded the more widespread foraminiferal funa from numerous exposures along the creek many years later. Bagg (1912), a year after joining the faculty at Lawrence College in Wisconsin, published another paper describing foraminifera from two sites in southern California. One place he referred to as Pliocene was Timma Point in San Pedro, Los Angeles County, based on observed parallels with the 'coralline' crug fauna of the St Erth beds in England (Jones et al., 1897), as well as the strata in the San Pedro area (Arnold & Arnold 1902; Arnold 1903).

Johan and Jorissen, F.J, 1996 The studies were conducted on Recent and ancient benthic foraminifera from the Adriatic Sea: distribution patterns in relation to organic carbon flux and bottom oxygen concentration. The current study's findings imply that benthic foraminiferal abundance in recent and fossil sediments provides a foundation for estimating present and past organic carbon flux at the seafloor. Whereas lateral organic carbon input may boost infaunal foraminifera production, epifaunal foraminifera abundance may be a more reliable metric of vertical organic carbon supply. When there is a lack of oxygen in the bottom water, the regular epifaunal population may be replaced by a community dominated by low-oxygen tolerant infaunal foraminifera. Under these conditions, it appears that reliable measurement of the vertical organic flux is impossible.

Rajiv Nigam, Neloy Khare 1999, Foraminifera spatial and temporal distribution in strata off India's central west coast, and use of their test morphologies for paleomonsoonal precipitation reconstruction. Foraminiferal composition and diversity were studied in 21 samples of surface sediments (varying in depth from 22 to 52 m) and two sediment cores of 4.80 m and 4.00 m (surface/subsurface) from the shallow region off India's central west coast. Scanning electron photo micrographs were used to identify and illustrate 177 different species. There are 72 genera, 47 families, 26 super families, and 5 sub orders. To gain insight into paleoclimatic changes in this location, quantitative spatial distribution data for morpho-groups

(angular-asymmetrical and rounded-symmetrical) were developed. The distribution demonstrated that angular-asymmetrical forms were less abundant near the river mouth, demonstrating an inverse association between angular-asymmetrical morpho-groups and river discharge (low salinity water). For rounded-symmetrical forms, the opposite is true. These metric's down core profiles revealed substantial wet periods around 3200 years BP and 1000 AD, interrupted by a dry interval around 2000 years BP. Our conclusion is consistent with the weather conditions recorded elsewhere in the world.

2.2 FORAMINIFERA FROM INDIA'S WEST COAST

Review on pollution ecology studies of Foraminifera of Trivandrum Coast, T S Satyanarayana Rao and K Kameswara Rao, In 1978, a study was conducted based on (1) the distribution and amount of foraminiferal species, (2) monthly differences in foraminiferal population, (3) the connections between foraminiferal assemblages and marine pollution, and (4) the effect of industrial effluents on foraminifera. Sediments were taken from beach sand and water depths of 5, 10, and 20m using a Van Veen grab along three crossovers off Thumba, Trivandrum Titanium Plant, and Shankhumugham, indicating the presence of 85 foraminifera species grouped into 42 genera and 26 families. Based on taxonomic assemblages, three faunal categories were reported: beach fauna at 0-1m, nearshore fauna at 1-5m, and offshore fauna at 5-20m depth. An electron microscope was used to investigate the effect of corrosion on foraminifera specimens obtained from contaminated areas. *Miliolids, Elphidium sp.,Operculina ammonoides, Amphistegina radiata, Nonion asterizans, Neoconorbina patelliformis, Ammonia beccarii, Hanzawaia concentrica, Hyalinea balthica, Textularia candeiana* were the most abundant along the coast, with *Clavulinoides jarvisi, Bolivina tortuosa, Spiril.* Overall foraminiferal population sizes were greater in February and March than in December. When compared with the stations along Thumba and Shankhumugham, the species diversity at the Trivandrum Titanium Plant site was quite low. It was found that the nearshore waters of Kochuveli beach were contaminated due to the substantial quantity of waste water discharged daily from the Trivandrum Titanium Plant. The primary constituents of effluents are ferrous sulphate and sulfuric acid.

Benthic Foraminifera in Beypore Estuary, Sreenivasulu Ganugapenta et al. 2019 evaluated the benthic foraminiferal diversity index in sediments from the Beypore Estuary. Using a grab sampler, sediments were collected from 16 sampling locations in the Beypore Estuary throughout the month of April, 2015. A total of 2 to 776 faunal species were observed, which were divided into 10 genera and three suborders. The most important species are*:*

Ammonia tepida (63%), Ammonia parkinsoniana(56%), Nonion grateloupi and Nonion scaphum (44%), Trochammina inflata, Ammonia becarii and Bolivina striatula (31%), and rare species are Quinqueloculina lata, T. agglutinans, Quinqueloculina stelligera. Because of the low salinity and high warmth that prevail in the habitat, the juvenile foraminifera very definitely died. The large number of stress-tolerant benthic foraminifera and the absence of *Elphidium* species in the estuary indicate that low-oxygen conditions exist. The ongoing low foraminifera diversity index shows that the ecosystem in the Beypore estuary is moderate to highly stressed. The low amount of tests in 60% of the estuary, as well as the poor variety, are highlighted by both inherent variances in ecological characteristics and human-induced activity. The investigation found that the river mouth had a larger foraminiferal variety.

Sreenivasulu, G., Praseetha, B. S., Daud, N. R., Varghese, T. I., Prakash, T. N., & Jayaraju, N. (2019). Benthic foraminifera as potential ecological proxies for environmental monitoring in coastal regions: A study on the Beypore estuary, Southwest coast of India. *Marine pollution bulletin*, *138*, 341-351.examined the foraminiferal assemblages in the Ashtamudi estuary. During the summer, sediment samples have been collected from 30 different locations in the Ashtamudi estuary. Using a Van-Veen grab, 2000. Estuarine bottom sediment samples were taken from several portions of the estuary, including the Ashtamudi entry, the central kayal, the southern kayal, the western kayal, and the eastern kayal. From estuarine sediments, 29 foraminiferal species belonging to seventeen taxa have been found. The genus Ammonia is the most prominent taxon in the Ashtamudi estuary. The following planktic foraminiferal species can be found in the Ashtamudi estuary: *Ammonia Beccaria, Ammonia dentata, Bolivina earlandi, Bulimina marginata, Cancris oblongus, Dyocibides sp., Elphidium discoidale, Elphidium hispidulum, , Eponides repandus, Globulina gibba, Nonion boueana*. Because these kayal were used for coir husk retting, faunal frequency and variety were low in the eastern, southern, and western kayal. The coir retting process produces hydrogen sulphide gas, which lowers the pH of the water and creates anoxic oxygen conditions. The fluctuation in faunal frequency reflects the random distribution of ecological factors and nutrients that regulate faunal dispersal.

Review of Benthic Foraminifera distribution and Palaeo productivity changes from Anthakara Nazhi beach sediment M. Ravichandran et al. 2020 investigated the distribution of benthic foraminifera and associated Palaeoproductivity variations in Anthakara Nazhi beach sediments from the Alappuzha area. Between September and October of 2018, one hundred beach core sediment samples were obtained. Standard Micropaleontological procedures were

used to process all materials. A total of 27 benthic foraminifera species were identified. *Ammonia beccarii, Ammonia gaimardii, Anomalina globulosa, Cancris oblongus, Gyroidinoides nitidula, Gyroidinoide scibaoensis, Quinqueloculina seminulum, and Textularia sp*. were found as the most dominant species. *Ammonia beccarii* and *gaimardii* are common in shallow-marine environments with sandy bottoms. Species *Cancris oblongus* has mesotrophic-eutrophic tolerance. *Gyroidinoides nitidula* indicates a high oxygen environment with low organic flow. The high organic productivity, fine sediment texture, and low salinity conditions all have a role in foraminiferal distribution in the Anthakara Nazhi beach zone. According to this study, fine sediment on Anthakara Nazhi beach is substantially more conducive to foraminiferal blooming. The faunal record of benthic foraminifera is strongly tied to the delivery of organic materials to the bottom and the oxygen concentration of the surrounding water. Thus, the distribution of benthic foraminiferal faunal records from Anthakara Nazhi beach samples provides important information for reconstructing Paleoclimatology and Palaeo productivity changes throughout India's west coast.

Nigam et al. (2000) examined the Vengurla-Cochin Sector of the Arabian Sea, identifying 204 foraminiferal species and generating paleo-depth proxy data using two distinct morphgroups. Kathal et al. (2000) used Q-mode cluster analysis on 160 foraminiferal species to distinguish two foram geographical regions for the west and east coasts. Based on the isotopic composition of planktonic foraminifera from the northeastern Arabian Sea, Luckge et al. (2001) estimated monsoonal variability in the northern Arabian Sea during the past 5000 years.Nigam et al. (2002) examined the impact of mining pollution on total foraminiferal number (TFN) in ten surface samples collected from the Mandovi Estuary in Goa. Peeters et al. (2002) investigated the effect of upwelling on the distribution and stable isotope composition of *Globigerina bulloides* and *Globigerinoides ruber* in the northwest Arabian Sea's modern surface waters.

Khare et al. (1995) investigated foraminifera off the coast of Mangalore and concluded that the distributional pattern of benthic foraminiferal morpho-groups is related to fresh water river discharge, which is related to rainfall. Khare et al. (1995) studied the distribution patterns of benthic foraminiferal morpho-groups in the shelf region off Mangalore using 45 surface sediment samples obtained at depths ranging from 20 to 86 m. Dredging for the navigational channel was blamed for an irregularity in the distribution pattern off New Mangalore Port. Nigam and Khare (1995) conducted a detailed analysis of foraminiferal research from Indian seas and published a tabular bibliography of such works, including their highlights, from 1951

to 1995. Nigam (1996) investigated the use of foraminiferal distribution patterns in marine sediment to predict paleo-sea levels from the Arabian Sea.

Mathur and Gupta (1989) reported the areal distribution of dominating foraminifera in sea bed samples from the Arabian Sea near Devgarh on India's west coast, as well as three major foraminiferal biofacies. Nigam et al. (1991) investigated surficial sediment samples obtained from the outer shelf from Vengurla to Mangalore and suggested that the growth of intertidal barnacles (*Cirripedes crustacea*) on foraminifera might be used to monitor palaeo-sea level fluctuations. Following a careful examination of three sediment cores from the shallow water zone off Karwar, Nigam and Khare (1992) concluded that microspheric generation prefers dextral coiling and that coiling in benthic foraminifera appears to be regulated by method of reproduction. Nigam and Khare (1994) investigated the effect of river discharge on the morphology of 148 benthic foraminiferal species taken from 21 surface sediment samples from the inner shelf zone off Karwa.

Nigam and Thiede (1983) described Recent foraminifera from the inner shelf of India's central west coast using factor analysis. Nigam (1984a) described 60 species of benthonic foraminifera from 23 samples obtained from the Damon-Bombay sectors tidally impacted inner shelf. Setty and Nigam (1984) described 45 intertidal foraminifera species from the Miramar Cananzalem shoreline in Goa. Setty and Nigam (1984) used benthic foraminifera as pollution indices in the maritime environment of India's west coast. Bhalla and Lal (1985) issued a preliminary note on Recent foraminifera from the Okhla beach sands in Gujarat, identifying 18 species while contrasting the fauna to that of other western beaches. Rao et al. (1985) investigated the frequency distribution of 52 foraminiferal species and faunal trends in relation to pollution off the shores of Trivandrum. Setty and Nigam (1985) identified 62 species of benthic foraminifera from a clastic shelf regime off the coast of Bombay. They also proposed that foraminifers may be used to effectively measure variety and hyposalinity, highlighting the consequences of river discharge. Bhalla and Lal (1985) published a preliminary note on Recent foraminifera from Gujarat's Okhla beach sands, naming 18 species and compared the fauna with that of other western beaches. Rao et al. (1985) studied the frequency distribution and faunal trends of 52 foraminiferal species off the coast of Trivandrum. From a clastic shelf regime off the coast of Bombay, Setty and Nigam (1985) found 62 species of benthic foraminifera. They also argued that foraminifers may be used to effectively measure diversity and hyposalinity, emphasising the effects of river discharge.

Rajiv Nigam, A. Mazumder, P. J. Henriques, 2003 studied about Distribution of Benthic Foraminifera in the Oxygen Minima Zone off India's Central West Coast. A total of 128 surface sediment samples [76 grab and 52 core top samples] from the region off Goa in the eastern Arabian Sea were analysed for benthic foraminiferal content up to a depth of 3300 m. There are currently 195 species of benthic foraminifera known. *Bolivina, Cassidulina, Lernella, Uvigerina*, and *Eponides* species were discovered to be the most abundant within the depth zone of 150 to 1500 m - a zone recognised as the Oxygen Minima Zone (OMZ) for the Arabian Sea. The abundance of benthic foraminiferal species in the Arabian Sea OMZ relative to other areas of the worldwide oceans offers some remarkable facts. *Bulimina marginata*, which has been known to be common in other locations of the world seas within the OMZ, accounted for only approximately 2% of the entire seabed foraminifera species in the current area. *Bulimina costata*, on the other hand, built more than 15% of all of the foraminifera, that has not been recorded to be common in any other location of the world's OMZ. This research verifies the presence of the oxygen least zone in the eastern Arabian Sea.

Rajeev Saraswat, Rupal Dubey, Dineshkumar P.K and Rajiv Nigam, 2018 studied about the Dwarf Foraminifera Off the West Coast of Kerala, India: A Reaction to Mudbank Formation. During the rainy season, a mudbank occurs off the shore of Alleppey, Kerala's coastal region. Mudbanks develop in the littoral seas within 15 metres of water depth. It is a small coastal zone with water that is undisturbed by the roughness of monsoon waves. In the mudbank area, the shoreline gets protection from monsoon wave erosion. Besides from the unusual tranquilly, the water column in the mudbank features a significant concentration of suspended sediments. Mudbank describes a peculiar marginal marine habitat with rich fish capture and is a source of income for fishermen in Kerala during the lean fishing season of monsoon. They examined the impact of mudbank formation on benthic foraminiferal morphology. Foraminifera have been identified in surface sediment samples in the area. The maximum diameter/length/width of foraminiferal group found in the mudbank was determined and compared to the type species. All of the present benthic foraminiferal species in the mudbank exhibited a maximum diameter/length/width that was smaller than the type species. Furthermore, foraminiferal quantity in the mudbank was low, which suggests a stressed environment. As a result, we conclude that dwarfism is a unique adaptation of foraminifera to mudbank formation. Thus, the reduced foraminiferal test size can be utilised as a technique for recognising past mudbanks as well as the geographic change of mudbanks.

S.M.Hussain, Merin Marin Maria Joy, A. Rajkumar, N. Mohammed Nishath and Shubhangi T. Fulmali, 2016 conducted studies about the Calcareous Microfauna (FORAMINIFERA AND OSTRACODA) Distribution from the beach sands of Kovalam , Thiruvananthapuram, Kerala South west coast of India. The geographic distribution of Recent calcareous microbes (Foraminifera and Ostracoda) from the Kovalam shoreline in Thiruvananthapuram, Kerala, is investigated in this research. Eleven shoreline sand samples were gathered from three different beaches in Kovalam, all separated by rocky terrain. Standard micropaleontological procedures were used for separating the Foraminifera and Ostracod species from the sediments. Individual species patterns of distribution were studied, and their sediment relationships have been identified for environmental analysis. Foraminiferal taxonomies, the classification proposed by Loeblich and Tappan (1987) was applied in the current study. A total of 24 foraminifera species have been identified, with 14 genera, 10 families, 8 superfamilies, and 3 suborders. CaCO3 along with additional sedimentological parameters, organic matter, and the sand-silt-clay ratio were estimated using established techniques. The ratio of carapaces to open valves is researched, as is predation on foraminiferal tests and ostracod carapaces, and the ecological consequences are examined. Several foraminiferal tests have been broken and abraded, showing the beach's heavy wave action.

Dr.Kurian C V, Antony A, 1979 the present study focuses on the distribution of foraminifera in the estuarine environment and the interstial area of sand beaches on India's south west coast, with the objective of correlating the transportation and level of presence of different kinds with hydrographic conditions and substrate characteristics. The foraminifera of the estuarine environment have been investigated in the Vembanad lake, an enormous estuary on India's south west coast that extends for about 60 km from Cochin Barmouth in the north to Alleppey in the south. For a period of two years (July 1973 to June 1975), fifteen locations were selected throughout the lake's length to collect hydrographic data and grab samples of bottom deposits.

2.3 GRAIN SIZE ANALYSIS

Gloria I. Lopez, 2017 studied about the Grain size analysis is a method of analysis that is widely utilised in the earth sciences and can be carried out as a standard laboratory research. Other disciplines, such as archaeology and geoarchaeology, make extensive use of it. It is a sedimentological investigation conducted to measure the size of the various particles which make up a specific unconsolidated sedimentary deposit, sedimentary rock, archaeological location, or soil unit. The primary purpose of this approach is to deduce the type of environment

and energy related to the transport mechanism at the time of deposition from the sizes and distributions of the particles of sediment analysed. Particle size is directly proportional to the type of environmental setting, carrying agent, length and time of transit, and depositional conditions. The primary objective of geoarchaeological research is to explain earlier natural and anthropogenic issues that occurred within an archaeological environment, either consecutively or intermittently. The environmental history of a site can be recreated from its beginnings using such information. Particle size analysis, as a primary analytical tool, should always be supported by other fundamental analyses that have the ability to improve comprehension of a specific locus or sedimentary unit within the archaeological context. Micropaleontology, as well as isotope and chemical examinations, are examples of such indicators. When numerous analytical laboratory processes are used together, the likelihood of obtaining data valuable in clarifying the depositional context as a whole improves, and the margin of error decreases. Underwater archaeological sites, particularly those near coastlines, are among the more difficult situations in which to recreate the stratigraphic succession of past ecosystems. This is related not just to the submerged situations, but also to the extremely dynamic processes that occur there, such as sea-level variations, powerful hurricanes, catastrophic occurrences such as tsunamis, littoral currents, and sediment movement, among other things. In addition to this, the (ancient) coastline's long and extensive human presence adds to the setting's diversity. Despite this, well-documented reconstructions of the lateral and/or vertical advancement of environments as a result of continuous environmental evolution, sudden natural changes, and man-made buildings can be found along ancient coastlines. Examples from the Mediterranean involve the rebuilding of the now-submerged ancient city and port of Alexandria on the Nile Delta in Egypt (Mostafa et al., 2000), the rebuilding of the harbour extensive of Caesarea Maritima in Israel - the biggest constructed manufactured harbour in the Mediterranean (Reinhardt et al., 2006), and the recognition of the destruction of the prehistoric Palaikastro in Crete following the great Santorini eruption in the Late Bronze Age (Bru).

The maximum amount that fundamental particle sizing technique is sieving. It involves moving the sediment through a succession of stacked sieve meshes with defined opening widths. Each sieve collects the size fraction that is bigger than its mesh size, breaking up the sample into diminishing size fractions. The sediment fraction retained in each filter is weighed to determine its percentage of the whole sample. This method can be utilised in both dry and wet environments. The benefits of sieving include its low cost and ease of usage when dealing

with coarse samples, and the physical separation of the sample as the final product. Its limitations include a poor resolution and accuracy, the difficulty of separating dry particles smaller than 50 m or cohesive materials using this technique, and the fact that results are influenced by the operator and the duration of agitation/shaking used, i.e., the technique itself (Folk, 1980; Krumbein and Sloss, 1963).

Burghard W. Flemming, 2007 studied about, implications for sediment trend analysis of grain-size analysis methodologies and sediment mixing on curve forms and textural characteristics. Deterministic physical models suitable of understanding the evolution of grain-size distributions during transport are still missing today. As a result, many features of particle frequency distributions, particularly curve forms and texture parameters, have been studied for years for possible information on sediment transport patterns and size-sorting processes in a variety of environments. Such approaches are mainly abstract, and so significantly depend on the reliability of the assumptions that underlie them. A factor that has largely gone undetected in this context is the reality that various techniques of grain-size analysis (e. g. sieving, laser intake and diffraction, settling velocity measurements) generate variable curve shapes and thus incongruous textural data when applied to the same sample material. This is demonstrated by a number of cases that demonstrate the differences between sieving and settling findings, the transformation of settling velocities into equivalent settling diameters (psi-phi-transformations), and the consequences of particle shape, particle density, and the temperature of the water. It is shown that particle-size distributions are not only method dependent, but also depending on the afterwards method used. As a result, only frequency curves made using the exact same technique and then processed using the same computations may be properly compared. Furthermore, computing textural parameters from bi- or multimodal size distributions yields incorrect results that are unconnected to the natural processes that contribute to the mixing of distinct size populations. Only decomposing such distributions into individual populations and spatially comparing such populations makes relevance in such instances. Because there is no physical explanation for the production of size distributions, the shape of a grain-size population's curve has no relevance on its own. Only a systematic examination of the progressively changing curve forms (together with associated textural properties) of sediments gathered on a tightly spaced grid may produce data adequate for sediment trend analysis.

Marina Navarro-Pons, Juan J. Muoz-Perez, and Jorge Roman-Sierra, 2013 Grain size is an essential characteristic of sediments and is frequently employed to characterise and

categorise sedimentary facies and habitats. Among the several traditional techniques used to establish grain-size frequency distributions, sieving is the most frequently employed. The accuracy of such assessments is highly dependent on the sieving duration, among other things. Yet, despite extensive research in this sector, suitable sieving periods for various types of sediments have yet to be determined. The effect of sieving duration on grain-size measurements of medium-grained microtidal and mesotidal beach and dune sands is investigated in the present paper. An error analysis was performed for different sieving times (2, 5, 10, 15, and 20 minutes) to measure the precision of essential textural metrics such as median grain size, sorting, skewness, and kurtosis. Significant variations were observed when the sieving time was less than 10 minutes after calibrating the analytical and sampling techniques. Such variations, however, were extremely slight, and grain-size distributions remained almost equal throughout sieving durations of 10 minutes or a longer time, with relative errors as low as 0% in some cases.

John Adams, 1977 studied about, Sieve Size Statistics from Grain Measurement. The examination of grain size in thin section is the most effective way to assess the size statistics of indurated sediments. The current study aims to relate thin section to sieve size statistics and expands on previous research in which the sieve size distribution was determined through sandstone disaggregation. In this study, loose sands with known sieve size distributions were added to produce artificial sandstones that were sectioned for size examination. A total of 72 sand samples were collected, impregnated, and thin sectionally determined. The average size, sorting, and skewness of the sand were altered, grains of various shapes were used, and two distinct types of grain orientation were examined. The study was expanded to include 11 gravel samples measured in cut slabs and 8 sand grain mounts. If all measurements are made in phi units, the empirical results confirm the theoretical premise that mean size measurements for similar samples are related by simple additive constants. Corrections, however, are required to account for differed grain shapes and grain positions, and those have been developed determined empirically. The sieve mean size can be calculated to within 0.3 phi at the 95% level for uniformly oriented grains of average form (B/A axial ratio = 0.7) by adding 0.34 phi to the total grain long axis taken from the thin section. The correlation coefficient among sieve and thin section measurements declines from 0.99 to 0.96 for the standard deviation, skewness, and kurtosis, suggesting that skewness and kurtosis cannot be confidently predicted from thin section measurements. By increasing the thin section statistic by 0.81, the sieve standard deviation can be approximated to within 0.24 phi at the 95% confidence level. Analytic

reasoning suggests that sieve estimations can be computed from thin section statistics using an appropriate equation, but that thin section size distributions cannot be transformed to corresponding sieve distributions in a straightforward manner.

Yu Liu, Xiaodong Zhou, Zhanping You, Biao Ma, Fangyuan Gong), 2019 done Using Sieve Analysis Discrete-Element Models to Determine Aggregate Grain Size. When accurate aggregate morphologies are represented, the grain size of aggregate particles is critical to the mixture gradation of discrete-element (DE) models. The goal of this work was to answer the question of how to quantify aggregate grain size utilising DE models based on virtual sieving analysis. First, virtual sieving analysis models with prolate ellipsoid, oblate ellipsoid, and cubic-shaped particles were created, and virtual sieving was done using three vibration patterns: vertical, horizontal, and hybrid vibration. Based on the virtual sieving analysis results, the influence and efficiency of the vibration patterns were investigated. The virtual sieving analysis was then performed with realistic aggregate forms. The shape sieving factor (Ssf) was generated from the test results and was used to calculate the grain size of individual particles. For additional validation, the grain size (Gs) of selected aggregates was measured manually in the lab and virtually sieved independently. The test results were then analysed and contrasted. The following are the key conclusions of this study: (1) vibration patterns had a significant impact on the virtual sieving analysis results, and vertical vibration is recommended for virtual sieving analysis; (2) particle shapes had a significant impact on the virtual sieving analysis results, and it was determined that aggregates with cubic shapes are relatively difficult to pass through the sieve meshes; (3) Most particles can pass through smaller sieve apertures than their equivalent-volume spheres; (4) the virtual sieving analysis approach developed in this study was validated by lab sieving tests, and the shape sieving factor (Ssf) derived from the virtual sieving analysis can be used to generate DE models with more accurate gradation.

H. Venkates et. Al, 1997 examined about, Textural properties of nearshore sediments off the coast of Honnavar, India's south west coast. Textural features of sediments off the coast of Honnavar, India's south-west coast, revealed that the sediments were mainly clayey in composition. It's skewed, positively skewed, and mesokurtic. The positive skewness of the sediments indicates low energy conditions in the nearshore zone, which promotes the accumulation of fine sediment fractions. Because of the poor sorting, the transportation agencies were unable to separate the sediments into distinct size grades. According to multigroup discrimination analysis, these sediments are of shallow marine origin and are influenced by salinity and differential settling velocities.

Mohan and Rajamanickam (1998) categorised the depositional areas of beaches and beach ridges along a 158-kilometer-long coastal strip extending from north of Pondicherry to Ennore, Tamil Nadu, on India's southeast coast, based on grain size characteristics. Selvaraj (1999) discovered a pale beach at 50 m deep in his research of the shelf sediments off the Kalpakkam coast, where a linear stretch of sand deposit was encountered.

Grain size criteria have been employed to characterise the sediments in the shelf environment (Nittrouer, 1983, 1984); additionally, the distribution and transport processes of the sediments present in the area affect the bottom topography of any current habitat (McCave, 1972). Textural parameter assessments, according to Koldijk (1968), are markers of environmental status since they are environmentally responsive. Because of fast industrial expansion, the estuaries and inner shelf sediments acquire a wide range of toxins, which are eventually concentrated and deposited on and sink the estuary or inner shelf floor.

2.4 CALCIUM CARBONATE ANALYSIS

According to S.M Hussain et.al. 2016, ostracods exist in an environment governed by temperature, bottom topography, depth, salinity, pH, alkalinity, dissolved oxygen, food supply, and substrate and sediment organic matter concentration. A grand total of 24 foraminifera species have been identified, divided into 14 genera, ten families, eight superfamilies, and three suborders. A total of 16 ostracod taxa have been laid out, with 14 genera, 10 families, 3 superfamilies, and 2 suborders. Each taxon's spread pattern was researched, and their sedimentary link was examined for ecologic/environmental research. The nature of the substrate for all 11 samples was assessed to see if it discloses the species supply, organic matter, and calcium carbonate concentration of sediments. The higher CaCO3 value and lower organic matter concentration in Kovalam beach sands support the largest population of Foraminifera and Ostracoda. Sand-silt-clay proportions were investigated, and only sand substrate was seen in this study region. In the above study it is analysed that that the population of Foraminifera is high. A shallow inner shelf to a neritic environment is observed.

Carbonate is a prevalent component of ocean sediments and has been observed to be a substantial indicator of terrigenous matter provenance and transfer in the Gulf of St. Lawrence (Loring and Nota, 1973). The author discovered calcium carbonate in the current study utilising the efficient titration method (Piper, 1947). Since the carbonate determined by this approach contains additional carbonates, such as magnesium, which is inconsequential, the total carbonate is referred to as calcium carbonate in the current study.

CHAPTER 3

METHODOLOGY

3.1 METHODOLOGY

3.1.1 FIELD WORK

A field study along the Vanchipura Beach (N 10.320317 and E 76.120466) in Kerala was conducted to examine the various characteristics of Foraminifera distribution. A total of one core sample and nineteen grab samples were collected from the beach in the month of May 2023. The core sample were collected by using a PVC pipe and the Grab sample by the scoup. The core sample depth is about 57 cm. Standard micropalaeontological techniques were used to separate the foraminifera taxa from the sediments. Aside from the taxonomy of the various species, stereo-binocular microscopy was used to closely examine their particular morphological and micro-structural characteristics. The taxonomy and systematic investigation were handled with the help of the Foraminifera treatise by Loeblich and Tappan, 1988, as well as other present publications. Individual taxon distribution patterns were studied, and their sediment relationships were determined for ecologic/environmental interpretation. The Krumbein and Pettijohn (1938) approach was used to estimate the sand-silt-clay ratio. The aim of the field work to analysis about the variations in the sand size and to analysis about the microfossil present in this region. Almost a day from morning to evening was taken to collect the samples, the grab sample that are collected by the scoup were put into a zip lock cover's.

The samples were collected from almost several location and from the first location we took the core sample by using the PVC pipe about 57 cm depth was taken. After the first location there were about a100 m gap to every location similarly grab samples were collected. The collected sample were brought to the lab and balance work were taken place there.

3.1.2 LABORTARY METHOD

3.1.2.1 Core Sample

The core sample that is collected is been cut into 3 cm each from the equal halves and the sample of core is about 19 small samples. These are transferred to the small zip lock covers. About 50 gm of sample weighted and washed through 230 mesh (63m opening) wet sieve using hand sprayer using light mist of water to remove fine mud (which include silt and clay) particles and avoid shell fracture. A light rubbing of small lumbs by hand is sometimes useful. The

samples were then placed in the oven at 50 degrees Celsius. The dried residue is placed on a picking tray for examination with a stereoscopic binocular microscope. The dried residue is placed on a picking tray for examination with a stereoscopic binocular microscope. The samples are mostly quartz, with a few heavy minerals and shell fragments. Only few microfossils of foraminifera were obtained.

Fig No.1 Showing the Core sample collected from the Vanchipura Beach

3.1.2.1 Grab Sample

The grab sample is been collected and 50 gm of sample is weighted and kept in oven overnight not more than 50 degree celsius. The dried samples are collected on the tray and small amount is taken in the picking tray and analysed in the stereoscopic binocular microscope. Unfortunately, no microfossils were discovered in these samples. Only several

quartz and small grain minerals were found. The procedure of the grab sample were same as the core sample.

3.1.3 DETERMINATION OF CALICUM CARBONATE

3.1.3.1 Procedure

The determination of calcium carbonate content in the sample is done by taking 5 gm of core sample and 10 gm of grab sample and these sample is collected to 250 ml beaker. The sample that is taken must be dried one. Take 87 ml of concentrated HCL and make up in to 1000 ml standard flask. The samples are placed in the beakers and to every samples 100 ml of HCl is poured. Then stir the sample with a glass rod and the process should be continued with 15 minutes of interval for 1 hour. After 1 hour place the sample solution without any shaking. 40 gm of NaOH is prepared and make up it into 1000 ml standard flask. The solution is poured into the Burette and the sample solution is taken by pipette (20ml) into a conical flask. The 20 ml sample solution is taken in the conical flask along with the bromothymol blue indicator about 6 to 8 drops. Then the titration is taken place along with NaOH. The hue of the indicator may fade when the end point blue - is near in some examples.

Fig No.2 Showing Calcium Carbonate analysis

More indicator is added in such situations, and the titration is finished. The following calculation calculates the proportion of calcium carbonate: Calcium carbonate percentage = (Blank titration - actual titration) × weight of sample. To determine the titre value of hydrochloric acid, a blank titration is performed.

Fig No.3 Showing samples with calcium carbonate

Fig No.4 Showing sample with peacock blue colour

3.1.4 DETERMINATION OF SAND SILT CLAY PERCENTAGE

Marine shallow sea sediments are typically composite types composed up of grains ranging in size from sand to clay in various combinations. In general, however, particle size decreases as depth increases.

3.1.4.1 Procedure

The samples are taken and dried in the oven for overnight, it is made sure that the moisture content in the sample is gone. The sample is washed in the 230 mesh sieve (0.063 mm) till we get a clear water. The washing is done clearly and the washed water is been poured to a cylindrical flask of 1000 ml. The sample retained on the sieve is dried and weighed to determine the weight of the sand fraction. Then 1000 ml in the cylindrical flask is stirred for some seconds, The stirring is done for the uniform mixing of particles. The time is recorded as soon as the movement is stopped, and exactly 2 hours and 3 minutes later, a 20 ml pipette is carefully inserted up to a depth of 10 cm into the solution and the sample is removed with uniform force to avoid turbulence. The sample that is taken is poured into a 50 ml beaker and kept in the oven over night in mild condition. The weight of the residue is estimated after complete drying, from which the weight of the clay fraction is computed. Subtracting the combined weight of the sand and clay fractions from the known sample weight yields the weight of the silt fraction.

Fig No.5 Showing the sieve analysis

3.1.5 STUDY AREA

Kerala is a state on the country's southwest coast. Its geology is diversified and has been sculpted by a variety of geological processes that have happened over millions of years. Kerala's geology includes a diverse spectrum of rock formations, including old crystalline rocks, sedimentary rocks, and coastal deposits. The western half of the state is mostly made up of ancient Precambrian crystalline rocks, which are among the oldest rocks on the planet. These rocks were created deep within the Earth's crust by extreme heat and pressure. The Western Ghats, a UNESCO World Heritage site, comprise Kerala's eastern border. This mountain range is a prominent geological structure consists of complicated rock formations such as gneisses, schists, and granites. The Western Ghats have shaped Kerala's landscape and climate. Coastal plains in Kerala's western region is distinguished by a thin stretch of coastal lowlands. Alluvial deposits, which are sediments deposited by rivers and streams over time, make up these plains. Because to its proximity to the Arabian Sea, the coastal region is also influenced by marine processes such erosion and deposition. Kerala also has various sedimentary basins, including the Cauvery Basin and the Warkali Basin. These basins contain sedimentary rocks such as sandstones, shales, and limestone that formed over millions of years as sediments accumulated in ancient oceans and river systems. Fossils and Paleoenvironments. The sedimentary rocks of Kerala frequently include fossils of ancient species, which provide vital insights into the state's previous ecosystems and the history of life on Earth. Kerala is known for its mineral resources, which include important amounts of ilmenite, monazite, and thorium-bearing minerals found in coastal sands.

Vanchipura Beach is located in the state of Kerala in southwestern India. The area's geological history stretches back to the Pre-Cambrian era, which lasted from around 4.6 billion years ago to approximately 542 million years ago. Vanchipura Beach's rocks are mostly granitic gneiss, a kind of metamorphic rock created by the transformation of pre-existing igneous or sedimentary rocks under high pressure and temperature conditions. Vanchipura Beach's granitic gneiss is thought to have originated 2.5 billion years ago during the Archean epoch. Over millions of years, the rocks at Vanchipura Beach have been subjected to numerous geological processes such as weathering, erosion, and sedimentation, which have contributed to the unique rock formations seen today. The action of the waves and weather has shaped the rocks, resulting in the construction of intriguing features such as caverns, arches, and pillars. The rocks' reddish-brown colour. This is due to the occurrence of iron oxide minerals such as

hematite and magnetite at Vanchipura Beach. These minerals originated as a result of the original rock's weathering and a change.

Fig No.6 Showing images taken from the field area Vanchipura Beach

Fig No. 7 Showing images taken from the field area Vanchipura Beach

Fig No.8 Showing images taken from the field area Vanchipura Beach

Fig No.9 Showing images taken from the field area Vanchipura Beach

Table No.1 Showing the sample location of the study area

LOCATION	LATITUDE	LONGITUDE
VANCHIPURA BEACH	N 10.3203	E 76.1205
L1	N10.3200	E76.1200
L2	N10.3213	E76.1197
L3	N10.3222	E76.1194
L4	N10.3230	E76.1191
L5	N10.3238	E76.1188
L6	N10.3250	E76.1186
L7	N10.3258	E76.1183
L8	N10.3263	E76.1180
L9	N10.3272	E76.1177
L10	N10.3280	E76.1175
L11	N10.3288	E76.1172
L12	N10.3297	E76.1166
L13	N10.3305	E76.1163
L14	N10.3313	E76.1161
L15	N10.3322	E76.1158
L16	N10.3309	E76.1156
L17	N10.3323	E76.1157
L18	N10.3337	E76.1153
L19	N10.3339	E76.1151

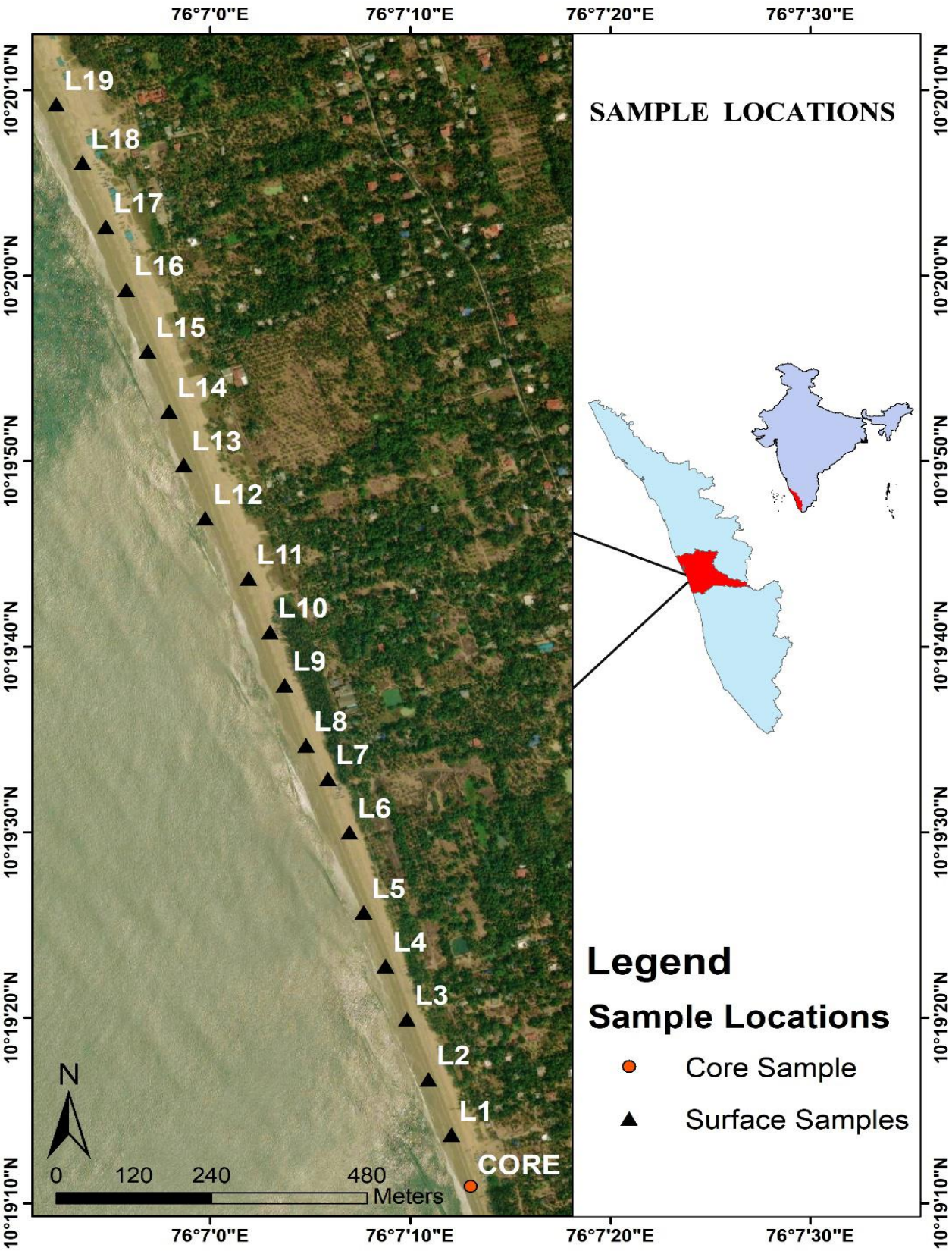

Fig No.10 Showing the sample location of the field

CHAPTER 4

RESULT AND DISCUSSION

4.1 SYSTEMATIC PALEONTOLOGY

4.1.1 CLASSIFICATION

In the following pages we discuss about the 15 foraminiferal species belonging to various genera, the core sample consist of 15 species were as the surface sample consist of 7 foraminiferal species.

Table No.2 Checklist of species in surface sample

1) *Textularia sp*
2) *Quinqueloculina lamarckiana d' Orbigny*
3) *Ammonia beccarii (Linnè)*
4) *Elphidium advenum (Cushman)*
5) *Elphidium crispum (Linnè)*
6) *Elphidium discoidale (d' Orbigny)*
7) *Elphidium norvanghi Buzas*

Table No.3 Checklist of species in the core sample

1) *Trochammina macrescens* (Brady, 1870)
2) *Textularia foliacea Heron – Allen & Earland*
3) *Spiroloculina bicostst d' Orbigny*
4) *Quinqueloculina lamarckiana d' Orbigny*
5) *Quinqueloculina bicostata d' Orbigny*
6) *Sorites orbiculus (Forskal)*
7) *Planorbulinella larvata (Parker and Jones)*
8) *Ammonia beccarii (Linnè)*
9) *Cribronoion simplex (Cushmam)*
10) *Elphidium advenum (Cushman)*
11) *Elphidium crispum (Linnè)*

12) *Elphidium discoidale (d' Orbigny)*

13) *Elphidium norvangi Buzas*

14) *Peneroplis proteus D' Orbigny, 1839*

15) *Parrellina hispidula (Cushman)*

4.2 TOTAL POPULATION OF FORAMINIFERA IN SURFACE SAMPLES AND CORE SAMPLES

In order to study the distribution of Foraminifera and the micro paleontological implication 19 surface samples and one core sample were collected from the Vanchipura Beach in Kerala. The population of foraminifera in all surface samples ranges from 65 to 76, and a total of 1268 individuals per 100g of wet sediments. The samples from location 14 contain maximum number Foraminifera, followed by samples from station 9,17. The foraminiferal population is equal at the 7,10,15 locations. The minimum number of species are from 8,19,12 station samples.

There are seven different specimens recognised from all the surface samples.In case of abundance, the species *Ammonia beccarii*, with a total population of 350, was found in all samples, followed by *Elphidium advenum* , with a total population of 230, and *Textularia* sp. with a total population of 173. The least abundant species is *Elphidium norvangi* with total population of 124. The total distribution in each sample shown in Table No. 4 and Fig No.11.

The foraminifera population in the core sample ranged from 75 to 91, with a total of 1558 specimens per 50 g of dried sediments. The core sample was divided into 19 sub- samples, each of which were analysed for additional analysis. At the depth of 54-57 cm, it shows good percentage of foraminifera. The other abundant locations are show. A total of 15 distinct species were detected in the core sample. When it comes to species distribution, *Ammonia beccarii* was discovered in all samples with a total population of 303, followed by *Elphidium advenum* with 255 and *Elphidium discoidale* with 232, *Sorites orbiculus* and *Trochammina macrescens*. The minimum population of foraminifera occur in 7,8 depths respectively. The total distribution of sample population is shown in Table No. 5.

In the study area, the species shows different salinity index.Different species can survive in different salinity. The genus like *Ammonia* and *Elphidium* mainly thrive at polyhaine to oligohaline zone and the genus *Spiroloculina, Sorites* shows hypersaline to mesohaline

environment which indicate the influx of fresh water and rain water runoff throughout the core varies and directly effecting the salinity index. Same time their morphological differences also noticeable in the study area. In the surface samples, angular forms are very less compare to rounded forms and the same trend is seen in the core sample also ie, angular forms were more abundant near the sea showing an reverse relation between angular morpho groups and river discharge. Several forms got deformed and shows colour variation in their shell due to the deposition of several minerals from the surroundings. This feature implies that shells undergone contamination.

SPECIES	**1**	**2**	**3**	**4**	**5**	**6**	**7**	**8**	**9**	**10**	**11**	**12**	**13**	**14**	**15**	**16**	**17**	**18**	**19**	**TOTAL**
Textularia sp.	10	8	9	10	8	7	9	10	9	9	9	7	8	9	9	10	10	11	11	173
Quinqueloculina lamarckiana d'Orbigny	9	9	8	10	11	9	9	9	10	9	9	7	8	9	9	9	9	9	9	171
Ammonia beccarii (Linné)	17	17	18	20	17	18	20	19	19	18	18	19	19	19	18	19	19	18	18	350
Elphidium advenum (Cushman)	12	12	11	12	12	11	11	11	11	12	11	11	12	14	13	13	14	13	14	230
Elphidium crispum (Linné)	9	8	8	7	8	7	8	9	10	9	8	9	10	9	8	8	8	9	9	161
Elphidium discoidale (d'Orbigny	7	9	7	7	9	8	7	7	7	7	6	6	6	9	9	7	8	6	9	141

Elphidium norvangi Buzas	6	5	6	7	4	7	8	6	9	8	6	7	5	7	6	7	6	7	7	124
TOTAL	70	68	67	73	71	67	72	65	75	72	67	66	68	76	72	73	74	73	66	1268

Table No.4 Shows the total population of Foraminifera in each surface samples

SPECIES	SAMPLE NUMBER																			
	1	2	3	4	5	6	7	8	9	10	11	12	13	14	15	16	17	18	19	total
Trochammina macrescens (Brady, 1870)	1	1	0	0	0	0	0	0	0	1	0	0	1	1	1	0	0	1	1	8
Textularia foliacea Heron- Allen & Earland	8	8	9	6	8	8	8	9	8	8	8	9	10	9	8	8	8	9	9	158
Spiroloculina affixa Terquem	1	2	1	1	2	2	1	1	1	0	0	0	0	0	0	0	0	0	1	13
Quinqueloculina lamarckiana d'Orbigny	6	7	9	8	10	9	9	9	9	7	8	9	9	9	9	9	9	9	9	163
Quinqueloculina bicostata d'Orbigny	8	8	9	8	7	9	9	9	9	9	9	9	8	8	8	8	8	8	8	159
Sorites orbiculus(Forskal)	2	0	0	0	1	0	0	1	1	1	1	0	0	0	0	0	0	0	0	7
Planorbulinella larvata (Parker and Jones)	1	1	1	1	1	1		1	1	1	1	0	0	0	0	0	1	1	1	13
Ammonia beccarii (Linné)	15	13	17	14	13	17	17	17	16	17	16	16	16	16	16	16	17	16	18	303
Cribrononion simplex (Cushman)	2	3	2	2	1	2	1	1	1	1	1	0	0	0	0	0	0	0	0	17
Elphidium advenum (Cushman)	12	13	12	12	13	14	12	14	13	12	14	13	14	14	15	14	14	15	16	255

Elphidium crispum (Linné)	10	9	9	9	9	9	9	6	8	9	10	9	7	8	7	8	10	9	10	165
Elphidium discoidale (d'Orbigny	9	8	9	8	6	7	8	9	5	7	9	8	9	7	9	8	9	8	9	232
Elphidium norvangi Buzas	6	5	6	5	7	6	8	9	7	9	7	6	8	9	8	9	8	7	9	139
Peneroplis proteus D'Orbigny, 1839	2	1	1	1	0	0	0	0	0	0	0	1	1	1	1	1	1	0	0	11
Parrellina hispidula (Cushman)	2	0	0	0	0	2	2	2	1	1	1	0	0	0	0	0	0	0	0	12
TOTAL	85	81	85	75	78	86	75	88	80	82	76	80	83	82	82	81	85	83	91	1558

Table No.5 Showing the total population of foraminifera in the core sample

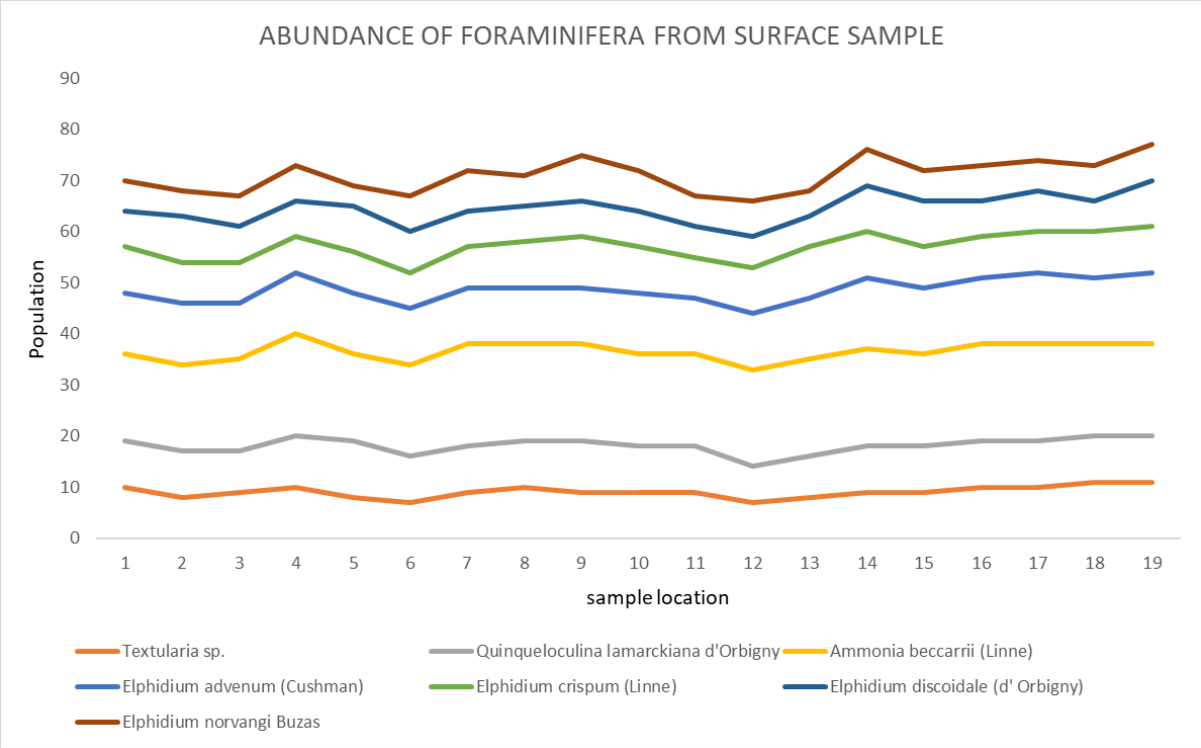

Fig No.11 Showing the total population of foraminifera in surface sample

4.3 SEDIMENT CHARACTERSTICS

Puri (1966) stated that the foraminifers exist in an environment influenced by temperature, bottom topography, depth, salinity, pH, alkalinity, dissolved oxygen, food supply, and substrate and sediment CaCO3 content. To determine if the calcium carbonate concentrations of the sediments and the type of the substrate reflect the number of foraminifera in them, sediment samples from Vanchipura beach were collected.

4.3.1 CALICUM CARBONATE

The main source of carbonate is the shells and shattered shell fragments of creatures and mollusks, as well as dilution of biogenic calcite by detrital material in the sediments. A similar kind of analysis was done by Sebastian et al. (1990), in their study on sediments of Mahe estuary, West coast of India. In the present study of CaCo3 percentage in the sediments of Vanchipura beach ranges from 0% to 3.25%. The lowest values were found in samples 8,16,17, while the highest values were found in samples 2,10,19. It is assumed that the calcium carbonate content of the area is one of the main characteristics that influence the foraminifera population, specifically its geographical distribution. Calcium carbonate content is often found

to be proportional to population size. The percentage of calcium carbonate is shown in Fig. No.12.

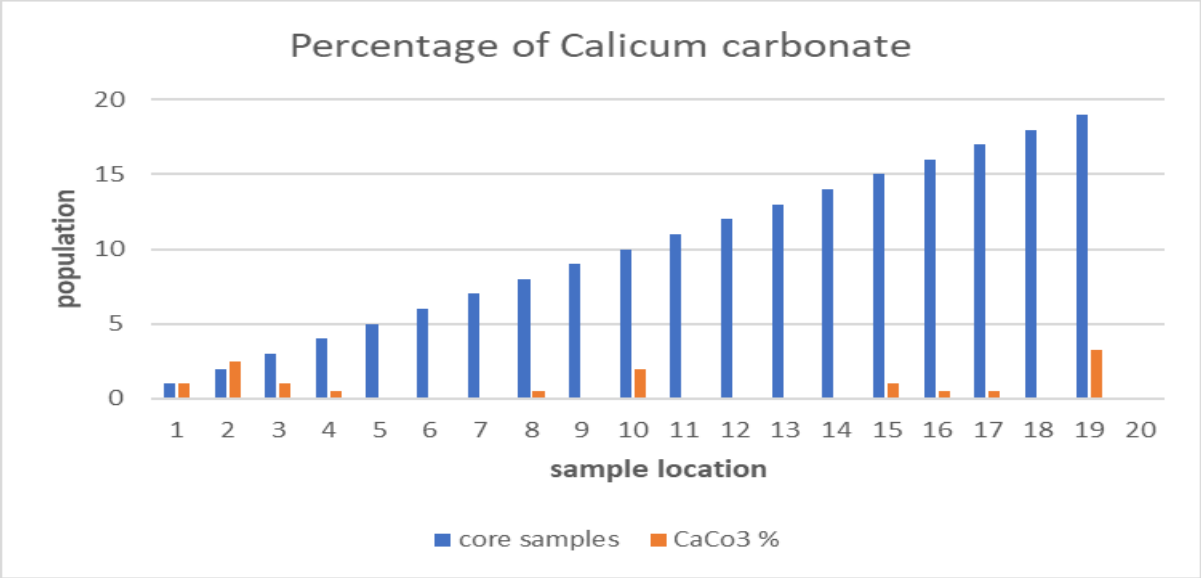

Fig. No.12 Showing percentage of calcium carbonate in samples

4.3.2. SUBSTRATE AND FORAMINIFERA POPULATIONS

According to Puri (1966), the characteristics of bottom sediments, such as particle size, sorting coefficient, and the presence or lack of bottom vegetation, influence the distribution of ostracods and foraminifers. The clay size particles tend to have more organic content in it than others. The clay composition of the sediment is thought to be a significant role in the distribution and quantity of benthonic organism Buzas (1966). The clay and silt content for the sediments may be too small about 2% or less than that.

In the Vanchipura Beach, the samples show various sand silt clay ratio. Among which the ratio varies from 79.3% to 94.3% in case of sand, 0.0075% to 0.0175% in case of clay and 5.687% to 20.685% in case of silt respectively. (Table No.6). The trilinear diagram of sand silt clay ratio of the core sample is shown in the (Fig No.13)

In the surface sample the sand silt clay ratio varies in sand by 71.46% to 98.15%, clay by 0.005% to 1.38% and the silt by 1.842% to28.517%. The table representing the percentage of sand silt clay ratio is given below (Table No.7) and the Trilinear diagram of sand silt clay ratio of the surface sample is shown (Fig No.14). In these areas the sediment type is observed as Sandy substrate only. From the above observations, it may be inferred that the most favourable sediment type for the population abundance is sand.

CORE SAMPLE NO	SAND %	CLAY %	SILT %	CaCO3 %
1	94.3%	0.0125%	5.687%	1%
2	88.64%	0.015%	11.345%	2.5%
3	90.16%	0.0125%	9.827%	1%
10	82.7%	0.0125%	17.287%	2%
11	80.32%	0.0175%	19.662%	0%
12	81.52%	0.0125%	18.467%	0%
17	79.3%	0.015%	20.685%	0.5%
18	79.5%	0.0075%	20.492%	0.5%
19	84.56%	0.025%	15.415%	3.25%
MAXIMUM	94.3%	0.0175%	20.685%	3.25%
MINIMUM	79.3%	0.0075%	5.687%	0%

Table No. 6 Showing sediments characteristics of Vanchipura Beach (Core sample)

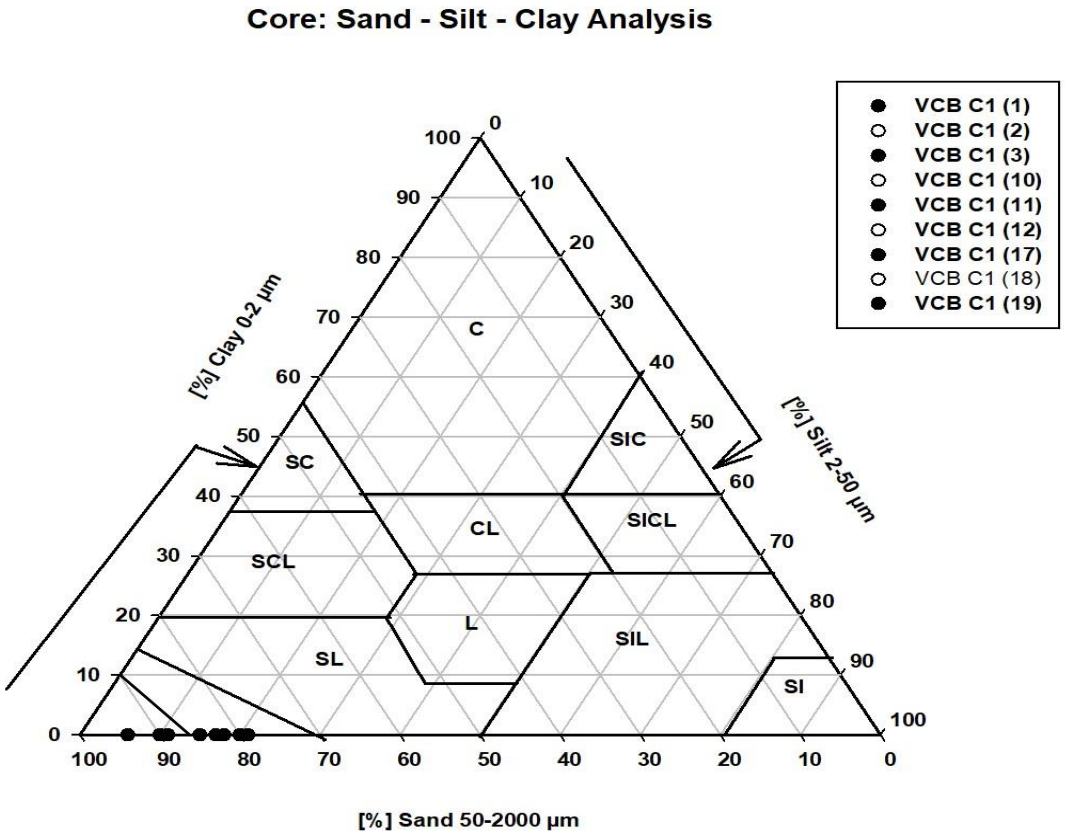

Fig No.13 Representing the sand silt clay ratio of core sample

SURFACE SAMPLE NO	SAND PERCENTAGE	CLAY PERCENTAGE	SILT PERCENTAGE
S1	96.84%	0.062%	3.097%
S2	98.15%	0.007%	1.842%
S3	96.58%	0.157%	3.262%
S10	80.57%	1.38%	18.05%
S11	81.71%	0.005%	18.285%
S12	81.8%	0.375%	18.162%
S17	71.46%	0.022%	28.517%
S18	75.93%	0.11%	23.96%
S19	76.94%	0.067%	22.992%
MAXIMUM	98.15%	1.38%	28.517%
MINIMUM	71.46%	0.005%	1.842%

Table No .7 Showing the sediments characteristics in Vanchipura beach (Surface sample)

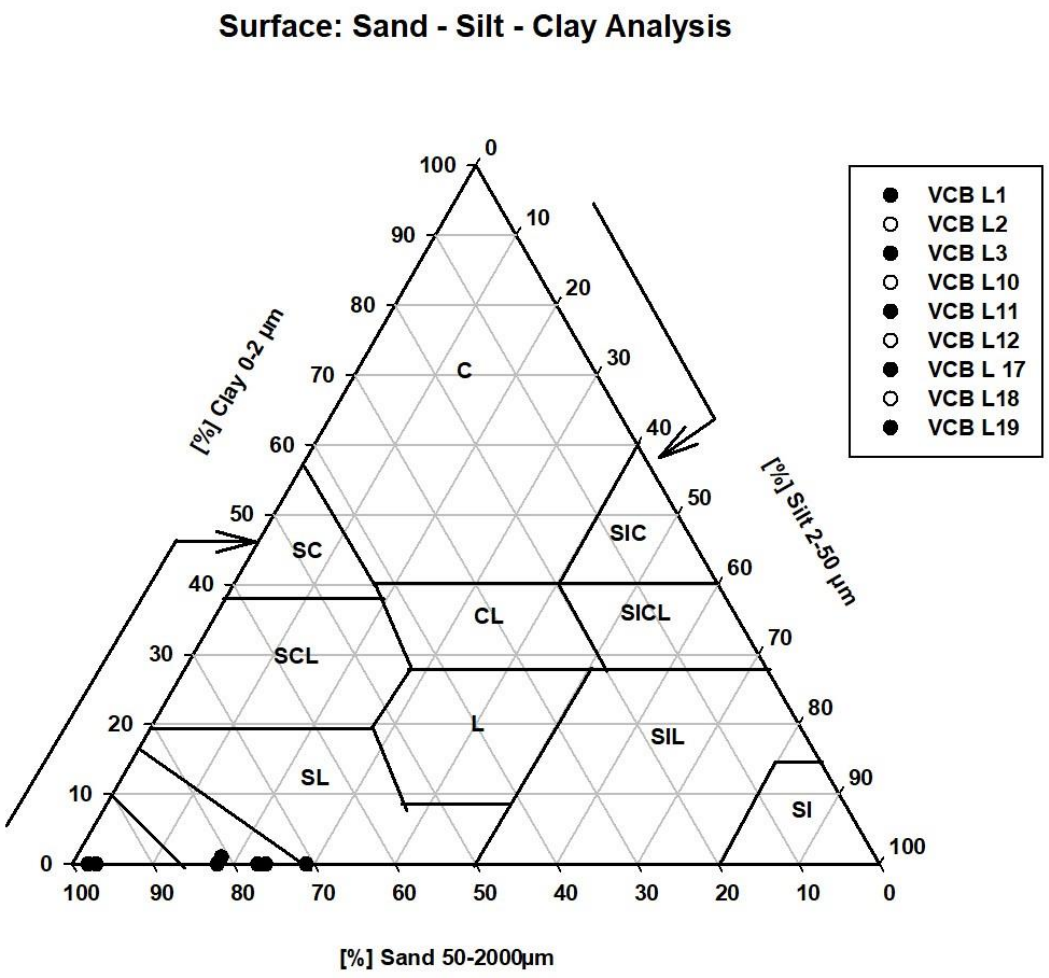

Fig No.14 Representing the sand silt clay ratio of surface sample

CHAPTER 5

CONCLUSION

Marine and brackish water microfossils have a high practical relevance due to their small size, vast geographical range, extremely prolific occurrence, and sensitivity in sediments of all ages and in nearly all situations. As an outcome, even a little sand sample will obviously provide considerable data for quantitative techniques of investigation. Microfossils, particularly Foraminifera, have been demonstrated to be exceedingly useful in ecological and paleoecological applications. Foraminifers, which are essentially marine unicellular protists with a hard calcium carbonate covering known as test, have been widely used in paleoclimatic reconstruction, sediment transport, and other studies. Because of their amazing sensitivity to minute changes in the physicochemical qualities of their surroundings, foraminifers are ideal for such research. They are especially useful for environmental reconstructions and have been used for stratigraphic correlation at various stages.

Formainifera found in the present study area are typical of a shallow, shelf to beach habitat and and core samples. The distorted morphologies and colour diversity in their shells demonstrate the research area's polluted nature, which is caused by the usage of fishing boats. The colour of foraminiferal tests indicates that the sediments were deposited in an oxygenated environment. The diverse species represent distinct salinity indexes ranging from mild to hypersaline. The availability of fresh water flow to the research region is indicated by their physical properties.

The calcium carbonate content in this region is thought to be one of the major characteristics that determine the population of foraminifera, particularly its geographical distribution. In this case, the calcium carbonate concentration is shown to be exactly related to population size. Based on the kind of sediment samples, it is predicted that sediment deposition in the Vanchipura beach occurs under medium to high energy circumstances. It also considers the preservation as well as the damaged, corroded, and very corrosive foraminifera testing.

Based on the findings made in the research region, the faunal assemblage appears to be entirely compatible with deposition under tropical/subtropical shallow water environmental

conditions and on sandy substrates. Furthermore, the forms prefer coarse-grained sediments, whereas the highly calcified and covered forms prefer fine-grained sediments.

REFERENCE

Adams, J. (1977). Sieve size statistics from grain measurement. *The Journal of Geology*, *85*(2), 209-227.

Alve, E. (1995). Benthic foraminiferal responses to estuarine pollution; a review. *The Journal of Foraminiferal Research*, *25*(3), 190-203.

Bhalla, S. N., Khare, N., Shanmukha, D. H., & Henriques, P. J. (2007). Foraminiferal studies in nearshore regions of western coast of India and Laccadives Islands: A review.

Bunt, J. A., Larcombe, P., & Jago, C. F. (1999). Quantifying the response of optical backscatter devices and transmissometers to variations in suspended particulate matter. *Continental shelf research*, *19*(9), 1199-1220.

Buzas, M. A., Hayek, L. A. C., & Culver, S. J. (2007). Community structure of benthic foraminifera in the Gulf of Mexico. *Marine Micropaleontology*, *65*(1-2), 43-53.

Dubey, R., Saraswat, R., Nigam, R., & DineshKumar, P. K. (2018). Dwarf foraminifera off Kerala, India: a response to mudbank formation.

Finger, K. L., Flenniken, M. M., & Lipps, J. H. (2008). Foraminifera used in the construction of Miocene polychaete worm tubes, Monterey Formation, California, USA. *The Journal of Foraminiferal Research*, *38*(4), 277-291.

Flemming, B. W. (2007). The influence of grain-size analysis methods and sediment mixing on curve shapes and textural parameters: implications for sediment trend analysis. *Sedimentary Geology*, *202*(3), 425-435.

Ganugapenta, S., Nadimikeri, J., Ballari, L., Nageshrao, P. T., Tiju, V. I., & Addula, N. R. (2021). Ecological modeling based on benthic foraminifera from Tupilipalem coast, southeast coast of India: Implications for ecological trajectory.

Hussain, S. M., Joy, M. M., Rajkumar, A., Nishath, N. M., & Fulmali, S. T. (2016). Distribution of calcareous microfauna (Foraminifera and Ostracoda) from the beach sands of Kovalam, Thiruvananthapuram, Kerala, Southwest Coast of India. *J Palaeontol Soc Ind*, *61*, 267-272.

Jorissen, F. J. (1987). The distribution of benthic foraminifera in the Adriatic Sea. *Marine Micropaleontology*, *12*, 21-48.

Jorissen, F. J., Barmawidjaja, D. M., Puskaric, S., & Van der Zwaan, G. J. (1992). Vertical distribution of benthic foraminifera in the northern Adriatic Sea: the relation with the organic flux. *Marine Micropaleontology*, *19*(1-2), 131-146.

Liu, Y., Zhou, X., You, Z., Ma, B., & Gong, F. (2019). Determining aggregate grain size using discrete-element models of sieve analysis. *International Journal of Geomechanics*, *19*(4), 04019014.

López, G. I. (2017). Grain size analysis. *Encyclopedia of geoarchaeology*, 341-348.

Mazumder, A., Henriques, P. J., & Nigam, R. (2003). Distribution of benthic foraminifera within oxygen minima zone, off central west coast, India. *Gondwana Geol. Mag*, *6*, 5-10.

Mendes, I., Gonzalez, R. J. M. A. D., Dias, J. M. A., Lobo, F., & Martins, V. (2004). Factors influencing recent benthic foraminifera distribution on the Guadiana shelf (Southwestern Iberia). *Marine Micropaleontology*, *51*(1-2), 171-192.

Minhat, F. I., Ghandhi, S. M., Ahzan, N. S. M., Haq, N. A., Manaf, O. A. R. A., Sabohi, S. M., ... & Abdullah, M. M. (2021). The occurrence and distribution of benthic foraminifera in tropical waters along the Strait of Malacca. *Frontiers in Marine Science*, *8*, 647531.

Mohan, P. M., & Rajamanickam, G. V. (1998). Depositional environments: inferred from grain size along the coast of Tamil Nadu. *Geological Society of India*, *52*(1), 95-102.

Nigam, R. A. J. I. V. (2005). Addressing environmental issues through foraminifera–case studies from the Arabian Sea. *Journal of the Palaeontological Society of India*, *50*(2), 25-36.

Nigam, R., & Thiede, J. (1983). Recent foraminifers from the inner shelf of the central West Coast, India: A reappraisal using factor analysis. *Proceedings of the Indian Academy of Sciences-Earth and Planetary Sciences*, *92*, 121-128.

Nigam, R., Saraswat, R., & Kurtarkar, S. R. (2006). Laboratory experiment to study the effect of salinity variations on benthic foraminiferal species-Pararotalia nipponica (Asano). *J. Geol. Soc. India*, *67*, 41-46.

Prabhu, H. V., Hariharan, V., Katti, R. J., & Narayana, A. C. (1997). Textural characteristics of nearshore sediments off Honnavar, south west coast of India.

Radhakrishnan, K., Hussain, S. M., Sivapriya, V., Rajkumar, A., Nazeer, M. N., & AKRAM, N. (2022). Distribution of recent Ostracoda from the sediments of Gulf of Mannar, Tamil Nadu, southeast coast of India. *Journal of the Palaeontological Society of India*, *67*(1), 229-236.

Rao, K. K., & Rao, T. S. (1979). Studies on pollution ecology of foraminifera of the Trivandrum coast.

Saraswat, R., Kouthanker, M., Kurtarkar, S. R., Nigam, R., Naqvi, S. W. A., & Linshy, V. N. (2015). Effect of salinity induced pH/alkalinity changes on benthic foraminifera: A laboratory culture experiment. *Estuarine, Coastal and Shelf Science*, *153*, 96-107.

Setty, M. G., & Nigam, R. (1982). Foraminiferal assemblages and organic carbon relationship in benthic marine ecosystem of western Indian continental shelf.

Sreenivasulu, G., Praseetha, B. S., Daud, N. R., Varghese, T. I., Prakash, T. N., & Jayaraju, N. (2019). Benthic foraminifera as potential ecological proxies for environmental monitoring in coastal regions: A study on the Beypore estuary, Southwest coast of India. *Marine pollution bulletin*, *138*, 341-351.

Suokhrie, T., Saalim, S. M., Saraswat, R., & Nigam, R. (2018). Indian monsoon variability in the last 2000 years as inferred from benthic foraminifera. *Quaternary International*, *479*, 128-140.

Suokhrie, T., Saraswat, R., Nigam, R., Kathal, P., & Talib, A. (2017). Foraminifera as bio-indicators of pollution: a review of research over the last decade. *Micropaleontology and its Applications.-Scientific Publishers (India)*, 265-284.

Yanko, V., Kronfeld, J., & Flexer, A. (1994). Response of benthic foraminifera to various pollution sources: implications for pollution monitoring. *Journal of Foraminiferal Research*, *24*(1), 1-17.

GEOCHEMICAL STUDIES ON SILICICLASTIC FORMATIONS OF THE PROTEROZOIC KALADGI SUPERGROUP, KARNATAKA

Dissertation submitted to Christ College (Autonomous), Irinjalakuda, Kerala,
University of Calicut in partial fulfillment of the degree of
Master of Science in Applied Geology

By,

VARSHA KRISHNAN

Reg No. CCAVMAG015

2021-2023

DEPARTMENT OF GEOLOGY AND ENVIRONMENTAL SCIENCE
CHRIST COLLEGE (AUTONOMOUS), IRINJALAKUDA, KERALA 680125
(Affiliated to University of Calicut and re-accredited with by NAAC with A++)

JULY 2023

GEOCHEMICAL STUDIES ON SILICICLASTIC FORMATIONS OF THE PROTEROZOIC KALADGI SUPERGROUP, KARNATAKA

Dissertation submitted to National Centre For Earth Science Studies, Akkulam
Thiruvananthapuram in partial fulfillment of the degree of
Master of Science in Applied Geology

By,

VARSHA KRISHNAN

Reg No. CCAVMAG015

2021-2023

DEPARTMENT OF GEOLOGY AND ENVIRONMENTAL SCIENCE
CHRIST COLLEGE (AUTONOMOUS), IRINJALAKUDA, KERALA 680125
(Affiliated to University of Calicut and re-accredited with by NAAC with A++)

JULY2023

CERTIFICATE

This is to certify that the dissertation entitled **" GEOCHEMICAL STUDIES ON SILICICLASTIC FORMATION OF THE PROTEROZOIC KALADGI SUPERGROUP, KARNATAKA"** is a bonafide record of work done by Ms. VARSHA KRISHNAN (Reg. No. CCAVMAG015), M.sc. Applied Geology, Christ College (Autonomous) Irinjalakuda under my guidance in partial fulfillment of requirements for the degree of Master Science in Applied Geology during the academic year 2021-2023.

Dr. Linto Alappat
Dean of Research and Development of TLC
Internal Supervisor

Dr. Anto Francis
Coordinator Geology (S)
Christ College (Autonomous) Irinjalakuda

Place:.....

Date:.....

External Examiners;

1. ……

2. …….

DECLARATION

I **Varsha Krishnan** hereby declare that this dissertation titled "**GEOCHEMICAL STUDIES ON SILICICLASTIC FORMATIONS OF THE PROTEROZOIC KALADGI SUPERGROUP, KARNATAKA**" is an original and authentic work carried out by me under the guidance of Dr. Linto Alappat, Christ College Irinjalakuda and Dr. Bivin G. George, NCESS, Thiruvananthapuram. The research was conducted as a partial fulfillment of the requirements for the degree of Msc. Applied Geology. It has not formed the basis for the award of any other degree or diploma, in this or any other Institution or University. I further declare that the sources of information, data, and materials used in this project have been duly acknowledged and referenced. Any contributions from other researchers or authors have been properly cited. I maintain that if any part of the report is found to be plagiarized, I shall take the full responsibility for it.

Place: Thiruvananthapuram VARSHA KRISHNAN

Date: Reg No. CCAVMAG015

ACKNOWLEDGEMENTS

I would like to express my heartfelt gratitude to all those who have contributed to the succession completion of my dissertation.

I am deeply indebted to my supervisor **Dr. Bivin Geo George**, Scientist B, SERG, National Centre for Earth Science Studies, Thiruvananthapuram and **Dr. Linto Alappat**, Dean of Research and Development of TLC (Former HOD), Department of Geology and Environmental Science, Christ College Autonomous, Irinjalakuda**,** for their supervision, support, and valuable guidance throughout the completion of dissertation work, their expertise and encouragement played a pivotal role in shaping the direction and scope of my research. I convey my sincere sense of gratitude to **Dr. Tomson J Kallukalam**, Scientist E & Group Head, SERG, NCESS for permitting me to do my dissertation work and use the facilities of the institution. I express my gratitude to **Prof. Jyotiranjan S Ray**, Director, NCESS for accepting my request for dissertation work at NCESS.

I am thankful to **Mr. Nishanth N**, Scientific Assistant, Grade B and **Mrs. Lakshmi G**, Scientific Assistant, Grade A for their valuable support in the preparation and analysis work. I would like to extend my thanks to **Ms. Haripriya J**, Research Scholar, NCESS for her support during the course of this work. I also like to thank all the staff members of NCESS for their support during this project. My sincere gratitude to **Dr. Anto Francis K Co-ordinator** , Department of Geology and Environmental Science, Christ College (Autonomous) Irinjalakuda and **Mr. Tharun R.** Head of Department of Geology and Environmental Science, Christ College (Autonomous) along with all my teachers and staff members of the Department of Geology and Environmental Science, Christ College Autonomous, Irnjalakuda for their encouragement and help.

Last but not the least, I would like to thank my family and friends for supporting me and for being by my side in all ups and downs. I ascribe millions of gratitude to the almighty for the abundant blessing which is poured up on me.

VARSHA KRISHNAN

ABSTRACT

The Kaladgi Basin which is situated in Karnataka stands a notable geological landmark distinguished by its diverse assortment of sediment configuration, rock classification and mineral reserves. Over millions of years the basin underwent a series of tectonic activity and environmental conditions that played an important role to mold the basin into its present form. The Proterozoic Kaladgi Supergroup in Karnataka, India, put forward a significant geological setting to elucidate Earth's ancient sedimentary processes. This study presents a comprehensive geochemical investigation focused on the siliciclastic formations within the Kaladgi Supergroup. The objective of the study was to classify the Kaladgi siliciclastic rocks using their major oxide, understand the weathering intensity of the source area and to decode the provenance of the sediments.Through the laboratory analysis this study go through the detailing of siliciclastic rocks, by techniques such as X-ray diffraction (XRD) and X-ray fluorescence (XRF) spectroscopy. The findings of the geochemical analysis and interpretation reveals environmental conditions during deposition, as well as the tectonic setting and climatic influence that mold the formation of the Kaladgi Supergroup. Geochemical Indices including Chemical Index Alteration(CIA) and Chemical Index of Weathering (CIW), suggest the degree of alteration and weathering throughout deposition. These help to contribute to the palaeoenvironmental conditions during the sedimentation process.

CONTENTS

List of Figures

List of Tables

1. INTRODUCTION

The present exposures of the Purana basins of Peninsular India occupy nearly $1.5*10^5$ km^2 area in the Indian subcontinent, with an equal area being concealed under younger cover or lost to ensuing erosion. The Archean history of Peninsular India is recorded in the five distinct cratonic nuclei, namely Aravalli, Bundhelkand, Bastar, Singhbhum, and Dharwar. And now the Purana basins are representatives of the contemporary geological record from the Indian Peninsula (Kale and Phansalkar, 1991; Miall et al., 2015; Chakraborty et al., 2020). The seven basins are (1) Vindhyan (Aravalli-Bundhelkand Craton), (2) Chhattisgarh, (3) Khariar-Indravati (Bastar Craton), (4) Cuddappah, (5) Bhima, (6) Kaladgi (Dharwar Craton), (7) Pranhita-Godavari (intercratonic between Bastar and Dharwar cratons) basins. The Proterozoic basins of India are significant features which played an important role in the formation and evolution of the Indian Subcontinent. The Proterozoic basins characterized sedimentary rock formations that hold valuable geological history about the region. These basins are distributed throughout the country and recognized by their vast economic importance, mineral reserves and hydrocarbons.

One of the prominent basins in India is the Vindhyan basin located in Central India and it's known for extensive sedimentary rock sequence, which give valuable perception to the depositional environment and palaeoclimate of Proterozoic era. This basin also hosts economical minerals like coal, limestone and bauxite. Another important Proterozoic basin is the Cuddapah Basin, situated in southern India. This basin is renowned for its thick sedimentary rock succession, which includes shales, sandstones, and limestones. The Cuddapah Basin is rich in mineral resources like limestone, barites, and uranium, making it economically significant. The Proterozoic basins of India also include the Bhima Basin, the Pranhita-Godavari Basin, and the Kaladgi Basin, among others. These basins exhibit diverse geological features and hold significant reserves of minerals and hydrocarbons, contributing to India's economic growth and development. Aside from their economic significance, the Proterozoic basins in India play a crucial role in understanding the geological past and tectonic development of the Indian subcontinent. They provide valuable information about the ancient continental structures, sedimentary processes, and climatic conditions that prevailed during the Proterozoic Eon. The

Khariar-Indravati Basin is made up of several isolated outcrops that are dispersed over the Bastar Craton and are collectively known as the Bastar basins (Khariar, Abujhmar, Keskal, Ampani, Sukma, and Indravati) (Ramakrishnan, 1987). Large portions of the Vindhyan Basin, the western and northwestern expansions of the Pranhita-Godavari Basin (PG), and the northward extensions of the Kaladgi and Bhima basins and the Dharwar Craton are all hidden by the Deccan Traps. While the northern limits of Vindhyan Basin are covered by Late Cenozoic Indo-Gangetic alluvium, portions of the PG Basin (along its axis) are buried beneath Gondwana (Late Palaeozoic to Mesozoic) sediments. Beside the Purana basins, Precambrian sedimentary records in India also include; (1) deformed, meta-sedimentary successions hosted in greenstone belts (Bababudan, Chitradurga etc.), fold belts (Aravalli-Delhi Fold Belt) and mobile belts (CITZ, Eastern Ghats) and (2) Paleoproterozoic to early Phanerozoic Lesser Himalayan succession as part of Cenozoic Himalayan orogen, bounded between Main Boundary Thrust (MBT) in the south and Main Central Thrust (MCT) in the north, respectively.

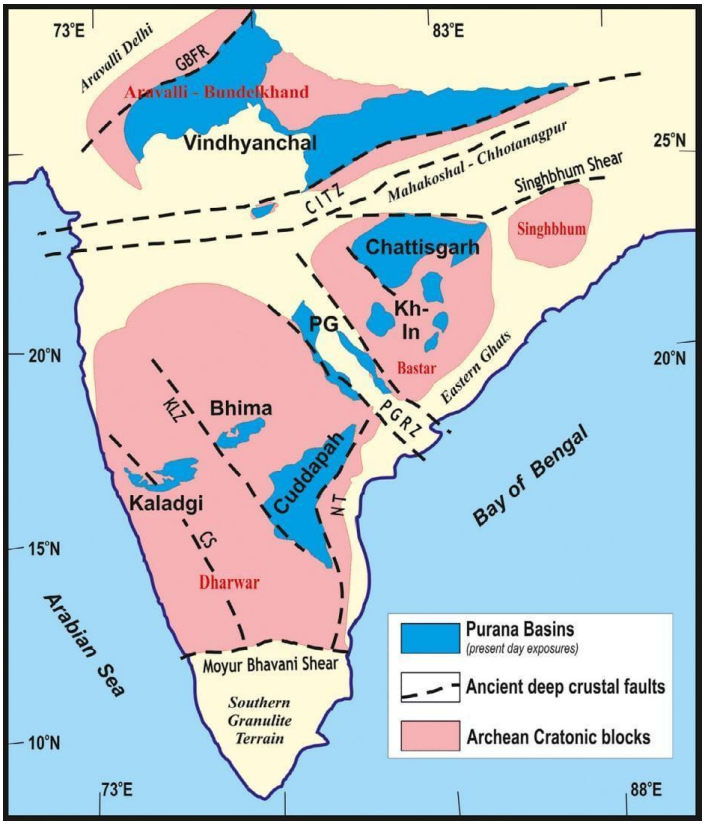

Fig 1: Proterozoic basins in India (modified after Kale and Chakraborty et al., 2021)

1.1 KALADGI BASIN

Kaladgi basin is an E-W trending irregular basin underlain by the basement granitoids (Peninsular Gneiss and Dharwar Batholiths) of the Dharwar Craton in the south and east, and overlain by the Deccan traps in the north. The basin covers an area of 8300 sq.km and is made of an older Kaladgi sequence and younger Badami sequence occurring in separate sub-basinal areas, like the older Cuddappah and young Kurnool sequences in Cuddappah basin. The Kalagdi basin stands out from other Purana basins due to its lack of significant deformation, as it is not closely linked to either mobile belts or terrane boundaries in terms of spatial association. The sedimentary rocks found in the Kaladgi basin include sandstones, shales, and limestones, which were deposited over millions of years in ancient marine, fluvial, and lacustrine environment.

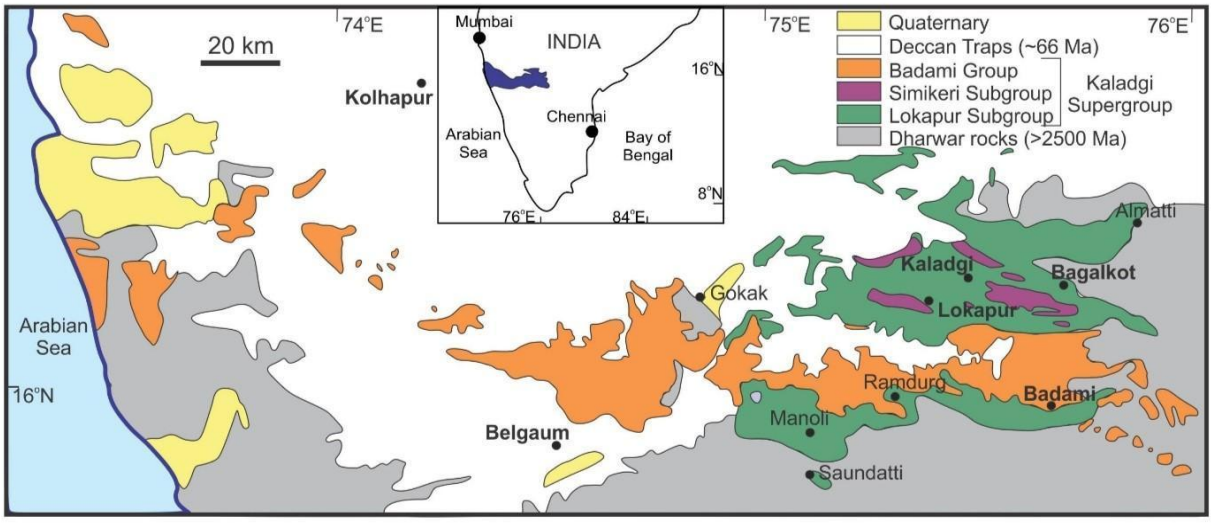

Fig 2: Simplified geological map of Kaladgi Basin (modified after Patil-Pillai and Kale, 2011)

1.2 GEOLOGY OF KALADGI BASIN

The Kaladgi basin is exposed between the longitude 73° E to 76° E and the latitudes of 15° 30'N to 17° N. The Kaladgi basin is divided into Bagalkot (Foote,1876) and Badami groups (Vishwanathiah, 1968) which have a maximum thickness of about 4500 m and 500 m, respectively. As they lie unevenly on the older Precambrian rocks, the Kaladgi sediments are exposed in a synform with a WNW-ESE orientation. The sedimentary deposits found in the Belgaum, Bijapur, and Bagalkot districts of Karnataka, extending from Almatti in the east to

Ajra in the west, over a distance of approximately 100 km in the east-west direction, are collectively referred to as the 'main basin'. In general, the sediments of the basin consist of conglomerates, sandstones, quartzites, limestones and shales and are regarded as equivalent to the Cuddapah system of Andhra Pradesh. The study region is a portion of the Kaladgi Basin and includes the districts of Yadwad in Belgaum, Lokapur, Kaladgi, and Bagalkot in Bagalkot. Based on an angular and erosional unconformity between them, the sedimentary sequence in the Kaladgi Supergroup is divided into the older Bagalkot and younger Badami Groups. This distinction was made by (Viswanathiah 1968) from Torgal Tanda (15°55′39″N:75°16′08″E) and east of Kendur (15°58′12″N:75°45′11″E). They are unevenly overlaid by the Deccan lava flows that have spread out in the form of horizontal beds. They are unevenly underlain by the Archean suite of rocks. Inside the Kaladgi basin, a few small outlying areas are composed of compact and dense flows of basalt. These flows typically have amygdaloidal holes as well as prismatic and columnar joints. Within the Kaladgi basin, less compact formations contain fillers such as calcite, zeolites, and other minerals. In the entire region, there is obvious spheroidal weathering. Stromatolites or microfossils from the Badami Group have been reported by Viswanathiah (1976) and Raha et al. (1982). The Simikeri and Lokapur Subgroups of the Bagalkot Group are split from one another by a disconformity. (Jayaprakash 2007) divided the Simikeri Subgroup into three formations with seven members having a total stratigraphic thickness of 1140 m, and the Lokapur Subgroup into six formations comprising thirteen members with an aggregate stratigraphic thickness of 3094 m based on extensive mapping of the basin. Two formations and six component members made up the Badami Group, which had an overall stratigraphic thickness of 286 m.

1.3 LITHOSTRATIGRAPHY

1.3.1 KALADGI SUPERGROUP

The name Kaladgi Supergroup has originated from the previous classifications of (Viswanathiah, 1977 and Jayaprakash, et al., 1987); for the entire succession of sediments occurring in the Kaladgi Basin. The name has been derived after a place called Kaladgi, which is located almost in the center of the basin and is extended towards the southwest of Parasgarh, Western Ghats in the west and Amingarh in the east. The base is bounded by the erosional and

angular unconformity (“the Great Eparchean Unconformity " of Foote,1876), while at top, another regional unconformity, separates it from the Deccan Traps. The Kaladgi basin also includes three sets of sedimentary cycles consisting of quartzite, argillite, carbonates, and chert breccias. These sedimentary cycles were deposited in a shallow marine environment. The Kaladgi Supergroup has been subdivided into two distinct groups, namely the lower Bagalkot and upper Badami Groups. This division is based on the presence of an intrabasinal unconformity, which is characterized by an erosional surface and a clear angular boundary between the sediments above and below it.

1.3.2 BASEMENT

The basement complex of the Dharwar Craton, comprising granites, metavolcanics, and metasediments, is found beneath the basin in an unconformable relationship. The Kaladgi Basin in southwestern India is an intracratonic sedimentary basin with an Archaean basement and a Mesoproterozoic sedimentary cover that is deformed and overlain by relatively undeformed Neoproterozoic sediments separated by unconformities. The Peninsular Gneissic Complex (PGC), which covers a significant portion of the Western Dharwar craton, consists of extensively deformed and migmatized gneiss. It exhibits a diverse range of compositional enclaves and is intruded by more recent mafic rocks.

1.3.3 BAGALKOT GROUP

The name Bagalkot Group has been originated as per the previous classification of (Viswanathiah, 1977 and Jayaprakash, et al., 1987) as it includes two cyclic successions of quartzite-shale carbonate-chert breccia intervened by a ‘disconformity’. The names come after the town Bagalkot, as the type succession of Bagalkot Group is exposed in the area. The lower boundary of the group is defined by a widespread erosion and angular nonconformity, corresponding to the 8th order surface hierarchy as proposed by (Miall 1985, 1988). On the other hand, the upper boundary of the group is characterized by an intrabasinal unconformity of the same order, which is also erosional and angular in nature. The Bagalkot group which divided into two subgroups namely Lokapur subgroup and Simikeri subgroup. The lowermost Lokapur Subgroup is the thickest sequence (~4200m) that occurs through the basin. The Simikeri

subgroup is confined in the east central part of the basin and is separated from the underlying Lokapur subgroup by a disconformity. The Lokapur and Simikeri subgroups are of Mesoproterozoic age as determined from stromatolite biostratigraphy (cf. Pillai, 1997, Kulkarni and Borkar, 1999) and C/Sr isotope data from carbonates and shale (cf. Padmakumari et al., 1998, Rao et al., 1999).

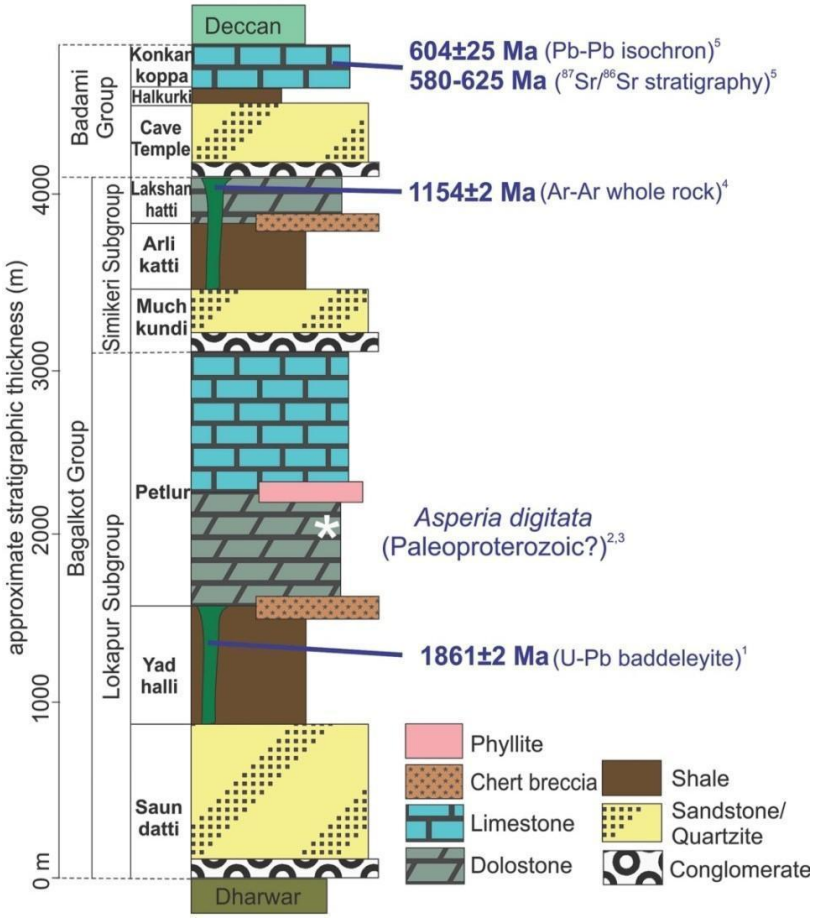

Fig. 3: Stratigraphy of Kaladgi Basin (from George et al., 2023)

1.3.4 LOKAPUR SUBGROUP

The lower sequence of quartzite, argillite, chert breccia, and carbonate facies found within the Bagalkot Group is referred to as the Lokapur Group. This succession was not

recognised as a subgroup by Viswanathiah (1977), and he directly divided the Kaladgi Group into three formations (Bagalkot, Lokapur and Mudhal Formations) based on transitional facies contacts between them. According to his classification, the lower part of the quartzite-argillite-chert breccia and carbonate sequence is referred to as the Bagalkot and Lokapur Formations. In contrast, the upper part of these lithofacies is represented by the Mudhol Formation. This was revised by (Jayaprakash et al., 1987), and the two cycles of the four lithofacies were combined under the Bagalkot Group. Each succession was further designated as Lokapur and Simikeri Subgroups. In present study, the four identified lithotypes, classified as microfacies, have been designated as "Formations" based on their mappable characteristics. The four facies of the lower cycle form the Lokapur Subgroup. The contact between the Lokapur and Simikeri subgroups is characterized as a disconformity. The lowermost coarse siliciclastic formation of the Lokapur Subgroup is situated directly above the crystalline rocks of the Archaean basement. The two are separated by an erosional and angular nonconformity. This is the thickest unit of the Kaladgi Supergroup (~ 4200 m). A detailed description of the four formations within the Lokapur Subgroup are discussed in the following:

1.3.5 Saundatti Quartzite Formation

The basal Saundatti Quartzite consists of conglomerate and quartzite. This formation contains the basal rudaceous and arenaceous siliciclastic rocks that can be traced along the boundary of the Kaladgi Basin. This having a thickness of about a ~1000 m thick. The member of this formation are exposed along the Ramdurg – Mullur where all the three members are represented. An erosional and nonconformity surface marks the boundary between the underlying crystalline rocks and the siliciclastic sediments that make up this formation. In most exposed areas, the Yadhalli formation transitions horizontally and vertically into finer argillaceous sediments. This gradational transition is evident in the hilly regions where the Saundatti Formation exhibits a slope-break, while the flatter areas are characterized by the Yadhalli Argillates underneath. Due to this break, there is a notable increase in the proportion of the argillaceous component, which has been identified and classified as a separate formation. The Saundatti Quartzite are interbedded within the argillates or dolomite limestone, with sharp lithological boundaries.

The name of the Formation comes after a town which is situated at the south-west tip of Kaladgi Basin. The majority of the layers within this formation, accounting for approximately 90% by thickness and over 95% by exposure, are identified as Saundatti Quartzite according to Jayaprakash et al. (1987). The siliciclastic unit, characterized by its sedimentary nature, forms the basal terrigenous detritus observed along the edges of the Kaladgi Basin, particularly in its main eastern exposures. This unit directly forms contact with the underlying basement rocks.

1.3.6 Yadhalli Formation

A significant portion of the basin is covered by the Almatti Quartzite, which has silty intercalations and grades laterally and vertically into a thick succession (about 1000 m) of argillites. The argillites display a range of subfacies, which encompass buff-colored calcareous shales exhibiting slaty cleavage, bluish-purple ferruginous shales that transition into clayey and fine-grained siliceous siltstones with a dull appearance. One particular subfacies of these argillites also includes phyllites with a sheeny texture and slaty cleavage. This outcrop extends extensively across the broad cultivated plains of the Bagalkot-Kaladgi area. It can be observed along the northern and southern flanks of a syncline with a double-dipping structure situated southeast of Bagalkot. Since this Formation can be found in extensive unbroken exposures in the "youngest" Formation of the Lokapur Subgroup, this name was chosen from that given to it by Jayaprakash et al. (1987). This formation has a gradational connection with both the Saundatti Formation under it and the Petlur Formation above it. It frequently makes sharp contact with the Mahakut Formation. This formation has been classified into three parts based on the subfacies compositions, including the Manoli Ferruginous Shale, Jalikatti phyllite and Yargatti Shale.

1.3.7 Petlur Formation

This formation is composed of dolomite and limestone. It is extensively spread in the Bagalkot-Kaladgi-Lokapur sector of the basin. The calcareous shales within the Lokapur Subgroup transition into carbonates, which are typically identified as the termination point of the Lokapur Subgroup. This Formation encompasses various members, including the Chitrabhanukot Dolomite, Chikshellikeri Limestone, and Petlur Limestone, as defined by (Viswanathiah 1977). Additionally, (Jayaprakash et al. 1987) further classified it into, including

the Chitrabhanukot Dolomite, Chikshellikeri Limestone, Nagnur Dolomite, Petlur Dolomite, and Bamanbudni Dolomite Members. The rocks found in this formation display significant deformation and low-grade metamorphism. In the areas surrounding Kaladgi and Lokapur, the carbonates within this formation exhibit intense folding, characterized by prominent parasitic folds. These carbonates also display a diverse range of primary structures, including convolute bedding, climbing ripple laminations, flame structures, intraformational limestone breccias as described by Kale et al. (1998), and dish and cone structures. These primary structures are indicative of carbonate facies that were deposited on a shallow marine carbonate platform.

1.3.8 SIMIKERI SUBGROUP

The Simikeri Subgroup, which represents the second cyclic succession within the Bagalkot Group, overlays the argillites and carbonates of the Lokapur Subgroup. The contact between the Simikeri Subgroup and the Lokapur Subgroup is marked by a clear disconformity, indicating a noticeable interruption or gap in the deposition between the two. It is restricted to the northern sector of basin and having a thickness of about 1000 m which is extended from Muchkundi Formation to Lakshanhatti Formation. The Simikeri Subgroup derives its name from Simikeri village, which serves as the stratotype for this subgroup. The most representative and well-exposed sections of the Simikeri Subgroup can be observed in the Bagalkot-Simikeri sector. The succession originally identified as the Mudhol Formation by Viswanathiah (1977) was subsequently renamed by Jayaprakash et al. (1987) as the Simikeri Subgroup. This renaming was retained in the current classification due to the fact that the Simikeri Subgroup represents a succession of four macrofacies within the region. The layers within the Simikeri Subgroup display noticeable deformation, characterized by tightly plunging folds. The folded members of the Simikeri Subgroup are exposed in multiple small synsedimentary subbasins, which demonstrate doubly plunging orientations aligned in an east-west direction. The Simikeri Subgroup has been divided into Muchkundi Quartzite, Arillikatti Shale and Lakshanhatti Dolomite Formations.

1.3.9 Muchkundi Formation

The Simikeri Subgroup comprises rudites and coarse siliciclastic lithofacies, which are positioned above the Yadhalli Argillites and Petlur Carbonates of the Lokapur Subgroup. The contact between them is disconformable. The Formation previously referred to has undergone a name change and is now recognized as the Muchkundi Formation. This designation was chosen based on the exposure of the stratotype for this Formation, which is located to the south of Muchkundi village. In this formation the conglomerate directly overlies the Yadhalli shales of Lokapur Subgroup. The estimated thickness of the Muchkundi Formation is approximately 600 meters. This Formation is considered equivalent to the Vajramatti Quartz arenite Member described by Viswanathiah (1977) and is also recognized as a component of the Kundargi Formation as classified by (Jayaprakash et al. 1987). The Muchkundi Formation includes conglomerates that are present as pebbly beds, transitioning into coarse and gritty quartzites. These quartzites typically exhibit a yellowish-brown color and possess a glassy texture. They are highly deformed due to geological processes. The quartzites grade laterally and vertically into finer argillites. Consequently, the Muchkundi Quartzite Formation has been divided into two distinct members: the Bevinmatti Conglomerate and the Tulsigeri Quartzite.

1.3.10 Arlikatti Formation

The Tulsigeri Quartzite exhibits lateral and vertical gradations into fissile ferruginous shales, which in turn transition into a calcareous-rich variety. These ferruginous and calcareous shales are primarily found at the core of the large doubly plunging folds that host the Simikeri Subgroup. The shales within this formation form extensive deposits that are widespread throughout the region, although their exposure levels are limited. The type-section of the Muchkundi Formation can be observed near the village of Arlikatti, located south of Lokapur. The ferruginous type of this formation is readily noticeable and extensively exposed in the surrounding area of Simikeri village. The Muchkundi Formation has an estimated thickness of approximately 300 meters. For instance, Viswanathiah (1977) designated certain horizons within the Muchkundi Formation as the Muchkundi Argillite Member of the Mudhol Formation. Meanwhile, Jayaprakash et al. (1987) referred to these horizons as the Govindkoppa Argillite (part of the Kundargi Formation) and Dadanhatti Argillite (part of the Hoskoti Formation)

Members. Within the Muchkundi Formation, the argillites exhibit lateral transitions from ferruginous siltstones to soft, fissile, finely laminated bluish purple ferruginous shale. These shale layers gradually transform into buff-colored, fissile, and friable calcareous shales. Both types of shales are characterized by the development of bedding plane cleavages, and in some locations, they exhibit characteristics of phyllites due to the intense deformation and development of slaty cleavage.

1.3.11 Lakshanhatti Formation

The Arlikatti argillites are overlain conformably by the Lakshanhatti Dolomites. The thickness of the formation is about approximately 200m. The Dolomite within the Muchkundi Formation consists of multiple varieties, including stromatolitic dolomites and non-stromatolitic dolomites. These variations in composition contribute to the overall diversity and characteristics of the dolomite present within the formation. The name comes after by village Lakshanhatti which located in the west of Lokapur –Yargatti. The stromatolitic dolomites of this Formation contain colonies of Collenia and stratifera forms are seen. The dolomites are interbedded with argillite beds.

1.3.12 BADAMI GROUP

The sediments of the Bagalkot Group, which have undergone deep erosion, are overlain by younger undeformed sediments. The boundary between these two units is defined by an intrabasinal unconformity, indicating a period of erosion and non-deposition between them. The name "Badami Group" was originally assigned to these sediments by Viswanathiah (1977) and Jayaprakash et al. (1987), and this classification has been retained in the current framework. The sediments belonging to the Badami Group are predominantly located in the southern portion of the eastern continuous exposures of the basin. These sediments have a thickness of approximately 550 meters. The lithology comprise of this group is of coarse argillites and limestones. Badami Group has been divided into three formations, namely the Cave Temple Arenite Formation, the Halkurki Shale Formation and the Konkankoppa Limestone Formation.

1.3.13 Cave temple Formation

The Cave Temple Formation comprises both conglomerate and sandstone facies. The conglomerates are observed as thin lens-like bodies, resting on the deeply eroded and deformed sediments of the Lokapur Subgroup within the southern sector of the basin. The contact between the conglomerates and the underlying sediments is marked by an intrabasinal unconformity, indicating a hiatus or a period of non-deposition. The sandstones within this formation are present as isolated occurrences, resting directly on the underlying crystalline rocks of the basement. It is important to mention that in various areas; the Deccan Traps volcanic rocks conceal or hide these sedimentary formations. The Badami Formation corresponds to the Ramdurg Formation as described by Viswanathiah (1977) and partially to the Kerur Formation as classified by Jayaprakash et al. (1987). The distribution of this Formation is limited to the southern part of the Kaladgi Basin, extending from Gokak in the western region to Parasgarh fort located south of Saundatti, and further extending eastward to Patadkal. The sandstones found in the Badami Formation have served as the foundation for the creation of magnificent cave temples, giving rise to the name "Cave Temple Arenite Formation." This formation has been categorized into three members based on color, texture, and primary sedimentary structures; the Torgal Conglomerate, Kendur Sandstone and Gokak Sandstone Members. The sandstones found within this formation are characterized by their coarse-grained, gritty, and friable nature.

1.3.13 Halkurki Formation

The Halkurki Shale consists of various varieties, including greenish-brown siltstone enriched with glauconite and bluish-purple ferruginous shales. These shales gradually transition into buff to white-colored calcareous shales. The beds within this shale formation exhibit thin lensoid bedding as well as occasional ripple bedding, with a notable presence of fissility, indicating the tendency to split along parallel planes. The name comes after by the type locality of this Formation of village Halkurki which is given by Viswanathiah (1977) and Jayaprakash et al. (1987). It grades laterally and vertically into Konkankoppa Limestone. The shale in this formation exhibits a fissile nature with exceptionally fine lamination. In certain areas, particularly to the east of Muchalgud hamlet and south of Katageri ridge, glauconitic siltstones can also be observed. These rocks, known as siltstones, are dull, earthy brown, thinly laminated,

and have slight dips. The Cave Temple Arenites also contain a few intercalated thin strata of the Halkurki Shale.

1.3.14 Kokankoppa Formation

This Formation is the uppermost and youngest unit of Badami Group as well as Kaladgi Supergroup. These are black, thinly bedded, parallel laminated limestones which having gentle dip of 5 to 10°. The name Konkankoppa Limestone of Jayaprakash et al. (1987) has been retained as it is best exposed in a stream called Hire Halla, flowing south of Konkankoppa village and also having stratigraphic thickness of approximately 80m. Bidirectional ripple marks, suspicious trace of fossil and nodular iron segregation is seen in this Limestone.

1.4 REVIEW OF LITERATURE

Based on stromatolite biostratigraphy and their correlation with the stromatolites from the Tadpatri Formation of the adjacent Cuddapah Basin, a Lower Mesoproterozoic age (1600 Ma) was assigned to the Kaladgi stromatolites (Viswanathiah and Sreedhara Murthy 1979; Jayaprakash et al. 1987; Sharma et al. 1998). Sharma et al. (1999) concluded that the stromatolites of the Lokapur and Simikeri Subgroups do not indicate a major temporal difference in the age and are all indicative of a Late Palaeoproterozoic to Early Mesoproterozoic age. Padmakumari et al. (1998) and Sambasiva Rao et al. (1999) gave model Rb–Sr isotopic age calculated with respect to CHUR for the shales from Bagalkot Group; and suggested that their deposition was younger than 1800±100 Ma. Kale (2015) put forward a contrasting viewpoint suggesting a significantly younger age for the Kaladgi Supergroup. The author also highlighted gaps and deficiencies in the assumptions that supported the previously proposed older age.

Carbon and strontium isotopic composition of the carbonates from this basin, suggested a Post-Sturtian age (≤600 Ma) for Konkankoppa Limestone of Badami Group and a Mesoproterozoic age (between 1600 and 1000 Ma) for the carbonates of Bagalkot Group (Kumar et al. 1999). Isotope studies (George et al., 2023) focusing on the marine carbonate successions within this basin, including

Chitrabhanukot, Chikshellikeri, Lakshanhatti (Bagalkot Group), and Konkankoppa (Badami Group), have been conducted to examine the C–O–Sr isotopes. The results of these studies indicate that the $\delta^{13}C$ values of all the carbonate formations have retained the original marine signature. The limited variation of $\delta^{13}C$ observed in the carbonates of the Bagalkot Group suggests a relatively stable organic carbon burial process. On the other hand, the wider range of $\delta^{13}C$ variation in the Konkankoppa Limestone of the Badami Group indicates a more dynamic organic carbon burial scenario. These isotopic signatures align with the C-isotope stratigraphy observed during the Meso-Neoproterozoic era. The ^{206}Pb-^{207}Pb dating analysis conducted on the Konkankoppa Limestone, the youngest unit of the Kaladgi Supergroup, revealed a depositional age of 604 ± 25 million years ago. The obtained age of 604 ± 25 million years ago, combined with the primary $^{87}Sr/^{86}Sr$ ratio of 0.70781, indicates that the sedimentation of the Badami Group continued during the Ediacaran Period. These data confirm the existence of a long duration depositional hiatus, of >500 million years, between the Bagalkot and the Badami Groups. The findings of this study contradict the assertion that sedimentation in the majority of Proterozoic basins in peninsular India ceased around 1000 Ma.

The identification of framework clasts such as quartz, K-feldspar, tourmaline, sphene, zircon, and biotite indicates a granitic source for the sediments found along the northern margins of the basin. On the other hand, the presence of Banded Hematite Jasper, Banded Hematite Quartzite, chert, and other minerals suggests that the metasediments originating from the Hungund Schist Belt are a secondary source of sediment towards the central eastern part of the basin. The granitic rocks forming the basement might have undergone uplift along the northern boundary of the basin, leading to the formation of rugged terrain in that area. Singh and Rai (2000), focuses on the study of sedimentary facies, palaeoenvironment reconstruction and basin analysis of the lower Kaladgi basin, providing insights into the depositional process and palaeoclimate of the region. Also, they present the lithostratigraphy, sequence stratigraphy and basin analysis of the middle Kaladgi basin. The recent studies of basal Salgundi Conglomerates

gives the product of terrestrial scree formed along the margins of the basins and fan deposits that graded downslope to form braided sediments (Bose et al., 2008); this also conclude that the tectonic influence on the gradient of the marginal slope of the basin controlled the nature of the sedimentary package and a subsequence build-up of the sequence.

The Kaladgi Basin's aquifer systems, groundwater dynamics, and water quality are all examined in the hydrogeology section. It integrates research on the distribution of aquifer types, the potential for groundwater recharge, and the geological controls of groundwater occurrence and flow. It also explores the toxins including fluoride, salinity, and other water quality issues. The surface water resources of the Kaladgi Basin, emphasizing the river systems, reservoirs, and their hydrological characteristics. It presents studies that investigate streamflow patterns, sediment transport, and water availability in the basin. Furthermore, it discusses the impact of anthropogenic activities on surface water quality and the need for sustainable water management practices. Also, the basin is known for extensive gas and oil reserves. Mineral resources of the Kaladgi basin highlights exploration and exploitation of minerals such as limestone, bauxite, and manganese. Many researchers have conducted studies on the petroleum potential of the Kaladgi Basin. These studies have found that the basin contains significant amounts of oil and gas reserves, particularly in the Lower Cretaceous formations. Shivanna et al., (2011) employed a 3D GIS technique to investigate the Proterozoic sedimentary Kaladgi Basin. Their study involved the construction of three-dimensional geological models using surface-mesh, wire-mesh, and TIN (Triangulated Irregular Network) in a 3D GIS environment. The aim was to decipher the ancient marine terrain surface within the study area of the Kaladgi Basin. To achieve this, a comprehensive database comprising approximately 20,522 point elevations and several kilometers of line elevation contours was utilized.

The Kaladgi Supergroup plays a crucial role in understanding the paleogeographic changes that occurred in the Indian subcontinent during the Proterozoic era. It offers valuable insights into the past locations of India, its interactions with neighboring landmasses, and the dynamic shifts in continental configurations throughout geological history.

1.5 OBJECTIVES OF THE STUDY

In this project work, I intend to

1. Classify the Kaladgi siliciclastic rocks using their major oxide composition,
2. Understand the weathering intensity of the source areas of the Kaladgi sedimentary rocks,
3. Decode the provenance of the sediments and thereby understand the evolutionary history of the basin using major oxide geochemistry.

2. METHODOLOGY

For the present study, samples were collected in and around Lokapur, Gaddankeri, Badami and Bagalkot. Sample details and methods used during the study are summarized below;

2.1 SAMPLES

The samples KD18-4,5,6,7,129,134,135,236,237,238,239 which belong to the basal Lokapur subgroup consist of the lithology quartzite, shale, phyllite, sandstone. Samples KD18-110,130,131,132,133,248 & 249 of Simikeri subgroup bears the lithology of quartzite and shale. Four samples from Badami group KD18-232,233,234,235 comprise of shale and sandstone.

Table1: Details of Kaladgi Samples

Sample ID	Formation	Group/Subgroup	Lithology
KD18-4	Saundatti	Lokapur Subgroup	Quartzite
KD18-5	Manoli	Lokapur Subgroup	Shale
KD18-6	Manoli	Lokapur Subgroup	Shale
KD18-7	Yargatti	Lokapur Subgroup	Shale
KD18-110	Tulsigeri	Simikeri Subgroup	Quartzite
KD18-129	Jallikatti	Lokapur Subgroup	Phyllite
KD18-130	Tulsigeri	Simikeri Subgroup	Quartzite
KD18-131	Arliketti	Simikeri Subgroup	Shale
KD18-132	Arliketti	Simikeri Subgroup	Shale
KD18-133	Tulsigeri	Simikeri Subgroup	Quartzite
KD18-134	Manoli	Lokapur Subgroup	Shale

KD18-135	Manoli	Lokapur Subgroup	Shale
KD18-232	Halkurki	Badami Group	Shale
KD18-233	Halkurki	Badami Group	Shale
KD18-234	Halkurki	Badami Group	Shale
KD18-235	Badami	Badami Group	Sandstone
KD18-236	Manoli Shale	Lokapur Subgroup	Shale
KD18-237	Manoli Shale	Lokapur Subgroup	Shale
KD18-238	Saundatti	Lokapur Subgroup	Quartzite/Sandstone
KD18-239	Manoli	Lokapur Subgroup	Shale
KD18-248	Arliketti	Simikeri Subgroup	Shale
KD18-249	Arliketti	Simikeri Subgroup	Shale

2.2 DETERMINATION OF LOI

The Loss on Ignition (LOI) is an analytical technique which is used to detect the volatile components in the sample. LOI represents the weight loss experienced by the sample when it is heated at 900 ^{0}C. By this, volatile components like carbon dioxide, water, organic matter and other volatile compounds get removed.

2.2.1 Procedure for determination of LOI

1. **Sample Preparation:** The sample is usually collected in solid form such as rocks, minerals, sediments etc. It should be collected properly, cleaned and ground into fine powder to set the seal for homogeneity.
2. **Weighing:** Initially, take the weight of an empty crucible (crucible is a ceramic or metallic container in which the samples are subjected to high temperature) which is cleaned either with water or acetone. After weighing the empty crucible, a representative portion of the sample around 1-3 grams were added. Accurately measure the weight by using analytical balance and record the initial weight.
3. **Heating**: The crucibles are then placed in a muffle furnace or oven which is specially designed for LOI determination. The temperature is then raised up to around 900^0 C and held for a specified period (1-2 hours).
4. **Cooling and Weighing:** After heating the samples, the crucible is removed from the muffle oven and it is left to cool in a desiccator to prevent moisture absorption. Once the crucible reaches the room temperature, it is weighed again on the analytical balance.

5. **Calculation:** The LOI is calculated by subtracting the final weight of the sample after heating from the initial weight of the sample and expressing the loss of weight in percentage. The formula for calculation of LOI is given by;

LOI = {Wt of sample (before LOI) – Wt of sample (after LOI)}*100/Wt of sample (before LOI)

The resultant LOI value represents the volatiles which are expressed in weight percentage during heating. This also gives important information about the composition of samples, especially its organic content and volatile matters.

Fig4: Samples placed in the Muffle Furnace for LOI

Table2: LOI calculation

Sample no.	Weight of empty crucible (g)	Weight of crucible with sample (g)	Weight of sample before LOI (g)	Weight of sample with crucible after LOI (g)	Weight of sample after LOI (g)	LOI value in %
KD18-4	37.44	40.01	2.57	40.01	2.57	0.07
KD18-5	33.96	36.06	2.10	36.03	2.07	1.42
KD18-6	37.02	40.01	2.99	39.98	2.95	1.28
KD18-7	34.10	37.00	2.90	36.98	2.87	0.99

KD18-110	36.36	39.09	2.73	39.09	2.73	0.05
KD18-129	34.30	37.02	2.72	37.00	2.70	0.76
KD18-130	43.15	46.01	2.86	46.00	2.85	0.16
KD18-131	34.54	37.12	2.58	37.09	2.55	0.90
KD18-132	32.84	35.20	2.36	35.18	2.34	0.46
KD18-133	32.84	35.82	2.98	35.81	2.97	0.31
KD18-134	33.96	37.07	3.10	37.06	3.10	0.17
KD18-135	36.49	39.50	3.01	39.49	3.00	0.21
KD18-232	39.09	40.61	1.52	40.59	1.49	1.38
KD18-233	34.78	37.78	3.00	37.75	2.97	0.97
KD18-234	36.57	39.52	2.95	39.48	2.91	1.54
KD18-235	35.19	38.14	2.95	38.13	2.94	0.08
KD18-236	32.58	35.53	2.96	35.51	2.94	0.71
KD18-237	37.55	40.61	3.06	40.60	3.05	0.34
KD18-238	39.31	42.36	3.05	42.36	3.05	0.10
KD18-239	38.49	41.49	3.00	41.46	2.97	0.80

KD18-248	40.19	43.21	3.03	43.19	3.00	0.72
KD18-249	37.44	40.47	3.03	40.45	3.01	0.66

2.3 MAJOR OXIDE ANALYSIS

Major oxide analysis refers to the evaluation of composition of materials and substance. Sedimentary rocks generally contain major oxides that are derived from weathering and erosion from their parent rocks. These analyses provide valuable insights of depositional history and also help to understand processes involved in their formation.

2.3.1 Preparation of Pellet

The sample preparation method used in this study involves grinding and compression, which leads to a more uniform representation of the sample with no void spaces and reduced sample dilution. As a result, this method produces superior analytical findings compared to using loose powders. As a result of the sample preparation method, most elements exhibit higher intensities compared to when using loose powders. The examination of components in the ppm range works very well with pressed pellets. The only equipment needed to manufacture pressed pellets is a pulverizing mill and a sample press, which makes the process also rather easy and affordable.

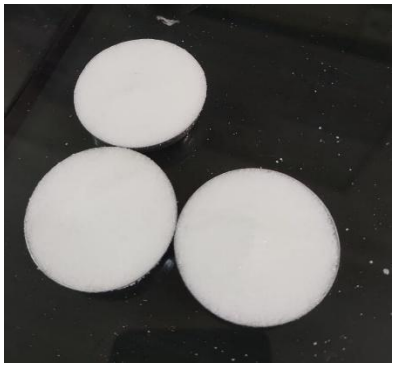

Fig 5: Aluminum cups filled with Boric acid

Fig 6: Pellet Presser

In order to do XRF analysis we need to prepare the sample as pressed pellets. Pellets are 40 mm aluminum cups. These pellets are filled using boric acid crystals. Boric acid crystals are found in nature as the mineral sassolite and appear as white powder or colorless crystals that dissolve in water. It is a weak acid that can react with alcohols to produce borate esters as well as a variety of borate anions and salts. These crystals act as a binding agent. The finely powdered samples are carefully sprinkled over the boric acid using a spatula. Then they are pressed in a 40-ton hydraulic press to produce a circular 40mm disc. These disc or pressed pellets are then used for the XRF analysis.

2.3.2 X- RAY FLUORESCENCE

X-ray fluorescence (XRF) is a non-destructive analytical technique used to determine the elemental composition of materials. It relies on the principle that when a material is exposed to high-energy X-rays, the atoms within the material emit characteristic X-rays that are unique to each element. The XRF instrument consists of a source that emits X-rays, a sample holder where the material is placed, and a detector that measures the energy and intensity of the emitted X-rays. When the X-rays interact with the atoms in the sample, the atoms absorb the X-ray energy and subsequently emit characteristic X-rays (Fluorescence). These characteristic X-rays are then detected by the instrument and analyzed to determine the elemental composition of the material. It can identify and quantify a wide range of elements, from light elements such as carbon and oxygen to heavy elements like lead and uranium. The technique is particularly useful for analyzing solid samples, including metals, minerals, soils, ceramics, and plastics.

One of the key advantages of XRF is its non-destructive nature, meaning that the sample remains intact and can be further analyzed or preserved after the measurement. Additionally, XRF instruments are relatively easy to operate and provide rapid results, making them valuable tools in both research and industrial applications. By analyzing the elemental composition of materials, XRF helps researchers and scientists gain insights into the chemical properties, quality control, and characterization of various substances. It plays a vital role in fields were accurate and efficient elemental analysis.

Fig 7: S8 Tiger WD-XRF

There are mainly two types of XRF;

- Energy dispersive X-ray fluorescence (EDXRF)
- Wavelength dispersive X-ray fluorescence (WDXRF)

Energy dispersive X-ray fluorescence

EDXRF is a popular and widely used technique in XRF analysis. In this method, the sample is bombarded with high-energy X-rays, causing the atoms in the sample to emit characteristic fluorescent X-rays. These X-rays are then dispersed by an energy-sensitive detector, which measures their energy and intensity. The detector records the full spectrum of

emitted X-rays simultaneously, allowing for rapid analysis of multiple elements. EDXRF instruments are typically compact, portable, and offer relatively fast analysis times. They are commonly used in applications such as alloy identification, environmental analysis, and quality control in industries.

Wavelength dispersive X-ray fluorescence

WDXRF is a technique that utilizes a crystal monochromator to separate the fluorescent X-rays based on their wavelengths. The X-rays emitted by the sample are diffracted by the crystal, and different wavelengths are directed towards separate detectors. Each detector is optimized to detect a specific wavelength, allowing for highly precise and accurate measurements of individual elements. WDXRF instruments are often used in laboratories and research settings where high analytical performance is required. They are suitable for applications such as quantitative analysis of major, minor, and trace elements in a wide range of samples, including geological samples, metals, and advanced materials. The sample of present study were measured in a S8 Tiger WD-XRF at NCESS.

Both EDXRF and WDXRF techniques have their advantages and are suited for different applications. EDXRF offers portability, simplicity, and lower cost, making it suitable for routine analysis and fieldwork. On the other hand, WDXRF provides excellent sensitivity, accuracy, and precision, making it suitable for demanding analytical tasks and research purposes. The choice of technique depends on the specific requirements, sample types, and analytical goals of the user.

2.3.3 Principle

X-ray fluorescence (XRF) is an analytical technique that operates on the principle of the interaction between high-energy X-rays and atoms within a sample. When a material is exposed to X-rays, the atoms in the sample absorb the X-ray energy, resulting in the displacement of inner-shell electrons. Once the inner-shell electrons are displaced, the atoms return to a more stable state by filling the vacancies in the inner shells. During this relaxation process, the atoms emit X-rays with energies characteristic of the elements present in the sample.

XRF analysis involves two main stages: excitation and detection.

- Excitation: In an XRF instrument, an X-ray source, often an X-ray tube, emits high-energy X-rays. These X-rays are directed towards the sample being analyzed. When the X-rays interact with the atoms in the sample, they undergo various processes such as photoelectric absorption and scattering.

Photoelectric absorption occurs when an inner-shell electron is ejected from an atom, leaving behind a vacancy in the electron shell. The energy of the ejected electron, known as a photoelectron, is determined by the energy of the incident X-ray minus the binding energy of the inner-shell electron. Each element has a specific binding energy, and thus, the energy of the emitted X-rays during relaxation is characteristic of the elements present in the sample.

- Detection: Following the excitation process, the atoms in the sample undergo relaxation and emit fluorescent X-rays with discrete energies corresponding to the specific elements. These characteristic X-ray are collected by a detector, which measures their energy and intensity.

Bragg's law, formulated by Sir William Henry Bragg and Sir William Lawrence Bragg, relates the angles of incidence and diffraction of X-rays by a crystal lattice. It states that when X-rays encounter a crystal lattice, they will undergo constructive interference if the following condition is satisfied:

$$\mathbf{n\lambda = 2d \sin(\theta)}$$

In this equation:

- n represents the order of the diffraction peak (n = 1 for the primary peak, n = 2 for the second-order peak, and so on).
- λ is the wavelength of the incident X-ray.
- d is the interplanar spacing of the crystal lattice planes.
- θ is the angle between the incident X-ray beam and the crystal lattice planes.

In XRF analysis, Bragg's law is utilized in wavelength dispersive X-ray fluorescence (WDXRF). WDXRF employs a crystal monochromator to separate the fluorescent X-rays based on their wavelengths. The crystal monochromator is typically made from a single crystal, such as

quartz or lithium fluoride. When X-rays emitted by the sample interact with the crystal monochromator, the crystal lattice planes diffract the X-rays according to Bragg's law. By adjusting the angle of incidence (θ) and the crystal orientation, a specific wavelength of X-ray can be selectively diffracted toward a detector. This wavelength selection allows for precise measurements of individual elements in the sample. The detector, optimized for the specific wavelength, records the intensity of the diffracted X-rays, providing information about the elemental composition of the sample. Bragg's law, together with the crystal monochromator, enables WDXRF instruments to achieve high accuracy and resolution in elemental analysis. By measuring the diffracted X-rays at different angles, WDXRF instruments can quantitatively analyze the concentration of major, minor, and trace elements in a wide range of materials.

Depth of Sampling

Sampling penetration depth in X-ray fluorescence (XRF) refers to the distance that X-rays can effectively penetrate a material during analysis. Understanding the sampling penetration depth is crucial for ensuring accurate and representative measurements. The penetration depth of X-rays is influenced by various factors, including the energy (wavelength) of the X-rays, the density and composition of the material being analyzed, and the specific absorption characteristics of the elements of interest. In general, higher energy X-rays have greater penetration depth compared to lower energy X-rays. This means that high-energy X-rays can penetrate deeper into the sample before being absorbed or scattered. However, the actual penetration depth is also affected by the density and composition of the material. Dense materials with high atomic numbers tend to attenuate X-rays more strongly, resulting in shorter penetration depths. It is important to note that XRF analysis typically provides information about the elemental composition of the material near its surface. This is because the X-rays used in XRF have limited penetration depth, and their intensity decreases exponentially as they travel deeper into the material. As a result, XRF analysis is well-suited for analyzing surface layers or thin coatings on samples.

To obtain representative measurements and minimize errors, proper sampling techniques are employed in XRF analysis. The sample surface is typically prepared by grinding, polishing, or other methods to ensure a consistent and clean surface. The X-ray beam is then focused on the

desired area of the sample, taking into account the expected penetration depth. Precautions are taken to avoid regions that may contain surface contaminants or non-representative layers, which could potentially impact the accuracy of the analysis. In cases where a deeper analysis is required, techniques like micro-XRF or X-ray depth profiling can be employed. These techniques use focused X-ray beams to analyze specific regions of interest within a sample, providing information about the elemental distribution at different depths. Overall, understanding the sampling penetration depth in XRF is essential for selecting appropriate measurement parameters, optimizing sample preparation, and obtaining accurate elemental composition data from the near-surface layers of materials.

Calibration Standards

For X-ray analysis of sediments there are several International sedimentary rock standards used. It includes SCo-1, SDC-1, SDO-1, MAG-1, SO1, BX-N, JSd-1, JSd-2, JSd-3, JSl-1, JSO-1, JMS-1, JMS-2 and JLk-1.

Detectors in XRF

X-ray fluorescence (XRF) analysis detectors play an important role in capturing and measuring the characteristic X-rays emitted by a sample. These detectors are designed to convert the X-ray photons into electrical signals that can be further processed and analyzed. Scintillation counters are one of the detectors used in XRF analysis. These detectors consist of a scintillator material that emits light when struck by X-ray photons. The emitted light is then converted into an electrical signal using a photomultiplier tube (PMT) or a silicon photodiode. Scintillation counters offer fast response times, good energy resolution, and are capable of handling high count rates.

Analyzing crystals:

In X-ray fluorescence (XRF) analysis, different types of crystals are employed as analyzers to diffract X-rays and separate them based on their wavelengths. In S8 Tiger model XRF there were seven analyzing crystals and includes LiF 200, LiF220, PET, XS-55, XS-N, XS-C and XS-B.

Table3: Certified values of reference standards used for calibration

Code	SCo-1	SDC-1	SDO-1	SGR-1	MAG-1	SO1	BX-N
Name	Cody Shale	Mica Schist	Devonian Ohio Shale	Green River Shale	Marine Sediment	Soil	Bauxite
SiO_2	62.80	65.80	49.28	28.24	50.40	54.98	7.40
TiO_2	0.63	1.01	0.71	0.53	0.75	0.88	2.37
Al_2O_3	13.70	15.80	12.27	6.52	16.40	17.59	54.21
MnO	0.04	0.10	0.04	0.034	0.10	0.11	0.05
Fe_2O_3	5.13	6.32	9.34	3.03	6.80	8.58	23.17
CaO	2.62	1.40	1.05	8.38	1.37	2.46	0.17
MgO	2.72	1.69	1.54	4.44	3.00	3.83	0.11
Na_2O	0.90	2.05	0.38	2.99	3.83	2.70	0.04
K_2O	2.77	3.28	3.35	1.66	3.55	3.18	0.05
P_2O_5	0.21	0.16	0.11	0.33	0.16	0.15	0.13
LOI	9.9	1.62	21.7	33.13	14.33	4.4	12.17
Total	101.38	99.23	99.77	89.28	100.69	98.86	99.87

Code	JSd-1	JSd-2	JSd-3	JSI-1	JSO-1	JMS-2	JMS-3	JLK-1
Name	Stream Sediment	Stream Sediment	Stream Sediment	Slate	Soil	Marine Sediment	Marine Sediment	Lake Sediment
SiO_2	66.55	60.78	76.00	59.47	38.37	53.74	41.78	57.16
TiO_2	0.64	0.61	0.40	0.73	1.23	0.70	1.40	0.67
Al_2O_3	14.65	12.31	9.91	17.60	18.06	15.82	14.18	16.73
MnO	0.09	0.12	0.15	0.06	0.20	0.10	2.26	0.27
Fe_2O_3	5.06	11.65	4.37	6.76	11.38	6.90	10.96	6.93
CaO	3.03	3.66	0.56	1.48	2.55	2.13	4.68	0.69
MgO	1.81	2.73	1.17	2.41	2.11	2.87	3.24	1.74
Na_2O	2.73	2.44	0.41	2.18	0.67	4.07	5.79	1.05
K_2O	2.18	1.15	1.97	2.85	0.34	2.24	2.70	2.81
P_2O_5	0.12	0.11	0.08	0.20	0.48	0.18	1.26	0.21
LOI	3.14	3.52	4.79	5.68	24.38	10.4	11.26	12
Total	100	99.08	99.81	99.42	99.77	99.15	99.51	100.2

2.3.4 Calibration of XRF:

The calibration of X-ray fluorescence (XRF) involves the process of establishing a relationship between the measured X-ray intensities and the concentrations of elements in a sample. It begins with the selection and preparation of calibration standards, which are well-characterized reference materials with known compositions. The XRF instrument is then set up with the appropriate parameters, and the calibration standards are measured to record X-ray intensities. Data analysis is performed to correct for various factors and construct a calibration curve relating the measured intensities to the known concentrations. The calibration curve is validated using additional reference materials, and it is subsequently used for quantitative analysis of unknown samples. Regular recalibration is necessary to maintain accuracy. The specific calibration procedures may vary depending on the instrument and application. The calibration lines of the major oxides constructed by using sedimentary rock sample are shown below;

Calibration line of SiO_2:

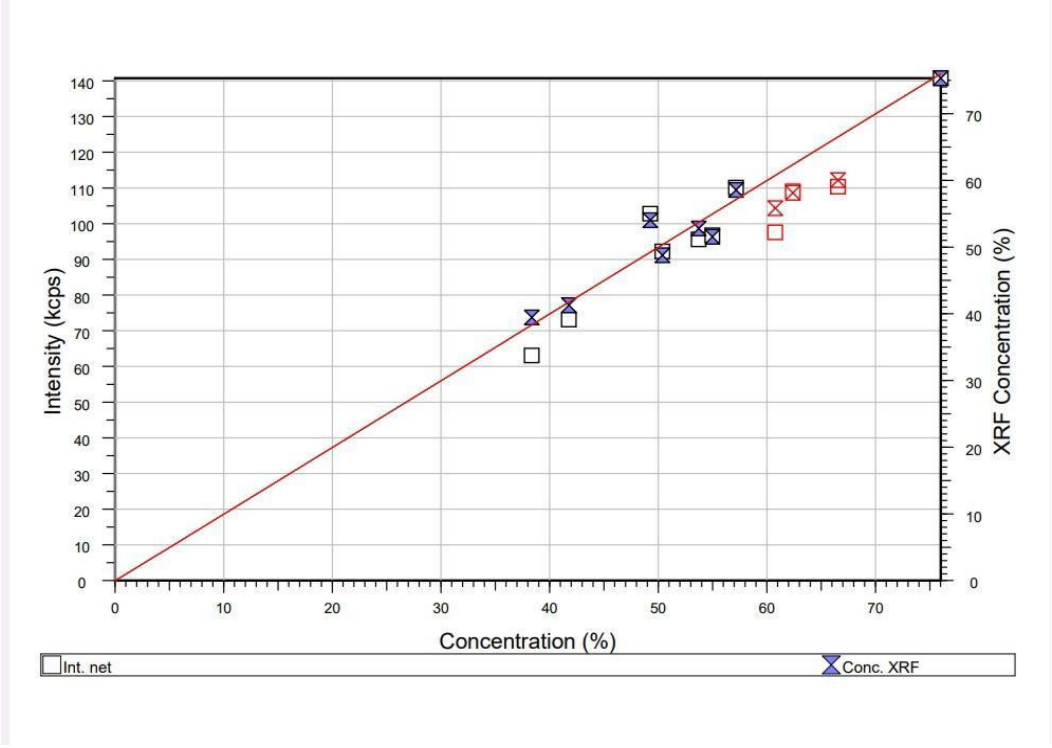

Calibration line of TiO_2

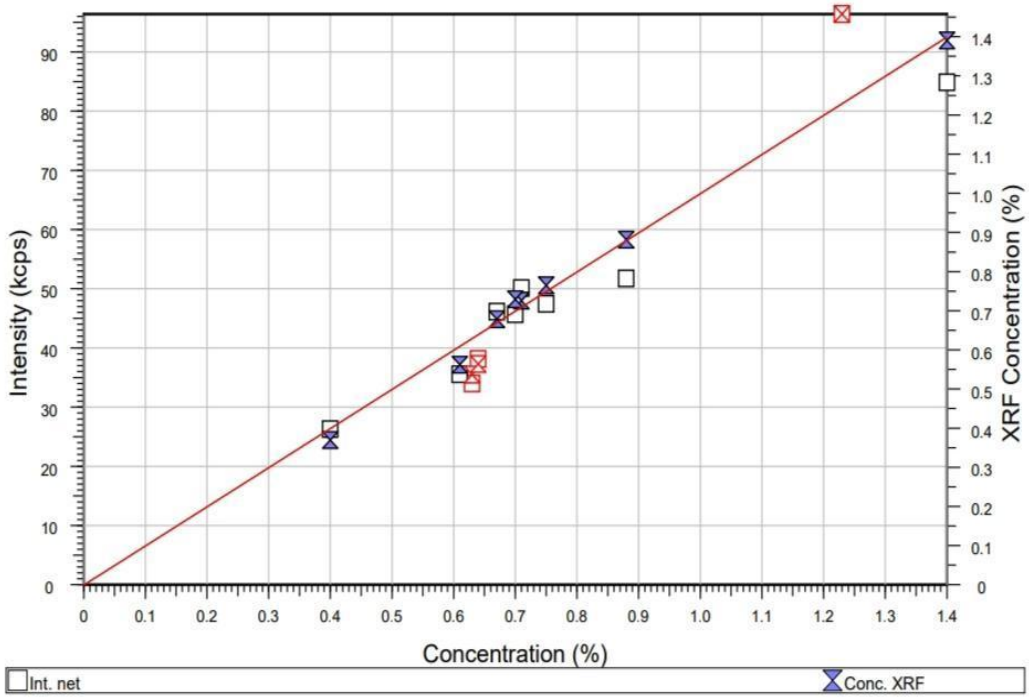

Calibration line of Al_2O_3

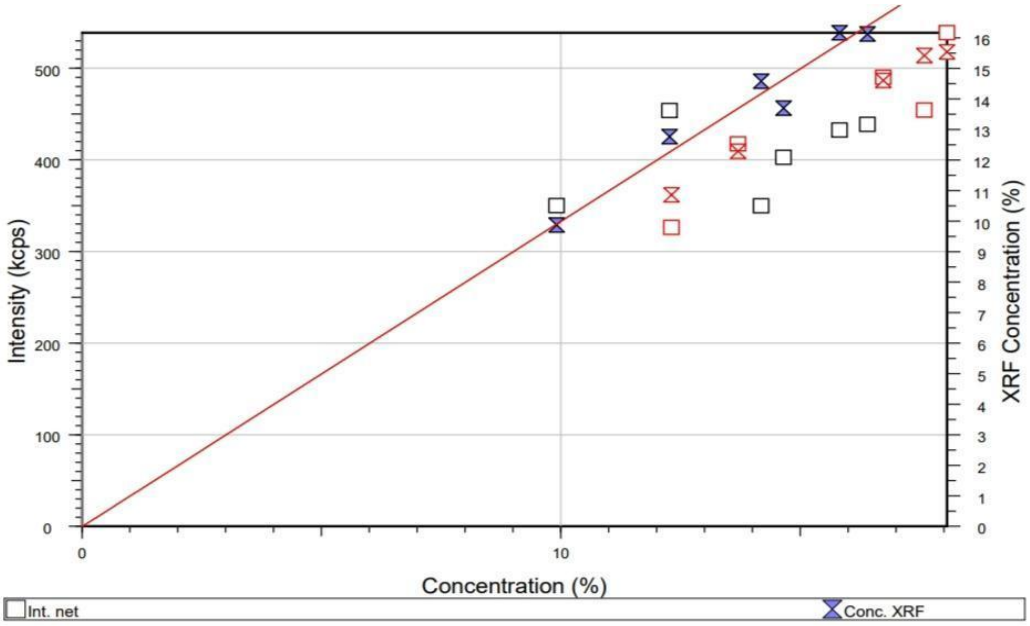

Calibration line of MnO

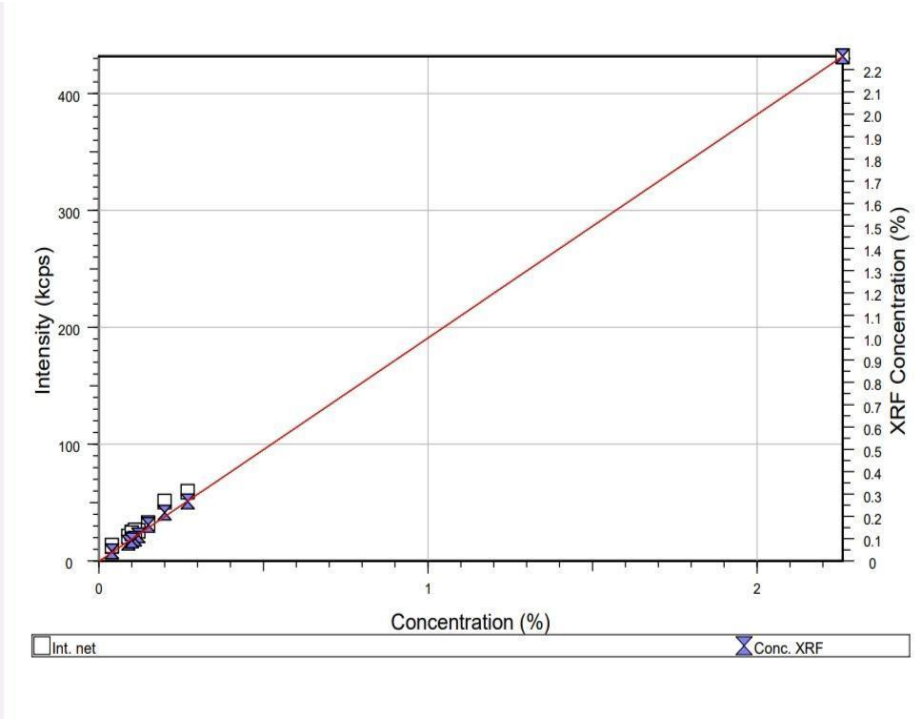

Calibration line of Fe_2O_3

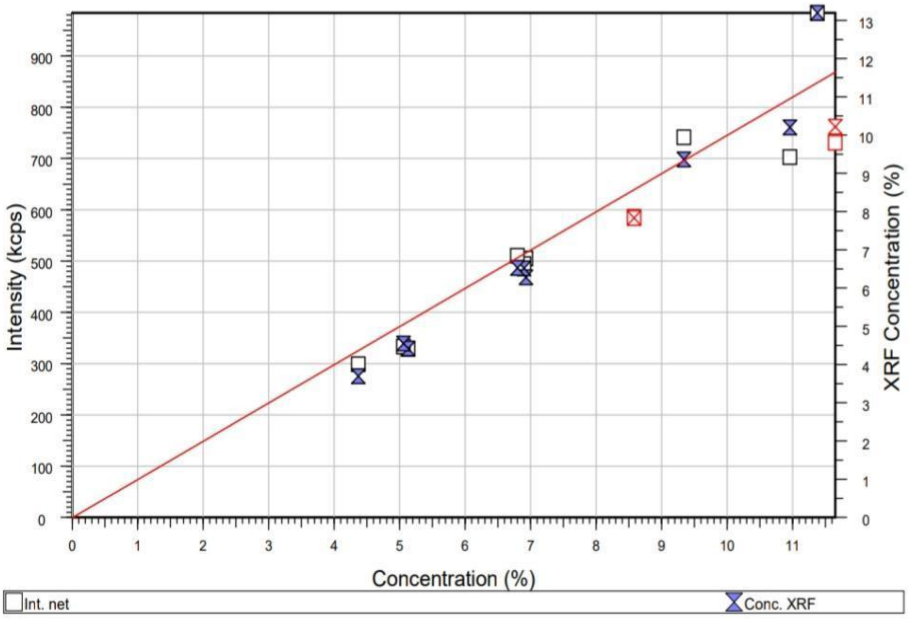

Calibration line of CaO

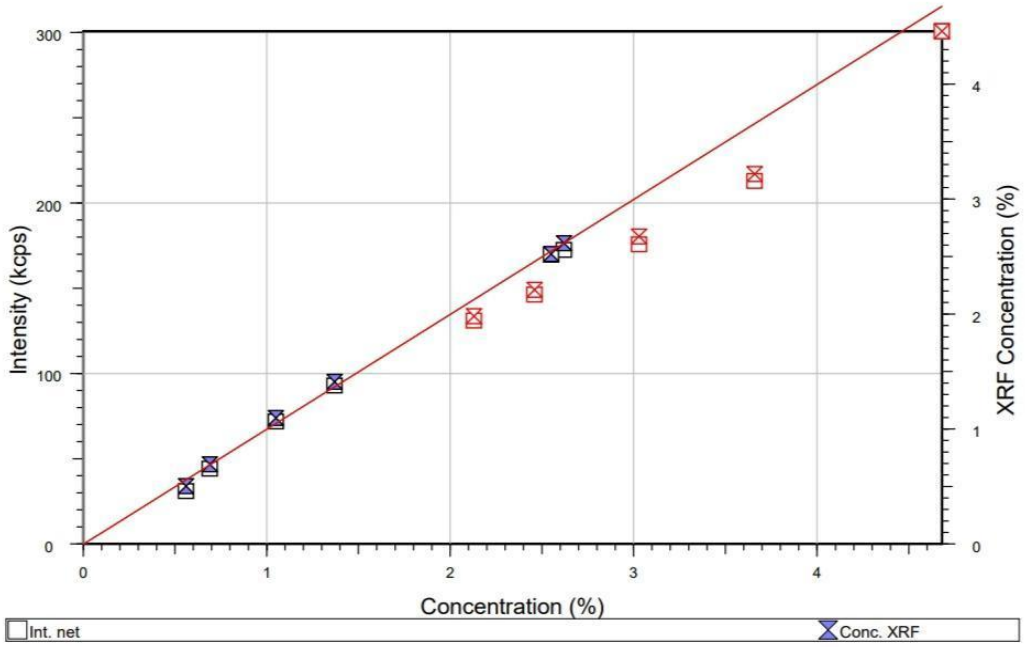

Calibration line of MgO

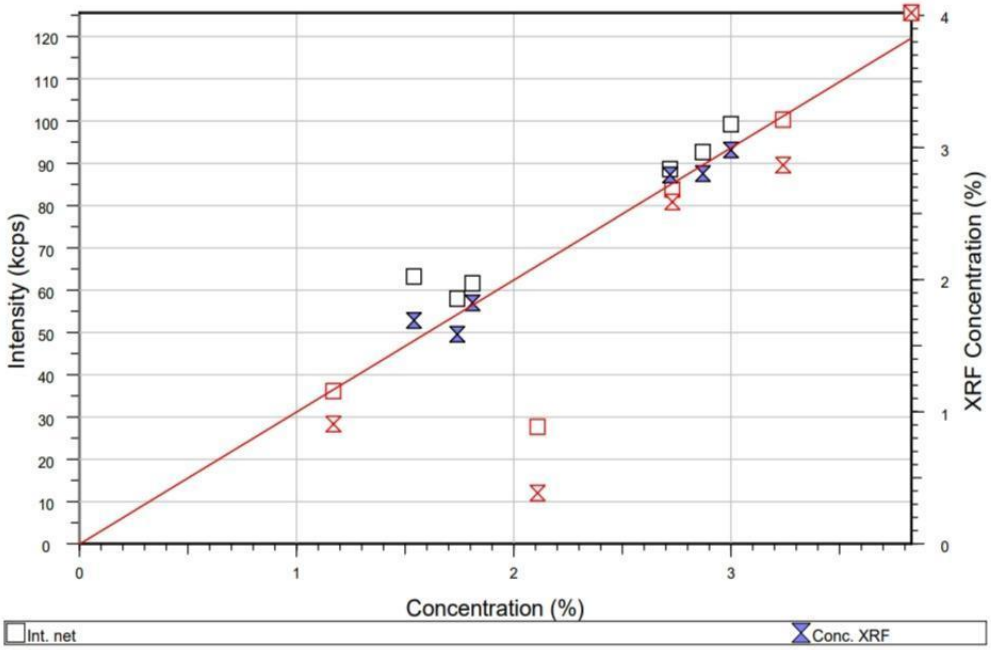

Calibration line of Na_2O

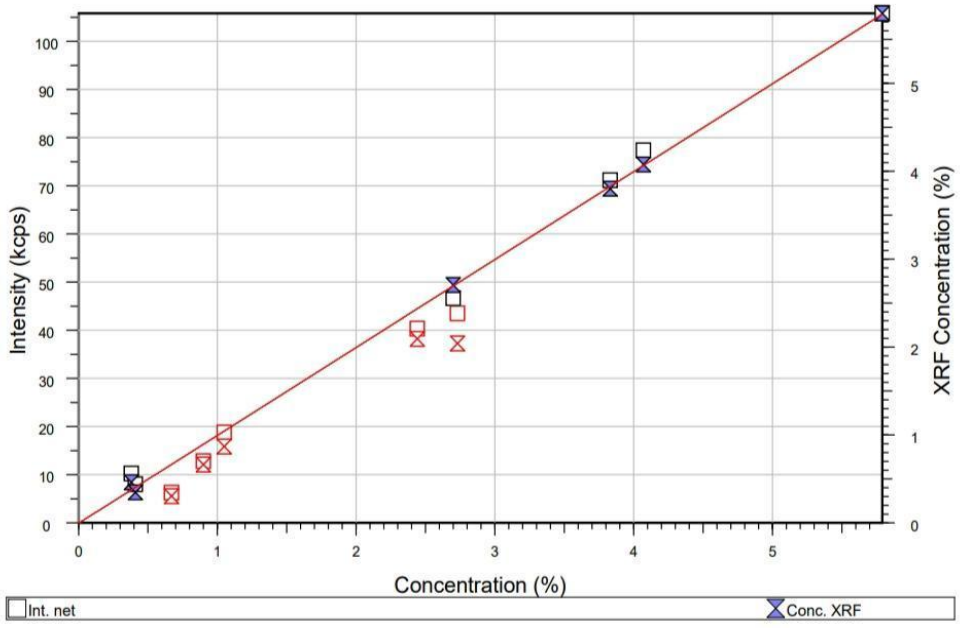

Calibration line of K_2O

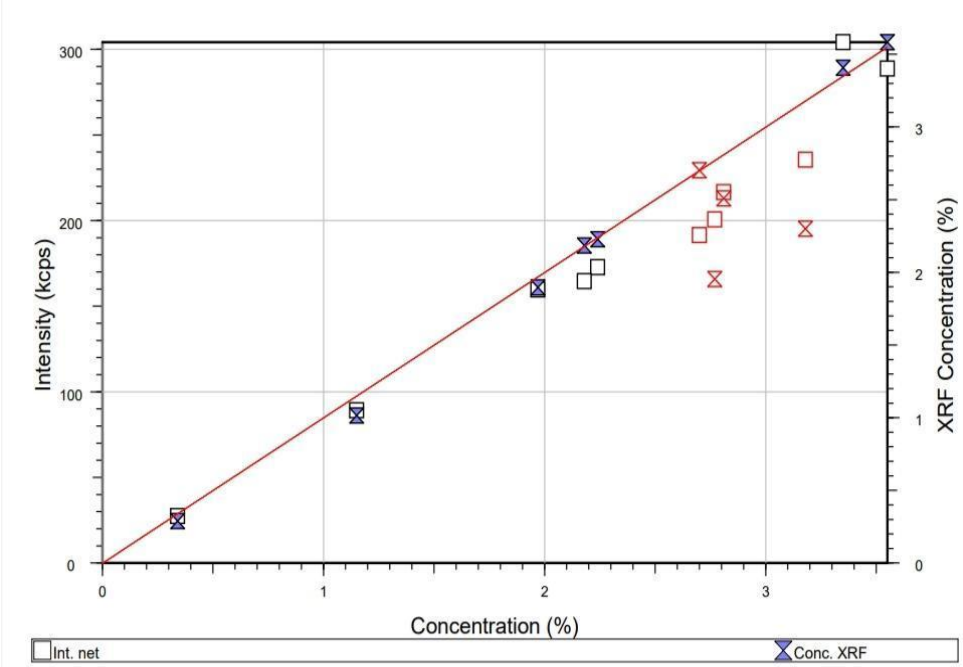

Calibration line of P_2O_5

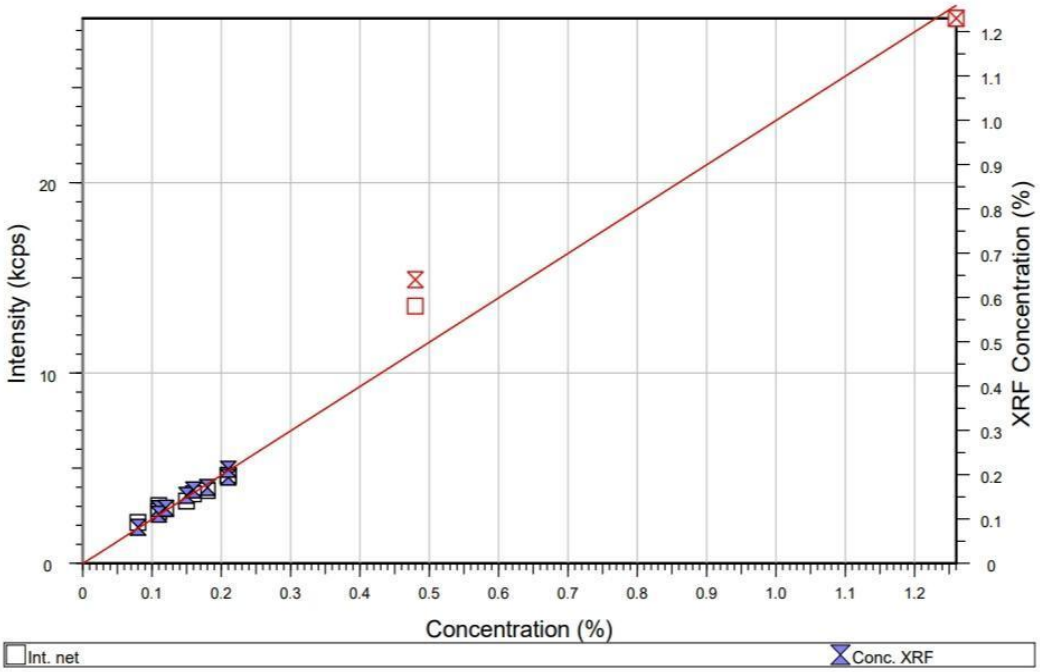

Fig 8: Calibration curves of major oxides

The pellets prepared from the Kaladgi samples were analyzed in S8 Tiger XRF at NCESS. The calibration lines were constructed using international standards SCo-1, SDC-1, SGR-1, MAG-1, BXN, JSd-1, JSd-2, JSd-3, JSI-1, JSO-1, JMS-1, JLK-1 and JSD-3. SDO-1, a shale standard, was measured as the unknown for accuracy and precision check.

2.4 Chemical Weathering Indices

Weathering indices are quantitative measures used to assess the degree of weathering or alteration undergone by rocks, minerals, soils, or other materials exposed to the Earth's atmospheric and environmental conditions over time. Different weathering indices focus on specific aspects, such as mineralogical changes, elemental composition, or physical properties.

Common weathering indices include the Chemical Index of Alteration (CIA), the Weathering Index of Parker (WIP), the Index of Weathering (IW), and the Plagioclase Index of Alteration (PIA). These indices typically involve calculations based on elemental abundances or ratios derived from geochemical data obtained through laboratory analyses or field measurements. Weathering indices help scientists and geologists better understand the extent and nature of weathering processes, which has implications for landforms, soil development, mineral exploration, and environmental studies.

Chemical Index of Alteration

Nesbitt and Young (1982) developed the Chemical Index of Alteration which defined the ratio of immobile to mobile elements. This quantifies the alteration of silicate minerals which are the primary constituents of rocks by evaluating the relative abundance of major elements. It is calculated based on the concentration ratios of certain oxides, typically silica (SiO_2), alumina (Al_2O_3), and sodium oxide (Na_2O), using the following formula:

$$\mathbf{CIA = [Al_2O_3 / (Al_2O_3 + CaO^* + Na_2O + K_2O)] * 100}$$

Where all the variables represent the molar amount of major element oxides and the CaO* represent the CaO fraction in silicate minerals only excluding CaO from carbonates and phosphates minerals.

The CIA ranges from 0 to 100, with higher values indicating more intense chemical weathering. A CIA value of 100 suggests complete chemical breakdown of primary minerals and the dominance of secondary mineral phases. Conversely, lower values indicate minimal weathering or the presence of unaltered primary minerals. The CIA is widely used in geological and environmental studies to evaluate weathering processes, paleoclimate reconstructions, and soil development, providing insights into the history and conditions of Earth's surface environments. However, the CIA value cannot give any details about instantaneous chemical weathering and seasonal climatic change (Nesbitt and Young,1982).

Chemical Index of Weathering

This provides information about the intensity of weathering processes and the degree of chemical alteration of the rock material. The CIW is calculated based on the elemental compositions of certain major oxides, typically including silica (SiO_2), alumina (Al_2O_3), iron oxide (Fe_2O_3), calcium oxide (CaO), magnesium oxide (MgO), sodium oxide (Na_2O), and potassium oxide (K_2O). The index is determined using the following formula:

$$\mathbf{CIW = ([(Al_2O_3 + Fe_2O_3) / (Al_2O_3 + Fe_2O_3 + CaO + MgO + Na_2O + K_2O)] * 100)}$$

Where all the variables represent molar amounts of major element oxides.

A higher CIW value indicates a greater degree of chemical weathering, with increased dissolution and removal of easily weathered minerals, leaving behind more resistant minerals in the sediments. A lower CIW value suggests limited chemical weathering and a higher proportion of unaltered or less weathered minerals in the sediment. The difference in the value of CIW between source rock and sediment reflects the chemical weathering experienced by the weathered material (Harnois,1987).

Plagioclase Index of Weathering

The PIA is a geochemical index used to evaluate the degree of chemical alteration specifically in plagioclase feldspar minerals within sedimentary rocks. Plagioclase feldspar is a common mineral found in many sedimentary rocks, and its alteration can provide valuable information about the weathering processes and the conditions under which the sediments were deposited. The PIA is calculated based on the relative abundances of specific elements within the plagioclase feldspar, typically including aluminum (Al), sodium (Na), and potassium (K). The index is determined using the following formula:

$$\mathbf{PIA=[(Al_2O_3-K_2O)/(Al_2O_3+CaO^*+Na_2O-K_2O)] * 100}$$

A higher PIA value indicates a greater degree of alteration or weathering of the plagioclase feldspar, with an increased loss of sodium and potassium and an enrichment of aluminum. A lower PIA value suggests minimal alteration or the presence of relatively unaltered

plagioclase feldspar. PIA is a modification of CIA which is equivalent to projecting the solid circle onto the A-CN join from the K-feldspar composition (Fedo et al., 1995).

Weathering Index of Parker

$$\mathbf{WIP = (Al_2O_3 + Fe_2O_3) / (Al_2O_3 + Fe_2O_3 + CaO + Na_2O) * 100}$$

Where the major element oxides are represented in molar proportion and CaO* represents the fraction in silicate minerals only. A higher WIP value indicates a greater degree of chemical weathering and suggests that the sedimentary rock has undergone significant alteration, with the loss of more easily weathered elements like calcium and sodium. Conversely, a lower WIP value suggests a lesser degree of weathering and the presence of less altered or more pristine sediments. The WIP has the opposite trend in comparison with CIA, CIW and PIA. High WIP values suggest low degree of chemical weathering whereas lower WIP value indicates intense weathering.

Ruxton Ratio

Ruxton (1968) proposed a simple weathering index, which has been termed the Ruxton Ratio. Ruxton stated that his simple weathering index is best suited for weathering profiles developed on uniform acid to intermediate bedrock. The Ruxton Ratio relates silica loss to total element loss and considers alumina to be immobile during weathering. Ruxton tested R on weathering profiles developed on igneous and metamorphic rocks from humid regions and found that R correlated well with total-element loss.

Index of Compositional Variability

The Index of Compositional Variability (ICV) can be used to interpret the compositional maturity of a source rock (Cox et al.,1995). It is calculated by using the equation as follows:

$$\mathbf{ICV=(Fe_2O_3+K_2O+Na_2O+MgO+CaO+MnO+TiO_2)/Al_2O_3}$$

ICV measures the transition of minerals from the primary phase to the secondary phase. The lower ICV value (<1.0) indicates a compositionally mature rock which has undergone several weathering cycles. When ICV is high (>1.0), the rock is immature and likely experienced a single weathering cycle.

W index

The W index is a geochemical weathering index developed by the statistical analysis of elements' behavior during igneous rock weathering (Ohta and Arai, 2007). This is different from other chemical indices (except ICV) because the W index is based on 8 major oxides whereas others depend on three or four major oxides. The W index can be explained by using MFW diagram (Ohta and Arai,2007). The M F and W can be calculated using following equation;

$$M = -0.395*\ln SiO_2+0.206*\ln TiO_2-0.316*\ln Al_2O_3+0.160*\ln Fe_2O_3+0.246*\ln MgO+ 0.368*\ln CaO+0.073*\ln Na_2O-0.342*\ln K_2O+2.266$$

$$F = 0.191*\ln SiO_2-0.397*\ln TiO_2+0.020*\ln Al_2O_3-0.375*\ln Fe_2O_3-0.243*\ln MgO+0.079*\ln CaO+0.392*\ln Na_2O+0.333*\ln K_2O-0.892$$

$$W= 0.203*\ln SiO_2+0.191*\ln TiO_2+0.296*\ln Al_2O_3+0.215*\ln Fe_2O_3-0.002*\ln MgO- 0.448*\ln CaO-0.464*\ln Na_2O+0.008*\ln K_2O-1.374$$

Palaeotemperature

CIA values can also be used to calculate the paleotemperature by using the formula of Cao et al., (2019).

$$\mathbf{T\ (^0C) = 0.56*CIA - 25.7}$$

This relationship is only applicable for the value of CIA range of approximately 50 to 90, corresponding to a paleotemperature range of ~3 ^{0}C to 25 ^{0}C with an uncertainty of approximately ±5 ^{0}C (Cao et al., 2019).

MIA

MIA is another weathering index proposed by Voicu et al., (1997) to measure the intensity of chemical weathering. MIA has a close relationship with CIA. It is represented using an equation;

$$\mathbf{MIA = 2*(CIA-50)}$$

When the MIA ranges from 0 to 20%, they are designated as incipient, whereas 20-40% are weak, 40-60% are moderate and 60-100% are intense weathering.

3. RESULTS

3.1 Major Oxide Geochemistry

The geochemical composition of the Kaladgi sediments is presented in Table 4. The sediments show high concentration and affinity towards SiO_2 ranging from 57.55% to 98.76% with average value of 72.43%, and with that Al_2O_3 shows moderate composition compared with other oxides with range of 0.81% to 22.74% and having an average concentration of 12.93%. The presence of other major elements shows a great deviation from Si and Al concentration. TiO_2, FeO and MgO vary from 0.85% to 1.06%, 0.15% to 12.16%, 0 to 3.28%, with average concentration of 0.47%, 5.48%, 1.23%, respectively. The concentration of K_2O, Na_2O and CaO are relatively low with the range of 0.03% to 3.21%, 0.07% to 6.25% and 0.05% to 4.3%. MnO and P_2O_5 shows an average range of concentration 0.008%, 0.095%. The LOI values of the sediments ranges from 1.78% to 0.05 which expresses the relatively low amount of volatile components present in the sediments. The high silica content in the sediments suggests that it is predominantly silica rich and has undergone intense weathering where silica is resistant to weathering, and other less resistant minerals have been altered.

Table 4: Major oxide data of Kaladgi sedimentary rocks

Formation and Lithology	Saundatti Quartzite	Manoli Shale	Manoli Shale	Yargatti Shale	Tulsigeri Quartzite	Jallikatti Phyllite	Tulsigeri Quartzite
Sample ID	KD18-4	KD18-5	KD18-6	KD18-7	KD18-110	KD18-129	KD18-130
	Wt%	Wt%	Wt%	Wt%	Wt%	Wt%	Wt%
SiO_2	61.05	61.05	60.71	65.01	98.76	63.490	96.06
TiO_2	0.85	0.85	0.83	0.71	0.02	1.06	0.07
Al_2O_3	17.04	17.04	17.91	17.39	0.81	16.11	2.91
MnO	0.01	0.01	bdl	bdl	bdl	bdl	bdl
Fe_2O3	12.16	12.16	11.97	6.62	0.15	9.8	0.62
CaO	0.09	0.09	0.08	0.12	0.06	0.09	0.05
MgO	2.39	2.39	1.37	3.21	bdl	2.31	bdl
Na_2O	0.13	0.13	0.12	0.14	0.03	0.12	0.04
K_2O	4.42	4.42	5.27	5.46	0.11	0.96	0.07
P_2O_5	0.09	0.09	0.09	0.08	0.01	0.12	0.01
LOI	1.78	1.78	1.64	1.26	0.05	0.96	0.15

NB: bdl- below detection limit

Arlikatti Shale	Arlikatti Shale	Tulsigeri Quartzite	Manoli Shale	Manoli Shale	Halkurki Shale	Halkurki Shale	Halkurki Shale
KD18-131	KD18-132	KD18-133	KD18-134	KD18-135	KD18-232	KD18-233	KD18-234
Wt%	Wt%	Wt%	Wt%	Wt%	Wt%	Wt%	Wt%
57.55	69.45	89.20	94.34	86.980	74.14	65.990	68.64
1.04	0.67	0.1	0.07	0.08	0.56	0.7	0.68
21.89	15.75	8.05	2.04	4.97	14.65	16.52	15.61
bdl	bdl	bdl	bdl	bdl	bdl	bdl	bdl
9.92	7.68	1.46	2.79	6.27	2.34	8.11	6.25
0.08	0.07	0.05	0.05	0.05	1	0.92	1.06
1.89	1.26	bdl	bdl	bdl	1.97	1.96	1.8
0.12	0.1	0.05	0.04	0.06	0.29	0.26	0.22
6.25	4.36	0.74	0.49	1.34	2.94	3.97	3.57
0.09	0.1	0.01	0.02	0.03	0.46	0.39	0.27
1.17	0.57	0.32	0.17	0.21	1.65	1.19	1.9

Badami (Cave Temple Arenite) Sandstone	Manoli Shale	Manoli Shale	Saundatti Quartzite	Manoli Shale	Arlikatti Shale	Arlikatti Shale
KD18-235	KD18-236	KD18-237	KD18-238	KD18-239	KD18-248	KD18-249
97.26	62.86	65.77	91.62	68.40	66.99	60.17
0.02	0.69	0.37	0.03	0.51	0.67	0.62
1.97	20.48	22.74	6.37	17.33	19.01	21.76
bdl	bdl	bdl	bdl	bdl	0.07	0.05
0.16	6.2	1.53	0.32	5.97	6.24	8.93
0.05	0.08	0.07	0.05	0.3	0.18	0.56
bdl	2.53	1.78	bdl	3.28	1.73	1.82
0.03	0.14	0.16	0.04	0.18	0.59	0.45
0.43	6.04	7.11	1.45	3.17	3.56	4.75
0.01	0.05	0.05	0.01	0.09	0.08	0.08
0.08	0.91	0.43	0.1	0.98	0.87	0.82

4. DISCUSSION

4.1 Classification of Kaladgi siliciclastic rocks

According to Herron and Pettijohn classification diagrams, most of the Kaladgi sediments comes under wacke, litharenite to quartz arenite, and arkose to subarkose. Shales from Simikeri and Lokapur subgroup namely Manoli Shale and Yargatti Shale shows $\log(SiO_2/Fe_2O_3)$ from 0.5 to 0.7 which fall in the field of wacke. Not only Manoli Shale and Yargatti Shale falls in wacke classification, Halkurki Shale from Badami Group also show the same trend (Figs. 9 and 10). One of the Tulsigeri Sandstone samples from Simikeri Subgroup indicates litharenite and Saundatti Sandstone from Lokapur Subgroup falls in subarkose field. Saundatti Sandstone from Lokapur Subgroup and Tulsigeri Sandstone plots in Fe-sand field. The shales which fall on wacke may contain a significant proportion of lithic fragments derived from various source rocks and may have been deposited in mixed sediments environment. Saundatti Sandstone which falls in subarkose have presence of feldspar, along with varying amounts of quartz and lithic fragments. Tulsigeri Sandstone which shows a transformation from litharenite to quartz arenite with decrease in lithic content and increase in quartz content. Both Saundatti Sandstone and Manoli Shale fall in the field of Fe-sand which indicate elevated levels of iron oxide or iron bearing minerals in them.

In the Pettijohn's classification diagram, most shales fall in litharenite to arkose fields. Two shales from Simikeri Subgroup (Arlikatti) show wacke composition. Halkurki Shales and one of the shales from Lokapur Subgroup fall in litharenite field which indicate considerable amount of lithic fragments likely present in it. Along with the shales, Tulsigeri and Saundatti Sandstones show subarkose which represent an intermediate stage between arkose (high feldspar content) and litharenite (quartz rich). Badami Sandstone, Manoli Shale and Saundatti Sandstone fall in the field of sublitharenite and represent well sorted and matured compositions compared to litharenite and subarkose. According to Na_2O and K_2O composition ratio, it appears that alkali feldspars are more abundant than sodic feldspars in the sandstones. Therefore, compositionally the Kaladgi Sandstones plot in the potassic side than sodic (Fig. 11).

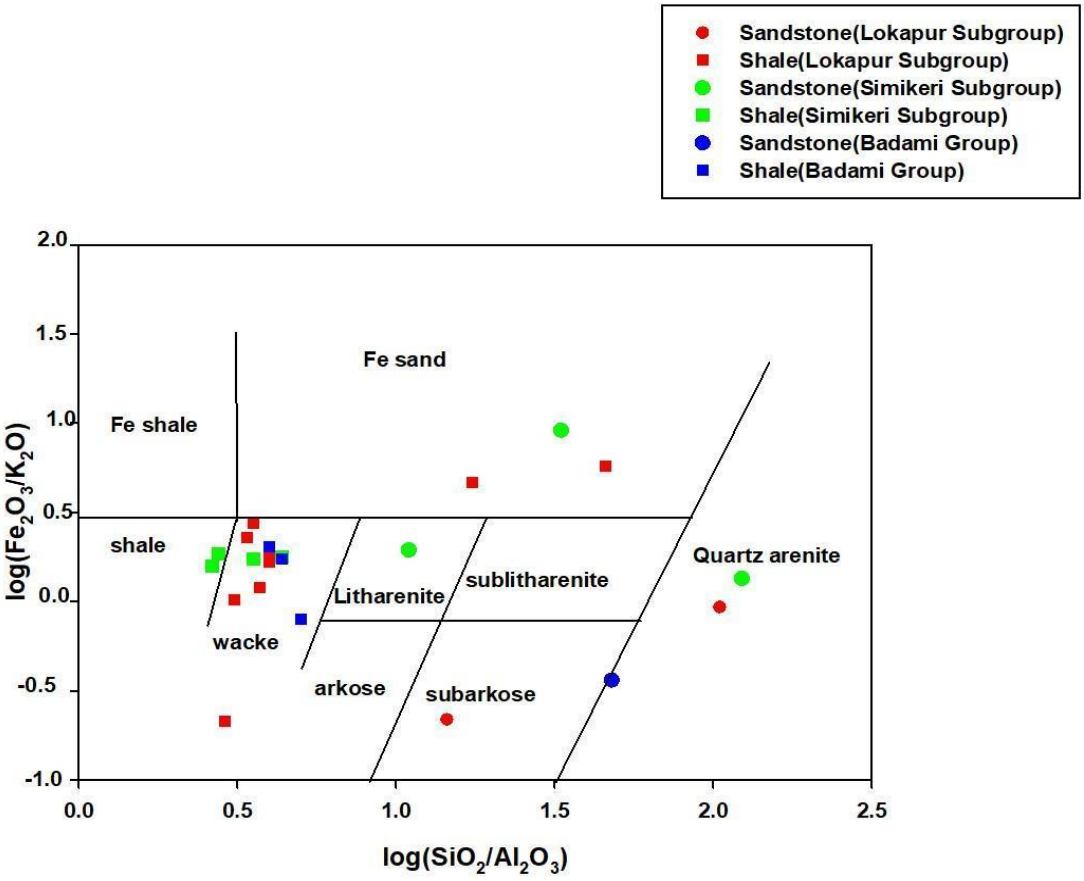

Fig. 9: Kaladgi siliciclastic rocks plotted in Herron's classification diagram

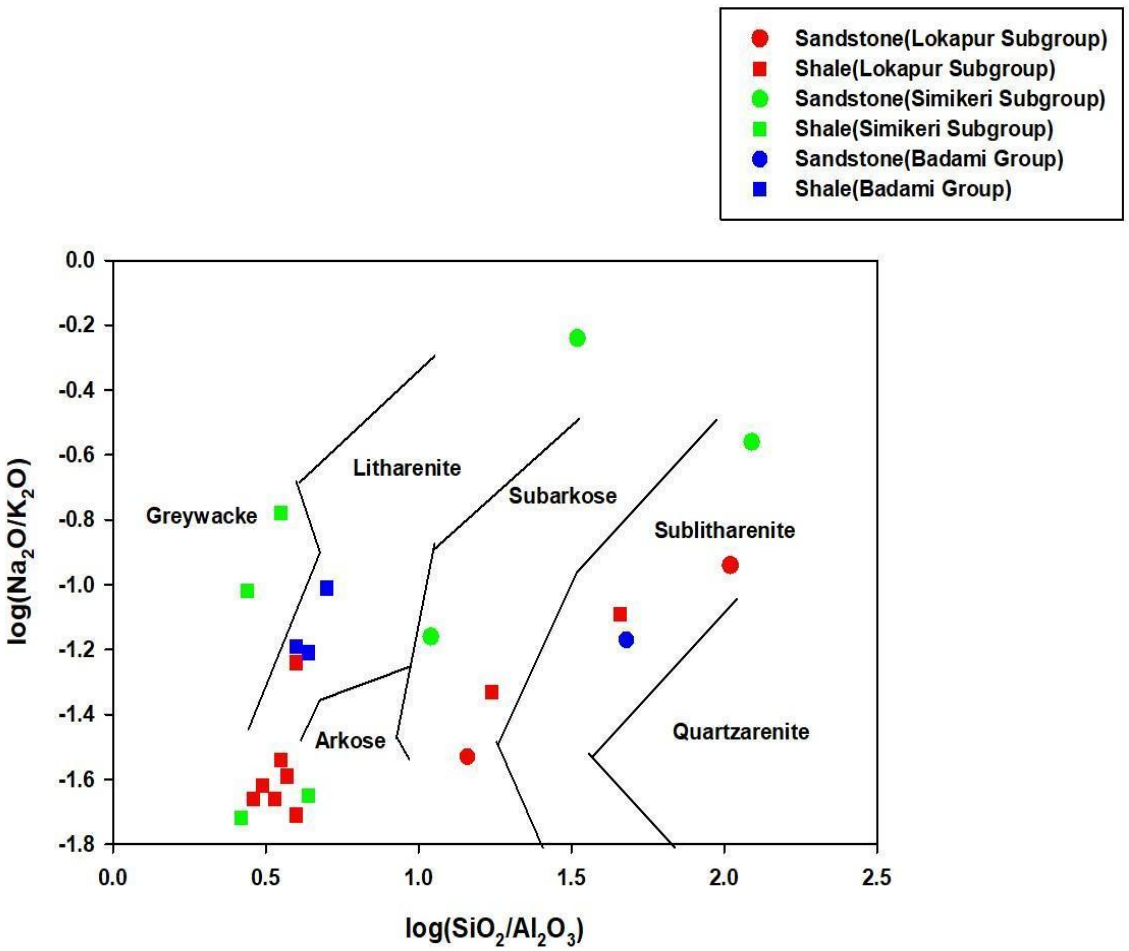

Fig. 10: Kaladgi siliciclastic rocks plotted in Pettijohn's classification diagram

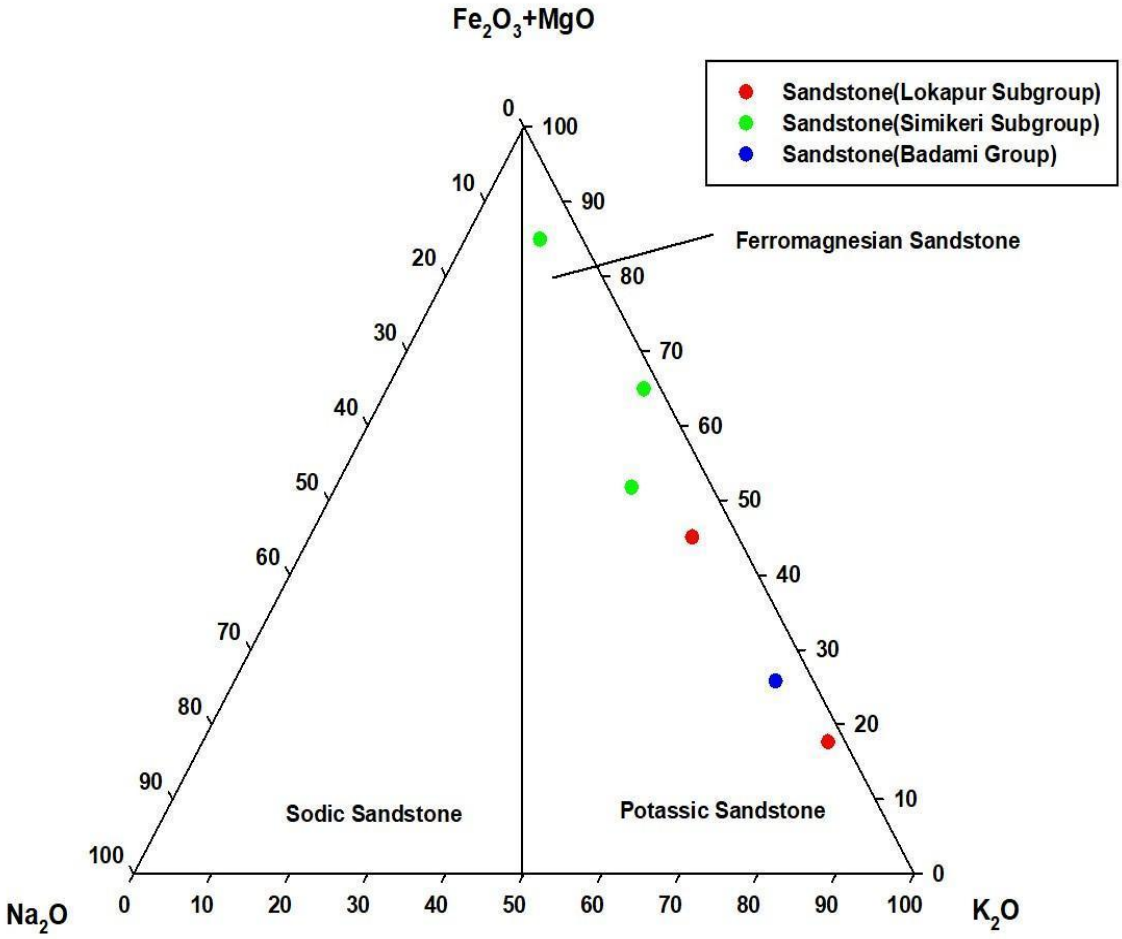

Fig. 11: Compositional classification of sandstones of Kaladgi basin

4.2 Weathering Intensity in the source area

The results from major element analysis are further used to calculate the chemical weathering indices. The chemical weathering indices calculated for Kaladgi sedimentary rocks are shown in Table 5. The CIA values of sediments range from 69.03 to 92.60. This reveals that the source areas of sediments have undergone moderate to strong chemical weathering rate. It implies that most of the feldspar has been weathered in to clay. The CIW values of sediments range from 98.46 to 83.64 indicating high weathering in the source area. It is also possible that the sediments have undergone more than one weathering cycle. The PIA value ranges from 81.35 to 97.78 indicating that most of the plagioclase in the sediments got altered to clay. A higher PIA value suggests that the source area experienced increased chemical weathering. The Ruxton ratio of the sediments range from 104.73 to 2.70 which reveals that intensive to weak weathering.

Table 5: Chemical weathering indices of Kaladgi sedimentary rocks

Sample ID	KD18-4	KD18-5	KD18-6	KD18-7	KD18-110	KD18-129	KD18-130
CIA	69.03	76.75	73.80	73.23	74.48	70.35	92.60
CIW	87.02	97.83	97.56	97.49	83.64	97.81	94.89
PIA	82.44	97.01	96.40	96.24	81.35	96.41	94.76
WIP	0.01	6.78	4.01	9.09	0.01	6.63	0.01
RUXTON RATIO	104.70	3.58	3.39	3.37	121.93	3.94	33.02
ICV	0.63	1.18	1.10	0.94	0.46	1.20	0.29
W INDEX	-1.56	-0.20	0.43	0.20	-1.66	0.49	-0.83
Vogt Ratio	14.88	9.20	14.76	7.38	10.22	9.76	33.11
K/Al	0.27	0.26	0.29	0.31	0.14	0.37	0.02
M	1.85	2.73	2.80	2.05	2.16	8.43	2.88
F	0.59	0.14	0.67	0.34	1.10	0.30	0.36

Table 5 contd.

Sample ID	KD18-131	KD18-132	KD18-133	KD18-134	KD18-135	KD18-232	KD18-233
CIA	75.49	75.86	89.21	74.81	75.19	72.79	72.08
CIW	98.46	98.18	97.89	92.87	96.33	86.46	88.72
PIA	97.78	97.42	97.67	90.60	94.89	83.32	85.34
WIP	5.48	3.67	0.04	0.02	0.06	5.60	5.61
RUXTON	2.63	4.41	11.08	46.25	17.50	5.06	3.99

RATIO							
ICV	0.88	0.90	0.30	1.69	1.57	0.62	0.47
W INDEX	-0.89	0.60	-0.50	-0.70	-0.60	-0.06	2.95
Vogt Ratio	15.09	16.13	8.79	28.11	57.36	10.22	11.63
K/Al	0.29	0.28	0.09	0.24	0.27	0.20	0.24
M	7.92	6.42	1.93	3.22	5.64	4.80	11.24
F	0.12	0.33	0.44	0.37	0.40	0.51	0.40

Table 5 contd.

Sample ID	KD18-234	KD18-235	KD18-236	KD18-237	KD18-238	KD18-239	KD18-248
CIA	71.73	76.48	74.76	73.77	78.68	81.59	78.68
CIW	87.21	93.35	98.20	98.31	97.60	97.32	93.61
PIA	83.69	91.47	97.38	97.47	96.84	96.68	92.11
WIP	5.15	0.02	7.24	5.22	0.06	9.19	4.95
RUXTON RATIO	4.40	49.37	3.07	2.89	14.38	3.95	3.52
ICV	0.87	0.35	0.77	0.48	0.29	0.76	0.68
W INDEX	-0.35	-1.50	0.28	-0.11	-1.11	0.31	-0.19
Vogt Ratio	11.94	30.00	10.70	17.00	86.89	6.53	13.82
K/Al	0.23	0.22	0.29	0.31	0.23	0.18	0.19
M	9.40	0.49	5.64	1.80	0.62	6.48	30.33
F	0.41	0.69	0.65	0.54	0.73	0.36	0.48

Table 5 contd.

Sample ID	KD18-249
CIA	75.93
CIW	92.52
PIA	90.43
WIP	5.25
RUXTON RATIO	2.77
ICV	0.79
W INDEX	-0.35
Vogt Ratio	15.58
K/Al	0.22
M	10.67
F	0.45

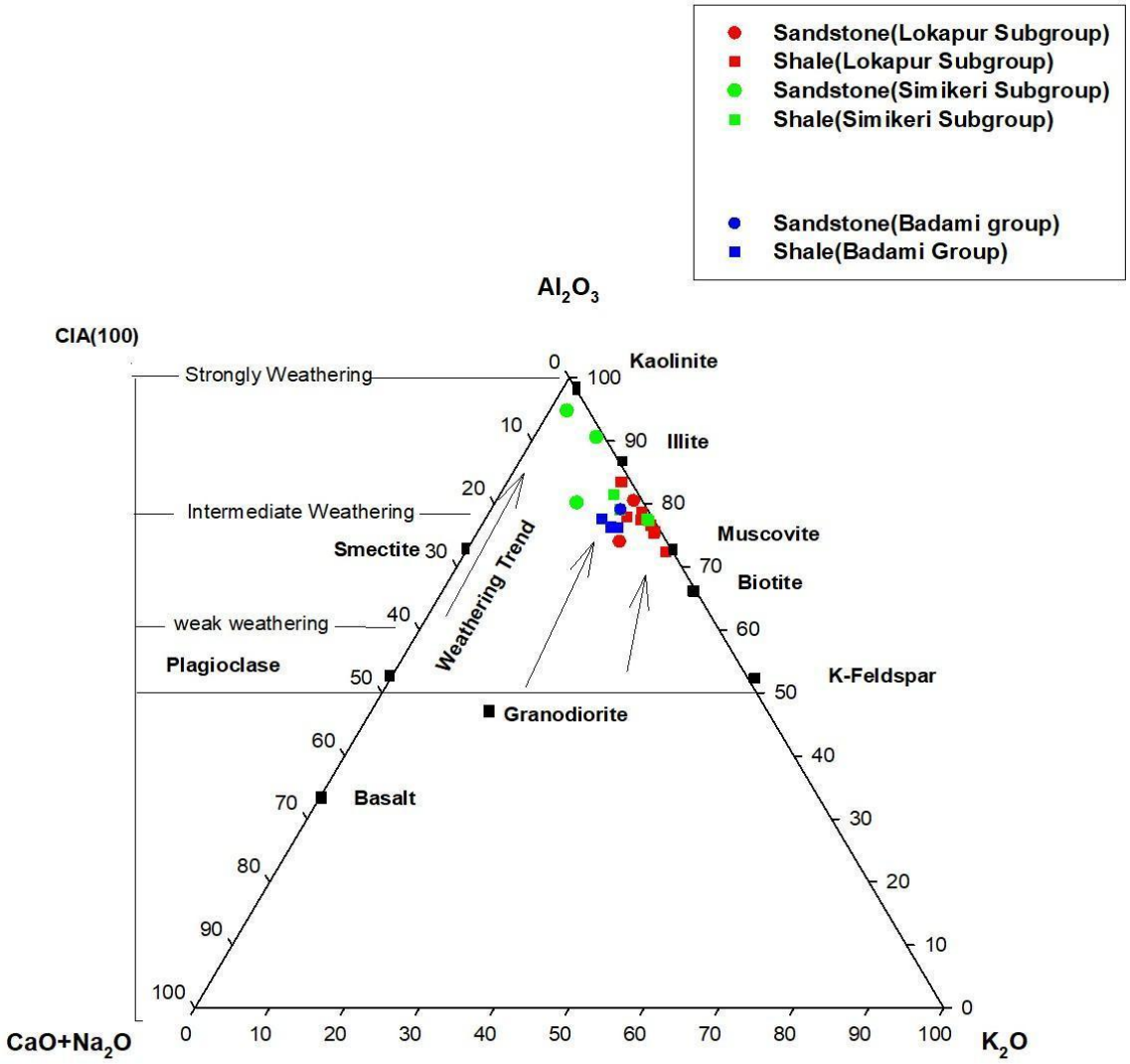

Fig. 12: A-CN-K diagram

From the A-CN-K diagram (Fig. 12), it shows a general weathering trend towards Al_2O_3 which indicates high clayey content that have experienced significant chemical weathering and alteration. These rocks may indicate a mature sedimentary system with a long weathering history. And the CIA values reach nearly 100 and indicates high weathering intensity. The Tulsigeri sandstones from the Simikeri Subgroup has undergone strong weathering (Fig. 14). Most of the shales show similarities in their composition and have undergone intermediate to

strong weathering. All sediments shown have >70% Al_2O_3 content and represent a proportionality towards alumina compared to calcic, sodic and potassic fields.

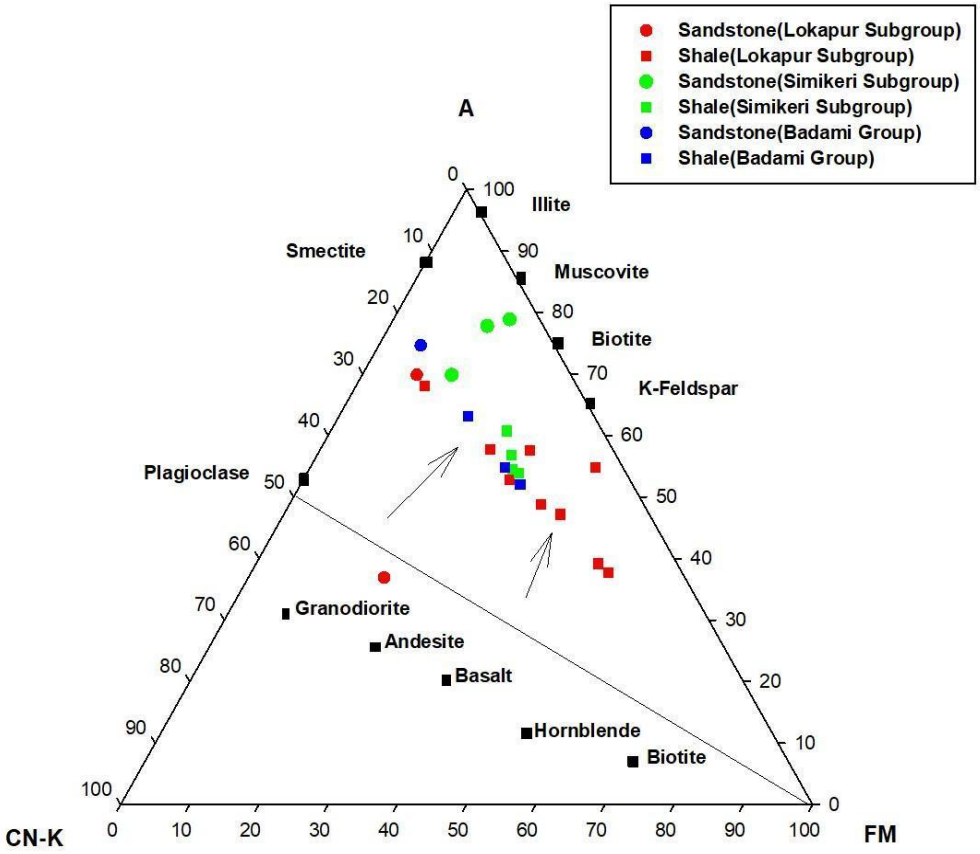

Fig. 13: A-CNK-FM Diagram

The A-CNK-FM diagram (Fig. 13) reveals a strong trend towards the A end member of A-CNK-FM. The shales from Lokapur Subgroup, Simikeri Subgroup and Badami Group fall in the A end member which suggests that they contain a significant amount of Al_2O_3. Analyzing the mineral composition of shales, including the presence of alkali feldspar, can provide insights into their origin, the rocks they were derived from, the environment of deposition, and the subsequent diagenetic processes they have undergone. The diagram shows that the sandstones from Lokapur Subgroup, Simikeri Subgroup, Badami group also have a trend towards the A endmember which indicate that they contain a relatively higher proportion of Al_2O_3 rich clay minerals and has undergone high degree of chemical weathering.

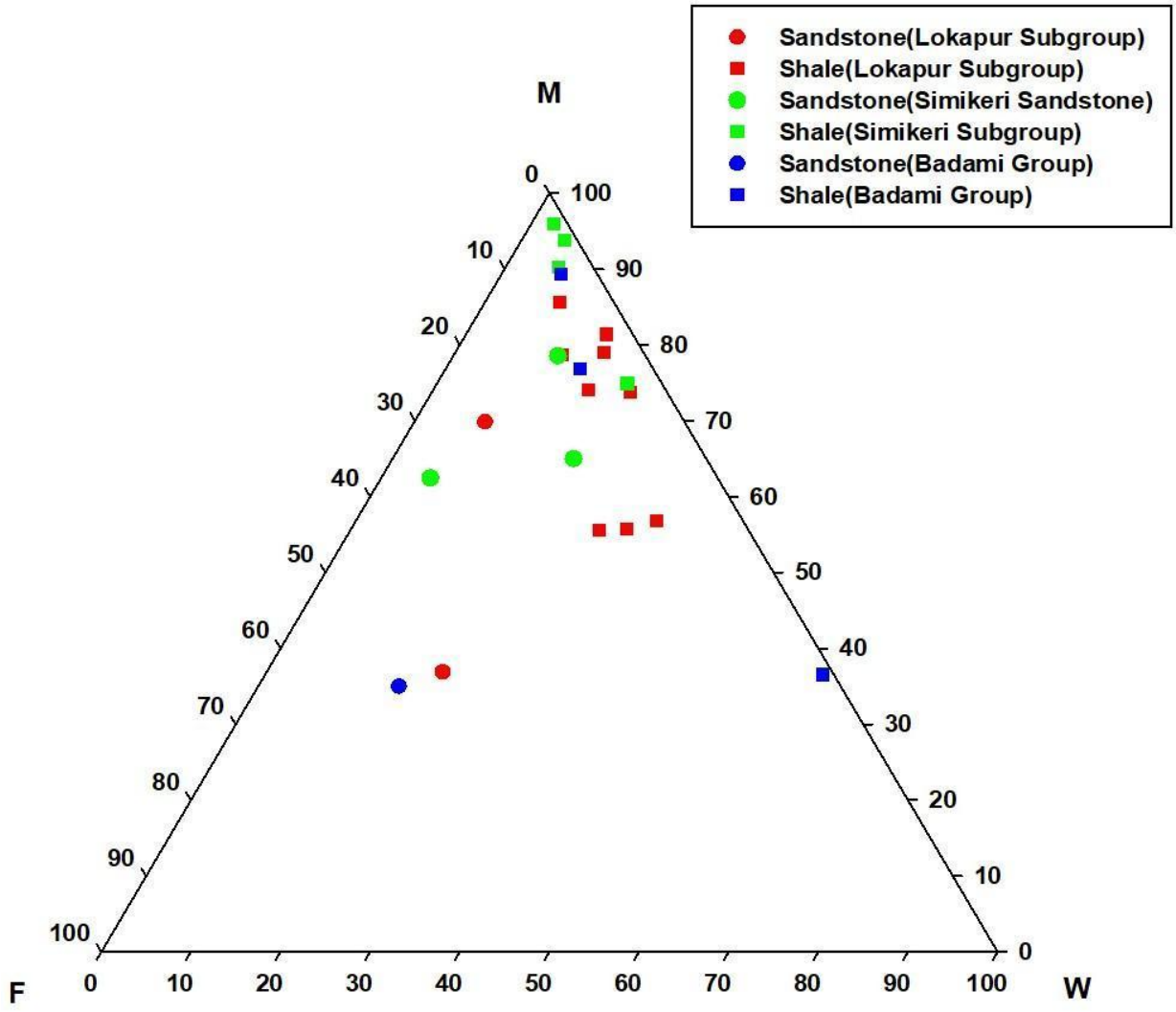

Fig. 14: MFW diagram of Kaladgi sedimentary rocks

The MFW diagram (Fig. 14) suggests that the Kaladgi sediments have undergone high weathering and has intermediate composition. The diagram shows a trend towards intense weathering. The intense weathering can lead to the breakdown and alteration of minerals, resulting in the formation of secondary minerals and the release of soluble ions. The diagram implies that the sediments have undergone transportation and deposition which selectively removed mafic and felsic minerals while concentrating the weathering products. This could occur when sediments are transported over long distances. The diagram also reveals the

composition of the source rock/s as intermediate from which the sediments evolved and it can to help identify the parent rocks that underwent weathering processes.

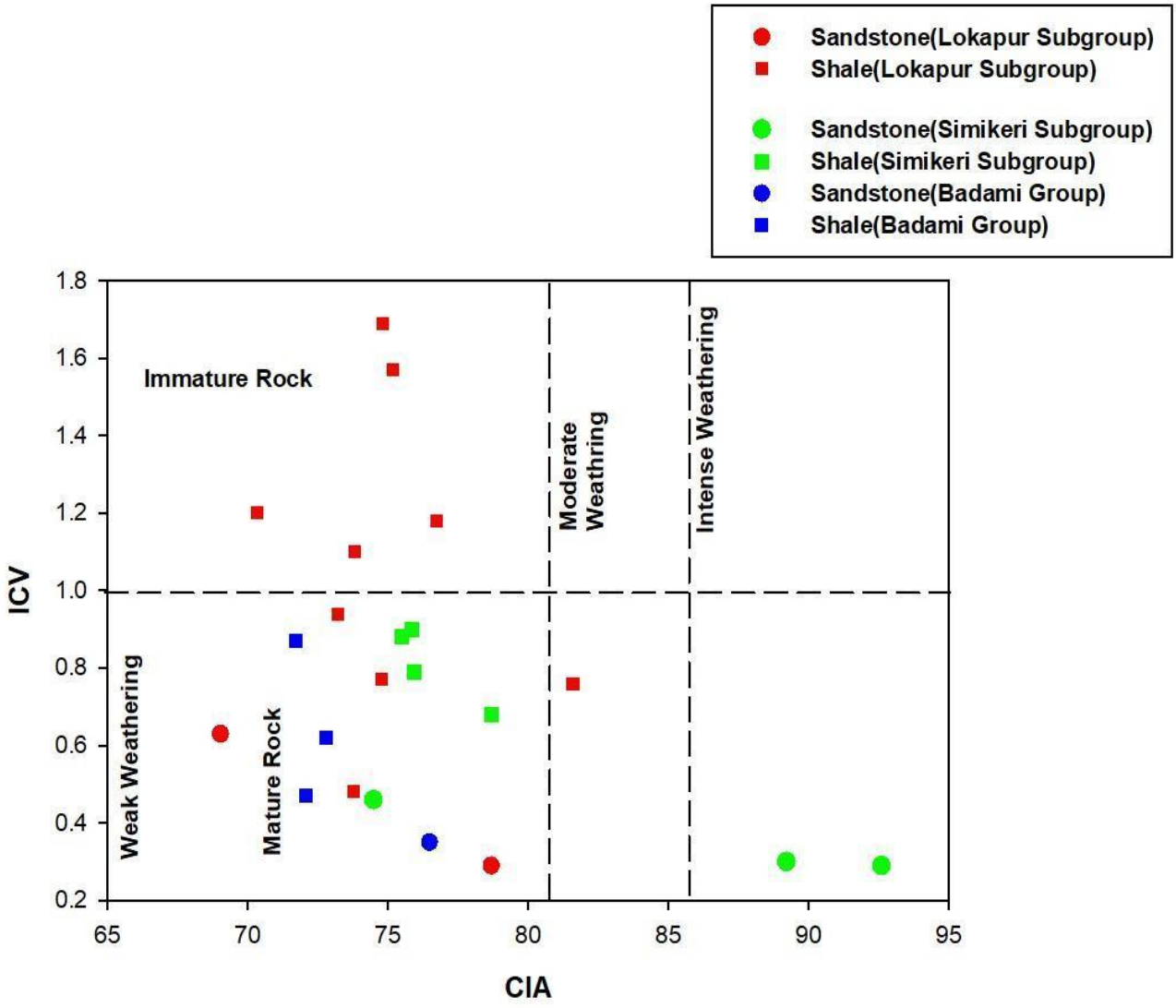

Fig. 15: ICV vs CIA plot

The ICV of Kaladgi sediments varies from 0.25 to 1.65. This shows that most of the Kaladgi sediments show high maturity. In the ICV vs. CIA diagram (Fig. 15), implies that majority of the Shales from Lokapur Subgroup are immature. As shales, being fine-grained, typically have low ICV values because their mineral composition is relatively homogenous. Whereas the Shales from Badami Group and Simikeri Subgroup shows maturity. The sandstones

from Lokapur Subgroup and Badami Group shows compositional maturity but underwent moderate to strong weathering but sandstones from Simikeri Subgroup underwent intense chemical weathering and also shows compositional maturity.

4.3 Provenance of sediments

The TiO_2 vs. Al_2O_3 diagram (Fig. 16) shows that the Kaladgi sediments have felsic to intermediate provenance. From the major oxide composition and the chemical weathering indices, it is evident that Kaladgi basin sediments were derived from a highly weathered felsic dominant complex. The cratonic basement rocks of Dharwar Craton and the late Archean granitoids of the craton fall into such a category. It is likely that those rocks along with some amount of mafic rocks would have contributed majority of the sediments to Kaladgi basin during its evolution.

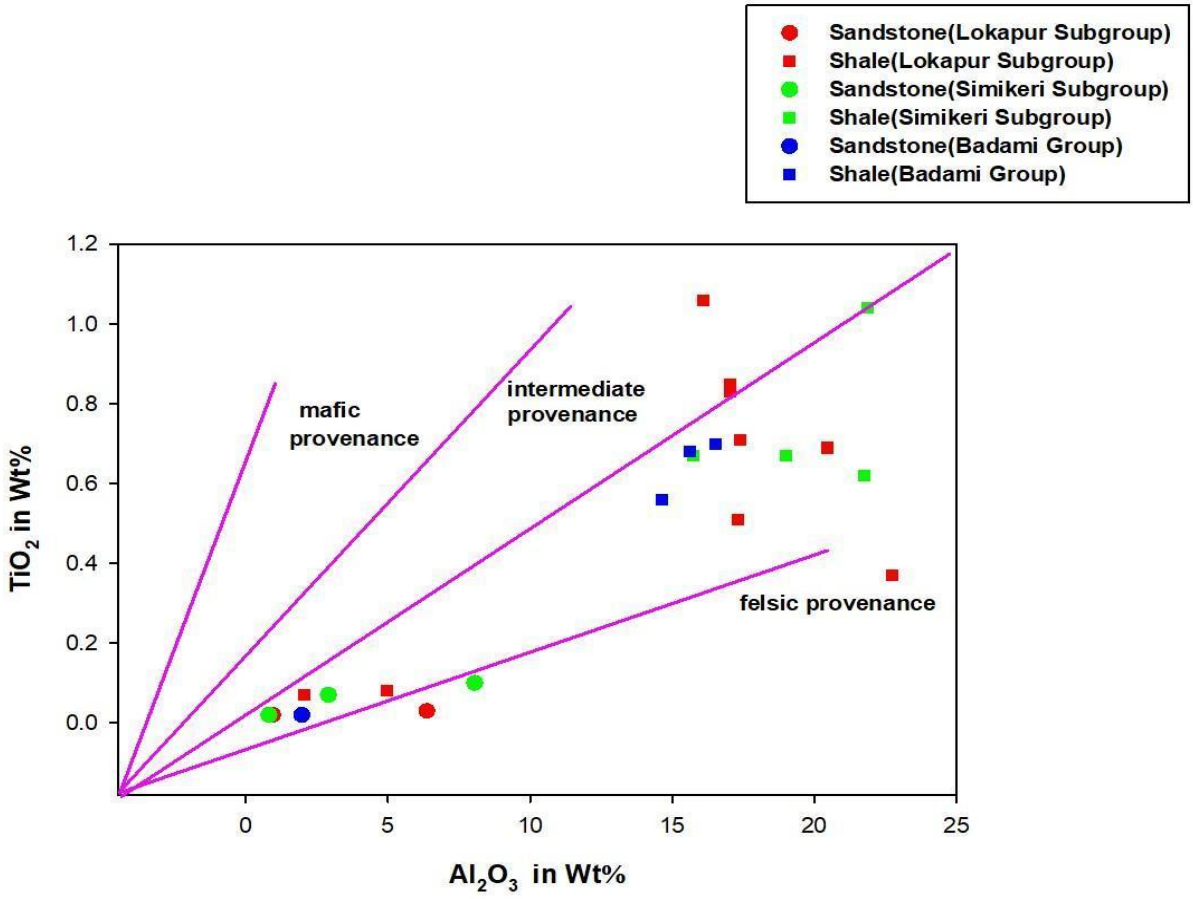

Fig. 16: TiO_2 vs Al_2O_3 plot

5. CONCLUSIONS

The geochemical studies conducted on the siliciclastic rocks of the Proterozoic Kaladgi Supergroup in Karnataka have provided valuable insights into the composition and evolution of these rocks. Through careful analysis and interpretation of various geochemical parameters, several conclusions can be drawn from these studies.

1. The geochemical data reveals a mature nature of the siliciclastic rocks, characterized by high quartz content and low proportions of unstable minerals. This maturity can be attributed to extensive weathering and erosion processes that occurred over an extended period.
2. The Al_2O_3 content of the siliciclastic rocks provides insights into the degree of chemical weathering. Higher Al_2O_3 values imply intense weathering, suggesting a long period of exposure and erosion of source rocks before deposition. This indicates that the sediments underwent extensive chemical breakdown processes during transportation.
3. Most of the Kaladgi sedimentary rocks exhibit intermediate to felsic provenance which indicates high Al_2O_3 content while some contain intermediate provenance which reveals a mixture of felsic and mafic source rocks.
4. The major element composition of the Kaladgi siliciclastic rocks indicates a predominantly old cratonic source, likely the Dharwar rocks, contributed most of the sediments to the basin.

6. REFERENCES

Absar, N., & Sreenivas, B. (2015) Petrology and geochemistry of greywackes of the~ 1.6 Ga Middle Aravalli Supergroup, northwest India: evidence for active margin processes. International Geology Review, 57(2), 134-158.

Adegbe, OC, Jinoih, YA, (2013) Geochemical Fingerprints, Implication for Provenance. Tectonic and Depositional Settings of Lower Benue Trough Sequence, Southeastern Nigeria. Journal of Environment and Earth Science, 3,10.

Balesh, K.B. Das, S.S., Dayal, AM, Kale, VS, (1999) Occurrence of tiny digitate stromatolite [Yelma digitate grey, 1984], Yargatti Formation, Bagalkot Group. Kaladgi basin, Karnataka, India Current Science, 75, 360-365.

Baulaz, B., Mayayo, MJ, Fernandez-Nieto, C. Lopez, JMG, (2000). Geochemistry of Precambrian and Paleozoic siliciclastic rocks from the Iberian Range (NE Spain) implications for source-area weathering sorting provenance and tectonic setting Chemical Geology, 168, 135-150.

Cao, Y., Song, H., Algeo, T. J., Chu, D., Du, Y., Tian, L., ... & Tong, J. (2019). Intensified chemical weathering during the Permian-Triassic transition recorded in terrestrial and marine successions. Palaeogeography, Palaeoclimatology, Palaeoecology, 519, 166-177.

Chakrabarti, R., Basu, A. R., & Chakrabarti, A. (2007). Trace element and Nd-isotopic evidence for sediment sources in the mid-Proterozoic Vindhyan Basin, central India. Precambrian Research, 159(3-4), 260-274.

Chandrasekhara Gowda, M. J., & Govinda Rajulu, B. V. (1980). Stromatolites of the Kaladgi Basin and their significance in Palaeoenvironmental studies. *Miscellaneous publication-Geological survey of India*, (44), 220-239.

Derakhshan-Babaei, F., Nosrati, K., Tikhomirov, D., Christl, M., Sadough, H., & Egli, M. (2020). Relating the spatial variability of chemical weathering and erosion to geological and topographical zones. *Geomorphology*, *363*, 107235.

Devli, M. S. (2018). *Sedimentology and Provenance Studies of Lower Part of the Bagalkot Group of Kaladgi Basin: Implications of Tectonic and Sedimentation History* (Doctoral dissertation, Goa University).

Dey, S. (2015). Chapter 19 Geological history of the Kaladgi–Badami and Bhima basins, south India: sedimentation in a Proterozoic intracratonic setup. *Geological Society, London, Memoirs*, *43*(1), 283-296.

Dey, S., Rai, A. K., & Chaki, A. (2009). Palaeoweathering, composition and tectonics of provenance of the Proterozoic intracratonic Kaladgi–Badami basin, Karnataka, southern India: evidence from sandstone petrography and geochemistry. *Journal of Asian Earth Sciences*, *34*(6), 703-715.

Garcia, D., Ravenne, C., Maréchal, B., & Moutte, J. (2004). Geochemical variability induced by entrainment sorting: quantified signals for provenance analysis. *Sedimentary Geology, 171(1-4)*, 113-128.

George B.G., Ray, J.S., Patil-Pillai, S., Mahala, M.K., Kumar, S., Kale, V.S., (2023) C-Sr-Pb isotope systematics of carbonate formations of Kaladgi Supergroup: implications for basin evolution and correlation with Proterozoic global events. *Precambrian Research, 388, 107014.*

George, T. S. (1999). Sedimentology of Kaladgi basin. In *Field workshop on integrated evolution of the Kaladgi and Bhima basins. Geol. Soc. India, Bangalore* (pp. 13-17).

Hounslow, M. W., & Morton, A. C. (2004). Evaluation of sediment provenance using magnetic mineral inclusions in clastic silicates: comparison with heavy mineral analysis. Sedimentary Geology, 171(1-4), 13-36.

Jayaprakash AV. Sundaram V., Hans, K. Mishra, RN. 1987 Geology of the Kaladgi-Badami Basin, Karnataka Purana Basin of Peninsular India (middle to late Proterozoic) Geological Society of India, Memoir & 201-225.

Jayaprakash, M. C., Channabasappa, K., & Natashekar, D. (2011). Three-dimentional (3D) model of the proterozoic kaladgi basin, Southern India-a gis approach. *Journal of Applied Geochemistry*, *13*(1), 42-47.

Kale, V. S., & Phansalkar, V. G. (1991). Purana basins of peninsular India: a review. *Basin Research*, *3*(1), 1-36.

Kale, V. S., & Pillai, S. P. (2022). Sediments from Purana basins, India: Where were they derived from. Geosystems and Geoenvironment, 1(4), 100069.

Li, C., & Yang, S. (2010). Is chemical index of alteration (CIA) a reliable proxy for chemical weathering in global drainage basins. American Journal of Science, 310(2), 111-127.

McLennan, S. M., Hemming, S., McDaniel, D. K., & Hanson, G. N. (1993). Geochemical approaches to sedimentation, provenance, and tectonics. Special Papers-Geological Society of America, 21-21.

Miall, A. D., Catuneanu, O., Eriksson, P. G., & Mazumder, R. (2015). Chapter 23 a brief synthesis of Indian Precambrian basins: classification and genesis of basin-fills. *Geological Society, London, Memoirs*, *43*(1), 339-347.

Meunier, A., Caner, L., Hubert, F., El Albani, A., & Prêt, D. (2013). The weathering intensity scale (WIS): An alternative approach of the chemical index of alteration (CIA). American Journal of Science, 313(2), 113-143.

Ohta, T., & Arai, H. (2007). Statistical empirical index of chemical weathering in igneous rocks: A new tool for evaluating the degree of weathering. *Chemical Geology*, *240*(3-4), 280-297.

Ohta, T. (2004). Geochemistry of Jurassic to earliest Cretaceous deposits in the Nagato Basin, SW Japan: implication of factor analysis to sorting effects and provenance signatures. Sedimentary Geology, 171(1-4), 159-180.

Patil Pillai, S., George, B. G., Ray, J. S., & Kale, V. S. (2019). Comments on Paper: "Depositional history and provenance of cratonic ‘Purana’ basins in southern India: A multipronged geochronology approach to the Proterozoic Kaladgi and Bhima basins” by Joy et al., 2018. Geological Journal, https://doi. org/10.1002/gj. 3415. *Geological Journal*, *54*(5), 3167-3169.

Patil-Pillai, S., & Kale, V. S. (2007). Tectonic Controls on Sedimentation in the Proterozoic Kaladgi Basin of South India. In *Abstract International Conference on Precambrian Sedimentation and Tectonics and second GPSS Meeting, IIT Bombay* (pp. 10-12).

Patranabis-Deb, S. (2015). Origin and sequences of sedimentary structures of shelf macrotidal sandstone bars in the Neoproterozoic Kerur Formation of the Badami Group, Kaladgi Basin, India. In *31st IAS Meeting of Sedimentology* (pp. 22-25).

Pettijohn, FJ, Potter, PE. Siever, R. 1972 Sambands. Springer-Verlag New York.

Perri, F. (2020). Chemical weathering of crystalline rocks in contrasting climatic conditions using geochemical proxies: an overview. Palaeogeography, Palaeoclimatology, Palaeoecology, 556, 109873.

Pillai, S. P., Pande, K., & Kale, V. S. (2018). Implications of new^ 40 Ar/^ 39 Ar 40 Ar/39 Ar age of Mallapur Intrusives on the chronology and evolution of the Kaladgi Basin, Dharwar Craton, India. *Journal of Earth System Science*, *127*, 1-18.

Peshwa, V. V., Phadke, A. V., Phansalkar, V. G., Soman, G. R., & Deolankar, S. B. (1989). Geology of the Kaladgi Basin and associated rocks in parts of northern Karnataka and western Maharashtra: A study based on remote sensing techniques. *ISRO-RESPOND Proj. Rep., Poona Univ., Pune, India*.

Pujar, A., Puniya, M. K., Hiremath, M., & Anjanappa, S. (2021). Study of structural, deformation temperature, and strain analysis of the quartzarenites of south-central Kaladgi basin, exposed at and around Mullur ghat and Kallur village of Belgaum district, Karnataka, India. Arabian Journal of Geosciences, 14(9), 744.

Ramachandran, A., Madhavaraju, J., Ramasamy, S., Lee, Y. I., Rao, S., Chawngthu, D. L., & Velmurugan, K. (2016). Geochemistry of Proterozoic clastic rocks of the Kerur Formation of Kaladgi-Badami Basin, North Karnataka, South India: implications for paleoweathering and provenance. Turkish Journal of Earth Sciences, 25(2), 126-144.

Sathyanarayan, S., Arneth, J. D., & Schidlowski, M. (1987). Stable isotope geochemistry of sedimentary carbonates from the Proterozoic Kaladgi, Badami and Bhima Groups, Karnataka, India. *Precambrian research*, *37*(2), 147-156.

Sharma, M., Banerjee, D. M., & Santosh, M. (2014). Proterozoic basins of India. Journal of Asian Earth Sciences, 91, 227-229.

Sharma, M., & Pandey, S. K. (2012). Stromatolites of the Kaladgi Basin, Karnataka, India: systematics, biostratigraphy and age implications. *The Palaeobotanist*, *61*, 103-121.

Velmurugan, K., Madhavaraju, J., Balaram, V., Ramachandran, A., Ramasamy, S., Ramirez-Montoya, E., & Saucedo-Samaniego, J. C. (2019). Provenance and tectonic setting of the Proterozoic clastic rocks of the Kerur Formation, Badami Group, Mohare area, Karnataka, India. *Geological evolution of the Precambrian Indian shield*, 239-269.

Verlekar, P. A., & Mahender, K. (2020). Provenance, tectonics and palaeo environment of Mesoproterozoic Saundatti Quartzite Member of Kaladgi Basin, India: A petrographic view.

Verma, S. P., & Armstrong-Altrin, J. S. (2013). New multi-dimensional diagrams for tectonic discrimination of siliciclastic sediments and their application to Precambrian basins. *Chemical Geology*, *355*, 117-133.

Vivek, S., NAIR, S. A., & Patil, S. (1998). Testimony of intraformational limestone breccias on Lokapur-Simikeri disconformity, Kaladgi Basin.

Weltje, G. J., & von Eynatten, H. (2004). Quantitative provenance analysis of sediments: review and outlook. Sedimentary Geology, 171(1-4), 1-11.

Whitmore, G. P., Crook, K. A., & Johnson, D. P. (2004). Grain size control of mineralogy and geochemistry in modern river sediment, New Guinea collision, Papua New Guinea. Sedimentary Geology, 171(1-4), 129-157.

Yang, J., Cawood, P. A., Du, Y., Feng, B., & Yan, J. (2014). Global continental weathering trends across the Early Permian glacial to postglacial transition: Correlating high-and low-paleolatitude sedimentary records. Geology, 42(10), 835-838.

RADIOLARIAN DIVERSITY AND ITS CLIMATIC REPERCUSSIONS OF THE SOUTHERN BAY OF BENGAL

Dissertation submitted in partial fulfilment of the degree of

Master of Science in Applied Geology

Submitted By

Haifa Abdul Kareem Valassery

Reg. No. CCAVMAG016
2021-2023

Under the Supervision of

Dr. N R Nisha

Micropaleontology Laboratory
Dept. of Marine Geology and Geophysics
School of Marine Science
Cochin University of Science & Technology
Kochi-16, Kerala

DEPARTMENT OF GEOLOGY AND ENVIRONMENTAL SCIENCE
CHRIST COLLEGE (AUTONOMOUS), IRINJALAKUDA, KERALA, 680125
(Affiliated to University of Calicut and re-accredited with by NAAC with A++)

AUGUST 2023

Cochin University of Science and Technology

DEPARTMENT OF MARINE GEOLOGY AND GEOPHYSICS

MICROPALEONTOGY LABORATORY

SCHOOL OF MARINE SCIENCES, FINE ARTS AVENUE, KOCHI - 682 016, INDIA

Dr. N. R. NISHA
Assistant Professor

Phone : 0484-2366478 (Extn. 3316)
Mobile : 9846929649
Email : nrnishacusat@gmail.com
nrnisha@cusat.ac.in
nisharavindran@yahoo.com

MGD/ MICROPAL/23-24/15

Date: 24.08.2023

CERTIFICATE

This is to certify that the dissertation report entitled "**Radiolarian diversity and its climatic repercussions of the Southern Bay of Bengal**" is a bonafide record of project work done by Ms Haifa Abdul Kareem Valassery (Reg.No.CCAVMAG016), M.Sc. Applied Geology, Department of Applied Geology and Environmental Science, Christ (Autonomous) College, Irinjalakuda 680125. The work was carried out under my supervision and guidance at the Micropaleontology Laboratory, Department of Marine Geology and Geophysics, School of Marine Sciences, Cochin University of Science and Technology, Kochi-16, from April 2023 to August 2023, for the partial fulfilment of the requirements for the award of the degree of Master of Science in Applied Geology during the academic year 2021-2023 of Christ (Autonomous) College, Irinjalakuda, Kerala.

(Nisha. N.R)

Flat No. 1008, Oceanus Maple, Vattekunnam, Edappally North, Kochi - 682 024

DECLARATION

I hereby declare that this project report entitled "**Radiolarian diversity and its climatic repercussions of the Southern Bay of Bengal** " is an authentic work carried out by me from April 2023 to August 2023, under the supervision of **Dr N. R. Nisha**, Assistant Professor, Micropaleontology Laboratory, Department of Marine Geology and Geophysics, School of Marine Science, Cochin University of Science and Technology, Kochi-16, Kerala, in partial fulfilment of the requirements for the award of the degree of Master of Science in Applied Geology of Christ (Autonomous) College, Irinjalakuda, Kerala. No part of the report is reproduced from other resources. All information included from other sources has been duly acknowledged. I maintain that if any part of the report is found to be plagiarized, I shall take full responsibility for it.

Place: Irinjalakuda **HAIFA ABDUL KAREEM VALASSERY**

Date: **Reg. No. CCAVMAG016**

CERTIFICATE

This is to certify that the dissertation report entitled "**Radiolarian diversity and its climatic repercussions of the Southern Bay of Bengal**" is a bonafide record of project work done by Ms Haifa Abdul Kareem Valassery (Reg.No.CCAVMAG016), M.Sc. Applied Geology, Department of Applied Geology and Environmental Science, Christ (Autonomous) College, Irinjalakuda 680125. The work was carried out under my supervision and guidance in partial fulfilment of the requirements for the award of the degree of Master of Science in Applied Geology during the academic year 2021-2023.

Dr Sunitha D

Internal Supervisor

Dr Anto Francis K

Co-ordinator

Department of Applied Geology and Environmental Science

Christ College (Autonomous),Irinjalakuda

Kerala-680125

Place: ……

Date : ……

External Examiners

1. ……..

2. ……

ACKNOWLEDGEMENT

I would like to express my sincere gratitude to my supervisor **Dr N. R. Nisha**, **Assistant Professor, Department of Marine Geology and Geophysics, School of Marine Science, Cochin University of Science and Technology, Kochi-16**, for the supervision, cooperation, support, and valuable guidance throughout the completion of this work. I convey my sincere sense of gratitude to **the Head, Department of Marine Geology and Geophysics, School of Marine Sciences, Cochin University of Science and Technology, Kochi-16** for permitting me to do my dissertation work and use the facilities of the institution. I am also thankful to the **Inter-University Accelerator Centre, New Delhi for extending the AMS facility for 14 C funded by the Ministry of Earth Science (MoES), Govt. of India** with reference numbers **MoES/16/07/11(i)-RDEAS and MoES/P. O (Seismic)8(09)-Geochron/2012**. I am also grateful to **the Director, National Centre for Polar and Ocean Research NCPOR, Goa** for providing the gravity core for this study. I sincerely acknowledge **the Director, Geological Survey of India, Mangalore for extending the SEM facilities.**

I am thankful to **Ms Kavya Aravind, Research Scholar, Department of Marine Geology and Geophysics, CUSAT, Kochi** for her valuable support in the preparation and analysis of the work. I would like to extend my thanks to **Ms. Veena G Vishwam** and **Ms. Puja Vijay, Research Scholars, Department of Marine Geology and Geophysics, CUSAT, Kochi,** for their support during this work. I also like to thank all the staff members of the Department of Marine Geology and Geophysics, CUSAT for their support during this project.

My sincere gratitude to all my teachers and staff members of the Department of Geology and Environmental Science, Christ College Autonomous, Irnjalakuda for their encouragement and help. I express my gratitude to **Dr Sunitha D, Assistant Professor, Department of Geology and Environmental Science, Christ College (Autonomous) Irinjalakuda, for her support**. I express my heartfelt gratitude **to Dr Linto Alappat, Dean of Research and Development of TLC (**Former HOD**), Department of Applied Geology and Environmental Science, Christ College (Autonomous), Irinjalakuda** for his valuable support throughout the course of work. I would extend my deepest gratitude to **Dr Anto Francis K, Co-ordinator, Department of Applied Geology and Environmental Science, Christ College (Autonomous), Irinjalakuda.**

Last, but not least, I would like to thank my family and friends for supporting me and for being by my side in all ups and downs. I ascribe millions of gratitude to the Almighty for the abundant blessing which is poured upon me.

HAIFA ABDUL KAREEM VALASSERY.

INDEX

List of Figures

List of Plates

ABSTRACT

The southern Bay of Bengal (BoB) is famous for its biodiversity. The present study is the first report of radiolarians of the southern BoB. The present investigation mainly focuses on the taxonomic identification and temporal distribution pattern of these siliceous organisms. We recorded 18 radiolarian species belonging to 12 genera and 5 families. Based on the available radiolarian dates the average sedimentation ratio of the study are 625 cm/Kyr and the examined core spans up to 44 Kyr BP.

The temporal distribution pattern records the overall dominance of spummellarians over nassellarians. The dominant species recorded from the study area are *Acanthosphaera actinota*, *Acrosphaera spinosa*, *Dictyocoryne truncatum*, *Dictyocoryne euclidis* and *Spongaster tetras tetra* (Hollis and Neil, 2005; Rogers, 2016). We could also mark the Younger Dryas (YD, Bolling, Allerged (B/A), Henrinch events (H1, H2, H3 and H4) and the Last Glacial Maximum during 4A layer from the southern Bay of Bengal.

CHAPTER 1

INTRODUCTION

The Indian Ocean was a poorly studied area before the establishment of the International Indian Ocean Expedition (IIOE). The Bay of Bengal (BoB) is a complex and dynamic body of water extending to an area of 2.2 million km^2, about 2090 km long and 1610 km wide (LaFond, 1966). It has great significance in terms of climate and its marine ecosystems, where the surface currents are substantially affected by the monsoon winds and Coriolis effect (Chowdhury, 2023). The BoB is considered as a hotspot for palaeoceanographic and paleoclimatic studies. Both the Indian summer monsoon and the winter monsoon systems largely influence the oceanographic processes of the BoB (Shankar et.al., 2002). Marine microfossils particularly foraminifera had been mainly used and had gained wide attention among the Quaternary researchers whereas the radiolarian group of microfossils is the less attempted faunal representation of the BoB.

1.1 Oceanographic Setting

The Southern Bay of Bengal is an oceanic region that lies between the southern tip of the Indian Peninsula and the northern coast of Sri Lanka. It is surrounded by the Indian Ocean to the west and the Bay of Bengal to the east. The region is characterized by its unique oceanographic conditions, which contribute to a highly diverse and complex ecosystem. The region experiences two distinct seasons, the southwest monsoon season generally occurs between June and September, while the northeast monsoon season occurs between October and December. During the southwest monsoon season, the region experiences intense rainfall, high winds, and strong ocean currents, which are mostly driven by the southeast trade winds. The region is also influenced by the Indian Ocean Dipole - a climate phenomenon that results from differences in sea surface temperature across the equatorial Indian Ocean. Surface water in the Bay of Bengal is characterized by low salinity caused by excess precipitation and freshwater runoff. Contrary to the Arabian Sea, where salinity exceeds 36.5%, salinity in the Bay of Bengal reaches very low values of 30% (Wyrtki et.al., 1971; Ittekkot et.al., 1991; Murty et.al., 1992; Suryanarayana et.al., 1993). Surface water in the Bay of Bengal is characterised by low salinity caused by excess precipitation and freshwater runoff. Contrary to the Arabian Sea, their

salinity exceeds 36.5‰, salinity in the Bay of Bengal reaches very low values of >30‰ (Wyrtki et.al., 1971; Ittekkot et.al., 1991 Murty et.al., 1992; Suryanarayana et.al., 1993).

The Southern Bay of Bengal is home to a diverse range of marine organisms. Among these organisms are the radiolarians, a group of microorganisms that are found throughout the world's oceans. They are widely seen in shallow to open ocean regions (Wang, 2012) and dispersed horizontally across all world oceans and vertically up to 8000 m water depth (Suzuki and Aita, 2011; Suzuki and Not, 2015; Wang et.al., 2003). Several attempts were done on radiolarians of world oceans to document their morphology, evolutionary changes, biostratigraphic zonations and paleoceanographic and climatic significances (Mullineaux and Smith, 1986; Petrushevskaya and Swanberg, 1990; Sharma and Daneshian, 1998; Gupta et.al., 2002; Wang and Abelmann, 2002; Afanasieva, 2006, 2007; Lüer et.al., 2008; Lazarus et.al., 2009; Almeida et.al., 2017; Johnson and Knoll, 1974; Danelian and Frydas, 1998; Lazarus, 2005). The biogeographical and depth distribution patterns of radiolarians of the BoB are little-attended areas of concern to researchers. The present investigation focuses on the systematics and temporal distribution pattern of radiolarians of the southern BoB during the past 44 Kyr. Studies have shown that the distribution and abundance of radiolarians in the Southern Bay of Bengal are strongly influenced by the physical properties of the water column, such as temperature, salinity and nutrient content. The region's warm, low-salinity surface waters support a diverse range of shallow marine organisms, while the deep waters are characterized by high salinity and low nutrients. Overall, the Southern Bay of Bengal is a complex and dynamic oceanic region that is home to a diverse range of marine organisms, including the radiolarians. Understanding the oceanographic conditions and biological diversity in the region is critical for managing its resources effectively and conserving its unique ecosystem.

1.2 Review of Literature

The studies on radiolarians across the oceans took a turn with the taxonomic works of Ernst Haeckel, 1862. The monograph ‘Die Radiolarian’ which was then followed by ‘The Voyage of H.M.S. Challenger’ report dedicated to radiolaria (Cavalier et.al., 2018; Adl et.al., 2019; Biard, 2022). This massive work inspired and set a path for new-generation researchers. Radiolaria are marine species inhabiting saline waters (salinities above 30 PSU) (Boltovskoy et.al., 2017). Ecological relationships of these fossils have been used to reconstruct the paleoenvironment (Lazarus et.al., 2020). The last few decades have seen a growing interest in

modern radiolaria, likely thanks to large-scale studies that highlighted their apparently substantial contribution to marine biodiversity and carbon pooling (Biard et.al., 2016; Cavalier et.al., 2018). Radiolarian skeleton, now fossilised, will record the imprint of its surrounding environment and save it for millennia, providing excellent tools to reconstruct the past environment (De Wever et.al., 2002). Along with foraminifera, Radiolaria have the most extensive fossil record (starting as old as 521 million years ago) of any other protist lineage (Suzuki and Not, 2015). We lack very basic knowledge concerning their ecology, this point being hampered by the lack of reliable estimates of their abundances across the various size classes (Biard et.al., 2016). Knowledge of their contribution to contemporary biogeochemical cycles is more advanced. Radiolaria are active and important contributors to the carbon (Lampitt et.al., 2009) and silicon cycles (Takahashi, 1987) of the ocean.

The majority of radiolarians occur in the upper 100m, the surface hydrographic properties should influence the temporal variation of radiolarian fluxes. The prevailing hydrographic conditions, salinity and >80% of the terrestrial monsoon rains result in freshwater run-off through the rivers into the Bay of Bengal causing a hypo-saline condition in the Bay of Bengal (Gupta and Gahalaut, 2009). Radiolarian abundance is a monsoonal proxy responding to the Earth's orbital forcing. It is assumed that the shift in radiolarians varied in accordance with the monsoonal SST and salinity (Gupta and Fernandes, 1997

). A study of radiolarian fluxes collected during 1991–93 from time-series sediment traps deployed at 1071 and 3010 m water depth in the southern Bay of Bengal (SBBT) yielded 40 species/groups of radiolarians. The radiolarian flux had a response to the salinity and SST variations due to the precipitation received during monsoon and from the freshwater runoff from the Indian rivers which in turn caused a hyposaline condition in the Bay of Bengal, these results prove that more studies on radiolarian assemblages in the down core data can reveal the monsoonal history in the geological past (Gupta et.al., 2002).

CHAPTER 2

RADIOLARIANS

2.1 Radiolarians

The radiolarians are marine unicellular zooplankton having a skeleton of hydrous amorphous silica or celestite which are more resistant when compared to calcareous skeleton thus being well preserved in the marine sediments (Ishitani et.al., 2016). These protists inhabit both surfaces as well as deep water regions and have a worldwide distribution (Krabberød et. al., 2011). Whereas few species are restricted to certain ecological conditions and are very helpful in finding surface water properties like temperature, salinity, primary productivity, and reconstruction of paleo monsoon (Anderson, 2001; Matul and Mohan, 2017). Although researchers have attempted to study the radiolarians from the deep sea, their studies were confined to the surface sediment and lacked temporal distribution data from the modern Indian Ocean (Gupta, 1996).

Radiolarians are single-shelled holoplanktonic species with sizes varying from <100 mm to 1-2 mm in diameter (Anderson, 2001). They have a structure that enhances their buoyancy. The taxonomic identification is primarily done based on the skeletal morphology and morphology of the central capsule (Haeckel, 1887; Nigrini and Johnson, 1982; Boltovskoy, 1998; Krabberød et.al., 2011). Radiolaria has two orders; they are Polycystina, with a skeleton formed from pure opal which in turn makes the skeleton resistant towards dissolution, therefore making it the most preserved fossil radiolarians (Armstrong and Brasier, 2004). The second order is Phaeodaria, having skeletons of hollow silica bars connected by organic matter which are therefore not preserved in the fossil record (Armstrong and Brasier, 2004). The order Polycystina is further divided into 3 suborders they are Collodaria (spherical-like structure), Nassellaria (conjoining skeleton with a ring or cone structure), Spumellaria (spongy irregular spherical chamber in centre and having pseudopodia-like structures) (Swanberg and Anderson, 1985).

2.2 Lifestyle of Radiolarians

In live radiolarians, the cytoplasm is divided into outer cytoplasm and inner endoplasm which is separated by a central capsule (unique feature) (Armstrong and Brasier, 2004).

Thread-like Filopodia/axopodia (pseudopodia) is seen radiating from the central capsule (Armstrong and Brasier, 2004). Calymma acts as a float action feature for radiolarians. The skeleton formed from mineralization is in its simplest form which is radial or tangential (Armstrong and Brasier, 2004). The composition of skeletons differs from $SrSO_4$ in class Acantharean to opaline silica in polycystina (Armstrong and Brasier, 2004). Reproduction occurs either by fission or by swarming (sexual reproduction, flagellated cell release) (Armstrong and Brasier, 2004). There is a wide range of radiolarians from herbivores to omnivores (Casey, 1993; Lipps, 1993). They capture surrounding prey by paralyzing them using axopodia passing them to food vacuoles, from where it is digested and nutrients are further passed through the central capsule. Spherical and discoidal shape, fat-globe accumulation, gas-filled vacuoles, and skeletal cavities maintain the species' buoyancy (Armstrong and Brasier, 2004).

2.3 Distribution and Ecology

Radiolaria first appeared in the Cambrian period and were one of the first groups to change from a benthic to free-floating mode of life (Lipps, 1993). They are found in oceanic conditions from the photic zone to the abyssal plains, they are abundant in the continental slope, in depths where nutrients brought up by diverging surface currents are seen, multiple forms are found at equatorial regions and seen associated with diatoms at the subpolar regions (Armstrong and Brasier, 2004). Based on the nutrient intake habit, they are found in different areas of the ocean i.e.

- Herbivores: Mostly found at 200m of the upper portion of the ocean waters (Armstrong and Brasier, 2004).
- Symliotrophs: Found at warm shelf portions and in subtropical gyres (Armstrong and Brasier, 2004).
- Detritivores and bacterivores: Found in high latitudes of shallow sub-surface of ocean waters. Their abundance fluctuates in accordance with the availability of food, mineral content ($SrSO_4$, Silica), water current, depth, and water mass differences. It is recorded that they do not bloom in cold water and the peak was recorded at the equatorial belt (Armstrong and Brasier, 2004).

2.4 Significance of Radiolarians

The study of radiolarians gives a correlation of the biostratigraphy of ocean sediments (Sanfilippo, 1985). It helps in the study of deposits which do not contain any calcareous fossils (Ishitani et.al., 2016). They are good proxies for paleotemperature, paleoclimate, paleo-productivity, etc (Casey et.al., 1990). The complex nature of the radiolarian skeleton and an almost complete Mesozoic to Recent geological record makes this group ideal for charting microevolutionary changes (Knoll and Johnson, 1975). They show radiolarian provincialism in Cenozoic sediments (Casey et.al., 1990). They have also been used to indicate palaeogeographic and tectonic changes in ocean basins. For example, radiolarian stratigraphy gave early support to the hypothesis of sea-floor spreading (Riedel, 1967). The resistant nature of radiolarian chert to tectonism and diagenesis means Radiolaria are often the only common fossils preserved in orogenic belts and within accreted terranes (Murchey, 1984).

CHAPTER 3

MATERIAL AND METHODS

3.1 Core Location

The present investigation was carried out in a sediment core (SK 329/1), retrieved from the northern tip of the Ninetyeast Ridge, (09°31' N, 90°49′ E) during the 329th cruise of the ORV *Sagar Kanya*. The 2.55 m long core was recovered from a water depth of 3452 m (Fig.1). The core was subsampled on board at 1 cm regular intervals up to 100 cm, 2 cm intervals up to 200 cm, and 5 cm intervals to the entire length of the core. A total of 50 samples were analysed for the present investigation.

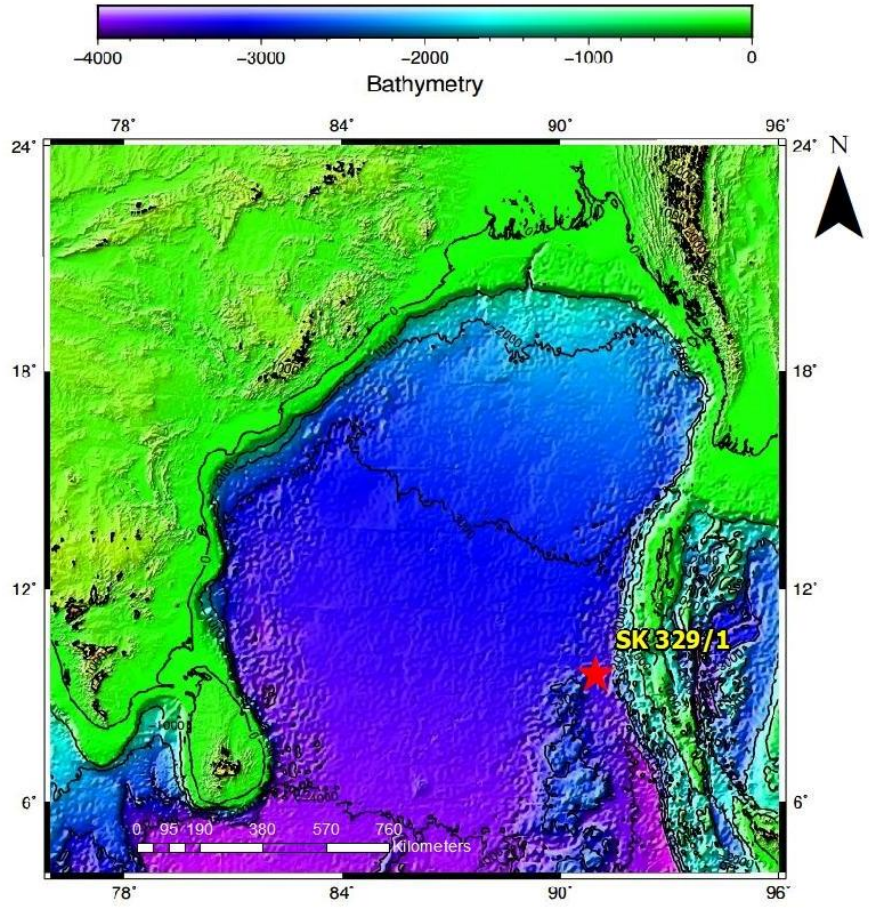

Fig. 1 Location of the gravity core recovered from the southern Bay of Bengal

3.2 AMS Dating

The age model of the core SK329/1 was established using the AMS radiocarbon ages. Samples of mixed planktonic foraminifera were analysed at the Inter-University Accelerator Centre (IUAC), New Delhi. For the AMS C^{14} dating the samples were processed at the AMS Pelletron facility at IUAC. The samples were graphitized with the help of the Carbonate Handling System (CHS) in the IUAC facility. For graphitization, the surfaces of mixed planktic foraminiferal species were leached by 0.1 M HCl to clean and then produced CO_2 is flushed with Helium. The remaining sample was hydrolysed by 85% phosphoric acid, and CO_2 was transferred to the zeolite trap in the AGE system. This trapped CO_2 through thermal expansion was transferred through an in-situ glass tube in the reactor filled with iron powder. The CO_2 is reduced by H_2 gas on the surface of iron powder at 580°C. Graphite is formed and water vapours were removed with the help of Peltier coolers (Sharma et.al., 2019). These iron powders were transferred to pellets and installed in the 500 KV Pelletron Accelerator for Accelerator Mass Spectrometry (AMS). The primary standards (OXII), IAEA reference samples, alpha graphite, and Ph blank samples are installed along with the unknown samples (Sharma et.al., 2019). The obtained raw data concerning radiocarbon dating was converted to calibrated calendar ages using Calib 8.2 Software.

3.3. Faunal Analysis

For the faunal analysis, 20 g of each dried sample was treated with 5 % hydrogen peroxide and kept overnight. These treated samples were boiled, cooled, and sieved through a 120 µm sieve. The sieved samples were dried and kept in plastic containers. After splitting the sample using a micro auto splitter, the radiolarian analysis was done. The entire sample was analysed wherever there was a rare occurrence of radiolarians. All radiolarian specimens were picked, and assemblage slides and reference slides were prepared. Scanning Electron Micrographs (SEM) were prepared for the surface ultrastructure studies of all the recorded species. SEM analysis was carried out using the SEM-EDX-CL LAB facility (Make and model: JEOL JSM-IT200) of the Geological Survey of India (GSI), Operation West Coast-I, Marine and Coastal Survey Division OPWC1, Mangalore, Karnataka.

3.2 Objectives

1. To study radiolarian assemblages (qualitatively and quantitatively) from the southern Bay of Bengal.
2. To study the temporal distribution pattern of radiolarians to understand the monsoonal history of the southern Bay of Bengal of during the past 44 Kyr.

CHAPTER 4

SYSTEMATICS OF RADIOLARIANS

The taxonomic identification is primarily done based on the skeletal morphology and morphology of the central capsule (Haeckel, 1887; Nigrini and Johnson, 1982; Boltovskoy, 1998; Krabberød et.al., 2011). In the present investigation, we recorded 18 radiolarian species belonging to 12 genera, 5 families and 2 suborders (Table 1). In the examined core, the Spumellarians were dominated by Nassellarians. The most dominant species are *Acanthosphaera actinota* and *Acrosphaera spinosa*. Radiolarian assemblages were dominated by tropical-subtropical warm water species such as *Acanthosphaera actinota, Acrosphaera spinosa, Dictyocoryne truncatum, Dictyocoryne euclidis* and *Spongaster tetras tetras* (Hollis and Neil, 2005; Rogers, 2016). All dominant specimens were illustrated by Scanning Electron Micrographs (Plate 1) and all the specimens are preserved at the respiratory of the Micropaleontology Laboratory, Department of Marine Geology and Geophysics, Cochin University of Science and Technology, Kochi, Kerala, India.

Table 1 List of radiolarian species recorded in the present study

Acanthosphaera actinota Haeckel, 1860	*Acrosphaera murrayana* (Haeckel) Hilmers, 1906
Acrosphaera spinosa Caulet, 1986 (Fig is not included in plates)	*Axoprunum stauraxonium* Haeckel, 1887
Axoprunum pierinae Clark and Campbell, 1942	*Cenosphaera cristata* Haeckel, 1887
Collosphaera huxleyi Muller, 1855	*Dictyocoryne euclidis* Haeckel, 1887
Dictyocoryne profunda Ehrenberg, 1872	*Dictyocoryne truncatum* (Ehrenberg) Nigrini & Moore, 1979
Dictyocoryne sp Ehrenberg, 1872	*Euchitonia elegans-furcata*
Heliodiscus asteriscus Haeckel, 1887	*Hexacontium armatum-hostile*
Hexacontium hexactis (Stoehr) Dumitrica, 1978	*Lamprocyclas maritalis* Haeckel, 1887
Peripyramis circumtexta Haeckel, 1887	*Pterocanium korotnevi* (Dogel) in Dogel & Reshetnyak, 1952
Spongaster tetras tetras Ehrenberg, 1860	

Kingdom	Protista Haeckel, 1887
Phylum	Sarcodina Hertwig and Lesser, 1874
Class	Actinopoda Calkins, 1909
Subclass	Radiolaria Müller, 1858
Order	Spumellaria Ehrenberg, 1875
Superorder	Polycystina Ehrenberg, 1838
Family	Actinommidae Haeckel, 1862, emend. Riedel, 1967
Genus	*Acanthosphaera* Ehrenberg, 1858

4.1 Species: *Acanthosphaera actinota* Haeckel, 1860 (Plate 1. Fig. 1)

Shell very thin-walled, about ten times as broad as one mesh. Pores regular, hexagonal, with thread-like bars; six to eight on the radius. Radial spines at the nodal points of the network, bristle-shaped, scarcely broader than the bars; about twenty main spines as long as the diameter of the shell, only one-third to one-half as long as the former.

Family	Collosphaeridae Müller, 1858
Genus	*Acrosphaera* Haeckel, 1881

4.2 Species: *Acrosphaera murrayana* (Haeckel) Hilmers, 1906 (Plate 1. Fig. 2)

Shell spherical, with large circular or rounded pores of unequal size, two to four times as broad as the bars. Ten to twelve pores in the half meridian of the shell. The margin of every pore with a coronal of six to nine short and acute spines not longer than the half diameter of the pore. No spines between the pores.

4.3 Species: *Acrosphaera spinosa* Caulet, 1986 (Plate 1. Fig. 3)

Spherical shell, with irregularly rounded pores, and numerous short oblique spines. Most specimens are easily distinguished by the presence of numerous short spines.

4.4 Species: *Axoprunum stauraxonium* Haeckel, 1887 (Plate 1. Fig 4)

Shell ellipsoidal, one and one-third times as long as broad, with a smooth surface. Network regular, with circular meshes, four times as broad as the bars. Two polar spines are three-sided pyramidal, half as long as the shell, and as thick at the base as a single mesh. Four inner radial beams (lying, two in the major and two in the minor axis of the ellipsoid) are very thin, at the central free ends knob-like and thick. The distance between two opposite beams equals one-third of the minor axis and indicates probably the diameter of the lost spherical medullary shell.

4.5 Species: *Axoprunum pierinae* Clark and Campbell, 1942 (Plate 1. Fig. 5)

Shell ovate, with two opposite thick equal polar spines, round in cross-section. The tip of the spine is bluntly sharpened. Dense cortical shell, surface nearly smooth, wall is with about fourteen pores across the equator and eighteen from pole to pole. Unequal subcircular pores, with very thin rims, thick wall, with extremely short sub-sepaloid projections bounding the faint sub hexagonal areas from whose centres the pores arise; medullary shell wall is very thin, with faint sub hexagonal pores and thin bars, supporting beams. Six, arranged in two nearly equatorial pairs, and two strong polar ones.

Genus *Cenosphaera* Ehrenberg, 1854

4.6 Species: *Cenosphaera cristata* Haeckel, 1887 (Plate 1. Fig. 6)

Thick-walled spherical shell and thorny. Pores are subcircular or circular, variable in size, 10-24 on the half-equator, as wide to five times as wide as the intervening bars. Pores surrounded by raised polygonal frames bearing short thorns at the corners. Recorded specimens with irregular subcircular pores, ridges, and hexagonal framing.

Genus *Collosphaera* Müller, 1858

4.7 Species: *Collosphaera huxleyi* Müller, 1855 (Plate 1. Fig. 7)

Shells with small to medium-sized pores scattered about the surface only; no spines or tubes. Shell is very irregular, between subspherical and polyhedral in form, but with irregular impressions, boils or bosses, and between these different rounded prominent tubercles and ridges. Network irregular, strong, with rounded, subcircular or nearly polygonal meshes. The diameter of the meshes is half to four times as broad as that of the thick bars.

Family Spongodiscidae Haeckel, 1862 emend. Riedel, 1967

Genus *Dictyocoryne* Ehrenberg, 1860

4.8 Species: *Dictyocoryne euclidis* Haeckel, 1887 (Plate 1. Fig. 8)

Discoidal test with three arms of nearly equal size and similar shape separated by nearly equal angles; a layered spongy patagium generally present but rudimentary or absent in several specimens, thicker distally along its margin than proximally where it is thin and delicate when fully developed subtriangular in shape. The central region of the test is circular to sub triangular in outline, consisting of 4-5 concentric discoidal latticed shells, therefore, biconvex inside view. Arms very narrow proximally, increase only gradually in breadth for most of their length, terminating in broad bulbous tips, a few of which were observed with 3-4 internal concentric shells or rings. In most specimens, the internal structure of the test is not distinct and the centre as well as the arms appear spongy. The arms and centre are covered with a generally distinguishable, small-pored latticed sheath.

4.9 Species: *Dictyocoryne profunda* Ehrenberg, 1872 (Plate 1. Fig. 9)

Three spongy, unchambered arms radiating at equal or almost equal angles from a central disc. Arms are much broader proximally with a much shorter region of narrow breadth; terminations of arms spatulate or lanceolate, coming to a point distally in fully developed forms. Position of arms varies from nearly equally disposed to bilaterally disposed of, generally a larger distinct odd arm present. A layered spongy patagium is either partially developed, rudimentary, or absent. In those with patagium partially developed it showed no increase in its thickness distally.

4.10 Species: *Dictyocoryne truncatum* (Ehrenberg) Nigrini & Moore, 1979 (Plate 1. Fig. 3) (Plate 1. Fig. 10 a, b)

Similar to *D.profunda*, but differs in having much broader arms and usually a well-developed patagium. Stars with 3 radii truncate at the apex. The specimens show a broader, spatulate-type arm.

Genus *Euchitonia* Ehrenberg, 1860 emend. Nigrini, 1967

4.11 Species: Euchitonia *elegans – furcate* (Plate 1. Fig. 11 a, b)

Shells are bilaterally symmetrical with 3 arms of approximately equal length. Arms increasing in breadth distally and having a blunt or irregularly rounded termination; sometimes with 1-3 slender terminal spines. Proximally arms appear chambered, but a rather dense mesh of subcircular pores generally obscures distal chambers, and gives arms a spongy appearance. Paired arms form the smaller angle opposite the odd arm and often curve slightly towards each other. Differs from *D. profunda* in that the 3 arms are slenderer, longer, and their orientation defines two larger angles and one smaller.

Family *Heliodiscidae*

Genus *Heliodiscus* Haeckel, 1862 emend. Nigrini, 1967

4.12 Species*: Heliodiscus asteriscus* Haeckel, 1887 (Plate 1. Fig. 12)

Disk with smooth surface, three times as broad as the medullary shell. Pores are regular, circular, and ten to twelve on the disk's radius. Marginal spines are fifteen to twenty, conical, often double contoured, of variable size and disposition, the largest as long as the disk’s radius.

Genus *Hexacontium* Haeckel, 1881

4.13 Species: *Hexacontium armatum-hostile* (Plate 1. Fig. 13)

Cortical shell with regular honeycomb-like network. Meshes are funnel-shaped, with circular inner and hexagonal outer aperture, as broad as the bars. Main spines are strong,

three-sided prismatic, as long as the radius of the outer shell. Short, bristle-like by-spines are present at every nodal point. Usually, 6 main spines are opposite in pairs in three-dimensional axes perpendicular to one another.

4.14 Species: *Hexacontium hexactis* (Stoehr) Dumitrica, 1978 (Plate 1. Fig. 14)

Cortical shell is thick-walled, smooth, or a little rough. Pores are regular circular, of the same breadth as the bars; five to seven on the radius. Both medullary shells are of the same structure but have smaller pores. Six spines are triangular pyramidal, nearly as long as the diameter of the outer shell, three times as broad at the base as one pore. The medullary shell wall of the present specimen is the same in structure with smaller pores.

Order	Nassellaria Ehrenberg, 1875
Family	Pterocorythidae Haeckel, 1881
Genus	*Lamprocyclas* Haeckel, 1881

4.15 Species: *Lamprocyclas maritalis* Haeckel, 1887 (Plate 1. Fig. 15)

Shell campanulate, but not so slender and with different peristome. Cephalis is subspherical, with a very stout, pyramidal horn of twice the length, the edges of which are spirally convolute. Outer coronal structure of the peristome is with twelve to fifteen short, divergent feet and the inner is with many convergent longer feet.

Genus *Peripyramis* Haeckel, 1881 emend. Riedel, 1958

4.16 Species: *Peripyramis circumtexta* Haeckel, 1887 (Plate 1. Fig. 16)

Shell slender, pyramidal, with nine strong radial beams, connected by fifteen to twenty transverse horizontal rings, which are partly complete, partly interrupted. Meshes are subregular and square. From the nodal points of the surface there arise branched spines, which at equal distances from it are connected by thin threads, forming a delicate outer arachnoid shell with large irregular polygonal meshes.

Genus *Pterocanium* Ehrenberg, 1847

4.17 Species: *Pterocanium korotnevi* (Dogel) in Dogel & Reshetnyak, 1952 (Plate 1. Fig. 17)

Thorax in the form of a cupola or a perforated pot with rounded, small pores of uneven size. Three massive, faceted and slightly convex (outward) basal spines extending from the lower rim of the cupola. The spines extend from the rim of the cupola at an angle of 120° to each other. The length of the basal spines somewhat exceeds the combined length of the cupola and the apical spine. The surface of the cupola is nodose with short conical protrusions. From the lower margin of the thorax to the base of the cephalis, there are 5-6 horizontal rows of pores; these pores decrease in size in the direction of the mouth aperture. The cephalis has the form of a small dome-like, reticulate superstructure above the cupola of the thorax. This superstructure consists of pores which are larger than those on the thorax; they are triangular or tetragonal instead of rounded, with narrow bars between them. The number of pores on the cephalis is small, obviously not over 6-8. From the apex of the cephalis arises an apical spine; it is smooth, massive and somewhat shorter than the basal spines.

Genus *Spongaster* Ehrenberg, 1860

4.18 Species: *Spongaster tetras tetras* Ehrenberg, 1860 (Plate 1. Fig. 18)

Tests similar to that of *D. truncatum* except for the four equally disposed spongy arms. In the former the three arms arise from the circular central region, with complete or partially developed spongy patagium. Test with a square outline having rounded corners. Arms appear to be spongy, without concentric rings or shells, generally of equal size, and without definite margins. The present species lacks concentric rings in arms. No specimens were observed without a patagium.

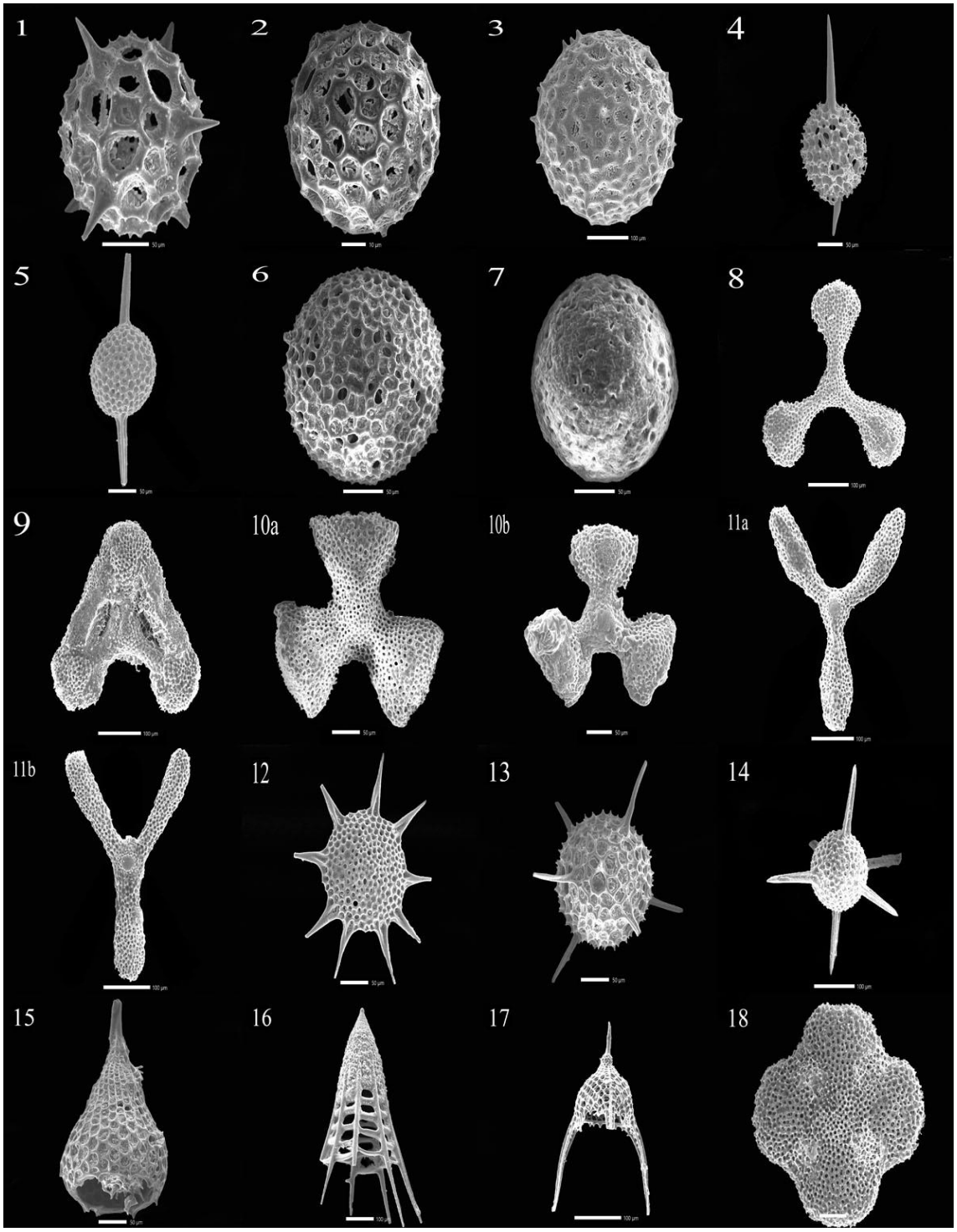

Plate 1 Dominant radiolarians of the Southern Bay of Bengal: **(1)** ***Acanthosphaera actinota*** Haeckel, 1860 (50µm); **(2)** ***Acrosphaera murrayana*** (Haeckel) Hilmers, 1906 (10 µm); **(3)** ***Acrosphaera spinosa*** Caulet, 1986 (100 µm); **(4)** ***Axoprunum pierinae*** Clark & Campbell 1942 (50 µm); **(5)** ***Axoprunum stauraxonium*** Haeckel, 1887 (50 µm); **(6)** ***Cenosphaera cristata*** Haeckel, 1887 (50 µm); **(7)** ***Collosphaera huxleyi*** Müller, 1855 (50 µm); **(8)** ***Dictyocoryne euclidis*** Haeckel, 1887 (100 µm); **(9)** ***Dictyocoryne profunda*** Ehrenberg, 1872 (100 µm); **(10 a, b)** ***Dictyocoryne truncatum*** (Ehrenberg) Nigrini & Moore, 1979 (50 µm, 100 µm); **(11 a, b)** ***Euchitonia elegans-furcata*** (100 µm, 100 µm); **(12)** ***Heliodiscus asteriscus*** Haeckel, 1887 (50 µm); **(13)** ***Hexacontium armatum-hostile*** (Stoehr) Dumitrica, 1978 (100 µm); **(14)** ***Hexacontium hexactis*** (Stoehr) Dumitrica (50 µm); **(15)** ***Lamprocyclas maritalis*** Nigrini 1967 (50 µm); **(16)** ***Peripyramis circumtexta*** Haeckel, 1887 (100 µm); **(17)** ***Pterocanium korotnevi*** (Dogiel) in Dogiel & Reshetnyak, 1952 (100 µm); **(18)** ***Spongaster tetras tetras*** Ehrenberg 1860 (50 µm).

CHAPTER 5

TEMPORAL DISTRIBUTION PATTERN OF RADIOLARIANS

The micro faunal composition in marine sediments has been known to change with environmental conditions. Any fluctuation in the environment is reflected by the variation in micro faunal assemblages. Like the most widely used foraminifera, radiolarians are also found to be a potential tool for deciphering the palaeoceanographic conditions of certain areas of the marine realm. The southern Bay of Bengal is the least studied area in respect of radiolarian diversity and distribution. In the present investigation a detailed study has been done on the radiolarian diversity and its temporal distribution of the southern BoB during the past 44 kyr BP. The radiolarian assemblage comprises both spumellarians as well as nassellarians. Spumullarians are circular forms and nassellarians are flask or funnel shaped forms.Of the recorded 18 radiolarian species, 10 species belong to spumellaria and 8 species belong to nassellarians (Table 2).

Table 2 List of recorded spumellrians and nassellarians of the Southern Bay of Bengal

SPUMELLARIANS	NASSELLARIANS
Axoprunum pierinae	*Acanthosphaera actinote*
Axoprunum stauraxonium	*Acrosphaera spinosa*
Hexacontium armatum-hostile	*Acrosphaera murrayana*
Hexacontium hexactis	*Pterocanium korotnevi*
Dictyocoryne euclidis	*Collosphaera huxleyi*
Dictyocoryne profunda	*Heliodiscus astericus*
Dictyocoryne truncatum	*Lamprocyclas maritalis*
Dictyocoryne sp.	*Peripyramis circumtexta*
Euchitonia elegans- furcate	
Spongaster tetras tetras	

The percentage abundance of spumellarians and nassellarians were also analysed and the spumellarains are dominating over the nassellarians in the southern BoB during the past 44 Kyr (Fig.2).

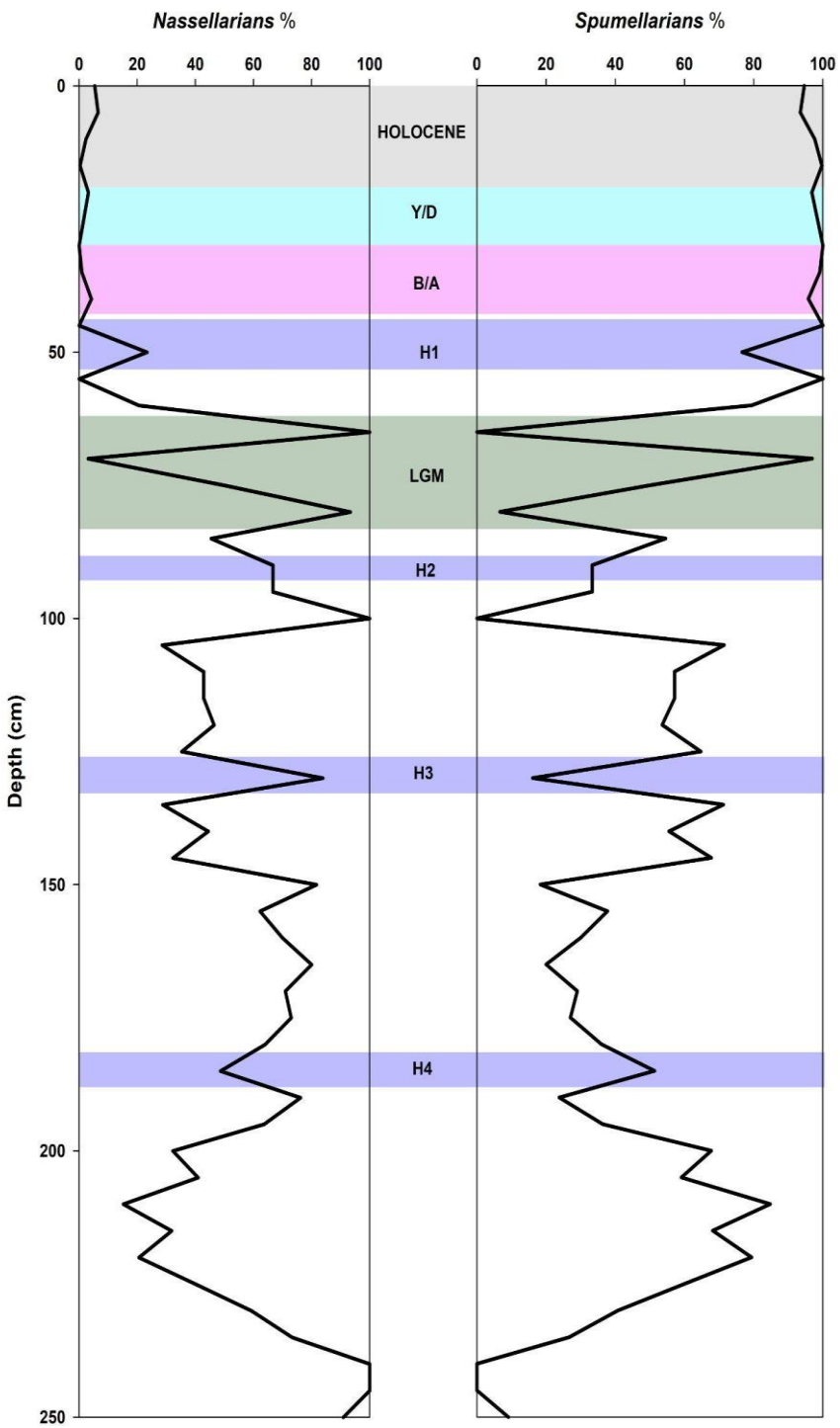

Fig. 2 Percentage abundance of spumellarians and nassellarians of the examined core

The percentage distribution of fauna exhibited a dominance of spumellarians over nassellarians in the upper portion of the core, while this abundance of spumellarians decreases with depth towards the bottom. In contrast, nassellarians show an opposite trend with an

increased abundance towards the bottom of the core. This temporal distribution pattern may be associated with the transport of cool deep water during Holocene.

The radiolarian assemblages were dominated by *Acanthosphaera actinota*, *Acrosphaera spinosa*, *Dictyocoryne truncatum*, *Dictyocoryne euclidis* and *Spongaster tetras tetras* in the examined core (Fig.3).

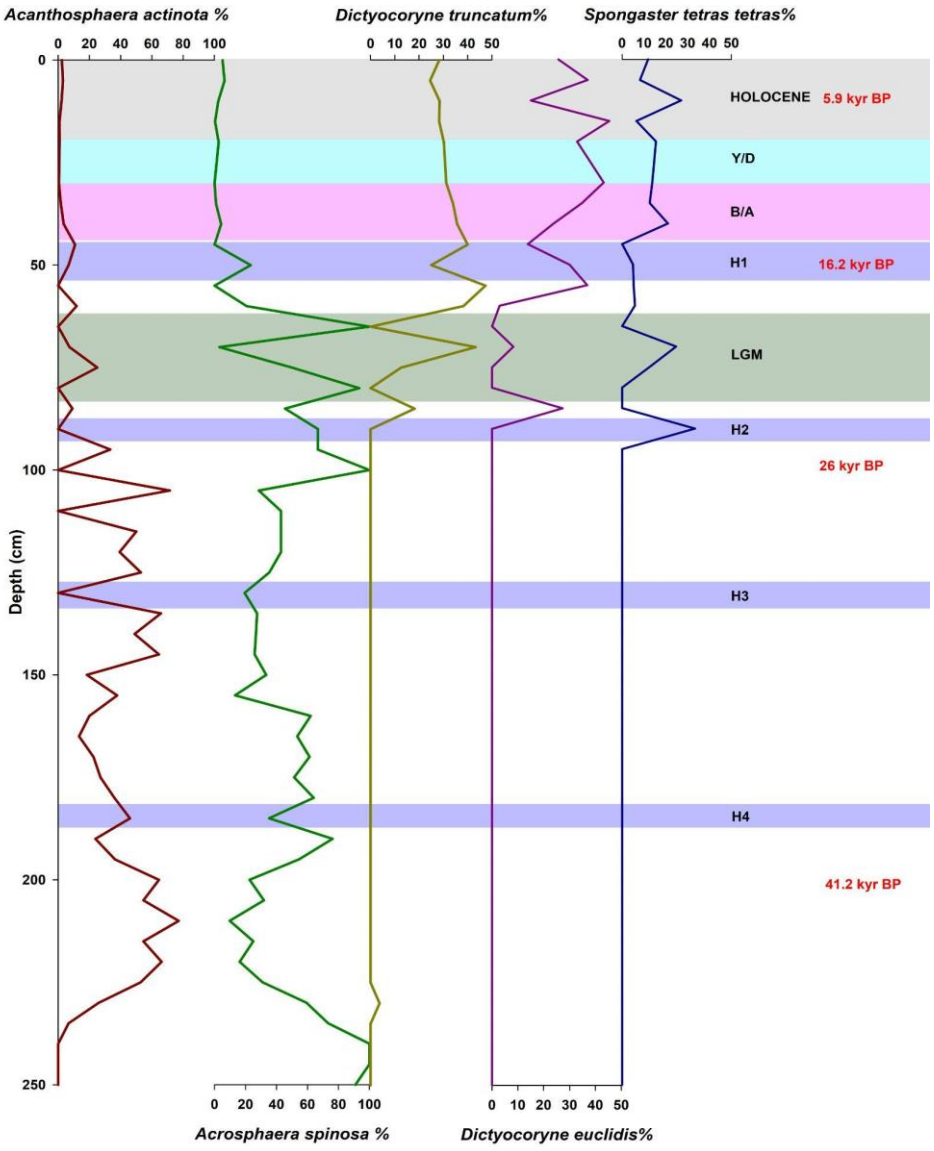

Fig. 3 Temporal distribution pattern of *Acanthosphaera actinota*, Acrosphaera spinosa, *Dictyocoryne truncatum, Dictyocoryne euclidis* and *Spongaster tetras tetras* along the examined core.

The Holocene is marked by the dominance of spumellarians such *Dictyocoryne truncatum*, *Dictyocoryne euclidis* and *Spongaster tetras tetras* (Fig.3). In the mid Holocene *Dictyocoryne euclidis* and *Spongaster tetras tetras* exhibit an opposite trend with each other. Among spumellarians, the family Spongodescidae are dominant, with species *Dictyocoryne*

truncatum, Dictyocoryne euclidis and *Spongaster tetras tetras.* Spongodiscids prefer low salinity and high sea surface temperature waters characterized by an increase in monsoonal rainfall (Sharma and Devi, 2007). Hence this period indicates a predominance of shallow warm water surface dwellers. *Acanthosphaera actinota* and *Acrosphaera spinosa*, the most abundant nassellarains of the examined core, show very low abundance during the Holocene.

The Younger Dryas (YD), also known as the Younger Dryas stadial, was a cold phase that occurred between approximately ~12.9–11.8 kyr BP (Bakke et.al., 2009; Haridas et.al., 2022). In the examined core, a slight increase is marked in abundance of species *Dictyocoryne truncatum* and *Dictyocoryne euclidis. D. truncatum* is largely a surface-dwelling species surviving optimally in warmer water that supports optimum skeletal growth and maturation. The tolerance of cooler water, however, may also reflect biological adaptations related to variations in habitat during the reproductive cycle. In the southern Bay of Bengal near the end of the Pleistocene Epoch a dominant warming was recorded.

The Bølling–Allerød interstadial (B/A), also called the Late Glacial Interstadial, that occurred during ~14.8–12.9 Kyr BP (Haridas et.al., 2022), was an abrupt warm, and moist interstadial period. It was noted in the final stages of the Last Glacial Period. It began with the end of the cold period known as the Oldest Dryas and ended abruptly with the onset of the Younger Dryas. (Naughton et.al., 2023). In southern BoB, *D. truncatum* the species that prefer warm climatic conditions are found to be the most abundant one.

Heinrich events are the intense and quasiperiodic pulses that primarily originated from the Laurentide ice sheet (Bond et.al., 1993; Heinrich, 1988; Maslin and Gornitz, 2009) which occurred against the unstable glacial climate and represent a brief expression of the most extreme glacial conditions in the North Atlantic (Hemming, 2004). Heinrich events are characterised by further drop in temperature from the already cold glacial climate (Bond et.al., 1993; Dansgaard et.al., 1993). In the present investigation, we recorded an increase in the abundance of *Acrosphaera spinosa* and *Acanthosphaera actinota* during Heinrich event 1 (H1). Both these species prefer colder waters for thriving.

Last Glacial Maximum (LGM) (~19–23 Kyr BP) is considered as a cold period. LGM was accompanied by a marked decline in Sea Surface Temperature (SST) (Haridas et.al., 2022). *Acrosphaera spinosa* shows its maximum abundance during LGM. These are organisms that mostly prefer cold climatic conditions. So, their abundance is very less in the Holocene and

abundance increases during glacial intervals. The warm water species *Dictyocoryne truncatum, Dictyocoryne Euclid is* and *Spongaster tetras tetras* shows decrease in their abundance during LGM. During Heinrich event 2 (H2) *Spongaster tetras tetras* are the most abundant species. Towards the close H2, *Dictyocoryne truncatum, Dictyocoryne euclidis* and *Spongaster tetras tetras* are absent and the radiolarian assemblages are dominated mainly by *Acrosphaera spinosa* and *Acanthosphaera actinota.* During H3 events, *Acanthosphaera actinota* reaches nearly zero in their abundance where as in H4 both *Acanthosphaera actinota* and *Acrosphaera spinosa* shows moderate abundance. Further investigation is needed for clarifying the absence of Acanthosphaera *actinota* during H3.

CHAPTER 6

SUMMARY AND CONCLUSION

The present investigation is the first report on the temporal distribution pattern of radiolarians of the southern Bay of Bengal. In this investigation, we reported 18 radiolarian species belonging to 12 genera and 5 families. Based on the AMS C^{14} dates measured from mixed planktic foraminifera of the examined gravity core, the average sedimentation rate of the study area is 6.25 cm/Kyr. The examined sediment core spans up to 44 Kyr BP.

We also analysed the temporal distribution pattern of radiolarians. *Acanthosphaera actinota, Acrosphaera spinosa, Dictyocoryne truncatum, Dictyocoryne euclidis* and *Spongaster tetras tetras* are the most abundant species. From the faunal data and the already available stable isotope data (not included in present report), we have marked various climatic events that are recorded during the past 44 Kyr in the southern Bay of Bengal. They are Younger Dryas (YD), Bølling–Allerød (B/A), Heinrich event 1 (H1), Last Glacial Maximum (LGM), Heinrich event 2 (H2), Heinrich event 3 (H3), and Heinrich event 4 (H4). The vertical distribution pattern of radiolarians shows variations at different intervals at different depths which indicates varying environmental conditions and associated monsoonal fluctuations. Spumellaraians are abundant over nassellarains in the examined core. The dominant nassellarians are *Acanthosphaera actinota* and *Acrosphaera spinosa.* Whereas spumellarians are dominated by the family Spongodiscidae with *Dictyocoryne truncatum, Dictyocoryne euclidis* and *Spongaster tetras tetras* species. The percentage distribution of fauna exhibited a dominance of spumellarians over nassellarians in the upper portion of the core, while the abundance decreases with depth towards the bottom. In contrast, nassellarians show an opposite trend with an increased abundance towards the bottom of the core. Thus, the abundance of radiolarians shows a fluctuating relationship with depth. During Younger Dryas, the warm water radiolarians such as *Dictyocoryne truncatum* and *Dictyocoryne euclidis* dominate the assemblage. This may be due to the warming episode that happened during the end of Pleistocene epoch in the southern Bay of Bengal. The Bølling–Allerød is marked by the presence of warm water species *D. truncatum.* During Heinrich event 1 (H1) *Acrosphaera spinosa* and *Acanthosphaera actinota*, the cold loving radiolarians dominate. *Acrosphaera spinosa* shows its maximum abundance during LGM. They prefer a cool environment.

BIBLIOGRAPHY

Adl, S.M., Bass, D., Lane, C.E., Lukeš, J., Schoch, C.L., Smirnov, A., Agatha, S., Berney, C., Brown, M.W., Burki, F. and Cárdenas, P., 2019. Revisions to the classification, nomenclature, and diversity of eukaryotes. *Journal of Eukaryotic Microbiology*, *66*(1), pp.4-119.

Afanasieva, M.S., 2006. Radiolarian skeletons: Formation and morphology of skeletal shells. *Paleontological Journal* 40 (5), 476–489. https://doi.org/10.1134/S0031030106050029.

Afanasieva, M.S., 2007. Radiolarian skeleton: Morphology of spines, internal framework, and primary sphere. *Paleontological Journal* 41, 1–14. https://doi.org/10.1134/S0031030107010017.

Almeida, H.I., Cortese, G., Yu, P.S., Chen, M.T. and Kucera, M., 2017. Environmental determinants of radiolarian assemblages in the western Pacific since the last deglaciation. *Paleoceanography* 32, 830–847. https://doi.org/10.1002/2017PA003159.

Anderson, O.R., 2001. Protozoa, Radiolarians. *In*: *Encyclopedia of Ocean Sciences*, 2315–2320. https://doi.org/10.1006/rwos.2001.0193.

Armstrong, H.A. and Brasier, M.D., 2004. Radiozoa (Acantharia, phaeodaria and

Bakke, J., Lie, Ø., Heegaard, E., Dokken, T., Haug, G.H., Birks, H.H., Dulski, P. and Nilsen, T., 2009. Rapid oceanic and atmospheric changes during the Younger Dryas cold period. *Nature Geoscience*, *2*(3), pp.202-205.

Biard, T., 2022. Diversity and ecology of Radiolaria in modern oceans. *Environmental Microbiology* 24 (5), 2179–2200. https://doi.org/10.1111/1462-2920.16004.

Biard, T., Stemmann, L., Picheral, M., Mayot, N., Vandromme, P., Hauss, H., Gorsky, G., Guidi, L., Kiko, R. and Not, F., 2016. In situ imaging reveals the biomass of giant protists in the global ocean. *Nature*, *532*(7600), pp.504-507.

Boltovskoy, D., 1998. Classification and distribution of South Atlantic recent polycystine Radiolaria. *Palaeontologia Electronica* 1(2), 1-116. https://doi.org/10.26879/98006.

Boltovskoy, D., 2017. Vertical distribution patterns of Radiolaria Polycystina (Protista) in the World Ocean: living ranges, isothermal submersion and settling shells. *Journal of Plankton Research* 39 (2), 330–349. https://doi.org/10.1093/plankt/fbx003.

Bond, G., Broecker, W., Johnsen, S., McManus, J., Labeyrie, L., Jouzel, J. and Bonani, G., 1993. Correlations between climate records from North Atlantic sediments and Greenland ice. *Nature*, *365*(6442), pp.143-147.

Campbell, A.S., Clarck, B.L., 1944. Miocene radiolarian faunas from southern California. *Geological Society of America, Special Papers* 51, 1-76.

Casey, R.E., 1993. Radiolaria. *Fossil Prokaryotes and Protistis*.

Casey, R.E., Weinheimer, A.L. and Nelson, C.O., 1990. Cenozoic radiolarian evolution and zoogeography of the Pacific. *Bulletin of marine Science*, *47*(1), pp.221-232.

Caulet, J.P., 1986. Radiolarians from the Southwest Pacific. In R. B. Blakeslee (Ed.). *Initial Reports of the Deep-Sea Drilling Project* 90, 835-861. https://doi. org/10.2973/dsdp.proc.90.114.1986.

Cavalier Smith, T., Chao, E.E. and Lewis, R., 2018. Multigene phylogeny and cell evolution of chromist infrakingdom Rhizaria: contrasting cell organisation of sister phylum Cercozoa and Retaria. *Protoplasma, 255*, pp.1517-1574.

Chowdhury, Aniruddha., 2023. Variability of Ocean Surface Currents in the Bay of Bengal. https://www.researchgate.net/publication/369794546_Variability_of_Ocean_Surface_ Currents_in_the_Bay_of_Bengal

Clark, B.L. and Campbell, A.S., 1942. Eocene radiolarian faunas from the Mt. Diablo area, California. *Geological Society of America* 39, 1-112

Danelian, T. and Frydas, D., 1998. Late Quaternary polycystine radiolarians and silicoflagellates of a diatomaceous sapropel from the Eastern Mediterranean, Sites 969 and 971. *Proceedings of the Ocean Drilling Program: Scientific Results* 160, 137-154. https://doi.org/10.2973/odp.proc.sr.160.007.1998.

Dansgaard, W., Johnsen, S.J., Clausen, H.B., Dahl-Jensen, D., Gundestrup, N.S., Hammer, C.U., Hvidberg, C.S., Steffensen, J.P., Sveinbjörnsdottir, A.E., Jouzel, J. and Bond, G., 1993. Evidence for general instability of past climate from a 250-kyr ice-core record. *nature*, *364*(6434), pp.218-220.

De Wever, P., Dumitrica, P., Caulet, J.P., Nigrini, C. and Caridroit, M., 2002. *Radiolarians in the sedimentary record*. CRC Press.

Dogel, V.A. and Reshetnyak, V.V., 1952. Materialy po radiolyariyam severo-zapadnoy chasti tikhogo okeana. *Issledovanya Dalnevostochnykh Morei SSSR* 3, 5-36.

Dumitrica, P., 1978. Badenian Radiolaria from Central Paratethys. *In: E. Brestenská (ed.) Chronostratigraphieund Neostratotypen. Miozän der Zentralen Paratethys*, 231-261.

Ehrenberg, C.G., 1838. Über die Bildung der Kreidefelsen und des Kreidemergels durch unsichtbare Organismen. *Abhandlungen der Königlichen Akademie der Wissenschaften zu Berlin*, 59-147.

Ehrenberg, C.G., 1847. Über die mikroskopischen Kieselschaligen Polycystinen als mächtige Gebirgsmasse von Barbados und über das Verhältnifs der aus mehr als 300 neuen Arten bestehenden ganz eigenthümlichen Formengruppe jener Felsmasse zu den jetzt lebenden Thieren und zur Kreidebildung. Eine neue Anregung zur Erforschung des Erdlebens. *Bericht Über Die Zur Bekanntmachung Geeigneten Verhandlungen Der Konigliche Preussische Akademie Der Wissenschaften Zu Berlin*, 40-60.

Ehrenberg, C.G., 1854. Die systematische Characteristik der neuen mikroskopischen Organismen des tiefen Atlantischen Oceans für den Monatsbericht zum Druck zu übergeben, deren Verzeichnifs im Monat Februar bereits mitgetheilt worden ist. *Bericht Über Die Zur Bekanntmachung Geeigneten Verhandlungen Der Konigliche Preussische Akademie Der Wissenschaften Zu Berlin*, 236-250.

Ehrenberg, C.G., 1860. Über den Tiefgrund des stillen Oceans zwischen Californien und den Sandwich-Inseln aus bis 15600’ Tiefe nach Lieutenant Brooke. *Monatsberichte der Konigliche Preussische Akademie der Wissenschaften zu Berlin*, 819-833.

Ehrenberg, C.G., 1872. Mikrogeologische Studien als Zusammenfassung seiner Beobachtungen des kleinsten Lebens der Meeres-Tiefgründe aller Zonen und dessen geologischen Einflufs. *Monatsberichte der Konigliche Preussische Akademie der Wissenschaften zu Berlin*, 265-322.

Gupta, H. and Gahalaut, V., 2009. Is the northern Bay of Bengal tsunamigenic? *Bulletin of the Seismological Society of America, 99*(6), pp.3496-3501.

Gupta, S.M. and Fernandes, A.A., 1997. Quaternary radiolarian faunal changes in the tropical Indian Ocean: inferences to paleomonsoonal oscillation of the 10 degrees S hydrographic front.

Gupta, S.M., 1996. Quantitative radiolarian assemblages in surface sediments from the Central Indian Basin and their paleomonsoonal significance. *JOURNAL-GEOLOGICAL SOCIETY OF INDIA*, *47*, pp.339-354.

Gupta, S.M., Mohan, R. and Guptha, M.V.S., 2002. Radiolarian fluxes from the southern Bay of Bengal: sediment trap results. *Deep Sea Research Part I: Oceanographic Research Papers* 49, 1669–1688. https://doi.org/10.1016/S0967-0637(02)00085-7.

Haeckel, E.H.P.A., 1860. Fernere Abbildungen und Diagnosen neuer Gattungen und Arten von lebenden Radiolarien des Mittelmeeres [Supplementary illustrations and diagnosis of new genera and species of living radiolarian of the Mediterranean Sea]. *Monatsberichte der Konigliche Preussische Akademie der Wissenschaften zu Berlin*, 835-845.

Haeckel, E.H.P.A., 1862. Die Radiolarien (Rhizopoda Radiaria) Eine Monographie. Tafel 1, *Berlin: Reimer*. Berlin, ist Edition. 1-572.

Haeckel, E.H.P.A., 1881. Prodromus Systematis Radiolarium, Entwurf eines Radiolarian Systems auf Grund von Studien der Challenger-Radiolarien. *Jenaische Zeitschrift Für Naturwissenschaft* 15(8), 418-472.

Haeckel, E.H.P.A., 1887. Report on the Scientific Results of the Voyage of H.M.S. Challenger during the years 1873–76. *Zoology* 18(40), i-clxxxviii [188], 1-1803. http://www.19thcenturyscience.org/HMSC/HMSC-Reports/Zool-40/README.ht

Haridas, N.V., Banerji, U.S., Maya, K. and Padmalal, D., 2022. Paleoclimatic and paleoceanographic records from the Bay of Bengal sediments during the last 30 ka. *Journal of Asian Earth Sciences* 229, 105169. https://doi.org/10.1016/j.jseaes.2022.105169.

Heinrich, H., 1988. Origin and consequences of cyclic ice rafting in the northeast Atlantic Ocean during the past 130,000 years. *Quaternary research*, *29*(2), pp.142-152.

Hemming, S.R., 2004. Heinrich events: Massive late Pleistocene detritus layers of the North Atlantic and their global climate imprint. *Reviews of Geophysics*, *42*(1).

Hertwig, R. and Lesser, E., 1874. Bemerkungen zur Organisation und systematischen Stellung der Foraminiferen: Jenaische Zeitschr. für Nat. 10(3), 41-55.

Hilmers, C., 1906. Zur Kenntnis der Collosphaeriden. Inaugural-Dissert. Doktorwurde hohen philosoph. Fak. Christian-Albrechts Univ., Kiel, 5-93.

Hollis, C.J. and Neil, H.L., 2005. Sedimentary record of radiolarian biogeography, offshore eastern New Zealand, *New Zealand Journal of Marine and Freshwater Research* 39(1), 165-192. https://doi.org/10.1080/00288330.2005.9517299.

Ishitani, Y., Febvre-Chevalier, C. and Febvre, J., 2016. Radiolaria. *In*: John Wiley & Sons, Ltd (ed.) *ELS*. 1–6. https://doi.org/10.1002/9780470015902.a0001985.pub2.

Ittekkot, V., Nair, R.R., Honjo, S., Ramaswamy, V., Bartsch, M., Manganini, S. and Desai, B.N., 1991. Enhanced particle fluxes in Bay of Bengal induced by injection of fresh water. *Nature*, *351*(6325), pp.385-387.

Johnson, D. and Knoll, A., 1974. Radiolaria as Paleoclimatic Indicators: Pleistocene Climatic Fluctuations in the Equatorial Pacific Ocean. *Quaternary Research* 4(2), 206-216. https://doi.org/10.1016/0 033-5894(74)90008-8.

Knoll, A.H. and Johnson, D.A., 1975. Late Pleistocene evolution of the collosphaerid radiolarian Buccinosphaera invaginata Haeckel. *Micropaleontology*, pp.60-68.

Krabberød, A.K., Bråte, J., Dolven, J.K., Ose, R.F., Klaveness, D., Kristensen, T., Bjorklund, K.R. and Tabrizi, K.S., 2011. Radiolaria Divided into Polycystina and Spasmaria in Combined 18S and 28S rDNA Phylogeny Lopez-Garcia, P. (ed.). *PLoS ONE* 6(8), e23526. https://doi.org/10.1371/journal.pone.0023526.

LaFond, E.C., 1966. Bay of Bengal, The Encyclopedia of Oceanography. *Fairbridge R. W.*, New York, 110–118.

Lampitt, R.S., Salter, I. and Johns, D., 2009. Radiolaria: Major exporters of organic carbon to the deep ocean. *Global Biogeochemical Cycles*, *23*(1).

Lazarus, D.B., 2005. A brief review of radioliarian research. *Paläontologische Zeitschrift* 79 (1), 183–200. https://doi.org/10.1007/BF03021761.

Lazarus, D.B., Kotrc, B., Wulf, G. and Schmidt, D.N., 2009. Radiolarians decreased silicification as an evolutionary response to reduced Cenozoic Ocean silica availability. *Proceedings of the National Academy of Sciences* 106 (23), 9333–9338. https://doi.org/10.1073/pnas.0812979106.

Lazarus, D.B., Suzuki, N., Ishitani, Y. and Takahashi, K., 2020. *Paleobiology of the Polycystine Radiolaria*. John Wiley & Sons.

Lipps, J.H., 1993. Fossil prokaryotes and protists.

Lüer, V., Hollis, C.J. and Willems, H., 2008. Late Quaternary Radiolarian Assemblages as Indicators of Paleoceaonographic Changes North of the Subtropical fronts, Offshore Eastern New Zealand, Southwest Pacific. *Micropaleontology* 54 (1), 49-69. http://www.jstor.org/stable/30135298.

Maslin, M. and Gornitz, V., 2009. Quaternary climate transitions and cycles. *Encyclopedia of Palaeoecology and Ancient Environments. Springer, Dordrecht*, pp.841-855.berg, C.G., 1875. Fortsetzung der mikrogeologischen Studien als Gesammt- Uebersichtder mikroskopischen Palaontologie gleichartig analysirter. Gebirgsarten der Erde, mit specieller Rucksicht auf den PolycystinenMergel von Barbados. *Abhandlungen der Königlichen Akademie der Wissenschaften zu Berl*in, 1-225.

Matul, A., and Mohan, R., 2017. Distribution of Polycystine Radiolarians in Bottom Surface Sediments and Its Relation to Summer Sea Temperature in the High-Latitude North Atlantic. *Frontiers in Marine Science* 4, 330. https://doi.org/10.3389/fmars.2017.00330.

Müller, J., 1855. Über die im Hafen von Messinabeobachteten Polycystinen. Bericht Über Die Zur Bekanntmachung Geeigneten Verhandlungen Der Konigliche Preussische Akademie Der Wissenschaften Zu Berlin, 671-676.

Mullineaux, L.S. and Westberg-Smith, M.J., 1986. Radiolarians as Paleoceanographic Indicators in the Miocene Monterey Formation, Upper Newport Bay, California. *Micropaleontology* 32 (1), 48-71. https://doi.org/10.2307/1485701.

Murchey, B., 1984. Biostratigraphy and lithostratigraphy of chert in the Franciscan Complex, Marin Headlands, California.

Murty, V.S.N., Sarma, Y.V.B., Rao, D.P. and Murty, C.S., 1992. Water characteristics, mixing and circulation in the Bay of Bengal during southwest monsoon. *Journal of Marine Research*, *50*(2), pp.207-228.

Naughton, F., Sánchez-Goñi, M.F., Landais, A., Rodrigues, T., Riveiros, N.V. and Toucanne, S., 2023. The Bølling–Allerød Interstadial. In *European Glacial Landscapes* (pp. 45-50). Elsevier.

Nigrini, C. and Johnson, D.A., 1982. Radiolarian biogeography in surface sediments of the eastern Indian Ocean. *Marine Micropaleontology* 7(3), 237-281. https://doi.org/10.1016/0377-8398(82)90004-4.

Nigrini, C., Moore, T.C., 1979. A guide to modern Radiolaria. *Cushman Foundation for Foraminiferal research Special Publication* 16, 107-116. http://gdcmp1.ucsd.edu/geol_coll/radlit/nm79titl.html.

Nigrini, C.A., 1967. Radiolaria in pelagic sediments from the Indian and Atlantic Oceans. *Bulletin of the Scripps Institution of Oceanography of the University of California* 11, 1-125.

Petrushevskaya, M.G. and Swanberg, N.R., 1990. Variability in Skeletal Morphology of Colonial Radiolaria (Actinopoda: Polycystinea: Collosphaeridae). *Micropaleontology* 36(1), 65-85. https://doi.org/10.2307/1485665.

Radiolaria) and heliozoa. *Microfossils*, pp.188-199.

Riedel, W.R., 1958. Radiolaria in Antarctic sediments. *B.A.N.Z. Antarc. Res. Exped. Rep. Ser. B* 6(10), 217-255.

Riedel, W.R.,1967. Some new families of Radiolaria. *Proceedings of the Geological Society of London* 1640, 148-149.

Rogers, J., 2016. Monsoonal and other climatic influences on radiolarian species abundance over the last 35 ka, as recorded in core FR10/95-GC17, off North West Cape (Western Australia). *Revue de micropaléontologie.* http://dx.doi.org/10.1016/j.revmic.2016.05.003.

Sanfilippo, A. and Riedel, W.R., 1970. Post Eocene "Closed" Theoperid Radiolarians. *Micropaleontology* 16(4), 442-462. https://doi.org.10.2307/1485072.

Sanfilippo, A., 1985. Cenozoic radiolaria. *Plankton stratigraphy*.

Shankar, D., Vinayachandran, P.N. and Unnikrishnan, A.S., 2002. The monsoon currents in the north Indian Ocean. *Progress in Oceanography* 52 (1), 63–120. https://doi.org/10.1016/S0079-6611(02)00024-1.

Sharma, R., Umapathy, G., Kumar, P., Ojha, S., Gargari, S.F., Joshi, R., Chopra, S. and Kanjilal, D., 2019. AMS and upcoming geochronology facility at Inter University

Accelerator Centre (IUAC), New Delhi, India. *Nuclear Instruments and Methods in Physics Research Section B: Beam Interactions with Materials and Atoms* 438, 124-130. https://doi.org/10.1016/j.nimb.2018.07.002.

Sharma, V. and Daneshian, J., 1998. Radiolaria as tracers of ocean–climate history. *Current Science* 75(9), 893–897. http://www.jstor.org/stable/24101662.

Sharma, V. and Devi, L.B., 2007. Neogene oceanographic and climatic changes in the northern Indian Ocean: Evidence from Radiolaria.

Suryanarayana, A., Murty, V.S.N. and Rao, D.P., 1993. Hydrography and circulation of the Bay of Bengal during early winter, 1983. *Deep Sea Research Part I: Oceanographic Research Papers*, *40*(1), pp.205-217.

Suzuki, N. and Aita, Y., 2011. Radiolaria: achievements and unresolved issues: taxonomy and cytology. Plankton and Benthos Research 6(2), 69-91. https://doi.org/10.3800/pbr.6.69.

Suzuki, N. and Not, F., 2015. Biology and ecology of radiolaria, in *Undefined Marine PROTISTS*, eds S. Ohtsuka, T. Horiguchi, N. Suzuki, and F. Not (Tokyo: Springer), 179–222. https://doi.org/ 10.1007/978-4-431-55130-0_8.

Suzuki, N. and Oba, M., 2015. Oldest fossil records of marine protists and the geologic history toward the establishment of the modern-type marine protist world. *Marine protists: Diversity and dynamics*, pp.359-394.

Swanberg, N.R. and Anderson, O.R., 1985. The nutrition of radiolarians: Trophic activity of some solitary Spumellaria 1. *Limnology and Oceanography*, *30*(3), pp.646-652.

Takahashi, K., 1987. Radiolarian flux and seasonality: climatic and El Nino response in the subarctic Pacific, 1982–1984. *Global Biogeochemical Cycles*, *1*(3), pp.213-231.

Wang, J.B., 2012. Study on the Ecology and Taxonomy of polycystine Radiolaria from three areas of the South China Sea. D. Phil. Thesis, Institute of Oceanology, Chinese Academy of Sciences.

Wang, R. and Abelmann, A., 2002. Radiolarian responses to paleoceanographic events of the southern South China Sea during the Pleistocene. *Marine Micropaleontology* 46 (1-2), 25–44. https://doi.org/10.1016/S0377-8398(02)00048-8.

Wang, R., Clemens, S., Huang, B. and Chen, M., 2003. Quaternary palaeoceanographic changes in the northern South China Sea (ODP Site 1146): radiolarian evidence. *Journal of Quaternary science* 18(8),745-756. https://doi.org/10.1002/jqs.784.

Wyrtki, K., Bennett, E.B. and Rochford, D.J., 1971. Oceanographic atlas of the international Indian Ocean expedition.

Wyrtki, K., Bennett, E.B. and Rochford, D.J., 1971. Oceanographic atlas of the international Indian Ocean expedition. *(No Title)*.

Xiping, D., Knoll, A.H. and Lipps, J.H., 1997. Late Cambrian Radiolaria from Hunan, China. *Journal of Paleontology*, *71*(5), pp.753-758.